

DTIC FILE COPY

1

MINUTES OF THE TWENTY-SECOND EXPLOSIVES SAFETY SEMINAR

AD-A181 275

Volume II



**Anaheim Marriott Hotel
Anaheim, California
26-28 August 1986**

DTIC
ELECTE
MAY 5 1987
A

This document has been approved
for public release and sale; its
distribution is unlimited.

**Sponsored By
Department of Defense Explosives Safety Board
Alexandria, Virginia**

87 5 1 039

COMPONENT PART NOTICE

THIS PAPER IS A COMPONENT PART OF THE FOLLOWING COMPILATION REPORT:

TITLE: Minutes of the Explosives Safety Seminar (22nd) Held in Anaheim,
California on 26-28 August 1986. Volume 2.

TO ORDER THE COMPLETE COMPILATION REPORT, USE AD-A181 275

THE COMPONENT PART IS PROVIDED HERE TO ALLOW USERS ACCESS TO INDIVIDUALLY AUTHORED SECTIONS OF PROCEEDING, ANNALS, SYMPOSIA, ETC. HOWEVER, THE COMPONENT SHOULD BE CONSIDERED WITHIN THE CONTEXT OF THE OVERALL COMPILATION REPORT AND NOT AS A STAND-ALONE TECHNICAL REPORT.

THE FOLLOWING COMPONENT PART NUMBERS COMPRISE THE COMPILATION REPORT:

AD#: POOF 350 thru POOF 393 AD#: _____
AD#: _____ AD#: _____
AD#: _____ AD#: _____

Accession For	
NTIS GRA&I	<input checked="checked" type="checkbox"/>
DTIC TAB	<input type="checkbox"/>
Unannounced	<input type="checkbox"/>
Justification	
By _____	
Distribution/	
Availability Codes	
Dist	Avail and/or Special
A-1	

This document has been approved
for public release and sale; its
distribution is unlimited.

DTIC FORM 463
MAR 85

OPI: DTIC-TID

MINUTES OF THE
TWENTY-SECOND EXPLOSIVES SAFETY SEMINAR

Volume II

Anaheim Marriott Hotel

Anaheim, California

26-28 August 1986

Sponsored by
Department of Defense Explosives Safety Board
Alexandria, Virginia 22331-0600

Approved for public release; distribution unlimited

TABLE OF CONTENTS

the following sessions → VOLUME II OF the Minutes includes

SESSION - ORDNANCE DISPOSAL; Moderator - Milton Van Slyke

ASSESSMENT OF THE FEASIBILITY OF PERFORMING INFILDT
NONDESTRUCTIVE EVALUATION TO DETERMINE THE PRESENCE
OF EXPLOSIVES MATERIALS WITHIN CASED MUNITIONS 1185
Harold J. Gryting, Ph.D.

HAWTHORN ARMY AMMUNITION PLANT, NEW BOMB OPEN BURNING/ 1223
OPEN DETONATION GROUNDS EOD SURFACE SWEEP - A PROJECT
OVERVIEW
C.D. Douthat

SESSION - REDUCING THE MAXIMUM CREDIBLE EVENT; Moderator - William R. Hammer

SUPPRESSION OF PROPAGATION BETWEEN STACKS OF BOMBS 1237
Kenneth R. Shopher and Edward M. Jacobs

TEMPORARY TANK AMMUNITION STORAGE FACILITY 1279
David L. Collis

PROPAGATION TESTING OF M61 ROCKETS IN SINGLE ROUND 1329
CONTAINERS
D.B. Hill

SESSION - WATER SPRINKLER/DELUGE SYSTEMS; Moderator - Robert A. Loyd

DELUGE SPRINKLER SYSTEM, TIMED INTERVAL OPERATION ADDITION 1347
Wayne R. Sueker

PYROTECHNIC FIRE SUPPRESSION SYSTEM EVALUATION 1365
Joseph P. Caltagirone, Luis M. Vargas & Luis R. Garza

ULTRA HIGH SPEED DELUGE FIRE PROTECTION SYSTEM FOR 1397
MUNITIONS, EXPLOSIVES, PYROTECHNICS
Gary A. Fadorsen

SESSION - EXPLOSIVES CLASSIFICATION AND QUANTITY-DISTANCE; Moderator - Dr. N. J. M. Rees

CLASSIFICATION OF EXPLOSIVES UNDER THE UN SCHEME - 1429
A NEED FOR UNIFORMITY OR FLEXIBILITY
Dr. R. J. Smallwood

UK MOD EXPLOSIVE STORAGE PRINCIPLES 1437
Dr. J. M. Rees

AN AUDIT OF THE QUANTITY DISTANCES USED FOR THE STORAGE OF AMMUNITION AND EXPLOSIVES
Lt. Col. F. Cantrell

SESSION = LARGE SCALE EXPLOSION TESTING;
Moderator - John Eddy

EXPANDED SIMULATION TECHNIQUES
Robert A. Flory

DAMAGING DISTANT AIRBLAST FROM MINOR SCALE 1513
Jack W. Reed

SESSION - HAZARDS FROM WEAPONS FRAGMENTS
Moderator - Patricia K. Bowles

FRAGMENT HAZARD INVESTIGATION PROGRAM: PREDICTION
OF QUANTITY DISTANCE REQUIREMENTS FOR MASS-DETONATING
AMMUNITION USING A MONTE CARLO SIMULATION MODEL
W.D. Smith

DRAG COEFFICIENTS FOR IRREGULAR FRAGMENTS 1549
Frank McCleskey

FRAGMENT HAZARDS EVALUATION PROPOSAL 1591
A. G. Papp, Richard P. Guarienti and Fred Krach

SESSION - RISK ASSESSMENT
Moderator - Peter J. Rutledge

THE APPLICATION OF RISK ASSESSMENT IN THE FIELD OF
EXPLOSIVES AND AMMUNITION SAFETY
F.R. Hartley, F. Cantrell, P.A. Moreton, J.J. Clifton and
J.N. Edmondson

WARTIME MISSION OF EXPLOSIVES SAFETY 1605
Captain Susan J. Kaufman, USAF

WHO IS AFRAID OF RISK CRITERIA
H.A. Merz



ACCESSION FOR

NTIS GRA&I ☒

DTIC TAB ☐

Unannounced ☐

Justification

By _____

and/or for _____

Availability Codes

Avail and/or

Dist _____ Special _____

Al

Cont'd

SESSION - EFFECTS OF BLAST AND DEBRIS ON STRUCTURES
Moderator - Walter C. Buchholtz

BLAST TESTING OF EXPEDIENT SHELTERS IN MODEL SCALE Edward D. Esparza	1641
BLAST LOADING ON ABOVE GROUND BARRICADED MUNITIONS STORAGE MAGAZINES - II G. A. Coulter, C. N. Kingery and P. C. Muller	1681
ESKIMO VII TEST RESULTS R. N. Murtha	1731

SESSION - SAFETY CONCERNS FOR INITIATING DEVICES
Moderator - Roger H. Goldie

INSENSITIVE CONDUCTING COMPOSITION (CC) PRIMERS R. J. Spear and J. R. Bentley	1785
IRON-WIRE RF-PROTECTION AND TRANSMISSION LINE EQUATIONS Klaus G. Rucker	1801
SAFETY CONSIDERATIONS FOR IN-LINE MECHANICAL FUZES Dr. B. W. Thorpe and Mr. J. R. Bentley	1823

SESSION - INDUSTRY EXPLOSIVES SAFETY
Moderator - A. K. Siler, Jr.

HAZARDS AND OPERABILITY STUDIES AND THEIR APPLICATION TO AN EXPLOSIVE PLANT R. E. Knowlton	1833
MANUFACTURE AND STORAGE OF LEAD AZIDE BY A COMPUTER INTEGRATED SYSTEM B. Bobasch	1847
ORDNANCE INDUSTRY SAFETY PROBLEMS; THE CAN'T BE SOLVED ALONE Thomas S. Denison	1857

SESSION - DEBRIS HAZARDS FROM STRUCTURES
Moderator - J. P. McLain

JOINT AUSTRALIAN/UK STACK FRAGMENTATION TRAILS PHASE TWO REPORT J. Henderson, J. Walker, Dr. N. J. M. Rees and R. A. Bowe	1867
--	------

Cont'd p. vi

TECHNICAL EVALUATION OF THE LIMITS OF THE HAZARDOUS AREAS AS TO PROJECTIONS F.X. Boisseau, D. Houdusse and R. Kent	1887
VELOCITY MEASUREMENTS OF ACCEPTOR WALL FRAGMENTS FROM THE MASS DETONATION OF A NEIGHBORING ABOVEGROUND BARRICADED MUNITIONS STORAGE MAGAZINE MODEL G. Bulmash, C. N. Kingery and G. A. Coulter	1909
<i>Cont'd</i>	
SESSION - THERMAL HAZARDS	
Moderator - Hyla S. Napadensky	
PREDICTIVE MODELS FOR THERMAL HAZARDS J. L. Janney and R. N. Rogers	1955
MULLER MIXER FIRE, 'LESSONS LEARNED' B. V. Diercks, J. E. Hawley and M. L. Naron	1967
FLASH BURN HAZARD CRITERIA RE-EVALUATION FOR PROPELLANT FIRES R. B. Crockart	1979
SESSION - CHEMICAL AGENT SAFETY	
Moderator - Mark M. Zaugg	
SYSTEMS SAFETY CONSIDERATIONS FOR THE DESIGN OF A CHEMICAL SURETY MATERIEL LABORATORY G. E. Collins, Jr.	1997
SAFETY CONSIDERATIONS FOR THE OPERATION OF A THERMAL DESTRUCTOR UNIT FOR CHEMICAL SURETY MATERIEL 3" X" ITEMS G. W. St Pierre	2013
SESSION - CLOSE-IN AND CONFINED BLAST LOADS	
Moderator - Richard L. Lorenz	
AIRBLAST MEASUREMENTS AND EQUIVALENCY FOR SPHERICAL CHARGES AT SMALL SCALED DISTANCES Edward D. Esparza	2029
SAFETY ANALYSIS FOR VENTED DUST EXPLOSIONS James J. Kulesz and Dr. Wilfred E. Baker	2059

cont'd	TNT EQUIVALENCE OF TWO PLASTIC-BONDED EXPLOSIVES FOR INTERNAL BLAST AND GAS PRESSURES Dr. Wilfred E. Baker and Donna W. O'Kelley	2073
SESSION - ENERGETIC MATERIALS HAZARDS TESTING ; and		
Moderator - William P. Yutmeyer		
	HAZARD ANALYSIS OF EXPLOSIVES BY ACCELERATING RATE CALORIMETRY Jack L. Johnston and Maria P. Flores	2085
	DETERMINATION OF METAL SPARKING CHARACTERISTICS AND THE EFFECTS ON EXPLOSIVE DUST CLOUDS C James Dahn and Bernadette N. Reyes	2107
	WC-814 PROPELLANT BURNING IN A SCAMP-TYPE HOPPER C. James Dahn	2119
SESSION - DEMILITARIZATION/DISPOSAL OF AMMUNITION/EXPLOSIVES		
Moderator - Dr. James J. Mikula		
	AN AUTOMATED EXPLOSIVE REMOVAL SYSTEM USING CAVITATING WATER JETS Dr. A. F. Corn	2133
	IDENTIFICATION AND CHARACTERIZATION OF EMISSIONS AND RESIDUES FROM OPEN BURNING AND DETONATION OF MUNITIONS Mark M. Zaugg	2151
BACKUP PAPER		
	TOMAHAWK (BGM-109 B/C-2) SYMPATHETIC DETONATION TESTING AND HAZARD ARC DETERMINATION Michael Swisdak, Jr.	2165
	CHAIRMAN'S CLOSING REMARKS	2189
	ATTENDANCE LIST	2191

AD-P005 350

Harold J. Gryting, Ph.D.

**Paper for DDESB
Anaheim Meeting
26-28 August 1986**

DISTRIBUTION STATEMENT:
"Approved for public release;
distribution is unlimited."

1185

ABSTRACT

Progress in explosives vapor detection is reviewed. The NAVSEA problems of detecting live explosives in sealed ordnance and differentiating them from inert materials are considered and detection techniques useful in their solution presented. Recommendations for vapor detection improvements and for development of new techniques and instrumentation are given.

Portable on-the-fly measurements of vapor from bombs will not at present assure live vs. inert differentiation.

ACKNOWLEDGMENTS

The writer is indebted to NAVSEA 06H3 and NAVSEA 6423 for support and encouragement especially Mr. Ken Range and Mr. Ed. Daugherty. The encouragement of SwRI management and staff and especially Mr. Alex Wenzel, Director Department of Energetic Systems and Dr. George Matzkanin, Director NTIAC. Miss Deborah Stowitts edited the reports and Mrs. Lynette Ramon and Mrs. Barbara Gryting typed the reports on which the paper is based. Both government and industrial scientists contributed information used herein, many of them are listed in the referenced reports.

I. INTRODUCTION

The majority of explosive detection studies in the past as well as those currently underway are concerned with terrorist activities of one kind or another. A great insurgence of effort therefore has accompanied the increase in national and international crime. There are already a great many detectors on the market and many others in various stages of research and development.

Other detection needs include those of detecting buried mines at various depths below the surface. The Fort Belvoir Research and Development Center has conducted research in this area since the 1960's. The Naval Sea Systems Command is concerned with ordnance used at its testing facilities present and past including bombing ranges. It is concerned as well in transportation of ordnance items and in their ultimate disposal. It is necessary to know if these ordnance items (whether they be bombs, flares, projectiles or other items) are loaded with energetic materials or have been freed from such explosives or may be loaded with an inert material.

In previous work on this problem at NWC⁽¹⁾ several commercial instruments were investigated to determine whether any suitable ones could be found for determining explosives (Comp B or TNT for examples) loaded in closed warheads or bombs.

This study covered ion mobility spectrometry, the U.S. Customs thermionic acetone vapor detector and a non-commercial Gas Chromatograph with electron capture detection as the main types. Each had some value for detecting bare or recently loaded explosives, however, none were suitable for use in on-the-fly measurements for explosives loaded into MK 82 bombs (Comp B loaded). The best for our purposes was the GC Electron Capture Detector which could detect dinitrotoluene and trinitrotoluene down to a few picograms (10^{-12} g). Even this would not pick up enough vapors without first encasing the ordnance in a tank and evacuating for several hours and catching the effluent vapors in a dry ice trap. The head space in the trap would then be sampled by pumping the vapors for the GC.

The customs detector would only detect RDX or HMX or other explosives that had residual solvent with an alpha keto group like acetone or methylethyl ketone. Characteristics of some other methods including nuclear gauging, NMR, FTIR, and acetone wash with GC were considered along with some other methods and a proposal was written covering a multi-instrument development and

evaluation for both vapor and non-vapor methods. The NAVSEA was not prepared to engage in a comprehensive study but did fund a review of improved instruments and methods that might later be developed for the attainment of their objectives. They also supported a small experimental study by IRT Corporation for a nuclear gauging effort.

This paper is a summary of the literature review on instruments and concepts for solving explosives detection problems that the NAVSEA has encountered. Recommendations are given for methods that best warrant further development. Limitations of instruments commercially available are described in reference to the NAVSEA requirements for portable, rapid action detectors.

The study described here covers a comprehensive literature review from 1980-1983 with some papers and techniques looked at since that time.⁽²⁾ Two separate studies were made: (1) vapor detectors and (2) non-vapor detectors. (Phase II Non-Vapor Detectors will be described in a later paper.)

II. DATA BASES SEARCHED

The data bases searched by computer included: (1) INSPEC DATA BASE, which is the largest data base in the English language in the fields of Physics, Electrotechnology, Computers and Control. (2) Chemical Abstracts Search Data Base. This covers bibliographic data from all documents covered by the Chemical Abstract Service. (3) NTIS Data Base. This covers government research, development, engineering, plus analyses by Federal agencies, their contractors and grantees. (4) Compendex Data Base which is from the Engineering Index with a worldwide coverage of 3500 journals, publications of engineering societies and organizations including papers from the proceedings of conferences, and selected Government reports and books. In addition to the above data base, contact was made by phone or visit to people at organizations involved with detection of explosives in some manner. A summary from a meeting of scientists at Cambridge, Mass. to discuss potential solutions to the FAA problems was obtained. This meeting, held April 19, 1983, brought several potential contractors together to pool their knowledge and suggestions as to worthy approaches for the FAA. Both abstracts and complete papers were also obtained from the FBI-sponsored detection meeting held at Quantico, W. Va. (March 29-31, 1983.) These two conferences were directed primarily at detection of explosives that might be brought in by terrorists or saboteurs. A meeting attended in August 1983 primarily concerned NDE for materials in general and essentially all papers concerned non-vapor types of detection. Much of the vapor pressure data on explosives stems from work at BRL. Fort Belvoir has been associated with most of the

conventional methods of detection of materials although they are less concerned with the detection of explosives than they are with more readily detected mines which contain explosives. Their problems are, therefore, for the greater part at least different from those of the Naval Sea Systems Command. Fort Belvoir does not ignore explosives detection as will be made clear later, as they have some very basic and interesting on-going studies related to TNT detection.

III. VAPOR DETECTION METHODS

The various methods for vapor detection that have been used or that have potential for use for explosives inside of closed ordnance items are reviewed to see whether they might be considered in their present state or by modification of either the instruments or techniques. Differentiation between live explosives listed previously^(1,2) and inert simulants^(1,3) is the major problem involved in both the safety and the cleanup and recovery methodology required by the Naval Sea System Command. When methods and instrumentation are selected for detection, this factor must be borne in mind and will be considered in the analysis that follows for the various classes of instruments or methodologies reported on here.

A. ION MOBILITY SPECTROMETRY

Recent literature describing instruments by Ion Track or Pye Dynamics⁽¹⁾ (the latter has been changed to Grasbey Dynamics at the same location and the same products), does not reveal any major improvements since these instruments were reviewed previously. Appendix I of Ref. 1 describes these as does Table I. Fig. 1 gives the general diagram showing how the Ion Mobility Spectrometer also known as the Plasma Chromatograph operates. It measures mobility of ions drifting through an electric field. Mobility is proportional to the inverse square root of the ion mass. More sophisticated instruments are available as the Phemto-Chem and the T. M. Franklin GNO Corporation instruments which have been reported to give 10^{-12} mole/mole for TNT which is the same as 2.27×10^{-10} g. These are larger non-portable instruments and although still viable as concepts for future portable instruments, would be currently unsuitable for detecting less than picogram quantities as required in a field portable instrument. The two first mentioned instruments are mainly portable detectors designed to detect such materials as nitroglycerine or 2,4-dinitrotoluene which they can detect down to 10^{-7} . The small portable instruments have their place in detecting noncased explosives, explosives carried on a person's body, and in detecting scattered explosive after a dud operation of some sort where a deflagration occurred rather than a detonation. They have been found of little use for discerning where explosive or inert materials are loaded in a closed bomb or warhead.

B. GAS CHROMATOGRAPHY

Gas Chromatography along with other chromatographic methods is finding increased use in analysis of materials in which picogram quantities may be all that is available for the sample. Gas chromatography is accompanied by detectors useful for the range of concentrations available for measure. The electron-capture is still among the most sensitive or the most sensitive of the detectors used with gas chromatography. Campbell and Lee⁽⁴⁾ have used capillary columns in the gas chromatographic determinations of a number of nitro-polycyclic aromatic hydrocarbons and applied it to their determination from diesel exhaust extract. Silicic acid column chromatography combined with the reduction of the nitro compounds by means of potassiumborohydride catalyzed with Copper II chloride derivitization with pentafluoropropionic acid anhydride yielded the enriched nitro fraction needed. Gas chromatography with electron capture detection as well as nitrogen selective thermionic and flame ionization detection and GC/mass spectrometry together with low-resolution mass spectral data were used to positively identify ten nitro polycyclic compounds. More than 120 such compounds were thus tentatively identified. The authors indicate that the best selective detection system for the nitro polycyclic aromatic compounds may be the negative chemical ionization mass spectrometry (NICIMS). However, although NICIMS has excellent sensitivity, many interfering compounds frequently detected by common selective detectors are not detected by NICIMS. This technique would probably be precluded on the basis of expense and high sophistication from competition with GC for our purposes in explosives detection in ordnance. HPLC was also found to fail to detect many nitro-PAC isomers. These authors suggest an ideal scheme for such compounds should include a high selective preparative procedure that isolates nitro-PACs while eliminating all non-nitro compounds from the isolated material. Final resolution with gas chromatography is recommended (using a capillary gas chromatograph).

Gross and others⁽⁵⁾ in their summary of instrumentation for detecting hazardous materials indicate several showing promise for further development. among these were included the non-remote portable gas chromatograph/mass spectrometer and a remote passive IR analyzer. At the time of the study (1980) they indicated that no instrument existed in portable ready form to detect all of the 115 materials considered to pose significant hazards in emergency operations management. This study has many parallels to future recommended studies for the Naval Sea Systems Command. Because of some similarity their objectives for emergency detection are given: 1. Compilation of hazardous materials most likely to be encountered in FEMA emergency missions. 2. Determination of exploitable chemical and/or physical characteristics of those materials. 3. Evaluation of

the state of pertinent detection technology. 4. Establishment of operational and performance requirements for any detection technique deemed practical. Major emphasis was applied to gathering data on the hazardous materials that could be used in their studies. Emphasis was also placed on types of instruments that could be made portable, easy to use and suitable for the first emergency group to arrive on the scene of an accident. Instruments evaluated included: Passive IR Absorption; Active Double-ended Direct Absorption; Laser Raman Spectroscopy; Non-dispersive or Discrete Frequency Absorption; Dispersive Absorption; Mass Spectroscopy or GC/MS; Gas Chromatography; Detector Kits; Chemical Kits; Combustible Gas Detector; and IR Hot Spot Detectors. An ideal instrument would be a small black box with a few controls, usable by an inexperienced person, which could be pointed at a material or vapor cloud, and which would immediately identify the material and simultaneously give its concentration. Although no such instrument is available, the potential may exist.

Bourne and others⁽⁶⁾ have evolved a system known as Matrix Isolation Gas Chromatography. Modern GC/FTIR systems have used a gold-coated light pipe for "on-the-fly" measurements. There are commercial versions which now approach the theoretical limits of dead volume and light throughput which ultimately limit the sensitivity of these systems. Unfortunately this sensitivity limit is insufficient to match the performance of GC/MS. The light-pipe dead volume and flow rate place severe restrictions on the possibilities for optimization of the gas chromatography. A new technique has recently been developed for interfacing a GC to an IR spectrometer using Matrix Isolation. The first commercial unit, the Cryolect from Cryolect Scientific can be used with any high performance FTIR Spectrometer. Matrix Isolation interfacing offers a significant enhancement in sensitivity over light-pipe systems and allows much greater chromatographic flexibility. The basic principles of Matrix Isolation referring to the trapping of atoms, molecules, or free radicals in a crystalline cage at temperatures near absolute zero and in which the "cage" is made up of a frozen inert gas as argon or nitrogen and discussed in reference 6.

Saadat and Terry⁽⁷⁾ have contributed considerably to the development of miniature gas chromatographs. The instrument is the Michromonitor (Microsensor Technology Inc.), a computer-controlled, portable gas analyzer for field or laboratory use. A miniature gas chromatograph, many components of which are fabricated on a silicon wafer, constitutes the heart of the instrument which fits upon a human hand, and up to five GC modules can be used in one Michromonitor. The detector at the output of the GC columns is an integrated thermal conductivity detector. The detector is capable of detecting 15 femtograms of pentane. Its potential for use in explosives is not indicated in the article. If this sensitivity can be achieved for

explosive compositions or for their common impurities such as the dinitrotoluenes in TNT or in Composition B for example, it might be possible to obtain detection on single pass measurements from closed bombs. Their methods of obtaining positive identification without use of infrared, Raman, or Mass Spectroscopy is to set the instrument to operate two of the columns packed with different substrates. The peak is positively identified as caused by a particular compound only if it is detected at the expected retention time on both columns. From information fed the computer previously concerning retention times as functions of temperature, predictions of retention times at other temperatures can be made. This would greatly simplify concern over differing ambient temperatures during a day of checking for explosives. As used for quantitative determination of gases, the Michromonitor is capable of running in automatic mode at intervals selected by the user. Statistical information such as maximum, minimum, mean, and % standard deviation of the concentration results are calculated for each gas and stored in memory. Extensive software diagnoses the integrity of the system and reports any possible malfunction. The analyzer can be configured variously, e.g., it can be used as a BTU analyzer. The parameters for calculating BTU can be entered into the computer's memory through keyboard dialog. In the BTU mode, specific gravity and compressibility factors of the natural gas mixture are displayed along with the individual gas concentrations. More than one hundred chemical compounds encountered in the work place can be determined. Although femtogram sensitivity has been previously indicated, the minimum detection limits for most commonly occurring solvents and similar compounds lies between 5 and 20 ppm or 9 (nine) orders of magnitude higher. It is not known whether the ppm values were because quantitative measurements may require that much more material or whether the femtogram detections with pentane was something very unusual. Picogram qualitative detections are common for certain explosives using high quality GC or HPLC instruments.

Anspach⁽⁸⁾ and others conducted an evaluation of solid sorbents for use in sampling low levels of explosives in water. About 27 sorbents were obtained from several companies. These represented many types of materials. The best ones were Porapak S or Porapak R depending upon the explosive to be determined. The Hewlett-Packard GC-EC was used and the most effective sorbent for each of eight explosives was used and subjected to precision testing as well as for accuracy of results. Detection limits were not of low enough minimum value for our purposes but are included in our report⁽⁹⁾. Most of these detection limits whether by GC-EC or by HPLC are below 10 micrograms per liter. Their detection limits ranged from 0.81 $\mu\text{g/l}$ for 2,6-DNT to 10.3 $\mu\text{g/l}$ for PETN.

No suitable method was found for Picric acid, Tetrazene, or Lead Styphnate. Interferences from major contaminants proved to be the largest problem in the evaluation of various sorbents. Douse^(10,11) used handswab extracts samples with GC with electron capture to detect explosives.

Meyers and Meyers⁽¹²⁾ in a project to identify manufacturers of smokeless powders have used a combination of gas chromatography and proton magnetic resonance (PMR). They also reviewed methods used previously for the detection of smokeless powders and their components as the nitrated products of glycerine. Use of the two techniques enables identification not only of the manufacturer of the powder but also the various powders manufactured by the manufacturer. Thin-layer chromatography was used to determine whether the material was single base or double-base propellant. For a gas chromatograph they used the Hewlett-Packard 5880A which is described in Hewlett-Packard HP Source⁽¹³⁾. This instrument uses a combination of internal method software and integral BASIC programming. Capillary columns are employed for improved sensitivity, and resolution. To perform an automated identification, the 5880A performs two distinct steps. First, searching the chromatogram for the presence of specific peaks (a qualitative step) and second, comparing peak areas or heights to reference values, a quantitative step. These steps have been combined in a BASIC program written for the 5880A Gas Chromatograph. Data files for each sample type are stored on the integral cartridge tape. The program is started upon completion of an analysis. A tentative match is reported if all reference peaks in a given data file are found in the sample chromatogram. The program then compares the normalized area or height percentage of each calibrated peak with lower and upper bounds stored in the calibration table. Deviations are summed over all the peaks. If the sum is less than the specified recognition window, the match is confirmed. After this confirmation has been achieved, a report identifying the sample is generated. This Hewlett-Packard Gas Chromatograph can analyze rapidly both qualitatively and quantitatively for explosives that are brought into the laboratory; however, it suffers from lack of portability for direct determination of explosives in closed ordnance.

The use of multiple detectors with gas chromatography for analysis of organic nitro compounds and explosives is discussed by Krull et al.⁽¹⁴⁾. They have used a parallel arrangement of electron-capture detection (ECD) with photoionization detection (PID) together with certain Permabound GC packing materials, for the resolution and specific identification of numerous organic nitro compounds and other explosives. They used a Varian Model 3700 gas chromatograph equipped with conventional Varian FID and ECD detectors. A separate PID unit was mounted external to the main GC oven, on top of the GC with external heating tape applied

to the interface preventing condensation of GC effluents after their exit from the column oven. The PID was from HNU Systems Inc., Model PI-51-01. The detection quantities and minimum levels detected were not as low as believed to be required in our work with bombs and warheads although their detection minimum levels for dinitrotoluenes were as good as we had obtained before⁽¹⁾. Their values for the DNT isomers were three picograms in each of the 2,3-, 2,4- 2,6-, and 3,4-dinitrotoluenes. The greater sensitivity of the ECD was noted however, the compound detection and selectivity were generally better via the PID. They point out that in deciding which detector to use, provided only one is used, one must decide whether detectability or selectivity is of greatest concern. Relative response ratios can be used when these two detectors are both used in parallel and such numbers are better to differentiate explosives from each other. The use of several detectors is important in other ways. When the amount or concentration of vapor is totally unknown it is better to use a detector that requires a larger sample (if available) or that can measure over a larger range or both. Then the sensitive electron capture detector (ECD) would not be swamped out so often by high concentrations which it cannot handle. Picograms require ECD whereas micrograms would swamp the ECD while being readily detected without dilution by several other less sensitive detectors.

Penton⁽¹⁵⁾ describes the advantages of using the newer fused silicon dioxide capillary columns as opposed to the packed column. Capillary columns give better resolution, yielding taller and narrower peaks, lower detection limits, and smaller errors in quantitation. Capillary columns are usually made with pure silicon dioxide without metal contaminants found in glass columns; this in turn leads to less tailing of polar compounds and fewer reactions with column ingredients. Penton analyzed nitroglycerine, lowest detection level 35 femtograms, TNT, lowest detection level 0.11 picogram, PETN, lowest detection level 0.38 picogram, and RDX, lowest detection level 0.39 picogram. Analyses were all performed using a Varian 6000 gas chromatograph equipped with a Model 1095 on-column injector and electron capture detector. A Varian 401 chromatography data system was used for quantitation. The column was of fused silica coated with a half micron thick coating of SE 30. No noticeable degradation was evident after two month's use.

Tung-ho Chen of U.S. Army Armament Research and Development Command, having been involved with the analysis of an unknown liquid explosive mixture, has outlined the methodologies used for the identification, structural determination, and quantification of the constituents of the mixture⁽¹⁶⁾ which emphasizes what can be done when a large number of analytical instruments are at one's disposal. This also further surfaces the problem of determining whether an explosive is present versus

some other non-explosive material. Fast atom bombardment mass spectrometry (FABMS) and Fourier transform mass spectrometry (FTMS) were only used in a cursory examination. GC/EIMS provided considerable structural information, however, the lack of molecular weight information required the use of direct inlet probe high resolution electron impact mass spectrometry which provided unequivocal data concerning the exact elemental compositions of the fragment ions and also the structural data necessary for elucidation of the structure of the unknown compounds in the mixture. Next most powerful tools to the HREIMS were positive ion chemical ionization (PCI) MS and the negative ion chemical ionization (NICI) MS from which key molecular weight information was deducted. Close behind these techniques in usefulness were GC/EIMS and GC/PICIMS which permitted rapid separation and characterization of nonlabile constituents of the explosive. Supplementary structural data were provided by NMR and IR which facilitated identification of the known, although the lower sensitivity of the commercial instruments representing these methods limited their usefulness.

Reutter et al., of the FBI Laboratories have shown the problems that can arise when a terrorist uses little known explosives or propellant ingredients which may not have been previously characterized or its characteristics had not been compiled in an FBI laboratory. One of these⁽¹⁷⁾, hexamethylenetriperoxidediamine, whose potential as a military explosive had been shown in 1904, and although too unstable for military use was selected apparently because of ease of synthesis. Complications of instability made GC/MS characterization difficult and infrared spectrophotometry showed only C-H stretch vibrations together with a peak later shown to be from an impurity. High resolution mass spectrometry together with NMR and some fine chemical sleuthing nailed the structure down to the tricyclicdiamine noted above. The other explosion occurred outside the contiguous 48 states and resulted in considerable loss of life. After HPLC separations showed none of the ordinary explosives, GC/MS found a peak which on a library search through EPA-NIH records matched well with diethyleneglycoldinitrate (DEGDN). An electron impact mass spectral determination was made for the second component of this explosive and found a spectrum indistinguishable from those of EGDN, NG, and PETN. The mass spectrum was consistent with a nitrate ester of mass of 255 daltons. Metriol trinitrate (MTN) was found to match this value; the most probable source was then found to be "Hercudyne," a dynamite made by Hercules. Standard samples of DEGDN and MTN were then obtained and both GC/MS and HPLC with pure samples together with debris extract spiked with them gave results indicating these two ingredients as the two components of the terrorist concocted explosive. Ironically, although these explosives were in standard reference tests, none was in the extensive FBI files and no spectral data had been compiled in any of the standard spectra reference libraries.

Goff and Fine in a series of articles describe analyses of explosives by means of use of GC or HPLC together with the Thermo Electron Analyzer, Model 610 as the detector. The latter pyrolyzes the separated products from either type chromatograph, ozonizes them to nitrogen dioxide or to nitric oxide^(18,19) which are detected as previously described therein. Minimum detectable levels were found for TNT and RDX 4 pg, for EGDN, NG, and DNT 5 pg, and for tetryl 25 pg. Possible advantages of this detector over some very highly sensitive detectors as electron capture are that it can be used over a range of nanogram down to low picogram range without dilution or concentration and without extensive sample cleanup procedures prior to analysis, and that it would not be "swamped out" so readily by exposure to slightly high concentrations. The TEA analyzer has been designed to respond only to nitro and nitroso compounds and thus there are not peaks for other compounds which may be in the same sample which otherwise obscure the identifying peaks of the explosive. The GC/TEA as well as the HPLC/TEA served adequately to detect explosives in acetone or methanol solution and also post-blast debris from methylene chloride solutions concentrated from debris extracts. Post-blast air samples taken in an air-sampling cartridge developed by Rounbehler, and handswab extracts were both adequately analyzed using either GC/TEA or HPLC/TEA.

The analysis of explosives residues by electron impact gas chromatography mass spectrometry (EIGC/MS) and on line computer searching of spectra has been reported by Messler⁽²⁰⁾ using a Hewlett-Packard Model 5992A GC Mass Spectrometer containing an electron ionization source and quadrupole mass analyzer used to collect standard spectra. The instrument is controlled by a 98255A microprocessor, having a 16K memory. Software used was Hewlett-Packard ON-Line Search Tape 05992-10012. This software allowed the GC/MS to perform scanning experiments where a library of up to 50 compounds is searched as each GC peak elutes. The software was modified so that the St. Louis Metropolitan Police Library now handles a capacity of 12999 pollutants and explosives.

Martz and others have established a smokeless powder library of about one hundred powders in their GC/MS system at the FBI laboratory in Washington⁽²¹⁾. Identification of a smokeless powder is effected by computer searching the composite spectrum of the unknown powder against the library. Confirmation follows by comparing the relative amounts of the various components as found by the GC/MS analysis and also by comparison of physical properties. Typical mass spectra are shown in the reference from a Finnigan 4021 quadrupole/mass spectrometer equipped with a Finnigan INCOS 2300 data system. Their gas chromatograph was equipped with a Scientific Glass Engineering, Inc., on-column

injector and a 20-meter, 0.20 mm ID, SE-54 bonded phase-fused silica column. In these analyses the powder was extracted with 0.5 ml of chloroform and 0.1 to 0.2 microliter injected on-column. In these analyses the powder was extracted with 0.5 ml of chloroform and 0.1 to 0.2 microliter injected on-column at ambient temperature.

A group at NWC as part of the Navy's pollution abatement has been fingerprinting the products of detonation for propellants and explosives as well as the products from burning for disposal. In recent studies related to underwater detonations, (22) molecular TNT has been found in the detonation products from TNT detonations in nitrogen and also in detonations in air; whereas, RDX and PETN are not found as detonation products from their explosive mixtures. The formation of products such as naphthene and other substances absent in the original mixture is hypothesized as occurring in reformation reactions from the fragments which include atoms and portions of molecules.

Cumming and Park have indications (23) that negative ion mode monitoring in the GC/MS detection process improves both detection limits and the degree of discrimination possible. Gas chromatography has made greater use of mass spectrometry possible in several ways. Yino (24) and Hunt (25) have reviewed mass spectrometry for characterization of unknown explosives. Electron impact (EI), in which ionization is caused by electron bombardment at 70 eV under high vacuum, produces fragmenting of most explosive molecules into smaller moieties of molecular fragments with corresponding simplified spectra limiting its usefulness in detection. This is caused by the poor charge stabilizing effect of the nitro group. Molecular ions from nitroalkenes eject the nitro group so easily that a molecular ion (M^+) is seldom observed. As examples, at 70 eV electron impact and at standard conditions with high vacuum, none of the nitrate esters give a molecular ion. Major peaks from nitro-alkane fragments are identified as:

NO^+ mass unit = 30

NO_2^+ mass unit = 46

$(H_2C-O-NO_2)^+$ mass unit = 76

Most aromatic nitro compounds do give molecular ion peaks and are thus easier to analyze using electron impact.

The fragmentation of TNT (26) forming a base peak at $m/z = 210$ corresponds to $(C_7H_4N_3O_5)^+$ which corresponds to the loss of OH from the molecular ion. This requires the efficient separation of the mixtures prior to optimizations, a function usually well performed by gas chromatography. Negative ion mass spectrometry has evolved because of improvements (23,26) in both

ionization and instrument techniques which allow instruments designed for positive ion operation to be readily adaptable to produce and detect negative ions. The reason for preferring negative ion (NI) rather than positive ion (PI) mass spectrometry is because the NI has greater selectivity combined with picogram level of sensitivity. The predominating mechanism of ion production is electron capture in which the NI behaves similarly to the gas chromatographic electron capture detector which is one of the most sensitive of explosives detectors available.

The development of portable GCMS instruments is described by Drew and Stevens⁽²⁷⁾. Most commercial instruments have been developed for the laboratory where a highly controlled environment and few limitations on space and power requirements are the norm. Among its carefully selected instruments for a Mars trip in search of evidence for the presence of life or its precursor NASA chose a portable GCMS instrument to fit into its very compact and light weight landing system capable of heat-soak sterilization, launch vibrations and accelerations, and of traversing interplanetary space for about six months, shock landing on Mars, and functioning millions of miles from earth in an unfriendly atmosphere of blowing dust. A current terrestrial man-portable GC/MS is largely based upon the Viking instrument. Specifications for the fully portable instrumentation are set up for a concept validation stage which has been ongoing at the Jet Propulsion Laboratory. The specifications include a desired femtogram detection sensitivity in an instrument which is expected to weigh 25-30 kg plus 0.9 kg for each hour of operation for the batteries. Although this weight would not be ideal for someone to carry around on the back, it may be a starting point for constructing a gas chromatograph/mass spectrometer suitable for identification of explosives. It is noted that for explosives detection, a vapor inlet probe and a pre-concentrator would be needed possibly together with certain extraction techniques possible for separation of interferences. Such an instrument should be of value for several applications relating to explosives detection.

Sullivan and Watson⁽²⁸⁾ describe portable detectors available from Xon Tech Inc. that can detect most organonitrate explosives present in open containers. The Model GC-710 detector measures the presence of explosives such as TNT, C-4, dynamite, and Deta Sheet for a time period as long as 30 minutes after sampling. The GC-710 weighs 43 pounds, costs around \$10,000, and requires only one operator. A personal sampler with attachable sampling cartridges can be used to extend the search area.

Ziegler et al.,⁽²⁹⁾ have described an extensive and organized chromatographic data processing command language. Nearly any manipulation of chromatographic data and results can be conveniently conducted using sensible instructions.

Karanek et al.,⁽³⁰⁾ have thoroughly reviewed fundamental developments (with 811 references) in the field of gas chromatography for 1982 and 1983 and the extent of GC use is evident from sales of about \$300 million in 1983 projected to \$425 in 1986. As an example of the scientific and technology improvements, electron-capture detection of aromatic hydrocarbons can now be predicted based upon known ionization potentials⁽³¹⁾. The detection limits for electron-capture detection have been reported for some strong electrophores as being in the attogram range⁽³²⁾.

Yang⁽³³⁾ describes the Varian models 3300 GC and 3400 GC. These instruments feature builtin self diagnostics and are the smallest size offered having fully automatable microprocessor controlled GC operations. The GC 3400 (20 in. H x 20 in. W x 24 in. D) with builtin printer/plotter and large column oven (10 in. H x 9 in. W x 7 in. D) will accommodate two 4 meter packed columns, two glass columns, or two capillary columns or combinations of these. Detectors range from electron capture detectors with sensitivity to <0.07 picograms through lesser sensitivity broader range detectors as thermal conductivity or flame ionization detectors.

Twibell has noted that gas chromatography with electron-capture detection was found to be the most accurate and sensitive technique for analyzing handswab extracts of nitroglycerine. Residues could be detected for 20 hours after handling the explosive. The lowest detection limit under these circumstances was 10 nanograms⁽³⁴⁾. Reviews on gas chromatography also include references 35 and 36, Smith's "Handbook of Chromatography"⁽³⁷⁾ and the use of gas chromatography in the analyses of polymers is reviewed by Smith⁽³⁸⁾.

C. HIGH POWER LIQUID CHROMATOGRAPHY

High power liquid chromatography has been used in numerous analytical procedures for detection and analysis of energetic materials and is the chromatographic method of choice for many other materials. Although many more papers have been published on HPLC than on gas chromatography, it may not be as readily miniaturized for the intended applications related to the current project. Explosives analysis methods can be covered only briefly here. Brueggmann⁽³⁹⁾ separated HMX, RDX and other explosives by use of RAD-PAK A (C18) column and made 70-76% recoveries with a lower detection limit of 100 nanograms. While more than adequate for the wastewater determination the lower limit would have to be picogram or better for determining these same explosives from vapor sampling from bombs and warheads.

Krull and others applied HPLC in complex matrices including post-blast residue debris⁽⁴⁰⁾. A joint project between Israel

Police Headquarters Laboratories and Northeastern University included development of the method, and study of various mobile phases from which toluene was tentatively chosen as best pending full health effect studies and NIOSH regulations. Toluene is not generally used by others as an HPLC mobile phase. Conditions for detecting 2,4-DNT, 2,6-DNT, TNT, PETN, NG, tetryl and other explosives were investigated. Retention times varied from 3.5 to 8.6 min. for 2,6-DNT depending upon the column type, solvent used, mobile phase composition, and other factors. The equipment used was standard laboratory type instrumentation (virtually HPLC system and any GC-ECD instrument can be used). No attempt was made to miniaturize for field work.

A composition analysis for TATB/HMX/Estane was developed by Schaffer⁽⁴¹⁾.

HPLC-UV methods have also been defined for quantitative determination of RDX, DNT and TNT in animal tissues and plants. Detections at the 5 to 100 ng level were obtained. Tetryl could not be determined from any of the mixtures as it adsorbed too strongly to protein or other macromolecule⁽⁴²⁾.

Concentration of trace organics from water was worked out by the Kaplans⁽⁴³⁾ who chose the primary and secondary products of the microbial transformation 2,4,6-TNT. These were extracted with SEP-PAK C-18 (Waters) Cartridges and quantitated with HPLC down to 30 ng quantities.

At the FBI symposium a number of papers covered HPLC analyses. Krull⁽⁴⁴⁾ compares the various types of detectors for HPLC much as he also did for GC⁽¹⁴⁾ for explosives as well as with other aliphatic and aromatic nitro compounds and aliphatic nitrate esters. Reductive liquid chromatography and electrochemistry detectors were used as well as a new technique they developed consisting of post column, on-line, real time, photolysis/derivitization generating organic nitrite from virtually all explosives and organic compounds after they have been eluted from the analytical HPLC column. The nitrite is then detected via conventional thin layer flow-through electrode detection in oxidative liquid chromatography-electro-chemistry using single and dual cells in the oxidative and/or reductive modes. Lower detection limits ranged from 25 to 200 ppb (or 500 pg to 4 ng).

The pendant mercury drop electrode (PMDE) detector was used with HPLC for screening explosives components⁽⁴⁵⁾. Detection limits are quite good (2-20pg).

Use of ammonium picrate (Explosive D) in projectiles has become obsolete with subsequent demilitarization by burning or dump containment. The Bureau of Medicine and Surgery, Dept. of the Navy, as response to its Assessment and Control of Installation of Pollutant Programs at US Naval Station, set an

interim target maximum contaminant level for nitrophenols including ammonium picrate and picramic acid at 0.001 mg/l (1 ppb). An appropriate analysis was therefore required for picrate in ground water. Hoffsonner and Glover⁽⁴⁶⁾ developed a simplified liquid chromatography method using a modified paired Ion Chromatography (PIC) method for the picric acid determination. A Hewlett-Packard, Model 1084A, HPLC was used with a 254 nm UV detector and an RP-8 column (25 cm long and 4.6 mm ID) maintained at 40°C. Since polynitrophenoxide ion is not retained it could not be separated without use of a reagent (tetrabutylammonium phosphate) which being completely ionized forms a neutral ion pair complex with the polynitrophenoxide ion is separated on the reverse phase (RP) column. Detection level of 0.6 to 1 ppb was achieved.

Kissinger has conducted numerous studies on nitro compounds⁽⁴⁷⁾ using liquid chromatography with electro-chemistry detection. He concludes it to be a viable approach for many explosive applications. He cites advantages of using two working electrodes to improve both qualitative and quantitative results. Used either in parallel or in series, dual electrodes provide many opportunities to study explosives because of the wide range of redox properties involved. Some compounds are easy to reduce (picric acid) and others (nitramines, nitrate esters) are difficult. Kissinger has provided a recent text⁽⁴⁸⁾ for a very detailed review of this mode of detection in liquid chromatography. Whitnack⁽⁴⁹⁾ has also researched the electro-chemical analysis field and developed many polarographic procedures for analysis of nitroglycerine, TNT, HMX and other materials.

A sub-discipline of high pressure liquid chromatography (HPLC), Ion Chromatography (IC), uses an analytical column packed with a low capacity ion exchange resin. The mobile phase is an aqueous buffer solution which may contain an organic solvent as methanol or acetonitrile. Ions are partitioned between the ion exchange resin and the eluent (mobile phase). Conductivity detection is most commonly used as it responds to all ions in aqueous solution. This method can be very valuable in the analysis of post blast residues and has been shown by Reutter et al.,⁽⁵⁰⁾ to have advantages over other techniques when the ionic residues are volatile or electrochemically active. Energetic materials such as ammonium nitrate, potassium nitrate, sodium nitrate, potassium chlorate, potassium perchlorate, barium chlorate, barium nitrate and strontium nitrate, amines and their salts can be analyzed by high power liquid chromatography-ion chromatography version. The material sampled can be as vapor or from the solid. The method has been used for water based explosives including such sensitizers as ethylenediaminedinitrate and diperchlorate and values down to 0.5 ppm have been determined with linearity for quantitative analysis between 0 and 15 ppm. The FBI laboratory is constantly updating their information on commercial explosives so that when

a new one comes on the market, if no adequate analysis method suffices for FBI purposes, a research project is initiated to develop one. Excellent review articles for ion chromatography are given by Small et al.,^(51, 52) and by Williams⁽⁵³⁾. Interferents and capabilities are described in Dionex literature^(54, 55).

Barsotti et al.,⁽⁵⁶⁾ have used the Wescan Model 26 ion chromatograph with dual column and dual detectors for simultaneous determinations of monovalent cations as sodium ion, methylammonium ion, ammonium ion and of bivalent cations as calcium ion, using dual conductivity detectors. They conclude that ion chromatography can form the basis for a method to control process and quality in the manufacture of water gel explosives.

Rudolph⁽⁵⁷⁾ has used DIONEX Model 16 ion chromatograph for determination and characterization of "low explosives" such as black powder, potassium chlorate/sugar mixtures and the commercial black powder and its substitute, Pyrodex. Conductivity detectors together with electrochemical and ultraviolet-visible spectrophotometric detectors were used. These materials could be detected from their burned residues. There is no evidence, however, in the last two references that ion chromatography is sensitive to less than parts per million.

GC/MS has been discussed as possibly the ultimate method of vapor detection and specific identification. Yinon⁽⁵⁸⁾ indicates certain circumstances where LC/MS can be used while GC/MS is not suitable. Thermally sensitive or non-volatile compound exemplify such cases. LC/MS also has some interface problems between the liquid at high pressure and the reduced pressure of the mass spectrometer. Special interfaces have been designed, some of which are commercially available. One such interface splits the LC effluent so only 1 or 2% enters the mass spectrometer through a 5 micrometer aperture in a stainless steel diaphragm. Sensitivity is of course reduced using such an interface by a factor of 50-100.

Powermex and Tovex, commercial blasting agents have been confiscated in labor-related bombing incidents. These materials are sensitized with ethyleneglycol mononitrate (EGMN) and monomethylaminenitrate (MMAN). Prime and others⁽⁵⁹⁾ have described detection methods using HPLC. Large samples of MMAN can be determined by X-ray diffraction and infrared spectrophotometry. Smaller samples are more difficult although spot tests and GC and derivative HPLC have been suggested. Prime et al., selected derivitization (using Dansylchloride as derivitization agent and following with separation by HPLC) for method development. Advantages of derivitization in chromatography were explained in an earlier report⁽¹⁾. It effectively provides sensitization for the type of detector used as well as better separation in the chromatographic option

chosen. Recovery of EGMN was also found enhanced by a four fold-factor by using a 55°C purge of the explosive debris.

HPLC is often used with infrared detection specific materials as the IR spectrum can often be considered positive evidence for identification of specific compounds. The Fourier Transform-Infra-Red Spectroscopy (FTIR) is a powerful tool for this. The resultant spectrum is compared with reference spectra via computer library search of various standard explosive IR spectra. Riddell et al.,⁽⁶⁰⁾ have taken head space concentration samples over explosion debris as well as solvent extracted material and analyzed using HPLC-FTIR which greatly improved selectivity over HPLC alone with UV detection at 254 nm. Using a Varian Model 5000 Chromatograph (HPLC) with a Nicolet 7199 FTIR with a KBR-GC beam splitter and including a laser-referenced Michelson Interferometer with absolute wave number accuracy specified to better than 0.01 reciprocal centimeters, on-the-fly real time measurements were taken using the FTIR to monitor several absorption bands simultaneously in real time. Complete IR spectra were also storable for future use. Detection using these techniques is unfortunately only at the microgram level and although very useful when sufficient explosive is present as in terrorist bombing residues, does not at present represent a viable method for detection of less than picogram quantities which would be required for analysis of unconcentrated vapors over most sealed ordnance such as bombs and warheads.

Smokeless powders have been the focus for detection by FBI Laboratory's Bender⁽⁶¹⁾ with tandem ultraviolet/Thermal Energy Analyzer (TEA) detectors. Diphenylamine, 2-dinitrodiphenylamine, N-nitrosodiphenylamine, nitroglycerine, 2,6-dinitrotoluene and 2,4-dinitrotoluene have been separated, identified and their relative quantities used to characterize the gun powder. Detection was found possible to the low nanogram range. This is still more than three orders of magnitude too high a concentration for the very low levels we require to determine explosives in bombs. Its usefulness in the present state is that the method is powerful enough to differentiate between ball powders of the same components differing only in percentage of ingredients, and in DuPont IMR (Improved Military Rifle) single base powder, it is identified and distinguished from others in the IMR series by the relative ratios of lesser components 2,6-dinitrotoluene, N-nitrosodiphenylamine and n-butylphthalate.

Majors⁽⁶²⁾ reviews general trends in HPLC usage based upon a survey of 200 users responding early in 1984. Reverse phase HPLC, making use of water and acetonitrile, is used more than other types. It is used primarily for nonpolar and hydrophobic compounds and has increased in popularity because of its application to ionic and ionizable compounds through ion-pair, ion suppression, complexation, and other ion interaction techniques. Other HPLC modes are used mainly for more specialized applications such as those involving water sensitive

compounds, isomers, polymers, and metallic ions. The lifetime of HPLC columns is gradually increasing, and that for reverse phase chromatography on octadecylsilane bonded-phase columns has increased from early times life of two months to from six months to a year and some columns have been observed to have been used much longer than this. Batch-to-batch variation in columns can be a problem. In some instances standardization is required for similar peak dimensions with each new column.

Dolan⁽³⁾ reviews theoretical plates in HPLC columns which with 5 m packing typically run from 60,000 to 100,000 and for 3 m packing, 150,000 plates may be available. He relates total variance to the sum of variances due to column, injector, detector and tubing.

The Appendix I⁽¹⁾ contains a profile of various explosives and analyses available using liquid chromatography/electrochemistry for qualitative and quantitative analysis as present by Bioanalytical Systems, Inc.

D. BIOCHEMICAL METHODS

1. Enzymes and Related Methods Using a Chemiluminescence Output Signal.

The use of chemiluminescence in explosives detection has been studied in different ways by several groups; detectors have been made which are sold commercially. Antek, Houston, TX has an instrument detecting TNT at the ppm level. Therma Electron Corporation, Waltham, MA also has an instrument available. Antek instrument will not determine explosives at levels we require (vapors from closed bombs or other ordnance)⁽⁴⁾. The Antek instrument, however, may be suitable for analyzing for liquid propellant mixtures of the types developed at BRL.

The Los Alamos National Laboratory has an interesting study going on chemiluminescence reactions⁽⁵⁾. The project centered on detecting high explosives at nuclear power reactors to thwart terrorist activity. The HE analysis developed relies on coupling the chemistry of the HE with that of the luminol chemiluminescence reaction.

⁽⁴⁾ Private communication from Randy Wrayford of Antek to Harold Gryting.

The accomplishments of LANL program are cited as⁽⁶⁴⁾:

1. Success in coupling HE and CL chemistry reliably.
2. Capability to use a micellized solvent to concentrate HE.
3. Establishment of the basis for design instrumentation that may exhibit better sensitivity and lower levels of detection than exhibited by the laboratory apparatus used for this study.

Heller^(65,66) and others have studied methods for determining explosives in water. A system using fluorescent ionic resins was used to detect TNT and similar nitroaromatics. They indicate development of luminescent methods requires finding chemical reactions from normally non-luminescent explosives that either produce light, produce products which produce light or quench other chemiluminescent reactions. The break down of explosives to nitrogen dioxide which yields inactive nitrogen dioxide plus a photon was studied and this technology later became the basis for the instruments previously described. Other reactions including thorium oxide catalyzed oxidation of CO and the metal reduction of CO were investigated. The photochemistry of TATB was also studied.

Chemiluminescence has been used by Rhoton⁽⁶⁷⁾ to determine presence or absence of a reaction during machining and related operations for plastic bonded explosives.

Dr. Heinrich Egghart⁽⁶⁸⁾ used the coupling of a light emitting indicator reaction (chemiluminescence) with reactions specific to TNT or DNT which are facilitated by an antibody or an enzyme. Appendix II of reference 1 provides Dr. Egghart's description. The laboratory work is done by the University of California (Dr. Marlene DeLuca). The best detection is 10^{-17} mole of TNT (see Appendix II of reference 1) equating 2.3×10^{-15} g of TNT which is about two orders of magnitude better than that of on-the-shelf gas chromatographs. Unfortunately, this method presents difficulties in obtaining for the reaction a detector suitable for field use. Another technique, however, also biochemical in origin and using "TNT reductase" enzyme for specificity and bacteria fed on TNT used to synthesize the enzyme is being considered for use in a small portable instrument. Change in NADH level (which occurs by consumption by TNT presence) is shown by change in luciferase light emission. About 10^{-14} mole of TNT can be detected which translate to 2.3×10^{-12} gram of TNT as minimum detectability level which unfortunately is from borderline to an order of magnitude or more too large for our detection purposes and about the same sensitivity as gas chromatography with electron capture detectors.

2. Animals as Detectors of Explosives.

In reference 1 the use of dogs, rats, gerbils and other animals was briefly described including tests pitting dogs and handlers against instruments with their operators. Discussions with Dr. Ray Nolan of Fort Belvoir R & D Center revealed that the Army is no longer continuing the study in which rats were being trained to reveal the presence of explosives from direct brain wave pattern transmission to an appropriate oscilloscope. This was one of the most intricate of the many studies involving animals.

The effort on rats from FY76-FY81 is given by Nolan⁽⁶⁹⁾. These experiments were devised to improve the reliability and versatility of that class of detector system currently known as in vivo bio-sensor. The target substance of interest in this research was the military explosive TNT. The research was designed to prove and did prove the validity of four theses: (1) Rats can detect TNT via their olfactory function; (2) Trained rats will operantly signal the arrival of TNT vapor at their nares; (3) Rats may be trained en mass to function as bio-sensor systems; (4) The electroencephalogram (EEG) of trained rats contain specific signals uniquely related to their awareness of TNT vapor. Ablino male rats were equipped with four chronic indwelling brain electrodes, three of which were electroencephalograph (EEG) pick-off electrodes juxtaposed to the dura mater, while the fourth lead was a stimulus electrode embedded in the medial forebrain bundle (MFB). Electrical brain stimulation (EBS) was applied to the MFB (which has been termed a pleasure center), as a conditioning stimulus during training and reinforcement sessions. Subjects were first conditioned by operant methods to associate the presence of TNT vapors with EBS and to signal awareness of the target substances by treadle pressing. Properly conditioned rats can, in fact, be utilized as sensory elements in bio-sensor explosives systems.

Gerbils are still under investigation at the University of Toronto with Dr. Biedermann⁽⁷⁰⁾. They are reported to be able to work an eight hour shift whereas dogs normally rest after a much shorter time. One file drawer of gerbils used in conjunction with electronic reporting of their findings has been found to work well at airports. We are not aware of any recent in depth study of gerbils for detecting sealed explosives.

Smith⁽⁷⁰⁾ indicates the use of dogs for explosives detection in the protection of nuclear plants. By developing a test area for dog and handler, flushing between tests and regulating scent entry rate, detection at the 90-95% level and false alerts at 4-7% range were achieved. On commercial dynamite with 720 trials a 100% detection rate was achieved with 1.9% false starts.

Dean and Tomlinson⁽⁷¹⁾ at SwRI describe the progressive learning sequence that trains dogs to become sensitive, communicative detectors of vapors. The dog then becomes a portable, mobile biological vapor detector. The paper indicates that a trained dog has the sensitiveness of at least one femtomole (10^{-15}) which for TNT is 2.3×10^{-13} gram or an order of magnitude better than most of the better instruments available. The reason for such sensitiveness is easier to imagine in noting that a German Shepherd has 2×10^{-9} olfactory receptors and that each cell has 125 cilia giving a total ciliary surface area of 7.85 square meter which is several times the dogs surface area. One molecule of a certain vapor was noted to be sufficient to stimulate a single olfactory cell. In studies with EGDN most dogs were insensitive beyond 10^{-14} mole or 1.6×10^{-12} gram; however, one dog sustained a 98% efficiency rate at 10^{-17} mole but gave no indication of detection of EGDN vapor at 10^{-19} mole (1.6×10^{-17} gram). Dean has cited Russian literature from 1958 that notes that dogs receiving caffeine or amphetamines under certain conditions showed much enhanced detection sensitivity. This enhancement was said to continue for eight hours. Two to three orders better sensitivity were reported for those given caffeine or amphetamines. Training of dogs also continues at the Lackland Air Force Base^(c), San Antonio, TX. They are flown to various locations in response to needs for detection of explosives or drugs.

(b) Private communication from Dr. G. Biedermann to H.J. Gryting.

(c) Private communication from Sergeant G. Wilson to H. J. Gryting.

D. OPTICAL

1. Infrared (IR) and Fourier Transfer Infrared (FTIR) Spectrometry.

The Chemical Systems Division, Edgewood, APG, MD has sponsored contracts concerning development of instruments that take advantage of the small differences in temperature between the target material and its background for the detection of chemical warfare agents⁽⁸⁾. Passive LOPAIR for Long Path Infrared and a later developmental model, the XM21, are described together with derivation of equations and diagrams depicting principles. A list of some remote instruments used on space missions is given as: IR Filter Wheel Spectrophotometer; UV diffraction Grating Spectrometer for Water Vapor Determination; UV Spectrometer with Grating Monochromator. These have all been used in one or more spacecraft.

Of further interest is the fact that for examination of hazardous materials in a field environment, the remote passive IR analyzer was one of two recommended methods for further development in the future. (The other as indicated under gas chromatography was gas chromatography with mass spectroscopic identification.) In gathering IR spectra for most of a list of 115 hazardous materials it was determined that over 90% of the materials could be determined by means of IR spectra measurements.

E. SENSOR COMPILATION

Norton⁽⁷²⁾ has compiled relevant information on: instrumentation systems, transducer fundamentals, solid mechanical quantities, fluid mechanical quantities, acoustic, thermal optical magnetic, electrical, nuclear quantities, sensing methods, design, and operation. In addition, descriptions of the various analyzers for chemical properties and compositions covering many of the instrument types discussed in this paper are explained in principle. these condensed summaries aid in selecting options when designing new instruments for specific purposes.

CONCLUSIONS AND RECOMMENDATIONS

Of the vapor detectors, gas chromatography with electron capture detection supplemented by mass spectroscopy appears to be the farthest along; there being versions described herein which have high detectability and with use of concentrators to be developed may be close to desired detectability for sealed bombs. On-the-fly measurements would still be slowed by the need for placing the concentrators ahead of time. Negative chemical ion mass spectrometry, successful in identifying nitro

polycyclic aromatic compounds, has been suggested as the possible best selective system for positive explosive identification.

The NASA work has accelerated miniaturization of Gas Chromatography/Mass Spectroscopy detection instruments. Man portable instruments were made for space satellites that weigh about forty pounds. The relatively new capillary columns and reduced dead space measurements seem a good way to obtain samples especially from explosive detonation residues.

Miniaturization of an Ion Mobility Spectrometer which has recently been reported to be sensitive to one picogram in a microprocessor-controlled system weighing under thirty pounds is another likely possibility for future detection especially if even greater sensitivity can be achieved.

Use of enzymes in detection together with chemiluminescence holds promise of better specific response to TNT than has been achieved with the available detectors. For this to be practical for a large range of explosives, either a more general reaction applicable to many explosives or many specific enzymes each developed for use with its own explosive compound would be required. As long as TNT or compositions made with TNT are present in mines, the Army may find the TNT specific enzyme system highly desirable, however, the Navy, having large amounts of PBX materials in warheads cannot be locked into one such detector or detecting mechanism.

Little new material on insects as explosives detectors was found. Very early work had indicated great promise, however later work tended to indicate that insects have not been studied for training them as gerbils, rats, pigeons and especially dogs have been trained. The way ants can migrate over distances to ferret out food suggest that labeling with food smelling substances might produce another useful detection system especially for shallow buried items. Placentious suggests that insects may be the most sensitive of all detectors^(d).

Dogs have held their own against instruments with occasional dog sensitivity showing up as high or higher than the experimental techniques involving conventional detectors or such other bio-sensor systems as enzymes with chemiluminescence. Contrary to some previous information, dogs can be trained to work 12 hours with 10 minute breaks at hourly intervals. One man and his dog searched the Notre Dame Field House in 12 hours^(e) page 213.

^(d) Private communication from Bob Placentious, National Bureau of Standards to Harold Gryting.

(1) It is recommended that an R&D program for detection of explosives in Mark 80 series bombs and in other prioritized weapons be initiated.

(2) It is recommended that an instrument based on chromatography and mass spectroscopy be developed with detector sensitive to femtogram quantities.

(3) It is recommended that methods be investigated to provide small orifices in weapons for examination of explosive vapors or for use with other NDE methods to be discussed in a separate paper⁽¹⁾.

(4) It is recommended that a pump-tube or other self-contained sampling device designed to attach with a vacuum-tight seal over threaded sections of loading ports of warheads and bombs be developed for ease in securing sufficient quantity of vapor samples.

(5) It is further recommended that acetone wash techniques as described in reference 1 be studied in detail for at least the top ten important ordnance items.

More recent studies with explosives debris also show solution in acetone as a very good method to dissolve explosives for detection by Gas Chromatography/Electron Capture Detector and and/or Gas Chromatography/Mass Spectroscopy.

With respect to assessment of feasibility of determining presence of explosives material within cased ordnance from in field tests, we pose the question:

What is Feasible and What is Not?

• It is feasible to detect explosives in open warheads with science and technology available today.

• It may be feasible to detect cased munitions including sealed bombs and warheads provided sufficient vapor can escape through the threaded sections. (This may require that improved laboratory instruments be made portable.)

Furthermore, should insufficient vapor be escaping naturally, a hole could be made which would allow detection by vapor detectors (or by non-vapor type NMR detector.)

• A possible alternative is to develop and apply a concentrator of vapors which applies suction at the threaded loading port.

What appears not feasible is the detection and identification of sealed warheads and bombs using currently

available small (man-portable) detectors on an on-the-fly basis without a sampler for sampling and concentrating the vapors to a detectable concentration. In fact without such a sampler/concentrator the most sophisticated laboratory vapor detector now marketed will not detect vapors directly from cased munitions such as the Mark 80 series bombs and some of the warheads described before⁽¹⁾. Table I, II, III give examples of the detectability by some such instruments. With a sample/concentrator device and/or with capability to make safe in-field small openings in a bomb or warhead case the feasibility of detection of several explosives could be reasonably assured. This could be accomplished by using available instrumentation, which would certainly appear feasible. Alternatively, instrumentation designed, from information that is state-of-art, to be used for ordnance to be found on bombing or missile ranges could provide the kind of instrument most needed for groups involved in range cleanup and range safety.

The problem of unexploded ordnance escaping recognition and being found by children who at times cause an accidental and sometimes fatal explosion to occur has not been totally overcome as Appendix V San Antonio Express News of January 29, 1984⁽²⁾ reports. Another incident reported in the Express New concerned a shell, handled in a military school, exploding and killing several people. This one was thought to be inert and had been handled in classes several times.

Terrorists' bombings, the bombs remaining undetected in time to prevent detonation, occur at frequent intervals around the world. Appendix VI⁽³⁾ covers the bombing in the Montreal train station by terrorists. Development and use of proper instruments together with trained dogs, and possibly other trained animals, together with trained personnel and education of those involved with our transportation system should reduce and help eliminate both accidental and terrorist caused detonation. Terrorism can be reduced also if those who plan those activities can be made aware that their bombs will be detected. The manned vehicle crash detonations occurring in the past should also be reduced by ensuring that the area near the embassies or troop concentrations are kept under observation by TV camera and by the most sensitive explosives detectors we can develop in the near future.

The conclusions and recommendation of reference 1 representing earlier work both experimental and an analytical review of detection concepts and instruments are subscribed to as continuing to be viable. There are some obvious things we can do and these will help us to detect more explosives and to differentiate them better from inert stimulants

We have noted the development of many new instruments and improvement of a few of those that have been commercialized or that have been under development for extended periods of time.

Information available on chromatographic methods leads us to believe that we could start with the technology described herein plus that from recent symposia and reference 1 and construct a detection system (GC/ECD) which will be man-portable, and with development of proper accessories and program, it should then become feasible to detect the vapor from explosives inside of sealed bombs and warheads without moving them to evacuation chambers.

REFERENCES

1. Gryting, H. J., "Detection of Energetic Materials," Final Report Contract N60530-81-309 for Naval Weapons Center, China Lake, CA, Southwest Research Institute, San Antonio, TX, December 1981.
2. Drimmer, B. E., Navy Bank of Explosives Data Vol. I, II, III, and IV. VSE Corporation for Naval Surface Weapons Center, Silver Spring, MD, 10910 NSWC MP 83-230, June 1983.
3. "The Physical Properties of Explosives and Inert Materials Whose Physical Properties Resemble Those of Explosives," The Journal of the JANNAF Fuze Committee (Joint Army-Navy-Air Force) Serial No. 17.0, March 1960.
4. Campbell, R.M. and M. L. Lee, "Capillary Column Gas Chromatographic Determination of Polycyclic Aromatic Compounds in Particulate Extracts," Anal. Chem. 56, pp 1026-1030, 1984.
5. Gross, G.J., D.E. Harris, G. Lachs, and R. Dillman, "Instrumentation for Detecting Hazardous Materials," Final Report June 1980. Locus Inc. for Federal Emergency Management Agency, Washing, D. C.
6. Bourne, S., G. Reedy, P. Coffey, and D. Mattson, "Matrix Isolation GC/FTIR," American Laboratory pp. 90-101, June 1984.
7. Saadat, S. and S.C. Terry, "A High-Speed Chromatographic Gas Analyzer," American Laboratory, pp. 90-101, May 1984.
8. Anspach, G.L., W.E. Jones II and J.F. Kitchens, "Evaluation of Solid Sorbents for Sampling and Analysis of Explosives from Water," ARC 49-5028, April 1982.
9. Gryting, H.J., "Assessment of the Feasibility of Performing Infield Nondestructive Evaluation to Determine the Presence of Explosive Materials within Cased Munitions, Phase II Vapor Detection," SwRI Final Report (Phase II) Project 15-5607-825, Department of Energetics Systems, Southwest Research Institute, San Antonio, TX, November 1983.

10. Douse, J.M.F., J. Chromatogr. 208, p. 83, 1981.
11. Douse, J.M.F., "Trace Analysis of Explosives in Handwab Extracts using Amberlite XAD-7 Porous Polymer Beads, Silica Capillary Column Gas Chromatography with Electron Capture Detection and Thin-Layer Chromatography," Journal of Chromatography, 234, pp. 415-425, 1982.
12. Meyers, R.E. and Meyers, J.A., "Instrumental Techniques Utilized in the Identification of Smokeless Powders, Proton Magnetic Resonance (PMR) and Gas Chromatography (GC)," Federal Bureau of Investigation, Proceeding of the International Symposium on the Analysis and Detection of Explosives, pp 93-106, March 29-31, 1983.
13. Hewlett-Packard HP SOURCE p. 6, Aug. 1984.
14. Krull, I.S., M. Swartz and K.H. Xie, "The Use of Multiple Detection in the Gas Chromatographic Analysis of Organic Nitro Compounds and Explosives (GC-ECD/PID). Federal Bureau of Investigation, Proceedings of the International Symposium on the Analysis and Detection of Explosives, pp. 107-122, March 19-31, 1983, FBI Academy, Quantico, VA.
15. Penton, Z. IBID. pp. 123-127, 1983.
16. Chen, Tung-ho, IBID. PP. 143-147, 1983.
17. Reutter, D.J., E.C. Bender, and T.L Rudolph, IBID. pp. 149-158, 1983.
18. Goff, E.U., W.D. Yu, and D.H. Fine, "Description of a Nitro/Nitroso Specific Detector for the Trace Analysis of Explosives," IBID. pp. 159-168, 1983.
19. Fine, D.H., W.C. Yu, and E.U. Goff, "Applications of the Nitro/Nitroso Specific Detectors to Explosive Residue Analysis," IBID. pp. 169-179, 1983.
20. Messler, H.R., "On-Line Computer Search System Applied to Explosives," IBID. pp. 241-244, 1983.
21. Martz, R.M., and L.D. Lasswell III, "Smokeless Powder Identification," pp. 245-254, 1983.
22. Johnson, J.H., E.D. Erickson, C.A. Heller, S.R. Smith, and L.A. Mathews, "Fingerprints of Detonation Products from Navy Explosives," IBID. pp. 255-258, 1983.

23. Cumming, A.S. and K.P. Park, "The Analysis of Trace Levels of Explosive by Gas Chromatography/Mass Spectrometry," IBID. pp. 259-265, 1983. RARDE, Woolich, London.
24. Yinon, J., and Zitris, S., The Analysis of Explosives, Pergamon Press (Oxford) 1981.
25. Hunt, D.F. and F.W. Crow, "Trace Organic Analysis. A New Frontier in Analytical Chemistry," NBS 9th Materials Research Proceedings 1978.
26. Bulusu, S. and T. Axenrod, Org. Mass. Spec. 14 (11) 585, 1979.
27. Drew, R.C. and C.M. Stevens, "A Man Portable GC/MS for Explosives Detection," Proceedings of the International Symposium on the Analysis and detection of Explosives pp. 419-427, FBI Academy, Quantico, VA, March 29-31, 1983.
28. Sullivan, R.J. and G.W. Watson, "Sampling of Explosives with Multiple, Portable Preconcentrating Cartridges," IBID. pp. 431-440, 1983.
29. Ziegler, E. et al., Anal. Chim. Acta., 147, 91, 1983.
30. Karasek, Onusha, Young and Clement, "Gas Chromatography," Anal. Chem. Fundamental Reviews, 56, pp. 174b-199r, 1984.
31. Wojnarovits, L. and Toldack, G., Journ. Chromatogr. 234, pp. 451-453, 1982.
32. Corkill, J.A. et al., Anal. Chem. 54, pp. 481-485, 1982.
33. Yang, F.J. et al., American Laboratory, p. 102, May 1984.
34. Twibell, J.D. et al., J. Forensic Sci., 27 (4) 792, 1982
35. Bretell, T.A. and Saferstein, Anal. Chem. Application Reviews, 55, 19r-31r, 1983.
36. Risby, T.H. et al., "Gas Chromatography," Anal. Chem. Fundamental Review, 410r-423r, 1982.
37. Smith, C.G. et al., CRC Handbook of Chromatography, 1982.

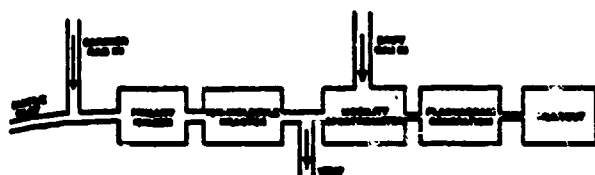
38. Smith, C.G., N.H. Mahle, and C.D. Chow, "Analysis of High Polymers," Anal. Chem. Applications Reviews 55 (5) 156r-164r, 1983.
39. Brueggmann, E.E., "HPLC Analysis of SEX, HMX, TAX, RDC and TNT in Wastewater," Technical Report 8206, Jan. 1983, US Army Medical Bioengineering R&D, Ft. Dietrich, MD.
40. Krull, I.S. et al., Analytical Letters, 14(A16) 1363-1376, 1981.
41. Schaffer, C., "Compositional Analysis of RX-26-AF a TATB/HMX/Estane PBX," MHSMP-80-61 Mason and Hanger--Silas Mason Co. Nov. 1980.
42. Lakings, D.B. and O.V. Gan, Final Report MRI Project 4549-A, Midwest Research Institute for ARRADCOM, Jan. 1981.
43. Kaplan, D.L. and A.M., Analytical Method for Concentration from Water," TRNATICK/TR-81/014 April 1981.
44. Krull, I.S. et al., FBI International Proceedings, IBID. pp. 11-29, 1983.
45. Lloyd, J.B.F., IBID. pp. 31-30, 1983.
Also J. Chromatogr. (No. 2) 227-236, 1983.
46. Hoffsommer, J.C. and D.J. Glover, FBI International Proceedings, IBID. 41-44, 1983.
47. Kissinger, P.T., IBID. pp. 45-48, 1983.
48. Kissinger, P.T., Liquid Chromatography/Electrochemistry: Principles and Applications, BAS Press, W. Lafayette, IN, 1984.
49. Whitnack, J., "Explosive Research and Development, Applied Polarography," NWCTP 6087, pp. 33-35, 1978.
50. Reutler, D.J. and R.C. Buechele, FBI International Proceedings, IBID. pp. 199-207, 1983.
51. Small, H., T.S. Stevens, and W.D. Bauman, Anal. Chem. pp. 1802-1809, 1975
52. Small, H., Anal. Chem. 55, pp. 235-242, 1983.

53. Williams, R.J., Anal. Chem. 55, pp. 851-854, 1983.
54. Dionex Application, Note 18R, Dionex Corp., Sunnyvale, CA, March 1978.
55. Dionex Application, Note 6, Dionex Corp., Sunnyvale, CA, March 1978.
56. Barsotti, D.J., R.M. Hoffman, and R.F. Wenger, FBI International Proceedings, IBID. pp. 209-212, 1983.
57. Rudolph, T.L., IBID. pp. 213-219, 1983.
58. Ynon, J., "Analysis of Explosives by LC/MS," IBID., pp. 227-234, 1983.
59. Prime, R.J. and J. Krebs, IBID., pp. 285-288, 1983.
60. Ridell, R.H. and T. Mills, "Analysis of Explosives by HPLC-FTIR," IBID., pp. 289-307, 1983.
61. Bender, E., "Analysis of Smokeless Powders Using UV/TEA Detection," IBID., pp. 309-320, 1983.
62. Majors, R.E., "Trends in HPLC Column Usage," LC Vol. 2 No. 9, pp. 660-666, Oct. 1984.
63. Dolan, J.W., "Chromatographic Theory as a Problem Isolation Aid: Part I," Liquid Chromatography, Vol. II No. 9, pp. 668-669, 1984.
64. Neary, Michael P., "Summary of Activities, Final Report: A Proposal to Develop a Method for the Detection H. E. Employing Chemiluminescence Reactions," Jan. 1981.
65. Heller, C.A., "Impurity Analysis by Chemiluminescence," NWCTP 6087, pp. 37-40, 1978.
66. Heller, C.A., "Trinitrotoluene Detection In Water. Design of an On-Stream, Automated Instrument Based upon Fluorescent Ion-Exchange Resins," NWCTP 6035, July 1978.
67. Rhoton, N.O., "Evaluation of Machining Safety: PBX 9404 and LX-10 Process Development: Endeavor No. 301." Report No. MHSNP-81-31, Mason and Hanger--Silas Mason Co., Inc., Amarillo, TX, July 1981.
68. Egghart, H., Private Communication to H.J. Gryting, June 1984.

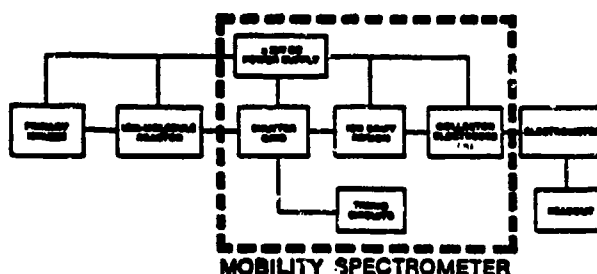
69. Nolan, R. "Investigation of Behaviorally Modified Rats for Use in Explosives Detection Systems," Report MERADCOM-2343, Dec. 1981, Fort Belvoir, VA.
70. Smith, J., "Remote Detection of Explosives Using Trained Canines," FBI Proceedings, IBID., 441-457, 1983.
71. Dean, E.E. and S.J. Tomlinson, "The Scientific Development through Olfaction and Behavioral Modification," IBID., Moulton, D.G., "Enhancement of Olfactory Discrimination." Final Report Grant No. AFOSR 73-2425 1-2.
72. Sharma, J., "X-Ray Photoelectron Spectroscopic (XPS) Detection and Identification of Explosives Residue," FBI Proceedings, IBID., pp. 181-185, 1983.

ION MOBILITY SPECTROMETER LABORATORY INSTRUMENT

PLASMA CHROMATOGRAPH SYSTEM DIAGRAM



PLASMA CHROMATOGRAPH ELECTRONICS



SAMPLE AND GAS FLOWS

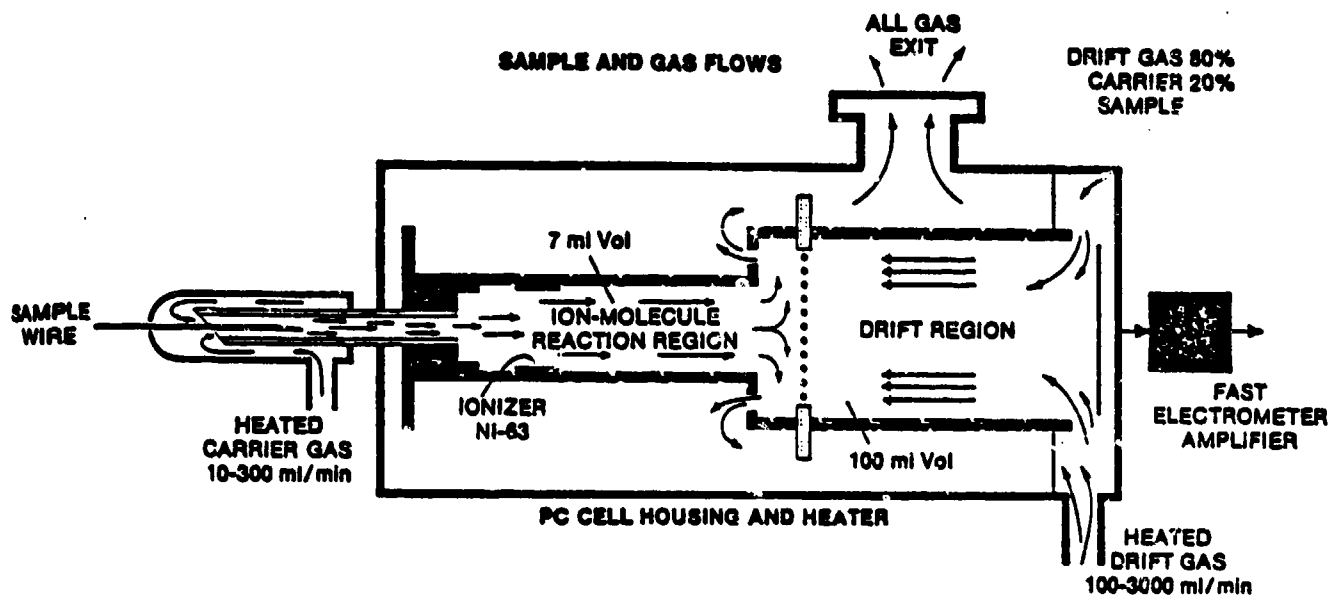


Figure 1.

ION MOBILITY SPECTROMETER SIMPLE FIELD MODEL

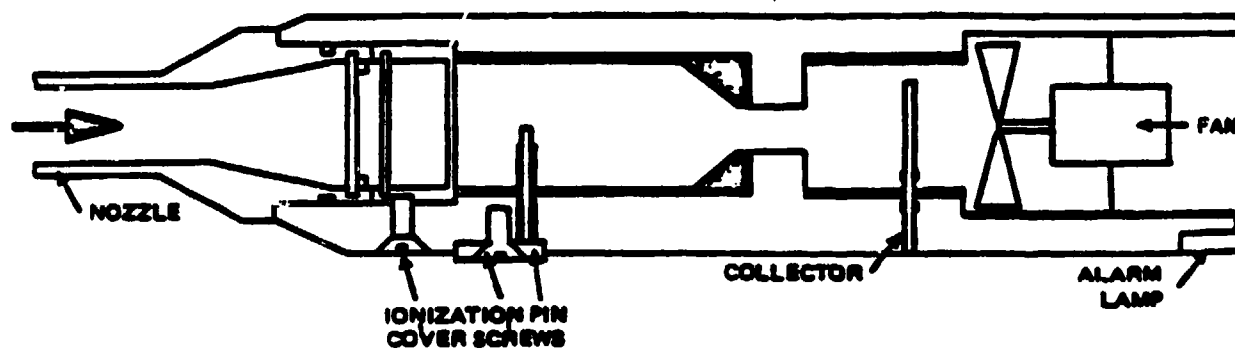


Figure 2.
Cross Section of Ion Mobility
Spectrometer.

AD-P005 351

Hawthorne Army Ammunition Plant, New Bomb
Open Burning/Open Detonation Grounds
EOD Surface Sweep - A Project Overview

Presented at the 22nd Annual
DOD Explosive Safety Seminar

by

C. David Douthat, P.E.
U.S. Army Corps of Engineers
Huntsville Division
Huntsville, AL

Table of Contents

	<u>Page</u>
I. Introduction	1
II. Background Information	1
III. Discussion	2
IV. Surface Sweep Data	8
V. Conclusion	8

List of Illustrations

	<u>Page</u>
Figure 1. Site Sector Map	3
Figure 2. Search Interval vs. SEP	6
Figure 3. Fragment and Ordnance Sector Tally	7
Figure 4. UXO Quantity Tally	9

List of Tables

Table 1. Support Equipment Requirements	4
---	---

I. Introduction

→ The U.S. Army Corps of Engineers, Huntsville Division recently completed a contract for an Explosive Ordnance Disposal (EOD) Surface Sweep of the Hawthorne Army Ammunition Plant (HWAAP), Nevada, New Bomb Open Burning/Open Detonation Grounds (OB/OD). This is the first EOD contract operation of this type ever undertaken by the Corps of Engineers.

↘ The scope of the contract required the location and rendering safe of approximately 5000 tons of ordnance fragments and 25,000 items of unexploded ordnance. This was a manual labor intensive operation under the direct supervision of civilian EOD qualified supervisors.

→ The completion of this project has demonstrated that what was once an exclusive military function can be done in a safe and effective manner by civilian forces.
↗

II. Background Information

Hawthorne Army Ammunition Plant is a government-owned/contractor-operated (GO/CO) facility located on 154,000 acres of Federal land south of Walker Lake in Mineral County, NV. Its mission includes loading, storing, maintaining and demilitarizing military munitions.

The New Bomb open burning/open detonation area is located 19 miles south of Hawthorne City limits on Nevada State Route 31. The area is within the Toiyabe National Forest and is leased to the Army by the U.S. Department of Agriculture. The actual leased area is approximately 800 acres.

The New Bomb Area is situated in a deep box canyon, which is a section of the Wassuck/Anchorite Hills. This area is where all open detonation of high explosive ordnance occurred.

As part of routine operations, DOD produces, stores, and uses large quantities of munitions and explosives. Each year, large quantities of these materials must be disposed of as waste. These wastes include out-of-date explosives and propellants, items in storage or manufacture which have failed quality assurance tests, out-of-date and obsolete munitions items, and any unsafe munitions items, components or explosives. Other related wastes also include materials which may have become contaminated by contact with these items. At present, OB/OD of explosive wastes are the most effective means of destroying many items, decontaminating large metal objects, and reducing most combustibles to a smaller volume. OB/OD is the most economical and in some cases, the only safe method currently available for the effective destruction, decontamination, and reduction of explosives and explosive wastes.

The OB/OD operations have been conducted at the New Bomb site since 1947. These grounds were operated by the Department of the Navy from 1947 to 1977 at which time ownership was transferred to the Department of the Army and the

grounds were continued for this use until the fall of 1984. Numerous types of ordnance, munition and explosive items were destroyed at this site during that time frame. Although disposal procedures were to prohibit kick-out of items that were destroyed by demolition, large quantities of fragments, intact unexploded ordnance and bulk explosives could be found throughout the site. This condition presented an undesirable environmental condition as well as a safety problem to the personnel operating the site and to the general public which had easy unauthorized access to the area.

III. Discussion

A competitively negotiated service contract was awarded to UXB International Inc., Washington, D.C. on 1 July 1985 to perform the EOD sweep. The qualifications of the contractor required that they have previous EOD work experience and that all management and supervisory personnel be Naval School, Explosive Ordnance Disposal, NAVSCOLEOD, Indianhead, Maryland trained and certified to perform all operations necessary under the contract.

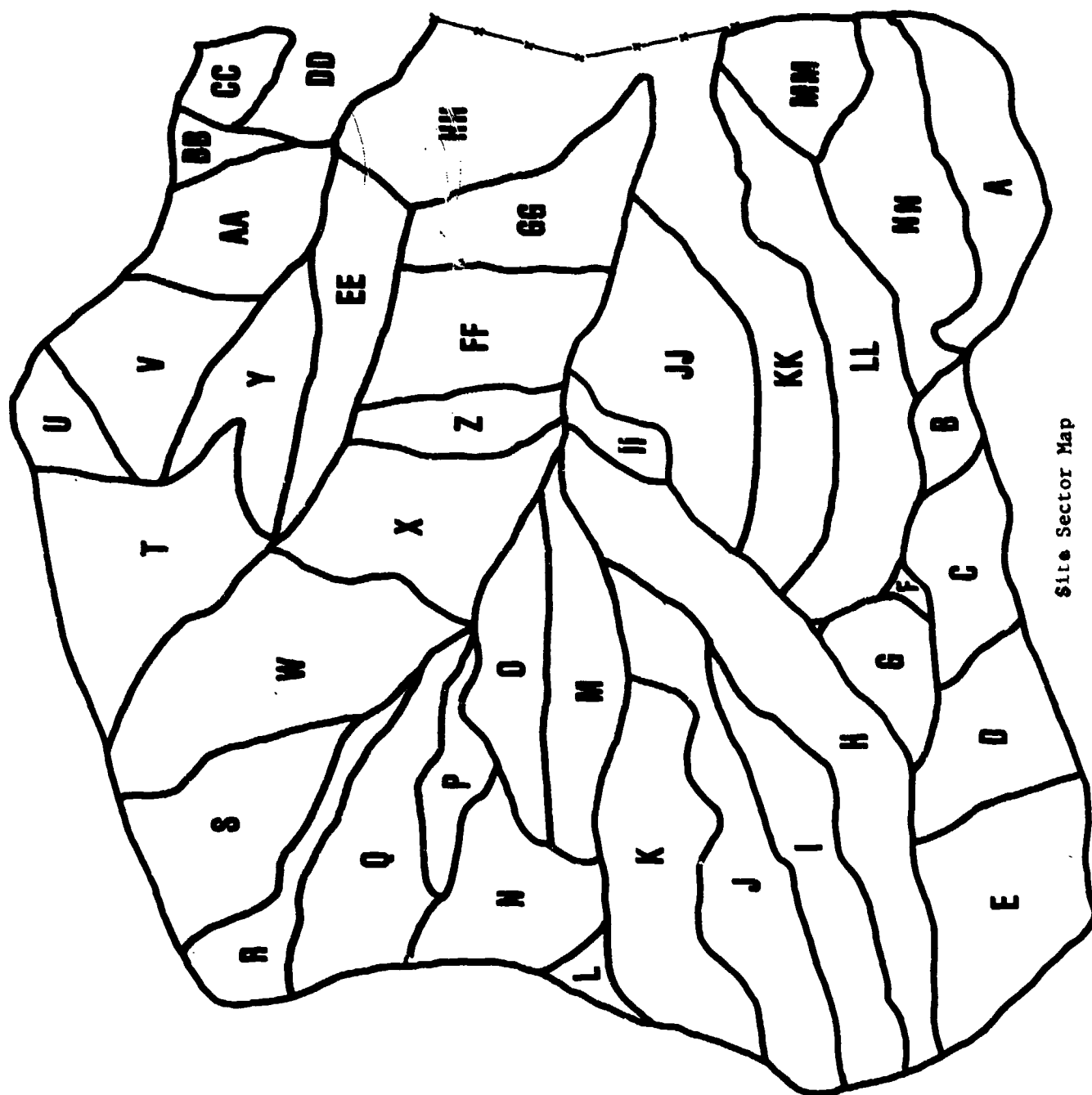
Prior to any ordnance operations on the site, the contractor was required to submit for approval Technical Plans, Management Plans, Safety Plans and SOP's to address all phases of the projected work. This was necessary to ensure the safety of all personnel during work activities and define management structure, responsibilities, work procedure, training, operating procedures, etc. during performance of the contract.

As a part of the preparation of the technical plans, the contractor was required to divide and mark the entire range into sectors and grids. This was required to measure the project progress and provided a basis for project completion payment. The methodology used in sector definition was to establish search/sweep sectors utilizing the natural or man-made boundaries (i.e., roads, fire lanes, mountain peaks and valleys). A total of forty (40) sectors were identified as shown on figure 1. In order to estimate the level of effort required to sweep each of the sectors preliminary surveys were performed to estimate the level of scrap metal contamination expressed in numbers of items per square feet of area.

In support of this project the contractor established facilities within the city of Hawthorne and at the site. The main office was located at Hawthorne and served as the recruitment center and Program Managers' office. The site field trailer served as the command post for the field work, first aid station, radio station and equipment station. Other equipment and materials required to support the project are shown in table 1.

Sweep Procedures

The initial EOD sweep of areas was conducted by EOD qualified personnel. This sweep located and marked the explosive material and identified those items that were to be destroyed in place. These sweeps were normally conducted on Saturdays or after the general labor force left the range. Those ordnance



Site Sector Map
Figure 1.

Table 1
Equipment Requirements

Facilities

Explosive Storage Magazines (2)
Maintenance Traylor (1)
Pallet Weighing Station (1)
Sani-Huts (6 to 10)

Equipment

IT-28 Forklift
Lift All Forklift
Rough Terrain Forklift
5 Ton Truck
10 Ton Truck
Jeeps (2)
Chevrolet Suburban (2)
Honda 4 Wheel Cycles (2)
Honda Trailers (2)
Portable Generators for Radio Transmitters
Water Tanks 1-300 gal., 1-1000 gal.
Fuel Support Tanks 500 gal. (2)
Radios
 Portable (AM) - 7
 Base Station (HF) - 1
 Portable Radios (HF) - 8
 Repeater Station (HF) - 1

Miscellaneous Equipment

Safety Glasses
Hard Hats
Rakes
Wheelbarrels
Fire Fighting Equipment
Picks (6)
Shovels (20)
Buckets (300)
Gloves (50 Doz.)
Safety Rope
First Aid Equipments
Water Coolers (16)

items that could be moved were placed in designated pallets for UXO and transported to the detonation pits for destruction. Those items to be destroyed in place were conspicuously marked for later destruction.

Follow-up sweeps were conducted by teams consisting of an EOD qualified team leader and laborers. These teams performed sweep operations using standard military EOD line abreast procedures. Spacing depended on the density of fragment, ground cover and terrain of the area. Any ordnance located during this follow-up sweep was flagged for later removal or destruction.

As a quality assurance measure, check sweeps were performed prior to government inspection. When the site supervisor was satisfied that the clearance was complete, governmental inspection was requested for sector sweep acceptance.

Sweep Effectiveness Probability (SEP)

The structure of the scope of work required the contractor to clean up all visible fragment greater than one inch in length in any direction and to locate and render safe all unexploded ordnance and explosive material. From this standpoint, the contractor was required to achieve a SEP of 100 for the entire range. This method was somewhat contrary to military ordnance sweep projects where a desirable SEP is established usually 80 to 90 and the area is swept until that SEP is accomplished at which time the area is considered clean.

Prior to this project completion it was decided to collect some data on sweep effectiveness from three different areas of approximately equal size but with varying terrain, ground cover and level of contamination. The three sectors were selected and were swept based on the following:

- Sweep 1: EOD sweep for potentially hazardous items. Time, personnel, item number, and item types were recorded.
- Sweep 2: Clearance sweep; search line with one EOD supervisor for every 10-15 laborers. Time, personnel, pounds of scrap, and EOD item number and types were recorded.
- Sweep 3: Check sweep; search line with one EOD supervisor for every 10-15 laborers. Time, personnel, pounds of scrap, and EOD item number and type were recorded.
- Sweep 4: Inspection sweep; the technical escort representative of the contract officer swept the lane with the site supervisor and one laborer. Pounds of scrap and EOD items and types, if any, were recorded.

Search Effectiveness Probability (SEP) was calculated as the ratio (%) of pounds of scrap collected on Sweep 2 to total pounds of scrap collected on all the sweeps. These SEPs ranged from 93.6 to 97.6. Separate SEPs were also calculated for potentially hazardous items using the ratio (%) of items collected on Sweep 1 to all hazardous items collected. These SEPs ranged from 20 to 83, but were not considered particularly meaningful since the searcher spacing interval was large (6 to 18 ft.) and the EOD searchers were confident that any UXO that was missed would be identified on subsequent sweeps. A comparison of this data with other sweep projects at Kahoolawe Island (Ref 1) and Cuddeback, CA (Ref 2) is shown in Figure 2.

SEARCH RATE VS. SEP

KAHOOLAWE, CUDEBACK, & HWAAP SURFACE

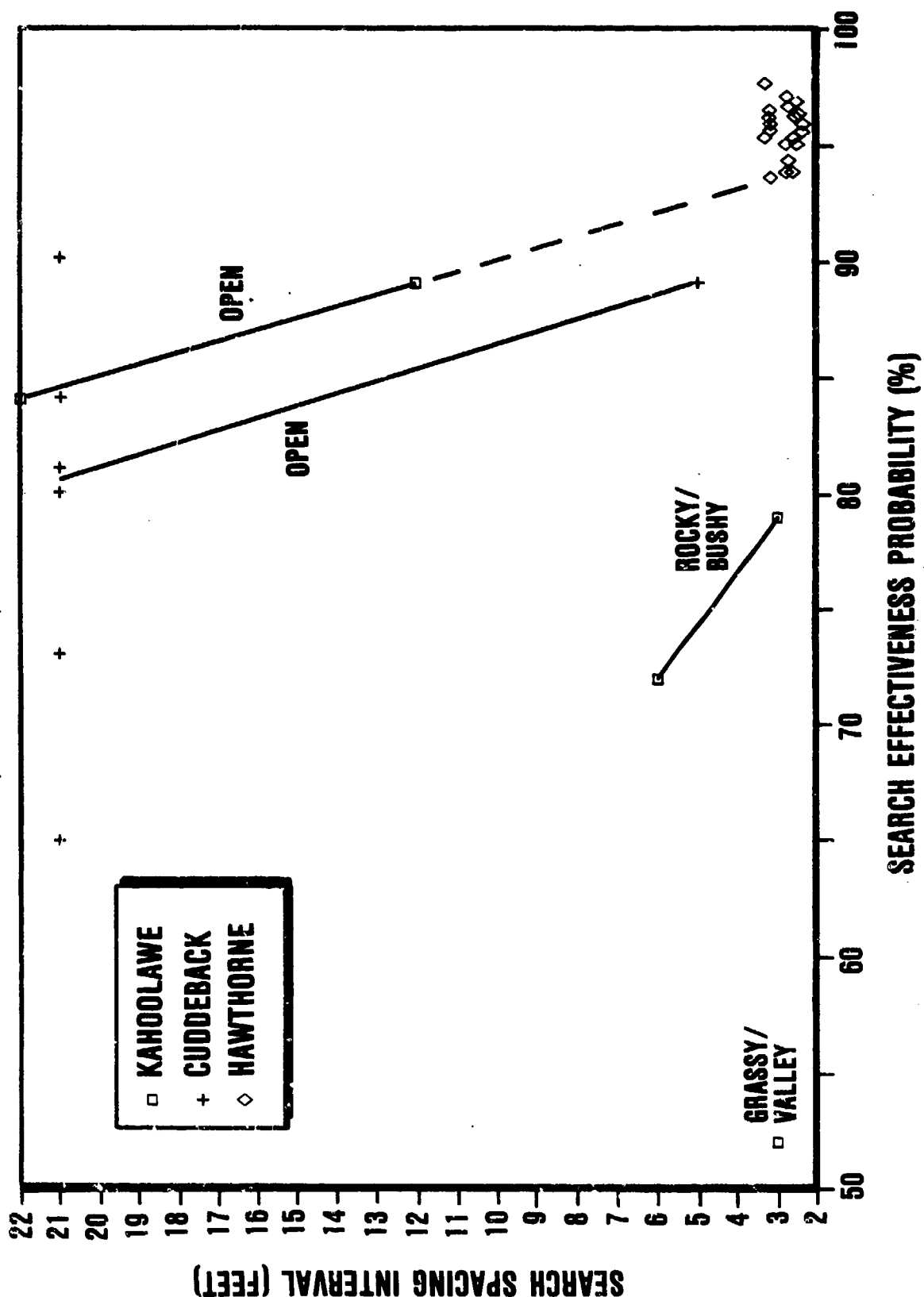


Figure 2.

**Fragment and Ordnance
Sector Tally**

SECTOR (# of Grids)	AREA (SQ. FEET)	SCRAP METAL (POUNDS)	BULK EXPLOSIVES (POUNDS)	DISPOSAL BY DETONATION (ITEMS)
A(14)	660000	8084	0	0
B(9)	150000	256	0	0
C(26)	650000	70520	0	2
D(23)	800000	134876	0	10
E(37)	1100000	269916	0	16
F(5)	22000	3095	0	0
G(25)	505000	77440	0	0
H(92)	1760000	1063546	0	25
I(70)	1070000	418363	0	1882
J(71)	1440000	754528	0	941
K(68)	1200000	439158	0	10
L(6)	85000	10273	0	0
M(93)	1100000	615773	0	6
N(23)	850000	440793	0	5
O(80)	800000	603852	0	5
P(30)	420000	366647	0	3
Q(42)	970000	390363	0	7
R(12)	370000	76462	0	3
S(18)	900000	269794	0	8
T(12)	1200000	319221	80	2087
U(1)	300000	0	0	0
V(20)	820000	27186	0	0
W(11)	1760000	732044	0	18
X(16)	1060000	396091	0	12
Y(13)	700000	35792	0	1
Z(7)	420000	86782	0	3
AA(7)	660000	5822	0	0
BB(3)	190000	0	0	0
CC(7)	250000	2394	0	0
DD(8)	700000	8526	0	0
EE(4)	760000	55562	0	1
FF(6)	950000	54377	0	2
GG(6)	820000	18136	0	0
HH(9)	1180000	447358	0	4381
II(2)	225000	74370	0	1
JJ(18)	1100000	260172	0	0
KK(25)	1388080	147380	0	5
LL(28)	1470000	51184	0	3
MM(6)	580000	4083	0	0
NN(14)	980000	8150	0	0
VARIOUS	0	0	7342	14991
SUBTOTAL	32365080	8748369	7422	24428
OPTION A	1524600	36179	0	0
OPTION B	5314320	0	0	207
TOTAL	39204000	8784548	7422	24635

* 4722 are Base Fuzes and are not counted as UXO

IV. Surface Sweep Data

The execution of the contract was completed in 228 days. This included mobilization, preliminary surveys, sweep time and demobilization. Personnel levels excluding management varied from 40 to 150 laborers per day. (Contract requirements limited no more than 15 laborers for each EOD supervisor.) Actual sector quantity amounts and ordnance types are shown in Figures 3 and 4. The average sweep rate for the project area was 0.05 acres/man-day which is slow compared to that at Cuddeback (Ref 2) of 0.58 acre per man day. This was to be expected since the contamination of HWAAP averaged over 12,000 lbs. per acre compared to that at Cuddeback of 2500 lbs. per acre. There were nearly 4000 pallets required to containerize the fragment. The final value of this contract was approximately \$2,500,000 for an average of \$3,125 per acre. This value is consistent with those costs identified in Ref 3.

V. Conclusion

The HWAAP New Bomb OB/OD Surface Sweep Project was successfully completed utilizing civilian forces operating under standard EOD military techniques. This project has demonstrated that where the need exists for ordnance cleanup, civilian forces are capable of performing the work. This capability will prove essential to the Department of Defense in the execution of the environmental restoration of present and formerly used ordnance sites.

UXO Quantity Tally

ITEMS	AMOUNT
AP Rounds	12
Base Fuzes	8674
Base Fuzes w/Dets	460
BD Fuze	1
Boosters (Various)	949
Booster Lead Ins	1
Burster Tubes	136
Cads	937
Detonators	35
Explosive Cartridges	227
FAH 30-53	1
Flare Ignitor	1
FMU 851B	1
HE Filled Rounds	2
Hedge Hog	1
Misc. Fuzes	419
Misc. Ordnance Items	811
M43A1 Blue Bomblets	2
M82 Bomb Nose	1
M83 Butterfly	1156
M100 Series Fuze	2
M103 Fuze (Nose)	4
M125A1 Booster	2
M344 PIBD Fuze	1
M904 Fuze	2
Mk 10 Army Device	1
Mk 44 Booster	27
Mk 230 Fuzes	58
Mortar Round	2
Nose Booster	4
Nose Det Fuzes	66
PD Fuze	5
Practice Depth Charges	3
Primers	134
Propellant Booster	1
Propellant Canisters	2
Propellant Cartridges	2
Special Fireworks	4
SQS.	1

Figure 4

UXO Quantity Table (cont'd)

ITEMS	AMOUNT
2.75 Rocket Fuze	1
2.75 Rocket Motors	1
2.75 Rocket Warhead	2
3" APHE Projectile	5
3" HE Projectile	285
3"50 HD Projectile	44
3.5 Fuzes (M404)	232
3.5 Rocket Motor	450
3.5 Rocket Motor & Fuze	79
3.5 Rocket W/H & Fuze	1
3.5 Rocket Warhead	16
3.75 Rocket Moror & Fuze	1
3.75 Rocket Warhead	220
5" HE Projectile	137
6" HE Projectile	217
8" HE Projectile	123
16" HE Projectile	1
20mm HE Round	126
221b. Frag Bomb	38
37mm HE Round	11
40mm HE Round	53
50mm HE Rcund	9
75mm Mortar	1
81mm Mortar	34
100lb. Bomb (old style)	23
106 Round	5

References

1. NAVEODTEHCEN Technical Report, TR-235, November 1980, "Study of Search Effectiveness of Surface Clearance Techniques on Kahoolawe Island."
2. Site Survey Plan, Cuddeback California, Air to Gunnery Range (AGGR), February 1986.
3. NAVEODTEHCEN Technical Report TR-275, January 1986, "Range Clearance Technology Assessment."

AD-P005 352

SUPPRESSION OF PROPAGATION BETWEEN STACKS OF BOMBS

KENNETH R. SHOPHER

EDWARD M. JACOBS

EXPLOSIVES SAFETY BRANCH
AIR FORCE INSPECTION AND SAFETY CENTER
NORTON AIR FORCE BASE, CALIFORNIA

ABSTRACT

Tests were conducted to determine if propagation could be prevented between stacks of MK 82 (500 pound) and MK 84 (2000 pound) bombs in storage. The effects of four variables were explored; orientation of the bombs, fuze well protection, distance between stacks of bombs, and placing material between stacks of bombs. A total of 19 tests have been conducted and conclusively prove that propagation between stacks of bombs in storage can be prevented.

BACKGROUND

Limited availability of land area for munitions storage at overseas bases, coupled with civilian encroachment, and the need to build additional facilities on available land has placed constraints on munitions storage capabilities. Many structures which can physically hold as much as 500,000 pounds of explosives are limited to 60,000 pounds or less by quantity distance constraints. One method of increasing the explosives capacity of limited structures is to place stacks of bombs in a structure in such a way that if one stack of bombs detonates the other stacks of bombs will survive. In this manner the maximum credible event (MCE) can be reduced to one stack of bombs and consequently required safety distances can be reduced.

TEST APPROACH

Two mechanisms are known to cause propagation between bombs, shock from the impact of high energy fragments and pressure/shock from blast. The easiest method of limiting pressure was to limit the size of the stacks of bombs. Consultation with Dr. Jerry Ward of the DDESB revealed that 60,000 pounds net explosives weight (NEW) was a conservative upper limit. We restricted our test to the 60,000 pound range. In order to reduce the effect of high speed fragments, material, which we will call buffer material, was placed between stacks of bombs. Buffer materials were limited to other munitions items and bomb components since they needed to be stored in the munitions areas in any case. Most fragments come from the sides of bombs, therefore the number of fragments transmitted from one stack of bombs to the next can be reduced by orienting the bombs so that the nose or tail of bombs in one stack are oriented toward the nose or tail of bombs in the other stack. Three stacks of bombs were used for each test; a center stack which we will refer to as a donor stack (in which one bomb is intentionally detonated), and two acceptor stacks which are the targets for the fragments.

MK 82 TEST SERIES

OVERVIEW

This test series was conducted in 1985. The goal was to determine if buffer material would prevent propagation between MK 82 bombs in storage.

TEST 1 (fig. 1)

The goal of this test was to determine what would happen to bombs in a normal storage configuration when one bomb in the donor stack was intentionally detonated. We were reasonably sure all bombs in the donor stack would detonate and the detonation

would propagate to the other stacks, but it was necessary to verify this before proceeding with the test series. The donor stack consisted of 108 MK 82 bombs, the acceptor stacks each consisted of 12 MK 82 bombs, and the stacks were separated by a nominal 30 inch aisle space. Bomb nose and tail fuze wells were protected only by plastic shipping covers.

All bombs detonated.

TEST 2 (fig. 2)

This was the first test using buffer material. The donor stack consisted of 108 MK 82 bombs, the buffers were one row of 20 MM TP ammunition and one row of CBU 58s. 12 MK 82s were used in each acceptor stack. Acceptor bombs were boosted and fuze as we felt this represented the most sensitive configuration for the MK 82.

The 12 bombs on the 20 MM side of the donor survived. One bomb on the CBU 58 side functioned low order, the others survived.

TEST 3 (fig.3)

This test was designed to be more representative of MK 82 bombs in storage. MK 82s were in their standard storage configuration (plastic nose and tail fuze well protectors). Two rows of 20 MM TP were used as the buffer on one side and 7 rows of MK 15 fins on the other. The acceptor stacks were 36 MK 82s.

All bombs in the acceptor stack on the MK 15 fin side survived. All bombs on the 20 MM side detonated.

We were unable to understand what caused the failure of the bombs on the side buffered by 20 MM. We had gone from the more sensitive fuze bombs and one row of buffer material to the less sensitive unfuzed bombs and two rows of buffer. We had, however, increased the size of the acceptor from 24 to 36 bombs which increased the number of targets for fragments. We decided to continue the test series using 36 bombs acceptors and see if we could determine the failure mode as the series progressed.

TEST 4 (fig. 4)

In previous tests buffer material was stacked in a standard manner and as a result an air space existed between columns of buffer material. We felt the failure mechanism might be bomb fragments coming through the spaces between columns of buffer material. In this test we staggered the buffer material horizontally to ensure that a fragment had to hit buffer material before it reached the acceptor bombs. Two rows of CBU 58s and 5 rows of MK 15 fins were used as buffers.

The bombs on the fin side survived. The bombs on the CBU 58 side detonated.

We were again faced by the dilemma of how less sensitive bombs with more buffer protection could fail. Perhaps we had erred when we considered fuze bombs more sensitive than unfuzed

bombs. Boosters and fuzes give more protection to the fuze cavities of bombs than the standard plastic shipping cap.

TEST 5 (fig. 5)

In this test we attempted to provide fuze well protection by placing plastic rods 2.75 inches in diameter by 6 inches long in the fuze wells of the bombs and covering these with the standard plastic shipping cap. We also staggered the buffer vertically in order to eliminate the possibility that fragments were transiting through the forklift holes in the pallets. The buffers were two rows of CBU 58 (which were now staggered both vertically and horizontally) and two rows of MK 15 fins (staggered horizontally only).

All bombs detonated.

The results of our tests to this point were inconclusive. We felt we needed to go back to our successful test and proceed from there. We were convinced that fragment attack was the mechanism causing the acceptors to detonate. We also felt that staggering the buffer material both horizontally and vertically would reduce the number of fragments reaching the acceptors.

TEST 6 (fig. 6)

In addition to fuzing and boosting the acceptor bombs we oriented bombs so that the nose of the acceptors were oriented toward the noses of the donors. We felt this might reduce the effect of the fragment attack by orienting the relatively smaller flat area on the front of the acceptor bombs toward the fragment attack. The acceptor stacks were composed of 24 MK 82s and the buffers were two rows of MAU 93 fins and three rows of 20 MM TP ammunition.

All bombs survived.

We are now convinced that fuze well protection is necessary.

TEST 7 (fig. 7)

In this test we used steel tail plugs in the noses of the acceptor/donor pair and steel nose plugs in the other. We retained the nose to nose orientation of the acceptor to donor. The size of the acceptor stacks was again increased to 36 bombs. Two rows of CBU 58 were used as one buffer and three rows of CBU 58 were used for the other. The buffers were staggered both horizontally and vertically.

All bombs survived.

CONCLUSION

It is possible to prevent propagation between stacks of bombs using fuze well protection, proper bomb orientation, and sufficient buffer material.

MK 84 TEST SERIES

OVERVIEW

This series started in the spring of 1986 and is ongoing at this writing. The goals of this series are to prove that the buffered storage concept works for the MK 84 bomb, determine if nose fuze well protection alone (no buffer material) will prevent propagation, to validate additional buffer materials, and test the effect of donor stacks with a net explosive weight of up to 60,000 pounds.

TEST 1 (fig. 8)

The goal of this test was to determine if steel nose fuze well protection alone would prevent propagation between stacks of bombs. Twenty four MK 84s were used as the donor and two stacks of 12 MK 84s were used as acceptors. Bombs were oriented nose to nose and separated by 15 feet, no buffer material was used. Steel nose plugs were used in both the donor and acceptor bombs.

All acceptor bombs survived. No significant damage was noted. Steel nose plugs were slightly eroded by fragments and jets (fig. 9). High speed photography revealed what looked like an aerodynamic flow of fragments around the pointed noses of the MK 84 bombs.

TEST 2 (fig. 10)

The goal of this test was to see if bombs with only nose and tail fuze well protection would survive if oriented so that the tail of one acceptor was exposed to the nose of the donor and if the nose of the other acceptor was exposed to the tail of the donor. The donor consisted of 24 MK 84s and the acceptors were 12 MK 84s. Bombs were placed 15 feet apart and no buffer material was used.

All bombs detonated.

TEST 3 (fig. 11)

After the failure of test 2 it was necessary to validate the results of test one to see if we should pursue testing with no buffer material. The test and results were the same as test 1.

TEST 4 (fig. 12)

This was an attempt to see what effect buffer material would have on bombs arranged with nose to tail and tail to nose

configurations. Five rows of empty 55 gallon drums were used to simulate bomb component containers. A thirty inch aisle space was maintained between the donor/acceptors and the buffer. This resulted in a distance of 13.5 feet between stacks of bombs.

One bomb in each acceptor stack reacted low order, all other bombs survived. Bomb noses and tails showed more damage than in test 1 and 3. (fig. 13, and 14).

TEST 5 (fig. 15)

Even though there was no stack to stack propagation in test 4, we wanted to prevent low order reactions if possible. In this test we added one row of drums to give us a total of six rows and increased the distance between bombs to 15 feet.

The results were identical to test 4. Based on this we decided to abandon the nose to tail and tail to nose configurations and continue the test series nose to nose orientation at 15 feet separation.

TEST 6 (fig. 16)

The DDESB had requested that we conduct this test in a simulated igloo. The igloo was simulated by a 20 x60 foot rectangular hole in the earth 10 feet deep. Three sides of the hole were lined with concrete slabs to make vertical faces and one 20 foot side was left open with a ramp sloping to ground level (fig. 17). Four rows of MK 20 cluster bombs were used as the buffer material. The MK 20 is packed 2 per metal container and has a net explosive weight of 100 pounds. Sixteen containers were used in each buffer for an explosive weight of 3200 pounds per buffer. Distance between stacks of bombs was 15 feet and the distance between the MK 20s and acceptors was 15 inches.

Acceptor bombs on the closed end of the simulated igloo detonated, MK 20s were completely consumed, and acceptors on the open end of the igloo survived with very little damage (less than that in test 1 and 3)(fig. 18).

We concluded that the detonation of the acceptor bombs at the closed end of the igloo was probably a pressure reaction caused by the relatively unyielding walls of the structure and the proximity of the MK 20s to the acceptor. Based on these results we felt that future tests should be conducted in a more realistically simulated above ground igloo.

TEST 7 (fig. 19)

The goal of this test was twofold. First to see if the donor would survive in an igloo with no buffer and to test 30 MM high explosive (HE) ammunition as a buffer. The test was conducted in a simulated igloo built above ground using concrete slabs. This igloo was 20 feet wide, 80 feet long, and 10 feet high, earth was mounded to the top on three sides, it had no roof, and a concrete slab was used for the door(fig. 20). Two rows of 30 MM HE ammunition were used as the buffer between the

donor and the acceptor at the door end of the igloo. No buffer was used between the donor and the acceptor at the rear end of the igloo, stacks of bombs were separated by 15 feet.

All acceptor bombs survived. Bombs on the closed end were damaged much like those in test 1 and 3. Some ammunition survived intact. Most cartridge cases and propellant were consumed, many projectiles appear to have reacted low order and only split the projectile case consuming most or all of the explosives inside.

From this we concluded that pressure was not a problem with a donor of 24 MK 84 bombs and that 30 MM HE ammunition was an acceptable buffer.

TEST 8 (fig. 21)

This was our first test above the 20,000 pound NEW range. The goal was to determine what effect a 48 bomb MK 84 donor would have on 24 MK 84 acceptors. The bomb fuze wells were protected with steel nose and tail plugs. Stacks of bombs were placed 15 feet apart. The test was conducted in a simulated above ground igloo. The igloo was the same dimensions as the one in test 7 but had a roof of concrete slabs. The steel superstructure used to support the roof was inside the igloo (fig. 22). A concrete slab was used as a door.

All acceptors survive. Several bombs sustained large dents in the side from collision with other bombs or the igloo (fig. 23). Many bombs had severe fragment damage to the nose, much like that seen in tests four and five.

We felt that most of the dents were caused by collisions with other bombs because there were few sharp edges that we would expect to see if the collisions were with the igloo superstructure. Several nose fuze wells had been eroded to the point that the fuze wells were visible (fig. 24).

TEST 9 (fig. 25).

Since the acceptors in test 8 had survived both the pressure and fragments from a 48 MK 84 donor we decided to increase the donor to 64 MK 84 bombs. We were concerned about the severe erosion of the nose plugs seen in test 8, so we decided to use a small quantity of buffer. Two rows of palletized MK 81 fins were used on each side. The test was conducted in a simulated above ground igloo with a roof, and a concrete slab for a door. The igloo had been redesigned so as to place the vertical support members outside of the igloo and decrease the amount of steel supporting the roof. We will call this igloo the Haymen Igloo (fig. 26).

Acceptor bombs on the door end detonated. Seven bombs from the rear stack reacted low order, many of the surviving bombs were dented and had severe nose erosion as seen in test 8.

Since the bombs at the rear of the igloo survived (these should have experienced the most pressure), we felt we could rule out pressure as the mechanism for the failure of the front stack.

We were convinced that the large quantity of fragments from 64 MK 84s simply overcame our buffer.

TEST 10 (fig. 27)

Two variables were changed in this test. The distance between stacks of bombs was increased from 15 feet to 20 feet and slightly more substantial buffers were used. The buffers were 3 rows of MK 81 fins and 3 rows of 20 MM TP ammunition. The donor was 64 MK 84s, and the acceptors 32 MK 84s. The test was conducted in a Haymen igloo.

The acceptors at the rear of the igloo(protected by the fins) detonated. The other acceptors survived in relatively good condition. Only four bombs had large dents in the sides, and one bomb had the base plate knocked off (it appeared to be a mechanical separation caused by impact with another metal object). Only two bombs had fragment damage to the nose.

A clear impression of a bomb base plate on the side of a bomb gave credence to our belief that many dents were caused by bomb to bomb collisions. We felt strongly that the failure was caused by fragment attack rather than pressure because the acceptor at the rear of the igloo had survived a 64 MK 84 attack with less buffer and less distance to the donor.

TEST 11 (fig. 28)

Since three rows of 20 MM TP ammunition had been a sufficient buffer we decided to try another fairly massive buffer. Three rows of CBU 58s were used for both buffers. The bombs were separated by 20 feet, and the test was conducted in a Haymen igloo.

All acceptors survived. Very little fragment damage was observed but several bombs were dented.

TEST 12 (fig. 29)

The success with CBU 58s led us to believe that MK 20s would work. Three rows of MK 20s were used in each buffer, the stacks of bombs were 20 feet apart, and the test was conducted in a Haymen igloo.

One acceptor bomb from the top row of each stack functioned low order, all other bombs survived. Again very little fragment damage was observed and several bombs were dented.

In this test the tops of the donor, buffer, and acceptor stacks were at virtually the same height and we believe the low order reactions were caused by fragments coming through the thin top of the buffer.

OVERALL TEST RESULTS

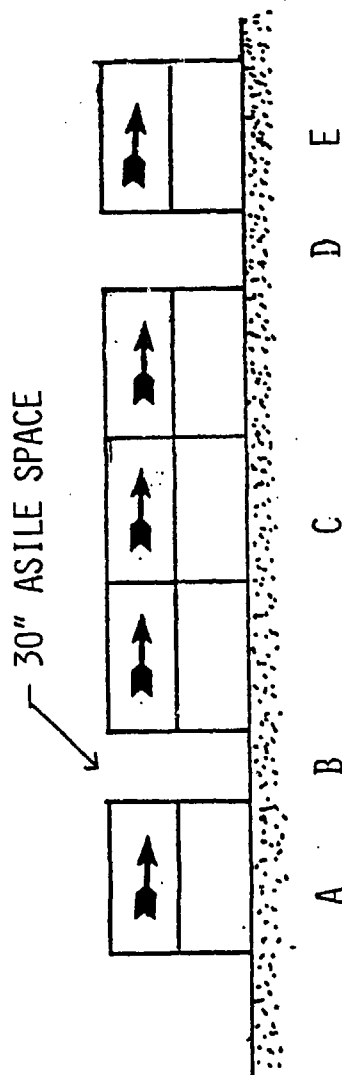
When stacks of bombs were arranged so the noses of the bombs in one stack were oriented toward the noses of bombs in the other stacks and steel nose and tail fuze well protectors were used, propagation between stacks could be prevented. Acceptor bombs survived the attack of pressure and fragments of up to 48 MK 84 bombs (45,360 pounds NEW) at 15 feet separation without using buffer material. Acceptor bombs also survived the attack of pressure and fragments from stacks of 64 MK 84 bombs (60,480 pounds NEW), even when coupled with the detonation of 96 MK 20s used as a buffer (9,600 pounds NEW) when stacks were separated by 20 feet and a proper buffer material was used.

CONCLUSION

Propagation can be prevented between stacks of MK 82 and MK 84 bombs when they are properly oriented, separated, steel nose and tail fuze well protection is provided, and buffer material proven adequate in this test series is used.

TEST NUMBER: 1

CONFIGURATION:



- A. ACCEPTOR: 12 MK 82 with plastic nose and tail plugs.
B. BUFFER: None. 30 inches between bombs
C. DONOR: 108 MK 82
D. BUFFER: None. 30 inches between bombs
E. ACCEPTOR: 12 MK 82 with plastic nose and tail plugs

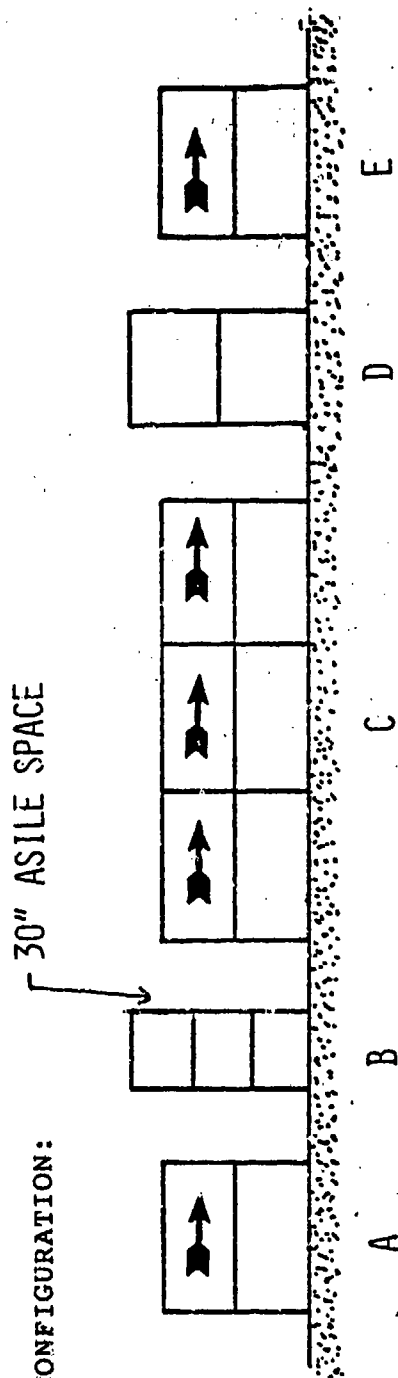
RESULTS: All bombs detonate.

CONCLUSIONS: All bombs in a stack of MK 82s will detonate if one bomb is initiated. Bombs in adjacent stacks will propagate.

FIGURE 1

TEST NUMBER: 2

CONFIGURATION:



- A. ACCEPTOR: 12 MK 82 boosted and fuze with 904 and 905 fuzes
- B. BUFFER: One row of CBU 58
- C. DONOR: 108 MK 82
- D. BUFFER: One row of palletized 20 mm TP ammunition.
- E. ACCEPTOR: 12 MK 82 boosted and fuze with 904 and 904 fuzes

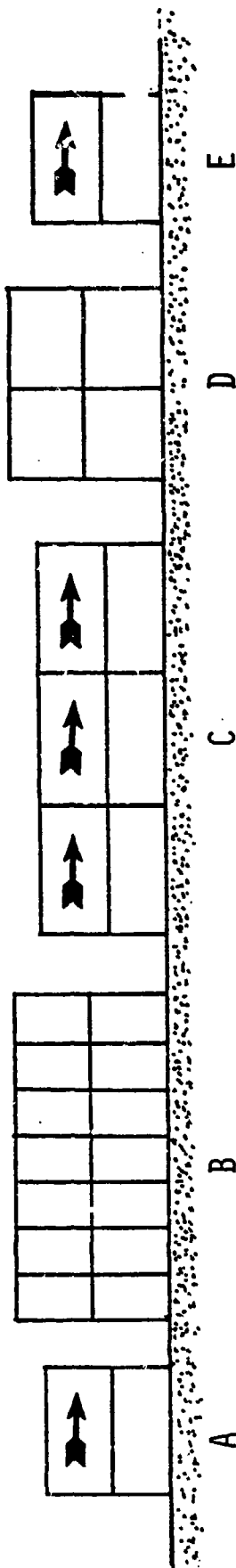
RESULTS: One bomb on CBU side functioned low order, all others survive.

CONCLUSION: Boosted and fuze bombs do not propagate when properly protected by buffer materials.

FIGURE 2

TEST NUMBER: 3

CONFIGURATION:



- A. ACCEPTOR: 36 MK 82 with plastic nose and tail plugs
- B. BUFFER: 7 rows of MK 15 bomb fins
- C. DONOR: 108 MK 82
- D. BUFFER: 2 rows 20 MM TP
- E. ACCEPTOR: 36 MK 82 with plastic nose and tail plugs

RESULTS: Bombs on fin side survive, bombs on 20 MM side detonate.

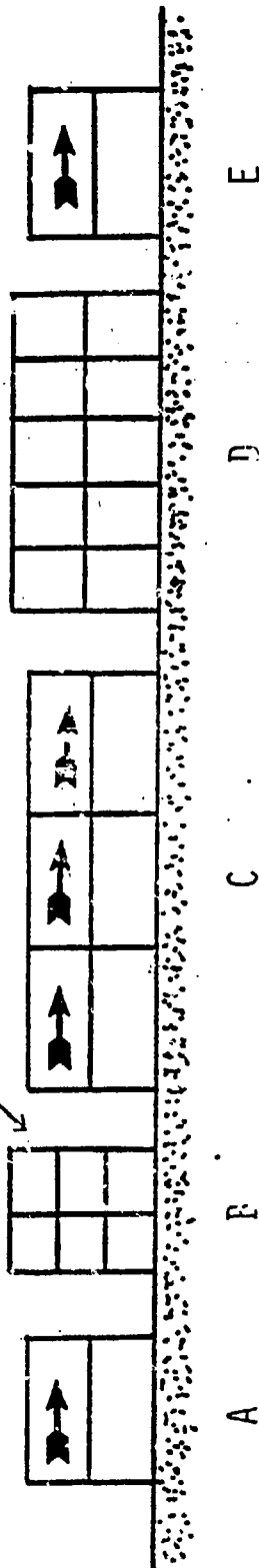
CONCLUSIONS: None. Why did less sensitive bombs fail when more of the same buffer was used? Did the change from 24 acceptors to 36 increase the probability of a lethal fragment? Continue testing with 36 acceptors. Stagger the rows of buffer horizontally so no line of sight exists between columns of acceptors.

FIGURE 3

TEST NUMBE' 1

CONFIGURATION:

30" ASILE (TYPICAL)



- A. ACCEPTOR: 36 MK 82 with plastic nose and tail plugs
B. BUFFER: 2 rows of CBU 58s, staggered
C. DONOR: 108 MK 82
D. BUFFER: 5 ROWS MK 15 bomb fins, staggered

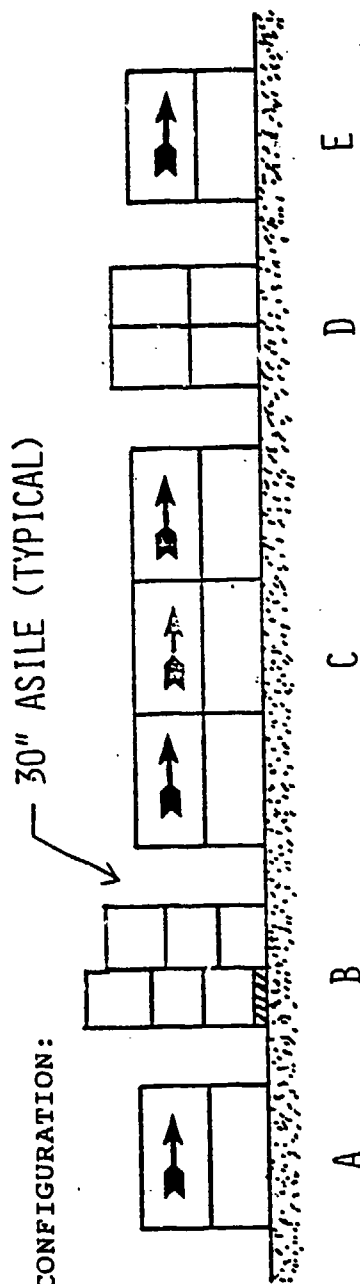
RESULTS: Bombs on CBU side detonate, bombs on fin side survive.

CONCLUSION: MK 15 fins are an acceptable buffer. Since test 2 was successful with the bombs boosted and fuze, perhaps fuze well protection will increase survival.
Try the next test with fuze well protection.

FIGURE 4

TEST NUMBER: 5

CONFIGURATION:



- A. ACCEPTOR: 36 MK 82 with 2.5" diameter 6" long plastic rods in fuze wells.
- B. BUFFER: 2 rows CBU 58, staggered both horizontally and vertically
- C. DONOR: 108 MK 82
- D. BUFFER: 2 rows MK 15 fins, staggered horizontally

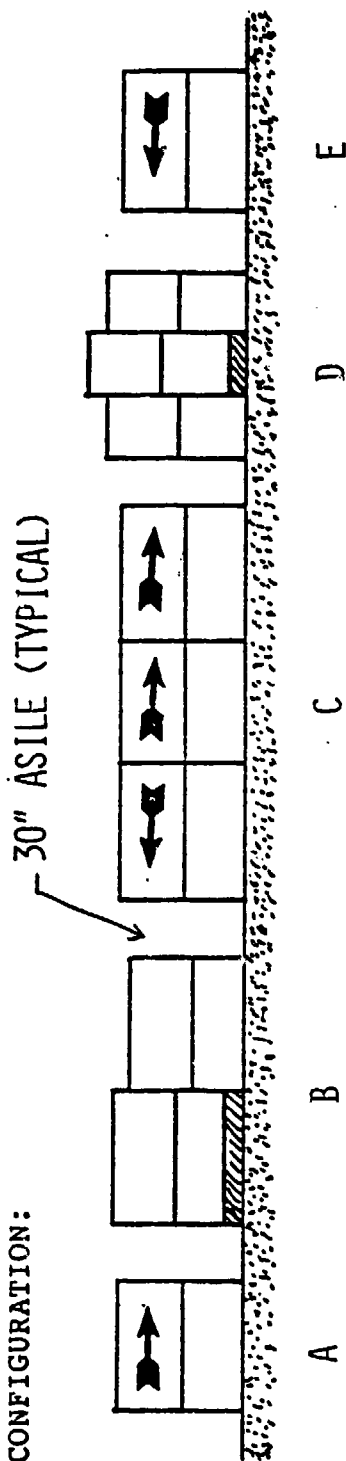
RESULTS: All bombs functioned high order.

CONCLUSIONS: Plastic rods were not sufficient nose fuze protection. Try fuzes and boosters again. Reduce acceptor stack to 24 bombs. Orient bombs so noses of the acceptors are exposed to noses of the donors.

FIGURE 5

TEST NUMBER: 6

CONFIGURATION:



- A. ACCEPTOR: 24 MK 82 boosted and fuze with 904 and 905 fuzes
- B. BUFFER: 2 rows palletized MAU 93 fins, staggered horizontally and vertically
- C. DONOR: 108 MK 82
- D. BUFFER: 3 rows 20 MM ammunition, staggered horizontally and vertically.
- E. ACCEPTOR: 24 MK 82 boosted and fuze with 904 and 905 fuzes

RESULTS: All bombs survive.

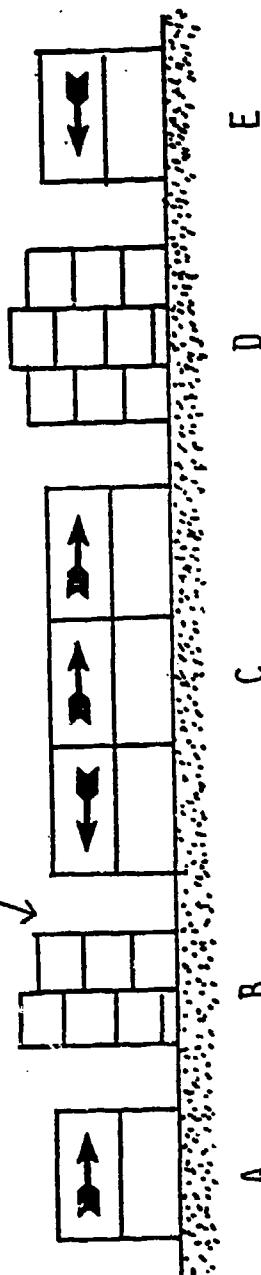
CONCLUSIONS: Fuze well protection works. Buffer stacks must be staggered to prevent a free path for fragments. Nose to nose orientation appears to work.

FIGURE 6

TEST NUMBER: 7

CONFIGURATION:

30" ASILE TYPICAL



A. ACCEPTOR: 36 MK 82 with steel tail plugs in nose fuze wells.

B. BUFFER: 2 rows of CBU 58, staggered

C. DONOR: 108 MK 82, steel tail plugs in noses of bombs facing acceptor with steel tail plugs in nose, steel nose plugs in noses of bombs facing acceptor with steel nose plugs.

D. BUFFER: Three rows of CBU 58, staggered

E. ACCEPTOR: 36 MK 82 with steel nose plugs in noses of bombs.

RESULTS: All bombs survive.

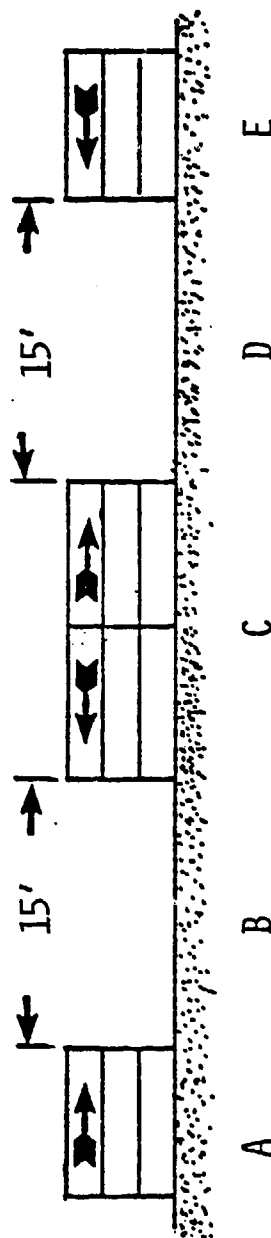
CONCLUSIONS: Propagation between stacks of bombs can be prevented. A combination of fuze well protection, and adequate buffers is necessary.

FIGURE 7

TEST NUMBER: 1

DATE: 1 April 86

CONFIGURATION:



- A. ACCEPTOR: 12 MK 84 with steel nose plugs
- B. BUFFER: 15' AIR
- C. DONOR: 24 MK 84 with steel nose plugs
- D. BUFFER: 15' AIR
- E. ACCEPTOR: 12 MK 84 with steel nose plugs

RESULTS: All acceptors survive. Noses of bombs show erosion from fragments and jets.

CONCLUSIONS: MK 84 bombs can survive attack by 24 MK 84 bombs without buffers at a distance of 15 feet, when oriented nose to nose and steel nose plugs are inserted in the nose fuze wells.
Try nose to tail and tail to nose exposures.

FIGURE 8



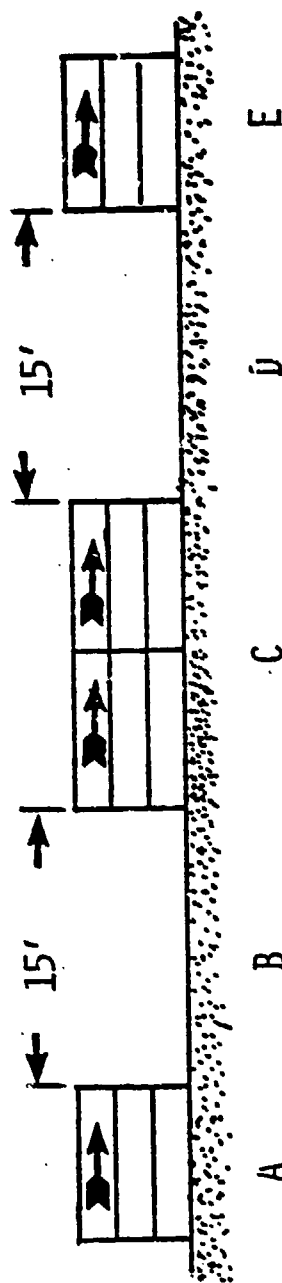
1255

FIGURE 9

TEST NUMBER: 2

DATE: 4 April 86

CONFIGURATION:



- A. ACCEPTOR: 12 MK 84 with steel nose plugs
- B. BUFFER: 15' Air
- C. DONOR: 24 MK 84 with steel nose and tail plugs
- D. BUFFER: 15' Air
- E. ACCEPTOR: 12 MK 84 with steel tail plugs

RESULTS: All acceptors detonate.

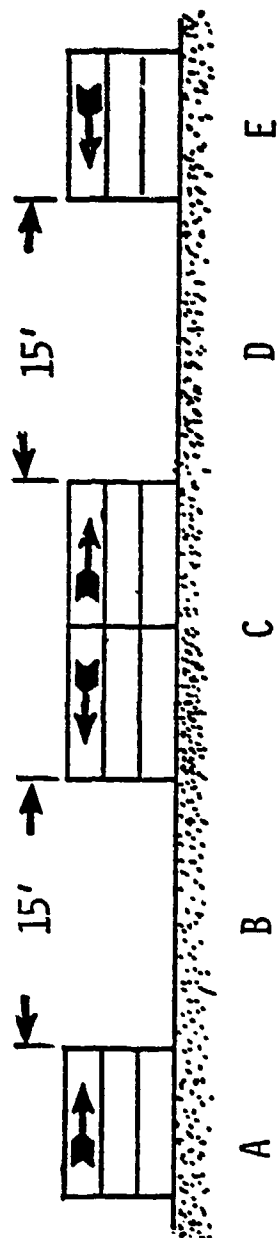
CONCLUSIONS: This is not an acceptable orientation. Were we just lucky with test one?
Reaccomplish test one.

FIGURE 10

TEST NUMBER: 3

DATE: 8 April 86

CONFIGURATION:



- A. ACCEPTOR: 12 MK 84 with steel nose plugs
- B. BUFFER: 15' Air
- C. DONOR: 24 MK 84 with steel nose plugs
- D. BUFFER: 15' AIR
- E. ACCEPTOR: 12 MK 84 with steel nose plugs

RESULTS: All acceptors survive. Nose plugs show erosion from fragment attack.

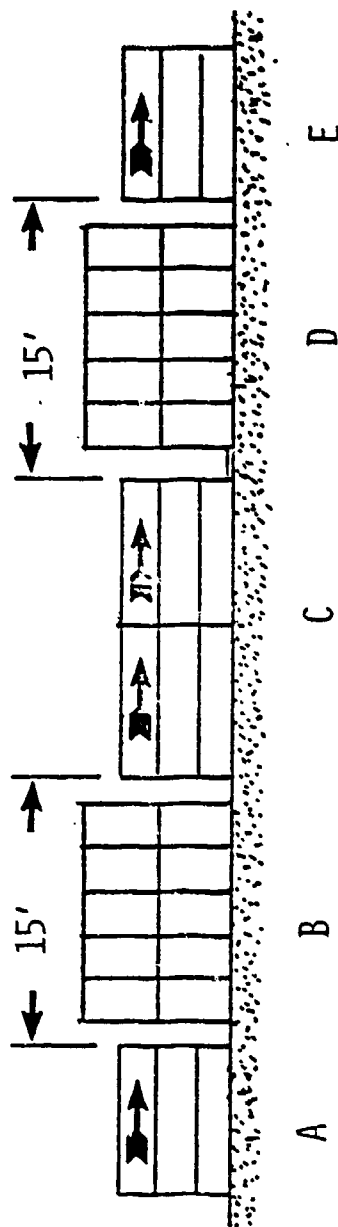
CONCLUSIONS: Nose to nose orientations are effective. Try orientations used in test two with buffer.

FIGURE 11

TEST NUMBER: 4

DATE: 10 April 86

CONFIGURATION:



- A. ACCEPTOR: 12 MK 84 with steel nose plugs
B. BUFFER: 5 rows of 55 gallon drums.
C. DONOR: 24 MK 84 with steel nose and tail plugs
D. BUFFER: 5 rows of 55 gallon drums.
E. ACCEPTOR: 12 MK 84 with steel tail plugs

RESULTS: One low order explosion in each acceptor stack. Many acceptor bombs show severe fragment damage.

CONCLUSION: This configuration could be successful with more buffer material. Try again with more buffer.

FIGURE 12



1259

FIGURE 13



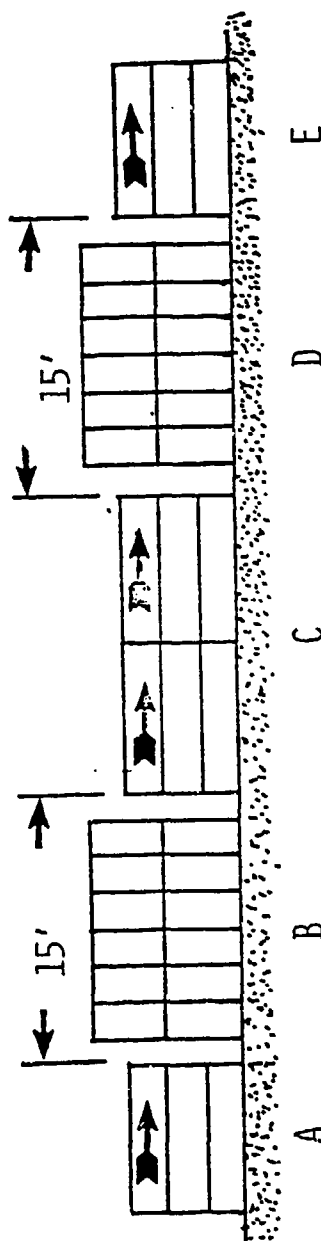
1260

FIGURE 14

TEST NUMBER: 5

DATE: 15 April 86

CONFIGURATION:



- A. ACCEPTOR: 12 MK 84 with steel nose plugs
B. BUFFER: 6 rows of 55 gallon drums
C. DONOR: 24 MK 84 with steel nose and tail plugs
D. BUFFER: 6 rows of 55 gallon drums
E. ACCEPTOR: 12 MK 84 with steel tail plugs

RESULTS: One low order in each acceptor stack. Severe fragment damage to many survivors.

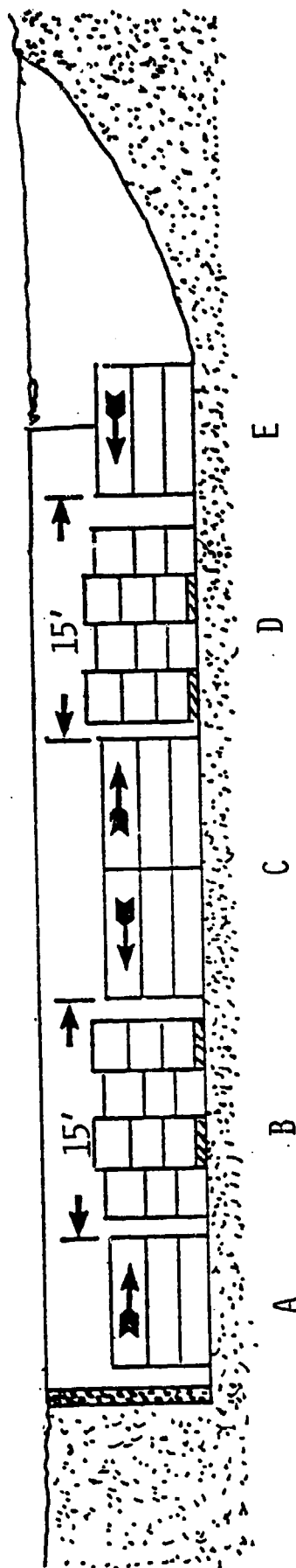
CONCLUSIONS: Since bombs oriented nose to nose survive with very little damage and no low orders abandon this configuration and continue the tests with nose to nose orientation and 15' separation.

FIGURE 15

TEST NUMBER: 6

DATE: 21 April 86

CONFIGURATION:



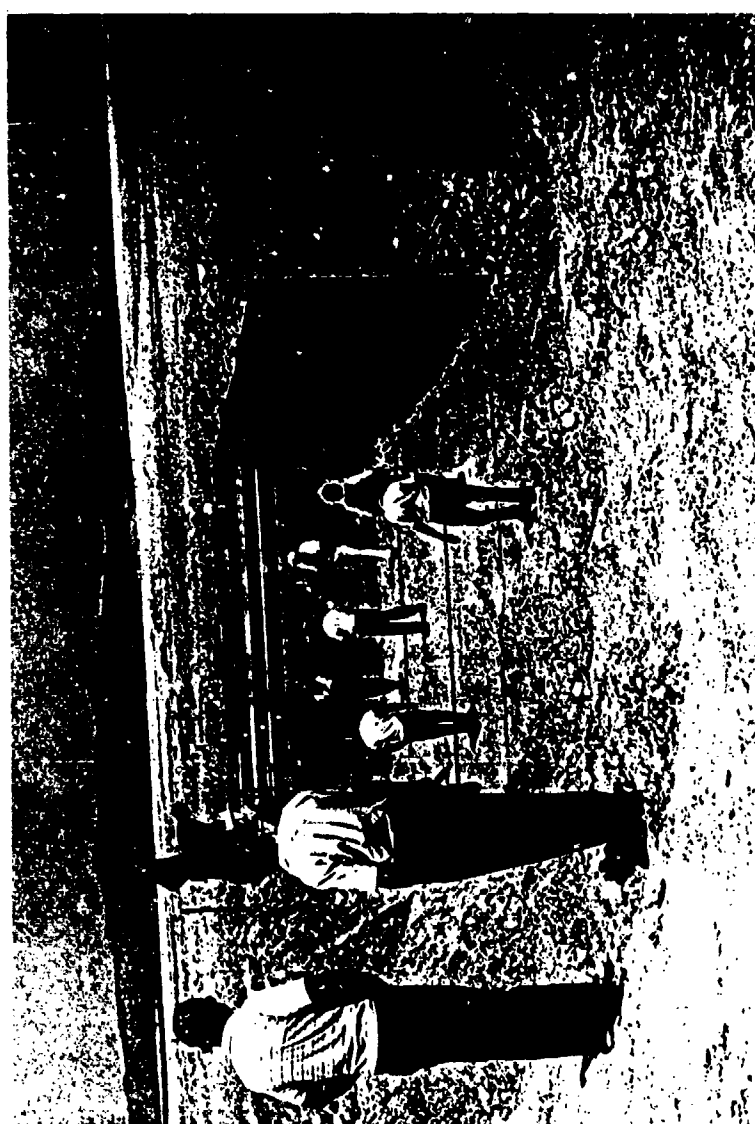
- A. ACCEPTOR: 12 MK 84 with steel nose and tail plugs
B. BUFFER: 4 rows MK 20, a total of 16 containers with 2 MK 20 per container. NEW of one MK 20 is 100 pounds.
C. DONOR: 24 MK 84 with steel nose and tail plugs
D. BUFFER: 4 rows MK 20
E. ACCEPTOR: 12 MK 84 with steel nose and tail plugs

SPECIAL CONDITIONS: Conducted in a simulated igloo. This igloo was constructed by digging a pit in the ground 10 feet deep, 20 feet wide and 60 feet long. The two long sides and one end was lined with concrete slabs to provide vertical walls. The remaining end was open with a ramp sloping to ground level.

RESULTS: Acceptors at closed end detonated. Acceptors at open end survived in very good condition. MK 20s appear to have mass detonated, there were a few intact metal components of the M118 bomblets but no unreacted explosives.

CONCLUSION: Acceptor bombs at closed end reacted due to pressures created by the combined MK 84 donor and the MK 20 acceptor. This pressure was not allowed to relieve due to the construction of the igloo. The lack of fragment damage to surviving bombs tends to rule out fragment attack as a mechanism. Try next test in a simulated igloo built above ground.

FIGURE 16



1263

FIGURE 17



1264

FIGURE 17



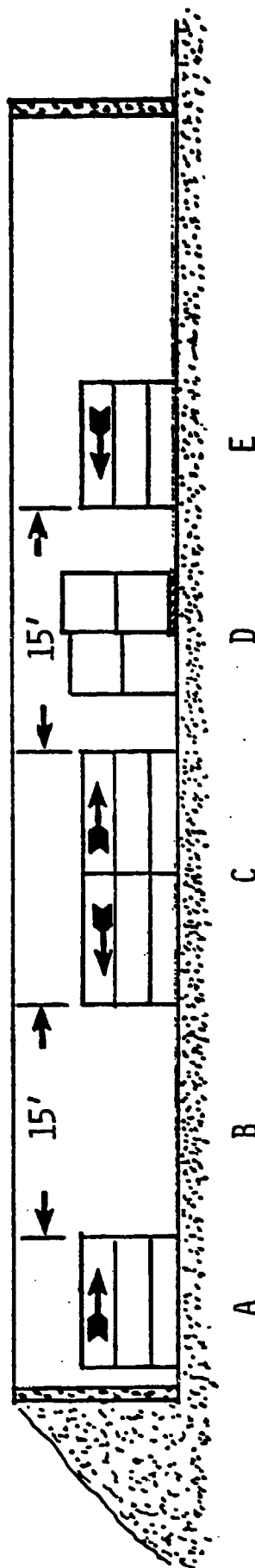
1265

FIGURE 18

TEST NUMBER: 7

DATE: 7 May 86

CONFIGURATION:



- A. ACCEPTOR: 12 MK 84 with steel nose and tail plugs
- B. BUFFER: 15' Air
- C. DONOR: 24 MK 84 with steel nose and tail plugs
- D. BUFFER: Two rows 30 mm HE
- E. ACCEPTOR: 12 MK 84 with steel nose and tail plugs

SPECIAL CONDITIONS: Conducted in simulated igloo built above ground using concrete slabs. Size 10 feet high, 20 feet wide, and 80 feet long. Earth is mounded against three sides and a concrete slab is used for the door. The structure has no roof.

RESULTS: All acceptor bombs survive. Bombs which were protected by 30 mm buffer suffer very little damage. Bombs on closed end are damaged much like those in tests 1 and 3. Some 30 mm rounds survived intact. Most cartridge cases and propellant were consumed. Many projectiles appear to have reacted low order and only split the projectile case and consumed most or all of the explosives inside.

CONCLUSIONS: Pressure is not a problem with 24 MK 84 bombs. 30 mm HEI is an effective buffer. Continue to test in above ground igloo and start increasing donor toward a goal of 64 MK 84.

FIGURE 19



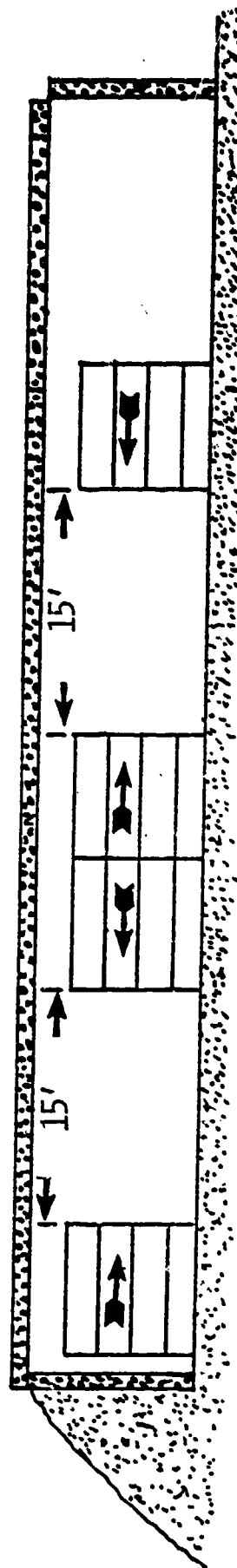
1267

FIGURE 20

TEST NUMBER: 8

DATE: 21 May 86

CONFIGURATION:



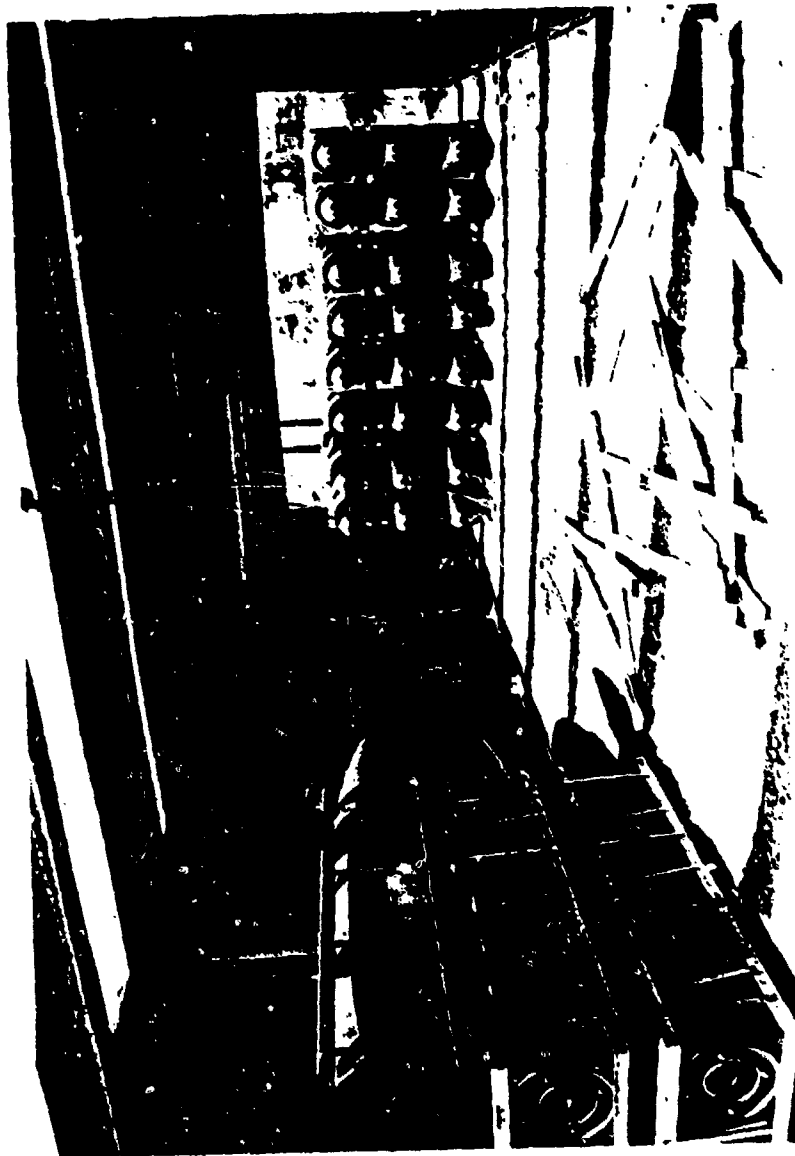
- A. ACCEPTOR: 24 MK 84 with steel nose and tail plugs
B. BUFFER: 15' Air
C. DONOR: 48 MK 84 with steel nose and tail plugs
D. BUFFER: 15' Air
E. ACCEPTOR: 24 MK 84 with steel nose and tail plugs

SPECIAL CONDITIONS: Conducted in simulated igloo. Construction similar to that in test 7, however, this igloo has a steel structure inside to support roof.

RESULTS. All acceptors survive, numerous large dents in sides of bombs which appear to be caused by interaction of bombs with the steel structure in the igloo or with other bombs. Many bombs have severe fragment damage similar to that seen in tests 4 and 5.

CONCLUSIONS: Most of the large dents were caused by bombs colliding with other bombs, very few sharp edged dents that one would expect from collisions with the steel structure. The severe fragment damage leads us to believe that we are near propagation caused by high energy fragments and must now use buffer. Pressure created by the donor bombs is not yet a problem. Continue tests in above ground igloo with roof, increase donor to 64 bombs, and use buffer material.

FIGURE 21



1269

FIGURE 22



1270

FIGURE 23



FIGURE 24



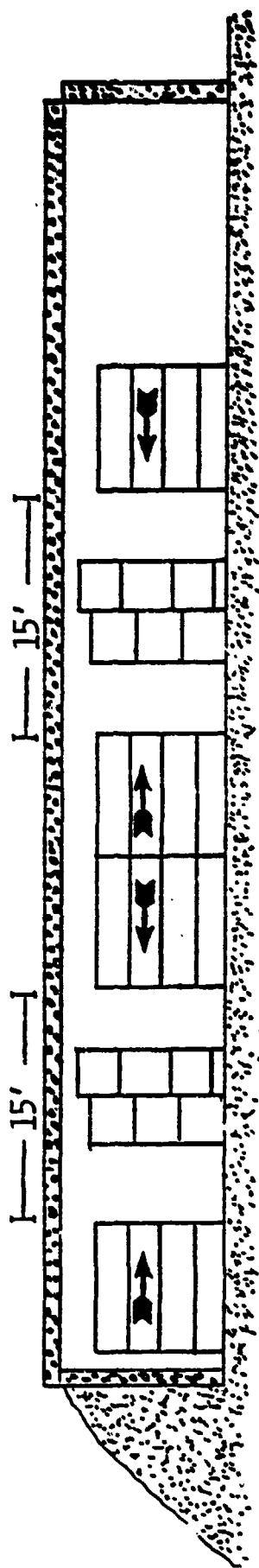
1272

FIGURE 24

TEST NUMBER: 9

DATE: 11 June 86

CONFIGURATION:



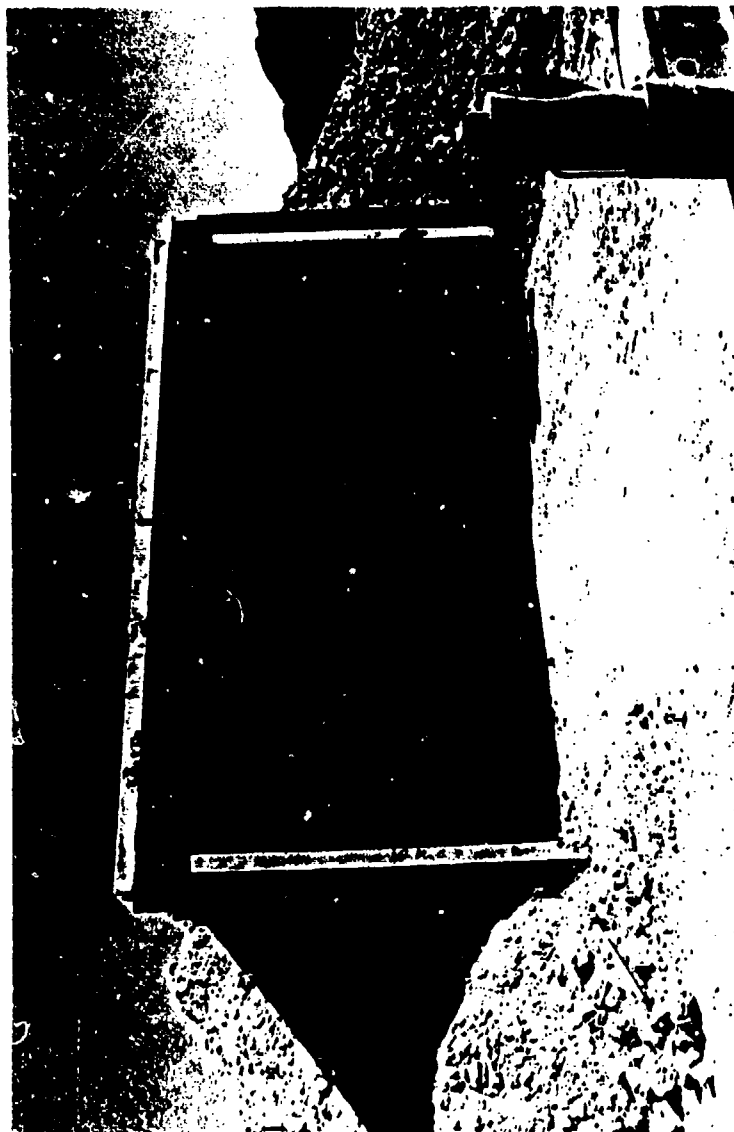
- A. ACCEPTOR: 32 MK 84 with steel nose and tail plugs
B. BUFFER: 2 rows palletized MK 81 fins
C. DONOR: 64 MK 84 with steel nose and tail plugs
D. BUFFER: 2 rows palletized MK 81 fins
E. ACCEPTOR: 32 MK 84 with steel nose and tail plugs

SPECIAL CONDITIONS: Conducted in a simulated igloo of the same dimensions as that in test 8. This igloo has the vertical metal superstructure used to support the roof beams outside the igloo. We will now call this igloo a Haymen igloo.

RESULTS: Acceptor bombs on the door end detonate. 7 bombs on the closed end sustain low order detonations (5 of which are on top row), 7 bombs have large dents in sides, still have fragment damage.

CONCLUSION: The large quantity of fragments generated by 64 MK 84 bombs overcame the buffer. Pressure was not a factor or we would have expected the donor at the closed end to mass detonate. Repeat the test using more substantial buffer.

FIGURE 25



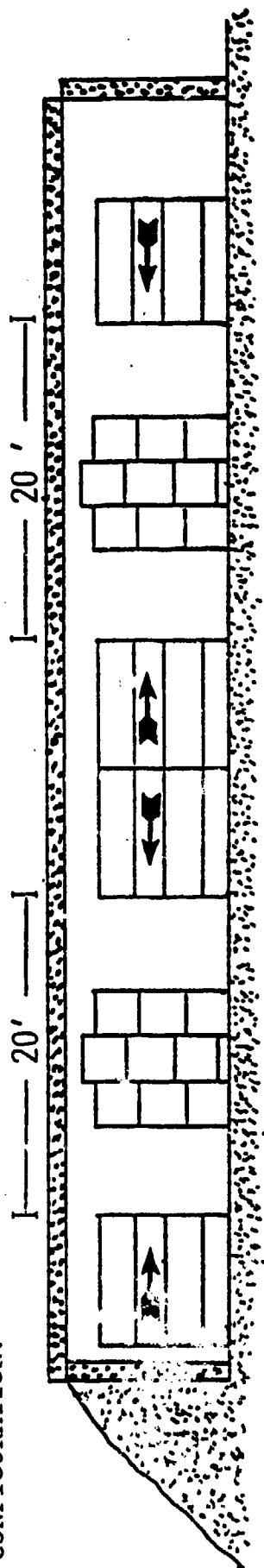
1274

FIGURE 26

TEST NUMBER: 10

DATE: 27 June 86

CONFIGURATION:



- A. ACCEPTOR: 32 MK 84 with steel nose and tail plugs
B. BUFFER: 3 rows palletized MK 81 fins
C. DONOR: 64 MK 84 with steel nose and tail plugs
D. BUFFER: 3 rows palletized 20 mm TP
E. ACCEPTOR: 32 MK 84 with steel nose and tail plugs

SPECIAL CONDITIONS: Conducted in a Haymen igloo.

RESULTS: Acceptors at closed end of igloo detonated. Acceptors at door end were in relatively good condition, 4 had dents in the side, 2 had fragment damage on noses, one had a fragment hole in the side, and one had the base plate knocked off by impact with another bomb or with the steel roof beams. Evidence of bomb to bomb interaction was indicated by the clear impression of a base plate on the side of one of the surviving bombs. A considerable amount of the 20 mm ammunition was unreacted. A few cans, with contents, survived virtually intact and were crushed by the pressure.

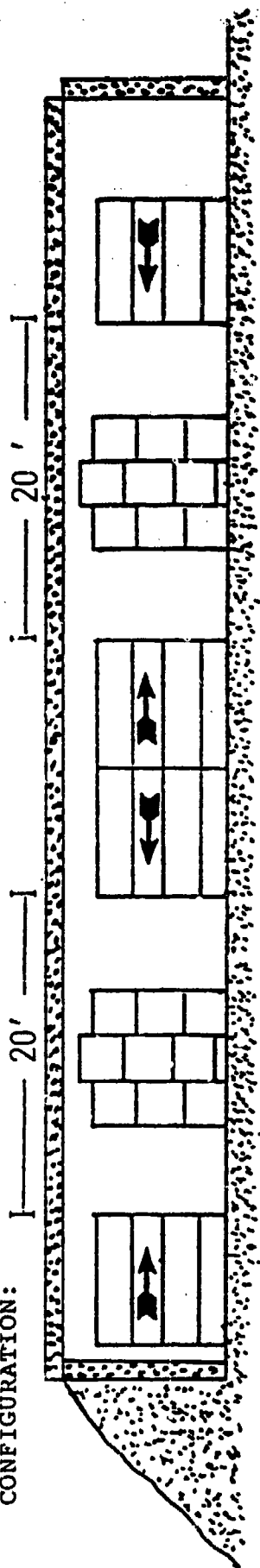
CONCLUSIONS: Three rows of palletized bomb fins are not a substantial enough buffer to prevent propagation. The mass provided by the 20 mm buffer was substantial enough to prevent propagation. Continue tests in igloo, use a more substantial buffer.

FIGURE 27

TEST NUMBER: 11

DATE: 17 JULY 86

CONFIGURATION:



- A. ACCEPTOR: 32 MK 84 with steel nose and tail plugs
B. BUFFER: 3 rows CBU 58s packed in metal shipping containers, two CBUs per container, NEW of each CBU 85 pounds. 24 total containers for a NEW of 4,080 pounds per buffer.
C. DONOR: 64 MK 84 with steel nose and tail plugs
D. BUFFER: 3 rows CBU 58
E. ACCEPTOR: 32 MK 84 with steel nose and tail plugs

SPECIAL CONDITIONS: Conducted in Haymen igloo.

RESULTS: All acceptors survive. Very little fragment damage occurred but several bombs sustained dents in the sides.

CONCLUSIONS: Substantial buffers will prevent propagation and also prevent fragment damage to bombs.
Since the 1.2 CBU 58 worked try the 1.1 MK 2C

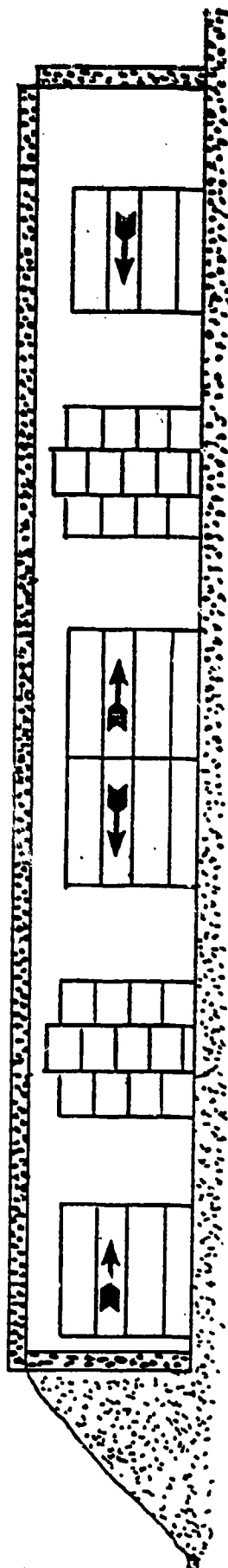
FIGURE 28

TEST NUMBER 12

DATE: 7 August 86 K — 20' —→

K — 20' —→

CONFIGURATION:



- A. ACCEPTOR: 32 MK 84 with steel nose and tail plugs
B. BUFFER: 3 rows MK 20
C. DONOR: 64 MK 84 with steel nose and tail plugs
D. BUFFER: 3 rows MK 20
E. ACCEPTOR: 32 MK 84 with steel nose and tail plugs

SPECIAL CONDITIONS: Conducted in Haymen igloo.

RESULTS: One bomb from the top row of each acceptor detonated low order. All other bombs survive with very little fragment damage. Several acceptors have dents in sides.

CONCLUSIONS: Three rows of MK 20s are an effective buffer. In this test the tops of the donor, buffer, and acceptor stacks were at virtually the same height. Only one row of buffer material(the one staggered vertically was at the same height as the acceptors. We feel the low order was caused by a fragment that passed through the one stack of buffer material.

FIGURE 29

AD-P005 353

TEMPORARY TANK AMMUNITION STORAGE FACILITY

By

David L. Collis

NEW MEXICO INSTITUTE OF MINING AND TECHNOLOGY
TERMINAL EFFECTS RESEARCH AND ANALYSIS GROUP

Presented To

TWENTY-SECOND DEPARTMENT OF DEFENSE EXPLOSIVES SAFETY SEMINAR

ANAHEIM MARRIOTT HOTEL

ANAHEIM, CALIFORNIA

26-28 AUGUST 1986

ABSTRACT

When vehicle maintenance is performed on combat ready tanks, all ammunitions must be offloaded in a safe area. An ammunition storage facility was developed for this purpose which would limit the maximum credible event to a reaction or detonation of only one H.E. warhead, thus limiting the explosion size and the fragment hazards. Tests were conducted to determine the physical parameters which would need to be implemented in order to satisfy the criteria of minimum explosion and fragment hazards, thus minimizing the inhabited building distance safety requirements.

An ammunition storage rack was designed and tested. It was determined from the results that with slight modifications a new rack design could be fabricated which would satisfy minimum safety requirements. The modified rack was fabricated and tested. The new rack limited the maximum credible event to a detonation of only one H.E. warhead, and reduced explosion and fragment hazards sufficiently to allow an inhabited building distance of 50 feet.

TEMPORARY TANK AMMUNITION STORAGE FACILITY

I. INTRODUCTION

Tank units currently stationed in the European theater of operations are permitted to remain in a combat-ready status with all standard ammunition stored on board. When vehicle maintenance is performed on these tanks, safety regulations require that all ammunition be offloaded and transported to an adequate storage facility which will satisfy the hazardous fragment and blast safety criteria. In some instances, safe storage facilities could be significant distances from the location of the maintenance operations.

To alleviate this problem, a temporary ammunition storage facility could be developed which would limit the maximum credible event to a reaction or detonation of only one H.E. warhead, thus limiting the explosion size and the fragment hazards. Tests were conducted to determine the physical parameters which would need to be implemented in order to satisfy the criteria of minimum explosion and fragment hazards, thus minimizing the inhabited building distance safety requirements.

Two ammunition storage racks were designed and tested. It was determined from the results that with slight modifications a new rack design could be fabricated which would satisfy minimum safety requirements. The modified rack was fabricated and tested. The new rack limited the maximum credible event to a detonation of only one H.E. warhead, and reduced explosion and fragment hazards sufficiently to allow an inhabited building distance of fifty feet.

The data presented herein includes a brief discussion of the preliminary sub-scale tests and first-trial rack tests, and a more detailed discussion of the subsequent rack designs which led to the final design.

II. PRELIMINARY SUB-SCALE TESTS

The purpose of the preliminary tests was to determine the physical parameters which would need to be implemented in order to satisfy the criteria of minimum explosion and fragment hazards. The primary hazard studied was the detonation of a 105mm, M456 HEAT warhead. Because the M456 HEAT projectiles are in the category of a mass-detonable munition, a special shielding and packaging arrangement would be necessary. Readily available shielding materials were considered; the standard shipping tube, wood, and PVC plastic pipe. To further reduce the fragment and blast hazard associated with the detonation of an H.E. warhead,

the HEAT cartridges were placed on the bottom, with the warhead to the rear of the rack. A sub-scale rack was constructed which would simulate the actual storage conditions including spacing and confinement. Figure 1 shows the basic setup for two of these tests. The center cartridge warhead was detonated by initiation of an M118 Rockeye submunition, 356mm behind the nose at a position directly in front of the base fuze of the warhead. (Several tests were conducted to verify a complete detonation of the warhead. Jet formation occurred in every case.) Table I lists the various tests conducted and combinations of shielding materials used. Several combinations were acceptable, but the 19mm wood box and the standard shipping tube separated by a 51mm air gap were the most desirable.

III. PRELIMINARY FULL-SCALE TESTS

The preliminary full-scale tests were designed to explore the feasibility of the rack design, and to test the shielding and packaging arrangement in an actual field condition.

Figure 2 shows the basic rack incorporating the wood shield design. In order to contain the fragments from both the warhead and the cartridge case, this basic rack was surrounded by a cinder block and earth wall. In front of the rack was positioned a wall of the same basic construction which was designed to stop cartridge case bases that would probably eject as a result of propellant ignition. Figures 3 and 4 show the details of the setup. Figure 5 shows the details of the kickout information which is further described in Table II. Cartridge case pieces went out in excess of 180m. There was a moderately long duration fire which resulted in several propellant charge cookoffs. The acceptor warheads were damaged but did not react or detonate.

Figure 6 shows the steel rack frame used to incorporate the standard shipping tube. The setup to contain the fragments was identical to the wood shield design. Figure 7 shows the basic test setup. The surrounding wall was identical to that used for the wood rack design. Figure 8 shows the details of the kickout information which is further described in Table III. There was a moderately long duration fire which resulted in several propellant charge cookoffs. The acceptor warheads were damaged but did not react or detonate, although two of the warheads did burn. Cartridge case pieces went out in excess of 50m.

The results from these two tests were similar. The maximum credible event was limited to one H.E. projectile, although several propellant charges reacted as a result of a sustained fire after the initial event. This resulted in cookoffs and additional debris spread. From these tests it was concluded that by moving in the front wall to the absolute minimum distance which would allow insertion of the cartridges into the rack, the throw-out pieces could be reduced to within a fifty-foot radius.

It was also surmised that the surrounding wall construction could be minimized in the front and on the sides, but should also be added to the top to aid in both cartridge protection and kickout reduction.

IV. FULL-SCALE TESTS

The full-scale tests would include eight M456 HEAT cartridges on the bottom row of the rack, and thirty-two K.E. cartridges on the four upper rows of the rack. Figure 9 shows the basic rack design used on the full-scale tests.

A. Rack with Single-Layer Sandbag Wall

Because a layer of sand six inches thick is adequate for protection against sidewall warhead fragments and cartridge case fragments, a single layer of sandbags would be adequate. However, the rear side of the rack must have a three-foot-thick barricade in order to stop fragments generated by the warhead jet. Figure 10 shows the basic setup used for this test. The top layer of bags was supported by a 0.062-inch-thick steel plate. As in the previous tests, a single H.E. projectile was detonated. Figures 11 and 12 show the details of the kickout information which is further described in Table IV. After analysis of the high-speed films, it was apparent that the sandbag walls did contain the initial explosion. Post-debris analysis showed that the initial maximum credible event was limited to one H.E. warhead. The sandbag wall did, however, collapse after several later propellant charge cookoffs. When this occurred, all fragment protection was gone, and subsequent cookoffs propelled cartridge parts in all directions. Figure 13 is a photograph of the setup, and Figure 14 is a view of the post-test area.

Although the end result of this test was not desirable, the conclusions were obvious. The sandbag wall, both top and sides, would have to be sturdier in design in order to withstand cookoff conditions. Some clear space around the rack would be necessary to allow venting of the propellant reactions, thus reducing the amount of explosion containment.

B. Rack with Multiple-Layer Sandbag Wall

Figure 15 shows the basic setup used for this test. Several modifications were implemented to the design used for the first full-scale test. A clear space was built into the rack which would allow a twelve-inch separation on the sides and rear of the rack between the cartridges and the sandbag wall. This was

reinforced by adding a 0.125-inch-thick steel sheet-metal plate on a frame around the basic rack, and welded to the rack. The multiple-layer sandbag wall was placed against the sheet metal. The sandbag wall was built in such a manner that the top row of bags was one layer thick, with each successive row down increased by one layer of bags.

The top layer of bags was increased to two layers and was supported by a 0.25-inch-thick steel plate. As in the previous tests a single H.E. projectile was detonated. Figure 16 shows the details of the kickout information which is further described in Table V. After analysis of the high-speed films, it was apparent that the sandbag walls did contain the initial explosion. Post-debris analysis showed that the initial maximum credible event was limited to one H.E. warhead. The sandbag wall partially collapsed after several later propellant charge cookoffs, but not sufficiently to allow large amounts of debris to escape the vicinity of the rack. Figure 17 is a photograph of the setup. Figure 18 shows details of the rack area after the test.

There was an improvement on the debris kickout. Since the sandbag shield did not completely collapse, the conclusion was that the continued propellant charge cookoffs were yielding the kickout fragments. Since the maximum credible event was confined to only one H.E. warhead, the propellant and the shipping containers were the only other cause for a sustained fire and resultant cookoffs. In order to reduce the cookoffs, both the shipping tubes and the propellant charges would have to be shielded from the fire hazards.

V. FINAL TESTS

The rack for the final tests would undergo further modification. In order to prevent the partial collapse of the sandbag walls, a thin steel support wall would be added on the sides. This wall would be fabricated from 0.125-inch-thick steel, welded to the basic rack framework, and tied to the sandbags with 0.15-inch diameter, No. 9 tie-down wires looped through the wall and placed flat within the sandbag array. This same basic setup was also used for the front wall. The top layers of sandbags were also reinforced by adding a 0.125-inch-thick steel sheet-metal box around the edges.

In order to reduce the sustained fire/cookoff condition, each layer of cartridges was separated from each other layer by placing a 0.125-inch-thick sheet metal divider under the cartridges. To further reduce the combustible-material exposed cross-section, each shipping tube was placed in a steel tube with 0.063-inch-thick side and end walls.

Figure 19 shows the rack final design before installation. Figure 20 shows the same rack after installation with all sand-bags in place. Figures 21, 22, 23 and 24 show the details for construction of the rack. Figure 25 is a photograph of the rack fully assembled. Three tests were conducted with this basic design, with a slight difference on the first test: the bottom divider floor was installed. On the second and third tests, the bottom divider floor was removed. After the damage assessment of the first test, the conclusion was made that further venting could be achieved if the row of H.E. projectiles were left open on the bottom. This would also allow the propellant from the donor cartridge to be dispersed, and consequently further reduce the sustained fire hazard.

A. Temporary Ammunition Storage Rack,
Final Design: Test No. 1

A single H.E. projectile was detonated. Figure 26 shows the details of the kickout information which is further described in Table VI. Only one piece of a cartridge case, weighing 81 grams, was found outside the fifty-foot radius circle at 105-ft. All other debris were contained inside a fifty-foot radius.

Post-debris analysis showed that the initial maximum credible event was limited to one H.E. warhead. There was considerable damage caused to the adjacent cartridges, but the cookoff hazard was confined to the lower two rows. Three of the H.E. warheads sustained no damage, two burned, and three had mild reactions. It appeared that with the increased confined area afforded by the sheet metal dividers, the propellant charge ignition focused the fire in the vicinity of the warheads, thus causing a cookoff reaction. There was also some unburned propellant in the immediate vicinity of the rack. There were several propellant charge reactions, but these appeared to be a result of the initial projectile detonation rather than from a cook-off condition. Figure 27 is a post-test view of the area around the rack.

B. Temporary Ammunition Storage Rack,
Final Design: Test No. 2

Test No. 2 was identical to Test No. 1, except that the bottom divider plate was deleted. Figure 28 shows the details of the kickout information which is further described in Table VII. Only one fragment, weighing 29 grams, was recovered outside the fifty-foot radius circle at 75-ft. This piece was believed to be a fragment from the fuze well of the donor projectile. All other debris were contained inside a fifty-foot radius.

Post-debris analysis showed that the initial maximum credible event was limited to one H.E. warhead. There was minimal damage caused to the adjacent cartridges, with most of the damage confined to those cartridges on either side of the donor. Five of the H.E. cartridges were virtually undamaged, with the remaining two sustaining minor damage. The propellant charges from the two adjacent cartridges appeared to cookoff, but the resultant reaction appeared to be more of a burn than a reaction. There was also some unburned propellant in the immediate vicinity of the rack. With a minimum of repair, this rack could still be used for the storage of ammunition. Figure 29 is a post-test photograph of the rack.

C. Temporary Ammunition Storage Rack,
Final Design: Test No. 3

Test No. 3 was identical to Test No. 2. Figure 30 shows details of the kickout information which is further described in Table VIII. Only one fragment, weighing 30 grams, was recovered outside the fifty-foot radius circle at 55-ft. This piece was believed to be a fragment from the fuze well of the donor projectile. All other debris were contained inside a fifty-foot radius.

Post-debris analysis showed that the initial maximum credible event was limited to one H.E. warhead. There was minimal damage caused to the adjacent cartridges, with most of the damage confined to those cartridges surrounding the donor. Five of the H.E. cartridges were virtually undamaged. The remaining two received some fragment damage in the propellant charge area and both the propellant charge and the warhead burned. One K.E. propellant charge above the donor cartridge also burned. This rack could be used for the storage of ammunition with a minimum of repair. Figure 31 is a post-test photograph of the rack.

VI. CONCLUSION

The rack design as configured in Figures 20, 21, 22, 23 and 24 will reduce and contain both explosion and fragment hazards generated from the detonation of an M456 HEAT projectile. The rack specified herein limits the maximum credible event to the detonation of one warhead, with a corresponding blast radius of 50 feet, and the fragment hazard radius, based upon one hazardous fragment per 600 square feet, is also reduced to 50 feet.

Therefore, when 105mm, M456 HEAT ammunition and other non-explosive conventional antitank ammunition are stored in the rack, in their fiber shipping tubes, with the warheads facing to the rack rear, on the bottom row, the hazard distance is 50 feet.

REFERENCES

1. DoD 6055.9 STD, DoD Ammunition and Explosive Safety Standards, July 1984.
2. AR 385-64, Ammunition and Explosive Safety Standards.
3. Howe, Philip M. and Collis, David L., "Temporary Tank Ammunition Storage Facility", BRL-MR-3424, January 1985.
4. Howe, Philip M., "Rack for Temporary Storage of 105mm HEAT Ammunition", BRL-SP-46, March 1986.

ACKNOWLEDGEMENTS

This work was done under contract with the U.S. Army Ballistics Research Lab, Contract No. DAAK11-84-D-0003, Terminal Ballistics Division, Explosives Effects Branch.

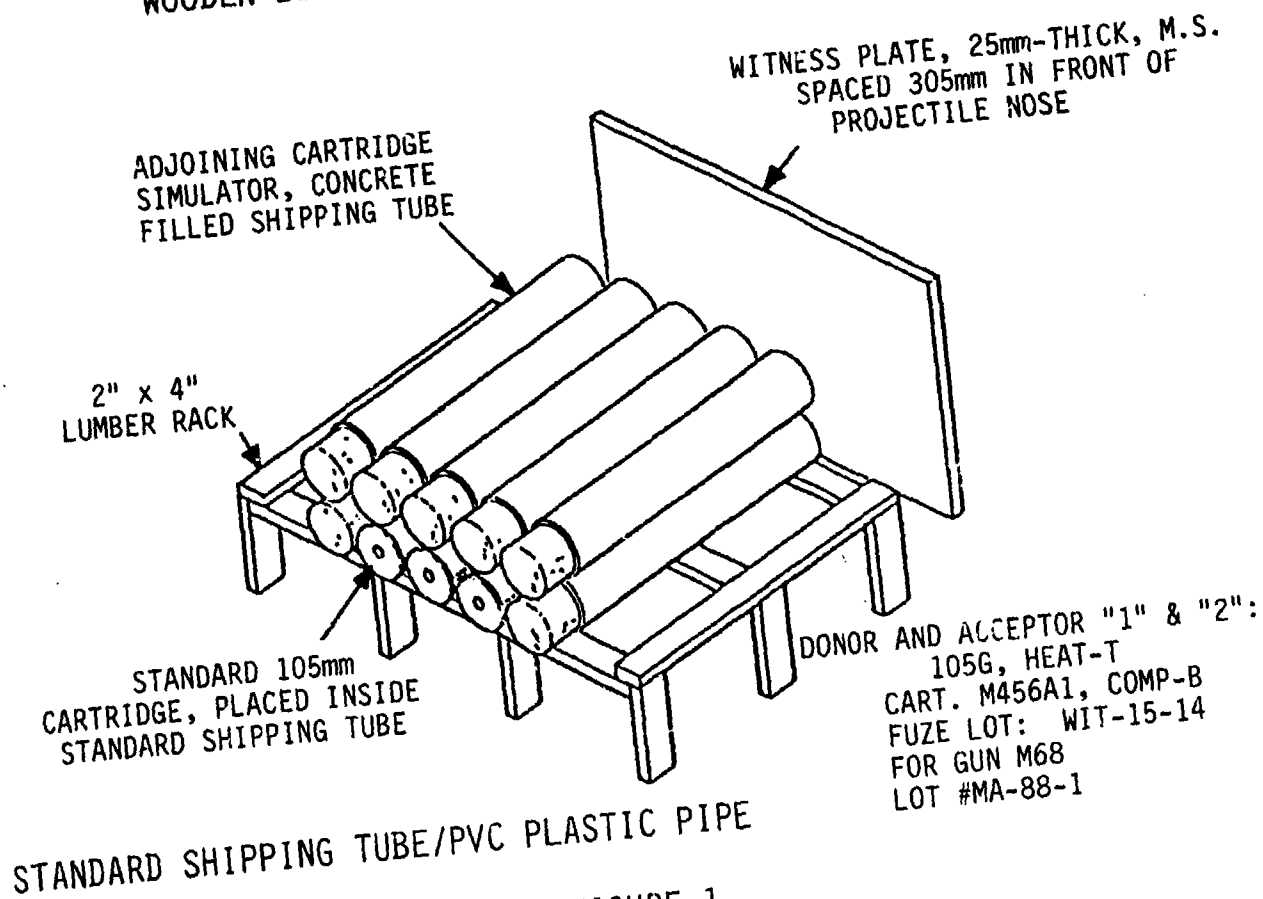
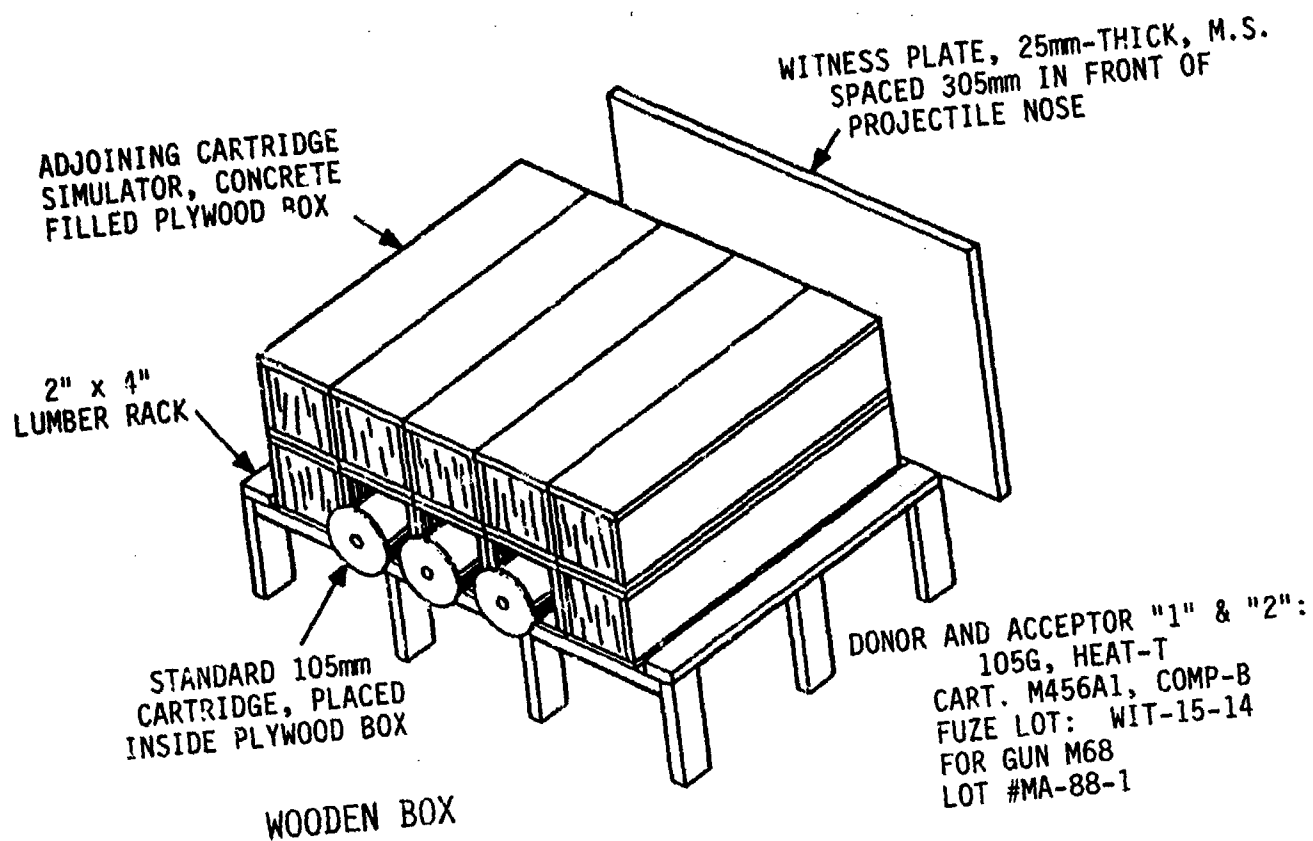


FIGURE 1

TABLE I

**TEMPORARY TANK AMMO STORAGE FACILITY
PRELIMINARY SUB-SCALE TESTS**

TEST NO.	SET UP	WARHEAD EFFECTIVE SHIELD	CASE EFFECTIVE SHIELD	R E S U L T S
FBA0801A3	19mm Wood Box	Wood 38mm	Wood 38mm	Acceptor warheads damaged, no reaction. Separated from cases.
FBA0802A3	Standard Shipping Tube	Tube 50mm	Tube 22mm	Acceptor warheads reacted. No jet formation.
FBA0802B3	7mm SCH 40 PVC	PVC 14mm	PVC 14mm	Acceptor warheads damaged, no reaction. Separated from cases.
FBA0803A3	10mm Wood Box	Wood 20mm	Wood 20mm	Acceptor warheads reacted, left one formed partial jet.
FBA0805A3	13mm Wood Box	Wood 26mm	Wood 26mm	Acceptor warheads reacted. No jet formation.
FBA0808A3	19mm Wood Box and Standard Shipping Tube	Wood 38mm Tube 50mm	Wood 38mm Tube 22mm	Acceptor warheads damaged, no reaction. Separated from cases.
FBA0810A3	8mm SCH 40 PVC and Standard Shipping Tube	PVC 16mm Tube 50mm	PVC 16mm Tube 22mm	Acceptor warheads damaged, no reaction. Separated from cases.
FBA0830A3	Standard Shipping Tube, Separated by 41mm Air Gap	Tube 50mm	Tube 22mm	A2 acceptor warhead damaged, and separated from case. A1 acceptor warhead reacted.
FBA0831A3	16mm Wood Box	Wood 32mm	None	Acceptor warheads reacted. No jet formation.
FBA0831B3	10mm Wood Box and 19mm Insert Wood Box	Wood 58mm	Wood 20mm	A1 acceptor warhead damaged, no reaction. A2 acceptor warhead burned, no jet formation.
FBA0901A3	Standard Shipping Tube Separated by 51mm Air Gap	Tube 50mm	Tube 22mm	A2 acceptor and case slight damaged. A1 acceptor damaged and separated from case. No reaction.

TEMPORARY TANK AMMUNITION STORAGE FACILITY,
WOOD RACK

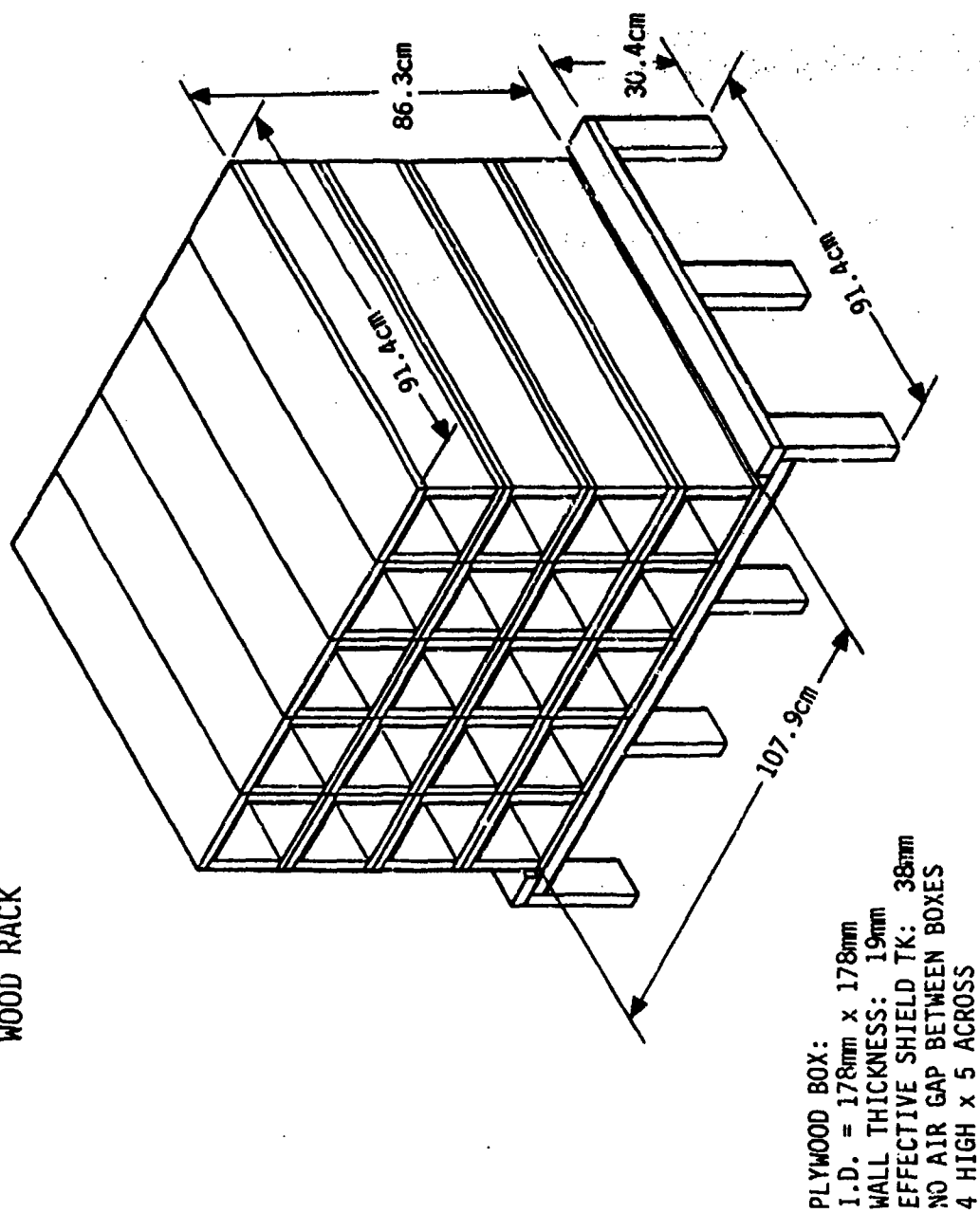


FIGURE 2

TEMPORARY TANK AMMUNITION STORAGE FACILITY, WOOD RACK

FRONT REVETMENT WALL:

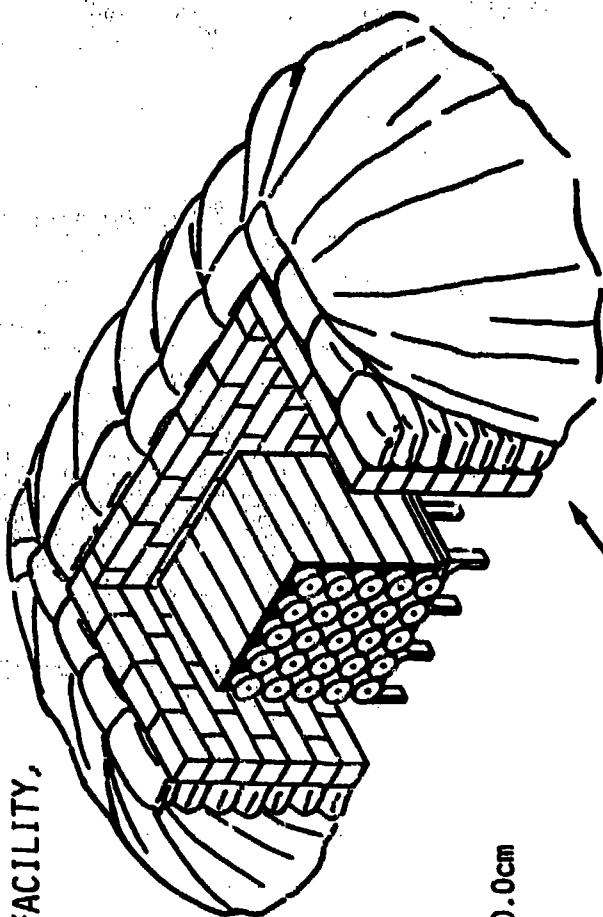
CINDERBLOCK WALL, SANDBAG AND EARTH FILL
NO MORTAR JOINTS BETWEEN BLOCKS, VOID IN
BLOCKS FILLED WITH SAND;

DIMENSIONS:

CINDERBLOCK WALL - LENGTH: 439.4cm
HEIGHT: 137.1cm
THICKNESS: 19.0cm

SANDBAG WALL - LENGTH: 439.4cm
HEIGHT: 137.1cm
THICKNESS: 30.0cm

EARTH FILL, AVERAGE DEPTH: 100.0cm



REVETMENT BUNKER:

OVERALL INSIDE DIMENSIONS - LENGTH: 195.5cm
HEIGHT: 137.1cm
DEPTH: 140.3cm

CONSTRUCTION DETAIL IS SAME AS
FRONT REVETMENT WALL

POSITION OF WOOD AMMUNITION RACK:

CENTERED IN REVETMENT BUNKER
AIR GAP TO BACK WALL: 30.4cm
AIR GAP TO SIDE WALLS: 43.8cm
AIR GAP ON BOTTOM: 30.4cm

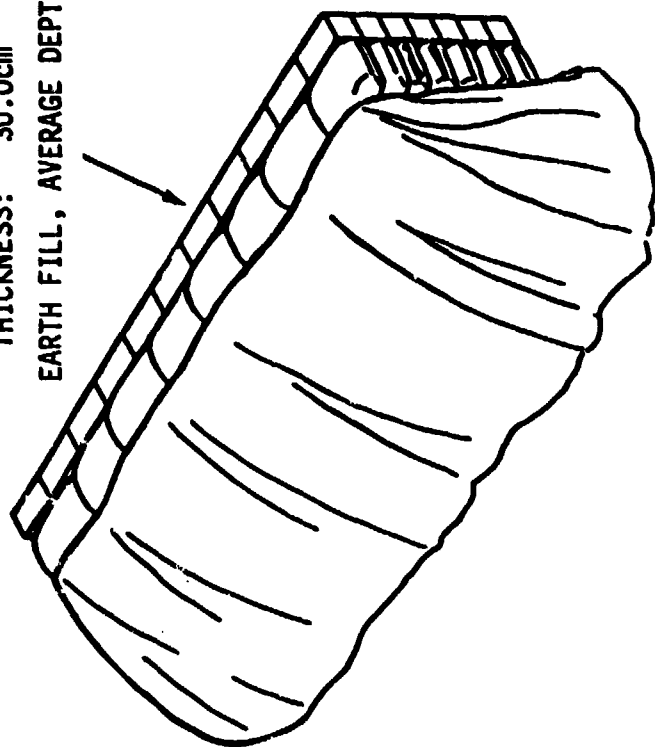
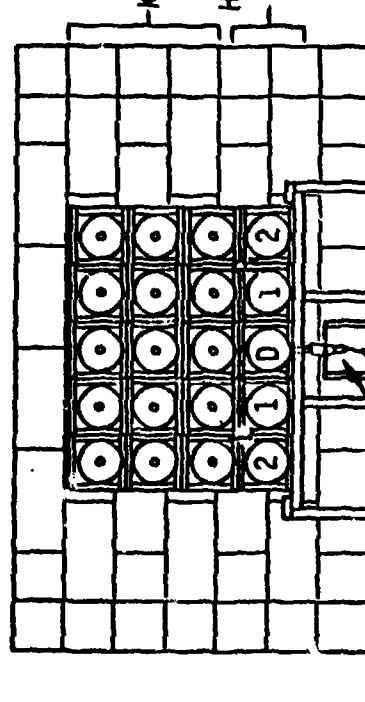


FIGURE 3

TEMPORARY TANK AMMUNITION STORAGE FACILITY. WOOD RACK

PLYWOOD BOXES:

O.D. = 21.5cm x 21.5cm EACH
BOX, STACKED 5 ACROSS AND 4
ROWS HIGH ON A 2"x4" LUMBER RACK



M118 ROCKEYE SUBMUNITION INITIATOR,
POSITIONED 356mm BACK FROM NOSE
OF DONOR ROUND. POSITION IS DIRECTLY
IN FRONT OF BASE FUZE.

KE PROJECTILE ROUNDS: 15 ea.

90mm TP-T, M353A1

HEAT ROUNDS: 5 ea.

105G, HEAT-T
CART, M456A1, COMP-B
FUZE LOT #WIT-15-14
FOR GUN M68
LOT #MA-88-1

PLYWOOD BOX:

I.D. = 178mm x 178mm
WALL THICKNESS: 19mm
EFFECTIVE SHIELD TK: 38mm
NO AIR GAP BETWEEN BOXES.

FIGURE 4

TEMPORARY TANK AMMO STORAGE FACILITY

- Δ - CARTRIDGE CASE
- - KE PROJECTILE
- - HEAT PROJECTILE
- ⊖ - COMPLETE HEAT ROUND
- ⊕ - COMPLETE KE ROUND

WOOD RACK

DEBRIS RECOVERY ZONES

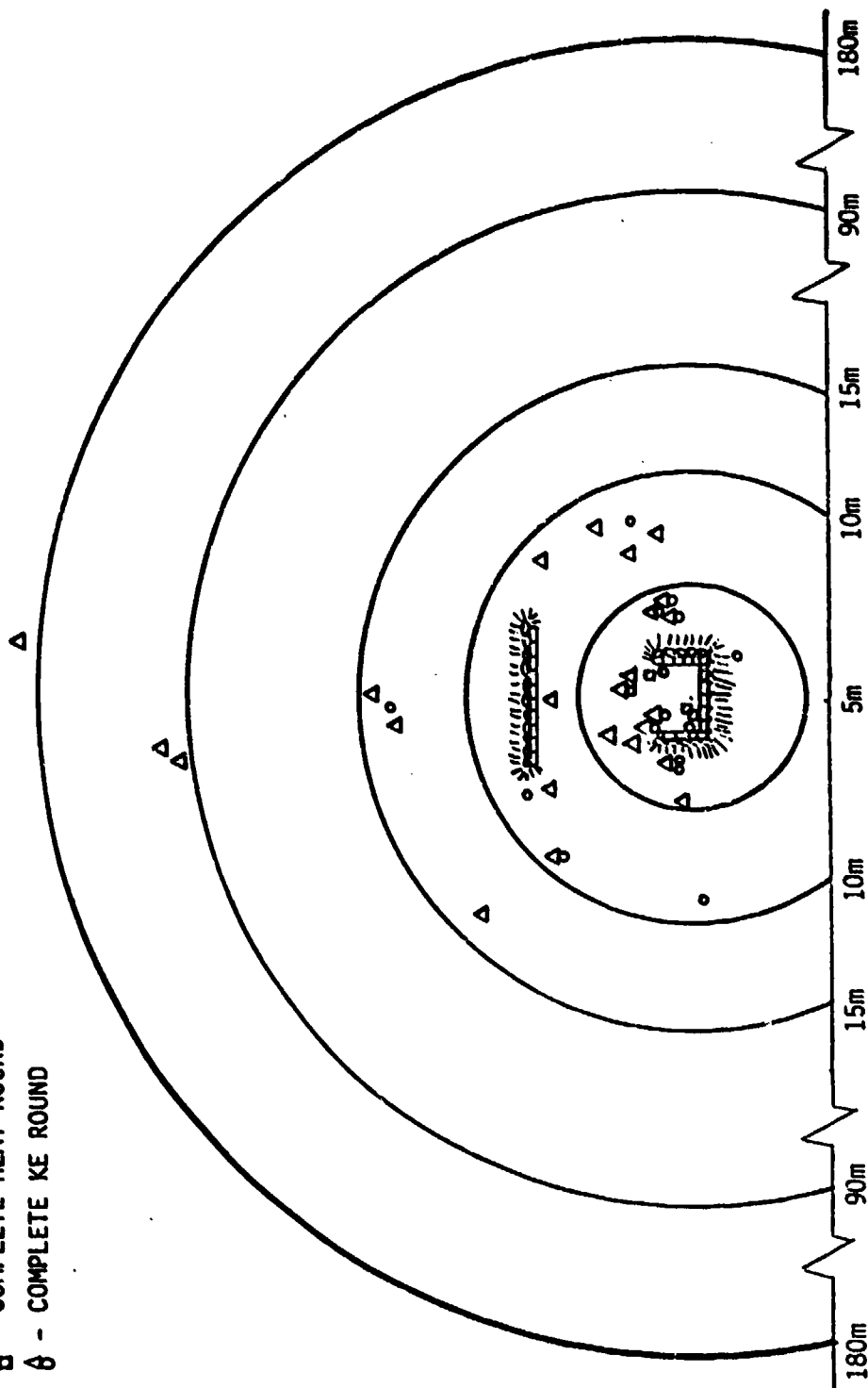


FIGURE 5

TABLE ii
TEMPORARY TANK AMMUNITION STORAGE RACK

WOOD RACK

DEBRIS RECOVERY

ALL MEASUREMENTS TAKEN FROM POINT OF ROCKEYE INITIATION
OF DONOR WARHEAD

5m Radius of Ground Zero	- 3 Acceptor HEAT Warheads; 5 KE Projectiles; 1 Acceptor, Complete Round; 5 KE, Complete Round; 5 Cartridge Cases
5m - 10m Zone	- 3 KE Projectiles; 1 KE, Complete Round; 6 Cartridge Cases
10m - 15m Zone	- 1 KE Projectile; 3 Cartridge Cases
15m - 90m Zone	- None
90m - 180m Zone	- 2 Cartridge Case Fragments from Acceptor R-2, Size: 254mm x 154mm, one at 94.1m, the second at 95.7m
180m Zone	- 1 Cartridge Case Fragment, Base and a 159mm x 110mm Section of Side Attached at 182.8m

TEMPORARY TANK AMMUNITION STORAGE FACILITY STEEL RACK

MATERIAL:

5.0cm x 5.0cm x 0.6cm ANGLE IRON,
AROUND OUTSIDE AND EACH SHELF
5.0cm x 0.6cm FLAT STRAP ON
CENTER SUPPORT AND
INSIDE LEGS ONLY

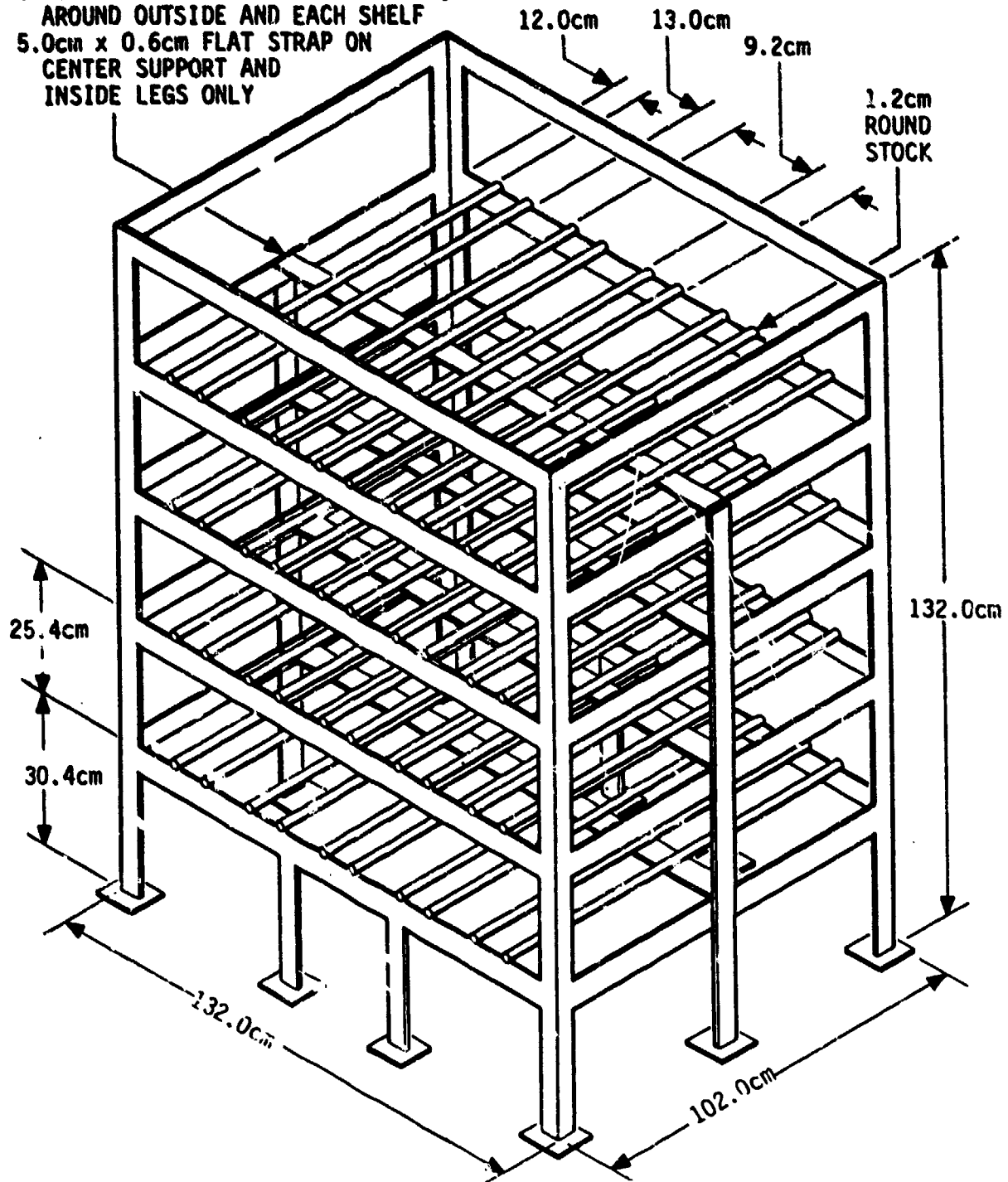
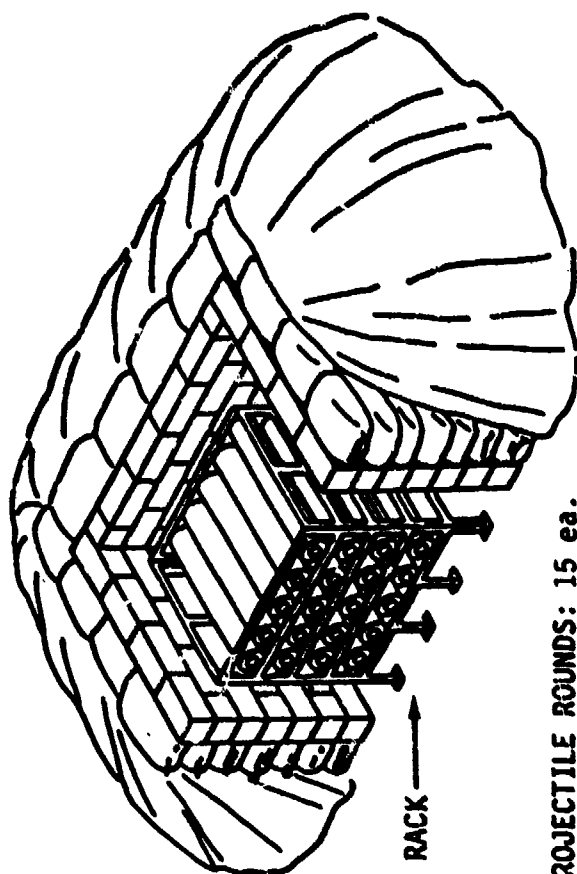
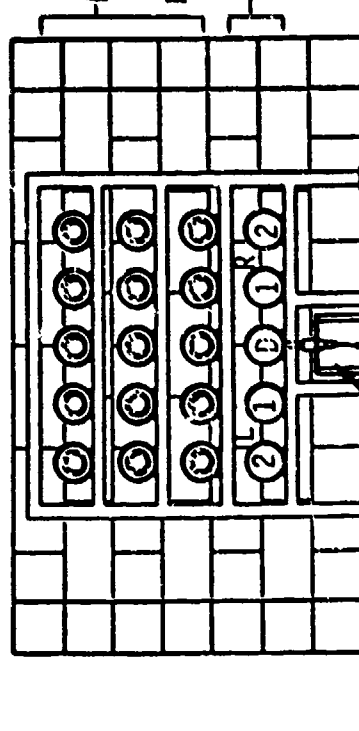


FIGURE 6

TEMPORARY TANK AMMUNITION STORAGE FACILITY, STEEL RACK



STANDARD SHIPPING TUBE
O.D. = 15.8cm
STACKED 5 ACROSS AND
4 ROWS HIGH ON STEEL RACK



— KE PROJECTILE ROUNDS: 15 ea.
90mm TP-T, M353A1

HEAT ROUNDS: 5 ea.

105G, HEAT-T
CART. M456A1, COMP-B
FUZE LOT #WIT-15-14
FOR GUN M68
LOT #MA088-1

M118 ROCKEYE SUBMUNITION INITIATOR
POSITIONED 356mm BACK FROM NOSE
OF DONOR ROUND. POSITION IS DIRECTLY
IN FRONT OF BASE FUZE.

STANDARD SHIPPING TUBE:

I.D. = 140mm

WALL THICKNESS:

AT CARTRIDGE CASE = 11mm

AT PROJECTILE = 25mm

EFFECTIVE SHIELD TK:

AT CARTRIDGE CASE = 22mm

AT PROJECTILE = 50mm

AIR GAP BETWEEN TUBES:

HORIZONTAL - 70mm

VERTICAL - 95mm

FIGURE 7

TEMPORARY TANK AMMO STORAGE FACILITY

STEEL RACK

DEBRIS RECOVERY ZONES

- Δ - CARTRIDGE CASE
- - KE PROJECTILE
- ◻ - HEAT PROJECTILE
- ⊕ - COMPLETE HEAT ROUND
- ⊙ - COMPLETE KE ROUND
- - FUZE

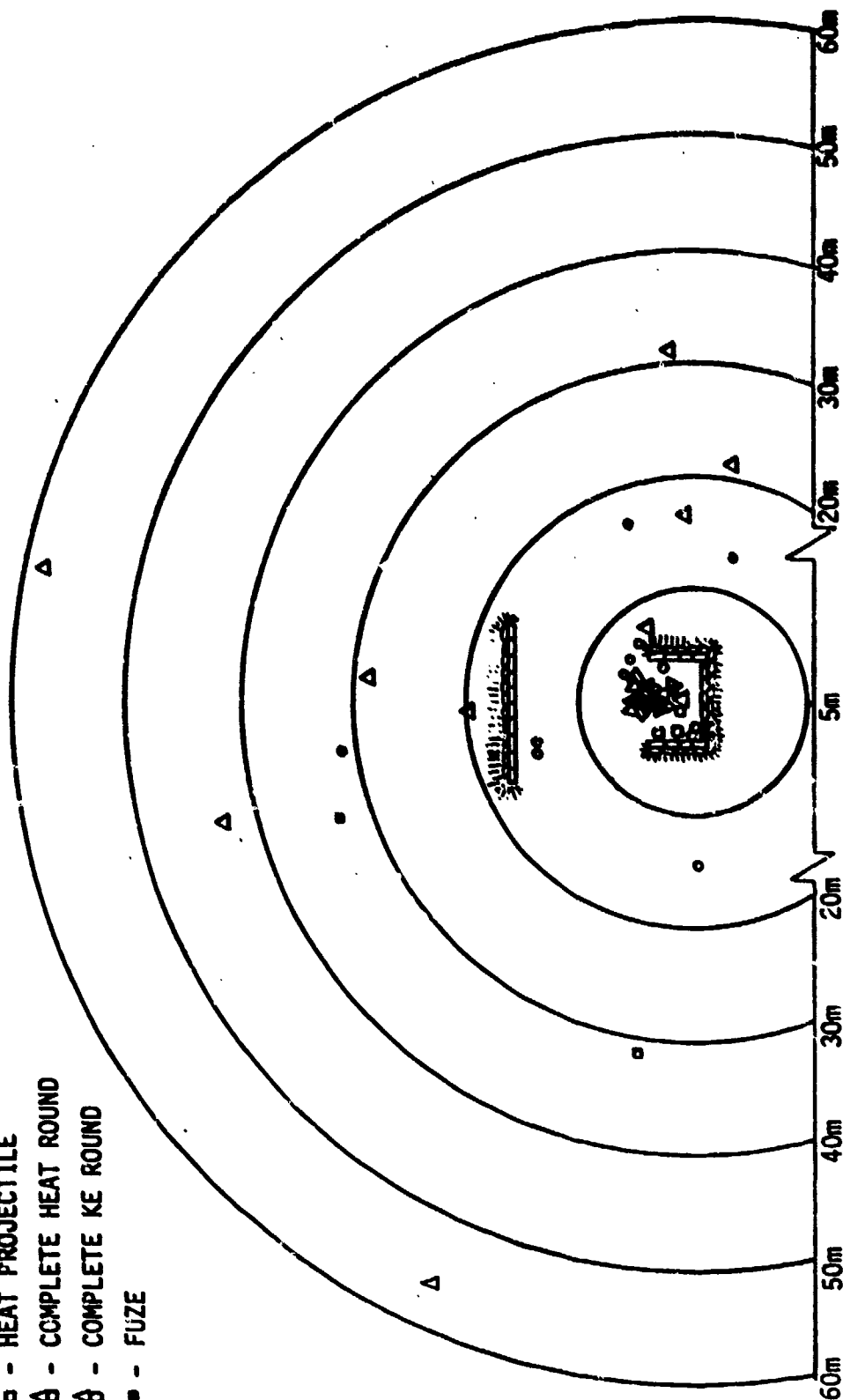


FIGURE 8

TABLE III
TEMPORARY TANK AMMUNITION STORAGE RACK
STEEL RACK

DEBRIS RECOVERY

**ALL MEASUREMENTS TAKEN FROM POINT OF ROCKEYE INITIATION
OF DONOR WARHEAD**

5m Radius of Ground Zero	- 3 HEAT Warheads; 9 KE Projectiles; 15 Cartridge Cases
5m - 20m Zone	- 6 KE Projectiles; 1 Cartridge Case Fragment (Base Only)
20m - 30m Zone	- 1 Cartridge Case; 2 Cartridge Case Fragments, 10cm x 5cm and 20cm x 10cm
30m - 40m Zone	- 1 HEAT Warhead (33.8m); 1 HEAT Fuze (34.4m); 2 Cartridge Case Fragments, 36cm x 10cm and 42cm x 8cm (30.1m)
40m - 50m Zone	- 1 Cartridge Case Fragment (42.9m)
50m - 60m Zone	- 1 Cartridge Case (56.3m); 1 Cartridge Case Fragment, 4cm x 6cm (59.1m)

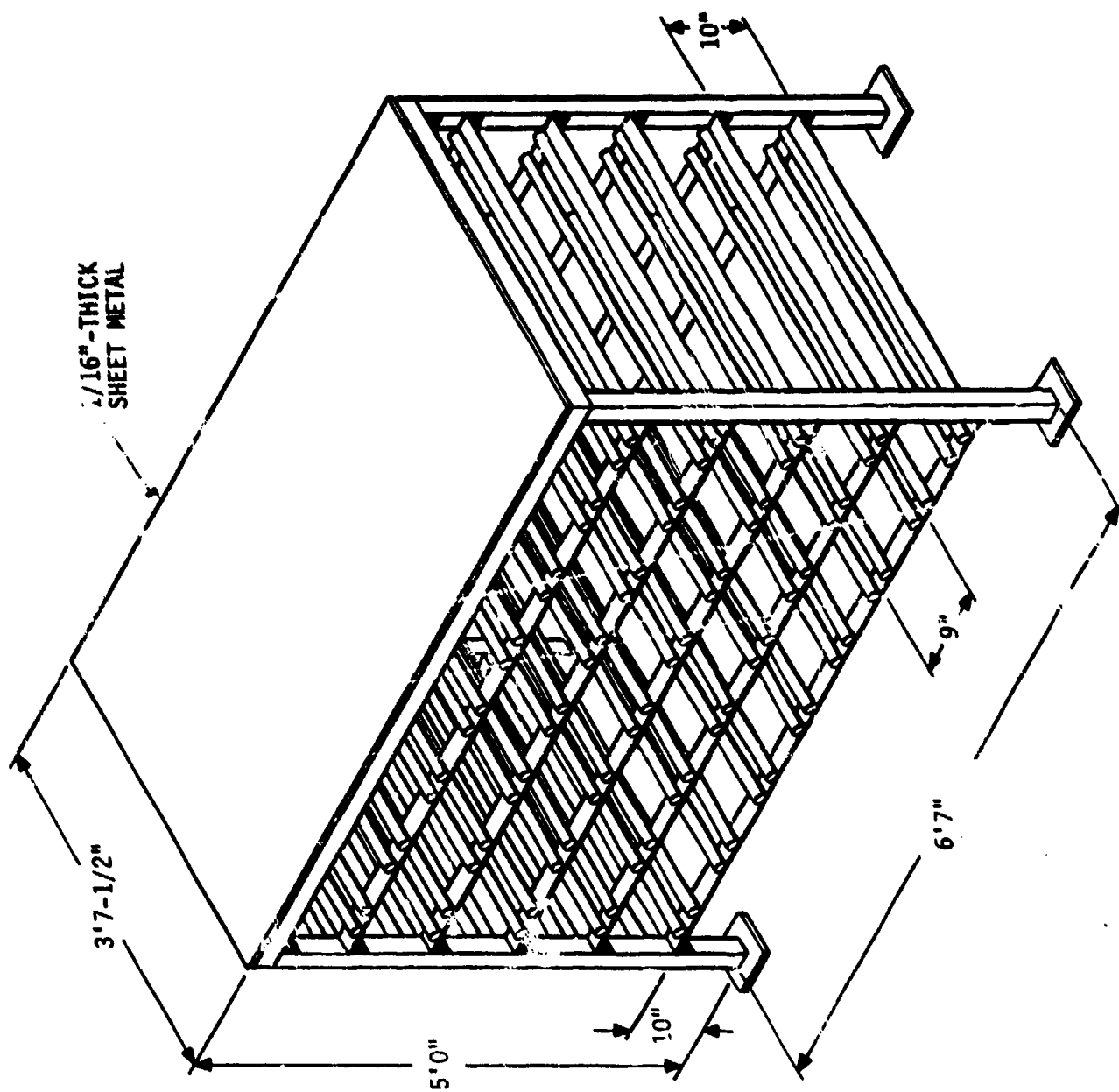


FIGURE 9. BASIC STEEL RACK

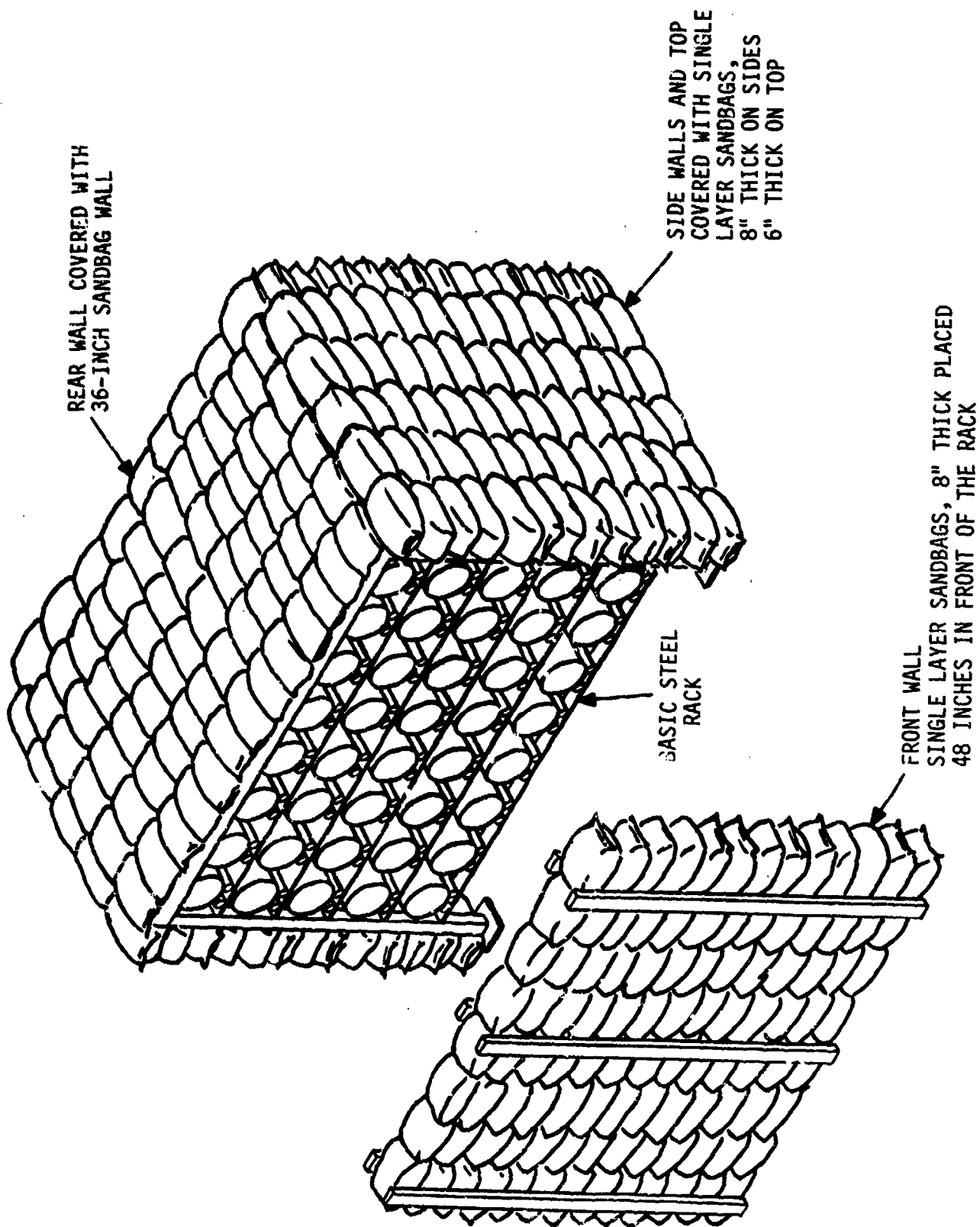


FIGURE 10. RACK WITH SINGLE LAYER SANDBAG WALL

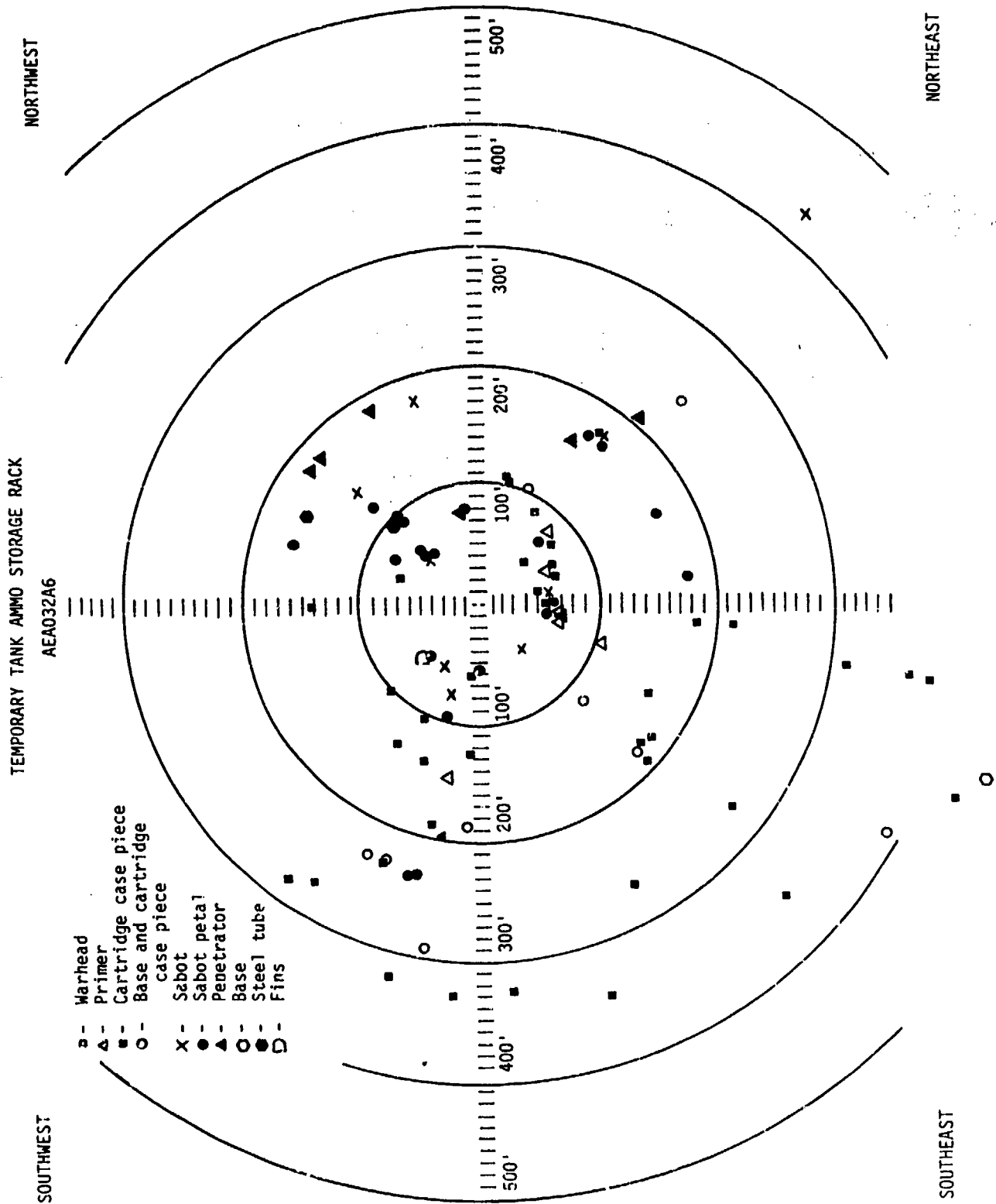


FIGURE 11

TEMPORARY TANK AMMO STORAGE RACK

NORTHWEST

NORTHEAST

AEA0326A6

SOUTHWEST

SOUTHEAST

- - Warhead
- △ - Primer
- - Cartridge case piece
- - Base and cartridge case piece
- X - Sabot
- - Sabot petal
- ▲ - Penetrator
- - Base
- - Steel tube
- D - Fins

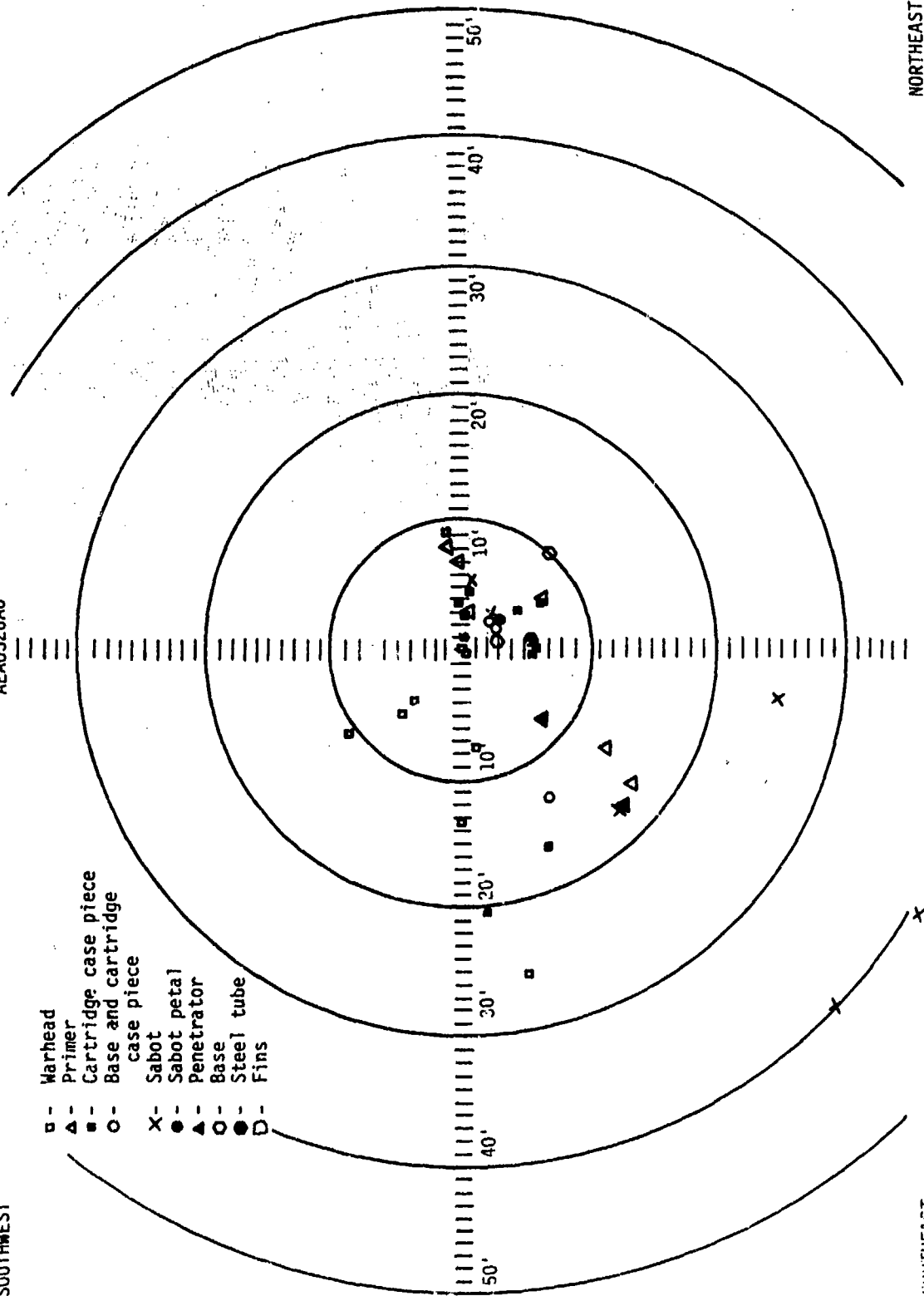


FIGURE 12

TABLE IV
TEMPORARY TANK AMMUNITION STORAGE RACK

DEBRIS RECOVERY

ALL MEASUREMENTS ARE TAKEN FROM POINT OF ROCKEYE INITIATION
OF DONOR WARHEAD

50-ft Radius of Ground Zero	Six complete K.E. cartridges; one shipping tube with HEAT round; 4 primers, 5 cartridge case pieces; three cartridge case pieces with base attached; 4 complete sabots; one sabot piece; one sabot with penetrator; one sabot in case without penetrator; 2 penetrators; one base only from cartridge case; one base only from cartridge case with primer; one cartridge case from K.E. round inside shipping tube; two cartridge cases; one empty tube, 2 complete K.E. cartridges without penetrator; K.E. projectile without a case.
50-ft - 75-ft Zone	Three complete sabots; one sabot in tube, and 8 sabot petals; one set of fins; 4 primers; 7 pieces from cartridge cases (3"x2-1/2", 8"x5", 6"x2-1/2"x 5"x6-1/2", 18"x9")
75-ft - 100-ft Zone	One complete sabot; one penetrator; one primer; one tube piece; 5 sabot petals; 2 pieces from cartridge cases (8"x3")
100-ft - 125-ft Zone	One sabot petal; one primer; 3 pieces from cartridge cases (10"x8", 11"x6", 10"x5") 2 pieces from cartridge cases with base (12" and 5-1/2" high)
125-ft - 150-ft Zone	One complete sabot and two sabot petals; 4 pieces from cartridge cases (4"x3", 9"x3", 11"x6", 4-1/2"x3-1/2"); one primer
150-ft - 175-ft Zone	One complete sabot, one partial sabot in tube; 4 sabot petals; one penetrator; one piece from cartridge case with base (2-1/2" high)
175-ft - 200-ft Zone	One sabot in tube; one sabot petal; 3 penetrators; one partial base with piece of cartridge case (14"x7-1/2"); one base with piece of cartridge case (7" high); 6 pieces from cartridge cases (7-1/2"x4-1/2", 4"x3-1/2", 12"x5", 12-1/2"x7", 9"x3-1/2", 21"x13")

TABLE IV (cont):

200-ft - 225-ft Zone	One penetrator; one piece of cartridge case (4"x2-1/2")
225-ft - 250-ft Zone	One piece of cartridge case (5"x7-1/2"); one partial base with piece of cartridge case (17"x9"); 2 bases with piece of cartridge case (24-1/2" and 4-1/2" high)
250-ft - 275-ft Zone	Three pieces from cartridge cases (12-1/2"x8", 3-1/2"x12", 5"x3")
275-ft - 300-ft Zone	One piece of cartridge case (3"x2-1/2"); one base with piece of cartridge case (3-1/4" high)
300-ft - 325-ft Zone	Two pieces from cartridge cases (12"x5-1/2", 9"x4-1/2")
325-ft - 350-ft Zone	Three pieces from cartridge cases (7"x4", 5"x4-3/4", 11-1/2"x8-3/4")
350-ft - 375-ft Zone	Two pieces from cartridge cases (6"x4-1/2", 11-1/2"x5-1/2")
375-ft - 400-ft Zone	One piece of cartridge case (10-3/4"x4"); one base with a piece of cartridge case (2-1/2" high)
400-ft - 425-ft Zone	One sabot
425-ft - 450-ft Zone	One piece of cartridge case (3-1/2"x2-1/4")
450-ft - 475-ft Zone	No debris
475-ft - 500-ft Zone	One base

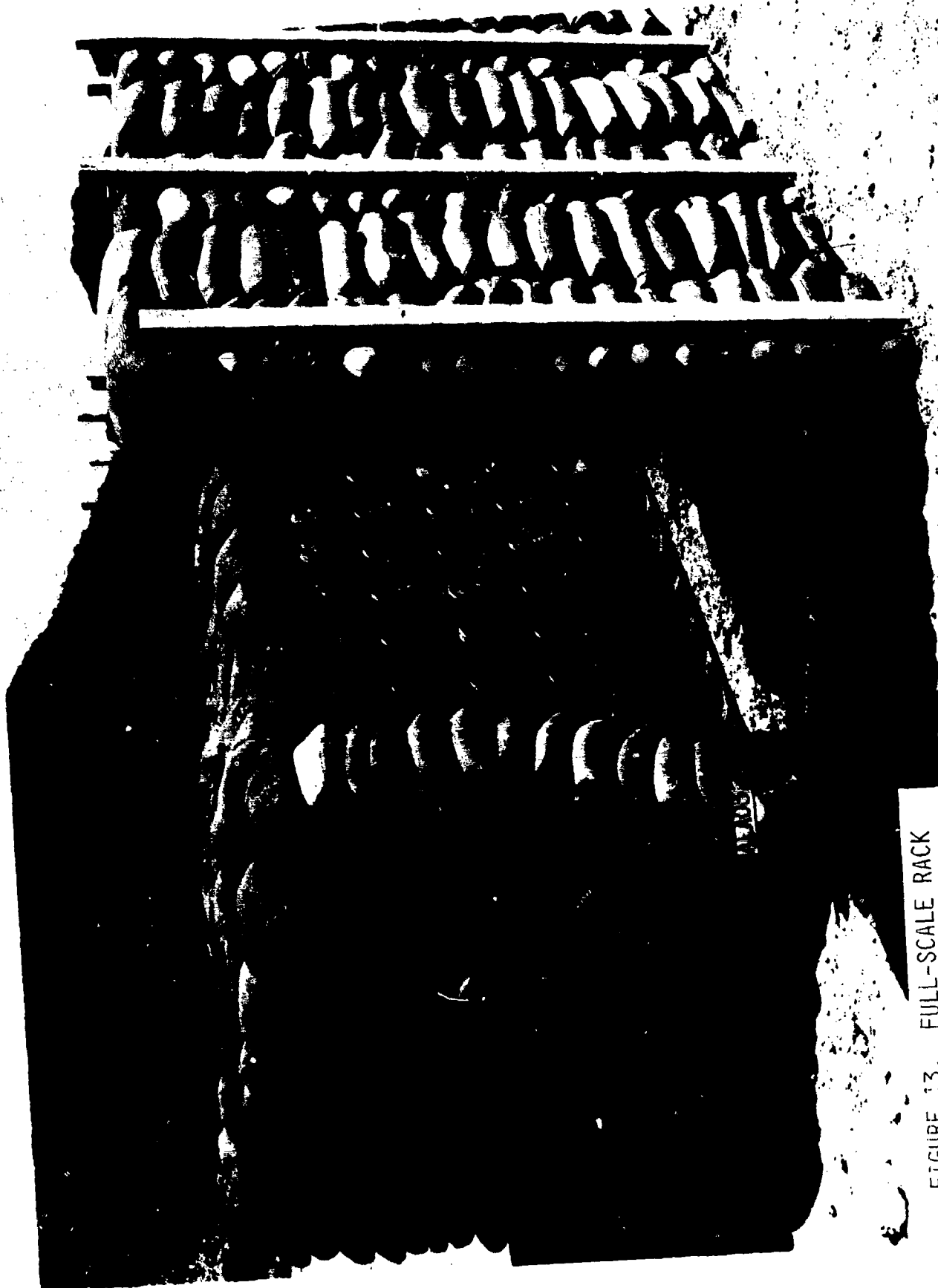


FIGURE 13. FULL-SCALE RACK
WITH SINGLE-LAYER SANDBAG WALL



FIGURE 14. FULL-SCALE RACK
WITH SINGLE-LAYER SANDBAG WALL
POST-TEST AREA

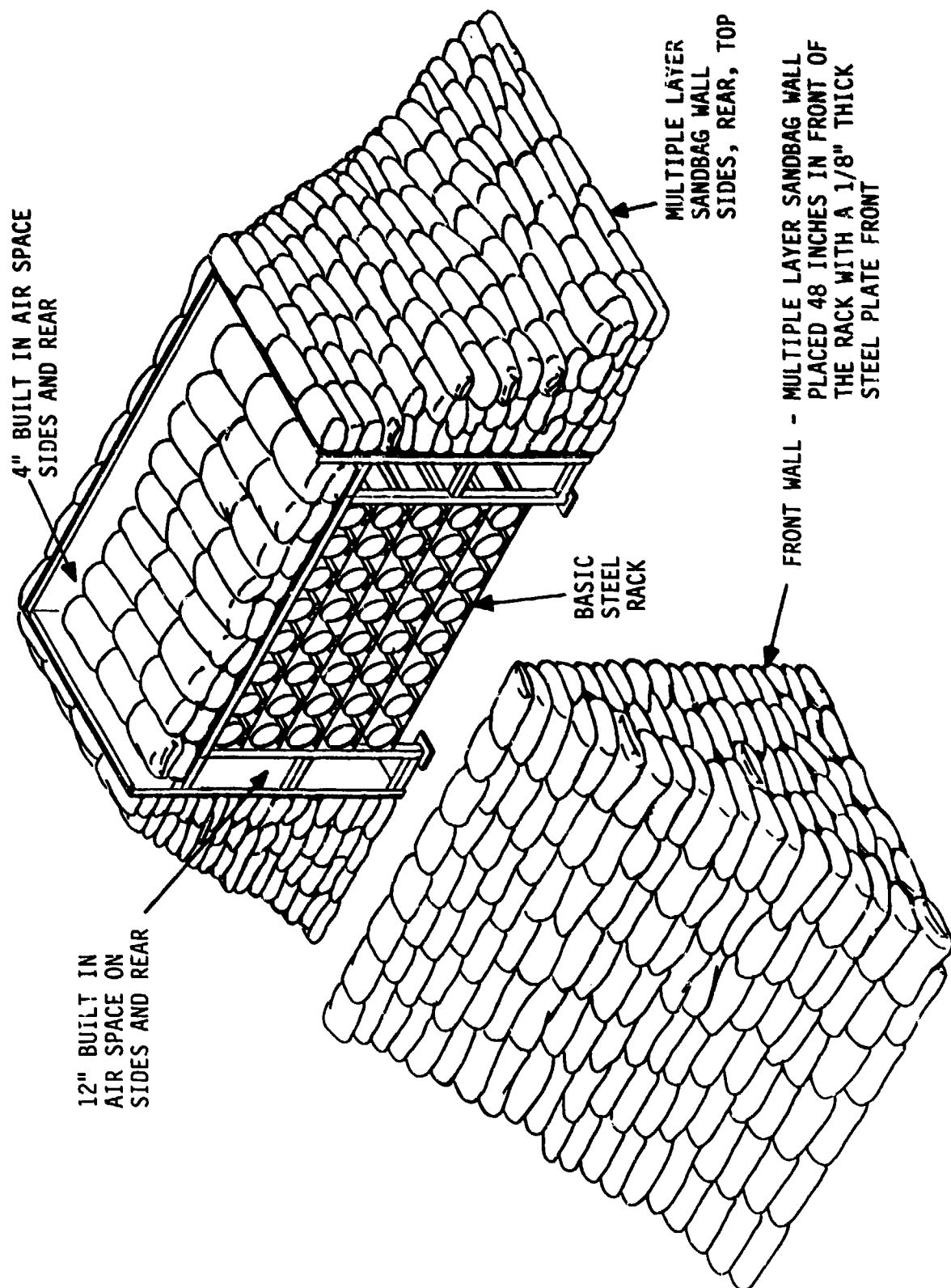


FIGURE 15. RACK WITH MULTIPLE LAYER SANDBAG WALL

NORTHEAST

SOUTHWEST

SOUTHEAST

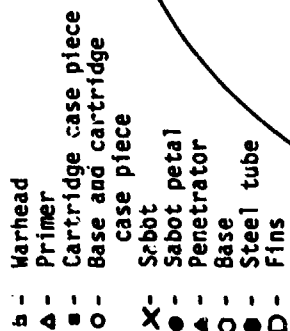


FIGURE 16

TABLE V

TEMPORARY TANK AMMUNITION STORAGE RACK

DEBRIS RECOVERY

ALL MEASUREMENTS ARE TAKEN FROM POINT OF ROCKEYE INITIATION
OF DONOR WARHEAD

50-ft Radius Of Ground Zero	Three primers; 10 pieces from cartridge cases (13-1/2"x11", 20"x9", 9-1/2"x3-1/2", 7-1/4"x3-1/4", 6-1/2"x4-3/4", 11-1/2"x5-1/2", 7"x6-1/2" (donor), 5-1/4"x5", 18-1/2"x7-1/2", 17"x9"); one piece of H.E. cartridge case; 2 bases with pieces from cartridge cases (11" and 23-1/2" high); 2 burned H.E. warheads
50-ft - 75-ft Zone	One sabot; one piece of cartridge case (7-3/4" x 6-3/4"); one H.E. base with cartridge case piece (22-1/2" high)
75-ft - 100-ft Zone	One primer; 2 pieces from cartridge cases, one from donor (9-7/16"x6-1/8"); one H.E. cartridge case base with cartridge case piece (22-1/2" high)
100-ft - 125-ft Zone	One sabot; one piece of cartridge case from H.E. cartridge (9"x2")
125-ft - 150-ft Zone	One complete sabot and one sabot petal; 5 pieces from cartridge cases (7-1/2"x3", 6-1/2"x3", 21-1/4"x16", 7"x3-3/4")
150-ft - 175-ft Zone	Two sabot petals; one piece of cartridge case (5"x8-1/2"); one primer
175-ft - 200-ft Zone	One penetrator; one cartridge case base (2-1/4" high); one piece of cartridge case (12-1/2" x 4-1/2"); one base with cartridge case piece (5" high)
200-ft - 225-ft Zone	Three pieces from cartridge cases (7"x5", 7"x10" 9"x5-1/2"); one base with cartridge case piece (7-1/2" high)
225-ft - 250-ft Zone	Three pieces from cartridge cases (6-3/4"x9-1/2" 10-1/2"x4-1/2", 14-1/2"x5")

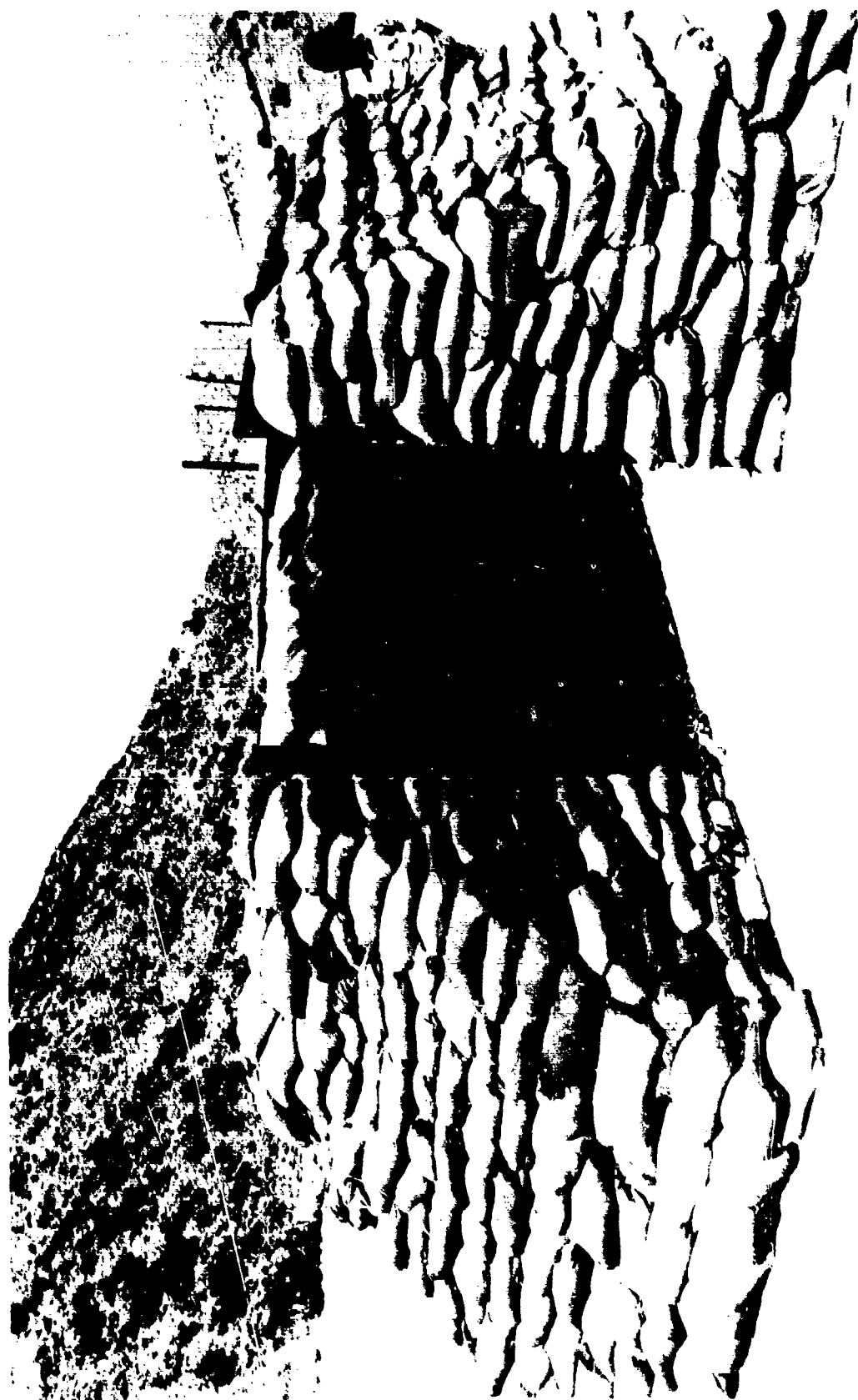


FIGURE 17. FULL-SCALE RACK
WITH MULTIPLE-LAYER SANDBAG WALL



FIGURE 18. FULL-SCALE RACK
WITH MULTIPLE-LAYER SANDBAG WALL
POST-TEST AREA

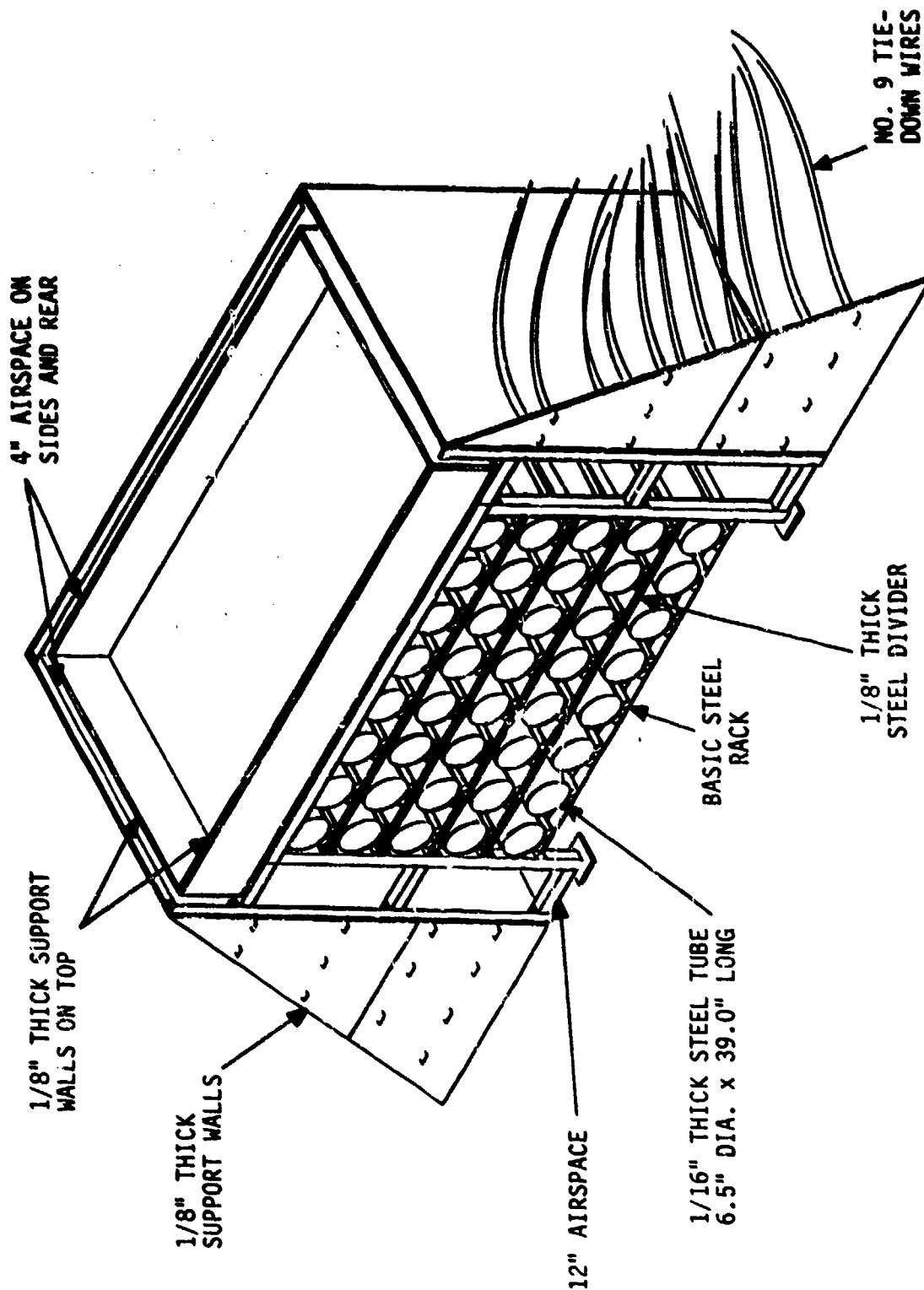


FIGURE 19. TEMPORARY AMMUNITION STORAGE RACK;
FINAL DESIGN - BEFORE INSTALLATION

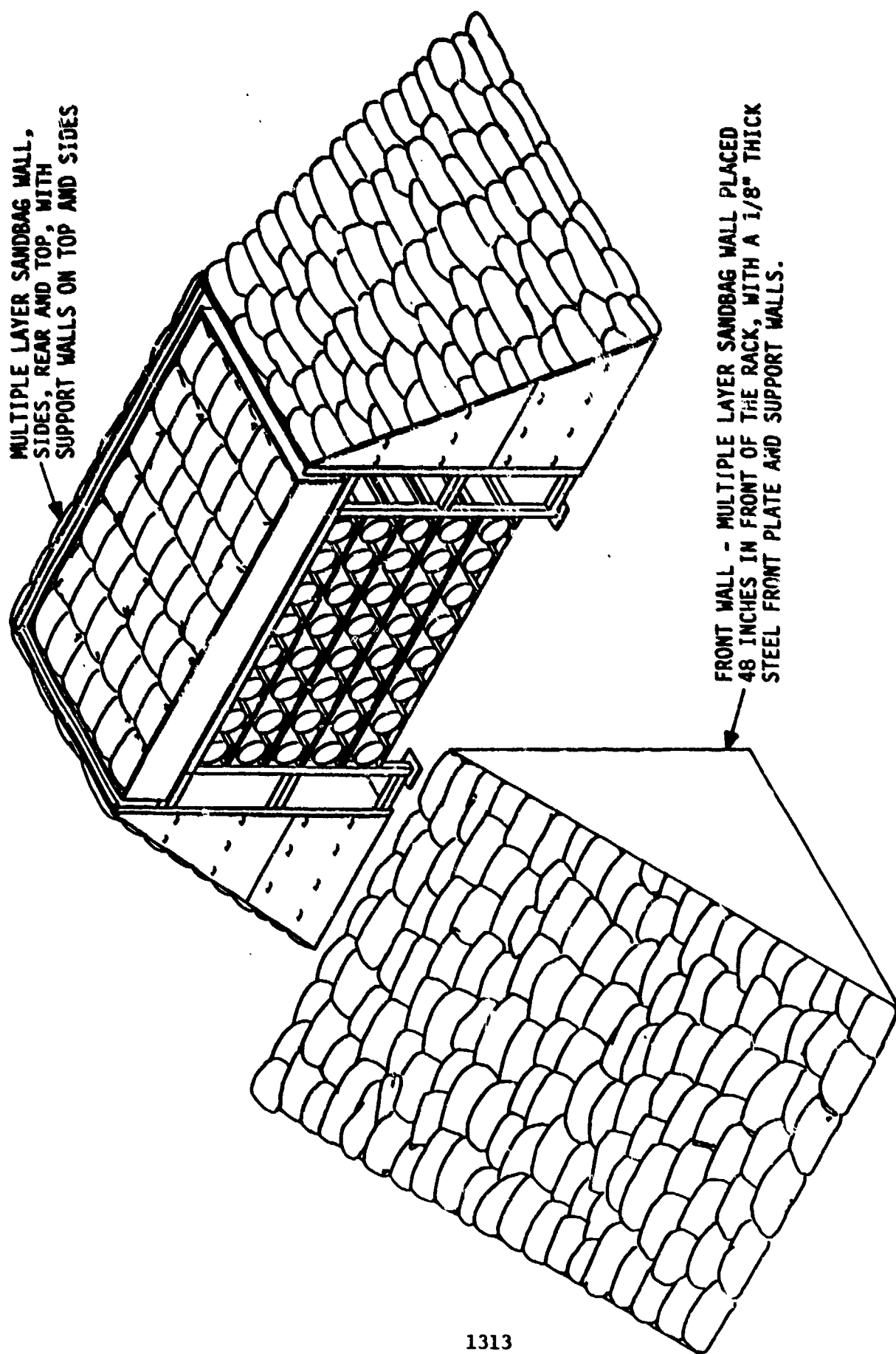


FIGURE 20. TEMPORARY AMMUNITION STORAGE RACK:
FINAL DESIGN - AFTER INSTALLATION

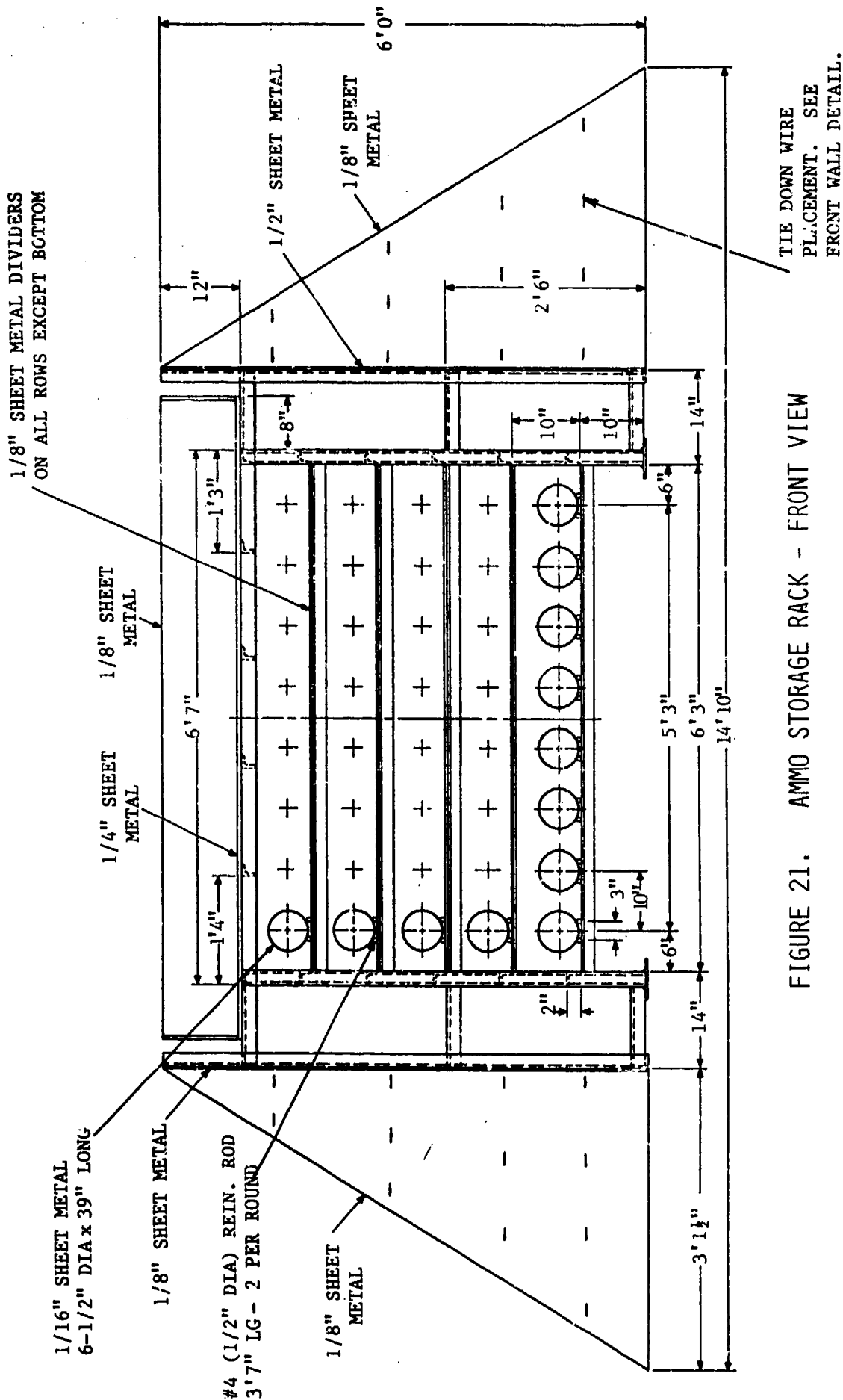


FIGURE 21. AMMO STORAGE RACK - FRONT VIEW

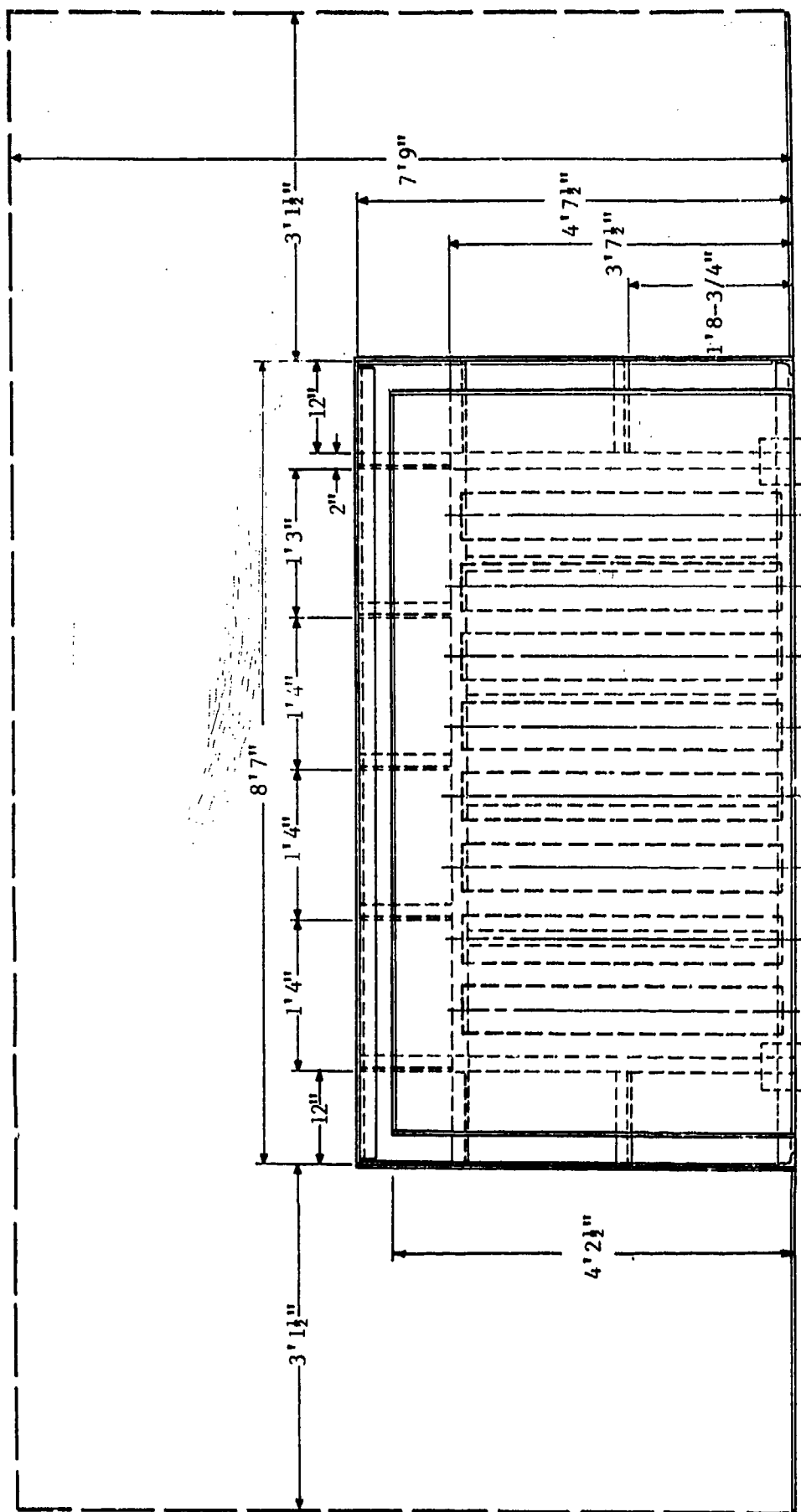


FIGURE 22. AMMO STORAGE RACK - TOP VIEW

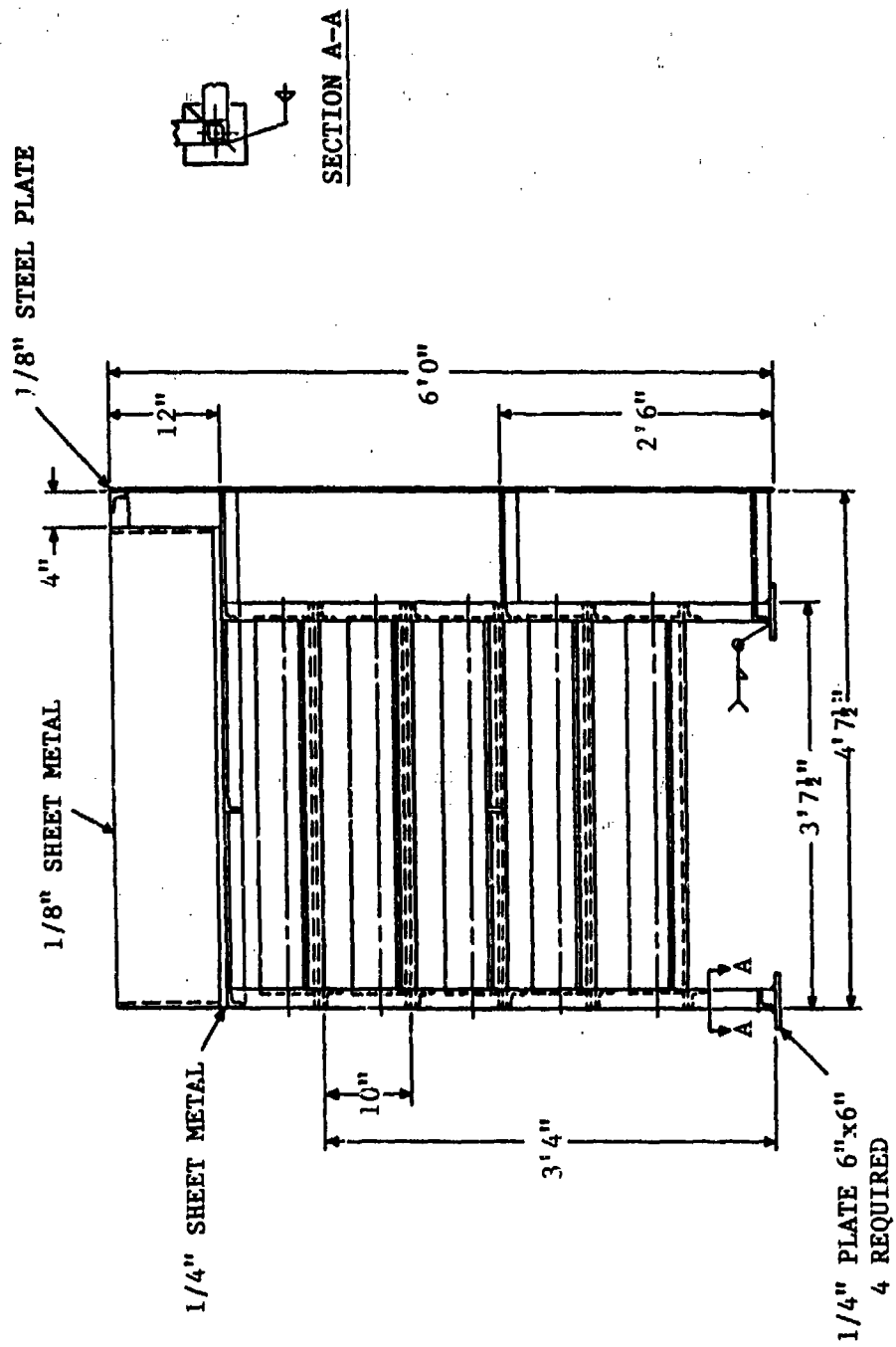


FIGURE 23. AMMO STORAGE RACK - SIDE VIEW

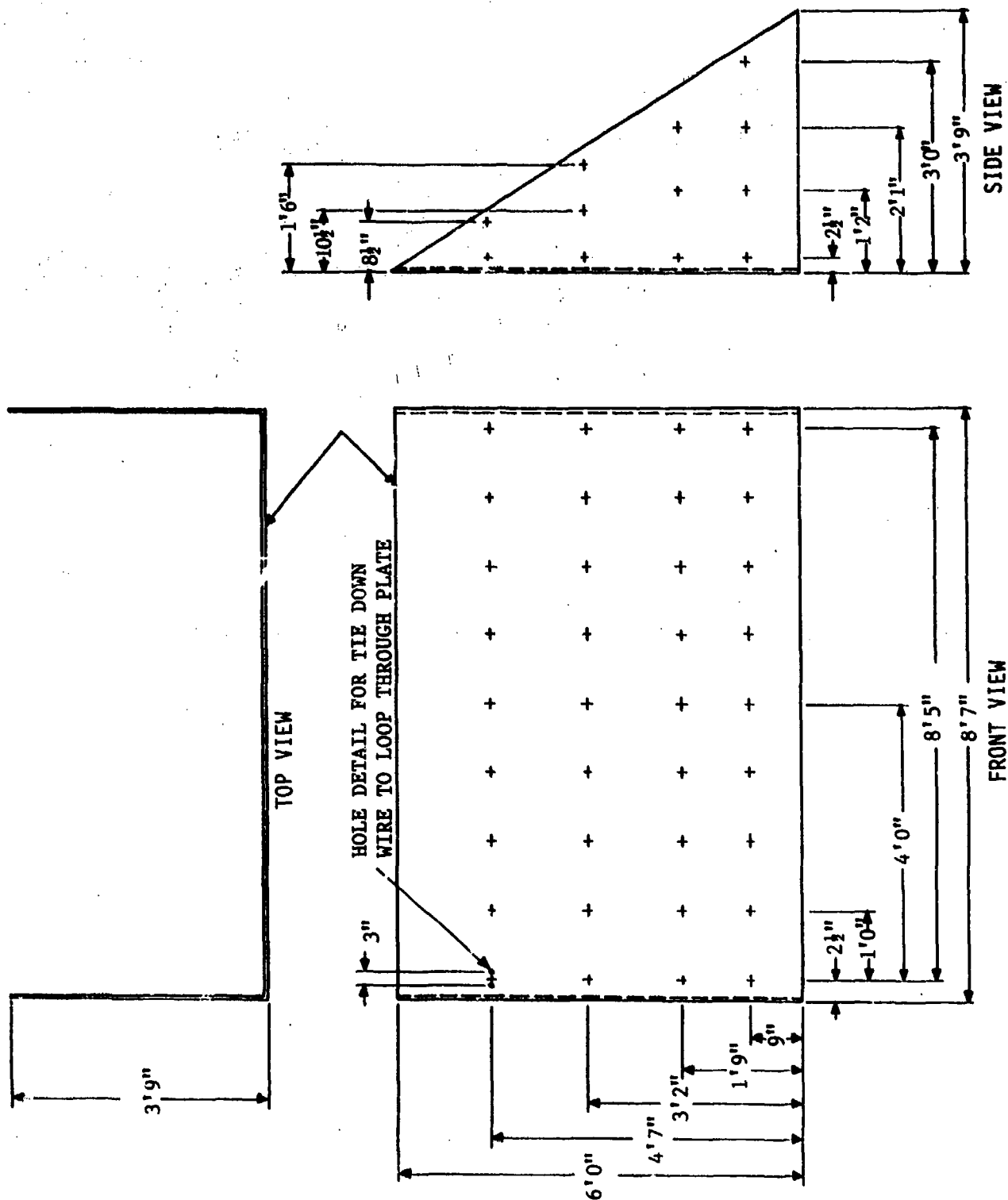
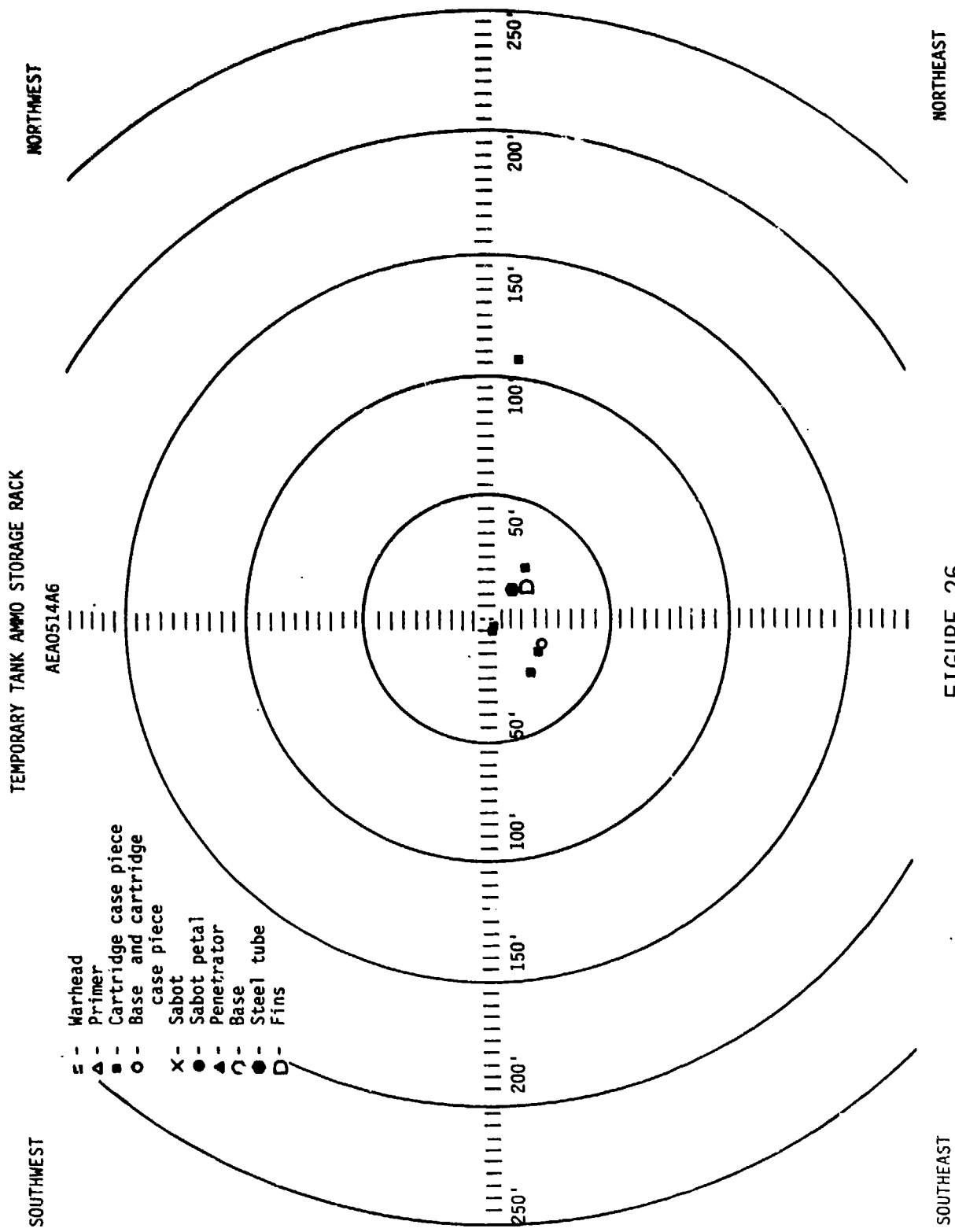


FIGURE 24. AMMO STORAGE RACK - FRONT WALL



FIGURE 25. TEMPORARY TANK
AMMO STORAGE FACILITY



NORTHEAST

FIGURE 26

SOUTHEAST

TABLE VI
TEMPORARY TANK AMMUNITION STORAGE RACK

DEBRIS RECOVERY

ALL MEASUREMENTS ARE TAKEN FROM POINT OF ROCKEYE INITIATION
OF DONOR WARHEAD

50-ft Radius of Ground Zero	One steel tube; fins from heat round; 5 pieces from cartridge cases (15-1/2"x13"; 6-1/2"x 4-1/2", 10"x5", 21"x7-1/2", 10-1/4"x7-1/2"); one base with piece of cartridge case (4" high)
50-ft - 75-ft Zone	No debris
75-ft - 100-ft Zone	No debris
100-ft - 125-ft Zone	One piece of cartridge case



FIGURE 27. FINAL DESIGN:
TEST NO. 1 - POST-TEST AREA

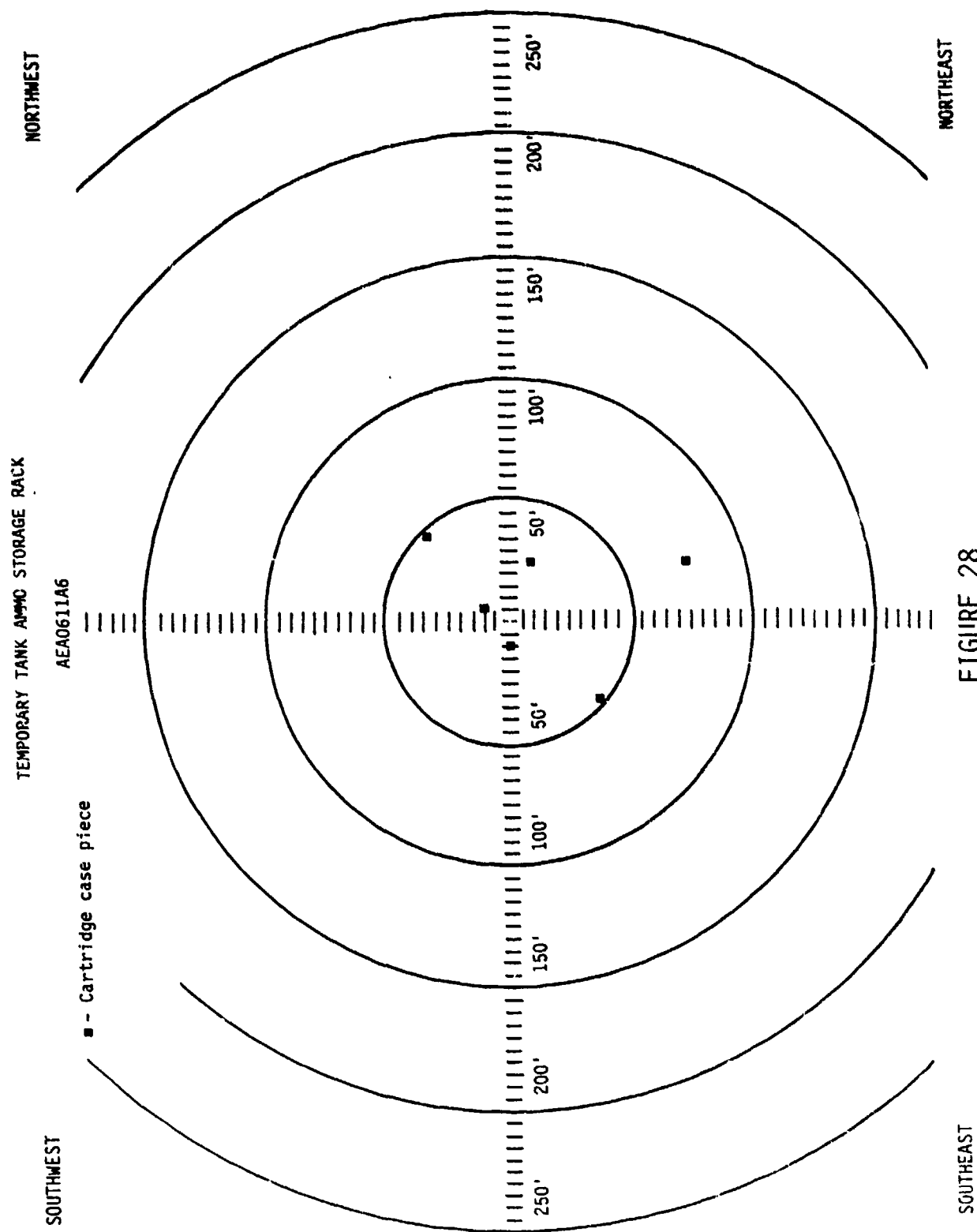


FIGURE 28

TABLE VII
TEMPORARY TANK AMMUNITION STORAGE RACK

DEBRIS RECOVERY

ALL MEASUREMENTS TAKEN FROM POINT OF ROCKEYE INITIATION
OF DONOR WARHEAD

50-ft Radius of Ground Zero	5 pieces of donor cartridge case (7-3/4"x6", 4-1/2"x2-1/2", 4"x1-3/4", 4-1/4"x2", 2-1/2"x1-1/2")
50-ft - 75-ft Zone	One piece of donor warhead (1-1/2" x 1")

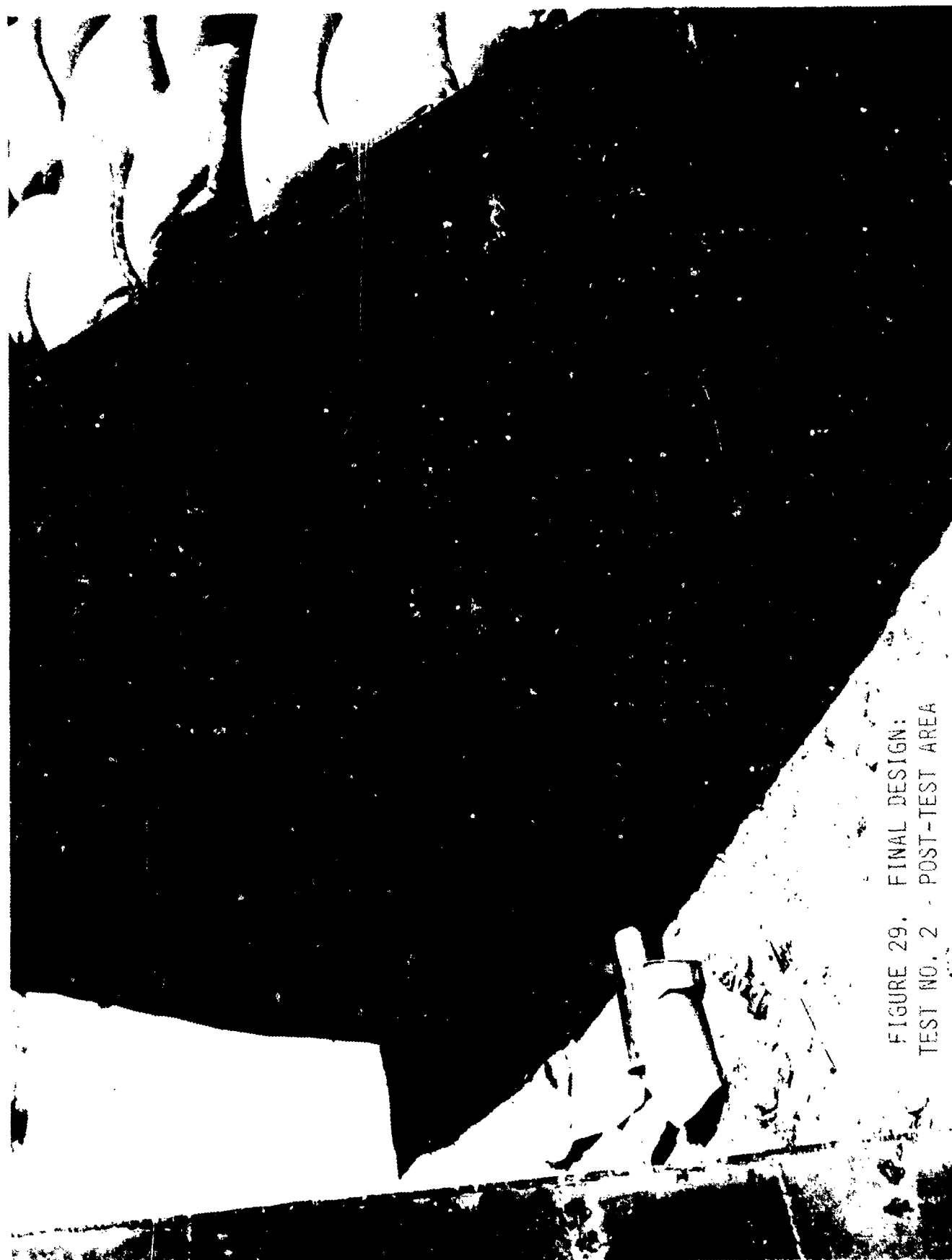


FIGURE 29. FINAL DESIGN:
TEST NO. 2 - POST-TEST AREA

NORTHWEST

NORTHEAST

TEMPORARY TANK AMMO STORAGE RACK

AEA0702A6

□ - Warhead piece
■ - Cartridge case piece

SOUTHWEST

SOUTHEAST

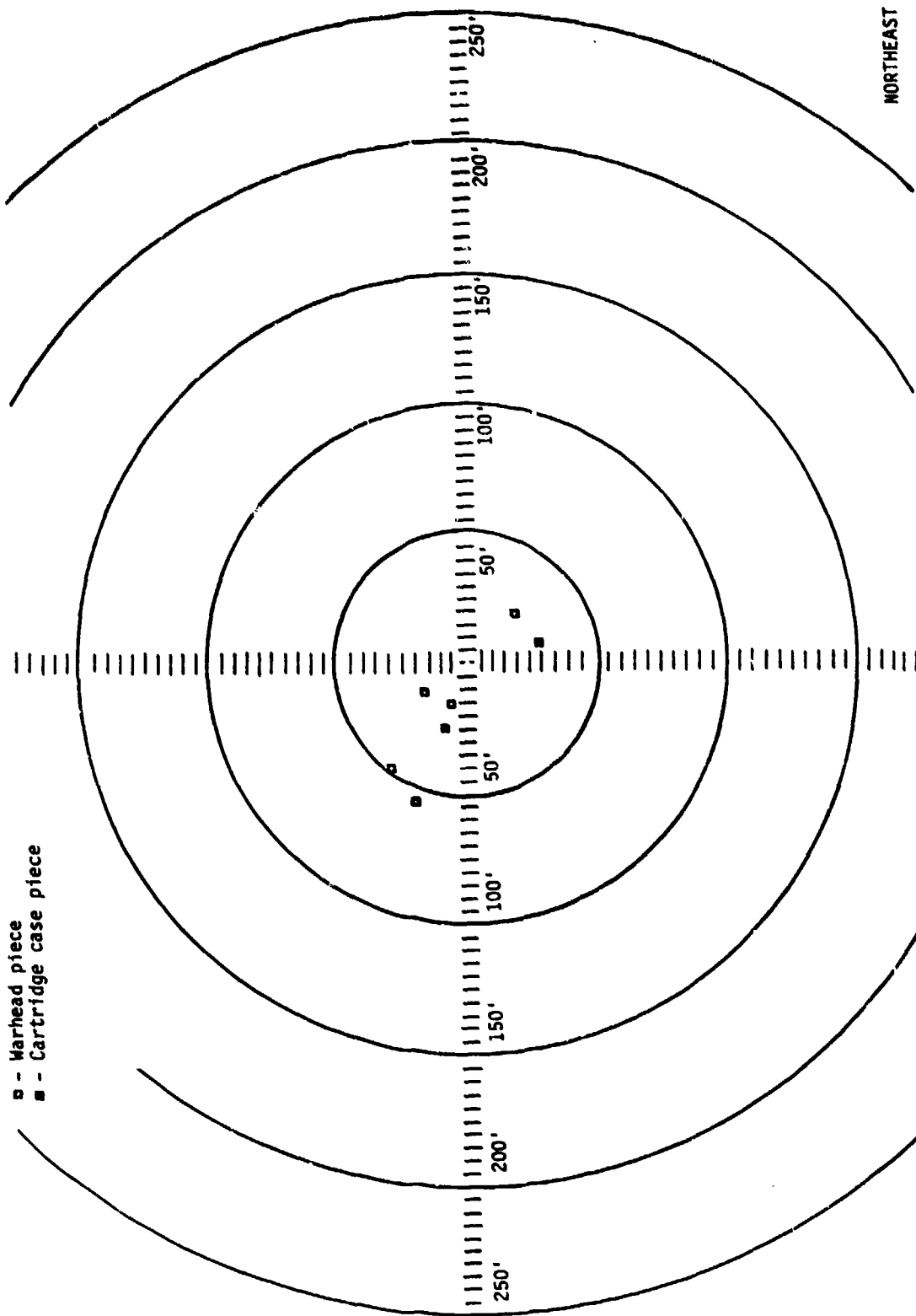


FIGURE 30

TABLE VIII

TEMPORARY TANK AMMUNITION STORAGE RACK.

DEBRIS RECOVERY

ALL MEASUREMENTS TAKEN FROM POINT OF ROCKEYE INITIATION
OF DONOR WARHEAD

50-ft Radius of Ground Zero	2 pieces of donor cartridge case (6"x4", 7"x4"); 4 pieces of donor warhead (3"x1-1/4", 1-1/2" x 1-1/8", 2"x1", 1-1/2"x1/2")
50-ft - 75-ft Zone	One piece of donor warhead (1-1/2"x1")



AEAG702A6

FIGURE 31. FINAL DESIGN:
TEST NO. 3 - POST-TEST AREA



AD-P005 354

PROPAGATION TESTING OF M61 ROCKETS
IN SINGLE ROUND CONTAINERS

D.B. HILL
Ammunition Equipment Directorate
Tooele Army Depot, Utah

Presented at:
TWENTY-SECOND DOD EXPLOSIVES SAFETY SEMINAR
Dept. of Defense Explosives Safety Board
Anaheim, California

ABSTRACT

Maximum Credible Event

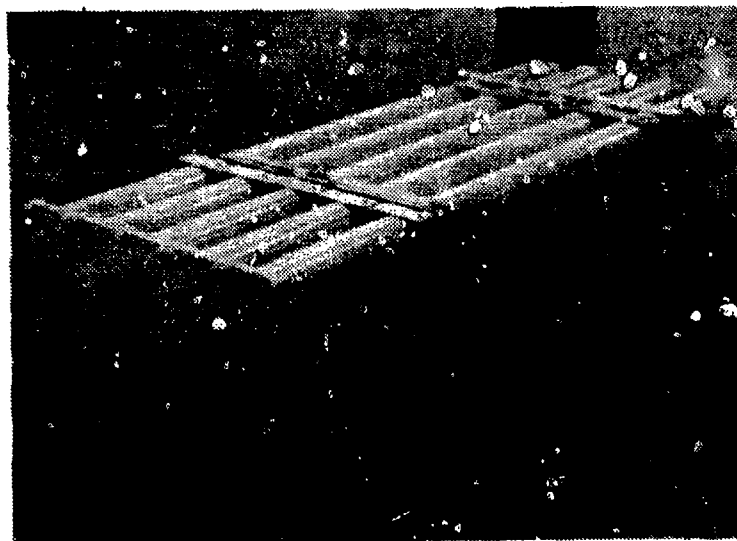
A need potentially exists for overpack containers for 115mm M55 Rockets. A single round overpack system has been designed and a series of tests were conducted, utilizing M61 Rockets, to determine effect of the overpack on the previously-established MCE for palletized M55 Rockets; and to provide data for storage hazard classification of rockets stored in the overpack containers. This paper presents results of those tests.

PROPAGATION TESTING OF M61 ROCKETS IN SINGLE ROUND CONTAINERS

INTRODUCTION

This paper presents results of a series of tests conducted to assess the potential for propagation between 115mm rockets confined in newly-designed overpack containers. The tests were conducted by the Ammunition Equipment Directorate at Tooele Army Depot, Utah in late 1985-early 1986.

The 115mm rocket at issue is the obsolete, lethal chemical agent filled M55 rocket. A need potentially exists for some type of overpack to contain agent that may leak from the rocket's existing shipping and firing container. The U.S. Army Defense Ammunition Center and School, acronym USADACS, located at Savanna Depot Activity, Savanna, IL designed an overpack system consisting of stackable, cylindrical steel tubes referred to as Single Round Container (SRC); see Figure 1. In order for the SRC to be qualified as an overpack system for M55 rockets, it must be subjected to a variety of tests, one of which is the subject of this paper.



PALLETIZED SRC
FIGURE 1

The Army's TB 700-2, entitled Dept. of Defense Explosives Hazard Classification Procedures, outlines the tests required to assign an explosives hazard classification to ammunition and explosives. The tests discussed herein were intended to address only the storage hazard classification requirements. A second major objective of the test program was to determine a "maximum credible event" (MCE) for a pallet of rockets each contained in SRC.

DESCRIPTION OF ROCKET

Because the M55 rocket is filled with lethal chemical agent, the tests were conducted with M61 rockets. The M61 rocket is the practice simulant for the chemical agent-filled M55 rocket. It is used for training personnel in the techniques of loading, preparation for firing, and firing of rockets from the M91 launcher. The fuze, explosive bursters, and propellant are identical in both rockets. The only difference is that the warhead in the M61 rocket is filled with an ethylene glycol simulant for the agent. A description of the M61 rocket follows; see Figure 2:

M67 Motor containing M28 Propellant, 19.3 pounds (M28 propellant is double base solid propellant with a cellulose acetate restrictive container)

M34 Burster, 2.7 pounds Composition B4

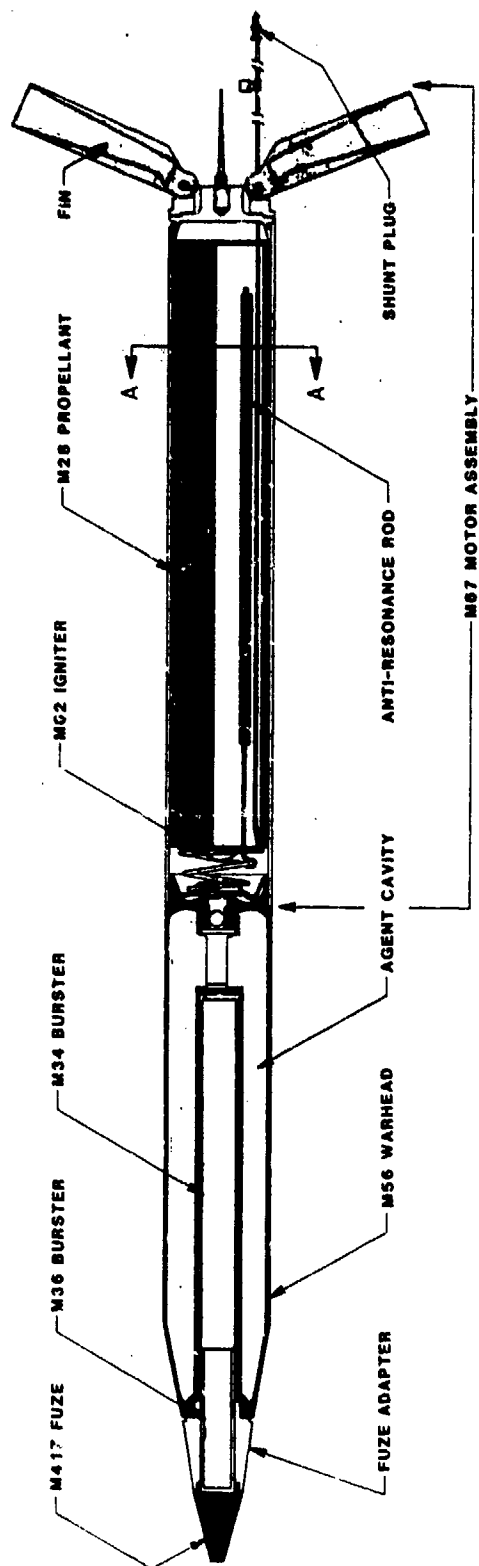
M36 Burster, 0.5 pounds Composition B4

M417 Fuze, 190 grains RDX

M56 Warhead, containing approximately 10.7 pounds ethylene glycol

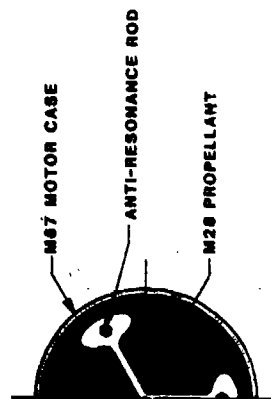
M62 Igniter, 25 grams ignition mixture

The rocket is approximately 4.5" diameter by 78" long and weighs 58 pounds. It requires a 24 volt DC power source for firing the electric squib in the igniter assembly of the motor. The rocket is stored in and fired from its M441 fiberglass shipping and firing container which is approximately 5" diameter by 82" long. The rockets are normally palletized for storage, fifteen rockets to a wooden pallet; see Figure 3.



M55/M61: ROCKET COMPONENTS

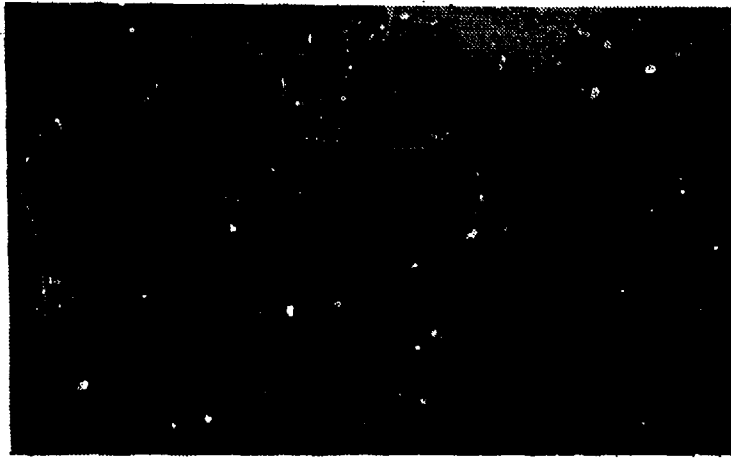
M67 MOTOR - 19.3 LBS M28 PROPELLANT (DBL BASE)
 M34 BURSTER - 2.7 LBS COMPOSITION B4
 M36 BURSTER - 0.5 LBS COMPOSITION B4
 M62 IGNITER - 25 GRAMS IGNITION MIXTURE
 M417 FUZE - 190 GRAMS RDX
 M56 WARHEADS - 10.75 LBS GB
 10.1 LBS VX
 10.75 LBS EG (SIM)



SECTION A-A

M55/M61 ROCKET

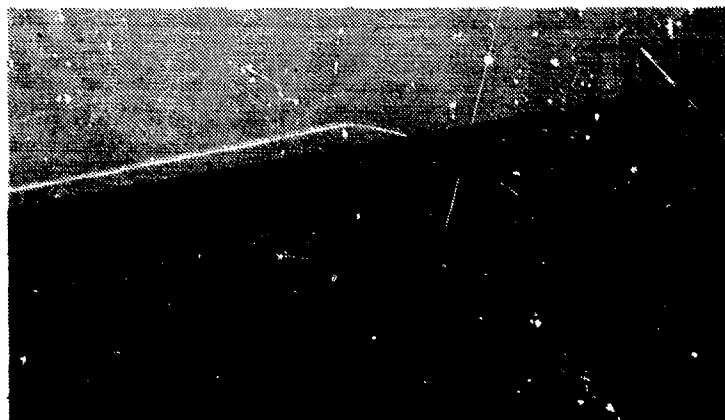
FIGURE 2



PALLETIZED M55/M61 ROCKETS
FIGURE 3

DESCRIPTION OF SRC

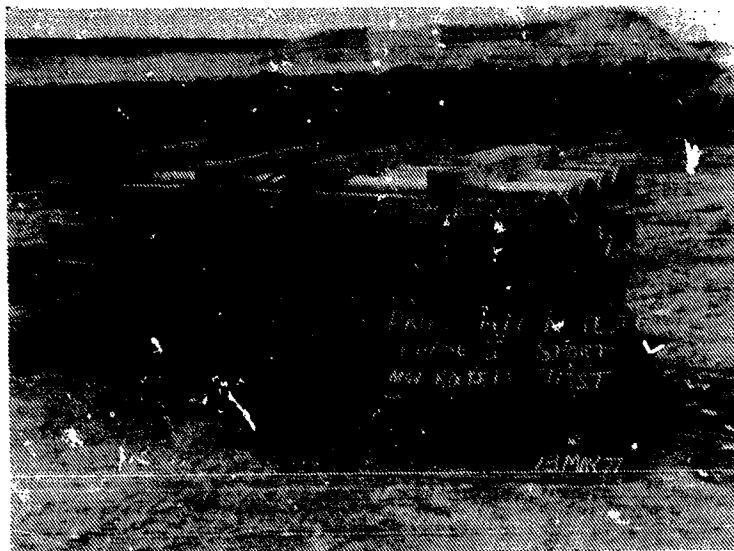
The SRC is fabricated from low carbon cold rolled steel, 5 3/8" inside diameter, 16 gage wall thickness. A dome is welded to one end; and a square flange is welded to the other end, with four bolts welded to the flange for affixing a blind flange for closure. An o-ring is installed in the face of the blind flange to effect a liquid and vapor tight seal. Further, a spring is attached to the blind flange to apply retention pressure to the rocket contained within the SRC. Square stacking brackets with guide pins permit stacking of fifteen SRC in a three row array similar to the standard pallet of rockets without SRC; see Figure 4.



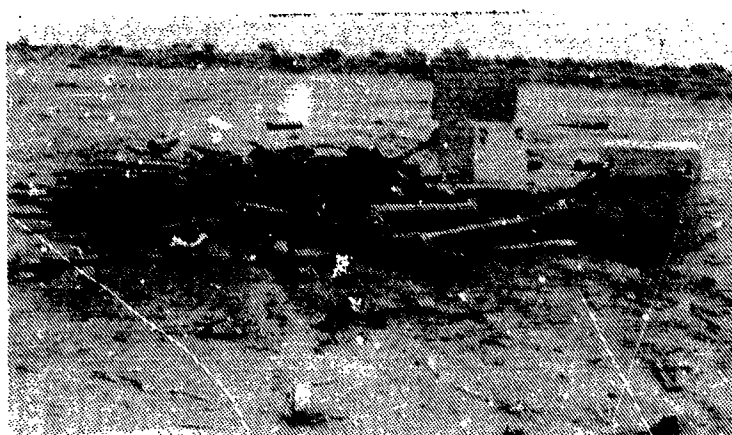
SINGLE ROUND CONTAINER
FIGURE 4

DISCUSSION

In early 1977, a series of tests were conducted at Tooele Army Depot to determine the MCE for a standard pallet of 15 M55 rockets contained only in their standard fiberglass shipping and firing containers. Those tests, conducted with M61 rockets, established the MCE as the spontaneous detonation of one rocket with a sympathetic detonation of another rocket warhead, and massive leakage of agent from the remaining thirteen rockets. See Figures 5 and 6. These tests were reported in AED Report 24-77 (Ref. 1).



1977 TEST SETUP
FIGURE 5



1977 TEST RESULTS
FIGURE 6

One objective of the recent 1985-1986 series of tests was to see if the SRC overpack altered the MCE.

The tests conducted on the SRC were as follows:

- *three baseline tests - for establishing baseline pressure data for single rockets contained in SRC
- *three single package tests (IAW TB 700-2) - tests were conducted with nine rockets per pallet
- *fragment search - conducted after each single package test

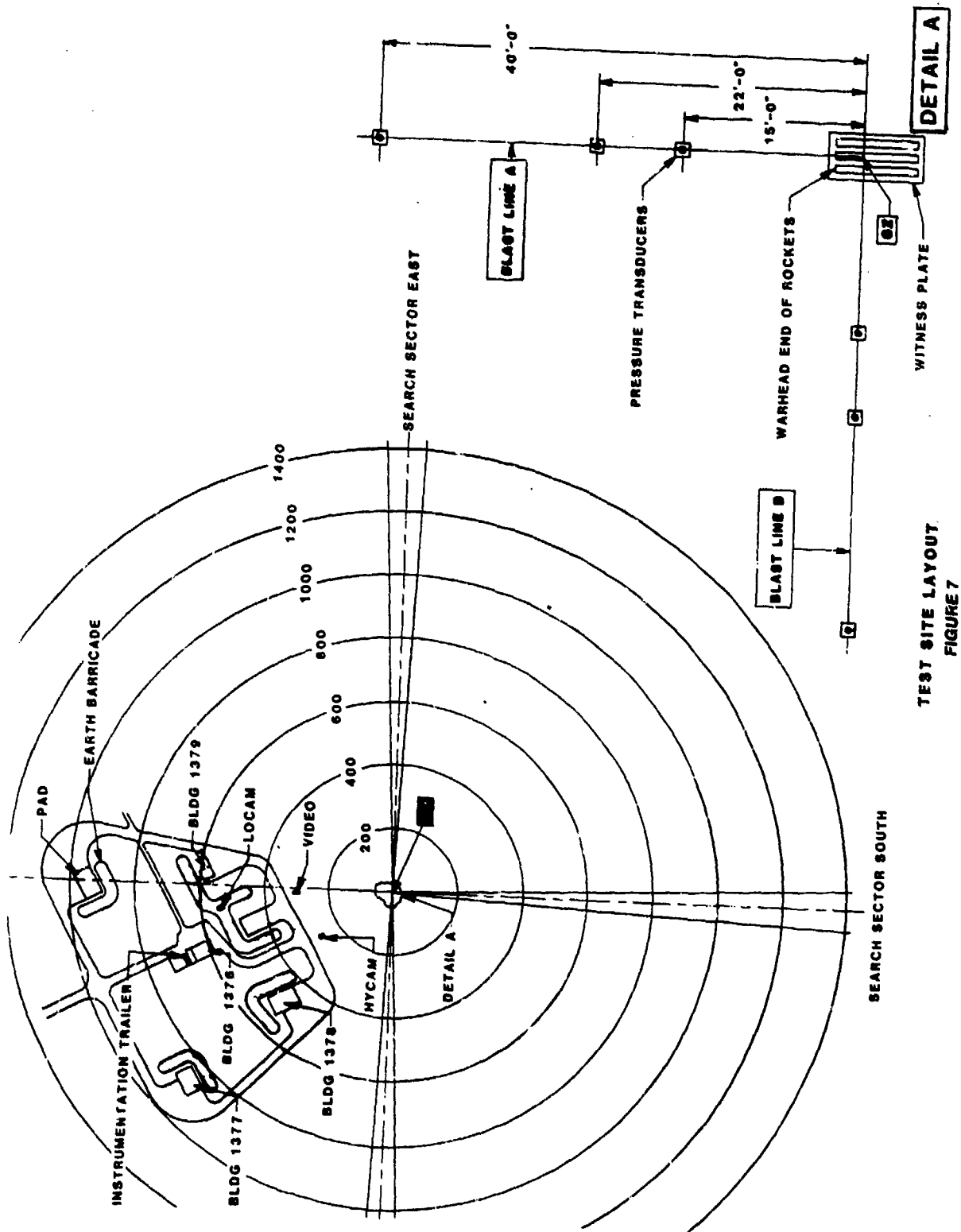
The tests yielded the following results:

- *No propagation from donor rocket to in-pallet acceptors; i.e. total explosive yield of only one warhead burster.
- *Complete rupture of all acceptor warheads.
- *Propellant grain ejected from donor in two of the three pallet tests and burned freely; i.e. non-propulsive.
- *No propellant initiated or burned in any acceptor rocket.
- *Significant damage to all acceptor SRC.
- *Massive fireball.

TEST PREPARATIONS

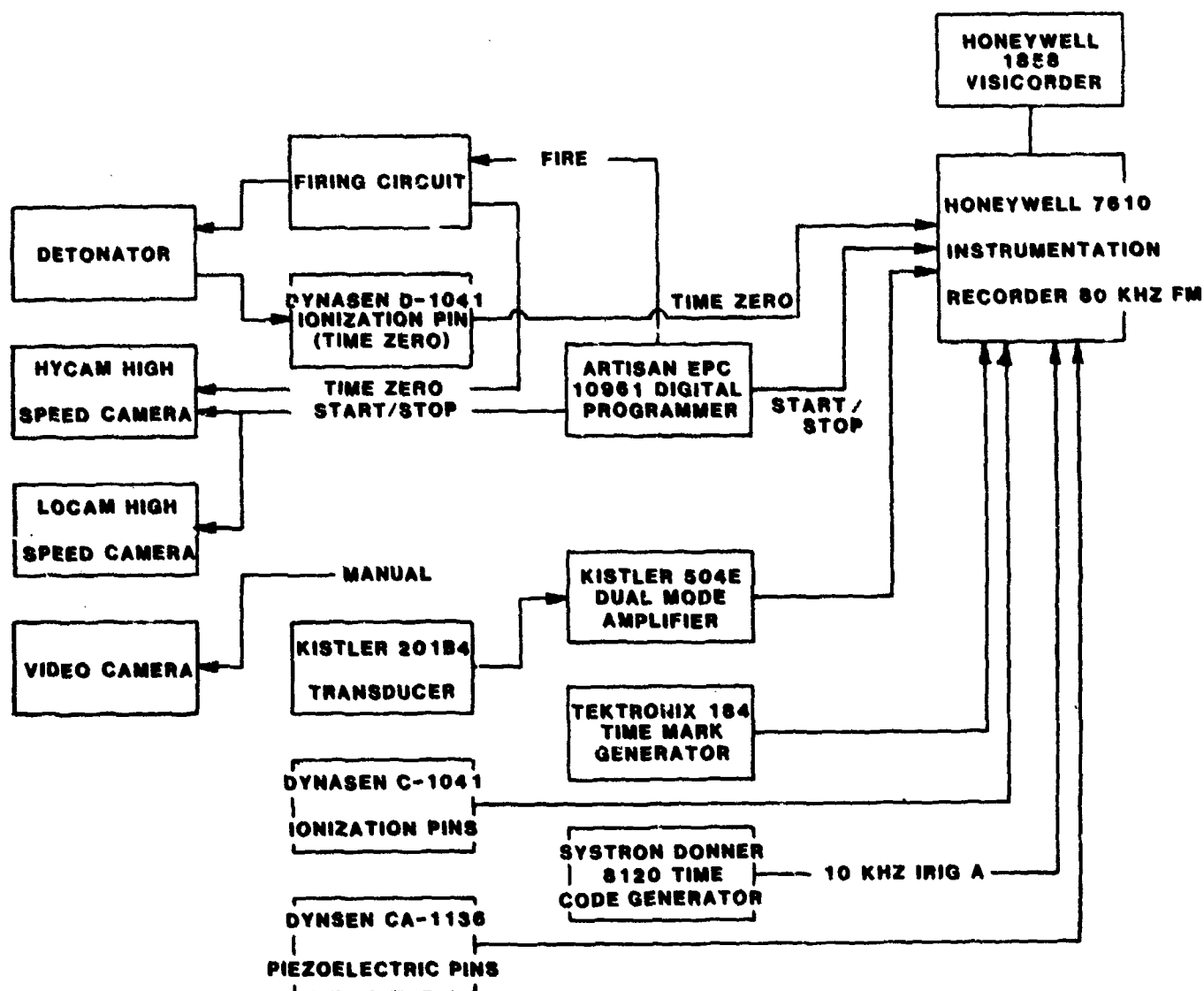
Setup for all tests was as shown in Figure 7. A piezoelectric pressure transducer array measured free-field overpressures along two blast lines: one parallel to, and one at right angles to the burster in the initiated rocket. All test items were placed on heavy steel witness plates. The test site was prepared by clearing a large area of vegetation and setting stakes to define three search sectors as described in TB 700-2 for fragment search. Tests were controlled and monitored from the data acquisition trailer. Two high-speed movie cameras and one video camera were used for documentation.

Pressure transducers used in the free-field blast measurement array were low-impedance piezoelectric devices, Kistler Piezotron Model 210B4 (100 kHz



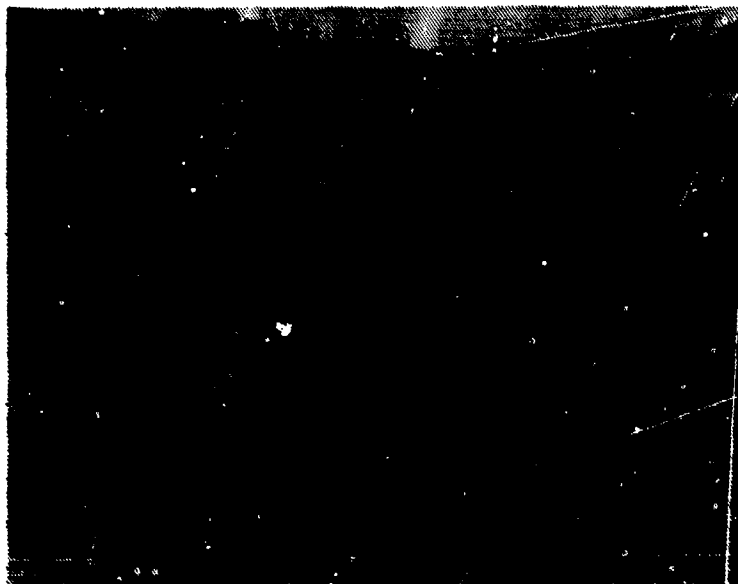
TEST SITE LAYOUT
FIGURE 7

frequency response). The instrumentation recorder was Honeywell Model 7610 (80 kHz frequency response). Dynasen Model CA-1136/1137 piezoelectric blast pins were used in the acceptor warheads to detect burster function if propagation occurred; and Dynasen Model CA-1041 ionization probes were used in the rocket motors to detect motor initiation; see Figure 8.



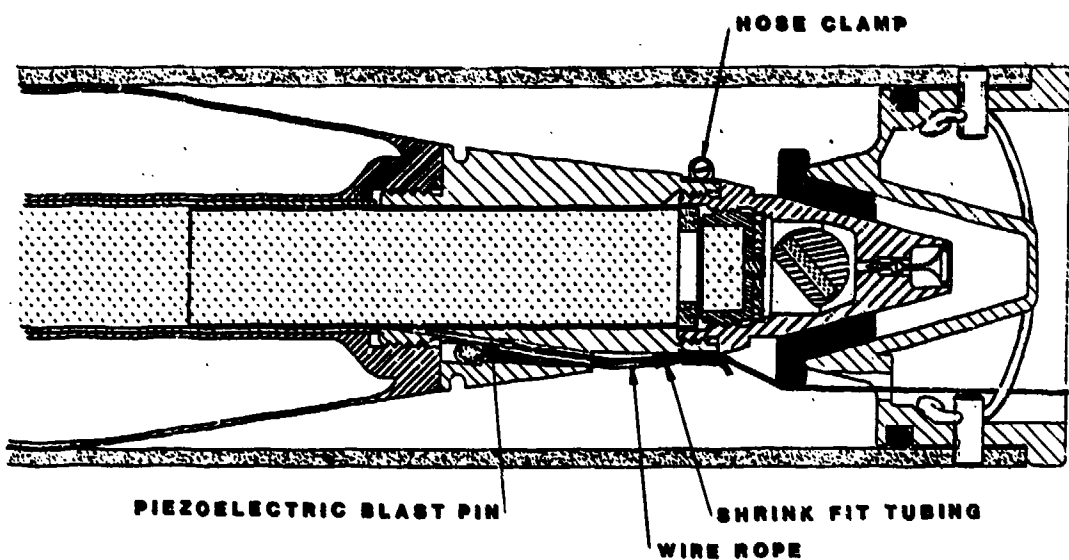
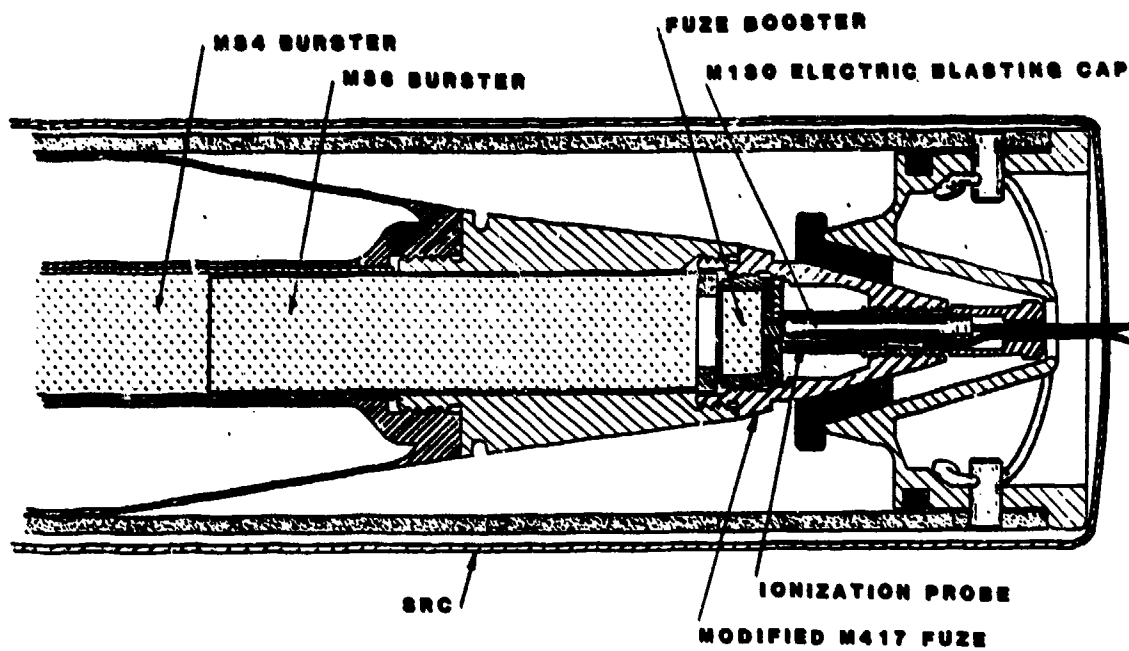
INSTRUMENTATION SCHEMATIC
FIGURE 8

Single M61 rocket/SRC configurations were used for the baseline tests (three replicates); see Figure 9. The M417 fuze was modified to accept an electrical blasting cap clamped against the fuze booster charge; and an ionization probe adjacent to the blasting cap to provide a Time Zero generator for instrumentation; see Figure 10. No explosive overcharge was used. The threads were machined from the fin-nozzle assembly of the rocket motor to preclude propulsion if the M28 propellant had ignited.



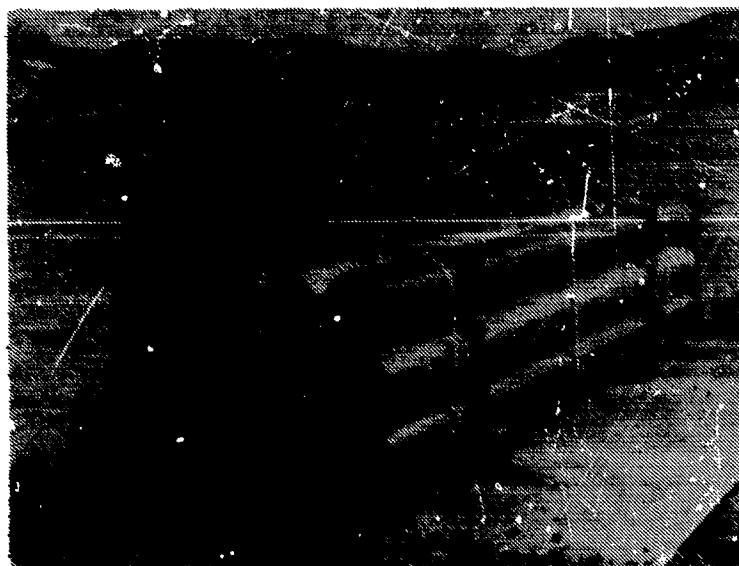
**BASLINE TEST SETUP
FIGURE 9**

The pallets, or single packages, were configured, colored, and numbered as shown in Figure 11. The donor, or central rocket was modified as described for the baseline test rockets. The eight acceptor rockets, for the first test only, were prepared as follows (see Figure 10). The fuze adapter was modified to allow insertion of a piezoelectric blast pin against the M36 burster. The blast pin was held tightly against the burster by attaching its electrical lead to a short length of wire rope with shrink-fit tubing, and then clamping the assembly to the fuze adapter with a hose clamp. The electrical lead was passed through the existing inspection hole in the fiberglass container's



M61 ROCKET MODIFICATIONS
 FIGURE 10

endcap and then through a hole drilled in the dome end of the SRC. An ionization probe (to detect motor ignition) was inserted into a void in the M28 propellant grain, near the vicinity of the black powder igniter charge; and its electrical lead passed through inspection ports in the fiberglass container endcap and the SRC flanged end. The blast pins were not used for the next two tests because of a false indication of propagation given in the first test. The ionization probes were determined to be unnecessary instrumentation because visual inspection would reveal if a motor initiated. The threads were machined from the fin-nozzle assembly in all rockets for all tests to preclude propulsion in event of motor ignition. The rockets were then placed in SRC and the flanged end plates secured with the nuts tightened to 20 ft-lbs. The nine SRC for each test were palletized and banded in three locations with 3/4" banding. The pallet was then placed on wooden 4 x 4s on a witness plate, oriented as shown in Figure 11.



PALLET TEST SETUP
FIGURE 11

TEST/RESULTS

Problems were encountered in the three single-rocket baseline tests; see Figure 12. One test failed because the M34 burster did not detonate when the blasting cap was functioned; and the pressure measurements from Blast Line B

(stations 4, 5, and 6) on the other two tests were unuseable because of pressure transducer problems. There was sufficient confidence in the remaining data, however, to proceed with the single package or pallet tests. That decision was made based on validation of the Blast Line A pressure transducers with bare spherical charge tests, and comparison with data from baseline tests conducted in 1977.



BASELINE TEST RESULTS

FIGURE 12

In the three pallet tests, both blast lines were functioning properly. Pressure yields in the three pallet tests were consistent with, and in some cases slightly lower than the pressure yields from the baseline tests. The conclusion, based on comparison of pressure yields with those of the baseline tests, is that there was no propagation from the donor to any acceptor, i.e. total explosive yield of only one warhead; and that propagation is unlikely.

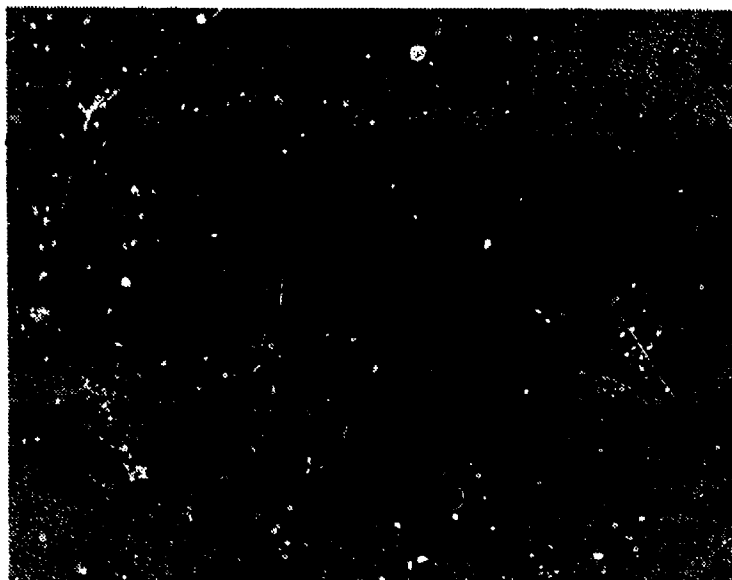
Table 1 provides comparisons of blast pressure data from the 1977 tests and the recent, 1986 tests. For convenience of comparison only, the values

presented are numerical averages of several tests in each series; e.g. the values for each peak positive incident overpressure and positive incident impulse for the 1977 baseline series is a numerical average of 4 tests. Four pressure measurements, at each transducer location, were averaged for the value presented in the table. The reader is referred to the final report of these tests for detailed presentation of data (Ref. 2).

TABLE 1 - PRESSURE DATA

	TRANSDUCER	1977		1986	
	No.	Baseline	Pallet	Baseline	Pallet
PEAK POSITIVE INCIDENT OVERPRESSURE psi	1	7.22	7.86	6.80	6.19
	2	3.74	3.88	3.64	3.47
	3	1.47	1.49	1.42	1.41
	4	4.47	5.13	--	5.48
	5	2.47	3.18	--	3.17
	6	1.32	1.45	--	1.54
POSITIVE INCIDENT IMPULSE psi-ms	1	6.88	8.66	6.31	6.19
	2	4.79	5.59	4.80	4.14
	3	2.38	2.72	3.14	2.42
	4	5.10	7.14	--	5.50
	5	3.58	5.00	--	3.55
	6	1.93	2.96	--	2.05

All acceptor warheads were totally destroyed with the exception of acceptor number 8 in each pallet test (acceptor number 8 being directly beneath the donor); see Figure 13. Those acceptors, however, were badly ruptured, releasing their ethylene glycol fill. The conclusion is that in a pallet of rockets contained in SRC, all warheads can be expected to be ruptured in event of a detonation of one warhead.



PALLET TEST RESULTS
FIGURE 13

Large quantities of unburned or unexploded explosive burster were found in all three tests; see Figure 14. The burster cases show evidence of secondary partial detonation or pressure rupture. Review of high speed films reveals sporadic flashes within the fireball of the initial detonation that may be burning or detonating pieces of explosive. Burster cases recovered in the 1977 tests did not show similar evidence of low-order detonations.

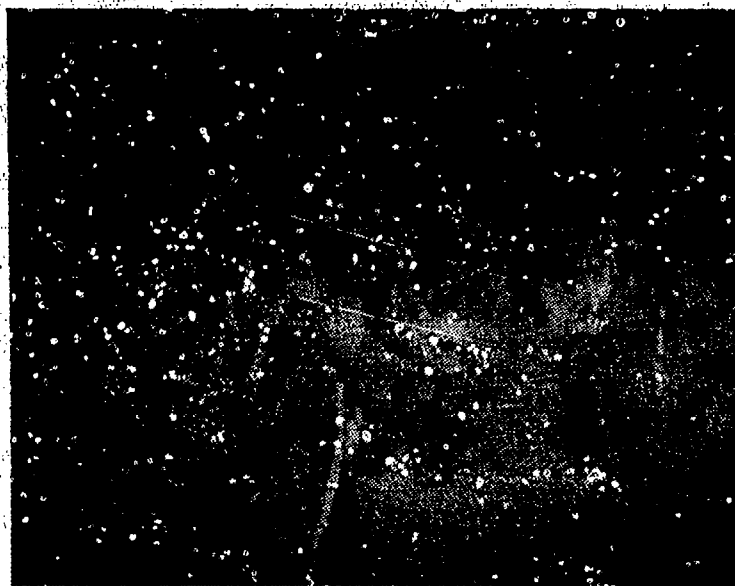


TYPICAL BURSTER RESIDUE
FIGURE 14

No motors burned within their SRC. Only two motors ignited...in two tests, the propellant grains were ejected from the donors at initial detonation and burned up completely on the ground. Review of the high speed films does not reveal when or where ignition occurred. In one test, the inside of the donor motor casing was charred and blackened as though the motor may have been burning while in the case, whereas the motor casing of acceptor number 2, from which a propellant grain also ejected, was clean. Inasmuch as the burning propellant grain remained at ground zero, it apparently was not confined sufficiently to be propulsive. The conclusion is that propellant burning can occur and that hazard must be considered.

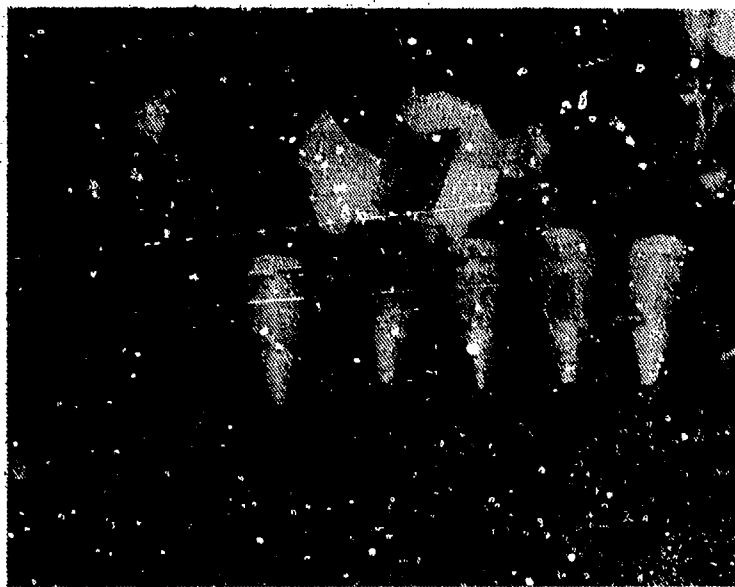
All tests, including baseline, exhibited tremendous fireballs (burning ethylene glycol) which were not seen in reviewing high speed films of the Mar-Jun 1977 tests. The fireball in the first pallet test was significantly larger than was seen in the other pallet tests, particularly the third in which more liquid ethylene glycol was observed at ground zero than in the other tests. The absence of fireball in the 1977 tests, suggests that brief confinement by the SRC when the warheads ruptured caused vaporization of the ethylene glycol, enhancing ignition into the fireball observed in these tests.

Fragmentation patterns and distances appeared to be similar to those in the 1977 tests except that more fragments were recovered in those tests. The majority of fragments in both series (1977 and current) were in a 200-600 ft. radius of ground zero, and to the east and west of ground zero. One piece, in the recent series, was found at 1190 feet. The greatest distance recorded in the 1977 test report was 1030 feet. There was a greater scattering of major components (SRC, shipping/firing container, motor casing) around ground zero in the current series of tests. Figure 15 shows that significant damage was incurred by all the acceptor SRC. The motor half of the SRC generally remained intact with the motor housing and propellant grain staying within the SRC while the warhead half was totally destroyed. In all three tests the acceptor immediately beneath the donor remained completely assembled; i.e. the entire rocket remained within the SRC. The warhead and warhead end of the SRC were flattened and ruptured; and the burster burned up completely within the warhead.



TYPICAL PALLET TEST RESIDUE
FIGURE 15

Figure 16 shows unfunctioned fuzes and fuze adapters recovered in one of the tests. Two of the fuzes remain in their respective SRC. The photo depicts 7 fuzes. The eighth fuze belonged to the donor, thereby accounting for all but one fuze in one test. Results were similar in a second test; 3 fuzes were not found in the third test.



RECOVERED FUZES
FIGURED 16

SUMMARY

In conclusion, it appears that the Single Round Container does not significantly alter the MCE for fifteen palletized 115mm rockets:

MCE

Original Configuration

*Spontaneous detonation of one warhead, sympathetic detonation of another

*Leakage of agent from remaining thirteen warheads

In SRC Overpack

*Spontaneous detonation of one warhead

*Leakage of agent from remaining fourteen warheads

Test data was provided to the AMCCOM Safety and AMC Field Safety Activity offices for their use in establishing storage hazard classification for M55 Rockets overpacked in SRC.

REFERENCES

1. Smith, Kenneth T., Propagation Between Munitions for Palletized M61 Rockets, AED Report No. 24-77, 3 October 1977.

2. Hill, D. B., Tests to Determine Extent of Propagation Between 115mm M61 Rockets Confined in Single Round Containers, AED Report No., 01-86.

AD-P005 355

A

PRESENTATION

TO

DEPARTMENT OF DEFENSE
EXPLOSIVES SAFETY BOARD

"DELUGE SPRINKLER SYSTEM
TIMED INTERVAL OPERATION ADDITION"

By

WAYNE R. SUEKER P.E.
HONEYWELL INC.

At

ANAHEIM, CALIFORNIA

AUGUST 27, 1986

VU-GRAPH PLEASE (Honeywell Logo)

Hello: I am Wayne Sueker, a professional engineer for Honeywell. I work at both our metal parts manufacturing facilities at the Twin City Army Ammunition Plant near New Brighton, Minnesota and at our load, assemble and pack facility at the Joliet Army Ammunition Plant near Joliet, Illinois.

VU-GRAPH 1 PLEASE (Pic of HJA)

~~Deluge Sprinkler Systems for the~~ ^{are described}
This is our recently established load, assemble and pack facility on a portion of the Joliet Army Ammunition Plant. When we rehabilitated these areas, we designed and installed a number of unique deluge sprinkler systems. These systems protect the following:

- ✓ people operated ammunition assembly machines.
- ✓ people operated explosive material handling systems.
- ✓ remotely controlled machines that load explosives into ammunition components.

Deluge sprinkler systems installed at other than our Joliet location, when "tripped", continue to flow water in large quantities after the need for that flow has passed. This flow continues until either the control valves are turned off (if you can get to them - more about this later) or the water supply is exhausted. (And this has happened at some facilities)

A very real problem with all deluge sprinkler systems is that many times the thing that set off the system is not a fire. The extreme spark/flame sensitivity of these ultraviolet or infrared fire detectors also means that they are subject to nuisance trips from electrical shock, excessive humidity, interior faults, etc. Many times the large quantity of water now all over your facility never had a fire to put out. Moreover any explosive material present in the deluged area may now be spread all over the place. This causes a tremendous safety hazard when the explosive dries out. The dispersed explosive also can cause a pollution problem.

The systems ~~Honeywell designed and~~ installed at Joliet have electronic timers, fast acting pneumatic valves and back-up electronic circuitry to control the length of the deluge water flow. The systems can restart deluge water flow for a number of conditions, as later explained.

~~Our systems~~ ^{They} have back-up fail-safe modes that allow for main power failure, air pressure failure and manual reaction to damaged equipment.

Let's see what happens at most other deluge sprinkler protected facilities.

VU-GRAPH 2 PLEASE (Picture of a lake)

Is this what your plant looked like the last time your deluges tripped?
The boat is anchored to building #3!

Most other deluge sprinkler systems have a continuous flow thru the deluge heads once the system is tripped. The only way to stop the flow is to turn off the water supply valves or run out of water.

Unfortunately, the appropriate water supply valves are usually located close to the accident area. If there is explosive material in the accident area, permission from the safety department must be obtained before your mechanic can enter the area. If your safety engineers are not on site (it may be 2 A.M. Sunday with no lines operating). You may run out of water before you can get permission to close the valves.

This possible loss of water supply could jeopardize other operating lines that draw fire protection water from that supply. It even could force production lines to stop operation and force the workers to evacuate their area.

As stated earlier, excessive deluge sprinkler water flow in areas containing explosives also can cause widespread pollution problems.

Again remember, many of these deluge water flows may be the result of an accidental "trip". There may never have been a fire.

VIEW GRAPH 3 PLEASE - (Pic of hopper with deluge protection)

Let's see how Honeywell's system operates

Something trips the deluge system. It may be a fire or it may be a nuisance trip. The deluge sprinkler water flows for a preset time and the panel turns off the water supply. Any continuing fire or any new fire is detected by the system and water is automatically reflowed. Water also can be manually flowed under unusual circumstances.

No one has to get into an area possibly contaminated with explosive materials to shut off valves, you do not take the chance of exhausting your water supply and your facilities are not under water.

How was our system designed?

Honeywell has been making inert metal parts and fuzes for 20 plus years. We always subcontracted our production requirements for load, assemble and pack (LAP).

When we entered the LAP end of the small caliber ammunition business several years ago, we reviewed the existing manufacturing procedures in use at other ammunition loading facilities. We found that some of these procedures had not been upgraded to current technology.

My end of the business is facilities, so let's see what we had to build on. Our "new" facilities at Joliet, were composed of six (6) 1940's built WWII fuze and booster assembly groups. Two (2) of the groups last had explosive assembly work in the 70's, one (1) in the 60's, one (1) in the 50's and two (2) were basically "abandoned in place" (as far as explosive assembly work) at the end of WWII.

As our needs didn't match the best that was left, you can see we had an excellent opportunity to consider new techniques for facilitization as we were almost starting from "scratch".

We reviewed the most recent "state-of-the-art" electrical and mechanical equipment/designs to see if they were applicable.

Our foremost design criteria, of course, was

SAFETY

Honeywell's proposed LAP procedures stated that we would, at Joliet, handle our explosive materials in a "maximum credible incident" (MCE) mode. This mode is defined in the AMC-R 385-100 Safety Manual.*

This MCE mode is based on the concept that when you can prove non-propagation between piles or stacks of explosives, you can use the weight of the largest pile or stack for your quantity distance calculations. You do not have to use the total explosive weight in the building or even in various bays.

Consult with your safety people if you think you could apply this concept.

These explosive unit-weight reductions can result in the following:

- less costly barricade/separation walls
- less distance required between operation buildings
- less explosive hazard exposure to employees
- less amounts of explosives involved in the event of a fire or detonation.

The last item, less amounts of explosives involved in a fire or detonation, was the one that I keyed on to try to develop a new deluge sprinkler fire protection system. I felt we could control or limit water flow if we designed proper safeguards into the system. These safeguards would have to let the system perform as a manual system in the case of a catastrophic accident, but be responsive to our needs in a less serious situation.

After consulting our in-house experts on explosive material behavior in burn (deflagration) and hi-order (explosion) modes, we calculated the deluge sprinkler water flow time intervals. We used the individual deluge nozzle characteristics and the burn time of the explosive amount to be protected. Yes, explosives burn, a lot faster than wood, but they will burn. Given their choice, they often burn easier than they explode.

*As described in the AMC-R 385-100 (2-56) and (17-7) safety manual.

To make sure we could get more water if the fire burned longer than we calculated we added a circuit to allow the U/V detectors to continuously scan. If the fire was still burning when the system tries to turn "off", the system recycles. If fire shows up after the system shuts down, the extra circuit restarts the cycle and reflows the system.

We also planned to use these controlled flows to wet down explosive materials present in hoppers on the machines. This "wet-down" would render inert many of the explosives we use and would greatly reduce the sensitivity of the rest of them.

Working with our deluge sprinkler contractor, we did the following:

VU-GRAPH 4 PLEASE (pic of detection panel)

We combined a U/V detector panel system with additional timer circuits and over-ride circuits with

VU-GRAPH 5 PLEASE (Pic of valves)

a regular fast acting deluge valve and a fast acting pneumatically closed, spring opening valve.

VU-GRAPH 6 PLEASE (Pic of detection head)

Controlled by a self-checking (to see if the lens is clear) ultraviolet detector system

VU-GRAPH 7 PLEASE (Pic of deluge sprinkler nozzles over hopper)

that can deliver deluge quantities of water where we want it and with a controlled length of flow.

As stated before, the extra circuits allow the detector system to recycle the timer if fire is present when the water flow is scheduled to turn off. They also restart the flow cycle if fire shows up after the system has turn-off. Control buttons were added to allow manual control water flow if some fire is observed,

VU-GRAPH 8 PLEASE (Pic of TV camera)

say, when we use a remotely controlled TV camera to scan an area of an incident. The incident may have caused debris to block the U/V detector's view.

We also designed "fail-safe" features into the system. The basic detector-control circuitry has battery back-up systems so that power failure will not affect the operation of this primary function. The Honeywell added timed-interval system was designed to be "fail-safe" to an open-flow mode if power or air pressure were lost. Any loss of power or air would automatically cause spring loaded valves to go to a position that allows deluge water to flow. This power or air loss will not flow an untripped system, only timed out systems would automatically open and flow deluge sprinkler water.

We may not need this extra water, but we will get it until, to paraphrase Mr. John Houseman, "we get our water flow stoppage the old fashioned way, we turn it" (the valve to "off", that is).

Does it work?

VU-GRAPH 9 PLEASE (Pic of HJA)

In a machine area of one of our production lines at Joliet, we press pre-pelleted tracer pellets into projectile bases. The quantity of tracer pellets in the machine hopper is reasonably small (three (3) to four (4) pounds) and any fire that would start in the hopper would be over very quickly (about three seconds). Once a fire has started in the hopper, it probably could not be put out. In this case, we would only want to protect the equipment and personnel and prevent the spread of the fire to other areas in the room.

The machine is in a barricaded room with interlocks on all access doors. There are no people in the machine area while the machine is operating and we monitor the machine by explosion-proof remote controlled TV cameras.

Using all this data, we are limiting this zone's deluge sprinkler water flow to five (5) seconds. Remember we have all the back-up systems to flow more water if needed.

We had an accidental trip of the deluge system in this tracer charge area some time ago. We "think" that a reflection off a polished brass belt buckle from an arc-welding repair about 300' away got through several "open at the same moment" doors and caused a U/V detector to dump the system. The machine was in a stopped condition at that moment.

We, of course, evacuated the area and upon "all clear" started investigative and explosives clean-up procedures. All the while timed-out deluge system was still active and was protecting our personnel.

After the clean-up and the investigation was completed, our technician shut the system down, reloaded the explosively operated water valve and we resumed production. The clean-up time was minimal, the water damage to the machine was minimal, the explosive contamination of surrounding areas was minimal and we did not compromise our water supply. More importantly, we had full sprinkler deluge protection during the whole clean up time.

Does it work, Part II

As in most explosive handling facilities, we have had some small "incidents" with explosive materials. Our barricades and shields have prevented any personnel injuries but we have suffered some minor machine damage.

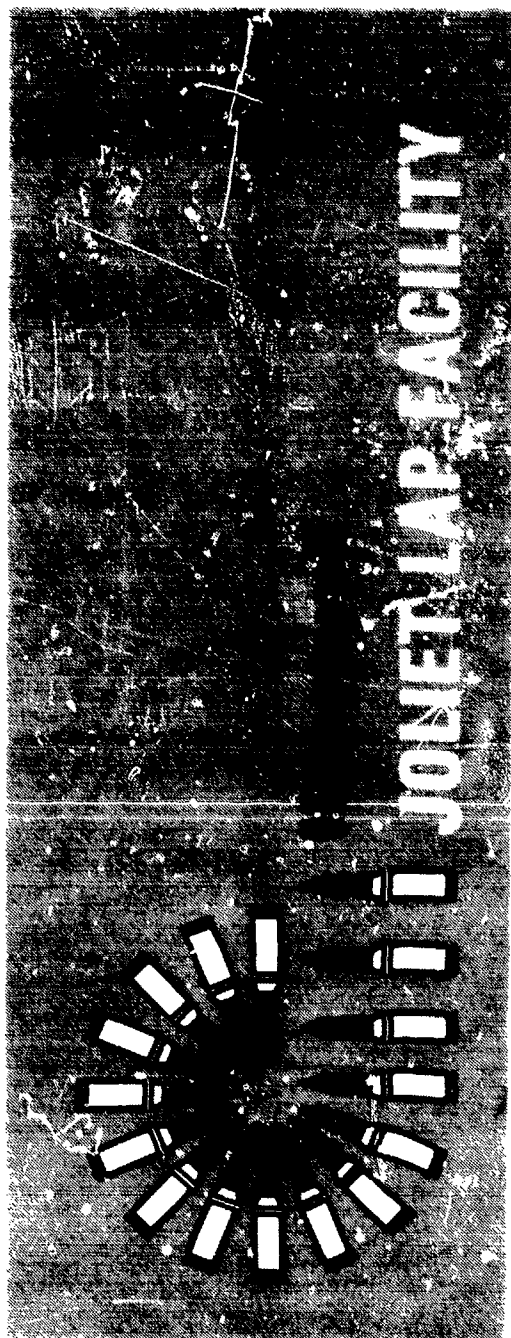
More important, to this discussion, the flow controlled deluge sprinkler systems have performed as required and have done all the things we designed into them. We have protected our people, put out the fires, prevented propagation to hoppers containing explosives, kept explosive contamination problems to a minimum, kept clean-up to a minimum, reduced machine damage, reduced structure damage and kept down time as low as possible.

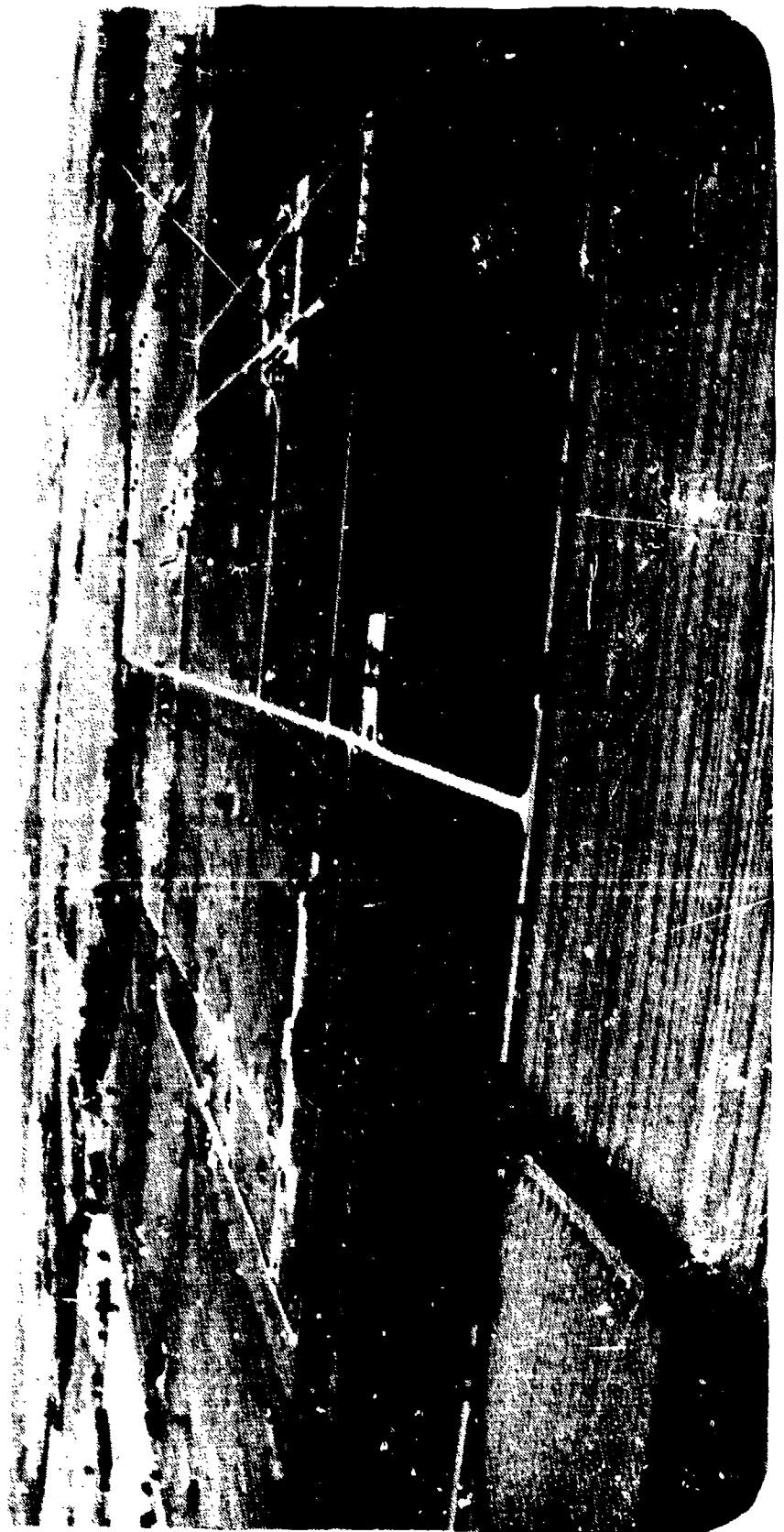
In conclusion

The timed interval control systems that we added to our recently installed deluge water sprinkler systems at Joliet, were well worth the small extra cost of the equipment and installation.

We have a safer system and a system more responsive to our needs.

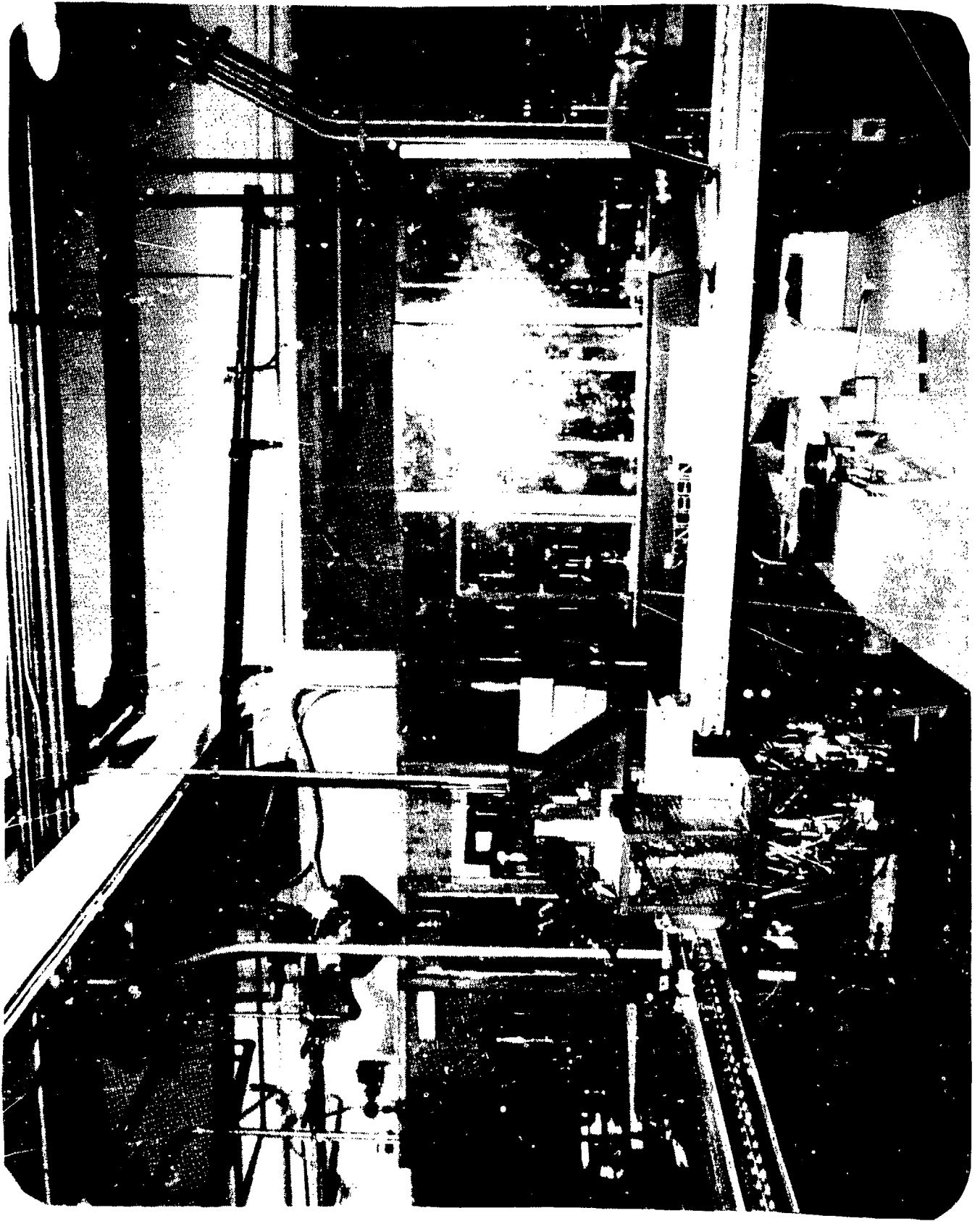
Any questions?

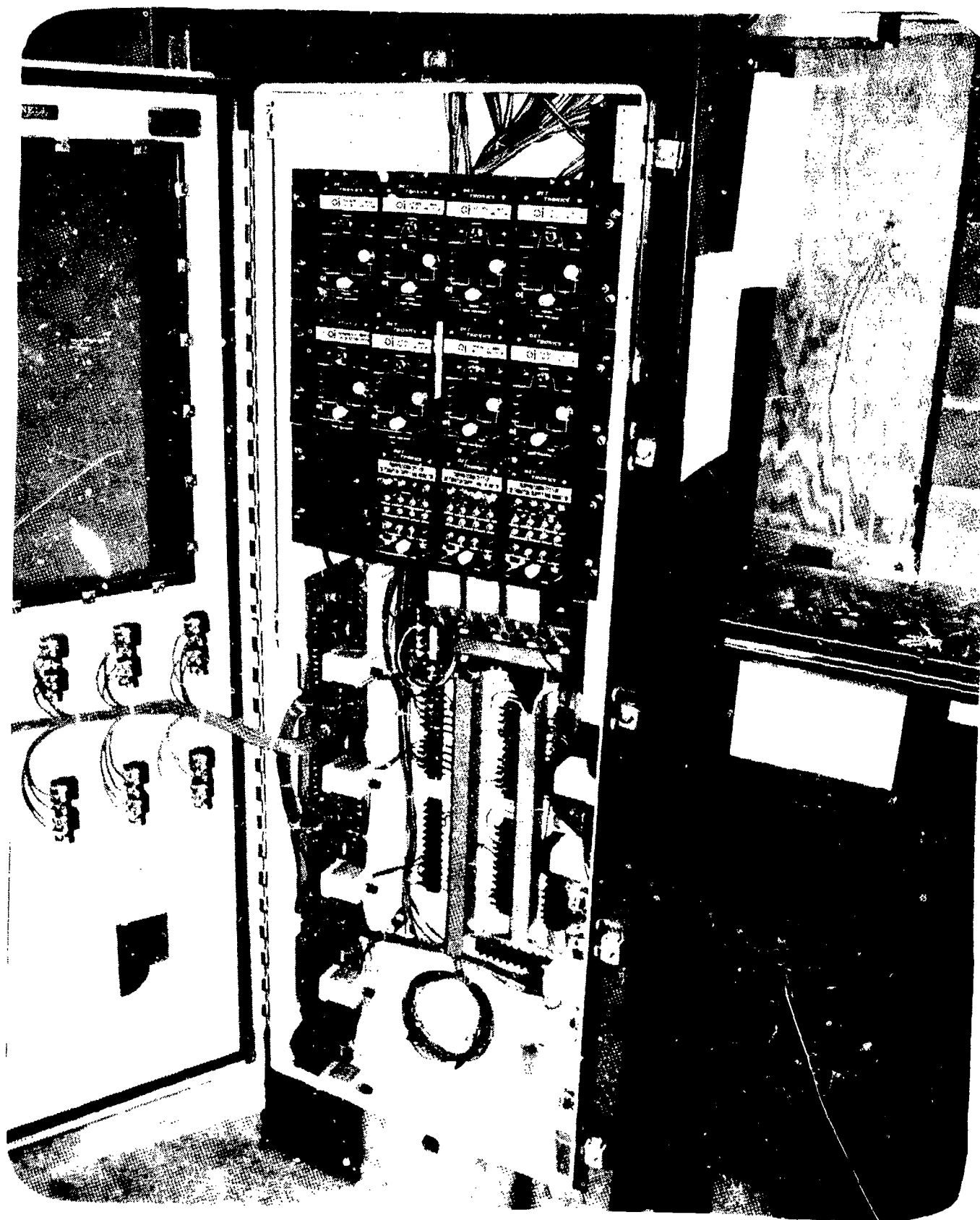


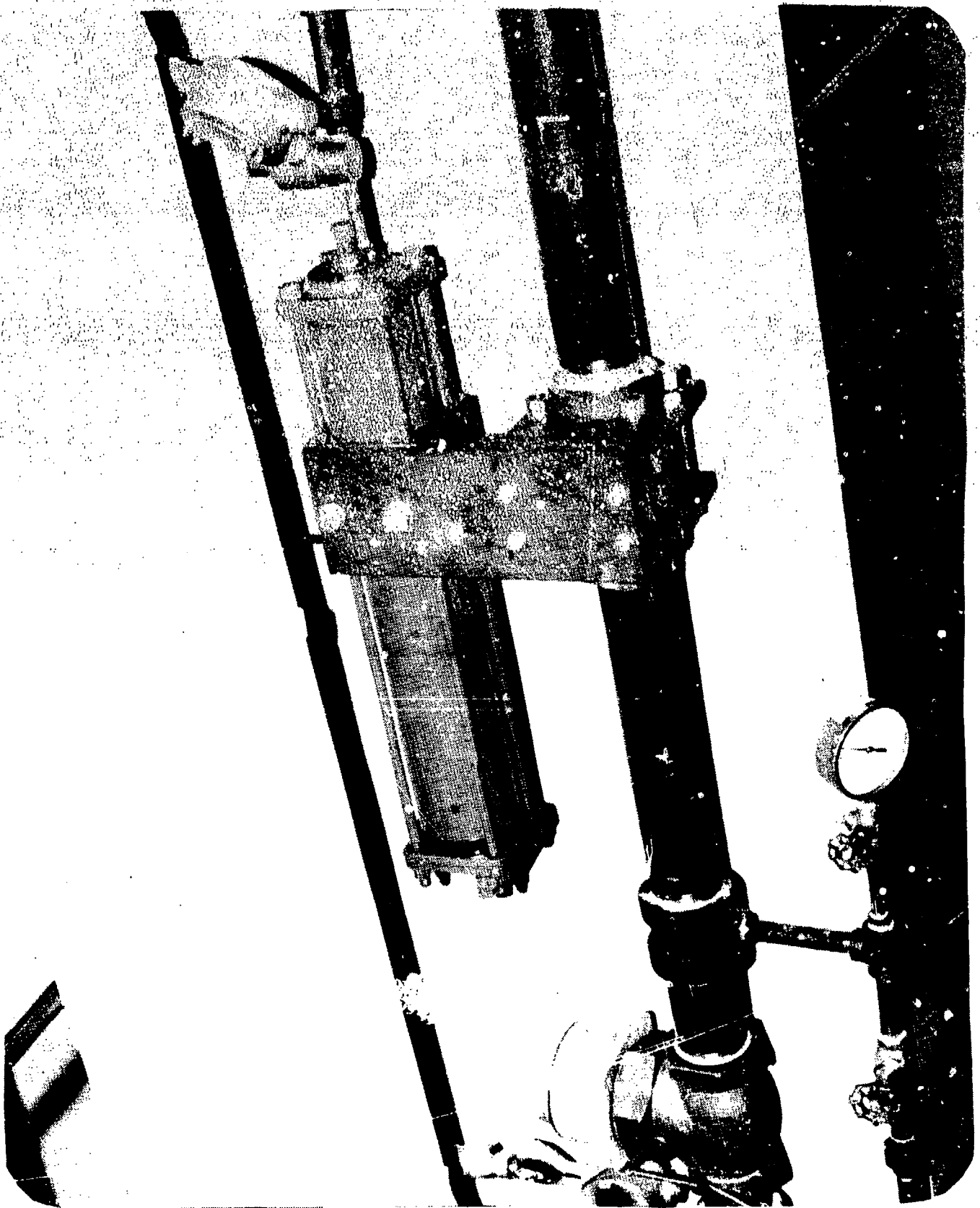


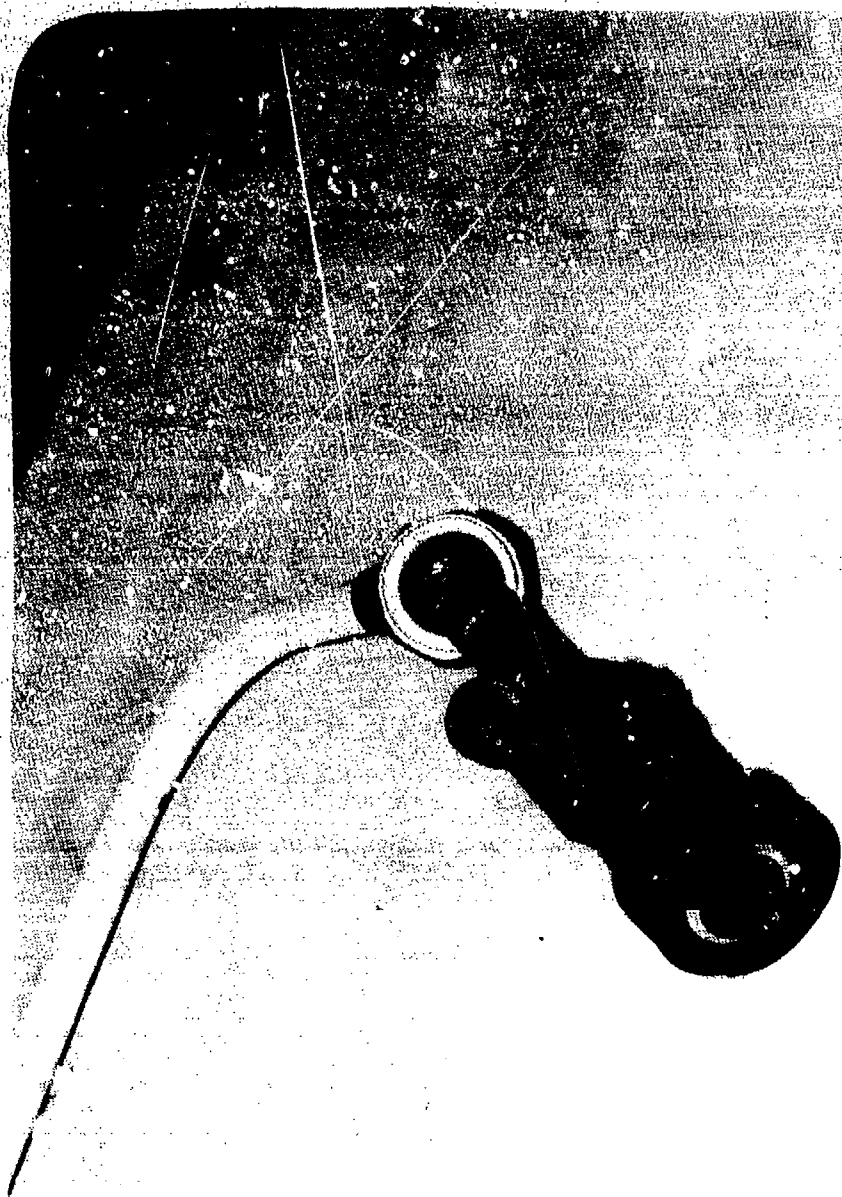


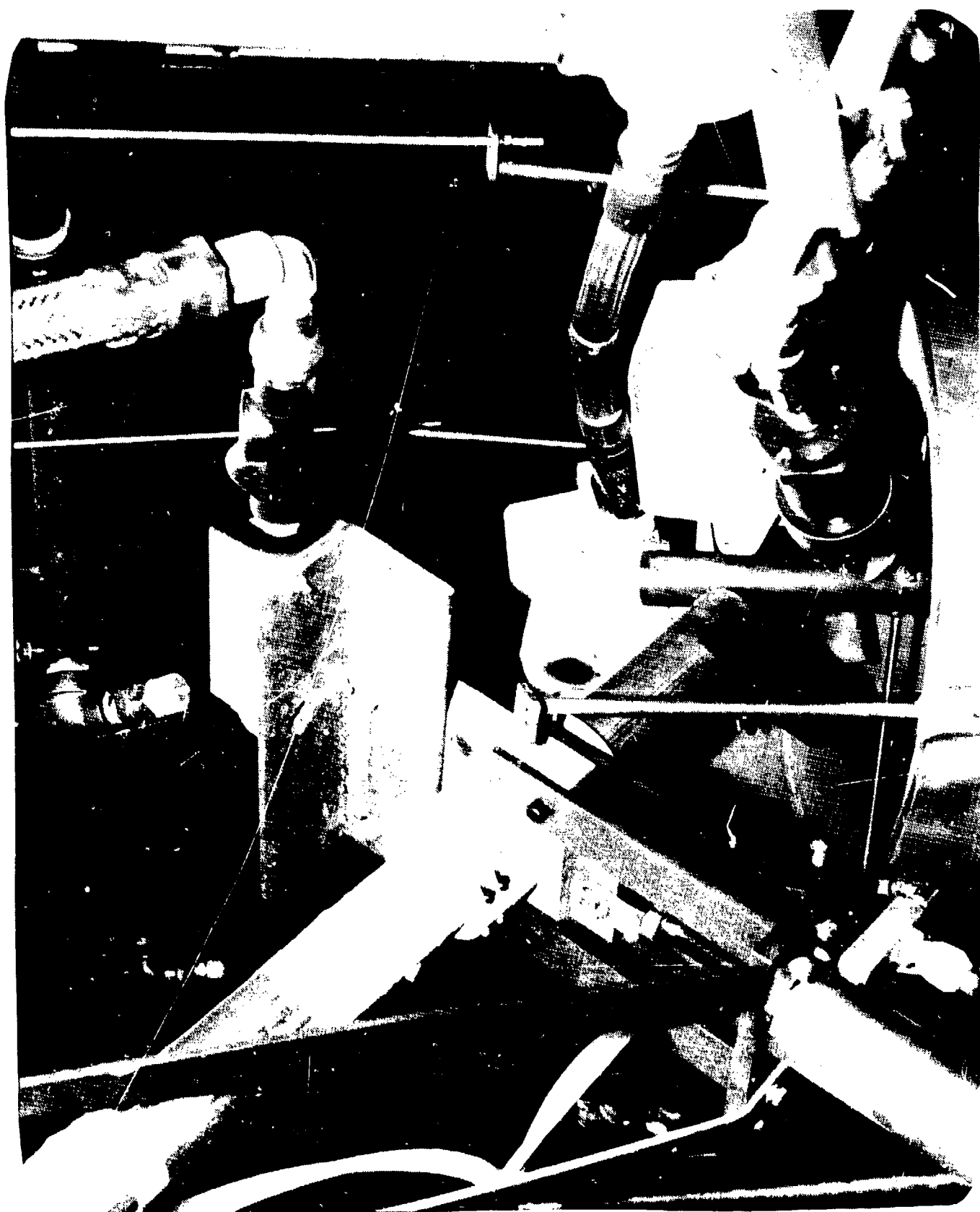
1356

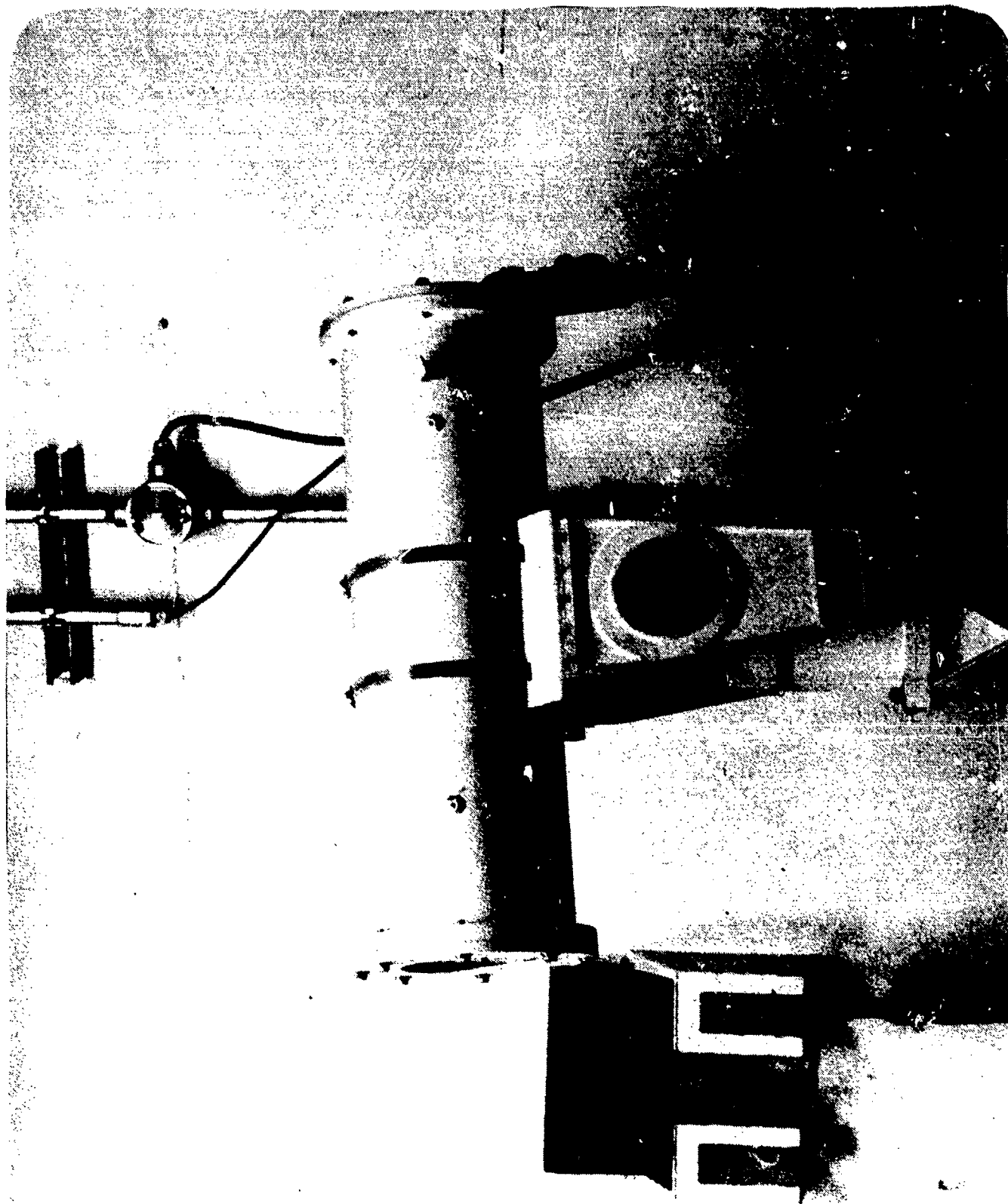














AD-P005 356

PYROTECHNIC FIRE SUPPRESSION SYSTEM EVALUATION

Joseph P. Caltagirone
U.S. Army Armament Research, Development and Engineering Center
Dover, New Jersey 07801-5001

Luis M. Vargas
Luis R. Garza
Southwest Research Institute
San Antonio, Texas

Abstract

The manufacture and processing of pyrotechnic mixes has been marked in the past by accidents due to the inherent sensitivity of the materials to stimuli such as friction, impact and static electricity discharge. A program was undertaken to evaluate the effectiveness of a fire suppression system in fighting pyrotechnic fires. This paper summarizes test results on several compositions using different deluge components and configurations and efforts that have resulted in improving the response time and effectiveness of fire suppression systems.

PYROTECHNIC FIRE SUPPRESSION SYSTEM EVALUATION

Introduction

The manufacture and process of pyrotechnic materials has been marked in the past by accidents, primarily fires caused in part by the inherent sensitivity of the materials to stimuli such as friction, impact and static electricity discharge. The day-to-day handling of pyrotechnic materials during their manufacture greatly enhances the probability of an incident and the probability of injuries and fatalities.

To improve the manufacturing of pyrotechnics from a personnel safety standpoint, either the sensitivity of the pyrotechnic must be reduced through changes in the formulation, or the human contact with the pyrotechnic can be eliminated or at least reduced through protective isolation of the equipment, or through the use of fire detection or suppression systems to extinguish or at least control any fire that may result. The use of water deluge systems in the manufacturing and processing of explosives and propellants has been extensively investigated and water deluge systems have become an integral part of explosives and propellant manufacturing. The application of water deluge systems for pyrotechnic applications however, had not received the same level of attention and experimental evaluation. This multi-year effort was therefore designed by the Army to fill this gap, i.e., to develop a water deluge system for pyrotechnics and to experimentally evaluate the effectiveness of the system. The program was divided into the following tasks: 1) Survey existing GOGO and GOCO pyrotechnic manufacturing facilities to determine what fire suppression capabilities were on line, 2) assemble a "typical" fire suppression system currently installed at the plants and evaluate its effectiveness against pyrotechnic fires, and 3) improve the response time of the fire suppression system. This paper presents an overview of the work performed as part of this program.

Survey and Test Setup

As part of this program, five facilities that manufacture pyrotechnics were visited: Longhorn Army Ammunition Plant, Lone Star Army Ammunition Plant, Lake City Ammunition Plant, Pine Bluff Arsenal and Crane Army Ammunition Activity. Of these five facilities, only Longhorn and Lone Star AAPs had any extensive type of deluge system in their manufacturing and process bays. Briefly, the types of fire suppression systems installed consisted of a manifold system with sprinkler type nozzles or protector nozzles strategically positioned over the mixers, granulators, blenders etc. Figure 1 shows a typical mixer bay used in manufacturing a magnesium based flare mix and the water deluge nozzles positioned over the mixer. The deluge system is functioned by a UV detector/controller system. Once the UV detectors have sensed a fire, the controller issues a "FIRE" alarm which closes a solid state relay thereby powering an explosive actuated valve that then releases water through the manifold and out of the nozzles. Southwest Research Institute assembled a water deluge system for experimental verification as shown in Figure 2. This system consists of a flow loop powered by a standard Hale fire pump, an in-line Primac high-speed explosive actuated valve, a manifold system with five nozzles each equipped with rupture disks or blowout caps. Figure 3 shows the assembled water deluge system with the UV detectors and a simulated mix muller. Water deluge tests were also

conducted with the pyrotechnic materials in a simulated granulator and in drying trays. Typical water delivery rates for the deluge system were 40 gpm per nozzle at line pressures of approximately 60 psi.

Experimental Evaluations

Test Plans:

The water deluge system was evaluated using various types of pyrotechnic materials: an aluminum based starter mix, a magnesium based flare mix M206 (both wet with a solvent and in a dry granulated condition), a second magnesium based flare mix (MK45), and three smoke mixes. The system was evaluated varying the following parameters:

- Type of pyrotechnic material
- Quantity of material involved
- Condition of the pyrotechnic (wet with solvent or dry)
- Ignition scenario (bottom or top ignition)
- Number of UV detectors
- Water pressure
- Nozzle spray pattern
- Deluge height

Multiple Detector Tests:

A series of tests were performed to determine the effect that the use of multiple UV detectors would have on the system response time. The UV detectors used were DET-TRONICS Corp. model DE 1777 sensors with a DET-TRONICS Corp. model 7303 controller. Small pyrotechnic charges were placed in view of the detector(s) on a drying tray and ignited using electric matches. The elapsed time required for the controller to sample and declare a fire was recorded for each test performed. Tests were conducted using one, two, and four detectors. Based on the results of the test series, it was very obvious that the use of multiple detectors improves the detection system overall response time. The controller counts UV pulses from the detectors and must reach a pre-set number of counts before it will issue a fire alarm. When multiple detectors are used, the controller will sum the UV counts transmitted from each detector thereby responding much faster than if only one detector is used because the controller must wait for that one detector to transmit all of the necessary counts.

Starter Mix Tests

A total of 11 tests were conducted using the starter mix and varying the quantity of mix, the point of ignition, the nozzle spray pattern, and the quantity of water applied. In all of the tests, the mix was contained in a typical drying tray as shown in Figure 4 and ignition of the starter mix was performed remotely using an electric match. A number of preliminary tests were performed in order to optimize the nozzle type for use in the deluge testing. Tests were performed using 45 degree spray nozzles, 30 degree spray nozzles, 15 degree vee shape nozzles and 15 degree full cone nozzles. Tests showed that the 15 degree full cone nozzles were the most effective in delivering concentrated high velocity water that could penetrate an intense fireball such as that produced by pyrotechnics. The decision was made to perform all of the starter mix tests using the 15 degree full cone nozzles,

each equipped with a gold leaf rupture disk and using two UV detectors. The deluge system was successful in extinguishing the pyrotechnic fire in each of the 11 tests. The average detection time was 221 msec after ignition of the electric match and the average Primac response time was 234 msec after ignition. The average water-at-the-nozzle time for the 11 tests was 127 msec after UV detector actuation. A summary of these tests is presented in Table 1.

Six additional tests were performed using the starter mix in a simulated mix muller as shown in Figure 5. This series of tests utilized four UV detectors and the controller was set to trigger at a more sensitive rate of 10 counts instead of the 25 previously used. The use of a high walled mixer had no appreciable effect on the response of the deluge system. The deluge successfully controlled and extinguished all 6 fires with no difficulties. The average UV detection time for these tests was 173 msec which was faster than the previous series run with only two detectors. For this series of tests, the deluge system controller was equipped with a solid state relay instead of a mechanical relay and the Primac response time was basically the detector response time i.e., the average Primac response time was the same as the average detection time, 178 msec. The average water-at-the-nozzle time was 122 msec after UV detector actuation which is very close to the average times recorded in the earlier work. Table 2 presents a summary of the results of these tests.

M206 Tests

A total of 16 tests were performed using the M206 pyrotechnic mix which is a magnesium based illuminating flare mix. Tests were conducted on the mix wet with a solvent (simulating the actual mixing conditions) and also dry and granulated into a specific size. In the actual test program, important parameters such as the following were varied: quantity of material, quantity of solvent (% ratio), water application rates, height of the nozzles from the mix, and ignition point. Throughout this portion of the test program, the nozzles on the deluge system were equipped with blow-off caps instead of the previously used rupture disks and a total of four UV detectors were used to further decrease the detector response time. All tests were performed with the mix in the simulated mix muller and ignition was accomplished using an electric match/starter mix booster combination.

Of the 16 tests performed, seven tests involved the dry, granulated M206 mix (three of these tests were performed with the deluge manifold lowered by 0.61m (2 ft)) and nine tests were performed with the M206 wet with solvent. For the seven dry mix tests, the time required by the UV system to sense the pyrotechnic fire varied from a minimum of 75 msec to a maximum of 375 msec after ignition of the electric match. The detection times for the remaining five of the seven tests were very close with a minimum time of 87 msec, a maximum of 112 msec and an average of 99.6 msec. Water-at-the-nozzle times were measured on four of the tests with the times varying from a minimum of 50 msec to a maximum of 138 msec after detector response. On all of the tests involving the dry mix, the deluge system did not respond fast enough to make a difference and the fireball lofted and burned above the manifold. The mix burned so fast and so violently that the deluge had no chance in putting out the fire. Figure 6 is a sequence of pictures of one of the tests using the dry M206 and as can be seen, the fireball lofts and burns above the manifold.

The UV detector response times for the nine tests performed using the solvent wet M206 mix varied from a minimum of 71 msec to a maximum of 238 msec after ignition of the electric match. The average response time for the nine tests was calculated to be 132 msec. If the minimum and maximum times are eliminated, the average for the remaining seven tests is 125 msec which is slightly faster than the total average time. Water-at-the-nozzle times varied from a minimum of 34 msec after fire detection to a maximum of 183 msec. The average water-at-the-nozzle time was calculated at 108 msec after detection which is approximately 17 msec slower than the dry mix times. Actual burn times for these tests varied from a minimum of 3.85 sec to a maximum of 60.1 sec. and these variations were dependant on both the water application rate and on the percentage of solvent used, where the burn times were less for those tests with the higher solvent ratio. In all of the wet mix tests the water deluge system was very effective in controlling the subsequent fires and in eventually extinguishing them. Some of the tests resulted in fires that burned for a long period of time, however the burn was a controlled burn and a very survivable one. Figure 7 is a sequence of pictures of one of the longer burning "wet" mix tests. This particular test burned for over 11 seconds. Figure 8 is a sequence of pictures showing one of the tests using actual wet mix made by SWRI. As shown in the pictures, the fire is quickly extinguished. The mesh seen in the pictures was installed around the mixer to help catch some of the mix washed overboard. The three tests performed with the lower deluge showed no appreciable change or reduction in the burn time. Table 3 presents a summary of the M206 mix (dry and wet with solvent) water deluge test results.

MK45 Flare Tests

A total of 15 tests were performed using the MK45 flare mix which is another magnesium based mix. The tests were conducted varying the quantity of mix, the shape of the pile of mix (cone shaped or flat), the water application rate, and the height of the deluge. The tests showed that the fire ball height was greatly affected by the shape of the mix prior to ignition with the cone shaped tests having the larger fireball heights. The time required by the UV detectors to sense the fires varied considerably from a minimum of 283 msec to a maximum of 829 msec. This variation is much larger than in any of the materials previously tested. The average UV response time was calculated at 490 msec after ignition of the electric match. Detection times for nine of the 15 tests were within 22% of the average time. Water-at-the-nozzle times were measured for 14 of the 15 tests and the fastest time measured was 51 msec after detection of the fire and the slowest time was 149 msec after detection. An average water-at-the-nozzle time was calculated and found to be 81 msec after detection of the fire. Eight of the 14 tests had water-at-the-nozzle times within 23% of the average time, while 13 out of the 14 tests had water-at-the-nozzle times within 37% of the calculated average. In all of the cone shaped tests, the water deluge system was ineffective in extinguishing the fire since the bulk of the mix became involved before the UV detectors could sense the fire. On those tests where the mix was in a flat configuration, the water deluge system did have an appreciable affect on the fire and some unburned residual material was recovered. Figure 9 is a sequence of pictures showing the results of one of the "flat" tests and as can be seen, the deluge does have some affect on the fire even though there is a very large initial fireball. Table 4 summarizes the results of the 15 tests with the MK45 mix.

Smoke Mix Tests

A large number of tests were conducted using three smoke mixes: green smoke, yellow smoke and HC smoke. Tests were performed with the smoke mixes in the simulated mix muller out in the open and in the mix muller in a simulated mixing bay. Two types of detectors were used, the standard UV detector and a prototype dual mode smoke/UV detector manufactured by DET-TRONICS Corp. In the tests with the standard UV detectors, only the HC smoke fires were recognized promptly. Since the actual combustion of the green and yellow smokes was rather mild yet produced vast quantities of smoke, detection of any fire did not occur until the combustion was practically over and the detectors were not shielded by the smoke. The HC smoke burned much more violently and flames were plainly visible to the detectors early in the test. Table 5 presents the results of the tests using the standard UV detector.

A total of 17 tests were performed using the dual mode smoke/UV detectors. These tests were performed in the simulated mixing bay and tests were performed with the detector in six different positions in order to maximize its effectiveness. In all of the tests with the green and yellow smoke mixes the detector was ineffective in sensing the fire. These particular mixes created large quantities of dense smoke that fooled the detector into thinking that the optics were dirty and subsequently issuing erroneous smoke "fault" alarms instead of "fire" alarms. Table 6 presents the results of the 17 tests performed with the dual mode smoke/UV detector.

Improved Deluge Design

The earlier work demonstrated that the existing deluge design, i.e., the design utilizing the Primac valve did not respond fast enough to effectively combat certain pyrotechnic fires especially those involving dry mixes. It was therefore decided to modify the existing deluge in order to speed up the response time and then experimentally evaluate these modifications to see if the system response was adequate to extinguish the dry pyrotechnic mix fires. Several "fixes" were investigated, among those being the use of a combination UV/IR detector in an attempt to speed up the detection time, and the use of explosive actuated valves at the nozzles in lieu of the standard Primac valve to speed up the water delivery time.

UV/IR Detector Tests

A prototype UV/IR detector manufactured by ARMTEC Industries, Inc. was experimentally evaluated to see if the dual mode detector was faster responding than the standard UV detector manufactured by DET-TRONICS Corp. and used on all the previous work. Comparison tests were performed using both systems and the DET-TRONICS UV detector system with multiple detectors, i.e., 4 detectors were repeatedly slightly faster than the ARMTEC dual mode detector. In the comparison tests, both systems were mounted side-by-side and subjected to the same pyrotechnic fire scenario to insure that no one system would see a different fire. The test setup is shown in Figure 10.

Explosive Actuated Valve Evaluations

The use of explosive actuated valves at the nozzles was evaluated and experimentally verified using two different dry pyrotechnic mixes and one wet with a solvent. As part of the evaluation process, manufacturers of explosive actuated valves were contacted in order to evaluate off-the-shelf valves in terms of design, effectiveness, and cost. The off-the-shelf valve shown in Figure 11 proved to be cost prohibitive so a modified explosive actuated valve was designed by SWRI. Figure 12 shows the modified valve disassembled and it consists of a commercially available rupture disk holder, a rupture disk and an explosive cap that is placed in contact with the rupture disk. Figure 13 shows the fully assembled modified explosive actuated valve. The cap, which is a directional fragmenting explosive is functioned by the UV detector controller electronics. Comparison tests between the Primac system and the modified explosive actuated valve system were performed and showed that the explosive actuated valve responded much faster than the Primac system ever could. In the previous work done with the Primac system, the Primac valve was 12 to 15 feet upstream of the manifold and due to the hydraulics involved with the system and the resistance given by the blow-off caps covering the nozzles a typical response time for water-at-the-nozzle from detection time was 120 to 150 msec. With the explosive actuated valve system at the nozzle, the water-at-the-nozzle time was reduced to approximately 5 to 6 msec which is the time that it takes the explosive cap in contact with the rupture disk to function. In effect, the water-at-the-nozzle time was reduced by over 110 msec. These results were so favorable that it was decided to experimentally evaluate the deluge system equipped with explosive actuated valves.

Explosive Valve Deluge Tests

A series of tests were performed using the improved deluge design to determine the effectiveness of the deluge in combatting dry pyrotechnic fires. Tests were conducted with the dry M206 flare mix and with the dry MK45 flare mix in a simulated granulator as shown in Figure 14 and varying the quantity of mix, the shape and the ignition point. The tests with the dry M206 used 1 lb and 3 lb of mix and were ignited at the bottom and at the top of the mix respectively. The tests with the ignition at the bottom showed that even though the deluge system responded within 50 msec after detection, the mix burned so fast laterally that by the time it had burned vertically a sufficient amount for the detectors to view the fire, the bulk of the mix was involved and was lofted such that the deluge was ineffective. Ignitions of the mix just below the surface, however were successfully extinguished without the bulk of the mix becoming involved. Tests with the MK45 flare mix also yielded similar results in that the mix would burn before the deluge had a chance to function. Figure 15 shows a sequence of pictures of a test with the M206 mix in a granulator and ignited at the bottom and as can be seen in the sequence, the event is not controlled by the deluge. Figure 16 however is a sequence of a test with M206 ignited near the surface and as can be seen, the deluge quickly extinguishes the fire.

Full Scale Wet M206 Test

A full scale test of wet M206 was tested to simulate conditions as mixed. This test involved 125 lb in a simulated mix-muller and mixing bay.

The booster was placed 3 in. from the surface of the mix, which was 5 in. deep. At 317 msec after ignition of the booster, the UV detector issued a fire alarm and the deluge functioned. The system immediately extinguished the fire which appears to have been an MKK fire before the M206 itself had a chance to get involved. If the deluge system had been slower responding, the M206 mix would have gotten involved and deluge would have taken longer to extinguish the fire and if there were no deluge system the mix would have ignited when the MKK burned off.

Conclusions

Based on the finding of the experimental program conducted, a number of conclusions were drawn:

- Nozzles with a tight spray pattern such as the 15 degree full-cone nozzles and with a high delivery rate are much more effective in penetrating a pyrotechnic fireball and in subsequently controlling and extinguishing the fire.

- The standard state-of-the-art UV detectors appear to be adequate for detecting most pyrotechnic fires ignited at or near the top of the mix. The use of multiple detectors greatly enhances the response time of the detection system. However, for some of the dry magnesium based mixes, fires especially those ignited near the bottom of the mix (primarily the deeper mixes) are not detected fast enough by current state-of-the-art detectors to allow the deluge enough time to extinguish the fire before it becomes fully involved.

- The deluge system design used in this program was very effective in controlling and extinguishing fires involving the Pine Bluff starter mix, the M206 mix wet with solvent, and the shallow depth MK45 mix (less than 1.5 in).

- The deluge system design using the explosive actuated valves responded much faster than did the design using the Primac valve. This design however, was not fast enough to extinguish the deeper dry M206 mix fires that were ignited at the bottom of the mix nor did it extinguish the deeper MK45 mix fires.

- The Southwest Research Institute modified explosive actuated deluge valve design was comparable to the commercially available valve in response time, however, in cost, the SWRI design was much cheaper.

REFERENCES

1. Vargas, L.M.; Rindner, R.; Stirrat, W., "Fire Suppression System Safety Evaluation," ARLCD-CR-83031, Dec 83.
2. Vargas, L.M.; Caltagirone, J., "Evaluation of Pyrotechnic Fire Suppression System for Six Pyrotechnic Compositions," ARLCD-CR-85006, Mar 85.
3. Vargas, L.M.; Garza, L. R.; Caltagirone, J.P., "Evaluation of an Improved Pyrotechnic Fire Suppression System," ARAED-CR-86016, Jun 86.

Table 1. Deluge Tests of Aluminum Starter Mix in Drying Trays

Test No.	Quantity of Mix	Igniter Type/Position	Nozzle Type	Engine (rpm)	Line Pressure	Flow Rate	Detector Time (msec)	Prime Valve Time (msec)	Water at Nozzle Time (msec)	Total Burn Time (sec)
1	4.54 kgm (10 lb)	BN/Top Corner	15° Pull	2100	N/A	863 liter/min (228 gpm)	279	250	308	1.75
2	6.81 kgm (15 lb)	BN/Top Corner	15° Pull	2100	N/A	829 liter/min (219 gpm)	158	171	297	1.98
3	11.35 kgm (25 lb)	BN/Top Corner	15° Pull	2100	435 kPa (63 psi)	874 liter/min (231 gpm)	182	195	342	No Video
4	11.35 kgm (25 lb)	BN/Top Corner	15° Pull	2100	455 kPa (66 psi)	916 liter/min (242 gpm)	236	251	294	5.9
5	4.54 kgm (10 lb)	BN/Bottom Center	15° Pull	2100	N/A	N/A	183	193	N/A	N/A
(Prime Detonator Failed to Fire)										
6	6.81 kgm (15 lb)	BN/Bottom Center	15° Pull	2100	469 kPa (68 psi)	923 liter/min (244 gpm)	289	223	326	0.5
7	11.35 kgm (25 lb)	BN/Bottom Center	15° Pull	2100	504 kPa (73 psi)	787 liter/min (200 gpm)	271	284	404	5.27
8	4.54 kgm (10 lb)	BN/Bottom Center	15° Pull	1900	345 kPa (50 psi)	780 liter/min (206 gpm)	263	276	346	0.43
9	4.54 kgm (10 lb)	BN/Bottom Center	15° Pull	1400	221 kPa (32 psi)	511 liter/min (135 gpm)	284	298	416	0.61
10	4.54 kgm (10 lb)	BN/Bottom Center	45° Pull	2000	407 kPa (59 psi)	537 liter/min (142 gpm)	201	214	337	18.4
11	9.08 kgm (20 lb)	BN/Bottom Center	45° Pull	1900	345 kPa (50 psi)	492 liter/min (129 gpm)	169	183	368	16.7
(One Nozzle Rupture Disk did not Function)										
(One Nozzle Rupture Disk did not Function)										

Table 2. Summary of Starter Mix Tests
in Simulated Mix-Muller

Test No.	Charge Size kg (lb)	Igniter	Engine rpm	Line Press kPa (psi)	Detector Time (msec)	Flow lit/min (gal/min)	Water Nozzle (msec)	Burn Time (sec)
1	100 gm	2 EM	N/A	N/A	222	N/A	N/A	2.53
2	2.27 (5)	2 EM	N/A	N/A	108.3	N/A	N/A	6.16
3	4.54 (10)	1 EM-BTM Corner	1800	359 (52)	176	863 (228)	314	1.12
4*	6.81 (15)	2 EM-BTM Center	1800	366 (53)	256	825 (218)	456	0.65
5	11.35 (25)	2 EM-BTM Center	1800	338 (49)	144	840 (222)	167	1.26
6	4.54 (10)	2 EM-BTM Center	1800	331 (48)	163	848 (224)	292	0.36

Table 3. Summary of M206 Mix Tests in Simulated Mix-Muller

Test No.	Detector No.	Charge Size	Igniter	Engine rpm	Line Press kPa (psi)	Detector Time (msec)	Flow lit/min (gpm)	Motor Nozzle (msec)	Burn Time (sec)
1	4 @ 1.22 m (4 ft)	2.27 kg (5 lb) Dry	2EH 1-1/2 CC MEX	1800	303.6 (44)	100.0	840.3 (222)	230	0.88
2*	2 @ 2.44 m (8 ft) w/hoods	1.36 kg (3 lb) Dry	2EH 3CC MEX	N/A	N/A	75.0	N/A	N/A	1.82
3*	2 @ 1.52 m (5 ft) w/hoods 2 @ 3.05 m (10 ft) w/o hoods	1.36 kg (3 lb) Dry	2EH 3CC MEX	1800	303.6 (44)	87.0	828.9 (219)	N/A	0.7
4*	4 @ 1.52 m (5 ft) w/hoods	2.27 kg (5 lb) Dry	2EH 3CC MEX	N/A	N/A	100.0	N/A	N/A	1.63
5*	2 @ 1.52 m (5 ft) 2 @ 2.44 m (8 ft)	0.59 kg (1.3 lb) Wet (25% MEX)	2 EH	1800	331.2 (48)	713.0	794.9 (210)	321	11.4
6*	2 @ 1.52 m (5 ft) 2 @ 2.44 m (8 ft) w/hoods	1.77 kg (3.9 lb) Wet (25% MEX)	2 EH	1800	365.7 (53)	82.4	878.1 (232)	190	3.86
7*	2 @ 1.52 m (5 ft) 2 @ 2.44 m (8 ft)	2.95 kg (6.5 lb) Wet (25% MEX)	2 EH	1800	324.3 (47)	116.0	825.1 (218)	228	22.7
8*	2 @ 1.52 m (5 ft) 2 @ 2.44 m (8 ft) w/hoods	5.90 kg (13 lb) Wet (25% MEX)	3 EH	1800	331.2 (48)	101.0	825.1 (218)	231	36.2
9*	2 @ 1.52 m (5 ft) 2 @ 2.44 m (8 ft) w/hoods	2.95 kg (6.5 lb) Wet (25% MEX)	2 EH	1400	200.1 (29)	112.0	412.6 (109)	146	60.1
10*	2 @ 1.52 m (5 ft) 2 @ 2.44 m (8 ft)	4.54 kg (10 lb) Wet (25% MEX)	2 EH	1800	385.4 (56)	71.0	821.3 (217)	176	19.5
11*	2 @ 1.52 m (5 ft) 2 @ 2.44 m (8 ft) w/hoods	2.59 kg (6.5 lb) Wet (35% MEX)	3 EH	1800	351.9 (51)	181.0	787.3 (208)	364	13.6

Table 3. Summary of M206 Mix Tests in Simulated Mix-Muller (Continued)

Test No.	Detector No.	Charge Size	Igniter	Engine rpm	Line Press kPa (psi)	Detector Time (msec)	Flow lit/min (gpm)	Meter Nozzle (msec)	Burn Time (sec)
12*	2 @ 1.32 m (5 ft) 2 @ 2.44 m (8 ft) w/hoods	5.90 kg (13 lb) Wet (35% MEK)	3 EM	1800	393.3 (57)	238.0	832.7 (220)	304	7.2
13*	2 @ 1.54 m (5 ft) 2 @ 2.44 m (8 ft) w/hoods	9.08 kg (20 lb) Wet (35% MEK)	3 EM	1800	393.3 (57)	73.0	840.3 (222)	116	11.8
14**	4 @ 1.75 m (5.75 ft)	0.454 kg (1 lb) Dry	1EM & 5 gr booster	2200	545 (79)	112.0	904.6 (239)	170	
15**	4 @ 1.75 m (5.75 ft)	0.454 kg (1 lb) Dry	1EM & 5 gr booster	2200	527.7 (83)	375.0	927.3 (246)	494	
16**	4 @ 1.75 m (5.75 ft)	1.59 kg (3.5 lb) Dry	1EM & 5 gr booster	2200	524.4 (76)	99.0	881.9 (233)	149	

NOTE: All tests were performed using the 15, Full Cone Nozzles

* Blow-off cap released prematurely and wet mix with water. Test was performed with mix still wet.

** Tests were performed with a lowered manifold.

Table 4. Summary of MK45 Flare Mix Tests

Test No.	Charge kg (lb)	Line P kPa (psi)	Flow liter/min (gal/min)	Detector Time (msec)	Water at Nozzle (msec)	Burn Time (sec)
1 Cone	0.91 (2)	426 (61.7)	729 (192.5)	416	519	1.54
2 Cone	0.91 (2)	433 (62.7)	847 (223.7)	793	942	1.5
3 Flat	1.23 (2.7)	454 (65.8)	786 (207.7)	287	387	1.12
4 Cone	1.36 (3)	471 (68.3)	806 (213)	411	510	1.17
5 Cone	2.27 (5)	460 (66.7)	806 (213)	434	521	1.59
6 Cone	2.27 (5)	466 (67.5)	825 (218)	447	527	2.0
7 Cone	2.27 (5)	460 (66.7)	806 (213)	431	483	1.66
8 Flat	2.27 (5)	483 (70.0)	825 (218)	466	531	1.67
9 Flat	2.27 (5)	449 (65)	825 (218)	339	422	2.05
10 Cone	2.27 (5)	656 (95)	988 (261)	600	675	1.55
11 Flat	4.54 (10)	662 (96)	988 (261)	721	801	2.98
12 Flat	4.54 (10)	587 (85)	924 (244)	829	882	2.77
13 Flat*	2.27 (5)	545 (79)	943 (249)	520	575	0.98
14 Cone*	2.95 (6.5)	531 (77)	882 (233)	381	432	1.18
15 Flat*	4.54 (10)	587 (85)	924 (244)	283	400	N/A

Note: Test 1 had 2 UV detectors located 1.82 m (6 ft) from center of mixer.
 Tests 2-12 had 2 UV detectors located 1.82 m (6 ft) and 2 UV detectors located 2.44 m (8 ft) from center of mixer.

• All tests were performed using the 15° Full Cone nozzles

• All tests were ignited using 1 electric match and a 5 grain booster of IMR 4227 located at the bottom center of the mix.

* Manifold lowered - UV detectors located 1.75 m (5.75 ft) from center of mix.

Table 5. Summary of Smoke Mix Tests
Using UV Detectors

Test No.	Smoke	Charge	Igniter	UV Detection Time
1	Green (10 lb)	4.54 kg Booster	1 EM & 5 gr	63.7 sec
2	Green (5 lb)	2.27 kg Booster	1 EM & 5 gr	118.0 sec
3	Yellow (5 lb)	2.27 kg Booster	1 EM & 5 gr	35.1 sec
4	Yellow (10 lb)	4.54 kg Booster	1 EM & 5 gr	10.7 sec
5	Yellow (5 lb)	2.27 kg Booster	1 EM & 5 gr	32.1 sec
6	HC (1 lb)	0.454 kg Booster	1 EM & 5 gr	425.0 msec
7	HC (1 lb)	0.454 kg Booster	1 EM & 5 gr	458.0 msec
8	HC (1 lb)	0.454 kg Booster	1 EM & 5 gr	423.0 msec

**Table 6. Summary of Smoke Mix Tests
Using Dual Mode Detector**

Test No.	Smoke	Charge	Igniter	Detector Position	Smoke/Flame Detection Time
1	Green	0.454 kg (1.0 lb)	EM & 5 gr Booster	Center over Mixer	No Detection
2	Green	0.908 kg (2.0 lb)	EM & 5 gr Booster	Centered over Mixer	No Detection
3	Yellow	0.454 kg (1 lb)	EM & 5 gr Booster	Centered in Bay Facing Mixer	Flame - 30 sec
4	Yellow	0.454 kg (1.0 lb)	EM & 5 gr Booster	Centered in Bay Facing Mixer	Flame - 194.5 sec
.5	Yellow	0.454 kg (1.0 lb)	EM & 5 gr Booster	Centered in Bay Facing Mixer	Flame - 11.6 sec
.6	Yellow	0.454 kg (1 lb)	EM & 5 gr Booster	Across Doorway	Smoke - 33.0 sec
.77	Yellow	0.454 kg (1.0 lb)	EM & 5 gr Booster	Across Doorway	Smoke - 129.2 sec
.8	Green	0.454 kg (1 lb)	EM & 5 gr Booster	Across Doorway	Smoke - 141.2 sec
.9	White	0.454 kg (1 lb)	EM & 5 gr Booster	Across Doorway	No Detection
10	Green	0.454 kg (1 lb)	EM & 5 gr Booster	Top Front Wall	No Detection
11	Yellow	0.454 kg (1.0 lb)	EM & 5 gr Booster	Top Front Wall	Smoke - 179 sec
12	Green	0.454 kg (1 lb)	EM & 5 gr Booster	Centered Across Mixer	Smoke - 140 sec
13	Yellow	0.454 kg (1 lb)	1 EM & 5 gr Booster	Centered Across Mixer	Smoke - 141 sec
14	White	0.454 kg (1 lb)	1 EM & 5 gr Booster	Centered Across Mixer	Smoke - 90 sec
15	Yellow	0.454 kg (1.0 lb)	1 EM & 5 gr Booster	Top Backwall	Smoke - 90 sec
16	Green	0.454 kg (1 lb)	1 EM & 5 gr Booster	Top Backwall	Smoke - 120 sec
17	White	0.454 kg (1.0 lb)	1 EM & 5 gr Booster	Top Backwall	Smoke - 82 sec

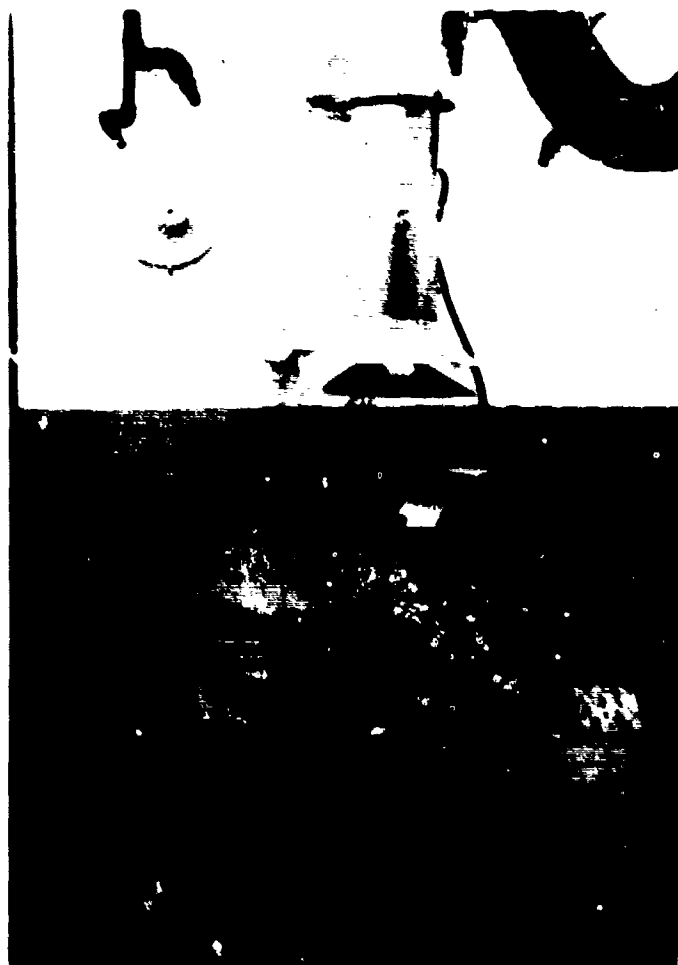


Figure 1. Typical Pyrotechnic Mixing Bay

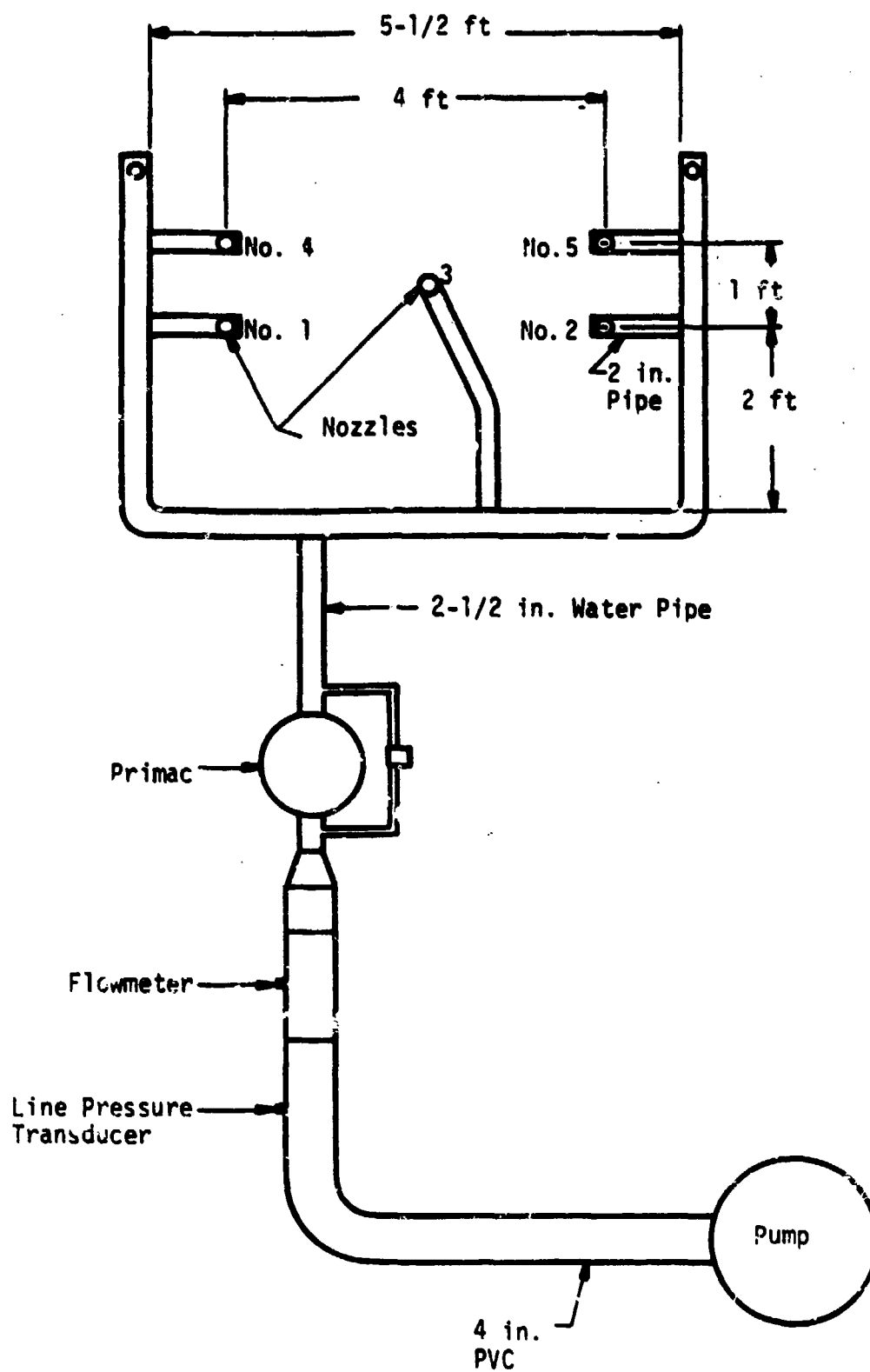


Figure 2. Flow Loop for Water Deluge System

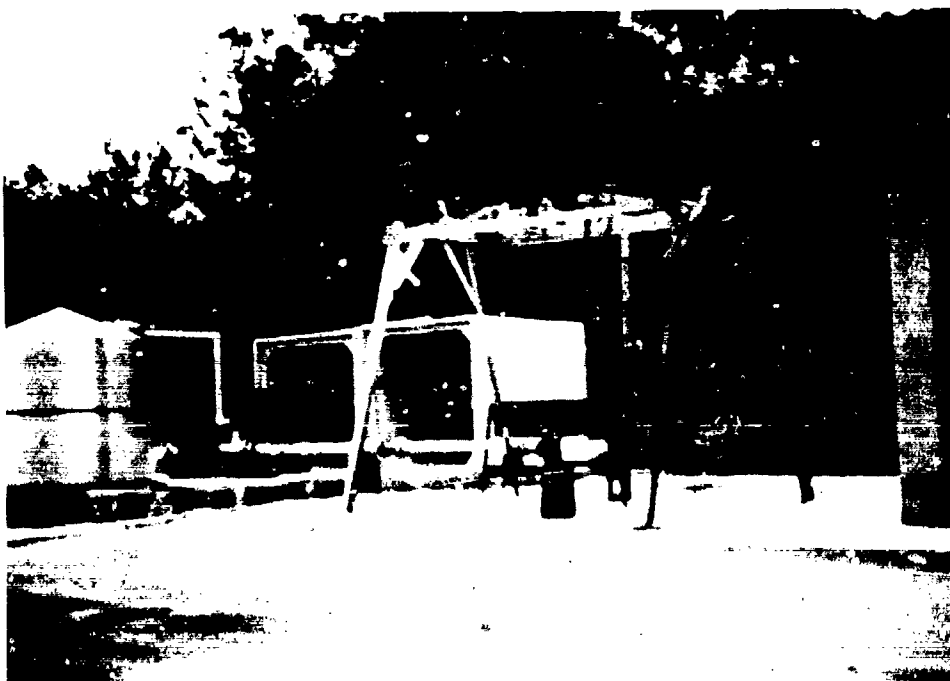


Figure 3. Assembled Water Deluge System
1383



Figure 4. Drying Tray Test Setup



Figure 5. Deluge Setup with Simulated Mix-Muller



Figure 6. Sequence of Dry M206 Test

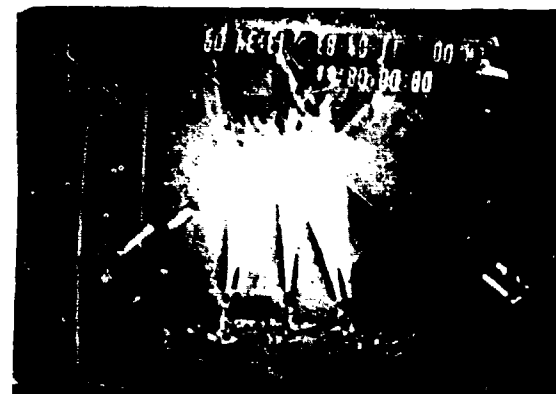
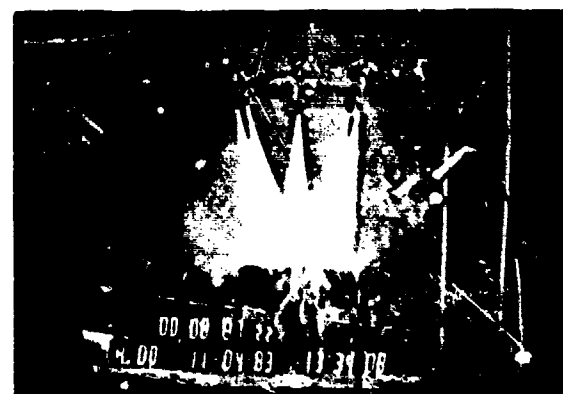
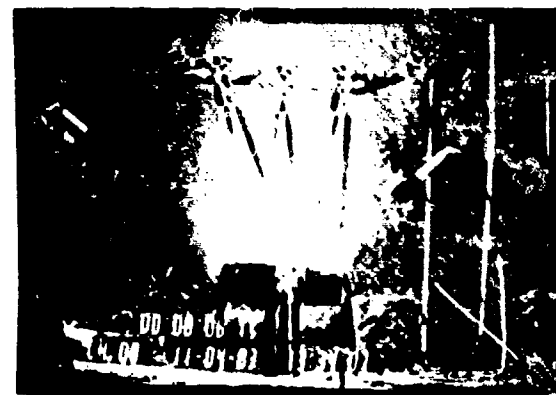
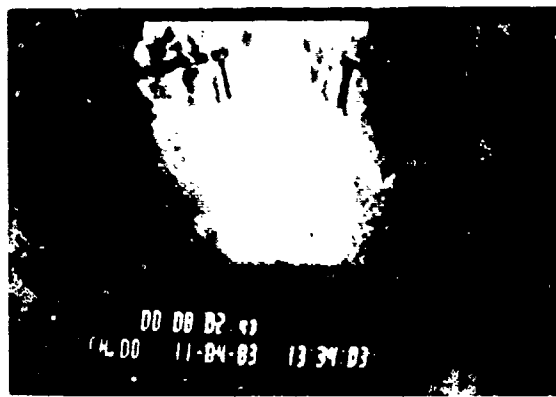
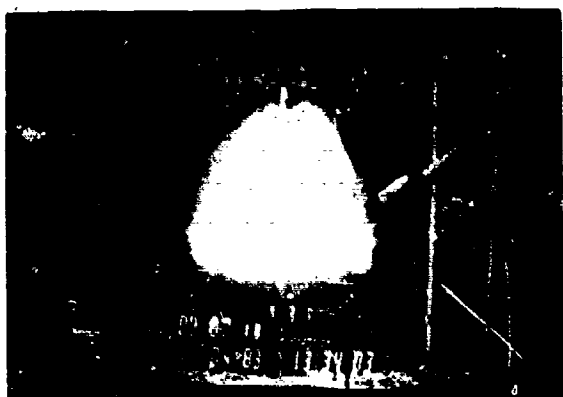
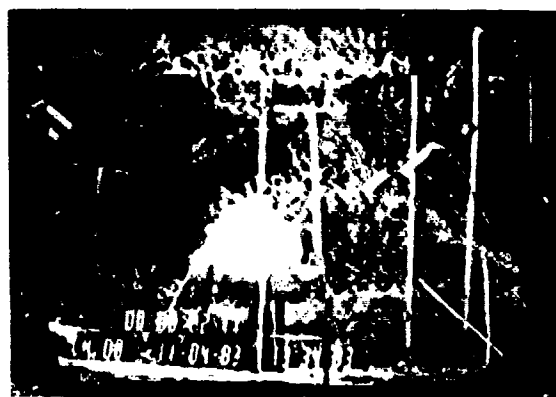


Figure 7. Sequence of M206 "Simulated Wet" Mix

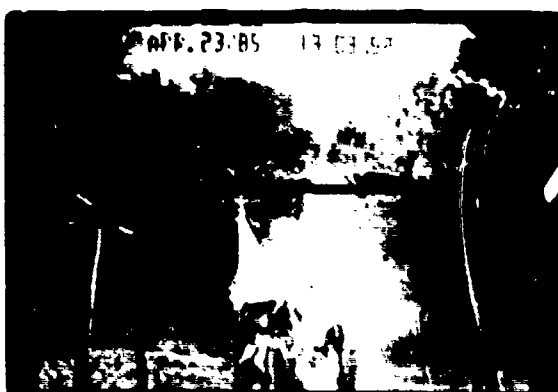


Figure 8. Sequence of Wet M206 Mix as Manufactured

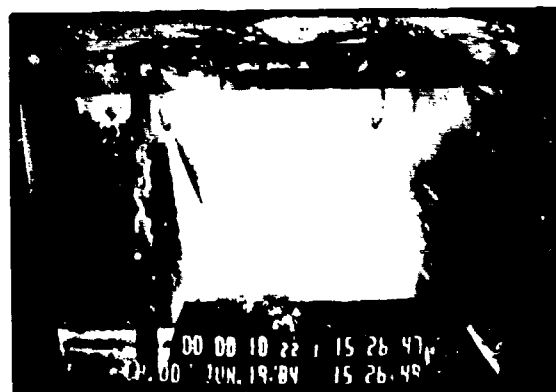
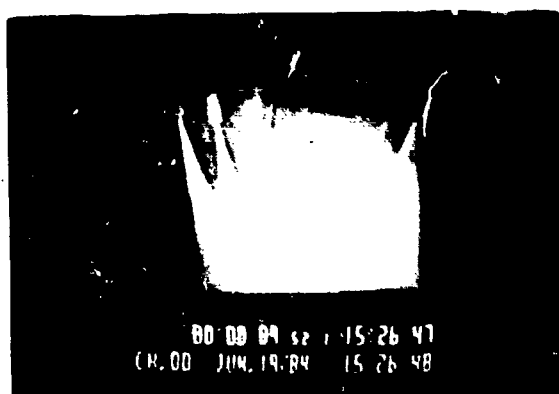
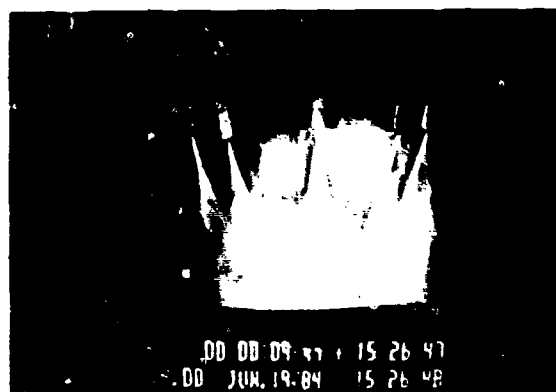
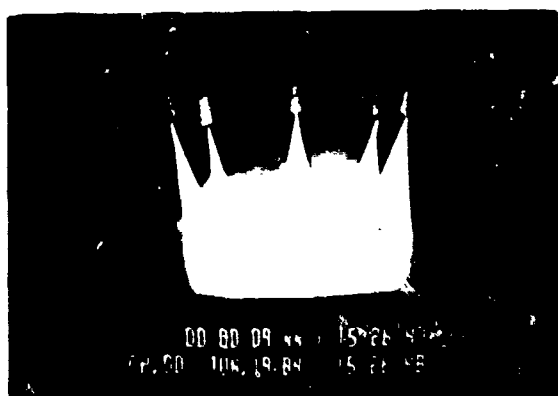
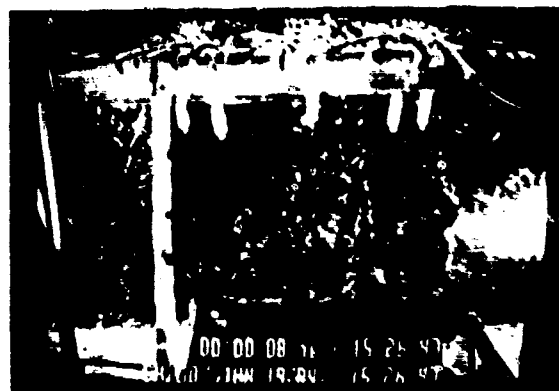
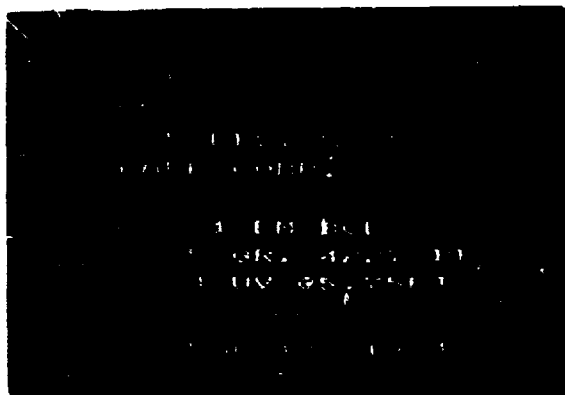


Figure 9. Sequence of MK45 Mix (Flat)

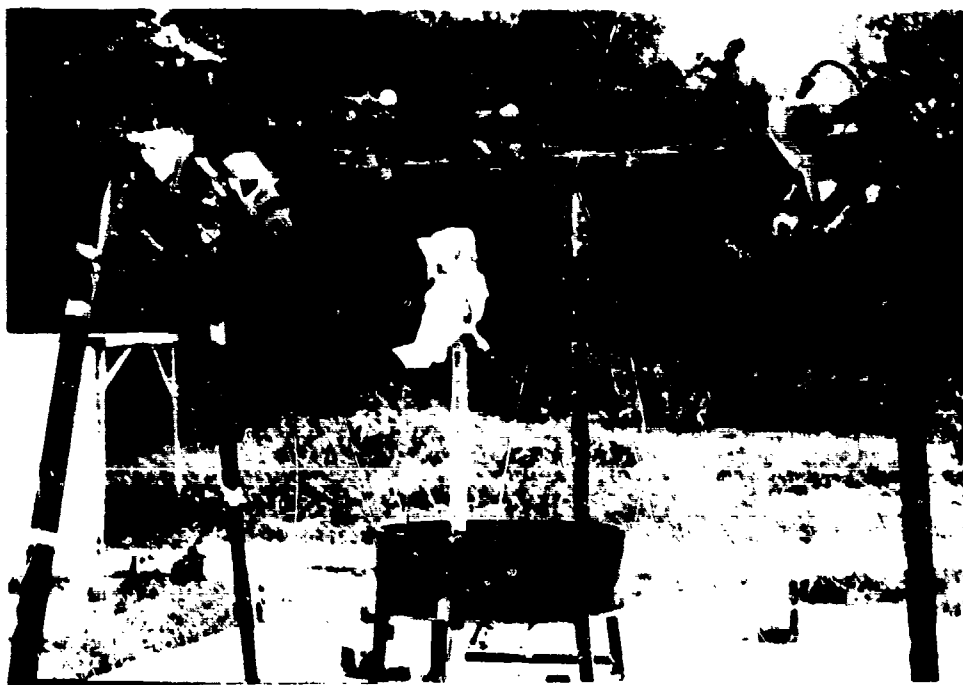


Figure 10. UV/IP Detector Test Setup

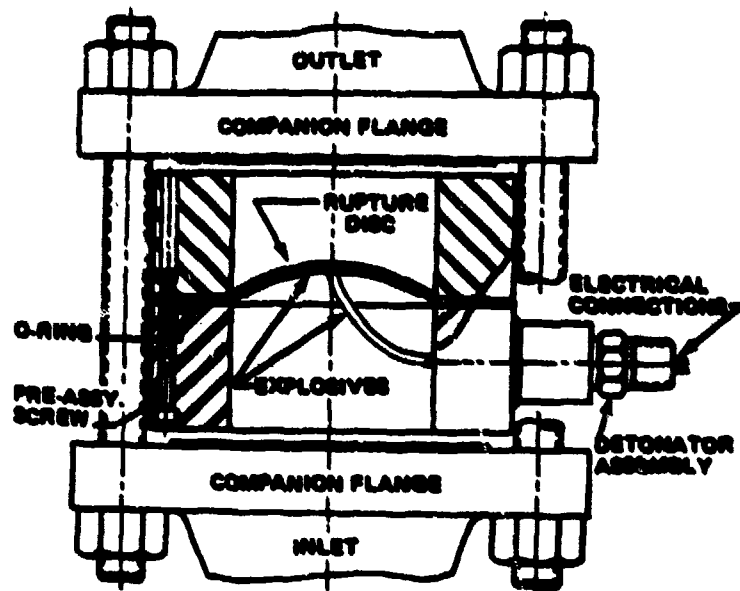


Figure 11. Fike A10 Deluge Valve



Figure 12. Threaded Rupture Disk Assembly.

(Left to Right: Nozzle, Threaded Half, Rupture Disk, Right Half, and Explosive Cap)



Figure 13. Explosive Cap in Contact with Rupture Disk



Figure 14. MK45 Composition in Simulated Granulator



Figure 15. Sequence of Dry M206 Mix in Granulator
(Bottom Ignition)



Figure 16. Sequence of Dry M206 Mix in Granulator
(Top Ignition)

AD-P005 357

PILOTEX
ULTRA HIGH SPEED DELUGE
FIRE PROTECTION SYSTEM FOR
MUNITIONS, EXPLOSIVES, PYROTECHNICS

GARY A. FADORSEN

"AUTOMATIC" SPRINKLER CORPORATION
PILOTEX SYSTEMS DEPARTMENT
1000 EDGERTON RD.
BROADVIEW HTS., OHIO 44147
(216) 526-9900

August 25, 1986

1397

DESCRIPTION

THE ~~9~~ AUTOMATIC SPRINKLER PILOTEX SYSTEM, IS AN ULTRA HIGH SPEED FIRE SUPPRESSION DELUGE. Operation from release actuation to delivery is accomplished in the millisecond range.

High pressure priming of fire main pressure and simultaneous opening of all nozzles connected to one pilot line make the PILOTEX Deluge System unique.

When a fire is detected, the solenoids are activated, pressure is relieved in the pilot line, which normally holds the valve closed in each discharge head. Because the detection is electronic and water is immediately available at the nozzle, an extremely fast response time is possible.

Each PILOTEX piping system is specially designed to cover the hazard effectively. Different discharge patterns are available simply by adapting AUTO-SPRAY nozzles to the PILOTEX head.

The basic components of the Ultra High Speed PILOTEX Deluge System are:

- PILOTEX valves with nozzles.
- High Speed Module (HSM)
- Detection System
- Solenoids

APPLICATIONS

The PILOTEX Ultra-High Speed Deluge is used where rapid

August 25, 1986

1398

discharge of water is required, such as in high hazard applications where speed of operation measured in milliseconds is needed to control or extinguish the combustion reactions of high energy fuels, liquid or solid fuel propellants, gaseous fuels, metal powders, munitions products, grains and dust handling systems and others.

Detection and operation can be achieved in various ways depending upon time requirements:

1. By Race-of-Rise - H.A.D.'s send a pneumatic pressure impulse to trip an "AUTO-SENTRY" release dumping pilot pressure. This type can be reset after operation (operation in seconds).
2. By Fixed Temperature Units, such as sprinklers, installed on pilot line at acceptable spacing. They must be of a type where the fusible element is directly connected with the water in the pilot line. These, if fused, must be replaced before restoring pilot pressure. (slowest configuration)
3. By Electronic Detection (UV, or IR or Thermal) opening a solenoid-operated relief valve. (millisecond response time)
4. By manual means - either electrically by use of push button and solenoid valve or by manually opening a ball valve, (releases pilot pressure).

The speed of operation of this system is particularly suited for the protection of special hazards. It has the advantage of a primed deluge system, it may be installed as

August 25, 1986

1399

a modular section of a larger sprinkler system, such as a deluge extension to a wet pipe system.

Fire alarm may be obtained by use of Water Motor Alarm, Water Flow Indicator, Pressure Switch on the pilot line or electronically via control panel.

August 25, 1986

1400

OUTLINE OF THE HISTORY OF HIGH SPEED SYSTEMS

I. Conventional Wet & Dry Pipe Systems

- A. Wet Systems - 3 - 5 minutes to set off sprinkler
- B. Dry Systems - Water to sprinkler head 60 seconds
after sprinkler head is set off.

II. Deluge Systems

- A. Open Head Systems - 15 seconds to 2 minutes depending
on detection.
- B. Primed Deluge System - with U.V. or I.R. detection
this system could be as fast as
1 - 2 seconds.
- C. Squib Operated Primed Deluge - with flame detectors
this system can be
made to work under 1
second.
- D. Pilot Operated Primed Deluge (Pilotex)-
with U.V. or I.R. detection, this system (if
designed and installed correctly) will give
consistent response times of well under 50
milliseconds.

Note: System response time is defined as: The elapsed time
from instant detection of flame to flow at worst case nozzle.

"AUTOMATIC" offered squib operated valve - "SPECTRONIC"
from 1960 to 1968. However, due to high maintenance,
cumbersome resetting and unreliable response times, the valve
was dropped from the "AUTOMATIC" product line.

The Pilotex nozzle originally developed as an "on-off" sprinkler
for archives in Washington, has found extensive use in munitions.

The system was then used manually or with rate-of-rise
release.

August 25, 1986

With the advent of sophisticated electrical detection and control equipment we operate using a solenoid release valve.

Features:

1. System can be set up using any of the modern electrical detection and alarm system including ultra violet, infra red, gas detectors or pressure sensors.
2. System can be discharged in the event of a total power failure.
3. System is reset with a push of a local or remote push button. No squibs to replace, no rupture discs or caps to replace, no re-priming of the system piping to be done. No replacement parts after a discharge.
4. System has full supervision of the electrical circuits unlike squib operated systems where you cannot supervise the squib.
5. At any given test pressure Pilotex will outperform any squib operated valve.
6. Due to quick reset feature a large number of systems can be tested in a short amount of time.

The following is a comparison of features of the Pilotex pilot operated system as compared to the Spectronic explosive squib operated system.

PILOTEX
(PILOT OPERATED SYSTEM)

Each head is an individual deluge valve(safety thru redundancy)

Redundant Solenoids (system will operate even if all but one solenoid fails).

SPECTRONIC
(EXPLOSIVE SQUIB OPERATED SYS)

Operation of complete system is dependent on operation of single valve.

Operation of complete system is dependent on operation of single valve.

August 25, 1986

**PILOTEX
(PILOT OPERATED SYSTEM)**

Electrically supervised for short, open and grounds.

System Reaction Time is not a function of supply pressure.

Available with mechanical manual release (electrical manual release also available). Mechanical manual release will operate without electrical power (line and/or standby).

System response time not affected by adjacent system firings.

Electrical reset (pushbutton reset achieved in seconds)

No reoccurring costs to reset system.

System can be tested and cycled quickly (less than 60 seconds per test)
No parts to replace

**SPECTRONIC
(EXPLOSIVE SQUIB OPERATED SYS)**

Electrical supervision of squib wiring for opens. Only wire is supervised. Explosive in squib cannot be supervised.

A drop in supply pressure will cause a drop in reaction time.

Manual release will not operate in the event of complete power loss.

Subsequent firing of adjacent system can cause loss of response time.

Manual reset:

1. Main must be turned off.
2. Gold rupture discs or blowoff caps must be replaced (at each nozzle).
3. Valve is then rearmed with explosive squib.
4. System is slowly filled to prime.
5. Air is vented from system.

Replacement parts needed every time system is fired.

- 2) Explosive squibs
1) Brass block
1) Break rod
plus gold disc's depending on number of nozzles.

Time required for testing is excessive, costly. Reset time between tests can go as high as 24 hours (when total air purge is necessary)

August 25, 1986

**PILOTEX
(PILOT OPERATED SYSTEM)**

No danger of handling explosives.

Automatic reset feature is available.

Indefinite shelf life.

**SPECTRONIC
(EXPLOSIVE SQUIB OPERATED SYS)**

Explosives must be handled each time valve is reset. (often in an explosive hazard area)

Not available.

Squibs have limited shelf life and must be rotated and/or replaced.

August 25, 1986

1404

PILOTEX VALVE SPECIFICATION

DESCRIPTION

The PILOTEX Pilot operated valve is a discharge device that incorporates a pressure differential valve.

The PILOTEX valve uses pilot pressure to seal off supply pressure. When pilot pressure is relieved, all PILOTEX valves connected to the one pilot line open instantly and simultaneously. When pilot pressure is restored, the nozzles close.

A PILOTEX valve consists of two-piece body threaded together and sealed with an O-ring. The upper body has a 1/2" NPT male connection for installation in standard pipe line fittings, and a 1/4" NPT female connection for the pilot line. It is through this pilot line connection that the cylinder and poppet that make up the differential valve receive pilot pressure. The poppet has a teflon face which seats against the orifice located in the lower body half of the valve. The lower body is interchangeable to accomodate various types of discharge devices.

*The male adapter is often used where there is a need for flange mount or to directly flood a melt kettle or mixer. The female adapter is most often used with the auto spray nozzles described later.

APPLICATIONS

The PILOTEX valve is used where rapid discharge of water is required, such as high hazard applications where speed of

August 25, 1986

1405

operation measured in milliseconds is needed to control or extinguish the combustion reactions of high energy fuels, liquid or solid fuel propellants, gaseous fuels, metal powders, munitions products and others.

OPERATION

When the PILOTEX valve is in its normally closed position, the poppet is held against the discharge orifice by the pressure within the poppet cylinder. When pilot line pressure drops, the fire main pressure overcomes the differential, forces the poppet up, and instantly starts full discharge.

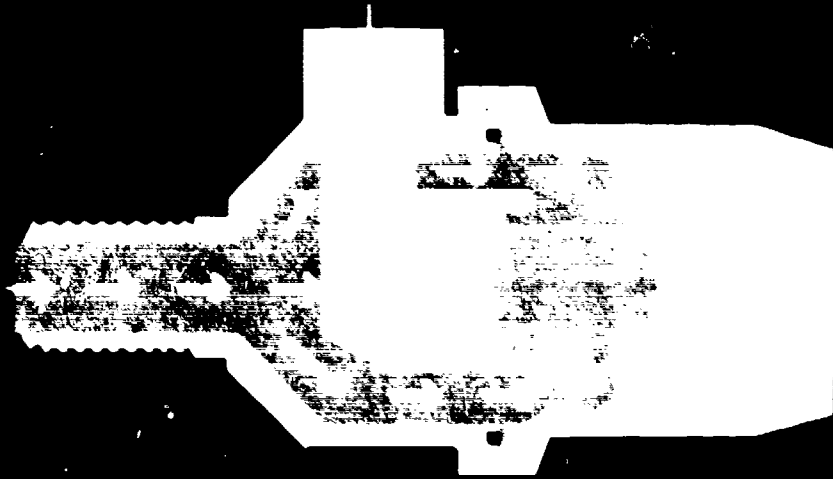
When pilot pressure is restored, the poppet reseats even against fire main pressure.

August 25, 1986

PILOTEX ULTRA HIGH-SPEED VALVE

Supply
(At System Pressure)

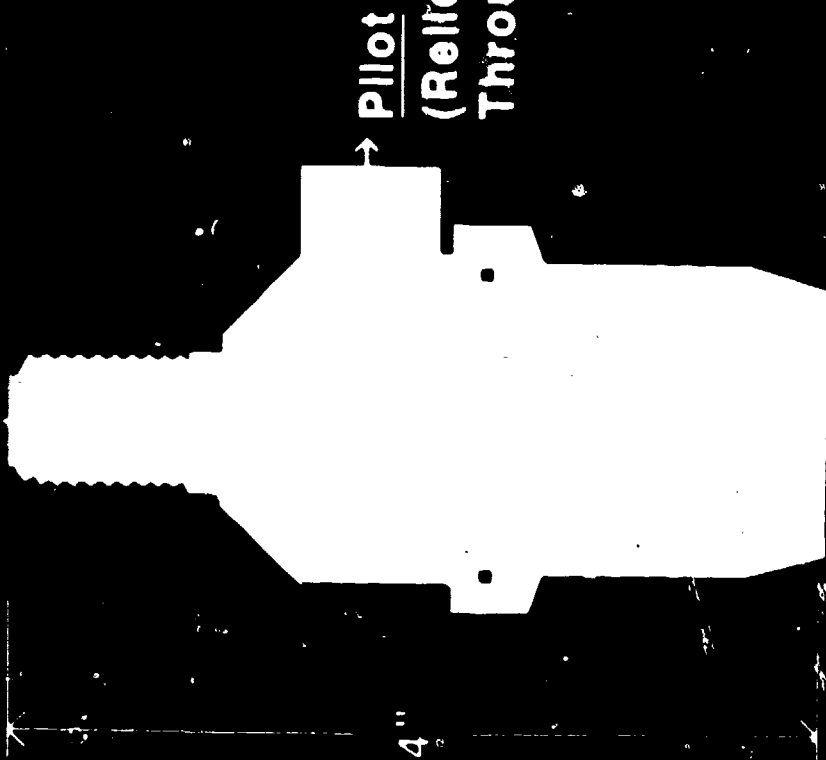
Pilot
(At System Pressure)



VALVE
CLOSED

PILOTEX ULTRA HIGH-SPEED VALVE

Supply



Pilot

(Relieve Pressure
Through Open Solenoid)

Flow To Hazard

VALVE
OPEN

August 25, 1986

PILOTEX VALVE SPECIFICATION (continued)

9000 SERIES (MALE)

3/4" 165-9075* upper body 165-0001
lower body 170-0020

1" 165-9100* upper body 165-0001
lower body 170-0021

1 1/4" 165-9125*
upper body 165-0001
lower body 170-0022

5000 SERIES (FEMALE)

3/4" 165-5075* upper body 165-0001
lower body 165-0020

1" 165-5100* upper body 165-0001
lower body 165-0021

1 1/4" 165-5125*
upper body 165-0001
lower body 165-0022

PILOTEX ULTRA HIGH SPEED VALVE PARTS LIST

165-0001	Upper Body Half
165-0020	3/4" Female Lower Body Half
165-0021	1" Female Lower Body Half
165-0022	1 1/4" Female Lower Body Half
170-0020	3/4" Male Lower Body Half
170-0021	1" Male Lower Body Half
170-0022	1 1/4" Male Lower Body Half
170-0019	Unmachined Male Body Lower Half
165-006	Brass Poppet Back
C5165-006	Poppet Assembly
1419189	"O" Ring for Poppet 3/32 x 5/8 x 13/16 (Buna -N, Teflon Coated)
1600117	"O" Ring for Body half Seal 1/16 x 1 1/2 x 1 5/8 (Buna -N)

*NOTE: All valve assemblies include: Poppet assembly, carton, label, upper/lower body halves, "O" ring for body half seal and Poppet "O" Ring (poppet "O" ring should be removed for munitions applications).

August 25, 1986

1409

AUTO-SPRAY SPECIFICATIONS

Fires involving flammable liquids are usually speedy, violent and stubborn to extinguish. Ordinary methods of fire protection are not effective.

"AUTO-SPRAY" is the most efficient method of applying water on such hazards. The Auto-Spray nozzle provides a high velocity directional spray. It is designed to impart sufficient velocity to the water spray to prevent dissipation of discharge before it reaches the surface to be protected. Interior spiral deflectors and a center jet break the water into the directional full cone spray.

"AUTO-SPRAY" NOZZLES are the high velocity solid cone type, and are available in the following designations or categories to suit specific requirements.

- NA - Narrow Angle
- MA - Medium Angle
- WA - Wide Angle
- LT - Long Throw
- F - Flat Type

"AUTO-SPRAY" NOZZLES are designed primarily for use with Pilotex systems operated by flame detection, but may be actuated by vapor, smoke, rate of rise, electronic or photo-electric detection units. They do not employ a fusible link arrangement, unless used with fusible link in the pilot system.

Possible objectives of an "Auto-Spray" system as per NFPA #15 are:

August 25, 1986

1410

AUTO-SPRAY SPECIFICATIONS

- a. Extinguishment of fire
- b. Control of burning
- c. Exposure protection
- d. Prevention of fire

"AUTO-SPRAY" is designed to satisfy these objectives by producing a coherent, uniform pattern which can be aimed at the specific area to be protected.

"AUTO-SPRAY" nozzles have relatively large water ways which make clogging from foreign material unlikely. It is therefore not necessary to remove and clean each nozzle after operation.

The internal construction of the "AUTO-SPRAY" NOZZLE is such that a stream of water entering the nozzle is split into two segments. The first segment is directed by turbine vanes at the second segment, which flows straight through the nozzle in such a way that a controlled turbulence is produced at the orifice and breaks up the stream. The arrangement and number of these internal vanes produces the great variety of available patterns, and also atomizes the water spray so that uniform discharge throughout the pattern can be achieved.

All nozzles are shipped individually packed in small cartons.

Nozzles are available for special application from most machineable materials at extra cost. Contact factory on specific materials, availability and delivery.

August 25, 1986

1411

AUTOSPRAY NOZZLES

<u>NOZZLE NUMBER</u>	<u>TYPE</u>	<u>PIPE CONN. MALE</u>	<u>PIPE CONN. FEMALE</u>	<u>ANGLE OF PATTERN</u>	<u>INVENTORY CODE NO.</u>
5NA	Narrow Angle	3/4	---	60	1415050
7NA	Narrow Angle	3/4	---	60	1415051
8NA	Narrow Angle	3/4	---	60	1415052
10NA	Narrow Angle	3/4	---	60	1415053
12NA	Narrow Angle	3/4	---	60	1415054
14NA	Narrow Angle	3/4	---	60	1415055
8MA	Medium Angle	1	---	90	1415058
13MA	Medium Angle	1	---	90	1415059
15MA	Medium Angle	1	---	90	1415060
19MA	Medium Angle	1	---	90	1415061
22MA	Medium Angle	1	---	90	1415062
26MA	Medium Angle	1 1/4	---	90	1415066
28MA	Medium Angle	1 1/4	---	90	1415067
38MA	Medium Angle	1 1/4	---	90	1415068
10WA	Wide Angle	1	---	120	1415063
14WA	Wide Angle	1	---	120	1415064
18WA	Wide Angle	1 1/4	---	120	1415069
29WA	Wide Angle	1 1/4	---	120	1415070
15LT	Long Throw	1	---	40	1415056
22LT	Long Throw	1	---	40	1415057
31LT	Long Throw	1 1/4	---	40	1415065
187 F	Flat Type	1/4	1/4	11 x 60	N.C.
218 F	Flat Type	1/4	1/4	11 x 60	N.C.
250 F	Flat Type	3/4	---	11 x 60	1415001
375 F	Flat Type	3/4	---	11 x 60	1415002

August 25, 1986

1412

AUTOSPRAY NOZZLES

K-FACTORS OF PILOTEX SPRINKLER WITH MODEL 165
(FEMALE THREAD) ADAPTOR AND AUTO-SPRAY NOZZLES

<u>NOZZLE</u>	<u>K-FACTOR NOZZLE ONLY</u>	<u>K-FACTOR WHEN USED WITH PILOTEX SPRINKLER ADAPTER</u>
5NA	0.9	0.8
7NA	1.2	1.1
8NA	1.4	1.3
10NA	1.8	1.6
12NA	2.2	2.0
14NA	2.6	2.4
8MA	1.5	1.4
13MA	2.3	2.0
15MA	2.7	2.4
19MA	3.4	2.9
22MA	4.0	3.6
26MA	4.8	3.8
28MA	5.1	4.2
38MA	7.0	4.7
10WA	1.8	1.5
14WA	2.6	2.4
18WA	3.3	3.2
29WA	5.3	4.4
15LT	2.8	2.5
22LT	4.1	3.2
31LT	5.7	4.4
250F	1.4	1.3
375F	3.1	2.9

August 25, 1986

SPECIFICATIONS SOLENOIDS

DESCRIPTION

Solenoids are 2-way, normally closed internal pilot operated solenoid valves. Valve bodies and bonnets are of brass construction.

The solenoids are equipped with an enclosure which is designed to meet NEMA type 4, watertight, NEMA type 7 (Cor D) Hazardous Locations - class I, Group C or D and NEMA type 9 (E, F, or G) Hazardous Locations - class II, Groups E, F, or G.

OPERATION

Normally closed: Valve is closed when solenoid is de-energized and opens when solenoid is energized.

POSITIONING/MOUNTING

This valve is designed to perform properly when mounted in any position. However, for optimum life and performance, the solenoid should be mounted vertical and upright so as to reduce the possibility of foreign matter accumulating in the core tube area.

PIPING

Connect piping to valve according to markings on valve body. Apply pipe compound sparingly to male pipe threads only; if applied to valve threads, it may enter the valve and cause

August 25, 1986

1414

operational difficulty. Pipe strain should be avoided by proper support and alignment of piping. When tightening the pipe, do not use valve as a lever. Wrenches applied to valve body or piping are to be located as close as possible to connection point.

IMPORTANT: For the protection of the solenoid valve, install a strainer or filter suitable for the service in the pilot line. Periodic cleaning is required depending on the service condition.

WIRING

Wiring must comply with Local and National Electrical Codes. Housings for all solenoids are provided with connections for 1/2 inch conduit. The general purpose solenoid enclosure may be rotated to facilitate wiring by removing the retaining cap or clip. CAUTION: When metal retaining clip disengages, it will spring upwards. Rotate to desired position. Replace retaining cap or clip before operating.

August 25, 1986

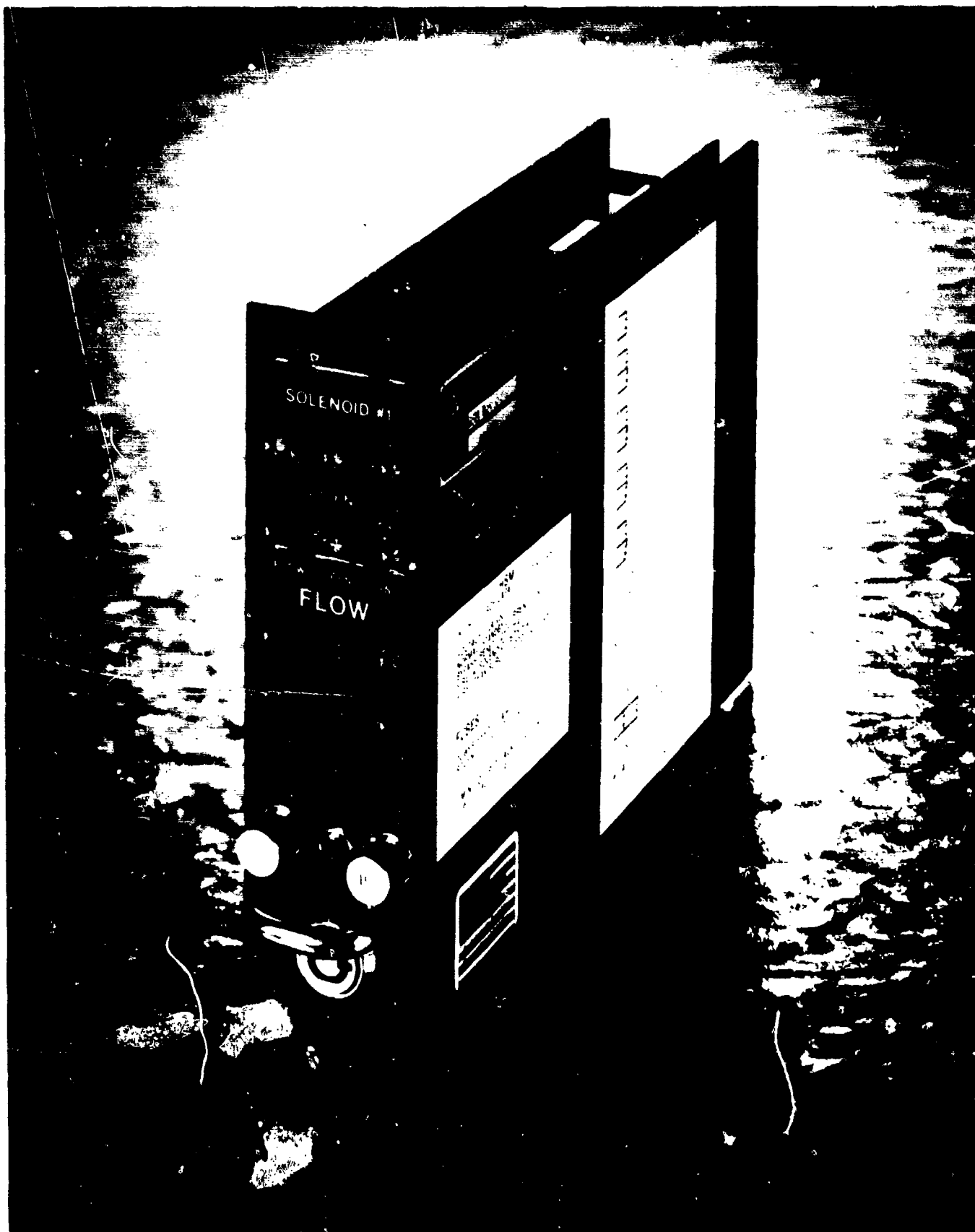
1415

SPECIFICATIONS
HIGH SPEED MODULE (HSM)

High Speed Modules (HSM): High speed modules shall be solid state modular 19" rack mountable units. They shall be specifically designed to interface between the UV zone controllers and the pilot valve solenoids. HSM's shall supervise solenoid wiring for shorts, opens and grounds. They shall monitor the UV zone controllers for fault and fire conditions. HSM's shall also monitor manual pull stations, flow switches, pressure switches and tamper switches. HSM during fire conditions shall provide a high voltage pulse to operate the pilot solenoid valve. Relay output circuit shall be form C rate 3 amperes. They shall have replaceable fuses on the front panel in both the input power feed circuit and the pilot solenoid circuit. HSM's shall have LED status lights on the face for fault conditions, fire conditions and manual power on conditions. They shall also be equipped with a timing test plug on the front face. HSM's shall be suitable for 24 VDC with a maximum power draw at 30 watts. Furnish Automatic Sprinkler #HSM.

August 25, 1986

1416



August 14th 25, 1986

SPECIFICATIONS
HIGH SPEED MODULE (HSM) (continued)

Solenoid Resistance Approximately 50 ohms.

End of Line Resistance 10 K Ohms.
(at auxillary device)

Relay output contacts rated a 3 Amps.

Circuitry: Solid State C-MOS logic and discrete switching components.

DC-DC Converter output 180 VDC.

Fuses: (One spare of each on Main Circuit Board)

Power Feed 2 Amp
(Microtype)

Solenoid Circuit 1 Amp
(Microtype)

VOLTAGE: 24 VDC
NORMAL/STANDBY CURRENT: 210ma
BYPASS/RESET: 250ma
FIRE W/SOLENOID: 520ma
FIRE - PEAK SURGE: 1.2 amp (instantaneous)
LAMP TEST: 400ma

TIMING OUTPUT JACK: 100ms
(open collector to ground)

CURRENT DRAW FROM INPUTS: 10ma

CAUTION!!
STATIC SENSITIVE CMOS CIRCUITRY
DO NOT REMOVE COMPONENTS FROM SOCKETS

DO NOT PLUG IN WITH POWER ON

OBSERVE HANDLING PROCEDURES FOR STATIC SENSITIVE EQUIPMENT

PHYSICAL DIMENSIONS

Height 177mm. (7")
Width 50mm. (2")
Depth 245mm. (9 3/4")

Shipping Weight 1.2 kilograms (2.5pounds)plus packaging

August 25, 1986

1418

HIGH SPEED MODULE (HSM)

FEATURES

The front panel of "AUTOMATIC" SPRINKLER'S High Speed Module contains ten light emitting diodes. (L.E.D.'s)

When illuminated, the six amber L.E.D.'s indicate fault conditions within the system. The two red L.E.D.'s indicate a fire condition and the two green L.E.D.'s indicate a normal power on condition. The common fault L.E.D. indicates any module fault and external fault if so connected.

Lamp test pushbutton illuminates all L.E.D.'s. In addition to the lamp test pushbutton provided on each HSM, a remote lamp test feature enables all high speed modules inside an enclosure to be lamp tested from a single pushbutton switch mounted on the outside of the enclosure.

The miniature jack on the front of the HSM is used to operate the solid state timer during system time tests. It may also be used for chart recorders, or monitors if required.

The timing jack is an open collector to ground rated at 100 ma at 50 volts.

The timing output jack triggers the timer to start at the same instant the controller identifies the presence of flame, a flow switch at the PILOTEX nozzle stops the timer, thus measuring system response time.

August 25, 1986

1419

Digital timers are available from "AUTOMATIC" SPRINKLER CORPORATION OF AMERICA.

Total supervision of solenoids circuits. The HSM monitors for shorts, opens and grounds.

Two Form C fire relay outputs for Auxillary use.

Two Form C fault relay outputs for Auxillary use. The fault relays are normally energized so a loss of power would also cause a fault condition.

Normal/bypass key switch-disarms system for maintenance and testing.

Dual terminal strip for convenient daisy chain wiring.

Front mounted fuses.

Spare fuse holder located on main circuit board.

Interchangable identifier windows for easy labeling of L.E.D.'s, zones, buildings, etc.

Automatic reset option available.

August 25, 1986

1420

PORTABLE HIGH SPEED DELUGE

"AUTOMATIC" SPRINKLER has developed a portable high speed deluge unit capable of delivering water to the nozzles at well under 50 milliseconds. The system is designed to be supplied as a self-contained unit. Portable by use of casters or towmotor.

We believe this type of system could be very useful in the munitions industry. Since you have a better idea of your requirements, we would like to have your comments and recommendations. Please fill out the following form and send it to "AUTOMATIC" SPRINKLER along with your added comments.

The following is a brief description of the unit.

DESCRIPTION

The "AUTOMATIC" SPRINKLER Portable High Speed Deluge is a completely self-contained fire detection and suppression system. This portable unit is capable of delivering water at the nozzle well within 50 milliseconds from time of detection. The unit is designed to be portable either by use of casters or towmotor. Detection is accomplished by the use of ultra-violet detectors coupled to the Detronics 7404 ultra-violet controller. The suppression system utilizes "AUTOMATIC" SPRINKLER Pilotex nozzles which are actuated by solenoid release. The solenoids are supervised and energized with the "AUTOMATIC" SPRINKLER CORPORATION'S High Speed Module (HSM).

August 25, 1986

1421

The unit's water supply is approximately 100 gallons and is delivered by pressurized nitrogen gas at approximately 150 pounds.

All electronic components are explosion-proof rating. This system is supervised for low battery power, low water supply and low pressure. The detectors and solenoids are electrically supervised. The detector lenses are optically supervised and checked approximately every second, automatically.

The unit presently utilizes four (4) adjustable (moveable) nozzles and two (2) UV detectors also moveable.

SEQUENCE OF OPERATION

Upon sensing ultra-violet radiation, the detectors send a signal to the UV controller. If the amount of UV radiation meets a preset sensitivity requirement, the controller in turn signals the "AUTOMATIC" SPRINKLER High Speed Modules which send a 180V pulse to the solenoids. The duration of the 180V pulse is approximately 20 milliseconds; after that time the system drops the solenoid voltage down to 24V and maintains until the system is reset. Actuation of the solenoids releases pilot line pressure which allows the Pilotex nozzles to open. The water in the tank is pre-pressurized to approximately 150 pounds, forcing the water to flow through the nozzles. Again, system reaction time from detection of ultra-violet radiation to flow at nozzles is well under 50 milliseconds. System reset is accomplished by pushing reset button which de-activates the

August 25, 1986

1422

solenoids, thus restoring pilot pressure to close the Pilotex nozzles. The system is then ready and in stand-by mode.

APPLICATIONS

Basically, the system is designed to be used wherever fixed High Speed Suppression Systems are not feasible, either because of physical location, lack of fixed water supply or changing operations. The system should be especially useful in munitions depots where different operations are being done in different areas and portability is a requirement. The system could find use at overseas depots and temporary munitions installations along with shipboard or transport plane service.

August 25, 1986

1423

"AUTOMATIC" SPRINKLER PORTABLE HIGH SPEED DELUGE

YOUR NAME _____

COMPANY OR GOVERNMENT BRANCH _____

ADDRESS _____

TELEPHONE _____

1. Do you have uses or applications for portable high speed deluge? ☐ YES ☐ NO

If yes, please list: _____

2. What method(s) of portability would you require?

☐ TOWMOTOR ☐ CASTERS ☐ TRAILER ☐ OTHER(_____)

3. Should system connect to existing riser supply or use self-contained tank? ☐ FIXED ☐ TANK

Comments: _____

4. Tank capacity? _____ U.S. Gallons

5. Required response time? _____ Milliseconds

6. Maximum size? ☐ MAN DOOR ☐ SHIPPING DOOR

Comments: _____

7. Number of Nozzles? _____

8. Flow rate? _____

August 25, 1986

1424

9. Number of Detectors? _____
10. Explosion-proof rating? _____
11. Should detectors and nozzles be moveable?
Detectors? ☐ YES ☐ NO; Nozzles? ☐ YES ☐ NO
12. Equipment shutdown capability? ☐ YES ☐ NO
13. Indoor or outdoor use? ☐ INDOOR ☐ OUTDOOR ☐ BOTH
14. Average size of area to be covered? _____ SQ. FT.

Additional comments: _____

Send to:

"AUTOMATIC" SPRINKLER CORPORATION
1000 Edgerton Road
P.O. Box 180
Broadview Hts., Ohio 44147-0990
Attn: Gary A. Fadorsen
(216) 526-9900

Thank you for your help.

August 25, 1986

1425

HIGH SPEED DELUGE

A PRACTICAL STANDPOINT

The following is a list of items that we at "Automatic" have found useful in assuring that a high speed deluge is installed correctly and that start-up and operation go as smooth as possible. This list was compiled over the past few years from mistakes we have made, problems others have had and installation hints from other vendors. It is our hope that you will find at least one useful and that it may save you some time or expense. We are sure you agree that most of these "hints" are just common sense, but it is surprising how often they reoccur.

1. Study the hazard, detector sensitivity is inversely proportional to distance (inverse square). Keep the detector as close as possible to the hazard while keeping the hazard within the cone of vision.
Placing detectors in the four corners of the room is convenient but seldom effective.
2. The same goes for nozzels, why pay for a fifty millisecond response time, then put the nozzles 12 feet at the ceiling. Consider nozzle positions ie., keying on operators, melt kettles, mixer, flooding explosive from below, conveyor, etc.
3. Avoid detector obstructions. Glass, plastic, people, dirt, oil and smoke are very effective for blocking U.V. radiation.
4. Manual release (electrical or mechanical) should be fast acting and easily accessible. Ring-pull type at exits and operator stations have been successful. Avoid time consuming break or multi pull type.

August 25, 1986

1426

5. Installation mistakes will cause trouble during start-up but also will contribute to problems in the future.
 - a. Run detector wiring in separate conduit.
 - b. Run solenoid wiring in separate conduit.
 - c. Keep AC out of DC conduit.
 - d. Use drain seals on all detectors and solenoids.
 - e. Avoid splices, try to provide continuous runs between devices and panels.
 - f. Be sure wiring complies with manufacturer specification (current and voltage rating).
 - g. Megger all wiring.
 - h. Be aware explosion-proof is not necessarily water-proof.
 - i. Locate panels in non-explosive areas whenever possible.
 - j. Flush or clean piping before installing nozzels and solenoids.
 - k. Clean cutting oil from air lines before connecting air shields.
 - l. Use flexible conduit on detectors if reaiming will be needed.
 - m. Beware of Ambient Ultra Violet Radiation.
6. Supervision and redundancy is a must. Have at least two devices in a bay no matter how small. At least 2 detectors, 2 solencids and two nozzels. Supervise all circuits.

Many of the above should go without mentioning but we see some of them repeated from time to time. I am sure others have more suggestions. We welcome your ideas and suggestions. "Automatic" is strongly considering an "Ammo Plant News Letter" to help aid in communications between plants, depots, vendors, contractors, etc. If this would be of interest to you please send us your comments. Feel free to use the Portable High Speed Deluge Questionnaire for this purpose.

August 25, 1986

1427

 **Automatic Sprinkler**
CORPORATION OF AMERICA
A PPG INDUSTRIES COMPANY

"CLASSIFICATION OF EXPLOSIVES UNDER THE UN SCHEME -

A NEED FOR UNIFORMITY OR FLEXIBILITY?"

by Dr R J Smallwood, United Kingdom, Health and Safety Executive

1. Introduction

In the UK the United Nations scheme of classifying explosives is being increasingly incorporated into new legislative controls on explosives which are progressively replacing statutes whose origins lie in the 1875 Explosives Act. This reflects the extent of the success of the UN scheme in becoming increasingly adopted as the basis upon which explosives are classified for the purposes of international conveyance. It also indicates that there are advantages to be gained in framing domestic legislation so as to incorporate internationally accepted procedures.

In this paper ~~we~~ emphasises the advantages of adopting a uniform international approach towards the classification of explosives for international conveyance and illustrates, by example, the type of difficulty which might occur if such an approach is not adopted. It also explores difficulties which might be encountered in using classifications derived from UN tests as the basis for assessing the practical hazard presented by the explosives in situations other than international conveyance.

2. A unified international approach

The existing UN scheme of classifying explosives provides an internationally accepted method of classifying packaged explosives by assigning them to a particular hazard division and compatibility group. It is recognised that the precise packaging method is of fundamental importance in determining this classification. In some instances the method of confinement which is used in the UN class 1, series 6 tests can itself be a significant factor in determining the behaviour of the explosive in the tests. An example of such behaviour was observed in a trial in which a particular propellant, packed in cylindrical tubs and confined by sandbags, exhibited behaviour in the series 6 tests which resulted in the assignment of 1.1 hazard division. When the same packaged material was however confined not by sandbags, but by cylindrical tubs filled with sand, the propellant exhibited behaviour which resulted in the assignment of a 1.3 hazard division.

This was clearly one of those cases in which comparatively small variations in the extent of confinement had a significant effect on the behaviour of the material in the tests and hence on the hazard division to which it was assigned.

These results have been described in detail by a colleague at a presentation to the last DOD ESS, together with other examples of difficulties which had arisen in the UK during the importation of explosives. These arose as a result of differences which existed in different countries' interpretation of the classification procedure. In some cases the differences were comparatively minor but nevertheless resulted in significant difficulty for those involved.

The UK recognises there will inevitably be occasions when different competent national authorities interpret the classification procedures somewhat differently. However, since the UK has developed increasing confidence in the classifications assigned by other national competent authorities, it undertook to accept classifications assigned by other countries. In those cases where the classification differed from that assigned by the UK authorities, it was still accepted, provided that the classification was either supported by relevant test data or had been assigned by the national competent authority in the country of manufacture. In my opinion there still inevitably remains some areas which would benefit from further dialogue in order to resolve apparent differences in interpretation of the UN classification scheme. One such area is the tests and criterion which determine the assignment of a 1.4S classification. This was, incidentally, one of the examples quoted by my colleague two years ago.

In order to minimise these difficulties and to ensure safety during the conveyance of these goods it is clearly desirable to adopt, as far as is possible, a uniform approach to the performance and interpretation of the UN testing procedures. In the absence of such uniformity it is possible that countries will have less confidence than they currently have in the validity of the classification assigned by other national competent authorities.

A flexible UK domestic approach

I have emphasised above the advantages of adopting a uniform approach in the international application and interpretation of the UN scheme of classifying explosives. I would now like to outline the role that the UN classification scheme has played within the UK and go on to consider the significance that series 6 type tests might have in assessing the practical hazard posed by material in situations other than during international conveyance, eg during storage in purpose designed facilities.

The UN scheme of classification enjoys widespread application as the means of classifying explosives for the purpose of their international conveyance. This has been accompanied by an increasing use of the UN scheme within the UK as one of the methods by which explosives are classified, not only for the purpose of international conveyance, but also for the purpose of storage at licensed premises, and for conveyance.

Recently enacted UK legislation, entitled "The Classification and Labelling of Explosives Regulations 1983", requires that explosives be classified, not only in the form and packaging in which they are conveyed, but also in the form and packaging in which they are to be kept and supplied. Whilst, in most cases the classification might be the same for all of these situations, the regulations provide for the possibility that different classifications might be appropriate if, for example, material is stored in different packaging to that in which it is conveyed. These regulations also provide for the possibility of assigning different classifications to identical material in different situations, eg storage and conveyance. Since the UN series 6 test conditions are uniquely specified and invariant they cannot be used as a basis for assigning different classifications to material which, although identically packed, is nevertheless in different situations.

As well as being the UK competent national authority for classifying commercial explosives under the above regulations, we are also responsible for licensing sites at which explosives are manufactured and stored. This requires that we specify the safety distances which are to be maintained from buildings containing explosives to other facilities. Since it is the hazard division of the explosive which normally determines the safety distance to be specified, and the safety distances for explosives of hazard division 1.3 (HD 1.3) are

substantially less than those of HD 1.1, the effect of classifying materials as HD 1.1 rather than HD 1.3 can have considerable consequences for a particular site in terms of the quantity of explosive which can be kept, or the amount of land which is effectively sterilised of any development.

It is inevitable that individual examples will occur where the storage conditions at specific sites might be significantly different from the conditions of, for example, confinement, which apply in the UN series 6(a) and 6(b) tests. In such circumstances there might be justification for considering whether the hazard division derived from the UN tests is an appropriate basis upon which to assess the practical hazard presented by the material during its storage and thereby for deriving an appropriate safety distance.

An example which I will describe illustrates the type of consideration which might become increasingly necessary now that a formal test regime exists for classifying explosives.

An explosive stored at a factory had traditionally been assigned a 1.1 hazard division because it was known to detonate under particular conditions of confinement. The material was stored in quantities which enabled the maintenance of safety distances appropriate to HD 1.1 materials. A request was received from the company to store increased quantities of material, without increasing the safety distances, on the basis that burning trials which had been undertaken demonstrated that, under the proposed conditions of storage, no mass explosion of the contents of the storage building could occur. The trials had been performed several years ago prior to the widespread UK adoption of the UN scheme of classification and did not conform to the provisions of test series 6(a) or 6(b). There was therefore no question that the explosive could be reclassified as HD 1.3 rather than HD 1.1. However, the tests clearly provided useful information as to the behaviour of the packaged material under conditions of limited confinement and the consideration essentially became one of assessing whether the confinement provided in the tests adequately simulated that which could occur in practice during its storage.

These trials involved quantities of material of up to 400kg in different stacking configurations and with different levels of confinement. Three of the trials are described:-

Trial 1

Five powder boxes were laid side by side in a cruciform pattern. In addition sandbags were laid at the outer edge of each of the four outer boxes with the intention of preventing lateral, horizontal movement. One bag within the centre box was ignited and this was followed by successive, separate fires as each bag within separate boxes ignited. For all ten bags of powder to burn a time of 10 minutes 40 seconds was recorded. No explosions/detonations occurred.

Trial 2

Five boxes were laid side by side as in Trial 1 but with a further five boxes in similar orientation laid on top. The igniter was located in the lower central box. Again lateral horizontal movement of the outer boxes was restricted by sandbags and ignition achieved in the lower, central box. Once more separate bags of powder within each box ignited in turn with some boxes thrown about by the force of the fire. In this experiment 11 minutes 10 seconds were required for all the powder bags to ignite. No explosions/detonations occurred.

Trial 3

Again a cruciform pattern was employed but involving fifteen boxes i.e. packed three high. Confinement was increased by sand bagging all external surfaces of the powder boxes except the upward facing ones. In addition wooden stakes were used to reinforce the sand bagging and the whole structure wired together. Ignition of the lower central box was carried out and immediately one or two boxes were thrown clear of the stack but these did not ignite until much later. Once again there were individual fires at intervals as individual powder bags ignited and burned but in this experiment a minute long burn occurred two minutes thirty seconds after the start involving about seven powder boxes. A time of 13 minutes 50 seconds was required before the last powder bag ignited but once again there were no explosions/detonations.

The boxes were of fibreboard construction measuring approximately 50cm x 40cm x 25cm. Each box contained two bags each holding 12.5kg of explosive, separated by a fibreboard panel. Ignition was achieved by an electric fuze head packed in a small charge of black powder placed in the centre of one of the bags.

A number of conclusions were drawn from the results of these tests:-

1. The design of the approved transportation package for the explosive was effective in preventing rapid flame propagation of fire between individual boxes. Fire spread from one bag of powder to the other within a box was not immediate and up to a minute elapsed before the second bag ignited. Propagation of fire between boxes may be prevented for at least five minutes and in some cases much longer times were involved dependent upon the separation of the boxes.
2. With lateral confinement, a fire involving a stack of boxes three high did not result in a burning to detonation.

On the basis of the results from these tests the company proposed a system of racking and individual box restraint within their magazines which was designed to ensure that packages would not be subjected to confinement in excess of that provided in the trials.

It was considered that whilst the trials did not conform to the UN series 6 test conditions, they did nevertheless provide sufficient information to indicate that the practical hazard presented by the storage of a limited quantity of explosive, stacked and restrained in a particular manner, was more typical of a material of HD 1.3 rather than HD 1.1. It was therefore decided that in this instance the safety distances which would be specified would be those appropriate to a material assigned to HD 1.3. It should be emphasised however that the explosives remained classified and labelled as HD 1.1.

4. Conclusion

In this paper I have advocated the advantages of a uniform approach to the application and interpretation of the UN scheme of classifying explosives for international conveyance. This would avoid difficulties which have arisen in the past because of differences which have existed in interpreting the UN test regime. Such a unified approach is in my view not only desirable to avoid such difficulties but is also necessary to maintain safety standards.

Whilst arguing for a uniform international approach, I have also suggested that there are domestic circumstances where a flexible approach to the use of classifications resulting from UN series 6 tests is appropriate.

UK MOD EXPLOSIVE STORAGE PRINCIPLES

N J M Rees, BSc, PhD
Director, Safety Services Organisation,
Ministry of Defence, Procurement Executive,
St Mary Cray, Orpington, Kent.
Great Britain

1. THE AIM

MOD must control the storage and processing of explosives in such a way that the chance of a fire or an explosion is minimised; if a fire or explosion should occur whether it results from accident, enemy attack or sabotage, then the adjacent explosive stocks and facilities including personnel in the vicinity of the explosion site must be protected, to a predetermined, practical standard.

2. THE PRINCIPLES USED

These are relatively simple to state and understand but are difficult to apply because to define (say) the thicknesses of walls and traverses to stop fragments, and the distances between stacks of explosive that will prevent sympathetic detonation requires a sophisticated technical data base to arrive at practical economic solutions. It is very easy to overspend on protection and provide more than is necessary to fulfil our aim; on the other hand if sufficient protection is not available the entire explosives depot or factory together with a large proportion of its staff may be lost in the event of a single isolated explosion in one building. Building design and construction must strike a balance between adequate physical security and minimising the blast and thrown debris in the event of an explosion.

In the MOD Procurement Executive (PE) the principles used are:

- (a) To assume that if explosives are regularly present in a storage or processing activity then an explosion will take place at some time during the life of this activity.
- (b) To assess the distribution of the explosives present in a facility to decide what parts of the whole quantity will sympathetically detonate to effectively cause one explosion - these parts we define as the "Unit Risks" for that distribution of explosives.
- (c) To assess the design of the building containing the explosive, the processes to be carried out there, the adjacent buildings, the numbers and disposition of operating staff, and of any members of the public and their property that may be in the vicinity to see if the situation in the event of an explosion is acceptable.

Important considerations here are.

- (1) The explosion must not propagate immediately from one unit risk to adjacent ones.
- (2) Only the personnel working on that particular process or storage activity should be put at serious risk.
- (3) Serious structural damage to buildings should not extend beyond those buildings immediately adjacent to the explosion site.
- (d) If the assessment of a particular building and the processes carried out there are acceptable then the building and the process are inspected and if all is well then an Explosives Limit with appropriate conditions is authorised by myself as Chief Inspector of Explosives for the PE.
- (e) The inspection of the facility against the approved conditions and quantity of explosives and process is carried out at least once per year by my Inspectors.
- (f) To investigate any unexpected ignition or explosion which occurs and, depending upon its severity, set up a formal inquiry into its cause to establish the technical reasons for the incident and to make recommendations to prevent a recurrence. Blame is not apportioned at this inquiry but if any individual appears to be responsible, disciplinary action by Management is taken at a later stage.

3. THE TECHNICAL DATABASE

(1) Properties of Explosives

There are various types of explosives in existence and they behave in very different ways when they are initiated, as in enemy attack or ignited as in a fire. The latter is by far the most likely form of hazard which will be met under most circumstances. In order to simplify the assessment of the risks presented by the large number of different explosives that are manufactured at the present time, they are classified into a number of types depending on their behaviour under specially defined accident conditions. Up till about 8 years ago we in UK had our own system of Explosives Categories X, Y, Z and ZZ. Presently we use the UN system of Hazard Divisions, including the system of special Tests required to decide to which HD a particular explosive belongs.

Generally, when ignited, explosives burn and explode, producing the following effects:

- (a) Fast fragments from metal touching or near the explosive
- (b) Airblast

- (c) Cratering
- (d) Groundshock
- (e) Flame and Radiant heat
- (f) Lobbed building debris and explosive items.

The UN Classification Scheme using Hazard Divisions was originally for the transport of explosives though it now is almost universally used for the control of storage and manufacture as well. The definitions are given in "Transport of Dangerous Goods", 4th Revised Edition 1986 (1) on pages 2, 3 and 4.

Explosives are defined as:-

(a) An explosive substance is a solid or liquid substance (or a mixture of substances) which is in itself capable by chemical reaction of producing gas at such a temperature and pressure and at such a speed that will cause damage to the surroundings. Pyrotechnic substances are included even when they do not evolve significant amounts of gas.

(b) A pyrotechnic substance is a substance or a mixture of substances designed to produce an effect by heat, light, sound, gas or smoke or a combination of these as the result of non-detonative, self sustaining exothermic chemical reactions.

UN Class I Dangerous Goods are explosives and comprise:-

(a) Explosive substances (a substance which is not itself an explosive but which can form an explosive atmosphere of gas, vapour or dust is not included in Class 1), except those that are too dangerous for another class;

(b) Explosive articles, except devices containing explosive substances in such quantity or of such a character that their inadvertent or accidental ignition or initiation during transport shall not cause any effect external to the device either by projectiles, fire, smoke, heat or loud noise: and

(c) Substances and articles not mentioned under (a) and (b) which are manufactured with a view to producing a practical, explosive or pyrotechnic effect.

Transport of explosive substances which are unduly sensitive or so reactive as to be subject to spontaneous reaction is prohibited.

The objective of the recommended definition is to indicate which goods are dangerous and in which class they should be included, according to their specific characteristics. These definitions have been devised to provide a common pattern which it should prove possible to follow in the various national and international regulations. Used with the list of dangerous goods, the definitions should provide guidance to those who have to use such regulations; and they present a notable degree of

standardisation while retaining a flexibility that allows diverse situations to be taken into account.

The explosives in Class 1 are divided into 5 Hazard Divisions:

Division 1.1 Substances and articles which have a mass explosion hazard (A mass explosion is one which affects almost the entire load virtually instantaneously and fast fragments can be produced.) (Equivalent to the old Z and ZZ).

Division 1.2 Substances and articles which have a projection hazard but not a mass explosion hazard. (Equivalent to the old X and some Z).

Division 1.3 Substances and articles which have a fire hazard and either a minor blast hazard or a minor projection hazard or both, but not a mass explosion hazard (Equivalent to the old Y).

This division comprises substances and articles: (a) which give rise to considerable radiant heat, or (b) which burn one after another, producing minor blast or projection effects or both.

Division 1.4 Substances and articles which present no significant hazard (Equivalent to part of the old X).

This division comprises substances and articles which present only a small hazard in the event of ignition or initiation during transport. The effects are largely confined to the package and no projection of fragments of appreciable size or range is to be expected. An external fire must not cause virtually instantaneous explosion of almost the entire contents of the package. Substances and articles of this division are in Compatibility Group S if they are so packaged or designed that any hazardous effects arising from accidental functioning are confined within the package unless the package has been degraded by fire, in which case all blast or projection effects are limited to the extent that they do not significantly hinder fire-fighting or other emergency response efforts in the immediate vicinity or the package.

Division 1.5 Very insensitive substances which have a mass explosion hazard. This division comprises explosive substances which are so insensitive that there is very little probability of initiation or of transition from burning to detonation under normal conditions of transport. As a minimum requirement they must not explode in the external fire test.

The probability of transition from burning to detonation is greater when large quantities are carried in a ship.

Class 1 is unique in that the type of packaging frequently has a decisive effect on the hazard and therefore on the assignment to a

particular division. The correct division is determined by use of the methods outlined.

The different Hazard Division of explosives can behave in accident conditions in very different ways, and we therefore require different standards of protection for the different Hazard Divisions. The determination of the HD to which a particular explosive belongs is therefore most important, since if a HD 1.1 nature was allocated to HD 1.2 in error, then a fire could result in a mass explosion which would not have been allowed for in the protection provided during transport, storage or processing and could change an unpleasant incident to a disaster.

An incident of this kind occurred near Arles (Bouches de Rhone, France) in about 1917 (2). For a period from around 1900, TNT was not regarded as a true explosive, by the tests then being used to determine whether substances were explosives or not; it was accepted as a flammable substance. The explosives factory had 54 buildings laid out in two rows with just adequate separation to prevent sympathetic detonation spreading from building to building by airblast, but no traverses to stop fast fragments from the explosions. The process employed was to fill medium calibre shell with TNT and in present day terms shell were being treated as HD 1.3 whereas in fact, as the accident proved, they were really HD 1.1. The workforce was mainly Vietnamese. Each building contained 120 tonnes NEQ of TNT.

The accident is thought to have started on the filling line in one of the buildings in the middle of a row, with a fire possibly caused by someone smoking. The fire burned for a short period and the shell in that building exploded producing fast fragments which caused further explosions and fire in adjacent buildings. In all 46 buildings, each containing an NEQ of 120 tonnes TNT exploded, and the remaining 8 burned. Due to the peculiar local ground conditions the shallow craters are still there. About 1800 Vietnamese and 60 Frenchmen died. If the TNT had been treated as a detonating explosive of HD 1.1 and traverses provided between the buildings it is unlikely that the factory would have been lost and the casualty list would have been much smaller.

It is therefore most important to classify your explosives into the correct hazard divisions otherwise if one under-classifies your protection will not be effective, if one over-classifies excessive protection will be provided. Classification is done by testing in the case of important new natures, but because this is expensive and time consuming some new natures are classified by analogy and comparison with older ones that have already been tested, or with others classified by comparison only. Clearly errors in classification can arise and from time to time tests must be carried out to ensure that correct standards are being maintained.

In UK our testing generally follows the scheme in Chapter 4 of the UN "Orange Book"(1) to which UK has contributed a number of the tests used. The test series takes the form of a logical sequence of questions

and specified physical tests. Test Series 1 to 4 inclusive considers whether the substance or article in question is an "explosive" (i.e., suitable for Class 1), and if so, whether it is safe for transport. In our field of military explosives, substances and articles are not normally unduly sensitive, however the packaging can be changed from time to time and this may well affect the final Hazard Division assessment. Test Series 5 determines whether a substance can be included in HD 1.5, while Test Series 6 is in three parts and assesses whether the item in question should be allocated to Hazard Divisions 1.1, 1.2, 1.3 or 1.4. The three tests are:-

Test Series 6(a) - The Single Package Test

One package of, for example articles, is placed on the ground and one article in the centre is caused to function using its own means of initiation for non-detonating articles. Confinement of 0.5 metre sandbags is used in all directions (for packages larger than 1m, 1.0 metre confinement used). If the effect is so feeble that the other articles in the box are not functioned the test is repeated to make 3 tests in all.

If a significant event involving more than the initial donor article has occurred, then the 5 package stack test (6b) will follow; if not then Test Series 6(c) (see below) will be used to demonstrate that the effects are not magnified when the packaged explosives are burned.

Test Series 6(b) - The Five Package Confined Stack Test.

This determines whether an explosion or fire starting in one package will be communicated, package to package, in a stack. Five (or more, packages are placed together, preferably in a cross arrangement and one article in the centre package caused to function. The overall confinement by sandbags etc is 1 metre. Large articles carried unpackaged, e.g., HE bombs, are tested similarly. There may be a mass explosion of effectively all the packages or articles which would require a HD 1.1 classification. No further testing is then required. If this does not occur the test is repeated making 3 in all. Test Series 6c will then be used to demonstrate that no enhancement occurs in a fire situation. The allocation of Hazard Division 1.2, 1.3 or 1.4 will be made on the basis of the predominant hazard.

Test Series 6(c) - The Bonfire Test.

Five or more packages are placed on a metal grid about 1 metre above the ground and may be tied together by wire or metal strip fasteners. A wood fire is then constructed around the packages to at a thickness of at least 0.5 metres in all directions to ensure thorough soaking in the heat. After 15 minutes or so the wood usually settles to the height of the grid and the heap of glowing charcoal normally heats the packages, or articles if the packages

are of combustible materials for at least 30 minutes. It is customary to allow the fire to burn on to exhaustion but it can be terminated after 30 minutes using long throw fire hoses if this is desirable. This empirical test is difficult to quantify but the relevance to the realistic transport accident and storage situation fire hazard is undeniable. In particular the duration of 30 minutes plus makes it a far more searching test determining the eventual behaviour of munitions when involved in a fire than the Navy fuel fire tests which are of limited duration. In UK we consider that fires constitutes 80-90% of all dangerous incidents which involve explosives or munitions.

Thus the UN tests from 1 to 6 form an integrated series, the final tests assigning a Hazard Division to the item. If this is done then it implies that the earlier tests have been done and the item is safe for transport.

As you can see we have now come to the difficult part of our procedures - the day to day updating of the technical database. Because this Hazard Classification information and the separation rules for explosive buildings (the Quantity-Distances) are so important, there are certain statutory technical requirements and the job of ensuring that these tasks are fulfilled fall to specific MOD bodies.

4. MOD LEGAL RESPONSIBILITIES FOR EXPLOSIVES

In addition to the self interest of MOD in preserving its explosives against losses from accident, sabotage and enemy attack MOD is legally responsible for ensuring that its explosives are manufactured, stored and transported with the smallest reasonably practical risk to life and property. The Health and Safety at Work Act (1974) is applied to MOD in peacetime and is an enabling Act covering earlier Acts such as the Explosives Act (1875). It also allows regulations to be made under it, such as The Classification and Labelling of Explosives Regulations (1983). MOD is exempt from the requirements of the Explosives Act (1875) but has the usual interdepartmental agreement that standards at least as good as those in commercial industry are applied in MOD.

In order to ensure that MOD is complying with the HSW Act (1974), the MOD and HSE have set up a joint body, the Defence Explosives Safety Authority (DESA) to oversee and audit the MOD procedures. I am a member of the DESA Central Committee and am the Chief Inspector of Explosives for the Procurement Executive Department of the Ministry of Defence.

In addition since about 1925 MOD has maintained the Explosives Storage and Transport Committee (ESTC) with members from the HSE Explosives Inspectorate and the Department of Transport as well as its own experts. This committee is responsible in MOD for classifying Military Explosives and for recommending or "prescribing" adequate standards of safety for the processing, storage and transport of explosives throughout MOD. These "prescriptions" or recommendations (3)

are interpreted by the four Departments of MOD into their own mandatory explosives regulations (4). I am a member of ESTC and Chairman of their sub-committees for Explosion Effects and Port Explosives Limits. I also supply technical staff and effort to enable ESTC to carry out its functions. Currently my staff act as Technical Advisors for Explosives, Electrical Installations, Firefighting, and as secretaries to the Explosion Effects and Port Explosives Limits Sub-Committees (3). In addition my staff are conducting a major series of explosion effects trials in collaboration with the Australians at Woomera to assess the fragment throw from stacks of explosives detonated in different types of buildings (5).

5. ESTC PRESCRIPTIONS FOR QUANTITY DISTANCES

Over the last 60 years ESTC has put together all available technical safety information into its prescriptions and the present Royal Ordnance plc factories and PE explosives Research Establishments were built to the requirements of the draft version of 3/7/Explosives/43 available before and during the early part of the last war (6). This has been updated using some UK Wartime bomb damage information augmented by trials, accident records and much professional experience. The current version of the prescription (7) is now again under revision in parallel with the NATO QD rules (8), of which it forms the basis.

Different quantity-distance requirements are specified, depending on the nature of the receptor site under consideration. They are:

"Inside" Quantity Distances

1. Storage QDs
2. Process Building QDs.

"Outside" Quantity Distances

3. Public occupied buildings and Traffic Route QDs.

1. Storage Quantity Distances

Storage distances are those observed from any explosives building or stack (the "donor") to buildings containing explosives (the "receptor") in which no work is being done on the explosive and where there are few if any people present. The distances are those required to prevent propagation of explosion from one building to the next, and take no account of protection of personnel. The receptor building may, in fact, be destroyed and the explosives therein scattered and rendered unserviceable.

2. Process Building Quantity Distances

These are the distances observed from any explosives building or stack to buildings in which an explosive process or work in connection with the processing of explosive is being carried out. These distances are also

used to protect process workers from specially hazardous processes they may be carrying out and are greater than the corresponding storage distances. They are designed to provide a reasonable degree of protection from severe injury for the operation in the receptor building.

3. Public Occupied Building and Traffic Route Quantity Distances

Public building distances are those observed from any explosives building or stack to houses, railways, or major roads, and are intended to prevent severe structural damage to property, and to give a reasonable degree of protection from injury to members of the public in dwellings or in the open. Public building distances are also observed to buildings within the establishment used as main offices or engineering workshops where there are many personnel at hazard who are not directly involved in the explosives processes being carried out in the factory.

As you can see the complexities of the problems of a real factory are considerable. Already there are four different types of explosives - HD 1.1, 1.2, 1.3 and 1.4 together with three standards of quantity-distance as outlined above, and a wide range of different types of buildings which will give some degree of protection and influence the distances required.

Hazard Division 1.1

HD 1.1 items are the most complex and the current matrix is given as Table 1 of Ref 7. This is further complicated by the fact that the table includes distances appropriate to a number of obsolete buildings constructed of brick. Currently the storehouses for smaller quantities are not now normally built of brick; reinforced concrete is the preferred material because of the reduction in building debris in the event of an explosion, though is under review because of the results obtained from the joint Australian UK trials (5). In addition all 1.1 buildings must be traversed to stop fast fragments.

Storage Buildings

- (1) Igloos - Generally given $0.5Q^{\frac{1}{3}}$ (D3) for an igloo donor, but this may rise to $4.8Q^{\frac{1}{3}}$ (D9) for an open stack donor.
- (2) Earth Covered Buildings - Generally given $0.8Q^{\frac{1}{3}}$ (D4) for a similar or igloo donor but this can rise to $4.8Q^{\frac{1}{3}}$ (D9) for an open stack or other lightly enclosed explosives donor.
- (3) Heavy Buildings (self traversing) - Generally given $2.4Q^{\frac{1}{3}}$ (D7) for all types of donor.
- (4) Traversed Lightweight Buildings - Can sometimes be given $0.8Q^{\frac{1}{3}}$ (D4) but more usually $2.4Q^{\frac{1}{3}}$ (D7) is used.

Process Buildings:

Usually the composite table D9A ($4.8Q^{\frac{1}{3}}$ for $Q < 500\text{kg}$; $8.0Q^{\frac{1}{3}}$ for $Q > 4000\text{kg}$) is used although $8.0Q^{\frac{1}{3}}$ (D10) is preferable over this range, and may rise to $22Q^{\frac{1}{3}}$ (D13) with a minimum fragmentation distance of 270 or 400m for vulnerable receptor buildings.

Public Buildings and Traffic Routes

For little used traffic routes the composite D11 table with a minimum fragment throw distance of 180m is used. For busy routes and publicly occupied houses the composite D13 column is used with a minimum fragment throw distance of 270m for traversed donor sites and 400m for other donors.

Hazard Division 1.2 - Table 2 (7)

Here the major hazards arise firstly from a small number of fast fragments and lobbed ammunition which are projected from the donor explosion site and secondly from the number of such projections likely to arise from an incident. Less hazardous items, generally not containing a detonating explosive, and those containing it but which are below 60mm calibre are now identified by an asterisk (*) in the HD code and can be treated with less caution than the larger items. The more hazardous items are generally given $68Q^{\frac{1}{3}}$ (D2) though fixed distances of 10, 25, or 90m can be used for some storage and process receptor situations. Public traffic routes and houses occupied by the public generally require 135, or 270m respectively or $68Q^{\frac{1}{3}}$ (D2).

Hazard Division 1.3 - Table 3(7)

The major hazards arise from the radiation and flames, including jetting, which arise from military propellants. The distances in Table 3 (7) are based on the available data for propellants. Flame distances can be particularly capricious and can increase by as much as 50% above the indicated distances.

Earth covered or heavy walled buildings are the safest receptors and separation distances of 2 to 21 metres are acceptable. For receptor process buildings, whether traversed or not, a minimum of 60m or $3.2Q^{\frac{1}{3}}$ (D2) is required; again for a severe jetting situation up to 240m may be required. For traffic routes and houses occupied by the public a minimum of 60m or $6.4Q^{\frac{1}{3}}$ (D4) is required except where severe jetting is expected where the minimum is increased to 240m.

The effects of jetting are not generally recognised and a few years ago we carried out a trial in which a section of storage building was erected and stacked with boxes of propellant. The loading density was 63Kg/m^3 and the total weight was 4.5 tonnes. The expected flame radius was 15m (storage distance) but the flame jetted through a doorway to 50m. The process building distance was 53m for this quantity. Thus special

attention must be paid to jetting from large quantities of burning propellant.

Hazard Division 1.4

HD 1.4 items are relatively innocuous and only require building separations of 25 or 10m.

6. GENERAL SAFETY PROCEDURES

This section can really best be described as "common sense" for explosives managers. Under the pressures of production, staff cuts or a wartime emergency, a number of the normal procedures and safety requirements, perhaps not well understood by the local management, could be ignored under the pressures of the moment.

The following list is not exhaustive, but the bad practices described below have been found over the years to have often made the consequences of a minor accident or explosion much worse than one would have expected from the protection to be expected from following the other ESTC prescription requirements for quantity distances.

1. Storehouses illegally used for processing

Storage of explosives is a relatively benign operation, but processing, where bare explosive may be exposed, pressed or machined, or fuses inserted or removed from bombs or shells carries a much higher risk of initiation occurring. In a situation where HD 1.1 items are present this could easily lead to a larger explosion.

An unfortunate example is the RAF underground bomb storage at Fauld, Staffs, where on the 27 November 1944 the detonation of some 2,400 tonnes NEQ of miscellaneous bombs produced the largest explosively produced crater in Europe measuring 900 by 600 feet and 100 feet deep (Figure 1). This storage was licensed for unfused bombs only, and no process work should have been carried out in this storage facility. In addition a large number of separate caves were used for the bombs and although only about half the storage area was involved in the explosion it was much bigger than expected from the design and layout of the storage, and was a major disaster.

It is now thought that an illegal process of some kind was being carried out on one or more of the bombs in the store. One possibility is that some aircraft returned from a mission with full loads of fused bombs and that these were returned to the store on the narrow gauge train used for this purpose. The incompetent removal of a fuse from a bomb in a wagon on the train could have lead to the detonation of the train when it was standing across a number of adjacent cave entrances, thereby causing the initial simultaneous detonation of a large number of bombs, which then spread through the nearest storage caves.

2. Process Buildings Used for Storage

A production facility for land mines used a long continuously moving cooling line, a sealing station and a packing unit producing pallets of mines each having an NEQ of 1 tonne. All this took place in one large room and over 20 tonnes of cooling mines and finished pallets accumulated each day. The cooling line was divided up using dummy mines to limit the quantity that could detonate in one unit. External storage for the filled pallets was arranged and by moving them out as soon as one was filled the unit risk in the building was reduced to 1 tonne, thus considerably reducing the hazard to the adjacent buildings in the factory.

3. Use of Building Entrance Ways and Access Roads for Storage of Explosives

In a recent accident an entire storage depot containing a mixture of HD 1.1 and 1.2 was lost, because large quantities of boxed mortar bombs, grenades etc., were stored in the entrances to already overloaded storage buildings. Some boxes in a doorway were ignited and burning items were lobbed into other entrances full of more explosive stores etc. The buildings were traversed and they burned and exploded sequentially, the hazard from the exposed boxes preventing the fire being attacked in its early stages by the fire brigade.

4. Hidden Explosive in Old Buildings

Buildings that have been used for explosives manufacture and processing over a number of years can conceal large quantities of explosive, and any renovation, alteration or demolition work must be planned and carried out very carefully. Explosive can be carried down drains, through cracks in concrete floors into the subsoil, fill spaces between walls, all up to tonne quantities. Lesser hazards arise from penetration of explosive into mortar between bricks and other small gaps and into air extract ducts etc., but all must be carefully handled (4).

5. The Human Factor

The training of personnel employed in handling explosives is clearly as important as in any other occupation, however the potential for disaster following staff errors is greater than in most activities.

It is essential to have properly formulated, written and approved procedures to cover all regular operations involving explosives, and in addition to ensure that those handling the explosives fully understand the requirements for safe operation. The problem is often a genuine failure to understand rather than deliberate disobedience of procedures or instructions. This certainly applied in the case of the storeman in one factory in the

UK who could not accept that the new high energy propellants could be other than HD 1.3. He therefore continued to store the new HD 1.1 propellants together with the HD 1.3 types in spite of the appearance of the HD 1.1 labels on some of his stock. Fortunately this was corrected when it came to light at an inspection.

7. CONTROL OF EXPLOSIVES IN THE PROCUREMENT EXECUTIVE

From the preceding it is clear that it is not sufficient to have good guiding principles, and an up-to-date database giving sound quantity-distance requirements for storage and processing if the control of what is actually done with the explosives in the factories and storage depots is defective. In the UK MOD(PE), this control is effected by a licensing and inspection procedure carried out by my staff as laid down in the PE Explosives Regulations (4). Before the privatisation of the ROFs there were 49 sites with 2300 licences which has been reduced by their departure to 37 sites and 900 licences.

If an establishment wishes to work with explosives then the Safety Officer submits an application for an Explosive Limit Approval for the facility in which the work is to be done. The application is assessed at Safety Services Organisation (PE) and if agreed is authorised by me as Chief Inspector of Explosives. This assessment always involves envisaging the effects of the explosion of the contents of the building on the surrounding buildings. The procedure is complex and is shown in Figure 2. In difficult cases or where large sums of money are to be spent on new facilities scale model trials of the proposed new buildings are carried out. This is a specialist technique which required careful planning and interpretation (9). We also require the establishment to demonstrate that the processes they use for explosives are safe before they are licensed and put into use.

After the explosives facility has been licensed and put into use any accident or incident in which an unexpected ignition takes place is investigated. If it is a minor one then the factory will conduct the inquiry, if it is a major one I may carry this out myself. Recommendations are made to prevent a recurrence and if necessary the Explosives Regulations are changed to take account of the experience gained.

REFERENCES

1. "Transport of Dangerous Goods". Recommendations of the Committee of Experts on the Transport of Dangerous Goods. Fourth Revised Edition, United Nations 1986.
2. Burlot, "Memoires Artillerie Francaise, 9; 799, 1939.
3. List of ESTC Leaflets (Annex).
4. Explosives Regulations, for use in Procurement Executive Establishments AvP42, UKMOD.
5. Joint Australian-UK Stack Fragmentation Throw Trials. DODESB Safety Seminar 1986.
6. Notes on the Basis for Outside Safety Distances for Explosives involving the risk of Mass Explosion. 3/7/EXPLOS/43, 1965, UKMOD.
7. ESTC/220/Leaflet No.5 - Part 2. Quantity Distances for Military Explosives, UKMOD.
8. Manual on NATO Safety Principles for the Storage of Ammunition of Explosives (AC258).
9. A re-assessment of the existing underground explosive storage facility in the UK. C. F. Millington. US Department of Defense 20th Explosives Safety Seminar, Norfolk, VA 1982.



Figure 1: Crater left at the FAULD, Staffs Underground Bomb Storage Depot after the Accidental Explosion on 27 November 1944.

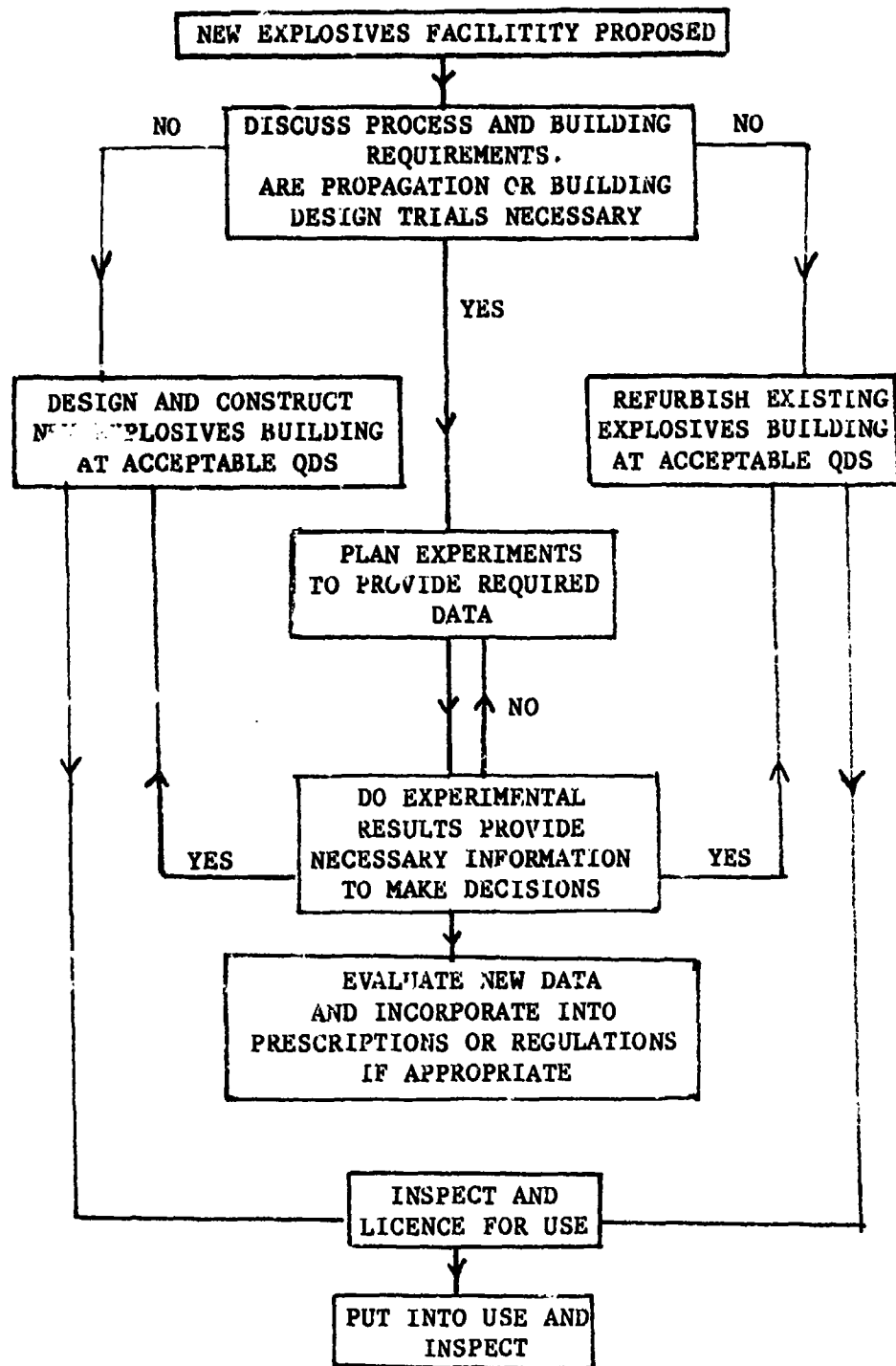


Figure 2: PE Procedures for Providing and Approving Explosives Buildings

LIST OF MOD EXPLOSIVES STORAGE AND TRANSPORT COMMITTEE LEAFLETS

<u>Leaflet No.</u>	<u>Title</u>
1.	Constitution, Terms of Reference and Rules of Procedure of the Explosives Storage and Transport Committee. Supplement: Constitution and Terms of Reference for Sub-committees of the ESTC.
2	Classification of Military Explosives for Storage and Transport Supplement: Comprehensive Tabulation of Ammunition and Explosives in accordance with the International System of Classification.
3	List of Permanent Classifications for Military Explosives
4	List of Temporary Classifications for Military Explosives
5	Quantity-Distances for Military Explosives Part 1: General Principles and Background Part 2: Above Ground Storage Part 3: Under Ground Storage Part 4: Quantity-Distances in Special Circumstances.
6	Buildings and Traverses for Military Explosives
7	Safety Conditions for Electrical Installations and Equipment for Buildings and Areas containing Military Explosives
8	Safety Conditions for Internal Combustion Engines in Military Establishments
9	Safety Conditions for Fire Fighting in Government Explosive Establishments
10	Notes for Guidance for Fire Fighting in Government Explosives Establishments
11	Packing of Military Explosives

- 12 Recommendations for the Carriage of Munitions on War in Civil Aircraft
- 13 Dangerous Goods of Non Explosive Categories stored in Explosives Storage Areas with Special Authorisation by Service Headquarters.
- 14 Rail Conveyance of Dangerous Goods other than Explosives
- 15 Notes on the Conveyance by Rail of Military Explosives Regulations
- 16 Cancelled
- 17 Notes on the Conveyance in Harbours of Military Explosives Regulations
- Supplement:
- 18 Notes on the Conveyance in Harbours of Military Explosives in Periods of Limited Emergency
- 19 Notes on the Conveyance by Road of Military Explosives Regulations
- 20 Notice in Crews of Road Vehicles Carrying Military Explosives including Ammunition
- 21 Conditions for the use of ISO Freight Containers for the Conveyance of Military Explosives.

AD-P005 360

✓

Lt Col F Cantrell
Royal Military College of Science
Shrivenham
Swindon
Wilts SN6 8LA
England

TWENTY-SECOND DEPARTMENT OF DEFENSE EXPLOSIVES SAFETY SEMINAR
PRESENTATION BY LIEUTENANT COLONEL FREDERICK CANTRELL RAOC
"AN AUDIT OF THE QUANTITY DISTANCE RULES FOR THE STORAGE OF AMUNITION AND
EXPLOSIVES"

1. I am certain that many of you here this afternoon play the game of chess, and for the few that do not I will explain that each player has 16 pieces to control. Some pieces can jump over others, both friend and foe, some move in straight lines any distances but in different directions, some pieces move in different directions when they take an opponents piece and once during the game, in a specific situation, a player can move two pieces at once. Theoretically the game can be lost or won by not removing a single piece from the board. A complicated game and rightly called the game of masters.

2. What has this got to do with a topic on the agenda at an Explosives Safety Seminar? Perhaps this vu-foil (vu-foil 1) will help explain, it is not a picture of a chess board, but a copy of one of the matrices used in the UK for determining quantity distances for the storage of ammunition and explosives. There are five such matrices, each one is made up of 120 cells, most cells have a least two entries and many three or even more. This adds up to about 1300 entries. The game of chess can be compared with the use of these matrices, but if you can visualise a game of three dimensional chess, then this I liken to the subject of my presentation - "An Audit of the Quantity Distances Rules for the Storage of Ammunition and Explosives". The requirement of such an audit being that there should be consistent relativities among all the cells, taking account of both vertical and horizontal comparisons in each table and the ranking among the tables themselves.

3. The quantity distances or QDs as they are called, have been in use for many years. Why therefore do we need an audit ?. The answer lies in questions asked at Ministerial level. Searching questions were asked with regard to the storage of ammunition. The basic questions asked were:-

"Why do we need expensive storage buildings?" and
"Why do we need so much real estate?".

To ask questions at Ministerial level is perhaps the best way to get some action - certainly in the United Kingdom. As a result a study group was set up to investigate risk analysis as it applied to the storage and handling of ammunition. As part of the study it was considered necessary to verify the consequence side of the risk equation, hence the audit of the QDs.

4. To consider the complete audit of the QDs in such a short session as this would be quite impossible, you will recall the 1300 individual entries in the matrices. I will therefore examine the derivation of distances currently used to safeguard the general public, and I will take a critical look at the QDs prescribed for earth covered buildings and I will then finish with a "commercial".

Quantity distances

5. It is important to note that the current OQDs do not attempt to provide absolute safety to the general public whether they be in buildings, in the open or in vehicles. It was for this reason that the terminology was changed in 1976 from "safety distance" to "quantity distance".

6. Firstly the derivation of the OQDs. This vu-foil (vu-foil 2) shows the UK OQDs for HD 1.1 as used today. At this stage I would like to point out that the same distances are required whether the munitions are stored in the open, in brick buildings or in earth covered magazines - in fact any type of above ground storage. I will return to this later.

7. The first question to ask is:

"what was the origin of the curve and how was it derived?".

From this vu-foil (vu-foil 3), it can be seen that the over pressure is not constant at the OQD for the whole range of NEQ, although the curve does level out to approximately 5kPa at about 6000kgs with the peak pressure as high as 40kPa at lower NEQs. Neither is the impulse constant over the whole range as can be seen from this vu-foil (vu-foil 4).

8. It is clear that in respect of the smaller NEQs, the higher overpressure is associated with a small impulse, whilst for the higher NEQs, the lower the over-pressure is associated with a higher impulse. This is illustrated on the iso-damage curve where values of impulse are plotted against pressure at the OQD for the range of NEQ. (vu-foil 5).

9. Although this explains the shape of the curve, it does not explain its derivation. For this it is necessary to go back in history over 40 years to the end of World War 2.

10. At the end of the war very large stocks of ammunition were held in the UK with no immediate outlet and it found quite impracticable to observe the pre-war safety distances. It was the general opinion that the distances could be reduced without incurring unreasonable hazards. In 1945 a Technical Sub Committee was set up with the aim of preparing new safety distances.

11. The Committee had at its disposal the work which had been done during the war on the assessment of damage from bombs as well as reports and records of accidents dating back to 1871. The Sub-Committee adopted the following standard for the assessment of the OQD (vu-foil 6):-

"That an explosion of the whole contents of a building or stack should not cause serious structural damage to the ordinary dwelling house, though minor damage such as broken windows, dropped ceilings or loosened slates would be accepted."

12. As a start point, the Committee took the formula developed during the war by the Ministry of Home Security which connected the average radius of damage (of a particular defined severity) with the net weight of explosives involved. It was stated that the formula had been derived from a very large number of enemy bomb incidents for which reliable data was available.

13. At this stage I must explain that the Ministry of Home Security had adopted damage classes to describe the effects of bombs at various distances. They are shown on this vu-foil (vu-foil 7):-

A Damage Almost complete demolition.

B Damage Such severe damage as to necessitate demolition of the building. 50 - 75 % of the external brickwork destroyed or rendered unsafe.

Cb Damage Damage so severe that the house was rendered temporarily uninhabitable and it was not found feasible to make it habitable during the war. Partial collapse of the roof, partial collapse of one or two external walls, severe damage to load partitions.

Ca Damage Damage so severe that the house was rendered temporarily uninhabitable but it was considered feasible to make it habitable during the war. Only minor structural damage to be expected.

D Damage Damage calling for urgent repairs but not rendering the house uninhabitable. This did not include houses which suffered only slight damage, to glass or ceilings for instance.

14. The formula mentioned is fairly well known, has been quoted on many occasions and is to be found in many documents. However its derivation is not so well known and I would now like to look at this aspect as the formula is the foundation of the QDs as used to-day.

15. It was argued that a specific impulse corresponded to a definite level of damage and therefore the distance between the explosion and the damage was directly proportional to the two-thirds root of the explosives weight. However tests showed that although the product of impulse and distance did approximate to two-thirds of the explosives weight, less damage was caused by large charges than by small charges when the distances were scaled.

16. For small charge weights it was further argued that it was reasonable to assume that the relationship between the damage done by each charge would depend on the relationship between the total areas under the pressure time curves (ie. impulse) as the duration would be small. Thus the two-thirds root relationship would hold good.

17. However, if large charges are considered, then the duration of the blast waves would be longer and the damage may occur well before the end of the positive phase. The relationship between the damage done by larger charges is then only related to the peak positive pressure, the total area under the curve being irrelevant. Thus for large charges, instead of distance being proportional to the two-thirds root of the explosives weight it would be proportional to the one-third root.

18. The problem which then presented itself was to determine a value of "n" in the formula where distance was proportional to the explosives weight raised to the power of "n". All that was known about "n" was that its value tended to two-thirds for very small explosives weights, and towards one-third for very large weights.

19. A hot sunny afternoon in California is neither the time nor the place to enter into the next stage of the problem in detail. Suffice to say that the expression as shown (vu-foil 8)

was found to fit the requirements. The only remaining task was to determine the values of k and c.

20. Because of uncertainty in explosive content of the bombs dropped, it was decided that only data from the general purpose 250kg and 1000kg bombs was reliable. At the higher end of the scale the data from an accident in 1917 at Silvertown, an explosives factory situated on the banks of the River Thames, was used.

21. From this data the constants in the formula were determined and the formula shown on this vu-foil (vu-foil 9) was adopted to forecast the distance at which the level of B Damage could be expected.

22. It must be realised that the formula was derived from only three sets of data for the range of explosive weights from 200lb to 100000lb. In addition the bomb damage data was obtained from only 10 incidents. The Silvertown accident is also worthy of further examination. The accident occurred in a TNT manufacturing plant. The total quantity of explosive material on site at the time of the explosion was about 83 tons, it was estimated that only 53 tons was involved in the actual explosion. This figure was calculated by assessing the damage to the plant and surrounding area - a rather circular argument, and consideration of the material recovered. It was also noted that several craters were produced indicating separate explosions.

23. At this stage there appeared to be no intention of using the formula to calculate safety distances. Its purpose was to relate damage to bombs dropped during enemy air attacks, for close in damage it appeared to be very successful. Although circular arguments are apparent in that damage was assessed, distances measured the explosive weight calculated. It was then said that a specific bomb would produce a certain level of damage at various distances.

24. It was recognised that the German general purpose bomb would not necessarily produce a formula applicable to accidents involving the detonation of large quantities of explosives, nevertheless it was decided, for want of anything better, to examine available accident data to ascertain whether or not the formula could be substantiated and related to the accident scenario.

25. A total of 24 reports on accidental explosions which had occurred in the war were examined by the Committee and it was considered that the formula gave a satisfactory estimate of the radius of B damage. Brief details of these incidents will be included in the report of the Seminar (Annex A). A further 79 explosions were then examined dating back to the year 1871. Finally the data to be examined was supplemented by the table given in the Appendix to "Explosives, their Anatomy and Destructiveness" by C S Robinson; the table included a record of 138 incidents.

26. After studying all the information available on damage from explosions, the Committee, at a meeting on 21 September 1945, decided that the revised safety distance to be adopted should be of the order of 3 to 3.5 times the radius of B damage. In drawing up the conclusions the following cautions were recorded:-

a. No detailed description had been given of the buildings involved in the list of "79 explosions".

b. No description had been given of any of the incidents referred to in "Robinson's List". The Sub-Committee considered it necessary to emphasise that very little was known about most of these incidents.

c. Some of the incidents listed in the "79 List" were duplicated in the "Robinson List"; in some cases there was excellent agreement however in others there was striking disagreement.

d. While the group of incidents reported by experienced observers was the smallest of the three, it was considered to give more definite information than either of the other two.

It was mainly the results of the smaller group, ie. the war time incidents, that lead the Sub-Committee to suggest that distances of the order of 3 to 3.5 times the radius of B damage should be adopted. It was also proposed that a further and more detailed study of the data should be made.

27. The result of this further study was that on 29 October 1945 the Sub-Committee tentatively adopted, subject to further revision, safety distance to inhabited building of 3.5 times the radius of B damage for barricaded sites and 4 times for unbarricaded. However the rational behind the change from 3 to 3.5 times the B damage distance for all situations, to 3.5 for barricaded and 4 for unbarricaded is very obscure. The distances were intended for quantities of 5000lb or more and for smaller quantities the distances were to be increased to bring them into accord with distances which the members of the Sub-Committee considered to be reasonable.

28. Although not brought out in the reports, the following breakdown of the "79 List" is pertinent:- (vu-foil 11)

Gun Powder	21	Dynamite	1
Nitro Glycerine	12	Ammonal	1
Gelignite	8	TNT/Amn Nitrate	1
Picric Acid	4	Cordite	1
Gun Cotton	4	Others	1
Unknown	25		

and for the "Robinson List" :- (vu-foil 12)

Dynamite	46	Nitrostarch	2
Black Powder	37	Tracer Composition	2
Nitro Glycerine	24	Gun Cotton	2
Gelignite	8	DNT	1
TNT	6	Chlorate	1
HE	4	Mixed	1
Smokeless Powder	3	Amn Nitrate	1

Many of these incidents were manufacturing rather than storage and I question whether the "79 List" and the "Robinson List" are really relevant in consideration of the QDs for modern munitions.

29. I have sifted through the recorded damage in respect of the 24 war time incidents and identified the data pertinent to the the level of B damage and the OQD. The detail is plotted on this vu-foil (vu-foil 13) along with the B damage curve and the OQD. In order to simplify the vu-foil I have categorised the damage as either A, B, C or D. I do not believe that the damage strongly supports the OQD curve, it could quite easily have been drawn at 3 or 3.5 times the B damage level as originally proposed.

30. During the period 1946-1947, the Explosives Storage and Transport Committee planned a series of trials. The main purpose of the trials was to obtain information on the prevention of propagation by the use of barricades. Arrangements were also made to include direct measurements of the magnitude and duration of the blast pressures and were possible, to record any damage to buildings as a check on the proposed OQDs. Unfortunately the limitations of the site excluded any useful deductions being made regarding the adequacy of the proposed QDs. The few structures within range were of concrete and already in a damaged condition. It was also necessary to curtail the trials programme and a serious gap in the data was acknowledged.

31. In 1948 the Explosives Storage and Transport Committee adopted the new distances, it was agreed on the evidence available that there was no justification for adopting different distances for barricaded and unbarricaded when the NEQ was above 3600kg and it was decided to adopt a standard distance of 4 times the radius of B damage for the OQD. For barricaded quantities not exceeding 3600kg it was considered justifiable to reduce the distance by 20% ie to 3.2 times the radius of B damage. It should be noted that the increased distances for smaller quantities proposed in 1945 was not pursued.

32. The distances have remained essentially the same to this day with the exception that they have now been metricated and:

a. The reduction permitted for barricaded explosives below 3600kg has been deleted.

b. A minimum distance has been introduced to take into account the hazards resulting from fragment attack. This minimum distance does not apply if adequate protection from fragment attack is provided.

33. I have covered quite considerable ground in the last 10 minutes or so and suggest it would be sensible to consolidate before proceeding further.

34. To summarise:

a. The QGDs are based on the formula derived to predict the level of damage to be expected from aerial bombs.

b. The formula was derived from analysis of 10 events, 5 involving 1000kg bombs and 5 involving 250kg bombs, and the accident at Silvertown in 1917.

c. The explosive involvement of the accident at Silvertown was assessed as 53 tons, this was based on material remaining on site after the explosion and consideration of the damage. Multiple explosions were apparent. It should be noted that beyond a distance of 2.8 times the radius of B damage, the damage was limited to broken window frames, doors and ceilings and was of a character that could be described as slight structural injury.

d. Many of the incidents in the "79 List" and the "Robinson List" involved NG or gunpowder, very few involved Military explosives. Many of the incidents were manufacturing rather than storage and the recorded data was of a very poor quality. The use of such data is questioned.

e. The proposals for the QGD varied from 3 to 4 times the radius of B damage. Justification for the various proposals is obscure and support for a value of 4 times the radius of B damage is no greater than it is for 3 times.

d. The value of $k = 22.2$ in the formula for QGDs above 4500kg implies a precision and accuracy that does not exist.

35. I believe that there is sufficient uncertainty in the derivation for an in depth study to be under taken which should include trials.

36. I mentioned earlier that the same OGDs apply to all types of above ground storage sites, ie open stacks, brick buildings and earth covered magazines. I would now like to discuss the situation with respect to earth covered magazines.

37. There have been a number of trials over the years involving earth covered buildings, both at full scale and one tenth scale. The main object of these trials was to determine the blast parameters seen by adjacent magazines and to confirm the inter magazine distances, however some free field blast measurements were also obtained. Additionally, model trials at 1/30 and 1/50 scale have also been carried to measure close in and far field pressures. In the interests of time I will not describe the specific trials, brief details of the trials I have considered will be included in the minutes of the Seminar (Annex B).

38. Ideally the TNT equivalence of the donor charge for each trial should be calculated and used in the analysis. The explosives used in all the trials was equal to or more energetic than TNT and conversion to TNT equivalence would increase the effective NEQ to be used in the assessment. However in some of the trials, in particular the ESKIMO Series, the donor charges were cased and this should also be taken into account in determining the TNT equivalence; this would have the effect of lowering the effective NEQ. Other factors can alter the effective NEQ, ie geometry of the charge, size of the charge, etc. The factors are many and varied and the effect of such factors are not sufficiently well understood at this stage to be applied with confidence as a general case, it is therefore considered prudent to use the actual donor charge weights rather than attempt a conversion. The model trials used bare charges (pentolite and CE/TNT) and thus use of the actual NEQ in the calculations introduces a "worst situation" which errs on the side of safety.

39. The full scale trial reported in technical paper 3843, 1965, was designed to provide maximum effect, ie the donor consisted of densely packed cans of Composition B. It is therefore considered acceptable to convert to TNT equivalence in this one instance. The fact that the charge was densely stacked and that multi-point initiation was used still makes the results err on the side of safety.

40. From a preliminary study of all the relevant data it was apparent that differing effects were obtained from the front, side and rear of the earth covered magazines. A plot of over-pressure against scaled distance for each trial was drawn. An example of the type of plot produced is shown on this vu-foil (vu-foil 14). The scaled distance at which a peak over-pressure of 5kPa would be obtained was determined for each situation. Again the detail is too much for this presentation but the figures will be included in the summary record (Annex C).

41. I will now look at each of the three orientations in turn.

42. Rear The plot of distance against NEQ for the rear orientation is shown on this vu-foil (vu-foil 15), the correlation using all the model results is good; the two full scale results are below the model curve. I suggest that there is sufficient evidence to adopt smaller OQDs than currently prescribed from the rear of earth covered magazines for the range of NEQ from 6000kg to 250000kg. The fact that the two full scale results are below the curve builds in a safety factor.

43. Side As for the rear orientation, this next vu-foil (vu-foil 16) shows the plot of distance against NEQ for the side orientation for the same constant value of the over-pressure. Again the correlation using all the model results is good and the four full scale trial results are again below the model curve. As for the rear orientation there is, I believe, sufficient evidence to adopt smaller OQDs from the sides of earth covered magazines.

44. Front The situation with regard to the front orientation is not as clear. This vu-foil (vu-foil 17) shows the plot of distance against NEQ for the same constant over-pressure of 5kPa. If the three low points at the high end of the plot are ignored, then a line with good correlation can be drawn through the remaining model results. It should be noted that the original BRL Report observed that higher NEQ produced pressure values lower than expected, but no reason was offered. It is possible that the higher charge weights produced a more disruptive effect on the building, thus reducing the strong directional effect to the front. The high charge weights in ESKIMO III and V also produced lower pressures to the front than expected. Three of the four full scale trials are below the model curve and the fourth - the bulk packed Composition B, is just above the curve. The evidence supports a reduction from the front - perhaps not as conclusive as from the side and rear. More trials data is required to increase the confidence level.

45. The next step is to suggest what the revised distances should be. Early in the presentation I indicated that above about 5000kg the damage to a normal dwelling from a bare charge of TNT was pressure dependent and therefore proportional to the cube root of the NEQ. It is not unreasonable to postulate that when a charge is suppressed by massive earth covering then the cube root law will no longer hold good. In fact the three curves I have just displayed fit the expressions as shown on this vu-foil (vu-foil 18).

46. Concern has been expressed in the UK at the departure from a simple cube root relation, although it is acknowledged that more suppression should be expected and is obtained when the NEQ is lower. Thus the value of K in the cube root expression will change as the NEQ increases.

47. My personal view is that if the facts fit a departure from the cube root relation, and they do, then we should revise the distances accordingly. However this is not a technical matter but a classical example of "we have always done it like that - why should we change now"

48. Another approach would be to relate either the total mass of cover, or the thickness of the cover, say at the mid point of the height of the magazine, to the NEQ and then calculate a relationship to the distance. This may prove to be a neater solution and allow a return to the cube root relation. This exercise I have programmed for the future.

49. Whatever method is used there is clearly mileage to be gained, these next three vu-foils (vu-foils 19-21) show the comparison of the current QQDs and proposed QQDs for each orientation.

50. Such reductions are perhaps of little significance in this part of the world where space does not seem to be a problem. But those of you who have been involved in siting of ammunition facilities in Europe will be aware of the grave difficulties with regard to real estate and will appreciate that any reduction in distances whilst still maintaining an acceptable level of safety will be most welcome.

51. A proposal to reduce the QDs has departed from the subject of the "Audit of the QDs". However I do tend to get carried away at times - my wife sometimes wonders why I sit looking at a computer screen for several hours during the evening.

52. My final overall summary of this very small part of the QD audit is as follows (vu-foil 22)

a. The general QQDs are not founded on such reliable data as is believed and they imply an accuracy and a precision that does not exist. It is likely that they are over cautious.

b. Different QQDs should be applied to different donor sites and in particular the evidence for introducing reduced distances from earth covered magazines is very strong, although more trials data may be necessary in respect of the front orientation in order to increase the confidence level.

53. Gentlemen that brings me to the end of my presentation, it has been detailed then the subject is complex. I have dealt with only about half a dozen entries in the QD matrices out of the total of 1300 - the road is long. How long I will continue on this audit I can't say, clearly I would like to see it through to the end. Now for my final plug, I did say that I would finish on a "commercial". The success of the audit depends upon a review of as much data as possible - trial results, accidents and subjective reasoning. I have amassed a considerable number of reports, nevertheless, copies of reports, both accidents and trials, opinions or even references will be most welcome and will be received most gratefully by me.

ANNEX A

BRIEF DETAILS OF 24 WAR TIME INCIDENTS

1. Rotherwas 12 September 1941. 300lb of TNT in a Royal Ordnance Factory.
2. Gravely 20 November 1943. 1000lb GP bomb filled 360lb 60/40 amatol.
3. Pembrey 23 November 1942. 2000lb TNT in a Royal Ordnance Factory, explosion occurred during the nitration of TNT.
4. Irvine 2 April 1940. 2240lb of bulk TNT.
5. Deenethorpe 5 December 1943. 12 x 500lb bombs, the explosion took place in an aircraft on the ground.
6. Offley 3 January 1945. 20 x 500lb bombs, the explosion took place in a rail wagon.
7. Catterick 4 February 1944. 397 boxes of grenades No. 75, filled burrowite total NEQ 6000lb. Explosion took place whilst loading a rail wagon from a road vehicle.
8. Waltham 18 January 1940. 6160lb guncotton.
9. Soham 2 June 1944. 44 x 500lb aircraft bombs DN-M64, filled amatol 50/50, NEQ per bomb 262lb total NEQ 11500lb. Charge weight ratio 53%.
10. Bootle 20 March 1945. 52 x 450lb depth charges, filled amatol total NEQ 18700lb. Explosion took place in a rail wagon.
11. Gascoigne Wood 18 April 1945. 98 x 500lb bombs, filled TNT total NEQ 27000lb.
12. JANAS B Abs:5. About 110 x 500lb bombs, filled Comp B total NEQ about 28000lb.
13. Hereford 30 May 1944. 12 x 2000lb aircraft bombs and 19 naval mines, total NEQ estimated at 33000lb of minol.
14. Igloo Magazine 13 August 1943. 20lb fragmentation bombs, filled TNT total NEQ 34000lb.
15. JANAS B Abs:9. 56 mines, filled torpex total NEQ 35860lb.
16. JANAS B Abs:14. 193 x depth bombs, filled torpex total NEQ 48000lb.
17. JANAS B Abs:8. Dynamite packed in boxes, total NEQ 70000lb.

18. Enemy action 23 February 1944. 3000 boxes grenades No. 75, total NEQ 48000lb.

19. Newhaven 21 November 1944. Nobels 822 bulk explosive, total NEQ 336000lb. The explosion took place on an ammunition barge.

20. JANAS P Abs:10. 2272 x 500lb bombs, filled Comp B total NEQ 591000lb. The explosion took place in a ship alongside a quay.

21. JANAS B Abs:7. 3339 x 350lb bombs, filled torpex total NEQ about 800000lb.

22. ANES B Abs:2. Miscellaneous ammunition, mostly torpex total NEQ 1100000lb.

23. ANES B Abs:1. Miscellaneous ammunition, total NEQ 3800000.

24. Buton-en-Trent 27 November 1944. Miscellaneous bombs, total NEQ about 5340000lb. Explosion occurred in an underground storage depot.

ANNEX B

DETAILS OF TRIALS

1. BRL Report 2680 1/50 scale trial. The donor charges of 0.8, 2.4 and 4.0lb pentolite (to represent 100000, 300000 and 500000lb at full scale) were contained in model earth covered steel arch igloos. The earth cover was carried from one half standard cover to double cover. Blast measurements were made in the near field and at scaled distances up to $30Q^{1/3}$. only measurements made with the standard cover were considered.
2. ARBRL Report TR 02453 1/30 scale trial. The donor charges of 0.227, 0.363, 1.088, 1.814 and 5.040kg pentolite (to represent 6130, 9800, 29370, 48980 and 136080kg at full scale) were contained in model earth covered steel arch igloos. Blast measurements were made in the near field and at scaled distances up to $19Q^{1/3}$.
3. ESTC/3/71 1/10 scale trial. Donor charge 64kg TNT slabs (to represent 64000kg at full scale) contained in a box type earth covered magazine. The trial involved four shots and far field blast effects were measured at nominal scaled distances of $8Q^{1/3}$ and $22Q^{1/3}$.
4. ESTC/3/76 1/10 scale trial. Donor charge of 8, 64, 125 and 216kg TNT slabs (to represent 8000, 64000, 125000 and 216000kg at full scale) contained in a box type earth covered magazine. The trial involved one shot at each charge weight and far field blast effects were measured at nominal scaled distances of $8Q^{1/3}$ and $22Q^{1/3}$.
5. ESKIMO I Full scale trial. The donor charge consisted of 155mm TNT filled projectiles, total NEQ 200000lb, contained in an earth covered steel arch igloo. Blast effects were measured at scaled distances up to $19Q^{1/3}$.
6. ESKIMO II Full scale trial. The donor charge consisted of tritonal filled M117 bombs with a total NEQ of 27800lb. The charge was contained in an open earth revetment. The trial was not considered.
7. ESKIMO III Full scale trial. The donor charge consisted of tritonal filled M117 bombs with a total NEQ of 350000lb contained in an earth covered steel arch igloo (lightweight 14 gauge deeply corrugated steel). Blast effects were measured in the near field and at scaled distances up to $20Q^{1/3}$.
8. ESKIMO IV Full scale trial. The donor charge consisted of 37000lb TNT stacked in the open in a hemispherical shape. The trial was not considered.
9. ESKIMO V Full scale trial. The donor charge consisted of 34000kg TNT stacked in the open in a hemispherical shape. The trial was not considered.

10. ESKIMO VI 1/2 scale trial. The donor charge consisted of Mark 16 torpedo warheads filled TNT, NRQ 44000lb (to represent 350000kg at full scale). The charge was contained in a large earth covered box type IIB magazine. Blast effects were measured in the near field and at scaled distances up to $19Q^{1/3}$.



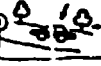

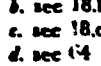
11. NOTS TP 3843 Full scale trial. The trial consisted of 6 tests, only test 6 is relevant to this paper. The donor charge consisted of 100000lb of Comp B packed in 2106 sealed, 9.5in cubical cans, 47.5lb NRQ per can. The cans were in a single stack to obtain maximum blast effects. The donor charge was contained in a steel arch earth covered igloo (1 gauge corrugated steel). The TNT equivalent of the donor charge was considered to be 113000lb. Blast effects were measured at scaled distances up to $29Q^{1/3}$. (Tests 1 and 2 were at full scale with donor charges of 998kg, however the donor igloos had acceptor igloos on each side at scaled distances of between 0.2 and 0.8 with a common earth cover over the donor and the two acceptors to a depth of about 0.6m. The configuration produced unusually high pressures to the front and unusually low pressures to the rear, the tests were not representative and were not considered).

ANNEX C

DISTANCES RELATED TO A PEAK OVER PRESSURE OF 5pKa

Trial	N	Rep. kg	Front		Side		Rear	
			SD	Dist- ance	SD	Dist- ance	SD	Dist- ance
US Model 1/50 Scale	.363	45375			18.3	653		
	1.088	136000			22.8	1173		
	1.814	226750			22.2	1354		
US Model 1/30 Scale	.227	6129	15.9	291	17.0	311	12.7	232
	.363	9901	18.0	385	17.4	372	13.6	291
	1.066	28782	18.1	555	17.9	549	13.9	426
	1.128	30456	18.2	568	18.0	562	14.3	447
	4.990	134730	15.5	795	20.8	1066	16.7	856
UK Model 1/10 Scale	8	8000	16.0	320	14.6	292	13.2	264
	64	64000	14.9	596	18.6	744	18.5	740
	125	125000	19.8	990	19.0	950	15.3	765
	216	216000	16.4	984	20.6	1236	21.4	1284
ESKIMO I	90720	90720	18.6	836	20.5	921		
ESKIMO III	158760	158760	14.8	801	20.2	1094		
ESKIMO VI	19958	159664	14.9	808	16.0	868	13.2	716
NOTS 3843	51257	51257	20.1	747	17.7	657	12.9	479

QUANTITY-DISTANCE TABLE FOR HAZARD DIVISION 1.1

POTENTIAL EXPOSURE SITE (ES)	(a)	(b)	(c)	(d)	(e)	(f)
 1	D3 _{es}	D3 _{es}	D6 _{es} or D7 _{es}	D6 _{es} or D7 _{es}	D6 _{es} or D7 _{es}	D4 _{es}
 2	D3 _{es}	D3 _{es}	D6 _{es} or D7 _{es}	D6 _{es} or D7 _{es}	D6 _{es} or D7 _{es}	D4 _{es}
 3	D4 _{esph} or D5 _{es}	D4 _{esph} or D5 _{es}	D4 _{esph} or D6 _{es}	D4 _{esph} or D6 _{es}	D4 _{esph} or D6 _{es}	D4 _{esph} or D6 _{es}
 4	D3 _{es}	D3 _{es}	D6 _{es} or D7 _{es}	D6 _{es} or D7 _{es}	D6 _{es} or D7 _{es}	D3 _{es}
 5	D3 _{es}	D3 _{es}	D6 _{es} or D7 _{es}	D6 _{es} or D7 _{es}	D6 _{es} or D7 _{es}	D3 _{es}
 6	D4 _{esph} or D6 _{es}	D4 _{esph} or D6 _{es}	D4 _{esph} or D6 _{es}	D4 _{esph} or D6 _{es}	D4 _{esph} or D6 _{es}	D3 _{esph} or D6 _{es}
 7	D4 _{es}	D5 _{es}	D8 _{es} , D9 _{es} or D12 _{es}	D8 _{es}	D8 _{es} , D9 _{es} or D12 _{es}	D8 _{es} , D9 _{es} or D12 _{es}
 8	D6 _{es}	D6 _{es}	D8 _{es} , D9 _{es} or D12 _{es}	D9 _{es}	D8 _{es} , D9 _{es} or D12 _{es}	D8 _{es} , D9 _{es} or D12 _{es}
 9	D4 _{esph} or D7 _{es}	D4 _{esph} or D7 _{es}	D9 _{es}	D4 _{esph} or D9 _{es}	D9 _{es}	D9 _{es}
 10	D4 _{esph} or D7 _{es}	D4 _{esph} or D7 _{es}	D9 _{es} or D12 _{es}	D4 _{esph} or D9 _{es}	D9 _{es} or D12 _{es}	D9 _{es} or D12 _{es}
 11	D4 _{esph} or D7 _{es}	D4 _{esph} or D7 _{es}	D9 _{es} or D12 _{es}	D4 _{esph} or D9 _{es}	D9 _{es} or D12 _{es}	D9 _{es} or D12 _{es}
 12	D4 _{esph} or D7 _{es}	D4 _{esph} or D7 _{es}	D4 _{esph} or D7 _{es}	D4 _{esph} or D7 _{es}	D4 _{esph} or D7 _{es}	D3 _{esph} or D7 _{es}
 13	D4 _{esph} or D7 _{es}	D4 _{esph} or D7 _{es}	D4 _{esph} or D7 _{es}	D4 _{esph} or D7 _{es}	D4 _{esph} or D7 _{es}	D5 _{esph} or D7 _{es}
 14	D4 _{esph} or D7 _{es}	D4 _{esph} or D7 _{es}	D4 _{esph} or D7 _{es}	D1 _{es} , D2 _{es} , D4 _{esph} or D7 _{es}	D1 _{es} , D2 _{es} , D4 _{esph} or D7 _{es}	D4 _{esph} or D7 _{es}
 15	D4 _{esph} or D7 _{es}	D4 _{esph} or D7 _{es}	D9 _{es} or D12 _{es}	D1 _{es} , D2 _{es} , D4 _{esph} or D7 _{es}	D9 _{es} or D12 _{es}	D9 _{es} or D12 _{es}
 16	D9A _{es} or D10 _{es}	D9A _{es} or D10 _{es}	D9A _{es} or D10 _{es}	D9A _{es} or D10 _{es}	D9A _{es} or D10 _{es}	D9A _{es} or D10 _{es}
 17	D10 (≥ 250 m)	D10 (≥ 270 m)	D10 (≥ 270 m)	D9A _{es} or D10 _{es}	D9A _{es} or D10 _{es}	D10 (≥ 270 m)
 18	D10 (≥ 270 m)	D10 (≥ 270 m)	D13 (≥ 270 m)	D9A _{es} or D10 _{es}	D13 (≥ 270 m)	D13 (≥ 270 m)
 19	D11 (≥ 270 m) _a or D13 (≥ 400 m)	D11 (≥ 270 m) _b or D13 (≥ 400 m)	D11 (≥ 270 m) _c or D13 (≥ 400 m)	D11 (≥ 180 m) _a or D13 (≥ 270 m) _a or D13 (≥ 270 m) _{im}	D11 (≥ 270 m) _b or D13 (≥ 270 m) _b or D13 (≥ 270 m) _{im}	D11 (≥ 270 m) _c or D13 (≥ 400 m) _c or D13 (≥ 400 m) _{im}
 20	D13 (≥ 400 m) _i	D13 (≥ 400 m) _i	D13 (≥ 400 m) _i	D13 (≥ 400 m) _{im}	D13 (≥ 400 m) _{im}	D13 (≥ 400 m) _i

a. sec 18.a. —virtually complete protection.

b. sec 18.b. —high degree of protection.

c. sec 18.c. —moderate degree of protection.

d. sec 14 —resistance of headwall and door(s) at ES.

e. sec 66 —effect of blast on structure at ES.

f. sec 16 —degree of protection depends on structure at ES and sensitiveness of its contents.

g. sec 6 —excluding primary explosive substances, etc.

h. sec 66 —excluding items at the ES vulnerable to attack by heavy spalling.

i. sec 37 —modular storage of bombs in open stacks.

j. sec 60 —untraversed storage of robust shell.

k. sec 26 —reaction of drivers on busy roads.

l. sec 29.a. —flying and falling glass, etc.

m. sec 29.b. —400 m minimum to built-up areas.

n. sec 56.c. —unless traverse effectively screens ES from projections.

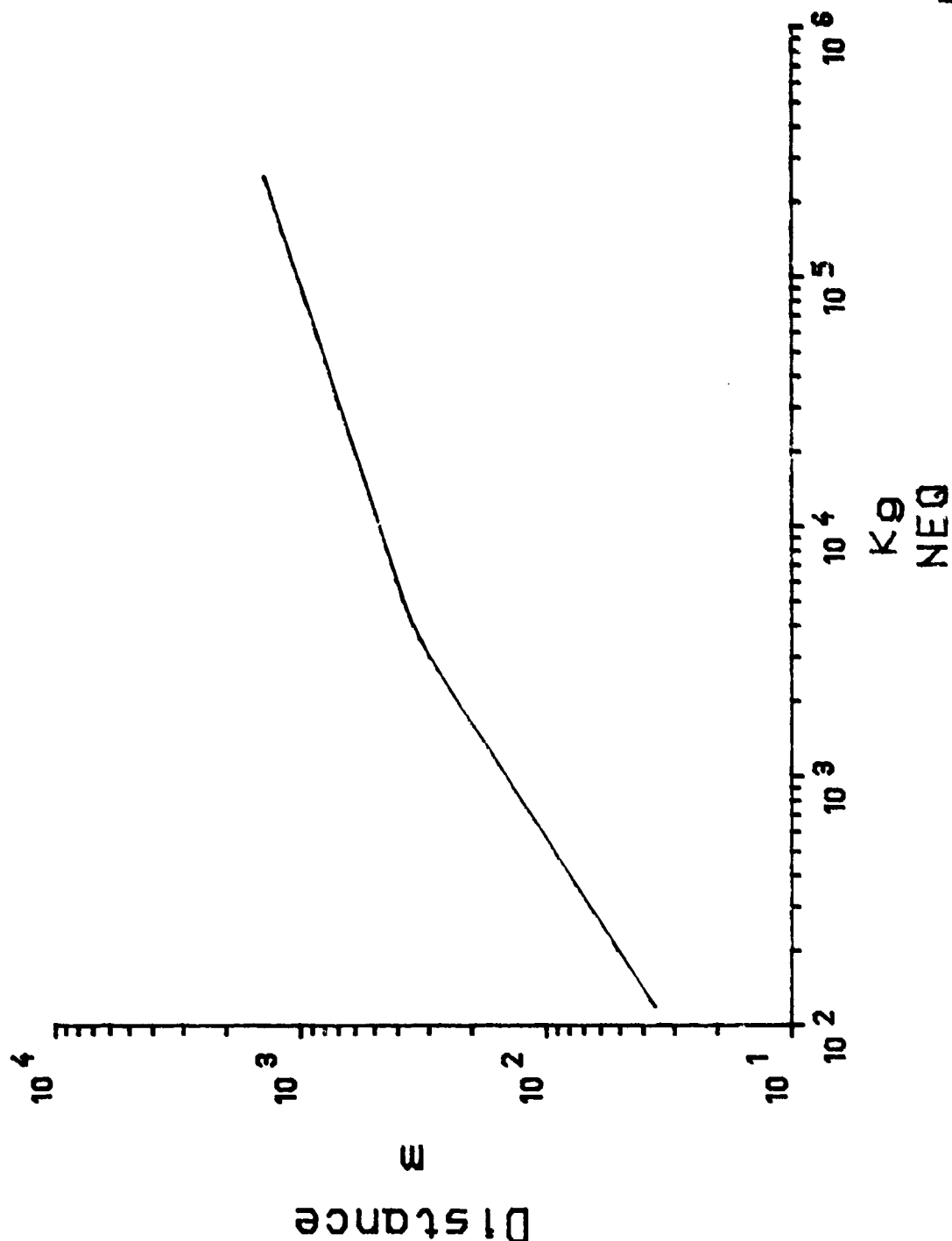
o. sec 10.a. —(in Preface)—less than D10 in many traversed situations when Q < 5000 kg.

p. sec 24.b(3) —risk to persons is tolerable in certain circumstances.

q. sec 24.b(4) —risk to persons is tolerable generally.

UK OUTSIDE QUANTITY DISTANCE

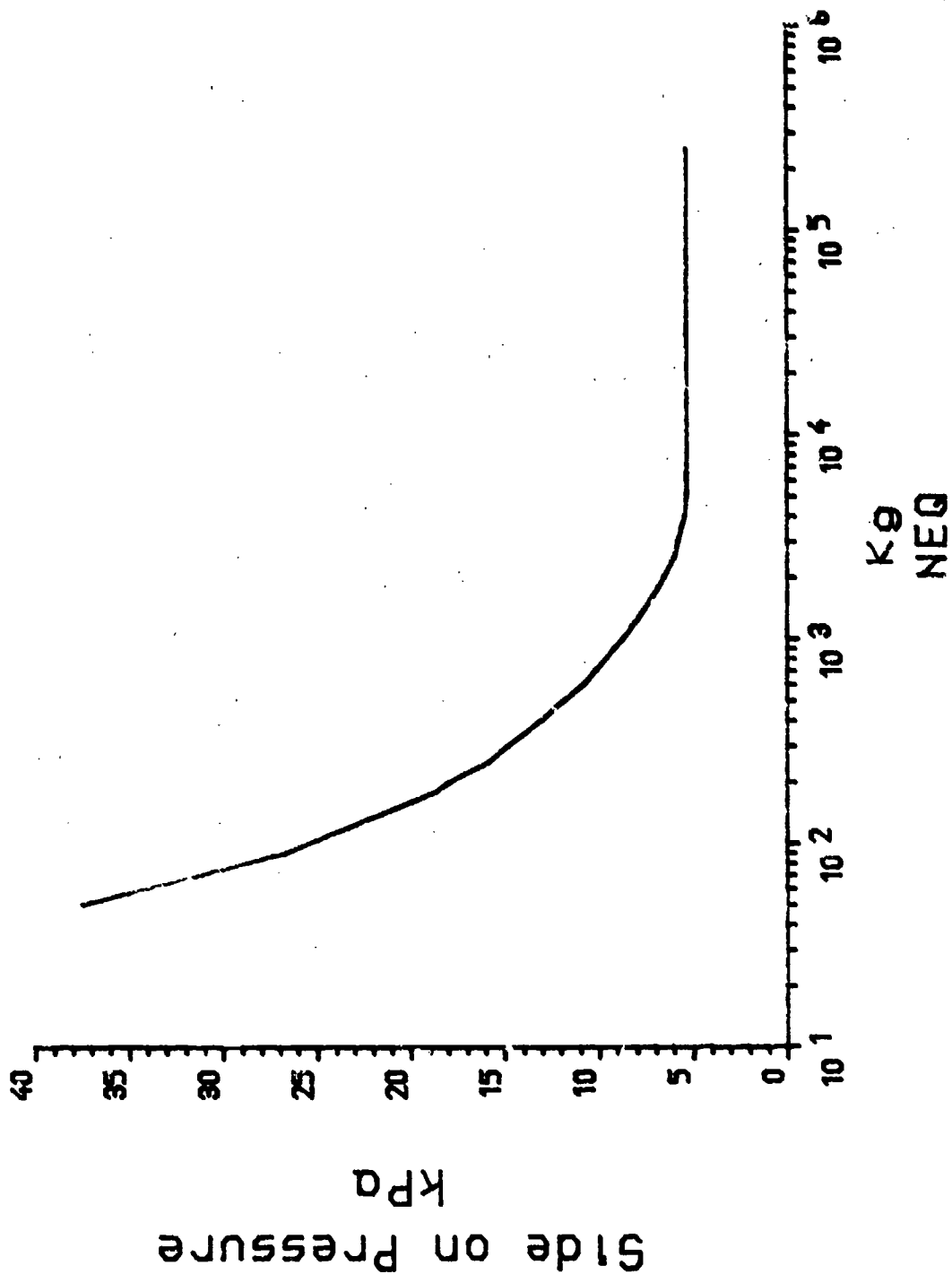
Hazard Division 1.1



Uu-Fo11 2

UK OUTSIDE QUANTITY DISTANCE

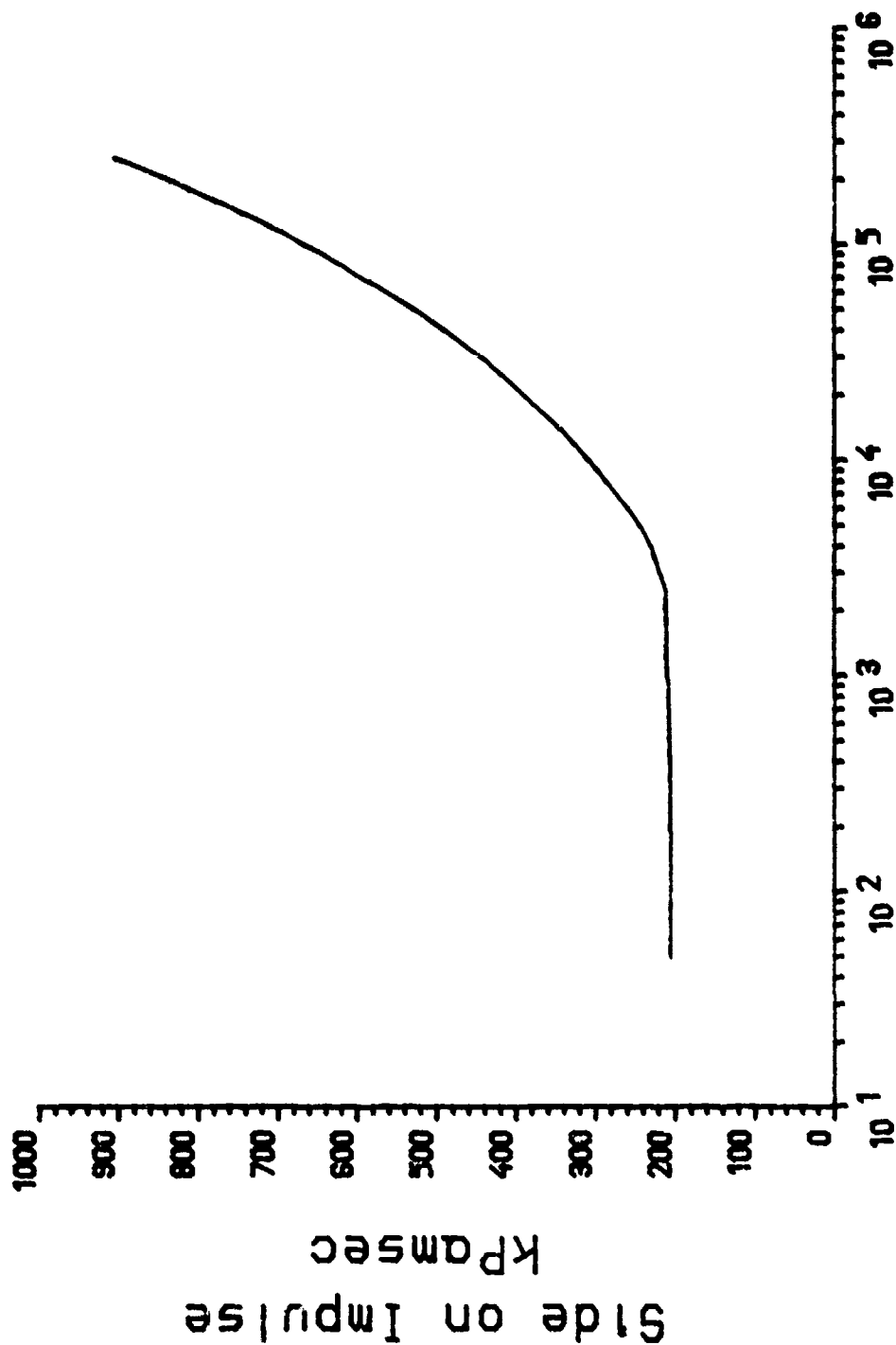
Hazard Division 1.1



UU-F011 3

UK OUTSIDE QUANTITY DISTANCE

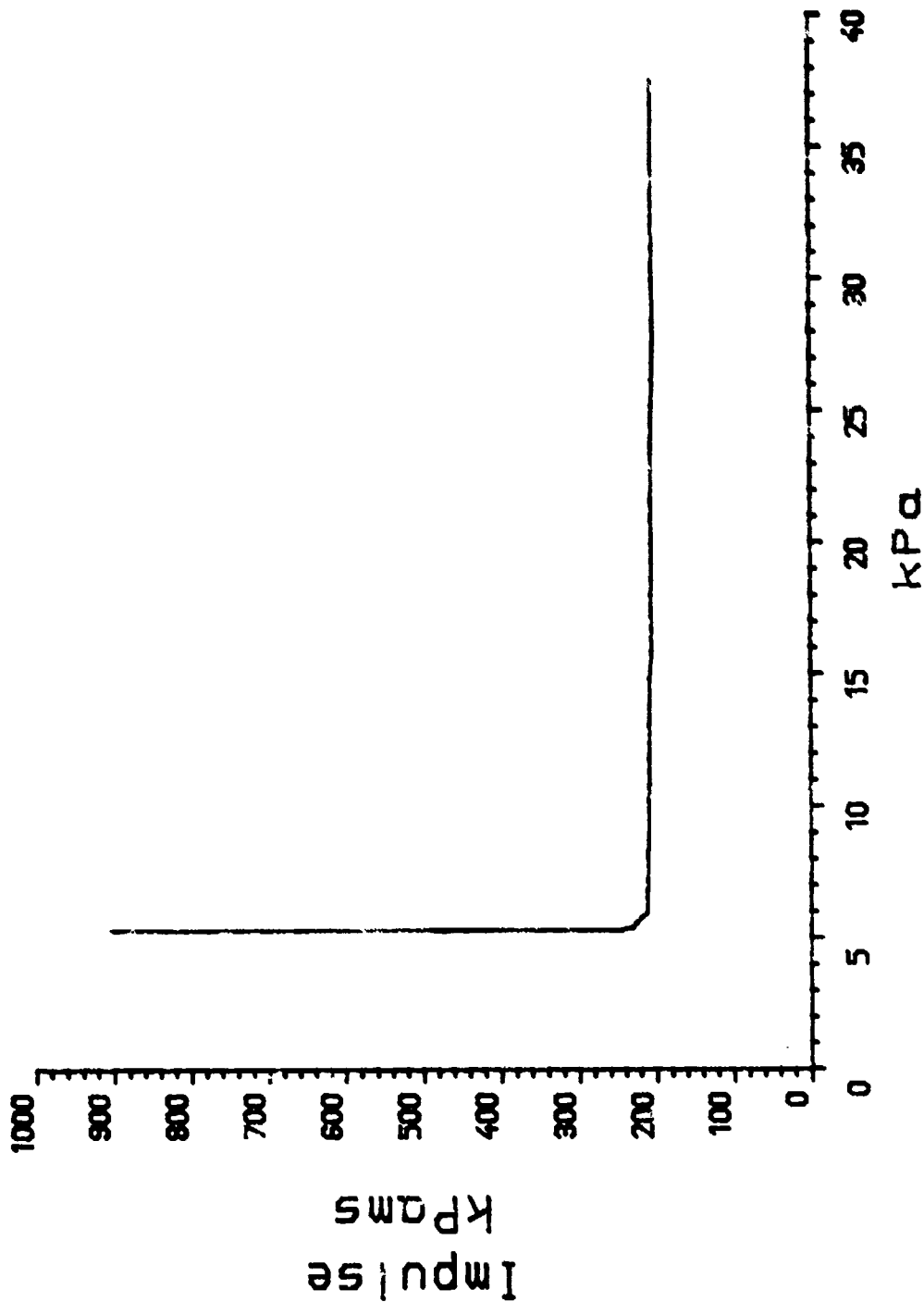
Hazard Division 1.1



K9
NEQ

UU-F011 4

ISO DAMAGE CURVE - 003
Impulse/Pressure (Side On)



Pressure

kPa

UU-F011 5

STANDARD FOR THE OGD

That an explosion of the whole contents of a building or stack should not cause serious structural damage to the ordinary dwelling house. Minor damage such as broken windows, dropped ceilings or loosened slates would be accepted.

MINISTRY OF HOME SECURITY
DAMAGE LEVELS

- A DAMAGE** Almost complete destruction.
- B DAMAGE** Severe damage.
50-75% external brick-work destroyed.
- Cb DAMAGE** Uninhabitable.
Partial collapse of roof.
Partial collapse of one or two external walls.
Severe damage to load partitions.
- Ca DAMAGE** Uninhabitable.
Only minor structural damage.
- D DAMAGE** Damage calling for urgent repairs.
Did not include ceiling and glass damage.

Vu-foil 8

BASIC EXPRESSION
FOR ANY DAMAGE LEVEL
DISTANCE - NEQ

$$D = \frac{kQ^{\frac{1}{3}}}{\left[1 + \left(\frac{C}{Q}\right)^2\right]^{\frac{1}{6}}}$$

EXPRESSION FOR B DAMAGE
DISTANCE - NEQ

$$D = \frac{14 Q^{\frac{1}{3}}}{\left[1 + \left(\frac{7000}{Q} \right)^2 \right]^{\frac{1}{6}}}$$

"THE 79 LIST"

GUN POWDER	21
NITRO GLYCERINE	12
GELIGNITE	8
PICRIC ACID	4
GUN COTTON	4
DYNAMITE	1
AMMONAL	1
TNT/AMM NITRATE	1
CORDITE	1
OTHERS	1
UNKNOWN	25

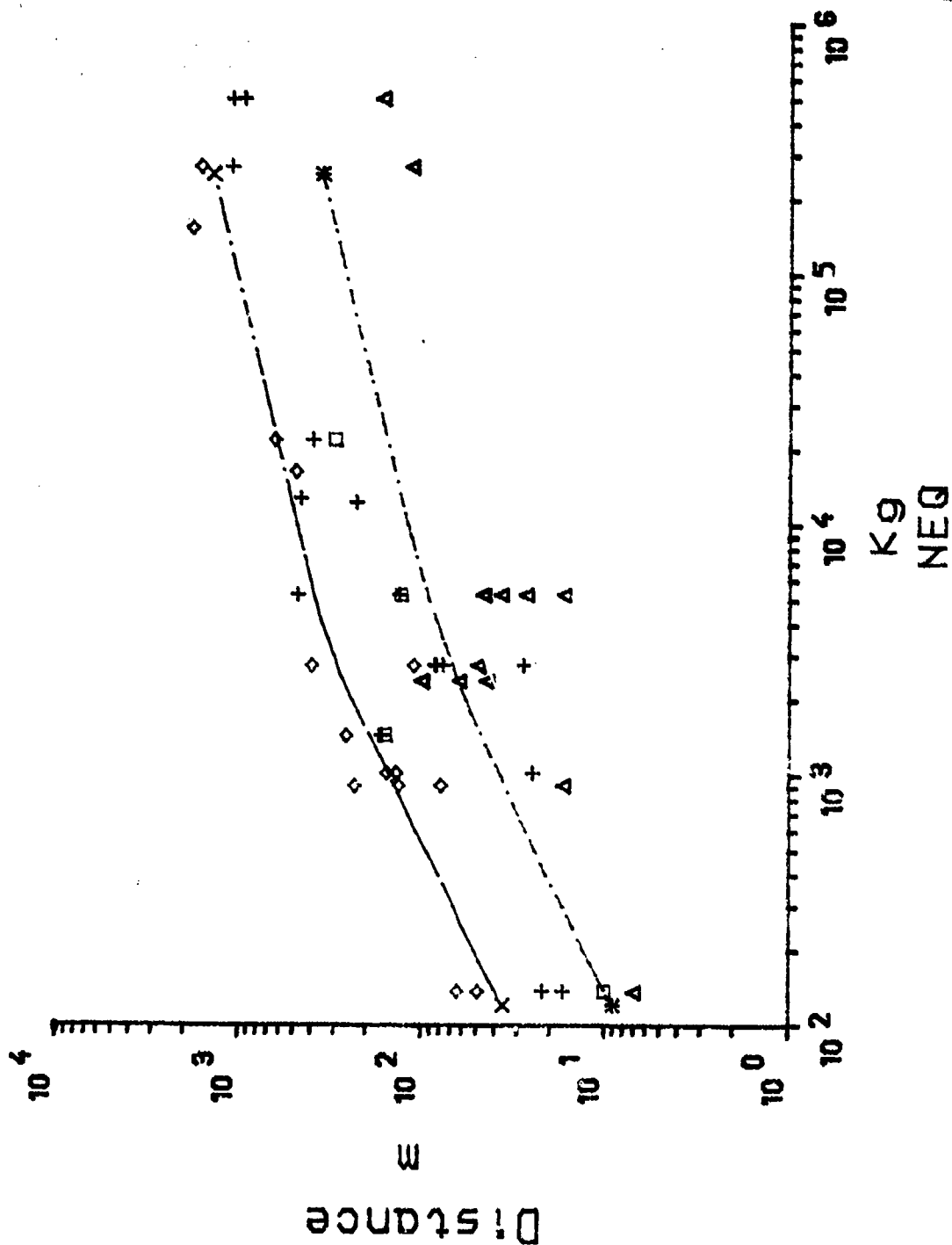
Vu-foil 12

"THE ROBINSON LIST"

DYNAMITE	46
BLACK POWDER	37
NITRO GLYCERINE	24
GELIGNITE	8
TNT	6
HE	4
SMOKELESS POWDER	3
NITRO STARCH	2
TRACER COMPOSITION	2
GUN COTTON	2
DNT	1
CHLORATE	1
MIXED	1
AMM NITRATE	1

DAMAGE PLOT "24" INCIDENTS UK OOD and 1 RB Curves

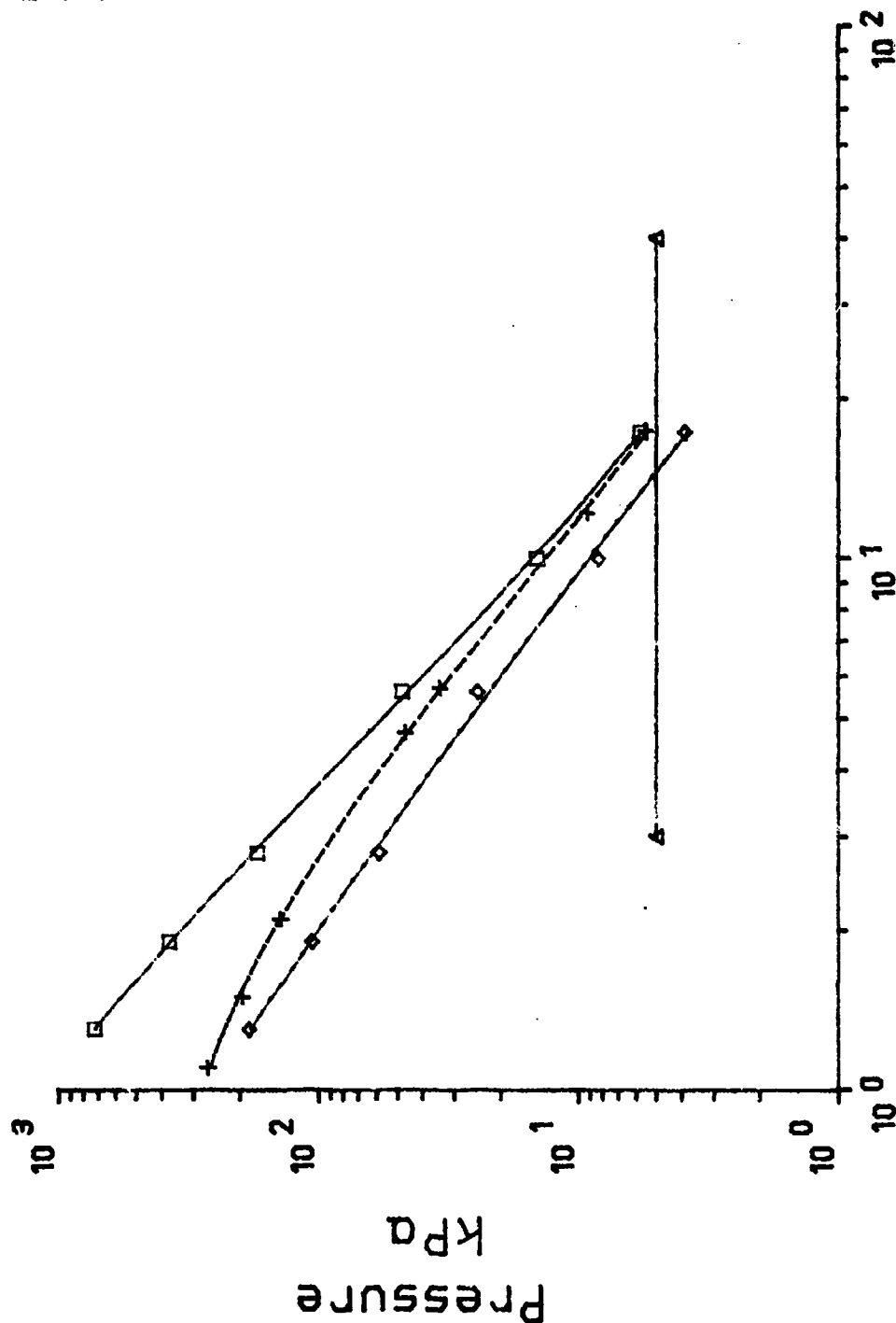
A Damage
 B Damage
 C Damage
 D Damage
 UK OOD
 1 RB



UU-F011 13

Model Trials 1/30 Scale NEQ 1.128kg (30456kg)

5kPa Line
 Front
 Side
 Rear

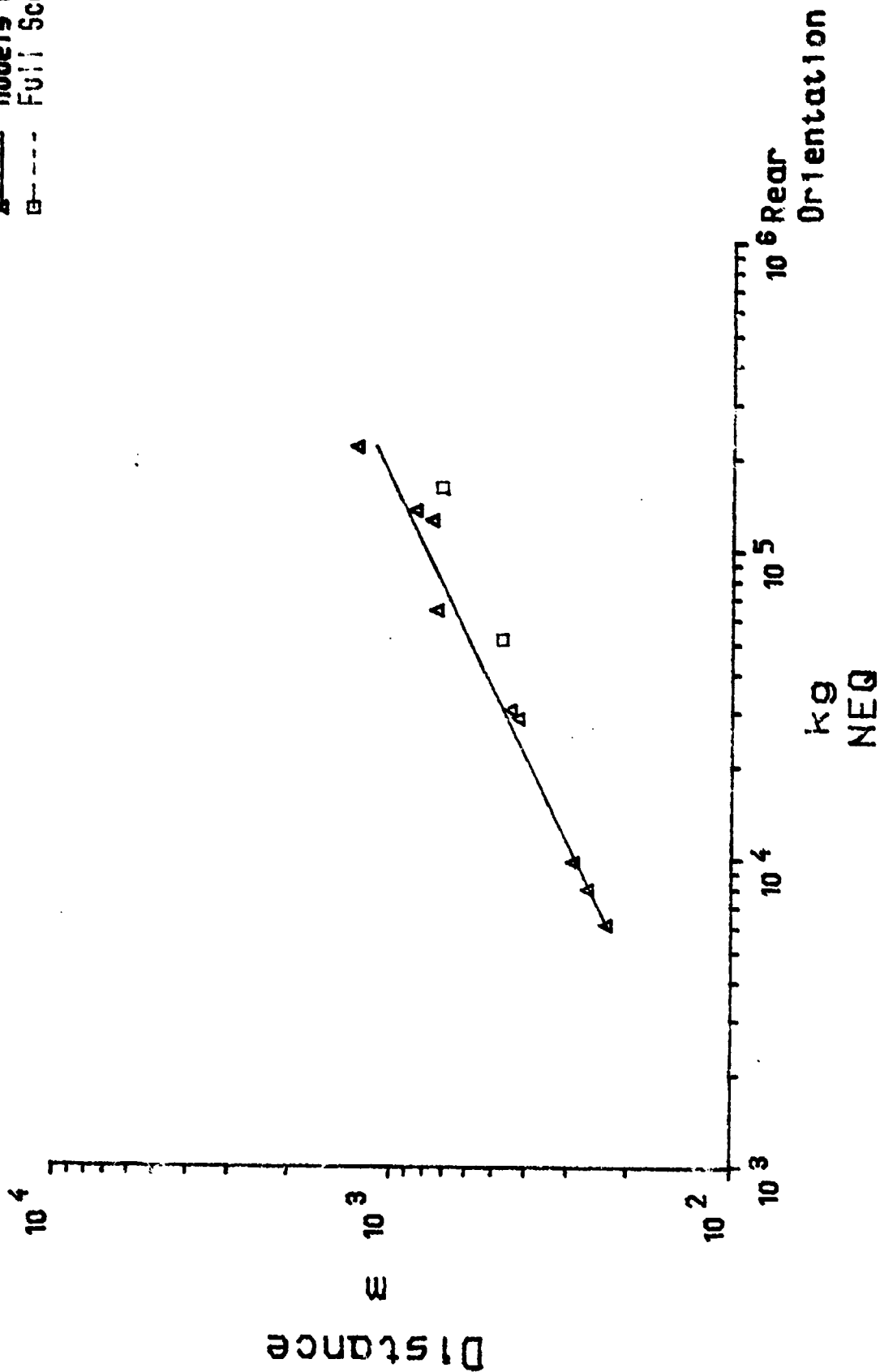


$m/Q^{1/3}$
 Scaled Distance

Uu-Foil 14

Earth Covered Building Distance/NEQ for 5kPa level

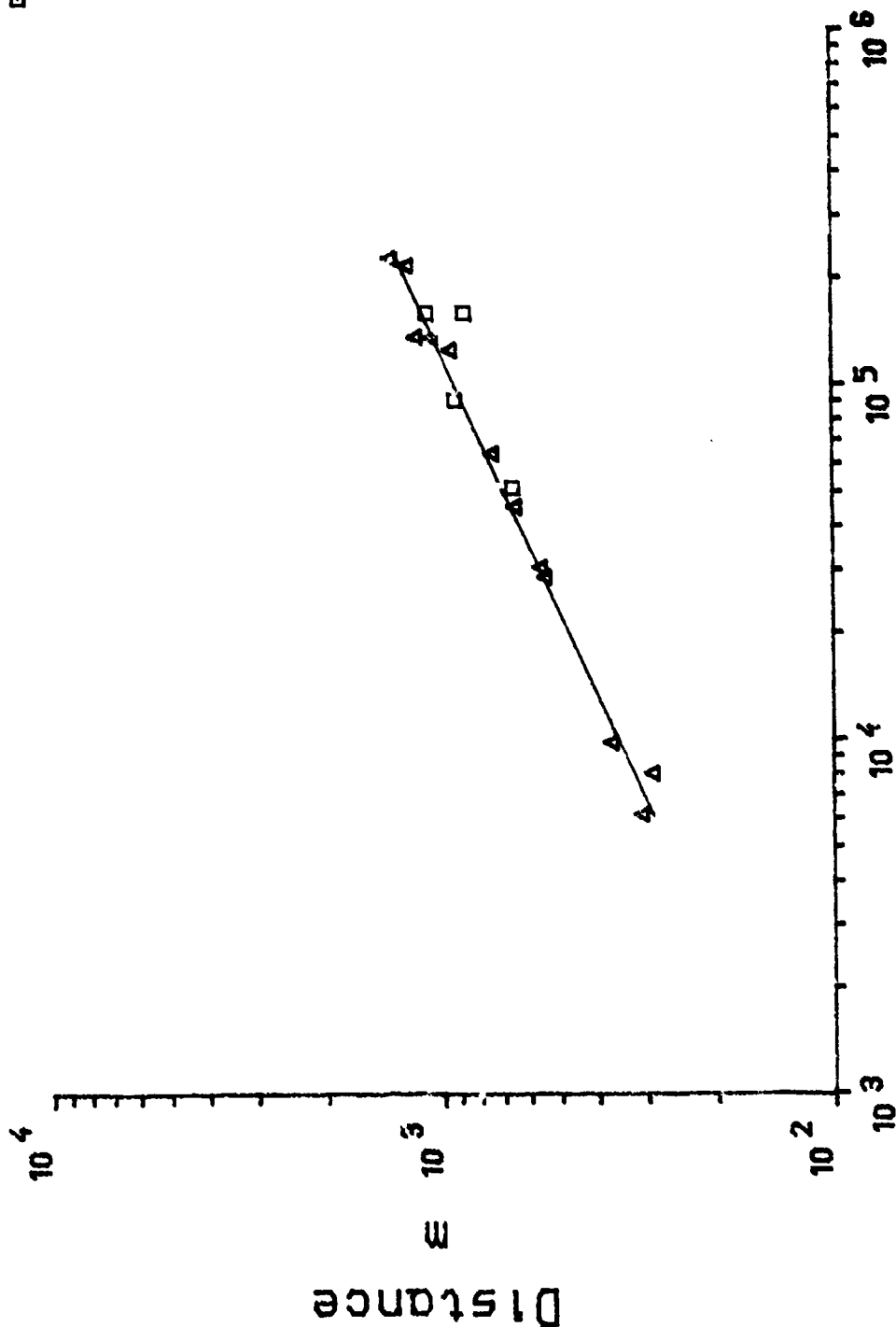
▲ Models US2UX
 □ Full Scale



Vu-Fo11 15

Earth Covered Building Distance/NEQ for 5kPa level

Models US20UK
Full Scale

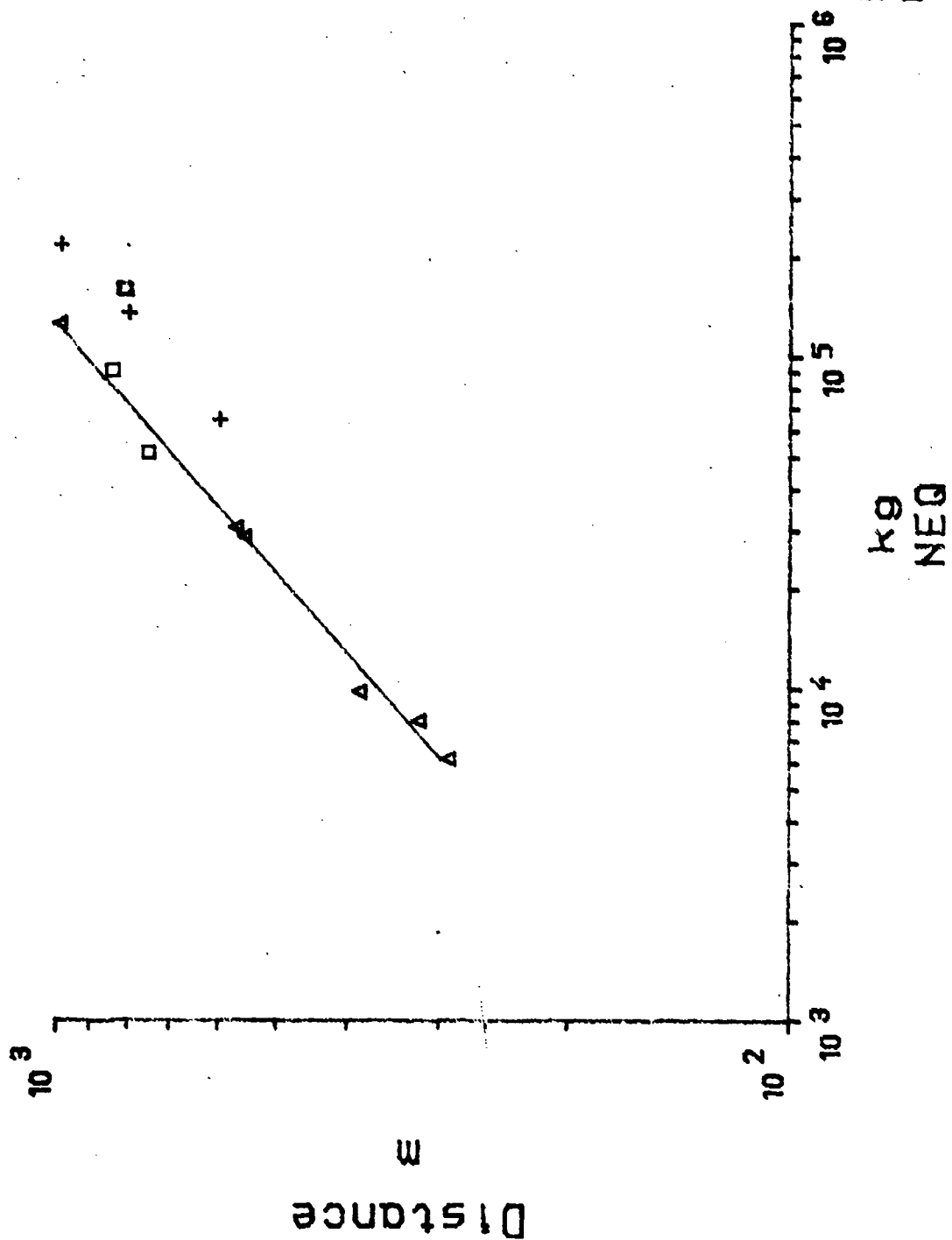


Side
Orientation

Uu-Foil 16

Earth Covered Building Distance/NEQ for 5kPa level

Model's US2UX
Full Scale
Low Points



Vu-Foil 18

DERIVED EXPRESSIONS

REAR $5.0 \times Q^{0.44}$

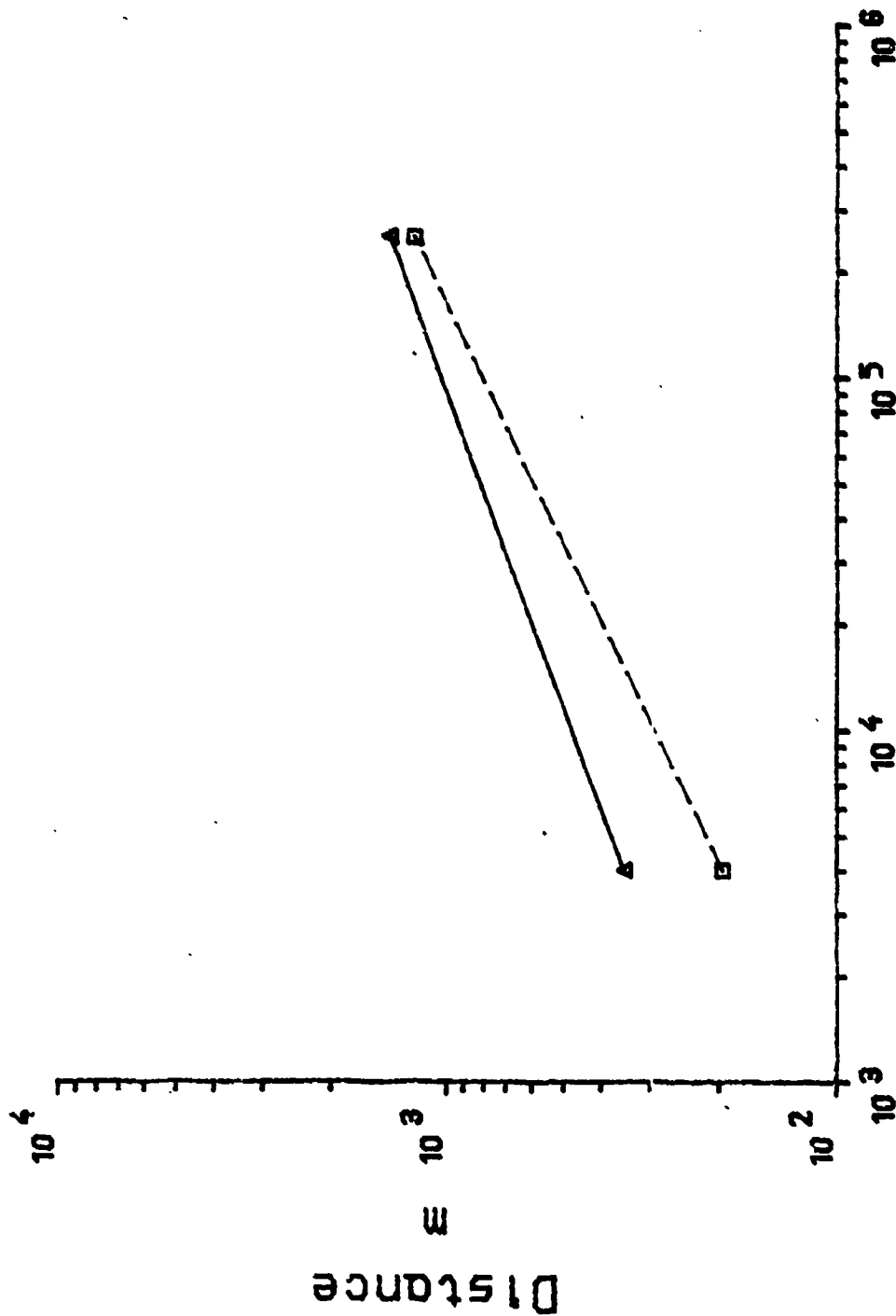
SIDE $7.4 \times Q^{0.42}$

FRONT $9.1 \times Q^{0.40}$

OOD FROM THE REAR OF MAGAZINE

Current and Proposed

A— Current OOD
 B--- Proposed OOD



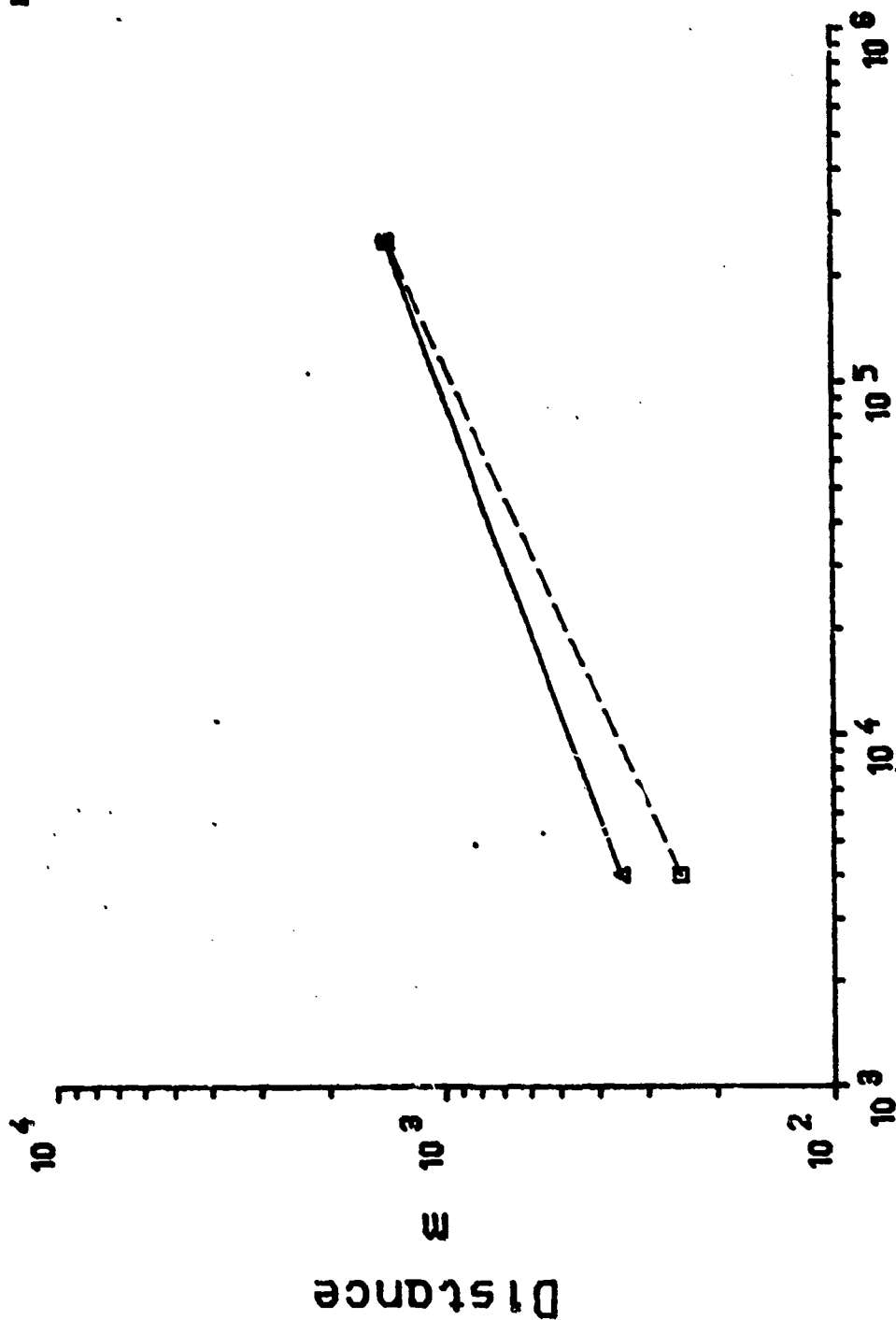
kg
NEQ

VU-F011 19

OOD FROM THE SIDE OF MAGAZINE

Current and Proposed

Current 800
Proposed 000

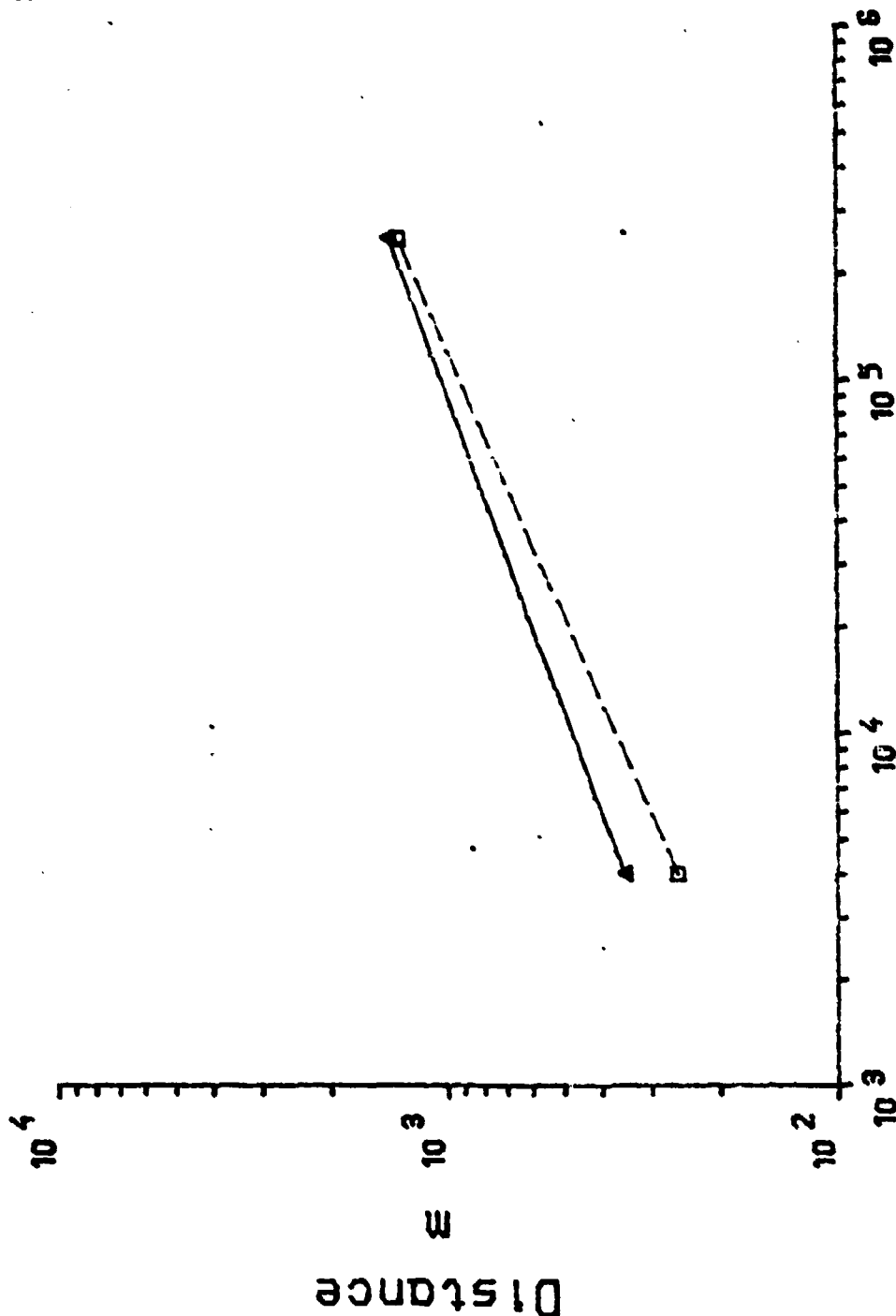


kg
NEQ

UU-F011 20

OOD FROM THE FRONT OF MAGAZINE Current and Proposed

A ——— Current OOD
 B - - - Proposed OOD



kg
NEQ

UU-F011 21

FINAL SUMMARY

1. The general OGDs are not founded on such reliable data as is believed and they imply an accuracy and a precision that does not exist. It is likely that they are over cautious.

2. Different OGDs should be applied to different donor sites and in particular the evidence for introducing reduced distances from earth covered magazines is very strong, although more trials data may be necessary in respect of the front orientation in order to increase the confidence level.

AD-P005 361

EXPANDED SIMULATION TECHNIQUES

**DIRECT COURSE - A 1 KT Height-of-Burst Nuclear
Blast Simulation**

**MINOR SCALE - An 8 KT Surface Nuclear Blast
Simulation**

**Robert A. Flory
Washington Research Center**

INTRODUCTION

→ In October 1983, DIRECT COURSE, the world's largest non-nuclear height-of-burst (HOB) event took place. In June 1985, ~~less than two years later~~, MINOR SCALE, the world's largest (8KT equivalent) non-nuclear surface event, took place. These two events represented a marked departure from the earlier rather standard and sporadic 1 KT equivalent surface events conducted by the Defense Nuclear Agency (DNA).

By developing these two new techniques as viable simulations, DNA has opened the door to further phenomenology research and airblast effects testing on a scale not previously attainable.

The 1 KT equivalent HOB technique offered the opportunity to examine on a large scale, the phenomenology associated with the regular reflection, irregular Mach reflection, and regular Mach reflection regions together with the associated flow fields, both dusty and clean.

The greater than 1 KT technique afforded an opportunity to examine structures, weapons systems, etc. at a significantly different impulse level than that previously available.

This paper will review the two new techniques and assess their simulation fidelity.

DIRECT COURSE AN HOB SIMULATION

DIRECT COURSE, a 1 KT equivalent HOB air blast simulation, took place on 26 October 1983 at White Sands Missile Range, New Mexico.

This event culminated two years of design effort, which among

other testing included a 24 ton scaled version of DIRECT COURSE entitled Pre-DIRECT COURSE, which was detonated on 7 October 1982. Discussion of the HOB simulation development as well as the Pre-DIRECT COURSE event is contained in a MABS-8 paper - entitled Large Scale Height of Burst Simulation (Reference 9).

DIRECT COURSE was quite simply 609 tons of ammonium nitrate with approximately 6% fuel oil added (ANFO), encased in a fiberglass sphere the center of which was 166 feet above the ground. The sphere was supported by a 6 foot square steel frame tower. Airblast and ground motion gages as well as photography were the primary methods utilized to determine the effects of the detonation.

AIRBLAST ENVIRONMENT

Figure 1 compares the DIRECT COURSE overpressures (corrected to sea level) recorded on all three blast lines (80 measurements) (Reference 1) with the standard curves contained in the DOD/DOE publication "The Effects of Nuclear Weapons" ("ENW") (Reference 2). The overall agreement is good, although the HE simulation produced slightly higher overpressures in the 150-15 psi region. As an additional comparison, REFLECT-4 code data points calculated for a 200 foot HOB (Reference 3) are also plotted in Figure 1. These data show a better correlation up to 50 psi but worse above that value.

Figure 2 compares the DIRECT COURSE dynamic pressures (corrected to sea level) on all three blast lines (41 measurements) with the standard curve contained in the "ENW". Agreement is quite good at the

lower dynamic pressure levels getting progressively worse as pressures increase. When the DIRECT COURSE data is compared against the REFLECT-4 data points however, a much closer correlation exists over the entire plotted range of values.

WAVEFORMS

On Pre-DIRECT COURSE, due to excessive fiberglass debris, very little useful airblast data were obtained in the regions above 100 psi. Fiberglass debris from the charge container was successfully mitigated on the DIRECT COURSE event by reducing the ratio of joint to panel density by a factor of two and by reducing the container mass to explosive mass ratio from 8.7 percent to 3.3 percent. As a result DIRECT COURSE wave forms in the regular reflection, Mach transition, and Mach reflection regions exhibited classical characteristics as shown in Figures 3, 4, and 5 (Reference 1).

GROUND MOTION

Two hundred and twenty two accelerometers were installed to measure the free-field ground motion produced by DIRECT COURSE. Two hundred and ten recorded usable data. For comparison purposes ground motion data from the PRISCILLA nuclear airblast event were scaled down to the DIRECT COURSE yield (Reference 4). As shown in Figures 6, 7, and 8 the vertical motion data showed generally good agreement with the scaled PRISCILLA data at shallow depths, however as depth increased the agreement disappeared. Although the reason for

this has not been fully determined, one possible cause is the geologic differences in the test sites. The PRISCILLA test site was generally uniform in nature with a low water table, while the DIRECT COURSE test site contained a more layered geology and a higher water table.

PHOTOGRAPHY

DIRECT COURSE charge disassembly photography (Reference 5) as shown in Figure 9 revealed that the shape appeared to be uniformly spherical, with the seam effects much less apparent than on Pre-DIRECT COURSE. Late exit of the shock wave from the fireball, first viewed on Pre-DIRECT COURSE reappeared on DIRECT COURSE and remained one of the major problem areas of this simulation. The fireball clearly impacted the ground before shock separation thus preventing at least the initiation of the irregular Mach reflection region from being photographically observable.

SEISMIC COMPARISON

There is one other interesting comparison of DIRECT COURSE to an actual nuclear event (Reference 6). In 1945, 5 Leet, 3-component, strong motion mechanical seismographs recorded the TRINITY motions at 5 separate locations. Mr. Leet gave the name "Hydrodynamic" wave to one unusual appearing section of one of the seismograms, suggesting that it might be useful in discriminating between the seismic waves produced by nuclear explosion versus naturally occurring earthquakes. Two of the original Leet instruments were found in the Los Alamos National

Laboratory (LANL) archives, reconditioned, and fielded on DIRECT COURSE. Comparisons between the Leet records for TRINITY and DIRECT COURSE and the digital records recorded by a modern electronic seismograph, as shown in Figure 10, indicate that the "Hydrodynamic" wave is real and not an instrument phenomenon.

HOB SIMULATION SUMMARY

DNA now possesses a reasonable technique for HE HOB nuclear simulations in the 1 KT range. Waveforms in the regular and Mach reflection regions are classical in nature, overpressure and dynamic pressure curves are close to the standard nuclear data curves as well as to the most recent computer code calculations, and vertical ground motions at shallow depths are in reasonable agreement with a nuclear event.

There are however, some areas where improvement is desirable. Examination of the effects on the ground immediately below the charge and a viewing of the transition from the regular reflection region to the mach reflection region are both areas of current interest which can not be accomplished with the present simulation.

A continued lowering of the container mass to explosive mass ratio may solve the transition region viewing problem by allowing the shock wave to separate from the fireball earlier, but an entire redesign of the charge holding system will be required to enable measurements to be made directly under the charge.

MINOR SCALE A "VERY LARGE EVENT"

The idea of a larger than 1 KT equivalent simulation is not a new one. With the increased emphasis on HE simulations by DNA and the successful development of an HOB simulation, the "very large event" became the next objective.

In an attempt to make the increase over 1 KT significant it was decided that a doubling of effects was the minimum acceptable. Because cube root scaling applies, planning for an 8 KT event was initiated. The event was given the nickname MINOR SCALE, and planning commenced with a June 1985 scheduled event date.

Designing the 8 KT simulation technique was a significantly easier task than designing the earlier HOB technique for two primary reasons. First, there was no tower to design with its associated charge holding device, and second, there was now some very recent experience with the use of fiberglass as a charge container.

Charge container shape was the first decision required. As shown in Figure 11 three container shapes were seriously considered and a detailed study effort by NMERI (Reference 7) was conducted. The hemisphere was studied as it had been used in the past and allowed a single point initiation with a uniform shock front in all directions. The hemispherical capped cylinder was studied, as it represented the past standard shape for DNA's simulations and had been selected as the best single shape that provided the most accurate simulation for both airblast and ground motion. The Flat Cylinder was studied as a new concept which would be easier to build and theoretically still provide

the correct airblast waveforms along the ground all around the charge.

After studying all aspects of the various shapes, it was agreed that the Flat Cylinder offered the cheapest and possibly the best solution for an airblast only event, however, it was also agreed that before a new design such as this could be used on a major event it must be tested and evaluated thoroughly, i.e., a scaled test of the event must be conducted. Time did not permit this approach. Geodesic hemispheres, a special case of hemispheres, were eliminated due to the many seams, potential constructability problems, and approximate geometry. Hemispherical capped cylinders offered potential perturbations due to the many initiation points required and the major change in configuration at the cap-base interface. The segmented hemisphere was selected as it offered the best opportunity to obtain a uniform waveform throughout the test bed.

Now that this shape had been selected ejecta became a potential problem. This potential problem was raised based on Operation Snowball (Reference 8), a 500 ton TNT hemispherical event that threw large chunks of clay out to the 10 psi level. Numerous solutions were examined, ranging from completely digging out the estimated crater and refilling it with sand, to excavating and refilling with sand various wedge shaped sections to a variety of depths. The ultimate decision to do nothing was based on the fact that the MINOR SCALE GZ was not over a soil that could be characterized as either rocky or capable of providing large independent masses of soil, and that the benefit to be gained by the use of substantial mitigation techniques was not worth

the rather significant associated cost and time.

The improvement in fiberglass containers has continued and the container for MINOR SCALE carried on where DIRECT COURSE left off. A much lighter cardboard filler was substituted for the balsa wood filler on DIRECT COURSE and a better understanding of strengths of fiberglass in this application are now known. As a result the ratio of container mass to explosive charge mass has now been reduced to .94%, a sizable reduction from pre-DIRECT COURSE's 8.7% and DIRECT COURSE's 3.3%. The seam to panel ratio on MINOR SCALE is 2 to 1, a slightly higher ratio than on DIRECT COURSE, but significantly lower than Pre-DIRECT COURSE.

GREATER THAN 1 KT SURFACE BURST SIMULATION SUMMARY

The design and construction of the MINOR SCALE charge and its firing will raise the simulation yield range from the present 1 KT level to the 8 KT level.

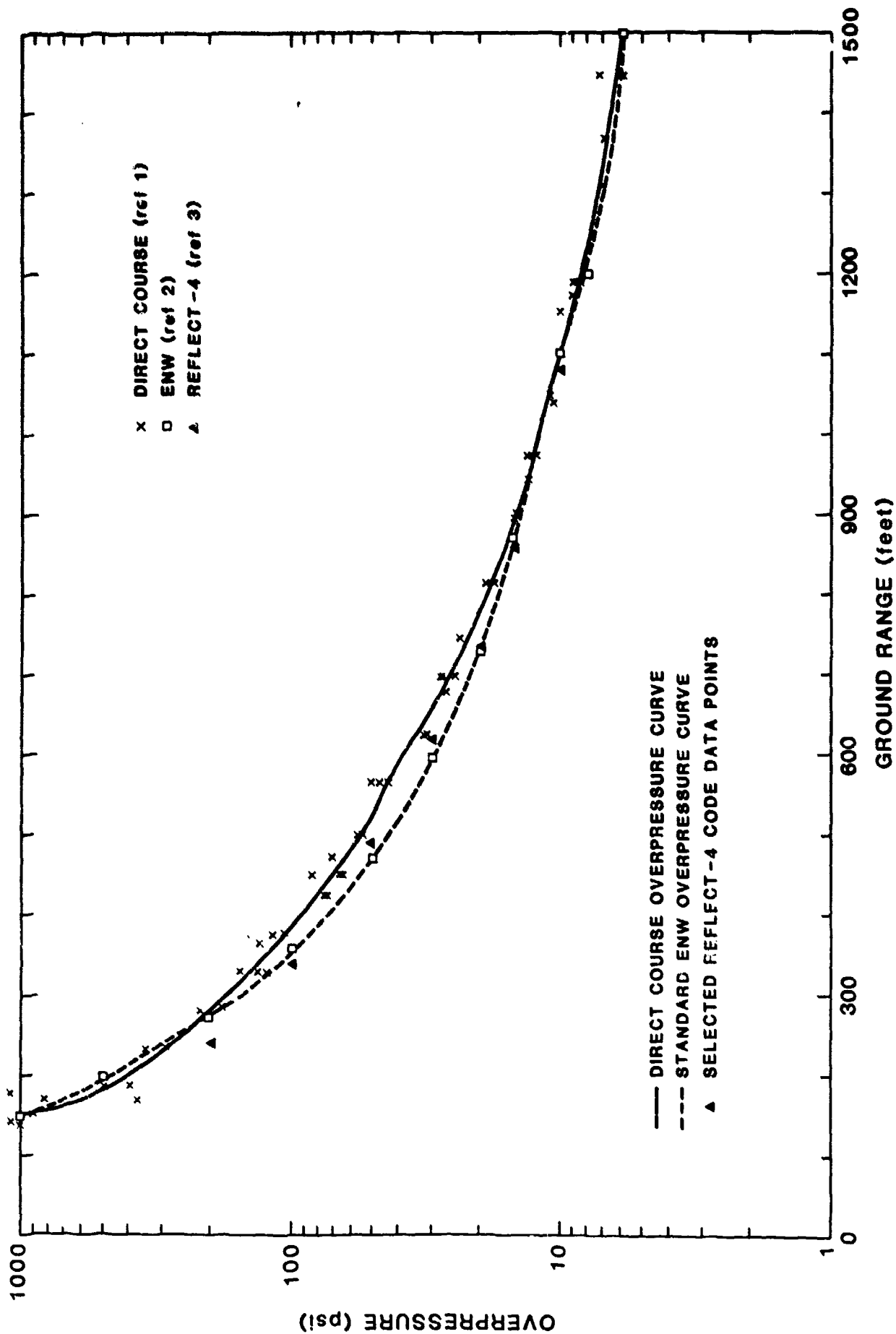


Figure 1

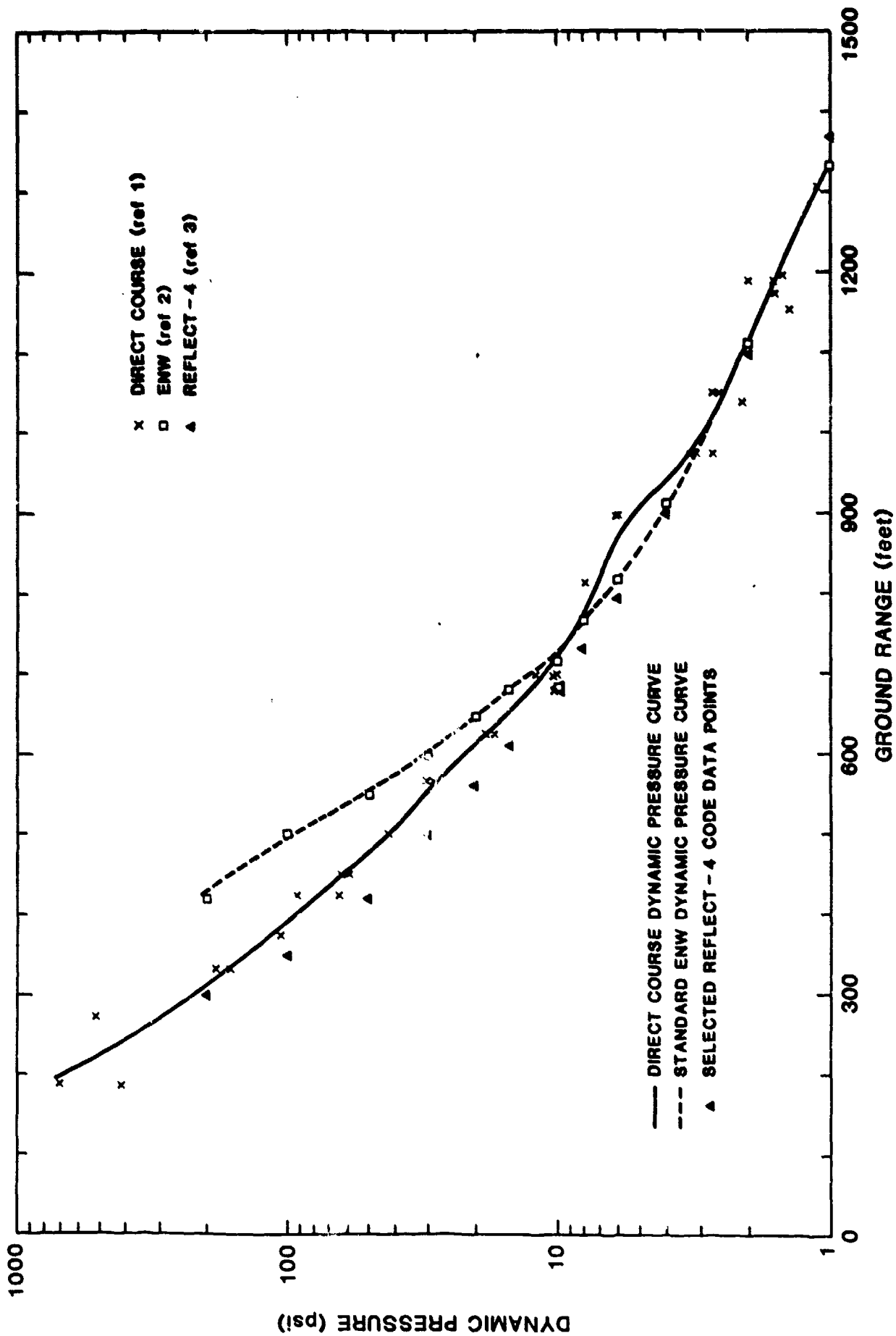
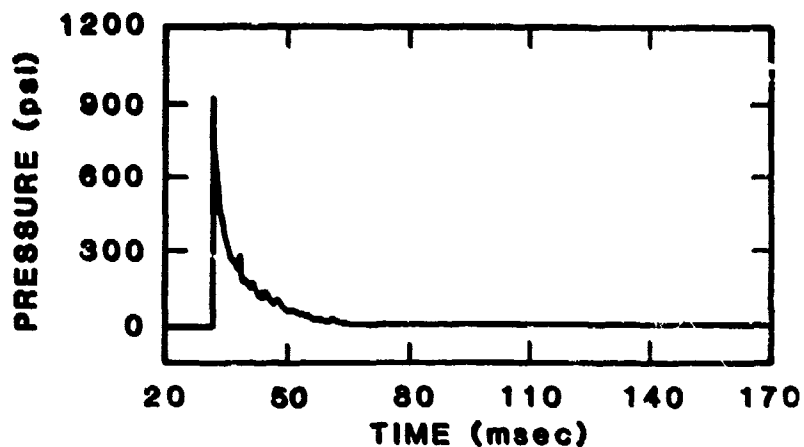


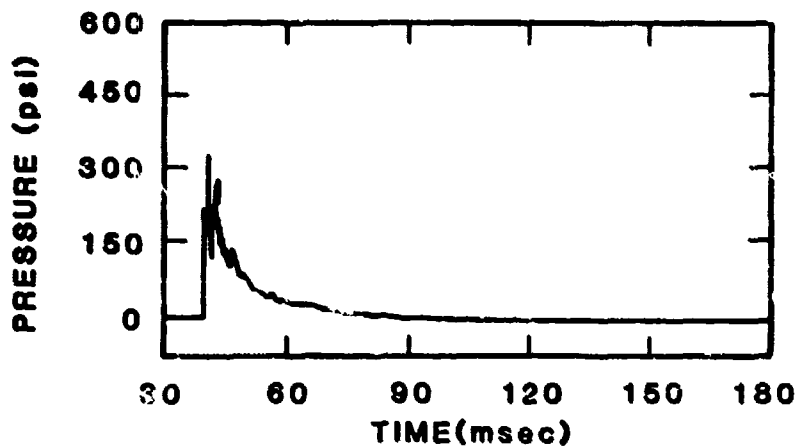
Figure 2

DIRECT COURSE WAVEFORMS - IDEAL SURFACE



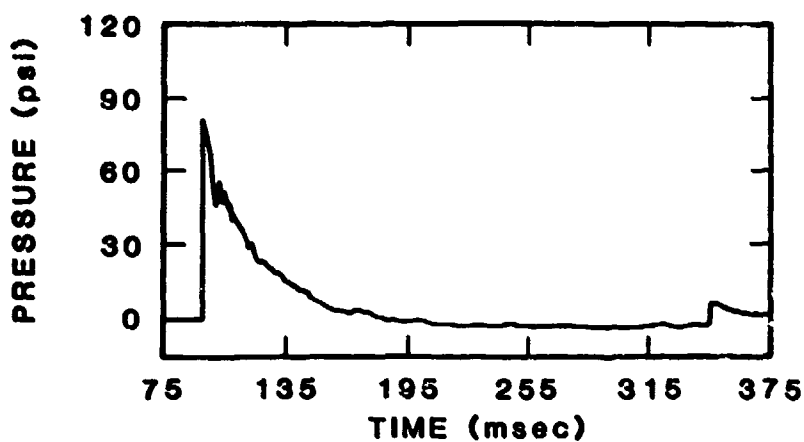
REGULAR REFLECTION REGION

figure 3



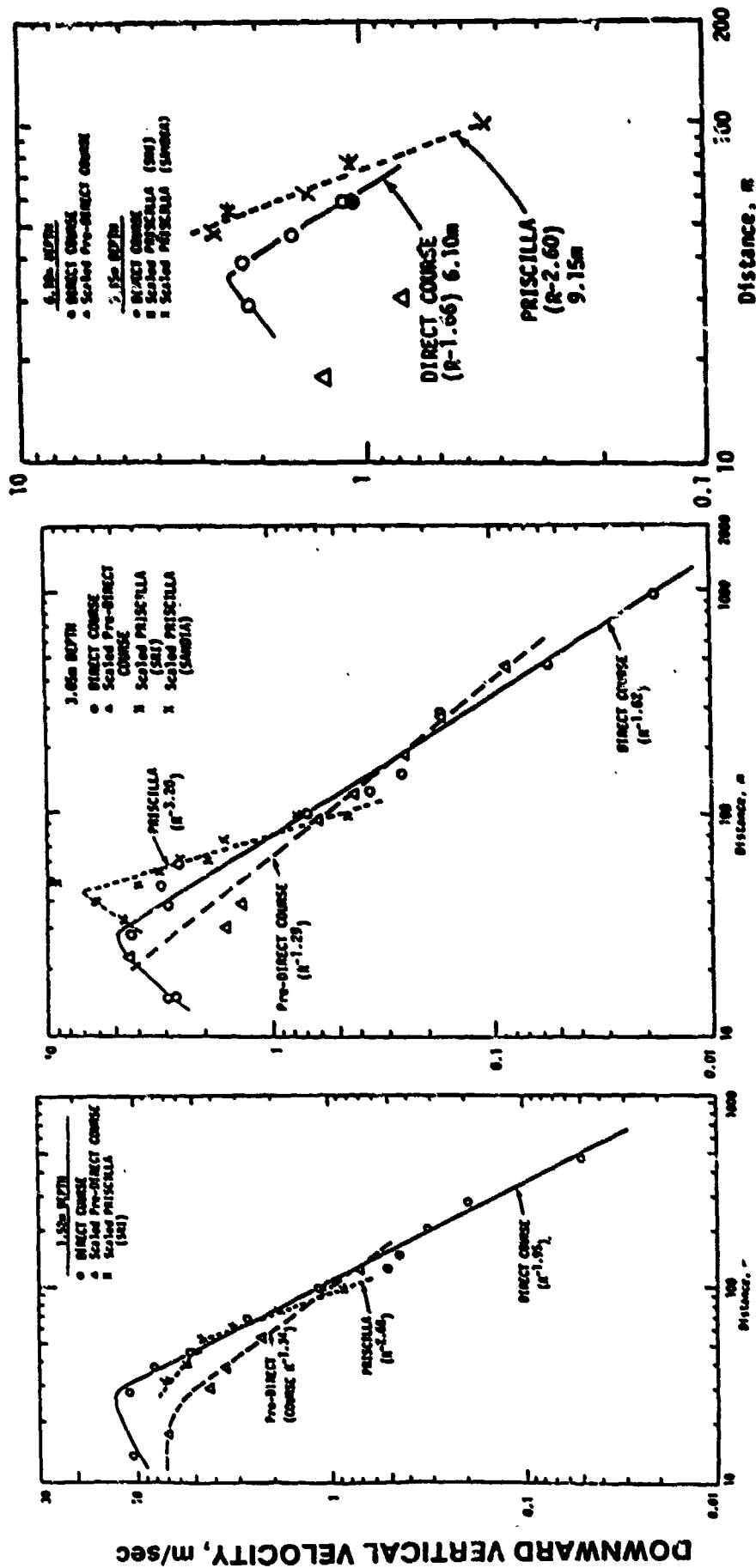
MACH TRANSITION REGION

figure 4



MACH REFLECTION REGION

figure 5



6.10 m AND 9.15 m DEPTH

3.05 m DEPTH

1.52 m DEPTH

Figure 6
Peak downward vertical velocity versus horizontal distance from GZ.
DIRECT COURSE, scaled PRE-DIRECT COURSE and scaled PRISCILLA.

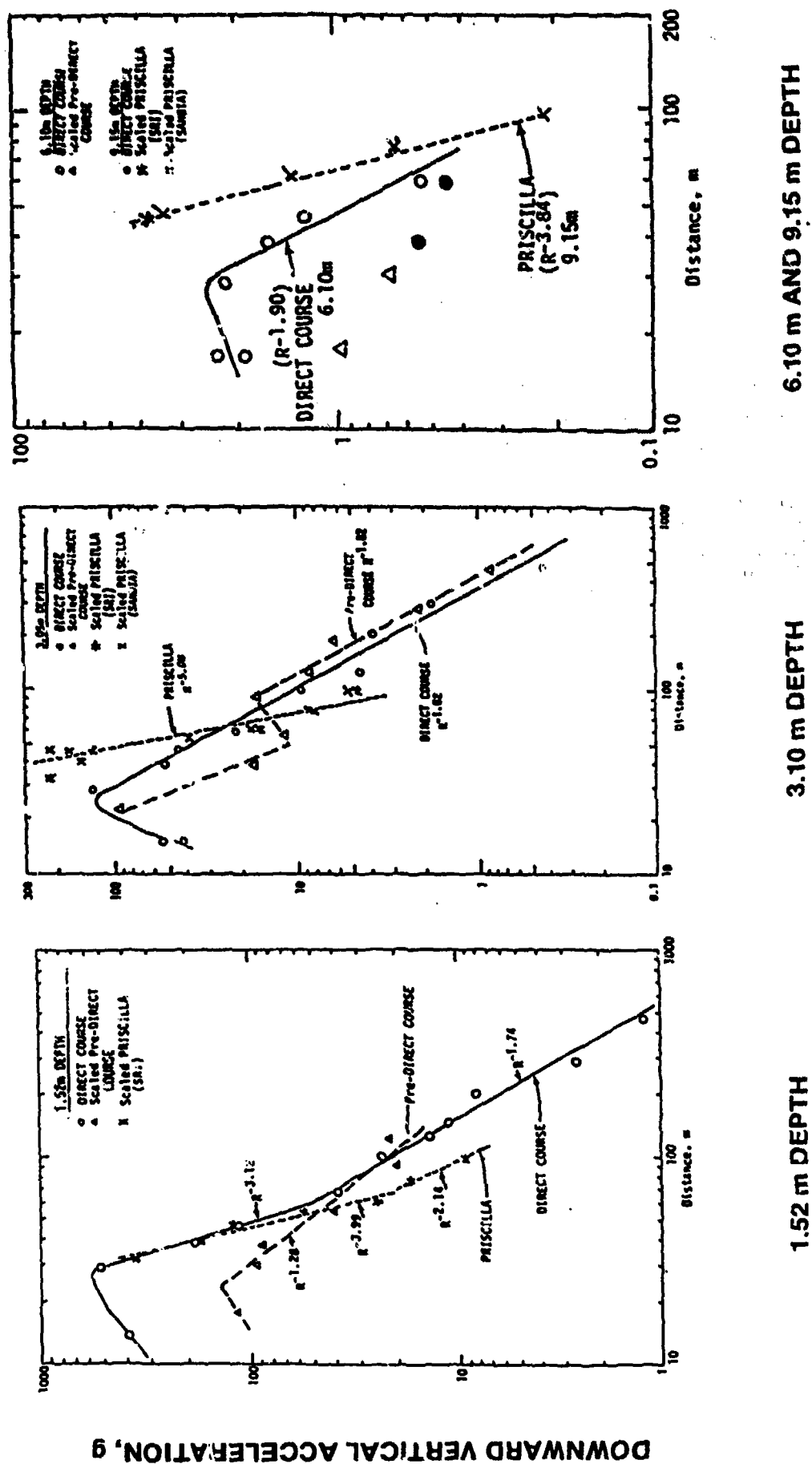
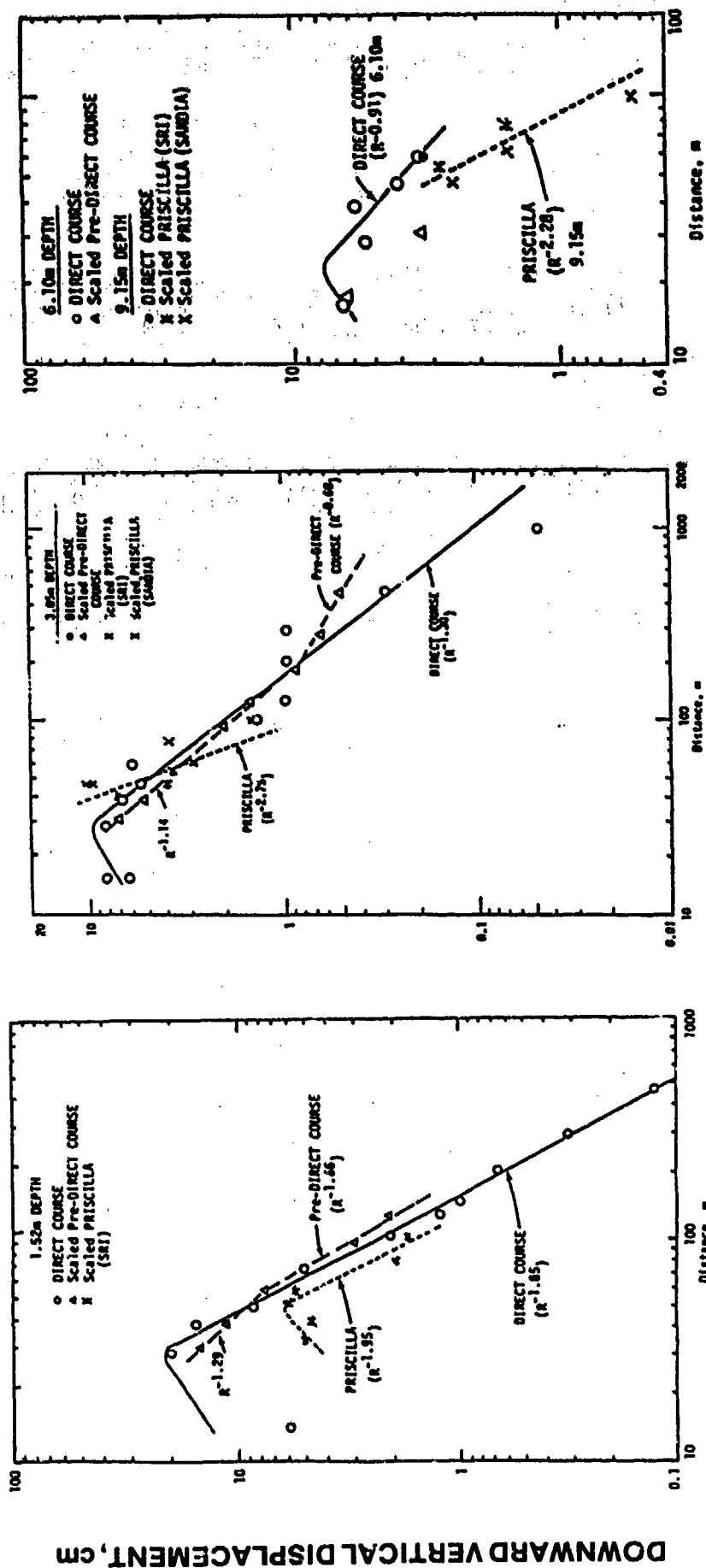


Figure 7
 Peak downward vertical acceleration versus horizontal distance from GZ.
 DIRECT COURSE, scaled PRE-DIRECT COURSE and scaled PRISCILLA.

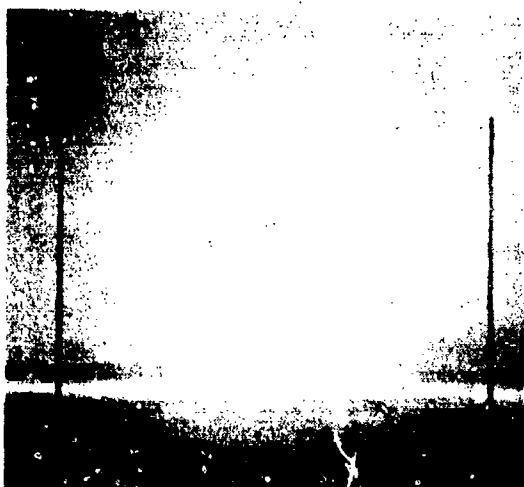


6.10 m AND 9.15 m DEPTH

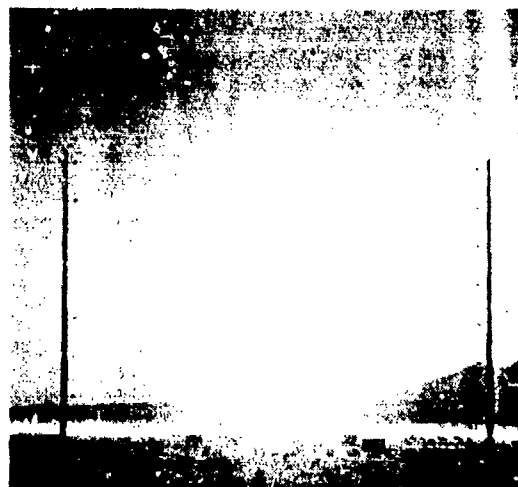
3.05 m DEPTH

1.52 m DEPTH

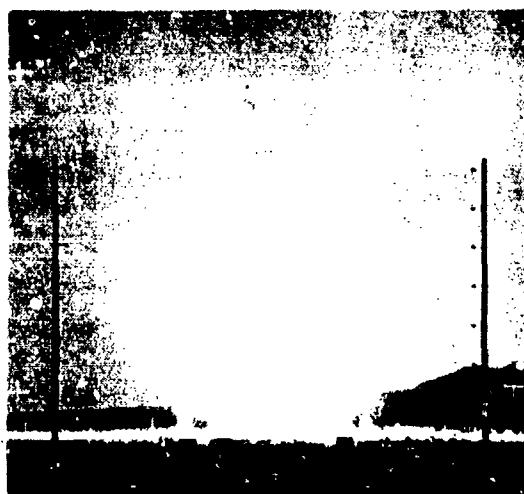
Figure 8
 Peak downward vertical displacement versus horizontal distance from GZ.
 DIRECT COURSE, scaled PRE-DIRECT COURSE and scaled PRISCILLA.



0.0122 sec



0.0149 sec



0.0205 sec

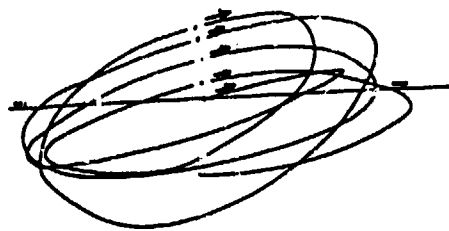


0.0288 sec

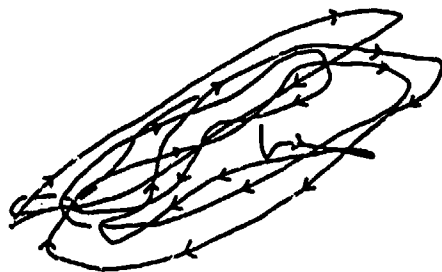
0 25 50 75
(meters)

DIRECT COURSE - FIREBALL EXPANSION SEQUENCE

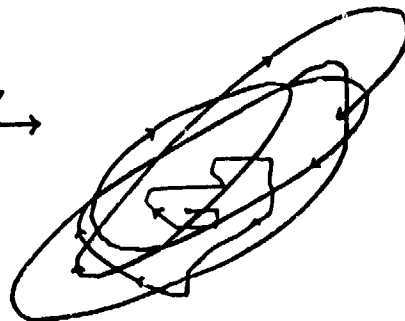
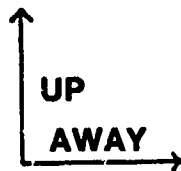
FIGURE 9



**LEET
TRINITY**



**LEET
DIRECT COURSE**

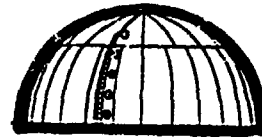


**DIGITAL
DIRECT COURSE**

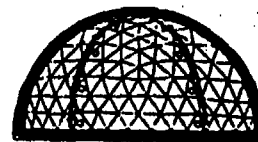
Figure 10
Hydrodynamic particle motion.

CONTAINER CONCEPTS

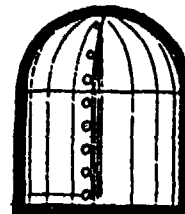
1. SEGMENTAL HEMISPHERE



2. GEODESIC HEMISPHERE



3. HEMISPHERICAL CAPPED CYLINDER



4. FLAT CYLINDER



Figure 11

REFERENCES

1. Teel, George. "Free Field Airblast and Thermal Definition for DIRECT COURSE, Experiments 7900 and 7901", Volume 1, Proceedings of the DIRECT COURSE Symposium 9-13 April 1984, in draft.
2. "The Effects of Nuclear Weapons", compiled and edited by Samuel Glasstone and Philip J. Dolan, Third Edition, prepared and published by the United States Department of Defense and Department of Energy, 1977.
3. Ruetenik, J.R., and Smiley, R.F., "Mach Shock Transition and HOB Knees", Proceedings of 8th MABS Symposium, Spiez, Switzerland June 1983.
4. Ingram, J., "Ground Motion Measurements, Experiments 7800 and 7850". Volume 1, Proceedings of the DIRECT COURSE Symposium 9-13 April 1984, in draft.
5. Dudziak, Walter F., "DIRECT COURSE Disassembly", Volume 3, Proceedings of the DIRECT COURSE Symposium 9-13 April 1984, in draft.
6. Reinke, R.E., Leverette, J.A., and Repichowski, J., "The DIRECT COURSE - TRINITY Seismic Experiment", Volume 2, Proceedings of the DIRECT COURSE Symposium 9-13 April 1984, in draft.
7. New Mexico Engineering Research Institute, "MINOR SCALE Preliminary Concepts for Charge Containers", 1984 draft report.
8. Keefer, John H., and Ethridge, Noel H., Aberdeen Research Center, Aberdeen, MD private communication.
9. Flory, Robert A., "Large Scale Height-of-Burst Simulation", Proceeding of the 8th MABS Symposium, Spiez, Switzerland June 1983.

DAMAGING DISTANT AIRBLAST FROM MINOR SCALE.

Jack W. Reed
Ground Motion & Seismic Division - 7111
Sandia National Laboratories
Albuquerque, New Mexico 87185

INTRODUCTION

An unexpected change in winds at 4-5 km MSL caused airblast ducting and focusing on Carrizozo, NM, 60 km east from MINOR SCALE. In result, this 4.8 kt ANFO (ammonium nitrate-fuel oil) explosion test, ~~sponsored by the Defense Nuclear Agency (DNA), and fired at 1220 MDT, 6/27/85,~~ rattled the town with 300 Pa (0.0435 psi) overpressure, according to the microbarograph records. Four large (8 x 10 ft) store windows were broken. Weather data which were collected during this event show that conditions changed near shot time, as needed to explain this result, but we have no clues for predicting such localized wind patterns.

Shock and acoustic waves are distorted by propagation through an atmosphere [ANSI, 1983] in which directed sound velocity varies with height, as it usually does. In a gradient condition, a vertical plane acoustic wave would travel faster near the ground than aloft, so that its wave normals (or rays) would be curved upward away from ground. The same effect bends all the emitted rays upward from a point source, or explosion.

Due to the divergence of the rays from ground level, overpressures would decrease faster with distance than would be expected from simple geometric spreading, as shown in Figure 1a. A so-called 'Standard' explosion, calculated for a calm atmosphere of uniform temperature and pressure [Needham, 1975], as shown in Figure 1b, would not have refracted or distorted rays but would have radial shock rays. Conversely, when sound velocity increases with height under an inversion as shown in Figure 1c, all emitted rays are bent downward toward the ground, in effect ducting the wave. Its spherical expansion is thus restricted, causing relatively increased overpressures to be observed along the ground.

When there is a complex dog-leg sound velocity versus height structure, as shown in Figure 2, the combination of gradient and inversion layers may focus the wave at some distance. Since this focusing occurs along a folding surface of the wave front in three dimensions and not at a point, it is properly called a caustic surface, but its intersection with the ground is often described as a focus. We do not know how intense these foci or caustics may be, but experience has demonstrated magnifications by several times above the expected Standard overpressures [Reed, 1969].

Directed sound velocity is the sum of the temperature-dependent sound speed and the directed wind component, and they both vary independently with altitude. Upper air temperature and wind reports are obtained from radiosonde balloon (raobs) ascensions.

MINOR SCALE PREDICTIONS

Figure 3 shows the Standard overpressure-distance curve, scaled to the MINOR SCALE yield of 4.8 kt ANFO or 8 kt NE (nuclear explosion). Potential weather effects on its propagation are shown by alternative curves for a strong gradient, a strong inversion, and an approximate upper bound for caustic con-

ditions. The window damage threshold shown at 200 Pa is only approximate and based on three incidents from atmospheric nuclear tests. This shows that there could be window damage to almost 200 km distance, depending on shot time weather conditions.

The area surrounding WSMR is shown in Figure 4. The largest communities within about 150 km range are Socorro (population 12,969), Carrizozo (pop. 1,222), Tularosa (pop. 2,536), Alamogordo (pop. 24,024), Holloman AFB (pop. 7,245), and Truth or Consequences (pop. 5,219).

WINDOW DAMAGE PROBABILITIES

The probability of breaking a window by airblast is shown by an empirical curve in Figure 5, as a function of incident overpressure [Reed, 1973]. Breakage appears with a lognormal probability distribution which decreases from a probability near unity at high overpressures to around 4×10^{-5} at 200 Pa (0.03 psi). There were about 19 window panes per capita in San Antonio, Texas, in 1964, when these data were assembled in a survey of damages from an accidental 50 ton HE explosion [Reed et al, 1968]. Target population census figures can thus be used to estimate the number of exposed panes, and the expected breakage can be calculated from a predicted airblast overpressure.

SHOT DAY WEATHER CONDITIONS

Upper air temperatures were not unusual, although there was only a weak temperature inversion near the surface on the morning of 6/27/85. Upper winds were unusual, ENE 26 knots at 7 kft MSL at 0400 MDT, following a cold air mass outbreak over the Great Plains [Reed & Church, 1986]. Upper wind speeds diminished to 13 kt by 1000 MDT. At 14 kft MSL winds were NW 10 kt at 0400 MDT, and they dropped to WNW 6 kt by 1000 MDT. Figure 6 shows these conditions, as translated to Carrizozo-directed sound velocities. The early morning dog-leg structure threatened airblast propagation enhancement, but by 1000 MDT surface warming gave a 18 ft/sec margin between the surface and 12 kft MSL sound velocities, to prevent any ducting. Conditions appeared equally good toward Alamogordo and Tularosa, and even better in all other directions. The shot-time raob showed a slight deterioration (increased upper level sound velocities) but no reason for concern. But, by the time this observation was in hand (shot time observations are made to balloon burst near 100 kft in about two hours), it had been discredited.

AIRBLAST AT CARRIZOZO

A microbarograph (MB) station was operated in Carrizozo and it obtained the pressure-time signatures shown in Figure 7. Three 2500 lb ANFO shots were fired before MINOR SCALE, at 0759 MDT (H-2 hours on the schedule) and 1114 MDT (H-1) to verify raob-based propagation calculations, and at 1218 MDT (T-2 minutes) to check yield scaling laws for long range propagation (5 MB stations were operated at 200 km range). The early shot gave an unexpectedly small wave at Carrizozo. Amplitude at 1114 MDT may have been 27 Pa as shown, but the high wind noise level makes it quite uncertain. The H-2 minute wave amplitude might have alerted our MB operator of what was coming (the cube root of yield multiplies 12.9 Pa to 202 Pa), but he was too busy changing the equipment to a less sensitive set range. At MS+150 seconds there was a small, explosion wave-shaped noise clearly recorded on the sensitive A-pen - MINOR SCALE was a dud! The ensuing bang quickly dispelled that thought. An overpressure of 297.5 Pa rattled windows and doors in spite of its slow compression, taking 400 ms from start to peak.

After this recording was completed with post-calls and time hacks, our MB operator called the city police to check on any damage reports. They had not received any calls, but they had thought their ceiling was going to fall from the blast which sprinkled their office and desks with dust and plaster powder. The sheriff had received a report of windows broken at a mid-town store. When the MB operator called these reports in, I had a credibility problem biased by the available weather information. At the scene of the damages, four large (about 8'x10') store windows were found broken of the seven which were exposed.

It was established that they had been about 1/4" or 3/8" thick plate glass, but the sheriff advised our man to leave town before he could make the detailed assessment and measurements which we had requested.

Two months later this store front had been completely remodelled with smaller panes, but the general dimensions of the original installation were verified. According to a WSMR attorney, they have settled this case with about \$2400.

IN EXPLANATION

The MB overpressure record indicates 2.13×10^{-4} window damage probability. Carrizozo's population of 1,222 (1980 census) leads to a guess that it also has around 23,218 window panes. Thus five should have been broken; only four were broken but they were big ones. A similarly good correlation with our prediction model was obtained at DIRECT COURSE in 1983, when 4.8% of the panes in the DNA Project Admin Park were smashed by an estimated overpressure around 2 kPa, which could be calculated to give from 4.5% to 7.8% breakage [Reed & Church, 1984].

But how did the overpressure get amplified to such an extent? It certainly is not explained by the shot-time raob made at Stallion, 28 km north of Ground Zero (GZ). There was, however, another raob made for another project at 1.25 hours after MINOR SCALE at Jallen Site, 50 km south of GZ. This observation showed, in Figure 8, a complex blast duct toward Carrizozo caused by a WNW 22 knot wind reported at 12 kft MSL. Only a narrow belt of the initial blast wave would have been ducted, according to ray path calculations, and it could have been focused near 30 km range after skipping above the 9000 ft Oscura Peak. But it apparently was reflected and repeated its atmospheric path to strike Carrizozo at 60 km range. Even the measurement errors and horizontal inhomogeneity of the atmosphere make these focal distance calculations uncertain by about 35%, but something quite similar likely occurred.

On the other hand, directed sound velocities calculated from the Jallen raob toward Tularosa and Alamogordo also showed very similar structures, while only very weak waves were recorded there by our MBs. Figure 9 shows these reports on the overpressure prediction graph, along with some yield-scaled points from DICE THROW [Reed, 1977]. That event almost broke some windows in Alamogordo, again - apparently - from wind effects that were not encountered by the shot time raob balloon. Had the MINOR SCALE yield been shot for DICE THROW, nearly 1000 windows would likely have been broken.

CONCLUSIONS

In spite of reliance on series of upper air weather balloon observations to predict distant airblast propagations from WSMR explosion tests, there have already been two incidents of wide misses.

Cont'd
It appears that the variability of winds over the mountainous region around WSMR is appreciably larger than over flatter terrain, so that airblast propagation predictions are subject to significant error.

Microbarographs are essential in surrounding communities, to document the explosion airblast strength when unexpectedly enhanced blasts occur.

The provided empirical model for estimating window damage from expected overpressure appeared to work well.

As expected, large windows were the first to fail from the blast. Large plates are indeed hazardous when they break, so that such window damage should be avoided, in spite of their relatively low replacement cost in comparison with test delays.

REFERENCES

American National Standards Institute, "Estimating Airblast Characteristics for Single Point Explosions in Air", ANSI S2.20-1983, Acoustical Society of America, New York City, NY, 1983.

Needham, C.E., Havens, M.L., and Knauth, C.S.; "Nuclear Blast Standard (1kt)", Report AFWL-TR-73-55 (Rev.), Air Force Weapons Laboratory, Kirtland Air Force Base, NM, Apr. 1975.

Reed, J.W., Pape, B.J., Minor, J.E., and DeHart, R.C.; "Evaluation of Window Pane Damage Intensity in San Antonio Resulting from Medina Facility Explosion on November 13, 1963", Ann. NY Acad. Sciences, Vol 152, 565-584, Oct. 28, 1968.

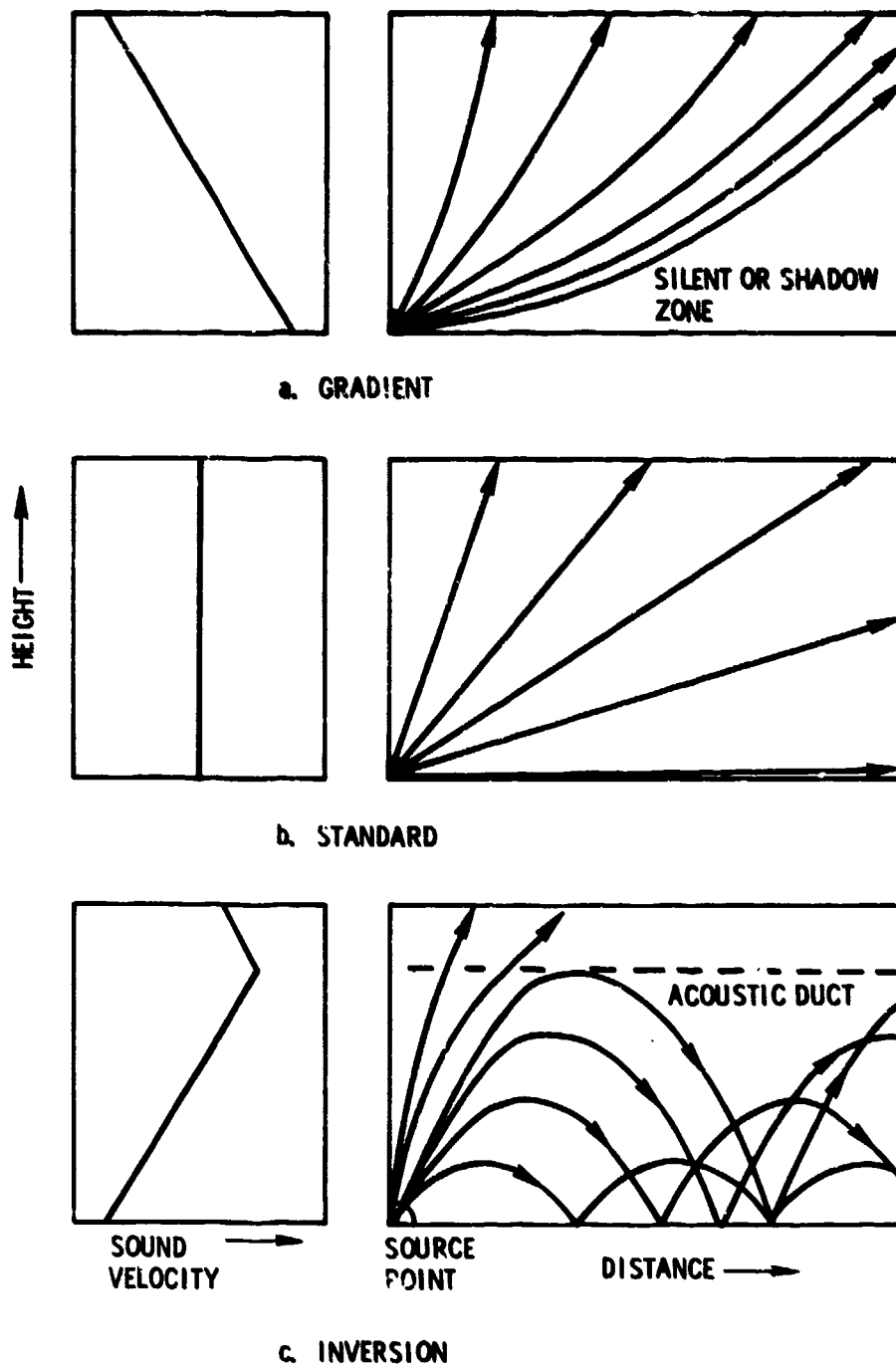
Reed, J.W.; "Climatology of Airblast Propagations from Nevada Test Site Nuclear Airbursts", SJ-RR-69-572, Sandia Laboratories, Albuquerque, NM, Dec. 1969.

Reed, J.W.; "Distant Blast Predictions for Explosions", in Vol.1, Minutes of DOD Explosives Safety Seminar, San Francisco, CA, U.S. DOD ESB, Washington, DC, Sept. 18-20, 1973.

Reed, J.W.; "DICE THROW - Off-Site Blast Predictions and Measurements", in Proceedings, DICE THROW Symposium, DNA-4377P-2, Vol.2, GE-TEMPC-DASIAC, Santa Barbara, CA, July 1977.

Reed, J.W., and Church, H.W.; "Airblast Predictions with Meteorological and Microbarograph Measurements", in Proceedings, Project DIRECT COURSE Results Symposium, Adelphi, MD, Apr. 9-13, 1984.

Reed, J.W., and Church, H.W.; "MINOR SCALE Weather-Watch & Microbarograph Project", in Proceedings, Project MINOR SCALE Results Symposium, Albuquerque, NM, Feb. 24-28, 1986.



**Figure 1. Atmospheric Refraction Effects on
on Sound Waves.**

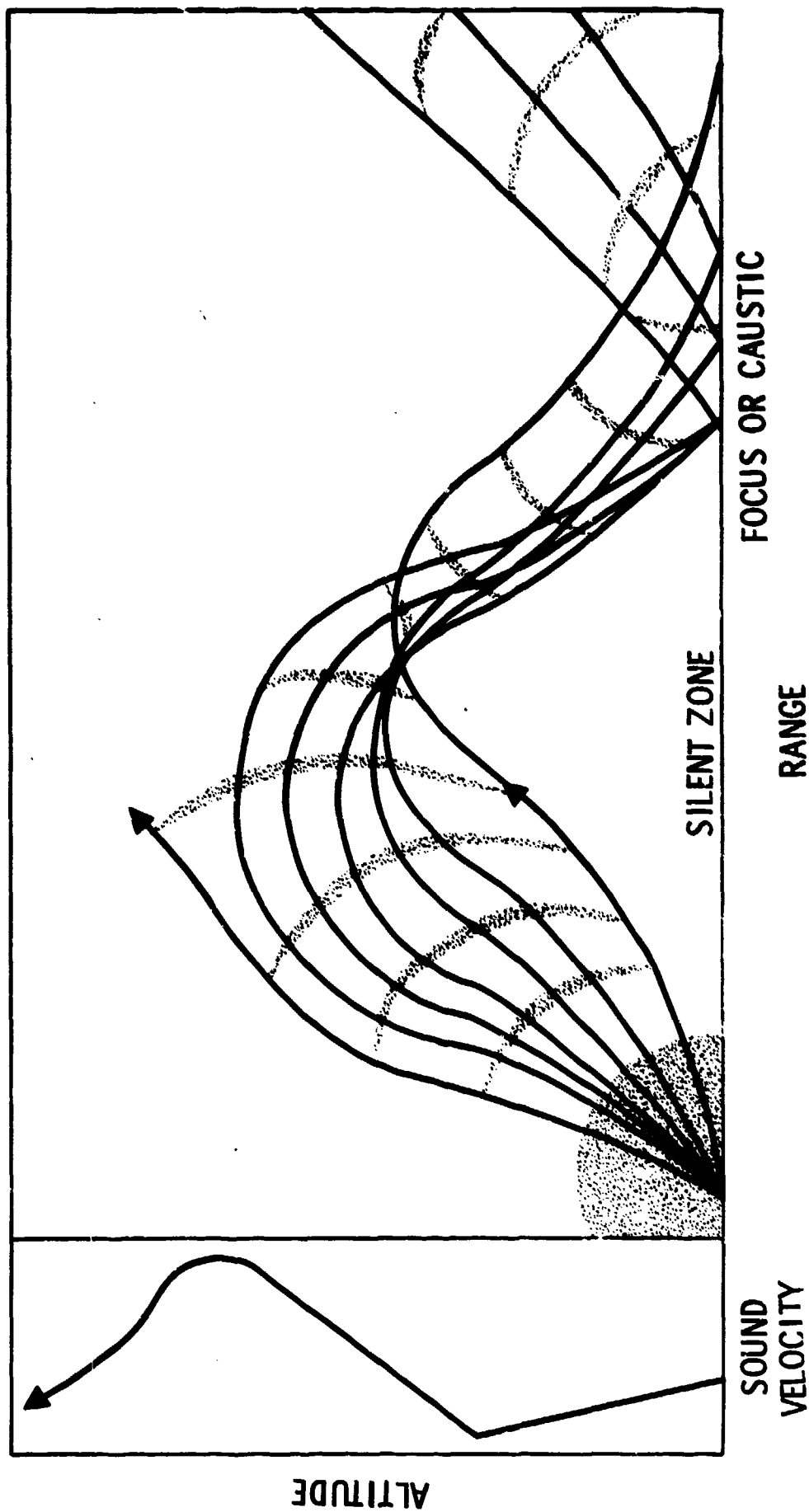
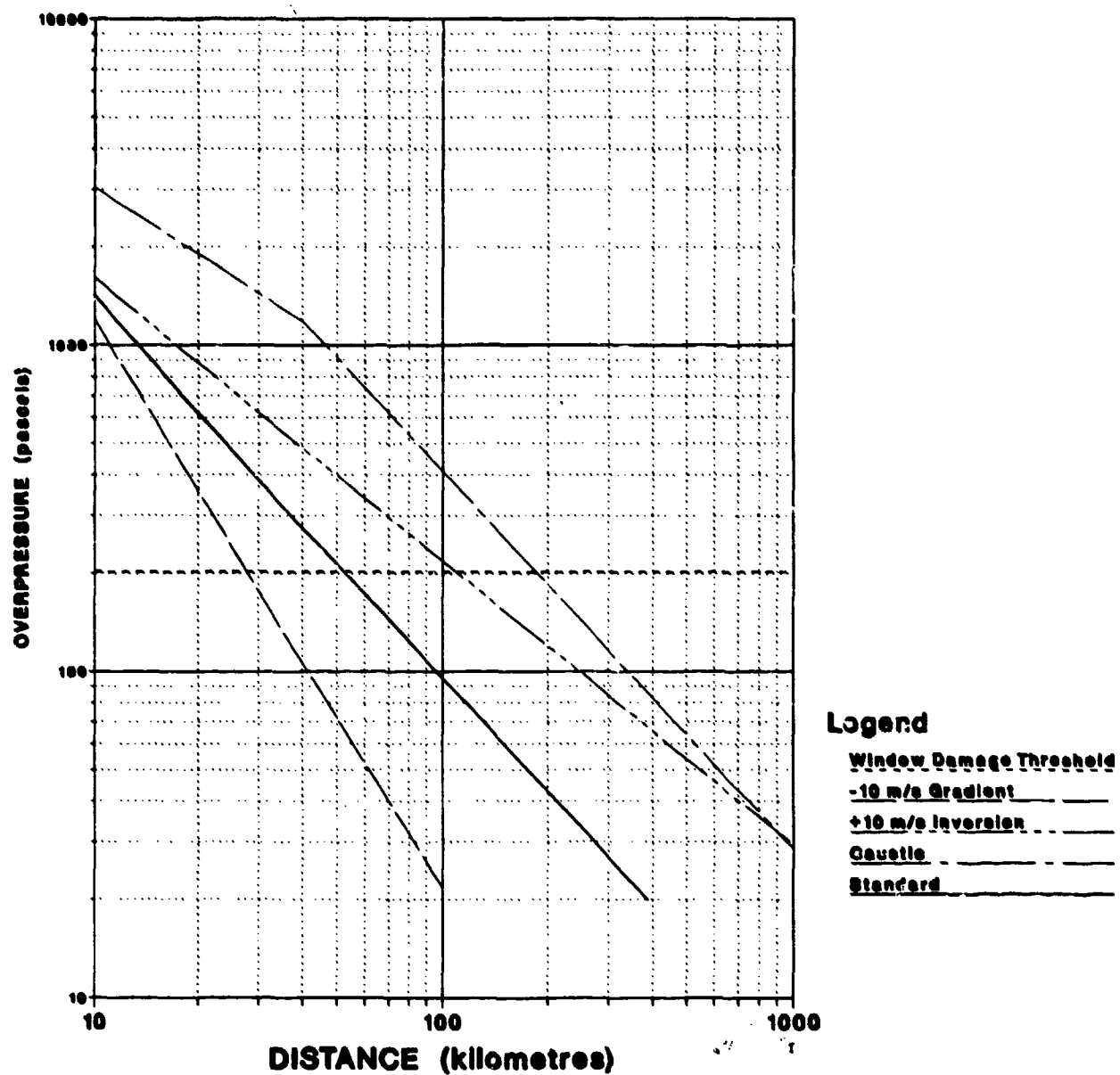


Figure 2. Typical Explosion Ray Paths under Complex Conditions.

Figure 3. Weather Effects on Overpressure-Distance Curve for MINOR SCALE, 4.8-kt ANFO Surface Burst.



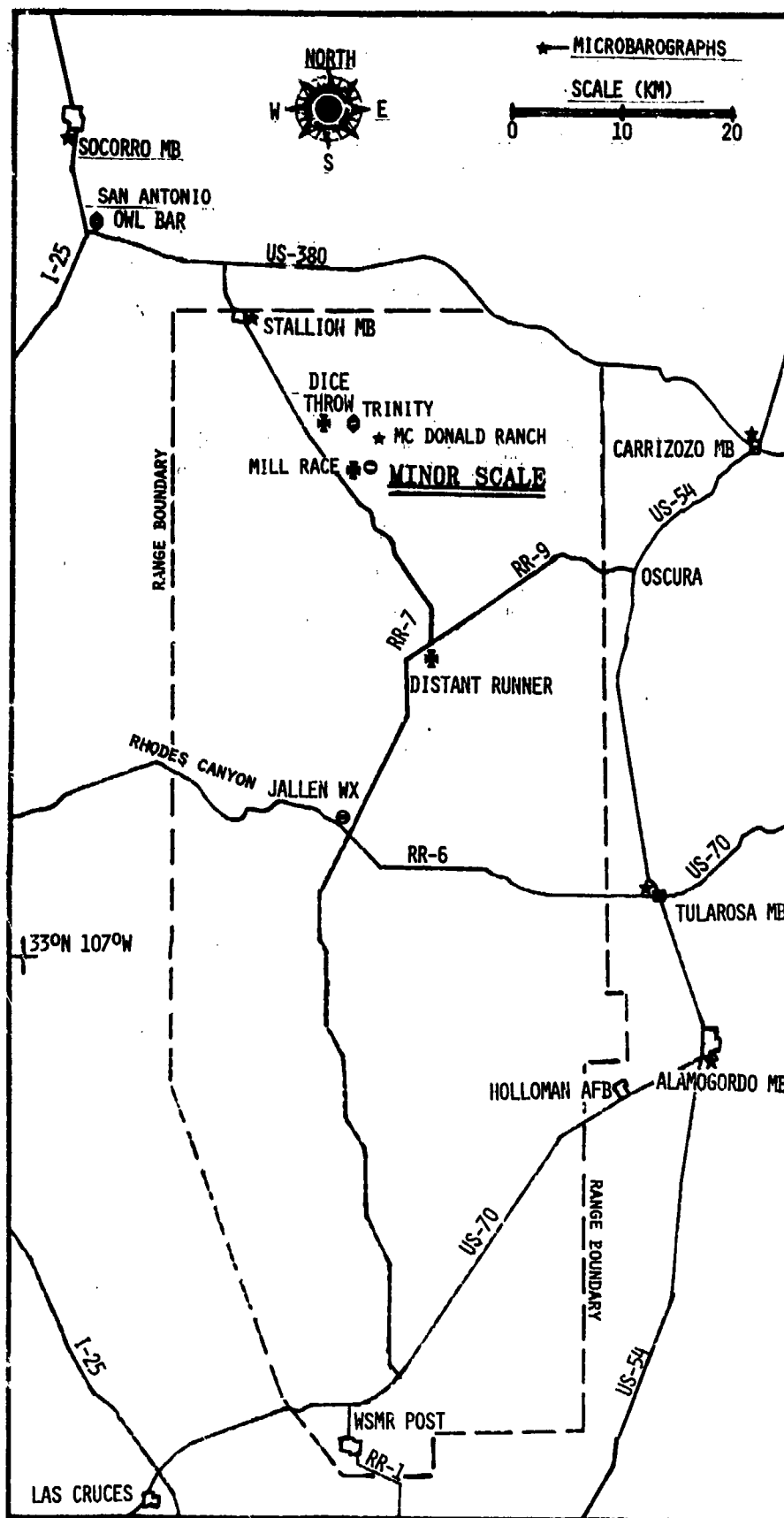
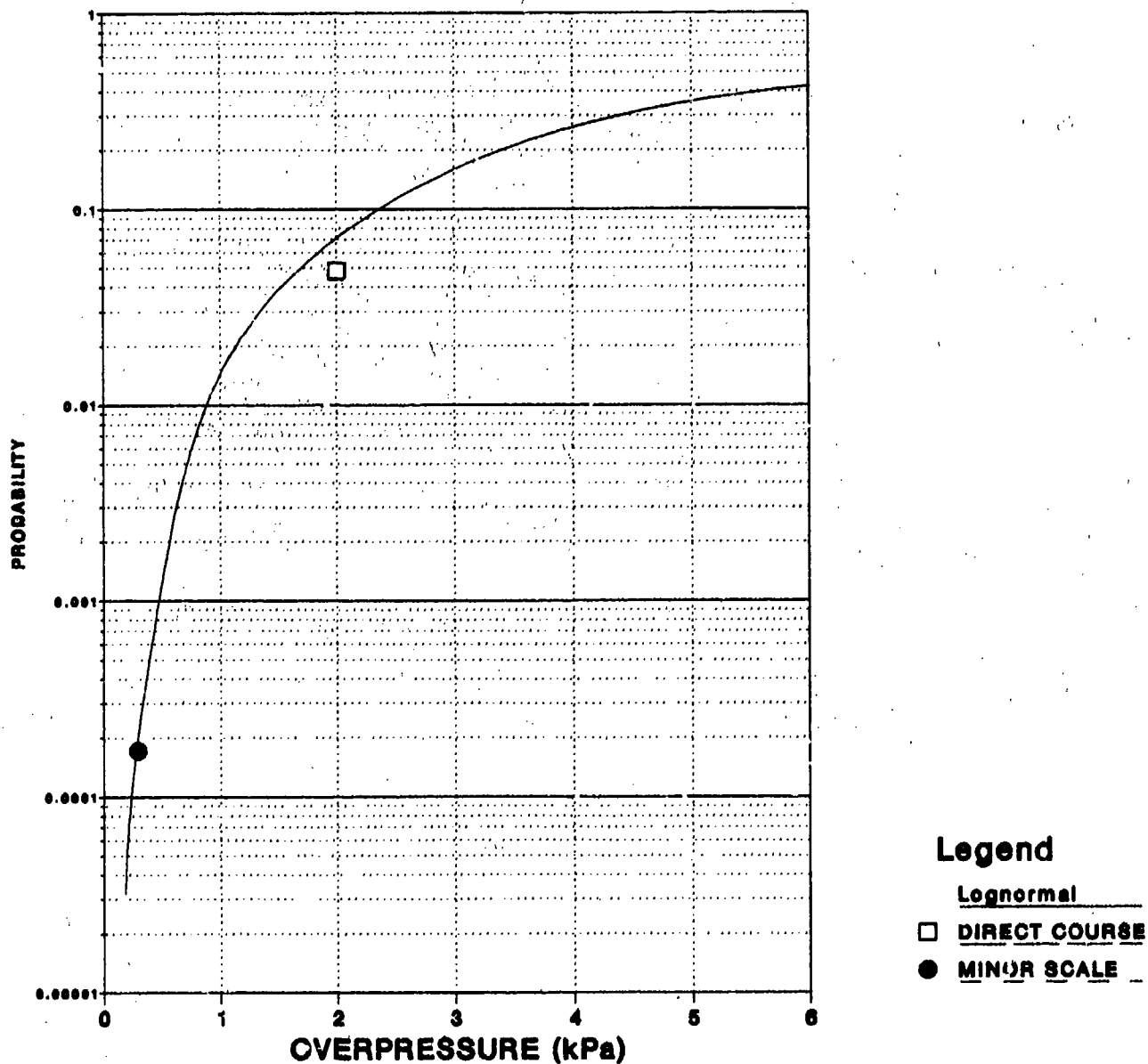
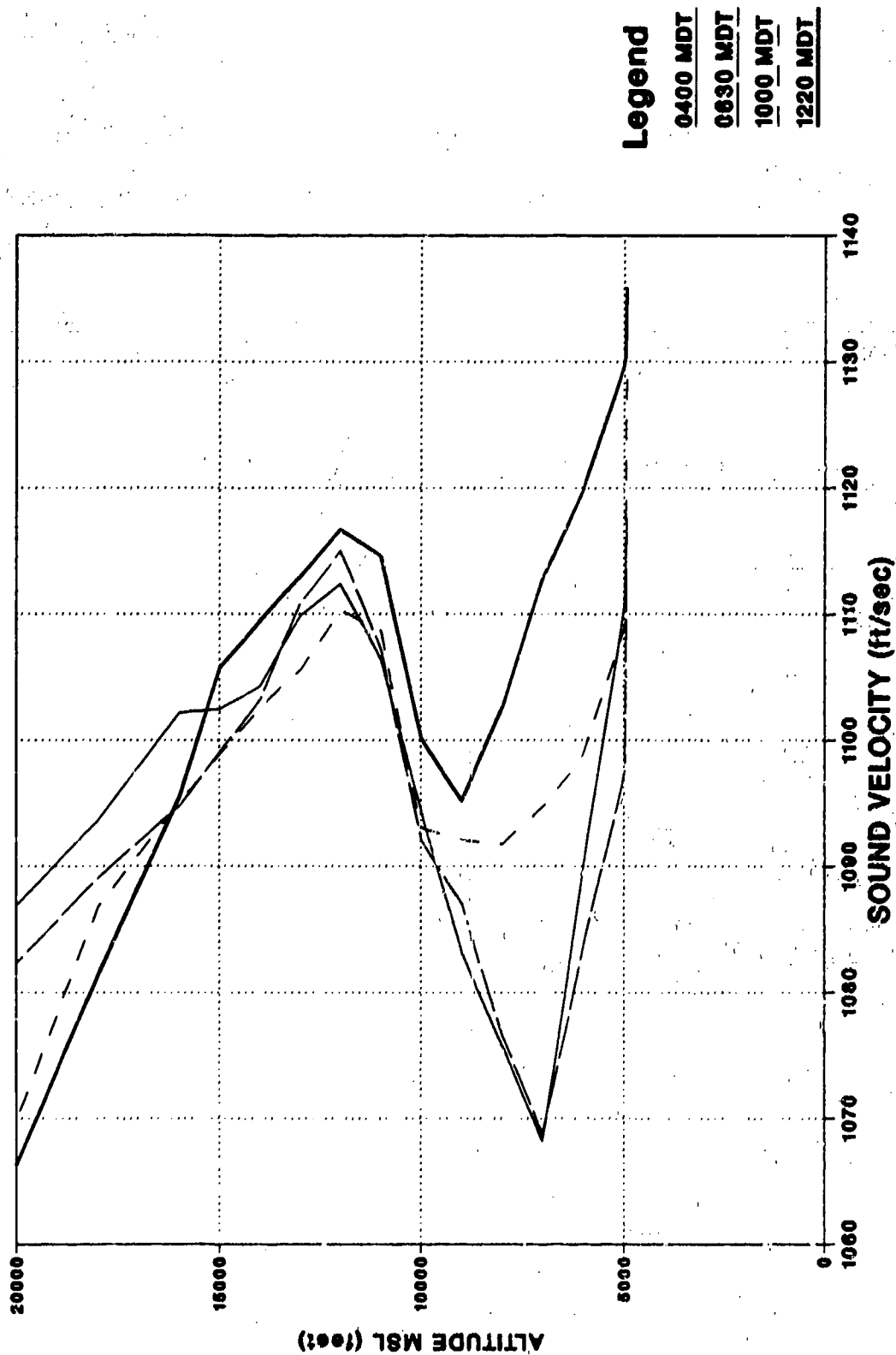


Figure 4. Map of White Sands Missile Range, New Mexico.

**Figure 5. Window Breakage from Airblast.
Based on 1964 Pane Size Distributions, San Antonio, TX.**



**Figure 6. DIRECTED SOUND VELOCITIES TOWARD CARRIZOZO.
AZIMUTH 087 DEG. - STALLION RAOBS**



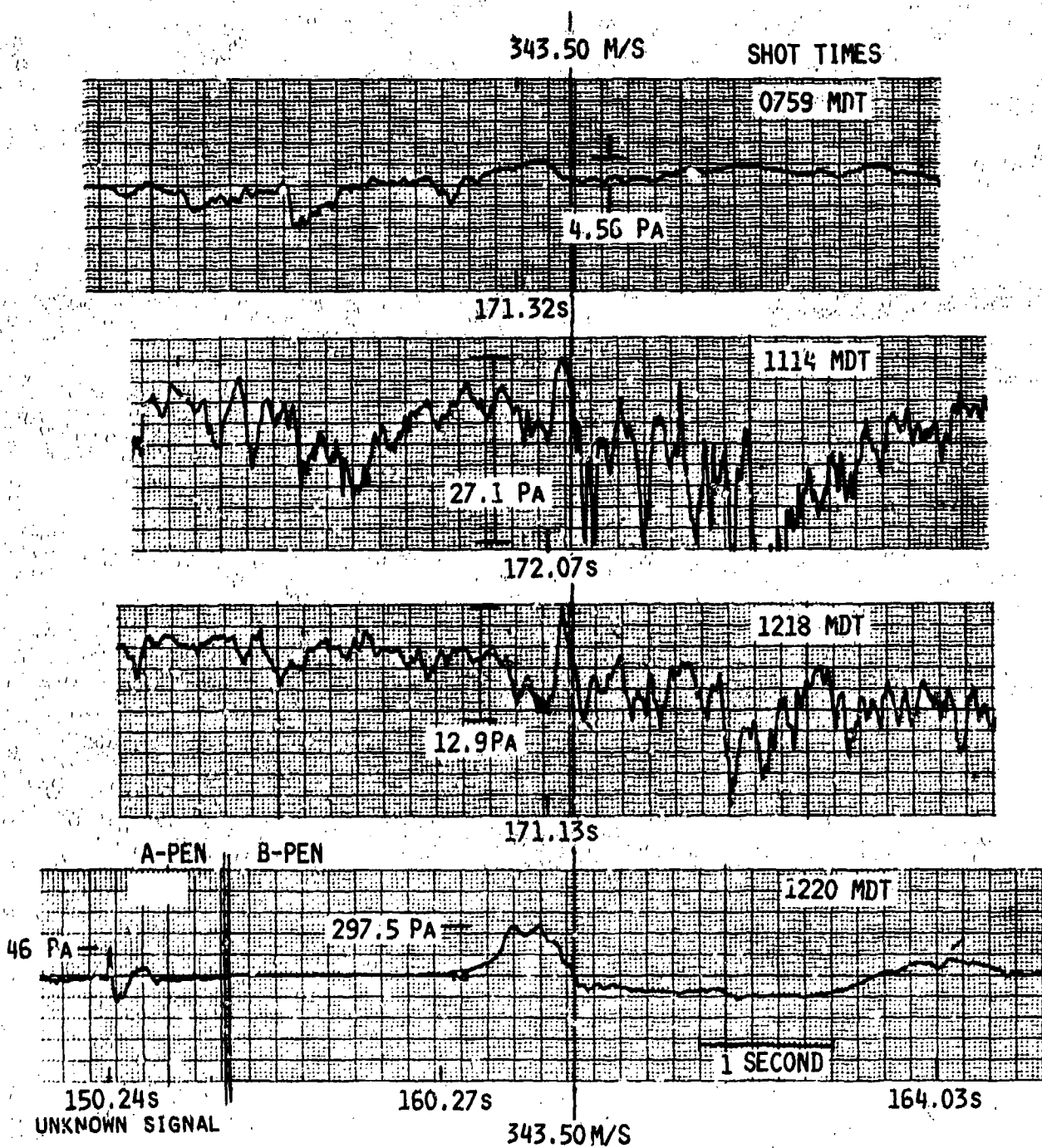
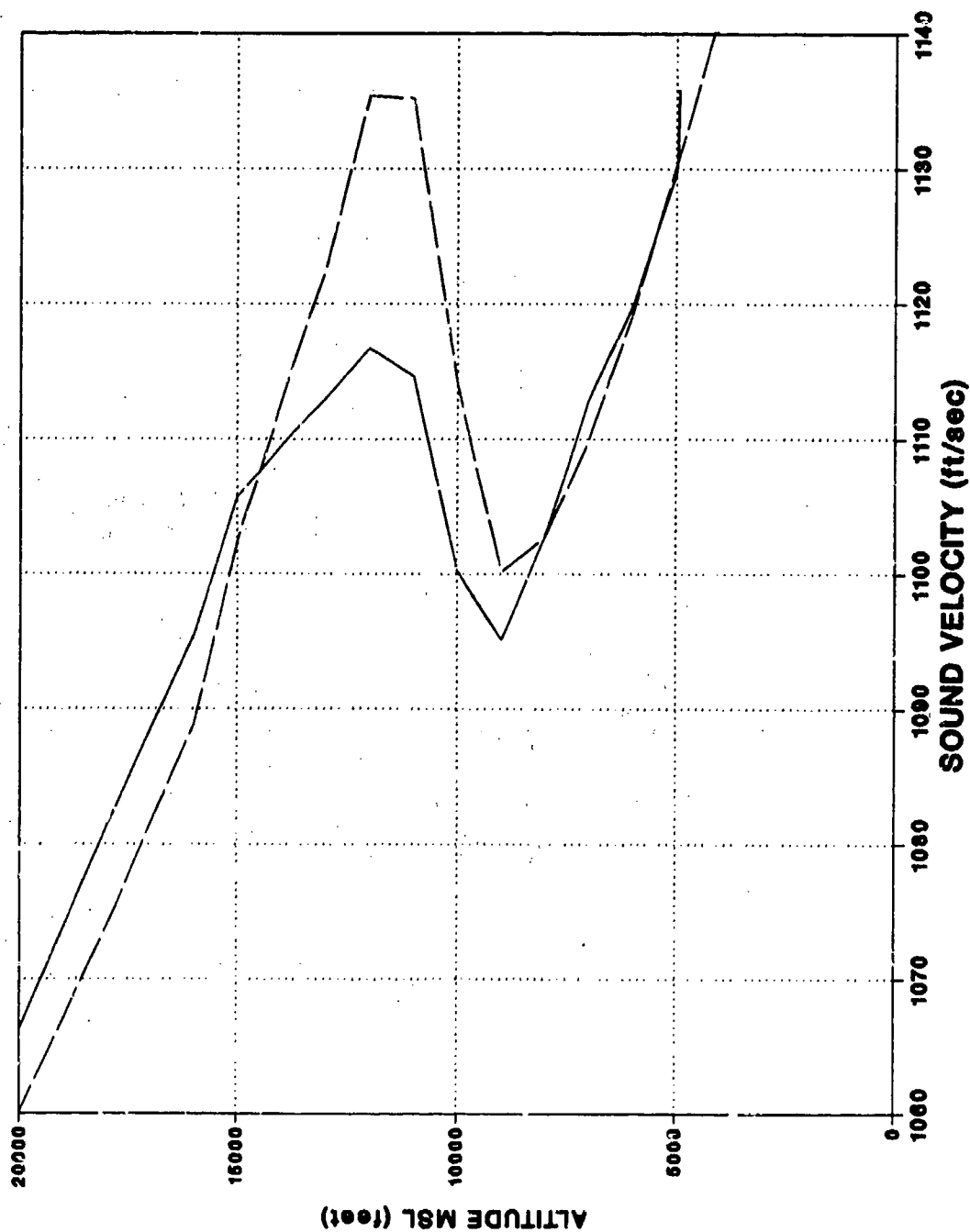


Figure 7. Carrizozo Microbarograms of MINOR SCALE and Pre-test Check Shots.

**Figure 8. DIRECTED SOUND VELOCITIES TOWARD CARRIZOZO.
AZIMUTH 087 DEG.**

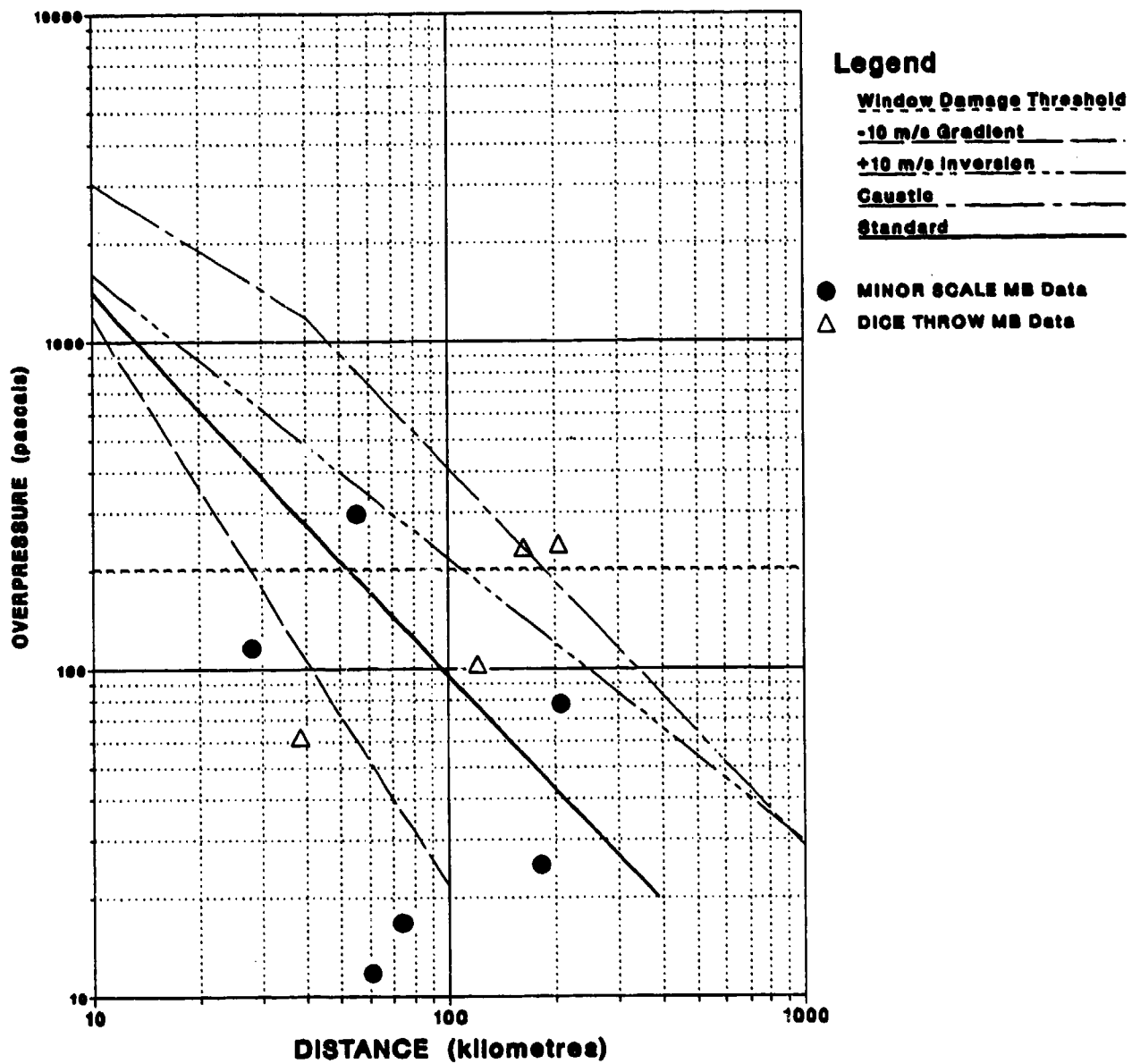


Legend

1220 MDT - STALLION

1336 MDT - JALLEN

Figure 9. Predicted and Observed Overpressures for MINOR SCALE, 4.8-kt ANFO Surface Burst.



**FRAGMENT HAZARD INVESTIGATION PROGRAM:
Prediction of Quantity Distance Requirements for
Mass-Detonating Ammunition Using a Monte Carlo Simulation
Model**

W. D. Smith, Naval Surface Weapons Center

INTRODUCTION

The Department of Defense Explosives Safety Board (DDESB) has funded a continuing study of the quantity distance (QD) requirements for Class 1, Division 1 ammunition (Mass-detonating) at the Naval Surface Weapons Center (NSWC). The main emphasis of the program has been methodology development using pallets of M107 155mm TNT loaded projectiles as a test vehicle. Previous reports have described the methodology developed to predict the far-field fragment hazards resulting from the detonation of stacks of projectiles. The initial deterministic methodology was based on the fitting of empirical relations to single pallet fragmentation data (weight-number and presented area distributions). Large-scale multiple pallet detonation tests conducted at the White Sands Missile Range (WSMR) and subsequent analysis showed that the far-field fragment density was directly proportional to the number of interaction areas (N_{ia} , spaces between projectiles in the face of the stack directed toward the fragment recovery zone). The empirical relations accurately predicted the total number of fragments recovered in the large-scale multiple pallet tests. However, prediction of the proportion of recovered fragments which would be considered hazardous ($KE \geq 58$ ft-lbf) was found to be unacceptably cumbersome. Consequently, it was decided to begin the development of a stochastic model to replace the original deterministic model. This report presents the results of the test and analysis effort pursued to validate the stochastic model. The details of the model development are presented elsewhere.

BACKGROUND

The deterministic methodology assumed that all fragments were ejected from the stack at optimum ejection angles (5 to 45 degrees) and that the kinetic energy of far-field fragments could be related to the calculation of terminal velocity in free-fall. Comparison of small-scale fragmentation characterization test data and the large-scale multiple pallet detonation test data from the WSMR indicated that a great number of fragments collected in the far-field were being ejected at other than optimum angles. These non-optimum ejection angle fragments possessed greater kinetic energy than the optimum ejection angle fragments and thus violated one of the basic assumptions used to develop the deterministic methodology. It was recognized that the event being simulated was actually a random event and that these problems could be reduced using a fragment trajectory

program modified to incorporate Monte Carlo simulation techniques. The development of this new approach (the stochastic model) encompassed approximately two years. The new model allows for the random behavior of the following parameters:

- a. initial fragment velocity
- b. fragment ejection angle
- c. fragment drag coefficient
- d. origin of fragments within the stack as a function of height
- e. soil conditions for fragment ricochet

Input data for the model is the standard data (fragment mass, initial fragment velocity, recovery zone and fragment presented area) obtained from fragmentation characterization tests.⁴ The user can specify the number of interaction areas in the stack (N_{ia}), the kinetic energy criterion and the hazardous fragment density criterion. The fragment trajectory calculation is a three-dimensional particle model that allows for a two-dimensional wind. Fragment ricochet effects are also included. Hit probability computations for striking a three-dimensional target (man, vehicle, building, etc.) are also incorporated in the model.

APPROACH

The Monte Carlo simulation model was validated by comparing the far-field fragment collection data from 155mm multiple pallet detonation tests and MK82 bomb single pallet detonation tests conducted at the WSMR to the far-field fragment densities predicted by the model. A series of small-scale fragmentation arenas was conducted to provide the input data for the model. The validated model was used to generate QD curves for stacks of 155mm projectiles and MK82 bomb pallets.

TEST AND ANALYSIS PROGRAM

155mm Projectile Pallets

Fragmentation Characterization

Two tests were conducted to determine the fragmentation characteristics of a two-pallet stack of 155mm projectiles configured identically to the detonation source used for the 36 pallet test at the WSMR (ie., two pallets positioned horizontally with the nose of one pallet beneath the bottom of

the other pallet). Figure 1 presents the fragment velocity distribution measured as a function of polar zone. The maximum velocity for the fragments was recorded in the 50 and 60 degree zone. The velocity distribution was comparable to the distribution recorded for the single pallet characterization test.² All collected fragments weighing greater than 300 grains had their presented areas measured. The 300 grain limit was chosen because it was determined by analysis that no fragment weighing less than 300 grains would be hazardous in the far-field.

Model Validation

The arena fragmentation characterization data was used as input to the Monte Carlo model to determine the number of replications necessary to obtain stable far-field fragment density results and to determine if the random number seed chosen had a significant effect on the predicted far-field density. Figures 2 and 3 provide the results of varying the number of replications and the random number seed. Stable fragment densities were obtained using a minimum of 30 replications. The predictions varied approximately 5% using a variety of random number seeds. The subsequent validation runs were made using 30 replications.

In order to compare the results of the Monte Carlo model with the large scale multiple pallet tests, the actual test data must be considered as a single replication of the random event simulated by the model. Consequently, simply comparing the average predicted far-field density to the actual test data would not conclusively demonstrate the accuracy or inaccuracy of the model. The model was designed to maintain a record of the minimum and maximum number of fragments as a function of range for each replication. Figure 4 presents a comparison of the far-field fragment collection data for the WSMR 36 pallet detonation test² with the minimum and maximum number of fragments predicted by the Monte Carlo model for an identical stack. It can be seen that the minimum and maximum predictions neatly bracket the actual recovery data. This indicates that the model accurately predicts the far-field fragment density resulting from the detonation of stacks of 155mm projectiles.

MK82 Bomb Pallet

Fragmentation Characterization

It became apparent during the development of the model that it would be beneficial to validate the model for another weapon in order to demonstrate the general utility of the model. A series of fragmentation characterization tests and far-field fragment recovery tests were conducted at the NSWC and the WSMR using single pallets of bombs as a cooperative effort with the Naval Explosive Safety Improvement Program (NESIP). A series of large-scale single pallet detonations

with far-field fragment pickup were conducted at the WSMR and a fragmentation characterization arena was conducted at the NSWC. The far-field collection tests were conducted with the pallet positioned horizontally. The center bomb in the bottom row was detonated. Fragments were collected in 36 ten degree wide collection zones 360 degrees around the pallet to a distance of 2700 feet. Six individual pallets were detonated and then the fragments were collected. The fragmentation characterization arena was conducted with the pallet positioned vertically. The center bomb in the row away from the celotex or steel plates was detonated. Figure 5 presents the fragment velocity distribution measured for the pallet of bombs as a function of polar zone. The maximum velocity (10900 ft/sec) was recorded between 20 and 40 and 60 and 80 degrees. The detailed fragmentation data and collection data are available.⁵

Model Validation

Figure 6 shows a comparison of the far-field collection data and the predictions of the Monte Carlo model for a single pallet of bombs. The model predictions generally bracket the actual test data. This indicates that the model can be used to predict the far-field fragment hazard for mass-detonating ammunition.

Quantity Distance (QD) Requirements

155mm Projectiles

The test and analysis program conclusively demonstrated that the far-field fragment density is directly proportional to N_{ia} in the stack. For large stacks N_{ia} is approximately equal to the number of projectiles in the face of the stack. Figure 7 presents a comparison of the Monte Carlo predictions for the number of projectiles in the face of the stack (N_p) and the corresponding blast criterion ($40W^{1/3}$) for a stack of the same size. It can be seen that the blast criterion apparently underestimates the hazard. However, it must be realized that the DDESB has established a minimum QD distance of 1250 feet for stacks containing less than 30000 lbs of explosive. Furthermore, the model indicates that for ranges greater than 2500 feet the fragment hazard is zero ($N_p = \text{infinity}$). This range corresponds to stacks containing 245000 lbs of explosive based on the blast criterion.

The Monte Carlo model was designed to be able to calculate the QD requirements using different hazard criteria. The results of this analysis is presented in Figures 8 thru 11 and are discussed below:

- a. Reducing the kinetic energy criterion from 58 to 10 ft-lbf increases the QD distance by approximately 200 feet (Figure 8).
- b. Reducing the hazardous density criterion from 1/600 sq ft to 1/6000 sq ft increases the QD distance by approximately 600 feet (Figure 9).
- c. Using the probability of hitting a standing man rather than the fragment density requirement does not significantly affect the QD criteria (Figure 10).
- d. Reducing the probability of hitting a man from .01 to .001 increases the QD distance by 600 feet (Figure 11).

Figure 12 compares the effect of tail wind on the QD curve for 155mm projectiles. It can be seen that a 90 ft/sec tail wind increases the QD requirement by approximately 900 ft.

MK 82 Bomb Pallet

Figure 13 presents the QD curve for MK82 bombs generated using both the existing DDESB density criterion and a probability of hitting a standing man of 0.01. The curves asymptotically approach 3500 feet for stacks with more than 200 bombs in the face. The curves indicate that the current blast criterion will underestimate the fragment hazard for stacks containing less than 670000 lbs of explosive. Furthermore, the current hazard criteria ($KE_{\text{haz}}=58 \text{ ft-lbf}$, Density = $1/600 \text{ ft}^2$) accepts a greater risk than does the .01 probability of hit criterion.

Figure 14 presents the effect of a 90 ft/sec tail wind on the QD curve. The tail wind will increase the distance required from 3500 ft to 4500 ft.

CONCLUSIONS

The Monte Carlo model has been shown to be an effective and accurate tool in predicting both the near and far-field areal fragment density resulting from the accidental detonation of stacks of Class 1, Division 1 (Mass-Detonating) ammunition. The model allows the user to easily assess the effect on the far-field fragment hazard of changes made to the hazard criteria (i.e, density or kinetic energy). Furthermore, the model eliminates the necessity of large-scale, multiple pallet tests

with far-field pickup. Properly designed small-scale fragmentation characterization arenas can be used to gather the necessary data.

The model has shown that the fragment hazard resulting from the detonation of Class 1, Division 1 ammunition exceeds the existing blast criterion (minimum 1250 feet) for relatively small stacks (less than 30,000 lbs of explosive). The fragment hazard asymptotically approaches a maximum (approximately 2500 feet for 155mm projectiles and 3500 feet for MK82 bombs) as the stack size grows larger. The blast criterion exceeds this distance for stacks containing more than 245,000 lbs of explosive for 155mm projectiles and 670,000 lbs for MK82 bombs. The fragment hazard for smaller stacks can be reduced by judicious stacking of the pallets to reduce the number of units in the face of the stack.

RECOMMENDATIONS

The explosive hazard classification procedures used by the DDESB⁶ should be modified to incorporate the test and analysis procedures developed by this program.

The instructions used by ammunition depots to stack ammunition in magazines should be reviewed and modified to reduce the number of units in the face of the stack to a minimum. Circular stacking of pallets should be studied as a means to minimize fragment hazards.

It is recommended that small-scale fragmentation characterization of additional Class 1, Division 1 ammunition be conducted and the Monte Carlo model used to generate new QD curves.

The Monte Carlo model should be used to generate QD curves for other classes of ammunition such as Class 1, Division 2 (Non-mass detonating). Minor modification of the model will be required.

The effect of magazine structures on the fragmentation characteristics of the ammunition studied should be determined. Small-scale fragmentation arenas should be used to develop the data required by the model.

REFERENCES

1. Ramsey, R. T., et al, *Fragment Hazard Investigation Program*, NSWC TR-3664, October 1978
2. Powell, J. G., et al, *Fragment Hazard Investigation Program: Natural Communication Detonation of 155mm Projectiles*, NSWC TR 81-54, July 1981

3. McCleskey, F., *Fragmentation Hazard Computer Model*, Minutes of the 21st DDESB Seminar, 1984

4. Ammerman, D. J., *Fragmentation Test Procedures Used at NSWC*, NSWC MP 81-16, June 1981

5. Smith, W. D., *Fragment Hazard Investigation Program: Validation of the Monte Carlo Simulation Model*, NSWC TR 86-187, Unpublished

6. Department of Defense Explosives Hazard Classification Procedure, Army TB700-2, Navy NAVSEAINST 8020.3, Air Force TO 11A-1-47, Defense Logistics Agency DLAR 8220.1, September 1982.

**MEASURED VELOCITY FOR 155MM
PROJECTILE PALLET**

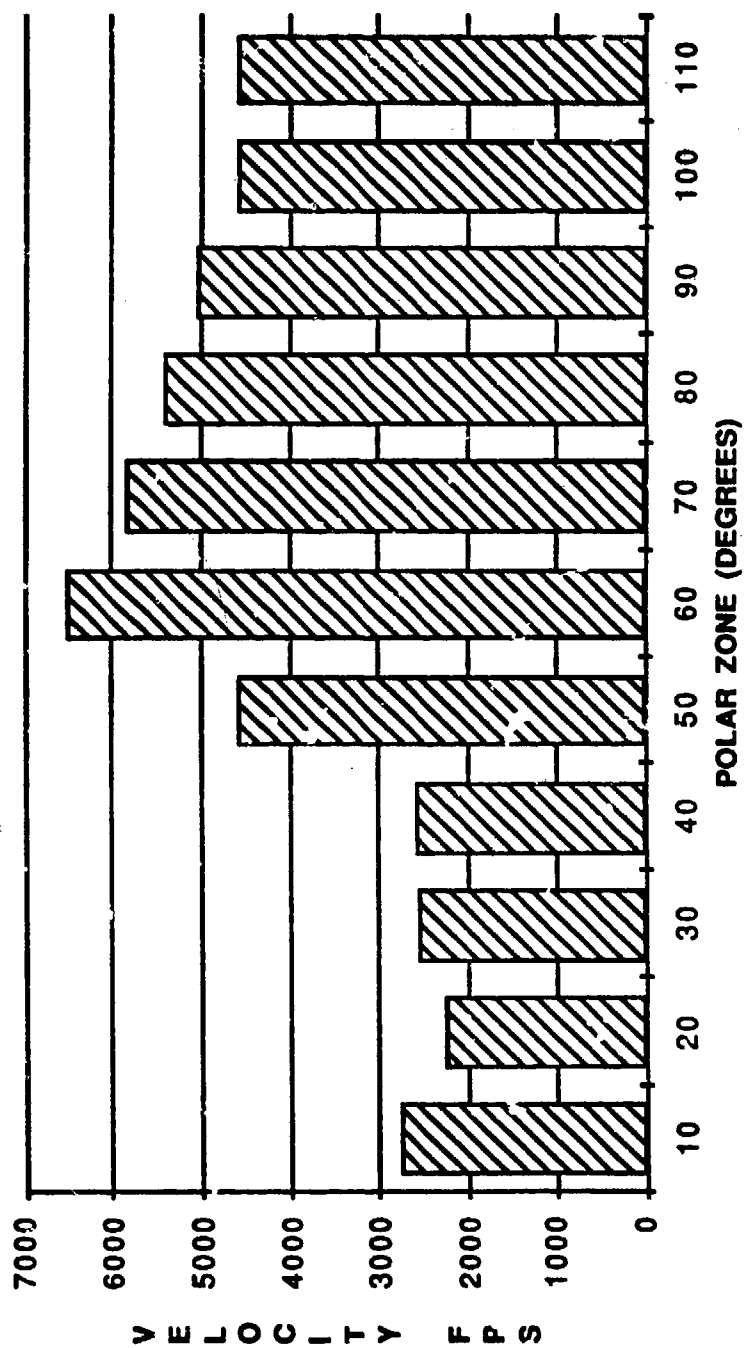


FIGURE 1

COMPARISON OF THE EFFECT OF THE NUMBER OF REPLICATIONS ON THE PREDICTIONS OF THE MONTE CARLO MODEL

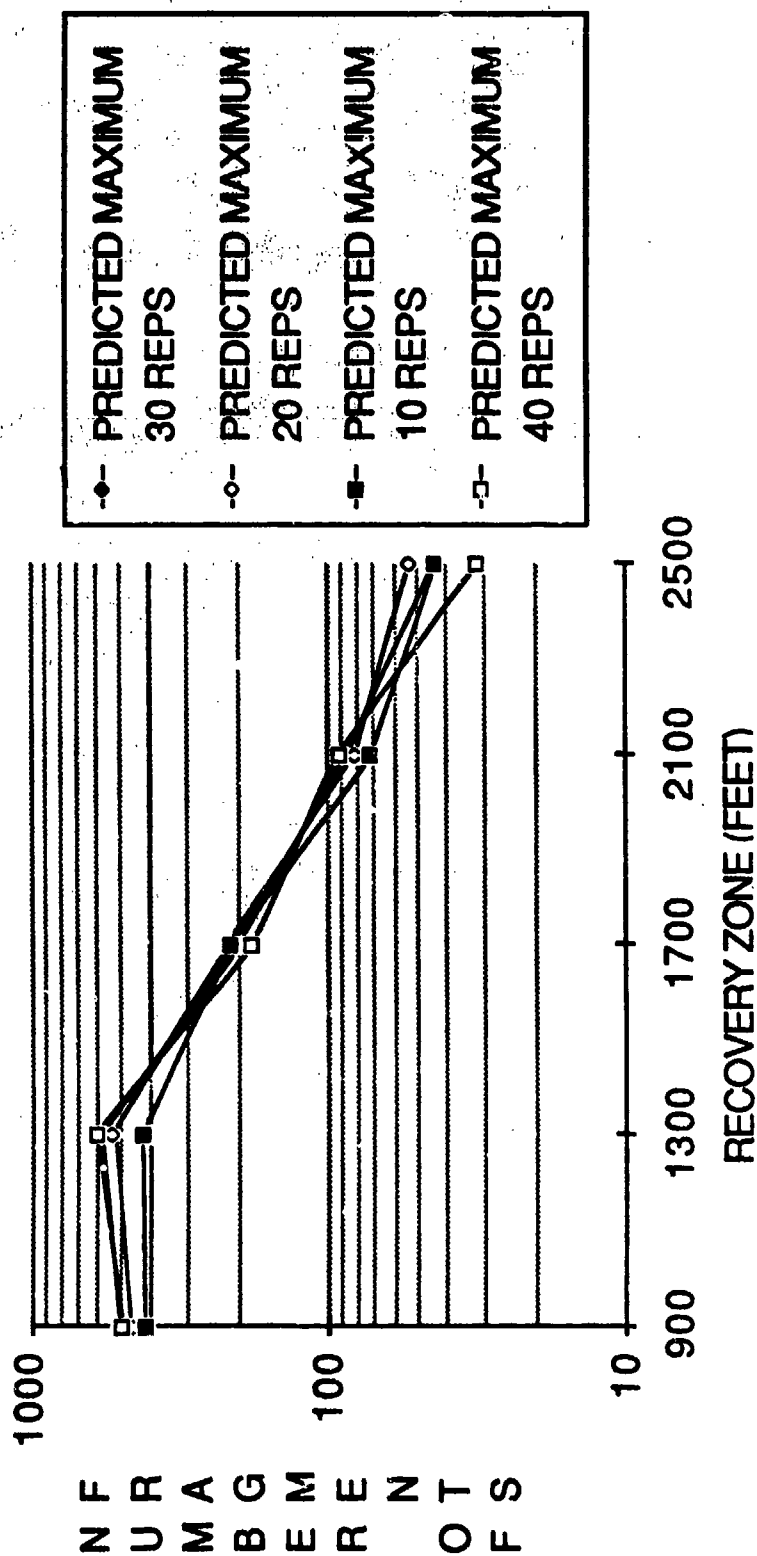


FIGURE 2

QD CURVE COMPARISON OF RANDOM NUMBER SEEDS FOR 36 PALLET CONFIGURATION OF 155MM PROJECTILES

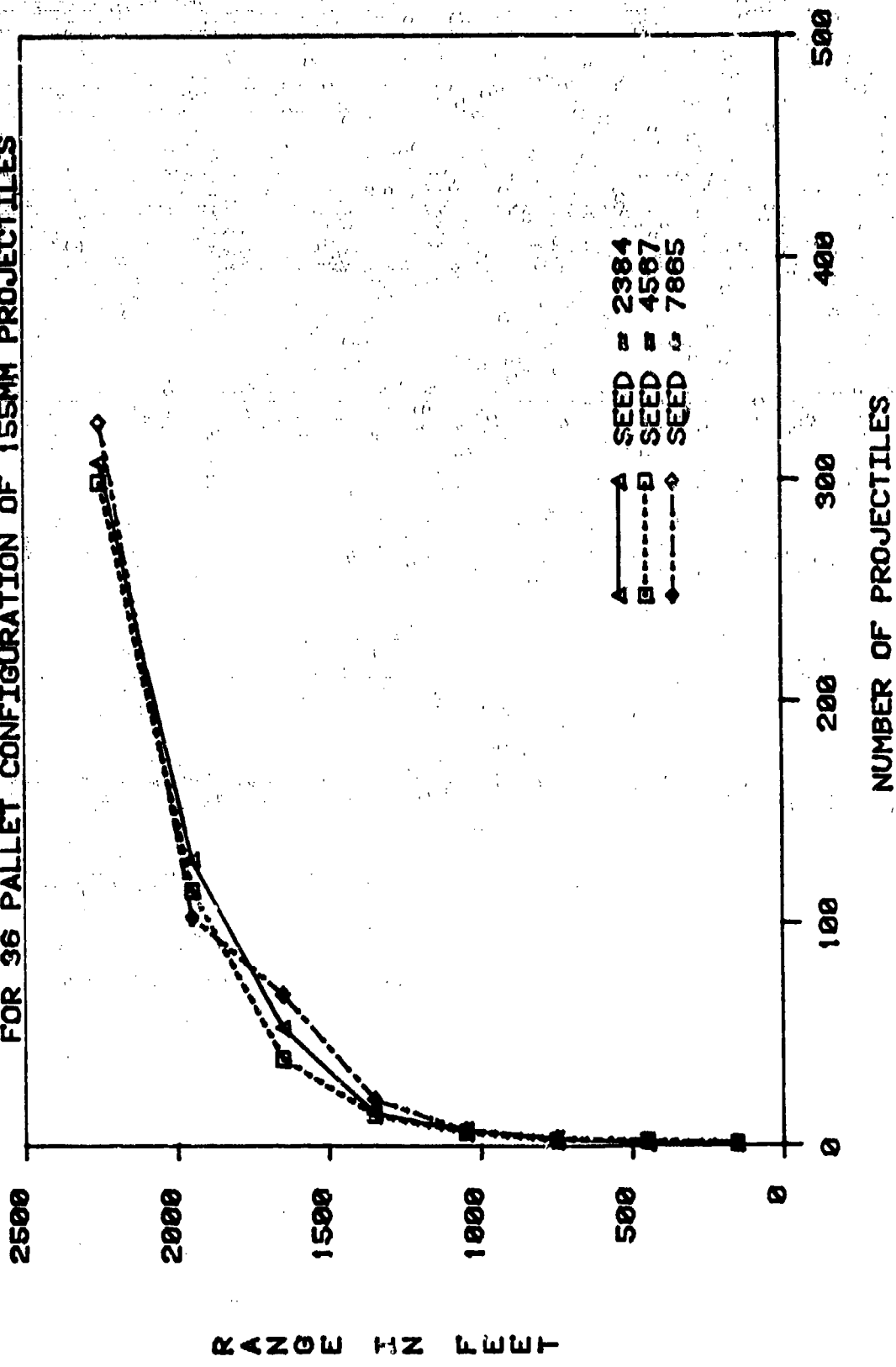


FIGURE 3

PREDICTED VERSUS ACTUAL RECOVERY DATA FOR 36 PALLETS OF 155MM PROJECTILES

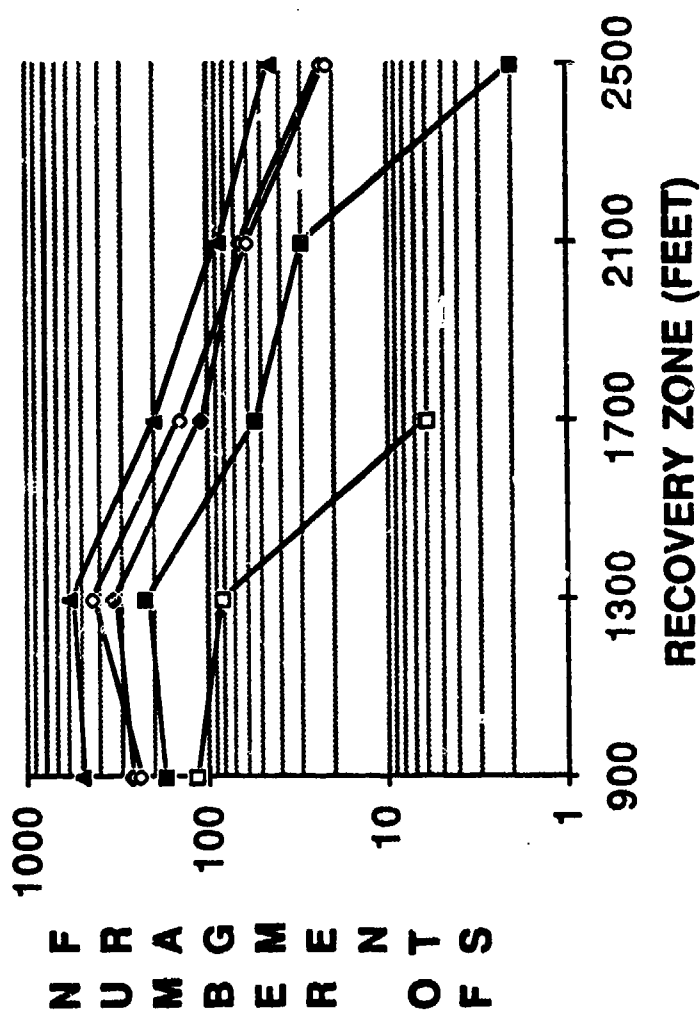


FIGURE 4

MEASURED VELOCITY FOR MK82 BOMB PALLET

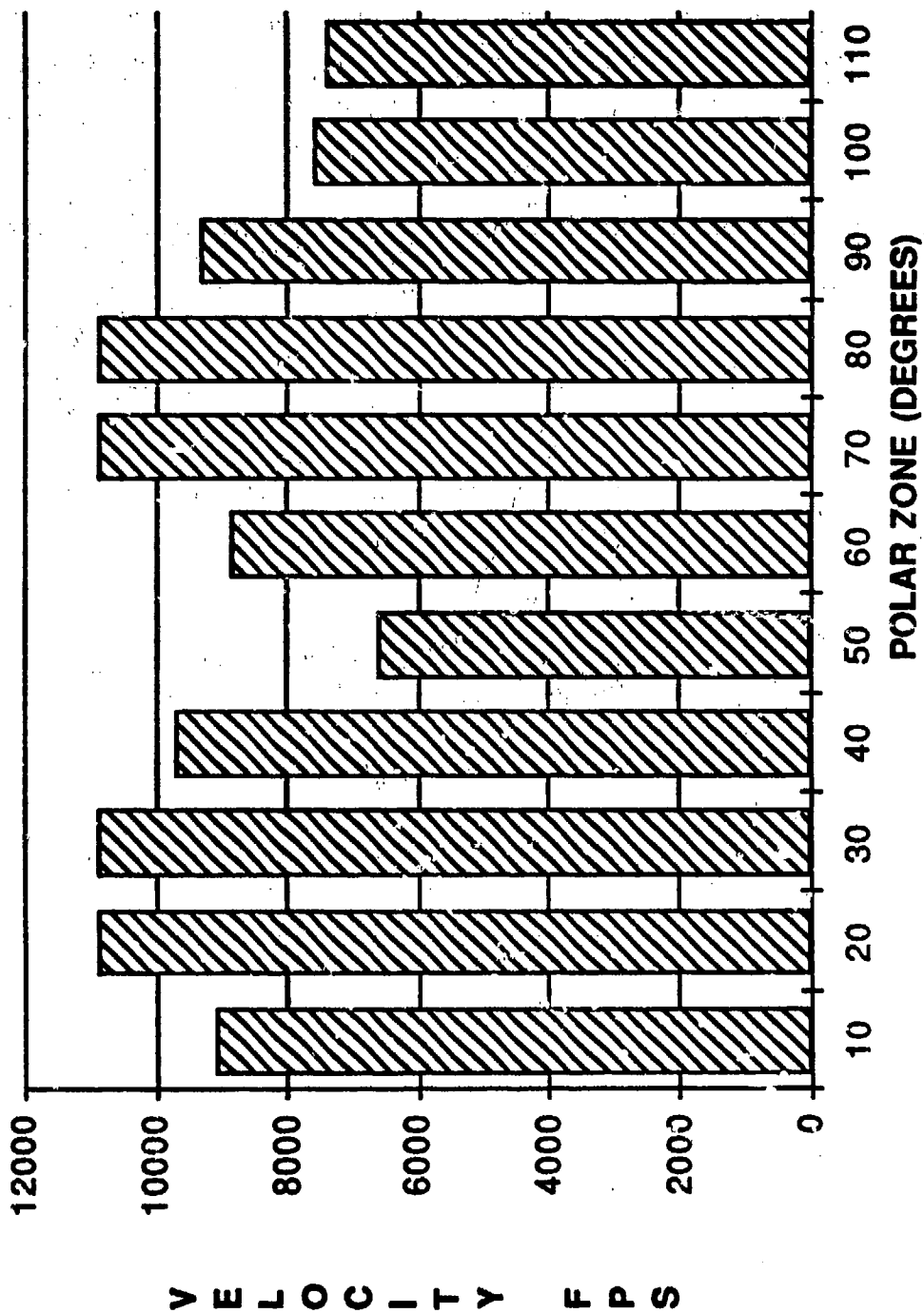


FIGURE 5

PREDICTED VERSUS ACTUAL RECOVERY DATA FOR MK82 BOMB PALLET

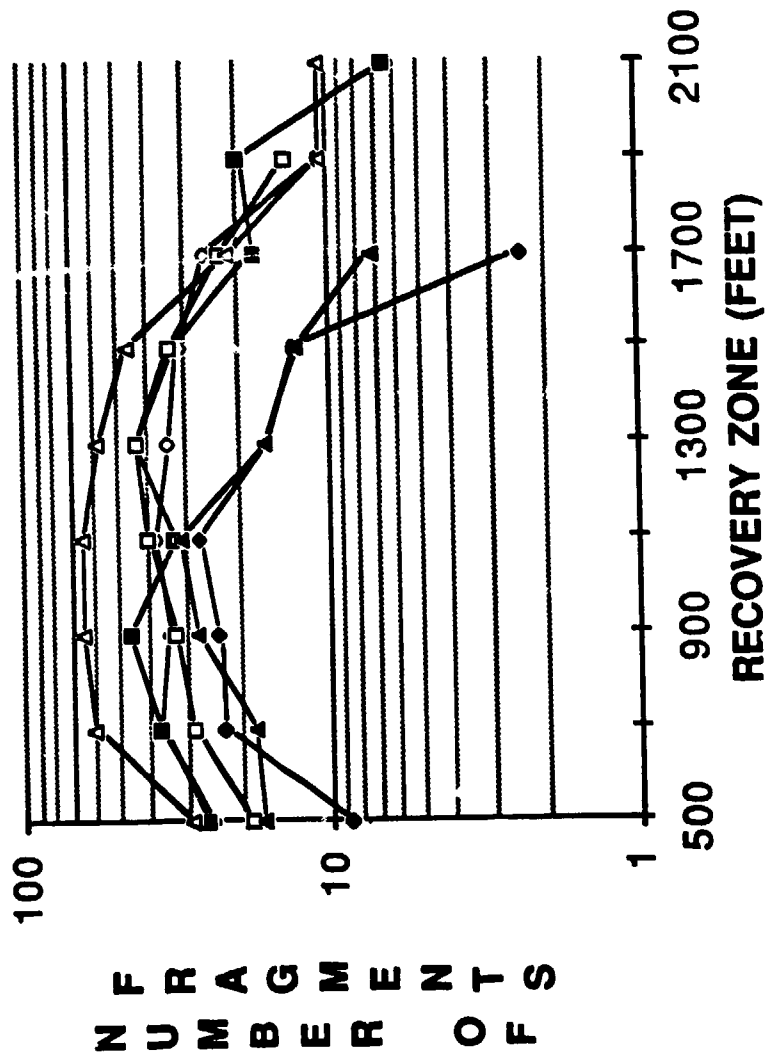


FIGURE 6

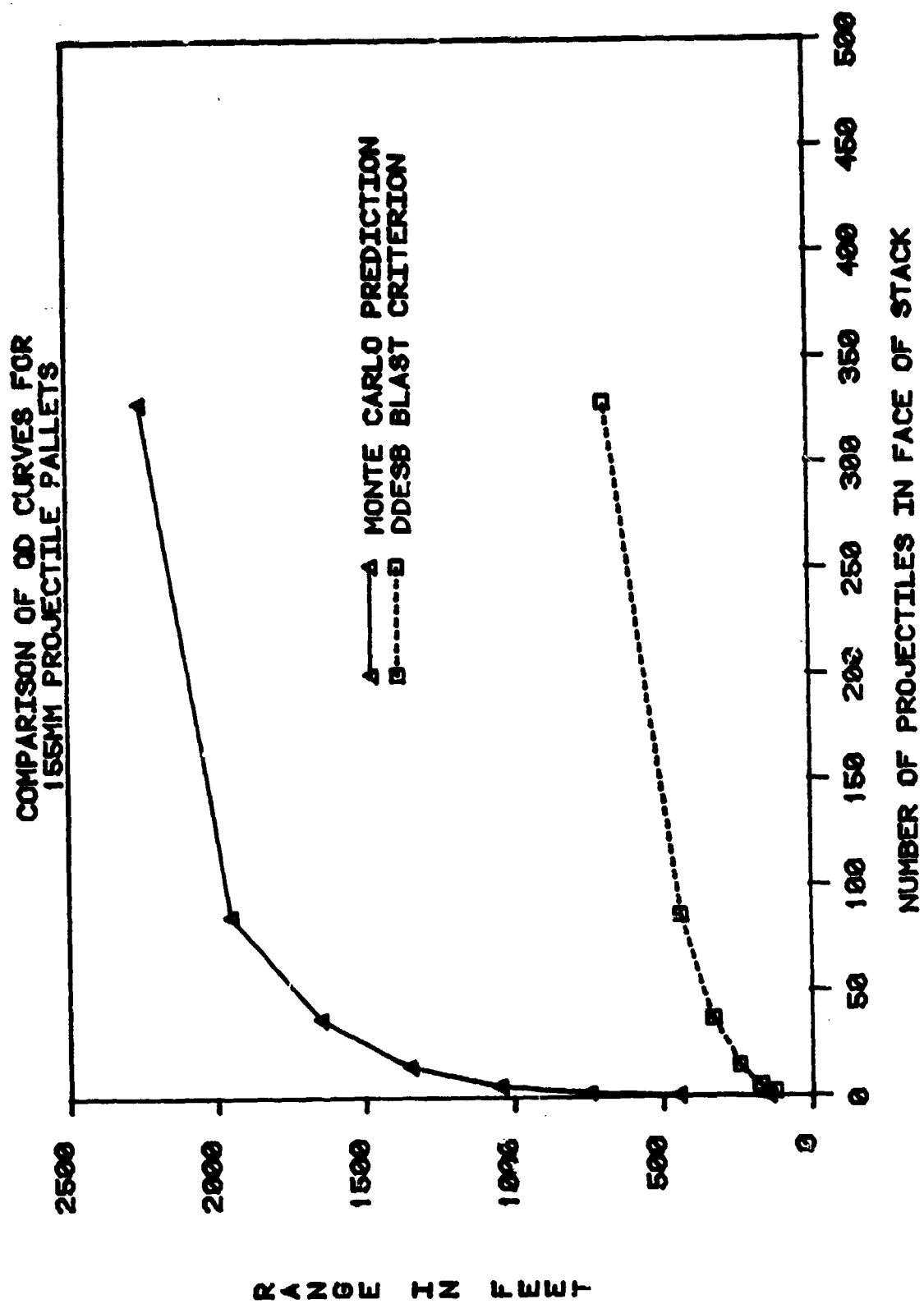
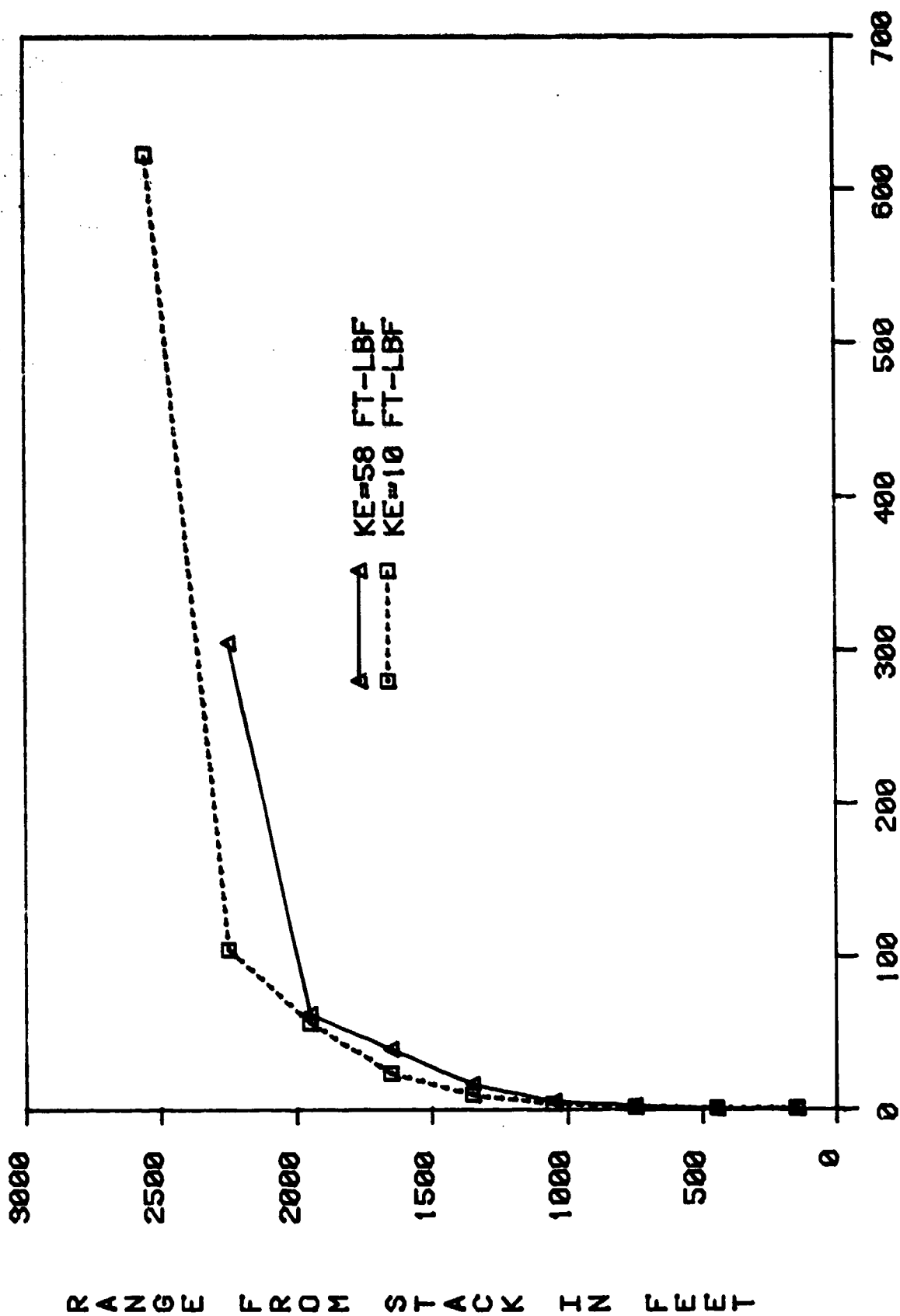


FIGURE 7

COMPARISON OF QD CURVES FOR 155MM PROJECTILES



NUMBER OF PROJECTILES IN FACE OF STACK

FIGURE 8

RANGE FROM STACK IN FEET

QD CURVE FOR 155MM TNT LOADED PROJECTILES COMPARISON OF DENSITY CRITERIA

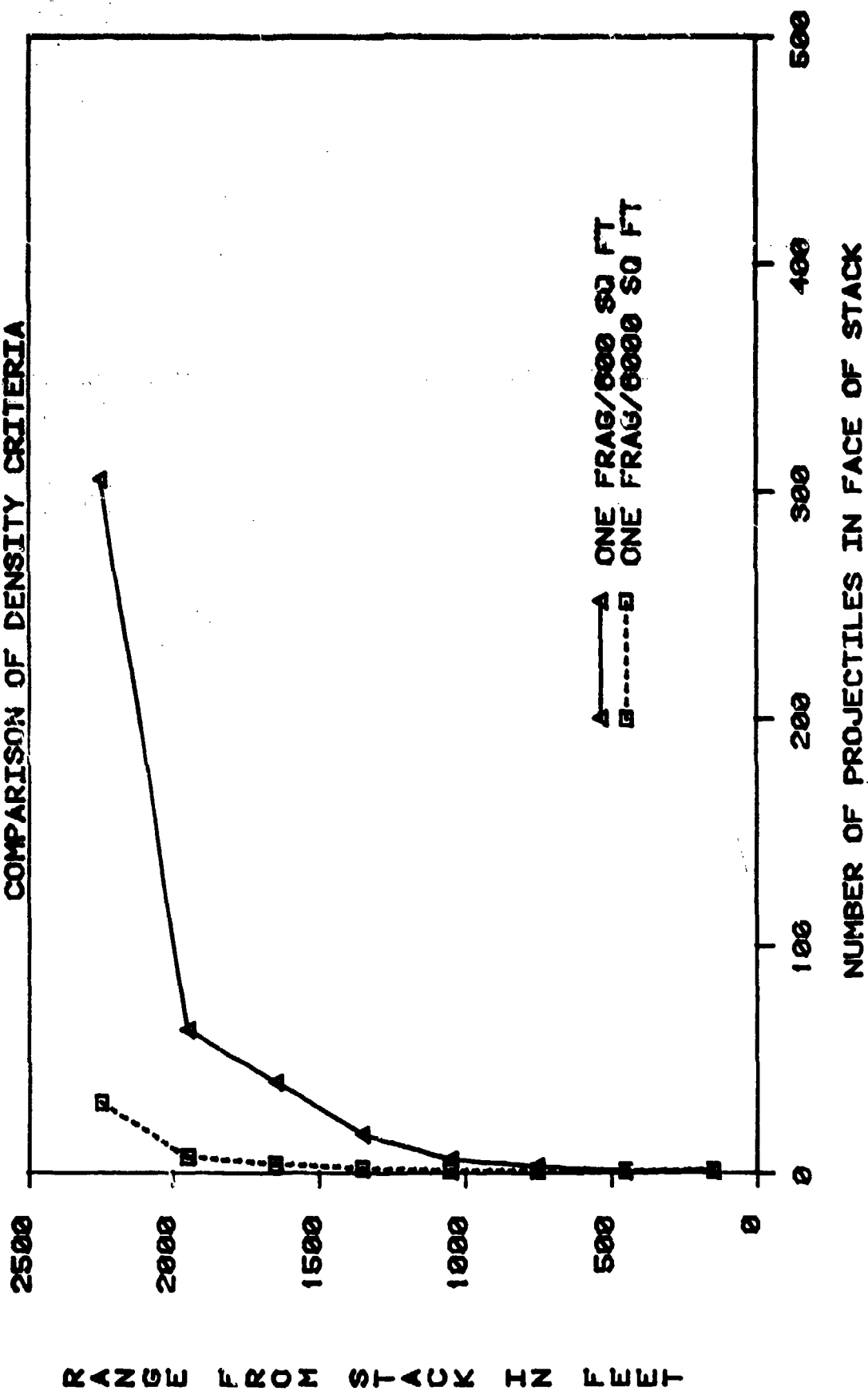


FIGURE 9

COMPARISON OF OD CURVES FOR 155MM PROJECTILES

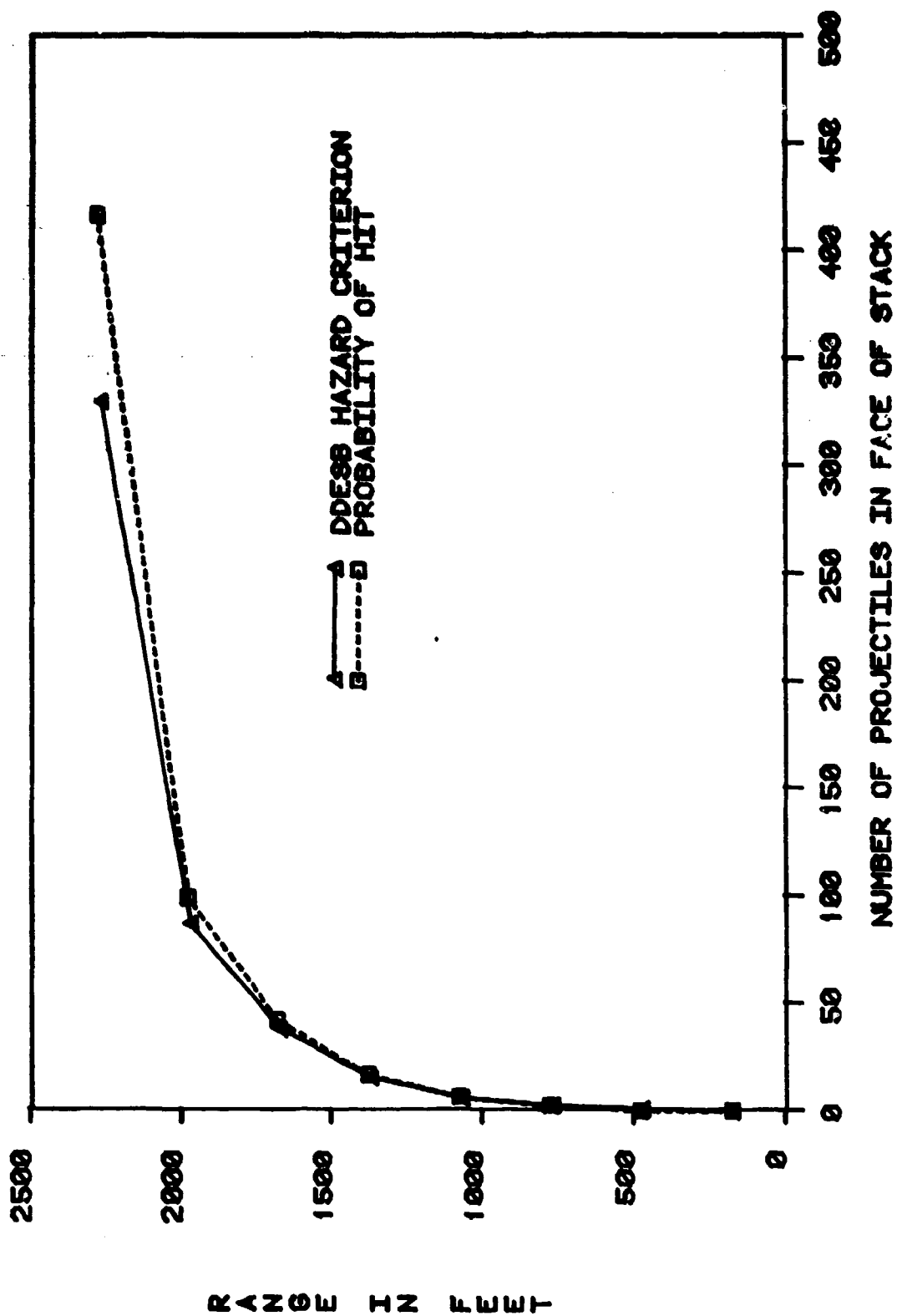


FIGURE 10

OD CURVE FOR 155MM TNT LOADED PROJECTILES COMPARISON OF PROBABILITY OF HIT CRITERIA

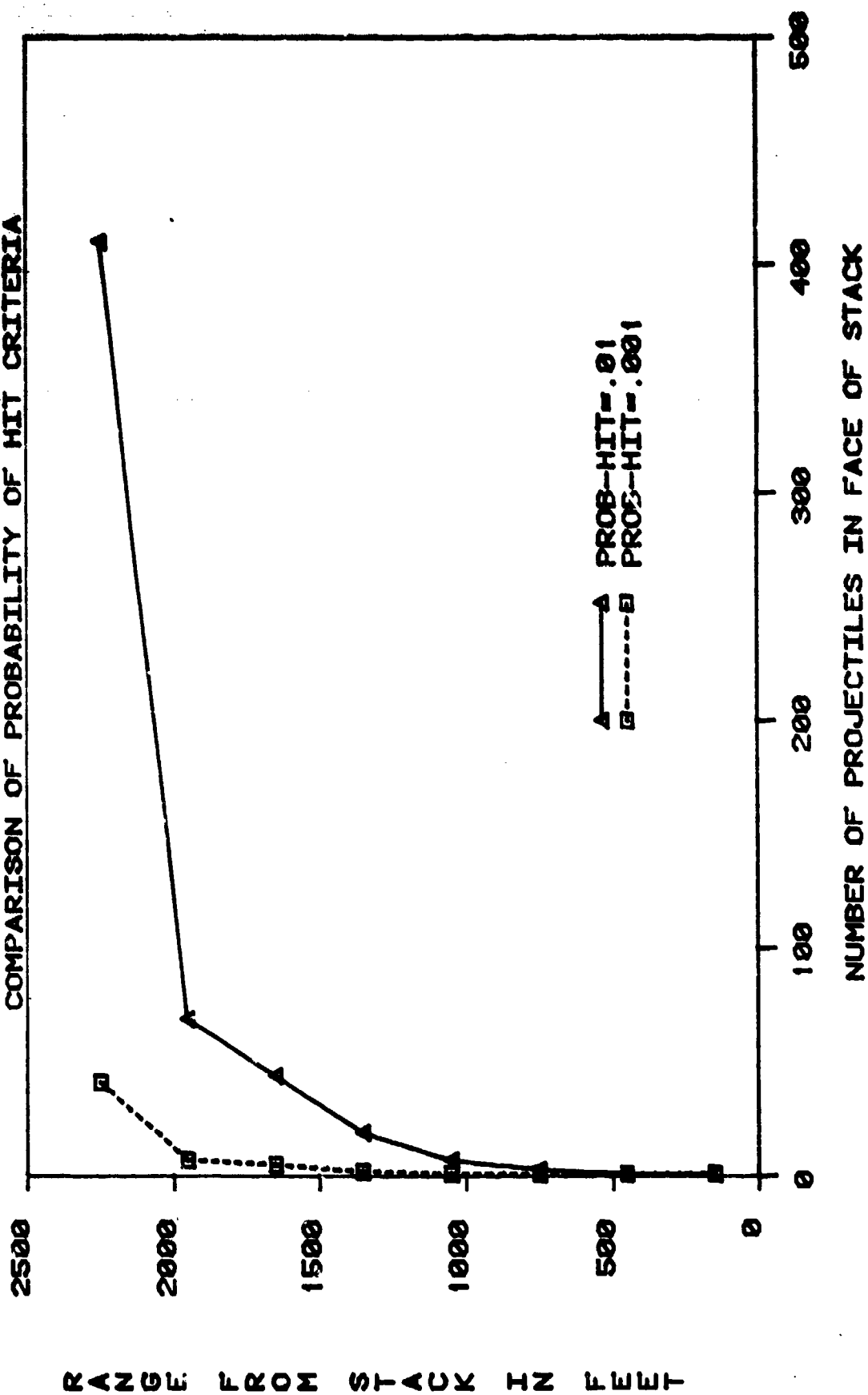


FIGURE 11

EFFECT OF TAIL WIND ON QD CURVE FOR 155MM PROJECTILES

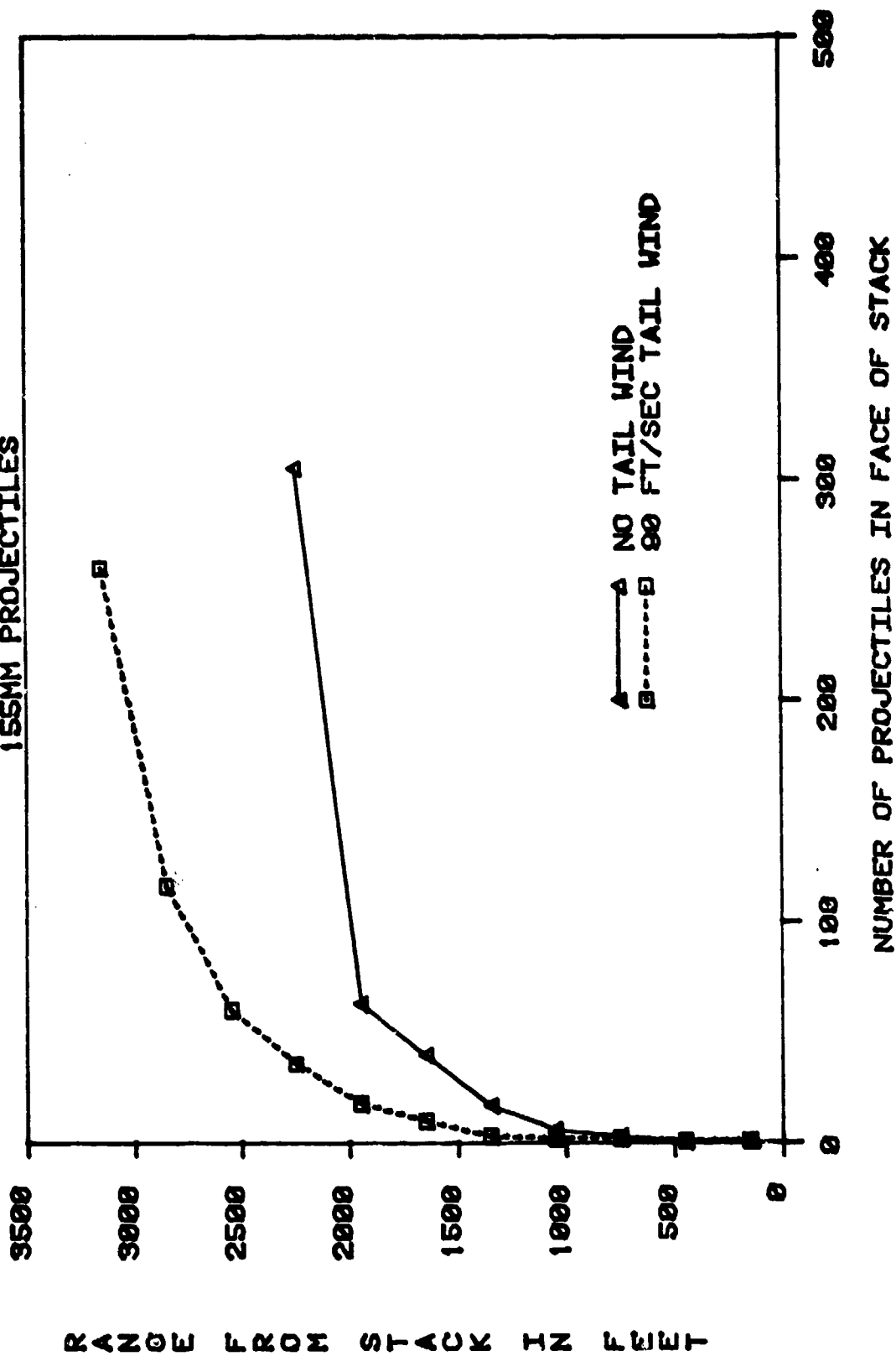


FIGURE 12

QD CURVE FOR MK82 BOMB PALLETS

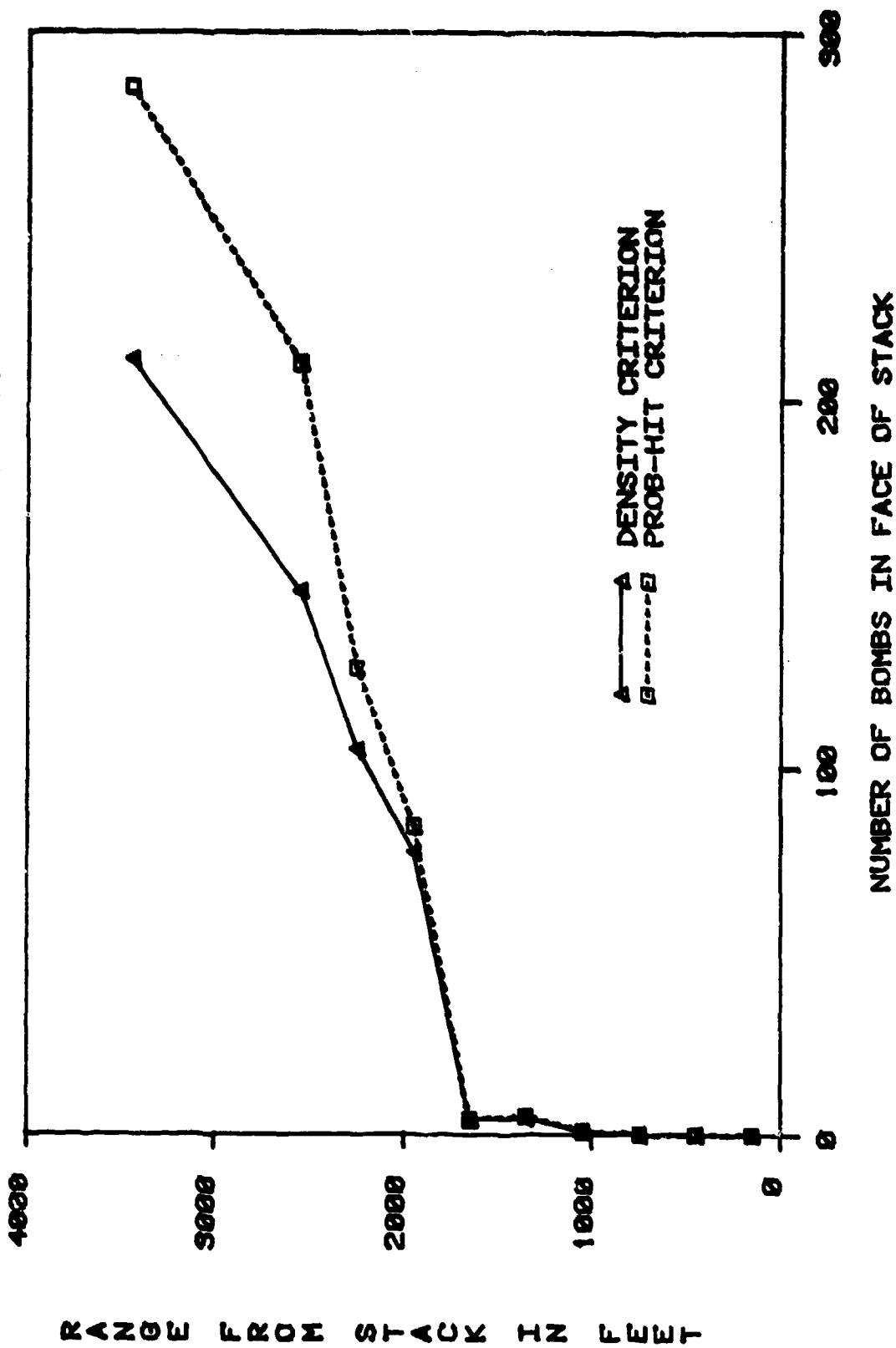


FIGURE 13

Effect of a Tail Wind on QD Curve for MK82 Bomb Pallet

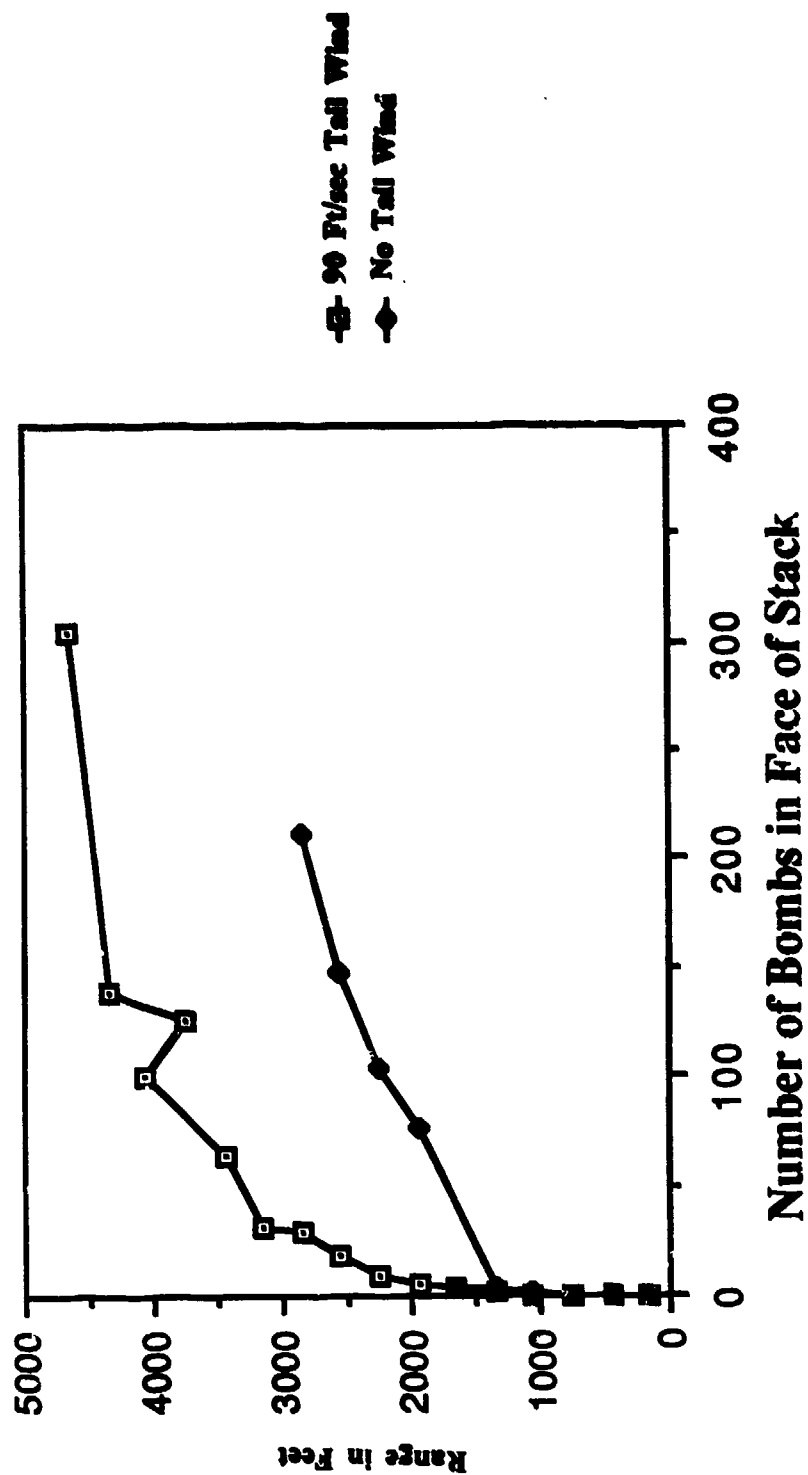


Figure 14

AD-P005 364

DRAG COEFFICIENTS
FOR
IRREGULAR FRAGMENTS

by

Frank McCleskey

Naval Surface Weapons Center
Dahlgren, Virginia 22448

Autovon 249-7993
Commercial 703-663-7993

The Naval Surface Weapons Center (NSWC) has a continuing task from the Department of Defense Explosive Safety Board (DDESB) to establish methods for predicting the fragment hazards due to the inadvertent explosion of ordnance items. As part of this task, NSWC has established a computer model which predicts fragment hazards. This computer model was explained in the minutes of the twenty-first DOD Explosives Seminar.

The computer model calculates individual trajectories for each fragment recovered in small-scale fragment arena tests. The following variables affect the individual fragment trajectories:

- EI - Initial Elevation Angle
- VI - Initial Velocity
- A/M - Area to Mass Ratio
- ALT - Altitude
- RHO - Air Density
- MN - Mach Number
- HO - Height of the Origin
- SC - Soil Constant (Ricochet)
- W - Wind Speed and Direction
- C_D - Drag Coefficient

Except for C_D , all of these variables can be defined with a fair degree of accuracy by tests, measurements, and calculations.

The drag coefficient for any fragment is a function of shape only. For regular fragments, like spheres or cubes, the drag coefficients are reasonably well defined. For irregular fragments, like those from bombs or concrete walls, no two fragments have exactly the same shape. As a result, no two irregular fragments have exactly the same drag coefficient. In all cases, drag coefficient is a function of Mach Number.

The drag coefficients for irregular fragments are not only uncertain but have a pronounced effect on far-field range. Figure 1 shows range versus C_D for a typical fragment. The range of low subsonic C_D varies from .5 to 1.5, a factor of three. Associated range varies by a factor of more than 2. This represents a large range uncertainty in trajectory calculations for establishing fragment hazards. If this uncertainty is to be reduced, some correlation must be established between C_D and the characteristics of the irregular fragments.

C_D is a function of shape only. Therefore any correlating parameter should be dimensionless; that is, geometrically similar fragments which have the same C_D should have the same correlating parameter. For example, we might take the ratio of the maximum presented area to the minimum presented area as a measure of shape. For a sphere this ratio would always be one no matter what the size of the sphere. For a cube this ratio would always be 1.732.

The impetus for this program was provided by an observation having to do with the data contained in reference (a). That report contained the first systematic look at air drag for fragments. Three regular fragments were studied in the report, i.e., a sphere, a cube and a bar. The bar length,

width and thickness were in the ratio of 5-1-1. Since these fragments were regular, exact ratios of maximum to minimum presented area could be calculated. The results were as follows:

FRAGMENT SHAPE

	SPHERE	CUBE	BAR (5-1-1)
C_D (MN .75)	.60	.88	1.12
A_{MAX}/A_{MIN}	1.00	1.73	7.14

Note that as the correlation ratio increases so does the C_D . The report also showed that the C_D for irregular fragments was greater than those for the sphere or cube. For irregular fragments the area ratio could be expected to be on the order of that for the bar. Everything seemed to support the idea that the C_D for irregular fragments could be correlated with dimensionless parameters.

To follow up on this idea, it was decided to choose 96 fragments with a wide variation of shapes for test in the vertical wind tunnel at Ballistic Research Laboratory (BRL) in Aberdeen, Maryland. Four different kinds of measurement were made on each fragment.

1. Linear Maxima: Length, width and thickness
2. Linear Averages: Length, width and thickness
3. Perimeters: (3 planes)
4. Presented Areas
 - a. Maximum
 - b. Average
 - c. Minimum
 - d. Variance
 - e. Standard Deviation

Linear dimensions were measured as shown in Figure 2. Note that in calculating average dimensions, the average thickness is calculated to produce an equivalent weight and volume rectangular parallelepiped.

Perimeters were measured in three planes as shown in Figure 3. Note that the perimeters do not exactly follow the contour of the fragment but represent a stretched string around the high points.

Fragment presented areas were measured in two ways. Measurements were made using an icosahedron gage, and calculations were performed on the equivalent weight and volume rectangular parallelepipeds. Figures 4 and 5 show the essentials of these measurements and calculations. The icosahedron gage is an optical device which throws a shadow of the fragment onto a sensing surface. The associated electronics produces a readout of presented area. The optical axis is positioned at 16 approximately equally spaced aspects so as to produce 16 distinct presented areas which can be analysed for a variety

of statistics. The icosahedron gage cannot mount a fragment weighing more than 1500 grains. For larger fragments, presented area statistics are calculated using the rectangular parallelepipeds as shown in Figure 5.

All of the linear, perimeter and area measurements for the 96 fragments are contained in Tables A-1, A-2 and A-3 of Appendix A.

The essential aspects of the vertical wind tunnel are shown in Figure 6. In operation, a fragment is placed on the fragment support screen in either the upper or lower test section depending on the air velocity necessary to raise the fragment. The air speed is controlled by opening the inlet vanes of the constant speed fan. The air speed is adjusted until the fragment rises from the screen and assumes a relatively constant height. At this time, the air stream velocity is read directly from the velocity calibrated manometer. Air density is calculated from the ambient pressure and temperature. Ambient conditions are acceptable because of the relatively low air velocities produced in the tunnel. These parameters together with the weight and average presented area of the fragment are then used to calculate the low subsonic drag coefficient (C_D).

Each fragment was tested in the vertical wind tunnel. The velocity of the air stream is increased until the fragment hovers in the air stream at near constant vertical height. In this vertical equilibrium position the drag and gravity forces will also be in equilibrium. From previous measurements we know the weight and average presented area of the fragment. From the wind tunnel we establish the density and velocity of the air stream. As shown in Figure 7, once we know these values, we can calculate C_D . Since we operate at a single air velocity we can only obtain a single point on the drag curve. This point is in the low subsonic region, roughly about a Mach Number of 0.1. The remainder of the drag curve must be inferred from other sources.

Three regular fragments (sphere, cube and bar) which were tested in reference (a) were also tested in the vertical wind tunnel. In reference (a) however, C_D was obtained at a Mach Number of approximately .75. The results were as follows:

	C_D Wind Tunnel	C_D Reference (a)	Delta
Sphere	.42	.60	+ .18
Cube	.64	.88	+ .24
Bar	.94	1.12	+ .18

As seen in the table, C_D at Mach .75 is about .2 higher than C_D at Mach .1 for all three fragments. Owing to the consistency in the rise of C_D from Mach .1 to Mach .75 for the three regular fragments, it seems reasonable at this time to accept the same rise in C_D for irregular fragments. In this way, the shape of the subsonic drag curve (as a function of Mach Number) for irregular fragments is established.

Experience shows that range is more sensitive to changes in subsonic C_D than to similar changes in supersonic C_D . This can best be seen in Figures 8 and 9. The shape of the transonic and supersonic portions of the drag curves in Figure 8 are approximations based on the study of scattered data in

reference (a) and (b). On the left side of Figure 8, the subsonic C_D is held constant while the supersonic C_D is allowed to vary $\pm .25$ about the mean. The range differences from the mean are both less than 100 feet. On the right side of Figure 8, the supersonic C_D is kept about the same as before and the subsonic C_D is allowed to vary $\pm .25$ about the mean. If subsonic and supersonic C_D were equally sensitive then the new range differences (deltas) should be about twice what they were before. In fact, they are about four times as large.

This range sensitivity can be further explained by the data in Figure 9 where velocity is plotted against range ratio for a typical far-field trajectory. The range ratio is the fraction of the total trajectory traversed. From the figure it can be seen that only 25 percent of the trajectory is supersonic while 75 percent is subsonic. Figures 8 and 9 demonstrate that the subsonic portion of the drag curve affects range much more than the supersonic portion.

Tables A-4, A-5 and A-6 of Appendix A list all of the dimensionless ratios considered to date. When plots of C_D versus the ratios were made, the best correlation was obtained with the ratio A_{MAX}/A_{AVG} ; that is, the ratio of the maximum presented area to the average presented area. This correlation is shown on Figure 10. The value for A_{MAX}/A_{AVG} is an average of the values obtained using the icosahedron gage and the equivalent rectangular parallelepiped calculations. The total range of uncertainty for all irregular fragments is from about 0.5 to 1.5. The range of C_D uncertainty at an average A_{MAX}/A_{AVG} of 1.45 to 1.5 is about 0.6. On average then, it can be said that the correlation reduces the uncertainty by about 40 percent.

It is important to know what a 40 percent reduction in C_D uncertainty means in terms of range uncertainty. Figure 11 shows this range uncertainty for a typical fragment trajectory with a presented area ratio of 1.5. The range differences are large, about 18 percent above the average and 28 percent below. In order to reduce the range uncertainty to an acceptable region of about ± 10 percent, it will be necessary to reduce the C_D uncertainty by about 75 percent.

In summary, the following observations can be made:

1. C_D is a function of shape only.
2. Range is more sensitive to subsonic than to supersonic C_D variations.
3. C_D correlates with dimensionless parameters.
4. The A_{MAX}/A_{AVG} parameter correlation reduces C_D uncertainty by approximately 40 percent.

Significant problems remain unresolved. For an acceptable range uncertainty of about ± 10 percent, it will be necessary to reduce the C_D uncertainty by about 75 percent. This might be done in a variety of ways. More efficient correlation parameters might be established. The typical motion of the fragments in the wind tunnel (Figure A-1 thru A-9 of Appendix A) might be used as an added correlation. Possibly, the use of presented areas

other than average might be used in calculating C_D . For example, in Figure A-3 of Appendix A all fragments exhibit a flat rotation such that the area presented to the air stream is much greater than the average presented area.

Another unresolved problem involves the shape of the transonic and supersonic portions of the drag curve. At present, the shape is only an approximation based on scattered data contained in references (a) and (b). A practical method is needed to test irregular fragments for C_D in a supersonic wind tunnel. The essential problem is the design of a fixture which will allow the fragment to move freely and, at the same time, continually measure drag force.

REFERENCES

a) Air Drag Measurements of Fragments, D. J. Dunn, Jr., and W. R. Porter, BRL Memorandum Report No. 915, D. J. Dunn, Jr., and W. R. Porter, (UNCLASSIFIED, August 1955).

b) Subsonic, Transonic and supersonic Drag Characteristics of Nine Shape Categories of Warhead Fragments, NSWC TR 81-112, Peter Daniels et al., (UNCLASSIFIED, May 1981)

CD - RANGE SENSITIVITY

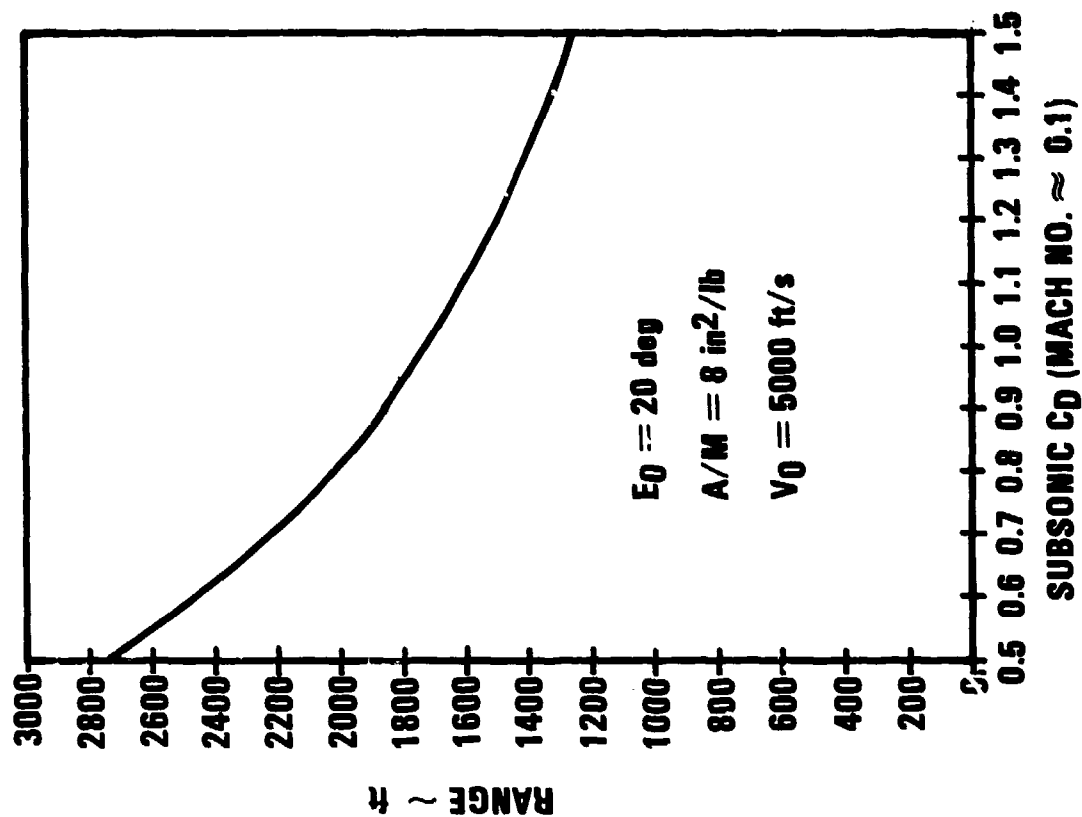
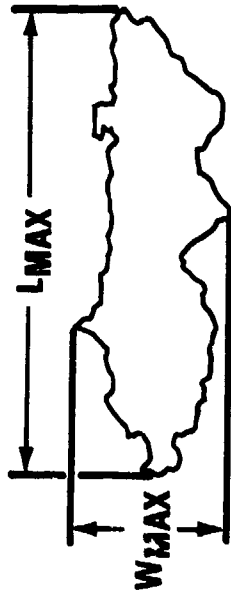


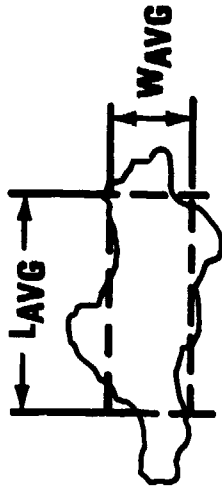
FIGURE 1

FRAGMENT LINEAR DIMENSIONS

MAXIMUMS



AVERAGES



FOR EQUIVALENT WEIGHT AND VOLUME

$$T_{AVG} = \frac{WT}{L_{AVG} \cdot W_{AVG} \cdot \rho}$$

WT = FRAG WEIGHT (lb)

L_{AVG} = AVERAGE LENGTH (in.)

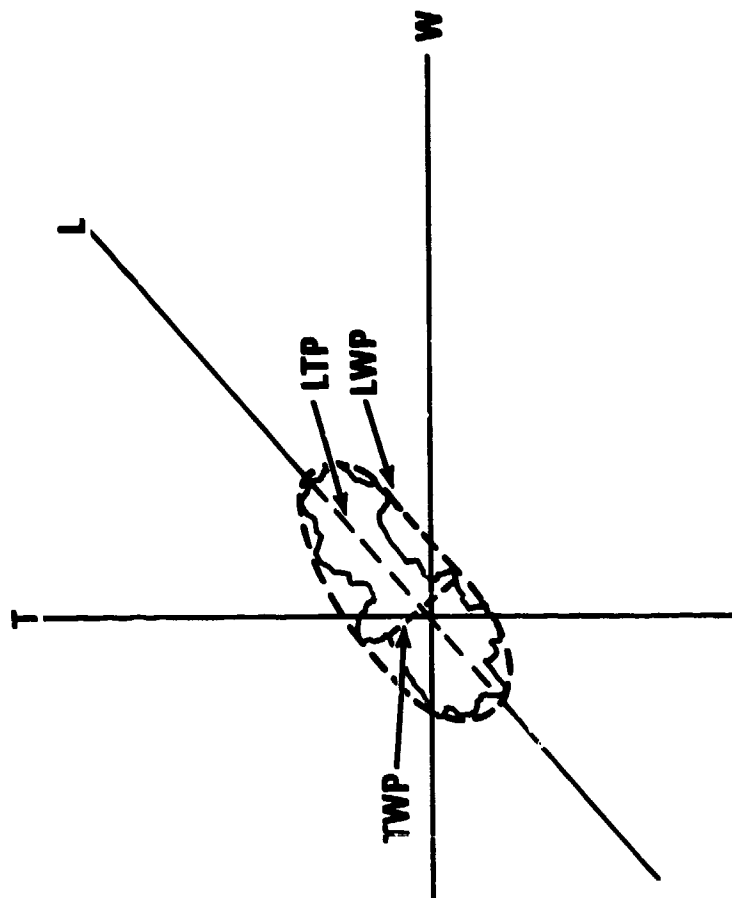
W_{AVG} = AVERAGE WIDTH (in.)

ρ = FRAG DENSITY (lb/in.³)

$\rho = 0.28$ (STEEL)

FIGURE 2

PERIMETER MEASUREMENTS



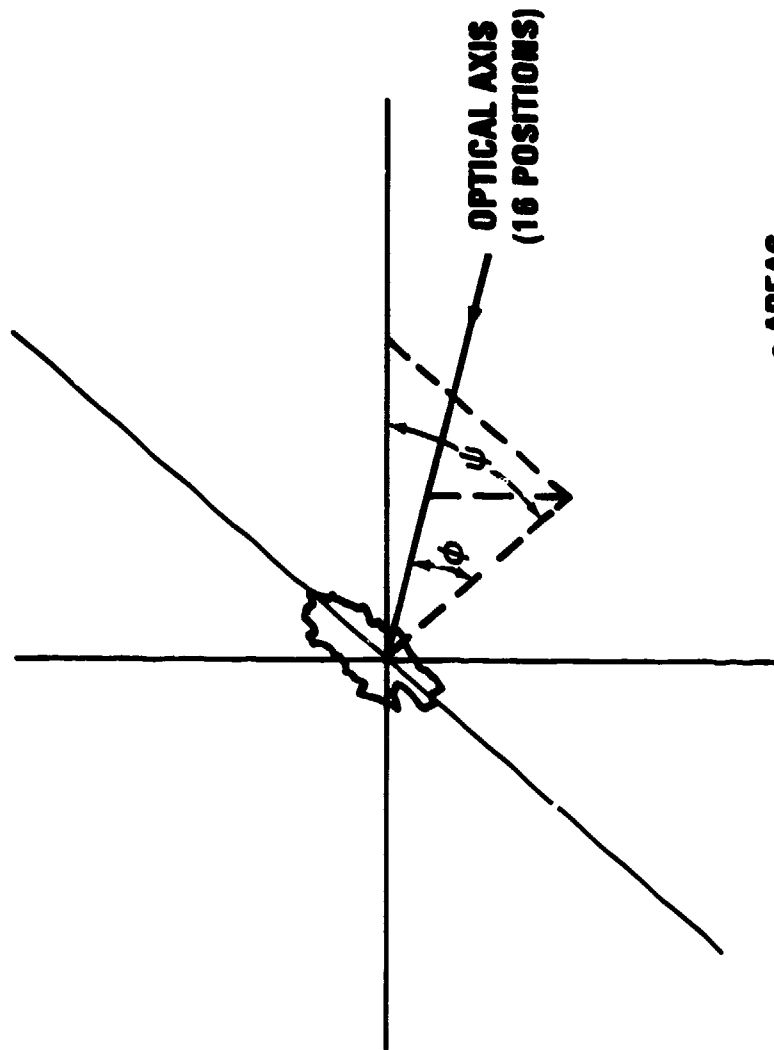
LWP - PERIMETER IN L-W PLANE

LTP - PERIMETER IN L-T PLANE

TWP - PERIMETER IN T-W PLANE

PRESENTED AREA MEASUREMENTS

(ICOSAHEDRON GAGE)

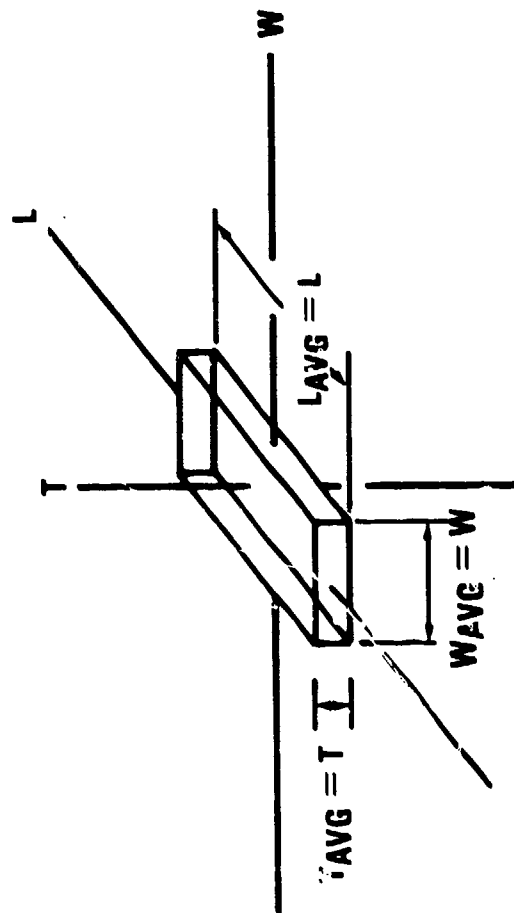


- AREAS
- MINIMUM
- AVERAGE
- MAXIMUM
- VARIANCE
- STANDARD DEVIATION

FIGURE 4

PRESENTED AREA MEASUREMENTS

(EQUIVALENT WEIGHT AND VOLUME RECTANGULAR PARALLELEPIPED)



AREAS

$$\text{MINIMUM} = W \cdot T$$

$$\text{AVERAGE} = 0.5 (L \cdot W + L \cdot T + W \cdot T)$$

$$\text{MAXIMUM} = ((L \cdot W)^2 + (T \cdot L)^2 + (T \cdot W)^2)^{1/2}$$

$$\text{VARIANCE} = 1/12 [(L \cdot T)^2 + (W \cdot T)^2 + (L \cdot W)^2] + [4/3\pi - 1/2] \cdot [L \cdot W \cdot (T)^2 + T \cdot W \cdot (L)^2 + T \cdot L \cdot (W)^2]$$

$$\text{STANDARD DEVIATION} = (\text{VARIANCE})^{1/2}$$

FIGURE 5

SUBSONIC VERTICAL WIND TUNNEL

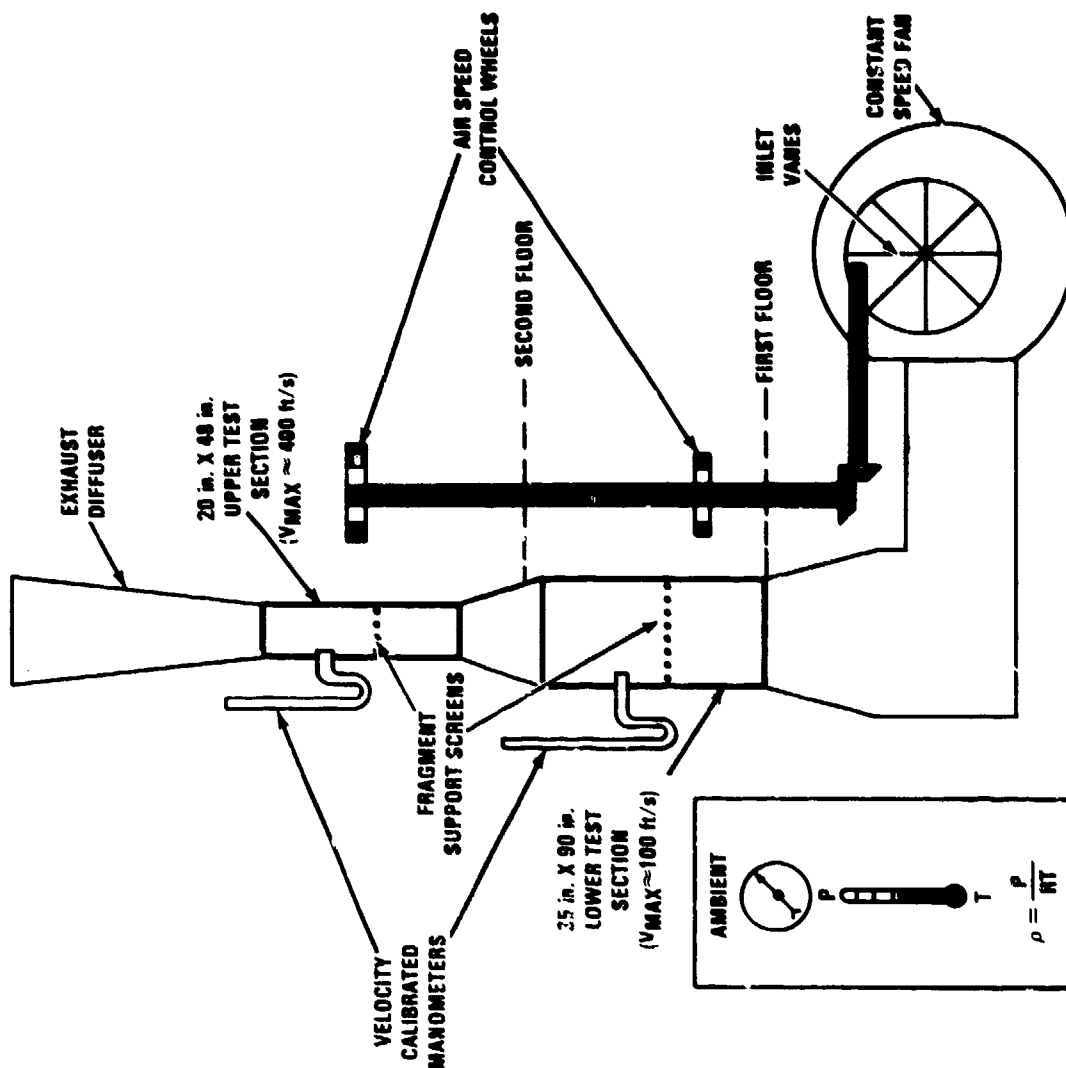
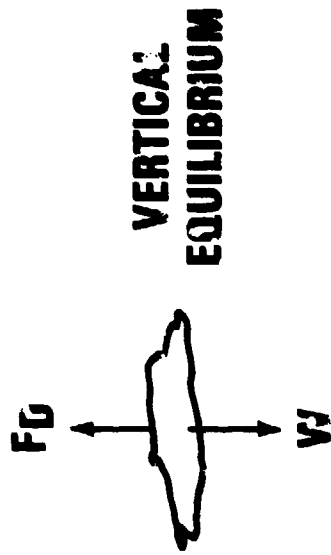


FIGURE 6

EXPERIMENTAL DRAG COEFFICIENT



$$F_D = \text{DRAG FORCE} = \frac{C_D \rho A V^2}{2}$$

$W = \text{FRAG WEIGHT}$

$$F_D = W = \frac{C_D \rho A V^2}{2}$$

$$C_D = \frac{2W}{\rho A V^2}$$

FIGURE 7

DRAG COEFFICIENT SENSITIVITY

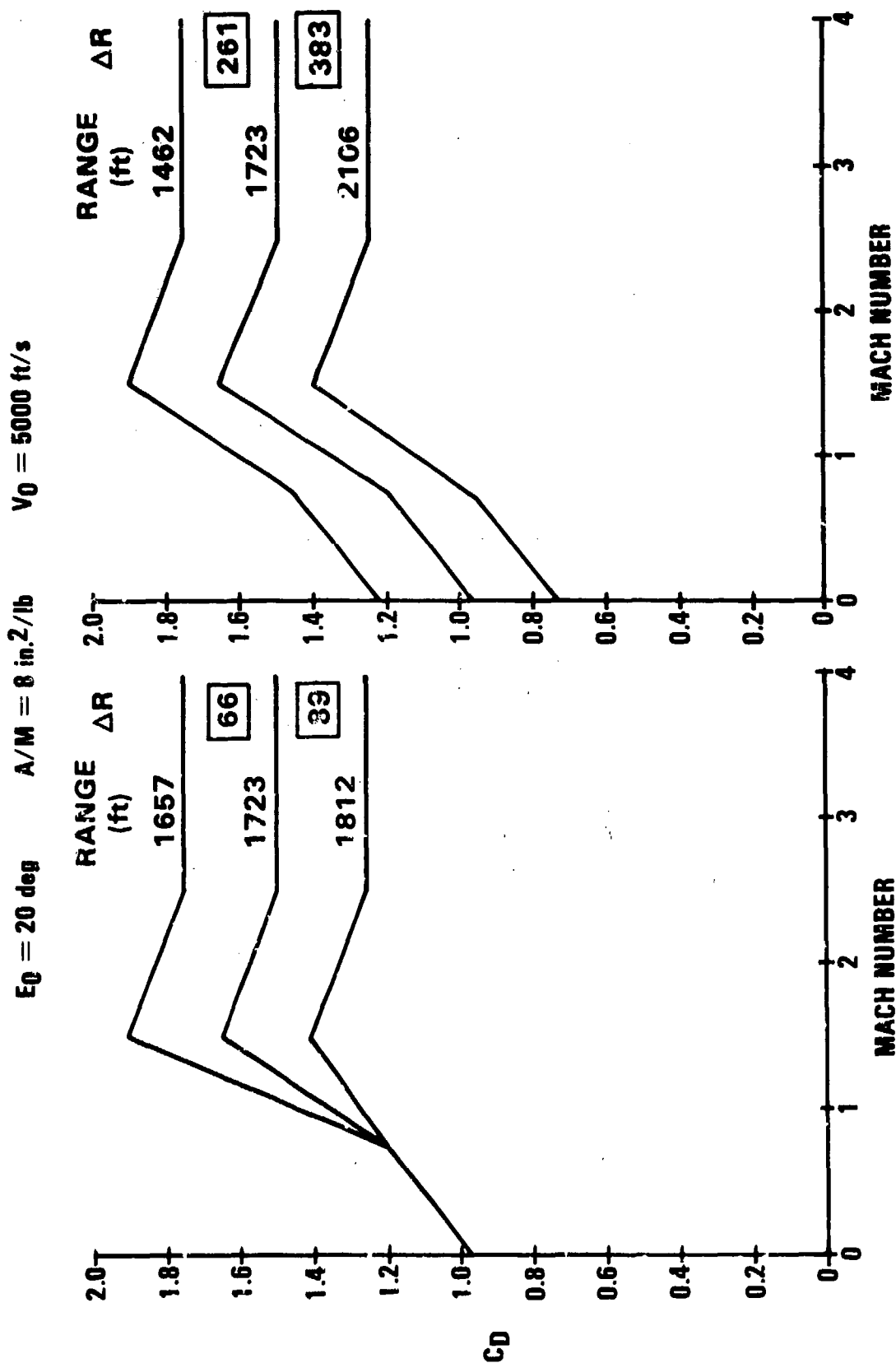


FIGURE 8

VELOCITY VERSUS RANGE RATIO

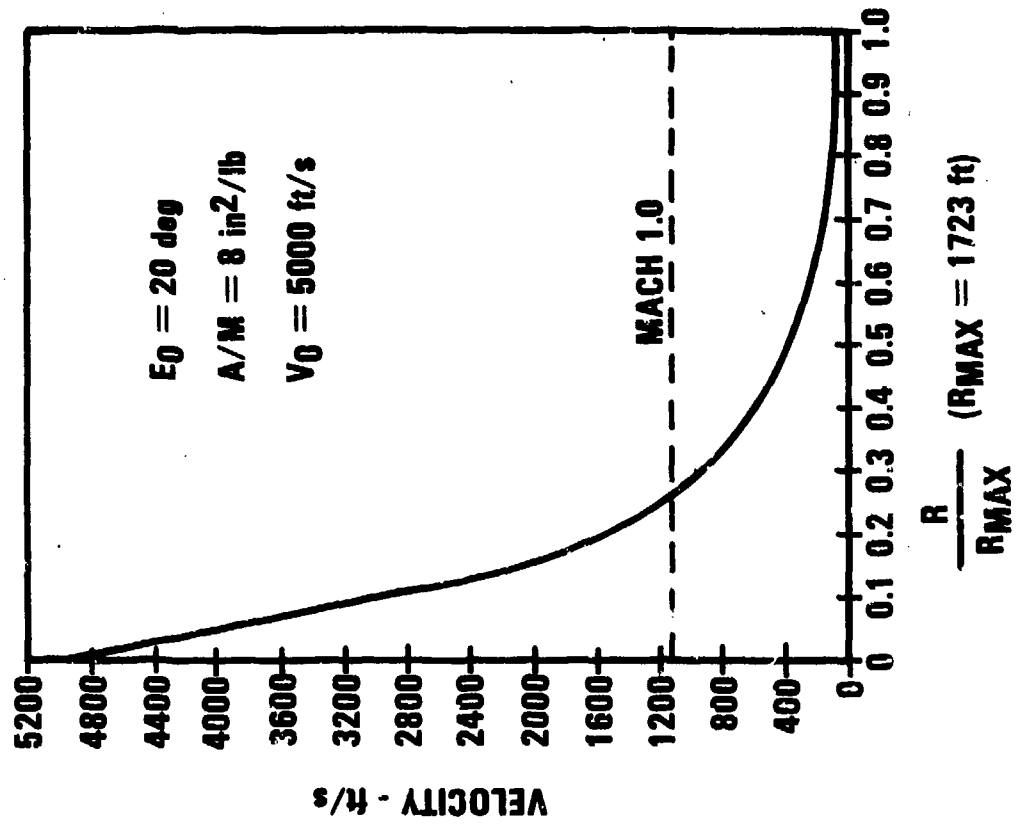


FIGURE 9

DRAG COEFFICIENT (C_D) vs. PRESENTED AREA RATIO (AR)

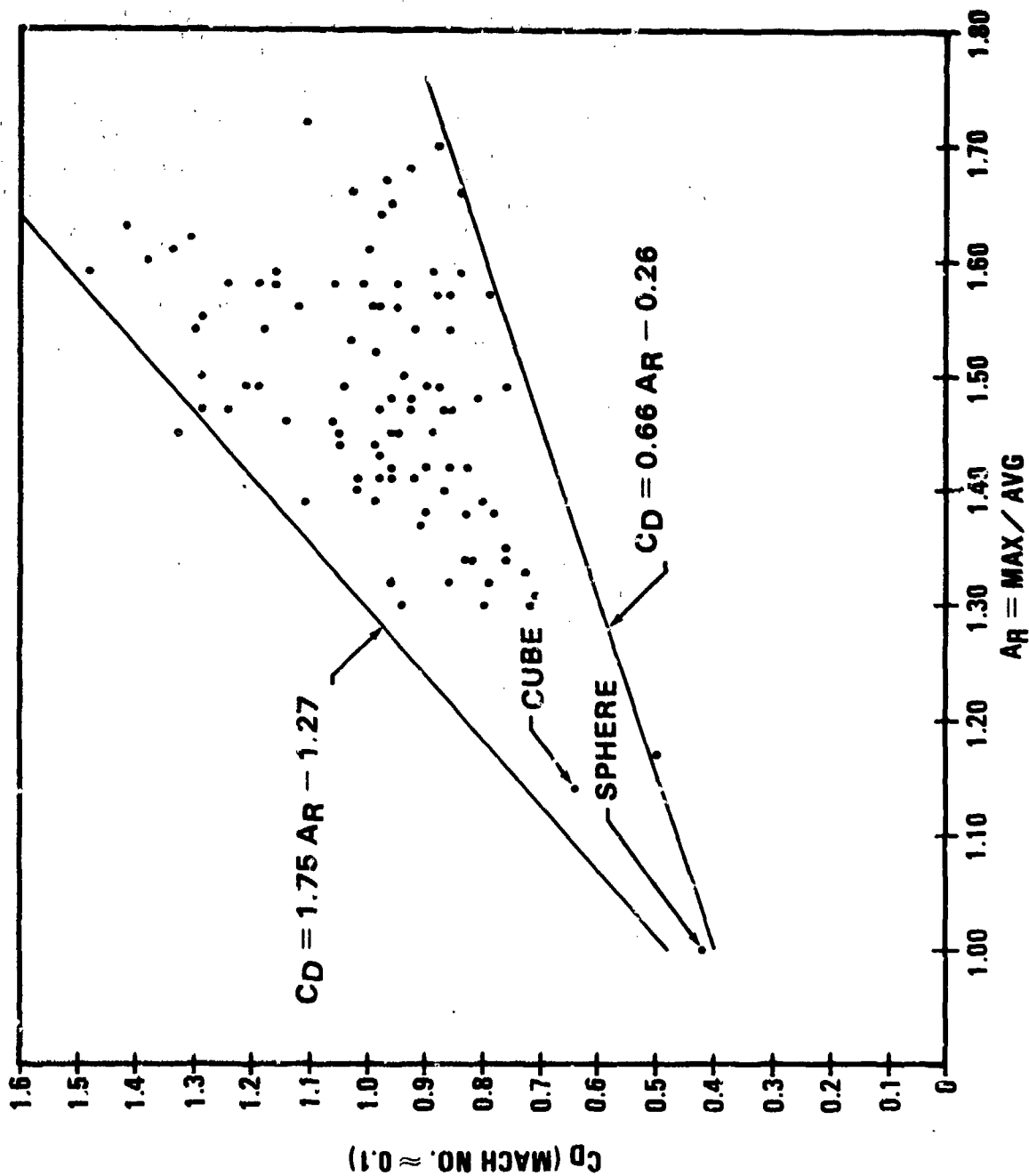


FIGURE 10

CD AND RANGE UNCERTAINTIES

$A_{MAX}/A_{AVG} = 1.5$
 $V_0 = 5000 \text{ ft/s}$
 $E_0 = 20 \text{ deg}$
 $A/M = 8 \text{ in.}^2/\text{lb}$

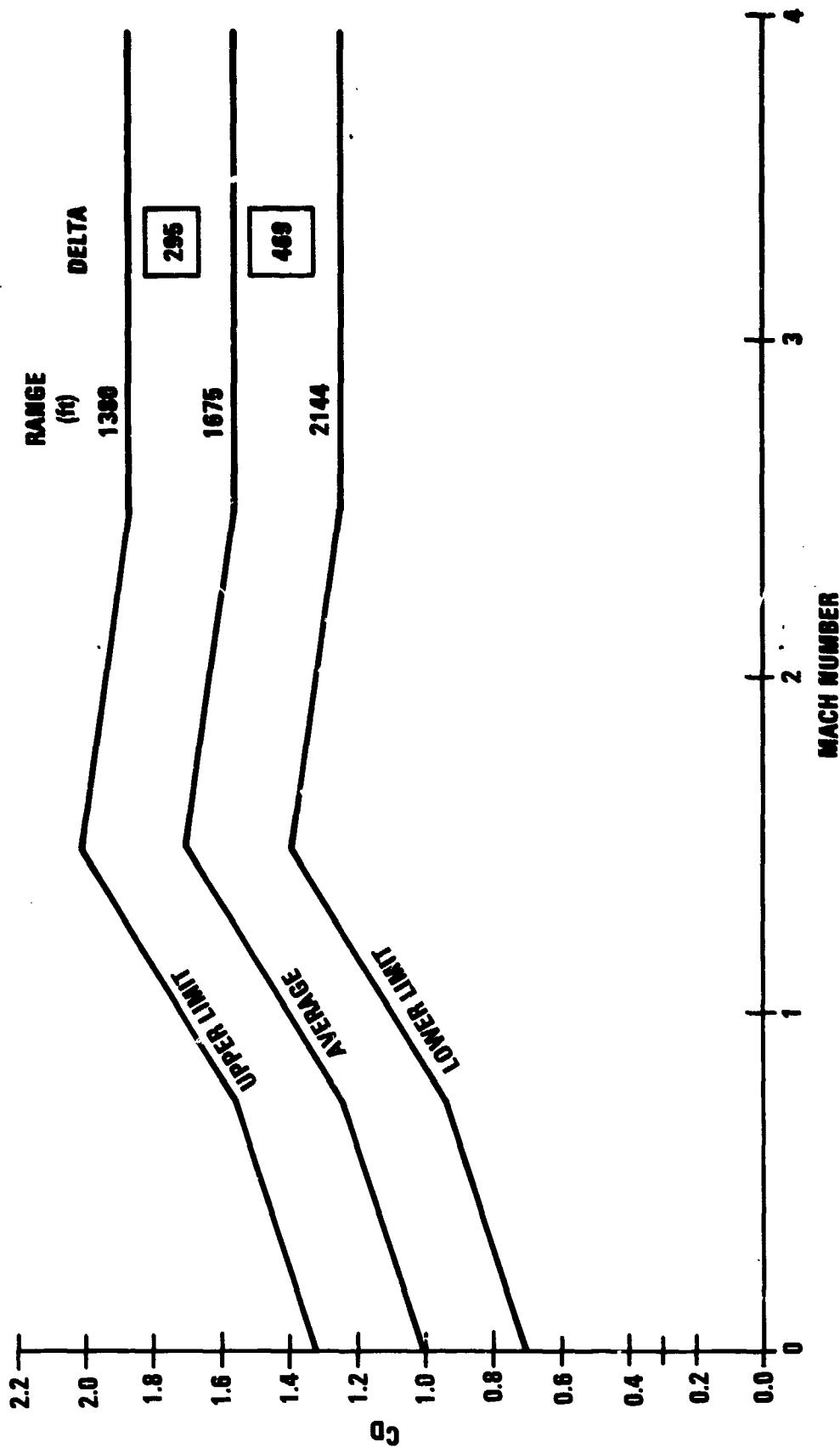


FIGURE 11

APPENDIX A

This Appendix contains 6 Tables and 9 Figures.

Table A-1 contains 16 presented areas measured by the icosahedron gage for the 84 fragments which could be mounted on the gage. Table A-2 presents the linear and perimeter measurements for all 96 fragments. LWP, LTP and TWP are the perimeter measurements in the LW, LT and TW planes, respectively. Table A-2 also contains the subsonic ($M = 0.1$) C_D measured for each fragment in the vertical wind tunnel. Table A-3 contains the presented area measurements for the 96 fragments obtained from the icosahedron gage and calculations using the equivalent rectangular parallelepipeds. Tables A-4, A-5 and A-6 contain the dimensionless ratios which were investigated as correlation parameters for C_D . Note that the fragments have been reordered in ascending C_D to help in the C_D correlation. The old frag number is that designated in Tables A-1, A-2 and A-3.

During the wind tunnel testing, the motion of each fragment was recorded. It was found that the motions could be defined in 9 distinct types. Each figure shows the plan views (L-W plane) of those fragments exhibiting the distinct motion indicated on the figure. Two numbers are given below each fragment. The first is the fragment number contained in Tables A-1, A-2 and A-3. The second number, in parenthesis, is the subsonic C_D measured in the vertical wind tunnel. It was hoped that knowing the shape, motion and C_D might provide an additional method for correlation. Currently, this has not been realized. It is interesting to note that only 35 percent of the fragments tumble randomly. This is at odds with the traditional assumption that all fragments tumble randomly in flight. It is because of the traditional assumption that C_D is calculated using the average presented area.

TABLE A1
PRESENTED AREA (SQ. IN.)
(ICOSAHEDRON GAGE)

FACE	PRESENTED AREA															
NO.	1	2	3	4	5	6	7	8	9	10	11	12	13	14	15	16
1	0.199	0.210	0.274	0.284	0.311	0.323	0.323	0.326	0.340	0.357	0.367	0.397	0.406	0.406	0.400	0.433
2	0.705	0.705	0.705	0.705	0.705	0.705	0.705	0.705	0.705	0.705	0.705	0.705	0.705	0.705	0.705	0.705
3	0.636	0.687	0.805	0.800	0.827	0.854	0.890	0.890	0.890	0.893	0.920	0.932	0.944	0.932	0.976	0.983
4	0.192	0.228	0.236	0.242	0.270	0.280	0.293	0.296	0.306	0.307	0.311	0.330	0.330	0.333	0.330	0.385
5	0.171	0.240	0.245	0.270	0.280	0.290	0.309	0.373	0.393	0.400	0.410	0.443	0.432	0.432	0.536	0.576
6	0.157	0.216	0.220	0.247	0.247	0.256	0.270	0.276	0.304	0.311	0.339	0.361	0.361	0.376	0.376	0.412
7	0.197	0.203	0.237	0.243	0.245	0.256	0.290	0.291	0.309	0.312	0.327	0.366	0.373	0.380	0.399	0.412
8	0.183	0.213	0.247	0.271	0.274	0.291	0.335	0.360	0.367	0.404	0.426	0.473	0.473	0.536	0.551	0.580
9	0.183	0.190	0.203	0.205	0.307	0.313	0.327	0.334	0.337	0.401	0.401	0.401	0.435	0.476	0.476	0.496
10	0.230	0.240	0.262	0.271	0.320	0.340	0.367	0.391	0.430	0.445	0.570	0.573	0.580	0.585	0.622	0.700
11	0.201	0.217	0.257	0.267	0.275	0.280	0.292	0.316	0.337	0.360	0.404	0.407	0.413	0.416	0.434	0.486
12	0.214	0.222	0.226	0.240	0.256	0.270	0.277	0.290	0.336	0.350	0.385	0.385	0.443	0.455	0.484	0.510
13	0.206	0.231	0.239	0.240	0.245	0.260	0.260	0.269	0.280	0.296	0.303	0.310	0.330	0.349	0.353	0.375
14	0.196	0.205	0.270	0.270	0.290	0.290	0.303	0.339	0.347	0.357	0.366	0.374	0.400	0.442	0.445	0.457
15	0.222	0.237	0.266	0.276	0.300	0.303	0.323	0.335	0.337	0.349	0.389	0.396	0.400	0.425	0.442	0.457
16	0.206	0.236	0.329	0.339	0.379	0.383	0.380	0.423	0.423	0.430	0.472	0.492	0.522	0.545	0.561	0.586
17	0.210	0.230	0.295	0.327	0.330	0.337	0.337	0.349	0.359	0.413	0.432	0.454	0.467	0.496	0.505	0.532
18	0.247	0.257	0.294	0.311	0.313	0.316	0.374	0.401	0.404	0.421	0.423	0.423	0.445	0.453	0.475	0.521
19	0.213	0.225	0.252	0.255	0.267	0.300	0.330	0.345	0.340	0.372	0.414	0.443	0.473	0.477	0.480	0.517
20	0.223	0.236	0.343	0.360	0.377	0.399	0.424	0.436	0.443	0.487	0.500	0.519	0.522	0.522	0.544	0.617
21	0.200	0.256	0.300	0.313	0.302	0.391	0.416	0.421	0.462	0.480	0.512	0.539	0.641	0.640	0.660	0.744
22	0.201	0.330	0.362	0.410	0.410	0.434	0.500	0.530	0.577	0.622	0.632	0.641	0.676	0.701	0.704	0.804
23	0.272	0.339	0.341	0.375	0.380	0.412	0.437	0.451	0.469	0.471	0.490	0.500	0.510	0.591	0.590	0.613
24	0.263	0.275	0.275	0.290	0.253	0.400	0.400	0.441	0.444	0.464	0.593	0.603	0.610	0.630	0.640	0.745
25	0.266	0.262	0.407	0.409	0.429	0.451	0.450	0.505	0.500	0.519	0.612	0.637	0.670	0.701	0.704	0.734
26	0.294	0.335	0.307	0.441	0.455	0.470	0.455	0.509	0.539	0.610	0.615	0.615	0.634	0.720	0.749	0.764
27	0.339	0.353	0.424	0.446	0.473	0.505	0.515	0.522	0.530	0.547	0.571	0.640	0.642	0.696	0.740	0.745
28	0.333	0.364	0.421	0.445	0.475	0.477	0.480	0.536	0.535	0.550	0.565	0.614	0.644	0.666	0.697	0.781
29	0.351	0.361	0.390	0.417	0.437	0.480	0.523	0.530	0.542	0.553	0.562	0.572	0.606	0.630	0.670	0.692
30	0.295	0.329	0.340	0.429	0.432	0.454	0.503	0.530	0.537	0.554	0.573	0.581	0.606	0.633	0.669	0.735
31	0.344	0.379	0.393	0.400	0.411	0.410	0.423	0.440	0.477	0.494	0.520	0.551	0.536	0.536	0.540	0.570
32	0.209	0.407	0.501	0.531	0.536	0.546	0.590	0.620	0.639	0.679	0.699	0.699	0.739	0.760	0.792	0.812
33	0.360	0.385	0.400	0.439	0.439	0.450	0.450	0.471	0.470	0.470	0.500	0.510	0.547	0.575	0.591	0.596
34	0.313	0.431	0.496	0.526	0.536	0.565	0.565	0.587	0.594	0.609	0.611	0.697	0.732	0.744	0.822	0.842
35	0.312	0.322	0.410	0.409	0.499	0.590	0.600	0.627	0.716	0.765	0.825	0.854	0.809	0.894	0.907	1.047
36	0.361	0.391	0.393	0.464	0.510	0.545	0.582	0.592	0.599	0.631	0.677	0.697	0.730	0.795	0.809	0.906
37	0.300	0.432	0.444	0.447	0.523	0.572	0.599	0.599	0.621	0.643	0.667	0.709	0.743	0.740	0.812	0.853
38	0.349	0.349	0.371	0.425	0.459	0.501	0.501	0.500	0.569	0.594	0.633	0.653	0.670	0.692	0.721	0.707
39	0.410	0.467	0.477	0.494	0.536	0.587	0.665	0.683	0.734	0.800	0.822	0.864	0.906	0.937	0.962	1.045
40	0.277	0.525	0.544	0.544	0.569	0.571	0.571	0.659	0.689	0.691	0.694	0.694	0.700	0.745	0.750	0.767
41	0.404	0.499	0.501	0.531	0.543	0.540	0.553	0.575	0.580	0.582	0.592	0.631	0.636	0.636	0.663	0.695
42	0.422	0.472	0.496	0.501	0.610	0.639	0.634	0.659	0.659	0.659	0.689	0.700	0.730	0.763	0.772	0.876
43	0.553	0.731	0.760	0.700	0.689	0.920	0.977	1.007	1.056	1.056	1.125	1.125	1.194	1.203	1.312	1.431
44	0.391	0.440	0.506	0.516	0.540	0.540	0.543	0.550	0.570	0.572	0.577	0.594	0.599	0.604	0.624	0.660
45	0.405	0.429	0.481	0.485	0.522	0.535	0.576	0.591	0.591	0.610	0.635	0.635	0.687	0.706	0.721	0.705
46	0.406	0.432	0.469	0.492	0.543	0.543	0.585	0.651	0.670	0.680	0.722	0.724	0.807	0.810	0.820	0.825
47	0.467	0.472	0.536	0.543	0.553	0.580	0.604	0.617	0.622	0.634	0.675	0.715	0.739	0.739	0.795	0.920
48	0.390	0.425	0.477	0.489	0.510	0.531	0.594	0.653	0.712	0.722	0.802	0.832	0.893	0.905	0.917	0.974
49	0.570	0.450	0.472	0.509	0.512	0.540	0.551	0.590	0.646	0.659	0.759	0.776	0.781	0.784	0.864	0.856
50	0.427	0.449	0.510	0.537	0.581	0.589	0.591	0.594	0.633	0.633	0.704	0.719	0.765	0.797	0.799	0.851

TABLE (CONTINUED)
PRESENTED DATA (SQ. IN.)
(ICOMATION GRADE)

NO.	1	2	3	4	5	6	7	8	9	10	11	12	13	14	15	16
21	0.482	0.487	0.490	0.490	0.737	0.737	0.737	0.821	0.821	0.821	0.821	0.821	0.821	0.821	0.821	0.821
22	0.488	0.488	0.488	0.488	0.578	0.578	0.578	0.635	0.635	0.635	0.635	0.635	0.635	0.635	0.635	0.635
23	0.543	0.548	0.557	0.715	0.725	0.725	0.725	0.725	0.725	0.725	0.725	0.725	0.725	0.725	0.725	0.725
24	0.338	0.381	0.535	0.619	0.634	0.653	0.747	0.821	0.821	0.821	0.821	0.821	0.821	0.821	0.821	0.821
25	0.485	0.476	0.533	0.573	0.683	0.742	0.785	0.821	0.821	0.821	0.821	0.821	0.821	0.821	0.821	0.821
26	0.338	0.644	0.684	0.713	0.773	0.882	0.882	0.921	0.921	0.921	0.921	0.921	0.921	0.921	0.921	0.921
27	0.458	0.458	0.582	0.685	0.646	0.676	0.748	0.734	0.778	0.784	0.818	0.888	0.888	0.888	0.888	0.888
28	0.288	0.619	0.619	0.713	0.725	0.738	0.777	0.918	0.948	0.948	0.918	0.884	0.884	0.884	0.884	0.884
29	0.482	0.535	0.535	0.588	0.635	0.728	0.827	0.825	0.885	0.875	0.912	0.912	0.912	0.912	0.912	0.912
30	0.485	0.585	0.588	0.614	0.674	0.688	0.635	0.723	0.742	0.757	0.772	0.882	0.882	0.882	0.882	0.882
31	0.335	0.335	0.684	0.732	0.742	0.821	0.948	0.948	0.948	0.948	0.948	0.948	0.948	0.948	0.948	0.948
32	0.538	0.688	0.732	0.841	0.835	0.861	0.878	0.885	0.935	0.935	0.935	0.935	0.935	0.935	0.935	0.935
33	0.338	0.447	0.713	0.718	0.733	0.882	0.837	0.835	0.945	0.935	0.884	0.888	0.888	0.888	0.888	0.888
34	0.317	0.638	0.635	0.688	0.773	0.783	0.882	0.988	1.197	1.237	1.434	1.537	1.517	1.738	1.884	1.942
35	0.435	0.488	0.618	0.638	0.577	0.637	0.727	0.785	0.785	0.823	0.884	0.938	0.938	0.938	0.938	0.938
36	0.531	0.588	0.535	0.535	0.634	0.733	0.762	0.772	0.782	0.732	0.853	0.888	0.888	0.888	0.888	0.888
37	0.622	0.637	0.735	0.788	0.888	0.834	0.838	0.848	0.888	0.932	1.188	1.288	1.214	1.348	1.253	1.431
38	0.535	0.688	0.619	0.634	0.653	0.733	0.887	0.976	0.835	0.935	0.938	0.884	0.888	0.888	0.888	0.888
39	0.575	0.585	0.737	0.737	0.757	0.835	0.871	0.888	0.978	0.884	0.843	0.883	0.883	0.883	0.883	0.883
40	0.434	0.572	0.687	0.661	0.788	0.788	0.725	0.778	0.788	0.788	0.814	0.833	0.873	0.888	0.985	0.912
41	0.585	0.545	0.732	0.882	0.882	0.978	0.938	0.878	0.878	0.878	0.878	0.878	0.878	0.878	0.878	0.878
42	0.614	0.653	0.678	0.712	0.934	0.938	1.013	1.087	1.338	1.353	1.355	1.685	1.738	1.822	1.938	2.035
43	0.533	0.671	0.788	0.718	0.728	0.853	0.922	1.085	1.031	1.088	1.341	1.331	1.438	1.488	1.488	1.632
44	0.635	0.678	0.788	0.759	0.912	0.912	0.951	0.976	1.038	1.033	1.088	1.188	1.237	1.272	1.335	1.438
45	0.588	0.681	0.834	0.838	0.873	0.883	1.035	1.031	1.138	1.188	1.327	1.375	1.381	1.411	1.411	1.648
46	0.457	0.688	0.748	0.738	0.738	0.882	0.831	0.844	1.217	1.232	1.241	1.488	1.577	1.688	1.735	2.088
47	0.482	0.571	0.837	0.916	1.085	1.025	1.035	1.064	1.133	1.262	1.291	1.311	1.538	1.685	1.745	1.735
48	0.838	0.948	0.977	1.087	1.035	1.135	1.234	1.234	1.385	1.333	1.412	1.388	1.938	1.988	1.747	1.835
49	0.682	0.761	0.888	0.988	0.988	1.117	1.105	1.105	1.195	1.294	1.688	1.638	1.719	1.788	1.788	2.074
50	0.674	0.634	0.961	0.971	1.119	1.158	1.287	1.227	1.267	1.385	1.415	1.464	1.494	1.523	1.563	1.781
51	0.682	0.838	1.045	1.075	1.185	1.125	1.125	1.134	1.174	1.283	1.322	1.342	1.571	1.588	1.548	1.688
52	0.685	0.763	0.913	0.842	0.872	0.837	0.985	1.085	1.088	1.188	1.183	1.281	1.255	1.488	1.583	1.935
53	0.688	0.618	0.776	0.838	0.888	0.988	1.023	1.314	1.343	1.357	1.447	1.624	1.688	1.876	1.985	1.979
54	0.693	0.871	0.838	1.038	1.038	1.157	1.195	1.195	1.374	1.312	1.718	1.729	1.828	1.937	2.045	2.285

TABLE A2
FRAGMENT DATA

FRAG NO.	SIZE	WEIGHT GRAMS	LONG IN.	WIDE IN.	THICK IN.	LONG IN.	WIDE IN.	THICK IN.	LIP IN.	LTP IN.	TIP IN.	CD	
1	1	122.3	1.29	0.29	0.25	1.3	0.3	0.25	3.25	3.19	1.13	0.94	
2	2	103.4	SPALLS				DIAMETER = 1.00 IN.				ALL PERIMETERS = 3.14 IN.		CD = .42
3	3	83.0	0.75	0.75	0.75	0.9	0.9	0.75	3.05	3.05	3.05	0.64	
4	3	102.7	0.95	0.60	0.40	0.9	0.5	0.13	2.30	2.19	1.75	0.54	
5	3	112.3	1.73	0.40	0.21	1.6	0.4	0.00	3.63	3.50	1.25	1.19	
6	3	113.2	1.02	0.05	0.25	1.0	0.5	0.12	2.55	2.13	1.50	1.05	
7	3	113.2	1.01	0.00	0.27	1.0	0.5	0.12	2.00	2.25	1.50	1.05	
8	3	113.7	1.25	0.01	0.21	1.2	0.6	0.00	3.25	2.75	1.75	1.34	
9	3	121.5	1.24	0.50	0.29	1.1	0.5	0.11	3.05	2.00	1.50	0.93	
10	3	121.0	1.40	0.72	0.22	1.2	0.7	0.07	3.44	2.30	1.50	0.97	
11	3	122.6	1.04	0.71	0.27	1.1	0.5	0.12	2.01	2.31	1.50	0.75	
12	3	122.8	0.94	0.73	0.20	0.9	0.0	0.10	2.75	2.00	1.75	0.80	
13	3	132.0	0.83	0.00	0.44	0.7	0.6	0.16	2.31	2.00	1.94	0.83	
14	3	132.9	1.00	0.73	0.33	1.0	0.5	0.14	2.00	2.31	1.94	0.95	
15	3	133.5	1.02	0.75	0.32	0.9	0.6	0.13	2.75	2.30	1.00	0.90	
16	3	134.1	1.74	0.55	0.20	1.7	0.4	0.11	3.00	3.50	1.50	0.95	
17	3	134.5	1.20	0.63	0.32	1.3	0.5	0.12	3.00	2.63	1.50	0.94	
18	3	134.6	1.35	0.71	0.34	1.4	0.4	0.14	3.05	2.75	1.01	0.83	
19	3	161.1	0.90	0.74	0.26	1.0	0.6	0.14	2.01	2.13	1.00	1.21	
20	3	170.2	1.43	0.02	0.37	1.3	0.6	0.12	3.30	2.01	1.01	1.29	
21	3	161.5	1.70	0.74	0.27	1.5	0.6	0.11	3.75	3.30	1.63	1.30	
22	3	203.7	1.04	0.65	0.30	1.5	0.6	0.12	4.00	4.00	1.44	1.10	
23	3	213.0	1.33	0.73	0.30	1.1	0.6	0.17	3.13	2.75	1.00	1.02	
24	3	214.6	1.07	0.50	0.26	1.0	0.0	0.14	3.19	2.30	1.94	1.40	
25	3	235.4	1.51	0.01	0.29	1.5	0.6	0.13	3.55	2.00	1.94	1.30	
26	3	236.4	1.40	0.73	0.41	1.5	0.6	0.14	3.00	3.05	1.75	1.19	
27	3	241.6	1.54	0.83	0.43	1.4	0.6	0.13	3.01	3.44	1.63	0.89	
28	3	244.0	1.30	0.70	0.40	1.3	0.6	0.16	3.50	3.31	2.05	1.33	
29	6	240.7	1.30	0.74	0.30	1.3	0.6	0.16	3.19	3.05	1.63	0.95	
30	3	253.1	1.74	0.77	0.35	1.7	0.5	0.13	3.94	3.63	1.75	1.24	
31	3	252.9	1.05	0.00	0.47	1.1	0.6	0.21	2.00	2.44	2.05	0.95	
32	3	277.4	1.07	0.77	0.46	1.9	0.5	0.13	4.05	3.94	1.94	0.90	
33	6	282.2	1.20	1.00	0.46	1.1	0.6	0.22	2.00	2.44	2.13	0.85	
34	6	291.1	1.49	0.00	0.44	1.4	0.7	0.13	3.94	3.31	2.05	1.29	
35	4	302.0	1.94	0.60	0.32	1.9	0.6	0.14	4.30	4.00	1.01	0.79	
36	4	304.0	1.60	0.00	0.36	1.5	0.7	0.13	3.75	3.44	1.75	1.15	
37	6	303.4	1.50	0.02	0.37	1.4	0.7	0.16	3.75	3.31	1.00	0.95	
38	4	313.1	1.54	0.05	0.30	1.3	0.7	0.10	3.44	3.19	1.01	0.90	
39	4	323.9	1.42	1.13	0.36	1.3	0.5	0.14	4.55	2.01	2.00	0.85	
40	3	325.7	1.55	0.70	0.57	1.4	0.6	0.20	3.44	3.44	1.01	0.82	
41	4	333.2	1.12	1.00	0.00	1.1	0.0	0.19	2.00	2.75	2.00	0.75	
42	6	333.0	1.73	0.65	0.33	1.5	0.6	0.19	4.25	3.94	1.75	0.90	
43	4	332.0	2.71	0.04	0.19	2.6	0.7	0.10	7.25	6.25	1.94	0.95	
44	4	334.0	1.17	0.02	0.74	1.1	0.7	0.23	3.31	3.05	2.25	0.72	
45	4	334.9	1.34	0.95	0.50	1.2	0.7	0.22	3.30	3.05	2.25	0.80	
46	3	337.9	1.33	1.14	0.51	1.3	0.7	0.20	3.01	3.05	2.25	0.83	
47	6	333.2	1.45	0.02	0.63	1.4	0.7	0.19	3.00	3.13	2.31	0.87	
48	3	353.2	1.30	1.23	0.46	1.2	0.9	0.17	4.00	2.00	2.01	1.04	
49	3	370.3	1.50	0.05	0.43	1.3	0.0	0.10	3.50	2.00	2.05	1.14	
50	4	381.0	1.12	0.99	0.62	1.2	0.0	0.20	3.60	2.94	2.55	1.11	

TABLE A2 CONTINUED
FRAGMENT DATA

FRAG NO.	SOURCE	WEIGHT GROSS	LNOM IN.	WNOE IN.	TKNO IN.	LNOM IN.	WNOE IN.	TKNO IN.	LMP IN.	LTP IN.	WTP IN.	CS
31	4	488.3	2.25	0.64	0.31	2.0	0.6	0.17	4.88	4.73	1.88	1.85
32	6	383.3	1.85	1.87	0.48	1.6	0.8	0.15	4.44	3.31	2.31	1.15
33	4	383.1	1.82	0.73	0.32	1.5	0.7	0.19	4.35	4.85	2.13	0.75
34	4	484.6	2.88	1.15	0.27	2.0	0.9	0.11	5.25	4.31	2.58	1.11
35	3	432.7	2.83	0.73	0.42	1.9	0.7	0.17	4.88	4.38	1.88	0.88
36	4	433.9	2.73	0.75	0.37	2.5	0.6	0.15	5.88	5.88	1.81	1.83
37	6	461.7	1.35	0.35	0.47	1.3	0.8	0.23	3.63	3.38	2.13	0.78
38	6	484.8	2.83	0.38	0.32	2.1	0.7	0.15	4.81	4.25	2.25	1.12
39	4	483.2	1.38	1.35	0.33	1.6	1.0	0.15	4.81	3.13	2.34	1.83
40	6	484.1	1.34	0.33	0.61	1.3	0.8	0.24	3.63	3.44	2.38	0.98
41	4	485.7	2.47	1.88	0.37	2.1	0.9	0.13	5.88	5.85	2.31	0.35
42	4	488.3	1.83	0.38	0.38	1.8	0.7	0.28	5.85	4.44	2.81	0.73
43	6	432.9	2.13	1.82	0.39	2.1	0.8	0.15	5.13	4.88	2.88	0.85
44	4	433.1	1.35	1.38	0.38	2.0	1.0	0.13	6.38	3.81	3.25	0.88
45	3	388.8	1.72	0.31	0.41	1.8	0.6	0.24	4.44	3.73	1.34	0.85
46	6	313.6	1.62	1.28	0.38	1.4	1.0	0.19	4.38	3.85	2.81	1.85
47	6	331.9	2.12	1.85	0.48	2.8	0.8	0.17	5.35	4.31	2.38	0.92
48	3	347.9	1.88	1.88	0.42	1.6	0.8	0.22	3.63	3.38	3.44	0.92
49	6	332.2	1.37	1.87	0.42	1.9	0.8	0.19	5.85	4.44	2.25	0.87
70	4	361.2	1.73	0.68	0.67	1.5	0.7	0.27	4.19	4.13	2.85	0.71
71	4	688.4	2.37	0.35	0.33	2.3	0.9	0.15	6.85	5.25	2.13	0.38
72	6	631.7	2.19	1.38	0.38	2.1	1.1	0.14	5.63	4.31	2.73	0.33
73	6	633.4	1.38	1.37	0.44	1.6	1.1	0.19	4.34	3.63	2.34	0.84
74	4	635.8	1.83	1.15	0.65	1.9	0.8	0.22	4.63	4.88	3.88	0.85
75	6	688.3	2.31	1.87	0.44	2.1	0.8	0.28	5.35	5.85	2.68	0.99
76	3	713.9	2.12	1.24	0.38	1.8	1.0	0.28	5.85	4.31	3.88	0.84
77	6	713.1	2.61	0.33	0.38	2.6	0.8	0.18	6.88	5.85	2.19	1.23
78	4	767.8	2.83	1.15	0.33	2.8	0.7	0.28	7.44	6.13	2.88	0.38
79	6	775.7	2.33	1.27	0.45	2.3	1.8	0.17	7.13	5.85	2.68	1.31
80	4	777.8	2.83	0.85	0.38	2.8	0.7	0.28	6.63	6.85	2.19	0.35
81	6	782.2	2.43	0.37	0.43	2.4	0.8	0.21	5.63	5.63	2.13	0.99
82	4	884.8	1.68	1.49	0.38	1.6	1.1	0.23	4.88	3.35	3.44	0.81
83	6	833.7	1.75	1.38	0.48	1.6	1.4	0.19	5.68	3.68	3.38	0.89
84	6	855.3	2.38	1.87	0.43	3.8	0.9	0.15	7.88	5.81	2.31	1.88
85	4	1617.7	3.23	1.27	0.35	2.7	1.1	0.28	7.81	6.73	2.81	0.33
86	6	1638.8	3.37	1.35	0.45	3.3	1.2	0.21	8.81	6.73	4.19	1.24
87	4	1738.4	3.33	2.85	0.65	3.3	1.2	0.23	8.88	6.35	3.68	0.38
88	6	1973.2	3.32	1.85	0.49	3.8	1.2	0.22	9.31	8.88	3.81	0.35
89	4	2883.7	2.38	1.49	0.37	2.5	0.9	0.45	5.73	5.68	3.88	0.78
90	6	2885.2	2.71	2.88	0.73	2.4	1.8	0.43	6.19	5.81	3.35	0.73
91	6	2833.6	3.38	1.84	0.45	3.8	1.4	0.23	8.88	6.23	3.88	4.99
92	4	2763.3	4.38	2.68	0.37	4.3	1.5	0.22	12.23	8.88	5.35	1.42
93	6	3148.8	4.38	1.38	0.45	4.1	1.5	0.25	13.85	18.88	3.31	1.81
94	4	3278.2	3.17	1.88	0.74	2.9	1.4	0.41	8.35	6.81	4.68	1.82
95	7	13333.1	3.17	2.81	2.33	3.1	2.8	1.28	9.63	8.88	8.19	0.38
96	7	23413.5	4.38	3.77	1.73	4.2	3.4	0.84	13.63	9.81	8.63	0.33

SOURCE CODE

1 - BAR (1/4 X 1/4 X 1 1/4)
2 - 1.88 IN. DIAMETER SPHERE
3 - .75 IN. PER SIDE CUBE
4 - 155MM M107 PROJECTILE

5 - 76MM MK 165 PROJECTILE
6 - MK 84 LOW DRAG BOMB
7 - MK 82 LOW DRAG BOMB

TABLE A3
ICOSAHEDRON VS CALCULATED AREAS

FRAG NO.	MIN AREA		MAX AREA		AVG AREA		STD DEV		VARIANCE	
	ICOS	CALC	ICOS	CALC	ICOS	CALC	ICOS	CALC	ICOS	CALC
1	0.20	0.07	0.43	0.50	0.34	0.30	0.07	0.09	0.005	0.000
2	0.79	0.79	0.79	0.79	0.70	0.79	0.00	0.00	0.000	0.000
3	0.64	0.50	0.90	1.00	0.07	0.07	0.10	0.09	0.009	0.000
4	0.19	0.06	0.37	0.47	0.30	0.31	0.05	0.11	0.003	0.012
5	0.17	0.04	0.50	0.66	0.37	0.41	0.11	0.16	0.013	0.027
6	0.16	0.06	0.41	0.52	0.30	0.34	0.07	0.12	0.005	0.015
7	0.20	0.06	0.41	0.52	0.30	0.34	0.07	0.12	0.005	0.015
8	0.10	0.05	0.50	0.73	0.37	0.44	0.12	0.19	0.015	0.036
9	0.10	0.06	0.50	0.57	0.35	0.37	0.09	0.14	0.009	0.019
10	0.23	0.03	0.70	0.05	0.43	0.49	0.15	0.22	0.023	0.050
11	0.20	0.06	0.49	0.57	0.34	0.37	0.00	0.14	0.007	0.010
12	0.21	0.00	0.51	0.65	0.33	0.40	0.10	0.16	0.010	0.027
13	0.21	0.10	0.36	0.44	0.20	0.31	0.05	0.10	0.002	0.009
14	0.19	0.07	0.46	0.52	0.34	0.35	0.07	0.12	0.006	0.014
15	0.22	0.00	0.46	0.56	0.34	0.37	0.07	0.13	0.005	0.017
16	0.21	0.05	0.57	0.71	0.42	0.46	0.11	0.17	0.011	0.029
17	0.21	0.06	0.55	0.67	0.30	0.43	0.10	0.16	0.009	0.026
18	0.25	0.06	0.52	0.60	0.30	0.41	0.00	0.13	0.007	0.010
19	0.21	0.00	0.52	0.62	0.36	0.41	0.10	0.15	0.010	0.021
20	0.22	0.07	0.62	0.00	0.44	0.50	0.10	0.20	0.010	0.039
21	0.20	0.06	0.74	0.92	0.40	0.56	0.16	0.23	0.026	0.054
22	0.20	0.07	0.00	0.92	0.55	0.57	0.16	0.23	0.025	0.053
23	0.27	0.10	0.61	0.69	0.45	0.47	0.10	0.16	0.010	0.024
24	0.27	0.11	0.75	0.02	0.46	0.52	0.16	0.20	0.025	0.040
25	0.26	0.03	0.79	0.93	0.53	0.59	0.17	0.23	0.029	0.051
26	0.29	0.00	0.76	0.93	0.54	0.59	0.14	0.23	0.020	0.051
27	0.34	0.09	0.75	0.07	0.54	0.57	0.12	0.21	0.015	0.043
28	0.33	0.10	0.75	0.01	0.54	0.54	0.12	0.19	0.014	0.036
29	0.35	0.10	0.69	0.01	0.52	0.54	0.11	0.19	0.011	0.035
30	0.30	0.00	0.74	0.09	0.51	0.59	0.12	0.21	0.016	0.043
31	0.34	0.12	0.57	0.71	0.46	0.51	0.07	0.15	0.005	0.022
32	0.29	0.07	0.01	0.99	0.62	0.65	0.14	0.23	0.019	0.055
33	0.36	0.13	0.60	0.71	0.40	0.51	0.07	0.15	0.005	0.022
34	0.31	0.11	0.04	1.01	0.61	0.65	0.14	0.24	0.010	0.059
35	0.31	0.00	1.05	1.17	0.60	0.74	0.23	0.29	0.053	0.004
36	0.36	0.10	0.99	1.00	0.62	0.69	0.10	0.26	0.031	0.063
37	0.30	0.11	0.05	1.01	0.61	0.66	0.15	0.24	0.023	0.050
38	0.35	0.12	0.79	0.95	0.55	0.63	0.14	0.22	0.019	0.040
39	0.42	0.13	1.05	1.19	0.71	0.74	0.20	0.30	0.040	0.009
40	0.20	0.12	0.77	0.09	0.62	0.62	0.12	0.20	0.015	0.039
41	0.40	0.15	0.70	0.92	0.50	0.62	0.06	0.21	0.004	0.043
42	0.42	0.11	0.00	0.95	0.65	0.65	0.12	0.21	0.015	0.046
43	0.55	0.07	1.43	1.04	1.02	1.07	0.24	0.49	0.056	0.236
44	0.39	0.16	0.66	0.03	0.55	0.60	0.07	0.17	0.004	0.029
45	0.41	0.15	0.70	0.09	0.59	0.62	0.11	0.19	0.012	0.037
46	0.41	0.14	0.03	0.96	0.64	0.66	0.14	0.21	0.020	0.046
47	0.47	0.13	0.02	1.02	0.63	0.69	0.11	0.24	0.012	0.055
48	0.40	0.15	0.97	1.11	0.60	0.72	0.19	0.27	0.037	0.071
49	0.37	0.15	0.90	1.00	0.64	0.71	0.16	0.25	0.025	0.064
50	0.43	0.16	0.03	1.00	0.64	0.60	0.12	0.23	0.015	0.052

TABLE A3 (CONTINUED)
ICOSAHEDRON VS CALCULATED AREAS

FRAG NO.	MIN AREA		MAX AREA		AVG AREA		STD DEV		VARIANCE	
	ICOS	CALC	ICOS	CALC	ICOS	CALC	ICOS	CALC	ICOS	CALC
51	0.48	0.10	1.05	1.25	0.78	0.82	0.19	0.30	0.037	0.000
52	0.41	0.13	1.20	1.31	0.77	0.83	0.26	0.32	0.060	0.104
53	0.54	0.13	0.90	1.10	0.75	0.74	0.11	0.25	0.012	0.004
54	0.34	0.10	1.67	1.82	0.96	1.07	0.41	0.48	0.169	0.220
55	0.45	0.12	1.20	1.37	0.85	0.80	0.23	0.33	0.051	0.111
56	0.36	0.09	1.39	1.55	0.93	0.95	0.27	0.30	0.072	0.144
57	0.46	0.10	0.96	1.10	0.73	0.76	0.15	0.24	0.022	0.050
58	0.29	0.11	1.34	1.51	0.87	0.96	0.26	0.37	0.069	0.138
59	0.45	0.15	1.55	1.63	0.92	1.06	0.35	0.41	0.121	0.169
60	0.49	0.19	0.97	1.10	0.73	0.77	0.14	0.24	0.020	0.057
61	0.53	0.12	1.66	1.91	1.03	1.14	0.36	0.50	0.131	0.246
62	0.64	0.14	0.99	1.32	0.86	0.80	0.10	0.31	0.010	0.094
63	0.40	0.12	1.39	1.71	0.93	1.06	0.30	0.43	0.089	0.187
64	0.52	0.13	1.94	2.02	1.15	1.19	0.47	0.53	0.225	0.260
65	0.45	0.14	1.13	1.17	0.79	0.83	0.20	0.25	0.040	0.063
66	0.53	0.19	1.36	1.44	0.85	0.93	0.26	0.35	0.067	0.120
67	0.62	0.14	1.45	1.64	0.97	1.04	0.25	0.40	0.064	0.164
68	0.59	0.17	1.14	1.34	0.86	0.90	0.20	0.31	0.039	0.094
69	0.57	0.15	1.20	1.57	0.92	1.01	0.21	0.30	0.044	0.143
70	0.43	0.19	0.91	1.14	0.75	0.82	0.13	0.24	0.010	0.035
71	0.51	0.13	1.00	2.10	1.15	1.27	0.42	0.54	0.174	0.290
72	0.61	0.16	2.09	2.34	1.26	1.39	0.49	0.61	0.242	0.370
73	0.52	0.21	1.69	1.80	1.06	1.14	0.36	0.44	0.127	0.196
74	0.64	0.10	1.44	1.59	1.01	1.06	0.24	0.37	0.059	0.136
75	0.51	0.16	1.65	1.74	1.10	1.13	0.31	0.42	0.097	0.173
76	0.47	0.20	2.00	1.85	1.14	1.10	0.44	0.45	0.196	0.202
77	0.48	0.14	1.76	2.13	1.17	1.34	0.30	0.53	0.147	0.201
78	0.84	0.14	1.86	2.04	1.29	1.33	0.30	0.49	0.000	0.230
79	0.60	0.17	2.07	2.34	1.30	1.43	0.42	0.59	0.175	0.352
80	0.67	0.14	1.70	2.05	1.24	1.33	0.30	0.49	0.090	0.230
81	0.60	0.17	1.61	1.99	1.20	1.29	0.26	0.40	0.067	0.227
82	0.69	0.26	1.55	1.82	1.00	1.19	0.20	0.43	0.070	0.104
83	0.61	0.27	1.90	2.20	1.27	1.40	0.46	0.57	0.216	0.329
84	0.60	0.15	2.20	2.75	1.41	1.67	0.46	0.70	0.210	0.494
85		0.31		3.00		2.01		0.73		0.535
86		0.26		4.03		2.45		1.03		1.053
87		0.20		4.04		2.50		1.02		1.034
88		0.26		4.64		2.83		1.10		1.400
89		0.41		2.55		1.90		0.50		0.245
90		0.43		2.64		1.93		0.54		0.286
91		0.35		4.20		2.64		1.00		1.161
92		0.33		6.53		3.06		1.71		2.900
93		0.39		6.25		3.01		1.60		2.549
94		0.50		4.27		2.92		0.96		0.925
95		2.57		7.00		6.37		1.11		1.232
96		2.04		14.90		10.32		3.33		11.070

EXPLANATION OF COLUMN HEADINGS

MIN AREA - MINIMUM PRESENTED AREA (SQ. IN.)
 MAX AREA - MAXIMUM PRESENTED AREA (SQ. IN.)
 AVG AREA - AVERAGE PRESENTED AREA (SQ. IN.)
 STD DEV - STANDARD DEVIATION OF PRESENTED AREA (SQ. IN.)
 VARIANCE - VARIANCE OF PRESENTED AREA (IN. 4TH)
 ICOS - AREAS CALCULATED FROM ICOSAHEDRON GAGE DATA
 CALC - AREAS CALCULATED FROM APPROXIMATING RECTANGULAR PARALLELEPIPEDS

TABLE A4
PRESENTED AREA RATIOS

FRAG NO.		CD	MAX / MIN		MAX / AVG		AVG / MIN	
NEW	OLD		ICOS	CALC	ICOS	CALC	ICOS	CALC
1	2	0.42	1.00	1.00	1.00	1.00	1.00	1.00
2	95	0.50		3.04		1.22		2.48
3	3	0.64	1.54	1.73	1.13	1.15	1.36	1.50
4	70	0.71	2.10	5.59	1.22	1.39	1.73	4.32
5	44	0.72	1.69	5.05	1.20	1.39	1.41	3.63
6	62	0.73	1.56	9.49	1.16	1.50	1.34	6.33
7	53	0.76	1.65	8.16	1.20	1.49	1.38	5.48
8	41	0.76	1.44	5.94	1.20	1.47	1.19	4.03
9	11	0.76	2.42	3.53	1.45	1.53	1.67	6.21
10	57	0.79	2.10	6.05	1.31	1.45	1.60	4.18
11	35	0.79	3.36	14.41	1.55	1.58	2.17	9.09
12	90	0.79		6.20		1.37		4.51
13	45	0.80	1.95	5.91	1.34	1.43	1.46	4.14
14	89	0.80		6.24		1.35		4.64
15	82	0.81	2.27	7.08	1.43	1.52	1.58	4.66
16	40	0.82	2.77	7.52	1.23	1.44	2.25	5.21
17	13	0.83	1.72	4.67	1.26	1.42	1.37	3.29
18	46	0.83	2.03	6.81	1.29	1.46	1.57	4.67
19	18	0.83	2.11	10.35	1.37	1.46	1.54	7.09
20	73	0.84	3.24	8.60	1.59	1.58	2.03	5.44
21	76	0.84	4.28	9.13	1.75	1.56	2.44	5.85
22	63	0.86	3.50	14.36	1.51	1.62	2.33	8.86
23	33	0.86	1.66	5.49	1.24	1.39	1.33	3.96
24	74	0.86	2.27	9.01	1.43	1.52	1.59	6.00
25	39	0.86	2.50	9.37	1.47	1.61	1.70	5.82
26	65	0.86	2.49	8.18	1.42	1.42	1.75	5.77
27	47	0.87	1.76	7.81	1.30	1.49	1.35	5.24
28	69	0.87	2.27	10.50	1.39	1.55	1.63	6.78
29	55	0.88	2.63	11.81	1.42	1.56	1.86	7.58
30	64	0.88	3.76	15.99	1.62	1.70	2.22	9.42
31	12	0.88	2.38	7.92	1.52	1.62	1.56	4.90
32	27	0.89	2.20	9.87	1.37	1.53	1.60	6.44
33	83	0.89	3.25	8.56	1.56	1.62	2.08	5.28
34	78	0.90	2.21	14.62	1.43	1.54	1.54	9.51
35	32	0.90	2.81	13.35	1.31	1.52	2.15	8.78
36	60	0.90	1.99	5.80	1.32	1.43	1.58	4.05
37	4	0.91	1.90	7.46	1.23	1.50	1.54	4.99
38	67	0.92	2.33	12.10	1.50	1.58	1.56	7.65
39	68	0.92	1.94	7.66	1.33	1.48	1.47	5.16
40	85	0.93		10.07		1.53		6.59
41	72	0.93	3.41	14.75	1.66	1.69	2.05	8.75
42	9	0.93	2.71	10.05	1.41	1.55	1.93	6.48
43	1	0.94	2.19	6.92	1.29	1.30	1.70	5.33
44	17	0.94	2.63	11.01	1.45	1.55	1.82	7.13
45	68	0.95		17.53		1.64		10.69
46	43	0.95	2.79	26.57	1.41	1.71	1.84	15.50
47	16	0.95	2.75	15.71	1.35	1.54	2.04	10.17
48	80	0.96	2.52	14.44	1.37	1.53	1.84	9.42
49	31	0.96	1.66	5.69	1.23	1.40	1.35	4.06
50	25	0.96	1.97	8.34	1.33	1.49	1.48	5.58

TABLE A4 (CONTINUED)
PRESENTED AREA RATIOS

FRAG NO.			MAX / MIN		MAX / AVG		AVG / MIN	
NEW	OLD	CD	ICOS	CALC	ICOS	CALC	ICOS	CALC
51	37	0.96	2.84	8.97	1.41	1.54	2.82	5.85
52	61	0.96	3.16	16.18	1.61	1.68	1.96	9.66
53	14	0.96	2.41	7.71	1.34	1.49	1.79	5.19
54	18	0.97	3.84	16.34	1.61	1.73	1.89	9.47
55	87	0.98		14.53		1.62		8.99
56	71	0.98	3.71	15.58	1.63	1.65	2.28	9.45
57	15	0.98	2.86	7.26	1.34	1.52	1.54	4.76
58	38	0.98	2.26	7.70	1.43	1.58	1.57	5.13
59	42	0.98	2.78	8.33	1.36	1.46	1.53	5.69
60	75	0.99	3.24	18.72	1.58	1.53	2.17	6.38
61	96	0.99		5.27		1.45		3.63
62	91	0.99		12.36		1.62		7.64
63	81	0.99	2.67	11.97	1.34	1.54	2.88	7.77
64	84	1.00	3.23	18.65	1.57	1.65	2.86	11.33
65	93	1.01		15.97		1.64		9.72
66	94	1.02		7.41		1.46		5.86
67	23	1.02	2.25	6.98	1.35	1.47	1.67	4.74
68	59	1.03	3.43	18.55	1.68	1.63	2.84	6.49
69	56	1.03	3.87	16.68	1.48	1.57	2.61	10.64
70	48	1.04	2.45	7.25	1.44	1.54	1.70	4.69
71	51	1.05	2.62	12.55	1.35	1.53	1.95	8.19
72	7	1.05	2.89	8.88	1.36	1.55	1.54	5.75
73	6	1.06	2.62	8.94	1.39	1.53	1.89	5.83
74	66	1.06	2.56	7.59	1.61	1.55	1.59	4.98
75	58	1.11	1.95	6.18	1.31	1.47	1.49	4.21
76	54	1.11	4.94	17.61	1.74	1.78	2.84	18.33
77	58	1.12	4.65	13.48	1.54	1.57	3.83	8.51
78	49	1.14	2.42	7.41	1.41	1.51	1.72	4.89
79	36	1.16	2.73	18.48	1.68	1.57	1.78	6.64
80	52	1.16	2.95	18.45	1.57	1.58	1.88	6.68
81	22	1.18	2.86	13.27	1.47	1.61	1.95	8.24
82	5	1.19	3.37	18.34	1.55	1.68	2.17	11.44
83	26	1.19	2.68	11.38	1.41	1.56	1.84	7.28
84	19	1.21	2.43	7.55	1.45	1.52	1.68	4.98
85	86	1.24		15.79		1.64		9.63
86	38	1.24	2.49	11.65	1.43	1.58	1.74	7.75
87	77	1.29	3.64	15.13	1.51	1.59	2.42	9.58
88	34	1.29	2.69	9.58	1.38	1.55	1.94	6.12
89	28	1.29	2.77	11.41	1.41	1.59	1.97	7.16
90	25	1.38	3.85	11.51	1.58	1.57	2.84	7.35
91	79	1.31	3.84	13.58	1.68	1.63	1.98	8.32
92	28	1.33	2.26	8.46	1.48	1.58	1.61	5.64
93	8	1.34	3.17	14.32	1.55	1.67	2.85	8.57
94	21	1.38	3.72	14.29	1.56	1.63	2.38	8.77
95	92	1.42		19.91		1.69		11.77
96	24	1.48	2.81	7.48	1.61	1.57	1.74	4.78

ICOS - PRESENTED AREA RATIOS CALCULATED FROM ICOSAHEDRON GAGE DATA
CALC - PRESENTED AREA RATIOS CALCULATED FROM APPROXIMATING RECTANGULAR PARALLELE
PIPEDS

TABLE A5
LINEAR AND STATISTICAL RATIOS

FRAG NEW	NO. OLD	CD	L/T	W/T	L'/T'	W'/T'	SD / ICOS	PAVG CALC	VAR / ICOS	PAVG+2 CALC
1	2	0.42	(SPHERE)							
2	95	0.50	2.42	1.56	1.74	1.33		0.17		0.03
3	3	0.64	1.00	1.60	1.00	1.00	0.11	0.10	0.01	0.01
4	70	0.71	5.50	2.57	3.43	1.46	0.10	0.29	0.03	0.10
5	44	0.72	4.69	2.90	2.33	1.56	0.12	0.29	0.01	0.14
6	62	0.73	9.03	3.53	4.61	2.03	0.11	0.35	0.01	0.14
7	53	0.76	7.81	3.65	4.38	2.04	0.15	0.34	0.02	0.16
8	41	0.76	5.69	4.14	2.24	1.90	0.11	0.33	0.01	0.10
9	11	0.76	9.22	4.19	5.90	3.11	0.25	0.37	0.06	0.36
10	57	0.76	5.74	3.53	4.11	2.53	0.20	0.32	0.04	0.13
11	35	0.79	14.02	4.43	8.36	2.81	0.34	0.39	0.12	0.21
12	90	0.79	5.63	2.34	4.42	2.66		0.20		0.00
13	45	0.80	5.57	3.25	3.55	2.31	0.18	0.31	0.03	0.15
14	89	0.80	5.50	1.98	3.57	1.60		0.26		0.07
15	82	0.81	6.86	4.71	4.03	3.18	0.26	0.36	0.07	0.11
16	40	0.82	7.00	3.03	3.86	1.80	0.20	0.32	0.04	0.16
17	13	0.83	4.41	3.78	2.55	2.34	0.16	0.30	0.03	0.30
18	46	0.83	6.48	3.49	3.73	2.59	0.22	0.33	0.05	0.16
19	18	0.83	9.69	2.77	5.70	2.29	0.21	0.33	0.05	0.26
20	73	0.84	8.42	5.79	5.06	3.92	0.34	0.39	0.11	0.13
21	76	0.84	8.90	4.94	5.58	3.19	0.39	0.38	0.15	0.12
22	63	0.86	14.09	5.37	7.85	3.38	0.32	0.41	0.10	0.16
23	33	0.86	5.08	2.77	3.40	2.50	0.15	0.29	0.02	0.16
24	74	0.86	8.63	3.63	4.24	2.23	0.24	0.35	0.06	0.11
25	39	0.86	9.20	6.37	5.43	4.05	0.28	0.40	0.08	0.22
26	65	0.86	7.55	2.52	5.43	2.33	0.25	0.30	0.06	0.11
27	47	0.87	7.49	3.74	3.49	1.86	0.17	0.34	0.03	0.17
28	69	0.87	10.18	4.29	6.38	3.08	0.23	0.37	0.05	0.14
29	55	0.88	11.45	4.22	6.71	2.47	0.27	0.38	0.07	0.16
30	64	0.88	15.84	7.52	5.32	4.14	0.41	0.45	0.17	0.17
31	12	0.88	7.79	7.79	4.55	4.15	0.30	0.41	0.09	0.41
32	27	0.89	9.54	4.09	5.10	2.48	0.23	0.37	0.05	0.24
33	83	0.89	9.43	7.37	5.70	5.07	0.37	0.41	0.13	0.12
34	78	0.90	14.02	3.51	7.74	2.55	0.23	0.37	0.05	0.10
35	32	0.90	12.75	3.36	6.19	2.09	0.22	0.36	0.05	0.20
36	60	0.90	5.47	3.37	3.35	2.04	0.19	0.31	0.04	0.13
37	4	0.91	7.17	3.98	2.97	1.79	0.17	0.35	0.03	0.30
38	67	0.92	11.79	4.72	7.23	3.27	0.26	0.39	0.07	0.15
39	68	0.92	7.33	3.66	5.01	2.82	0.23	0.34	0.05	0.13
40	85	0.93	9.72	3.96	7.08	2.83		0.36		0.13
41	72	0.93	14.59	7.64	9.66	5.41	0.39	0.44	0.15	0.14
42	9	0.93	9.76	4.44	5.81	2.68	0.27	0.37	0.07	0.30
43	1	0.94	5.17	1.15	5.16	1.15	0.21	0.23	0.04	0.14
44	17	0.94	10.65	4.10	5.84	2.56	0.26	0.37	0.07	0.32
45	88	0.95	17.21	5.44	10.86	4.31		0.42		0.17
46	43	0.95	26.29	7.08	18.39	5.33	0.23	0.45	0.05	0.19
47	16	0.95	15.10	3.55	8.76	2.42	0.25	0.37	0.06	0.30
48	80	0.96	13.84	3.46	8.05	2.22	0.24	0.37	0.06	0.10
49	31	0.96	5.29	2.89	3.17	2.18	0.15	0.29	0.02	0.17
50	29	0.96	7.99	3.69	4.94	2.47	0.20	0.35	0.04	0.22

TABLE A5 (CONTINUED)
LINEAR AND STATISTICAL RATIOS

FRAG NO.	NEW	OLD	CD	L/T	W/T	L'/T'	W'/T'	SD / AAVG	IC08	AVG	VAR / AAVG+2	IC08	AVG+2
51	37	0.96	8.69	4.35	5.61	2.86	0.25	0.37	0.06	0.20			
52	61	0.96	15.98	6.85	9.11	3.89	0.35	0.43	0.12	0.17			
53	14	0.96	7.37	3.69	4.30	2.68	0.22	0.34	0.05	0.33			
54	10	0.97	16.22	9.46	9.12	4.83	0.35	0.46	0.12	0.43			
55	87	0.98	14.23	5.18	7.65	3.64		0.41		0.17			
56	71	0.98	15.34	6.00	9.74	3.72	0.36	0.42	0.13	0.14			
57	15	0.98	7.03	4.69	4.29	3.04	0.21	0.36	0.05	0.35			
58	38	0.98	7.41	3.99	5.11	2.81	0.25	0.35	0.06	0.19			
59	42	0.98	7.88	3.15	5.98	2.32	0.19	0.33	0.04	0.17			
60	75	0.99	10.34	3.94	6.86	2.91	0.28	0.37	0.08	0.12			
61	96	0.99	5.02	4.06	3.34	2.73		0.32		0.10			
62	91	0.99	12.13	5.66	8.91	4.58		0.41		0.17			
63	81	0.99	11.55	3.85	7.57	2.77	0.22	0.37	0.05	0.11			
64	84	1.00	18.33	5.58	10.09	3.32	0.33	0.42	0.11	0.11			
65	93	1.01	15.70	5.74	12.05	4.83		0.42		0.18			
66	94	1.02	7.04	3.48	5.27	2.86		0.33		0.11			
67	23	1.02	6.66	3.63	4.46	2.44	0.22	0.33	0.05	0.24			
68	59	1.03	10.38	6.49	6.57	4.88	0.38	0.41	0.14	0.17			
69	56	1.03	16.12	3.87	10.00	2.59	0.29	0.38	0.08	0.15			
70	48	1.04	7.05	5.29	4.09	3.38	0.28	0.37	0.08	0.19			
71	51	1.05	12.06	3.62	6.38	1.83	0.24	0.36	0.06	0.16			
72	7	1.05	8.51	4.25	5.19	2.84	0.23	0.36	0.05	0.39			
73	6	1.06	8.66	4.33	5.53	3.23	0.24	0.37	0.06	0.40			
74	66	1.06	7.39	5.28	5.21	3.80	0.38	0.37	0.09	0.15			
75	30	1.11	5.91	3.94	2.82	2.18	0.19	0.33	0.04	0.16			
76	54	1.11	17.44	7.85	10.63	5.36	0.43	0.45	0.18	0.19			
77	58	1.12	13.02	4.34	6.06	2.47	0.38	0.39	0.09	0.16			
78	49	1.14	7.16	4.40	4.25	2.70	0.25	0.36	0.06	0.18			
79	36	1.16	10.13	4.73	6.26	2.95	0.29	0.38	0.08	0.21			
80	52	1.16	10.21	5.10	5.86	3.36	0.34	0.39	0.12	0.18			
81	22	1.18	12.99	5.20	8.04	3.01	0.29	0.40	0.08	0.28			
82	5	1.19	17.87	4.47	11.12	2.94	0.31	0.40	0.18	0.39			
83	26	1.19	11.05	4.42	5.46	2.55	0.26	0.38	0.07	0.24			
84	19	1.21	7.30	4.38	4.99	3.38	0.28	0.36	0.08	0.31			
85	86	1.24	15.52	5.64	10.07	4.75		0.42		0.17			
86	38	1.24	11.10	3.27	6.84	2.52	0.24	0.35	0.06	0.21			
87	77	1.29	14.74	4.54	9.36	3.11	0.33	0.40	0.11	0.12			
88	34	1.29	9.24	4.62	4.89	2.69	0.22	0.38	0.05	0.22			
89	20	1.29	11.15	5.15	5.61	2.92	0.23	0.40	0.05	0.31			
90	25	1.30	11.19	4.48	7.10	3.33	0.32	0.38	0.10	0.25			
91	79	1.31	13.35	5.80	7.76	3.65	0.32	0.41	0.10	0.12			
92	28	1.33	8.12	3.75	4.19	2.16	0.22	0.35	0.05	0.22			
93	8	1.34	14.15	7.07	8.45	4.78	0.33	0.43	0.11	0.43			
94	21	1.38	14.04	5.61	8.49	3.56	0.34	0.41	0.12	0.38			
95	92	1.42	19.67	6.86	11.16	5.31		0.44		0.28			
96	24	1.48	7.31	5.85	5.22	4.28	0.34	0.38	0.12	0.28			

HEADINGS

L - AVERAGE LENGTH W - AVERAGE WIDTH T - AVERAGE THICKNESS
L' = MAXIMUM LENGTH PLUS AVERAGE LENGTH
W' = MAXIMUM WIDTH PLUS AVERAGE WIDTH
T' = MAXIMUM THICKNESS PLUS AVERAGE THICKNESS
SD - STANDARD DEVIATION OF PRESENTED AREAS (SQ. IN.)
VAR - VARIANCE OF PRESENTED AREAS (IN. 4TH)
AAVG+2 - AVERAGE PRESENTED AREA SQUARED (IN. 4TH)
IC08 - AREAS CALCULATED FROM ICOSAHEDRON GAGE DATA
CALC - AREAS CALCULATED FROM APPROXIMATING RECTANGULAR PARALLELEPIPEDS

TABLE A6
PERIMETER RATIOS

FRAG NO. NEW	OLD	CD	LWP/LTP	LWP/TWP	LTP/TWP	LWP/LMAX	TWP/WMAX
1	2	0.42	1.00	1.00	1.00	3.14	3.14
2	95	0.50	1.00	1.18	1.00	3.04	2.91
3	3	0.64	1.00	1.00	1.00	4.03	4.03
4	70	0.71	1.01	2.03	2.00	2.42	3.03
5	44	0.72	1.00	1.47	1.36	2.83	2.74
6	62	0.73	1.25	1.98	1.58	3.04	3.12
7	53	0.76	1.12	2.14	1.91	2.81	2.84
8	41	0.76	1.05	1.07	1.02	2.57	2.47
9	11	0.76	1.22	1.87	1.54	2.70	2.11
10	57	0.78	1.07	1.70	1.59	2.33	2.22
11	35	0.79	1.10	2.42	2.21	2.29	2.66
12	90	0.79	1.07	1.74	1.63	2.28	1.71
13	45	0.80	1.10	1.50	1.36	2.52	2.37
14	89	0.80	1.01	1.40	1.47	2.22	2.60
15	82	0.81	1.37	1.42	1.03	2.90	2.31
16	40	0.82	1.00	1.90	1.90	2.21	2.32
17	13	0.83	1.16	1.19	1.03	2.78	2.43
18	46	0.83	1.25	1.69	1.36	2.82	1.97
19	18	0.83	1.11	1.69	1.52	2.25	2.55
20	73	0.84	1.36	1.68	1.23	3.11	2.15
21	76	0.84	1.17	1.69	1.44	2.39	2.42
22	63	0.86	1.09	2.57	2.35	2.41	1.96
23	33	0.86	1.18	1.35	1.15	2.40	1.95
24	74	0.86	1.16	1.54	1.33	2.53	2.59
25	39	0.86	1.62	1.70	1.04	3.21	2.38
26	65	0.86	1.18	2.29	1.93	2.58	2.13
27	47	0.87	1.24	1.68	1.35	2.68	2.82
28	69	0.87	1.14	2.25	1.97	2.57	2.10
29	55	0.88	1.11	2.89	2.59	2.40	2.25
30	64	0.88	1.67	1.96	1.17	3.26	2.04
31	12	0.88	1.38	1.57	1.14	2.93	2.22
32	27	0.89	1.11	2.34	2.11	2.47	1.96
33	83	0.89	1.54	1.63	1.05	3.23	2.20
34	78	0.90	1.21	2.58	2.13	2.61	2.48
35	32	0.90	1.03	2.09	2.03	2.17	2.52
36	60	0.90	1.06	1.53	1.45	2.36	2.56
37	4	0.91	1.09	1.36	1.25	2.56	2.92
38	67	0.92	1.29	2.34	1.81	2.62	2.25
39	68	0.92	1.04	1.05	1.02	2.27	3.44
40	85	0.93	1.16	2.78	2.40	2.42	2.21
41	72	0.93	1.31	2.05	1.57	2.57	2.12
42	9	0.93	1.14	2.04	1.79	2.47	2.59
43	1	0.94	1.02	2.88	2.82	2.52	3.92
44	17	0.94	1.14	2.00	1.75	2.34	2.38
45	88	0.95	1.16	2.44	2.10	2.37	2.05
46	43	0.95	1.16	3.74	3.22	2.68	2.31
47	16	0.95	1.05	2.46	2.33	2.12	2.73
48	80	0.96	1.09	3.03	2.77	2.33	2.55
49	31	0.96	1.10	1.31	1.18	2.56	2.34
50	29	0.96	1.04	1.96	1.88	2.31	2.20

TABLE A6 CONTINUED
PERIMETER RATIOS

FRAG NO. NEW	OLD	CD	LWP/LTP	LWP/TWP	LTP/TWP	LWP/LMAX	TWP/WMAX
51	37	0.96	1.13	1.39	1.76	2.37	2.29
52	61	0.96	1.12	2.46	2.19	2.38	2.28
53	14	0.96	1.25	1.48	1.19	2.88	2.59
54	18	0.97	1.45	2.29	1.59	2.32	2.88
55	87	0.98	1.35	2.41	1.78	2.52	1.88
56	71	0.98	1.15	2.85	2.46	2.36	2.22
57	15	0.98	1.16	1.63	1.41	2.78	2.22
58	38	0.98	1.88	1.98	1.76	2.23	2.18
59	42	0.98	1.88	2.43	2.25	2.46	2.65
60	75	0.99	1.18	2.87	1.88	2.41	2.51
61	96	0.99	1.39	1.58	1.14	2.98	2.29
62	91	0.99	1.42	2.29	1.61	2.69	2.11
63	81	0.99	1.88	2.64	2.64	2.32	2.28
64	84	1.00	1.36	3.41	2.52	2.64	2.16
65	93	1.01	1.31	3.95	3.82	2.85	1.67
66	94	1.02	1.26	1.83	1.45	2.78	2.48
67	23	1.02	1.14	1.66	1.46	2.35	2.58
68	59	1.03	1.54	1.64	1.86	3.84	2.16
69	56	1.03	1.83	3.25	3.14	2.14	2.38
70	48	1.04	1.39	1.42	1.82	2.98	2.28
71	51	1.05	1.83	2.89	2.81	2.16	2.64
72	7	1.05	1.28	1.79	1.58	2.66	2.58
73	6	1.06	1.28	1.71	1.42	2.51	2.21
74	66	1.06	1.47	1.68	1.89	2.78	2.34
75	58	1.11	1.26	1.44	1.15	3.29	2.59
76	54	1.11	1.22	2.18	1.72	2.51	2.16
77	58	1.12	1.13	2.14	1.89	2.37	2.38
78	49	1.14	1.35	1.88	1.48	2.98	2.42
79	36	1.16	1.89	2.14	1.97	2.23	2.19
80	52	1.16	1.34	1.92	1.63	2.67	2.16
81	22	1.18	1.88	2.78	2.78	2.17	2.22
82	5	1.19	1.84	2.98	2.88	2.18	2.68
83	26	1.19	1.27	2.22	1.75	2.62	2.22
84	19	1.21	1.32	1.66	1.26	2.87	2.28
85	86	1.24	1.31	2.18	1.61	2.61	2.15
86	38	1.24	1.89	2.25	2.87	2.26	2.27
87	77	1.29	1.19	2.74	2.31	2.38	2.35
88	34	1.29	1.19	1.91	1.61	2.64	2.31
89	28	1.29	1.28	1.87	1.55	2.36	2.21
90	25	1.38	1.24	1.84	1.48	2.36	2.48
91	79	1.31	1.41	2.65	1.88	2.82	2.12
92	28	1.33	1.86	1.78	1.61	2.54	2.64
93	8	1.34	1.18	1.86	1.57	2.32	2.16
94	21	1.38	1.11	2.38	2.87	2.21	2.28
95	92	1.42	1.38	2.28	1.68	2.72	2.87
96	24	1.48	1.34	1.64	1.23	2.98	2.16

HEADINGS

LWP - PERIMETER IN LW PLANE (IN.)

LTP - PERIMETER IN LT PLANE (IN.)

TWP - PERIMETER IN TW PLANE (IN.)

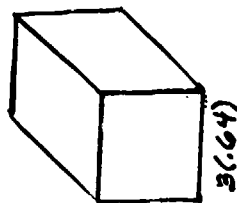
LMAX - MAXIMUM LENGTH (IN.)

WMAX - MAXIMUM WIDTH (IN.)

RANDOM TUMBLING



Figure A-1



3(.64)



4(.91)



6(1.06)



11(.76)



12(.88)



13(.83)



14(.96)



17(.94)



18(.83)



21(1.38)



27(.89)



34(1.29)



35(.79)



39(.86)



43(.95)



44(.72)



47(.87)



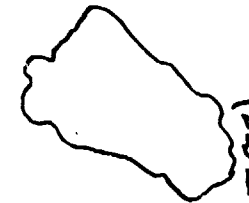
49(1.14)



53(.76)



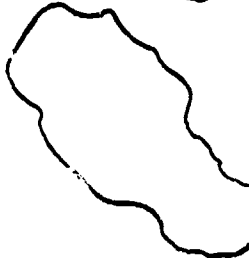
55(.88)



57(.78)



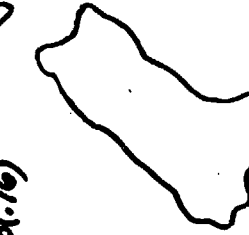
62(.73)



63(.86)



64(.88)



65(.86)

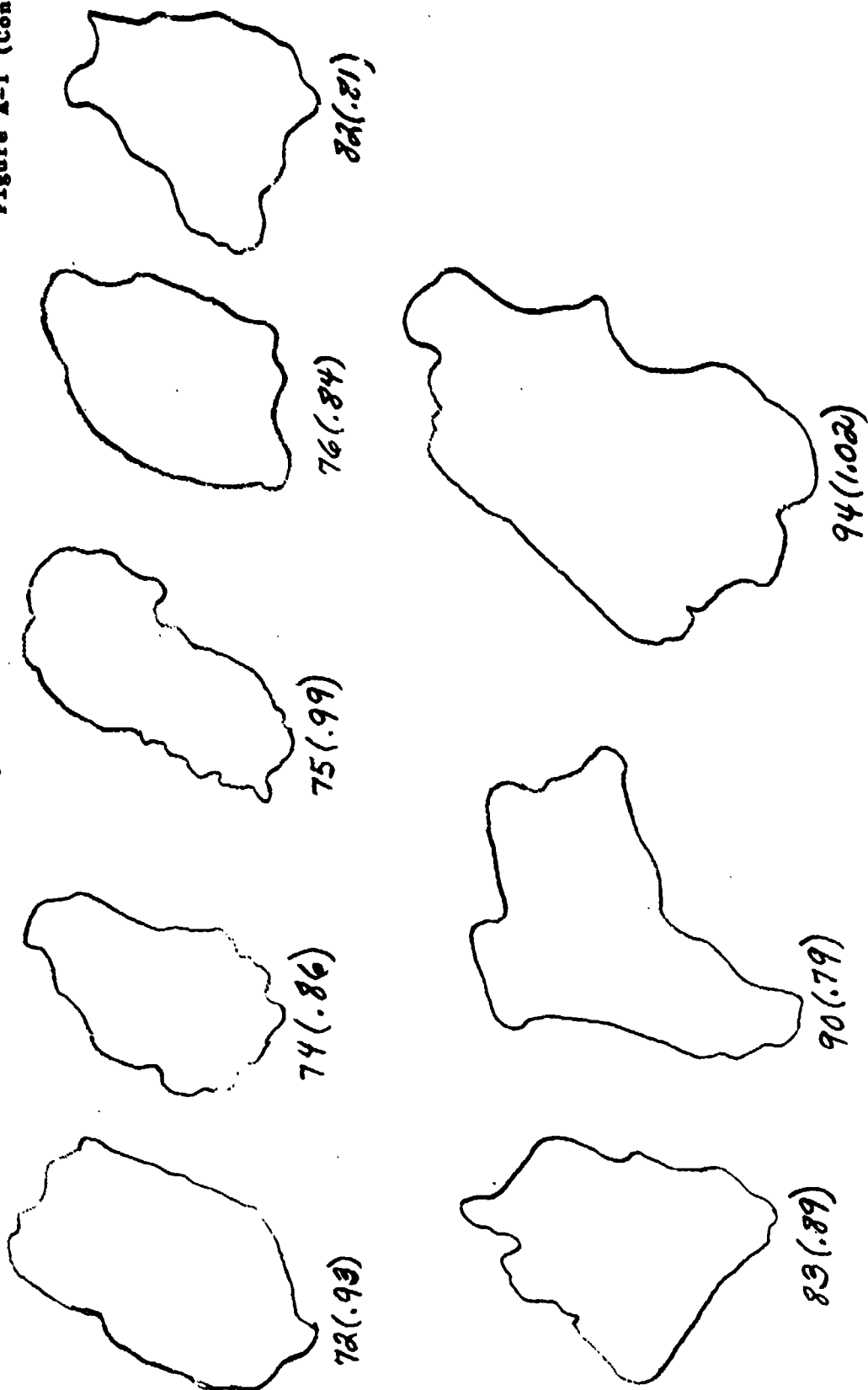


70(.81)

RANDOM TUMBLING

0 1 2 INCHES

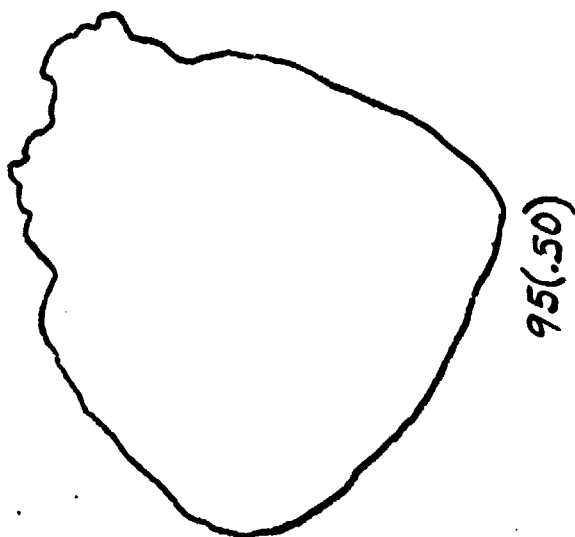
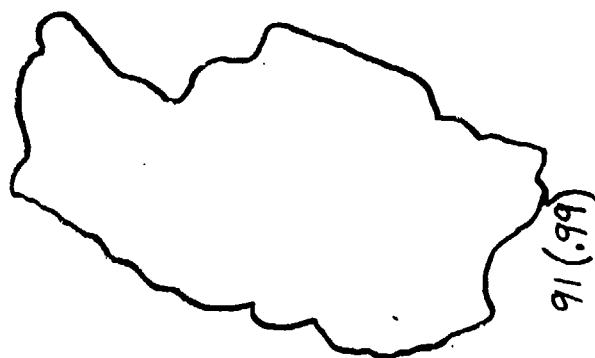
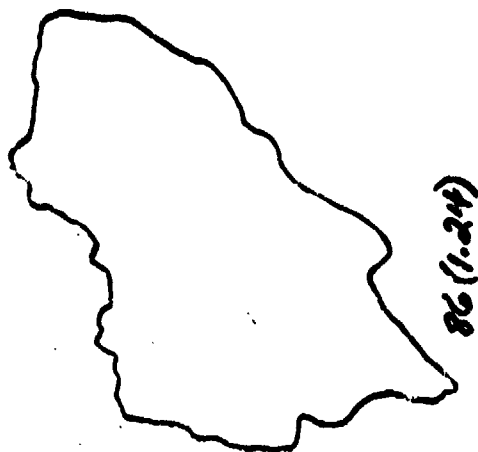
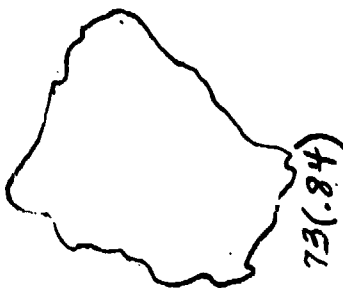
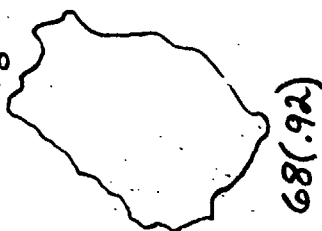
Figure A-1 (Cont'd)



FLOATS MOTIONLESS

0 1 2 INCHES

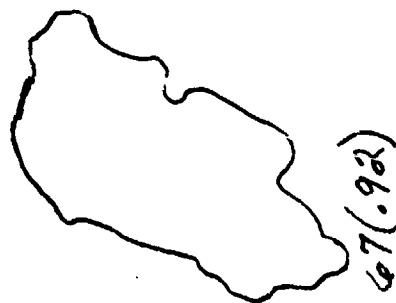
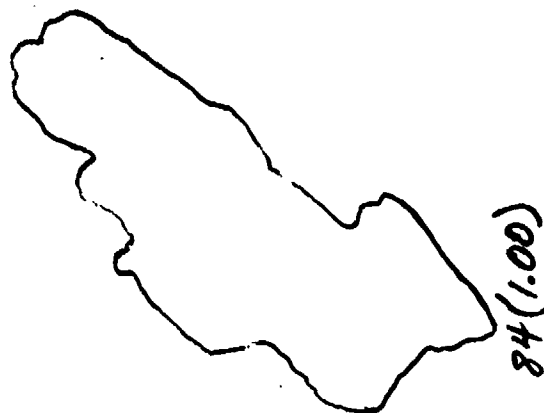
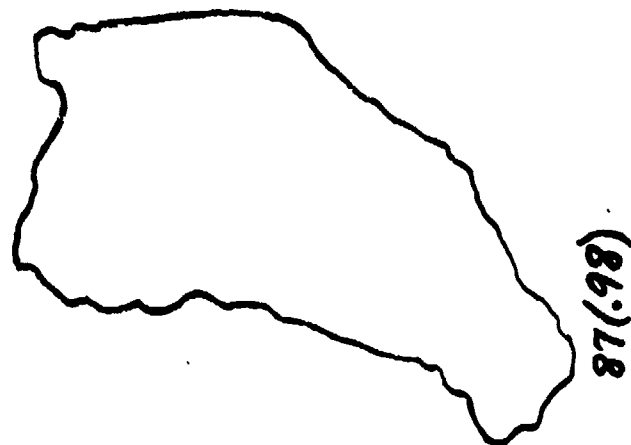
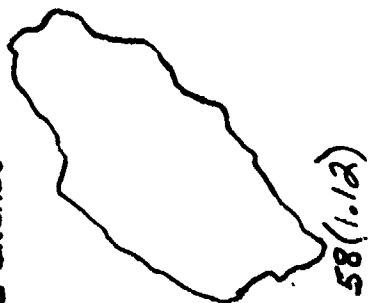
Figure A-2



FLAT ROTATION

0 1 2 INCHES

Figure A-3



ROTATES ABOUT THE LNT AXIS

0 1 2 INCHES



32(.90)



31(.96)



30(1.24)



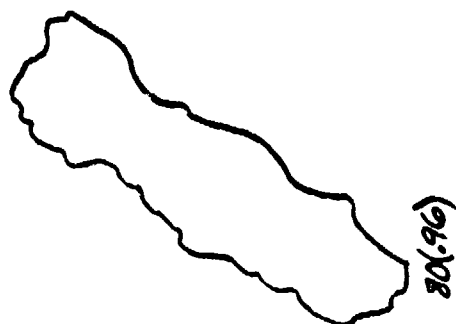
29(.96)



23(1.02)



16(.95)



80(.96)



59(1.03)



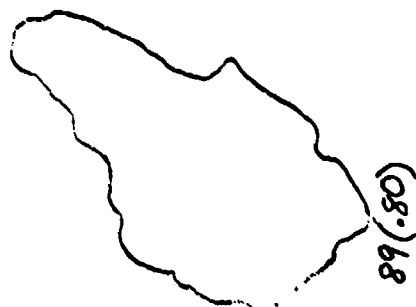
45(.80)



36(1.16)



33(.86)



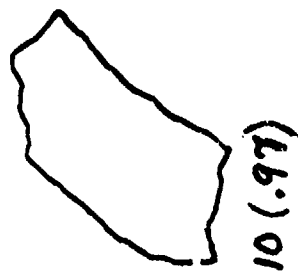
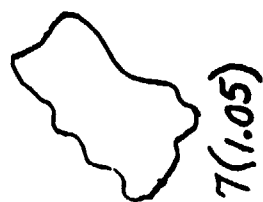
89(.80)

Figure A-4

ROTATES ABOUT THE LOW AXIS



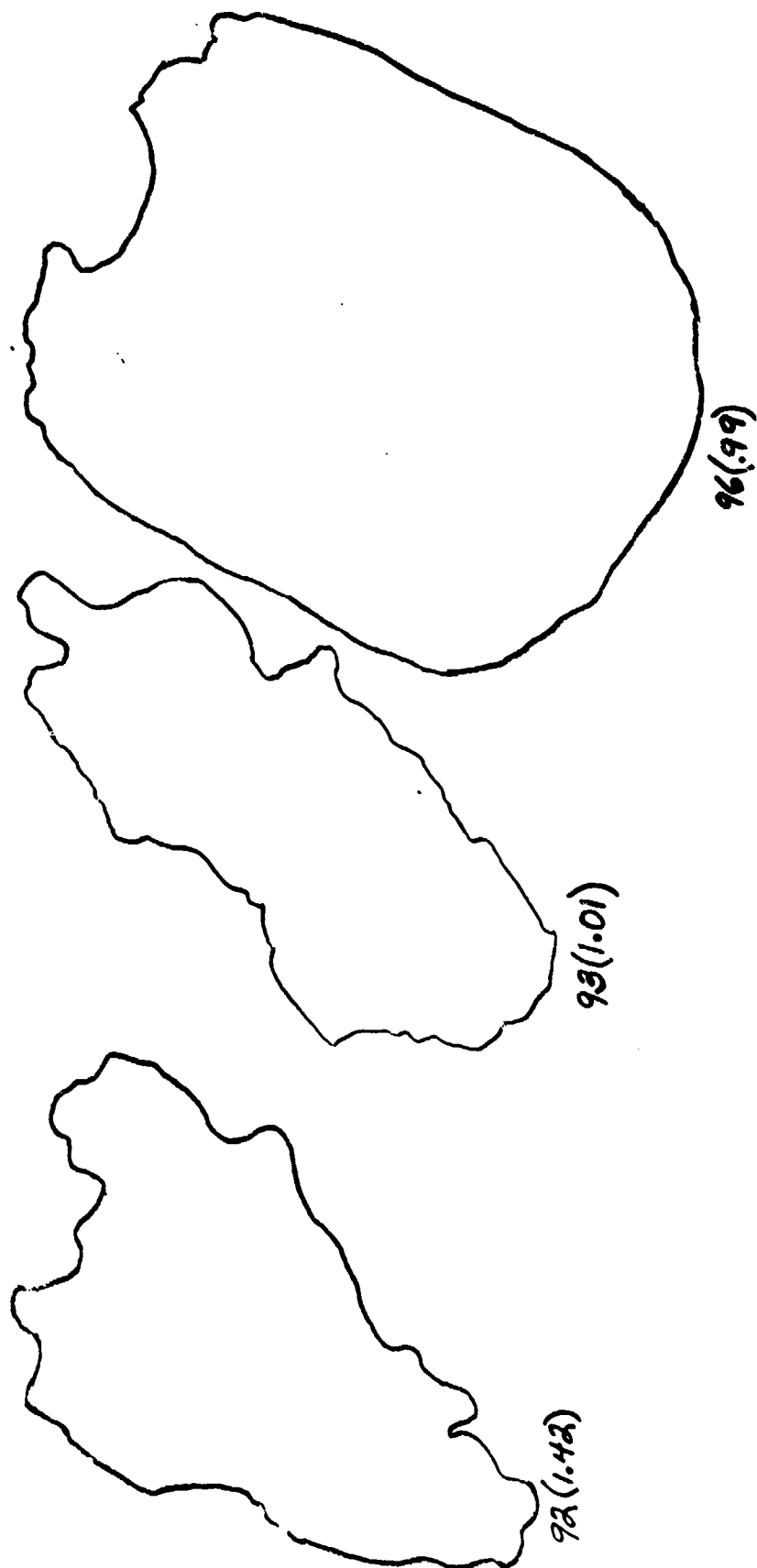
Figure A-5



ROTATES AROUND THE T-AXIS

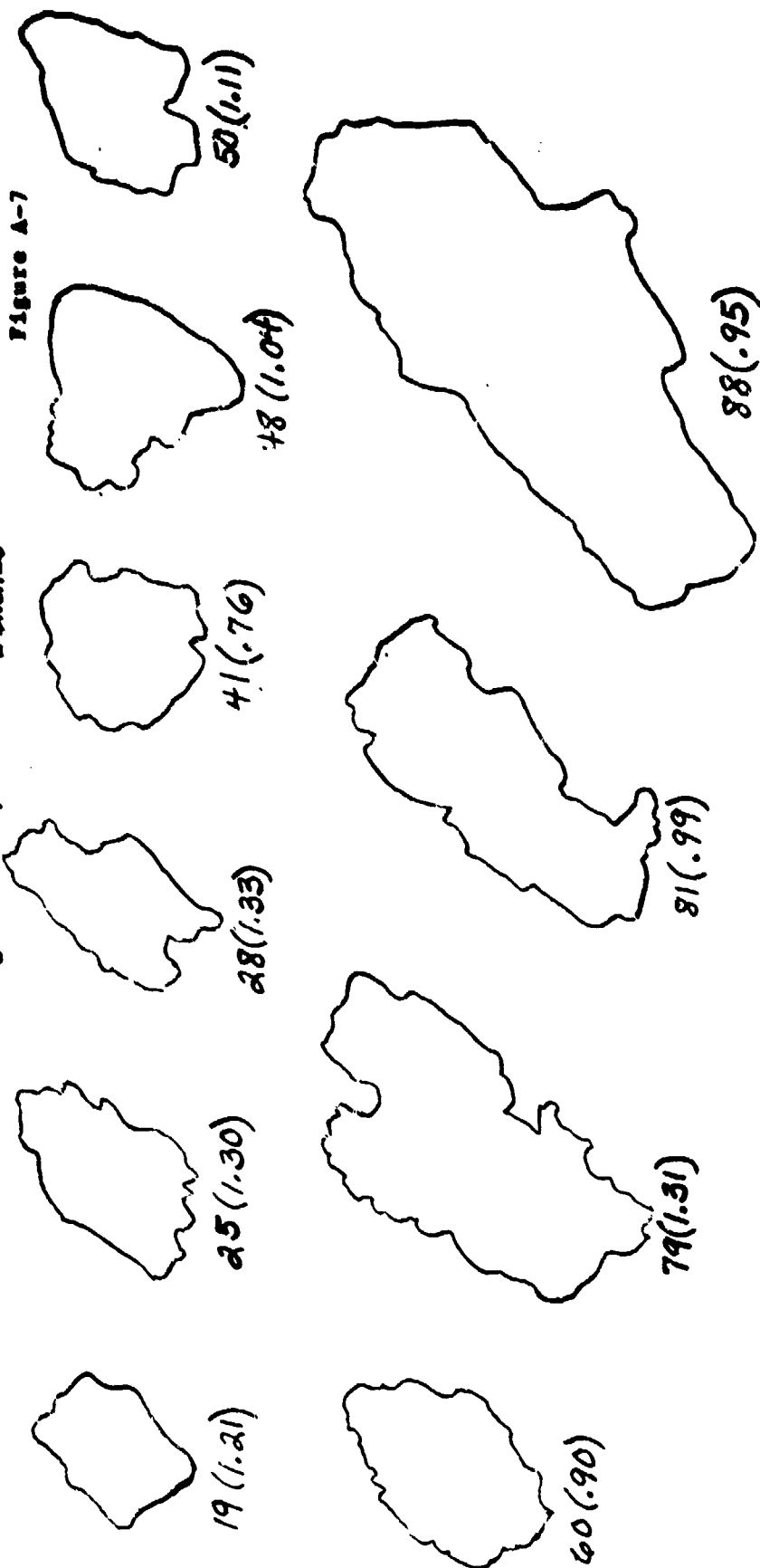


Figure A-6



ROTATES AROUND THE T-AXIS

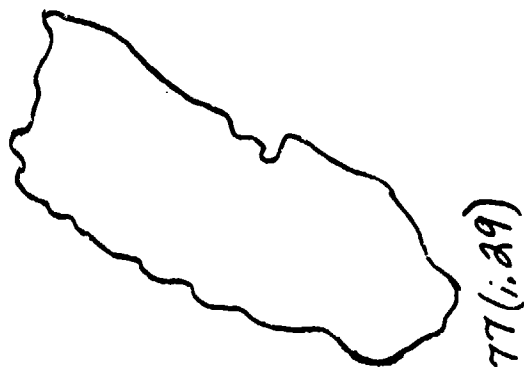
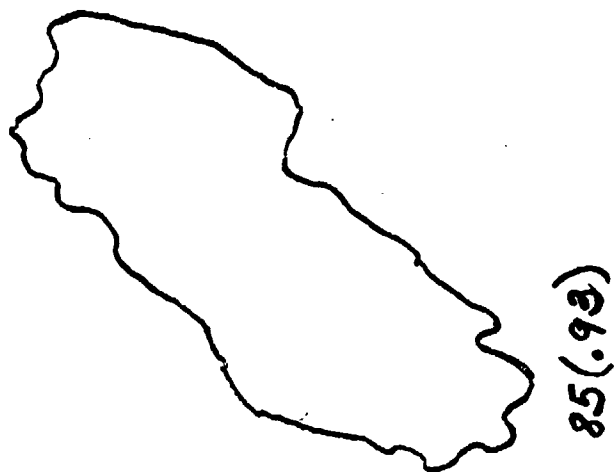
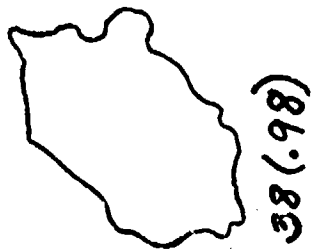
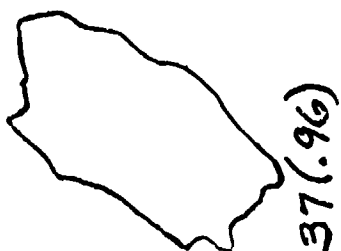
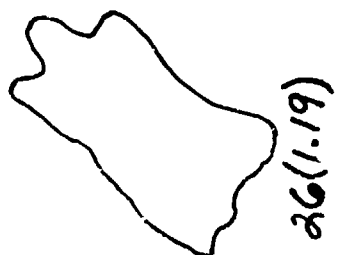
0 1 2 3 4 5 6 7 8 9 10 11 12 13 14 15 16 17 18 19 20 21 22 23 24 25 26 27 28 29 30 31 32 33 34 35 36 37 38 39 40 41 42 43 44 45 46 47 48 49 50 51 52 53 54 55 56 57 58 59 60 61 62 63 64 65 66 67 68 69 70 71 72 73 74 75 76 77 78 79 80 81 82 83 84 85 86 87 88 89 90 91 92 93 94 95 96 97 98 99 100
2 INCHES



ROTATES AROUND THE L-AXIS



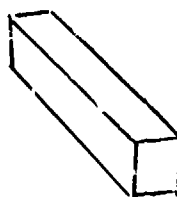
Figure A-8



CONING



Figure A-9



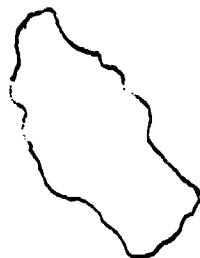
1(.94)



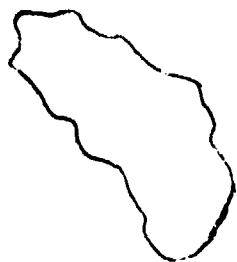
5(1.19)



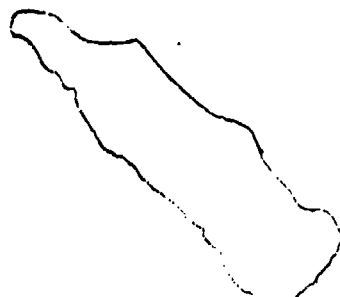
9(.93)



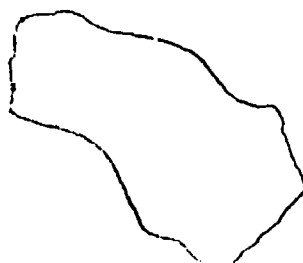
40(.82)



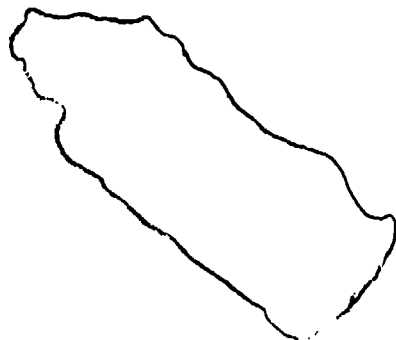
42(.98)



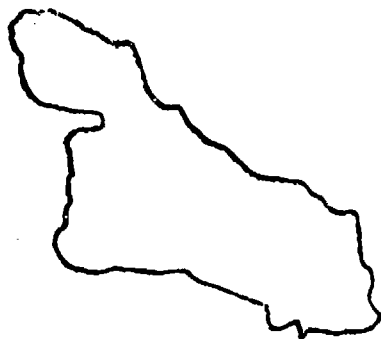
51(1.05)



69(.87)



71(.98)



78(.90)

AD-P005 365

FRAGMENT HAZARDS EVALUATION PROPOSAL

PRESENTED TO:

TWENTY-SECOND DOD EXPLOSIVE SAFETY SEMINAR

AUGUST 26 THROUGH 28, 1986

ANAHEIM MARRIOTT HOTEL

ANAHEIM, CALIFORNIA

BY:

A. G. PAPP

MASON & HANGER-SILAS MASON CO., INC.

PANTEX PLANT

AMARILLO, TEXAS 79177

RICHARD P. GUARIENTI

UNIVERSITY OF CALIFORNIA

LAWRENCE LIVERMORE NATIONAL LABORATORY

LIVERMORE, CALIFORNIA 94550

FRED KRACH

MONSANTO RESEARCH CORPORATION

MRC - MOUND

MIAMISBURG, OHIO 45342

INTRODUCTION

As the Department of Energy (DOE) adopted the Department of Defense (DoD) "Ammunition and Explosive Safety Standards," DoD 6055.9-STD, dated July 1984, in their "DOE Explosives Safety Manual," DOE/EV/06194-3, dated August 1985, it was emphasized to DOE contractors the need to provide safe clearance for hazardous fragments (both primary and secondary) which can evolve from accidental explosions from energetic materials (explosives, pyrotechnics, fuel, etc.).

Because the DoD generally deals with larger quantities of explosives, this proposal suggests smaller quantity breaks be studied. It is believed that the DoD 6055.9 criteria is very conservative and not realistic for most DOE applications, especially for explosive quantities of a few pounds or a few hundred pounds.

The proposed study is mainly aimed at developing criteria applicable to existing facilities because it is envisioned that new facilities will be designed to meet present criteria or the modified criteria that is expected as a result of this proposal.

PROBLEMS CAUSED BY PRESENT CRITERIA

An important consideration in the analysis of the hazard associated with an accidental explosion is the effect of the fragments generated by the explosion. To achieve a desired level of protection to surrounding facilities and personnel, explosives are required to be separated from these exposures at distances based on the maximum quantity of explosives permitted at the location.

DOE 6430.1, "General Design Criteria Manual" and DOE/EV/06194, "DOE Explosives Safety Manual" require that DoD 6055.9-STD, Department of Defense "Ammunition and Explosives Safety Standards" be used as mandatory siting criteria for determining minimum separation distances from explosives locations. The military criteria, which is based primarily on fragments from ordnance items, requires that specific minimum distances be maintained to protect people in the open and is applied to administrative areas, site boundaries, etc. For locations with mass-detonating explosives that have not been evaluated for fragment hazards, the following separation distances are required:

- o 670 ft for 100 lbs or less of thin cased or bulk explosives.
- c 1,250 ft for 101 to 30,000 lbs of explosives.
- o Table of distances for greater than 30,000 lbs of explosives.

When these criteria are applied to existing DOE contractor facilities, some of the problems include:

1. Some of these hazardous fragment distance circles go off-site and encompass public housing.

2. Assembly points for facility personnel (cafeterias, etc.) and roadways open to the public lie within these fragment distances.
3. Existing non-explosives operations fall inside these fragment distances.
4. Large land masses are consumed by these required fragment distances making future planning very difficult, especially if one wants to place a non-explosives facility in the area.

It is believed that the DoD 6055.9 criteria is very conservative and not realistic for most DOE applications, especially for explosive quantities of a few pounds or a few hundred pounds. An accidental explosion from these quantities should not project hazardous fragments near the required 670-ft or 1250-ft separation distance, but we have no evaluation to justify a reduction in the standard. The fragment hazard problem may be mostly "on paper." However, since it is DOE criteria, if an accident were to occur and a fragment were to strike a member of the general public or non-explosives worker, it could become a legal problem.

Thus, the evaluation proposed herein would develop realistic separation distance criteria from the relatively small quantities of explosives that typically are present in DOE operations. This should minimize the emotional public perception of the problem based on the present DoD conservative criteria for small quantities of explosives.

THE PROPOSED FRAGMENT HAZARD EVALUATION

A DOE separation distance criteria for explosives facilities can be developed by realistic assessment of the hazards created by fragments that can be generated in an explosives accident.

It is proposed that expert consultants be employed to develop realistic criteria. This evaluation would be coordinated by DOE contractor experts. During the first fiscal year (FY-1987) it is proposed that a literature search be conducted to assure total awareness of the present state of the art. The Department of Defense, Explosive Safety Board (DDESB) has agreed to work with DOE to assure that we are building on, and not duplicating, current fragment hazard technology. The literature search would be followed by a survey of present fragment hazards at DOE facilities and the survey would then be followed by a hazard refinement analysis to complete the first fiscal year.

The second fiscal year would include scale model testing to confirm and refine the analysis. A third fiscal year could conclude the scale model testing with full-scale testing, if necessary.

Constant monitoring of the project by DOE contractor experts, reviews by DOE HQ and coordinated efforts by DDESB will assure efficient application of funds. At any phase in the above-outlined effort, when adequate criteria is generated, the project may achieve its goal, and be terminated. Risk assessment principles will be applied to the project to assure that once a solution with a level of confidence acceptable to DOE HQ is achieved, the project can rapidly conclude with realistic fragment

hazard criteria. At this writing, however, it is felt that the efforts outlined above for the first fiscal year (through a hazard refinement analysis) will be the minimum effort required to provide meaningful technical guidance which could be accepted as a basis for a reduction in required separation distances.

BENEFITS OF THE PROPOSAL FRAGMENT HAZARD EVALUATION

It is anticipated that the project proposed herein would resolve the problems outlined in the initial part of this proposal.

A major benefit could be the elimination of negative public perceptions created by existing criteria. The proposed evaluation would show DOE efforts to develop realistic guidance for its contractors who deal with explosives. This could become extremely valuable in any legal actions which could arise if there were an explosives accident, especially the explosion generated fragments which caused severe injuries to members of the public.

Other advantages include:

- o Eliminate another fence-line issue before it is capitalized upon by state or other outside interests.
- o Provide efficient solutions to existing explosive facility non-compliance.
- o Focusing DOE technical resources and taking advantage of DoD assistance.
- o Reducing exemption requests, saving valuable time for DOE reviews.
- o Assuring minimal production vulnerability due to fragments generated by an accidental explosion.
- o Ease of auditing to a uniform code.
- o Open DOE land (presently covered by fragment distance circles) for productive use.
- o Provide meaningful fragment hazard design criteria for new facilities (creating more cost-effective designs).
- o Uniform guidance for contractors, avoiding expensive, repetitive solutions to similar problems.

These are some of the advantages, which collectively, will provide a very rapid pay-back for this proposed project.

CONCLUSION

↓ This proposed fragment hazard evaluation will develop a meaningful code for small explosive quantities in the range of interest to DOE operations with very probable spillover to DoD operations in the same range of explosive quantities. It will provide a uniform solution to fragment hazard mitigation.

The economic application of DoD 6055.9 criteria is of paramount importance. New facilities can be designed to meet the current DoD criteria; however, the upgrading of existing facilities to meet the current DoD criteria is not practically nor economically feasible.

Therefore, it is proposed to develop a design criteria to supersede and/or supplement DoD 6055.9 criteria for smaller quantities of explosives. ↗

BIBLIOGRAPHY

1. Department of Defense, "Ammunition and Explosives Safety Standards," DoD 6055.9-STD, Washington, D.C., July 1984.
2. Department of Energy, "DOE Explosive Safety Manual," DOE/EV/06194-3, Rev. 2, Washington, D.C., August 1985.
3. Department of the Army, Army Material Command, "Safety Manual," AMC-R 385-100, Alexandria, VA, August, 1, 1985.
4. Department of Energy, "General Design Criteria Manual (Chapter XXII, Explosive Facilities)," DOE Order 6430.1, Washington, D.C., August 26, 1985.
5. Department of Energy, Albuquerque Operations, Amarillo Area Office, "A Manual for the Prediction of Blast and Fragment Loading on Structures," DOE/TIC-11268, Amarillo, TX, April 1, 1982.
6. Department of the Army, the Navy and the Air Force, "Structures to Resist the Effects of Accidental Detonations," TM-5-1300, NAVFAC 197, AFM 88-22, Washington, D.C., June 1959.

The Application of Risk Assessment in the Field of Explosives
and Ammunition Safety

F R Hartley,⁽¹⁾ F Cantrell,⁽¹⁾ P A Moreton,⁽¹⁾ J J Clifton⁽²⁾ and
J N Edmondson⁽²⁾

(1) The Royal Military College of Science, Shrivenham, UK

(2) The Safety and Reliability Directorate, UK Atomic Energy
Authority, Culcheth, UK

SUMMARY

The four stages of risk assessment are described. These are:

1. What can go wrong?
2. How often can things go wrong?
3. What are the consequences of an incident?
4. So what, is it serious?

It is shown that each stage has value in enhancing safety even if the subsequent stages are not undertaken. Application of the full risk assessment procedure would bring the field of explosives and ammunition into line with current practices for safety assessment in the nuclear and chemical industries.

AIM

The aim of this paper is to describe a study of the applicability of risk assessment to the field of explosives and ammunition.

Introduction to Risk Assessment

The risk from a given event is a function of the frequency of that event and the consequences of its occurrence.

$$\text{Risk} = f (\text{Frequency}) (\text{Consequence})$$

Thus to reduce the risk from an event one can either seek to minimise the frequency of its occurrence, or ameliorate its consequences, or both. The former is achieved by careful design according to best practice prescribed in the UK by The Ordnance Board, by quality control, and by effective management throughout. The Quantity-Distance Regulations which are considered elsewhere in this symposium are designed to reduce the consequences of any incident to a level that is acceptable in terms of the damage caused to both people and property. A great deal of effort has been devoted to making explosives and ammunition as safe as possible. Although a lot of attention has been given to assessing the consequences of accidents the frequency side of the equation has not received much attention in the context of risk. This, of course, can be a perfectly acceptable position to adopt providing the costs of relying on consequence reduction by restricting land and facilities usage both within and outside explosives and ammunition facilities is not considered prohibitive. There are, however, several industries such as the nuclear and chemical industries where, as Chernobyl and Bhopal have demonstrated, such an approach is neither possible, acceptable to the General Public, or economically viable. For these industries quantitative risk assessment, using some of the techniques initially developed to determine the reliability of the Minuteman Launch Control System, has been adopted. Not only does it allow risks to be identified, but because of its quantitative nature, it allows corrective measures to be applied most cost-effectively by concentrating on those areas where the risk of an accident of large consequence is high.

Four Stages of Risk Assessment

Risk assessment falls into four stages which successively answer the questions:

1. What can go wrong?
2. How often can things go wrong?
3. What are the consequences of an incident?
4. So what, is it serious?

One of the key messages of this paper is that each stage of risk assessment

yields valuable insight into the problems inherent in coping with high energy materials. There will be many situations in which improvements in safety can be achieved through the greater insight that a systematic risk assessment gives, without the need to complete all four stages.

What Can Go Wrong?

What can go wrong? This is done by identifying all the possible incident situations. The first stage was to carry out a brainstorming session involving staff experienced in risk assessment and staff experienced in handling explosives and ammunition. Initially these sessions were truly brainstorming i.e. the random interaction of several brains. But gradually, as in the oil industry, the approach can be systematised by developing key prompt phrases. These are developed by taking the view that any problem be it a hazard or an operability one, can only arise when there is a deviation from the norm. The key prompt phrases are applied to search for every deviation. Eight key phrases are generally needed:

NONE
MORE OF
LESS OF
PART OF
MORE THAN
LESS THAN
WRONG ADDRESS
OTHER

Let us illustrate these by reference to MORE OF applied to a Road-Rail Transfer Point. MORE OF can arise when:

there is more explosive than expected,
more mechanical stress than is intended is applied, e.g. by dropping,
the temperature gets too high,
static electricity is present,
rf or ionising radiation is present,
overpressure is present,
there is flooding.

Having identified all the deviations that can occur the next stage is to look at their general causes, their specific causes and their consequences. Thus the general causes of overheating are fire and heat. The specific causes may be a grass fire, cigarettes, matches, fires in vehicles etc etc. The consequences are that a fire or heat may be communicated to the explosive contents which may themselves burn, burn to detonation, or burn to mass explosion.

In spite of its systematic approach the HAZOP technique would not normally be expected to identify every possible mechanism of failure. It should however identify most of the significant events by encouraging a systematic consideration of the relevant operations. The next stage is to fully systematise the operation by developing a series of Fault Trees. These take every top event possible and systematically determine all their possible causes. The top events are all "unintended initiation of explosives, propellants or detonators". A typical Fault Tree is shown in Figure 1. This shows a top event, communication of a 1.3 propellant fire to other storehouses and how it may be caused by a series of AND + or OR events. For example, the ignition of the contents of the storehouse may either occur directly, or by ignition of the storehouse building itself.

As staff become more experienced at the HAZOP study, so they find that more and more of the events in the Fault Trees have been identified in the HAZOP study. The result at this stage is a systematic and thorough understanding of what can go wrong in the facility being studied. The management of the facility will have been involved throughout the analysis and so it has a very detailed and thorough understanding of the problems it is trying to manage. Because it is systematic there should be no inadvertent gaps in it. And so, at the end of this first stage of risk assessment there is already a major advantage which would be worth having even if risk assessment is taken no further, namely a detailed and thorough knowledge of the problems that the staff are trying to manage when dealing with explosives and ammunition.

How often can things go wrong?

The second stage of risk assessment is to determine how often things can go wrong. This is done by quantifying the Fault Trees. In doing this allowance should be made for the quality of the material in the store and its packaging if, for any reason, these are not both A1. Broadly speaking the events on the Fault Trees fall into 2 major groups:

Those that are specific to the explosives industry, e.g. the probability of a munition that is dropped accidentally initiating.

Those that are more general e.g. the probability of a Fork Lift Truck accident.

Quantification of events that are specific to the explosives industry is difficult for two reasons:

1. Incidents are mercifully relatively rare.
2. Testing is usually insufficient to give quantitative probability for rare events. For example, dropping a given store 5 or 10 times from a given height does not give a lot of information about whether the probability of initiation is one in one hundred or one in a million. Remember the Russians designed the Chernobyl Reactor to a probability of initiation of one in ten thousand!

Quantification of events that are common to many industries is relatively easy as there is usually a fair amount of data available. Where no data exists, experts are asked to make guesstimates; in all cases guesstimates that err on the side of caution are used. Once these and the known probabilities are incorporated into the Fault Trees, two further checks are made.

1. It is important the frequency of the top event is compared with known historical experience. This is fundamental in showing whether absurdities have been introduced.
2. The sensitivity of the frequency of the top event to the guesstimated frequencies is determined by altering the guesstimates. Typically it is found that the frequency of the Top Event is only really sensitive to a few of the component Fault Tree frequencies. The frequencies are then examined with great care and if it is not possible to get a series of experts to agree on a reasonable value, then in the limit it may be necessary to undertake some trials to determine this.

The net result of quantifying all the Fault Trees is that it allows very low risk, intermediate risk and very high risk situations to be identified. This is very important in that:

1. It enables the very low risk situations to be neglected with confidence.
2. It enables limited available resources to be concentrated initially in tackling the very high risk situations.
3. Once the high risk situations have been eliminated resources can be devoted to determining how it is possible to reduce the risk levels of the intermediate situations. This will not always involve the expenditure of capital; careful analysis of the Fault Tree may well indicate that a change of procedure will reduce the level of risk very significantly.

Consequence Analysis

The third stage of risk assessment is that of consequence analysis. The consequences of an event are analysed to determine the effects upon people and structures due to blast overpressures, thermal radiation and missiles. All of these effects can also act as initiators for further events to produce and 'knock-on' or domino effect. Much of the data that underpins the Quantity Distance Rules are used in the analysis of the consequences of unwanted explosive and ammunition events.

So What, Is It Serious?

The final stage of risk assessment is to combine and summate the probabilities and consequences of all events considered to determine whether or not the risks posed by a facility are acceptable. Many many books and articles have been written on this subject and if they teach anything at all, it is that this is a virtually impossible task as events at inquiries concerning nuclear facilities in Europe especially the UK and West Germany have demonstrated. Our approach to this phase of risk assessment is therefore to follow the line of reasoning taken by the Health and Safety Commission in the UK and now enshrined in UK Law. The Health and Safety Commission were involved in a debate between the many companies involved in operating a particularly complex petrochemicals facility at Canvey Island in the estuary of the River Thames and the local residents who wanted to know "is it safe?". The approach that we are using is to attempt to determine what is an unacceptable risk. Any situation that gives rise to a higher level of risk than this MUST BE RECTIFIED. Whenever a situation is identified which offers a lower level of risk than the threshold level it must be examined to decide whether:

1. It is too inordinately expensive to do anything about it. If it is inordinately expensive then it must be accepted.
2. It is not too expensive to improve. In that case IT MUST BE IMPROVED and expenditure must be incurred in so doing.

The result is that all situations involving risk have been made as safe as is REASONABLY PRACTICABLE.

The results of a complete risk assessment as applied to explosive and ammunition storage are:-

1. It evaluates the total risk each facility poses to its employees and identifies the risk to which each employee is exposed depending upon their location within the facility.
2. It tells us the risk the facility poses to the general public outside the facility.

Since different stores containing explosives in the same hazard division (e.g.1.1) will have different risk levels associated with them, it may well be found at this stage that by repacking a facility such that high risk stores are placed in situations very remote from people (either within or outside the facility) whilst stores that pose a very low risk are placed closer to locations where people are usually to be found, that one or both of two desirable situations can be achieved.

1. The first is that the risk posed to people and other facilities is reduced.
2. The second is that it may well prove possible to get more material into a given facility. This must be financially attractive in many situations in crowded Europe if not in the US.

Summary

It was stated in the introduction that Risk Assessment is a four stage process and that each stage can be of significant value even if subsequent stages are not undertaken. Let us summarise this by looking at each stage in turn.

What can go wrong? HAZOP and Fault Tree Analysis give management a systematic and thorough understanding of the facility. Even at this stage some problems will be identified as in need of rectification.

How often can it go wrong? Quantification of Fault Trees identifies high, intermediate and low risk situations, allowing resources to be deployed to greatest effect in obviating the worst risk situations. Fault Tree Analysis also identifies the factors which give rise to high risk situations so enabling an essential task to be redesigned in order to reduce the risk involved.

Consequence Analysis. Identifies the risk to employees and to the public, knowledge of which may enable further risk reductions to be made and the facility to be used optimally.

So what, is it serious? Leads to the concept that risks are either unacceptable (and must therefore be eliminated) or must be reduced to as low a level as is REASONABLY PRACTICABLE.

Acknowledgement

In addition to the authors, three people have made particular contribution to this study: Brigadier J. Groom, formerly Chairman of the UK Explosives Storage and Transport Committee, Dr J Rees Director of Ministry of Defence's Safety Services Organisation and Mr B. Harvey formerly Chairman of the Major Hazards Committee in the UK.

AD-P005 366

WARTIME MISSION OF
EXPLOSIVES SAFETY

Capt Susan J. Kaufman, USAF
Air Staff, Office of Safety
& Nuclear Surety
AF/IGF
Room 5D273, The Pentagon
Washington D.C. 20330-5100
AV 227-7050
Comm (202) 697-7050

I. INTRODUCTION

The Air Force concept of explosives risk management has undergone major revision since 1983. The changes have been across the entire spectrum of safety management, from installation level analysis of the risk involved in specific explosives operations, to Secretary of the Air Force authorization of some explosives safety violations. In addition, safety factors in all combat explosives operations have been scrutinized in light of shifting from peacetime to wartime acceptable risk levels. Prior to 1983, installation level weapons safety officers had access to little specific information concerning the degree of risk to personnel and equipment. Air Force Regulation 127-100, Explosives Safety Standards, had tables that stated required separation distances for given net explosive weights, but if these distances could not be met, the safety officer had no quantitative way of expressing the additional degree of risk incurred. The only information provided to the commander was "this situation does not meet explosives safety standards." No attempt was made to determine the increased risk to the unit war fighting capability. In effect, the unit commander made decisions to violate DOD acceptable risk levels with no real knowledge of the impact of a mishap or enemy attack. In order to increase field level knowledge of explosives blast and fragment effects, the Air Force Inspection and Safety Center revised AFR 127-100 under a risk management concept. This paper outlines the development of this concept, its application at the field level, and its contribution to the Air Force warfighting capability.

II. Q-D and Probability

Quantity-distance criteria are the backbone of explosives safety risk assessment, in that they associate a given distance and explosives weight with the principal effects of blast overpressure and fragments. These criteria have been derived from empirical methods and, therefore, quite accurately determine the required separation for an assumed or permitted level of risk. The standard level of risk allowed for each type of exposed site is established by the Department of Defense to assure adequate protection of personnel and assets consistent with overall objectives. (1) Consequently, when deviating from these standards, proper authority within the Air Force must weigh the added risk against the strategic, or other compelling reasons that require such deviations.

The basic philosophy of explosives safety is that locations containing explosives, or potential explosive sites (PES), must be separated from each other and from other surrounding facilities and equipment, known as exposed sites (ES). This separation of the PES from the ES is referred to as quantity-distance (Q-D), and is based on a worst-case accident, known as the maximum credible event (MCE). The MCE, is expressed as the net explosives weight (NEW) which may be expected to react in a single event. These separations are determined by the formula $D = kW^{1/3}$ when D is the distance in feet, k is a factor identifying the risk assumed or permitted, and W is the NEW in pounds. With the known responses of individual ESs, (such as bombs, humans, aircraft,

facilities, etc) to specific levels of stimulus, a safe separation, i.e., assumed level of risks may be readily determined. DOD Q-D relationships define the acceptable risk with the assumption that the maximum credible event (MCE) will occur, that is the probability of occurrence is unity. An argument can be made that MCE=1 is not consistent with actual mishap experience. However, to use a probability of less than one requires some predetermination of how many times such an event is acceptable over a period of time, and how much loss one is willing to incur. That is the heart of the anomaly. Calculable disastrous results can't be acceptable on a probability basis, or more specifically, the DOD has not defined such acceptance. Thus, the central interest of risk assessment is the MCE, understanding what contributes to it, what will not contribute to it, and ultimately, measures that can be taken to limit or control it.

III. Hazard Properties

To pursue definition and control of the MCE, we must examine two specific hazardous properties of an explosion, blast and fragments. Testing has shown that the same blast overpressure is obtained at a distance proportional to the cube root of the weight of explosives involved in a detonation.

$$\frac{D_1}{W_1^{1/3}} = \frac{D_2}{W_2^{1/3}} = k$$

This is the derivation of K in the $D=kW^{1/3}$ formula used in Q-D calculations. A k-factor, then, indicates the level of overpressure, regardless of the quantity of explosives. This is a very useful concept as a k-factor (associated with a specific overpressure level) can readily be used to define expected damage at an ES. (Also note, the larger the k-factor, the greater the required distance.) Figure 1 is an example of several k-factors, and the associated PSI overpressure. Safe separation distance required is proportional to the NEW. With respect to the MCE, any method that demonstrates the ability to suppress blast may reduce the associated k-factor, thus reducing the required distance. For example, the standard earth-covered igloo functions as a blast suppresser, and a lesser k-factor is associated with this type of storage than would be used for the same explosives weight in above-ground (unsuppressed) open storage. Fragments on the other hand, exhibit different damage properties than blast. The DOD defines a lethal fragment as having 58 ft-lbs impact energy. The allowable hazardous fragment density to ESs not directly related to the combat mission is one per 600 feet. This can also be expressed as a probability of hit of less than 1%. Past explosives testing has demonstrated that in general, any amount of explosives between 100 and 30,000 pounds will propel lethal fragments 1250 feet. For a specific weapons configuration, the risk assessor must carefully compare the hazards from blast and fragments. (Figure 2)

There is another factor to consider in controlling a maximum credible event. If the risk assessor determines blast as the primary hazard, care must be taken to ensure that measures to suppress the blast do not contribute to the fragment hazard. This phenomena is demonstrated by hardened aircraft shelters (HAS). A HAS is constructed of reinforced concrete and heavy blast doors to resist overpressure from the outside, i.e., an enemy attack, and allow survivability

of the aircraft inside. For the purposes of risk assessment, one must consider the reverse situation. If the explosion occurs on the inside of a HAS, such as a weapons loaded aircraft accident, the failure mode of the heavily reinforced HAS walls contributes significantly to the fragment hazard. Explosives testing has demonstrated the need for increased k-factors for explosives if they are positioned inside a HAS.(2)

IV. Q-D Categories

We have demonstrated the proportionality between NEW, blast overpressure and distance. We must now turn our attention to the DOD mandated implementation of this principle.

Basically there are two cases to consider. The first case involves a sufficient degree of separation between neighboring PES, and the second case involves nonexplosive exposed sites, including facilities, work areas, roads, aircraft, equipment, etc., in the proximity of explosives storage, maintenance or employment areas.

Inhabited Building Distance (IB): This is the largest Q-D separation and is designed to protect civilian or unrelated base structures from blast and fragments. Associated k-factors range from 35 to 60.

Public Traffic Route (PTR): This Q-D separation applies to off-base roads, railroads, recreation areas and training areas. PTR is a lesser distance than IB, but still provides some protection from blast and fragments. Associated k-factors range from 24 to 30.

Intraline (IL): This separation is applied in several situations. It is used between explosive locations and maintenance areas where personnel are present as well as between explosives loaded aircraft and aircraft generation related facilities. It provides some protection from blast, but no fragment protection. The associated k-factor is usually 18.

Intermagazine (IM): This is the smallest Q-D separation, and it is used between explosives storage locations, and weapons loaded aircraft. It is the minimum distance required to prevent sympathetic detonation or propagation of explosion between PESs. It provides no fragment protection. The K-factor varies widely with the storage or employment situation, and ranges from 1.25 to 11.

Figure 3 is a summary of the Q-D separation categories, overpressure levels, and expected damage. This provides the basic tools of risk assessment.

In peacetime, the main thrust of explosives safety has been to protect civilians and unrelated base facilities from blast and fragments. In fact, the Secretary or Undersecretary of the Air Force must approve any Q-D violations involving off-base ESSs. A lower level of approval authority, generally at the AF Major Command is mandated for on-base violations. Therefore, at most Air Force locations, the funding priorities for correction of explosives safety problems tend to favor eliminating off-base civilian ESSs. In other words, enforcement of IB and PTR distances would appear to have priority over IL and IM requirements when working an explosives safety issue.

This has led to the impression that explosives safety is a peacetime function for protection of the civilian populace and has no real use for wartime operations. This is a serious misconception, and may adversely impact our warfighting capability if not alleviated. Explosives safety does, of course, have a peacetime obligation to limit loss of life and property damage, but it's really critical mission is preservation of combat capability. To understand the wartime mission, we must carefully examine the role of IL and IM Q-D separations in risk assessment.

V. RISK ASSESSMENT

To examine the value of installation level risk assessment, we will consider an accident that occurred 27 April 1969, at Danang AB, Vietnam. At 1030 on the morning of the accident, a security policeman observed a fire in the southeast corner of the Marine ammunition storage point (ASP), which was located next to USAF ASP-1 (See Fig 4). Attempts to fight the fire were unsuccessful, and the fire spread. Small explosions were heard, and burning debris was observed coming into USAF ASP-1. For the next seven hours, explosions spread throughout the Marine ASP, hurling large shrapnel fragments into USAF ASP-1 and starting small fires. (Figure 5) Delivery of munitions to the flightline stopped. At 1700, the initial explosion occurred at USAF ASP-1. An hour later, approximately 19 ammunition storage cells were destroyed (cratered, burning or buried). The explosions continued with diminishing intensity throughout the night.

The Marine ASP was almost completely destroyed. The USAF ASP-1 experienced extensive damage; the explosions destroyed or buried over 2.5 million pounds net explosives weight, and incurred costs of approximately \$5 million in facility repair (1969 dollars).

The two ASPs show very different damage patterns. The Marine ASP was completely destroyed, while damage to the USAF ASP-1 was limited. A comparison of the storage practices of the two services will account for the differences in the resulting damage. Figure 6 is a photograph of typical Marine ammunition storage at Danang AB. There were not enough storage revetments available, and ammunition was stacked in between the rows of revetments. This was a violation of established intermagazine distances and barricade (suppression) criteria. As a result, an explosion in one revetment propagated to the next revetment and so on. The improper storage rendered the revetments useless in suppressing sympathetic detonation and explosives propagation, and the entire Marine ASP was destroyed.

As mentioned in the account of the accident, burning debris and shrapnel were propelled from the Marine ASP into USAF ASP-1. The first high order detonation in the USAF area occurred approximately seven hours after the fire started. Figure 7 illustrates typical damage to USAF revetments. Out of 60 cells, 13 detonated high order, 4 burned, and 8 were buried. Although there are two sets of craters in adjoining revetments (row G, 8 & 9, and 5 & 6) eye witness testimony established that they were individual detonations caused by and shrapnel from the Marine ASP and, one did not propagate to the other. Some munitions items were improperly stored in between the revetments, and one stack of 2.75" rockets detonated sympathetically with the MK 82s in row G cell 5. (Figure 8)

The destruction of the Marine ASP compared to the more limited damage pattern in USAF ASP-1 is a good example of the role risk assessment plays in preserving the resources associated with combat capability. If munitions in USAF ASP-1 had not been properly warehoused very probably all 60 cells of munitions would have been lost instead of the 19 experienced in this mishap. Although this accident occurred from an accidental fire, an enemy attack could have produced similar results. Failure to follow intermagazine separations in a wartime situation can lead to a complete loss of combat capability.

VI. PLANNING FOR THE WARTIME MISSION

Reviewing the results of the Marine ASP disaster, and its impact on the Danang AB military operations, illustrates the importance of planning for preservation of combat capability. A weapons safety officer's responsibility to his commander is the identification of situations which have the potential to degrade warfighting ability.

When a Q-D problem is identified, several courses of action are possible. Reducing the Q-D by separating the explosives into smaller stacks may solve the problem. Figure 9 is an example of a 60,000 pound PES with an inhabited building ES violation. By separating the 60,000 pound PES into 2 stacks of 30,000 pounds spaced at intermagazine distance (to prevent propagation), the clear zone is reduced to accommodate the inhabited building ES. If this is not possible, an attempt may be made to suppress the mishap effects at the PES or the ES. Suppressing the mishap effects at the PES is difficult, because reinforcing or hardening explosives storage buildings may contribute to the fragment hazard, as evidenced in the HAS example earlier in this paper. However, earth barricades may be constructed at a PES and reduce Q-D requirements in some cases. Hardening at the ES may be as simple as protection with sandbagging, or may involve expensive real property modifications to walls and roofs. If smaller quantities of explosives or suppressing mishap effects are impractical, an explosives safety exception may be required.

Figure 10 outlines the steps the weapons safety officer follows in determining the degree of risk to the exposed sites. When the overpressure level is calculated, the chart at Figure 11 is used to predict the damage, and the resulting mission impact is provided to the Commander.

The weapons safety officer concentrates on three primary areas of activity; the weapons storage area, the flightline, and facility site planning.

Proper storage of ammunition is critical, as the Danang AB accident graphically illustrated. The weapons safety officer must constantly inspect all munitions storage areas for compliance with quantity-distance criteria. These inspections must also include general industrial safety and fire prevention efforts. If the military unit's mission calls for delivery of additional ordnance for specific combat scenarios, the weapons safety officer must ensure that the weapons storage area is capable of properly storing the ordnance as it is delivered, and provisions are made for build-up areas that will meet quantity-distance requirements.

On the flightline, review of aircraft parking plans and aircraft loading procedures is essential. An aircraft loaded with munitions is an explosives hazard, presenting a risk assessment problem similar to the storage situation. The aircraft must be positioned an adequate distance apart or barricaded to prevent an explosion of one propagating neighboring aircraft. This situation is often complicated with delivery of munitions to the flightline, and the position of explosives holding areas relative to the aircraft. The wing weapons safety officer must carefully analyze generation flow plans and explore ways to reduce risk by regrouping aircraft, or changing the sequence of aircraft loading. In the dynamic world of aircraft maintenance, on the spot risk assessment decisions may be necessary during wartime operations as aircraft are generated. If wartime clear zones must be expanded beyond peacetime limits, wing war plans should ensure provisions for evacuation of inhabited facilities exist. If functions not directly related to the combat aircraft generation activities can be temporarily relocated, capacity of hardened aircraft shelters and flightline holding areas may be increased.

Facility site planning is another area critical to wartime survivability. The obvious case is intermagazine and intraline spacing of facilities in the weapons storage area. However, many survivability gains can be made by planning flightline maintenance facilities and work areas. For aircraft generation facilities that must be near the flightline, design features can be incorporated into the construction plans to reduce the risk to personnel and equipment. Simple things, such as orienting windows and doors away from the ESs will greatly reduce personnel injury flying glass and debris. More expensive modifications, such as hardened roofs, reinforced walls or earth barricades may be feasible for protection of especially valuable test equipment or spare parts. Another aspect, often overlooked in long range planning, is natural terrain. Although airfields are generally "pool tables", it may be possible to position aircrew facilities, maintenance areas or supply warehouses into the sides of hills or underground where susceptibility to blast and fragment hazard is greatly reduced.

Many research and development projects and quantity distance tests are underway to develop technological solutions to explosives safety problems. Currently the Air Force is testing high explosive general purpose (GP) bomb propagation using inert material and low explosive cluster bombs as barricades (3). In some cases, stacking the barricade materials between stocks of GP bombs will increase the explosives storage capacity of igloos 2 or 3 times without increasing the risk of propagation. Also, testing of other munitions has demonstrated configurations and containers that prevent explosive propagation. Future test efforts of inventory items will be focused on real world Q-D problems encountered during wartime aircraft generation scenarios. Another research and development program is designing barricade materials that can be positioned within explosives pallets or, or between explosives stores loaded on aircraft (4). This will reduce the MCE to the explosion of one bomb, allow for greater flexibility on aircraft generation flow plans. A long range goal is development of an insensitive high explosive (IHE.) An IHE is an explosive that is so insensitive, an explosion or a fire will not cause sympathetic detonation or propagation. This will be a breakthrough in reducing the maximum credible event, but it is quite far in the future, and existing stocks of conventional munitions will complicate Q-D requirements.

VII. CONCLUSION

Although creative Q-D testing and technology efforts are aimed at reducing the NCE, there is no foreseeable panacea for eliminating the risk of accidental explosive propagation from wartime operations. Written was plans usually contain Annex N, which is the Safety Annex. This is an excellent format for weapons safety officers to document localized risk assessment considerations, and provide planners with information critical to survival of the combat capability. Review of base comprehensive plans maintained by civil engineering, and long-range military construction project submittals with an effort to preserve existing clear zones and maintain Q-D separations will minimize future risk management problems.

Wing weapons safety officers must be trained in risk assessment concepts, and work closely with operations personnel, maintenance and civil engineering community planners. It is not an easy job, and many difficult risk management decisions must be made by the wing commander.

FOOTNOTES

- (1) This guidance is found in DOD 6055.9-STD, Ammunition and Explosives Safety Standards. Specific Air Force implementation is found in AFR 127-100, Explosives Safety Standards.
- (2) This was established by the Distant Runner test, 1982.
- (3) This series of tests involving bulk storage of GP bombs started in 1985 and is still in progress.
- (4) This project is known as HAVE BLOCK. Tests started in 1984, and are still in progress.

<u>K-FACTOR</u>	<u>OVERPRESSURE</u>
6	27.0
18	3.6
40	1.2

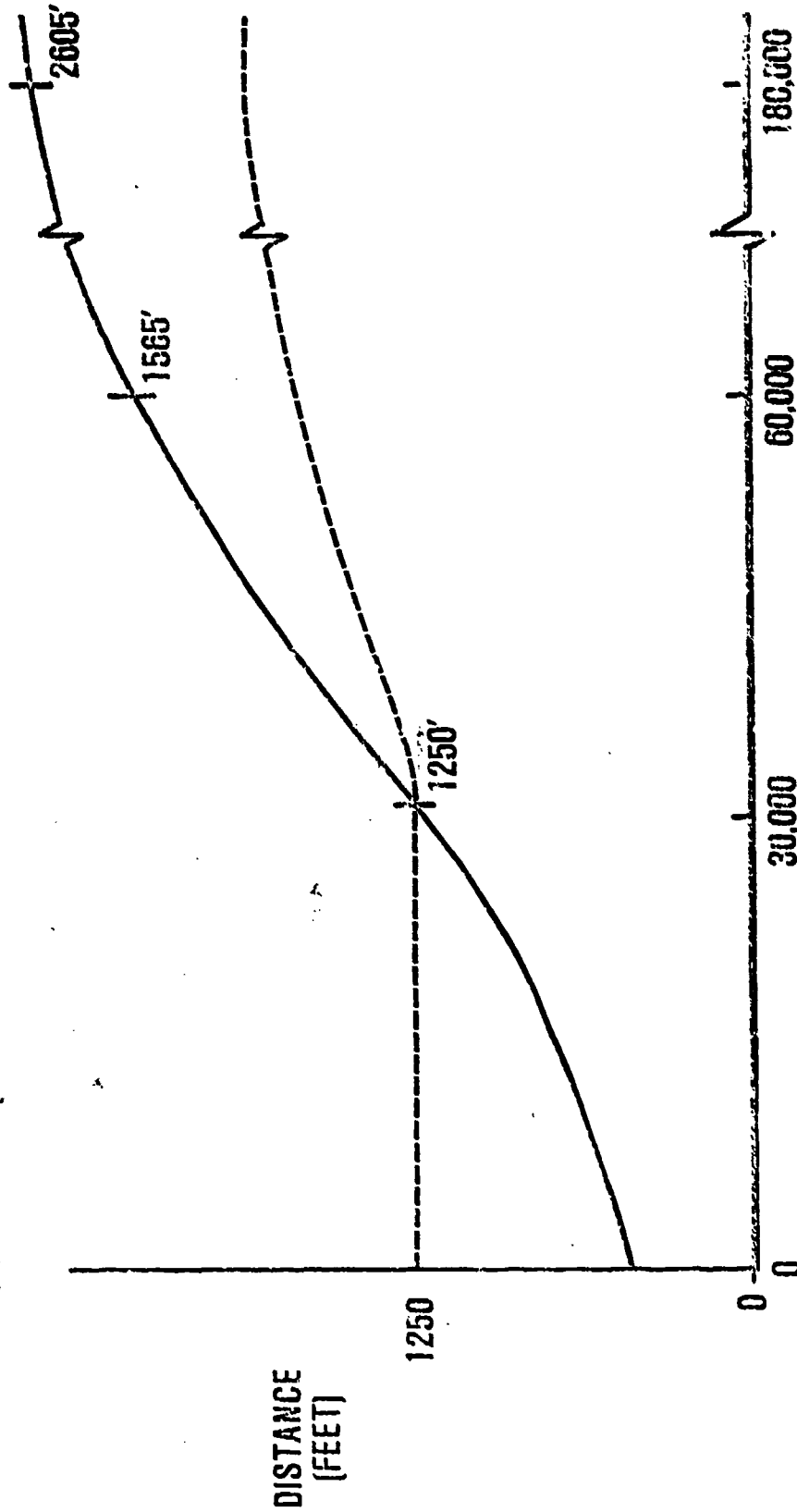
Figure 1

PRIMARY HAZARDS ASSOCIATED WITH EXPLOSIVES

○ DISTANCE REQUIRED FOR NET EXPLOSIVE WEIGHT (NEW)

— BLAST (GREATER THAN 1.2 PSI OVERPRESSURE - BROKEN GLASS/TEMP HEARING LOSS)

--- FRAGMENTS (ONE LETHAL FRAGMENT IN 600 SQ FT)



NET EXPLOSIVE WEIGHT

Figure 2

INHABITED BUILDING

PUBLIC TRAFFIC ROUTE

INTRALINE

INTERMAGAZINE

OVER 10 PSI

SOURCE

SYMPATHETIC DETONATION

3.5-10 PSI

DEATH

FACILITY DAMAGE

SERIOUS INJURY

1.2-3.5 PSI

INJURY

FACILITY DAMAGE

0.85-1.2 PSI

MINOR INJURY

BROKEN GLASS

Figure 3

Figure 4

Marine ASP

Row E

F

G

H

Air Force ASP-1

Figure 5: Ground view of explosions
in Marine ammunition
storage point





Figure 6: Aerial photograph of Marine ammunition storage point



Figure 7: Aerial photograph of Air Force ammunition storage point. Revetment E-19 detonated, burying neighboring revetments E-18 and E-20. Explosion did not propagate.

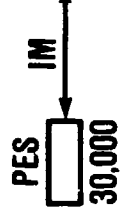
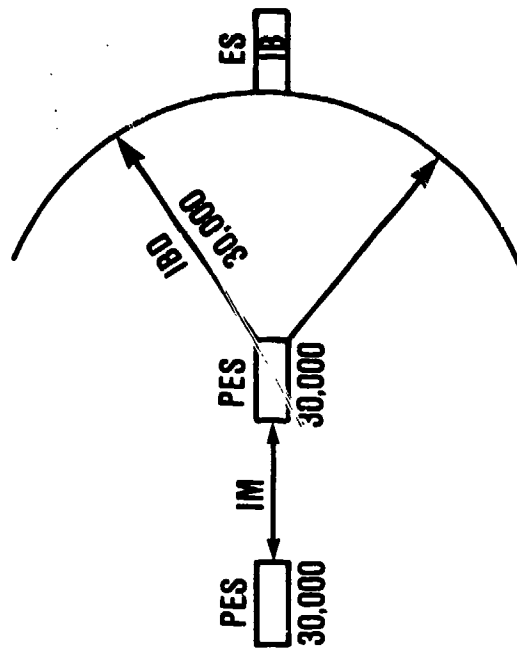
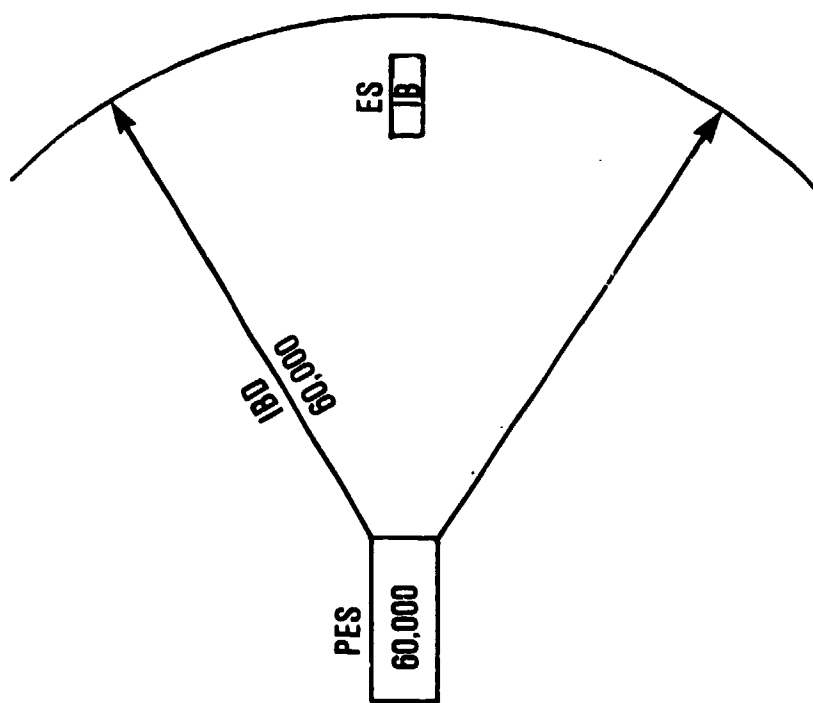


Figure 9

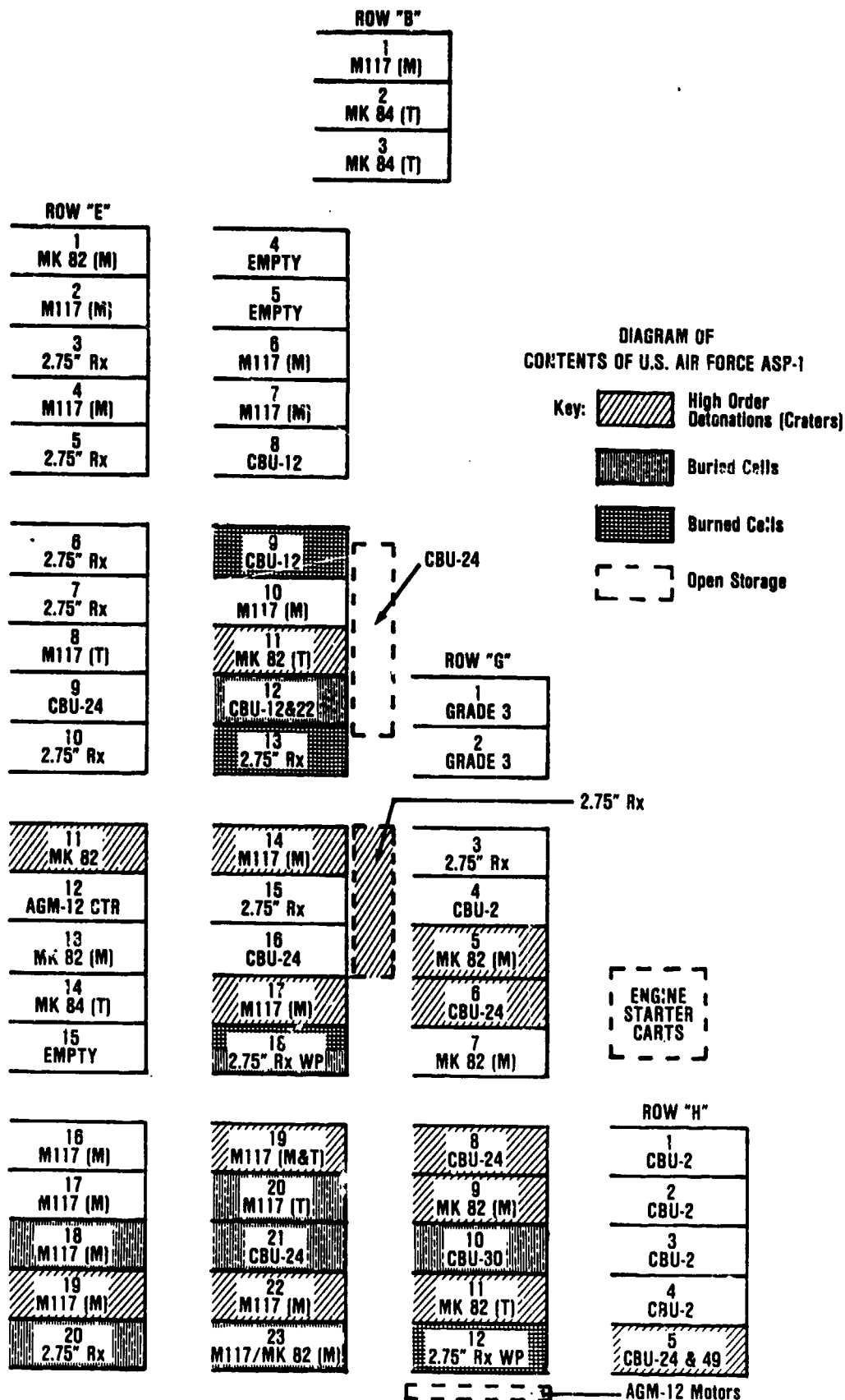


Figure 8
1622

RISK ASSESSMENT

- IDENTIFY PES
- IDENTIFY EXPOSED SITE
- USE $D = K \times \text{NEW } 1/3$
 - CALCULATE REQUIRED SEPARATION DISTANCES/NET EXPLOSIVES WEIGHTS
 - CALCULATE PROBABLE DAMAGE TO ES

ELEMENT	DAMAGE	SIDE ON OVERPRESSURE
Aircraft	Control Surface or other minor damage	1.0-2.0
	Major repair	2.0-3.0
	Complete destruction	4-10
Glass windows, large and small	Shattering, occasional frame failure	0.5-1.0
	Severe frame failure	1.5-3.0
	Roof rafters cracked	0.5-1.5
Wood frame structures	Studs and sheathing cracked	1.0-3.0
	Collapse	over 3.0
Metal (Butler type) buildings	Corrugated aluminum/steel paneling moderately buckled/joints separated	0.5-1.0
	Severe buckling/some panels torn off	1.0-2.0
	Complete destruction of siding/interior destroyed	over 3.0
Concrete block or brick wall, 8-12 inches (unreinforced)	Sever damage/shattering	1.0-2.0
	Collapse	7.0-8.0
	Shattering	1.0-2.0
Corrugated asbestos siding	Moderate cracking	3.0-4.0
	Severe spalling/wall displacement	6.0-8.0
	Concrete shatters, bare steel remains	10-14
Reinforced concrete walls	Complete destruction	14-20
	Slight damage	2.5-1.5
	Severe damage	3.0-4.0
Liquid storage tanks (unpressurized)	Collapse	8-10
	Complete destruction	10-14
	Moderate damage	6-8
Vehicles/trailers	Complete displacement	8-10
	Destruction	14-20
	Blown down	30

Figure 11

WHO IS AFRAID OF RISK CRITERIA?

by

Hans A. Merz
Ernst Basler & Partners
Consulting Engineers
Zurich, Switzerland

ABSTRACT

In recent years risk analyses using numerical probability estimates and consequence forecasts for accidental events have become a widely accepted technique for dealing with safety problems in the explosives industry. Considerable effort is put into acquiring data for the technical part of such analyses. When it comes to discuss the acceptability of the numerical risk estimates, differing opinions and even confusion can be observed.

This paper presents proposals for numerical risk criteria and their background. It will deal with the following fundamental aspects of risk appraisal:

1. In risk appraisal **different points of view** have to be considered:
 - a) The individual person exposed to a particular hazard (individual risk)
 - b) Society (collective risk)
 - c) The enterprise or operator (perceived collective risk)
2. **Risk acceptance depends on the characteristics of a risk situation.** Based on parameters such as the ability to control, avoid and influence a risk situation, different risk categories can be defined.
3. For a full risk appraisal the following **numerical risk criteria** have to be defined:
 - a) Maximum individual risk as a function of the risk categories
 - b) Willingness-to-pay for saving a human life as a function of the risk categories
 - c) Aversion function for low-probability/high-consequence events

Presented at the 22nd Department of Defense Explosives Safety Seminar, Anaheim, USA, 26-28 August 1986

INTRODUCTION

In recent years risk analysis techniques have gained increasing acceptance in many technical fields, including explosives safety. General consensus has been reached that safety of a process or a system is best described by the probability of accidents and their consequences. A steadily increasing number of papers are published dealing with methods and data to estimate probabilities and to determine the consequences of accidental explosions in manufacturing, transport and in the storage of ammunition and explosives.

However, when it comes to decide about the acceptability of a safety situation on the basis of calculated risk values, confusion and controversies can be observed. Some are calling for the politician to determine acceptable risk levels; others try to compare the risk values with risk from daily life. But nobody seems to be really happy. Even the opinion can be heard that the risk analysis technique will fail as a useful method in the future, because no consensus on risk criteria can be found.

This paper aims at clarifying the discussion about **RISK CRITERIA**. It presents the background and the general nature of such criteria and proposes numerical values. They have been developed in the course of the investigation of practical safety problems. They have been applied to a number of case studies in various technical areas and always lead to meaningful and acceptable solutions.

GENERAL MODEL OF SAFETY ASSESSMENT

The purpose of a safety assessment is to determine, if a process or a system can be considered safe enough or if additional safety measures are necessary. In order to answer this question it is essential to distinguish between the two parts of the assessment process (see figure 1):

1. The "objective" and technical part of **RISK ANALYSIS**: Its aim is to obtain a realistic view of the quantitative proportions of the risk involved. It involves the determination of the probabilities of accidental events and the quantitative description of their expected damage. Risk analysis is the domain of the technical experts. Here a large array of technical tools can be applied from fault-tree techniques, statistical analysis, simulation and field-trial to experience and expertise.
2. The "subjective" part of **RISK APPRAISAL**: Its aim is to discuss and define risk criteria in an explicit and quantitative way. Such criteria are the basis for the distinction between a safety situation to be considered as "safe and acceptable" or one to be considered as "unsafe and unacceptable". Risk appraisal is a question of our subjective value judgements and therefore does exceed the domain of the technical expert. Here, interdisciplinary expertise is necessary.

The distinction of these two parts is an important step toward clarifying the nature of safety assessments. However, this distinction should not lead to the wrong conclusion that risk analysis and risk appraisal are

completely independent elements. First of all it must be observed that a "common language" is indispensable: The result of a risk analysis must be such that it can be interpreted in the risk appraisal process or, the other way round, the input for risk appraisal must be defined such that it can be produced by risk analysis. Secondly, both parts are connected by the same important requirements of quantification. Risk assessment can only be successful if the risks as well as the risk criteria are expressed in quantitative terms.

THREE FUNDAMENTALS OF RISK APPRAISAL

1. Safety is a Matter of the Standpoint

Many publications on risk analysis start with the following definition of risk: risk is the product of the probability and the consequence of an accident. With other words, risk is equal to the expected damage. Though this is a correct statement it definitely is, at the same time, also an incomplete definition of risk.

When talking about risks we always have to distinguish between three different standpoints (see Figure 2).

1. Standpoint of an **INDIVIDUAL** exposed to a hazard:

An individual exposed to a hazard is primarily concerned with the questions: How large is the probability that I will be killed or injured in an accident? How much does my individual risk due to this hazard increase my normal fatality rate?

In order to account for this standpoint in a risk analysis it is therefore necessary to introduce the so-called **INDIVIDUAL RISK** defined as the (usually annual) probability that an identified person will be killed or injured as a consequence of an accident.

2. Standpoint of the **SOCIETY**

Besides being interested in guaranteeing minimum individual risk for each of its members, society is concerned about the total risk to the general public: How large are the total losses (e.g. per year) from a hazardous activity?

To describe this standpoint the afore-mentioned definition of risk as the expected damage of an activity applies. In the following this risk, describing the standpoint of society, will be called the real **COLLECTIVE RISK**. If expressed in terms of annual risks, it corresponds to the respective value shown in annual accident statistics.

3. Standpoint of the **INSTITUTION RESPONSIBLE FOR THE ACTIVITY**

The institution responsible for an activity can be a private company or a government agency. From their point of view it is not only essen-

tial to keep individual risks of employees or other persons and the collective risk at a minimum. An institution is also concerned to avoid catastrophic and spectacular accidents. As experience clearly demonstrates (Bhopal, Seveso, Challenger, etc.) that such catastrophic accidents damage the reputation, the image and even the prosperity of the institution responsible for the activity. Due to this, survival in the market can be threatened, or more stringent regulations called for by politicians might be the result. Therefore, an institution can even be interested in having higher safety standards than the individual or society request, especially when it comes to avoid rare but catastrophic accidents.

In order to account for this standpoint, the so-called **PERCEIVED COLLECTIVE RISK** must be introduced. In simplified terms, the perceived collective risk is the above mentioned collective risk weighted by a so-called risk aversion factor.

In summary it can be stated that for a complete description of a risk situation the risk values of all three identified standpoints have to be expressed in quantitative terms in a risk analysis, i.e.:

- The individual risk of all exposed persons
- The collective risk of accidents
- The perceived risk of accidents

2. Risk Valuation depends on the Nature of Risks

In many publications on risk acceptance elaborate tables can be found in which risks from various activities are compared. The risks from nuclear power are compared with the risks of flying in a aircraft, the risks from smoking are compared with those from chemical plants and so on. Experience clearly shows that such comparisons usually create more confusion than clarification. As a classical example of this confusion, the discussions about the radiological hazard to the population after the Chernobyl accident can be mentioned.

Risk comparisons are tricky, because not all risks are equal in their nature and therefore not all risks should be thrown into the same basket! There seem to be primarily two factors which determine the nature of a risk and its acceptance level (see figure 3):

- **DEGREE OF SELF-DETERMINATION** which itself depends on the ability of the involved people to know the risk, to avoid it and to influence it
- **DEGREE OF PERCEIVED BENEFIT** from the hazardous activity

So-called "voluntary" risks are characterized by a high degree both of self-determination and perceived benefit (eg. mountain climbing). So-called "involuntary" risks are on the other hand characterized by a very low to non-existent degree of self-determination and perceived benefit (eg. passing ammunition storage installation). Between the two extremes there are intermediate situations of risks.

Experience as well as our own intuition show that the acceptance of risk decreases with decreasing degrees of self-determination and perceived benefit. This explains why - for example - the comparison of risks from smoking (highly voluntary) with risks from a chemical factory (involuntary) is intuitively not accepted. The resulting confusion stems from the fact that the acceptance level of these two risks is not the same.

For the sake of practicality and based on experience collected in many case studies it is proposed to define four **RISK CATEGORIES** (see Figure 3) with decreasing risk acceptance from Category 1 to 4:

- CATEGORY 1 comprises the voluntary or nearly voluntary risks
- CATEGORY 2 comprises risks of high self-determination
- CATEGORY 3 comprises risks of low self-determination
- CATEGORY 4 comprises the involuntary or nearly involuntary risks

In summary, it can be stated that only those risks can directly be compared which fall into the same category, and that the level of the general risk acceptance depends on the category into which a particular risk falls. This applies to individual risks as well as to real and perceived collective risks.

3. Risk Appraisal requires Quantification of Risk Criteria

1. Risk Criteria for INDIVIDUAL RISKS

As mentioned before the individual risks are defined by the annual probabilities that identified individuals will be killed or injured by a hazardous activity. A characteristic feature of individual risk is the fact that very often large differences exist between the persons exposed to the same hazard (see Figure 4). In order to assure that the individual risk of a person is not the dominant part of his annual mortality rate and for reasons of equity it is essential that the size of the individual risks has to be limited for each individual. It is therefore not enough if the average individual risk of all exposed persons is below the limit, but that ALL individual risks are smaller or equal to it.

In setting the quantitative values for the **MAXIMUM ACCEPTABLE INDIVIDUAL RISKS** it has to be considered that not all risk are equal in nature and that these values must be a function of the previously mentioned risk categories. It is obvious that the maximum acceptable individual risk must decrease from Category 1 (voluntary risks) to Category 4 (involuntary risks).

Figure 4 proposes quantitative values for maximum acceptable individual risk as a function of the risk categories. For Risk Category 4 (involuntary risks) a value of 10^{-5} per year is proposed. Individual risks below this value are not of importance for an individual when compared with his total natural mortality rate. For Risk Category 1 (voluntary risk) a value of 10^{-2} per year is proposed. Experience shows that this value seems to be an "intuitive" upper limit, since

higher risks are rarely taken deliberately by persons. For risk situations located in Categories 2 and 3 the maximum individual risks lie in between these two numbers.

The line in figure 4 can also be interpreted as a dividing line between the responsibility of society and those of an individual. An individual striving for a negligible individual risk of 10^{-5} per year can take from this figure how much society will do to reach this goal and how much he must contribute himself. In a voluntary risk situation almost full responsibility rests with the individual. In an involuntary risk situation, however, he can rely on society, since most if not all responsibility rests with society.

2. Criteria for Collective Risks

In contrast to the individual risk, where the criteria consists in a fixed maximum acceptable limit, an absolute limitation of collective risks is not meaningful. There is no universal value for an acceptable collective risk, though it was often postulated in recent years. It can be shown that a fixed limitation is not reasonable if society is seeking to minimize the total collective risks.

The basis for any decision about the acceptability of collective risks is the so-called **RISK-COST DIAGRAM** shown in Figure 5. This diagram shows, how much an existing collective risk of a hazardous activity can be reduced if more and more safety measures were taken and therefore if more and more money would be invested in safety. The elaboration of such a risk-cost diagram is a mostly technical task and is part of the risk analysis. With other words, risk analysis is not finished when existing collective risks have been calculated, but only when it has been shown with this risk-cost diagram how and at what expenses the risk can be reduced.

The typical shape of the risk cost curve in Figure 5 indicates, that the collective risk could be reduced to negligible values, provided that the corresponding cost can be afforded. Since the resources of our society are limited, we face the well-known problem: Which strategy should we choose to obtain the least collective risk with limited resources? From economic theory it is known that in such situations the marginal costs must be the decision criteria.

With other words, this criteria tells us to stop our safety measures as soon as the marginal costs of the next safety measure exceed a - yet to be determined - value. This value, however, corresponds to the so-called **WILLINGNESS-TO-PAY** to save an additional life. It can therefore be stated that a collective risk can be considered as acceptable, if the costs of the next safety measures for saving an additional human life would exceed the determined willingness-to-pay.

In determining the quantitative values for the willingness-to-pay it has again to be considered that not all risks are equal in nature and that values must be a function of the previously mentioned risk categories. It is again obvious that the willingness-to-pay to save a human life is larger when the risks are involuntary than when they are voluntary.

Figure 5 proposes quantitative values for the willingness-to-pay as a function of the risk categories. For Risk Category 4 (involuntary risks) a value of 10 million Swiss francs or presently about 6 million US-Dollars is proposed. For Risk Category 1 (voluntary risks) a value of less than 1 million Swiss francs at current exchange rates of less 600'000 US-Dollars is proposed. For risk situations located in Categories 2 and 3 the values lie between these two numbers.

Two important comments have to be added at this place:

- The value of the willingness-to-pay does not imply a valuation of the human life. Such a valuation would be naïve. The criterion of the willingness-to-pay expresses, however, that our limited resources do not allow us to spend unlimited amounts of money to save a human life. Furthermore, it tells us how we should allocate our limited resources such that maximum risk reduction can be obtained.
- Determining the values of the willingness-to-pay is a matter of value judgements. There are not "correct" or "wrong" values. The proposed numerical values have been derived from past decisions about safety issues. They reflect the way how our western societies seem to think today intuitively about the willingness-to-pay to save a human life.

3. Risk Aversion Phenomenon

The risk aversion phenomenon appears as soon as the standpoint of the institution responsible for an hazardous activity is considered. It takes into account that an institution is in addition interested in avoiding catastrophic or otherwise spectacular accidents, since such events can damage reputation, image and the market position or could lead to more stringent regulation.

Risk aversion is an element of the formal decision theory and can be accounted for by **RISK AVERSION FACTORS**. Such factors lead to an increase of the collective risk and are usually a function of the number of fatalities. The perceived collective risk is therefore always higher than the real collective risk.

Determining the risk aversion factor is a matter of the institution responsible for the hazardous activity. It must be a value judgement by the management and take into account the special circumstances of the institution and of the hazards at stake. Therefore numerical proposals for risk aversion functions cannot be made.

In Figure 6 examples of risk aversion functions taken from actual case studies in Europe are presented.

Once perceived risks have been calculated, using an appropriate risk aversion function, the acceptable perceived risk value can be found with the same method as shown above and by applying the same values for the willingness-to-pay to save a human life.

CONCLUDING REMARKS

The ideas contained in this paper are not new. In previous seminars many of them have been presented in one way or another (Lit. 1, 3). At that time, however, these ideas were new and almost revolutionary. And the test of the practical application was limited to a few case studies. In the meantime much experience with this method has been collected in various fields, such as

- Fabrication of ammunition and explosives (Lit. 4)
- Storage of ammunition (Lit. 5)
- Transport of dangerous goods (Lit. 6)
- Railway Safety (Lit. 7)
- Railroad Grade Crossing Safety (Lit. 8)
- Traffic Safety (Lit. 9)
- Natural Hazards Safety (Lit. 10, 11)

In all these practical applications this method proved to be a most powerful instrument. In all cases it produced realistic and practical results, which could be accepted both by the responsible management as well as by the authorities.

The application of the method to safety problems in a number of different fields underlines its broad applicability. However, it must be stated that this method is limited to the assessment of hazard with predictable and immediate detrimental effects. The proposed risk categories and the risk criteria do therefore not apply to accidents with hardly predictable long-term hazards to health or life (e.g. accidents with radiological consequences, etc.)

LITERATURE

1. Th. Schneider, "How Much Should we be Willing to Pay for Explosives Safety?", 18th DDESB Seminar, San Antonio, Texas, 1978
2. Th. Schneider, "Practical Application of Quantitative Risk-Cost-Criteria to Explosives Safety", 19th DDESB Seminar, Los Angeles, California, 1980
3. H.A. Merz, "The Low Probability of Accidental Explosions: Isn't it worth a Cent in Explosives Safety?", 20th DDESB Seminar, Norfolk, Virginia, 1982
4. H.A. Merz, "Methods of Quantitative Risk Assessment: The Case of the Propellant Supply System", 21st DDESB Seminar, Houston, Texas, 1984
5. Eidgenössisches Militärdepartement: "Technische Vorschriften für die Lagerung von Munition (TLM 75)"
(Swiss Regulations for Ammunition Storage)

6. Gruppe für Rüstungsdienste/Bundesamt für Rüstungsbetriebe: "Sicherheitsmässige Beurteilung des Explosivstofftransportes zwischen einer Munitionsfabrik und ihrer Aussenlager", 1981
(Safety of Transport of Explosives between a Factory and their Storage Facilities)
7. Deutsche Bundesbahn: "Sicherheitskonzept für die Tunnel der Neubau-
strecken", München, 1983
(Safety of High-Speed Transportation Systems)
8. Deutsche Bundesbahn: "Sicherheitsanforderungen an Bahnübergängen",
München, 1985
(Safety of Railway Grade Crossings)
9. Schweiz. Beratungsstelle für Unfallverhütung: "Beurteilung des Un-
fallgeschehens aus der Sicht des individuellen und kollektiven Risi-
kos", Bern, 1985
(Assessment of Road Accidents with Respect to Individual and Collec-
tive risks)
10. Sanasilva: "Sicherheitsbeurteilung zur Erfassung von Naturgefahren im
Berggebiet", 1986
(Safety Assessment of Natural Hazards in Mountainous Regions)
11. Ernst Basler & Partners: "Risk Analysis - Is it a Useful Tool for the
Politician in Making Decisions on Avalanche Safety?" Paper to be pre-
sented to the International Avalanche Symposium, Davos, Switzerland,
14-19 September, 1986

The reports No. 5 to 10 are in German. They can be obtained from the author on request, provided that the sponsoring agency gives permission. A summary version in English exists for report No. 7.



Figure 1: General Model of Safety Assessment

1. Safety is a Matter of the Standpoint !

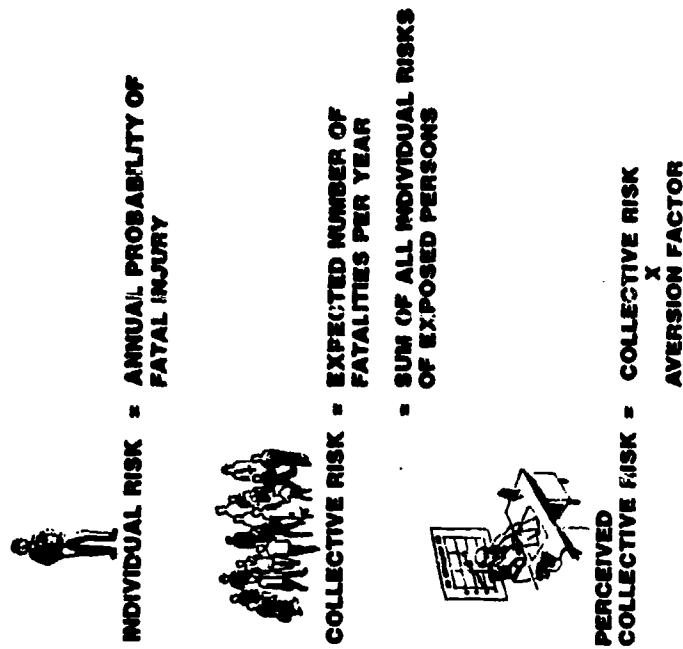
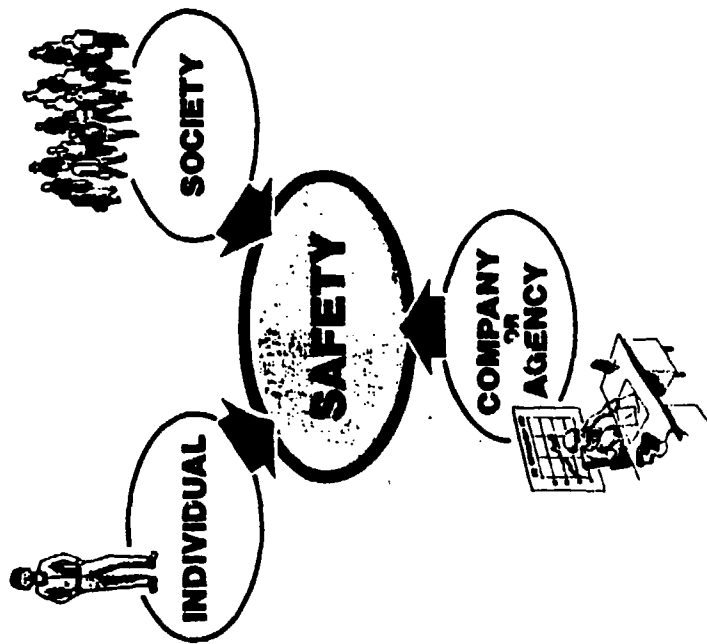
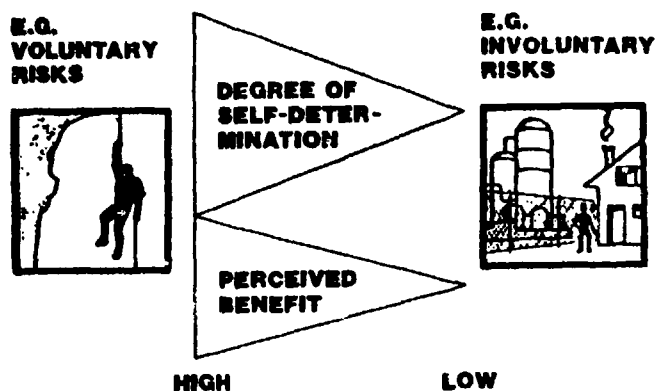


Figure 2: Standpoints towards Safety

2. Risk Valuation Depends on the Nature of Risks !



RISK CATEGORIES			
Category 1	Category 2	Category 3	Category 4
"Voluntary"	Large Degree of Self-Control	Small Degree of Self-Control	"Involuntary"

Examples

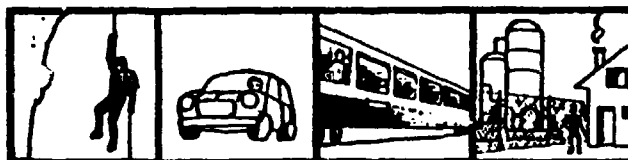


Figure 3: Risk Categories and Risk Acceptance

Quantification of Risk Criteria

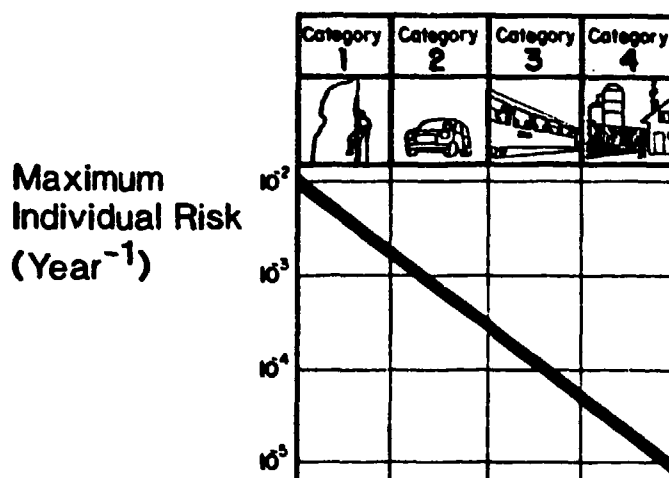
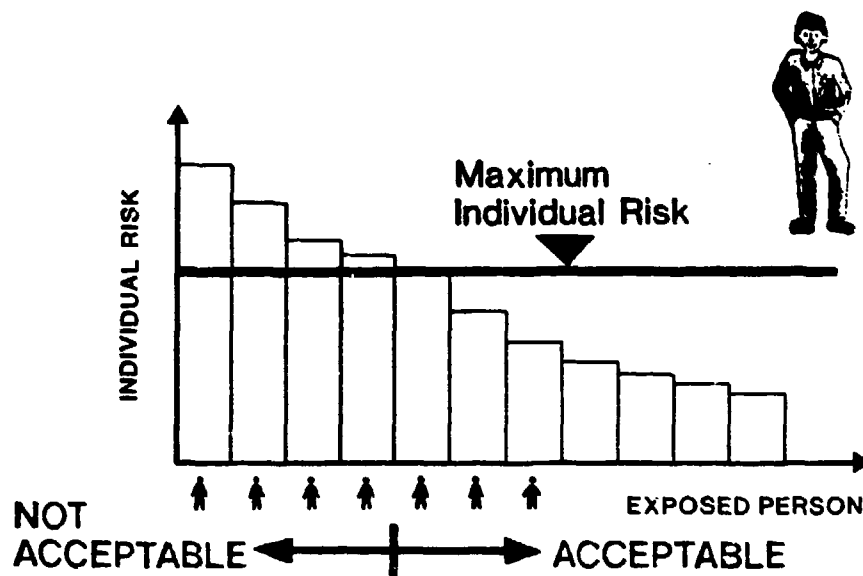
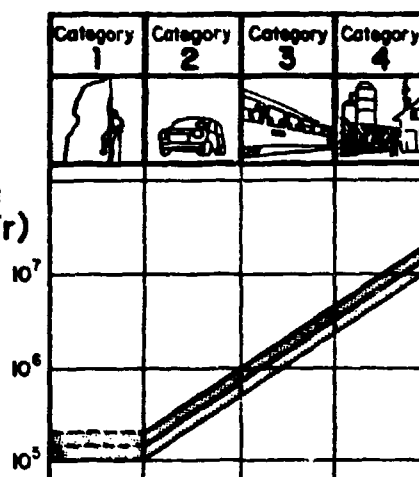
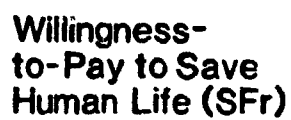


Figure 4: Criteria for Individual Risk



1638

Quantification of Risk Criteria



AVERSION

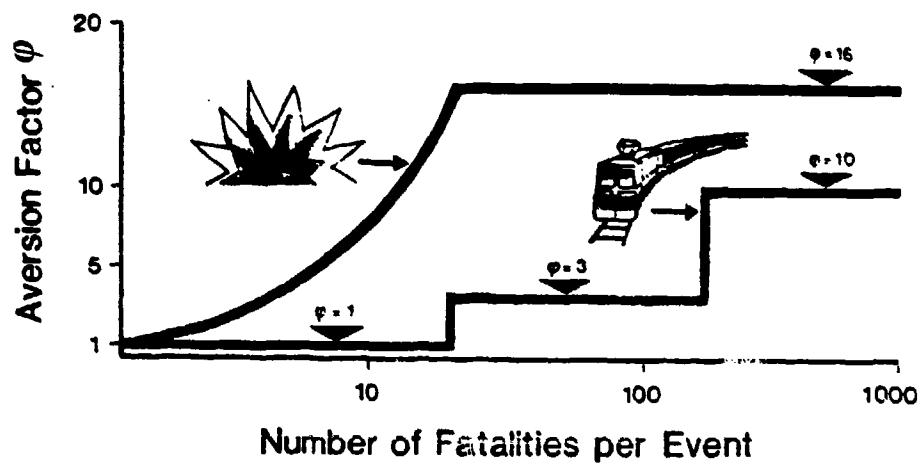


Figure 6: Example of Risk Aversion Functions

AD-P005 368

BLAST TESTING OF EXPEDIENT SHELTERS IN MODEL SCALE

by

Edward D. Esparza
Southwest Research Institute
San Antonio, Texas

22nd Department of Defense Explosives Safety Seminar
26-28 August 1986

ABSTRACT

A research program was conducted to evaluate the blast resistance of expedient fallout shelters designed for the civilian population in the event of a nuclear attack. As part of this research, model size shelters of six different designs were tested in a shock tunnel at average overpressure levels of 2.8, 4.6, and 8.8 psi. Measurements of the external blast pressures and internal pressure leakage into the model shelters were made. The expedient shelters tested utilize, in general, shallow soil excavation, load-bearing members of timber or doors, and soil-covered roofs. Replica model sizes were selected so that the shock tunnel load durations were long enough to test in the quasi-static load realm. An elevated soil section was used in the tunnel to test 96 response models in 12 experiments. Some of the shelter designs survived at every overpressure level very well, while other test items suffered structural failures in almost every case. This paper presents a brief description of the experiments, including some details of the shelters, of the model fabrication and pressure measurement system, and a summary of the results.

INTRODUCTION

A number of do-it-yourself shelters have been designed and recommended for providing protection to families or other small groups from deadly radiation and radioactive fallout generated by a nuclear detonation [1,2]. Shelter designs vary to accommodate different local soil conditions and available materials. For example, in areas where below ground shelters are impractical due to a shallow water table or bedrock, the expedient shelter recommended would be above ground. For areas with an abundance of small trees, the structural materials specified are wooden poles of various lengths. For areas where there is a shortage of small trees, household doors are used as the load-bearing members. However, for all designs, a thick earth cover and walls are used as the primary radiation shield.

Some of these shelters had been tested in high explosive nuclear simulation tests [3,4]. Generally, the results of these limited tests yielded qualitative results of a shelter at a particular overpressure range. To better evaluate the level of blast protection expedient shelters provide to occupants, an analytical and experimental program was conducted by Southwest Research Institute (SWRI) [5]. In this program, a literature search was conducted to identify expedient shelter designs. Eight selected designs were then evaluated analytically to determine expected failure mechanisms and to estimate the blast overpressures at which structural failures such as overturning, trench collapse, or roof collapse would be expected to occur. Six different shelter designs were then tested in a shock tunnel in model scale after several physical models were considered. Replica models were used because of the limitations on the available shock tunnel facility. The results from a series of twelve experiments involving 56 structural response models were used to determine the blast protection provided by each of the six types of shelters tested. Complete details of this shelter evaluation program are found in Reference 5. This paper presents brief descriptions of the six expedient shelters tested, an overview of the test program, some details of the experiments and pressure measurement system, examples of pressure traces, and a summary of the results.

DESCRIPTION OF EXPERIMENTS

Shelters

The six expedient shelters selected for testing are depicted in Figures 1-6 and were as follows:

- Door-covered trench shelter
- Above ground door-covered shelter
- Crib-walled shelter
- Ridge pole shelter
- Small pole shelter
- Log-covered trench shelter

The below ground shelters generally utilize an excavation with a soil-covered roof to provide protection from fallout. The earth cover is specified to be a minimum of 2 to 3 feet deep and is supported on a load-bearing roof of timbers or household doors. The excavations are about 4 to 6 feet deep with vertical walls. The above ground shelters have very shallow or no excavation specified in their construction. They use an earth-covered, load bearing roof of timbers or wooden doors about 1.25 to 2 feet deep, and an earth-mound or earth-filled walls about 2 to 4 feet deep.

For the shelters tested, the primary criterion for shelter acceptability was that occupants not be mortally injured. The damage mechanisms that were used to evaluate the level of protection the shelters afforded the occupants were classified as the exposure to overpressure, debris impact/burial, and occupant translation/impact. Because structural failures would create any or all of these occupant damage categories, failure modes for each of the shelters tested in model scale were identified and are listed in Table 1.

Scaling Considerations

A complete model analysis was conducted. Twenty parameters were used to describe the blast loading, ambient conditions, the soil, the shelter structure, and the shelter response. Using the Buckingham Pi Theorem [6], a set of 17 independent dimensionless ratios called pi terms was developed. Model and prototype systems are equivalent when the dimensionless ratios are the same in both. Sometimes this specific requirement cannot be satisfied

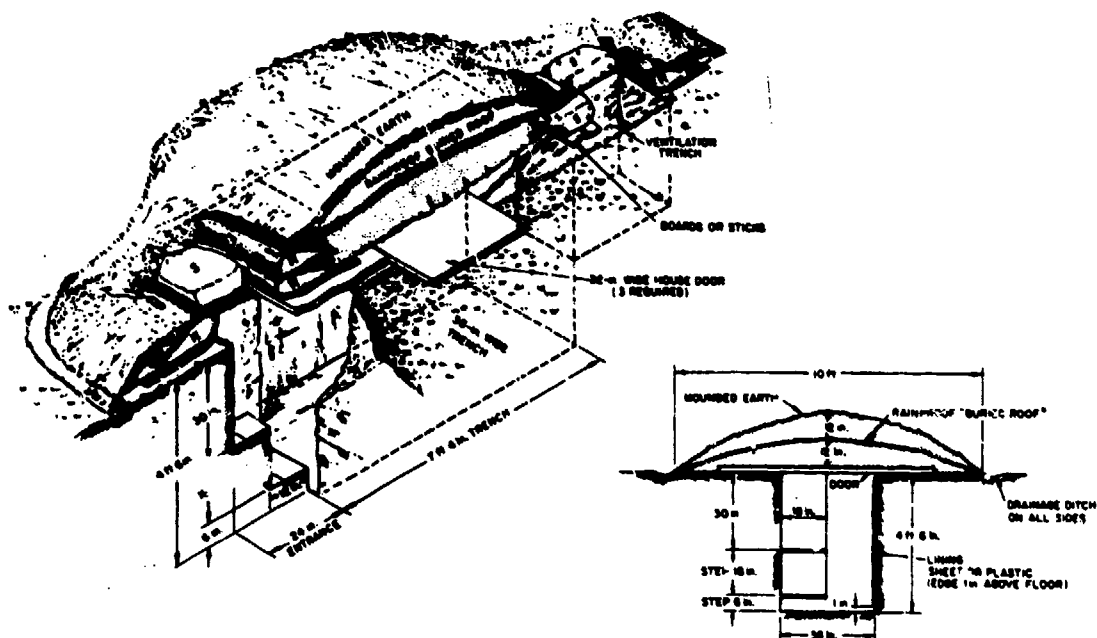


Figure 1. Door-Covered Trench Shelter (References 1 and 2)

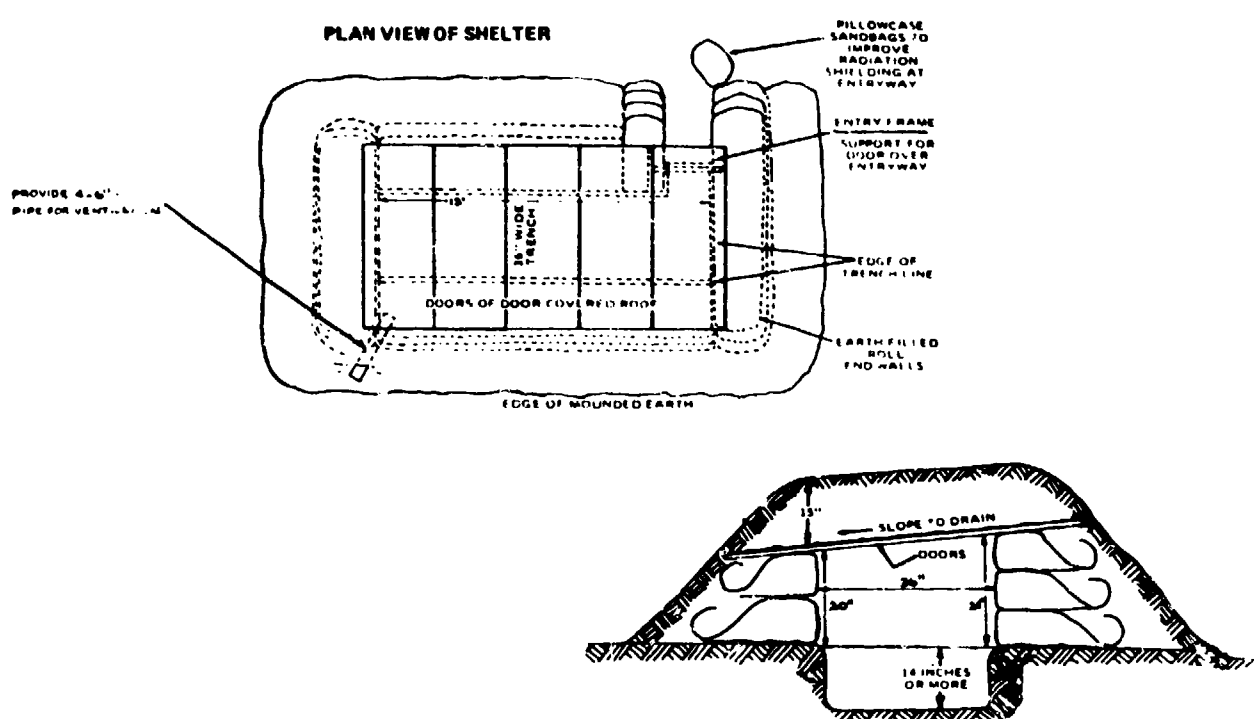


Figure 2. Above Ground Door-Covered Shelter (Reference 1)

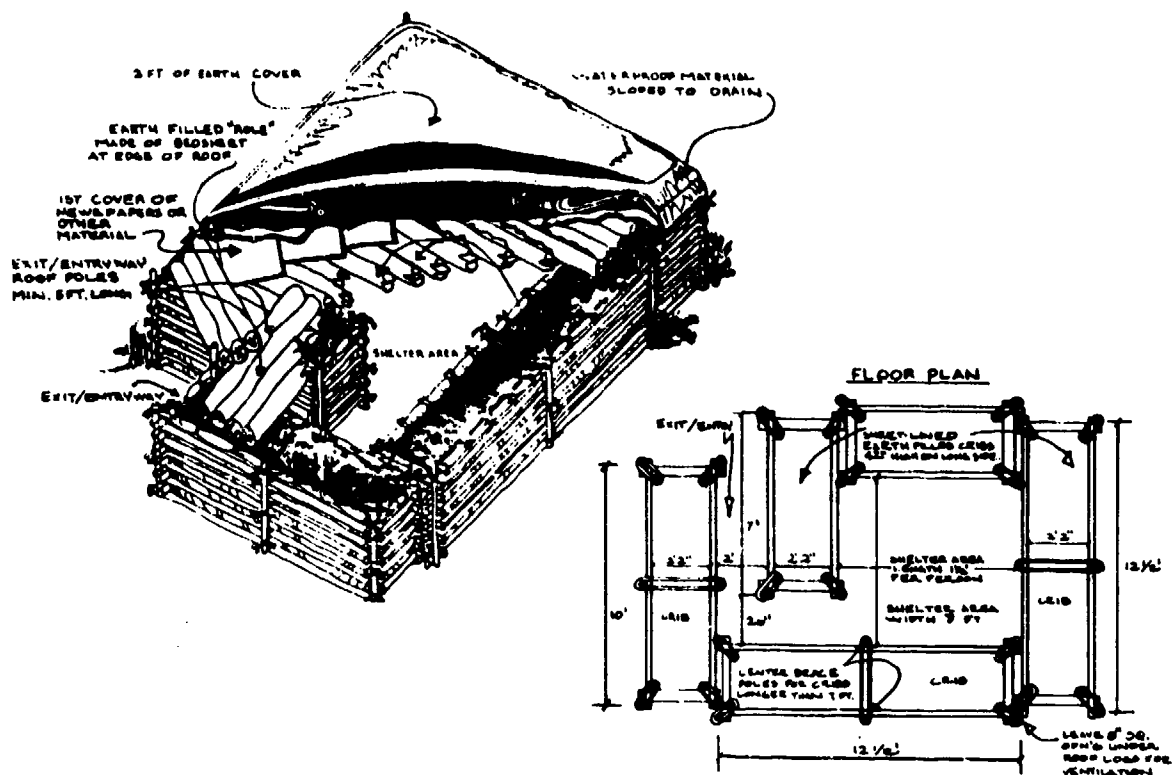


Figure 3. Crib-Walled Shelter (Reference 1)

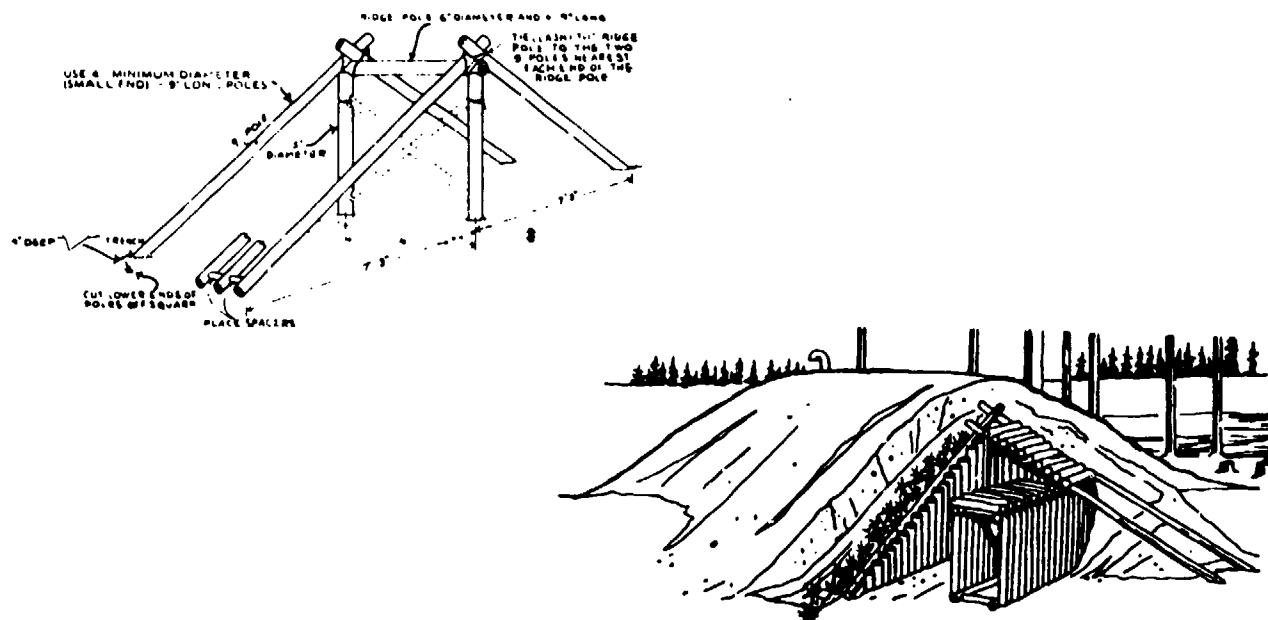


Figure 4. Ridge Pole Shelter (Reference 1)

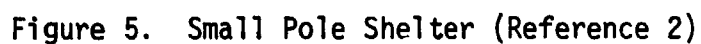


Table 1. Shelter Failure Mode Possibilities

<u>Shelter</u>	<u>Overturn/ Translation</u>	<u>Trench Collapse</u>	<u>Roof Collapse</u>
Door-covered trench		*	*
Above ground door-covered	*		*
Crib-walled	*		*
Ridge Pole	*		*
Small Pole		*	*
Log-covered trench		*	*

because of limitations in the test facility, in the physical properties of the materials, in having a constant gravitational field, in how small the model can be made, and in construction techniques.

Testing of the model shelters was intended to simulate loadings from a 1 megaton (MT) yield weapon at a distance where the side-on overpressure would be greater than 2 psi. A shock tunnel located at Fort Cronkhite, California [7], was provided by the government for testing. The shock tunnel has a maximum overpressure capability of about 8 psi with a positive duration of about 100 ms. Three different modeling approaches were considered: replica, Froude, and dissimilar material. Replica modeling was selected because it was the most practical and least affected by the limitations of the test facility.

In a replica model all components in the model are made of the same materials as in the prototype, and all geometries are similar. Therefore, all lengths and times are scaled by a factor λ ; density, stress, strain, and pressure remain invariant; and accelerations scale as $1/\lambda$. Because the acceleration of gravity cannot be varied in the test facility, gravitational effects were distorted between model and prototype. For the type of response expected from the shelter models, this distortion was considered to be of secondary importance.

Another problem for replica models caused by facility limitations was that the maximum overpressure of 8 psi that can be generated in the Fort Cronkhite tunnel has a 100 ms duration. Assuming that 1/10-scale shelter models were tested, this duration would correspond to 1.0 sec in full scale. A 1 MT nuclear explosion blast wave at the 8 psi level would have a duration of 2.8 sec. Fortunately, calculation of the response time of the various

structural components of the expedient shelters showed that the fundamental period for each full-scale shelter was considerably shorter than the duration of the overpressure load. Thus, the shelters were loaded in the quasi-static realm. Provided the response of the models was also in this domain, the duration of the loading did not have to be scaled rigorously. This was the case since the duration of the tunnel blast wave was about 4 to 45 times longer than the natural period of each model shelter depending on type.

The other two types of modeling considered were eliminated because in one case testing was required to be conducted in a reduced atmospheric pressure with model materials that were weaker by the scale factor, but of the same density, and with loading times that were longer than those required by the replica models. Evacuation of the expansion chamber in the shock tunnel was not possible. In the second case, to obtain longer scaled durations, a different, denser gas is required. This would have also required stronger model materials. However, because the shock tunnel could not be used practically with any gas other than ambient air, this modeling technique was eliminated.

Test Facility and Model Fabrication

The Fort Chronkrite shock tunnel located near San Francisco was specified and provided by the government for the model shelter evaluation program. The tunnel consists of a 63-foot long cylindrical compression chamber about 7 feet in diameter in which strands of Primacord® are used to generate the blast loads. The blast wave expands into a rectangular, 8.5 X 12 feet, cross-sectional expansion chamber about 100 feet long. A major consideration in test planning was the arrangement of model-scale test structures within the expansion chamber of the Fort Chronkrite facility, and the effects of this arrangement on blast loads on the structures. Some of the expedient shelters involve some sort of trenching, so that much of the shelter is below grade. To simulate such shelters within the test facility, a soil-filled test section was installed inside the shock tunnel to allow preparation or insertion of model-scale shelters underground. Nominal length and height dimensions of the test section are given in Figure 7. Laterally, the test section spanned the entire width of the tunnel (12 feet). To allow smooth shock wave loading approaching the models, a ramp was installed upstream at the front of the test bed. Downstream of the models, the test bed was continued to prevent

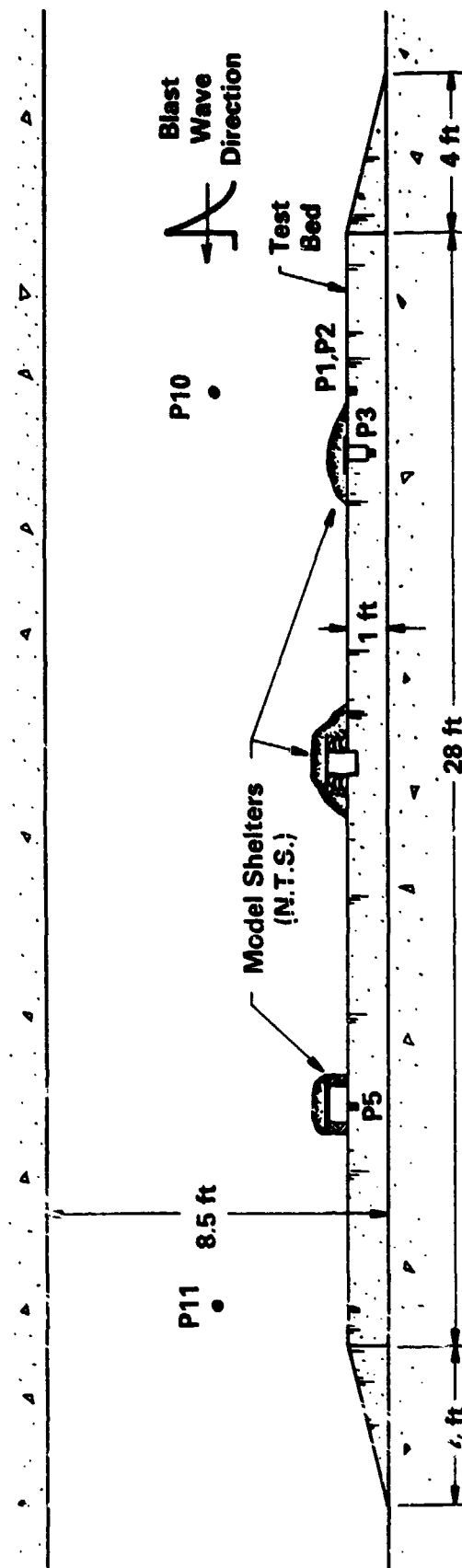


Figure 7. Elevation View of Soil Test Section in Tunnel

premature expansion of the incident shock wave and a down ramp was also installed. By providing a 1-foot high elevated floor over a 28-foot length of the tunnel floor, several models could be tested at one time.

An estimate of the flow over the models was made to approximate the worst-case shock loading that would occur. The blockage factor due to the elevated floor was small, and the elevated floor provided enough depth for sublevel structures to be incorporated into the earth. With a 1-foot elevated surface, side-on shock pressures were expected to be increased by less than 10 percent over the pressure that would be obtained were the tunnel to be used in the usual fashion.

By considering the interference drag that results between the models after the passage of the shock front, the spacing between models was determined. The spacing between models in tandem was that spacing necessary to eliminate interference drag. A similar approach was used to evaluate the spacing needed to eliminate interference drag in the tunnel axial direction. This method of determining spacing requirements followed procedures used to space obstacles in a conventional wind tunnel. By this technique, it was determined that ten, two-abreast models could be tested during one test run using the 28-foot long elevated test surface.

Axial spacing, based on this procedure, required that the test models be at least four to six feet apart on centers, with the first pair of models being four feet behind the transition from the 14-degree ramp up to the test surface. The last set of models was to be three feet forward on centers from a 14-degree ramp down to the shock tunnel floor. Recommended lateral spacing was based on having models with the lowest profile located toward the front edge of the elevated test bed. The last set of two models could be any of the models in pairs or in duplicate. The shelters were about three to four feet from a side wall to the edge of the model. Shock diffraction interference with these arrangements was expected not to be significantly different or altered from that found on an isolated model.

In determining the loading realm and selecting model sizes, response times were estimated for the shelters. Fundamental vibration frequencies were calculated for the main strength structural members. Wooden dowels of comparable strength were chosen to represent logs in the pole shelters. Main structural members in the shelters using wooden poles were generally specified

to be four inches in diameter. Use of 3/8-inch wooden dowels to model these poles resulted in a scale factor λ of 1/10.7 for these shelters. Several types and sizes of plywood were tested along with solid door sections to select modeling materials and sizes. Utile plywood, 3/16-inch thick, was selected to model doors serving as structural members. Using 3/16-inch plywood to model the nominal 1-3/8 inch thick doors resulted in a scale factor of 1/7.33.

Six different fallout shelters were tested in this project to determine their structural blast resistance. As indicated in the introduction, two other shelters were originally identified for evaluation, but were eliminated from testing. The eight shelters were numbered for identification, and the six that were tested are listed in Table 2 along with the scale factor used to size their components. The models of the six expedient shelters were prefabricated as much as possible at SwRI prior to departure to the Fort Cronkhite shock tunnel. In some cases, such as shelter 7, it was possible to assemble the complete wooden structure at SwRI. In other cases wooden subassemblies were put together before departure and later assembled at the test site. Finally, for some shelters (for example, shelter 2), only the model components for the logs and doors could be prepared at SwRI, and the complete assembly was effected at the test site. For those shelters which used soil trenches, wooden molds were fabricated at SwRI and used to form the trenches in the soil test bed.

Table 2. Model Expedient Fallout Shelters Tested

<u>Shelter No.</u>	<u>Shelter Name</u>	<u>Scale Factor</u>
2	Door-covered trench	1 : 7.33
3	Above ground door-covered	1 : 7.33
5	Crib-walled	1 : 10.7
6	Ridge pole	1 : 10.7
7	Small pole	1 : 10.7
8	Log-covered trench	1 : 10.7

The door-covered trench shelter is an example of one of the below ground designs for which a mold was made and used to form the trench. The procedure for making the trench was begun by digging a slightly oversized hole in the test bed, filling, and tamping the soil at the bottom of the hole to obtain the required depth for the trench. The mold was then placed in the hole and backfilled, and hand-tamped in layers with a two-by-four board. The soil used to backfill and to cover the shelters was sifted using a sieve made from 1/4-inch wire mesh. Water was then added to obtain a moisture content of about 10 percent, a level which provided the best soil workability in making the trenches with the mold. Figure 8 shows the trench for a No. 2 shelter. After all the trenches for these shelters were completed, their assembly followed strictly the plan illustrated in Reference 1. The earth-filled rolls were made using Saran Wrap® for the plastic material specified in the shelter plan [1]. The same type of wrap was used to rainproof the roof soil cover. Figure 9 provides an example of a completed No. 2 shelter just prior to testing. Shelters 3 and 8 were two other shelters whose assembly was done at the test site using a wooden mold to form a trench.

Shelter 5, the crib-walled above ground shelter, is an example of a shelter that was to a great extent, prefabricated in subassemblies at SwRI. The five required cribs for each of the five models made were all completed prior to arriving at the test site. In addition, the roof poles were precut in sets for each model shelter. Note that a significantly larger number of poles were required to make the roof than is specified in the instructions for the full-scale shelter in Reference 1. The cribs were assembled and filled with soil as specified in the shelter plan using plastic wrap to line each crib. Figure 10 shows a model of shelter 5 during assembly. The earth cover was then placed on the roof as specified. Figure 11 shows a completed model shelter 5 ready for testing. Shelter 6 was another shelter that was partially assembled at SwRI before completing at the test site.

Shelter 7, the small-pole shelter, was the only shelter evaluated in this program that is detailed only in Reference 2. Five models of this shelter were completely fabricated and assembled prior to departure from SwRI to the Fort Cronkhite shock tunnel. Each of these model shelters was installed in the test bed by first digging a slightly oversized hole of the specified depth, placing the assembled shelter in the hole, and then backfilling and

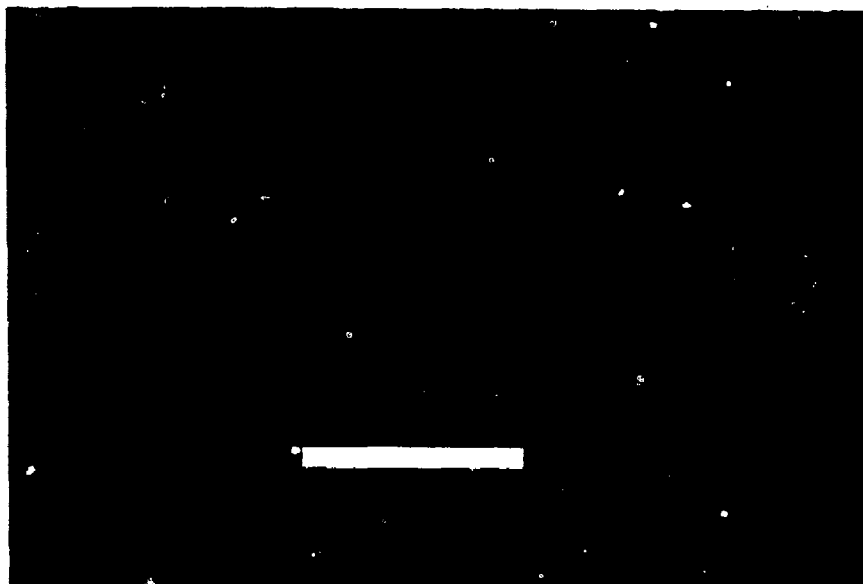


Figure 8. Soil Trench for Door-Covered Trench Shelter



Figure 9. Completed Model of Door-Covered Trench Shelter

data stored on the diskettes were then read into a DEC 11/70 minicomputer, and engineering plots were prepared using a Printronix 300 printer/plotter.

Test Matrix and Procedure

A total of 96 individual shelter response models were tested in the twelve experiments conducted at the shock tunnel. Each test consisted of setting up eight of the response models plus the two rigid models in the test section of the tunnel. To stay within the blast overpressure capabilities of the test facility, the tests were run at three nominal overpressures: 2, 4, and 8 psi. The number of shelters tested at each of these overpressures is listed in Table 3 together with the number of tests. The first five experiments were all at the lowest overpressure. Those shelter designs that survived easily were not tested as often. Also taken into consideration was the complexity of the erection procedure as well as the number of models that had been preassembled or for which parts had been fabricated. In general, those types of shelters that did not survive or appeared close to failure were tested in greater numbers. Three of the highest pressure tests were conducted next. For these tests, about the same number of samples were tested from each type of shelter.

The next three tests used the intermediate overpressure levels, and generally tested a similar number of samples from each type except the one type that had survived the best at the highest pressure level without a

Table 3. Response Models Tested

Shelter No	Nominal Overpressure (psi)			Total
	2	4	8	
2	7	5	5	17
3	16	7	5	28
5	2	4	5	11
6	5	4	6	15
7	2	0	5	7
8	8	4	6	18
No. of tests	5	3	4	12

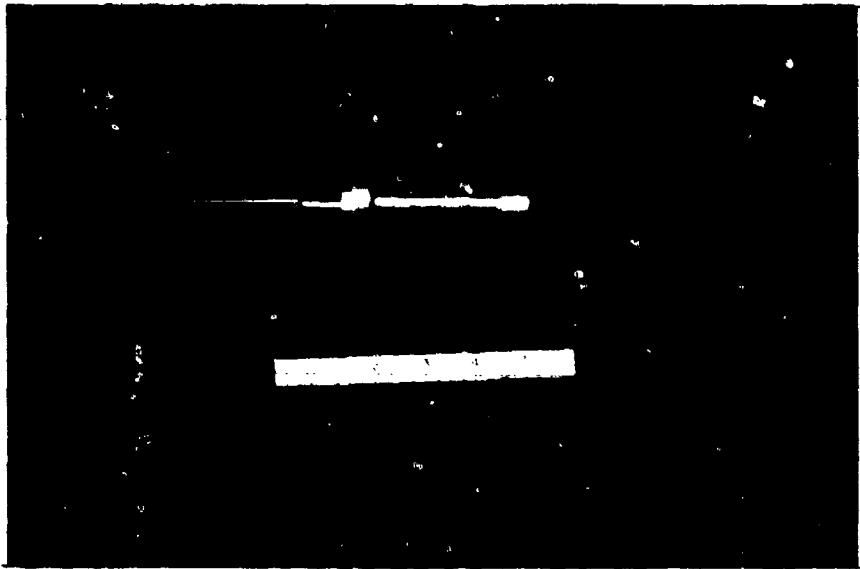


Figure 14. Pressure Transducer Canister

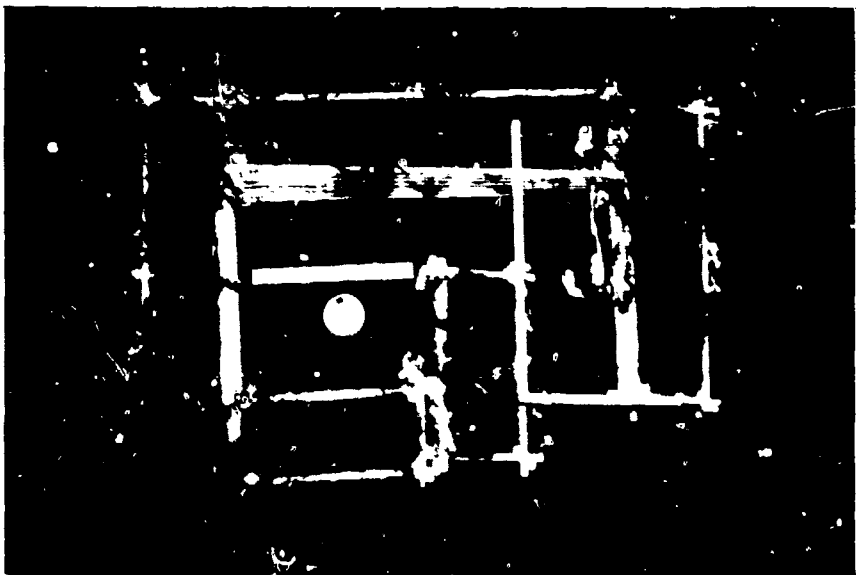


Figure 15. Typical Transducer Installation in Shelters

tamping the soil all around the shelter to obtain the results shown in Figure 12. Soil was then piled over the roof poles as specified in the shelter building instructions using plastic wrap for the rainproofing material in between the earth cover. A completed model shelter 7 is shown in Figure 13.

In addition to the response models of the six shelters listed in Table 2, two rigid models were used on each of the 12 blast experiments conducted in the shock tunnel. The two rigid models represented geometrically shelters 5 and 8. These rigid models were used to measure internal blast pressure leakage into these expedient shelters on every test. The rigid model of the crib-walled shelter 5 was fabricated from solid sections of wood with provisions for mounting pressure transducers on the roof and walls. The rigid model of the log-covered trench shelter 8 was constructed from thin aluminum plate.

Pressure Measurements System

Pressures were sensed and recorded on each test. In all twelve tests, five transducers were mounted to sense the blast overpressure on the test bed and on one wall of the tunnel as shown in Figure 7. In addition, up to seven other transducers were mounted in each test on the rigid and response models of the expedient shelters to sense internal blast pressures. Two types of transducers were used to sense these pressures, piezoresistive and piezoelectric. The piezoresistive pressure transducers used to make the majority of the measurements were Kulite Model HEM-375 with a pressure range of 0-25 psig. This sealed miniature transducer is an all metal, electron beam welded assembly featuring a metal diaphragm as a force collector with piezoresistive strain gages bonded inorganically. These transducers feature a high resonant frequency of approximately 50 kHz, good linearity, and static pressure response. Excitation voltage, bridge balance, and amplification for these pressure transducers were provided by Vishay Model 2310 signal conditioning amplifiers with the frequency response set at dc to 25 kHz (-5%).

The piezoelectric transducers used for the rest of the test measurements were all manufactured by PCB Piezotronics. Two Model 102A02 transducers were mounted on the tunnel wall, one near the front of the test bed and the other near the back. Their output was recorded by SWRI together with the output of the Model 102A05's and 102A15's installed on the test bed and in the model shelters. All three types of PCB transducers utilize an acceleration-

compensated, quartz sensing element coupled to a miniature source follower within the body of the transducer. The source follower converts the high impedance charge output into a low impedance, voltage output signal. The sensors have a rise-time capability of 1 microsecond. Each piezoelectric transducer was connected to a PCB Model 494A06 signal conditioner and amplifier. The amplifier has a specified frequency of 0.08 to 180,000 Hz (-3db) and a coupling time constant of 2 seconds.

Both types of pressure transducers were installed in protective steel canisters which simplified handling and installation in the soil test bed. Figure 14 shows a completely assembled transducer canister ready for burial. For those transducers used to sense the surface overpressure on the test bed, the steel canister was buried so that the transducer was flush with the ground surface. In a similar manner, the transducer canisters were mounted within the model shelters to sense the internal pressures. Figure 15 shows a typical installation in a crib-walled shelter.

The amplified signals from both the piezoresistive and piezoelectric pressure transducers were recorded at the test site on magnetic tape with an Ampex Model 2230 tape recorder with Wideband II, FM electronics. At a record speed of 30 inches/second, the specified data bandwidth capability was 0-100 kHz (+1, -2db). The pressure data were played back at the test site after each experiment using a Biomation Model 1015 four-channel transient recorder. The data traces were recorded on Polaroid film for quick-look analysis using a Tektronix Model 602 display unit. Upon return to SwRI from the Fort Cronkhite facility, the test data were played back and digitized using the system shown in Figure 16. Up to four channels of data were played back at one time through the analog filters into a Biomation Model 1015 four-channel transient recorder. This recorder digitizes the incoming analog signals at sample intervals of 0.01 milliseconds or greater. Since this unit has four separate analog-to-digital (A/D) converters, the samples for each of the four data channels are time correlated. Once the test data were properly formatted in digital form, a DEC 11/23 computer extracted the data from the transient recorder memory through the computer Automated Measurement and Control (CAMAC) data buss and stored them on a 8-inch flexible diskette. A graphics terminal was used to display each data trace for verification. The

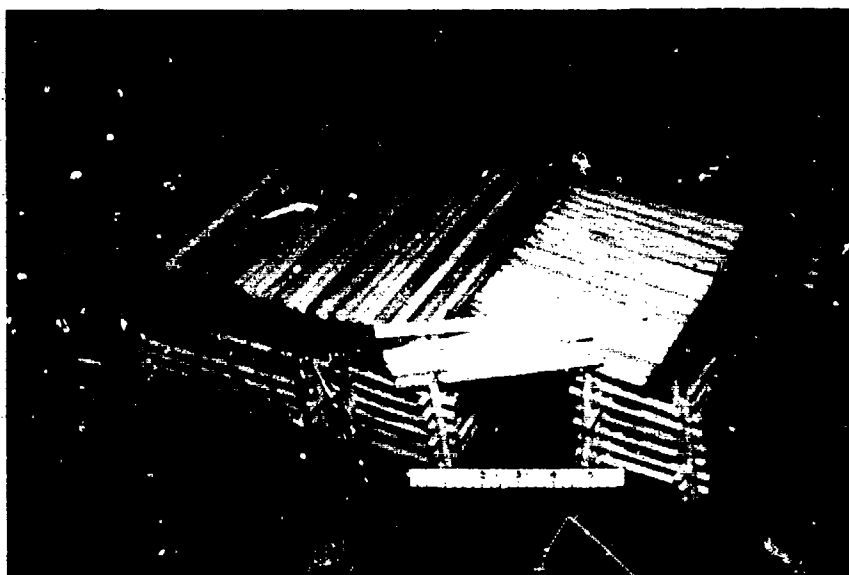


Figure 10. Assembling of Crib-Walled Shelter

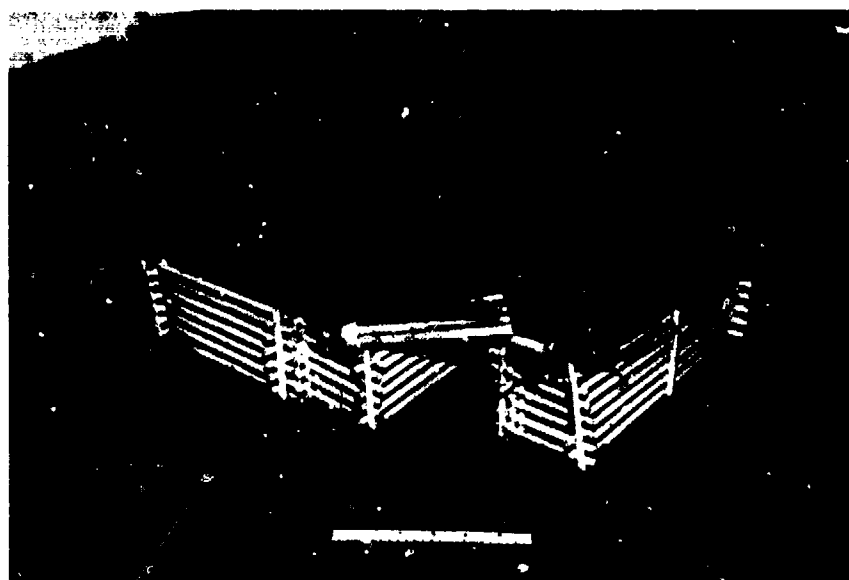


Figure 11. Completed Model of Crib-Walled Shelter

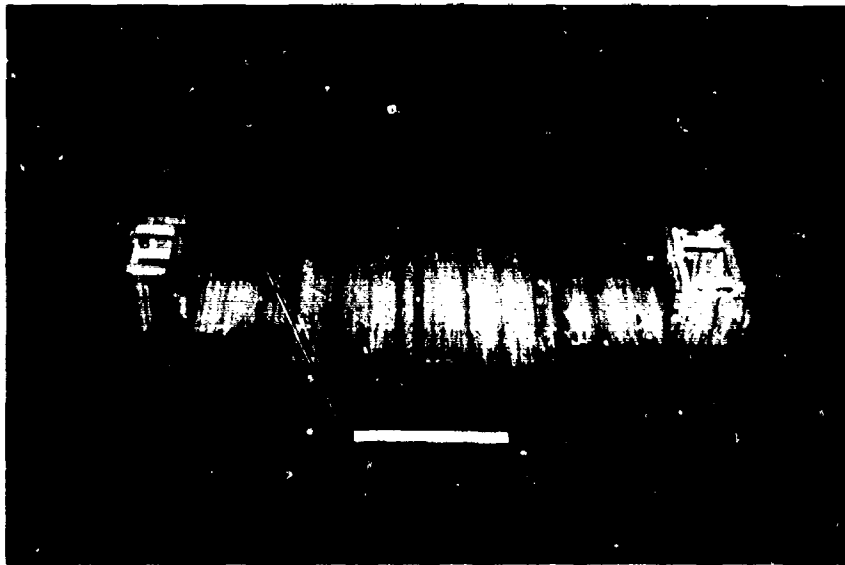


Figure 12. Burial of Small Pole Shelter Assembly

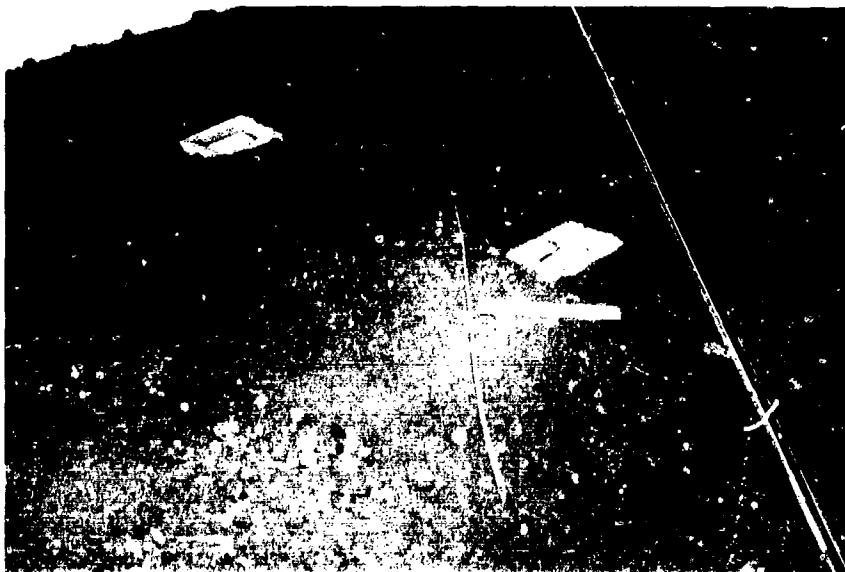


Figure 13. Completed Model of Small Pole Shelter

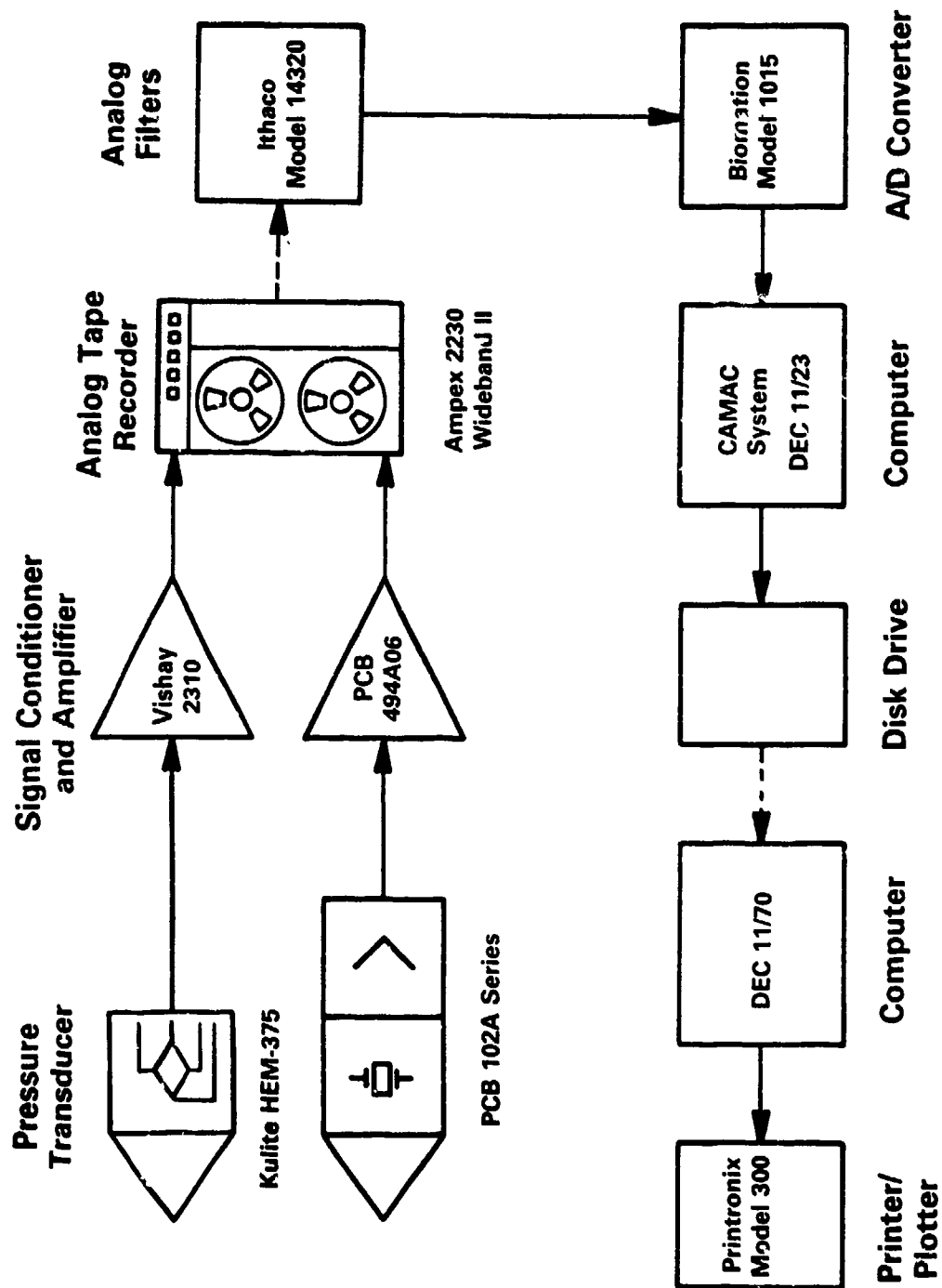


Figure 16. Data Recording and Processing System

failure. Included in this series of tests were two shelter models that were modified slightly to determine if their performance could be improved. The last test was at the highest pressure level and it included four of the shelters in slightly modified forms. A total of only six shelter models were tested in a slightly modified condition in the entire test program.

All 12 experiments in this program followed a similar test procedure regardless of which model shelters were being tested and which pressure level was used. As indicated previously, eight response shelters were installed in the test bed in each experiment along with two rigid models. The normal test sequence was begun by measuring carefully and marking on the soil test bed the location of each model shelter. Then, each model shelter was assembled or installed in place following the instructions provided in Reference 1 for five types of shelters and in Reference 2 for one type of shelter.

While all the model shelters were being installed, the pressure measurement system was set up and checked for proper end-to-end operation. Amplifier gain and tape recorder voltage levels were set to accommodate the peak pressure expected. After the model shelters were completed and the measurement system configured properly, the exit from the shock tunnel was closed and Primacord® explosive placed in the compression tube. The back door to the compression tube was then closed, and the area around the shock tunnel was secured. After a short countdown sequence, the explosive array was detonated, and the pressure data were recorded.

The tunnel exits and back door were then opened to allow natural ventilation of the explosion gases before test personnel would return to the test section of the tunnel to record the condition of the test shelters. In the meantime, the pressure data were played back into a transient recorder for quick-look analysis using Polaroid prints of the pressure-time histories. After it was safe to return inside the shock tunnel, SwRI personnel recorded the condition of each model shelter. The tested shelters were then carefully disassembled to determine their internal condition and then finally removed altogether from the test bed. The test bed was then readied for the next set of shelters to be tested.

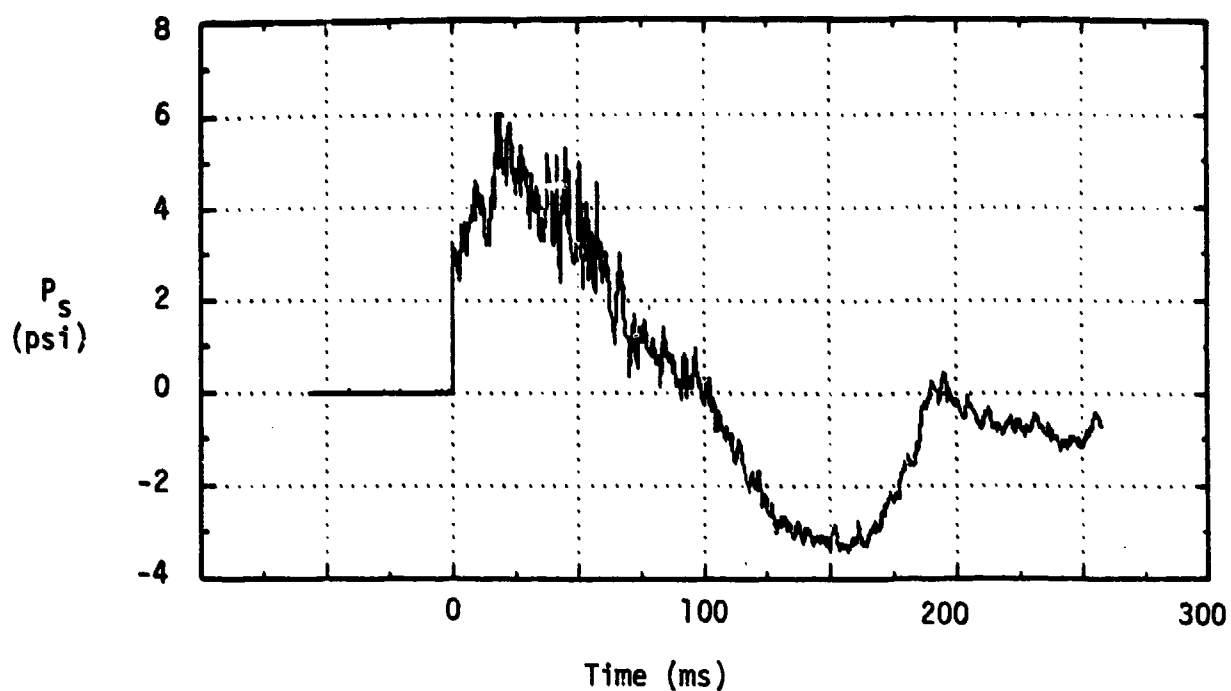
SUMMARY OF RESULTS

External Pressure Data

Up to 12 pressure measurements were made in each experiment. Five of these measurements were of external overpressures, two on one wall of the tunnel and three on the soil bed surface as shown in Figure 7. The rest of the transducers used on each test were installed on both the response models and the rigid models of the expedient shelters to measure the internal pressure leakage. Three different overpressure levels were used on the 12 tests. These were achieved by varying the number of Primacord® strands detonated in the compression tube of the shock tunnel. To achieve the lowest pressure level, two strands were used. The intermediate pressure load was achieved using four strands. For the highest pressure level, six strands were used. Analysis of the data traces for all three overpressure levels indicated a similar loading function in all cases. The five pressure transducers used for external measurements were P1 and P2 located on the soil surface at the front of the test bed, F10 located on the wall at the front of the test section, P9 located on soil surface at the rear of the test bed, and P11 located on the wall at the rear of the test section. Figure 17 shows two examples of the data recorded by P1 for an intermediate and a high overpressure test. These measurements made on the surface of the test bed just upstream of the first row of test shelters show oscillating high-frequency pressure pulses superimposed on the much lower frequency, larger amplitude pressure traces. These types of pressure records are quite similar to those recorded previously by various investigators using the Fort Cronkhite shock tunnel, and are representative of those made on each of the twelve tests at the five external locations on the various surfaces of the test section of the tunnel.

The peak overpressure for each of the five surface pressure transducers was obtained by a visual regression of the long duration pressure pulse through the high-frequency pressure oscillations. Table 4 summarizes the results of averaging the individual pressure measurements on each test. The corresponding estimated standard deviation for each set of measurements is also tabulated. As indicated by the deviation on this table, the measurements from each test were quite repeatable with most average overpressures having

(a) Intermediate Overpressure Test



(b) High Overpressure Test

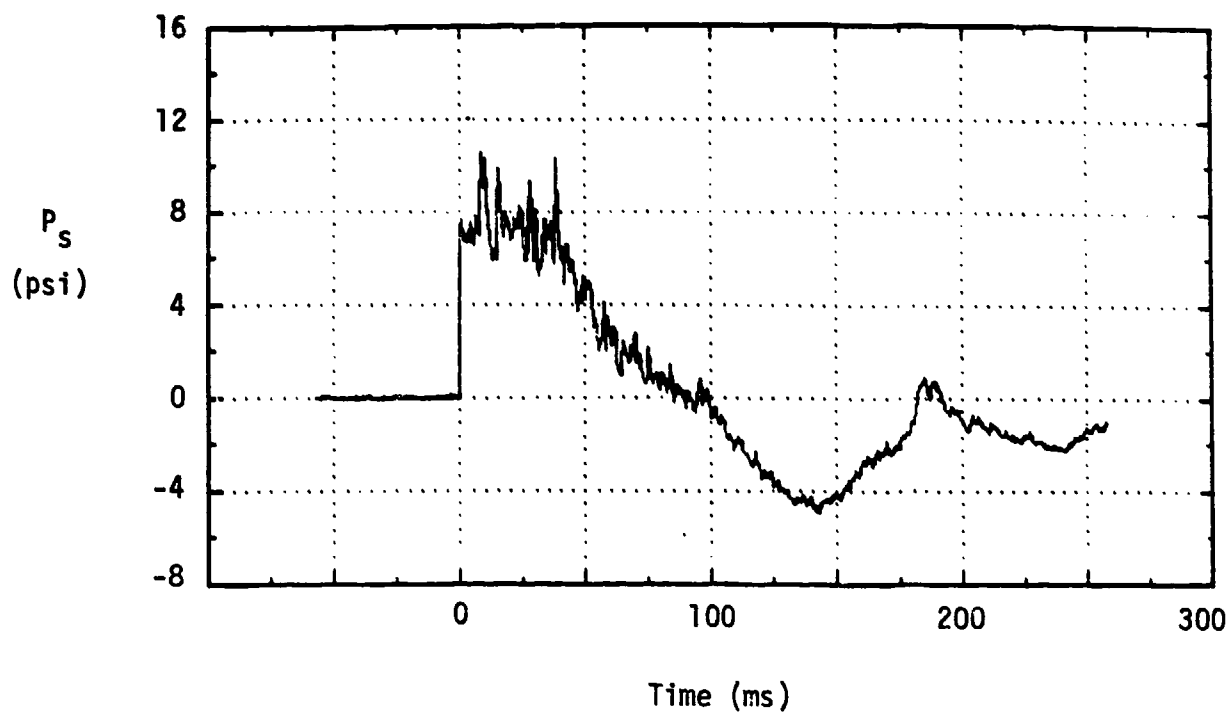


Figure 17. Test Bed Surface Overpressure Measurements

Table 4. Average Test Overpressures

<u>Test No.</u>	<u>Overpressure (psi)</u>	<u>Deviation ($\pm\%$)</u>
01	2.96	12
02	2.82	7
03	3.03	6
04	2.84	9
05	2.54	10
06	8.64	4
07	9.20	5
08	8.82	5
09	4.54	7
10	4.72	7
11	4.52	9
12	8.53	2

deviations considerably less than ten percent. By averaging every measurement made on the low, intermediate, and high pressure tests, respectively, the three nominal test overpressures loading the model shelters were 2.8 ($\pm 11\%$), 4.6 ($\pm 7\%$), and 8.8 ($\pm 5\%$) psig.

Internal Shelter Pressures

Measurement of the internal shelter pressures was made with transducers mounted on both the rigid and the response models. On every test, two transducers were mounted on each of the two rigid shelters, R5 and R8. In addition, up to three response models were instrumented in every test. The transducers used in the response models were rotated among the test items from test to test to obtain representative data from within each type of response model for as many pressure levels as was possible. In most cases, the peak pressure measured inside each shelter was essentially the same as measured by the external surface mounted transducers. Also, in most cases the time-histories recorded by the internal transducers was similar to that of the exterior ones with the exception that the high-frequency oscillations were filtered acoustically. In some instances the rise time of the pressure pulse is definitely slower within a shelter, and the peak pressure somewhat attenuated as compared to the external overpressure.

Figures 18 through 23 are examples of pressure-time records obtained from transducers sensing the internal pressure in each of the response and rigid models. The data traces in Figures 18 through 20 are for tests in which the surface overpressure measured was a nominal 4.6 psig. These records from shelters 2, 3, and 8, can be compared to those in Figure 17a to see how the internal geometry of each shelter affects the pressure buildup within the shelter. The data traces in Figures 21 through 23 are for a 8.8 psig nominal overpressure test. These data traces from shelters 5, 6, and 7 can be compared to those in Figure 17b to see the similarities and differences between the internal and external overpressures measured.

For example, the internal pressure in shelter 2, Figure 18, is quite similar to the external overpressures shown in Figure 17a. On the other hand, the internal pressure in shelter 3, Figure 19, shows a much slower rise time and considerably fewer high-frequency oscillations than the external overpressure records. These differences resulted primarily from the entrance to shelter 3 being mostly closed off by model sandbags as instructed in the building plans in Reference 1, while the entrances to shelter 2 are basically open. For shelter 6, the rise time in Figure 22 is somewhat slower than that in Figure 17b due to the relatively long entranceway for this shelter. An even slower rise time can be observed in Figure 23 for the pressure measured in shelter 7, which has even longer entrances leading into the shelter space.

For the two shelters, 5 and 8, for which rigid models were used to measure internal pressures, the pressure data from the rigid models were very similar in every respect to the data from the corresponding response models. The main difference observed was more reflections within the rigid models from the overstrength walls, floor, and roof as compared to the response models.

Shelter Structural Evaluation

Each of the 96 response model shelters was inspected thoroughly after being tested and an evaluation made as to the possible survival of the occupants. The criteria for survival were based primarily on whether the occupants would have been able to survive any structural or soil failures observed in the shelter after it was tested. In some cases it was obvious that unless the soil cover was replaced over the shelter after the blast loading, little or no fallout protection would have been available to the occupants. However, this was not used as part of the blast survival

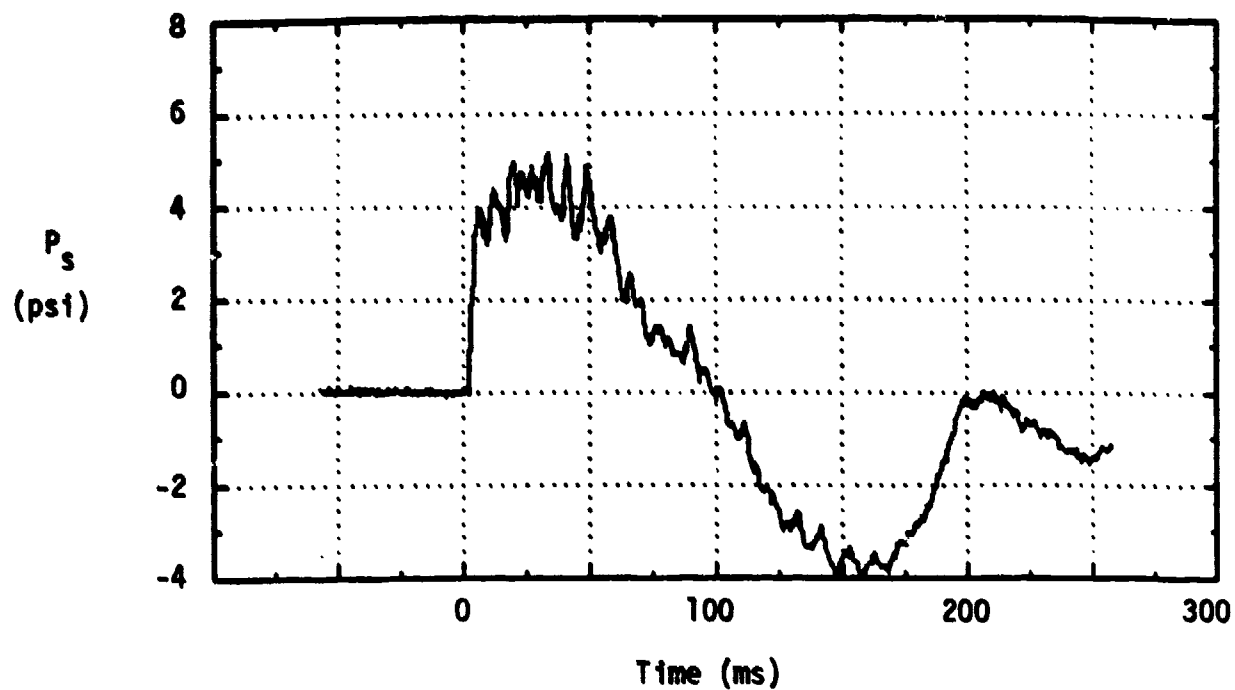


Figure 18. Internal Pressure for Door-Covered Trench Shelter

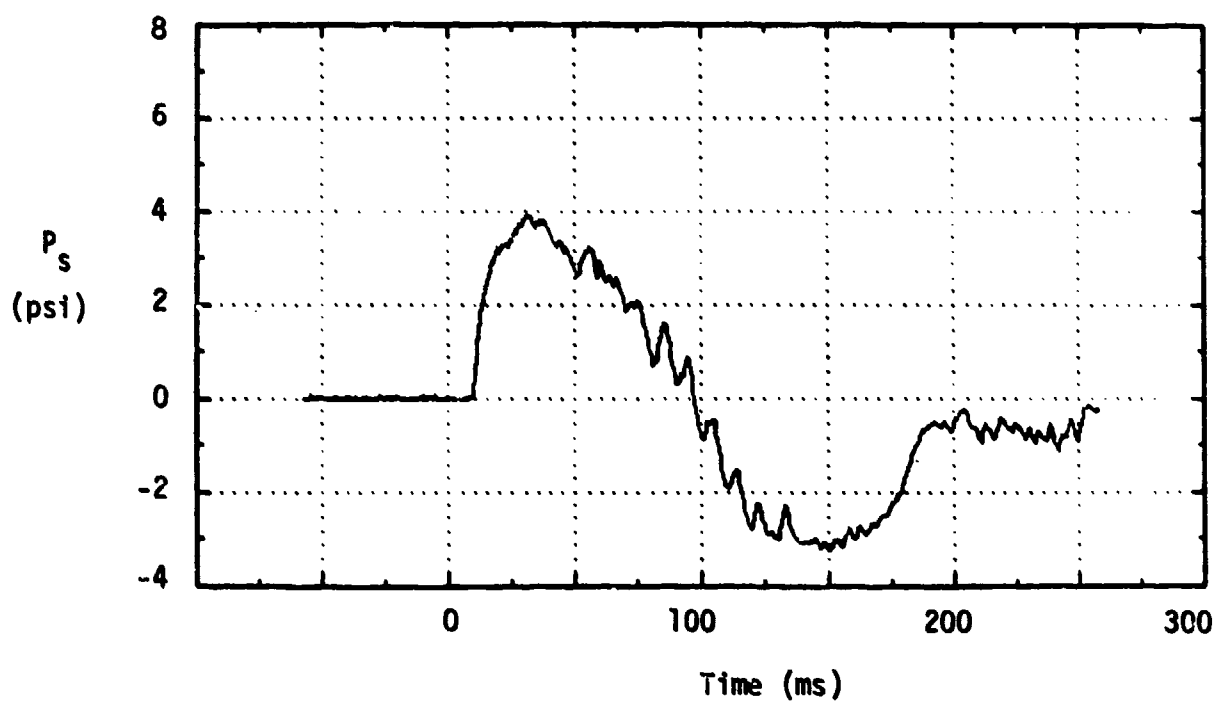


Figure 19. Internal Pressure for Above Ground Door-Covered Shelter

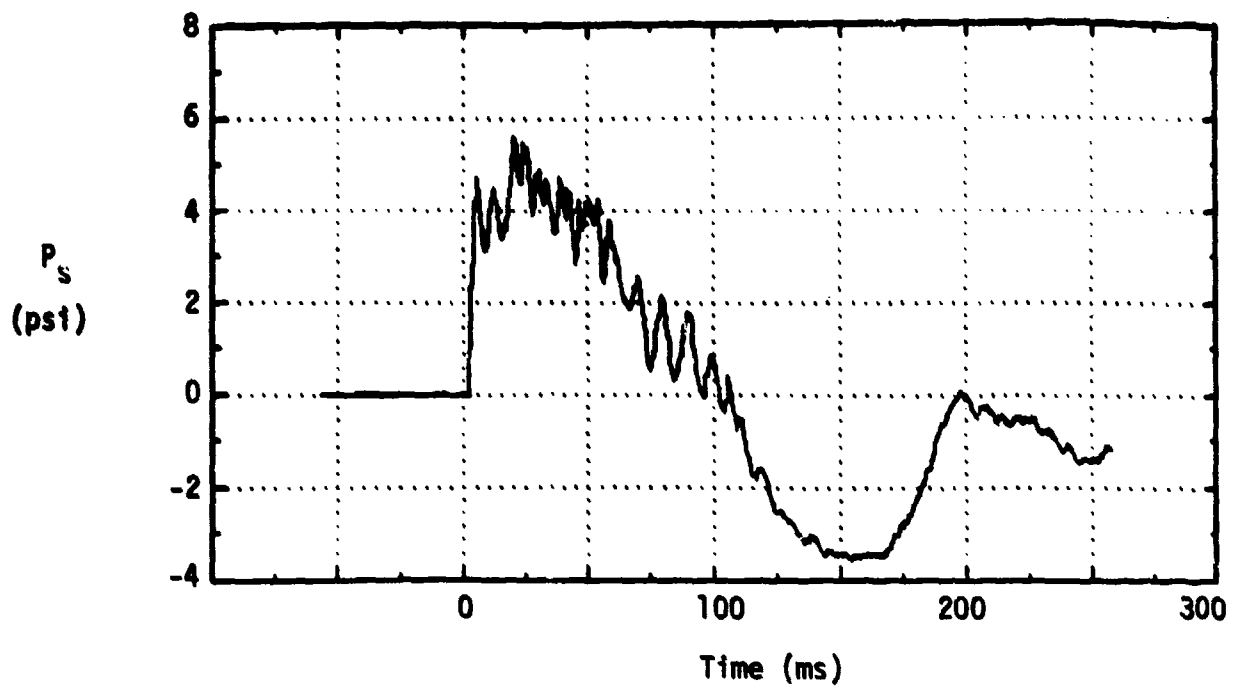


Figure 20. Internal Pressure for Log-Covered Trench Shelter

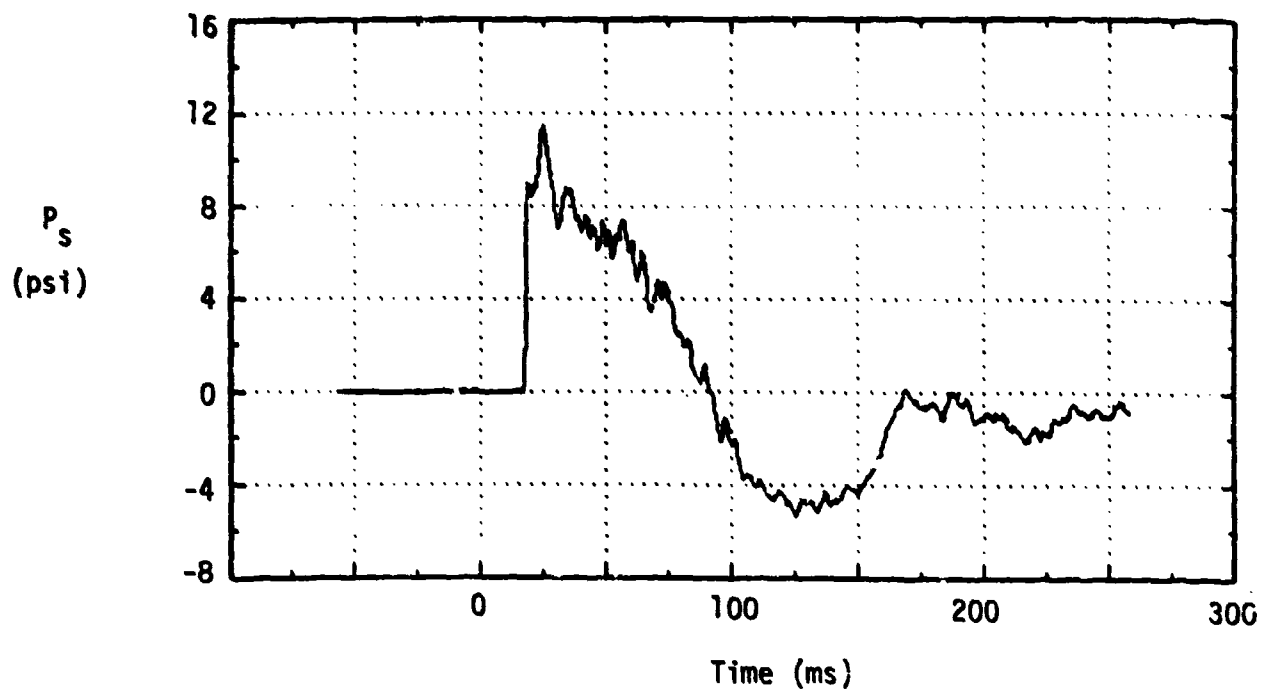


Figure 21. Internal Pressure for Crib-Walled Shelter

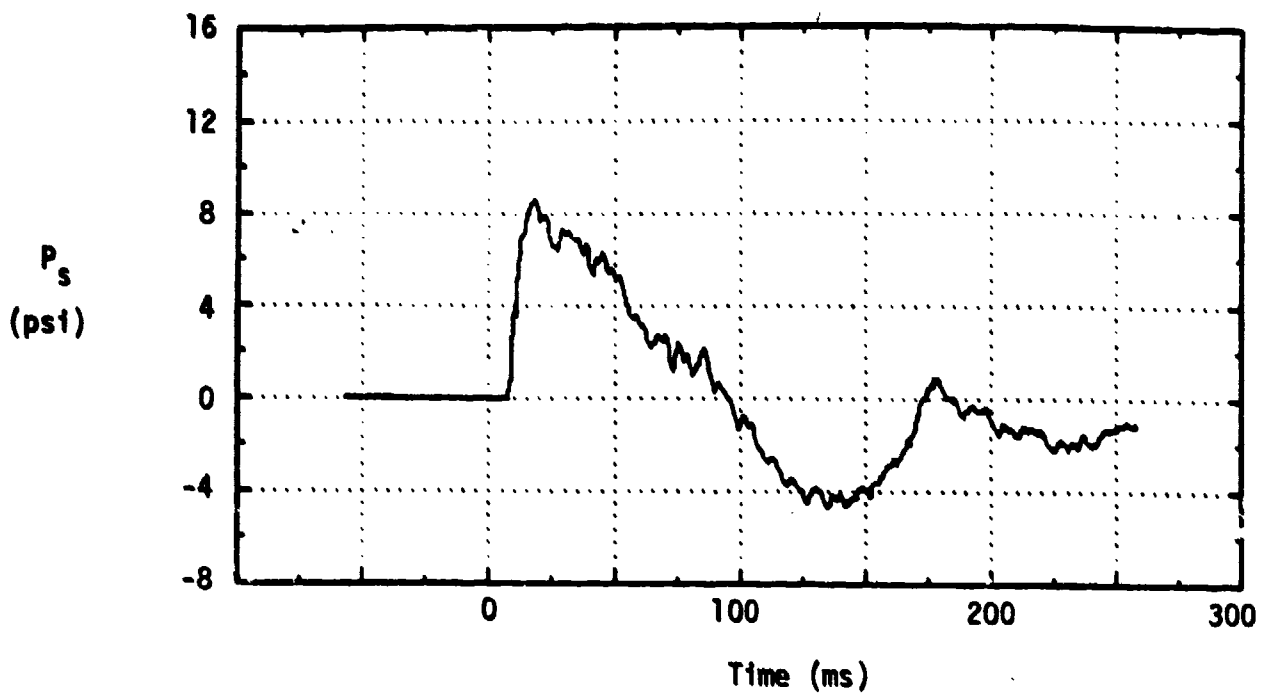


Figure 22. Internal Pressure for Ridge Pole Shelter

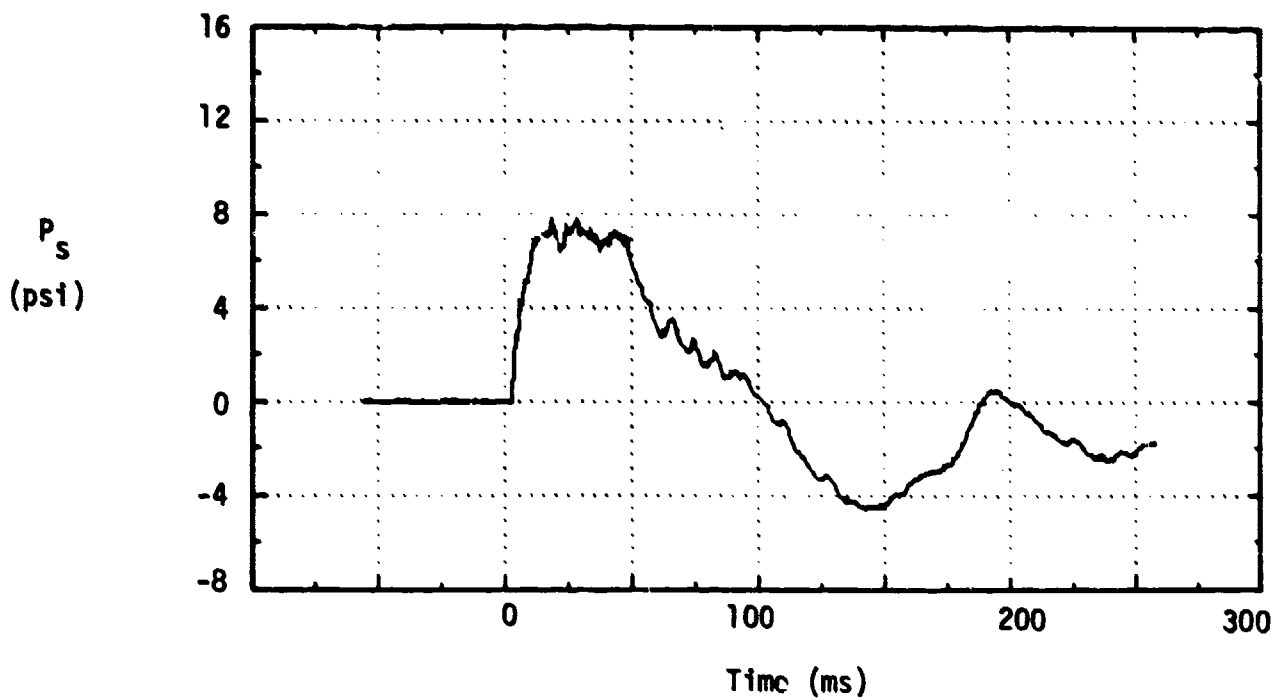


Figure 23. Internal Pressure for Small Pole Shelter

criteria. Similarly, as stated previously, the peak pressure inside most shelters during the the tests was essentially the external peak overpressure. Therefore, for some tests there probably would have been some ear damage to the shelter occupants, and to a much lesser extent, lung damage. However, up to the 8.8 psi maximum pressure tested, less than 20% of occupants would have ruptured eardrums [8, 9] and less than 1% would not have survived lung damage [10]. Therefore, structural failures listed in Table 1 were the only criteria used to determine the survivability of the shelters. Table 5 summarizes the survival assessment of the model shelters. In most cases, a yes or no rating was assigned. However, in a very few cases a marginal category also was used for shelters whose structural condition was such that the interior space appeared marginally safe for immediate survival, but perhaps not for long-term survival of its occupants.

The post-test evaluations of each shelter concentrated on the condition of the internal space of the shelter. Generally, a shelter was judged as not providing the occupants sufficient protection for survival if there was significant trench collapse, roof collapse, or rigid body translation. For example, failures for shelter 2 even at the low overpressures occurred from collapse of the door-covered, soil trench walls. For some of these model shelters, the exterior conditions after the test did not indicate major

Table 5. Model Shelter Blast Survival Evaluation

Shelter	2.8 psi Overpressure			4.6 psi Overpressure			8.8 psi Overpressure		
	Yes	Marginal	No	Yes	Marginal	No	Yes	Marginal	No
2	3	0	4	0	2*	3	1*	1*	3
3	16	0	0	1	1	5	0	0	5
5	2	0	0	1	0	3	0	1+	4++
6	5	0	0	4	0	0	5	1	0
7	2	0	0	-	-	-	5	0	0
8	1	1	6	0	0	4	0	0	6

* Doors added to shore trench sidewalls.

+ Roof poles attached to crib walls and additional soil around cribs.

++ Roof poles attached to crib walls on one test.

damage to the shelter. However, upon internal inspection, it was obvious that the shelter had not survived the simulated nuclear blast loading. The top picture in Figure 24 shows a plan view of shelter 2 after a low pressure test. The bottom photo shows the failed trench walls. Figure 25 is an example of a door-covered trench that survived the low overpressure loading. A modification tried on this shelter on the last two tests was to shore the trench walls with model doors. This simple modification does increase the survival of this shelter.

Shelter 5 is an example of a shelter that failed in some tests due to roof collapse or translation. This above ground crib-walled shelter survived very well in the low pressure tests, but did poorly at the higher pressures. Most failures of these shelters occurred due to the roof poles and soil falling into the shelter, and in some cases for the high pressure loads due to the entire shelter being translated by the blast wave. In the low pressure tests, some of the soil cover was blown away as indicated in Figure 26, but the rest of the shelter remained intact. On the other hand, in most of the intermediate pressure tests, most of the soil cover was either blown away or fell into the interior of the shelter along with many of the roof poles. Similar, though more severe, roof response was observed on the high pressure tests as indicated in Figure 27. In addition, the entire shelter was translated back about a shelter length and in some instances rotated slightly. Two modifications were tried on the last high pressure test. The roof poles of the two crib-walled shelters used in this test were glued along the edge of the cribs and to each other to represent their being tied down along the perimeter of the shelter. One of these shelters also was covered with additional soil around the cribs and the roof so that the entryway was the only part of the wooden framework that was visible from outside. In both cases most of the soil cover was blown away, but the roof poles remained in place as shown in Figure 28. However, significant shelter translation was observed. It is very probable that with the attached roof poles modification this shelter would have survived at the 4.6 psig overpressure level. Even at 8.8 psig, this shelter can probably survive if it can be anchored to avoid rigid body translations. For example, the entire shelter could be built in a shallow trench, and, with additional soil all around, would be kept from moving during blast loading.

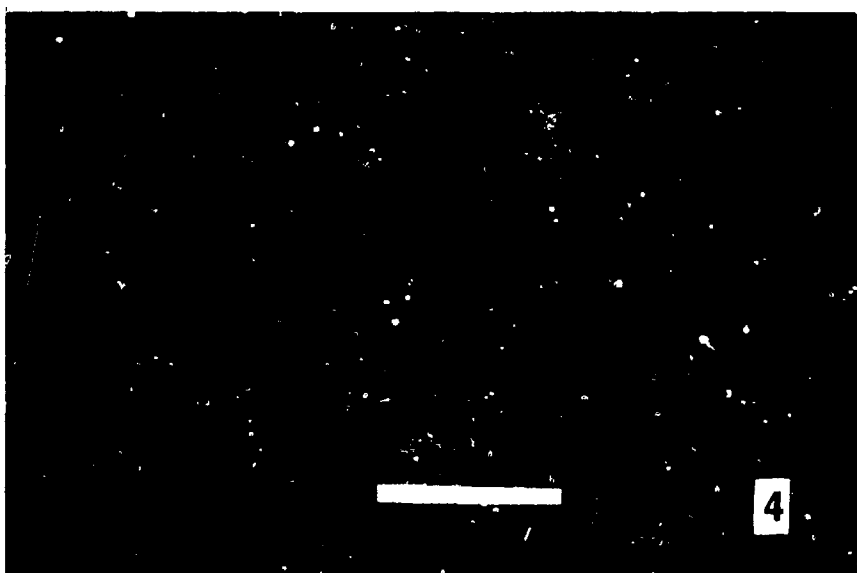


Figure 24. Non-Surviving Door-Covered Trench Shelter in Low Pressure Test

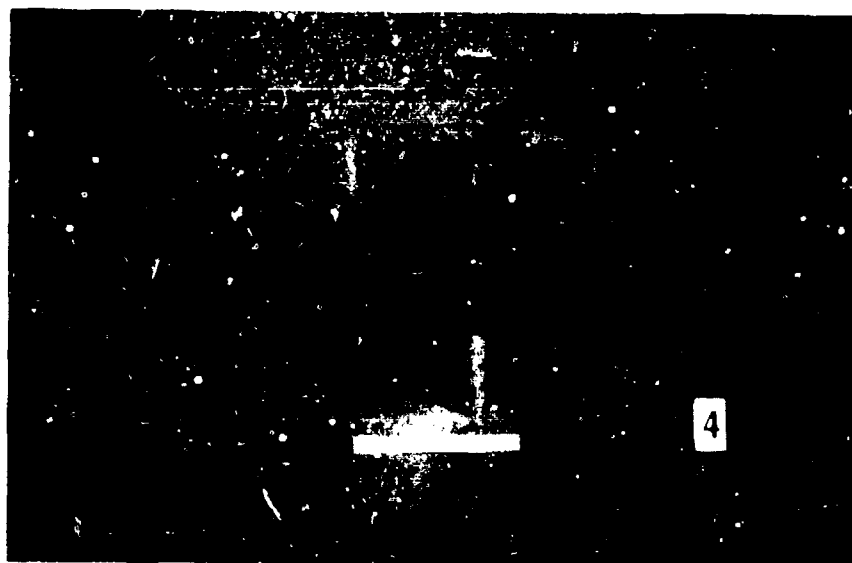
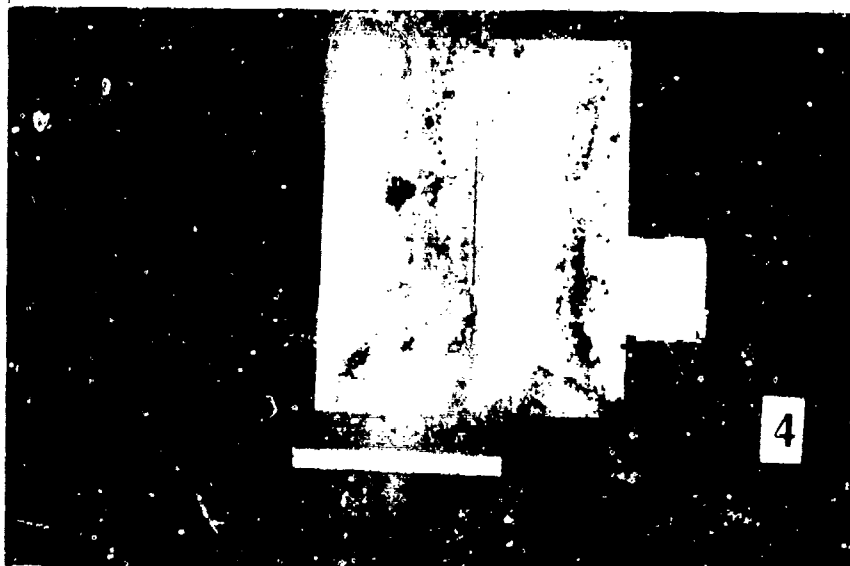


Figure 25. Surviving Door-Covered Trench Shelter in Low Pressure Test



Figure 26. Crib-Walled Shelter After Low Pressure Test

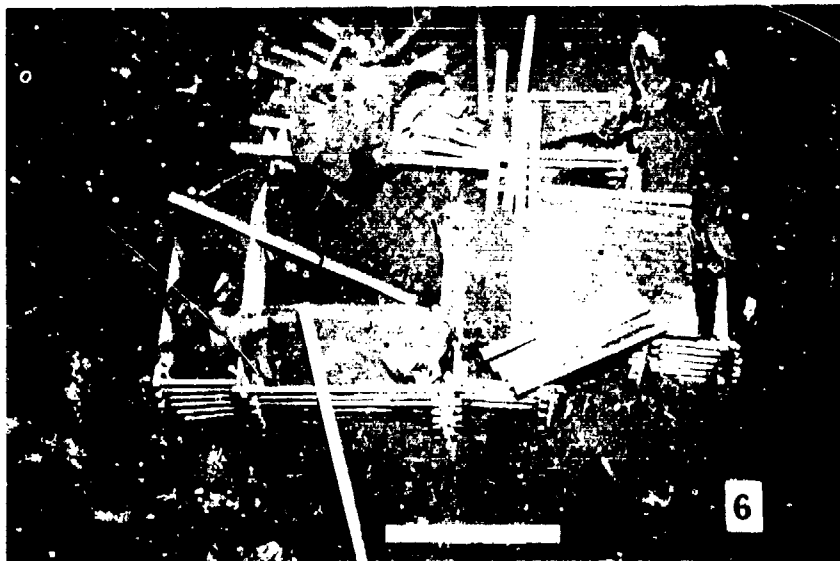


Figure 27. Crib-Walled Shelter After High Pressure Test

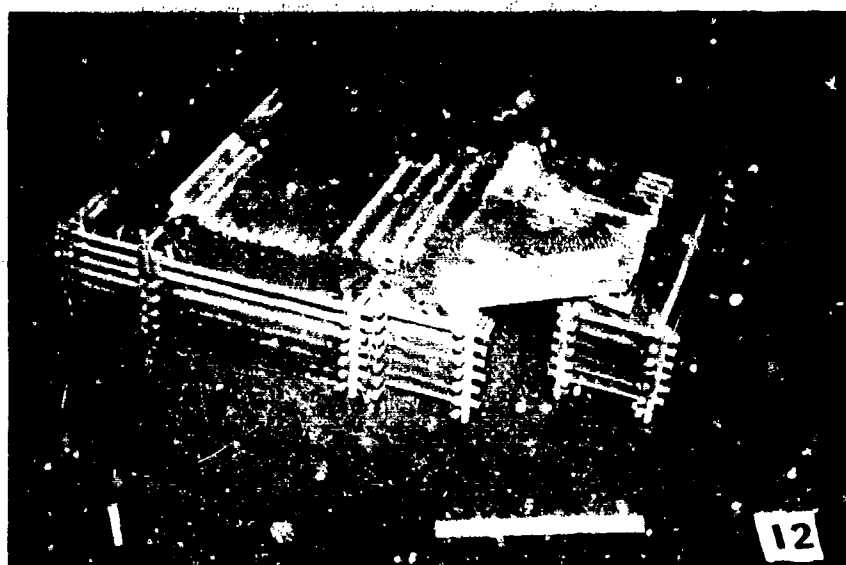


Figure 28. Modified Crib-Walled Shelter After High Pressure Test

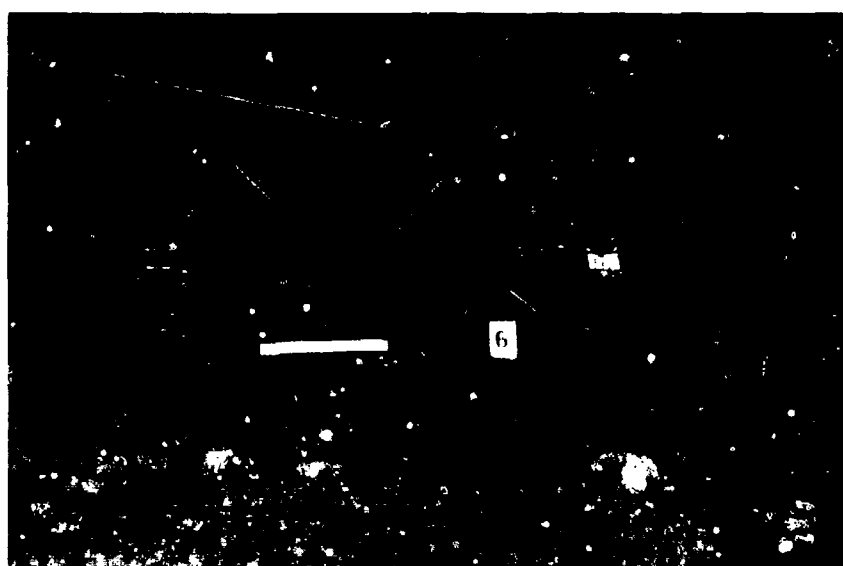


Figure 29. Small Pole Shelter After High Pressure Test

The small-pole shelter, shelter 7, provided the best blast protection in these tests. Not only did it survive structurally at the low and high overpressure loads, but it also kept most of its soil cover, even in the high pressure tests. Furthermore, as indicated earlier in the paper, the internal geometry of this shelter also provided some attenuation to the blast pressure leakage so that internal pressures were slightly lower in amplitude and had slower rise times than the external overpressures. Figure 29 shows a No. 7 shelter after a high pressure test. In these high pressure tests, some soil cover was blown away and into the entrance and vent openings. There was also some evidence of the floor soil being loosened slightly. In some case, a floor cross-frame pole was also loosened from the horizontal pole. Because this shelter always survived in the high pressure tests, it was not tested at the intermediate pressure level.

By treating the shelter survival results statistically, confidence limits can be determined for each shelter at each of the test overpressures. A binomial experiment is one in which there are only two outcomes. For the shelters, the outcome was survival or failure due to the blast loads. The estimate of the probability of survival \bar{S} for each shelter can be calculated from the results in Table 5. For example, \bar{S} for shelter 2 at the 2.8 psi overpressure is 3/7 or $\bar{S} = 0.43$. How much confidence can be placed on this estimate of the survival probability is a function of the number of shelters tested. The larger the number of trials, the closer that the estimated probability \bar{S} will be to the actual value S . In other words $|S - \bar{S}|$ becomes smaller with an increasing number of trials.

The results presented in Table 5 were used to compute 90-percent confidence limits that each shelter provides acceptable protection at least \bar{S} percent of the time when loaded by a given peak overpressure P_s . These confidence intervals on \bar{S} are shown in Figure 30. Note that none of the modified shelter results was included in computing the survival probabilities, and that the marginal shelters were counted as having survived to provide the two outcomes required of a binomial experiment. The point of interest is really the lower boundary of the confidence interval. For example, the results for shelter 3 at a 2.8 overpressure load indicate a 90-percent confidence that the shelter will survive 82-percent of the time. This is based on 16 shelters tested, all of which survived. As the number of shelters

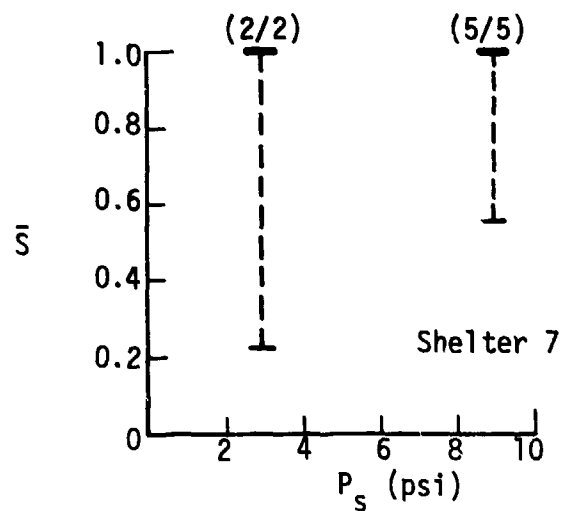
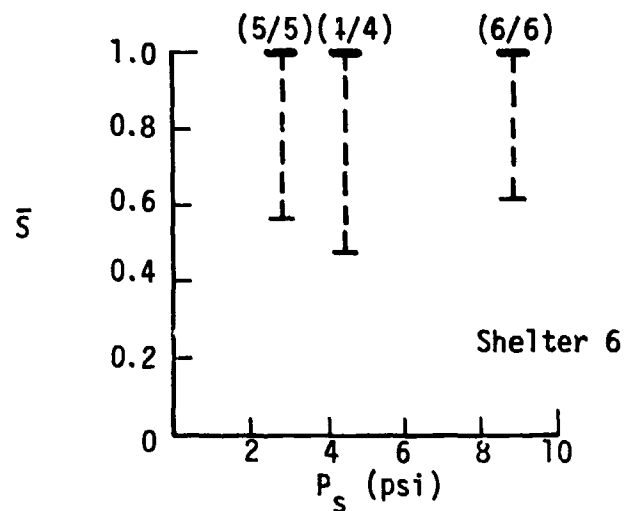
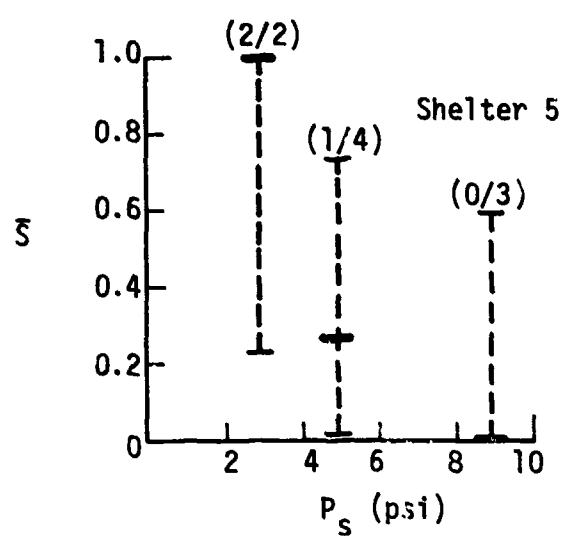
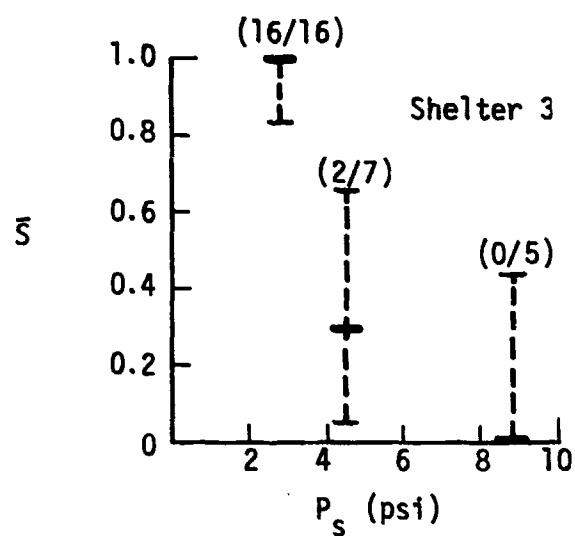
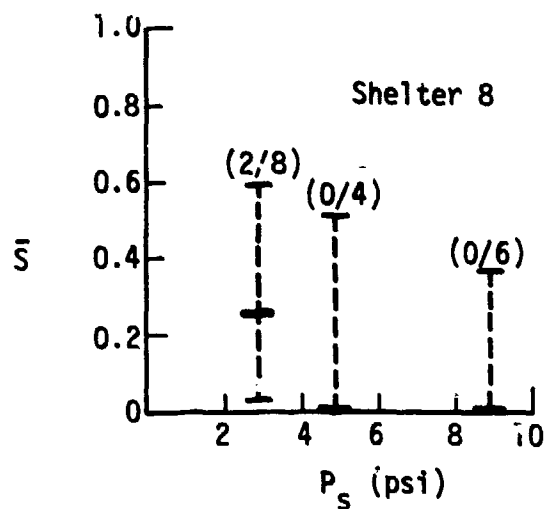
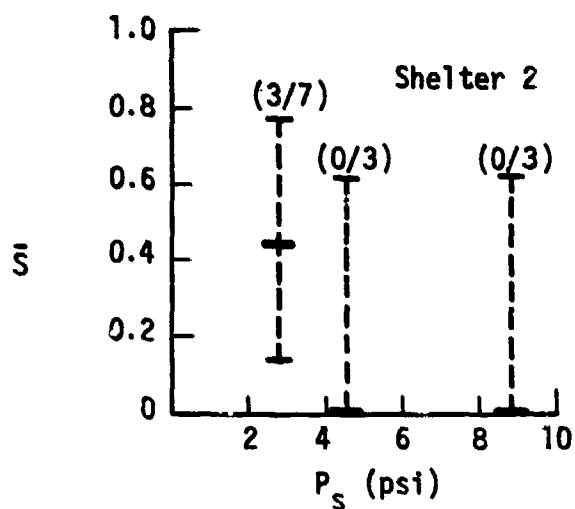


Figure 30. Confidence Intervals of 90-Percent

tested increases without a failure, the lower confidence limit at this pressure will approach 100-percent. Likewise, as shown in this figure, as the number of items tested decreases, the confidence interval will get larger. The estimated probability of survival for each shelter is denoted in Figure 30 by the bolder horizontal line at each pressure level tested. The results show very similar results for shelters 2 and 8, which performed the worst, for shelters 3 and 5, and for shelters 6 and 7, which did the best in this test program.

CLOSURE

All six expedient fallout shelters tested offer some level of blast protection. At least two model shelter of each type survived the 2.8 psig test overpressure. The log-covered trench shelter performed the worst, while the small pole shelter design proved to be best. The predominant failure mode for the shelters that did not survive was soil instability causing walls and roof to collapse. Roof collapse, in general, was another major cause of shelter failure. Translation of above-ground shelters caused some failures at the highest pressure levels. Pressures measured inside the shelters were similar to the external overpressures. Therefore, none of the wooden structural members failed since very little differential pressure developed. Results from the model tests were consistent with previous limited full-scale testing.

Some minor modifications that would improve blast survivability are recommended for the expedient shelter designs tested. Shoring the trench for all designs using trenches would significantly improve their performance particularly at the lowest and intermediate pressures tested. It is also recommended that the entrances for all shelter designs include a simple closure or other blast resistant restriction, such as sandbags, to reduce the internal pressure leakage during the blast wave passage. This would reduce eardrum damage and prevent any lung damage. Development of simple techniques for tying down shelter roof components to the walls and walls of above-ground shelters would increase their blast resistance and probability of survival even at the highest pressure tested. Because of the limitations on overpressure of the shock tunnel, it was not possible to test the small pole shelters at a pressure high enough for it not to survive. This and some of

the other designs with some of the modifications recommended should be tested in a higher pressure tunnel or high-explosive field tests. Replica modeling was successful in evaluating shelters at overpressures less than 9 psi, and should also be used in any future testing to afford testing more items and to increase the confidence of the results.

ACKNOWLEDGEMENTS

This paper is based on a research project conducted by Southwest Research Institute (SwRI) for the Lawrence Livermore National Laboratory (LLNL) and funded by the Federal Emergency Management Agency. Dr. R. G. Hickman was the LLNL contract technical manager, Mr. P. T. Nash was the SwRI project manager, and Scientific Service, Inc., fired the explosively driven shock tunnel. At SwRI, Dr. W. E. Baker performed the model analysis and model response calculations, Dr. R. E. White did the model shelter spacing analysis, and Mr. N. W. Blaylock carried out the statistical analysis. The author appreciates the contributions of all these individuals as well as those of the rest of the SwRI project team that successfully built the model shelters, and implemented and performed the shock tunnel experiments. In addition, the author thanks SwRI for providing the resources to prepare and present this paper.

REFERENCES

1. "Guide for Increasing Local Government Civil Defense Readiness During Periods of International Crisis," Defense Civil Preparedness Agency, Civil Preparedness Guide (CPG) 1-7, April 1979.
2. Kearny, C. H., Nuclear War Survival Skills, NWS Research Bureau, 1982.
3. Kearny, C. H., and Chester, C. V., "Blast Tests of Expedient Shelters in the DICE THROW Event," Oak Ridge National Laboratory, ORNL-5347, March 1978.
4. Kearny, C. H., Chester, C. V., and York, E. N., "Blast Tests of Expedient Shelters in the MISERS 3LUFF Event," Oak Ridge National Laboratory, ORNL-5541, January 1980.
5. Nash, P. T., Baker, W. E., Esparza, E. D., Westine, P. S., Blaylock, N. W., White, R. E., and Whitney, M. G., "Do-It-Yourself Fallout/Blast Shelter Evaluation," Final Report, Federal Emergency Management Agency, Southwest Research Institute Project 06-7531, San Antonio, Texas, March 1984.

6. Baker, W. E., Westine, P. S., and Dodge, F. T., Similarity Methods in Engineering Dynamics, Spartan Books, Hayden Book Company, Inc., Rochelle Park, New Jersey, 1973.
7. Wilton, C., Kaplan, K., and Gabrielson, B. L., "The Shock Tunnel: History and Results," SSI 7618-1, March 1978.
8. Hirsch, A. E., "The Tolerance of Man to Impact," Annals of the New York Academy of Sciences, Volume 152, Art. 1, pp. 168-171, October 1968.
9. White, C. S., "The Scope of Blast and Shock Biology and Problem Areas in Relating Physical and Biological Parameters," Annals of the New York Academy of Sciences, Volume 152, Art. 1, pp. 80-102, October 1968.
10. Baker, W. E., Kulesz, J. J., Ricker, R. E., Bessey, R. L., Westine, P. S., Parr, V. B., and Oldham, G. A., "Workbook for Predicting Pressure Wave and Fragment Effects of Exploding Propellant

AD-P005 369

BLAST LOADING ON ABOVE GROUND BARRICADED
MUNITION STORAGE MAGAZINES - II

by
George A. Coulter
Charles N. Kingery
Peter C. Muller

U.S. Army Materiel Command
Ballistic Research Laboratory
Aberdeen Proving Ground, Maryland 21005-5066

ABSTRACT

~~to the 1/3 power~~
This report presents the results of a study designed to measure the blast loading on above ground munition storage magazines. The magazines are sited at separation distances of K2 ($2W^{1/3}$ ft), K4 ($4W^{1/3}$ ft), and K6 ($6W^{1/3}$ ft) where W is the maximum allowable high-explosive weight in pounds mass. Earth barricades protect the structures. Responding and nonresponding 1/23.5 scaled models were used for the test program. Loading results are presented for the nonresponding barricaded model magazine. The highest loading measured on the nonresponding model was on the side-wall nearest the donor magazine. Maximum values of reflected pressure at Station 3 were found to be about 900, 600, and 360 kPa for separation distances of $0.8 Q^{1/3}$ m, $1.6 Q^{1/3}$ m, and $2.4 Q^{1/3}$ m, respectively. Whole wall translation velocities calculated from the measured wall loading forces ranged from 7-12 m/s. These velocities are well under the fragment velocities needed to cause detonation of the stored munitions in the acceptor magazine. This indicated the present siting criteria of $0.8 Q^{1/3}$ m ~~to the 1/3 power~~ is safe for this type of above ground barricaded magazine. Additional costly greater siting distances should not be necessary.

I. INTRODUCTION

A. Background

This study is a portion of a research program conducted at the Ballistic Research Laboratory (BRL) and sponsored by the Department of Defense Explosives Safety Board (DDESB). The purpose of the general program is to model and measure blast parameters pertaining to various types of munition storage magazines. This study concerns an above ground type barricaded storage magazine, but without earth cover. This type of magazine has been located in areas of Europe and in the United Kingdom. The particular one selected for study is located in Machrihanish, Scotland, Reference 1. Preliminary research at BRL was reported in Reference 2.

B. Objective

The primary objective of this phase of the research is to determine through scale model experiments the blast loading on an acceptor magazine with differing barricades in the event of an accidental explosion in a donor magazine. An assumption is made that all the stored munition (net explosive weight, NEW) in the donor magazine detonates together to create the blast wave. Effects of the munitions casing are not considered, although, for the particular contents of a known storage magazine it could be included.

All barricades were constructed of hard packed soil. Results from Reference 2 indicated a need to control this parameter. Safe separation distances of $0.8 Q^{1/3}$ m, $1.6 Q^{1/3}$ m, and $2.4 Q^{1/3}$ m, where Q is in kilograms, were to be modeled with the experiments. These distances correspond to K2 ($2W^{1/3}$ ft), K4 ($4W^{1/3}$ ft) and K6 ($6W^{1/3}$ ft) where w is in pounds mass.

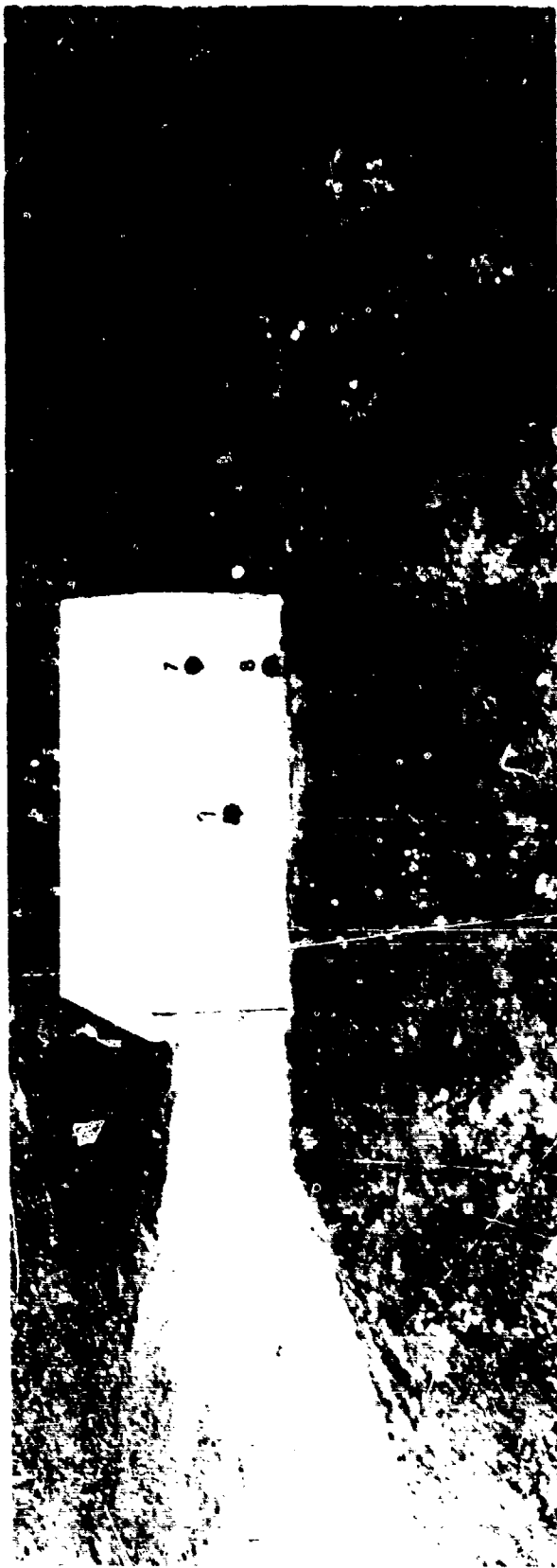
II. TEST PROCEDURES

The types of models, test site layout, instrumentation, and test matrix will be discussed in this section.

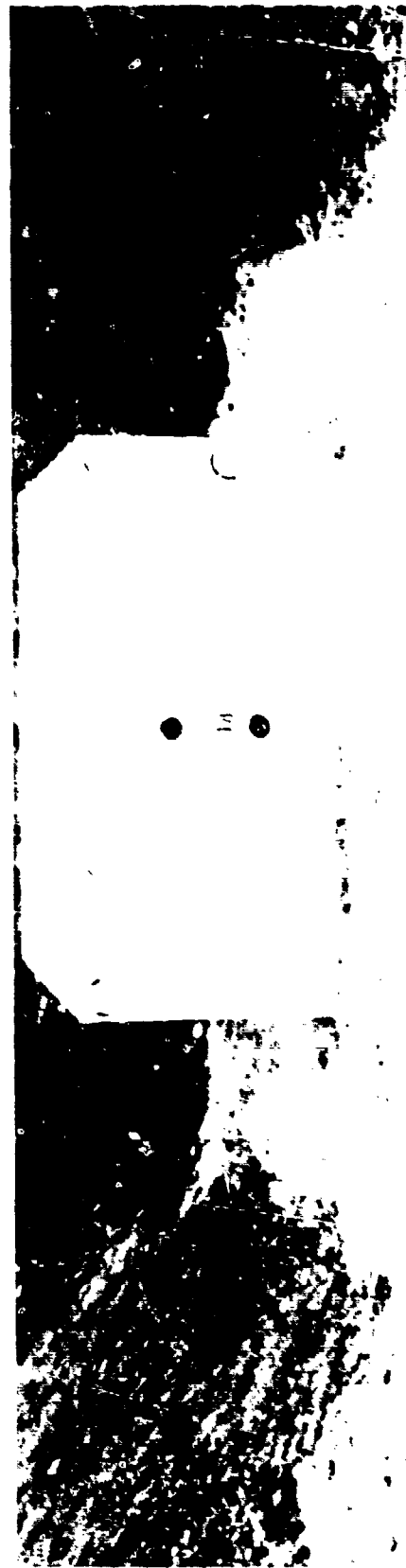
A. Models

Two types of scaled models were used for the test program. A steel nonresponding acceptor model was built and instrumented with piezoelectric pressure transducers. The second model was a scaled concrete model (density was same as full-size magazine) used both for the donor and the responding acceptor (Shot 1 only).

Figure 1 shows photographs and a sketch of the 1/23.5 scale nonresponding steel model of a munitions magazine located at the Machrihanish, Scotland site. The assumption is made that the variety of stored munitions in the full-sized magazine will be equivalent to 13,000 kg of bare hemispherical Pentolite. This amount is scaled down by the cube root or to 1/23.5 scale for the 1 kg charge that was used for these tests. The model dimensions and transducer locations are shown in Figure 1-C.

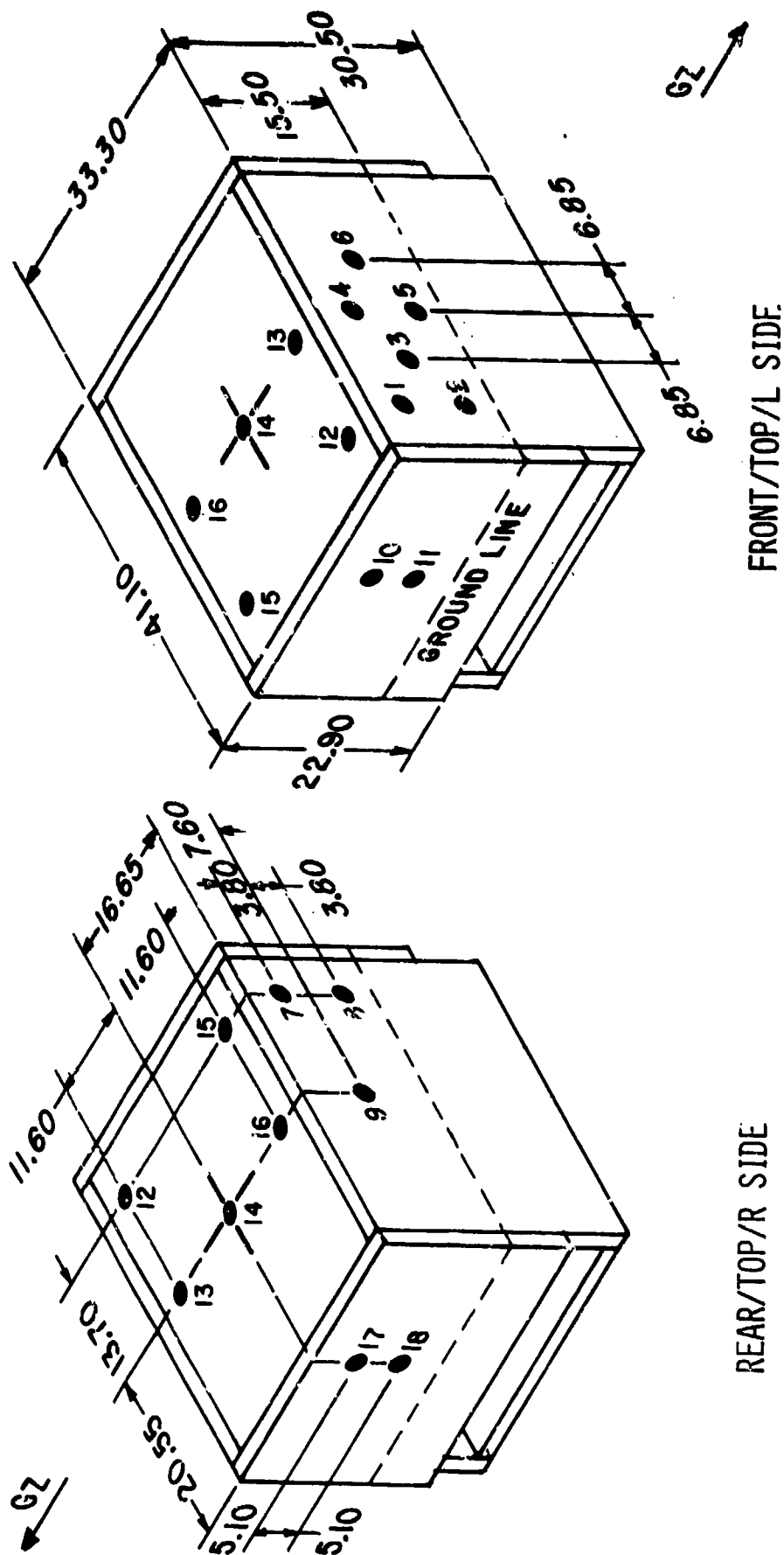


A. View of Back Side Wall



B. View of Right End Wall

Figure 1 Nonresponding Acceptor Model



C. Sketch Showing Station Locations

Figure 1. Nonresponding Acceptor Model (Cont.)

The near side-wall is defined as the wall closest to the magazine. All positions are defined as seen from the donor magazine.

The concrete donor/acceptor model was also 1/23.5 scale; it is shown in the photographs of Figures 2 and 3. The concrete models were cast as five separate slabs. The door opening was closed during the shot by a cardboard door. A ready-mixed mortar cement was used for the roof and wall portions. Copper wire was used as reinforcing for the roof slab only.

For Shot 1, the responding acceptor model had the near side-wall scored to control the break-up mode. Additionally, the model slabs were cemented at the joints with silastic cement to insure that the side wall would fail first as would be expected for the full-size magazine.

A styrofoam witness plate was placed against the back wall to catch any flying fragments. A simple indication of the break-up pattern might be obtained in this manner. A more sophisticated velocity screen system is planned for use during future tests.

B. Test Charges

The bare charges were cast in-house with a 50/50 mix Pentolite in a hemispherical mold. All charges were trimmed to be exactly 1 kg. Detonation was from the center of the flat surface of the charge placed on the donor's floor.

C. Test Layout

Figures 4-6 show sketches of the test site layout. All dimensions, including barricades, were scaled by the 1/23.5 factor chosen for the model and the charge. It was decided at a meeting with the DDESB Project Officer not to change the spacing between the models and the back barricade. Spacing was changed between the model magazines according to multiples of the safe separations distances: $0.8 Q^{1/3}$ m, $1.6 Q^{1/3}$ m, and $2.4 Q^{1/3}$ m.

D. Instrumentation

The instrumentation was standard for blast wave recording. The transducers were quartz PCB piezoelectric type, Models 113A24 and 113A28. These were coupled through preamplifiers into either a Honeywell 7600 or 101 FM recording system. The data were available from a visicorder immediately after the shot. Later the data were reduced to plots with engineering units for comparison. An analog-digital system coupled to a microcomputer accomplished this phase of the data reduction. See Figure 7 for a schematic.

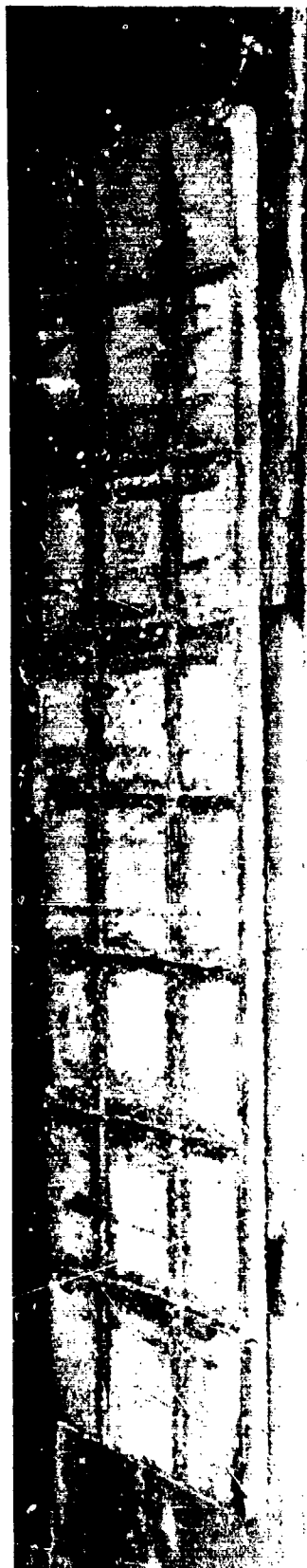


A. Donor without Roof Slab

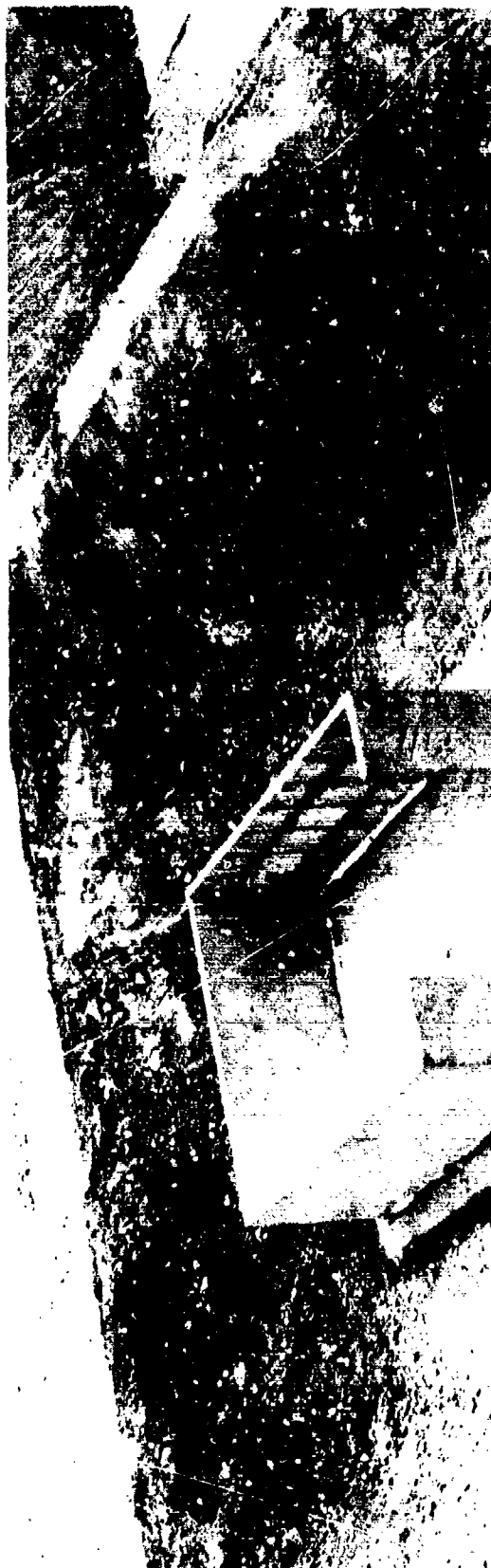


B. Acceptor

Figure 2. Concrete Donor/Acceptor Models



A. Scored Near Side-Wall



B. Installed Wall

Figure 3. Concrete Responding Acceptor Model



C. Reinforced Donor/Acceptor Roof

Figure 3. Concrete Responding Acceptor Model (Cont.)

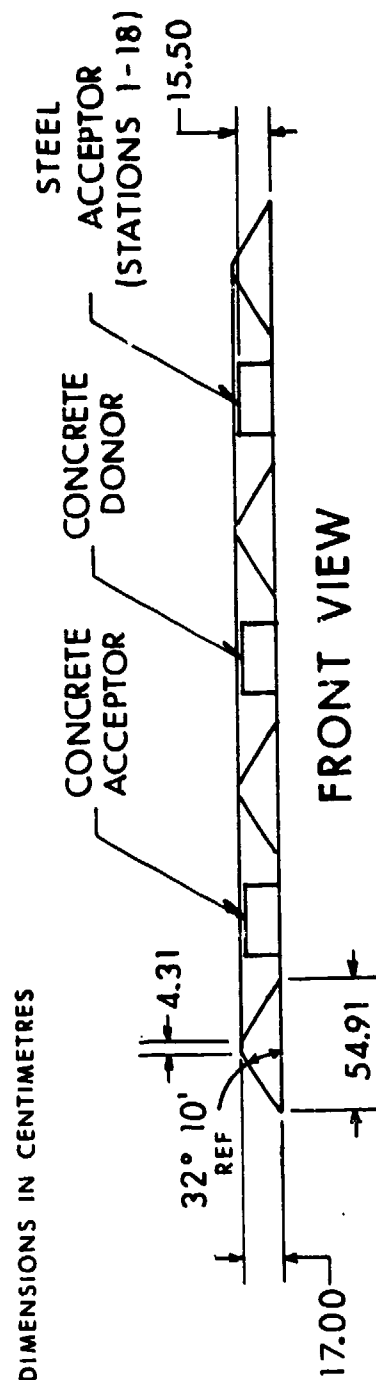
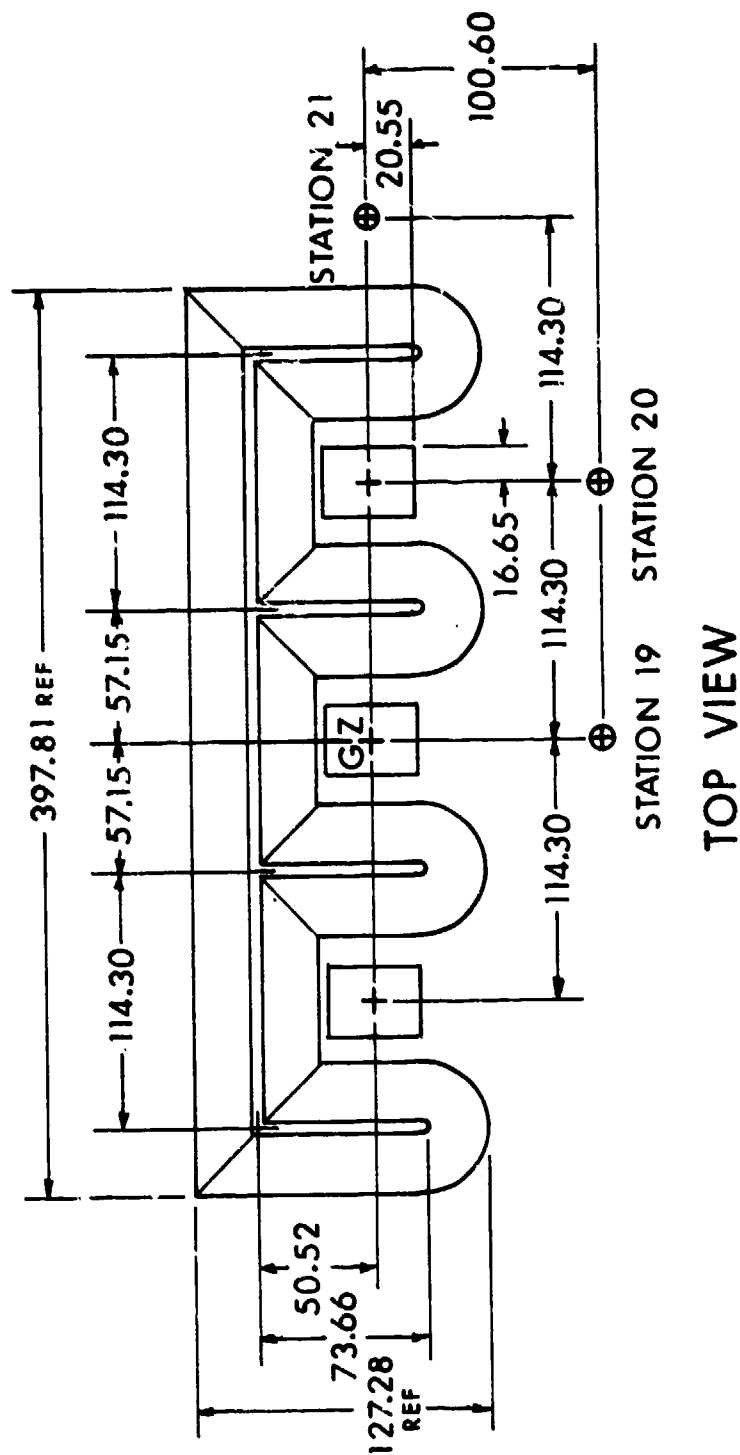


Figure 4. Test layout for a Separation Distance of $0.8 Q^{1/3}$ m

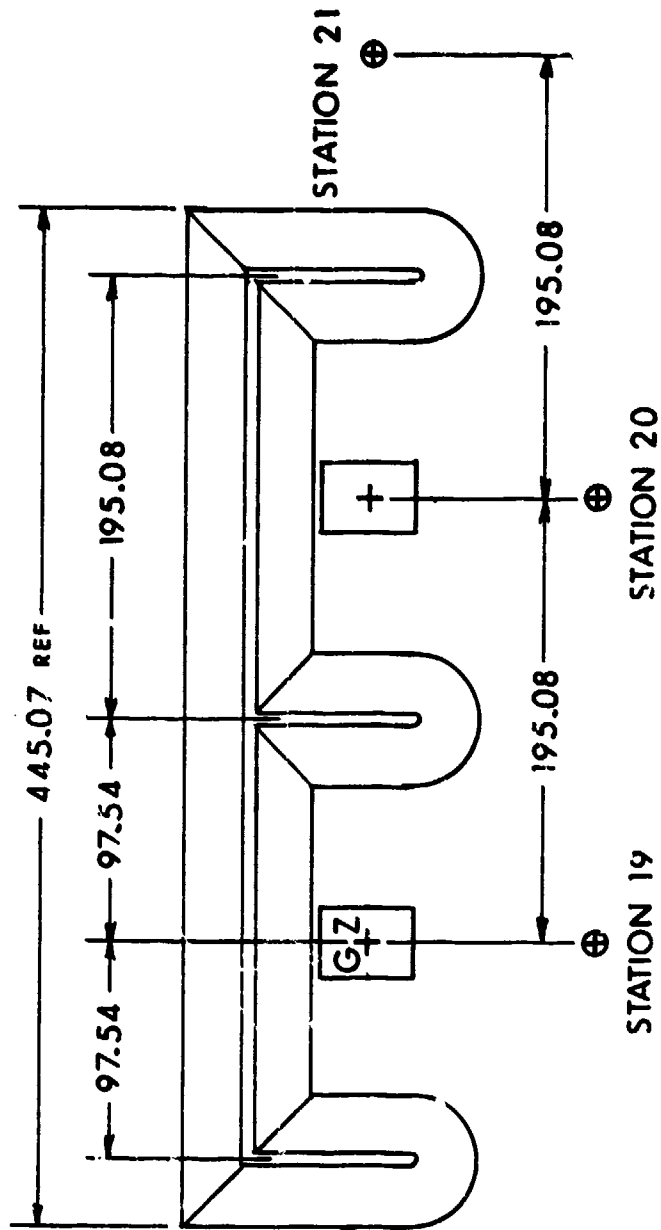


Figure 5. Test Layout for a Separation Distance of $1.6 Q^{1/3}$ m

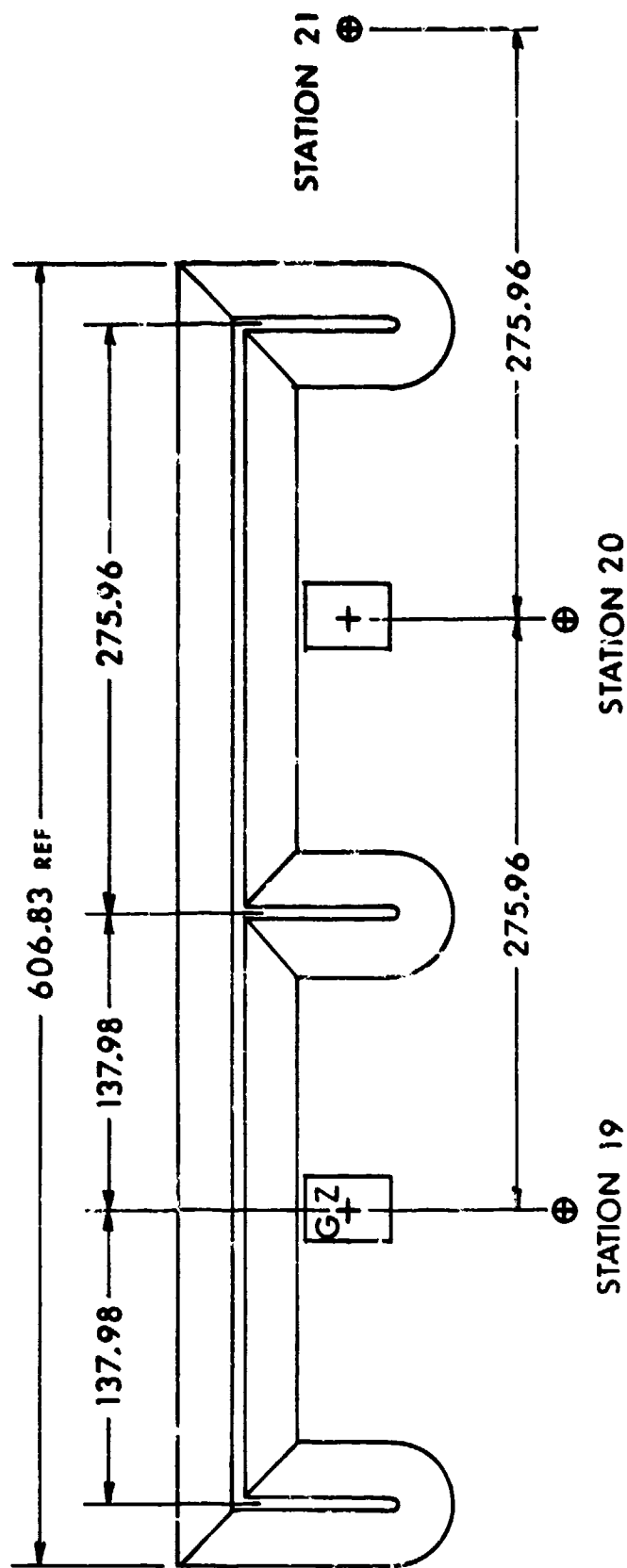


Figure 6. Test Layout for a Separation Distance of $2.4 Q^{1/3}$ m

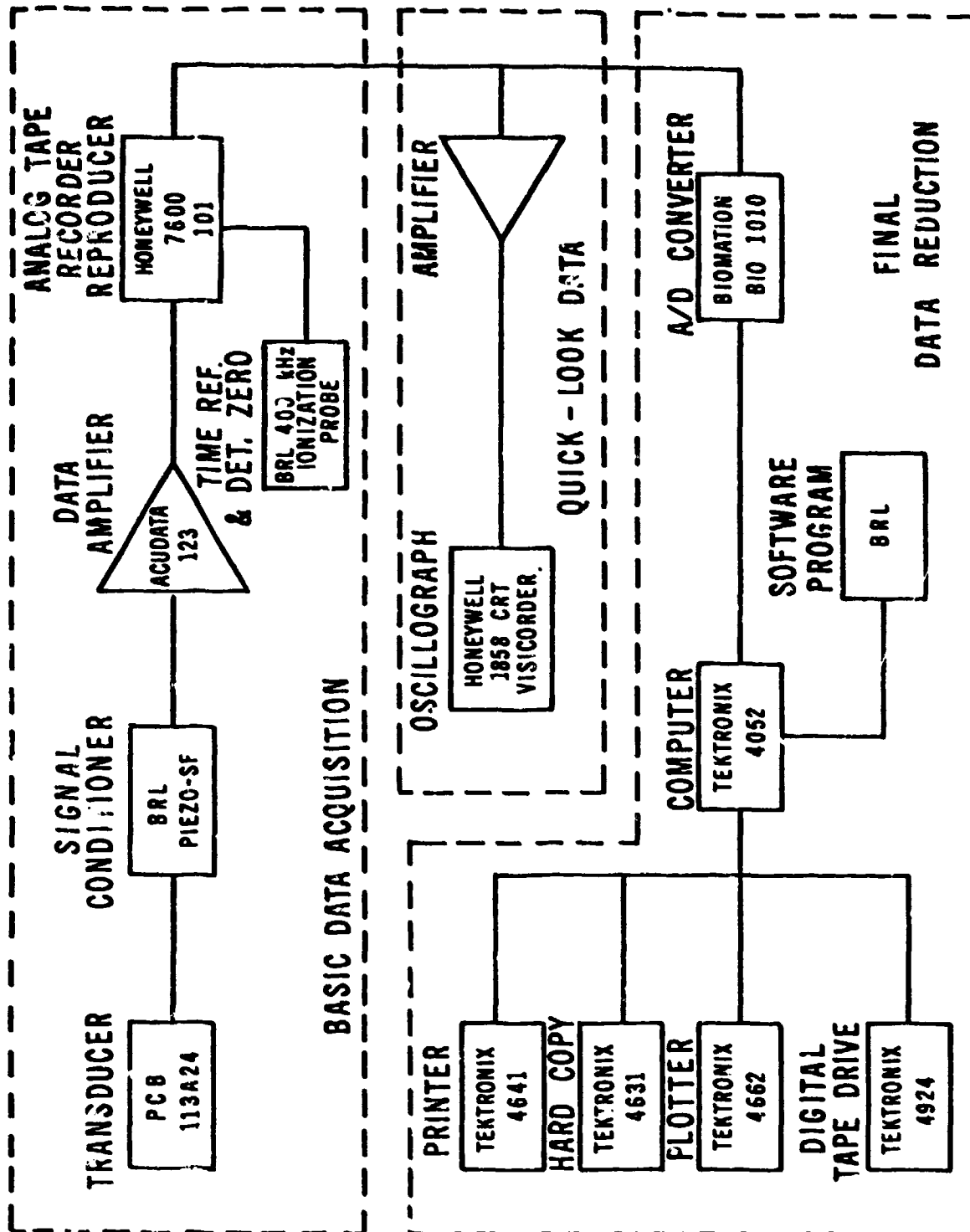


Figure 7. Data Acquisition/Reduction System

E. Test Matrix

A series of six shots was fired during the test period. For the test conditions at the Range 8 test site on Spesutie Island, see Table 1. A responding concrete acceptor model was used only on Shot 1. The remaining shots were made only with the non-responding instrumented steel acceptor. All Pentolite charges were cast and trimmed to be 1 kg hemispherical to make the test comparisons more exact. No scaling was needed between shots. All barricades were constructed of field soil, hard-packed.

TABLE 1. TEST MATRIX

Shot	Donor Cover kg	50/50 Pentolite Charge Weight kg	Concrete Acceptor	Ambient Pressure kPa	Ambient Temp. °C	Wind Speed km/h	Separation Distance Factor
1	5.72	1.00	Yes	101.5	30.0	12 @ 280°	K2
2	5.71	1.00	No	101.9	28.3	5 @ 190°	K4
3	5.33	1.00	No	102.9	25.0	3 @ 90°	K4
4	5.64	1.00	No	102.2	26.1	5 @ 90°	K6
5	5.50	1.00	No	101.8	30.3	5 @ 80°	K6
6	5.50	1.00	No	100.6	29.4	Calm	K6

English	Metric
Note: $K2 = 2W^{1/3}$ ft	$= 0.8Q^{1/3}$ m
$K4 = 4W^{1/3}$ ft	$= 1.6Q^{1/3}$ m
$K6 = 6W^{1/3}$ ft	$= 2.4Q^{1/3}$ m

for K2 English: $W = 2.204$ lbs, the $K2 = 2(1.30)$ ft = 2.60 ft.

for K2 metric: $Q = 1$ kg, the $K2 = .8 (1)$ m = 0.8 m

III. RESULTS

The results will be presented in photographs of site damage, in data tables, and in pressure-time records taken at various site locations and on the nonresponding model magazine.

A. Site Damage

Figures 8 - 10 illustrate the kind of damage that occurred to the responding model magazine. The donor magazine containing the 1 kg charge was destroyed completely. A crater was formed during each shot measuring 1.2 - 1.4 m across (measured to inside edge) and a depth of 0.26 to 0.28 m at the center. All craters were very similar from shot to shot.

The part of the barricade directly behind the donor charge model magazine was blown through on each shot. Both arms of the barricade on either side of the donor were crushed and moved away from the donor site (crater). The barricade behind and along the far side of the non-responding model was least disturbed of any part of the barricade. See Figures 9 and 10.

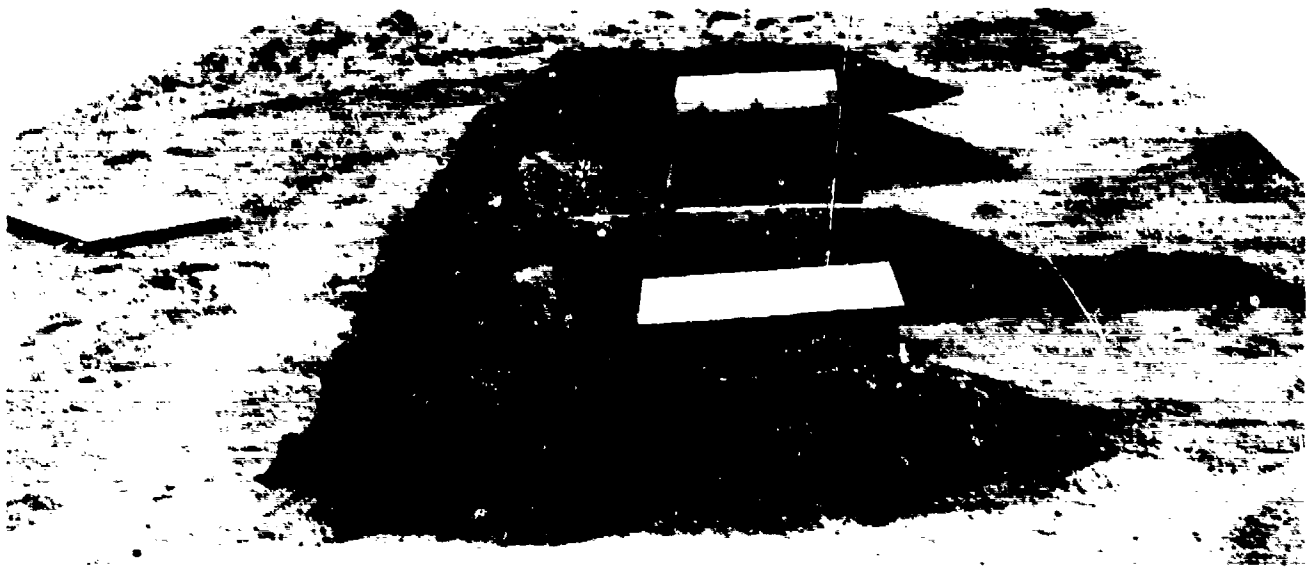
Figure 8-B illustrates the crushing and movement of the responding concrete model. Figure 8-C is a photograph of the reconstructed acceptor model showing the break-up of the various model components. The scored near side-wall did break as was anticipated, although the styrofoam witness plate (Figure 3-B) had almost no indentation from the movement of the wall segments. (The next series of tests planned will use velocity screens instead of the witness plate.)

B. Blast Loading on Acceptor Structure Near Side-Wall

Table 2 lists pertinent parameters at the three ground baffle stations. Station 19 is directly in front of the donor magazine. Station 20 is in front of the nonresponding acceptor model magazine, and Station 21 is on the other side of the barricade arm, past the nonresponding model. See Figures 4 - 6 above for the ground station locations for each of the three separation distances.

The peak pressures ranged from about 1500 kPa to 2300 kPa at Station 19 (where the distance remained the same) from 86 - 279 kPa at Station 20, and from 41 - 162 kPa at Station 21 over the three separation distances. For examples, see Figure 11.

Table 3 lists the parameters for the blast loading on the side-wall of the nonresponding model, nearest to the model donor magazine. Maximum values of reflected pressure peaks at Station 3 of about 900, 600, and 360 kPa were measured for separation distances of $0.8 Q^{1/3}$ m, $1.6 Q^{1/3}$ m, and $2.4 Q^{1/3}$ m, respectively. Typical pressure-time waveforms are shown in Figures 12 and 13 for two representative stations, Stations 1 and 3. The

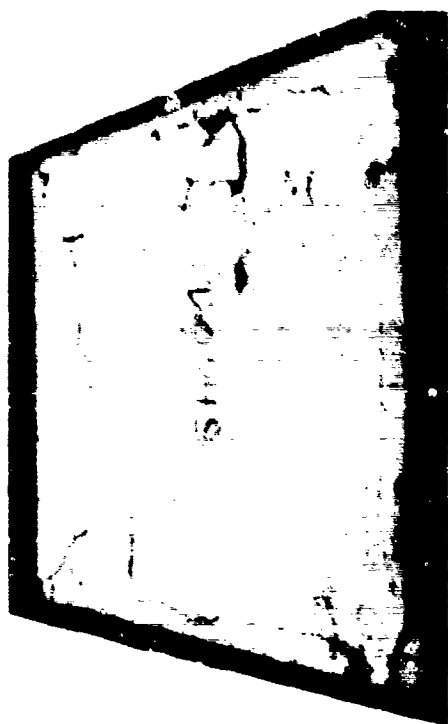


A. Preshot Site



B. Postshot Site

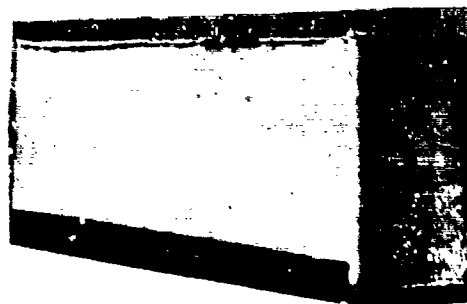
Figure 8. Photographs for a Separation Distance of
 $0.8 Q^{1/3} \text{ m (K2) 1695}$



Roof



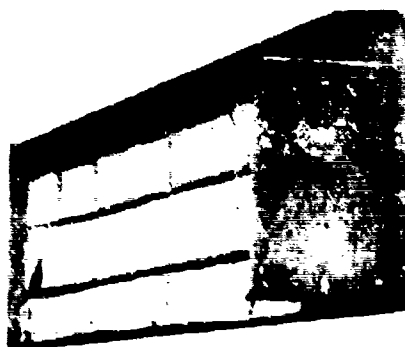
Back End Wall



Far Wall



Floor

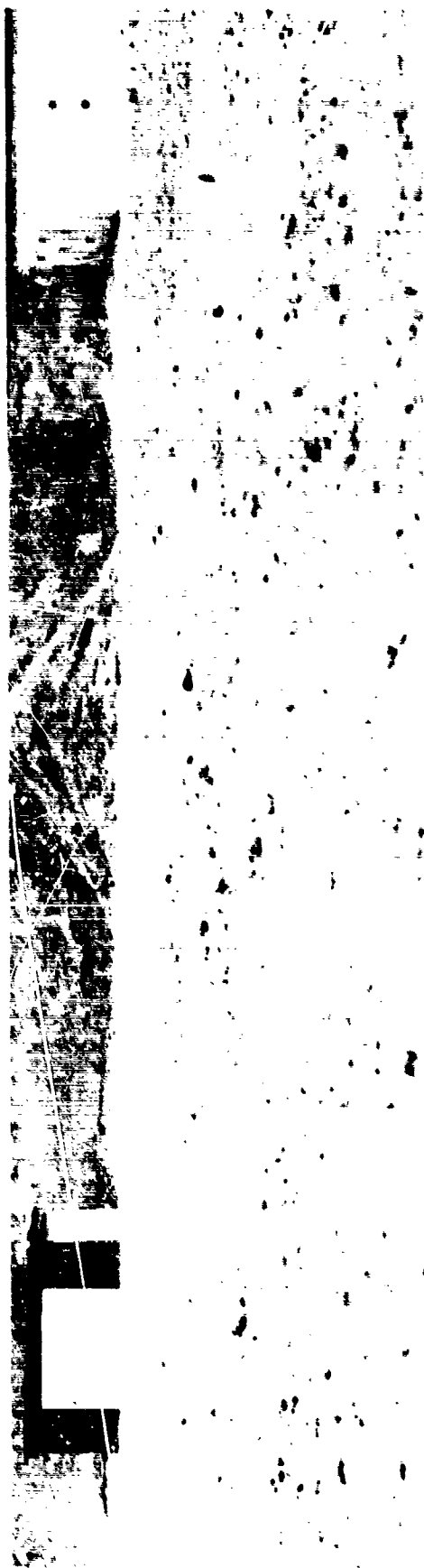


Near Wall

C. Postshot Acceptor Model Magazine

Figure 8. Photographs for a Separation Distance of

0.8 Q^{1/3} ± (K2) (Cont.)



A. Preshot Site



B. Postshot Site

Figure 9. Photographs for a Separation Distance of
 $1.6 Q^{1/3} \text{ m (K4)}$



A. Preshot Site

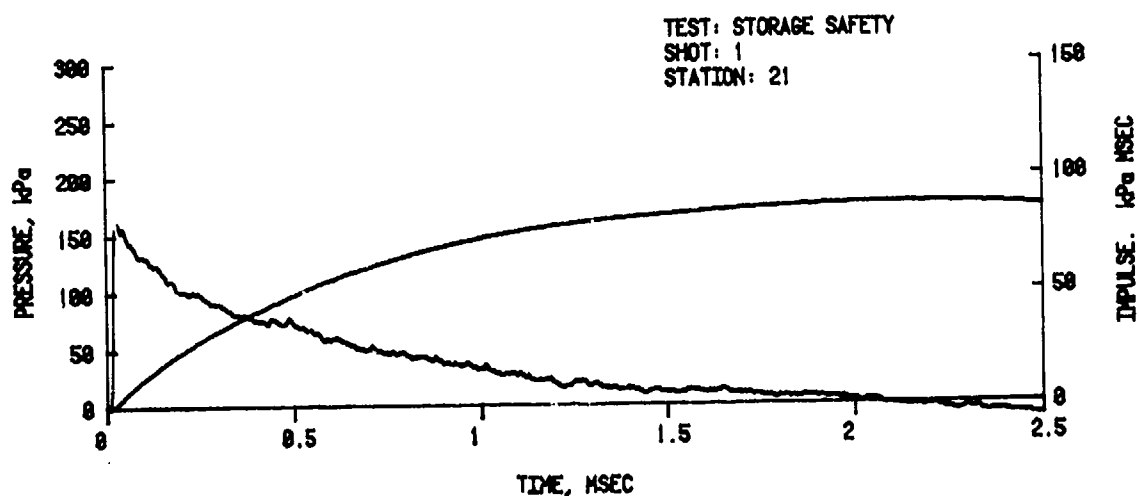
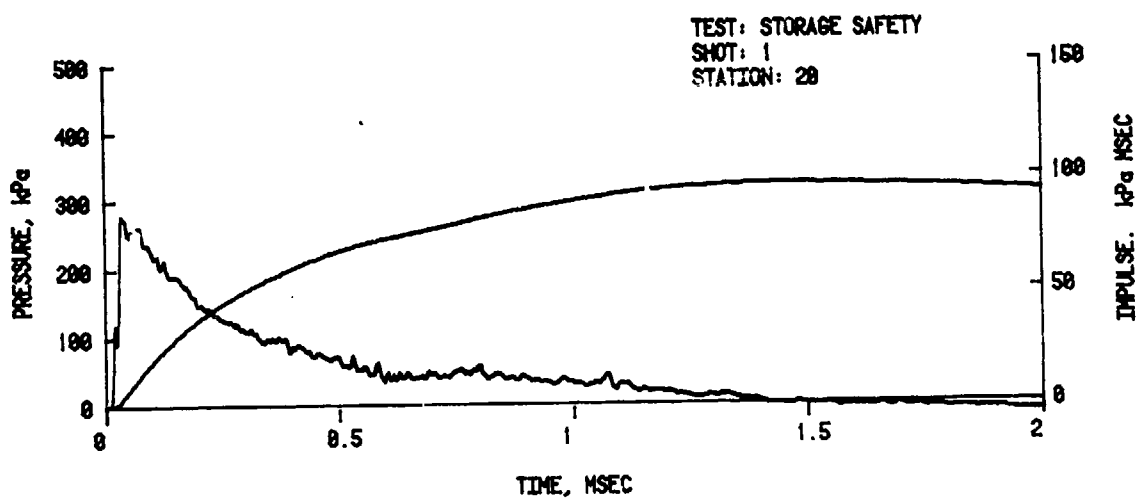
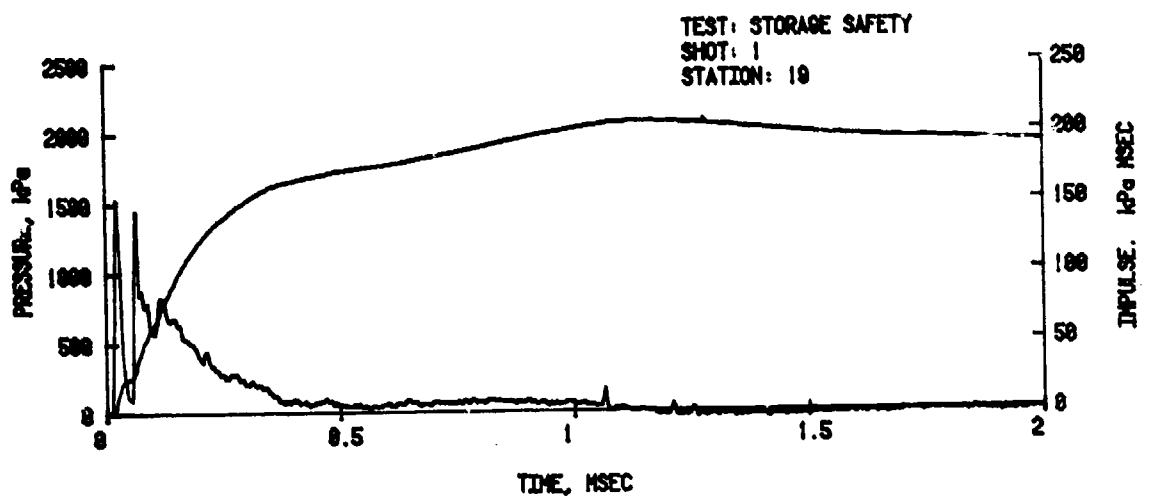


B. Postshot Site

Figure 10. Photographs for a Separation Distance of
 $2.4 Q^{1/3} \text{ m (K6)}$ 1698

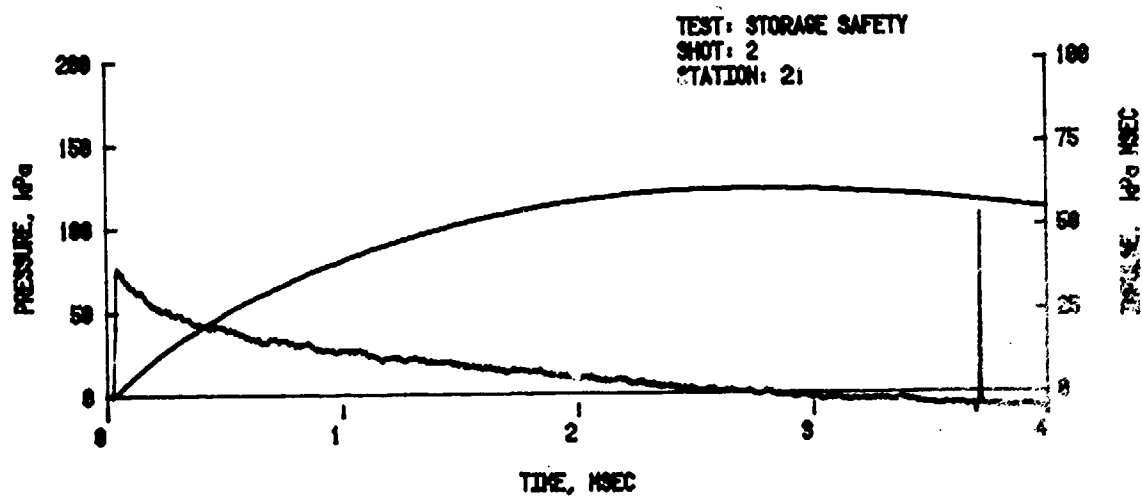
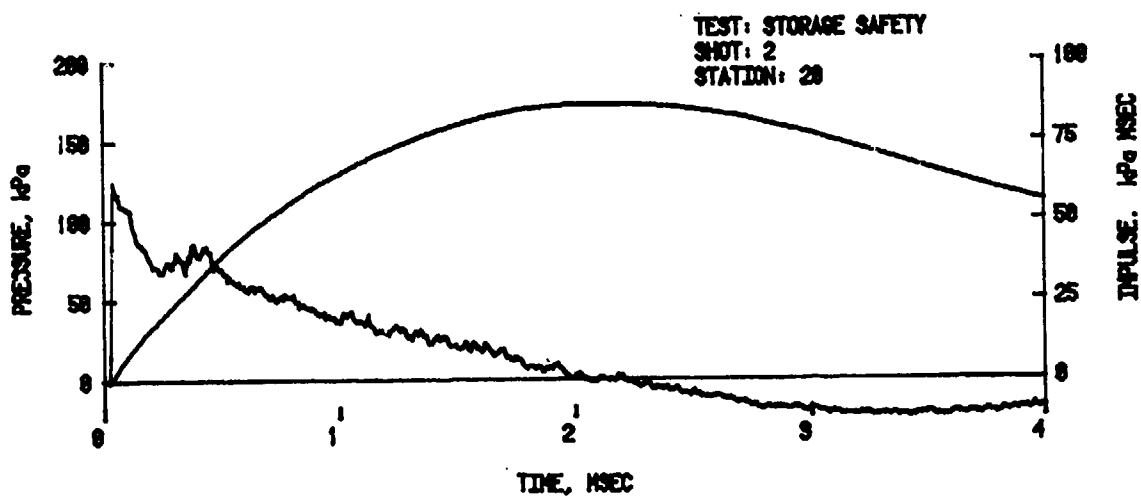
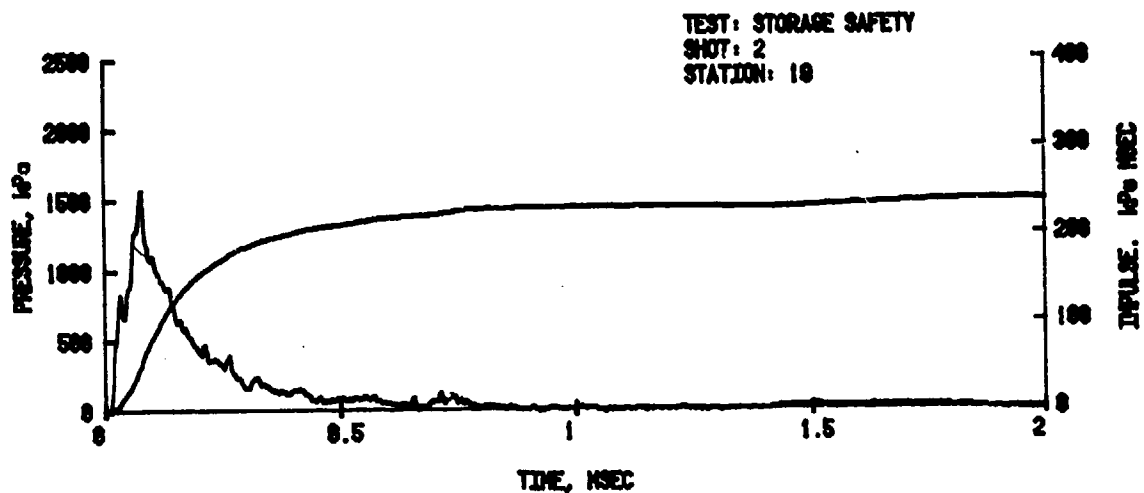
TABLE 2. FREE-FIELD BLAST PARAMETERS-WITH BARRICADES

Shot	Station	Distance m	Peak Overpressure kPa	Impulse kPa-ms	Arrival Time ms	Duration ms	Remarks
1	19	1.006	1537	207	0.48	1.16	$0.8Q^{1/3}_m$
	20	1.523	279	97	1.34	1.41	
	21	2.286	162	88	3.24	1.66	
2	19	1.006	501/1575	238	0.46	1.04	$1.6Q^{1/3}_m$
	20	2.195	125	86	2.43	2.21	
	21	3.902	76	61	6.74	2.83	
3	19	1.006	2280	312	0.45	0.64	$1.6Q^{1/3}_m$
	20	2.135	143	89	2.43	2.00	
	21	3.902	67	60	6.77	2.82	
4	19	1.006	2147	229	0.45	0.50	$2.4Q^{1/3}_m$
	20	2.427	93	78	4.16	2.35	
	21	5.519	28.7	40	10.51	3.10	
5	19	1.006	667/1582	252	0.44	0.71	$2.4Q^{1/3}_m$
	20	2.427	95	81	4.15	2.43	
	21	5.519	43	48	10.49	3.56	
6	19	1.006	2032	226	0.44	0.67	$2.4Q^{1/3}_m$
	20	2.427	86	75	4.03	2.40	
	21	5.519	41	46	10.64	3.26	



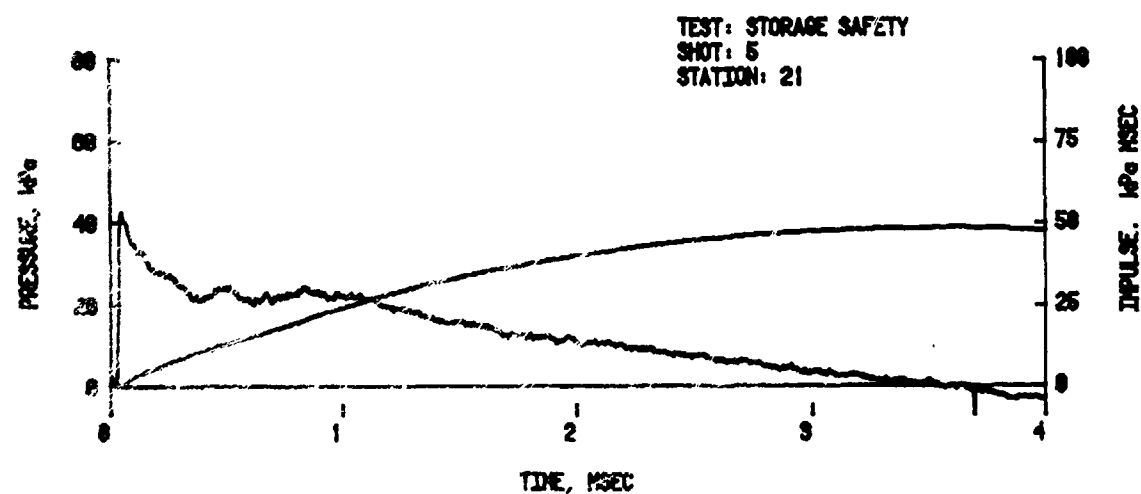
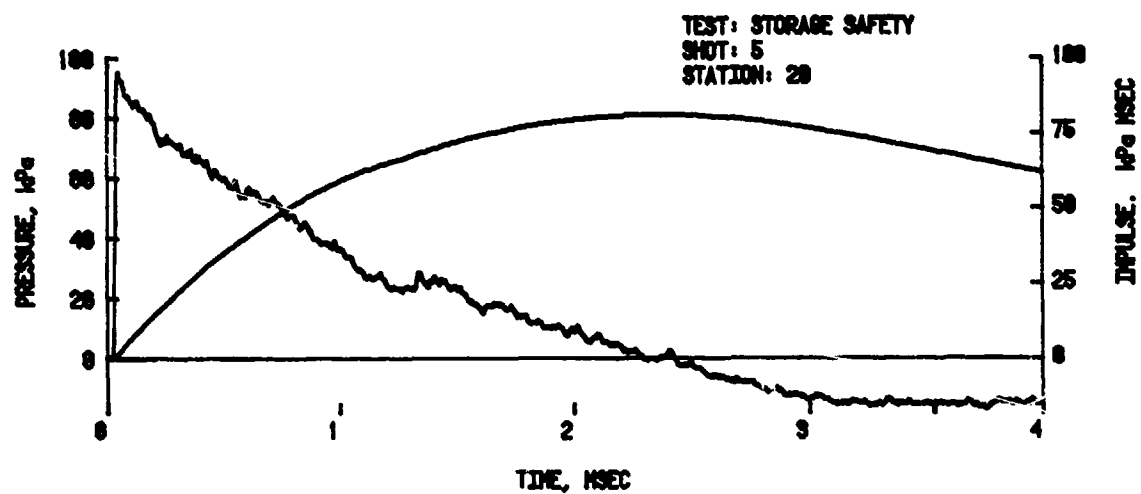
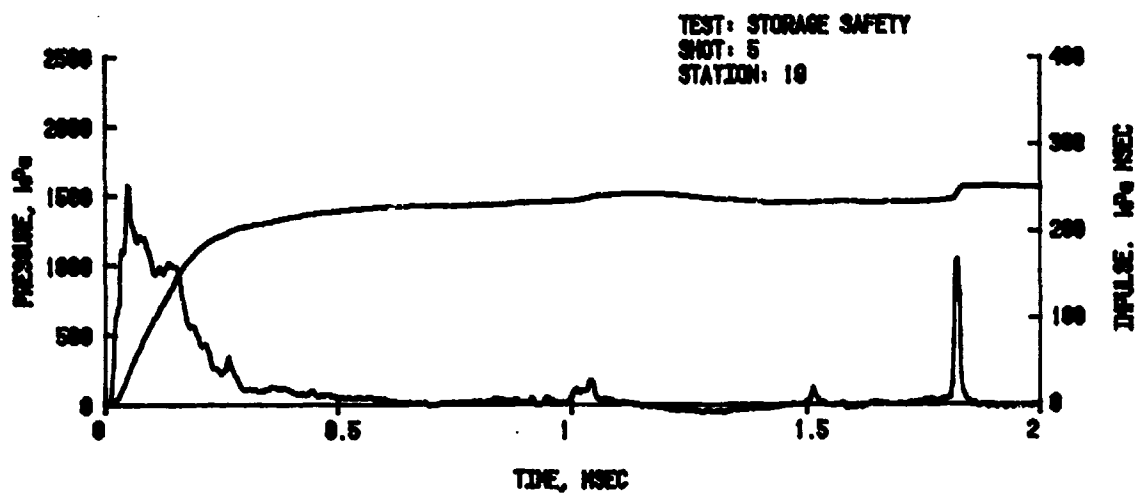
A. $0.8 Q^{1/3}_m$

Figure 11. Pressure-Time Records, Free-Field
with Barricades



B. $1.6 Q^{1/3} m$

Figure 11. Pressure-Time Records, Free-Field
with Barricades (Cont.)



$$C. 2.4 Q^{1/3} m$$

Figure 11. Pressure-Time Records, Free-Field with Barricades (Cont.)

TABLE 3. BLAST LOADING ON NEAR SIDE-WALL

Shot	Station	Peak Pressure kPa	Positive Impulse kPa-ms	Arrival Time ms	Positive Duration ms	Remarks
1	1	1128	182	0.80	0.56	$0.8Q^{1/3}$ m
	2	814/1707*	253	0.85	0.56	
	3	890	205	0.82	0.61	
	4	894	187	0.83	0.69	
	5	815	239	0.84	0.59	
	6	-	-	-	-	
2	1	300/565	165	1.96	1.13	$1.6Q^{1/3}$ m
	2	797/812	209	2.00	0.97	
	3	284/578	197	1.98	0.92	
	4	354/459	195	1.95	0.94	
	5	658	206	1.99	0.81	
	6	339/580	213	1.97	1.02	
3	1	339/513	156	1.88	1.17	$1.6Q^{1/3}$ m
	2	726	194	1.93	1.04	
	3	-	-	-	-	
	4	357/373	180	1.87	1.00	
	5	321/578	210	1.93	0.88	
	6	358/554	198	1.91	1.01	
4	1	488	125	3.40	1.89	$2.4Q^{1/3}$ m
	2	399/420	142	3.41	1.86	
	3	343/349	137	3.40	1.97	
	4	366	138	3.38	2.00	
	5	414/428	164	3.41	1.79	
	6	440	144	3.39	2.00	
5	1	319/416	119	3.49	1.58	$2.4Q^{1/3}$ m
	2	299/356	133	3.49	1.11	
	3	304/369	133	3.49	1.26	
	4	472	142	3.48	2.00	
	5	288/391	144	3.49	0.98	
	6	306/420	145	3.49	2.00	
6	1	243	106	3.40	1.96	$2.4Q^{1/3}$ m
	2	246	116	3.40	1.78	
	3	240	112	3.40	1.72	
	4	264	119	3.40	1.82	
	5	256/263	124	3.41	1.66	
	6	270	123	3.41	1.64	

*Second value refers to maximum reflected pressure peak if the initial peak is not the maximum.

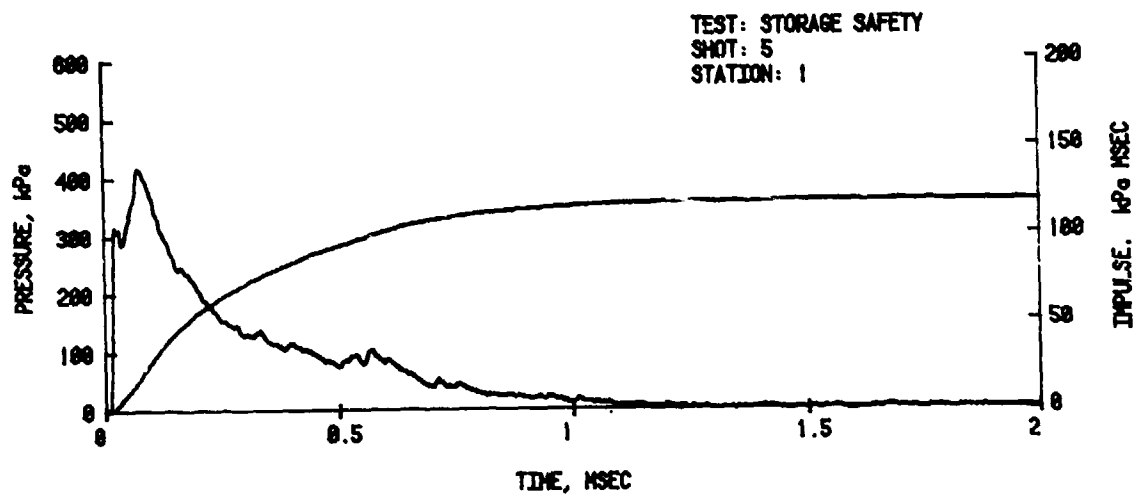
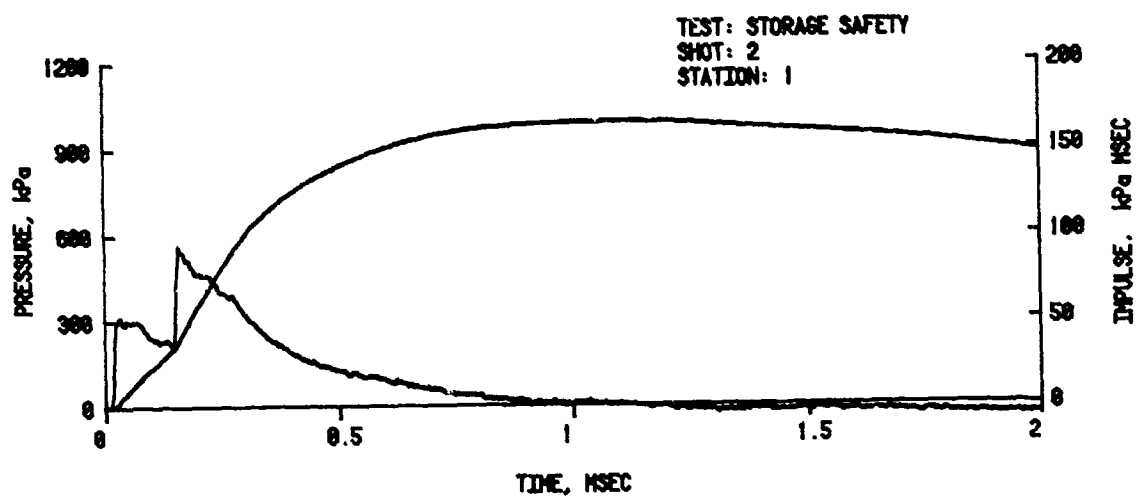
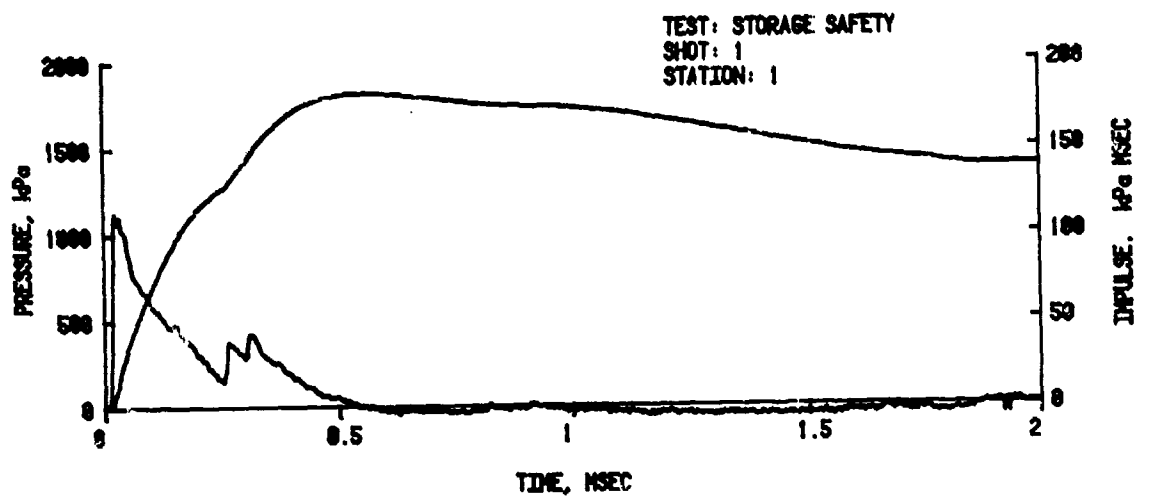


Figure 12. Pressure-Time Records from Near Side-Wall,
Station 1

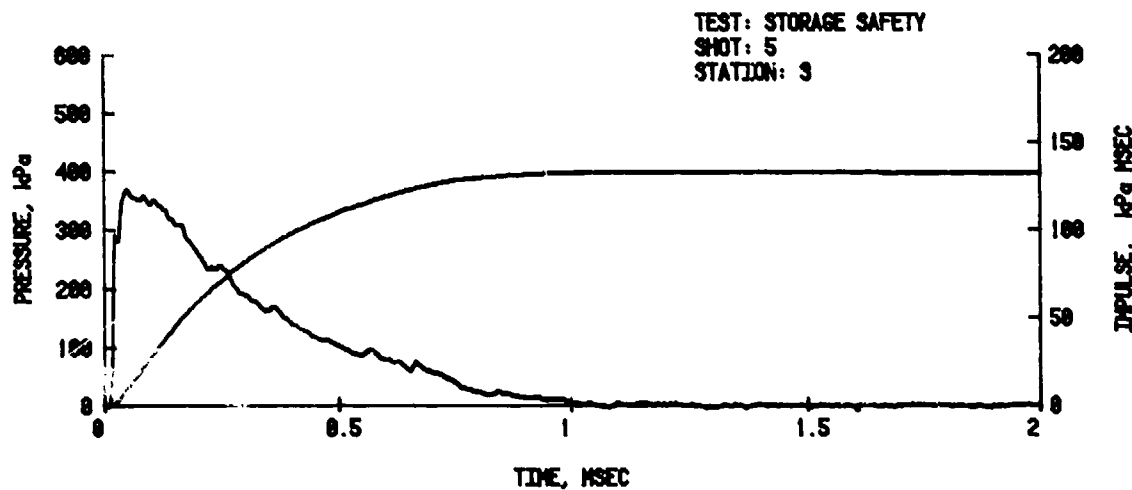
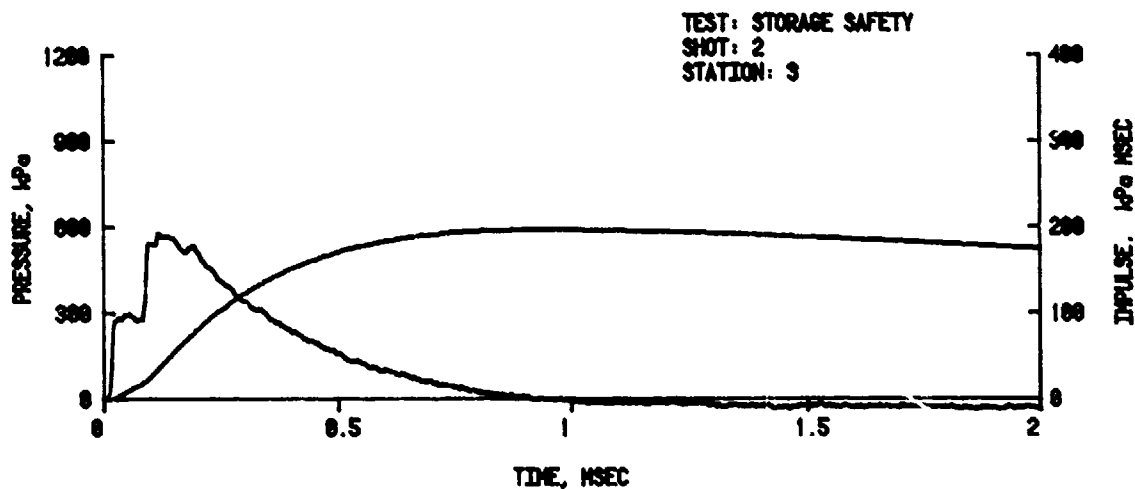
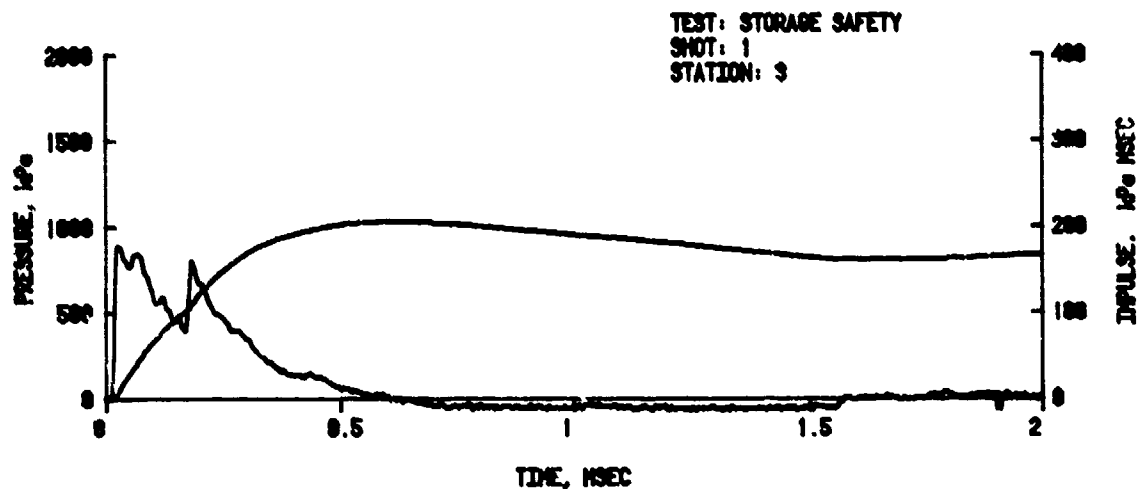


Figure 13. Pressure-Time Records from Near Side-Wall,
Station 3

waveform change as a function of separation distance is shown by the variation in peak formation: a large initial peak, a small initial peak and finally almost a single peak again. It should be pointed out that the difference in wave shapes at Stations 1 and 3 as shown in Figures 12 and 13 is because of the Mach reflection process where the reflection wave is catching up to the incidence shock as the distance from ground zero increases.

C. Blast Loading on Acceptor Structure - Roof

Table 4 lists the blast loading parameters for the roof of the acceptor model. Maximum values of about 480, 170, and 180 kPa were recorded at Station 13 for the three separation distances. Figures 14 - 16 are examples of the pressure-time curves recorded from Stations 13, 14, and 16. The waveforms are quite similar (for a specific shot) with some decay of peak pressure during the crossing of the roof.

D. Blast Loading on Acceptor Structure - Ends

Maximum peak pressure is seen to occur (Table 5) at Station 11 with a variation of about 500, 195, and 120 kPa corresponding to the three separation distances. The waveforms are shown in Figures 17 and 18. The general shape of the records from both ends of the acceptor magazine are quite similar, as were those on the roof.

E. Blast Loading on Acceptor Structure - Far Side-Wall

Table 6 lists the maximum peak pressure as measured on the far side-wall of the acceptor magazine. The values ranged from about 200 kPa for Station 9 at a distance of $0.8 Q^{1/3}$ m to a low of about 62 kPa at a distance of $2.4 Q^{1/3}$ m.

Figures 19 and 20 illustrate the variety of waveforms to be found on the far side-wall. A great many small reflections were recorded at the outer edge at Station 8 during Shot 1. At Station 9, near the center of the wall, large distinct reflections from the ground surface and the barricade were recorded for all three separation distances. No record approached the maximum pressure level measured on the near side-wall, however.

TABLE 4. BLAST LOADING ON ROOF

Shot	Station	Peak Pressure kPa	Positive Impulse kPa-ms	Arrival Time ms	Positive Duration ms	Remarks
1	12	418	99	0.84	0.86	0.8Q ^{1/3} m
	13	481	120	0.84	0.92	
	14	397	108	0.99	1.07	
	15	273	91	1.18	1.55	
	16	350	105	1.16	1.32	
2	12	143/147	62	2.03	0.70	1.Q ^{1/3} m
	13	146/149	63	2.03	0.70	
	14	152	91	2.25	1.32	
	15	125/141	78	2.51	1.86	
	16	140	80	2.49	1.92	
3	12	158	70	1.95	1.63	1.6Q ^{1/3} m
	13	169	74	1.97	0.80	
	14	148/160	84	2.18	1.41	
	15	125	75	2.43	2.00	
	16	128	72	2.41	1.96	
4	12	161	52	3.51	1.60	2.4Q ^{1/3} m
	13	39/156	50	3.45	0.90	
	14	35/146	71	3.64	2.52	
	15	126	70	3.94	2.76	
	16	135	73	3.84		
5	12	162	56	3.59	1.98	2.4Q ^{1/3} m
	13	179	58	3.58	0.91	
	14	149	73	3.79	2.59	
	15	136	66	4.04	2.59	
	16	166	68	4.02	2.61	
6	12	92/101	65	3.51	1.91	2.4Q ^{1/3} m
	13	103	54	3.52	1.24	
	14	93	71	3.76	2.51	
	15	77	64	4.04	2.58	
	16	88	67	4.02	2.51	

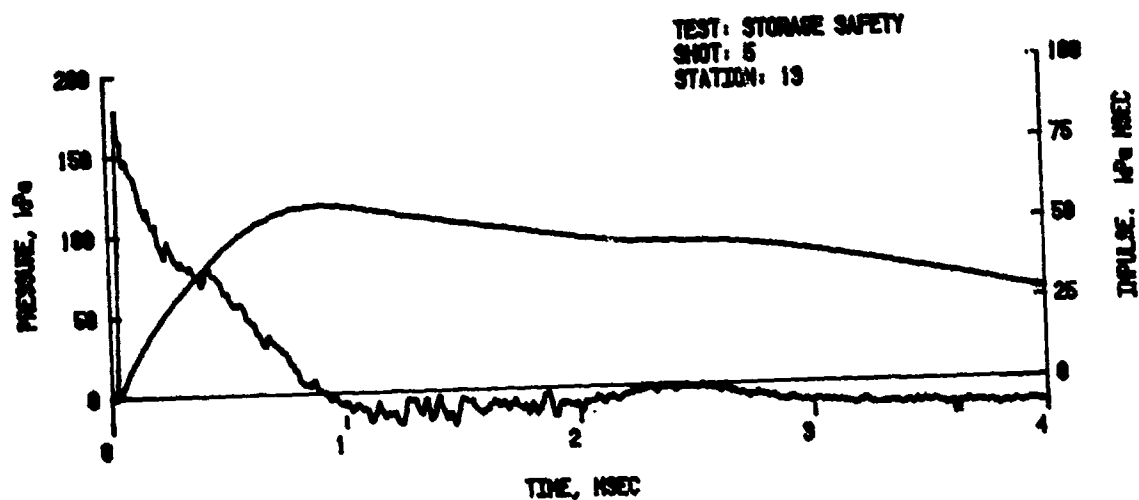
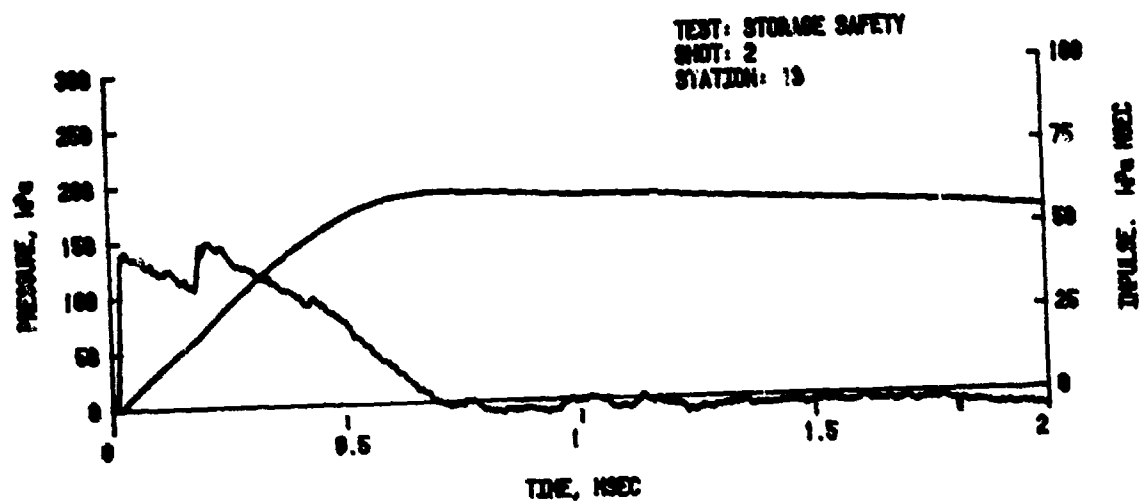
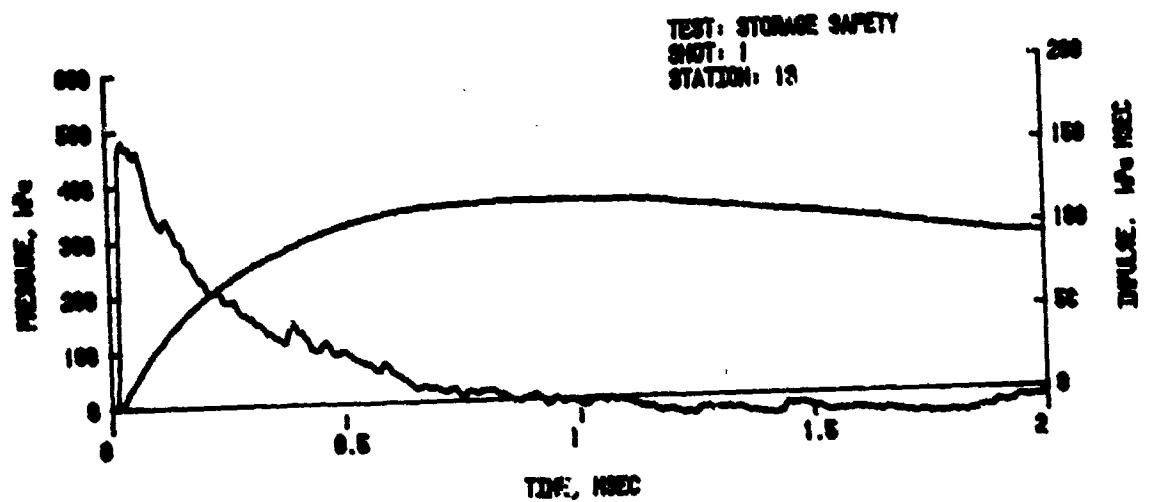


Figure 14. Pressure-Time Records from the Roof,
Station 13

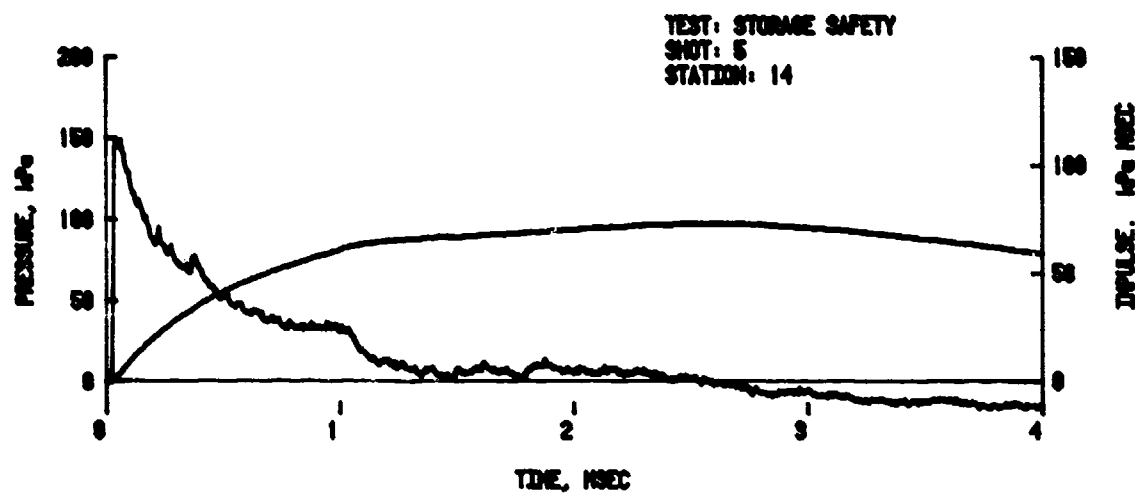
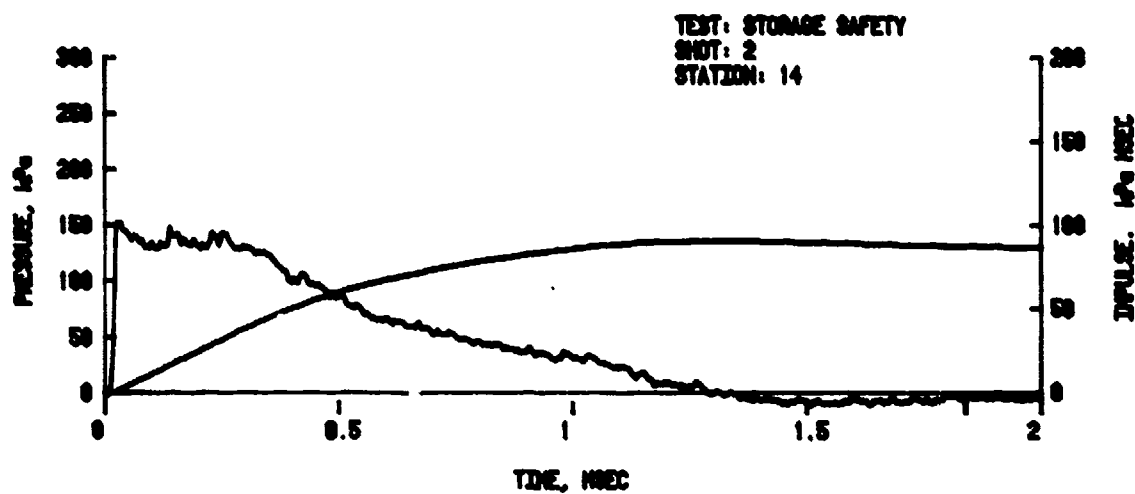
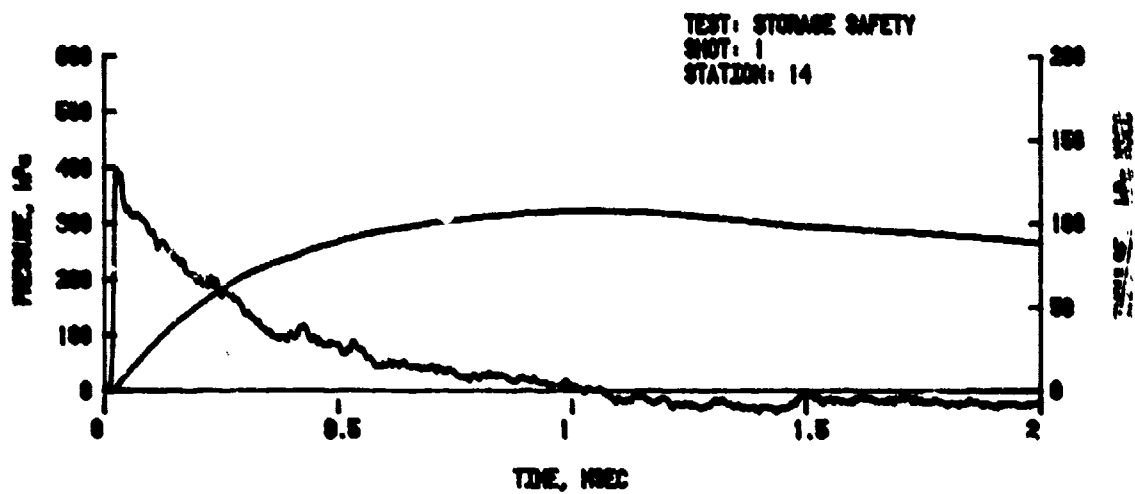


Figure 15. Pressure-Time Records from the Roof,
Station 14

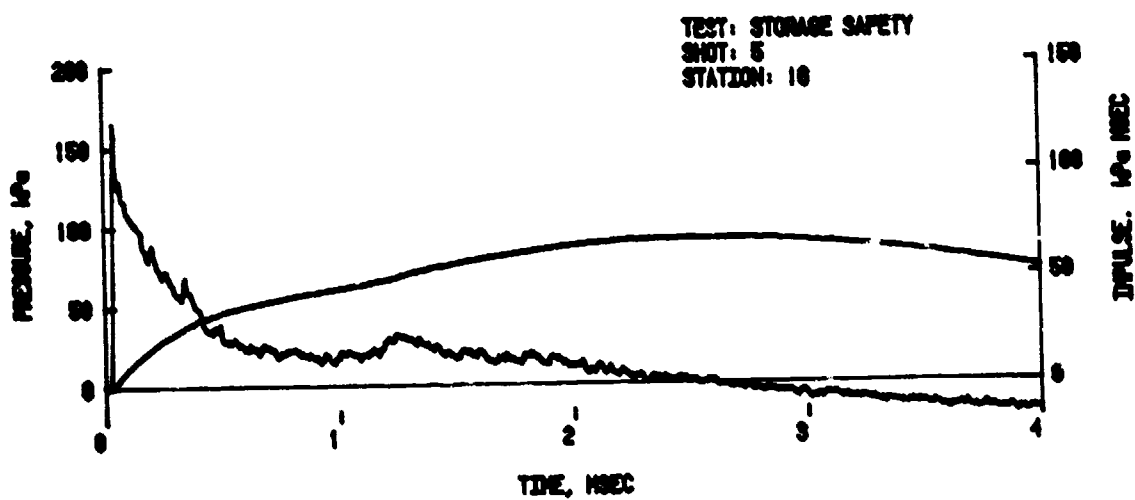
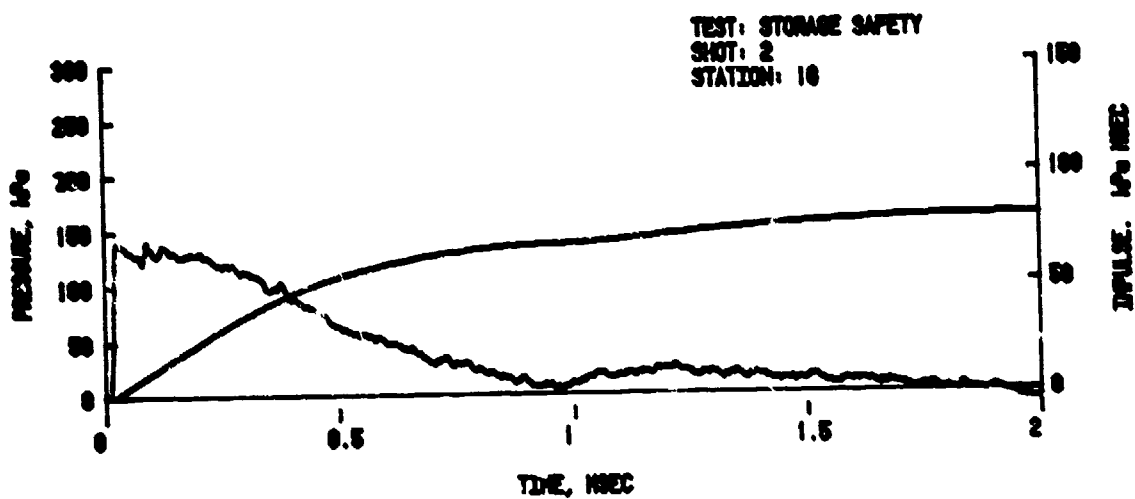
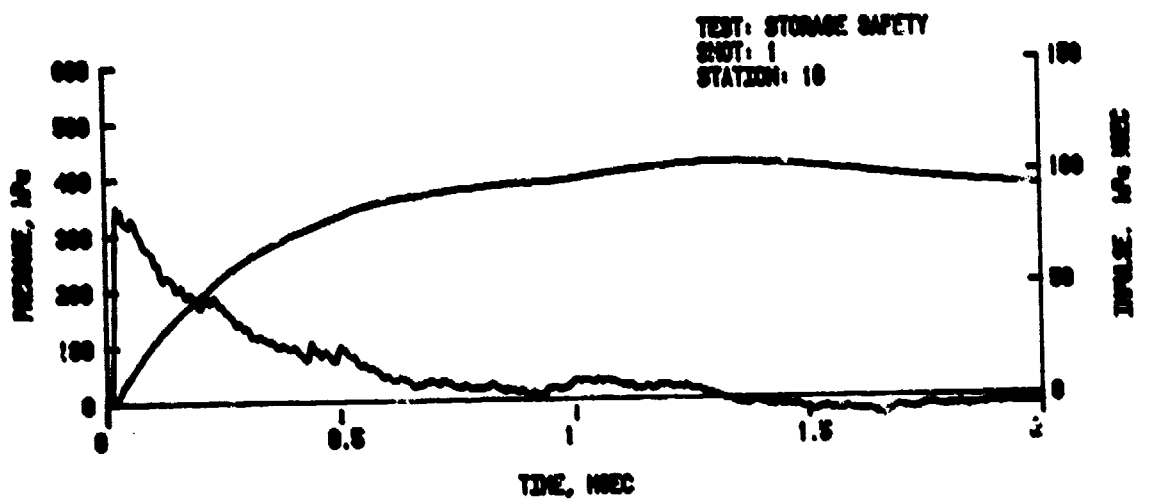


Figure 16. Pressure-Time Records from the Roof,
Station 16

Table 5. BLAST LOADING ON END WALLS

Shot	Station	Peak Pressure kPa	Positive Impulse kPa-ms	Arrival Time ms	Positive Duration ms	Remarks
1	10	240/478	104	1.06	0.99	0.8Q ^{1/3} m
	11	518	174	1.10	0.83	
	17	242/297	105	1.08	1.27	
	18	332	108	1.10	1.22	
2	10	189	88	2.29	1.37	1.6Q ^{1/3} m
	11	172/184	94	2.32	1.41	
	17	170	96	2.30	1.48	
	18	145/167	91	2.29	1.44	
3	10	188	81	2.22	1.33	1.6Q ^{1/3} m
	11	195	83	2.24	1.26	
	17	186	94	2.26	1.47	
	18	167	91	2.25	1.41	
4	10	117	70	3.76	2.36	2.4Q ^{1/3} m
	11	129	94	3.82	4.00	
	17	116	74	3.81	2.46	
	18	117	81	3.82	2.61	
5	10	127	72	3.85	2.85	2.4Q ^{1/3} m
	11	96/120	67	3.88	1.83	
	17	133	78	3.87	2.27	
	18	95/115	81	3.86	2.42	
6	10	84	64	3.77	2.48	2.4Q ^{1/3} m
	11	81	75	3.79	2.72	
	17	93	71	3.80	2.02	
	18	90	71	3.79	2.42	

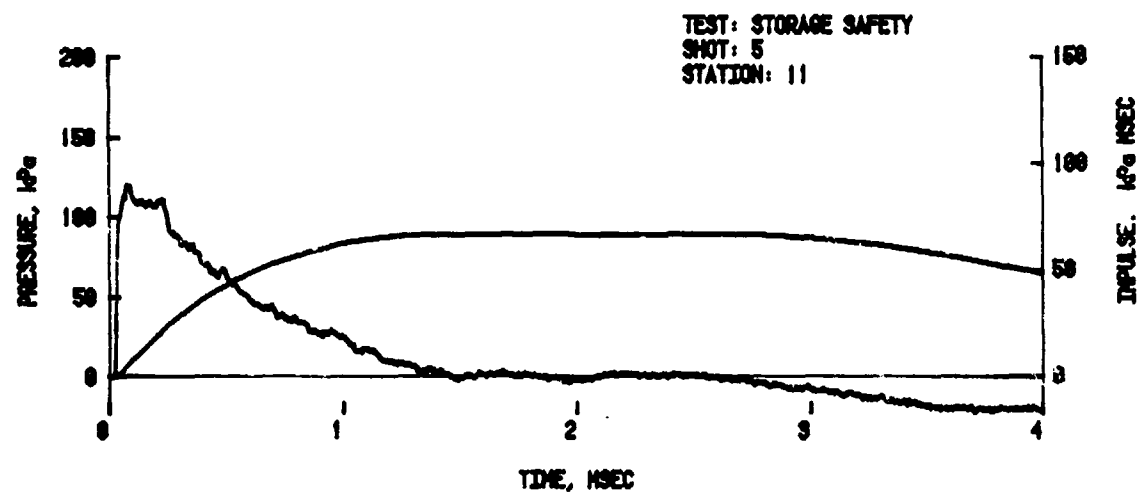
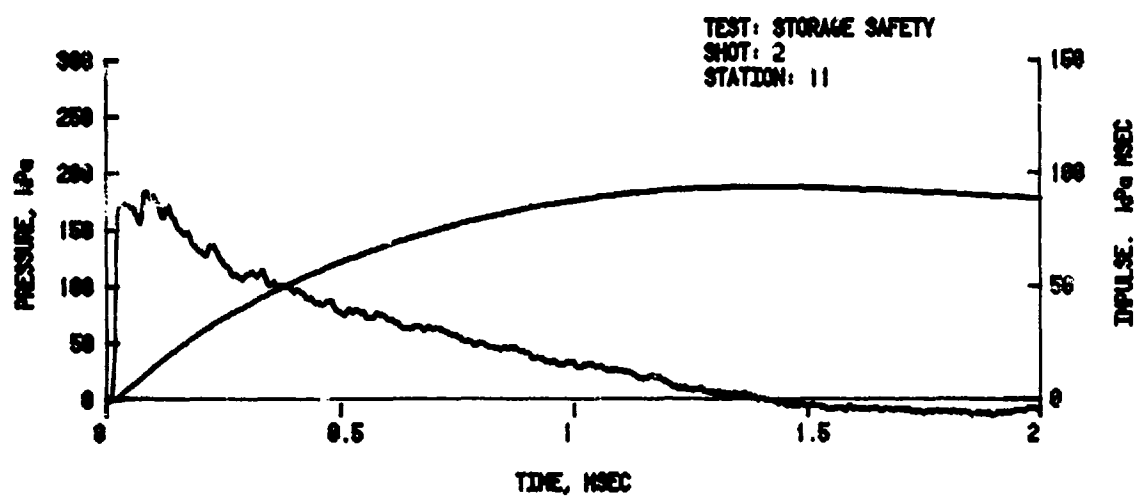
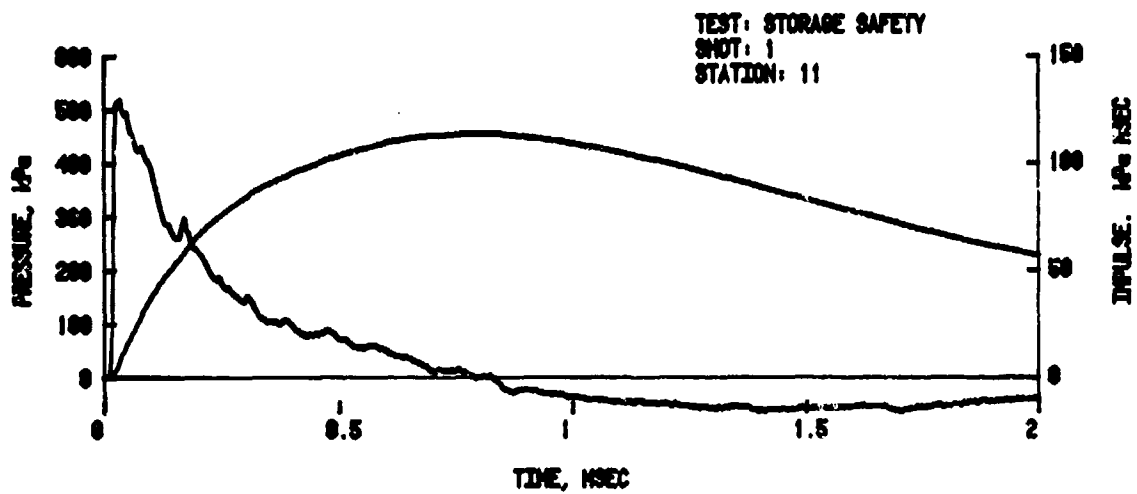


Figure 17. Pressure-Time Records from Back End-Wall,
Station 11

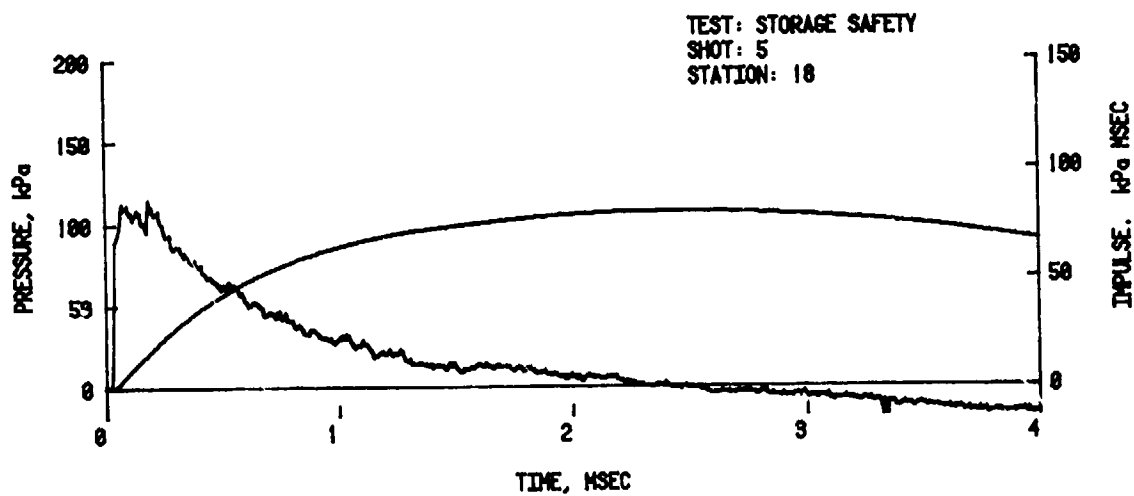
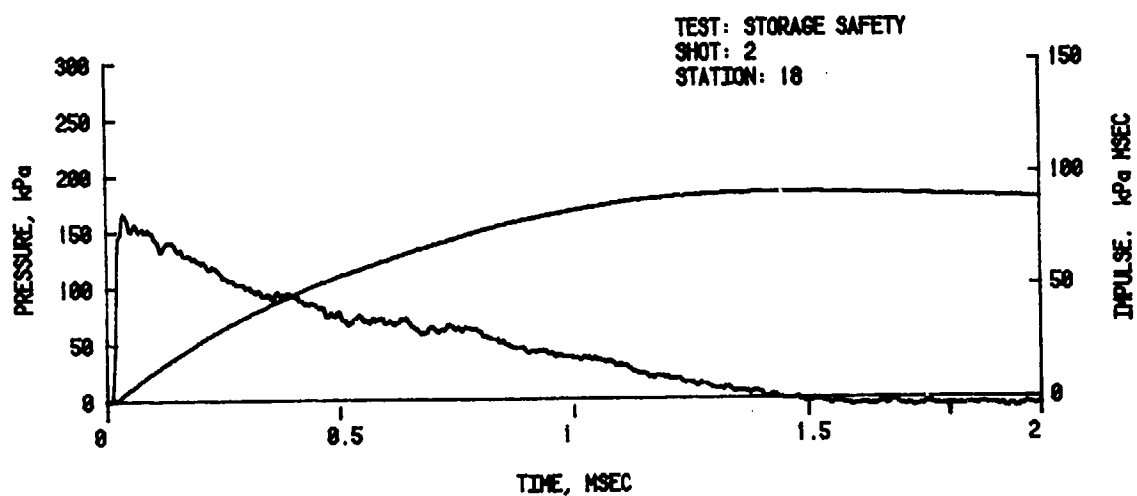
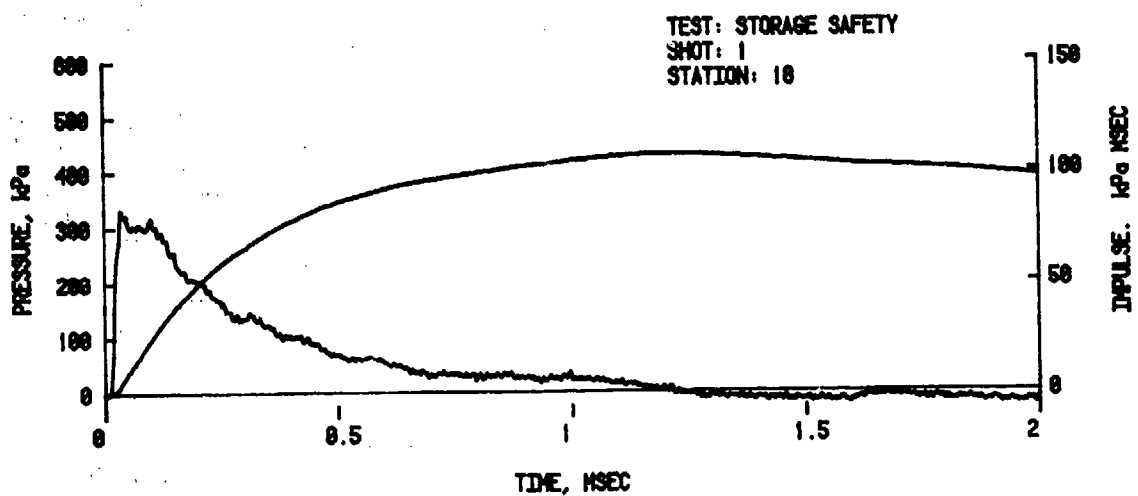


Figure 18. Pressure-Time Records from Front End Wall,
Station 18

Table 6. BLAST LOADING ON FAR SIDE-WALL

Shot	Station	Peak Pressure kPa	Positive Impulse kPa·ms	Arrival Time ms	Positive Duration ms	Remarks
1	7	63/81	70	1.33	1.85	$0.8Q^{1/3}$ m
	8	83/141	117	1.47	1.75	
	9	65/198	114	1.42	1.70	
2	7	27/64	30	2.70	1.68	$1.6Q^{1/3}$ m
	8	34/73	67	2.79	3.16	
	9	44/80	80	2.79	3.07	
3	7	34/61	32	2.62	1.71	$1.6Q^{1/3}$ m
	8	34/64	78	2.72	3.18	
	9	39/87	82	2.72	3.18	
4	7	28/42	59	4.09	2.49	$2.4Q^{1/3}$ m
	8	61	62	4.29	2.58	
	9	28/62	60	4.12	2.65	
5	7	31/43	56	4.23	2.85	$2.4Q^{1/3}$ m
	8	27/63	66	4.39	2.82	
	9	36/83	68	4.32	2.80	
6	7	18/42	61	4.24	2.89	$2.4Q^{1/3}$ m
	8	14/46	61	4.34	2.60	
	9	8.6/62	57	4.34	2.47	

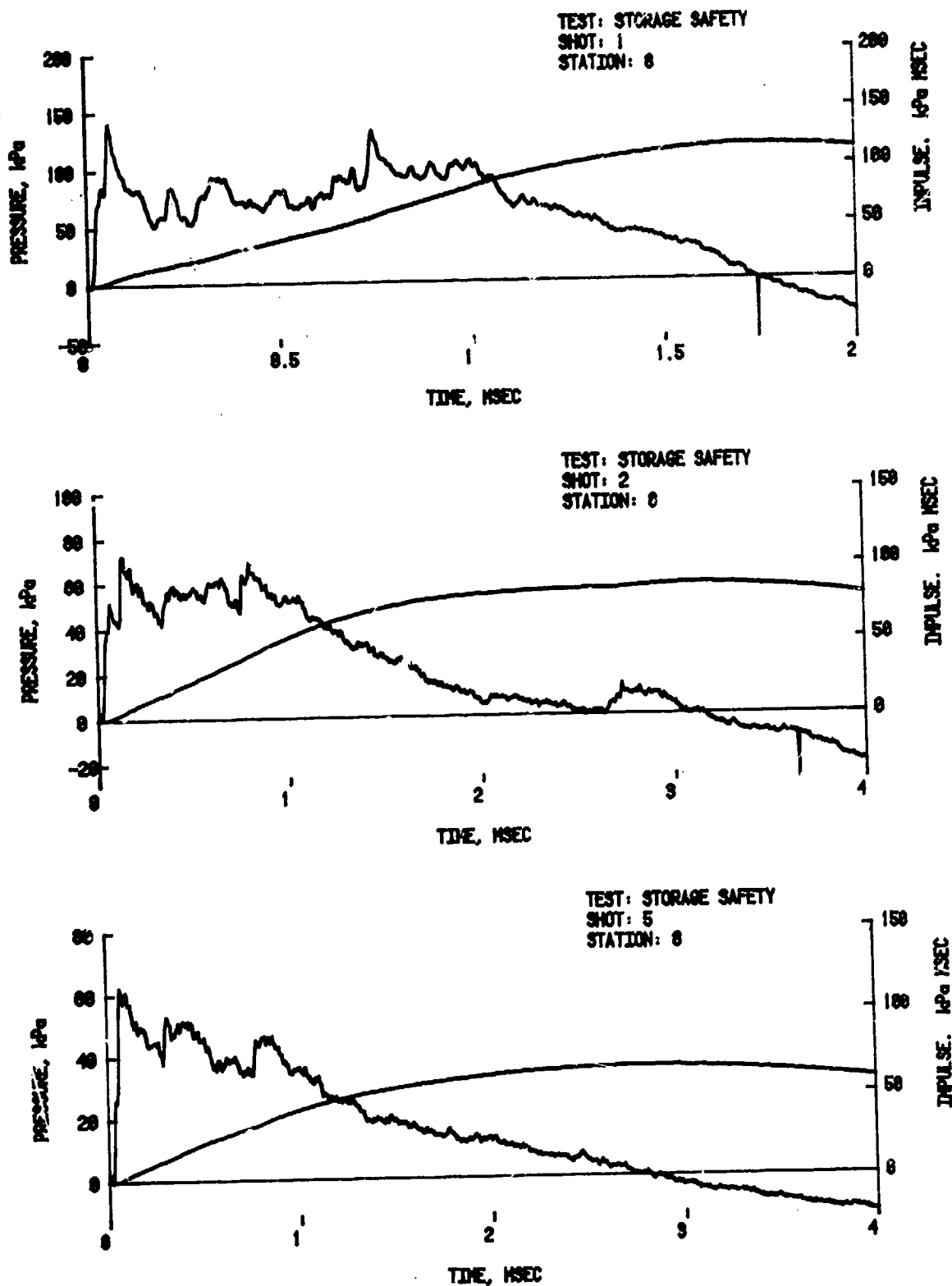


Figure 19. Pressure-Time Records from Far Side-Wall, Station 8

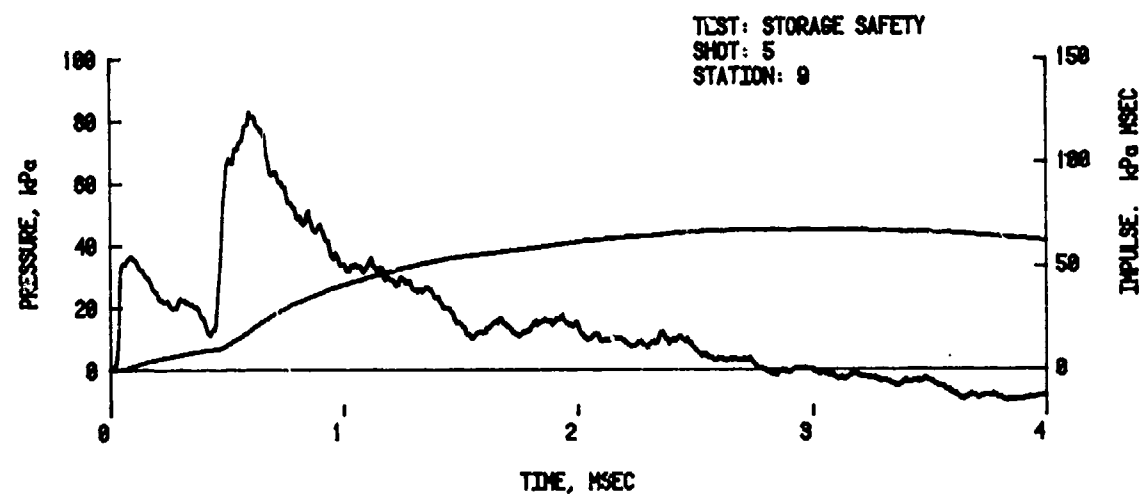
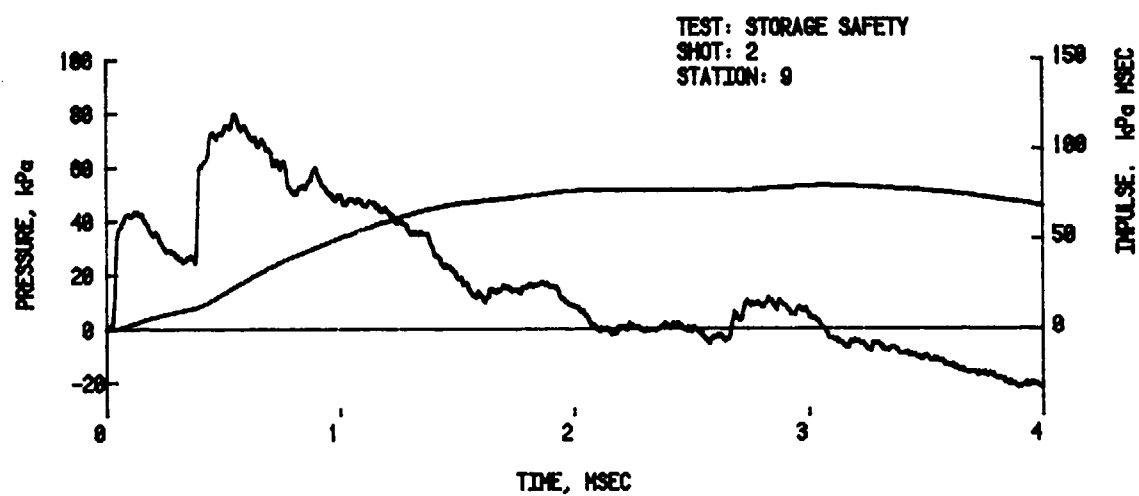
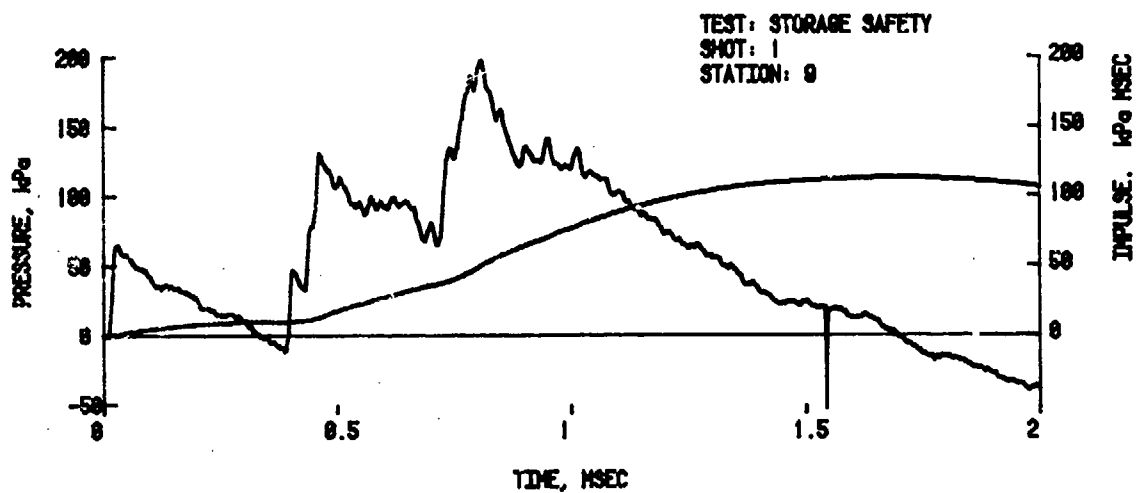


Figure 20. Pressure-Time Records from Far Side-Wall,
Station 9

IV. ANALYSIS

A. Blast Suppression Factors

The blast wave from the charge inside the donor magazine is suppressed to the sides and to the rear by both the presence of the cover and also the barricades. The cover effect is similar to that for a cased charge. Reference 1 gives an expression for a case correction factor, f_c , which will be used for the cover effect of the donor structure.

$$f_c = 0.02 + \frac{0.80}{1 + (W_{CT}/W_{NEW})}, \quad (1)$$

where W_{CT} is the total case weight (donor structure cover) and W_{NEW} is the net explosive weight. For an average value of 5.566 kg for W_{CT} and 1 kg for W_{NEW} , f_c is found from Equation 1 to be 0.321 kg.

The equivalent TNT weight, W_{TNT} , for a Pentolite charge and the donor structure is found from Equation 2.

$$W_{TNT} = f_c \times f_e \times W_{NEW}, \quad (2)$$

where the case factor, f_c , is taken as 0.321 and the pressure equivalent explosive weight factor, f_e , for Pentolite is 1.17 from Reference 3. The equivalent base TNT weight, W_{TNT} , is 0.375 kg of TNT, from Equation 2.

Alternate comparisons of the suppressive effects may be made by comparing the measured parameters at Station 20 (in front of the acceptor magazine model) with the free-field values from the standard curves for hemispherical TNT detonated on a hard surface. See References 4 and 5 for the scaling rules. The scaling rule used is given in Equation 3 for the charge mass-distance relationship. At a given peak overpressure

$$Q_2 = Q_1 \left(\frac{R_2}{R_1} \right)^3, \quad (3)$$

where R_1 is the distance from Q_1 (1 kilogram of explosive)

and R_2 is the distance from Q_2 (the equivalent mass of bare TNT needed to give the experimentally suppressed values for a 1 kilogram charge inside the donor magazine model).

The values of R_1 and R_2 are read from Figure 21A for Station 20 and 21B for Station 21. These are listed in Table 7 with the equivalent bare charge mass Q_2 . The average value for Q_2 of 0.43 at Station 20 compares quite well with the value of 0.38 calculated from Equation 2. It can be seen in Figure 21B that the suppressive effect is not evident at Station 21. The average value of Q_2 at Station 21 is 1.02 which implies no suppression of peak overpressure.

As noted in Reference 2 the impulse in the blast wave from the covered donor does not produce the same Q_2 values when standard scaling procedures are used. To determine the Q_2 based on impulse the following procedure was used.

A ratio of experimental values I_2/R_2 from Table 2 are determined for each shot. These are plotted along with the standard impulse/distance (I_1/R_1) versus distance curve in Figure 22. For a ratio of I_1/R_1 equal to I_2/R_2 , an R_1 is found. The values of R_2 and R_1 found in this way may now be put into Equation 3 to calculate Q_2 . These ratios of impulse and distance, and Q_2 values for Stations 20 and 21 are listed in Table 8. It can be seen that the Q_2 values for impulse are quite different from the Q_2 values calculated from the suppression of peak overpressure. The Q_2 values are also different for the two station locations. Table 8 can be summarized by stating that the impulse at Station 20 from a 1 kg covered donor can be matched with a 0.56 bare charge, and at Station 21 would require a 0.72 kg charge.

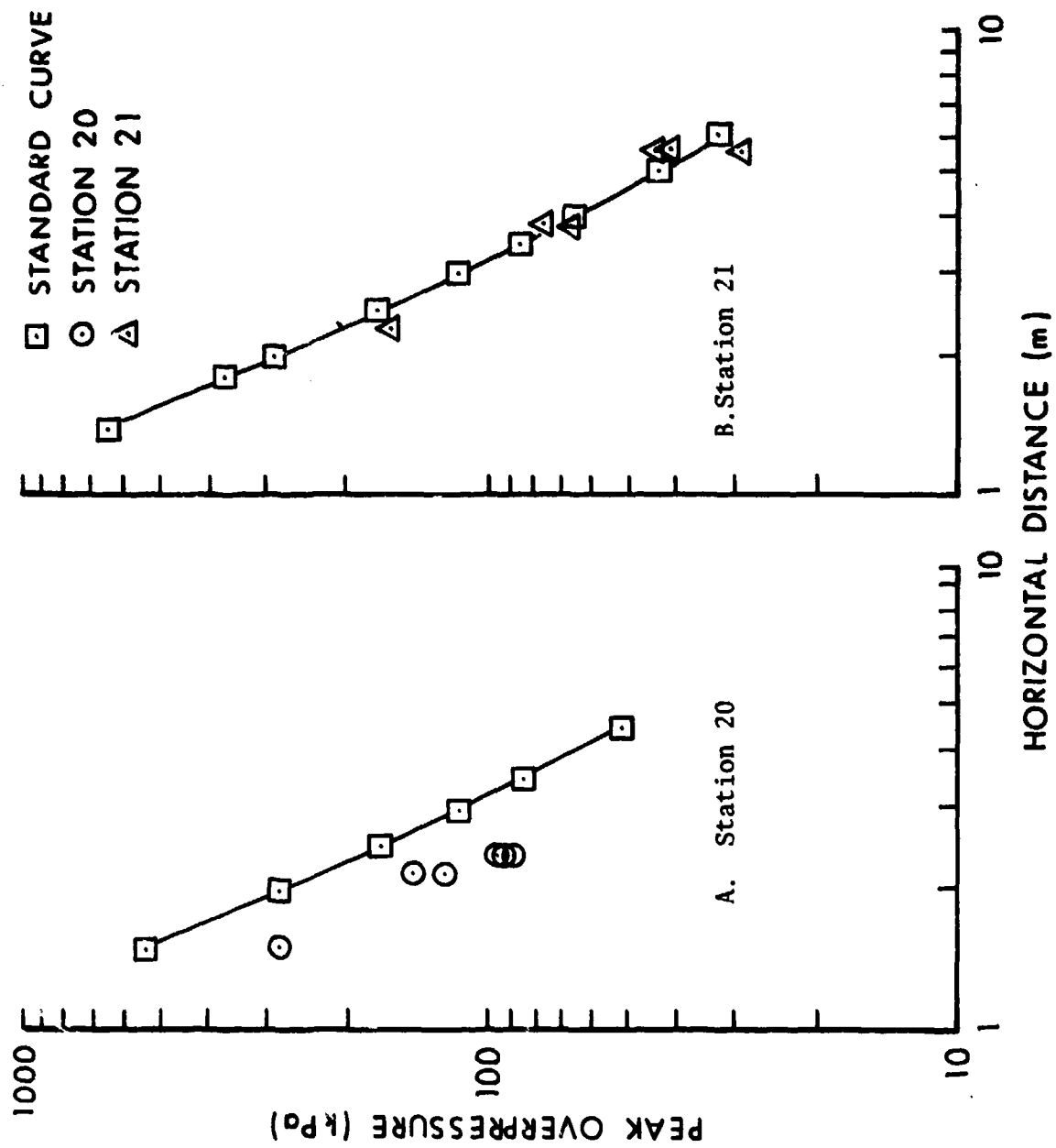


Figure 21. Comparison of Standard Free-Field Pressures to Data from Stations 20 and 21.

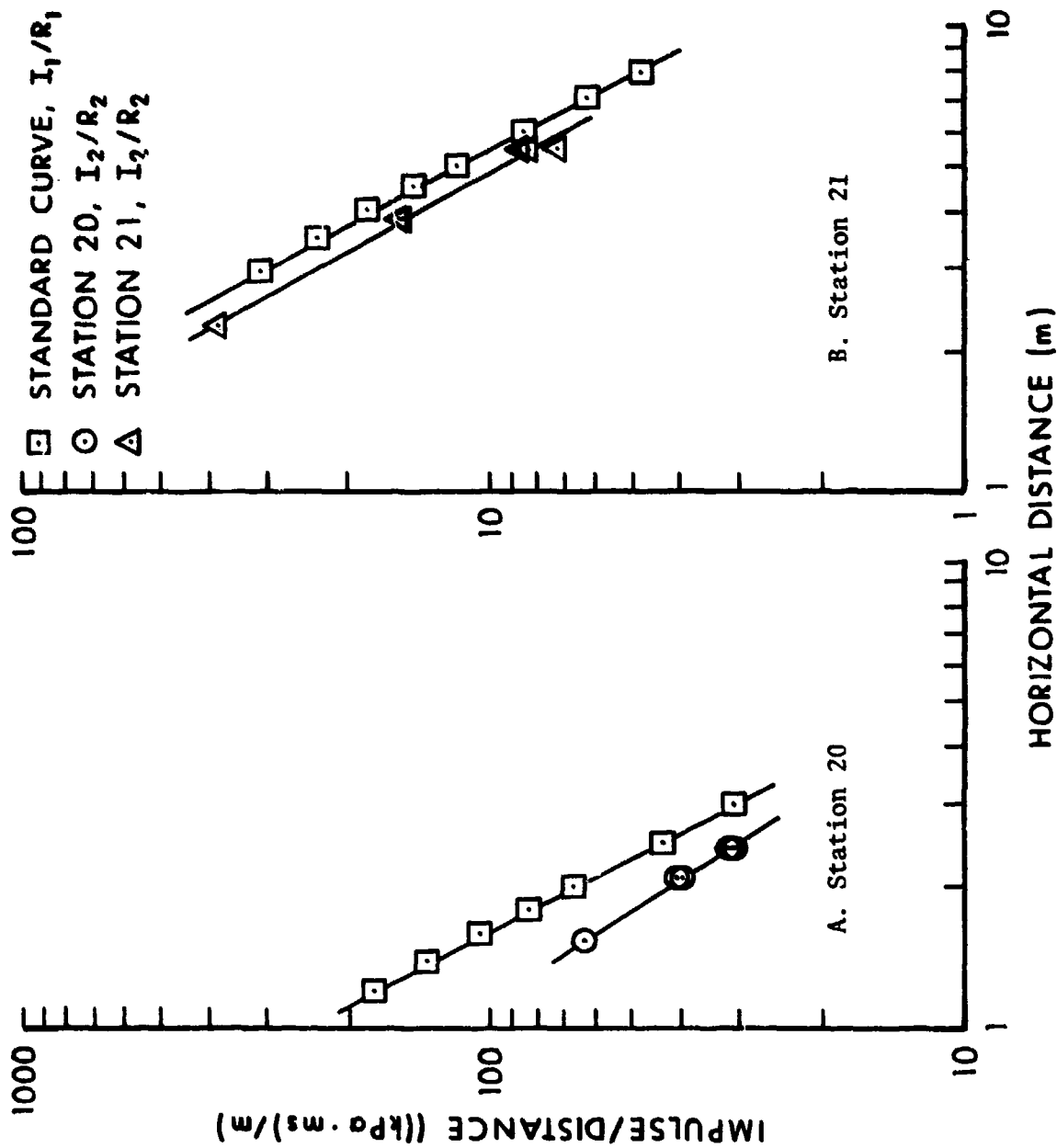


Figure 22. Comparison of Standard Free-Field Impulse to Data from Stations 20 and 21

TABLE 7. SUPPRESSION EFFECTS ON PRESSURE

Shot No.	Distance		Pressure	TNT
	R_1 m	R_2 m	kPa	Equivalence kg
<u>Station 20. Compared to Free Field Side-On Overpressure, $Q_1 = 1$ kg.</u>				
1	2.00	1.52	279	0.44
2	2.90	2.20	125	0.44
3	2.70	2.20	143	0.54
4	3.35	2.43	93	0.38
5	3.30	2.43	95	0.40
6	3.45	2.43	86	0.35
			Avg.	0.43
<u>Station 21. Compared to Free Field Side-On Overpressure, $Q_1 = 1$ kg.</u>				
1	2.55	2.29	162	0.72
2	3.70	3.90	76	1.17
3	3.95	3.90	67	0.96
4	6.35	5.52	29	0.66
5	5.00	5.52	43	1.35
6	5.15	5.52	41	1.23
			Avg.	1.02
<u>Calculated from Equation 2 Above - Analysis Section</u>				
A11	--	--	--	0.38

TABLE 8. SUPPRESSION EFFECTS ON IMPULSE

Shot No.	Experiment		Ratio	Standard		Ratio	Ratio	Q_2 $(R_2/R_1)^3$
	I_2 kPa-ms	R_2 m	I_2/R_2 kPa-ms/m	I_1 kPa-ms	R_1 m	I_1/R_1 kPa-ms/m	R_2/R_1	
<u>Station 20 Compared to Free-Field Side-On Impulse</u>								
1	97	1.523	63.69	131	2.05	63.69	0.74	0.41
2	86	2.195	39.18	102	2.60	39.18	0.84	0.59
3	89	2.195	40.55	103	2.55	40.55	0.86	0.64
4	78	2.427	32.14	94	2.92	32.14	0.83	0.57
5	81	2.427	33.37	96	2.88	33.37	0.84	0.59
6	75	2.427	30.90	93	3.00	30.90	0.81	0.53
							Avg.	0.56

Station 21 Compared to Free-Field Side-On Impulse

1	88	2.286	38.50	103	2.675	38.50	0.86	0.64
2	61	3.902	15.63	67.7	4.33	15.63	0.90	0.73
3	60	3.902	15.38	67.0	4.35	15.38	0.90	0.73
4	40	5.519	7.25	47.1	6.50	7.25	0.85	0.61
5	48	5.519	8.70	50.9	5.85	8.70	0.94	0.83
6	46	5.519	8.33	50.4	6.05	8.33	0.91	0.75
							Avg.	0.72

B. Translation Velocity Predictions for Near Side-Wall

A listing of the pressure-time loading records obtained from the experiment showed that the near side-wall had the highest load values. The pressure-time records for Stations 1-6 on the near side-wall were weighted, according to wall location, and summed to obtain a total load. From this load an average pressure load was calculated for the entire near side-wall. Figure 23 shows the resulting pressure-time curves for each of the separation distances.

The digitized versions of these loads were used in a translation program which was run on a microcomputer. The assumption was made that the near-wall started to move when the pressure load was applied. This assumption was made because of the inherent structural weakness of the brick wall of the full-size magazine which was modeled.

The computer program calculated the acceleration, a , from the model and loading parameters using Equation 4 for discrete intervals of the loading-time curve, P_L vs t_i . Time intervals of 10-25 μ s were used in the calculations.

$$a = 1000 \frac{A_w P_L}{M_w}, \quad (4)$$

where a is the acceleration (m/s^2) of the concrete model wall of area A_w ($0.050 m^2$) and mass M_w ($0.953 kg$) under a pressure loading of P_L measured in kPa. The incremental velocity, ΔV (m/s), was obtained from Equation 5 for an acceleration value over a time increment, $\Delta t(s)$.

$$\Delta V = a \Delta t, \quad (5)$$

where the time increment, Δt , is from a time t_1 to t_2 and so on. The incremental distance $\Delta D(m)$, is found from Equation 6.

$$\Delta D = \frac{\Delta V}{2} \Delta t, \quad (6)$$

where ΔV and Δt are defined above. The factor of $1/2$ is used to average the velocity changes over the time increment. The distance is then summed with each additional velocity and time increment.

The predicted motion parameters for the near-side wall are shown in Tables 9-11. The velocities are plotted in Figure 24. Generally, the velocity initially increases quickly, then reaches a maximum velocity at the end of the positive loading phase. Shot 2 had two major peaks in the pressure-time loading, which are seen in the wall velocity-time plot. When the second loading peak arrived, at 2 ms, the velocity sharply increased and reached a maximum above that of Shot 5 after it was lower initially. The maximum wall velocities reached ranged between 7-12 m/s.

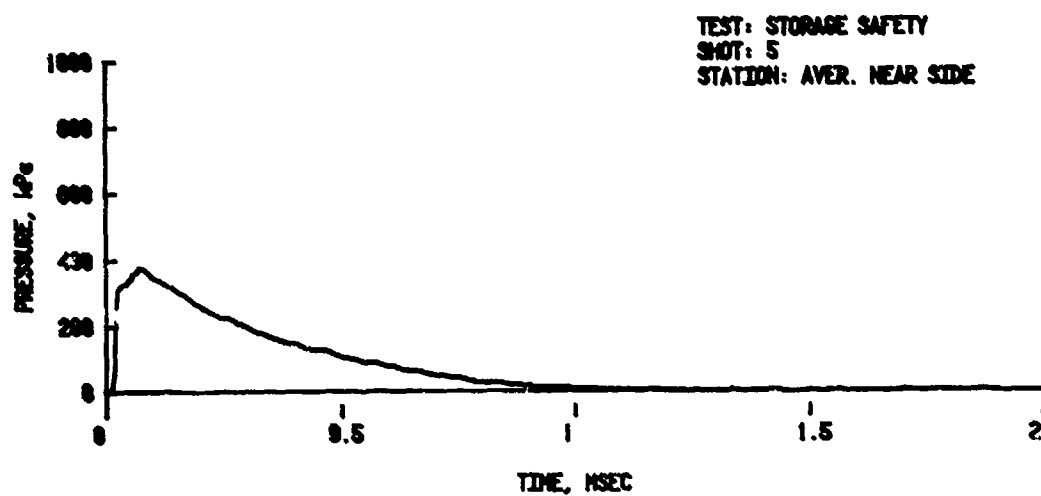
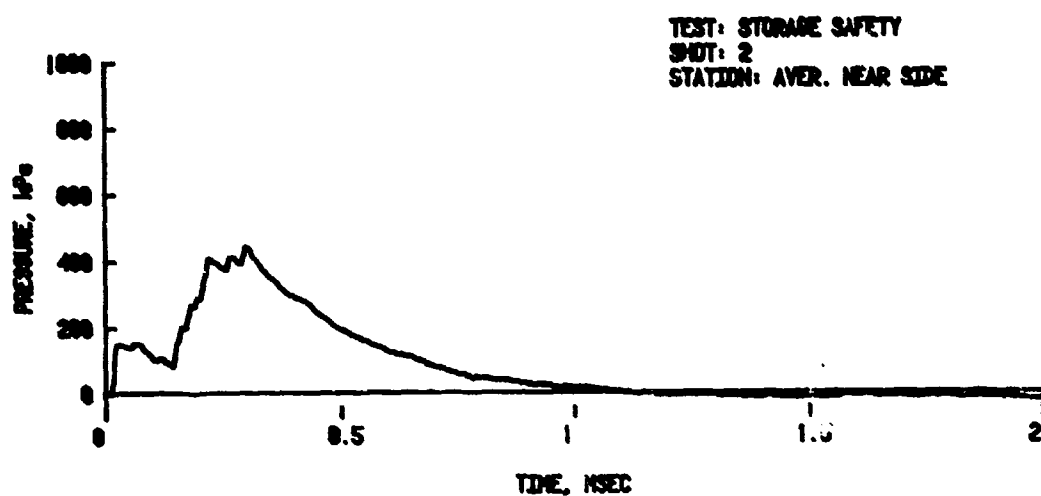
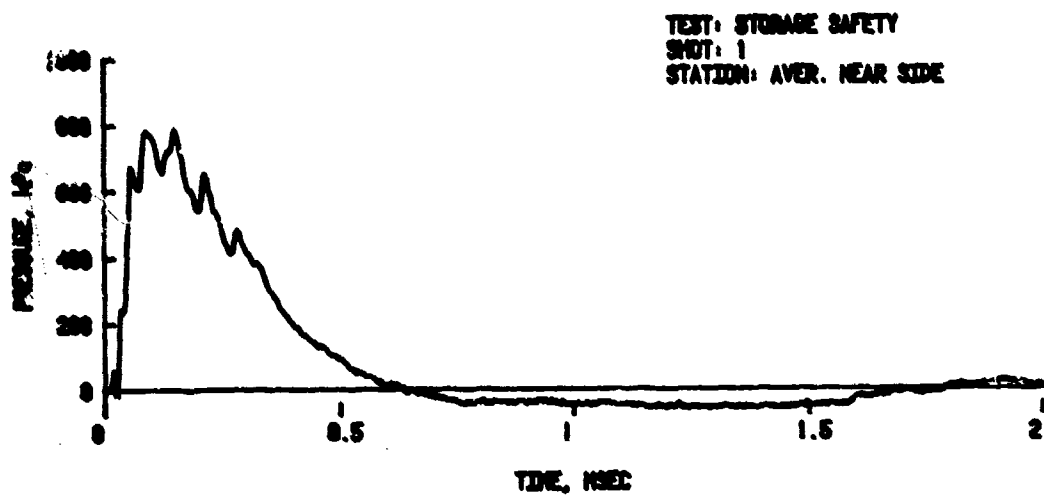


Figure 23. Average Loading on Near Side-Wall

Table 9. TRANSLATION OF NEAR SIDE-WALL, SHOT 1, $0.8 Q^{1/3}$ m.

Time, ms	Distance, cm	Velocity, m/s	Acceleration, m/s^2
0.00	0.00	0.00	0
0.03	0.01	0.71	35930
0.06	0.02	1.73	35930
0.10	0.03	3.32	36350
0.15	0.04	5.28	40350
0.19	0.06	6.61	29210
0.25	0.11	8.40	24790
0.30	0.15	9.57	22020
0.35	0.20	10.46	14390
0.40	0.25	11.02	9910
0.45	0.35	11.38	5600
0.50	0.36	11.57	2670
0.55	0.42	11.63	800
0.58	0.45	11.64	107

Table 10. TRANSLATION OF NEAR SIDE-WALL, SHOT 2, $1.6 Q^{1/3}$

Time, ms	Distance, cm	Velocity, m/s	Acceleration, m/s^2
0.00	0.00	0.00	0
0.03	0.00	0.19	7730
0.08	0.00	0.58	8000
0.10	0.01	0.74	6400
0.15	0.02	0.93	9530
0.19	0.03	1.36	15030
0.25	0.04	2.76	21590
0.29	0.05	3.27	19990
0.35	0.06	4.94	23450
0.45	0.10	6.84	15780
0.55	0.19	8.13	10450
0.65	0.27	8.96	7090
0.75	0.37	9.51	4420
0.85	0.47	9.83	2560
0.95	0.55	10.03	1870
1.08	0.65	10.16	910
1.12	0.75	10.19	267

Table 11.

TRANSLATION OF NEAR SIDE-WALL, SHOT D, $2.4 Q^{1/3}$ m

Time, ms	Distance, cm	Velocity, m/s	Acceleration, m/s ²
0.00	0.00	0.00	0
0.03	0.01	0.43	17060
0.08	0.02	1.38	20040
0.15	0.03	2.69	16470
0.20	0.04	3.43	14130
0.25	0.05	4.05	11990
0.30	0.07	4.60	10390
0.35	0.10	5.06	8850
0.40	0.12	5.45	7680
0.45	0.15	5.79	6660
0.50	0.17	6.09	5700
0.55	0.02	6.34	4690
0.60	0.22	6.53	3739
0.65	0.28	6.69	3200
0.70	0.30	6.82	2400
0.75	0.33	6.92	1870
0.85	0.42	7.06	1170
0.95	0.50	7.13	590
1.05	0.55	7.18	320
1.15	0.70	7.21	107
1.25	0.75	7.22	80
1.35	0.80	7.22	53

None of these maximum velocities appears great enough to initiate candidate munitions (Reference 1) that may be stored in this type of above ground, barricaded storage magazine.

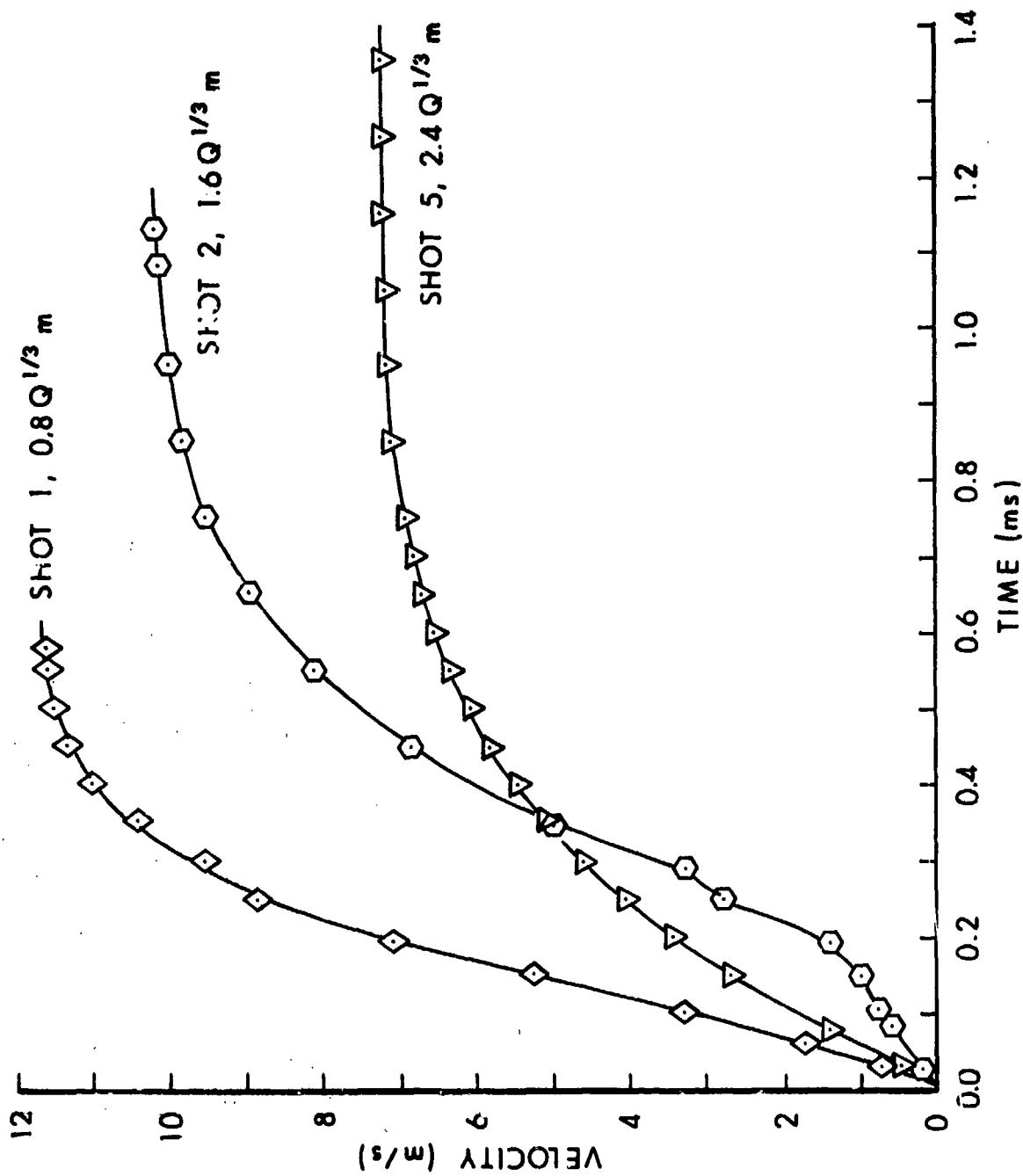


Figure 24. Predicted Translational Velocity of Near Side-Wall

SUMMARY AND CONCLUSIONS

A test series of six shots was fired with 1 kg bare 50/50 Pentolite hemispherical charges placed inside model concrete donor magazines. Measurements of pressure-time loading were obtained at several locations on a nonresponding barricaded model acceptor magazine. The experimental models were constructed at 1/23.5 scale of the full sized above ground barricaded munition storage magazine on site at Machrihanish, Scotland.

Calculations of charge suppression factors for Station 20 (using a pressure method), caused by the cover of the concrete donor model over the base charge, indicate values around 0.43 kg. A 0.43 kg free-field base hemispherical charge would have pressure equivalency to the covered 1 kg charge used during the experiments. At the greater distances, as calculated for Station 21, the average charge suppression factor was 1.02 kg indicating little or no effect of the donor model cover, or of the barricades around the model.

Whole wall translation velocities, calculated from the average near side-wall loading, ranged from 7-12 m/s. These low predicted velocities seem to be born out from the results of a preliminary shot with a responding concrete acceptor model magazine. Component wall debris translation appeared to be minimal. Tentatively, the observed and calculated values for the near side-wall (the highest loaded surface) velocities, indicated that the components of the wall would not attain hazardous velocities as quoted in the literature. This was true at a standard safe separation distance of $0.8 Q^{1/3}$ m. It would appear not necessary to increase the separation distance from this value to any larger separation distance. The $0.8 Q^{1/3}$ m separation distance appears adequate.

Further experiments are planned to better determine the velocities of wall debris from a number of responding model acceptor walls. Time constraints of the present experiments allowed only preliminary debris results to be obtained.

ACKNOWLEDGMENT

The authors wish to thank Mr. Kenneth Holbrook for the very extensive site and model preparation and also for being the explosive handler for the test series.

REFERENCES

1. F. B. Porzel and J. M. Ward, "Explosive Safety Analysis of the Machrianish Magazine," NSW TR 79-359, December 1979.
2. Charles N. Kingery, Gerald Bulmash, and Peter C. Muller, "Blast Loading on Above Ground Barricaded Munition Storage Magazines," Ballistic Research Laboratory Technical Report ARBRL-TR-0257, May 1984 (A141677).
3. "Structures to Resist the Effects of Accidental Explosions," Dept. of the Army Technical Manual TM 5-1300, June 1969.
4. Private Communication from Mr. Gerald Bulmash, USA Ballistic Research Laboratory, Aberdeen Proving Ground, MD 21005-5066.
5. Wilfred E. Baker, Explosions in Air, University of Texas Press, Austin, TX, 1973.

AD-P005 370

ESKIMO VII TEST RESULTS

by

Robert N. Murtha

Naval Civil Engineering Laboratory

Port Hueneme, CA

ABSTRACT

ESKIMO VII, seventh in the series of Explosive Safety Knowledge Improve-ment Operation Tests, was conducted to determine the safety and performance of Navy box-shaped ammunition storage magazines. The two magazines tested, the Type A (new design) and Type IIB (old design), were the remaining half-scale structures from the July 1980 ESKIMO VI test. The Type A magazine was tested using a foam High Explosive Simulation Technique (HEST) on its roof. The Type IIB magazine was tested one week later using a small hemispherical surface charge of 13,616 pounds of TNT. The two interior columns of the Type A magazine catastrophically collapsed when subjected to a HEST impulse approximately three times greater than the design impulse. Although the yield-line pattern and response predicted for the flat-slab structure never occurred, the roof remained intact while undergoing maximum support rotations of 16 degrees. These data indicate a high probability of eliminating the columns from future magazines by utilizing the tremendous energy absorbing properties associated with tensile membrane behavior of restrained slabs. The redesigned door and headwall system for the Type IIB magazine survived the blast loading conditions approximating those at the minimum side-to-side spacing of earth-covered magazines with only minor structural damage. These data indicate that the structural re-design used in this test is more than adequate to prevent sympathetic detonation.

INTRODUCTION

ESKIMO VII, seventh in the series of Explosive Safety Knowledge Improvement Operation test events of earth-covered magazine structures was recently completed at the Naval Weapons Center (NWC), China Lake, California. The box magazines tested were the two remaining structures, the Type IIB (designed in the 1950s) and the Type A (designed in the 1970s), from the July 1980 ESKIMO VI test. The Type A magazine was tested first using a foam HEST (High Expl-Sive Simulation Technique) (Ref 1). To obtain a test design impulse of 2,300 psi- μ sec acting on the roof, a charge density of 0.43 lb/ft³ was used. The Type IIB magazine was tested 7 days later using a hemispherically shaped surface charge of 13,616 pounds of TNT in a side-to-side orientation. The explosive effects (induced airblast loading, ground motion, debris, etc.) on the Type IIB magazine from the earlier HEST detonation was negligible. Results from ESKIMO VII will be used to evaluate the safety and performance under blast loading of box-shaped (smokeless powder/projectile) storage magazines. A description of the testing procedure and the results of the test are included in this report. If needed, additional pretest information can be found in the ESKIMO VII Test Plan (Ref 2).

Background

The Department of Defense Explosives Safety Board (DDESB) establishes explosives safety standards applicable to the military services and other Department of Defense (DOD) components. The quantity-distance standards for the separation of explosives storage magazines published in DOD Standard 5154.4S (Ref 3) depend on the construction of the magazines. Additionally, DOD 5145.4S allows higher explosive limits (up to 500,000 pounds) in certain standard earth-covered magazines of proven design that may be sited at the minimum intermagazine spacing permitted.*

ESKIMO VI showed that the door system design of Navy Smokeless Powder and Projectile Magazine Type IIB was inadequate to resist the loading resulting from detonation of 350,000 pounds in a similar magazine located at the minimum side-to-side spacing. The test also demonstrated an ample, possibly excessive, margin of safety in the Type A box magazine roof, which had been designed for a maximum support rotation of 2 degrees in accordance with the triservice manual on explosion-resistant structures (Ref 4).

*Prior to ESKIMO VI (1980), box magazines in the field had not been tested or specifically designed for overpressure loads. Safety policy, therefore, had required that they be sited at nonstandard intermagazine separation distances and that their storage capacity be limited to one-half the weight of explosives allowed in a standard magazine.

Objective

The objectives of ESKIMO VII were to:

1. Validate the performance of a redesigned door and headwall system for the Type IIB magazine under blast loading conditions approximating those at the minimum side-to-side spacing of earth-covered magazines.
2. Evaluate the reserve strength inherent in the Type A magazine design at roof slab deformations corresponding to large rotations at supports.
3. Provide test data to support improved load criteria, structural performance requirements, and design methods for the roofs, walls, and doors of more economical box-shaped magazines that can be sited at the minimum separation distances permitted by explosives safety standards.

High-explosive field test events are the only means, except for small-scale model testing, to evaluate the accuracy of calculational and empirical prediction techniques for the blast loading and response of magazine structures.

TEST A-ROOF

Type A Magazine

The Type A magazine (Ref 5) was designed to provide the same interior dimensions as the Type IIB magazine. The Type A magazine roof is supported by two interior circular columns with drop panels (see Figure 1). Aside from the Type A magazine being more massive and designed without pilasters, the major difference between the Type A and the Type IIB magazine is in the headwall design. The Type A magazine employs two sliding (built-up) doors that are supported on all four edges (the door sill, lintel, and jambs) by large beam elements. The two doors are located at the loading platform.

The Type A half-scale test structure duplicates the walls, roof, columns, footings, doors (without hanging mechanisms), and earth cover. The model structure used 1 foot of earth cover. Steel wing walls salvaged from the ESKIMO V test were designed to retain the earth cover. The interior floor slab, ramp, and loading platform in the model were replaced with compacted earth fill without concrete slabs, footings, or steps; all other nonstructural features were deleted. Construction drawings of the Type A structure used in ESKIMO VI are included in Reference 6.

In ESKIMO VI the roof parapet (a low wall used to retain the 1-foot soil cover on the roof) was severely damaged. The parapet was refurbished and increased in height from 1 foot 5 inches to a total height of 2 feet 9 inches. This modification was needed to retain the additional 12 inches of uncompacted native soil overburden required above the foam HEST cavity. The steel wing walls in the region adjacent to the structure were also increased in height (see Figure 2).

Foam HEST Design

To produce the required airblast loading, it was necessary to accurately simulate the overpressure component of the airblast generated by a high-explosive surface burst. A test procedure developed by the Air Force Weapons

Laboratory (AFWL) for the Defense Nuclear Agency (DNA) called HEST was used. The test involves distributing a high explosive over a relatively large surface area and covering the explosive with a soil overburden. Upon detonation, the surrounding soil berm forms a slowly expanding confinement chamber. The propagation rate, peak load, and rate of decay of the test bed loading forces are tailored to simulate a specific portion of the force fields radiating from a large natural or artificial disturbance.

The HEST test used in ESKIMO VII is more specifically described as a foam HEST test because a low-density plastic foam (1 pcf) was used in the construction of the charge cavity. The foam HEST configuration and the charge cavity are shown in Figures 3 and 4. The charge cavity consists of plastic foam sections hot-wire cut in a configuration with sufficient gaps to distribute the explosives uniformly and also support the overburden without crushing. The type of explosive used is pentaerthritoltetranitrate (PETN) made into 400-grains/foot detonating cord (Primacord). One strand of detonating cord was placed in each 1/2- by 1/2-inch groove that runs back to front across the charge cavity. Beyond the rear edge of the charge cavity, the 400-grains/foot detonating cord was pigtailed into one bundle and connected to a blasting cap. All pigtail leads were cut to equal lengths to ensure that detonation was initiated simultaneously along the rear edge of the charge cavity. The entire charge cavity was covered, after the explosives were placed, with a layer of 0.5-inch plywood on which 12 inches of uncompacted native soil overburden was placed (see Figure 5). The charge cavity was designed to overlap the roof by 1 foot on both sides and 5 feet on the backwall to minimize any edge effects.

Foam HEST "A-ROOF" was designed by NCEL using the HEST design lookup code developed at AFWL by Mr. Edward Seusy. The HEST design is done iteratively, changing the charge density, cavity depth, and overburden height until an acceptable match to the desired impulse history is found. A full description of the code is found in Reference 1. The charge density was designed to produce a peak pressure of 800 psi. An overburden of 12 inches was then computed to confine the blast long enough to simulate a 2,300-psi-msec impulse on the roof. The calculated outputs from the HEST design code of pressure and impulse are shown in Figure 6.

Instrumentation

Figure 7 is a schematic of the active instrumentation. A detailed description and purpose for each gauge is listed in Table 1. The bulk of the data gathered are airblast pressures, soil stresses, roof velocities, and ground motion velocities. Some low-frequency displacement transducers were also used to record late time gross relative deformation. A total of 16 gauges were used.

Velocity gauges are the pendulum-type gauges normally used in ground shock tests. A spring is included that compensates for gravitational effects on the pendulum. Airblast gauges record the pressure-time environment at the ground surface. Deflection gauges are linear-motion resistive gauges.

Motion Picture Photograph

The test was recorded photographically by ground 16mm cameras using color film at speeds ranging from 24 frames/second to 10,000 frames/second. Figure 8 illustrates the locations of the cameras.

TEST IIB-DOORS

Type IIB Magazine

The Type IIB magazine is a smokeless powder and projectile storage magazine in the Naval Facilities Engineering Command (NAVFAC) inventory (Ref 7). The full-scale Type IIB magazine is 52-feet deep and 97-feet wide with an inside height that varies from 13 feet at the rear wall to 15 feet 2 inches at the front wall. It has two interior columns and 10 pilasters with capitals. Three continuous drop panels are provided at the column lines between the side walls. Two doors are located at the loading platform.

The construction drawings for the Type IIB half-scale structure tested in ESKIMO VI are found in Reference 6. This test structure duplicates the walls, roof, columns, pilasters, floor slab, footings, both doors, and earth fill. The model structure used 1 foot of earth cover. Steel wing walls salvaged from the ESKIMO V test were designed to retain the earth fill behind them. The ramp and platform were replaced with compacted earth fill without concrete slabs, footings, or steps and all other nonstructural features were deleted.

The performance of the Type IIB test structure in ESKIMO VI showed that the current double-leaf hinged door design was inadequate for resisting the blast loads. These doors were forced inward, bending past the door stops, and were separated from their hinges, coming to rest in the corresponding rear corners of the magazine. A redesign of the door/ headwall was undertaken in connection with ESKIMO VII. In addition to satisfying explosives safety criteria, the new door design also satisfies physical security criteria for theft (Ref 8). The new door configuration shown in Figure 9 is similar to the sliding single-leaf system of the Type A magazine. The construction drawings for the half-scale components to be tested are shown in Figures 10 and 11. Construction photographs of the modifications are shown in Figures 12 and 13.

Hemispherical Surface Charge

The explosive charge configuration (orientation, size, shape, and range) was designed to provide a blast environment similar to that observed in the ESKIMO VI test. According to those test results, the centerline of the Type IIB headwall was subjected to an impulse of 382 psi-msec and a maximum overpressure of 50 psi. The charge configuration was designed by NCEL using Figure 18 from Reference 9. This figure appears as Figure 14 in this report. As a design aid, the relationship for peak positive incident overpressure (p_{so}) versus scaled unit positive incident impulse ($i/W^{1/3}$) was obtained from this figure and then plotted in Figure 15. At the desired peak overpressure level of 50 psi, the corresponding values for $i/W^{1/3}$ and scaled ground distance, $R/W^{1/3}$, are 16.2 and 4.6, respectively. Substituting 382 psi-msec for i in the first expression results in a desired charge weight (W) of 13,111 pounds. Substituting this value into the second expression results in a charge distance (R) of 108.5 feet from the headwall centerline. These values are valid for the ambient conditions at sea level. However, since the test site is about 2,000 feet above sea level, the mean ambient conditions differ measurably from those at sea level. To account for these differences, a computational procedure outlined in Reference 10 was followed.

Using this procedure the following parameters were obtained at the headwall centerline for $W = 13,616$ pounds and $R = 108.6$ feet:

$$P_{so} = 50.2 \text{ psi}$$

$$i_s = 382.4 \text{ psi-msec}$$

The values at both door centerlines were also calculated and are listed in Table 2 and shown in Figures 16 and 17.

The following equation for crater radius was derived from data found in Reference 11:

$$r_c = 0.452 W^{0.42}$$

where:

$$r_c = \text{crater radius (ft)}$$

$$W = \text{charge weight (lb)}$$

The calculated crater radius for a 13,616-pound charge is 24.6 feet. As shown in the proposed test configuration of Figure 18, cratering is of no concern.

The charge was constructed of 8-pound TNT blocks (2 by 6 by 12 inches) and is shown in Figure 19.

Instrumentation

Figure 20 is a schematic of the active instrumentation recording the blast environment at the Type IIB magazine. Surface airblast pressure gauges located along gage lines at 90 and 180 degrees recorded the free-field pressure-time environment (Figure 21, Table 3). These gauges were installed in heavy-gage mounts to read the side-on pressure loads. A detailed description and purpose for each gauge is listed in Table 4. A total of 31 gauges were used.

Motion Picture Photography

The test was recorded photographically by ground and air-based 16mm cameras using color film at speeds ranging from 24 frames/second to 10,000 frames/second. Figure 22 illustrates the locations of the ground cameras.

TEST RESULTS

The analog data signals from the test instrumentation were conditioned and recorded on 1-inch magnetic tapes. The tape recorders were 14-track, intermediate-band, with FM amplifiers, operated at either 60 or 120 ips, providing a maximum frequency response of 20 kHz or 40 kHz, respectively. Each tape contained a IRIG B time signal and a detonation zero signal. Time-history records of all data are not included in this report due to its bulk, but are available from the author on request. High speed films showing test results are located at NCEL. A full documentary film of test results should be available approximately January 1987.

Test A-ROOF

Observed Structural Response. Test A-ROOF took place on 5 September 1985. Figure 23 illustrates the sequence of the foam HEST event. The explosive source was designed to produce a maximum impulse of 2,300 psi-msec on the Type A magazine roof. The average measured impulse of 2,500 psi-msec was only slightly greater than predicted. A post-test view of the magazine interior is shown in Figure 24. Both interior columns catastrophically collapsed, changing the roof configuration from a flat slab to a rectangular two-way slab restrained on four sides. The large dynamic deflections that occurred resulted in the roof acting primarily as a tensile membrane member in the short direction (front to rear). None of the principal steel reinforcing bars were broken or showed signs of necking down. A view of the roof after excavating the left rear quadrant is shown in Figure 25. The permanent deflections of the roof surface measured along nine lines (A through I) are displayed in Figure 26 and listed in Table 5. The permanent center deflection at midspan of the roof was 45.5 inches. The maximum support rotation measured in the short direction along Line E equals 15.8° . The maximum support rotation measured in the long direction along Line 7 equals 9.1° .

Both the backwall and the headwall were forced inward by the tensile membrane action of the roof. The maximum inward displacement of these walls, measured at the magazine centerline near the roof elevation, were 8 inches and 2-1/2 inches for the backwall and headwall, respectively.

Response Instrumentation. Data recovery in general was poor. In view of the catastrophic collapse of the interior columns this loss of data was not unexpected. Data from only three of the recovered airblast pressure gages is considered useful. A summary of the airblast data is listed in Table 6 and a representative time history plot is shown in Figure 27. A summary of data derived from velocity gage output is shown in Table 7. Gage No. A-C2-V3 was attached to the column and was lost immediately confirming the sudden early collapse of the columns. All three vertical roof displacement gages functioned satisfactorily until reaching the established 18-inch limit of gage travel.

Test IIB-DOORS

Observed Structural Response. Test IIB-DOORS took place on 12 September 1985. The explosive source was designed to produce a maximum impulse of 382 psi-msec and peak overpressure of 50 psi on the centerline of the Type IIB magazine headwall. Generally, measurements of blast loading made during the test were slightly lower than the predicted levels. The measured impulse at the headwall centerline was 355 psi-msec with an initial peak overpressure of 58 psi. A comparison of the roof and headwall gage output for ESKIMO's VI and VII is quite similar. Figure 28 shows the magazine being engulfed by the fireball. A post-test view of the magazine and crater is shown in Figure 29. Crater dimensions were 9-foot depth and 20-foot radius. The redesigned door and headwall system remained intact and more than satisfied the explosives safety deficiencies uncovered in ESKIMO VI. Buckling of the exterior steel face plate of the near door is illustrated in Figure 30. Maximum permanent door deflections of the near and far doors were measured as 9/16 inch and 3/16 inch, respectively. The only significant magazine damage observed was to the capital of the near column. Several large concrete pieces had separated as shown in Figure 31.

Response Instrumentation. Data recovery in general was good. A summary of the pressure gage output is listed in Tables 8 and 9 and a representative time history plot is shown in Figure 32. A comparison of the measured air-blast impulse versus the predicted (from Ref 9) is shown in Figure 33. A summary of data derived from the velocity gage output is listed in Table 10 and a representative time history plot is shown in Figure 34. Displacement was established by integration of the velocity gage output. Displacement transducers were strategically positioned so as to measure the maximum displacement of the headwall, pilasters, and doors. A summary of the displacement gage data is listed in Table 11 and a representative time history plot is shown in Figure 35. A summary of the strain gage output is listed in Table 12 and a representative time history plot is shown in Figure 36.

DISCUSSION/CONCLUSIONS

Test A-ROOF

Although the intended purpose of the test was not achieved, significant findings in the areas of column design, slab deflection capacity, and tensile membrane behavior were uncovered. The loading capability of the NEST technique was awesome. A total of only 264 pounds NEW of primacord produced an impulse of 2,500 psi-msec on the magazine roof while in ESKIMO VI, 44,000 pounds NEW produced only 656 psi-msec impulse. Since the pressure pulse shapes from this NEST explosion and an HE magazine detonation are similar, the observed test results are considered appropriate. A post-test dynamic analysis of the column for the blast load acting directly on the column indicated column failure. The loaded area in this analysis was limited to the area of the drop panel. The current column design procedures (Ref 4) neglects this "early" loading condition and only considers a loading equal to the ultimate resistance of the roof acting over the tributary area supported by the column. Under most loading conditions, the direct blast loading would not control the column design. However, as demonstrated in ESKIMO VII, it is possible that for a high magnitude blast load acting on a relatively low resistance roof, the column could fail before the flat slab yield line patterns could develop and thus the direct blast loading would control. The column failures immediately transformed the roof slab into a rectangular two-way slab restrained on four sides with an aspect ratio L/H of 1.9. In order for this roof slab to develop tension membrane behavior, adequate lateral restraint of the reinforcement is mandatory. However, external lateral restraint is not required for elements supported on four edges provided the aspect ratio is not less than one-half nor greater than two. Within this range, the inherent lateral restraint provided by the element's own compression ring around its boundary is sufficient lateral restraint to develop tension membrane behavior. The Type A magazine roof satisfies both restraint conditions and thus, tensile membrane behavior is possible. The tensile membrane resistance function for the Type A magazine roof is shown in Figure 37. A dynamic response calculation using this function and the measured roof loading resulted in a predicted maximum displacement of 49.7 inches. This is only slightly greater than the measured post-test permanent displacement of 45.5 inches. Even though no stirrups were used, the concrete on the underside of the roof remained intact except for small regions of the column bands where the bottom steel was cut off.

Test. IIB-Doors

The redesigned door and headwall system of the Type IIB magazine was more than adequate to resist the load resulting from the detonation of 350,000 pounds NEW in a similar magazine located at the minimum side-to-side spacing. The pilasters, which were designed for a maximum support rotation of 4 degrees, sustained less than one-fourth-degree of rotation. Figure 38 shows the resistance function for the Type IIB magazine door. Initiation of plastic behavior for the built-up steel channel and face plates is predicted for 21.7 psi and 0.64 inch. The ultimate door resistance is reached when the oak boards rupture at 25.9 psi. The measured maximum strain, deflection, and permanent deflection for the near door are much smaller than predicted for the 12 degree design rotation (3 inches of displacement equals 12 degrees rotation).

ACKNOWLEDGMENTS

The testing described in this paper was conducted at NWC, China Lake, CA. Mr. Harry Laatz was the NCEL Field Test Coordinator, Messrs. Dale Johnson and Dan Goff were the NCEL Test Instrumentation Engineers, and Ms. Mary Beyer was the NCEL Data Reduction Engineer. Mr. Herman Hoffman was the NWC Project Engineer and Mr. Jack Brown was the NWC Range Operations Engineer.

REFERENCES

1. H.W. Wampler et al (1978). "A status and capability report on nuclear airblast simulation using HEST," in Proceedings of the Nuclear Blast and Shock Simulation Symposium, vol I, San Diego, Calif., 28-30 Nov 1978. Washington, D.C., Defense Nuclear Agency, 1978. (DNA 4797P-1)
2. R.N. Murtha (1984). The final FSKIMO VII test plan, Naval Civil Engineering Laboratory, Technical Memorandum M-51-84-23. Port Hueneme, Calif., Dec 1984.
3. Department of Defense, DOD 5154.4S (1978). Ammunition and explosives safety standards, Washington, D.C., Jan 1978.
4. Departments of the Army, Navy, and Air Force (1969). Structures to resist the effects of accidental explosions, TM 5-1300, NAVFAC P 397, and AFM 88-22. Washington, D.C., Jun 1969.
5. Naval Facilities Engineering Command (1978). Box magazine Type A standard, NAVFAC Drawing No. 1404000. Alexandria, Va., 1978.
6. Naval Weapons Center (1979). ESKIMO VI magazines, NAVFAC Drawing No. 6125900-6125910. China Lake, Calif., Jul 1979.
7. Bureau of Yards and Docks (1956). Standard magazine smokeless powder/projectile Type IIB, Drawing No. 749771. Washington, D.C., 1956.
8. T.L. Pickett (1983). Concepts for secure magazine doors, Naval Civil Engineering Laboratory, Technical Report R-901. Port Hueneme, Calif., May 1983.

9. C.N. Kingery (1966). Air blast parameters versus distance for hemispherical TNT surface bursts, Army Ballistic Research Laboratory, Report No. 1344. Aberdeen Proving Ground, Md., Sep 1966.

10. W.E. Baker et al (1980). A manual for the prediction of blast and fragment loadings on structures, Department of Energy, DOE/TIC-11268. Amarillo, Tex., Nov 1980.

11. L.K. Davis (1968). "Events 5, 6A, 6 and 1A; Project 3.01: Monitor crater studies," Operation Distant Plain Symposium II, Vicksburg, Miss., 24-26 Jan 1968. Washington, D.C., Defense Atomic Support Agency, May 1968. (DASA 2207)

Table 1. Instrumentation for Test A-ROOF

Channel No.	Gauge No.	Measurement	Manufacturer/Model	Location and Purpose of Gauge	Predicted Peaks
1, 2	A-A2-BP1 ^a	Airblast Pressure	Kulite/HKS-375-5000	Surface air pressure at center of left bay	800 psi
3, 4	A-A3-BP2	Airblast Pressure	Kulite/HKS-375-5000	Surface air pressure at rear of left bay	800 psi
5, 6	A-B2-BP3	Airblast Pressure	Kulite/HKS-375-5000	Surface air pressure at center of middle bay	800 psi
7, 8	A-D3-BP4	Airblast Pressure	Kulite/HKS-375-5000	Surface air pressure at rear of right bay	800 psi
9, 10	A-D2-BP5	Airblast Pressure	Kulite/HKS-375-5000	Surface air pressure at center of right bay	800 psi
11	A-B3-SE1	Soil Stress	Kulite/LQ-080U	Vertical soil stress at 1-in depth	800 psi
12	A-B2-SE2	Soil Stress	Kulite/LQ-080U	Vertical soil stress at 1-in depth	800 psi
13	A-B1-V1	Velocity	Bell & Howell/364142-0100	Vertical velocity of roof at front of middle bay	800 in/sec
14	A-D1-V2	Velocity	Bell & Howell/364142-0100	Vertical velocity of roof at front of right bay	300 in/sec
15	A-C2-V3	Velocity	Bell & Howell/364142-0100	Vertical velocity of right column below right bay	25 in/sec
16	A-B2-VF1	Velocity	Bell & Howell/364142-0100	Vertical velocity of ground at center of middle bay	25 in/sec
17	A-B1-VF2	Velocity	Bell & Howell/364142-0100	Vertical velocity of ground at front of middle bay	25 in/sec
18	A-D2-VF3	Velocity	Bell & Howell/364142-0100	Vertical velocity of ground at center of right bay	25 in/sec
19	A-B2-D1	Displacement	Bournes/2051941502	Vertical displacement of roof at center of middle bay	16.5 in.
20	A-B1-D2	Displacement	Bournes/2051941502	Vertical displacement of roof at front of middle bay	16.5 in
21	A-D2-D3	Displacement	Bournes/2051941502	Vertical displacement of roof at center of right bay	16.5 in

^a A = Test A-ROOF; A2 = Gauge location (A = headwall position, 2 = sidewall position); BP1 = airblast pressure gauge No. 1.

Table 2. Blast Parameters for W = 13,616 lb at
2,000 Feet Above Sea Level

Blast Parameter	Magazine Location		
	Near Door	Headwall Centerline	Far Door
Charge distance, R (ft)	92.5	108.6	124.7
Scaled distance, Z (ft/lb ^{1/3})	3.87	4.55	5.22
"Corrected" scaled distance, Z* (ft/lb ^{1/3})	3.78	4.44	5.09
"Corrected" ^a peak positive overpressure, P _{so} (psi)	66.9	50.2	35.0
"Corrected" ^b positive impulse, i (psi-msec) ^s	435.1	382.4	332.0
"Corrected" ^c positive duration, t _d (msec)	39.4	38.2	38.2
"Corrected" ^c arrival time, t _a (msec)	18.5	24.7	34.5

^aCorrection factor = 0.929.

^bCorrection factor = 0.959.

^cCorrection factor = 1.032.

Table 3. Free-Field Pressure Gauge Locations on Lines at 90 and 180 Degrees for Test IIB-DOORS

Range, R (ft-in)	Scaled Distance, ^a $Z = R/W^{1/3}$ (ft/lb ^{1/3})	"Corrected" Scaled Distance, ^b $Z^* = Z(13.66/14.70)^{1/3}$ (ft/lb ^{1/3})	"Uncorrected" Pressure Parameters				"Corrected" Pressure Parameters			
			Peak Positive Incident Overpressure, P_{so} (psi)	Unit Positive Incident Impulse, i_s (psi-msec) ^c	Arrival Time, t_d (msec)	Positive Duration, t_d (msec)	Peak Positive Incident Overpressure, P_{so} (psi)	Unit Positive Incident Impulse, i_s (psi-msec) ^c	Arrival Time, t_d (msec)	Positive Duration, t_d (msec)
71-8	3	2.9	140	573	11.0	39.4	130	550	11.3	40.6
95-6	4	3.9	70	454	19.1	38.2	65	435	19.7	39.4
119-5	5	4.9	43	370	29.9	37.0	40	354	30.8	38.2
143-3	6	5.9	28	310	45.4	39.4	26	297	46.8	40.6
167-2	7	6.8	20	263	52.5	46.6	19	252	54.1	48.0

^a $W = 13,616$ lb; $W^{1/3} = 23.88$ lb^{1/3}.

^b $Z^* = Z(13.66/14.70)^{1/3}$.

^cFrom Figure 14.

^dCorrection factor = 0.929.

^eCorrection factor = 0.959.

^fCorrection factor = 1.032.

Table 4. Instrumentation for Test IIB-DOORS

Channel No.	Gauge No.	Measurement	Manufacturer/Model	Location and Purpose of Gauge	Predicted Peaks
1	90-3-A1 ^a	Airblast Pressure	Bytrex/HFG-200	Surface air pressure at scaled distance of 3; 90-deg azimuth	130 psi
2	90-4-A2	Airblast Pressure	Bytrex/HFG-100	Scaled distance of 4; 90-deg azimuth	65 psi
3	90-5-A3	Airblast Pressure	Bytrex/HFG-100	Scaled distance of 5; 90-deg azimuth	40 psi
4	90-6-A4	Airblast Pressure	Bytrex/HFG-100	Scaled distance of 6; 90-deg azimuth	26 psi
5	90-7-A5	Airblast Pressure	Bytrex/HFG-100	Scaled distance of 7; 90-deg azimuth	19 psi
6	180-3-A6	Airblast Pressure	Bytrex/HFG-200	Scaled distance of 3; 180-deg azimuth	130 psi
7	180-4-A7	Airblast Pressure	Bytrex/HFG-100	Scaled distance of 4; 180-deg azimuth	65 psi
8	180-5-A8	Airblast Pressure	Bytrex/HFG-100	Scaled distance of 5; 180-deg azimuth	40 psi
9	180-6-A9	Airblast Pressure	Bytrex/HFG-100	Scaled distance of 6; 180-deg azimuth	26 psi
10	180-7-A10	Airblast Pressure	Bytrex/HFG-100	Scaled distance of 7; 180-deg azimuth	19 psi
11	B-C3A-BP1 ^b	Airblast Pressure	Senso-Metrics/SP68	Surface air pressure at center of middle bay	50 psi
12	B-C2A-BP2	Airblast Pressure	Senso-Metrics/SP68	Surface air pressure at front of middle bay	50 psi
13	B-A1D-BP3	Airblast Pressure	Senso-Metrics/SP68	Side-on air pressure on headwall at near door mid-height	67 psi
14	B-C1D-BP4	Airblast Pressure	Senso-Metrics/SP68	Side-on air pressure on headwall at centerline mid-height	50 psi
15	B-F1D-BP5	Airblast Pressure	Senso-Metrics/SP68	Side-on air pressure on headwall at far door mid-height	35 psi
16	B-C4E-BP6	Airblast Pressure	Bytrex/HFG-25	Interior magazine leakage pressure; centerline of floor at rear wall	0 psi
17	B-C2E-V1	Velocity	Bell & Howell/364142-0100	Vertical velocity of roof at front of middle bay	160 in/sec
18	B-D3C-V2	Velocity	Bell & Howell/364142-0100	Vertical velocity of right column at capital	50 in/sec
19	B-C1D-V3	Velocity	Bell & Howell/364137-0100	Horizontal velocity of headwall at centerline mid-height	515 in/sec
20	B-C2E-V4	Velocity	Bell & Howell/364142-0100	Vertical velocity of floor at front of middle bay	50 in/sec

Table 4. Continued

Channel No.	Gauge No.	Measurement	Manufacturer/Model	Location and Purpose of Gauge	Predicted Peaks
21	B-C3B-D1	Displacement	Bournes/200164W07	Vertical displacement of roof at center of middle bay	1.6 in
22	B-C2B-D2	Displacement	Bournes/2001564W07	Vertical displacement of roof at front of middle bay	1.6 in
23	B-A1D-D3	Displacement	Bournes/2051941502	Horizontal displacement at center of near door; inside face	10.5 in ^c 14.3 in ^d
24	B-B1D-D4	Displacement	Bournes/2001941501	Horizontal displacement of near door pilaster at mid-height; inside face	5.6 in
25	B-C1D-D5	Displacement	Bournes/2001941501	Horizontal displacement of headwall at centerline at mid-height; inside face	6.6 in
26	B-E1D-D6	Displacement	Bournes/2001564W07	Horizontal displacement of far door pilaster at mid-height; inside face	1.6 in
27	B-F1D-D7	Displacement	Bournes/2001941501	Horizontal displacement at center of far door; inside face	4.5 in ^c 5.6 in ^d
28	B-A1D-S1	Strain	Ailtech/SG129-65	Horizontal strain at center of near door; inside face	20,000 μ in/in
29	B-A1D-S2	Strain	Ailtech/SG129-65	Vertical strain at center or near door; inside face	10,000 μ in/in
30	B-F1D-S3	Strain	Ailtech/SG129-65	Horizontal strain at center of far door; inside face	20,000 μ in/in
31	B-F1D-S4	Strain	Ailtech/SG129-65	Vertical strain at center of far door; inside face	10,000 μ in/in

^a90 = 90° azimuth; 3 = scaled distance; A1 = airblast pressure gauge No. 1.

^bB = Test IIB-DOORS; C3A = gauge location (C = headwall position, 3 = sidewall position, A = elevation position);
BPI = Airblast pressure gauge No. 1.

^cRelative displacement.

^dGross displacement.

Table 5. Vertical Roof Deflection of the Type A Test Structure

Measurement Point	Vertical Displacement Along These Roof Lines ^a (feet)								
	A	B	C	D	E	F	G	H	I
1	0.26	0.28	0.36	0.45	0.40	0.41	0.58	0.38	0.33
2	0.84	0.85	1.03	1.17	1.14	1.27	1.26	1.05	0.92
3	1.13	1.67	1.93	1.98	1.94	1.97	1.90	1.74	1.15
4	1.26	2.13	2.50	2.70	2.74	2.74	2.38	2.11	1.23
5	1.35	2.25	2.80	3.16	3.28	3.07	2.60	2.23	1.25
6	1.48	2.43	3.00	3.48	3.63	3.27	2.75	2.33	1.29
7	1.61	2.55	3.16	3.61	3.79	3.35	2.88	2.42	1.33
8	1.72	2.72	3.33	3.69	3.77	3.49	3.00	2.54	1.40
9	1.84	2.91	3.13	3.38	3.45	3.24	3.02	2.66	1.46
10	2.00	2.43	2.56	2.93	2.84	2.88	2.49	2.29	1.52
11	1.34	1.66	1.90	2.09	2.15	2.06	1.85	1.58	1.30
12	0.66	0.94	1.13	1.40	1.32	1.33	1.14	0.89	0.60
13	0.27	0.29	0.32	0.71	0.61	0.79	0.56	0.27	0.21

^aSee Figure 26 for location of these displacements.

Table 6. Summary of Airblast Pressure Data for Test A-ROOF

Gage No.	Peak ^a Pressure (psi)	Impulse (psi-msec)
A-A2-BP1	1207/500	3500 ^b
A-A3-BP2	Bad Gage	—
A-B2-BP3	Bad Gage	—
A-D3-BP4	1570/400	2500
A-D2-BP5	1180/340	1550 ^c

^aThe first value is a maximum value read from the curve. The second value is a linearized estimate of the peak value based on an exponentially decaying pressure pulse.

^bResidual pressure equals +50 psi. Corrected impulse equals 2500 psi-msec.

^cResidual pressure equals -50 psi. Corrected impulse equals 2550 psi-msec.

Table 7. Summary of Velocity Data for Test A-ROOF

Gage No.	Peak Velocity (in/sec) ^a	Displacement ^a (in)
A-B1-V1 (roof)	460	37.2
A-D1-V2 (roof)	395	24.6
A-C2-V3 (column)	b	b
A-B2-VF1 (floor)	22	0.4
A-B1-VF2 (floor)	9	0.2
A-D2-VF3 (floor)	17	0.5

^aPositive values indicate downward motion.

^bGage lost during test.

Table 8. Summary of Free-Field Pressure Gage Data for Test IIB-DOORS

Gage No.	Gage Distance From Donor (ft)	Peak Overpressure ^a (psi)	Impulse (psi-msec)
90-3-A1 ^a	71.7	192/97	725
90-4-A2	95.6	73/58	403
90-5-A3	119.4	39/25	258
90-6-A4	143.3	24/21	226
90-7-A5	167.2	21/18	200
180-3-A6	71.7	165/90	580
180-4-A7	95.6	75/48	451
180-5-A8	119.4	42/30	258
180-6-A9	143.3	23/20	235
180-7-A10	167.2	18/16	235

^aThe first value is the maximum value read from the curve. The second value is a linearized estimate of the peak value based on an exponentially decaying pressure pulse.

Table 9. Summary of On-Structure Pressure Gage Data for Test IIB-DOORS

Gage No.	Location	Peak ^a Overpressure (psi)	Impulse (psi-msec)
B-C3A-BP1	Roof Centerline	82/46	382
B-C2A-BP2	Roof Centerline	55/41	390
B-A1D-BP3	Near Door	105/74	395
B-C1D-BP4	Headwall Centerline	58/42	355
B-F1D-BP5	Far Door	45/38	230

^aThe first value is a maximum value read from the curve. The second value is a linearized estimate of the peak value based on and exponentially decaying pressure pulse.

Table 10. Summary of Velocity Gage Data for Test IIB-DOORS

Gage No.	Location	Time from Zero to Maximum Peak Displacement (msec)	Peak Velocity ^a (in/sec)	Displacement (in)
B-C2B-V1	Roof Centerline	79	84 (-43)	1.49
B-D3C-V2	Far Column	79	17 (-21)	0.31
B-C1D-V3	Headwall Centerline	59	185 (-154)	2.00
B-C2E-V4	Floor	96	5 (-6)	0.12

^aPositive values indicate motions vertically down or horizontally toward the structure center.

Table 11. Summary of Displacement Gage Data
for Test IIB-DOORS

Gage No.	Location	Time from Zero to Maximum Displacement (msec)	Maximum Displacement (in)
B-C3B-D1	Roof Centerline	75	1.49
B-C2B-D2	Roof Centerline	77	1.49
B-A1D-D3	Near Door	43	1.62
B-B1D-D4	Near Door Pilaster	44	0.16
B-C1D-D5	Headwall Centerline	58	1.77
B-E1D-D6	Far Door Pilaster	53	0.16
B-F1D-D7	Far Door	69	2.24

^aPositive values indicate motions vertically down or horizontally toward the structure center.

Table 12. Summary of Strain Gage Data
for Test IIB-DOORS

Gage No.	Location	Direction	Time from Zero to Maximum Strain (msec)	Peak Strain ^a (μ in/in)
B-A1D-S1	Near Door	Horizontal	44	3270
B-A1D-S2	Near Door	Vertical	-	-
B-F1D-S3	Far Door	Horizontal	57	1895
B-F1D-S4	Far Door	Vertical	-	-

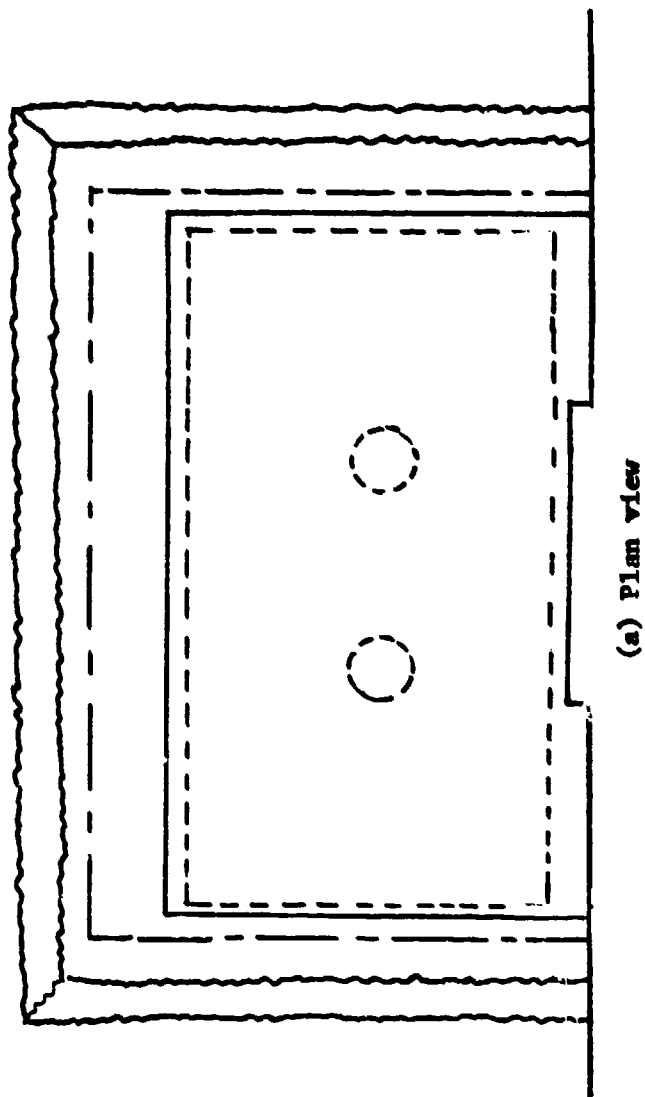
^aPositive values equal tension; negative values equal compression.



Figure 1. Interior view of Type A magazine before test.



Figure 2. Exterior view of Type A magazine before test.



Native soil overburden
 $D_{cav} = 4.5 \text{ in.}$ $H_{OB} = 12 \text{ in.}$

Charge cavity

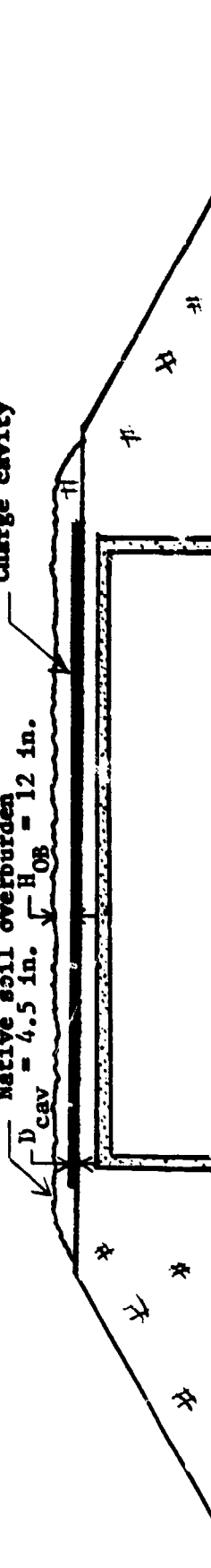


Figure 3. Foam HEST configuration and placement.

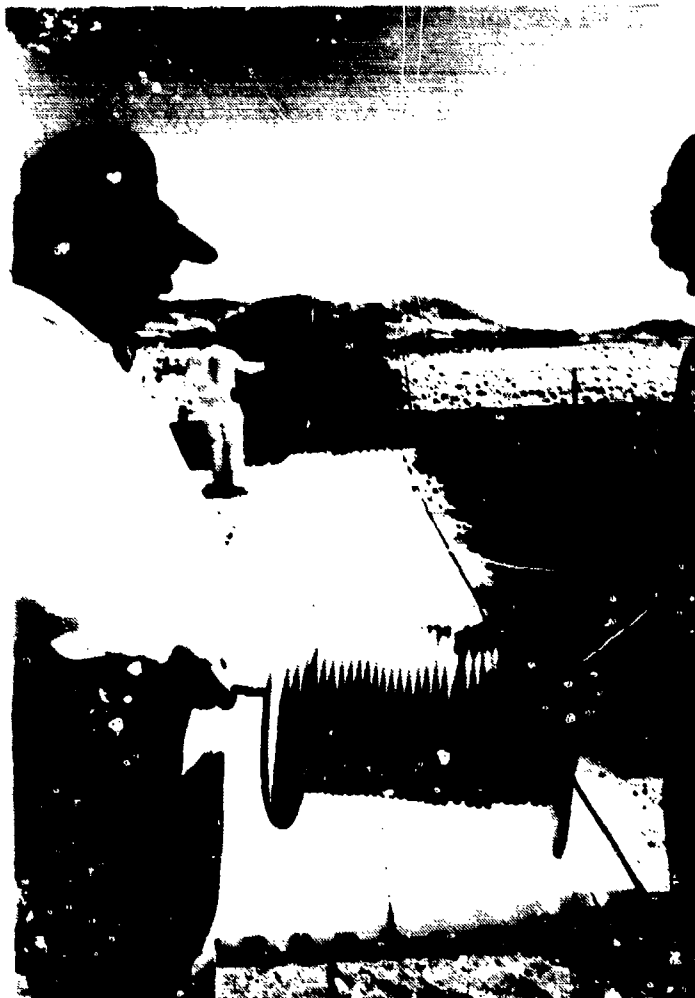


Figure 5. Construction of foam HEST charge cavity above Type A magazine roof.

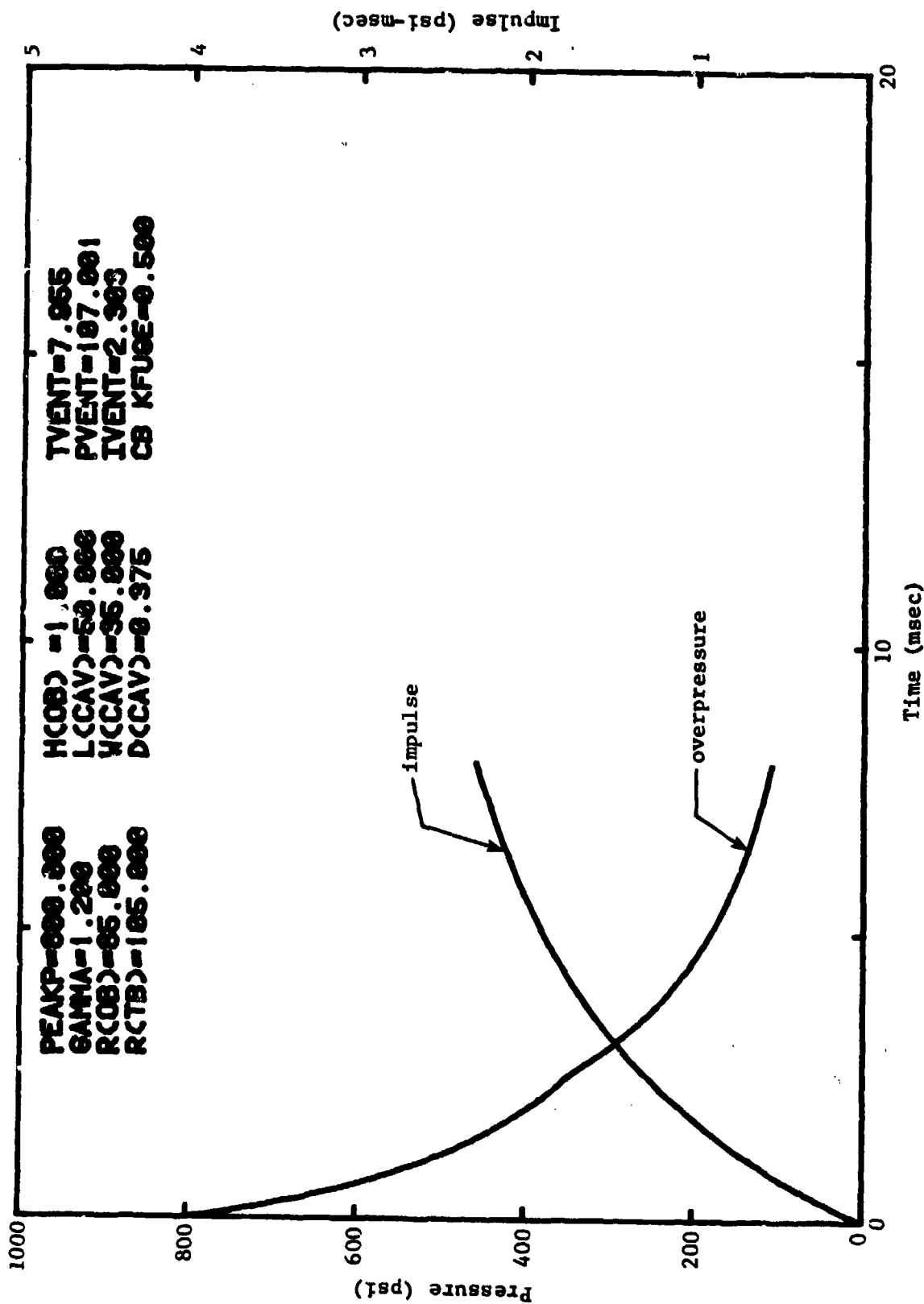


Figure 6. HEST design code output for foam HEST A ROOF parameters.

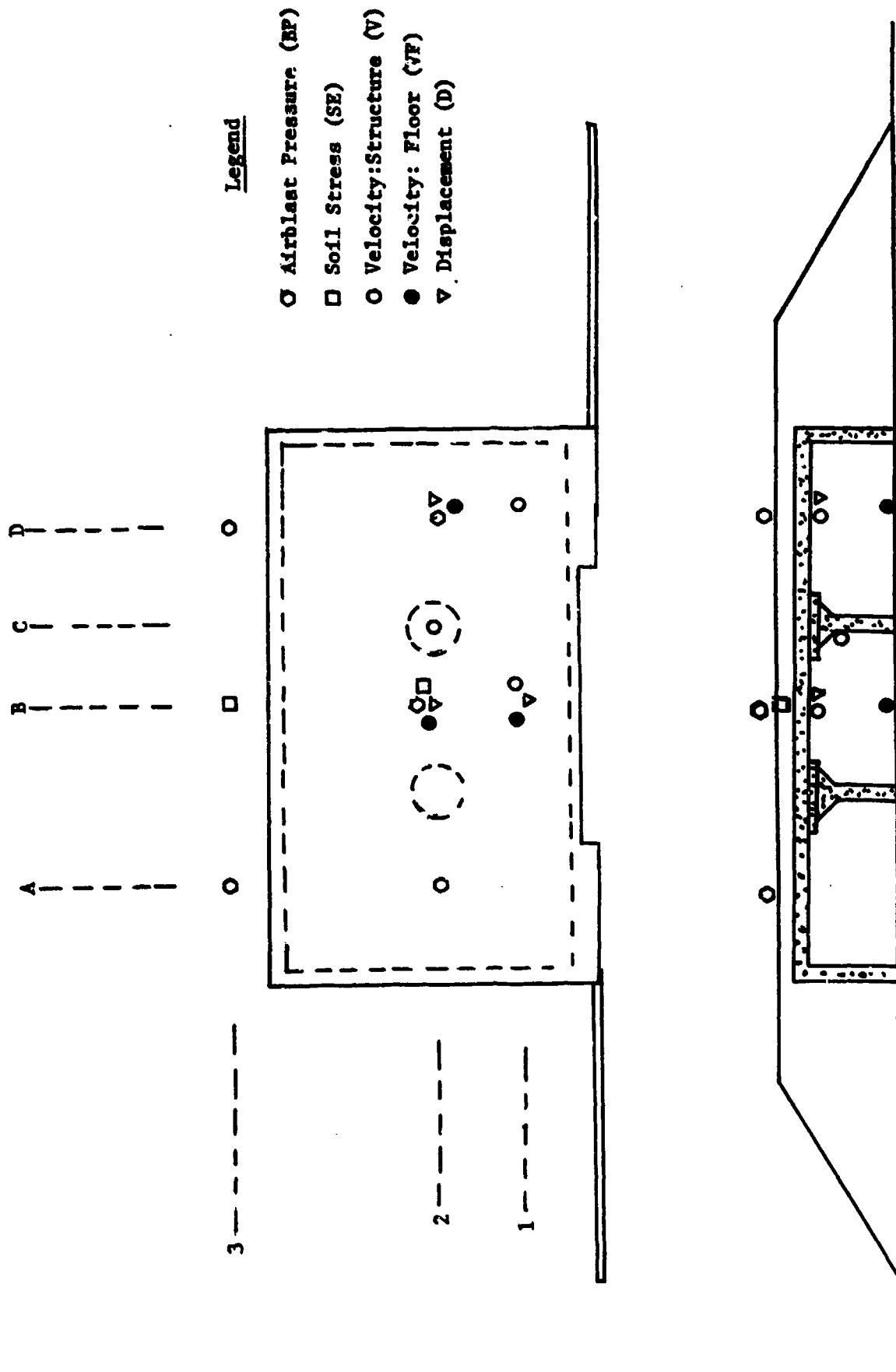


Figure 7. Type A magazine gauge locations for Test A-ROOF.

Test A-ROOF

Camera 1: View HEST Test Bed

Camera 2: View HEST Test Bed

Camera 3: Overall View of Type A Magazine

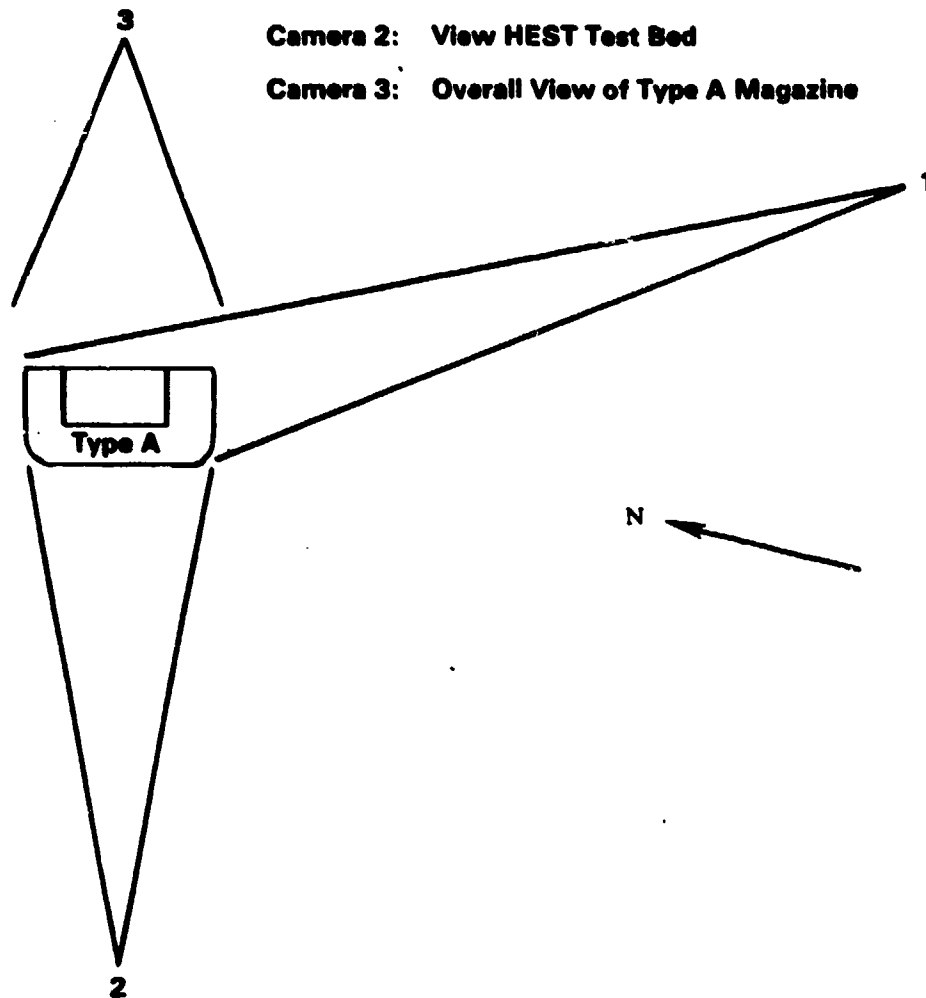
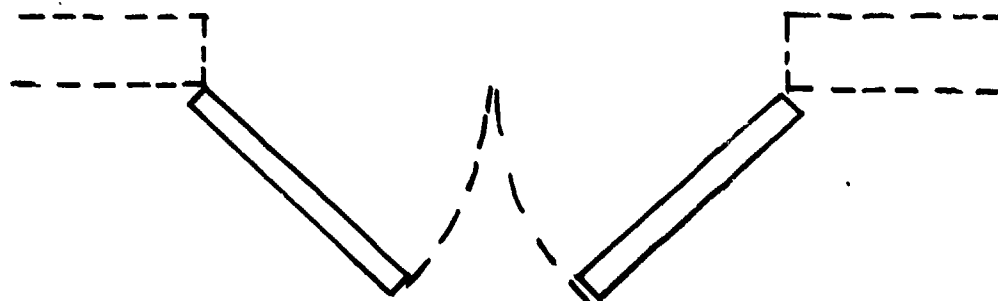
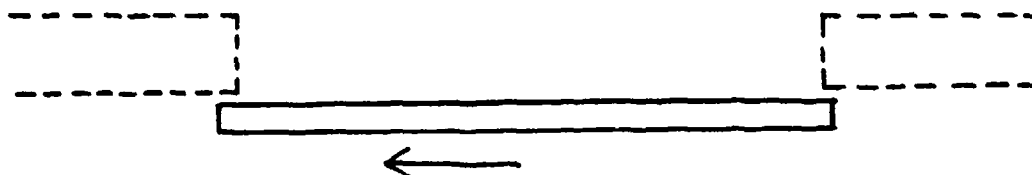


Figure 8. Test A-ROOF camera locations and field-of-view definition.

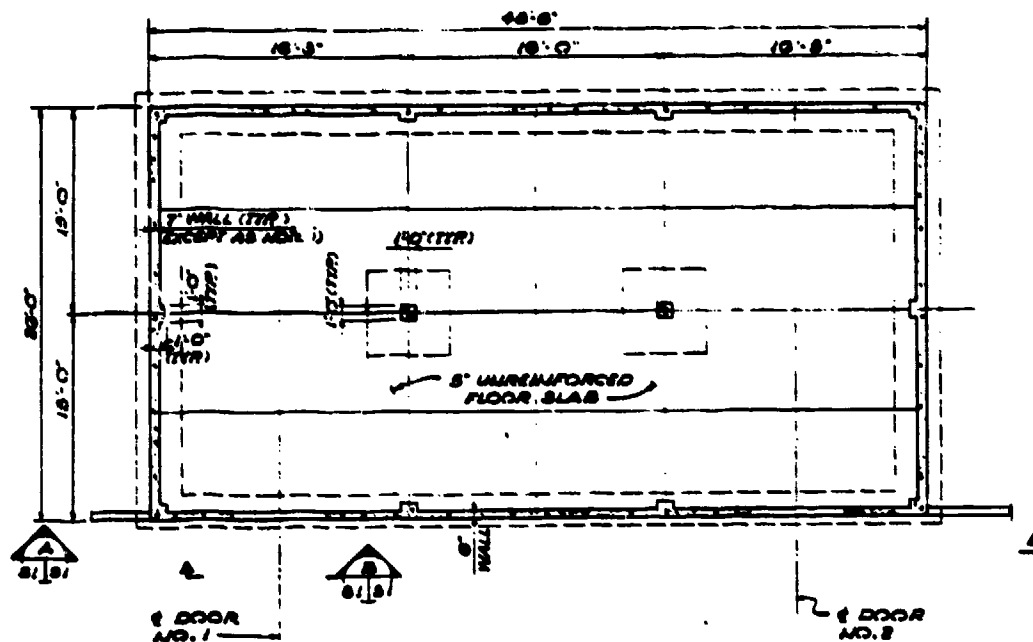


(a) ESKIMO VI: Double leaf/hinged

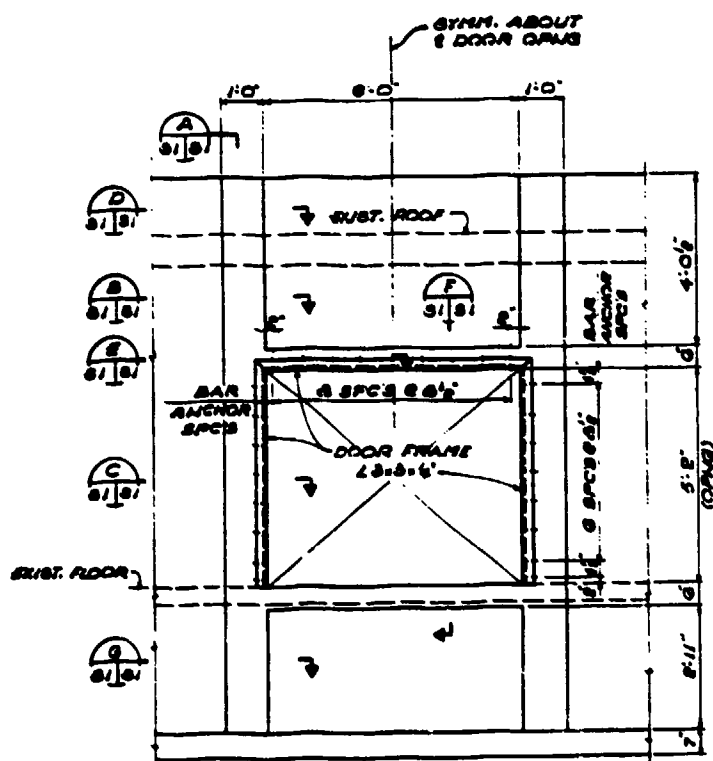


(b) ESKIMO VII: Single leaf/sliding

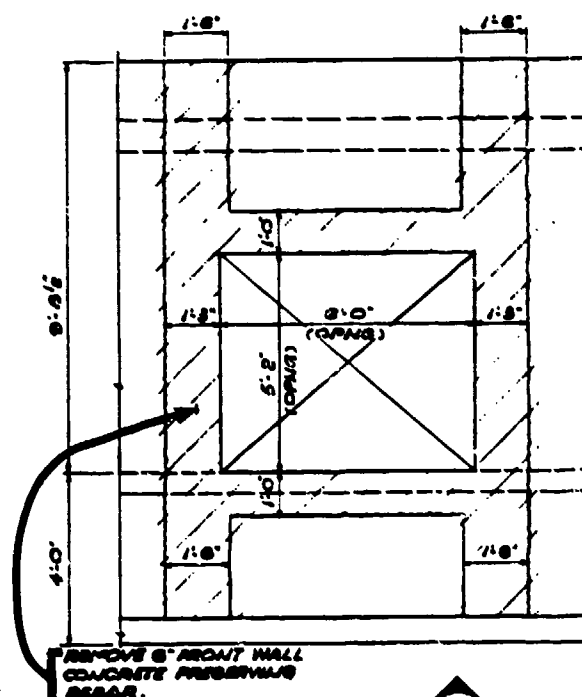
Figure 9. Type IIB magazine door.



EXISTING FIRST FLOOR PLAN
SCALE: 1/8" = 1'-0"

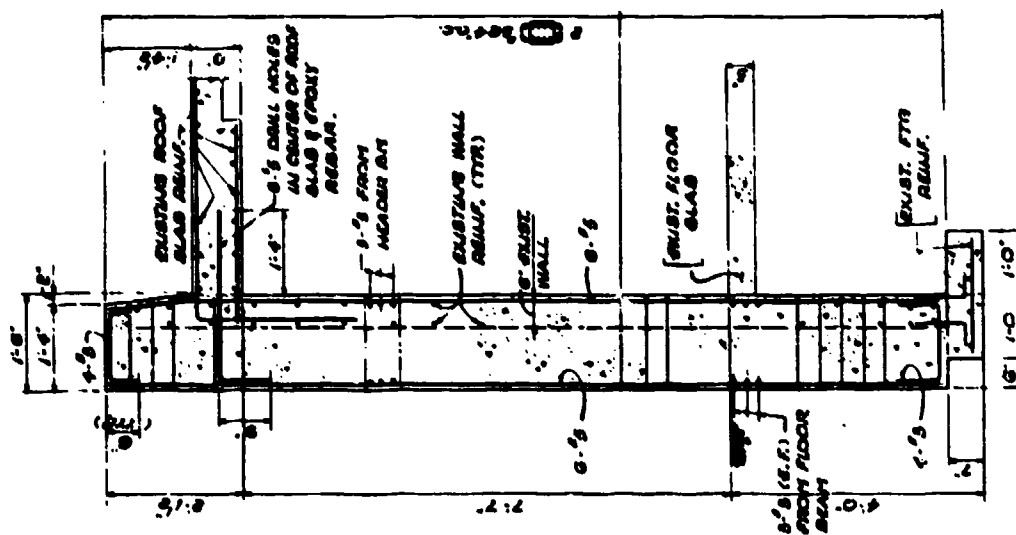


ELEVATION B
MODIFIED DOOR
(DOOR #1 SHOWN)
(DOOR #2 SIMILAR)
SCALE: 1/8" = 1'-0"

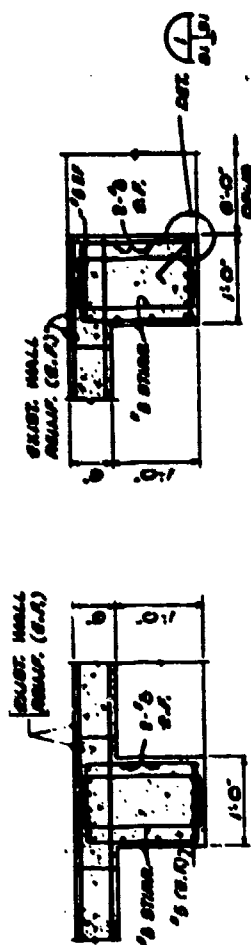


ELEVATION B
DEMOLITION
(DOOR #1 SHOWN)
(DOOR #2 SIMILAR)
SCALE: 1/8" = 1'-0"

Figure 10. Construction drawing of half-scale Type IIB magazine headwall modifications.

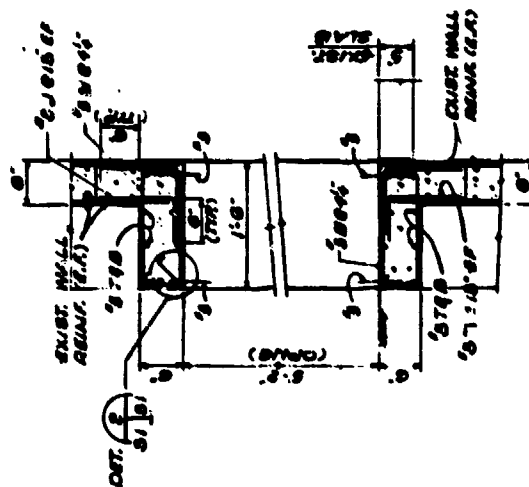


SECTION A
SCALE: 1/4" = 1'-0"



SECTION B
SCALE: 1/4" = 1'-0"

SECTION C
SCALE: 1/4" = 1'-0"



SECTION F
SCALE: 1/4" = 1'-0"

Figure 10. (Continued from previous page.)



1760



Figure 13. Completed headwall modifications of Type IIB test structure.



Figure 12. Pilaster and lintel beam reinforcement of the Type IIB test structure.

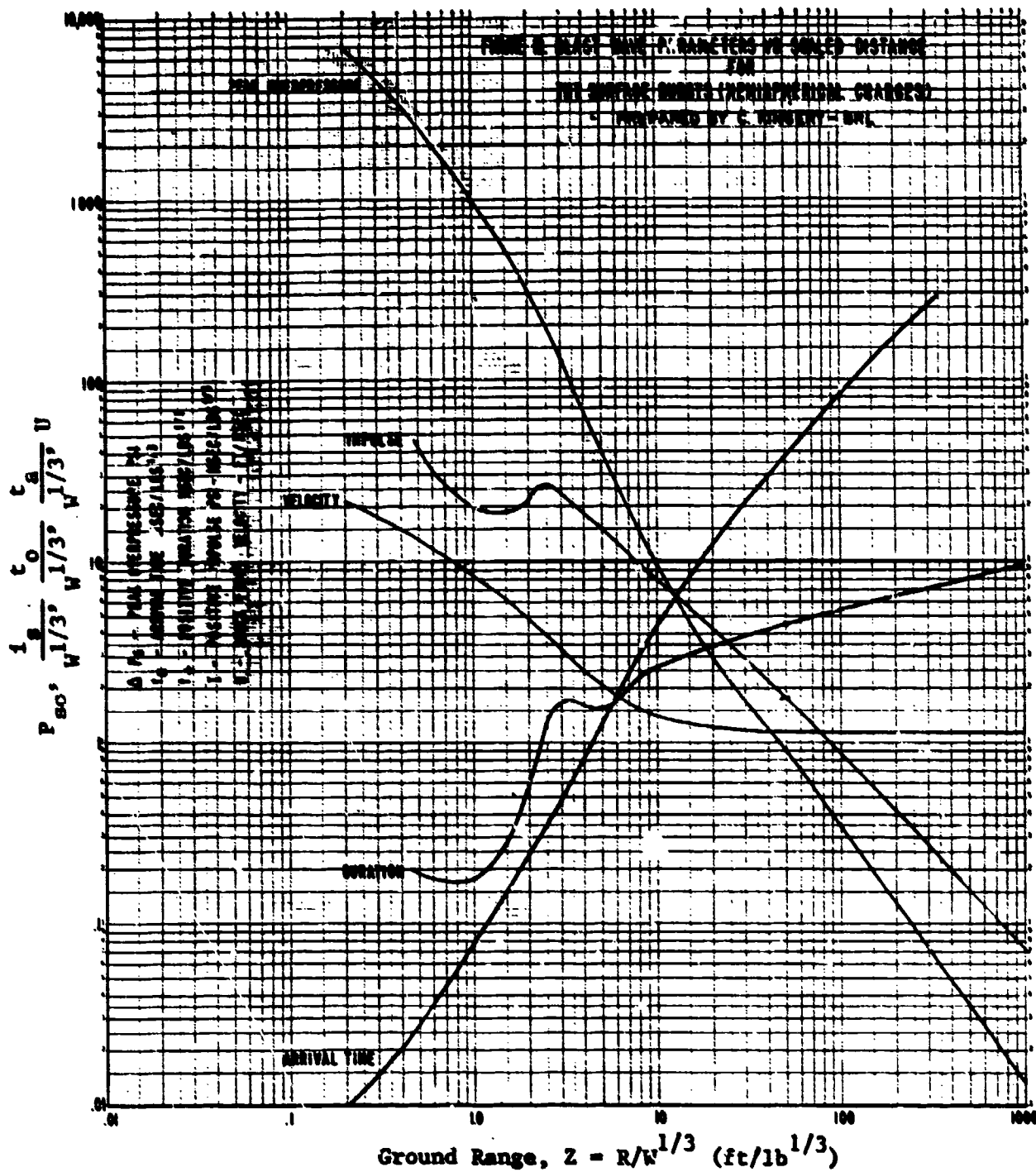


Figure 14. Blast wave parameters versus scaled distance for hemispherical TNT surface bursts (Ref 9).

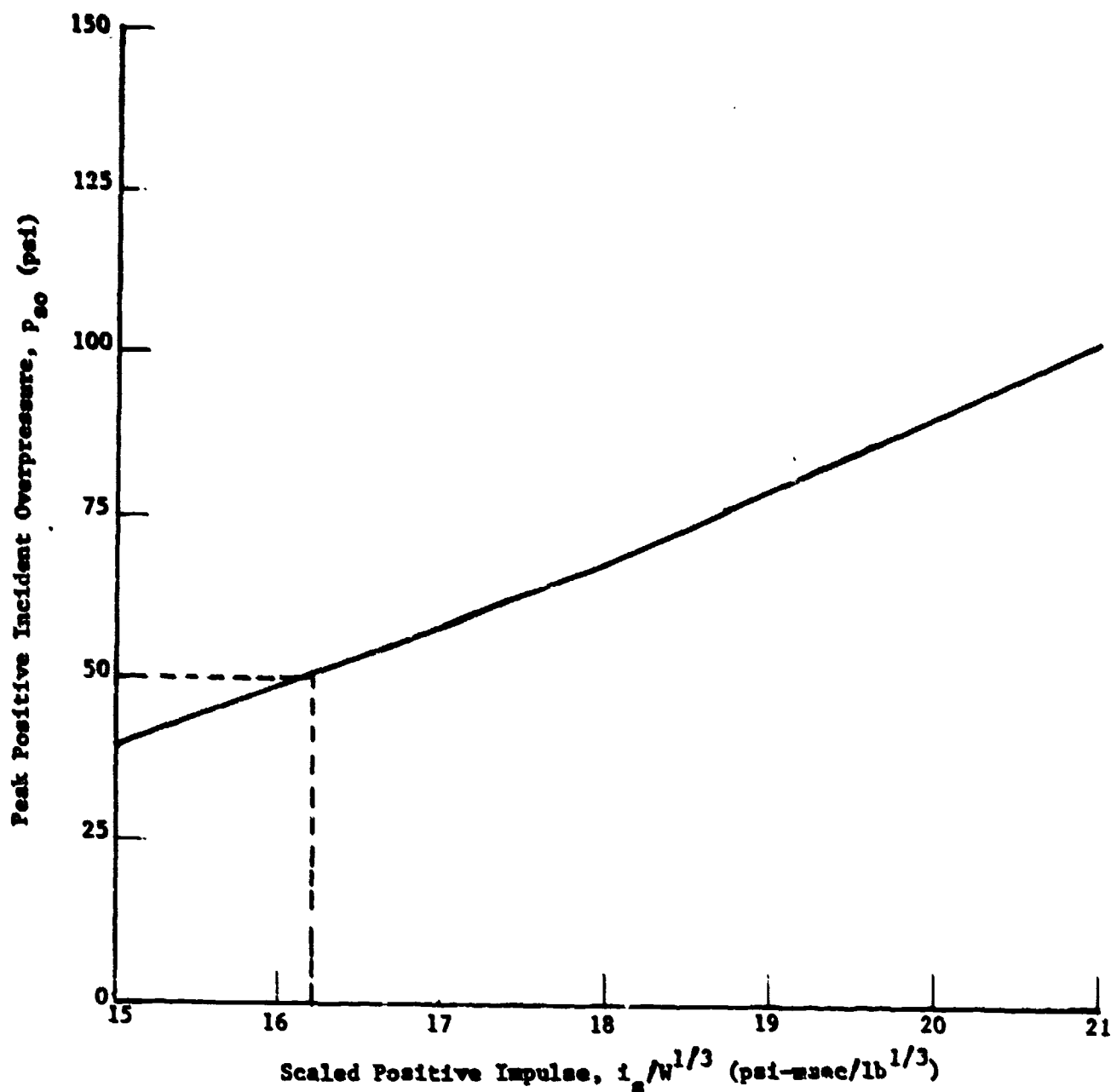


Figure 15. Peak positive incident overpressure versus scaled unit positive incident impulse for hemispherical charge (Ref 9)

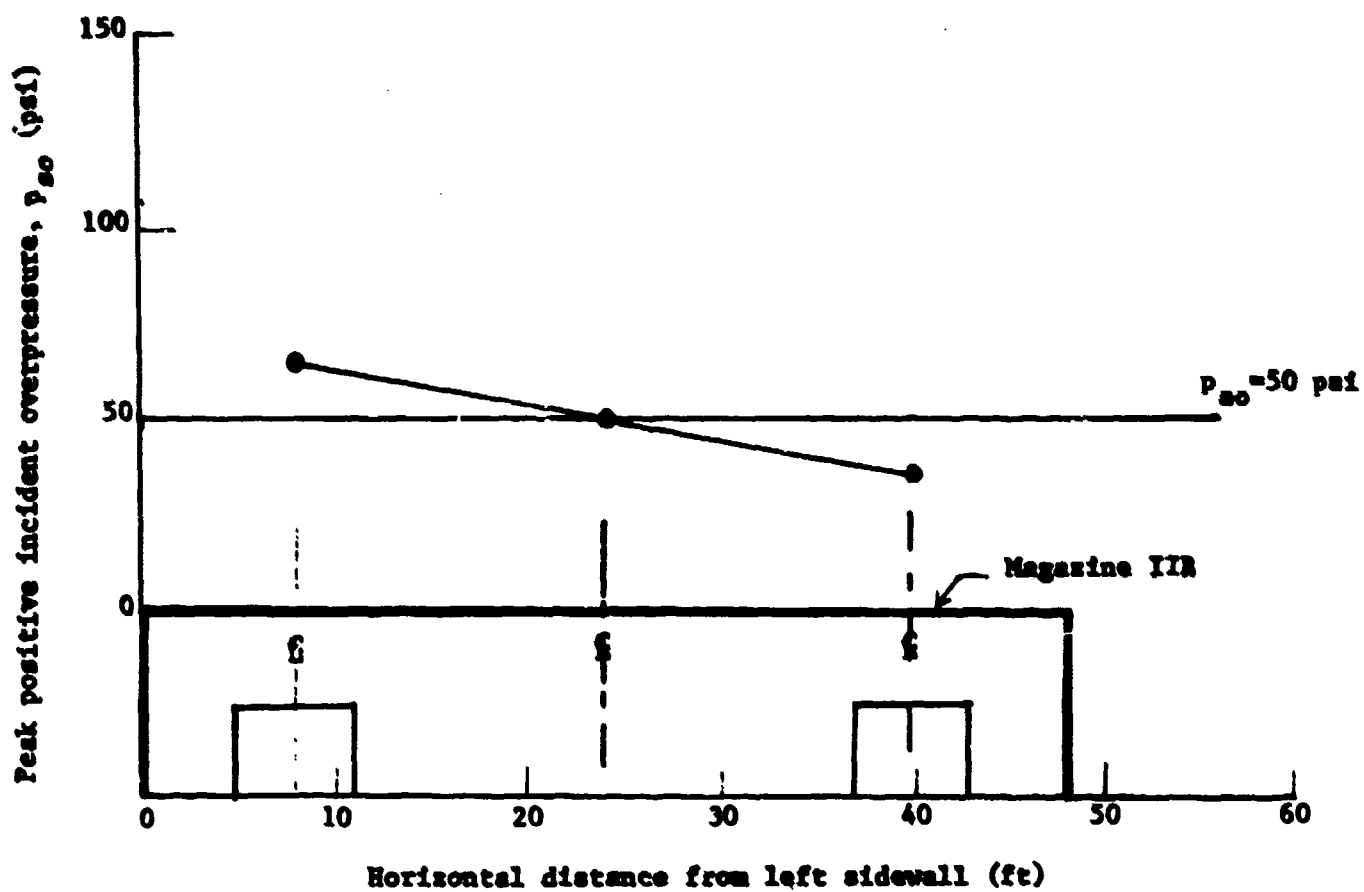


Figure 16. Peak positive overpressure acting along Type IIR magazine; $W = 13,616$ lb.

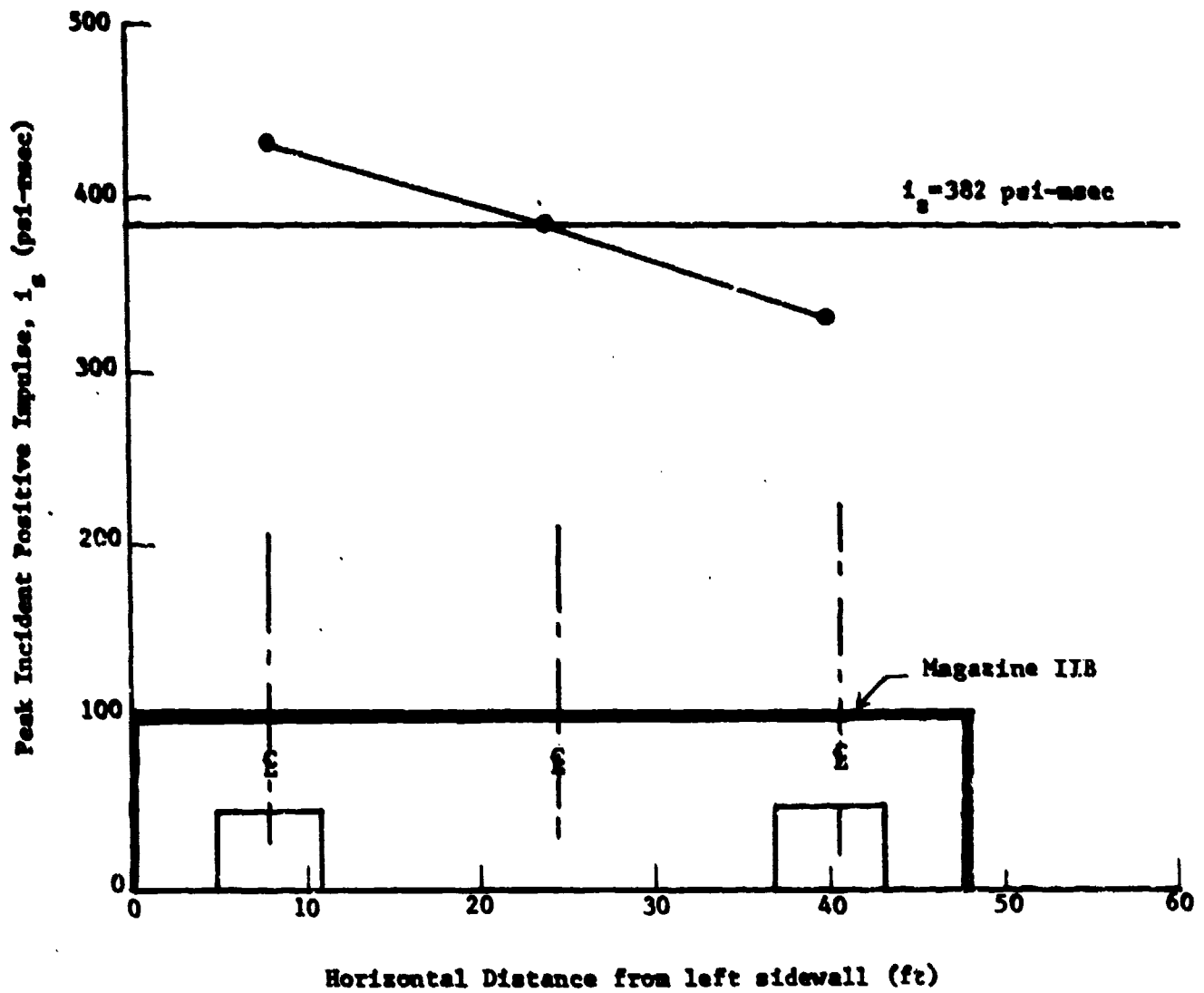


Figure 17. Impulse acting along Type IIB magazine; $W = 13,616$ lb.

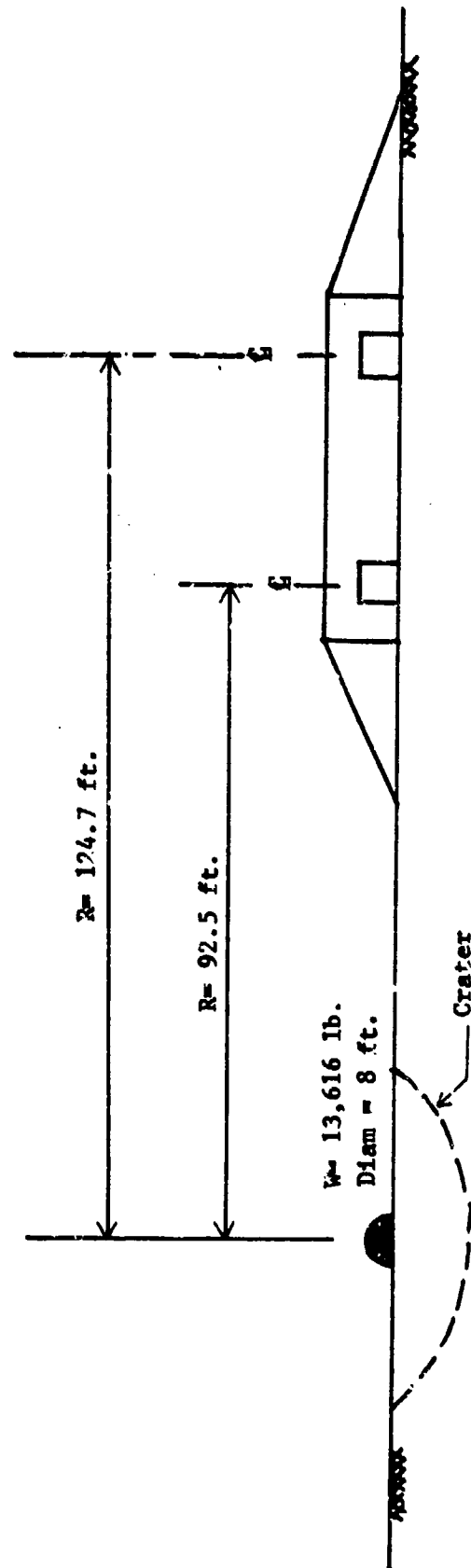


Figure 18. Test IIB-DOORS layout configuration.



Figure 19. Type IIB test structure and hemispherical surface charge.

A B C D E F

- Airblast Pressure (AP)
- Velocity: Structure (V)
- Velocity: Floor (VF)
- ▽ Displacement (D)
- Strain (S)

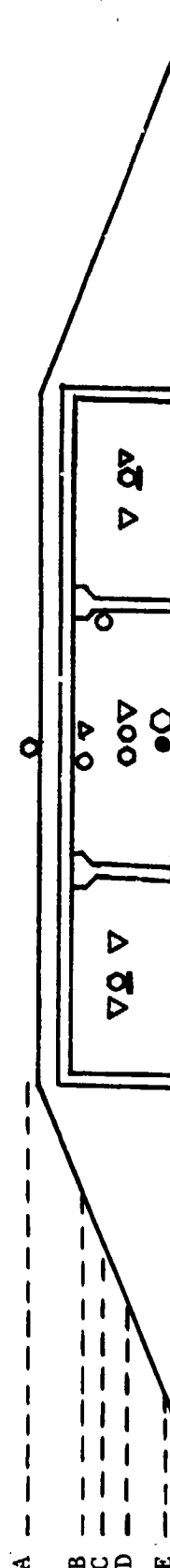
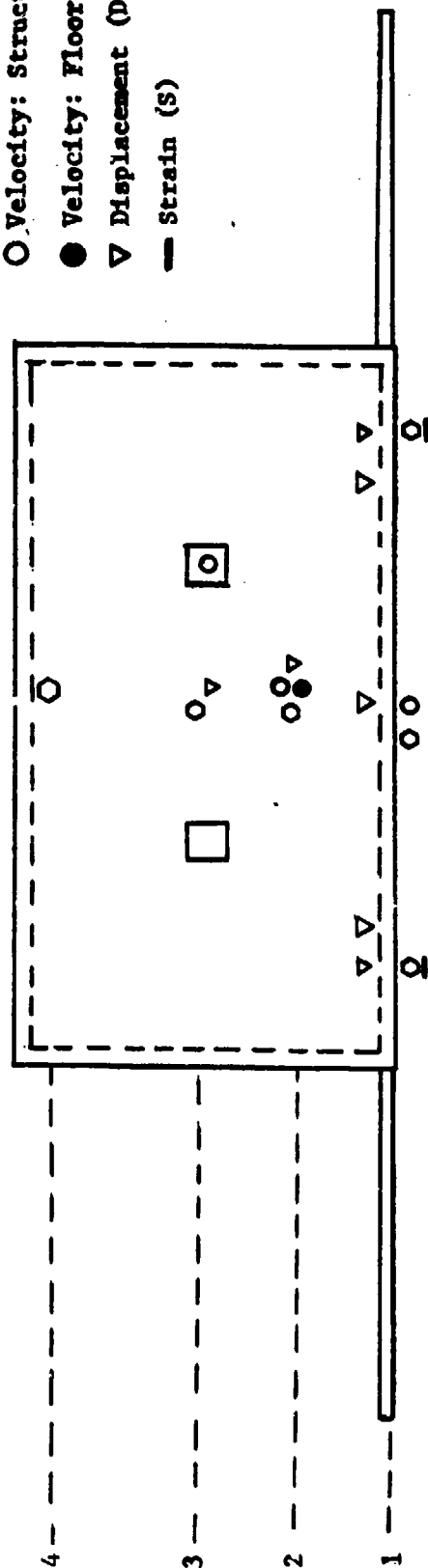


Figure 20. Type IIB magazine gauge locations for Test IIB-DOORS.

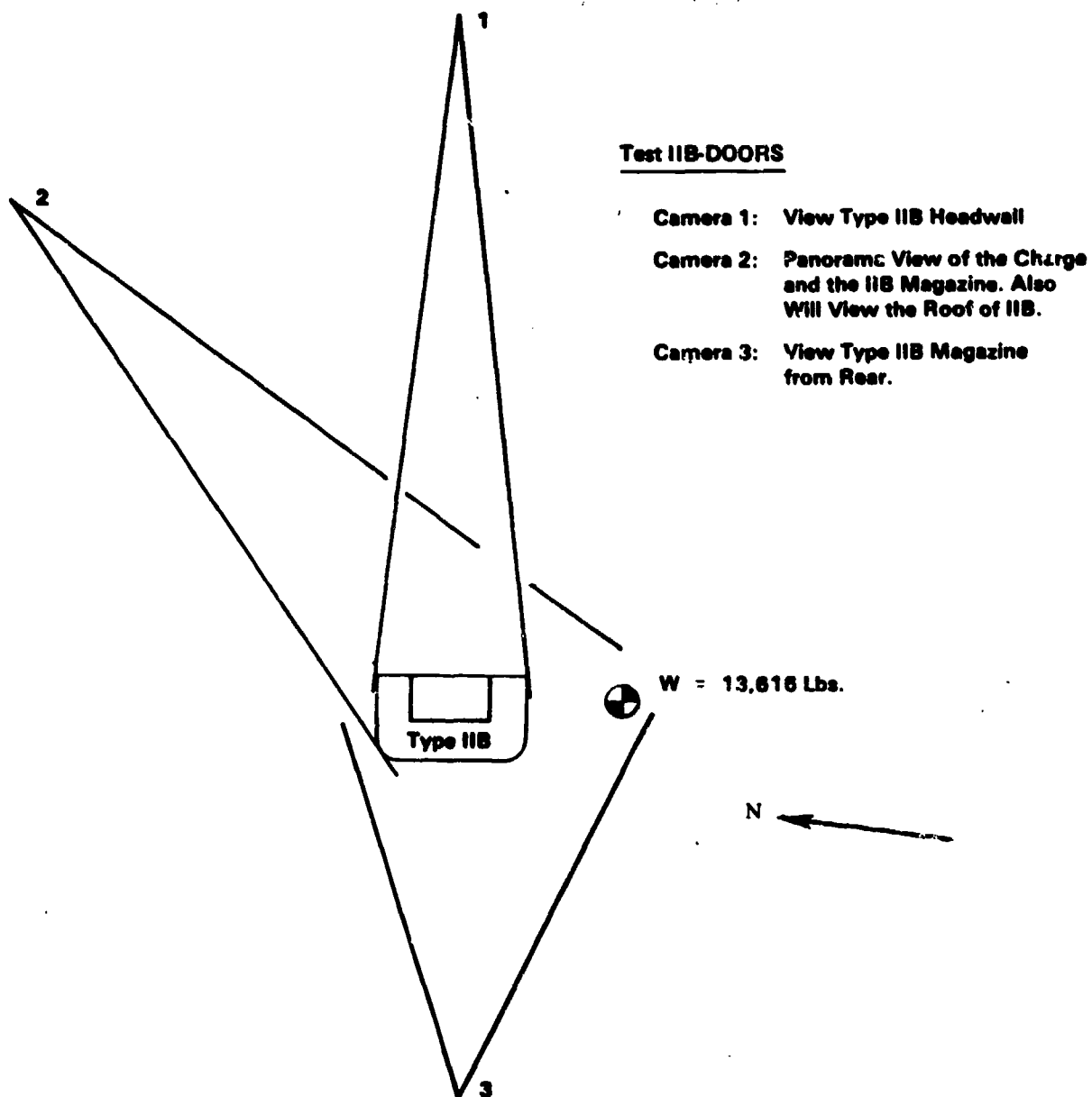


Figure 22. Test IIB-DOORS camera locations and field-of-view definition.

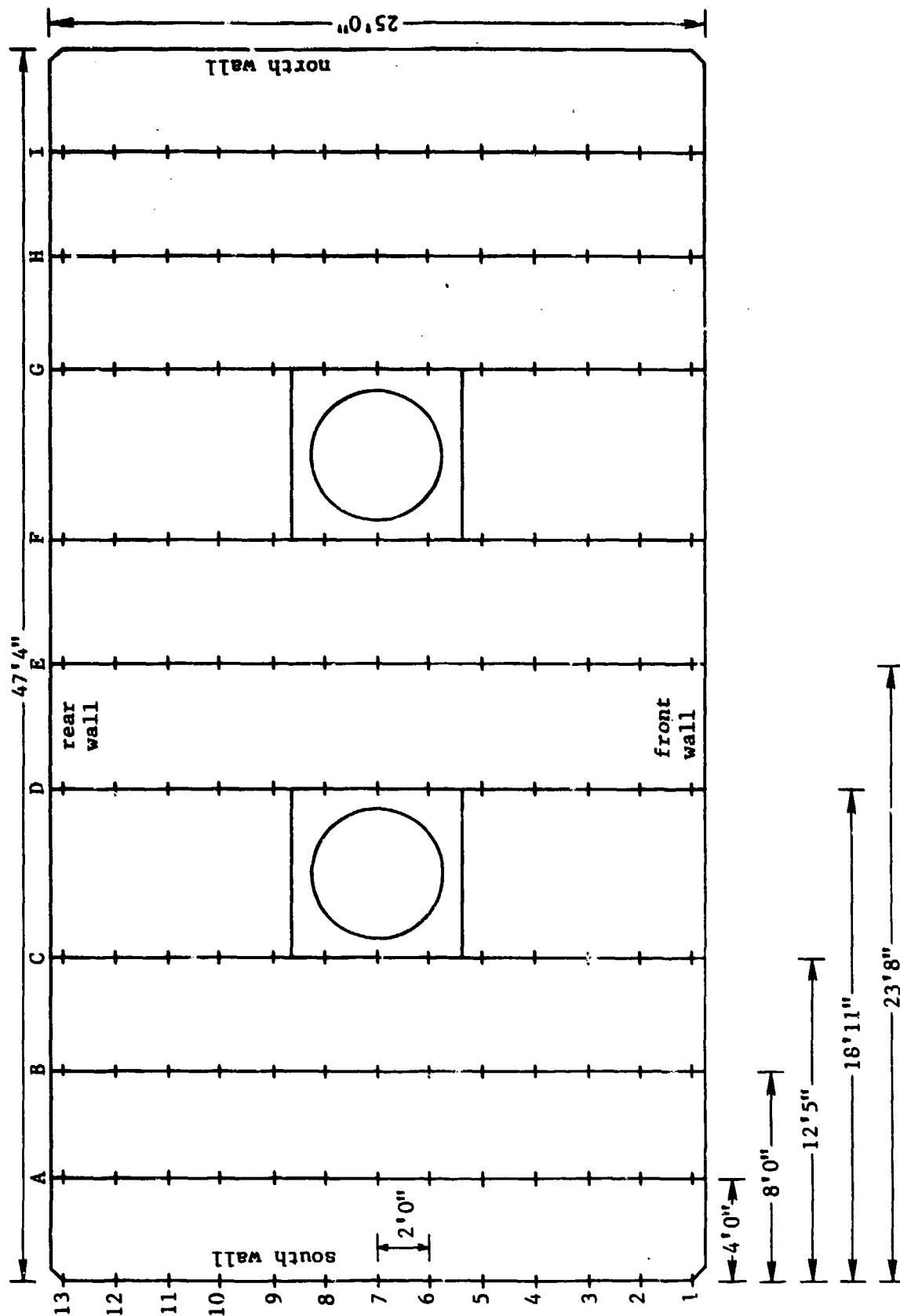


Figure 26. Deflection measurement locations and roof slab profiles for the Type A structure.

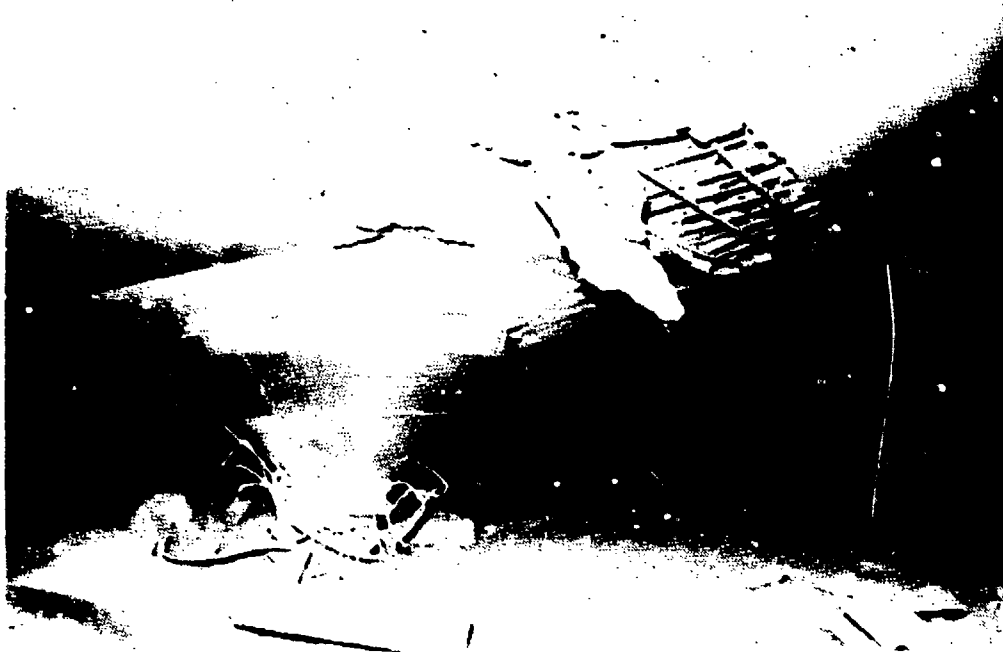


Figure 24. Post-test interior view of Type A test structure.

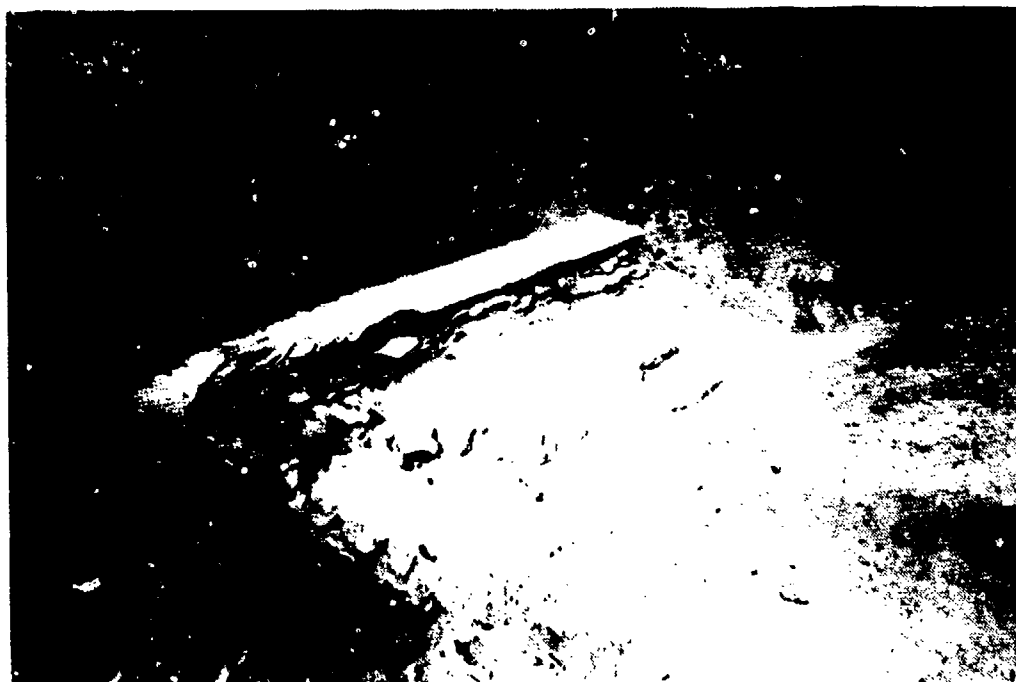


Figure 25. Post-test exterior view of the Type A test structure root quadrant taken from the south wall.



(a)



(b)

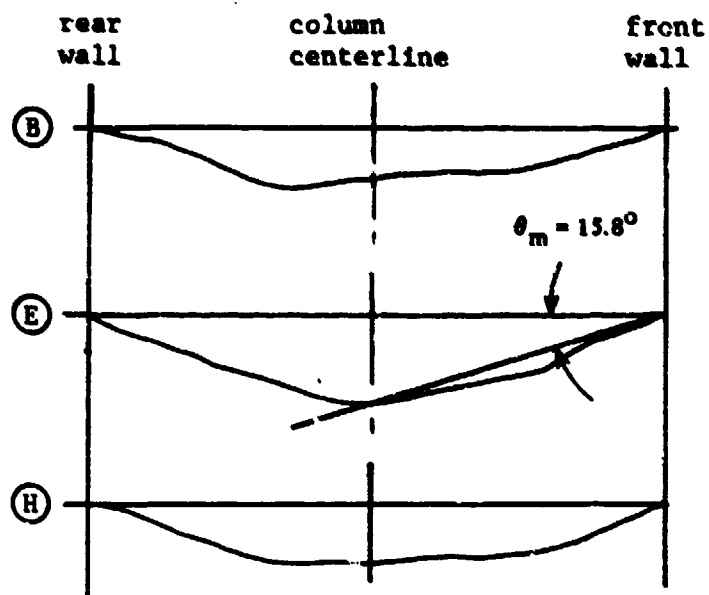


(c)



(d)

Figure 23. Test A - ROOF detonation sequence.



inches
0 10 20
10
20
inches

vertical and
horizontal scales
for profile

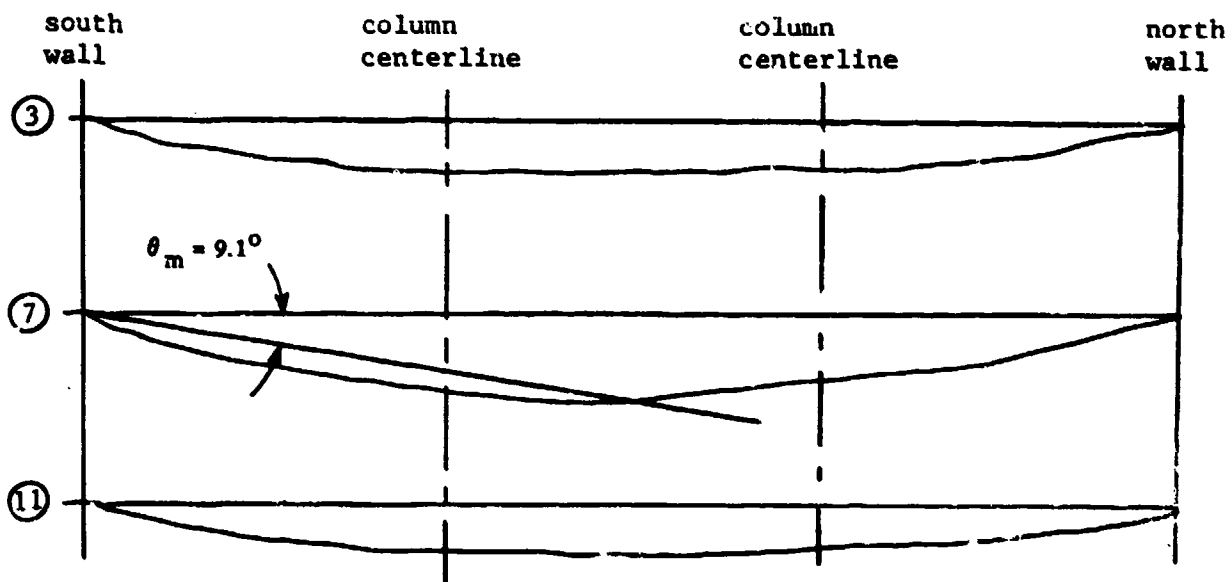


Figure 26. Continued.

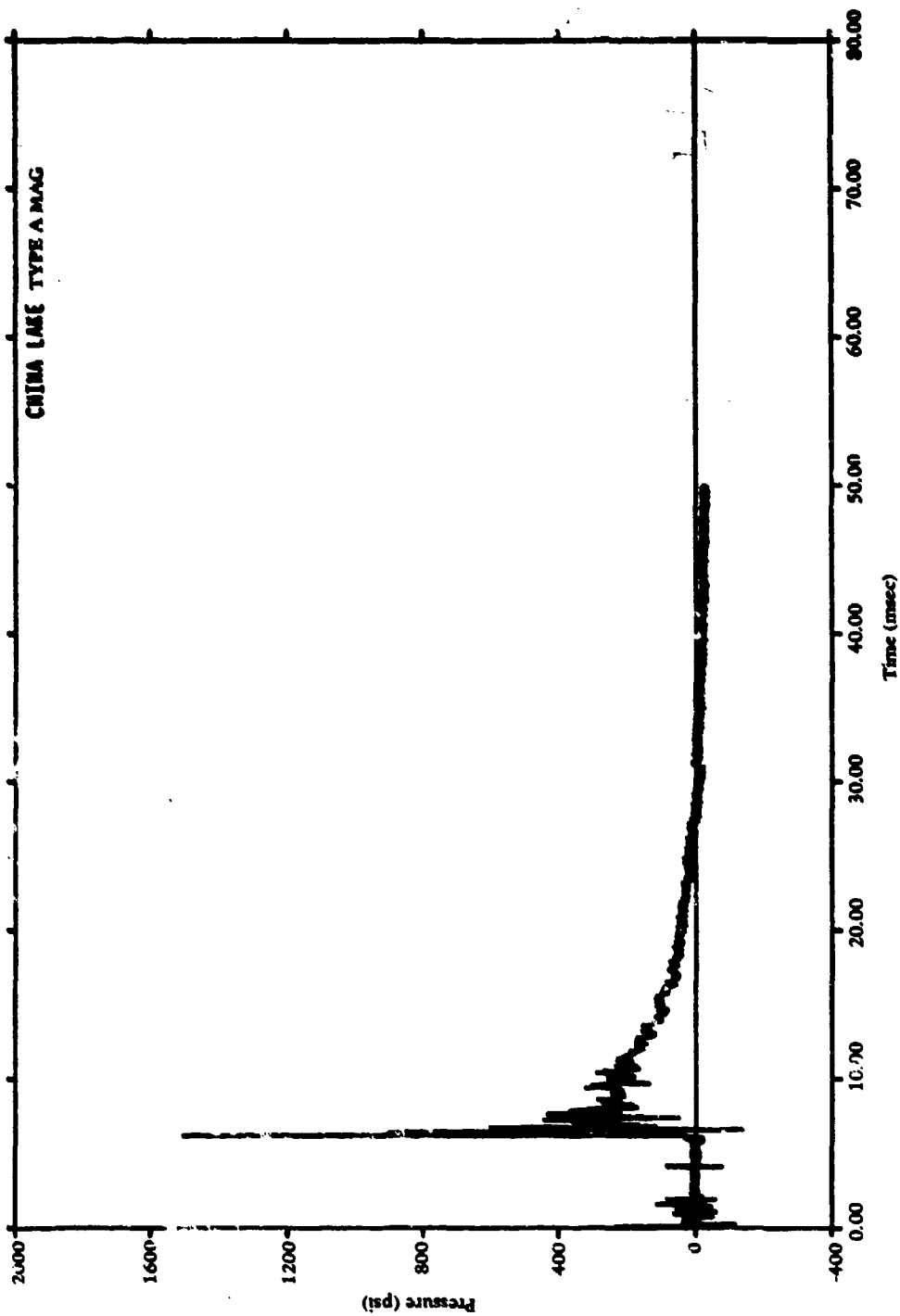


Figure 27. Typical airblast pressure gage output for Test A-ROOF, Gage No. A-D3-BP4.



Figure 28. Test IIB-DOORS fireball.

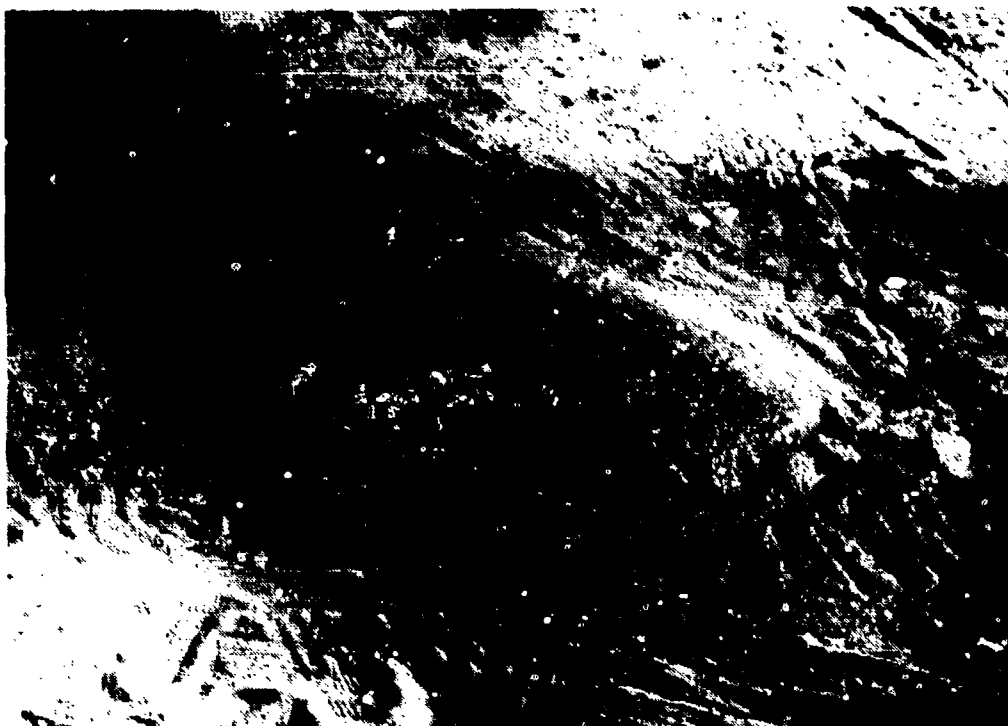


Figure 29. Post-test view of Type IIB test structure and crater.



Figure 30. Post-test view of near door of Type IIB test structure.

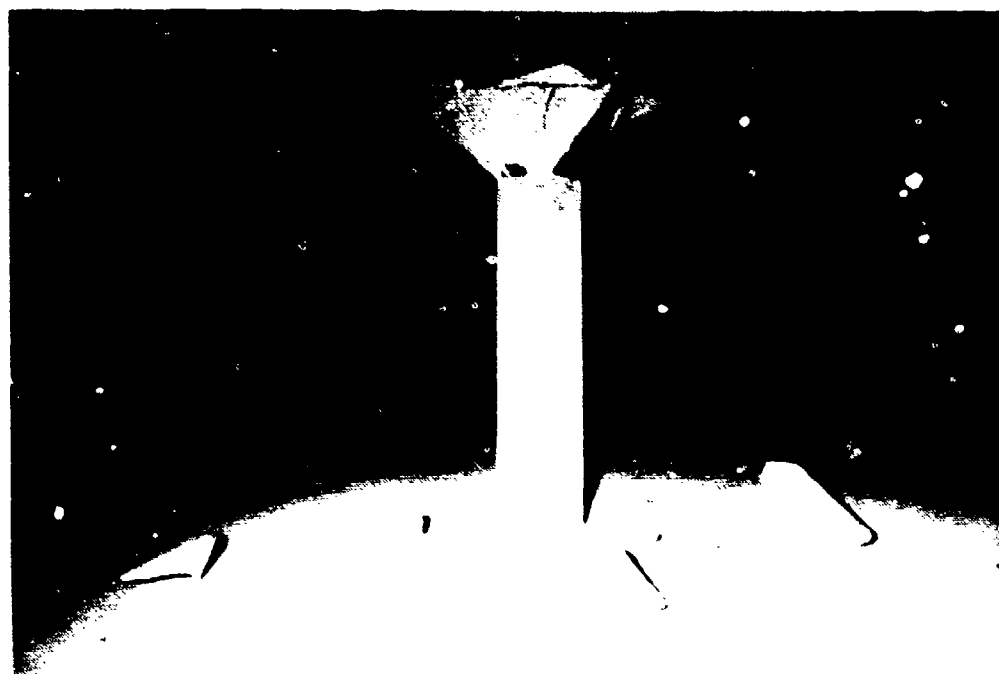


Figure 31. Post-test interior view of Type IIB test structure.

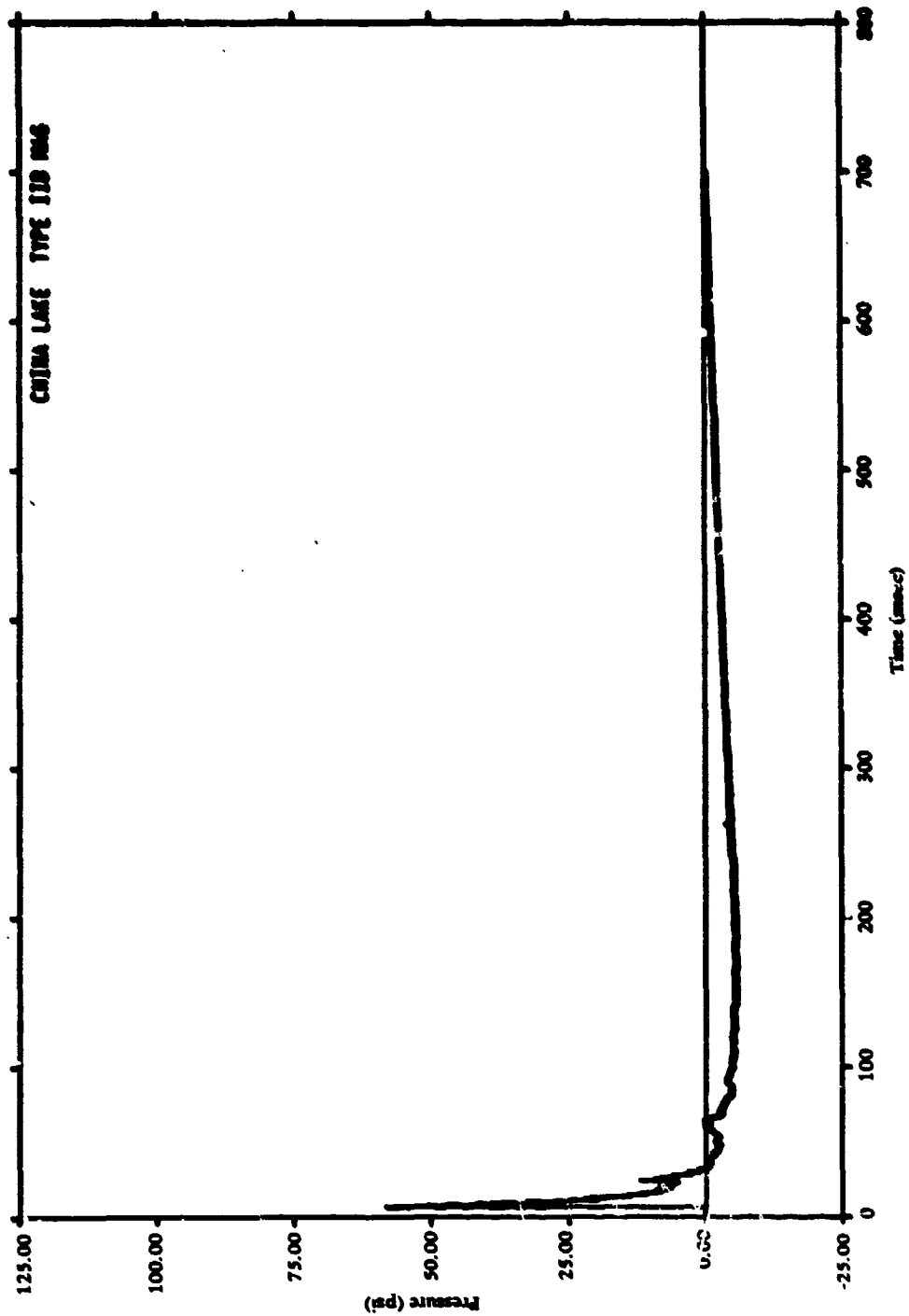


Figure 32. Typical airblast gage output for Test 11B-DOORS, Gage No. B-CID-BP4: headwall centerline.

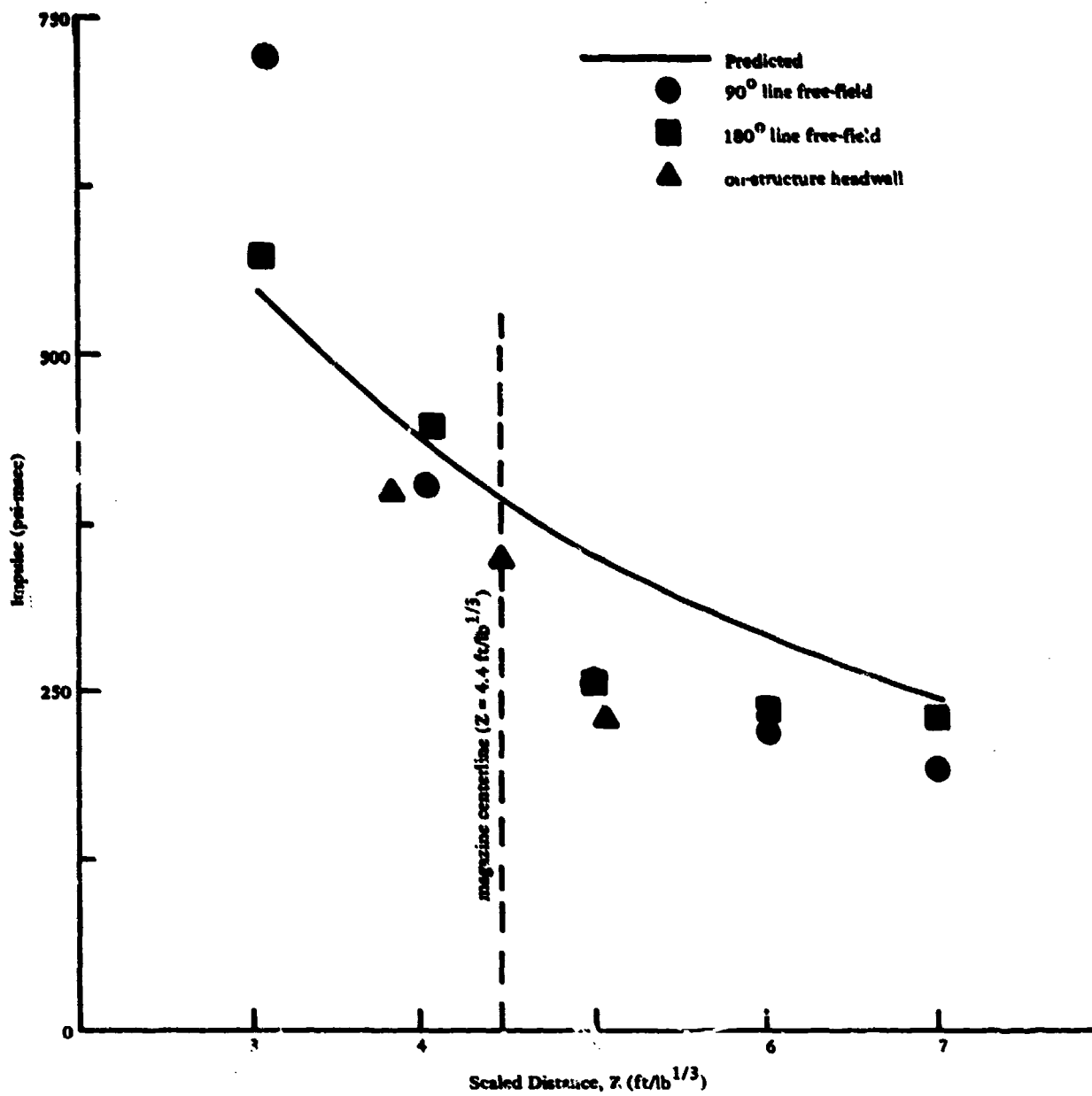


Figure 33. Measured versus predicted airblast loading for Test IIB-DOORS.

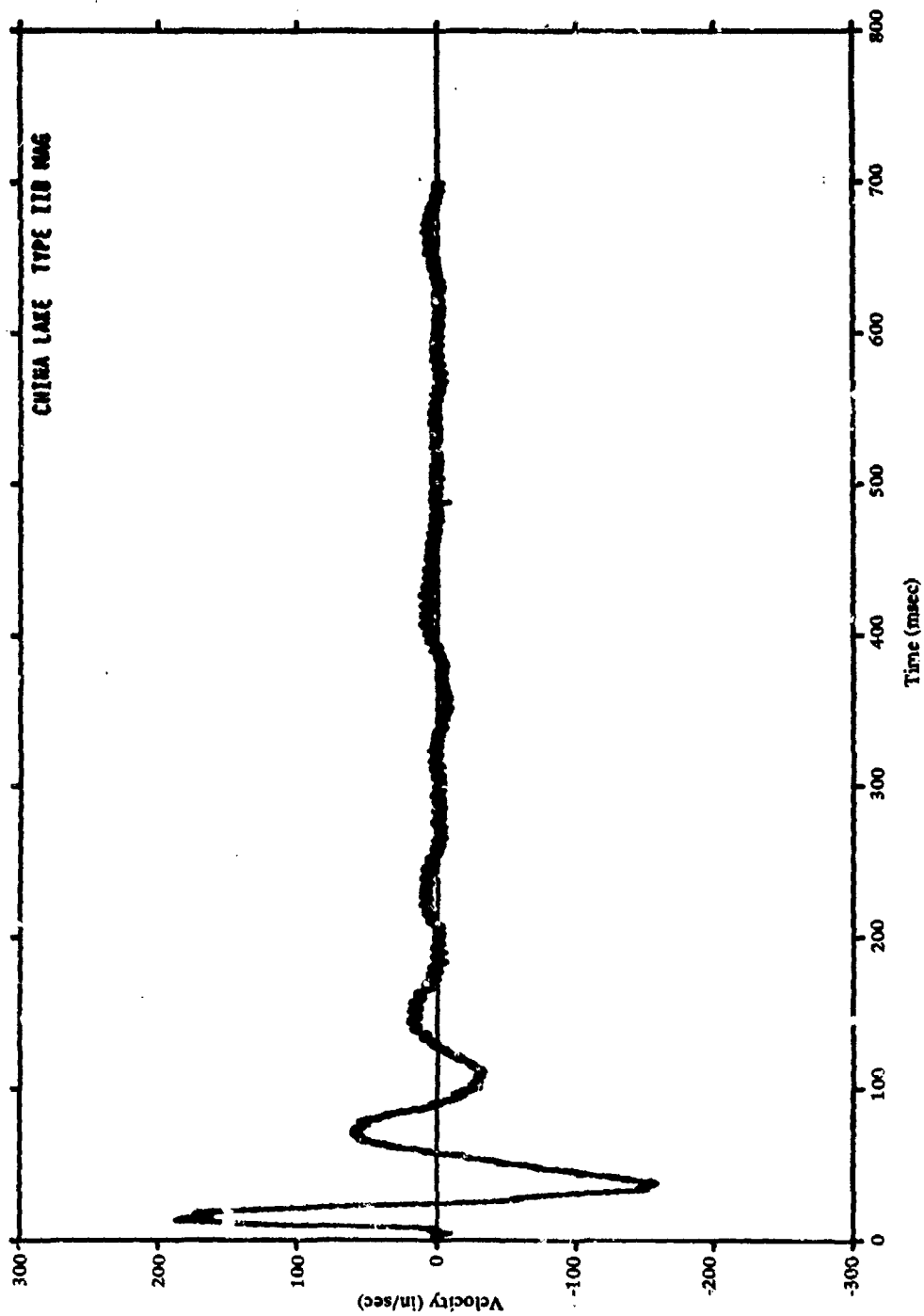


Figure 34. Typical velocity gage output for Test IIB-DOORS, Gage No. B-CID-V3: headwall centerline.

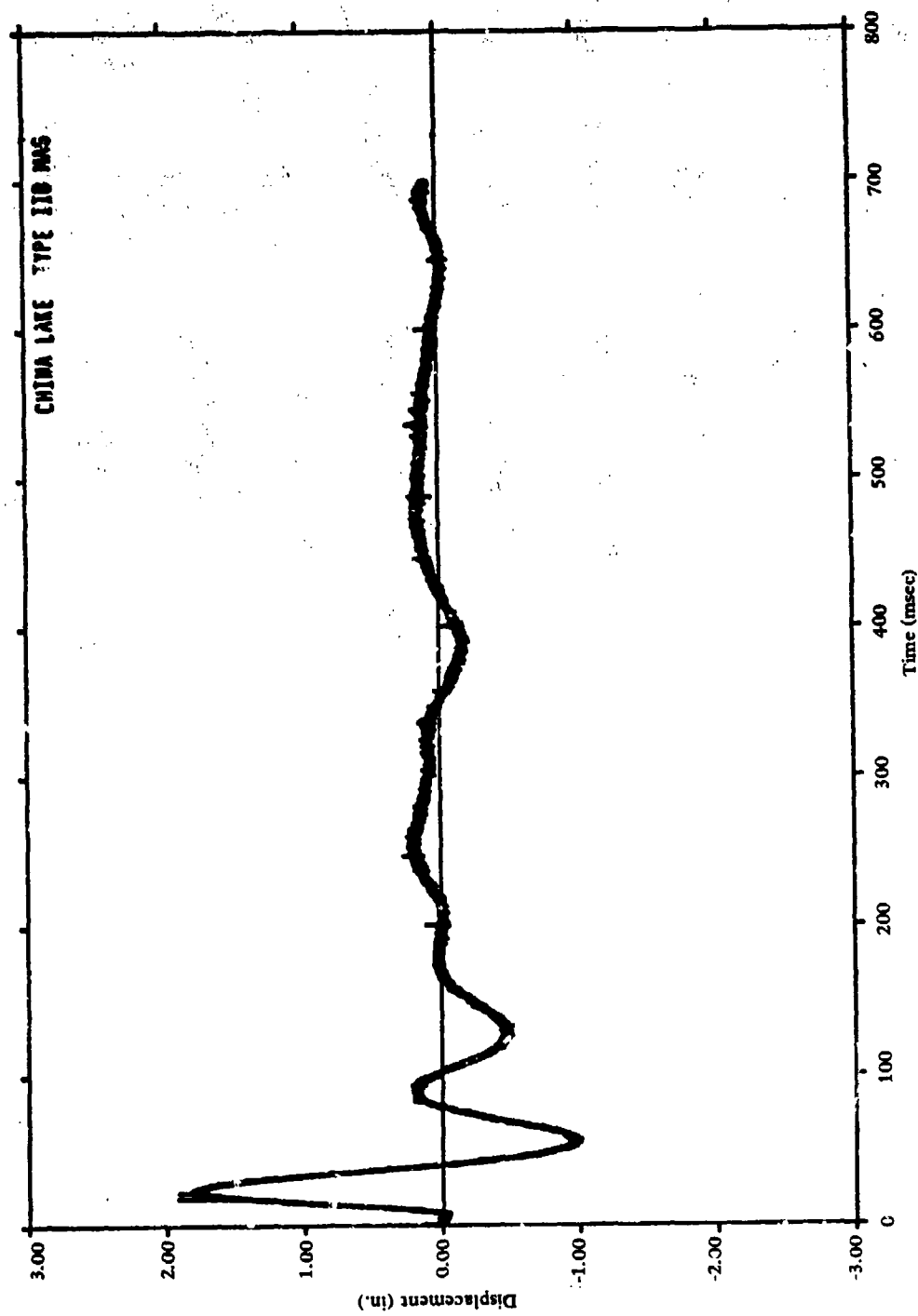


Figure 35. Typical displacement gage output for Test IIB-DOORS, Gage No. B-CID-D5: headwall centerline.

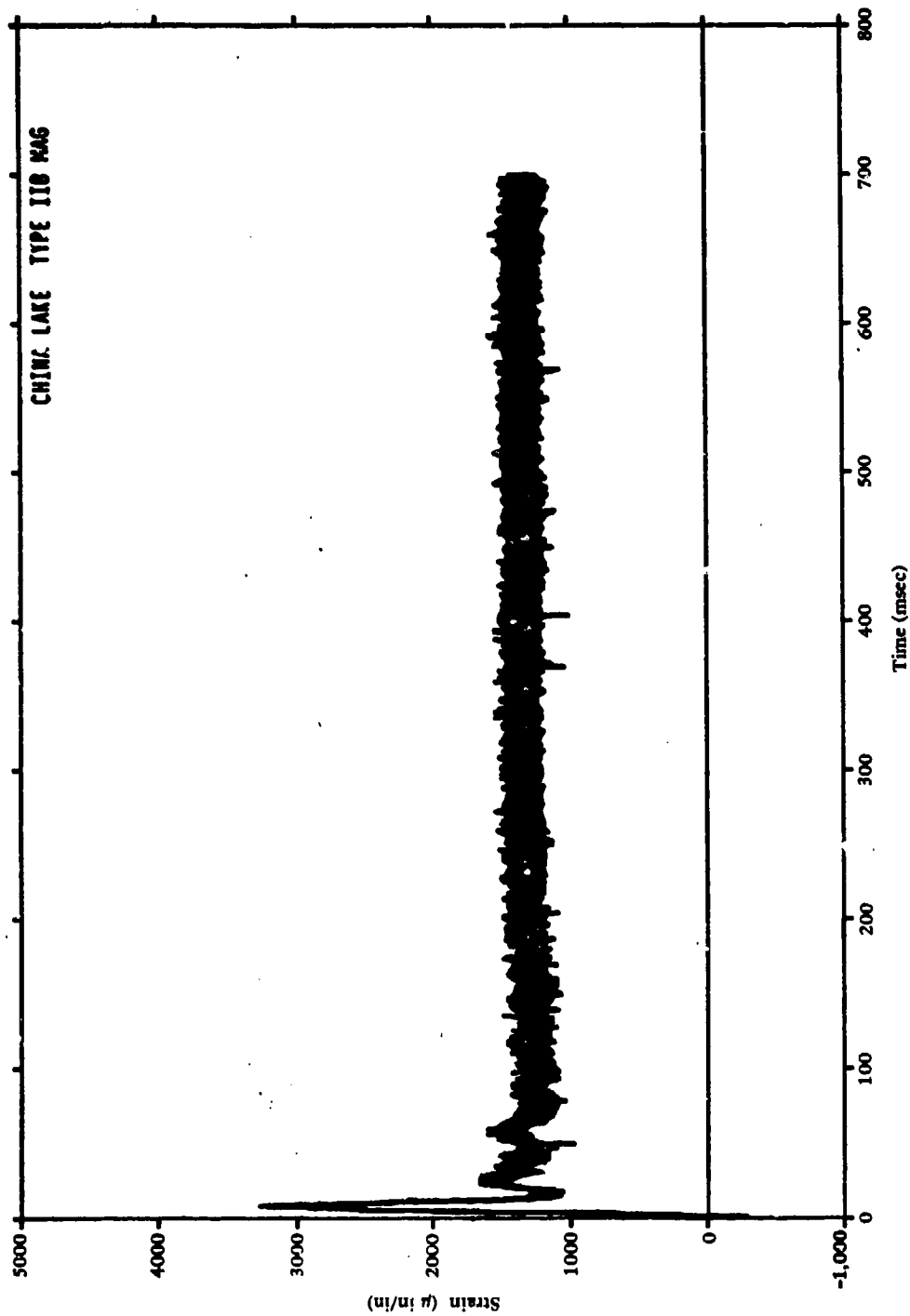


Figure 36. Typical strain gage output for Test IIB-DOORS; Gage No. B-AID-S1.

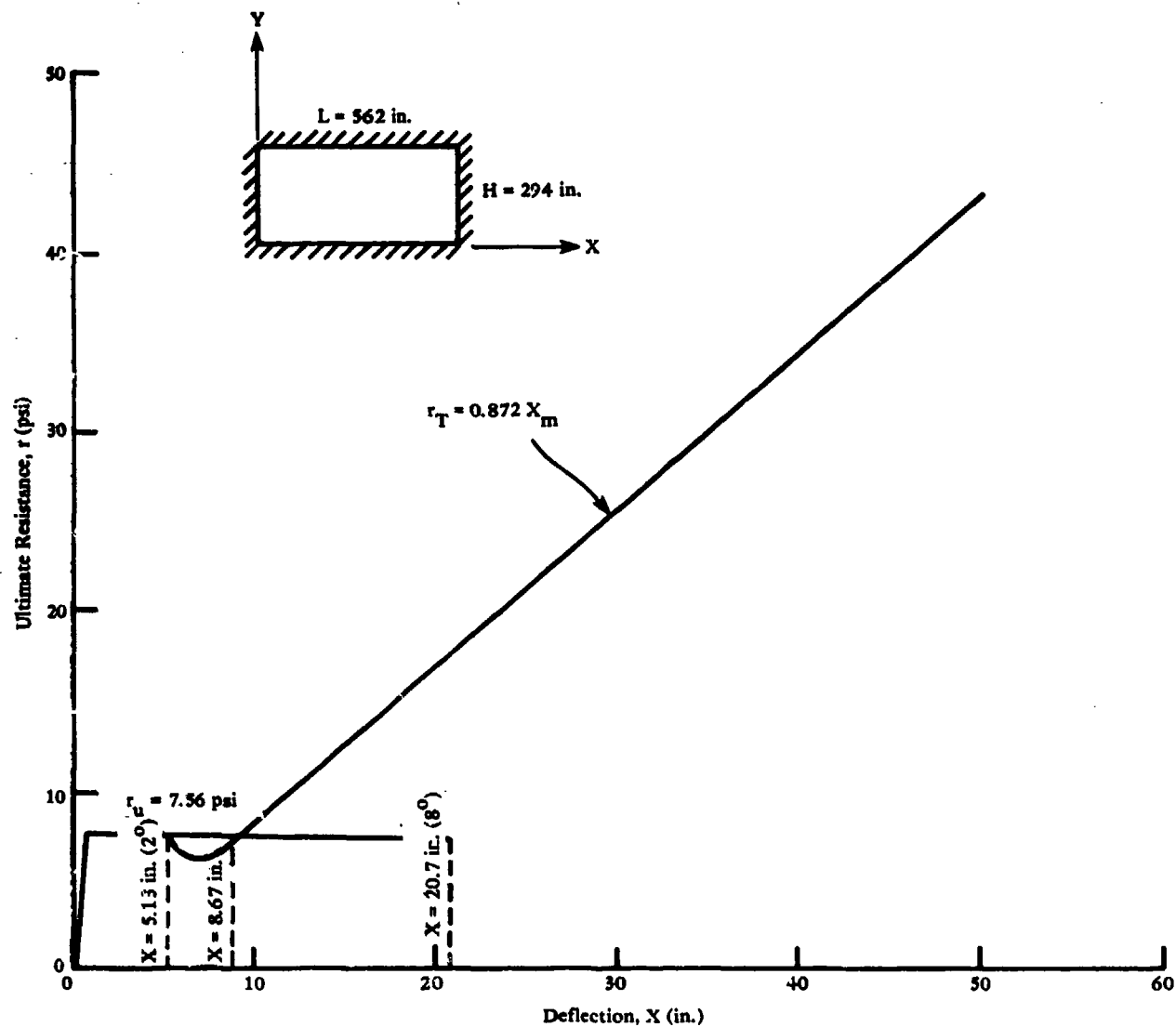


Figure 37. Available resistance-deflection curve for half-scale Type A magazine roof after column failure; two-way restrained slab.

AD-P005 371

INSENSITIVE CONDUCTING COMPOSITION (CC) PRIMERS

Robert J. Spear and John R. Bentley

Materials Research Laboratories, Maribyrnong
Victoria, Australia

ABSTRACT

RADHAZ is a serious problem in munitions using CC primers. An assessment of risk analysis is made. Development of two series of CC primers suitable for 20 mm cannon and 105 mm tank ammunition but which have markedly higher energy and power thresholds than current service primers is described.

1. INTRODUCTION

Electric primers for propellant cartridges are in-line, that is ignition of the primer will produce ignition of the propellant charge. All electric initiators are capable of initiation by unintended energy pulses. The most common sources of unintended energy are electrostatic discharge and energy induced in the firing circuit or leads from either pulsed power or continuous wave (CW) transmitters. Typical transmitters are RADAR, UHF, VHF, HF communication systems and switched high current sources. All of these sources represent a hazard when present in conjunction with electric initiators. In the case of medium and large calibre ammunition, such as 105 mm Tank, this hazard would be Category 1 - Catastrophic: may cause death or system loss [1]. Unintended initiation of smaller calibre ammunition such as 20 mm (Phalanx or aircraft carried) could also be catastrophic. The probability of an accidental initiation of the primer must therefore be very low for acceptable safety.

2. NO FIRE THRESHOLD

The risk associated with the use of a given electrical initiator is usually related to its no-fire threshold power (P_t) and energy (E_t) [2]. These should be as high as possible commensurate with the design of a given weapon. These threshold ignition values can range from about 1 μ J and 14 mW for sensitive initiators to 1 J and 1 kW for very insensitive systems. Most electric primers for propellant cartridges have threshold values between 2 μ J and 5 mJ for energy and 14 mW and 1 W for power. Threshold firing data for typical cartridge case primers are listed at Table 1. It can be seen that bridgewire (BW)

primers tend to have high E_t values, in excess of 1 mJ, and modest P_t values, in excess of 100 mW. Conducting composition (CC) primers tend to have very low E_t values, approximately 10 μ J, and P_t values similar to or slightly higher than BW primers. Both E_t and P_t values relate only to discharges through the intended firing circuits.

Electrostatic discharges can occur, usually to earth, and data in addition to E_t and P_t is required to estimate the risk from this source.

3. RISK ASSESSMENT

Risk assessment is carried out by relating the measured E_t and P_t values and electrostatic sensitivity to all perceived sources. This can be done either by calculation using the source characteristics, the distance of separation and assuming worst case coupling of the initiator or by measurement of the power/energy induced in the initiator when it is immersed in a representative field and a measurement of the field in the full service environment. These risk assessments are described in OP Proc 41273 [2] and NWS 6 [3].

Such risk assessments tend to be rather conservative due either to an assumption of worst case coupling ($1/2 \lambda$ antenna) in the case of calculation or additive instrumentation and experimental errors in the case of direct measurement. In addition conservative safety factors are called for with the intention of ensuring that the risk is very low. Despite this limitation, risk assessment by either calculation or susceptibility measurement are likely to remain as the

method of assessing risk from both pulsed and continuous wave electromagnetic radiation.

Electrostatic risk assessment is less well defined. One method (MIL-I-23659B) is a pin to pin and pin to case test involving a 500 pF capacitor charged to 25 kV with an in-series 5000 Ω resistor. This is intended to simulate the worst case electrostatic discharge from a charged person. It is considered to be a reasonable design objective but could be a little severe as an acceptance criterion, particularly for small initiators. Many CC and BW initiators currently in service would not pass this test. It should be noted that for cartridge case primers the body is used as the return electrode and pin to case discharges are not relevant. 25 kV represents an extreme charge for a person. 10 kV is more realistic for the Australian environment since the worst conditions for charge generation are cold and dry with very low relative and absolute humidity.

Any charged conductor can present an electrostatic hazard. Other sources, particularly large metal objects which would be a low impedance source, must also be considered.

Another possible source of electrical energy is capacitance coupling between the firing leads and current carrying conductors. The risk from such sources could be estimated by either calculation or direct measurement. Measurement is probably preferable due to the difficulty in defining the geometry of the conductors for theoretical assessment. E_t is the relevant parameter for switched DC power supplies and P_t the relevant parameter for AC power supplies.

A possible electrostatic hazard could arise with a bridgewire primer should the bridgewire break. This would create a high resistance discharge across the break. Quantifying such a risk would be difficult but bridgewires have been known to break during ramming. Such a failure mechanism is not associated with CC primers.

4. MIL-I-23659B

This specification establishes general guidelines for design and testing of electrical initiators. It mainly considers BW devices and prohibits the use of carbon unless specifically approved by the cognizant government contracting agency. It is considered to be generally applicable to CC initiators.

One of the main advantages of CC primers is their fast functioning time, as low as 10 μ s, which make them well suited to high rate of fire weapons, particularly 20-40 mm cannon. Fast functioning times are associated with relatively low values for E_c . It is most unlikely that CC primers which meet current specifications for cannon ammunition (MIL-P-1394E) can also meet the no-fire power values suggested in MIL-I-236659B for Group B (capable of ignition from 28 V power supply) initiators.

There is no requirement for microsecond functioning in most medium-large calibre ordnance and therefore MIL-I-23659B is considered to be a suitable standard for assessment of electric initiators in these systems.

MIL-I-23659B specifies the following for Group B initiators.

'The no-fire power shall not be less than 1 Watt'.
'The no-fire current shall not be less than 1 Amp'.
'The initiator shall not fire from a 500 pF
capacitor charged to 25 kV discharged through a 5000
resistor both from pin to pin and pin to case'.

It should be noted that no specific mention is made of E_t other than the 25 kV pin to pin test. For a low resistance device (1Ω) subjected to this test most of the energy will be deposited in the series resistor and only approximately 30 μJ will be deposited in the bridge. This will increase to a large proportion of the available 156 mJ for a high resistance path.

This test level is considered too low as a design criterion for electrical initiators which could be exposed to pulse power transmitters such as RADAR. Devices which have a low energy threshold can respond to a single pulse from a pulsed source. Thus CC primers which have a low E_t are particularly susceptible to pulsed sources with low pulse repetition frequencies. For worst case conditions if P_t is 1 W then E_t should be 2-5 mJ to ensure maximum protection. This is discussed in detail in [4].

5. DEVELOPMENT OF LOW SENSITIVITY CC PRIMERS FOR 20 MM AMMUNITION

Our initial development target was a primer for 20 mm ammunition for the 6-barrel M61 rapid fire gun system (RAAF F/A-18, RAN Phalanx). The current service primer is the M52A3B1 which is extremely sensitive (Table 1). The M52A3B1 specification (MIL-P-1394E) has the

key clause "the cap (primer) shall function in less than 0.3 ms when fired by a 10 μ s energy pulse from a 2 μ F capacitor charged to 160 V".

Previous work (5) indicated that CC primers could be produced which would meet MIL-I-23659. These primers had high P_c values (1-2 W) but were still quite sensitive to energy with E_c values of 50-100 μ J. All primers passed testing with the 25 kV equipment.

The M52A3B1 is filled with a multicomponent filling which functions both as conducting and priming increment (Table 2). In contrast, M52 DEFA has separate conducting and priming increments (Table 2). Both these options were investigated. Modification of the M52A3B1 filling by changing the conducting component and increasing its concentration was not successful since achievement of the desired sensitivity levels resulted in excessively long functioning times (cf MIL-P-1394E above). Success was achieved with a two increment filling using the key observations:-

- (i) Sensitivity increased greatly as lead styphnate particle size decreased. Material of mean particle size 115 μ m was used in the conducting increment.
- (ii) A oil furnace carbon black derived from heavy aromatic oil (Tintacarb 140 manufactured by Australian Carbon Black) exhibited an optimum balance of mixing and conducting.

The final two development options are listed in Table 2 and sensitivity characteristics are compared to M52A3B1 and M52 DEFA, including approximate safe separation distances from radar, in

Table 3. The substantial decrease in sensitivity relative to the two service primers is readily apparent. Full experimental details have been published previously [6,7] and the US patent has been granted.

6. DEVELOPMENT OF INSENSITIVE CC PRIMERS FOR 105 MM TANK AMMUNITION

Fast functioning is not normally a requirement for medium and large calibre ammunition, hence a further decrease in sensitivity could easily be achieved without this restriction. The specific target for such a primer was 105 mm tank ammunition.

UK 105 mm tank ammunition uses the L1A2 conducting composition primer. The quoted energy for 1 $\frac{1}{2}$ function is 18 μ J [8] thus E_c will be considerably less than this value. The average resistance is 50 Ω . Thus all primers would be expected to fire when subjected to the MIL-I-23659B electrostatic test which would deliver about 15 mJ to the primer. No data was available on the power sensitivity but it is probably in excess of 200 mW and thus not as relevant to safety as the low energy sensitivity.

The US designed a BW igniter, the M61, to replace the UK L1A2 primer. This device had no fire levels of about 130 mW and 4 mJ [8], rather similar to the UK type A, E & K fuseheads. The primer should not function when subjected to the 25 kV test; the US report no functions from static electricity from the human body. The M61 primer does not meet MIL-I-23659B. The E_c of M61 primers meets the level proposed in section 4 but the P_c value is well below the recommended 1 W and the primer will thus be moderately sensitive to power emitted from CW sources.

Experimental primers were prepared from the large particle size lead styphnate and tintacarb 140 in the ratio 92.5:7.5, 90:10 and 85:15. Results for energy and power sensitivity are listed, together with data for the 96:4 composition described previously, in Table 4.

It can be seen that the MRL insensitive CC primer using 10% tintacarb 140 as the conducting component and 90% large particle size lead styphnate offers significant reduction in RADHAZ compared to the US M61 BW electric primer. This is mainly due to the significantly higher values for no-fire threshold current (I_t) and P_t . Although E_t is higher for the M61 primer the circumstances where this will be of benefit are unlikely to be experienced in service (i.e. pulsed power sources with PRF > 50 pps). Both primers have good protection from electrostatic discharge and are unlikely to be initiated by discharges from charged personnel.

E_t for the MRL insensitive CC primer is approximately two orders of magnitude greater than the UK L1A2 primer and P_t is approximately one order of magnitude greater than the L1A2. The L1A2 has been introduced into service in the UK apparently with few problems. There is thus a strong indication that under all service conditions the MRL primer will have an extremely low rate of premature functioning.

7. CONCLUSIONS

The design of CC primers is very simple and it is probable that insensitive CC primers could be produced significantly more cheaply than BW primers. The most common problem, apart from electrical

sensitivity, is controlling production variables. It is apparent from our work on insensitive primers that performance parameters are more easily controlled using relatively large proportions of conducting component. The primers containing 7-10% tintacarb would be suitable for use in large calibre munitions, while the primers containing 4% tintacarb are clearly superior to current service primers for high rate of fire small calibre munitions. It is considered unlikely that production variables will cause a significant problem.

A possible problem with our experimental CC primers is the effect of ageing and rough handling on sensitivity. Preliminary tests on the 4% tintacarb primer indicate that it is less affected by ageing than current service CC primers [6] and we have seen no evidence to suggest rough handling is likely to produce super sensitive primers.

8. REFERENCES

1. Def Stan 08-3. Ordnance Board Safety Guidelines for Munitions, June 1979.
2. "Principles of Design and Use for Electrical Circuits Incorporating Explosive Components," OB Proc 41273 and Enclosure, November 1972 RESTRICTED.
3. Naval Weapon Specification No. 6(1978). "Standard RN Test Radio Frequency Environment and Acceptance Criteria for Weapon Design," MOD, Director General Weapons, UK. RESTRICTED.
4. Bentley, J.R. (1986). "Development of Insensitive CC Primers for 105 Tank Gun Ammunition," LRL-R-1001.
5. Bentley, J.R. (1980). "Insensitive Conducting Composition Igniters", 7th International Pyrotechnic Seminar, Vail, Colorado, USA.
6. Spear, R.J. and Redman, L.D. (1985) "A low Sensitivity Conducting Composition (CC) primer for 20 mm Ammunition", MRL-R-968, Materials Research Labs., Maribyrnong.

7. Spear, R.J. and Redman, L.D. (1985). "The Origin of Performance Differences Between Two Conducting Composition (CC) Primers", J. Energetic Mats., 3, 173.
8. Seeger, D.E. (1960). "Igniter for Tripartite 105 mm Tank Ammunition", PA-Report-89, Picatinny Arsenal, Dover, New Jersey.

TABLE 1

Threshold Sensitivity Data for Typical Propellant Primers

Primer	Resistance Range (Ω)	No-fire threshold values, 0.1%, 95% conf.		
		Energy (E_t , μ J)	Power (P_t , mW)	Current (I_t , mA)
M52A3B1	1 k - 1.2 M	2.2, 4.9	14	1
M52 DEFA	20-500	5.0	260	100
Igniter, Electric, CC, N8 MK2	500-2000	1	not available	not available
Igniter, Electric, CC, Nos, 1,2,3	20-60	30	not available	not available
Cap, No. 1 Mk 1	0.40 - 0.60	7500	340	750
Primer, No. 48, MK 2, No 50, MK 1	0.9 - 1.7	7000	200	450
Igniter, Type 100	0.9 - 1.6	2300	80	297

TABLE 2

A Comparison of Fillings in the M52A3B1, M52 DEFA and MRL
Low Sensitivity Primer for 20 mm Ammunition

Component/Parameter	M52A3B1	M52 DEFA		MRL Low Sensitivity	
		Conducting Increment	Priming Increment	Conducting Increment	Priming Increment (2 options)
Lead styphnate (%)	40 ± 2.5	95.0 - 95.5	48	96	48 40
Conducting Component (%)	0.75 ± 0.25 <u>a</u>	4.5 - 5.0 <u>b</u>	<u>b</u>	<u>c</u>	<u>c</u> 1
Barium nitrate (%)	44.25 ± 2.5		12		12 44
Potassium perchlorate (%)			28		28
Calcium silicide (%)	13.0 ± 2.5		10		10 13
Gum arabic/styphnic acid (%)	1.0 ± 0.25 ea				1 ea
Total mass (mg)	170	30	160	75	125 125

a acetylene black

b graphite

c oil furnace carbon black

TABLE 3

A Comparison of Performance Data for the MRL Low Sensitivity
Primer with M52A3B1 and M52 DEFA Primers

Parameter	Primer Type		
	MRL Low Sensitivity	M52 DEFA	M52A3B1
Resistance (Ω)	5-10	20-500	1.1 k - 1.2 M
E_t (μJ)	290	5	<5
P_t (W)	1.0	.26	.014
Functioning Time (μs)	49	43	81
Safe Separation Distance (m)			
1 MW X Band Radar	10	80	110
10 MHz VHF	30	140	190

TABLE 4

A Comparison of Performance Data for MRL Insensitive CC Primers.
Data for the 96:4 Low Sensitivity CC Primer and US and UK
105 mm Tank Primers are Included for Direct Comparison

Primer	E_t (mJ)	P_t (W)	I_t (A)
MRL DEVELOPMENT PROTOTYPES			
Lead Styphnate: Tintacarb 140			
85:15	3.0	3.6	
90:10	2.1	5.4	1.5
92.5:7.5	2.05	2.6	
96:4	0.3	1.0	
US M61	4	0.13	0.32
UK L1A2	< .018	> 0.20	0.05

AD-P005 372

IRON-WIRE RF-PROTECTION
AND
TRANSMISSION LINE EQUATIONS

KLAUS G. RUCKER
E. I. DU PONT DE NEMOURS
POMPTON LAKES, NJ 07442

1986

ABSTRACT:

A FORTRAN program of the exact transmission line equations shows that skin-effect resistance of iron wire protects electric detonators against radiofrequency stray energy.

CONTENT:

INTRODUCTION
SUMMARY
TRANSMISSION LINE EQUATIONS
FORTRAN PROGRAM
SKIN-EFFECT IN IRON WIRE

INTRODUCTION

Electric detonator legwires and their lead lines act as classic transmission lines when they carry microsecond electrical transients or high-frequency currents. Electrostatic discharges, radio-frequency hazards and capacitor-discharge blasting machine surges should be assessed with the full transmission line equations.

Most textbooks treat the simplified low-loss transmission line equations for communication applications. However, we use iron wire with high skin-effect losses in radio-frequency protection or we consider the action of legwires between the bridgewire and an antenna. Legwires in highly conductive blasting agents or mile-long iron-sheathed firing cables in oil wells are line structures outside of textbook geometries.

Exact transmission line equations account for all losses and use complex impedances, complex currents and complex voltages. Complex hyperbolic or exponential functions describe all conditions on a transmission line. Numerical calculations are very tedious when a range of conditions must be explored. Handling even a single problem on a modern calculator is very slow. The widely used SMITH-CHART graphic transmission line calculator considers only low losses and a real characteristic impedance.

Personal computers permit the use of BASIC or FORTRAN languages. The mathematical functions of most BASIC languages are too limited and cannot conveniently handle complex and/or hyperbolic functions. MICROSOFT-FORTRAN (versions 3.2 (1984) and later) for MS-DOS is a compiled language and offers exceptional value. It is installed on the 10 Mb hard disk of a DEC 100 + RAINBOW with 256 Kb RAM (without the 8087 coprocessor). It handles complex variable arithmetic, but only real arguments of hyperbolic functions.

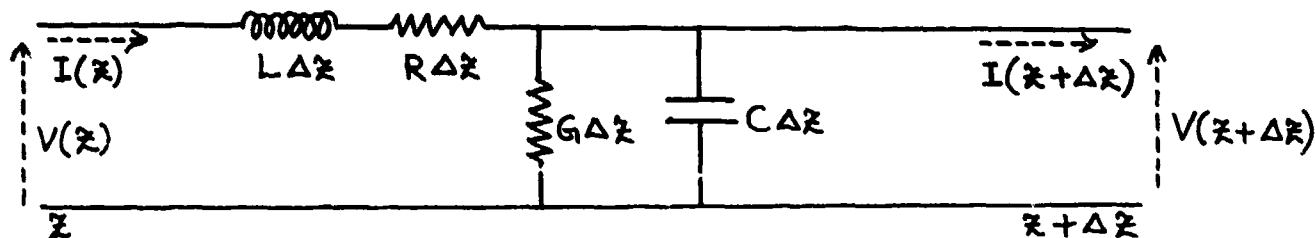
SUMMARY

The MS-DOS MICROSOFT-FORTRAN program of the exact transmission line equations accepts the line parameters: resistance, inductance, capacitance, leakage, line length, frequency and terminating impedance. It calculates and prints all transmission line functions of interest in electrical blasting reliability and safety. The Fortran Source Code listing is attached.

All iron and copper wire parameters are based on high frequency measurements. Increased skin-effect resistance provides most of the rf-protection because it can never be tuned out and it dissipates rf energy as heat away from the ignition charge. The impedance mismatch of approximately one ohm bridgewires and 100 to 1000 ohm characteristic impedances of legwires reflects most energy back onto the line. Iron's magnetic permeability and higher resistance cause better rf protection than copper.

TRANSMISSION LINE EQUATIONS

The physical structure of all transmission lines can be represented by equivalent circuits in the time and frequency domains. Treatment of transmission lines in the time domain is accomplished by solving hyperbolic partial differential equations and describes transient and steady state conditions. Treatment in the frequency domain is accomplished by solving ordinary differential equations and describes steady state conditions only. These steady state solutions however provide much insight into transient conditions and the travel of pulses along a line. A mental or actual Fourier analysis of a line problem can be based on a steady-state solution at many frequencies.



Using Kirchhoff's mesh and node equations, we derive

$$\frac{dV}{dz} = -(R + j\omega L) I$$

$$\frac{dI}{dz} = -(G + j\omega C) V$$

and from these

$$\frac{d^2 V}{dz^2} = (R + j\omega L)(G + j\omega C) V$$

$$\frac{d^2 I}{dz^2} = (R + j\omega L)(G + j\omega C) I$$

solutions of these equations are

$$V(z) = V_1 e^{-\gamma z} + V_2 e^{+\gamma z}$$

$$I(z) = I_1 e^{-\gamma z} + I_2 e^{+\gamma z}$$

where V_1, V_2, I_1, I_2 are complex number coefficients to be determined.

$$\gamma = \sqrt{(R + j\omega L)(G + j\omega C)} = \alpha + j\beta$$

$$\alpha = \sqrt{\frac{1}{2} [\sqrt{(R^2 + \omega^2 L^2)(G^2 + \omega^2 C^2)} - \omega^2 LC + RG]} \quad \text{NEPER/METER}$$

$$\beta = \sqrt{\frac{1}{2} [\sqrt{(R^2 + \omega^2 L^2)(G^2 + \omega^2 C^2)} + \omega^2 LC - RG]} \quad \text{RADIAN/METER}$$

γ (GAMMA) is the complex propagation constant with the real part α (ALPHA) attenuation constant and the imaginary part β (BETA) phase constant. ALPHA in

$$V_z = V_0 e^{-\alpha z}$$

indicates amplitude attenuation of the voltage after travelling along the line length BETA in

$$V_z = V_0 e^{-j\beta z}$$

indicates the phase shift in radian and also the wavelength on the line

$$\lambda = \frac{2\pi}{\beta}$$

Wavelengths on transmission lines are substantially shorter than those in air at the same frequency.

In evaluating γ , it is nowadays much simpler to perform the complex multiplication and complex square root and then to call for the REAL and IMAG parts of the result than to labor through the long equations for α and β .

It should be remembered that voltage and current also oscillate time-harmonically at the angular frequency $\omega = 2\pi f$, besides obeying their location determined attenuation α and phase constant β . The values for the line resistance R per meter, the line inductance L per meter, the line capacitance C per meter and the line leakage G per meter change with the geometry of a line and with frequency. The resistance R increases considerably with frequency because the skin-effect confines the current to a progressively thinner outer layer as the frequency increases. The computed examples are based on actually measured values of R , L , C , G .

Further evaluation of the set of ordinary differential equations leads to the definition of the characteristic impedance Z_0 , also called wave impedance or surge impedance. Voltage and current at any point of the line are related by the characteristic impedance Z_0 .

$$Z_0 = \frac{V}{I} = \sqrt{\frac{R + j\omega L}{G + j\omega C}} = R_0 + jX_0.$$

Although not used in the computer program, the characteristic admittance follows as

$$Y_0 = \frac{I}{V} = \sqrt{\frac{G + j\omega C}{R + j\omega L}} = G_0 + jB_0.$$

The absolute value of the characteristic impedance is

$$|Z_0| = \sqrt{\frac{R^2 + \omega^2 L^2}{G^2 + \omega^2 C^2}} \quad \text{ANGLE } \theta_0 = \frac{1}{2} \left(\arctan \frac{\omega L}{R} - \arctan \frac{\omega C}{G} \right)$$

The real part R_0 and the imaginary part X_0 of the characteristic impedance Z_0 are most readily derived nowadays through complex arithmetic. They are in longhand:

$$R_0 = \sqrt{\frac{1}{2} \left[\sqrt{(R^2 + \omega^2 L^2)(G^2 + \omega^2 C^2)} + \omega^2 LC + RG \right] / (G^2 + \omega^2 C^2)}$$

$$X_0 = \pm \sqrt{\frac{1}{2} \left[\sqrt{(R^2 + \omega^2 L^2)(G^2 + \omega^2 C^2)} - \omega^2 LC - RG \right] / (G^2 + \omega^2 C^2)}$$

Numerous sub-tabulations and calculating helps have been devised over the years to calculate γ , α , β , Z_0 , R_0 , X_0 . Also, numerous low-loss approximations were offered in textbooks to avoid some or most of these calculations. Personal computers and programmable calculators allow plowing straight through a problem without simplifying assumptions towards a precise answer.

High-frequency and low-loss assumptions yield

$$Z_0 = \sqrt{\frac{L}{C}} \quad \alpha \approx 0 \quad \beta = \omega \sqrt{LC}$$

They are listed here only as a limit condition.

The input impedance Z_i of a transmission line that is terminated by a load Z_L is

$$Z_i = Z_0 \left[\frac{Z_L \cosh \gamma l + Z_0 \sinh \gamma l}{Z_0 \cosh \gamma l + Z_L \sinh \gamma l} \right]$$

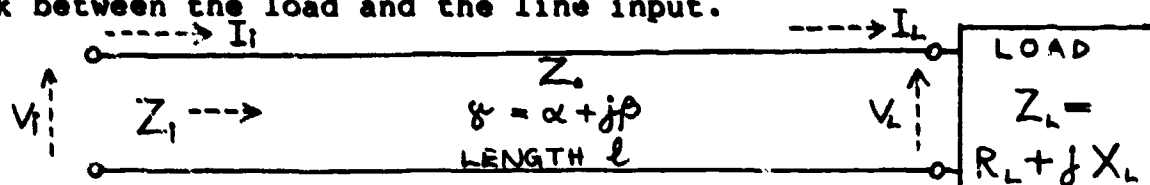
or in another form


$$Z_i = \frac{Z_L + Z_0 \tanh \gamma l}{1 + \frac{Z_L}{Z_0} \tanh \gamma l}$$

We use:

$$\tanh(a + jb) = \frac{\sinh 2a + j \sin 2b}{\cosh 2a + \cos 2b}$$

The transmission line section acts as a transformer or four-pole network between the load and the line input.



The load is in general the bridgewire with a resistance between 0.1 and 2 ohm. Duplex legwires  resemble 70 ohm twin-line, but casually deployed individual legwires have a characteristic impedance between 100 and 600 ohm. The low bridgewire resistance resembles a short circuit on a line whose characteristic impedance is hundred-fold higher. Most of the energy that travels from the input along the line is then reflected back onto the line and oscillates on the line until it is consumed in the loss and leakage resistance. The numerical relation is given in the reflection coefficient RFN

$$RFN = \frac{(Z_{LOAD}/Z_0) - 1}{(Z_{LOAD}/Z_0) + 1} = \frac{Z_{LOAD} - Z_0}{Z_{LOAD} + Z_0}$$

$RFN \approx 1$ when $Z_{load} \ll Z_0$.

The concept of TRANSFER or DRIVING IMPEDANCE is helpful because it connects the input Voltage V_i with the load current I_L

$$\frac{V_i}{I_L} = Z_0 \sinh \gamma l + Z_L \cosh \gamma l$$

We calculate the complex Voltage V_i necessary to drive 1 Ampere through the bridgewire load resistance R_L . Any other hazard current intensity can be scaled up or down with this information. We are always interested to know the real energy flow into the line; energy that oscillates in and out of the line (due to line reactance) does not heat the bridgewire. The computer program always displays the absolute, real and imaginary components of the complex voltages, currents, powers and impedances.

Two intermingling energy flows travel on a transmission line towards the load. One part of the energy flows in the wire as conduction current, the other part flows as an electromagnetic wave on and around the wire. Inspecting a series of printouts for different line lengths or frequencies gives insight into these phenomena.

The input current I_i follows from the input voltage V_i (for 1 Ampere through the bridgewire) and the input impedance Z_i :

$$I_i = V_i / Z_i$$

The 4th-6th last lines show the input current I_i that enters the line in order to drive 1 Ampere through the bridgewire.

Only real power that enters the line steadily contributes to bridgewire heating. We ask for the ratio of this power to the bridgewire power and thus define the protection factor PRFAC

$$\text{PRFAC} = \frac{\text{REAL POWER INTO LINE}}{\text{REAL POWER IN THE BRIDGEWIRE}}$$

The real power into the line RPWR is calculated as

$$\text{RPWR} = \text{RI} \cdot \text{CUR} \cdot \text{CUR} \quad (P = I^2 \cdot R)$$

where RI is the real part of the input impedance and CUR is the absolute value of the complex input current INCUR.

INCUR = complex input voltage U_{i1} / complex input impedance Z_i

PRFAC shows how much protection a transmission line confers on a bridgewire. The protection factor is always larger than 1 and frequently up in the hundreds! It is obvious that a passive device such as a transmission line can only diminish the energy that it carries to the bridgewire load. Tables 1 to 4 summarize the computer results.

A bridgewire at the far end of a transmission line has become physically inaccessible for us because it is in the detonator and the insulated legwires cannot be opened. We must determine now how much bridgewire current is flowing when a certain input voltage V_i across the line sends an input current I_i into the input impedance Z_i . This is the crucial problem that must be solved. We rephrase the question: Does the transmission line between the stray (hazard) current source I_i and the bridgewire increase or decrease the current? Does the transmission line "match" the stray source impedance to the bridgewire? Does a certain line length ($\lambda/4$ or $\lambda/2$) create a special hazard? Is there any condition where the transmission line creates a hazard?

Running the program for hundreds of conditions has shown very convincingly that a transmission line (e.g. the legwires):

1. delivers only a small fraction of the input energy to the bridgewire.
2. always protects the bridgewire because the line either dissipates or reflects energy.
3. does not have certain dangerous lengths, such as $\lambda/4$, $\lambda/2$, where it would create a worse situation for the bridgewire.
4. can sometimes increase the bridge current above the input current but at much higher input voltage and much higher input energy so that still a net protection remains.
5. introduces substantial losses in the 10-500 MHz range where EB cap wires are likely to abstract energy from an rf wave.
6. of iron wire practically eliminates the radio-frequency hazard for a bridgewire detonator.

The McGraw-Hill Schaum Outline Series book "Theory and Problems of Transmission Lines" by Robert A. Chipman 1968, 236 pages is excellent in every aspect and is by far the best book on the subject. Reading it is highly recommended.

A knowledge of transmission line theory leads to the understanding of electromagnetic wave propagation in lossy media such as snow, ice, water, rock, blasting agents, solids and liquids.

MICROSOFT-FORTRAN PROGRAM

MICROSOFT-FORTRAN on a personal computer is surprisingly powerful and is easily used when the compiler is loaded on the hard disk. A copy of the source program and several printouts are attached. Subscripts of the variables on the preceding pages have been written as appropriate two and three letter combinations in the source program. In-between variables were defined and used to handle parts of functions with complex arguments. Single precision calculations suffice and double precision is not available in some complex FORTRAN functions.

The slashes in FORMAT/WRITE commands 100 and 3100 are adjusted for an exactly repeating print pattern; a large number of tables can thus be presented report-ready. A comparison of the block of numbers on the upper left of a sheet with the printed output (200-3000 FORMAT) and with program lines 30 to 35 shows how values are entered.

All examples and tables are based on measured values of blasting cap legwires. The loss resistance is the most precise and reproducible value. Q-meters measured the skin-effect resistance at frequencies up to about 400 Megahertz. The leakage resistance is quite high and can be neglected in most cases. It represents the dielectric loss when wires pass through conductive blasting agents or ore bodies. Leakage resistance could also cover the radiation loss at higher frequencies. The line capacitance and inductance were measured with legwires casually deployed in parallel. Duplex wires and all cables and lines with well defined geometries allow calculation of capacitance and inductance from textbook equations.

A brief discussion of several problems is typed right under the computer printouts.

SKIN EFFECT IN IRON WIRE

Even though iron legwires are tin-coated, between 25 and 50 microinches (0.00064 to 0.0013 mm) thick, they still show a remarkable increase of resistance with frequency. Tin and iron have about the same resistivity, but iron's magnetism greatly contributes to the skin-effect. Graph 1 shows the resistance increase of copper and iron wire with increasing frequency; it is based on measured values of 23 ga (23 mil or 0.6 mm diameter) wires.

The graph clearly shows the contribution of iron's magnetism by the much larger resistance increase from DC to 1 MHz when compared to copper. For our calculations the external inductance of 1 meter of double iron legwire is 7.5 microhenry, that of copper is 1 microhenry. The capacitance of 25 picofarad/meter double line is the same for iron or copper. The leakage was arbitrarily set for $G=0.0001$ S/M or 10000 ohms/meter for both metals at all frequencies.

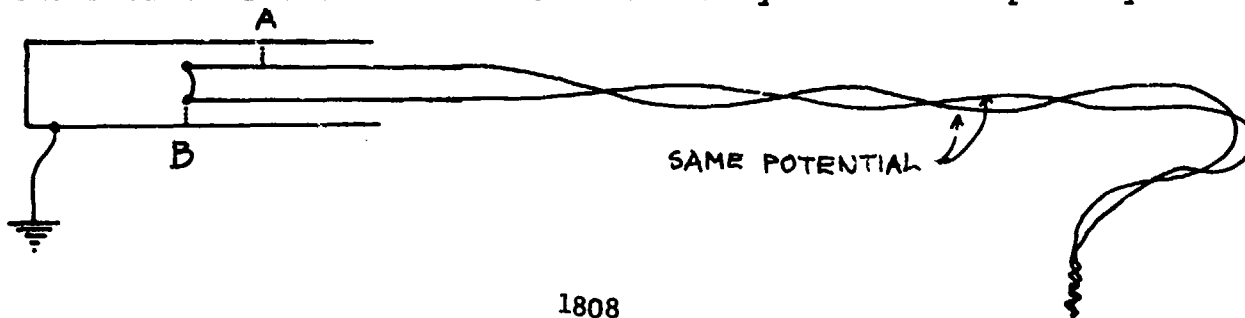
Four different bridgewire resistances were treated: 0.1 0.25 0.5 1.0 ohm. The two lower resistances are typically found in 1A-1W no-fire detonators and the two higher ones in regular commercial detonators. Tables 1 to 4 summarize the contents of about 200 computer runs and demonstrate the radio-frequency protection of iron wire at all frequencies.

Iron-wire based rf-protection can be designed in or it can be added as retrofit to an electroexplosive device. Wireless EED's can be attached to an iron wire lead line or at least to several feet of iron connecting wire. Iron wire is a poor antenna wire as well; its skin effect resistance dissipates most of the received energy as heat far away from the ignition charges. The wave length of an EM wave on iron wire is only one quarter that of the free space EM wave length. The iron wire wave length is only 37% of that on copper wires. The commonly used half-wave dipole covers a circular intercepting area of 1 unit when copper wire, but only 0.14 unit when iron wire.

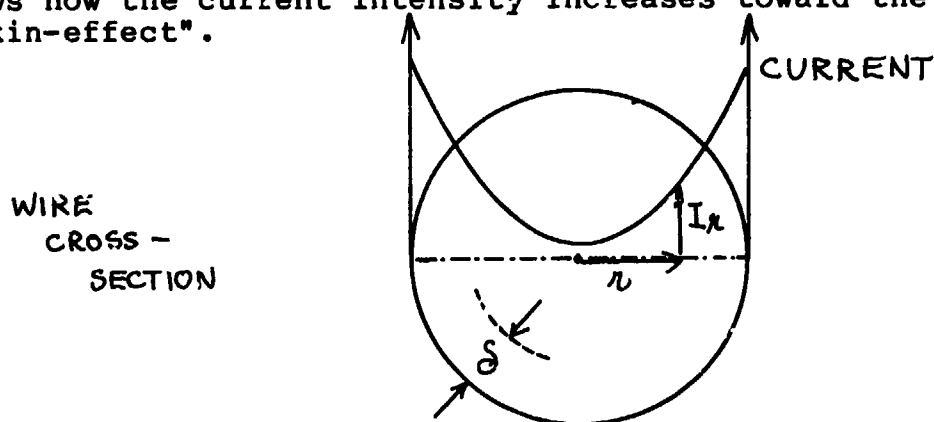
The added line resistance of iron wire usually does not require modified firing circuits. In oil well service work, for instance, 5 ohms (20 ft. double iron wire) increase does not matter when the firing cable has 300 or more ohms. Capacitor discharge firing circuits of specialty devices can be redesigned quite readily. Military detonators and weapons can be made rf-immune with iron legwires and/or lead lines that exceed about 10 ft. in length. Although iron is cheaper than copper as metals, the tinning and more difficult drawing process add a small cost increment to iron wire.

Conduction of rf currents above approximately 500 MHz on iron leg wires is practically impossible. UHF and RADAR pose no problem for an EED with iron leg wires, short of being in the near-beam of a high power antenna. The very limited radiation-intercepting area of a UHF dipole and the very high protection factors (see Table 1) of iron leg wires at these frequencies eliminate the rf hazard for an EED.

We should address the coaxial-mode hazard for an EED: voltages can appear between the legwires, who are joined by the bridgewire there, and the shell. The dotted lines show likely flash-over pathways



within the shell: "A" at a safe in-the-plug location and "B" through the ignition. RF-potentials must exceed maybe five hundred Volts to flash-over at these locations. A safe flash-over at "A" at a lower voltage than "B" flash-over through the ignition is the same engineering solution as is offered for electrostatic discharge protection. Such high voltages might only happen directly at a broadcast antenna or on an aircraft carrier deck. RF sparks from fingers and tools would immediately draw attention to such personally dangerous fields. The iron wire will protect the EED under these conditions as well, because the open circuit voltage at "A" and "B" is greatly lowered by losses on iron leg wires. The computer program could be used to give insight into this problem. The coaxial mode, as described here, is not a hazard in commercial blasting operations and might rarely be encountered on flight decks. The theory and the equations of skin-effect resistance as function of frequency are developed in textbooks of electrodynamics. The current intensity in a wire as function of the radius is described by complex-argument Bessel functions, the Kelvin functions. A typical current vs. radius plot shows how the current intensity increases toward the outside, hence "skin-effect".



The current-carrying skin-thickness δ in a flat plate is

$$\delta = \sqrt{\frac{\rho}{\pi f \mu}}$$

where ρ = resistivity

f = frequency

μ = permeability = $\mu_0 * \mu_{rel}$

At sufficiently high frequencies, δ also describes the skin thickness in a round wire.

HIGH-FREQUENCY RESISTANCE OF ONE METER OF 23 MIL DIA. WIRE

RESISTANCE (OHM)

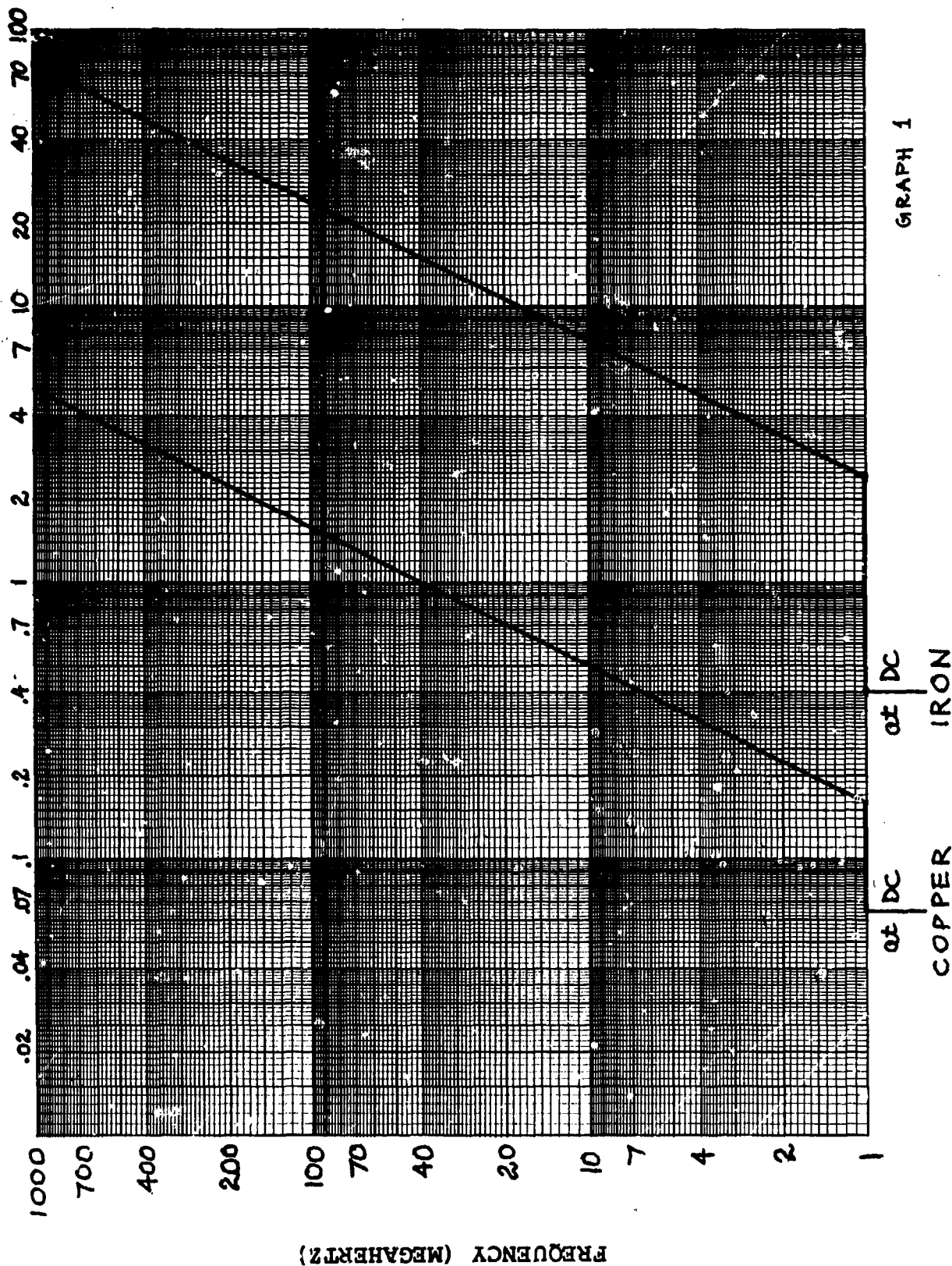


TABLE 1: PROTECTION FACTOR = ENERGY INTO LINE / BRIDGEWIRE ENERGY

BRIDGEWIRE (OHM)	LINE LENGTH: FREQUENCY (MHz)	0.3 METER		1 METER	
		COPPER	IRON	COPPER	IRON
0.1	0.5	1.6	10	3.0	31
0.1	1	2.0	15	4.2	49
0.1	2	2.3	21	5.4	69
0.1	5	3.1	32	8.3	116
0.1	10	4.0	46	12.0	181
0.1	20	5.3	66	18.2	260
0.1	50	8.0	96	32.0	322
0.1	100	11.2	112	37.0	382
0.1	200	13.5	141	43.0	484
0.1	500	17.5	203	56.0	669
0.25	0.5	1.2	5	1.8	13
0.25	1	1.4	7	2.3	20
0.25	2	1.5	9	2.8	28
0.25	5	1.8	13	3.9	47
0.25	10	2.2	19	5.4	73
0.25	20	2.7	27	7.9	105
0.25	50	3.8	39	13.4	128
0.25	100	5.1	45	15.4	154
0.25	200	6.0	57	17.8	194
0.25	500	7.6	82	23.0	268
0.5	0.5	1.1	3	1.4	7
0.5	1	1.2	4	1.6	11
0.5	2	1.3	5	1.9	15
0.5	5	1.4	7	2.5	24
0.5	10	1.6	10	3.2	37
0.5	20	1.9	14	4.4	53
0.5	50	2.4	20	7.2	64
0.5	100	3.0	23	8.2	77
0.5	200	3.5	29	9.4	98
0.5	500	4.3	41	12.0	135
1.0	0.5	1.1	2	1.2	4
1.0	1	1.1	2	1.3	6
1.0	2	1.1	3	1.4	8
1.0	5	1.2	4	1.7	12
1.0	10	1.3	6	2.1	19
1.0	20	1.4	8	2.7	27
1.0	50	1.7	11	4.1	33
1.0	100	2.0	12	4.6	39
1.0	200	2.3	15	5.2	49
1.0	500	2.7	21	6.5	68

TABLE 2: WAVE LENGTHS (METER)

FREQUENCY (MHZ)	AIR	WIRES	
		COPPER	IRON
0.5	600	355	131
1	300	193	71
2	150	99	36
5	60	40	15
10	30	20	7.3
20	15	10	3.7
50	6	4	1.5
100	3	2	0.73
200	1.5	1	0.37
500	0.6	0.4	0.15

TABLE 3: ATTENUATION OF DOUBLE LEGWIRE

(NEPER/METER)

FREQUENCY (MHz)	COPPER	IRON
0.5	0.0093	0.0271
1	0.0104	0.0307
2	0.0110	0.0332
5	0.0117	0.0368
10	0.0125	0.0409
20	0.0135	0.0466
50	0.0155	0.0575
100	0.0180	0.0703
200	0.0210	0.0876
500	0.0275	0.1214

TABLE 4: PROTECTION FACTOR FOR 1 OHM BRIDGEWIRE

LINE LENGTH: LEG WIRES:	QUARTER WAVE		HALF WAVE	
	COPPER	IRON	COPPER	IRON
FREQUENCY (MHz)				
0.5	183	579	989	3538
1	106	324	328	1069
2	56	171	129	404
5	25	75	49	155
10	14	42	26	84
20	8	24	15	48
50	4.1	13	7.2	24
100	2.8	8	4.6	15
200	2.0	5.4	3.1	9.8
500	1.6	3.4	2.1	5.9

Protection factors higher for bridgewires less than 1 ohm.

TYPE TLINE.FOR

```

C      TRANSMISSION LINE EQUATIONS
C      R =LINE RESISTANCE [OHM/METER]    INCLUDE SKIN EFFECT
C      L =LINE INDUCTANCE [MICROHENRY/METER]
C      C =LINE CAPACITANCE [PICOFARAD/METER]
C      G =LINE LEAKAGE [SIEMENS/METER]
C      F =FREQUENCY [MEGAHERTZ]
C      ZL =LOAD IMPEDANCE [OHM]
C      RL =RESISTIVE PART OF LOAD IMPEDANCE [OHM]
C      XL =REACTIVE PART OF LOAD IMPEDANCE [OHM]
C      LL =LINE LENGTH [METER]
C      ZZ =CHARACTERISTIC IMPEDANCE [OHM]
C      RR =RESISTIVE PART OF ZZ [OHM]
C      XX =REACTIVE PART OF ZZ [OHM]
C      ZI =INPUT IMPEDANCE [OHM]
C      RI =RESISTIVE PART OF ZI [OHM]
C      XI =REACTIVE PART OF ZI [OHM]
C      UI1=INPUT VOLTAGE TO OBTAIN 1 AMP THRU LOAD [VOLT]
C      RFN=REFLECTION COEFFICIENT AT LOAD
C      ALPHA =ATTENUATION [NEPER/METER]
C      BETA  =PHASE SHIFT [RADIAN/METER]
C      INCUR =COMPLEX INPUT CURRENT
C      RPWR  =REAL INPUT POWER
C      PRFAC =PROTECTION FACTOR
C      IMPLICIT REAL (L)
C      IMPLICIT COMPLEX (I)
C      COMPLEX ZL,ZZ,ZI,UI1,RFN,GAMMA,F1,F2,F3,F5,F6,F7,F8,F9,F10,INCUR
C      GAMMA=CMPLX(ALPHA,BETA)
C      ZZ=CMPLX(RR,XX)
C      ZI=CMPLX(RI,XI)
C      TYPE R,L,C,G IN ABOVE DIMENSIONS
50  READ(*,*) R,L,C,G
C      TYPE RL AND XL [OHM]
C      READ(*,*) RL,XL
C      TYPE FREQUENCY [MEGAHERTZ] AND LINE LENGTH [METER]
C      READ(*,*) F,LL
C      W=6.28318531E6*F
C      F1=CMPLX(R,W*L*1.E-6)
C      F2=CMPLX(G,W*C*1.E-12)
C      GAMMA=CSQRT(F1*F2)
C      ALPHA=REAL(GAMMA)
C      BETA=AIMAG(GAMMA)
C      ZZ=CSQRT(F1/F2)
C      RR=REAL(ZZ)
C      XX=AIMAG(ZZ)
C      ZZZ=CABS(ZZ)
C      ZL=CMPLX(RL,XL)
C      F3=CMPLX(SINH(2*ALPHA*LL),SIN(2*BETA*LL))
C      F4=COSH(2*ALPHA*LL)+COS(2*BETA*LL)
C      F5=F3/F4
C      F5 IS :TANH(A+JB)L      MEINKE P.292 (25.1)
C      F6=ZL+(ZZ*F5)
C      F7=ZL/ZZ
C      F8=1+(F7*F5)

```

```

ZI=F6/F8
RI=REAL(ZI)
XI=AIMAG(ZI)
AZI=CABS(ZI)
C CHIPMAN P.143 EQ.7.44 SOLVED WITH IT= 1 AMPERE
F9=CMPLX(SINH(ALPHA*LL)*COS(BETA*LL),COSH(ALPHA*LL)*SIN(BETA*LL))
F10=CMPLX(COSH(ALPHA*LL)*COS(BETA*LL),SINH(ALPHA*LL)*SIN(BETA*LL))
UI1=(ZZ*F9)+(ZL*F10)
AUI1=CABS(UI1)
VR=REAL(UI1)
VI=AIMAG(UI1)
RFN=((ZL/ZZ)-1)/((ZL/ZZ)+1)
INCUR=CMPLX(AR,AI)
INCUR=UI1/ZI
AR=REAL(INCUR)
AI=AIMAG(INCUR)
CUR=CABS(INCUR)
RPWR=RI*CUR*CUR
PRFAC=RPWR/RL
C NOTE THAT 1 AMP SQUARED = 1, THEREFORZ RL FOR POWER IN PRFAC
100 FORMAT(////////////////)
200 FORMAT('          TRANSMISSION LINE EQUATIONS'//)
300 FORMAT('          LINE RESISTANCE [OHM/METER]          R =',F14.7)
400 FORMAT('          LINE INDUCTANCE [MICROHENRY/METER] L =',F14.7)
500 FORMAT('          LINE CAPACITANCE [PICOFARAD/METER] C =',F14.7)
600 FORMAT('          LINE LEAKAGE [SIEMENS/METER]          G =',F14.7)
700 FORMAT('          FREQUENCY [MEGAHERTZ]          F =',F14.7)
800 FORMAT('          LOAD RESISTANCE [OHM]          RL=',F14.7)
900 FORMAT('          LOAD REACTANCE [OHM]          XL=',F14.7)
1000 FORMAT('          LINE LENGTH [METER]          LL=',F14.7)
1100 FORMAT('          COMPUTED VALUES :')
1200 FORMAT('          CHARACT.IMPED. [OHM]          ZZ =',F14.7)
1300 FORMAT('          RESISTANCE [OHM]          RR =',F14.7)
1400 FORMAT('          REACTANCE [OHM]          XX =',F14.7)
1500 FORMAT('          ATTENUATION [NEPER/METER]          ALPHA =',F14.7)
1600 FORMAT('          PHASE SHIFT [RADIAN/METER]          BETA =',F14.7)
1700 FORMAT('          LOAD CONDITIONS :')
1800 FORMAT('          INPUT IMPEDANCE [OHM]          AZI =',F14.7)
1900 FORMAT('          INPUT RESISTANCE [OHM]          RI =',F14.7)
2000 FORMAT('          INPUT REACTANCE [OHM]          XI =',F14.7)
2100 FORMAT('          REFLECTION COEFF. AT LOAD          RFN =',F14.5)
2200 FORMAT('          [VOLT] FOR 1 AMP THRU LOAD          AUI1 =',F14.7)
2300 FORMAT('          REAL INPUT VOLTAGE [VOLT]          VR =',F14.7)
2400 FORMAT('          IMAG INPUT VOLTAGE [VOLT]          VI =',F14.7)
2500 FORMAT('          INPUT CURRENT @ 1 AMP THRU LOAD [AMP] =',F14.7)
2600 FORMAT('          REAL CURRENT [AMP]          AR =',F14.7)
2700 FORMAT('          IMAG CURRENT [AMP]          AI =',F14.7)
2800 FORMAT('          REAL POWER INTO LINE [WATT]          RPWR =',F14.7)
2900 FORMAT('          PROTECTION FACTOR = REAL POWER / LOAD POWER')
3000 FORMAT('          PRFAC =',F14.7)
3100 FORMAT(////////////////)
      WRITE(*,100)
      WRITE(*,200)
      WRITE(*,300) R
      WRITE(*,400) L

```

```
WRITE(*,500) C
WRITE(*,600) G
WRITE(*,700) F
WRITE(*,800) RL
WRITE(*,900) XL
WRITE(*,1000) LL
WRITE(*,1100)
WRITE(*,1200) ZZZ
WRITE(*,1300) RR
WRITE(*,1400) XX
WRITE(*,1500) ALPHA
WRITE(*,1600) BETA
WRITE(*,1700)
WRITE(*,1800) AZI
WRITE(*,1900) RI
WRITE(*,2000) XI
WRITE(*,2100) RFN
WRITE(*,2200) AUI1
WRITE(*,2300) VR
WRITE(*,2400) VI
WRITE(*,2500) CUR
WRITE(*,2600) AR
WRITE(*,2700) AI
WRITE(*,2800) RPWR
WRITE(*,2900)
WRITE(*,3000) PRFAC
WRITE(*,3100)
GO TO 50
END
```

F>

47.7.5,25.0.0001
1.0
100.1

1 ohm bridgewire and 1 meter iron
legwire at 100 MHz.

PRFAC = 39

TRANSMISSION LINE EQUATIONS

LINE RESISTANCE [OHM/METER]	R =	47.0000000
LINE INDUCTANCE [MICROHENRY/METER]	L =	7.5000000
LINE CAPACITANCE [PICOFARAD/METER]	C =	25.0000000
LINE LEAKAGE [SIEMENS/METER]	G =	.0001000
FREQUENCY [MEGAHERTZ]	F =	100.0000000
LOAD RESISTANCE [OHM]	RL =	1.0000000
LOAD REACTANCE [OHM]	XL =	.0000000
LINE LENGTH [METER]	LL =	1.0000000

COMPUTED VALUES :

CHARACT. IMPED. [OHM]	ZZ =	547.7308000
RESISTANCE [OHM]	RR =	547.7299000
REACTANCE [OHM]	XX =	-.9879048
ATTENUATION [NEPER/METER]	ALPHA =	.0702908
PHASE SHIFT [RADIAN/METER]	BETA =	8.6036210

LOAD CONDITIONS :

INPUT IMPEDANCE [OHM]	AZI =	587.9349000
INPUT RESISTANCE [OHM]	RI =	83.3782300
INPUT REACTANCE [OHM]	XI =	-581.9927000
REFLECTION COEFF. AT LOAD	RFN =	-.99636
[VOLT] FOR 1 AMP THRU LOAD	AUI1 =	402.8460000
REAL INPUT VOLTAGE [VOLT]	VR =	-26.2129600
IMAG INPUT VOLTAGE [VOLT]	VI =	401.9923000
INPUT CURRENT @ 1 AMP THRU LOAD [AMP]		.6851881
REAL CURRENT [AMP]	AR =	-.6831484
IMAG CURRENT [AMP]	AI =	.0528301
REAL POWER INTO LINE [WATT]	RPWR =	39.1446400
PROTECTION FACTOR = REAL POWER / LOAD POWER		
PRFAC =		39.1446400

47.7.5.25.0.0001
0.5.0
100.1

0.5 ohm bridgewire and 1 meter iron
legwire at 100 MHz.

PRFAC = 77

TRANSMISSION LINE EQUATIONS

LINE RESISTANCE [OHM/METER]	R =	47.0000000
LINE INDUCTANCE [MICROHENRY/METER]	L =	7.5000000
LINE CAPACITANCE [PICOFARAD/METER]	C =	25.0000000
LINE LEAKAGE [SIEMENS/METER]	G =	.0001000
FREQUENCY [MEGAHERTZ]	F =	100.0000000
LOAD RESISTANCE [OHM]	RL =	.5000000
LOAD REACTANCE [OHM]	XL =	.0000000
LINE LENGTH [METER]	LL =	1.0000000

COMPUTED VALUES :

CHARACT. IMPED. [OHM]	ZZ =	547.7308000
RESISTANCE [OHM]	RR =	547.7299000
REACTANCE [OHM]	YX =	-.9879048
ATTENUATION [NEPER/METER]	ALPHA =	.0702908
PHASE SHIFT [RADIAN/METER]	BETA =	8.6036210

LOAD CONDITIONS :

INPUT IMPEDANCE [OHM]	AZI =	587.9477000
INPUT RESISTANCE [OHM]	RI =	82.3255800
INPUT REACTANCE [OHM]	XI =	-582.1555000
REFLECTION COEFF. AT LOAD	RFN =	-.99818
[VOLT] FOR 1 AMP THRU LOAD	AUI1 =	402.7982000
REAL INPUT VOLTAGE [VOLT]	VR =	-25.8714400
IMAG INPUT VOLTAGE [VOLT]	VI =	401.9666000
INPUT CURRENT @ 1 AMP THRU LOAD [AMP]		.6850920
REAL CURRENT [AMP]	AR =	-.6831035
IMAG CURRENT [AMP]	AI =	.0521604
REAL POWER INTO LINE [WATT]	RPWR =	38.6396000
PROTECTION FACTOR = REAL POWER / LOAD POWER		
PRFAC =		77.2792100

47,7.5,25,0.0001
0.25,0
100.1

0.25 ohm bridgewire and 1 meter iron
legwire at 100 MHz.

PRFAC = 154

TRANSMISSION LINE EQUATIONS

LINE RESISTANCE [OHM/METER]	R =	47.0000000
LINE INDUCTANCE [MICROHENRY/METER]	L =	7.5000000
LINE CAPACITANCE [PICOFARAD/METER]	C =	25.0000000
LINE LEAKAGE [SIEMENS/METER]	G =	.0001000
FREQUENCY [MEGAHERTZ]	F =	100.0000000
LOAD RESISTANCE [OHM]	RL =	.2500000
LOAD REACTANCE [OHM]	XL =	.0000000
LINE LENGTH [METER]	LL =	1.0000000

COMPUTED VALUES :

CHARACT. IMPED. [OHM]	ZZ =	547.7308000
RESISTANCE [OHM]	RR =	547.7299000
REACTANCE [OHM]	XX =	-.9879048
ATTENUATION [NEPER/METER]	ALPHA =	.0702908
PHASE SHIFT [RADIAN/METER]	BETA =	8.6036210

LOAD CONDITIONS :

INPUT IMPEDANCE [OHM]	AZI =	587.9540000
INPUT RESISTANCE [OHM]	RI =	81.7990300
INPUT REACTANCE [OHM]	XI =	-582.2361000
REFLECTION COEFF. AT LOAD	RFN =	-.99909
[VOLT] FOR 1 AMP THRU LOAD	AUI1 =	402.7745000
REAL INPUT VOLTAGE [VOLT]	VR =	-25.7006700
IMAG INPUT VOLTAGE [VOLT]	VI =	401.9537000
INPUT CURRENT @ 1 AMP THRU LOAD [AMP]		.6850442
REAL CURRENT [AMP]	AR =	-.6830810
IMAG CURRENT [AMP]	AI =	.0518255
REAL POWER INTO LINE [WATT]	RPWR =	38.3871000
PROTECTION FACTOR = REAL POWER / LOAD POWER		
PRFAC =		153.5484000

47,7.5,25,0.0001
0.1,0
100,1

0.1 ohm bridgewire and 1 meter iron
legwire at 100 MHz.

PRFAC = 382

TRANSMISSION LINE EQUATIONS

LINE RESISTANCE [OHM/METER]	R =	47.0000000	
LINE INDUCTANCE [MICROHENRY/METER]	L =	7.5000000	
LINE CAPACITANCE [PICOFARAD/METER]	C =	25.0000000	
LINE LEAKAGE [SIEMENS/METER]	G =	.0001000	
FREQUENCY [MEGAHERTZ]	F =	100.0000000	
LOAD RESISTANCE [OHM]	RL =	.1000000	
LOAD REACTANCE [OHM]	XL =	.0000000	
LINE LENGTH [METER]	LL =	1.0000000	
COMPUTED VALUES :			
CHARACT. IMPED. [OHM]	ZZ =	547.7308000	
RESISTANCE [OHM]	RR =	547.7299000	
REACTANCE [OHM]	XX =	-.9879048	
ATTENUATION [NEPER/METER]	ALPHA =	.0702908	
PHASE SHIFT [RADIAN/METER]	BETA =	8.6036210	
LOAD CONDITIONS :			
INPUT IMPEDANCE [OHM]	AZI =	587.9578000	
INPUT RESISTANCE [OHM]	RI =	81.4830300	
INPUT REACTANCE [OHM]	XI =	-582.2842000	
REFLECTION COEFF. AT LOAD	RFN =	-.99963	.00000
[VOLT] FOR 1 AMP THRU LOAD	AUI1 =	402.7603000	
REAL INPUT VOLTAGE [VOLT]	VR =	-25.5982100	
IMAG INPUT VOLTAGE [VOLT]	VI =	401.9460000	
INPUT CURRENT @ 1 AMP THRU LOAD [AMP]		.6850156	
REAL CURRENT [AMP]	AR =	-.6830675	
IMAG CURRENT [AMP]	AI =	.0516246	
REAL POWER INTO LINE [WATT]	RPWR =	38.2356100	
PROTECTION FACTOR = REAL POWER / LOAD POWER			
PRFAC =		382.3561000	

47,7.5,25,0.0001
1.0
100,C.182573864

Legwire length = λ at 100 MHz

548 volts at 15 MA is required to drive 1 ampere through the 1 ohm bridgewire. 8 watt power must be delivered to the 18 cm-legwire detonator to dissipate 1 watt in the bridgewire.

PRFAC = 8

TRANSMISSION LINE EQUATIONS

LINE RESISTANCE [OHM/METER]	R =	47.0000000
LINE INDUCTANCE [MICROHENRY/METER]	L =	7.5000000
LINE CAPACITANCE [PICOFARAD/METER]	C =	25.0000000
LINE LEAKAGE [SIEMENS/METER]	G =	.0001000
FREQUENCY [MEGAHERTZ]	F =	100.0000000
LOAD RESISTANCE [OHM]	RL =	1.0000000
LOAD REACTANCE [OHM]	XL =	.0000000
LINE LENGTH [METER]	LL =	.1825739

COMPUTED VALUES :

CHARACT. IMPED. [OHM]	ZZ =	547.7308000
RESISTANCE [OHM]	RR =	547.7299000
REACTANCE [OHM]	XX =	-.9879048
ATTENUATION [NEPER/METER]	ALPHA =	.0702908
PHASE SHIFT [RADIAN/METER]	BETA =	8.6036210

LOAD CONDITIONS :

INPUT IMPEDANCE [OHM]	AZI =	37370.3300000
INPUT RESISTANCE [OHM]	RI =	37370.2500000
INPUT REACTANCE [OHM]	XI =	-75.6040100
REFLECTION COEFF. AT LOAD	RFN =	-.99636
[VOLT] FOR 1 AMP THRU LOAD	AUI1 =	547.7887000
REAL INPUT VOLTAGE [VOLT]	VR =	.9879868
IMAG INPUT VOLTAGE [VOLT]	VI =	547.7878000
INPUT CURRENT @ 1 AMP THRU LOAD [AMP]		.0146584
REAL CURRENT [AMP]	AR =	-.0000032
IMAG CURRENT [AMP]	AI =	.0146584
REAL POWER INTO LINE [WATT]	RPWR =	8.0296810
PROTECTION FACTOR = REAL POWER / LOAD POWER		
PRFAC =		8.0296810

4.7,7.5,25.0.0001
1.0
1.1

A 1 ohm bridgewire and 1 meter iron
legwire in the AM broadcast band at
1 MHz.

PRFAC = 5.8

TRANSMISSION LINE EQUATIONS

LINE RESISTANCE [OHM/METER]	R =	4.7000000
LINE INDUCTANCE [MICROHENRY/METER]	L =	7.5000000
LINE CAPACITANCE [PICOFARAD/METER]	C =	25.0000000
LINE LEAKAGE [SIEMENS/METER]	G =	.0001000
FREQUENCY [MEGAHERTZ]	F =	1.0000000
LOAD RESISTANCE [OHM]	RL =	1.0000000
LOAD REACTANCE [OHM]	XL =	.0000000
LINE LENGTH [METER]	LL =	1.0000000

COMPUTED VALUES :

CHARACT. IMPED. [OHM]	ZZ =	504.3062000
RESISTANCE [OHM]	RR =	490.5912000
REACTANCE [OHM]	XX =	116.8118000
ATTENUATION [NEPER/METER]	ALPHA =	.0307104
PHASE SHIFT [RADIAN/METER]	BETA =	.0887431

LOAD CONDITIONS :

INPUT IMPEDANCE [OHM]	AZI =	47.5740100
INPUT RESISTANCE [OHM]	RI =	5.8038070
INPUT REACTANCE [OHM]	XI =	47.7186600
REFLECTION COEFF. AT LOAD	RFN =	-.99615
[VOLT] FOR 1 AMP THRU LOAD	AUI1 =	47.4140900
REAL INPUT VOLTAGE [VOLT]	VR =	5.6483240
IMAG INPUT VOLTAGE [VOLT]	VI =	47.0764500
INPUT CURRENT @ 1 AMP THRU LOAD [AMP]		.9966385
REAL CURRENT [AMP]	AR =	.9966344
IMAG CURRENT [AMP]	AI =	.0028791
REAL POWER INTO LINE [WATT]	RPWR =	5.7648540
PROTECTION FACTOR = REAL POWER / LOAD POWER		
PRFAC =		5.7648540

AD-P005 373

SAFETY CONSIDERATIONS
FOR
IN-LINE MECHANICAL FUZES

By

Dr. B. W. Thorpe, Australian Ordnance
Council, Canberra, Australia

and

Mr. J.R. Bentley, Materials Research
Laboratories, MoD, Melbourne, Australia

1. INTRODUCTION

A fuze is a device designed to initiate an explosive charge. Thus all explosive devices contain a fuze and since the fuze is responsible for initiating the explosive it normally contains safety features which are designed to prohibit initiation until the weapon has been deployed and has achieved a safe separation distance from the launcher platform.

For most conventional fuzes these safety features are embodied in a safe-arming unit (SAU) which keeps the initiator in a position where it cannot initiate the main charge until correct deployment and safe separation are achieved. Such systems are 'out of line' when safe and 'in line' when armed. Safety principles for these systems are well documented and have a long history of acceptable performance.

A more recent development is in-line electronic fuzing. These systems do not employ any sensitive explosives but use an electrically produced shock to initiate a secondary explosive. Such systems require extremely high power inputs and the SAU ensures that such a firing pulse cannot be delivered to the detonator until safe separation has been achieved. There is general agreement about the safety principles for such systems and in many respects they are similar to out-of-line fuze safety principles.

A large group of explosive initiation systems contain no safe arming unit. They are in effect in-line and are typically initiated either mechanically or electrically. Such systems have a significant risk of unintended functioning and it is common to employ operational constraints and procedures to reduce the risk of unintended initiation to an acceptable level. Examples of such a system are primed cartridge

cases and rocket motor igniters either electrically or mechanically initiated. The hazard of such a system may be quite low (small arms) or critical (large calibre shell). Electrically initiated devices are susceptible to various electromagnetic inputs including RADAR, electrostatic and other induced RF energies. In many instances quite low energies or powers can initiate the primer (10 J or 200 mW are typical) and various procedures are required to eliminate electrostatic and limit the RF environment so that the risk (probability of an unintended initiation) and hazard are kept within acceptable bounds.

2. PYROTECHNIC INITIATED EXPLOSIVES (PIE)

Australia, primarily the Royal Australian Airforce, are interested in procuring Raufoss MP70A1 20 mm ammunition (figure 1). This ammunition contains an initiation system which is mechanically initiated upon impact and does not include a safe arming unit. The initiation system is considered to be an In-Line Mechanical Fuze.

The Australian Ordnance Council (AOC) is required to establish safety criteria against which the ammunition could be assessed for safety and suitability for service. The currently accepted criteria for projectile fuzes [1,2] are of little relevance as they address only electronic in-line fuzes and out of line fuzes.

3. DESIGN SAFETY PRINCIPLES FOR IN-LINE MECHANICAL FUZES

A set of Design Safety Principles for in-line mechanical fuzes has been developed and promulgated as AOC proceeding 119/85. The major departures from similar principles for out of line fuzes are

(a) The absence of clauses relating to interruptors and shutters.

(b) The absence of clauses relating to safe separation distances.

(c) The inclusion of a clause relating risk and hazard.

(a) and (b) are clearly not appropriate to a system which has been designed with the intention of providing adequate and acceptable safety without shutters and safe separation systems. The major changes to conventional fuzing safety philosophy is the inclusion of hazard in the consideration of fuze safety.

4. HAZARD CATEGORIES

DEF STAN 08-3 gives the following qualitative hazard categories.

Category 1 - Catastrophic. May cause death or system loss.

Category 2 - Critical. May cause severe injury, severe occupational illness or major system damage.

Category 3 - Marginal. May cause minor injury, minor occupational illness or minor system damage.

Category 4 - Negligible. Will not result in injury,
occupational illness or system damage.

Design goals for conventional out of line fuzes are:

Safety system failure less than 1 in 10^6

Performance failure less than 1 in 10^3

No distinction is made on the basis of hazard. Thus a 20 mm projectile requires the same level of protection as a 155 mm shell and a 1000 kg bomb. This is probably a sensible approach as sympathetic detonation is an important factor in determining hazard.

PIE ammunition often contains low explosive loadings and little or no chance of mass explosions. This is true for Raufoss MP70A1 20 mm ammunition.

5. RELATIONSHIP OF RISK AND HAZARD

The accepted design goal for conventional fuzes of less than 1 in 10^6 for safety system failure is associated with stores which have a catastrophic hazard; this is an obvious criteria to apply to PIE ammunition given that a catastrophic hazard exists. At the other extreme of hazard category - negligible - a strong argument can be made for applying the performance failure rate goal of less than 1 in 10^3 . Intermediate hazard categories, critical and marginal, were assigned safety system failure rates of 1 in 10^4 and 1 in 10^5 respectively. These latter two relationships were somewhat arbitrary but it is

interesting to note that Brigadier MacKenzie Orr [3] came to similar conclusions and gives some statistical basis to the proposed relationship. Table 3 is reproduced from [3].

TABLE 3

Table of Acceptable Probabilities vs Effects of Malfunction
of Weapon Systems or Explosives Ordnance

EFFECT	ACCEPTABLE PROBABILITY OF OCCURRENCE PER EVENT
1. Catastrophic - Loss of life or total major equipment loss	1 in 10^6
2. Major - Serious injury or serious equipment damage	1 in 10^5
3. Minor - Injury causing temporary incapacitation or equipment damage requiring repair	1 in 10^4
4. Negligible - Temporary discomfort or inconvenience or minor degradation in equipment performance	1 in 10^3

6. SENSITIVITY OF EXPLOSIVE MATERIALS IN PIE AMMUNITION

The bench mark for explosives which may be used unshuttered in conventional fuzes and projectiles is tetryl. Explosives more sensitive than tetryl require shuttering. This is considered to be a reasonable design principle for PIE ammunition. The problem with this approach is defining what constitutes an explosive more sensitive than tetryl.

Qualification testing of an explosive involves a large number of sensitivity test including

- (i) Friction
- (ii) Impact - Figure of Insensitivity (F of I)
- (iii) Temperature - Ignition temperature
- (iv) Electrostatic
- (v) Thermal Stability
- (vi) Explosiveness
- (vii) Fragment Attack, bullet impact
- (ix) Cook-off
- (x) Shock - Gap Test

Such tests are quite good for ranking high explosives in terms of sensitiveness or likelihood of unintended initiation, i.e. in order of least sensitiveness.

TATB-TNT-Comp B (RDX/TNT)-Octol (HMX/TNT)-tetryl-RDX-HMX-PETN

This ranking will not be true for each test but is arrived at by considering the reaction of a given explosive to a range of stimuli.

Pyrotechnic materials have performance and sensitiveness characteristics quite different from high explosives. They tend to be more sensitive to friction and impact and less sensitive to temperature and shock. The criteria that pyrotechnics which are more sensitive than tetryl should not be used unshuttered in PIE ammunition is thus considered a good design goal but unfortunately one which is difficult

to quantify. A better judgement of which pyrotechnic materials are satisfactory unshuttered in PIE ammunition will be possible when a data base is available on PIE systems with a satisfactory service history. Until such information is available it is considered that the most relevant sensitiveness test is impact (F of I) and unless the materials are less sensitive than tetryl (F of I = 90) statistical data will be required to demonstrate that the risk of premature initiation lies within the bounds detailed in para 5.

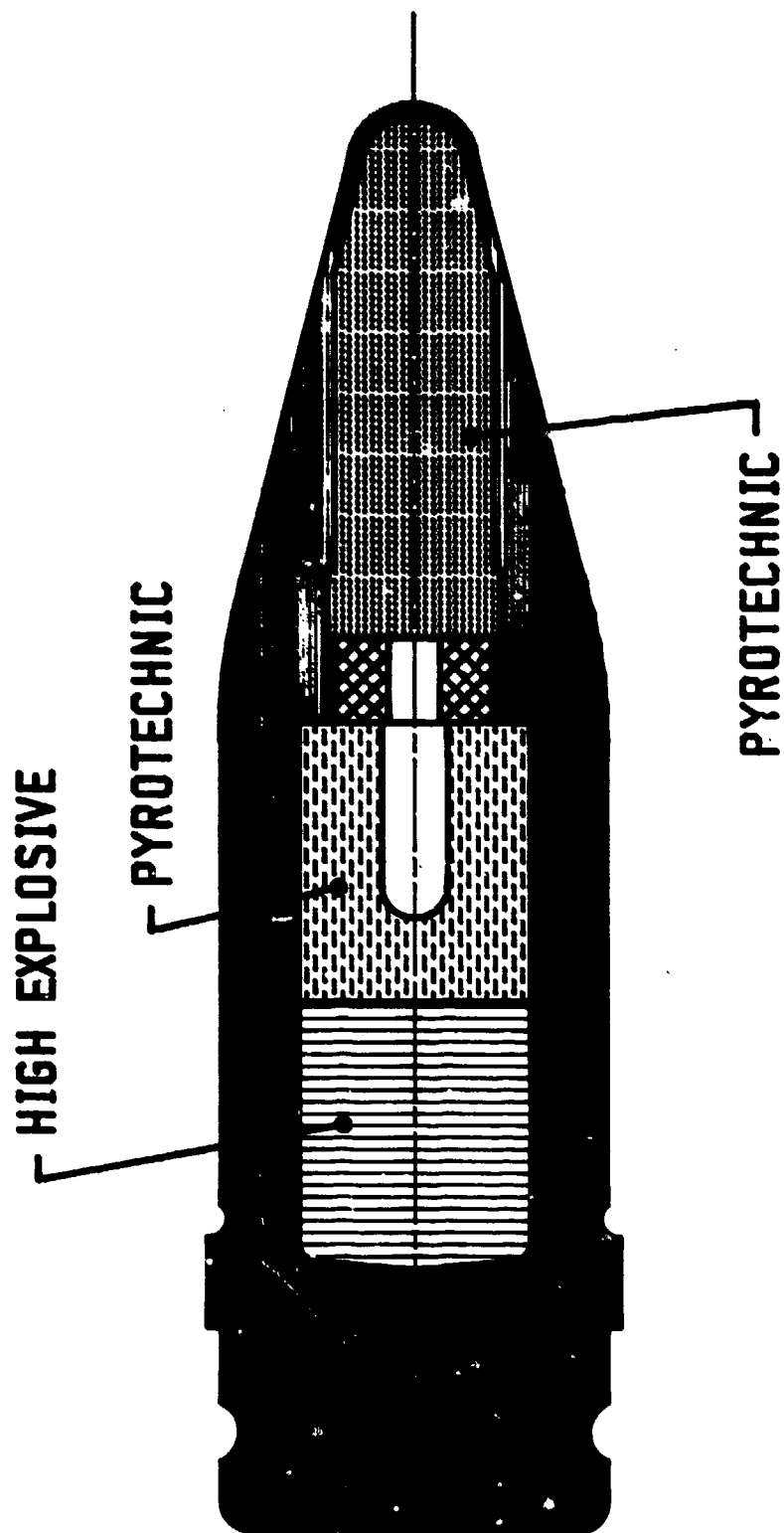
SUMMARY

Pyrotechnic Initiated Explosives

1. (PIE) ammunition is considered to contain a mechanical in-line fuze.
- Such systems are in principle similar to unshuttered electrically and mechanically initiated explosive systems currently in service.
- Design principles have been proposed for mechanical in-line fuzes.
- Tests are in hand to evaluate Raufoss 20 mm MP70 ammunition against these principles to determine safety and suitability for service.

REFERENCES

1. US Department of Defense (1984). "Military Standard. Fuze, Design Safety, Criteria For," MIL-STD-1316C.
2. UK Ordnance Board (1976). "Design Safety Principles for All Non-Nuclear Weapons Except Land Service Mines and Demolition Stores," OB Proc 41626.
3. First Australian Explosive Safety AOC Seminar, November 1985.



20mm PIE PROJECTILE

AD-P005 374

HAZARDS & OPERABILITY STUDIES
AND
THEIR APPLICATION TO AN EXPLOSIVES PLANT

By
R.E. Knowlton, Chemetics International
Company, Vancouver, Canada

ABSTRACT

↖ This paper is concerned with the use of Hazard & Operability Studies (HAZOP) in the Explosives Industry. The paper briefly describes a Pentaerythritol Tetranitrate (PETN) plant designed and built for Nobel Explosives Company, Ardeer, Scotland. This plant is unique as all the in-process materials handling and the processing itself, are carried out without any operators present in the unit.

Part of the checking of the design was carried out by Hazard & Operability Studies. This paper briefly describes the method itself, the application of the method to the plant and the results to date, including the use of this study as a national case example by the U.K. Health & Safety Executive ↗

INTRODUCTION

The chemical industry is a large and vital part of all industries, world wide. Its manufacturing processes often require the use of extremes of conditions e.g. temperatures and pressures. Many processes require the handling of materials which are hazardous, for example, flammable, explosive or toxic, often in considerable quantities. Furthermore, the industry is discovery-based, with many novel materials and processes.

Naturally safety is a high priority in the chemical industry in general. The explosives industry in particular, regards safety as the top priority in all its activities. Both the suppliers of explosives plants and the manufacturers of explosives, expend very considerable efforts ensuring that their design and operating methods conform to the stringent standards required by the nature of the materials which are being handled. Detonating materials, such as PETN and RDX, are particularly hazardous, being used to initiate explosions in materials such as TNT and AN/FO.

One approach to safety in say, a PETN plant is to design the unit so it will carry out the manufacture without any operators present.

This approach was accepted for a plant to be designed and built by Chemetics for Nobel Explosives Company (NEC), Ardeer, Scotland. NEC is a wholly owned subsidiary of Imperial Chemical Industries (ICI) London, England.

The requirements for a plant which operates without human intervention, mean that the checking methods must anticipate as far as possible all the hazards and operability problems. If these requirements are met, the final design and associated operating procedures will result in a plant producing at flowsheet rates consistently, reliably and safely.

The Aims of this Paper

The aims of this paper are:

1. To give a brief description of the PETN production plant.
2. To describe the safety and operability problems posed by the plant.
3. To describe briefly hazard & Operability Studies and the place of such studies in the safety of processes.
4. To illustrate the application of Hazop studies to the PETN plant.
5. To describe the overall effect of these studies on the commissioning and on the subsequent operation.

The Production Unit

The plant was designed for the production of 5 tons per day of PETN.

The process consists of the following steps:

1. Pentaerythritol (PE) is reacted with concentrated nitric acid to produce a slurry of crude PETN, in one of two, cooled, batch reactors.
2. The slurry is filtered and washed to give solid crude PETN.
3. The crude PETN is dissolved in acetone and subsequently precipitated in an acetone/water mixture.

4. The acetone is distilled off and the resultant PETN/water slurry is filtered and washed to give the final product.

The plant also includes waste acid stabilization, acetone recovery and effluent treatment units.

As far as possible, gravity flow is used throughout the plant to transfer material from one stage to the next. However, restrictions on the allowable height of the building meant that the gravity flow was in two "passes" with solid crude PETN being moved both vertically and horizontally from the bottom of the building to the purification equipment near the top of the building.

The PETN is moved in batches in stainless steel containers. The transfer sequence is as follows:

1. Crude PETN is discharged from a filter into a clean container fitted with a permeable liner.
2. The container is transferred to a station where recycle PETN is added.
3. The container is transferred to the interior of one of three dissolvers in which the PETN is dissolved leaving solid impurities in the liner.
4. The container with the solid impurities is transferred to a washing station, inverted and washed.
5. The clean container is righted and transferred to the filter ready for the next batch.

The above sequence involves the transfer of batches of PETN each weighing over 1000 lbs. in a complex series of vertical and horizontal movements. There is a total of four baskets moved by a single fork lift assembly with an overall vertical travel of 33 feet and an overall horizontal travel of 42 feet.

As mentioned earlier, a distinguishing feature of the design is that the complete process, including the materials handling, is carried out with no operators present. Apart from the introduction of PE to the unit and the final removal of the product, pure PETN, all the materials handling is performed automatically using hydraulically driven equipment. The processing and handling are controlled by a computer which provides the sequencing and safety checks at each stage.

In addition, a completely separate control system, verifying critical process steps and using a programmable logic unit (PLC), checks the computer system and is itself cross checked by the computer. This provides a high integrity system with both redundancy and diversity.

The Safety & Operability Problems

At a macro level, safety is provided for the operators by having the nitration and purification stages carried out within a blast mound. The operators are stationed in a central control room outside the mound during all periods when PETN is being processed. Therefore, the processing activities have to be handled and checked without the presence of operators. Furthermore, the unit has to work without fail for long periods of time.

The absence of operators in the unit itself made particularly stringent demands on the pre-start up checks. Once PETN was being produced, operators could not give "hands on" assistance during the commissioning. This meant that all possible eventualities had to be foreseen before the unit was started up.

At a more detailed level, some of the engineering requirements are severe. In common with many nitration units, "dump" systems have to be provided to render the unit safe in case a nitration reaction starts to exceed its working limits. In this unit, the dump system was custom designed so that all the components were checked by normal operation in every batch in order to confirm that the entire system would work on demand.

The whole production system of processing equipment, materials handling equipment, operating procedures and control system not only had to be safe while operating as intended but also had to be designed to remain safe during any excursions caused by

malfunctions and maloperations. However, these safety requirements could not be permitted to inhibit production so that the flowsheet rate was not achieved.

The requirements for safety, operability and productivity were met by a combination of the Hazard Identification technique of Hazard & Operability Studies and the checking approach of computer simulation. Only Hazard & Operability Studies are described in this paper.

Hazard & Operability Studies

One aspect of safety in the Chemical Industry is called "Process Safety". This means control of those hazards caused by malfunction and maloperation. Process Safety can be divided into four categories, namely:

- Process Hazard Management
- Hazard Identification
- Hazard Assessment
- Hazard Control

This paper concentrates on Hazard Identification i.e. finding the hazards. Broadly speaking there are four approaches to Hazard Identification, namely:

<u>Approaches</u>	<u>Examples</u>
Experience	Codes of Practice
Augmented Experience	Ask "what if?" questions
Analytical	Fault trees
Creative	Hazard & Operability Studies (Hazop)

Further information on Process Safety including the above approaches is given in Ref. 1.

Due to the novelty of the design for this unit, extensive use had to be made of the creative approach of Hazard & Operability Studies. Hazard & Operability Studies are aimed at making accidents and operational difficulties occur in the imaginations of members of a multidisciplinary team so that remedial action can be taken before real accidents occur. They are most effective at the design stage, by enabling team members

to visualize circumstances which do not yet exist and at a time when remedial actions can be taken at least cost.

They are a valuable supplement to and not a substitute for, sound experience-based practices.

The first Hazop system to be developed, called a "Guide Word" Hazop, is based on the assumption that hazards are caused by "deviations" from the intentions of the designers. If we could find all the deviations we would find all the hazards which could be caused by such deviations.

The Guide Word Hazop examination works as follows:

1. Break a design into suitable parts.
2. Select a part and specify its "design intention".
3. Find all possible "notional" or "hypothetical" deviations from that intention.
4. Determine whether any of the hypothetical deviations could occur in practice by seeking causes.
5. Explore the consequences of all practical deviations.
6. Identify potential hazards and operational difficulties.
7. Make a record so that suitable remedial action can be taken as a follow up to the identification exercise.
8. Repeat for all parts in the design.

The core of the technique lies in the method of generating all possible hypothetical deviations. This is achieved by associating each design intention with distinctive words or phrases called "guide words". Broadly speaking there are seven ways in which a piece of a plant can deviate and each of these has an associated distinctive word or phrase.

An example of the application of the methodology to the unit is described later. More detailed descriptions of the approach are given in refs. 1 through 9. Guide Word Hazard & Operability Studies are used, as a matter of policy on all Chemetics' designs and are in widespread use by the client, Nobel Explosives Company, its owner ICI and many parts of the chemical and process industries, world wide..

A second version of Hazard & Operability Studies is called a "Creative Checklist" approach. This retains the principle of stimulating creativity by associating a piece of data with a "triggering device". However, in this version, the triggering device of guide words is replaced by a list of potential hazards such as "fire", "explosion", "detonation", "toxicity", etc.

The method starts with an inventory of all the materials present.

Each item in the list of potential hazards is associated with each material to detect, qualitatively, which, if any, of the potential hazards could be caused by the material in question. When a hazard is detected, then a note is made of the quantitative numerical measurements of the intensity of each hazard, to create a "data base" of material properties. Thus the association of a particular material with the potential hazard of "fire" would, if the material were flammable, result in a note of relevant properties such as "flash point", "autoignition temperature", "flammable limits", etc. Any missing data can be highlighted and the collection of such data organized.

The same list of potential hazards is also associated with each major item of equipment in a block site plan. The aim is to detect whether extra precautions are necessary against specific hazards. Thus "fire", associated with a major item of equipment, could raise questions of spacing, fire fighting, fire containment, etc. The flow of hazards can be two way and highlight hazards to or from adjacent units and to or from the environment.

This second type of study may be used as a supplement to the guide word study under two circumstances.

1. As a very preliminary screen for major hazards prior to the detailed design.
2. When there is a need to detect hazardous "interactions" or domino effects, including the need for disaster plans.

Futher information on this type of hazard & operability study can be found in refs. 1,9 & 10.

The Hazard & Operability Studies on the PETN Unit

The first study was a "checklist" study on the materials. This was carried out not only on the raw materials such as PE and nitric acid and the finished product PETN but also on the solvents, by-products and effluents. In addition to highlighting the known hazards to all the team members, the method also revealed where there was a lack of some data and initiated a search for such data.

Because of the isolated nature of the unit, there was no checklist hazop on the site plan itself. This enabled more time to be allocated to the crucial guide word studies.

Hazard & Operability Studies are carried out by multidisciplinary teams under a trained study leader who is not a member of the design team. The team for this guide word study had the following composition:

Study Leader	a senior project engineer
Study Secretary	project drafting group leader
Study Members	design project manager
	senior process engineer
	mechanical design engineer
	instrument engineer
	electrical/control engineer
	operation engineer

The above composition is typical. In this study, the team was augmented by one or two further specialists for certain specific aspects.

The first operation to be examined was the hoist which raised a full bag of PE from the ground floor in the receiving bay and lowered the bag into the feed hopper so that the bottom valve could be opened to release PE. The Hazop examination of this operation will be described in detail to illustrate the "mechanics" of the methodology as applied to materials handling.

The Guide Word method requires a precise statement of what each operation and each item of equipment is designed to perform in order to be able to generate deviations. Deviations cannot be generated in vacuo.

The detailed design intentions for the hoist were:

1. Raise a full bag of PE vertically from the ground floor to the third floor.
2. Move the bag horizontally to a point directly over the PE storage hopper.
3. Lower the bag inside the hopper to a point where the bottom valve could be opened to release PE as the PE was extracted from the hopper.

Although the team members all had a general idea of the function of the hoist, this was the first time its function had been specified in such detail. This aspect of a Hazop Study will be referred to again later.

In order to illustrate the method, the guide words will be shown in upper case letters started with the negative of "don't" in table 1 below as applied to "raise a full bag of PE"

Table 1 - The application of the guide words to "raise a full bag of PE ..."

<u>Deviation</u>	<u>Meanings</u>	<u>Consequences & Actions</u>
DON'T raise	Failure of hoist	Process would eventually stop but no hazard, no action
	Hoist lacks capacity	Check capacity of hoist
MORE raise	Raise too far Raise too fast	Check limit switches Check speed of operation
LESS raise	Raise too little Raise too slowly	as above
AS WELL AS raise	Damage or tear bag	How would floor be cleaned?
PART OF raise	No logical meaning as there is only one activity	
REVERSE raise	Drop PE bag onto floor	No safety hazard because hoist control buttons are remote and the material will not explode. Would bag break and again, how would floor be cleaned?
OTHER THAN raise	Move bag horizontally instead of vertically	No hazardous consequences, no action.

The same procedure was applied to the other two aspects of the hoist operation with similar results.

The study continued with all the mechanical handling equipment being considered as well as all the various processing activities. For example, the PE feeder to the nitrator was a custom manufactured system provided by a reputable materials handling system designer and supplier. Yet 16 action items were identified concerned with the operation of the feeder.

The study on the very complex mechanical and control mechanisms for the container transfer system referred to earlier, identified many potential hazards and operability problems which would have caused serious startup delays and possibly serious accidents.

The complete Hazard & Operability examination was carried out in 20 sessions, each of which lasted about 4½ hours. Altogether 284 items were recorded for subsequent followup action. This is about the usual rate of 15 - 20 items per session.

An analysis of the items recorded is shown below in Table 2. Each item is classified by the nature of the problem i.e. "Safety, "Safety & Operability" or "Operability". The actions finally taken after the follow-up meetings are classified as "Revision to Manuals", "Process Design Change", "Project Design Change" or "No Action".

Table 2 - Classification of Action Items

<u>Nature of Follow-up Action</u>	<u>Nature of Problem</u>			<u>Total</u>
	<u>Safety</u>	<u>Safety & Operability</u>	<u>Operability</u>	
Revision to Manuals	6	15	15	36
Process Design Change	13	15	13	41
Project Design Change	13	22	16	51
No Action	<u>46</u>	<u>50</u>	<u>60</u>	<u>156</u>
Totals	78	102	104	284

Similar breakdowns are given in refs. 11 & 12 on totally different types of projects. As in these references, there are more "operability" problems to be resolved than safety problems. However, the PETN study was slightly unusual as just over half the items raised were, during the subsequent followup, classified as "no action". The proportion of "no action" items is usually in the range 10 - 30%. The higher proportion of "no action" items probably reflects the novelty of the design and the extreme concern of the team to record every item when there was the slightest degree of uncertainty.

Commissioning and History to Date

The computer and PLC were delivered to Chemetics in Vancouver in the middle of 1980. The programs were written and checked by simulation. The Guide Word Hazard & Operability Studies were carried out in parallel to the simulations. Some of the testing was to ensure that the software caused the equipment to operate exactly as specified. Some errors were detected. For example the control system closed two valves in the reverse sequence to that required. All the software errors were corrected.

The computer and PLC were delivered to the unit in April 1981. The plant was not yet mechanically complete but some water trials and the testing of some service units could be started. In addition, the linking of the control system to the mechanical items of equipment enabled the dynamic responses to be adjusted.

The commissioning checks were completed and the unit started the manufacture of product in November 1981. Only one hazard had escaped the Hazop Studies and pre-startup checks. It was found that a valve on the exit of a heated vessel had not been insulated and a choke occurred. This was quickly rectified. Guide Word Hazard & Operability studies typically detect between 90% & 99% of the residual hazards which exist in a well designed unit. The experience of this project to date suggests at least a 99% detection rate. The unit has now operated for over five years without any further problems and to the complete satisfaction of the client, Nobel Explosives Company.

The safety aspects of the PETN project have been considered so successful by the UK Health & Safety Executive that they will be used as a national "case example" in a forthcoming publication by the Executive.

Acknowledgements

The permission of the client, Nobel Explosives Company, Ardeer, Scotland to use their plant as the basis for this article is gratefully acknowledged.

The enthusiastic contribution of information by the Chemetics design team involved in the project has been greatly appreciated.

References

1. "Process Safety Management (control of acute hazards)" CMA, Washington, D.C. 1983.
2. Knowlton, R.E. "Hazard and Operability Studies and their Initial Application in R&D." R&D Management, Vol. 7, No. 1, October 1976.
3. Chemical Industries Association, Ltd. (U.K.), "A Guide to Hazard and Operability Studies 1977."
4. "Storingsanalyse Waarom? Wanneer? Hoe?" Directoraat-General van de Arbeid. The Netherlands 1979.
5. International Social Security Association. "Der Storfall im Chemischen Betrieb." Berufsgenossenschaft der Chemischen Industrie. "Heidelberg 1979.
6. Knowlton, R.E. "Hazard and Operability Studies, The Guide Word Approach." Chemetics International Company, Vancouver 1981.
7. Knowlton, R.E. "Hazop Poikeama Tarkastelu," Helsinki 1982.
8. Knowlton, R.E. "An Introduction to Guide Word Hazard and Operability Studies," Vancouver - CSChE Conference 1982.
9. Knowlton, R.E. "The Safety of Hydrogen as a Ground Transportation Fuel", ASME Winter Conference, New Orleans, 1984.
10. Knowlton, R.E. "An Introduction to Creative Checklist Hazard and Operability Studies," Vancouver - CSChE Conference 1982.
11. Knowlton, R.E. "Hazop and its Contribution to Plant Operability." AIChE Design '79 Conference. University of Aston Birmingham 1979.
12. Knowlton, R.E. & Wright, H.G. "Hazard Reduction & Operability Improvement in Pulp & Paper Plant Design." TAPPI Engineering Conference. Atlanta, GA. October 1981.

AD-P005 375

The Manufacture and Storage of Lead Azide
by a Computer Integrated System

B. Bobasch

Israel Military Industries

ABSTRACT

This paper describes a new approach to the production and storage of Lead Azide, by the use of a fully automatic computerized system.

The severe safety requirements necessary for handling this highly sensitive material necessitated the use of unconventional techniques for sensing and handling devices, including robots. In this pilot plant, the existing concept of batch work and small masses of material in process was retained. All production parameters, including lot details and storage data are automatically controlled and recorded by the system. One of the main goals achieved was the fact that no operator need come near the material during the process or during storage or withdrawal.

This concept has led to a very safe system for the production of Lead Azide as well as achieving good control and recording of parameters during production.

1. INTRODUCTION

The handling of very sensitive chemicals with robots and production of these substances with computer controls is little known in the western world.

The reasons for this are:

1. The profitability of these facilities is uncertain.
2. The strict safety requirements for these installations are above normal standards.

I.M.I. decided to develop plan and build a pilot plant for the full automatic production, handling, transporting and storing (CIM) to meet the special requirements and constraints which are required for the production of Lead Azide.

Emphasis was laid on the safety and quality of product by using the most modern production technologies. The intention was to use standard components available on the market.

It was soon found out that many components were not available. It was therefore necessary to develop several components that would comply with the special requirements. IMI Management understood these problems and allocated the necessary budget and support for the project.

2. INITIAL SITUATION

At the existing installation for the manufacture of this product, the production handling and storing of the material is carried out manually by conventional methods, applying all possible safety rules, as they are known at this branch. One of the reasons, for using robots is to avoid manual work, i.e. to remove the operator from the work cell. In order to achieve this it was decided to introduce full automatic computer-controlled production including robots. After a survey it was found out that there were many restriction and constraints on accomplishing the task.

The main restrictions are:

- The use of electrical energy in the work cells is restricted to very low energies.
- Handling and the transport must be executed with very gentle movements, without vibration and very low acceleration, and deceleration.
- The necessity for building components, with materials that are not commonly used in mechanical engineering.

The chemicals used in the manufacturing process cause deterioration of standard materials.

3. TECHNOLOGIES

3.1 Power for actuation

Because of restrictions on the use of electric energy, the technical solutions for actuation were accomplished with pneumatic and hydraulic power. All movements that handle Lead Azide use hydraulic power. This makes it possible to ensure very gently movements.

3.2 Actuator controls

All cylinders are controlled with flexible sequencing by direct programming of cylinder movement. By this system a very high degree of flexibility of operations for changing sequence is achieved by computer controls without the interference of the operator.

3.3 Sensors and signals

Because of the restrictions on the system, two types of signals were chosen. These signals are transformed into electrical input signals to the computer.

- Pneumatic limit switches (standard on the market).
- IR light conducted by fiber optics.
(Amplifiers were developed to answer the criteria. The equipment for production and quality control and fiber terminations were also developed. These components are standard with us and in production in our plant).
- Sensors for the chemical process that required the conversion into electrical energy located in the "Safe Area". They are of a type, that ensures that no medium which is in contact with the process has metallic contact with parts that are conducting electricity (fully insulated).

3.4 Controls

3.4.1 Computer

All processes and operations are controlled by the following computer system:

- Two micro computers,
linked by RS 232 C (Hand Shake)
- Three controllers connected to the micro computers.

The system has about 650 digital and analog In - and Outputs.

4. PLANT DESCRIPTION

4.1 Definitions

The plant has to produce powder by a chemical process. It must carry out the following operations:

- Feed solutions into reactor by dosing.
- Stir and mix the solutions with RPM and temperature control.
- Dry the slurry into powder.
- Fill the powder by weighing into containers.
- Take samples for quality control.
- Transport the product into storage.
- Store the product and keep stocks.
- Neutralize and destroy rejected lots.
- Transport and supply the product to users.

All the operations will be performed fully automatically.

4.2 Equipment

It was necessary to plan, construct and build the following work stations and equipment for automatic production, computer controlled as follows:

- Reactor with mixer
- Dosing and feeding systems for solutions
- Drying cell
- Filling and weighing cell
- Handling system,
one conveyor and five robots
- Automatic storing system
- Neutralization cell and waste solution
neutralization
- Heating and cooling systems for temperature control.

5. PRODUCTION CONTROL

Due to the fact that all production parameters are computer-controlled, production can be kept to narrow tolerances. This guarantees higher quality and permits accurate reproduction of each batch of Lead Azide.

6. SAFETY AND THE MAN / COMPUTER INTERFACE

All equipment handling sensitive material is located behind protecting walls.

The access to dangerous areas is through safety doors. controlled by the computer and permitted only under accepted corditions.

All required commands are given and received by the touch screen. with the aid of a menu. These commands are checked by the computer.

The computer is programmed so that it will not accept a wrong or invalid command.

The screen indicates the state of any cell operation with graphic symbols and text.

This includes:

- Temperatures
- Flows
- Mixer R P M
- Humidity
- Storage data
- Any irregular event or extreme condition during the process or handling of the material, etc.

For events like an "emergency stop" or a power failure etc. an immediate freeze of the whole system occurs.

For a restart the operator will have to decide according to the state of the freeze of the system whether to continue production or to abort the batch.

He will be guided by a menu on the screen. This procedure is checked by the computer and will not allow illogical decisions. *

The power for the computer is backed up with an UPS.

This will save all data and system conditions during power failure for a new start up.

All the data, i.e. production parameters, storage and stock details are recorded by the computer and can be traced on the screen or be printed in hard copy.

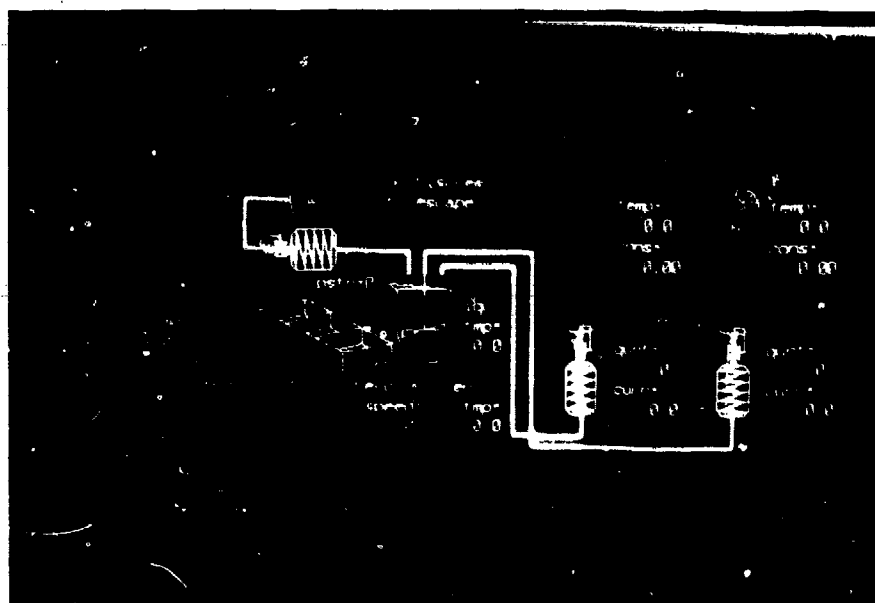


Fig. 1. Touch screen

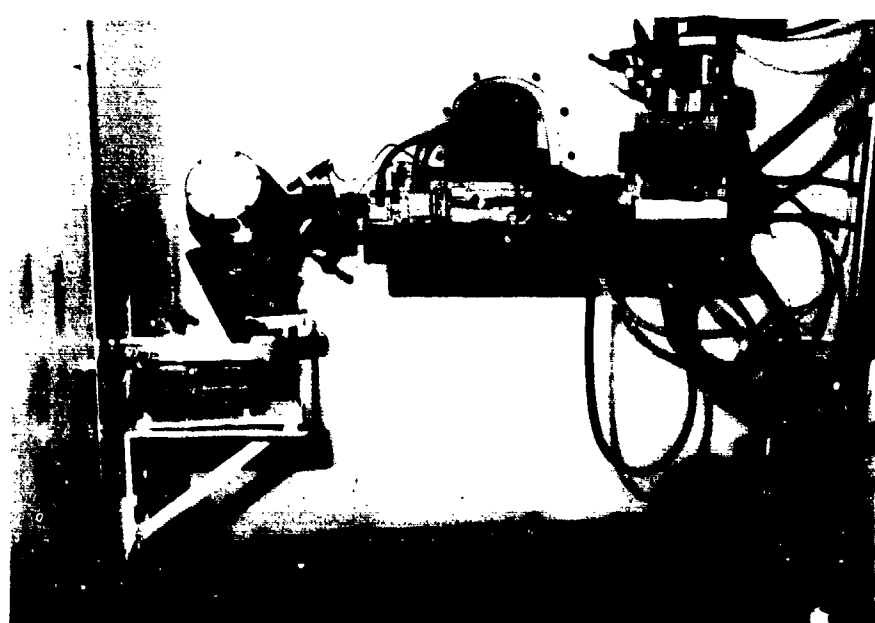


Fig. 2. Drying cell

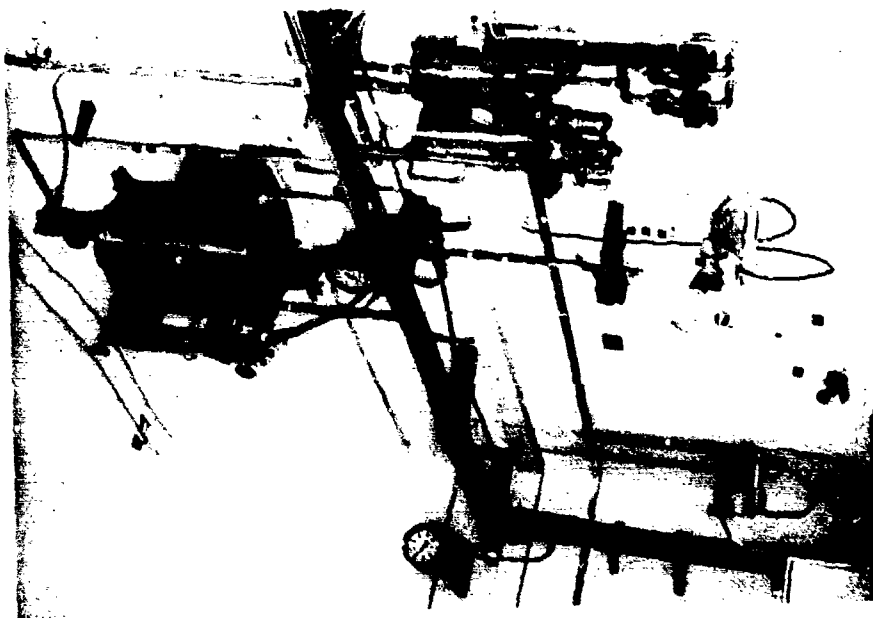


Fig. 3. Operators post

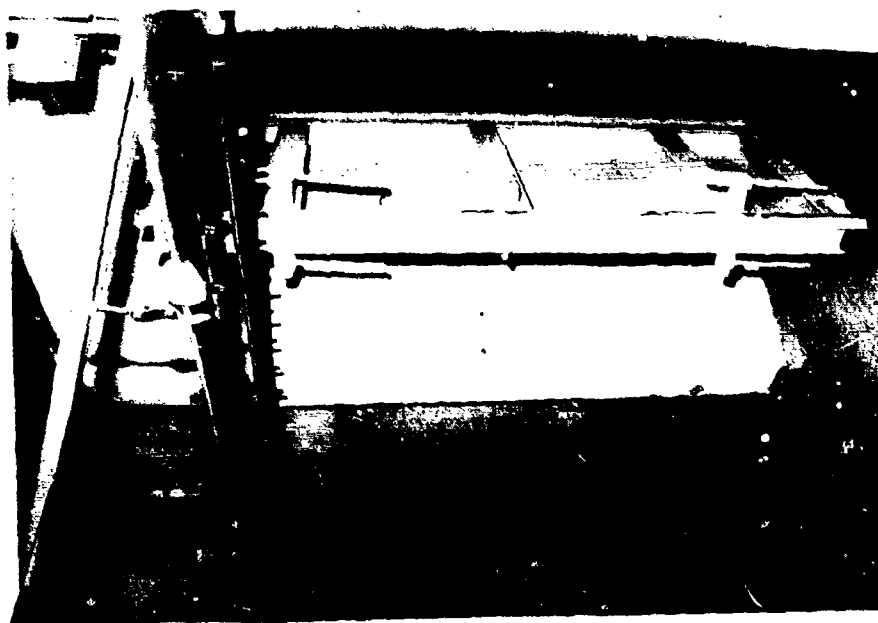


fig. 4. Safety door



Fig. 5. Conveyor rail

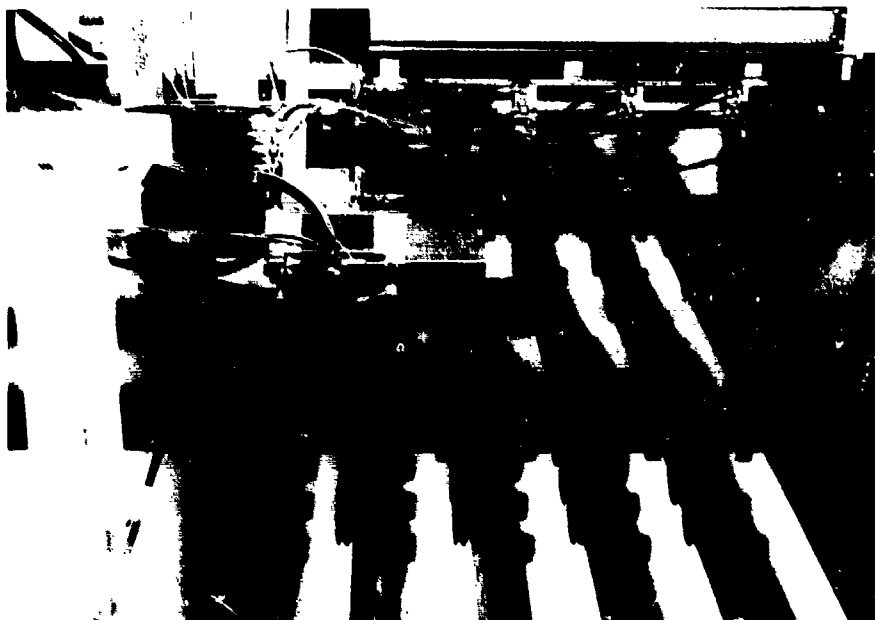


Fig. 6. Automatic storing system

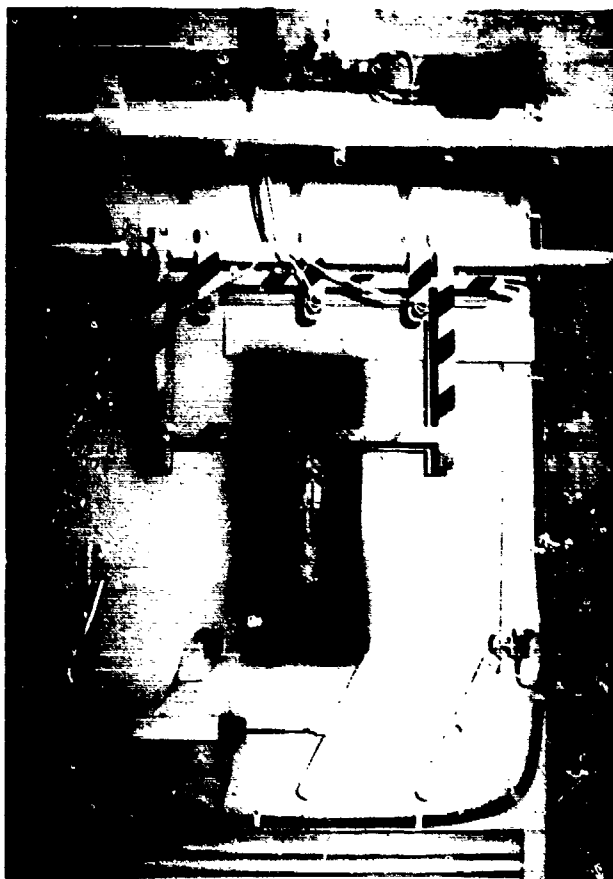


Fig. 7. Loading through safty hatch

If the Army controls only the top drawing of a technical data package, the only classification issued will be for the completed item. This has happened to both Honeywell and Ford on the 25mm Bushmaster program. Only the final assembly is granted a DOT Hazard classification, not the individual explosive assemblies which make up the round. It is difficult to build a complete round of ammunition when it's impossible to transport the propellant, fuses, high explosive and tracers from their manufacturer to the final assembly point. The problem is compounded when final assembly is on a GOCO plant, and there is no "official" DOD storage and compatibility data for magazine storage or for submission of a safety site plan.

Taking a look at the Navy, we feel that the Navy follows the Army a distant second place for granting DOT hazard classifications. The problem, however, appears to be that the Navy is severely understaffed. I would especially not want my observation here to be construed as a comment against the Navy's overall abilities, or technical knowledge, they do a good job.

Finally, taking a look at the Air Force, we find its hazard classifications to be the most elusive and difficult to obtain. In the past, when an interim classification was finally obtained, it was usually good for only one shipment. We are pleased to note that recently the Air Force has started to issue interim classifications for longer periods of time.

Now, I would like to turn to what we believe to be an example of good documentation for DOT/DOD hazard classifications. This is the Army's form of Hazardous Component Safety Data Sheets (HCSDS). This form provides a wealth of information, and is used for both interim and final hazard classifications. We believe it would be good for the other services to emulate this Army form. Unfortunately, obtaining the HCSDS sometimes proves to be difficult. Supposedly, the applicable HCSDS comes with the contract or proposal, but often this is not the case. Frequently, production or development is started on a letter contract which does not include HCSDS's. The 1 December 1980 version of this form states it is not valid unless issued as a part of a procurement/production package. This statement raises several questions for us. How can a DOT classification be valid one day and not the next? How can a DOT classification be valid for one contractor or the government and not another contractor? Does this mean that at contract conclusion all the storage and compatibility data from a HCSDS is invalid for residual items? Together, we should discuss the uses, limitations and critical need for HCSDS.

For planning, bid proposals, safety site plans, shipment of existing materials, and storage, HCSDS's are invaluable. Defense Contracts Administrative Services (DCAS) provides a vital service by providing HCSDS's as quickly as they can on request. The Army will also provide the HCSDS's via a request to the ACO. But, either route is rarely responsive to time sensitive matters and does not meet the needs of the industry. Could HCSDS's be located in DCAS Management Area offices? In many situations, a hard copy is not necessary, only some information from the form. We would suggest that HCSDS's be made available locally to a contractor. If this were done, a great service would be provided to the ordnance industry. When a final DOT/DOD hazard classification is issued, it should be incorporated into Hazard Classification of US Military Explosives and Hazardous Munitions, and when applicable OP5 Vol II.

An alternative for obtaining DOT Hazard Classifications is the DOT itself. More expedient and responsive than the DOD components, it is the only means available for contractors to receive a hazard classification for independent research and development items. When a classification is granted, their system of an "EX" number provides a ready reference to the original documentation. Shortcomings for the DOT are very few. Their dependence upon the Bureau of Explosives, American Railroad Association or the Bureau of Mines for recommending a classification, and the lack of DOD storage and compatibility information do present problems. With the impending closure of the Bureau of Explosives only the Bureau of Mines has an alternative laboratory that can recommend hazard classifications. A major crisis is brewing. Most contractors have never dealt with the Bureau of Mines and are concerned. Can the Bureau of Mines handle all the new work load, and what is their experience with ordnance products? There is a critical need for such a laboratory as the Bureau of Explosives. Alternatives for evaluating and recommending hazard classifications must be found now, or many IR&D programs, as well as some contract work will be affected. Lack of obtaining a DOD classification is not a true shortcoming of the DOT, for it is the DOD's responsibility to grant such information. It is a problem for contractors because they have to request hazard classification through dual channels, namely the DOT and the DOD.

A constant irritation experienced by many companies performing ordnance development work is the very narrow definition or interpretation in the DOT standards of what constitutes an engineering change to an item. When an engineering change occurs, as described by the standards, there is a need for a re-evaluation of the DOT hazard classification. This definition creates a needless administrative burden, when there is no change to explosive content or type, or effect to the arming and firing characteristics of the munition. Minor changes, additions or deletions of metal parts, or any change that will not increase the hazard for transportation or affect explosive content, should not be required for resubmission, particularly when the item is already a Class A explosive.

New performance-oriented packaging for ordnance items is approaching fast. A proposed regulation change (Docket Number HM181) would remove container specifications from CFR Title 49, and institute procedures more in line with United Nations and international civil air and maritime requirements. In essence, ordnance and explosive materiel packaging will have to be tested and certified against performance standards stated in these international regulations. Each specific type container used for a specific ordnance item or explosive component, will have to undergo drop, compression, and vibration testing. This differs from current DOT regulations which require packaging to conform to specific design standards. Such a regulation change, while not

yet in effect, will create formidable challenges for manufacturers. Research and development work may be impacted severely. In many cases hardware isn't available to perform the transportation test. Further, if there is hardware available, without a properly equipped and sited testing laboratory, it will be difficult to move the test items to a test location. This new standard will have a severe effect on many manufacturers. Movement of explosives, when defined as "reactive waste" by the EPA, for disposal, is another great problem facing our industry today. Contractors already face difficulty in obtaining DOT hazard classifications for explosive "reactive waste", but a monumental problem will result when performance packaging takes effect.

AD-P005 376

ORDNANCE INDUSTRY SAFETY PROBLEMS:

They Can't Be Solved Alone

**By
Thomas S. Denison
Principle Safety Engineer**

**Honeywell Inc., Defense Systems Division
Minneapolis, Minnesota**

Department of Defense contractors in the ordnance industry are being confronted with multiple safety-related issues that are currently or will very soon have a great impact upon the ability to produce ordnance material. ~~No one company~~ by itself can solve these issues. We at Honeywell believe fervently that safety issues affecting our industry can be resolved effectively with cooperation between government and industry. Together we can find the answers, and we must, for the health of our industry. Only by discussing our problems openly can we begin to resolve them. It is common to hear a contractor "cry", "Now look what the government is trying to do to us". It's also common to hear the government personnel say "That's the contractor's problem---not ours." We are in the same boat, why are we working at cross purposes? Our mutual objective is the same---the safe and efficient manufacture of ordnance material for defense.

This paper will address some problem areas in safety confronted by contractors within the ordnance industry. The paper does not speak for the industry or any particular association, but, it does represent our view of what are commonly known problems. The major areas where problems exist are: explosive hazard classifications, compliance standards, site plans, and training. Not all ordnance companies have experienced the problems that will be discussed, but many do, and these issues must be resolved.

While I will often be critical about the current situation, I hope to be even-handed in pointing out areas where both industry and the government can improve our working relationship. Most of all, I want to be solution-oriented in this paper. Thus, I've proposed at its conclusion a list of ten possible solutions, which, ~~I feel~~ will stimulate mutual problem solving for the benefit of ~~our entire industry~~ *are proposed.*

Explosive Hazard Classification

Ammunition and explosive hazard classification for over-the-road transportation is one of the greatest problems facing industry. There is a valid need to continue interim Department of Transportation (DOT) hazard classifications, particularly for research and development work. Often there is not enough hardware, or the design has not been formalized enough to perform the TB 700-2 test requirements. Only interim hazard classifications can respond easily to these changes during product development.

The need for obtaining interim DOT hazard classifications is critical. The problem we in industry face is in obtaining interim hazard classifications via the various DOD components. This process all too often has been disjointed, wrought with inconsistencies between the services, confused and time-consuming. In recent months, however, the "system" has started to straighten its self out. Progress has been made by all the services in processing requests for interim classifications, however, more work is needed.

It has been Honeywell's experience out of the various services, that the Army stands out as the best organized and prepared for dealing with the issuance of DOT hazard classifications. Their office seems to be understaffed, but of the services, we find them to be the most responsive. There is one area, however, that is still a problem.

When explosive wastes are involved, all EPA & DOT standards must be complied with and this becomes a very difficult challenge for ordnance contractors. If the explosive waste products are undamaged production scrap, essentially there is no problem. Such items are repackaged to meet DOT requirements, labeled, marked and properly shipped to an authorized and approved disposal site. Big problems occur when you have damaged explosive components, explosives suspended in water or other solvent, or worse yet, rags contaminated with explosives and cleaning solvent. In this instance a DOT hazard classification has to be obtained before you can ship, which causes delay and requires extensive administration time.

The worst possible situation occurs when ordnance products, damaged or rejected during production or development, are considered scrap and require disposal. Sometimes rework of scrap is successful but often rework is not feasible, it's uneconomical or otherwise impossible. If the manufacturing site is an approved and permitted disposal site, there is no problem, but few manufacturers are permitted disposal sites. It is virtually economically impossible to categorize every possible type of damage that could occur to an item, obtain a DOT classification and packaging requirements and ship the items.

Hard to find answers to this explosive waste problem must be found soon. A lot of valuable magazine storage space is being consumed in the temporary holding of scrap pending the obtaining of a DOT classification. This is another area where together we can discuss concerns and mutually find satisfactory answers for complex problems..

Compliance Standards

Standards are a vital and necessary part of our industry; they must exist. The history of the ordnance industry is marked with tragedy where standards did not exist. The DOD and DOD components perpetuate safety standards for both their own and industries' use. Problems for industry arise by application of these standards, their rigidity and inability to respond effectively to advancing technology, and how they come into existence.

The DOD components, because of their many types of facilities and operations, build into their standards an "acceptance of existing conditions" by either an outright grandfather clause or by a chain of command waiver/exemption system. DOD contractor safety standards have no built-in acceptance of existing facilities, other than by waiver or exemption from the appropriate PCO. With stable standards, request for waiver or exemption does not present much of a problem for contractors unless there are multiple DOD component PCO's involved. When more than one services PCO is involved, conflicts normally result from conflicting views of the various PCO's.

If standards are modified substantially like they have been just recently, and applied as of publication date, major problems result for the contractor. How government facilities respond to these changed standards is unknown. Doubtlessly, there will be a phase-in period, and based on funding and command attention, compliance at a future date.

In the industry sector the new standard appeared one day and enforced the next day. This left no phase-in period, nor any time to request, and have granted, allocation of funds to institute changes. Further, some of the new

standards will require contractors to modify extensively existing procedures and processes, and may require additional land. Like at the government facilities, all of this takes some degree of phase-in time, yet contractors are not permitted this grace period. Some government personnel may say "That is the contractors problem, not ours," but it is our mutual problem. As suppliers and manufacturers are affected by standards change, product, and production availability and capacity are affected.

Current ordnance industry standards are largely specification-oriented, and based usually on past unfortunate experiences or historically valid technology and procedures. By their nature, they are rigid and retrospective. As technology expands, the safety standards do not keep up. Contractor advances in technology, new materials, and processes, cause some of the tried-and-true safety guidelines to be outmoded. Outstepping the ordnance industries standards are new energetic compounds, different utilizations of propellants, automated factories, ultrasonic welding, wave soldering and the handling of assemblies containing integrated circuits and electro explosive devices.

Technology advances also bring to question the validity of existing standards in terms of what is known today. A lack of knowledge, technological advancement, or understanding of the problem and underlying cause, by some standards writers, has, in the past, called for use of a "what worked before will work again" attitude. Without due regard for technological advancement relative to existing standards, how can the field of safety advance? We believe that some standards in existence now should be re-evaluated in terms of today, not ten to forty years ago.

Performance oriented standards, not specification-oriented, can respond to technological change. Further, with performance-oriented standards, a contractor does not have to wait for the bureaucracy to catch up before something is accomplished.

DOD safety standards for the contractor are consensus standards developed by the services and DLA personnel. Since our industry's safety standards are consensus, we feel that industry should participate in the development of the standards. The leading edge of ordnance technology used to be in the government laboratories, today it is going on in both government and private industry. Industry safety professionals are by far more involved in the emerging technology and changes in production methods than some of the staff personnel who write safety standards. But, I want to admit right here that we in private industry are not without fault!

Private industry must accept a good portion of responsibility for non-progressive standards. Industry has not been proactive nor vocal in requesting to participate in the development of safety standards. We have tended to mind our own business and not be concerned with the affairs of our industry. Some of us bemoan the regulators and what "they" do but are not prepared to standup and participate in standards development. Perhaps through mutual participation of government and private industry in standards development, a mutual understanding of other issues which affect safety and the ability to produce will also result. Assuming government standards' writers are willing to open up the process of standards development to mutual participation, private industry must respond actively. Individually, ordnance companies must support these endeavors by allowing travel, funds and labor allocation for this vital task.

Safety Site Plans

Safety site plans are an effective safety management tool in which to develop and operate a safe facility. These plans are very labor intensive and time consuming to prepare, but the usefulness of this tool diminishes greatly because processing time is so lengthy. In today's environment, the time element lost in awaiting approval for a plan is a major headache for most contractors. Work does not stop while waiting for approval; manufacturing plans continue, production procedures are prepared, tooling and parts are ordered and facility modification is planned. Site plans need to be processed quickly and efficiently. If there are problems, contractors need to know now--not six to nine months after submission.

In fairness to the offices that process and approve plans, we recognize they are swamped with other duties and responsibilities, yet there has to be a higher degree of responsiveness and increased speed of processing. Perhaps redirection or increased allocation of personnel resources are necessary to answer this dilemma. Serious consideration should be given to increase the approval authority of lower command levels to lessen the amount of back-logged site plans at higher levels. I would recommend that site plans, when submitted for privately owned, privately operated (POPO) facilities, should be reviewed solely by the ACO. This avoids the conflicting views which often result when more than one PCO is involved. A single office at the DOD level should be available for mediation of differences between the ACO's safety representative and contractors.

Training Accessibility

Explosive safety training is the last issue to be addressed. The DOD maintains many fine schools for teaching explosive safety. They are acknowledged experts in a field where there are little or no alternatives for such education. The need for accessibility by contractors to these schools is critical and can increase the level of safety for the entire industry. Whether it is introducing explosives to a new safety professional or refresher training for an "old hand", access to DOD schools is vital to the safety performance of contractors while our need for this training is clear, we do find, however, that the system under which the schools operate has the effect of locking out private contractors. If contractors are not located on a GOCO installation, they are not given the opportunity to find out class schedules and request space allocation. Without allocation, attendance is virtually impossible. Some contractors have tried a "space available" approach to these schools only to find the doors closed to them due to course popularity. We feel that it would be a great service to the industry and fulfill a strong need if the DOD allowed free access to their safety-related schools.

We, especially, feel that there must also be accessibility to training on new standards. Defense Contracts Administration Services should sponsor seminars on the new 4145.26M, and subsequent changes, to acquaint contractors with the many new changes. To the best of my knowledge, only the Chicago Region has offered to familiarize contractors with this new information. This region should be commended for its dedication.

Conclusion

Issues addressed in this paper are not easy ones to solve, but through cooperation and mutual working of the problems, answers can be found. I would propose the following ten possible solutions:

1. DOD and DOT Hazard Classifications

A solution for streamlining and obtaining DOT/DOD interim and final hazard classifications would be to create a single unified tri-service office responsible for all hazard classifications. This office should be staffed appropriately, maintain an explosive's laboratory (much like the Bureau of Explosives), and be allowed to classify not only contract-related ordnance material but IR&D items destined for possible DOD usage.

2. HCSDS ACCESSIBILITY

HCSDS's fulfill a viable and important role. They should be maintained and expanded to all ordnance material from all DOD components. Accessibility to the data should be broadened with distribution down to the local DCASMA office and/or computer access to the database should be allowed.

3. Alternative for Bureau of Explosives

An alternative for the role played by the Bureau of Explosives must be located now. Possibly, the DOT can accept individual test data and recommendations from manufacturers or develop their own laboratory.

4. DOT Standards and Engineering Changes

DOT standards for Class A explosives, should be broadened to allow for engineering changes not affecting explosive content or type, causing an increased risk of transport, or effecting the arming and firing characteristics of ammunition.

5. DOD Panel for Packaging and Waste

DOD should create a panel to address performance oriented packaging and transportation of explosives deemed to be a reactive waste by the EPA. This panel should be comprised of all the services, DCT, EPA, and Industry. The complexity and impact of these issues cannot be understated. These problems need to be discussed and solutions coordinated among this group. Answers must be found quickly.

6. Safety Standards

Safety standards for contractors should be true consensus standards developed with representation and input from DOD contractors. Existing and new safety standards for contractors should be reviewed and revised as necessary to allow for a phase-in period of new standards, and be performance-oriented, not specification-oriented. Where appropriate as many specification standards as possible should be made advisory and not mandatory.

7. Safety Site Plans

Safety site plans must be reviewed on a priority basis by all reviewers. Difficulties in staffing must be solved. No site plan should require anymore than two months to complete its approval cycle. POPO site plans should be reviewed solely by the ACO. A single office at the DOD level should be available for mediation of differences between the ACO and contractors.

8. Safety Training

Contractors should be allowed access to DOD safety-related schools on an equal basis with current attendees. Contractors should either be advised of future schedules and permitted to request allocation of space or the DOD should obligate specific classes to be presented solely for the benefit of DOD contractors at designated locations.

9. DOD 4145.26M Familiarization

DCAS should conduct seminars in each region to familiarize contractors of the changes in DOD 4145.26m, and each subsequent change to that manual.

10. Communications Network

A current listing of the safety offices of all ordnance industry contractors should be maintained at a central location. Via this network, information should pass freely -- up, down, and between organizations, on accident information, request for guidance and assistance, and proposed standards changes.

In summary, I am confident that problem resolution is possible by talking and gaining a mutual understanding of each sides' views. Communication must flow freely, not only on standards, but also on accident causes and problems resolution. There appears to be no single office, or group who is dealing with all the safety issues we are confronted with today. Individual companies and various government offices take on problems and sometimes find solutions, but no one else knows about those solutions. As an industry, we reinvent the wheel or throwup our hands when a problem is too big. Only the DDESB Seminar offers a medium with which government and industry can communicate openly about safety problems and solutions.

The problems facing us are many; the solutions will be hard to come by, but of this I'm convinced ... much more open communication is needed, and in the long run, will be in both our individual and collective best interests. Together, we can find the answers.

AD-P005 377

JOINT AUSTRALIAN/UK STACK
FRAGMENTATION TRIALS
PHASE TWO REPORT

By

Mr. J. Henderson

Mr. J. Walker

Dr. N. J. M. Rees

Mr. R.A. Bowe

MOD, Procurement Executive
Safety Services Organization
Orpington, UK

1. BACKGROUND TO PHASE 2

1.1 The Explosion Effects Sub-Committee (EESC) of ESTC recommended in 1980 the investigation of fragments and debris arising from an untraversed bomb stack; one having a standard 2 degree traverse and also one with a 10 degree traverse. In addition, the effect of having such a stack inside a typical brick built storehouse with a protective concrete roof, under comparable traversed conditions, was also to be determined. Consequently Phase 1 was planned and carried out at DSC Woomera during May 1982 (Ref 2).

1.2 As a result of reservations expressed by RARDE concerning the symmetry of the bomb stacks used in Phase 1 it was decided to carry out a Phase 1B search over part of the sites used during Phase 1. RARDE's view was that it was probable that more lethal fragments, both in quantity and lethality, are generated by the nose and base of the bombs, many of which may be propelled by the blast more in a line radiating through the corners of the stack than in the line normal to the sides of the stack which was sampled in the trials. With these thoughts in mind a sampling plan was devised, utilising visual search and metal detection techniques, and was carried out at DSC Woomera during May 1984 (Ref 3).

1.3 Combination of the results from Phase 1 and 1B resulted in a recommendation to reduce minimum fragment throw distances (Ref 4) and showed that the RARDE reservations were unfounded. The trials to date had shown that there appeared to be no reason to apply a minimum quantity-distance of 270/400m for fragment/debris throw to a building, of construction similar to those tested and traversed preferably to the eaves, or an open stack traversed with the standard UK 2 degree traverse. The recommendation was to use D13 distances for fragment/debris throw, with a minimum of 270m for quantities less than the 1800kg tested in Phase 1, as determined in ESTC Leaflet 5 Part 2 (Ref 5). This would still give adequate protection from the effects of blast. The 270m minimum distance was an interim measure which was expected would be reduced when the results of Phase 2 were available.

1.4 A Phase 2 had been recommended because of some doubts as to the applicability of the trials to buildings which were considerably weaker than those tested, e.g. with 115mm brick walls and because it was not felt that the results allowed extrapolation down to small quantities of explosives (less than 1800 kg). Both of these doubts were based on the uncertainty over building break-up due to lighter construction or lighter loading.

1.5 Consequently Phase 2 was proposed using smaller quantities of explosives, typically of a few hundred kilograms, in a similar type brick built building to ascertain the effect of reduced loading. Similar trials were also proposed to ascertain the situation for a brick building of lighter construction and a concrete structure.

1.6 Approaches were made to the Australian Defence Authorities to continue the work of Phase 1 and 1B into a Phase 2 Trial. In November

1984 Dr N J M. Rees, Director SSO(PE) and Mr J Henderson, Secretary EESC, visited Canberra and the various Australian trials agencies involved to make the final planning arrangements for Phase 2. The proposals for the tests were approved by EESC and ESTC and are described in Section 3.

2. AIM OF PHASE 2

2.1 The prime aim of Phase 2 was to obtain additional data on the distribution of hazardous fragments and debris from an explosion in a building to supplement those obtained from Phases 1 and 1B. Phase 2 was intended to cover lower loading densities, with more typical explosives/ammunition, and more lightly constructed buildings.

2.2 From this data it was hoped to produce further recommendations to reduce or verify the existing Q-Ds based on fragment/debris throw considerations.

3. PHASE 2 TRIAL SPECIFICATION

3.1 Following discussions in UK and Australia the UK requirement for Phase 2 was finalised at a total of 4 trials as detailed below. Since Phase 1 consisted of Trials 1 to 4 the sequence was continued in Phase 2 consisting of Trials 5 to 8.

3.2 Trial 5: Building was constructed of 395mm cavity brick walls with a 150mm reinforced concrete roof to a design identical to that used for Phase 1. The explosive content of the building was sufficient fragmenting shell of Hazard Division 1.1 (Composition B filled) to give a total net explosives content for the building of 500kg TNT equivalent.

3.3 Trial 6: Building was constructed of 395mm cavity brick walls with a 150mm reinforced concrete roof to a design identical to that used for Phase 1. The explosive content of the building was sufficient boxed high explosives of Hazard Division 1.1 (Composition B) to give a total net explosive content for the building of 500kg TNT equivalent.

3.4 Trial 7: Building was constructed of 200mm reinforced concrete walls with a 150mm reinforced concrete roof. The explosive content of the building was sufficient fragmenting shell of Hazard Division 1.1 (Composition B filled) to give a total net explosives content for the building of 500kg TNT equivalent. The constructional details of the building probably utilising pre-cast concrete slabs assembled into the final structure on site are to be advised by the Australian Defence Trials Authorities.

3.5 Trial 8: Building was constructed of 280mm brick walls with a light-weight roof constructed of steel beams with corrugated iron and aluminium sheeting. The explosive content of the building was an incorporator loaded with 500kg TNT equivalent of high explosives of Hazard Division 1.1 (Composition B) and the building also contained pipes, etc to simulate a typical process environment. The constructional details of the building were advised by MFF St Marys who supplied the pre-fabricated steel frame and the incorporator.

3.6 All trial sites were virgin ground, with a minimum of 2000 metres between any two sites.

3.7 Trial sites 5, 6 and 7 were traversed to the level of the eaves of the building on two adjacent sides, the remaining two sides being left untraversed. In order to provide continuity and ease of comparison with Phase 1 the traverses were erected in the SE and SW sectors for each building and the door to the building was in the NE side. As in Phase 1 they were constructed of the local soil.

3.8 Trial 8 was traversed on the SW side to the eaves of the building and on the SE side to the standard two degrees from the level of the explosives in the incorporator. This orientation was required in order to provide continuity and ease of comparison with Phase 1 and similarly the door to the building was to be in the NE side. MFF St Marys proposed that identifiable surface debris should be placed on the traverse on the SW side of the building in Trial 8 to examine any effects of scouring that might take place during the explosion.

3.9 It was essential that all explosives used in any one trial, whether shell or HE, should be initiated virtually instantaneously. UK preferred that the initiation should follow a propagation mechanism as far as is possible, i.e. one shell or box should be initiated normally and detonating cord be used to ensure transmission of the detonation to the other shell or boxes present. This was in preference to each shell or box being initiated separately since this did not represent a practical accident situation. However it was necessary to initiate all shell simultaneously because of trial difficulties. The incorporator in Trial 3 had the charge cast into it at MFF St Marys and initiator pockets cast into the charge immediately below the access point in the lid of the incorporator.

3.10 The main requirement for each trial was the collection of fragments and building debris generated by the explosion of the building and its contents. There were minor variations between trials, principally in the subsidiary search areas. Actual collection methods were intended to be twofold, metal fragments to be detected by metal detector and building debris by a visual search. In common with Phase 1 it was quickly discovered that it was more efficient to collect the metal fragments by a simple visual search and the metal detectors were relegated to the role of checking the efficiency of this visual search. Sniffer dogs were also employed on one of the sites but proved useless because of the very large amount of explosives contamination present.

3.11 Additionally it was decided to carry out a search of the crater and its immediate surroundings on at least one site to determine the concentration of fragments which had been projected into the crater.

3.12 To complete the picture and obtain data which was not available from Phase 1 a search of the traverses on at least one site was proposed to determine the concentration of fragments projected into and stopped by the traverse.

3.13 Each trial was instrumented for blast to determine that a successful

detonation was achieved and to allow an assessment of the attenuations afforded by the different structures under test. An arrangement of two lines running to the NW and SW of each site was agreed with MRL Melbourne.

3.14 Each trial was recorded on video purely as a record of the trial. There was no intention to attempt to carry out any analysis of fragment velocities or trajectories from film records. Still colour photographs were taken after each detonation and during the collection phases as advised by the UK Scientist in Charge. A video record and still colour photographs of the construction phases were also taken.

3.15 The shell for the trials were American 175mm. These shell were supplied by USA and transported by UK at their own cost to a port of entry into Australia. These shell were transported in March 1985 through the good offices of Genchem Chartering Ltd to Australia and stored at DSC Woomera. The quantity shipped were 1200 shell, gross weight of approximately 15,000kg. It was proposed to use only 72 of these shell during Phase 2, the intention being to store the remainder for use during a possible Phase 3 in 1987.

4. FRAGMENT AND DEBRIS COLLECTION

4.1 The centre of explosion for each trial was established and a search pattern grid was laid. Each area was marked off with tape and searched by a visual sweep, backed up with a metal detector where appropriate.

4.2 In common with Phase 1 it was quickly established that shell fragments had attained a distinctive blue colour due to tempering by the heat of the explosion which made them readily identifiable against the red coloured earth and stone.

4.3 Trial 6 relied only on a visual search since the only metal fragments were pieces of door or roof reinforcement which were readily identifiable.

4.4 All fragments were identified by collecting them into a receptacle marked with search area in which they were found. They were taken back to base camp where they were sorted by type and weighed. Because of the large numbers of fragments collected and as it had been established from Phase 1B that the minimum weight of metal and masonry fragments of interest were 50g and 100g respectively, those fragments of each type under these weights were not weighed individually. Instead they were bulked together and a total weight for each type under the weight quoted was obtained. Subsequently two typical quantities of shell fragments were weighed individually to obtain the weighted distribution in the sample. For the masonry fragments photographs were taken of typical quantities.

4.5 All metal and masonry fragments over 50g and 100g weight respectively were weighed and recorded. To enable analysis and sorting by computer to be carried out all fragments were sorted into weight intervals by type and sector.

4.6 Full details of the results produced can be found in Section 9 of the full report. The data is too overwhelming to be reproduced here.

JOINT AUSTRALIAN/UK STACK FRAGMENTATION TRIALS

PHASE 2 REPORT

BY

J HENDERSON

J WALKER

DR N J M REES

R A BOWE

JUNE 1986

5. FRAGMENT AND DEBRIS CRITERIA AND ASSUMPTIONS

5.1 The fragment data was computer sorted using a VISICALC program on an Apple IIe microcomputer to calculate the numbers and densities of lethal fragments. The program will allow further analysis but for the present only totals of all potentially lethal fragments have been fully analysed. Various weights for fragment and masonry debris lethality were chosen and graphs produced of lethal density against distance, but for the sake of clarity only two sets of these graphs have been produced in the report.

5.2 In common with Phases 1/1B there is still some controversy over what these weights should actually be. However the following three assumptions are still valid:

ASSUMPTION 1

5.3 Fragments, whether metal or masonry, are considered potentially lethal, if their kinetic energy exceeds 80J (58ft lb). This value is based on pre WWI work in France (Ref 6) and is still the subject of debate although accepted internationally as a realistic hazardous fragment energy. Discussions are in progress within UK to assess whether this limit is too conservative. An American paper (Ref 10) suggests that it is but cannot provide any better estimate. It appears unlikely however that any new criterion will be established.

ASSUMPTION 2

5.4 All fragments are travelling at their free-fall velocities on impact which are in the range 50-60m/s for metal and 30-40m/s for masonry. These velocities are based on information used by Wing Cdr P Fairhurst in his fragment studies for the Explosion Effects Sub-Committee of ESTC (Ref 11).

ASSUMPTION 3

5.5 The potentially lethal fragment density is considered unacceptable if it rises above one potentially lethal fragment per 56 square metres (600 square feet). This figure is also accepted internationally and is equivalent to approximately a 1% chance of being hit by a potentially lethal fragment.

5.6 To simplify the analysis of the results each trial is considered separately in Section 6. Any comparisons between these trials and to other trials carried out will be made in the following Section 7. The reason for this is the extremely large number of fragments and debris which were collected. Some data will also be commented on in this section which have not as yet been analysed. When this additional analysis has been carried out it will be published as an addendum to the report.

5.7 Having accepted the two assumptions of paras 5.3 and 5.4 it is then necessary to interpret the values given to allow analysis of the fragments and debris collected. Phase 1B (Ref 4) recommended the use of 75 and 150g for metal and masonry fragments respectively. The relative velocities of the two fragment types would suggest a ratio in the range from 1.6 to 4

for masonry fragment weight to metal fragment weight. Thus in addition to the 150g masonry fragment weight a value of 250g has also been chosen for comparison. The choice of the metal fragment weight at 75g is still conservative in comparison to the criteria used by US (125g) (Ref 12). It is also understood that an even higher value is used by PhG.

6. FRAGMENT AND DEBRIS ANALYSIS AND DISCUSSION

6.1 For the sake of brevity only the most important analyses are discussed in this section. For a fuller discussion the overall report (Ref 1) should be consulted.

TRIAL 5

6.2 Figure 6.1 shows the average densities for the two levels of fragment weights chosen and it can be seen that at 270m with the lower masonry weight the density is marginally over the acceptable level and with the higher weight it is marginally under.

6.3 Increasing the masonry debris weight from 150g to 250g reduces the secondary debris problem but much of the problem is created by quarter, half and whole bricks, i.e. debris of 500g and over. Hence the overall reduction is significant but not as considerable as might be expected

6.4 Several radial searches were carried out on Trial 5 to establish the difference, if any, in the fragment distribution radially around the site. The basic symmetry of the fragment distribution which was noted in Phase 1 is still there but is now much more marked. Figure 6.2 shows some typical results. It is particularly important to note that the levels are much higher on the untraversed sides, and that the debris falls in a very limited 10 degrees sector centred on the line perpendicular to any side of the building.

6.5 It is interesting to note the contribution of the various types of fragments to the overall density on the traversed sides.

- a. Shell: At less than 150m these represent c.30% in the SE sector and 10% in the SW sector.
- b. Brick: Up to 270m these represent 60-80% of the fragments. Beyond 270m there are virtually none found.
- c. Beyond 270m it is only large concrete and shell fragments which are found. Beyond 500m no lethal fragments were found.

TRIAL 6

6.6 Figure 6.3 shows the average densities for the two levels of fragment weights chosen and it can be seen that, in common with Trial 5, the two masonry weights give density values at 270m marginally above and below the acceptable level.

6.7 Increasing the masonry debris weight from 150 to 250g again reduces the debris problem but once again the real problem is created by large

brick fragments over 500g.

6.8 Only one radial search was carried out on Trial 6 to establish the symmetry of the fragment distribution. Again the basic symmetry of the stack is obvious with the debris falling in the same limited 10 degrees sector for Trial 5.

6.9 The contributions of the various types of fragments to the overall density on the traversed side is as follows:

- a. Brick: Up to 150m these represent c.90% of the fragments, reducing to c.60% up to 270m. Beyond 270m again there are virtually none found.
- b. Concrete: From 150m to 250m these represent c.15-30% of the fragments. Closer in there are fewer fragments which are overwhelmed by the brick.
- c. Beyond 270m it is only large concrete fragments which are found. Beyond 400m no lethal fragments were found.

6.10 As a comparison, since Trials 5 and 6 were identical apart from the actual explosives stores used, Figure 6.4 shows the average densities for the two trials using the lower masonry debris weight. It can be seen that, apart from the significant increase at 230m in Trial 6 there is practically no difference between the results for the two trials. The results are virtually identical for the higher masonry debris weight

TRIAL 7

6.11 Figure 6.5 shows the average densities for the two levels of fragment weights chosen and it can be seen that the level of one lethal fragment per 56 square metres is not reached until c.330m. Certainly at 270m the level is well in excess of the acceptable value.

6.12 Increasing the masonry debris weight from 150 to 250g again reduces the numbers of lethal fragments. However some of the concrete debris produced was very large although the overall amount of debris was not as great as for the brick buildings. Unfortunately the debris produced seemed to be spread out over greater ranges than for the brick buildings.

6.13 Two radial searches were carried out at 270m and 350m. The search at 270m gives a clearer picture and can be compared directly to the similar searches in the other trials. The basic symmetry of the stack is again demonstrated with the debris falling in the same limited 10 degrees sectors.

6.14 At all ranges the concrete represents the major contribution to the fragment density and beyond 500m there are no lethal fragments on the traversed sides.

TRIAL 8

6.15 The results demonstrate that the comment is still valid that large

brick fragments create the major problem but in this instance they are projected neither in the quantity or to the ranges experienced in Trials 5 and 6. The level of one potentially lethal fragment per 56 square metres is achieved at 230m.

6.16 A radial search was carried out at 210m to establish the symmetry of the explosion and resulting debris. Again the basic symmetry of the distribution is obvious with the debris falling in the same limited 10 degrees sector as for the previous trials.

6.17 A significant large proportion of the incorporator was reduced to metal dust although there were also significantly large pieces, particularly from the lid which carried the gear box and, inlet/outlet points, located during the large metal debris search. The corners of the building frame were projected radially out from their positions and the centre roof support was cut into three pieces. No recognisable, lethal pieces of roof covering or the water tank were recovered.

6.18 The additional large metal debris search was conducted outside the main search areas and although large pieces, particularly of the building frame, were located none of them represented an unacceptable hazard since most fell within 270m, any outside this range being isolated fragments. On the untraversed side the maximum range occurred with a piece of the representative pipework of c.500g at 430m. On the traversed sides a metal fragment of c.2kg weight, identified as part of the incorporator was also found at 430m.

6.19 Painted and numbered rocks were placed on the surfaces of the two traverses to establish the effect of scouring on the traverses. For both traverses only the rocks in the central portion of the traverse were actually displaced significantly. Of those that were displaced some fell just over the traverse whilst several were projected up to 200m range. Mr Horoschun of the Australian Department of Housing and Construction has carried out a detailed analysis of this aspect (Ref 13).

6.20 For Trial 8 the brick did not create the level of problems as was seen in Trials 5 and 6 although it must be remembered that the walls were only 280mm thick and were not load-bearing.

FIGURE 6.1

TRIAL 5 AVERAGE DENSITY ON TRAVERSED SIDES

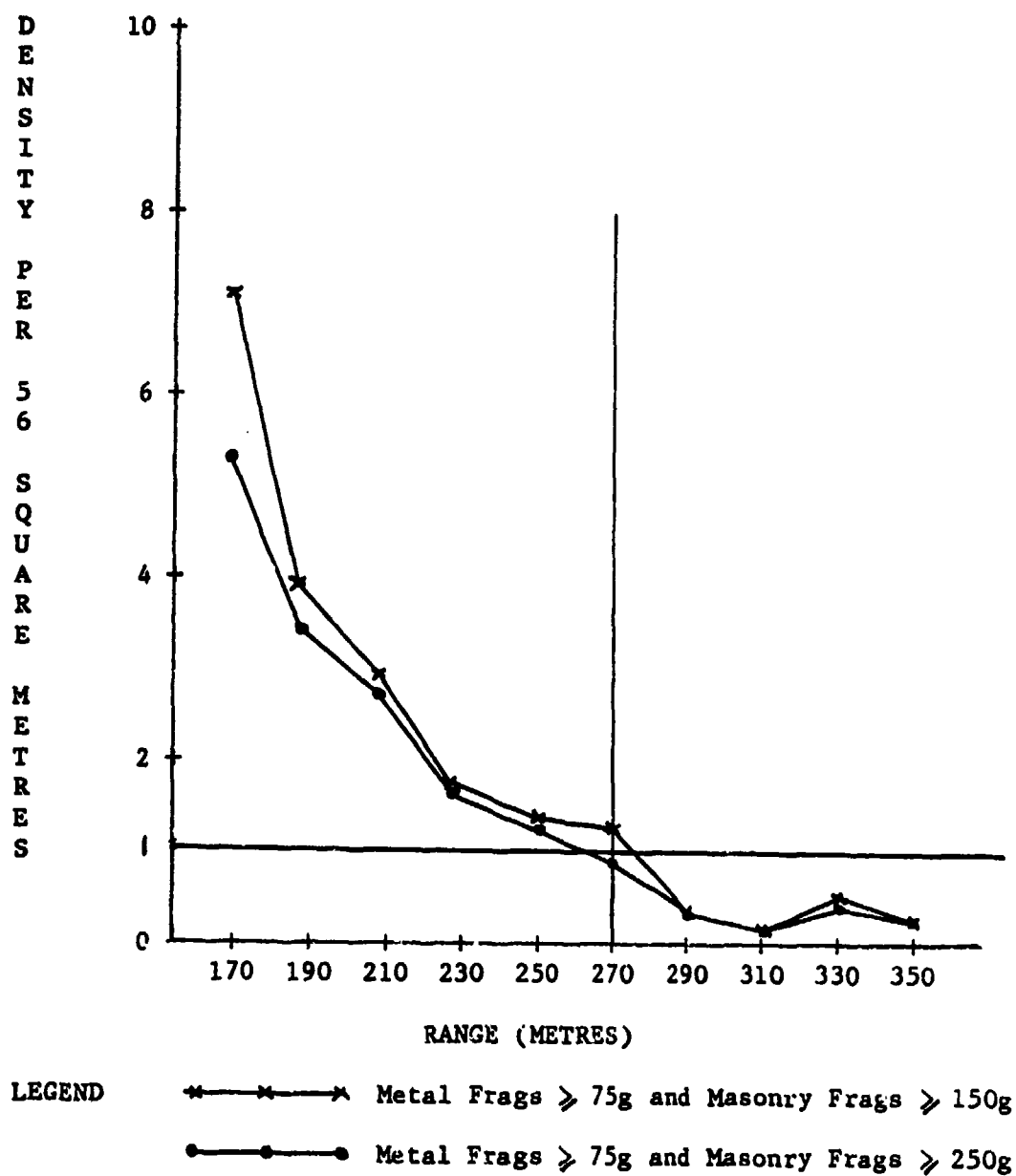


FIGURE 6.2

TRIAL 5 RADIAL DENSITY AT 290 METRES

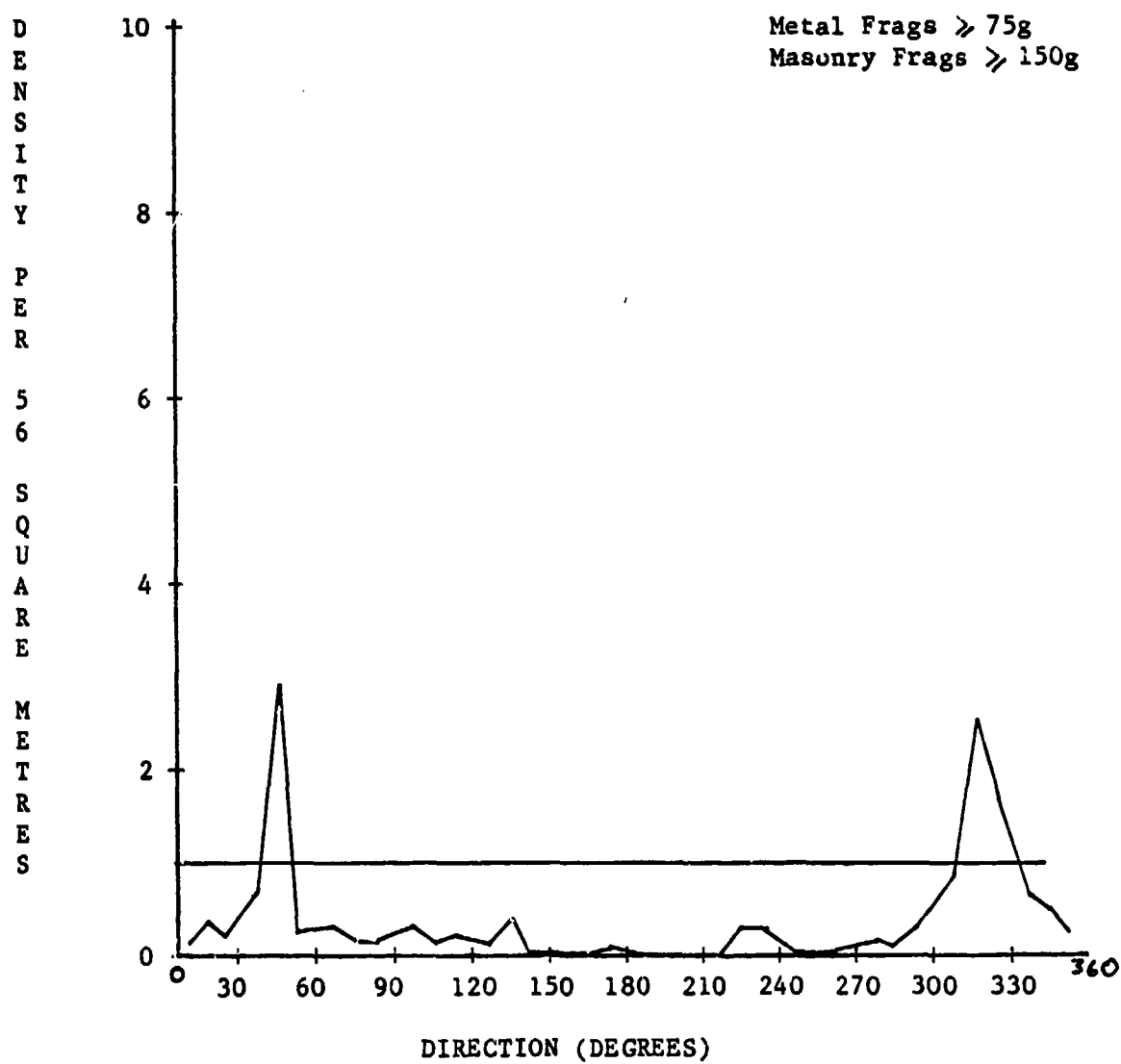


FIGURE 6.3

TRIAL 6 AVERAGE DENSITY ON TRAVERSED SIDES

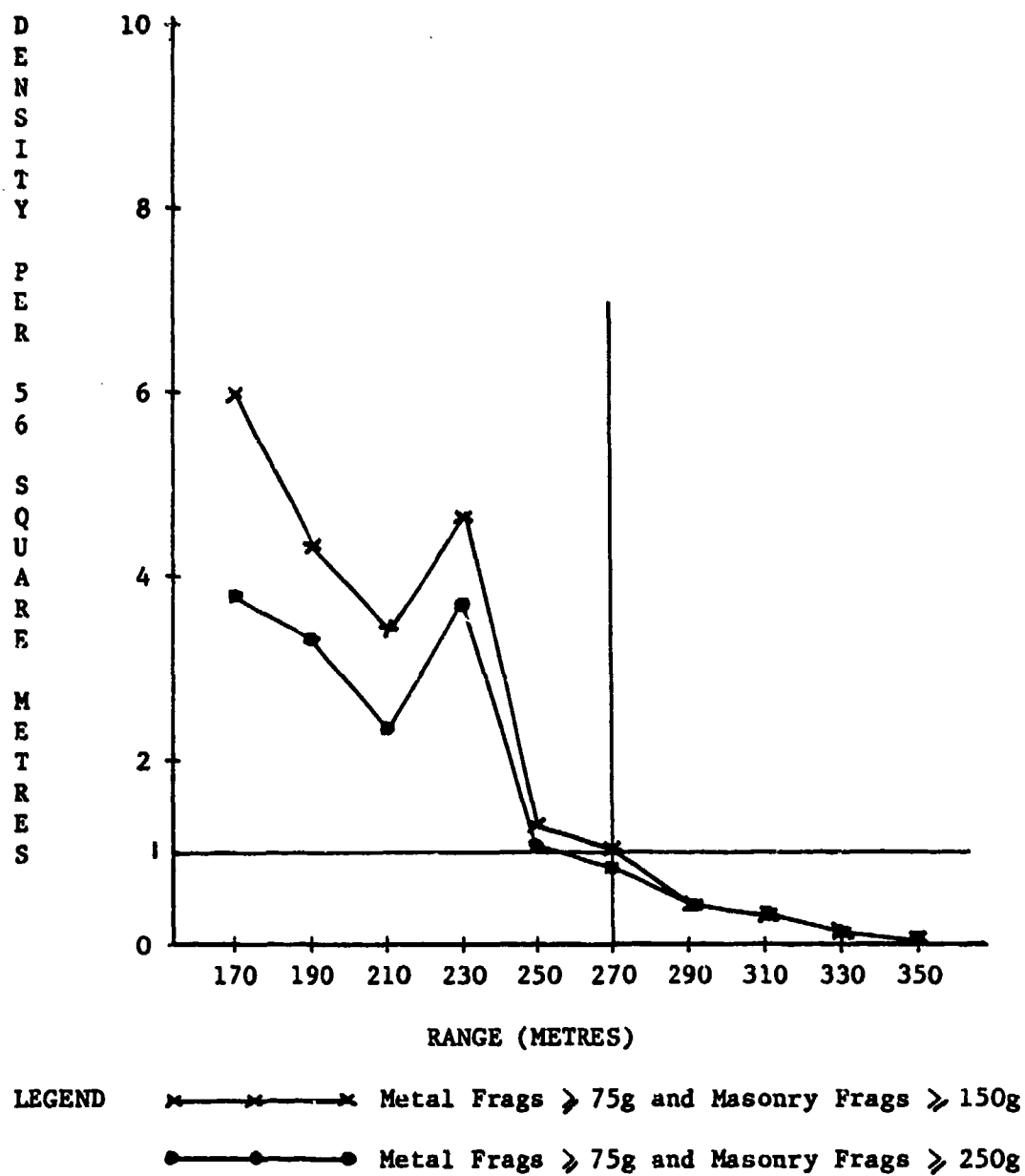


FIGURE 6.4

TRIALS 5/6 AVERAGE DENSITY ON TRAVERSED SIDES

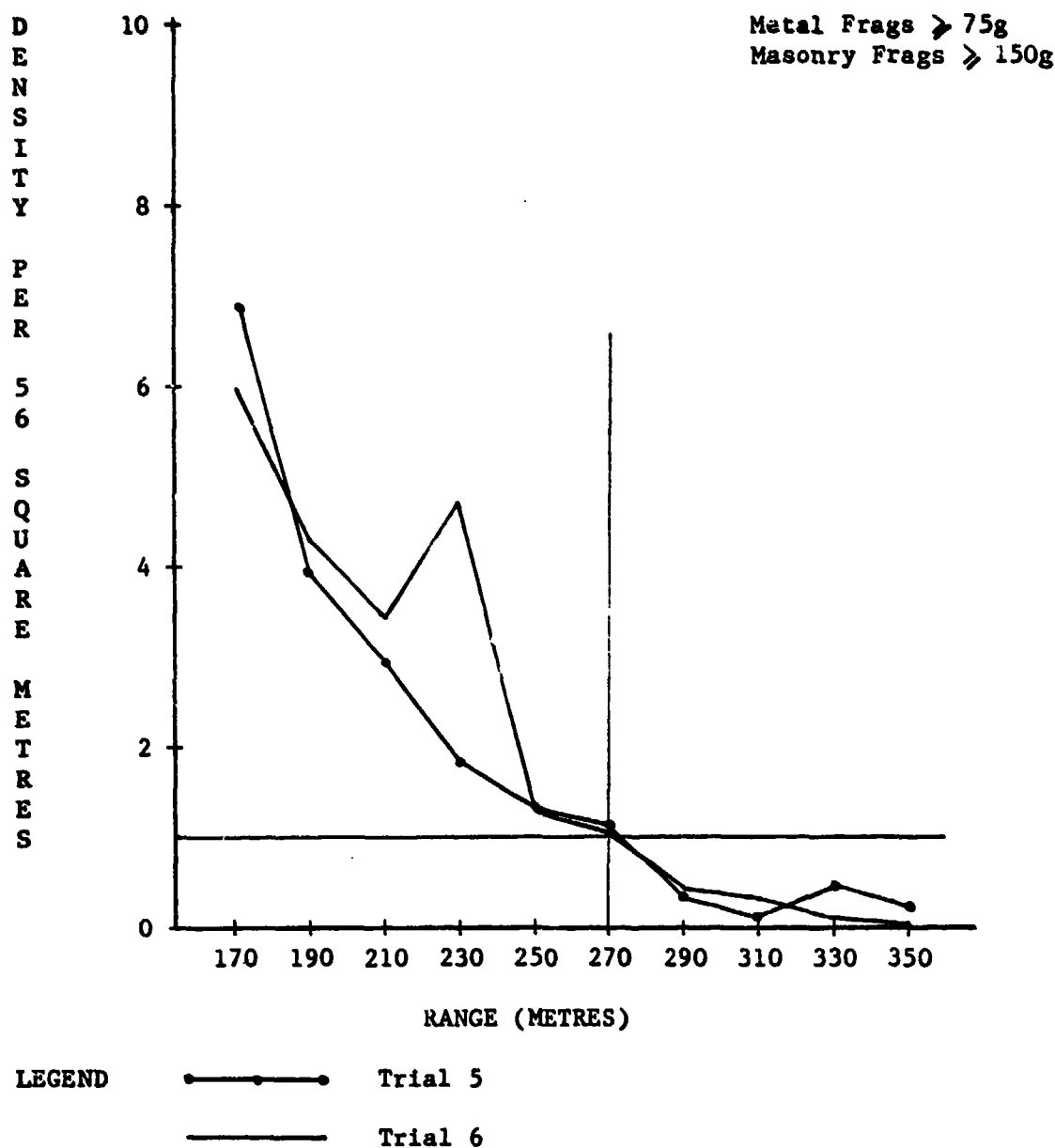
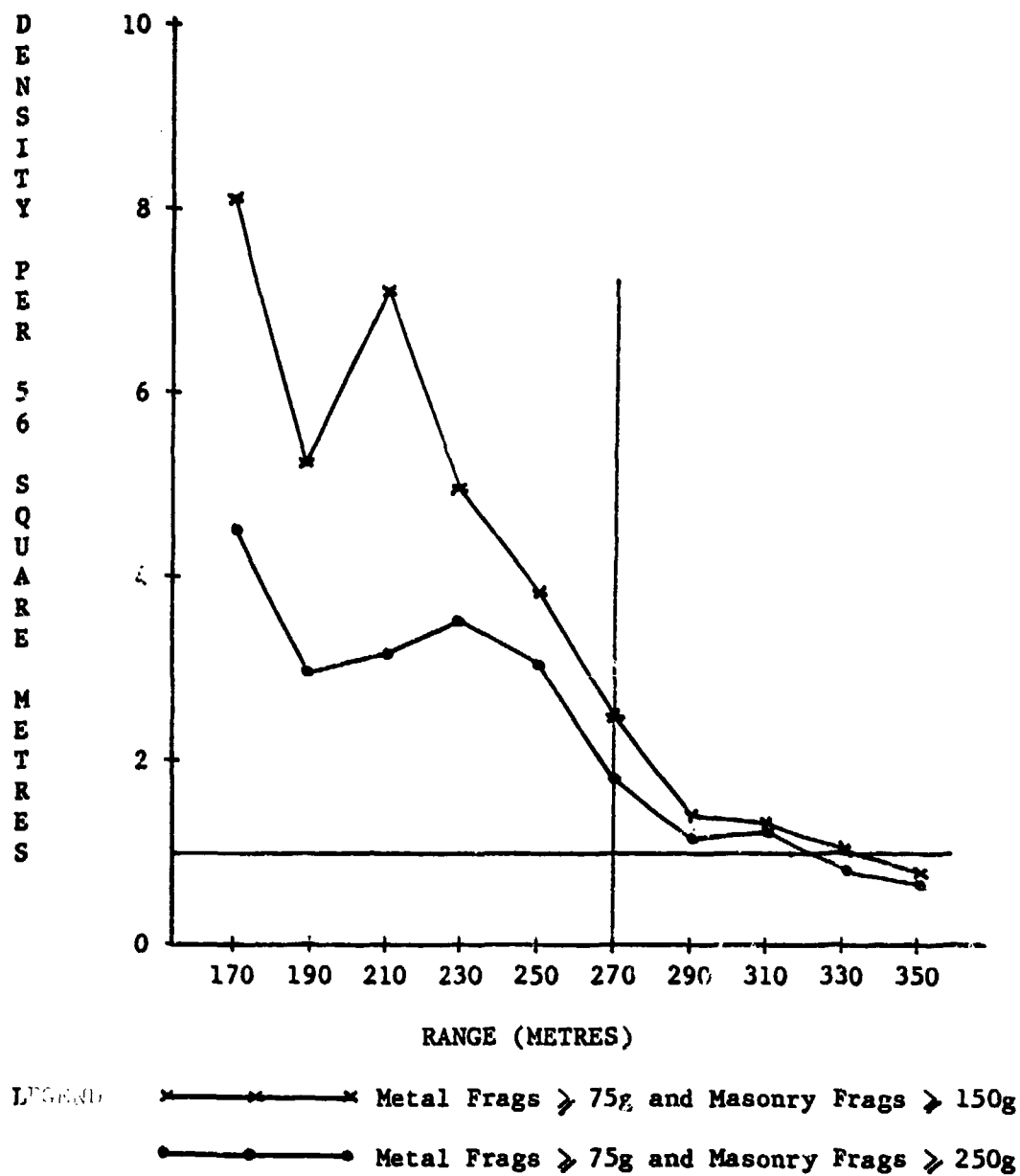


FIGURE 6.5

TRIAL 7 AVERAGE DENSITY ON TRAVERSED SIDES



7. CONCLUSIONS

7.1 The data appears to confirm the Phase 1/1B recommendation for the use of a 270 metre minimum distance for fragment and debris throw from brick buildings but does not confirm the reduced distance for concrete structures. There was in fact a considerable amount of building debris projected as had been intimated might be possible in the conclusions from Phase 1/1B. In particular the brick created an unacceptable debris hazard out to 270 metres on the limited 10 degree sectors centred on the lines perpendicular to each side of the building and in many instances reduced to almost zero outside this very restricted area. This last point is very important since it would be a gross mis-representation of the situation to say, even at 250m for instance, that the debris level was unacceptable since it is only unacceptable over approximately 10% of the area considered. This applies at all ranges and aerial photographs of Trials 6 and 8 showed that debris was being projected out perpendicularly to the sides of the building. The wall debris does spread out but not significantly and at 270m for example the total search front of 47m is more than enough to accommodate the spread of wall debris from its original 3m starting width at ground zero.

7.2 However there must remain some doubt that a brick structure would not produce unacceptable debris hazards beyond 270m. Phase 1 demonstrated that with 1800kg the bricks were pulverised to such an extent that they produced no significant hazard. Phase 2 has demonstrated that with 500kg the bricks are only broken up and produce a very serious hazard. Both trials indicate that brick debris will not go beyond c.270m and concrete, from a slab roof, will not go beyond 400-500m. It therefore seems reasonable to conclude that brick should not create a problem beyond 270m. However it should be remembered that the bricks used in Phase 1 and Phase 2 were not identical, the Phase 2 bricks being more typical of UK construction in general, although they were undoubtedly about 15-20% heavier. These bricks might not pulverise as effectively in the Phase 1 situation of 1800kg explosive loading.

7.3 There was no significant difference between the resultant debris patterns for Trials 5 and 6 and it is concluded that it is the amount of explosives which is the important factor not whether it is cased or even, it is inferred, how strong the case actually is.

Trial 7, using the concrete building demonstrated that even behind a traverse the debris hazard at 270m was unacceptable, the hazard extending out to some 350m. The overall number of building fragments produced from the concrete building was considerably less than from the brick buildings but it was distributed over a wider area, further out. It is concluded therefore that concrete buildings are not a sound concept, from a hazard point of view, for relatively small quantities of explosives (less than 6,000kg) unless only very small quantities (less than 50kg) are involved where the structures can be built to contain the effects of an explosion. Indeed there must be some doubt as to whether quantities larger than the 500kg tested would not project unacceptable levels of concrete debris to beyond 400m.

7.5 In the case of the portal frame building the level of debris is much reduced, principally because the walls were thinner and the roof was

constructed of almost frangible material instead of concrete. However it is still concluded that a distance of 270m is required to provide protection from lobbed debris provided there is a traverse at the potential explosion site. It might be possible to reduce this to around 180m if the brick infill was only 115mm since the amount of debris would be reduced by a further 50%. However this would require a detailed interpolation from the figures available or better still a further trial.

7.6 It is further concluded that for brick or concrete structures, when untraversed, a minimum distance of 400m is required to provide protection from lobbed debris.

7.7 It is also concluded that, as the traverses in both Phases 1 and 2 have remained practically undisturbed, there is no need to remove stones other than surface ones from the top third of a traverse used around buildings containing 1800kg or less of explosives. From other work currently being undertaken for Explosion Effects it would appear that such precautions may be unnecessary for any building traverse. The same may not necessarily be true for traverses around open stacks.

7.8 It is concluded that because of the reservations expressed in paras 7.2 and 7.4 the worst case situations may not, in fact, have been examined. Consequently further trials should be carried out to ascertain the following salient points:-

- a. To test a Phase 1 brick building, constructed of frogged bricks and loaded with 1800kg of shell, to determine whether the results from Phase 1 are reliable.
- b. To test the effect of a much larger loading, say 6000kg, in a typical brick storehouse.
- c. To test the effect of a much larger loading, say 6000kg, in a typical concrete storehouse.

7.9 It is also concluded that consideration should be given to carrying out at least one large test with, say 25 or 50 tonnes of bombs, as originally intended in Phase 1. This would probably be best done in a representative storehouse to ascertain that there is no specific problem created by debris at these quantities.

8. RECOMMENDATIONS

8.1 The results from Phase 2 confirm the Phase 1/1B recommendation for the use of D13 quantity-distance with a minimum fragment throw criteria of 270m for brick buildings or open stacks, traversed by the standard UK traverse. If there is no traverse the minimum distance should be 400m.

8.2 For concrete buildings the minimum distance should be maintained at 400m whether the building is traversed or not.

8.3 Further trials are recommended as detailed in paras 7.8 and 7.9 to verify that there are no additional debris problems created in buildings containing 1800-6000kg, particularly for concrete structures.

REFERENCES

1. Joint Australian/UK Stack Fragmentation Trials Phaser 2 Report
- J Henderson - D/Safety/11/55/22 of August 1985.
2. Joint Australian/UK Stack Fragmentation Trials Phase 1 Report
- F Bowman et al - D/Safety/11/55/22.
3. Joint Australian/UK Stack Fragmentation Trials Phase 1B
Preliminary Report
- ESTC/162/EE/77, WP7.
4. Joint Australian/UK Stack Fragmentation Trials Phase 1/1B
Recommendation to reduce Minimum Fragment Throw Distances
- Annex A to ESTC/163/EE/7.
5. Quantity Distances for Military Explosives
- ESTC Leaflet No.5 Part, June 1979.
6. Fragment Injury Criteria
- US(ST) IWP/11-79 dated 28 August 1979.
7. Letter Secretary EESC/Director of Trials
- D/Safety.11/55/22 dated 14 December 1984.
8. Defence Trial Directive, D/Trials, Canberra
- No.6/426 DST 85/11864 dated 18 April 1985.
9. Technical Instruction, D/Trials, Canberra
- DST 85/11864 dated 30 April 1985.
10. An Examination of Injury Criteria for Potential Application to
Explosives Safety Studies
- B R Rudolph, 21st DOD Explosives Safety Seminar.
11. Fragment and Debris Trajectories
- DWSE/188/1/3 dated 5 November 1980
12. Fragment Hazard Investigation Program
- R T Ramsey et al. 18th DOD Explosives Safety Seminar.
13. Investigation into the Debris hazard generated by rocks on Earthfill
traverses surrounding Potential Explosion sites
- G Horoschun, Department of Housing and Construction
Commonwealth of Australia

SUMMARY

Because of the restrictive nature of "minimum fragment throw criteria" and the expense of building traverses for which little credit was given, the UK Explosives Storage and Transport Committee (ESTC) decided in 1990 to conduct a series of fragment throw trials. Approaches were made to Australia resulting in Phase 1 of the trials which were fired in early 1982. As a result of reservations expressed by RARDE, UK, concerning the symmetry of the bomb stacks used in Phase 1 it was decided to carry out a Phase 1B search over part of the sites used during Phase 1. Phase 1B was carried out in early 1984.

Recommendations from the Phase 1 and Phase 1B trials resulted in a reduction of the minimum fragment throw criteria in UK Quantity-Distance tables. Additionally, Phase 2 trials were proposed to fill in missing data from the initial phases. The Phase 2 trials were fired in early 1985 and consisted of stacks of shell or explosive inside a variety of building constructions surrounded on two sides by traverses.

Fragments and debris were collected, on a sample basis, from the resulting explosions and these were then computer-sorted into a basic weight distribution against distance and direction. These results were further refined and are presented in tabular and graphical form in the full report (Ref 1). This paper is a much shortened version of the full report which contains the full basic computer sorted data and graphs of the results.

Further trials have also been proposed to consider other combinations of building constructions and stack sizes.

ACKNOWLEDGEMENTS

The UK authors wish to acknowledge the major contribution made by the Australian Department of Defence to the work reported here. The work was made possible by the use of the Woomera range and the effort provided by the Director of Trials, the Australian Army and the Materials Research Laboratories.

The trials were arranged through British Defence Research Scientific Staff Canberra (Dr R M Allen) with Director of Trials (Group Captain Coutts). The main contributors to the trials were the Australian Army (Project Officer Field, Major J Goodwin with EOD Staff and Lt P B Wright commanding the detachment from 21 Construction Squadron), Materials Research Laboratories, Melbourne (under Mr D J Hatt) and DSCW Personnel at Woomera (under Mr D Fall). Staff were also supplied from Australian Ordnance Factories to carry out weighing and sorting of fragments.

The trials would not have been possible without the aid of Department of Defense Explosives Safety Board who supplied surplus 175mm shell for use in the trials.

The trials proposals were discussed in detail with UK Ordnance Board, RARDE and ESTC. The results were endorsed by ESTC in June 1986.

AD-P005 378

TWENTY-SECOND DOD EXPLOSIVES SAFETY SEMINAR
26-28 AUGUST 1986, ANAHEIM - CALIFORNIA

TECHNICAL EVALUATION OF THE LIMITS OF THE HAZARDOUS
AREAS AS TO PROJECTIONS

BY

P.X. BOISSEAU*

D. HOUDUSQUE

R. KENT

SOCIETE NATIONALE DES
POUDRES ET EXPLOSIFS

* SNPE-CRB - P.O. BOX N° 2 - 91710 VERT LE PETIT - F R A N C E
TELEX 690479 Poudres F

1 - INTRODUCTION

↙ The French safety regulation on explosives gives fixed limits to the different hazardous areas as to projections. These fixed limits are under certain circumstances inadequate. This situation led the SNPE to develop a technical approach for the delimitation of the hazardous areas. This approach can be summed up in two parts :

* Elaboration of technical criteria for the limits of the different hazardous areas as to projections such as conditional probability of reaching person by hazardous fragments;

↘ Development of tools to predict fragments range and densities by computer codes and methods to assess experimental data like initial velocity of primary fragments, Gurney and Mott's coefficients, etc...

On one hand, this paper presents the technical criteria adopted by the SNPE, and on the other hand, the computer code DENSECLA. This software calculates the fragments densities, and then, evaluates the limits of the different hazardous areas through the conditional probability of lethality. ↗

2 - DISTANCES FIXED BY THE FRENCH REGULATION

The French regulation defines five areas of decreasing levels of potential damage towards persons and properties around the donor : Z1, Z2, Z3, Z4, Z5 and a sixth area, outside the five first must be considered

For example, Z1 corresponds to lethal injuries in more than 50 % of cases for person supposed to be present and unprotected, and Z2 corresponds to serious injuries which may be lethal.

The hazardous areas are circular or annular and the 5 radii of limits (R1, R2, R3, R4, R5) are fixed by the french regulation in function of the quantity of active substance and of the hazard division of the donor.

In this paper, the zone outside Z5 will be named "Low Danger Zone"

These fixed distances are described in the Table 1.

TABLE 1

FIXED DISTANCES AS TO PROJECTION HAZARDS (1.2 DIVISION)

Q in kg of active substance		RADII OF LIMITS (m)				
		Z1/Z2	Z2/Z3	Z3/Z4	Z4/Z5	Z5/LDZ
Q ≥ 100	A	15	90	200	$\frac{1}{6}$ 60 Q or 300 if 300 ≥ 60Q	$\frac{1}{6}$ 120 Q or 600 if 600 ≥ 120Q
	B	25	135	300	$\frac{1}{6}$ 75 Q or 400 if 400 ≥ 75Q	$\frac{1}{6}$ 150 Q or 800 if 800 ≥ 150Q
10 ≤ Q < 100	A	= 2/3 of the radii defined for Q ≥ 100 kg				
	B					
Q < 10	A	Radii have to be evaluated by a technical study				
	B					

- A - case of caliber not exceeding 60 mm or emitting projections of more than 150 g at more than 15 m. but emitting no projection of more than 250 g at more than 15 m.
- B - case of caliber greater than 60 mm or emitting projections of more than 250 g at more than 15 m.

3 - DISSATISFACTIONS CONCERNING THESE FIXED DISTANCES

In some cases, these fixed distances are inadequate :

- A given area can be reached by a high number of projections, or on the contrary there is a very low level of probability of hitting somebody.
- One possible fragment does not create by itself a hazardous area.
- There is no distance indicated when Q is less than 10 kg for 1.2 products.

All these dissatisfactions led the SNPE to develop a tool for predicting the fragments hazards.

4 - PROBABILISTIC APPROACH

The probabilistic approach is authorized by the french regulation, in general. Other regulations, accepting a probabilistic approach, do exist also. We can quote the DARCOM-385-100 of the US Army of 17 August 1981.

We can define the technical level of hazard of a given area by the probability of injuring or killing somebody supposed to be present. But before describing the technical criteria adopted by the SNPE, let us precise some definitions.

. Kinetic energy of the projection, E in Joule

. Frequency of explosion F

This is the probable number of explosions during a year.

. Conditional probability of reaching CPR

This is the probability of reaching somebody, supposing he is present in a given area, supposing the explosion has occurred, by one fragment or more.

. Conditional probability of reaching CPR_E

This is the probability of reaching somebody, supposing he is present in a given area, supposing the explosion has occurred, by one or more fragments of a given range of energy.

. Annual frequency of reaching AFR

This is the annual frequency of reaching somebody, supposing he is present in a given area, by one or more fragments.

. Annual frequency of reaching AFR_E

This is the annual frequency of reaching somebody, supposing he is present in a given area, by one or more fragments of a given range of energy.

. Degree of lethality of a fragment DL_E

The lethality of one projection can be described as the probability that it is lethal. We call this number "Degree of lethality" (lain between 0 and 1) and it is a function of the kinetic energy of the projection.

. Conditional probability of lethality CPL

This is the probability of killing somebody, supposing he is present in a given area, supposing the explosion has occurred, taking into account the degree of lethality of each projection.

5 - TECHNICAL CRITERIA USED BY S.M.P.E.

TABLE 2

TECHNICAL CRITERIA ASSOCIATED TO THE LIMITS OF THE
DIFFERENT HAZARDOUS AREAS

LIMIT	TECHNICAL CRITERIA	
Z1/Z2	CPL = 0.5	
Z2/Z3	CPL = 0.1	
Z3/Z4	CPR = $3 \cdot 10^{-2}$	} BY ONE PROJECTION OR MORE OF MORE THAN 8 JOULES OF ENERGY
Z4/Z5	CPR = 10^{-2}	
Z5/LDZ	AFR = 10^{-7}	

These criteria correspond to levels of potential damage towards persons. The CPL are evaluated taking into account all the fragments with a kinetic energy of more than 8 Joules. We will detail the lethality of projections in paragraph 6.2.4..

REMARK : The Z4/Z5 limit criterion corresponds to the criterion of one fragment or missile per 600 ft² ; the probability of hitting a man standing up and facing the explosion is approximately 1/100.

6 - THE COMPUTER CODE DESECLA

This computer code provides a flexible tool for predicting the fragment hazard of cylindrical explosive systems.

For example : propellant or explosive mixer, melt kettel, etc...

This code is bi-dimensional for vertical cylinder and tri-dimensional for horizontal cylinder.

6.1. Configurations

6.1.1. Vertical configuration

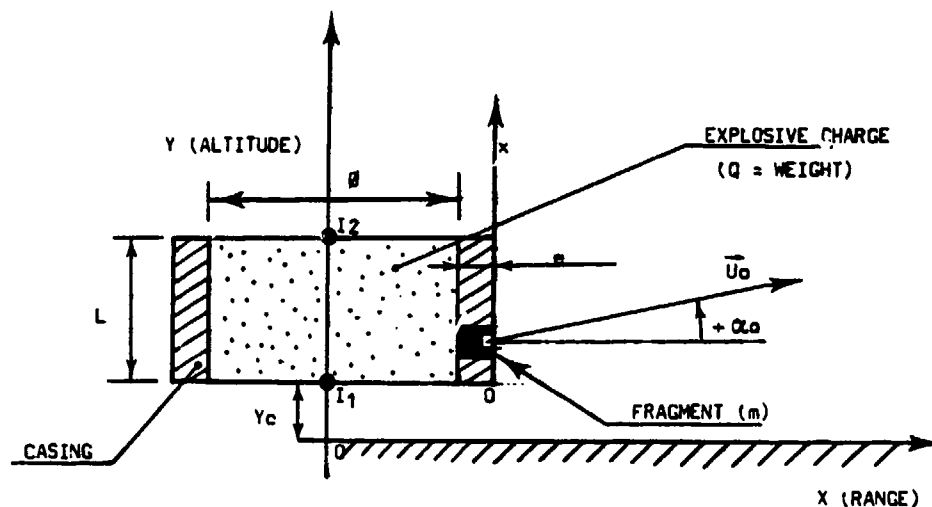


FIGURE 1
VERTICAL CONFIGURATION

Where

I_1 or I_2 = Local initiation point

Q = explosive weight

M = weight

Y_c = height

L = length

\emptyset = inside diameter

e = thickness

m = weight

x = location along casing

$U_0(x)$ = initial velocity

$\alpha_0(x)$ = initial trajectory angle

$Y_0 = Y_h + x$ = initial altitude

casing

fragment

6.1.2. Horizontal configuration

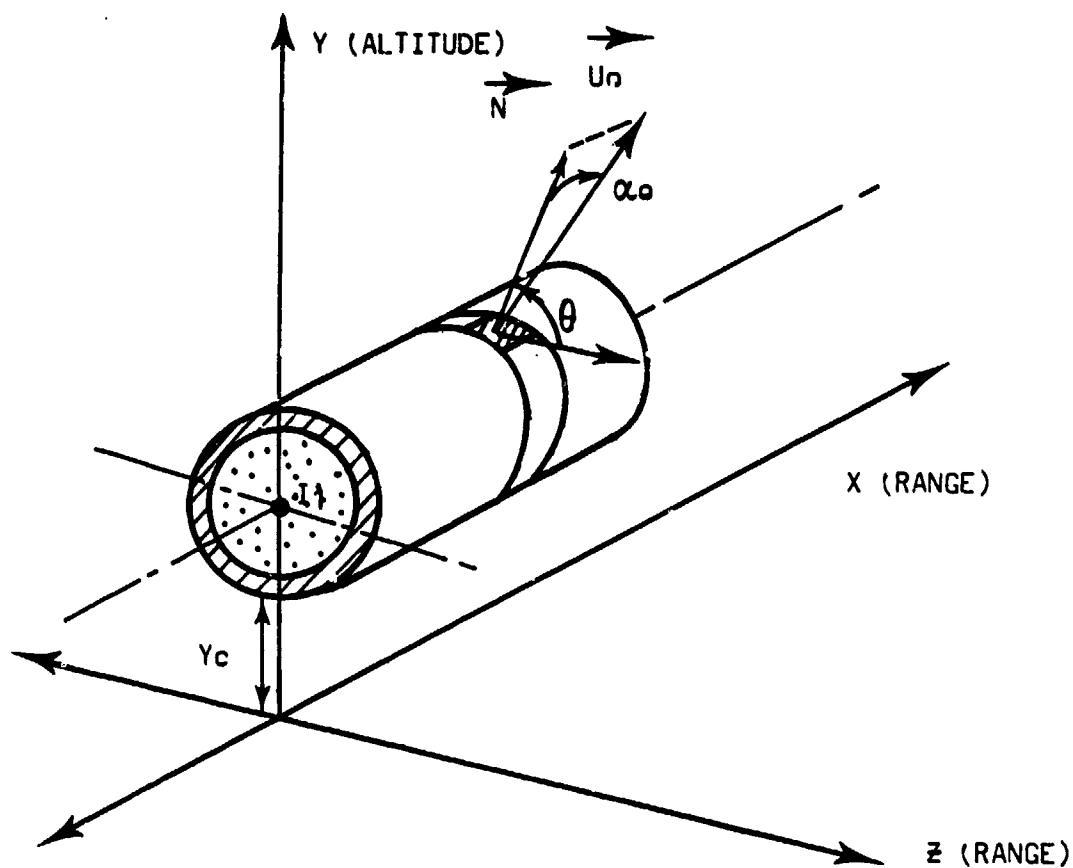


FIGURE 2

HORIZONTAL CONFIGURATION

Where

I_1, I_2, U_o, α_o same parameters as for vertical configuration

θ = angle between the normal to the fragment area and the horizontal direction.

6.2 Computation

6.2.1. Fragmentation and input data for ballistic calculation

- the fragment mass distribution is evaluated with the Mott formula and supposing a uniform radial distribution.

- the fragment initial velocity with the modified Gurney formula or with experimental data.

- the fragment initial trajectory angle with the modified Taylor formula or with experimental data.

6.2.2. Fragments trajectories

They are calculated with the fourth order Runge Kutta method and considering that :

C_x is function of the Mach number

\bar{A} , average presented area, is function of (fragment mass)^{2/3}

6.2.3. Fragments densities

Two fragments densities are calculated :

- a vertical density
- a ground density

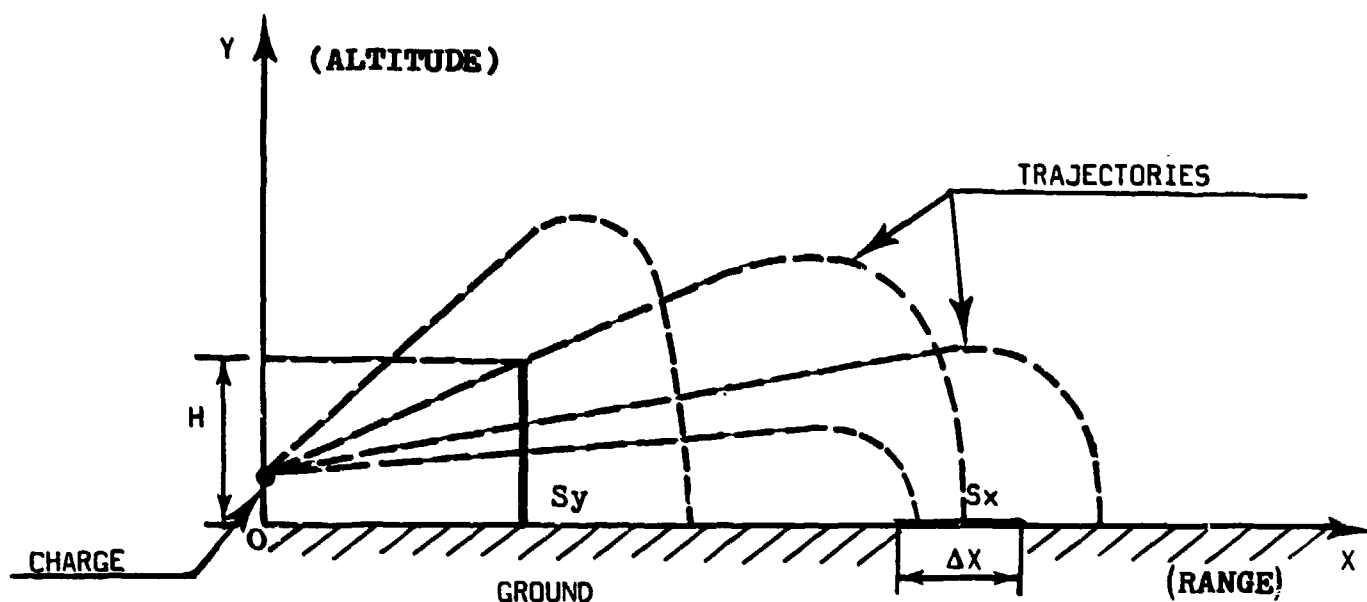


FIGURE 3

DEFINITION OF THE AREAS TAKED INTO ACCOUNT FOR THE FRAGMENTS DENSITIES

- Vertical density : $(dy)_E = (NE)_y / S_y$
- Ground density : $(dx)_E = (NE)_x / S_x$

with . $(NE)_y$ = number of fragments impacting S_y with a kinetic energy $\geq E$

. $(NE)_x$ = same definition but for S_x

. $S_y = Y_h \cdot \Delta X \cdot 2\pi$ = vertical area

. $S_x = X \cdot \Delta X \cdot 2\pi$ for the vertical configuration

= $\Delta X \cdot \Delta\beta$ for the horizontal configuration

where :

H = height of the vertical area S_y

ΔX = range increment calculation

$\Delta\beta$ = angular increment calculation (the ground area surrounding the horizontal cylinder is separated in different angular sectors of $\Delta\beta^\circ$ for the computation)

6.2.4. Probabilities

. conditional probability of reaching $(CPR)_E$
the conditional probability of reaching a volume defined by a vertical area
and a ground area, is calculated by the following relation :

$$CPR_E = (CPR_E)_x + (CPR_E)_y - (CPR_E)_x (CPR_E)_y$$

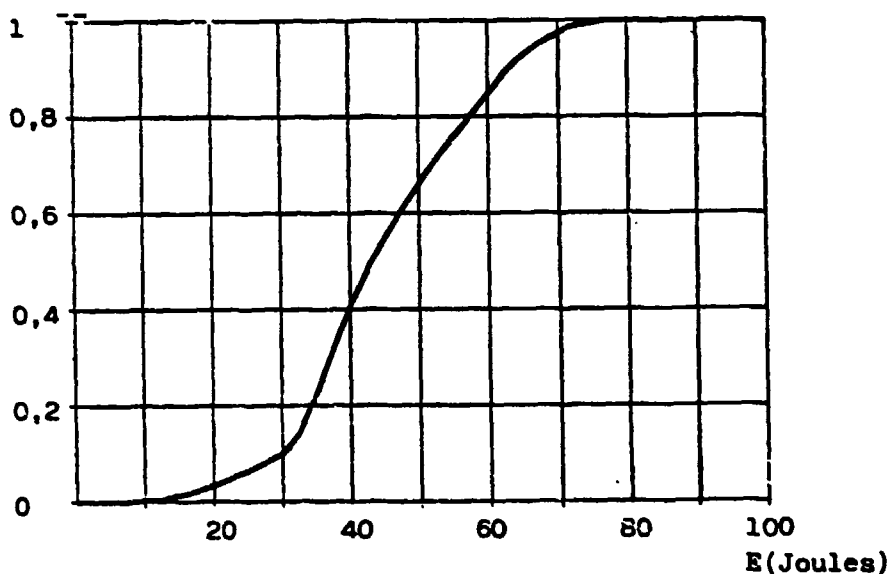
with, supposing a Poisson's distribution :

$$(CPR_E)_{x,y} = 1 - \exp - \left[\frac{(dx,y)}{E} \cdot S_{x,y} \right]$$

For a man standing up : $S_x = 0.26 \text{ m}^2$
 $S_y = 0.58 \text{ m}^2$
 $H = 2 \text{ m}$

. Conditional probability of lethality (CPL)

$$CPL = 1 - \frac{E_{max}}{E - 8J} (1 - CPR)^{DL_E}$$



DL = 1 → E = 79 J
DL = 0 → E = 8 J

FIGURE 4

DEGREE OF LETHALITY OF A FRAGMENT VERSUS ITS KINETIC ENERGY

. Annual Frequency of reaching

AFR = CFR . F

6.3. Examples of computation

6.3.1. Vertical configuration

. Input data

- | | |
|-------------------------------------|-------------------------------|
| - Mass of explosive charge | $Q = 3,000 \text{ kg}$ |
| - Detonation velocity | $UD = 7,657 \text{ m/s}$ |
| - Density of casing | $\rho = 7,800 \text{ kg/m}^3$ |
| - Inside diameter | $\phi_i = 1,625 \text{ m}$ |
| - Thickness | $e = 0.0225 \text{ m}$ |
| - Length | $L = 0.89 \text{ m}$ |
| - Height | $Y_c = 1.0 \text{ m}$ |
| - Experimental angular distribution | |
| - Point of initiation : bottom | |

. Output data

The calculated initial velocity of the fragment versus its location along casing and the experimental angular distribution are indicated on figure 5 here after.

The conditional probabilities of reaching and lethalties versus range are illustrated on figure 6 and table 3 describes the radii of the hazardous areas defined by the regulation and computed with Densecla.

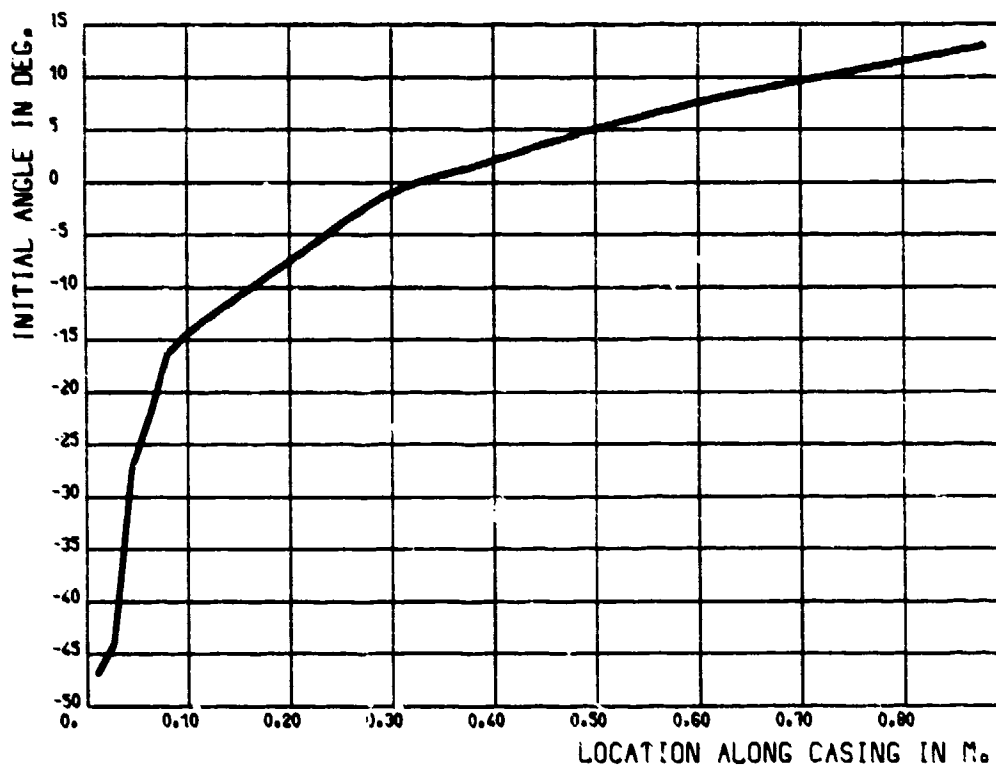
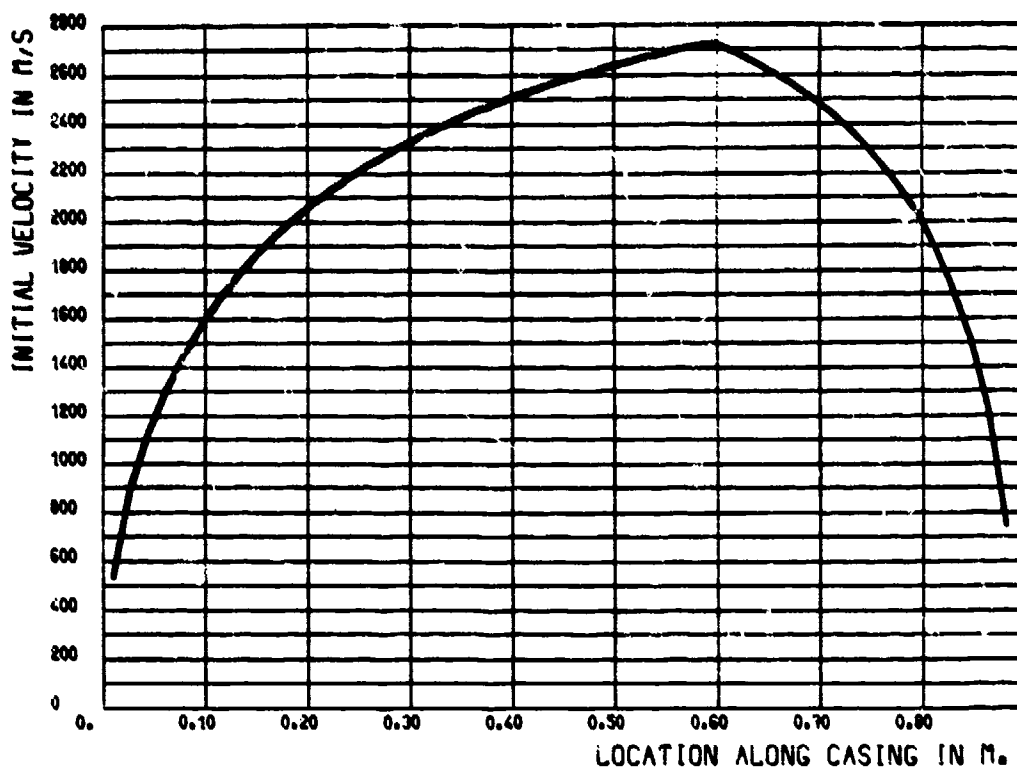


FIGURE 5

INITIAL VELOCITY AND ANGLE VERSUS LOCATION ALONG CASING

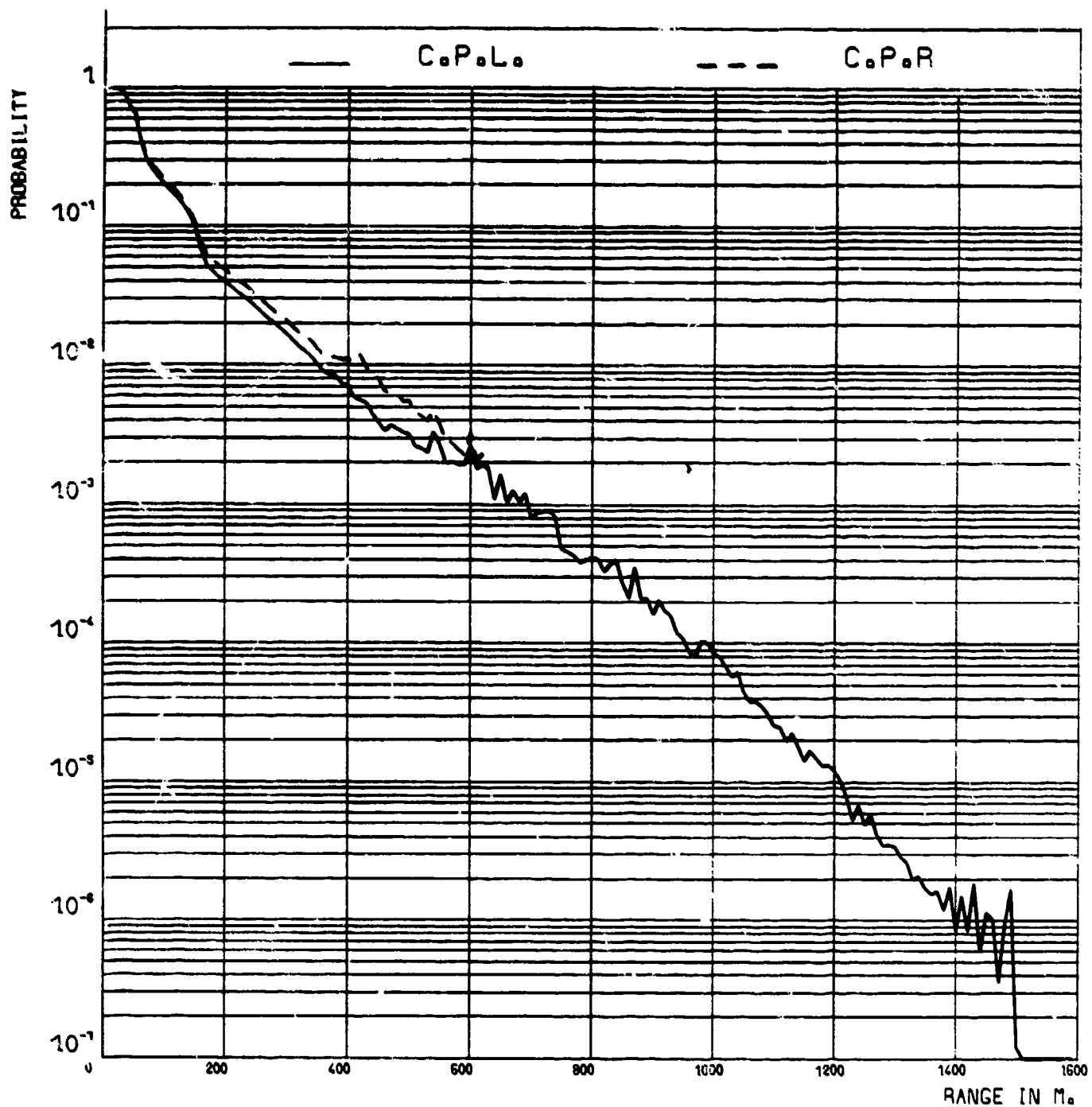


FIGURE 6
PROBABILITIES VERSUS RANGE

TABLE 3
RADII OF THE HAZARDOUS AREAS

RADII	PROBA.	VALUES OF THE RADII (M)		
		DENSECLA	FIXED	DISTANCES
			1.1	1.2
R1	CPL = 0.5	52	88	25
R2	CPL = 0.1	150	140	135
R3	CPR = $3 \cdot 10^{-2}$	255	260	300
R4	CPR = 10^{-2}	428	390	400
R5	AFR = 10^{-7}	988	772	800

6.3.2. Horizontal configuration

. Input data

- Mass of explosive charge
- Detonation velocity

$$Q = 13 \text{ kg}$$
$$U_D = 7,000 \text{ m/s}$$

- Mass of casing
- Density of casing
- Inside diameter
- Thickness
- Length
- Height

$$M = 20.6 \text{ kg}$$
$$\rho = 7,800 \text{ kg/m}^3$$
$$\phi = 0.20 \text{ m}$$
$$e = 0.01 \text{ m}$$
$$L = 0.40 \text{ m}$$
$$Y_c = 1.00 \text{ m}$$

- Experimental angular distribution
- Initiation point = right side

. Output data

The limit of the six areas are indicated in the figure 6 on 180° because of the symmetry presented by this configuration.

The figure 7 presents in three dimensions the CPR versus range for each angular sector of 10° .

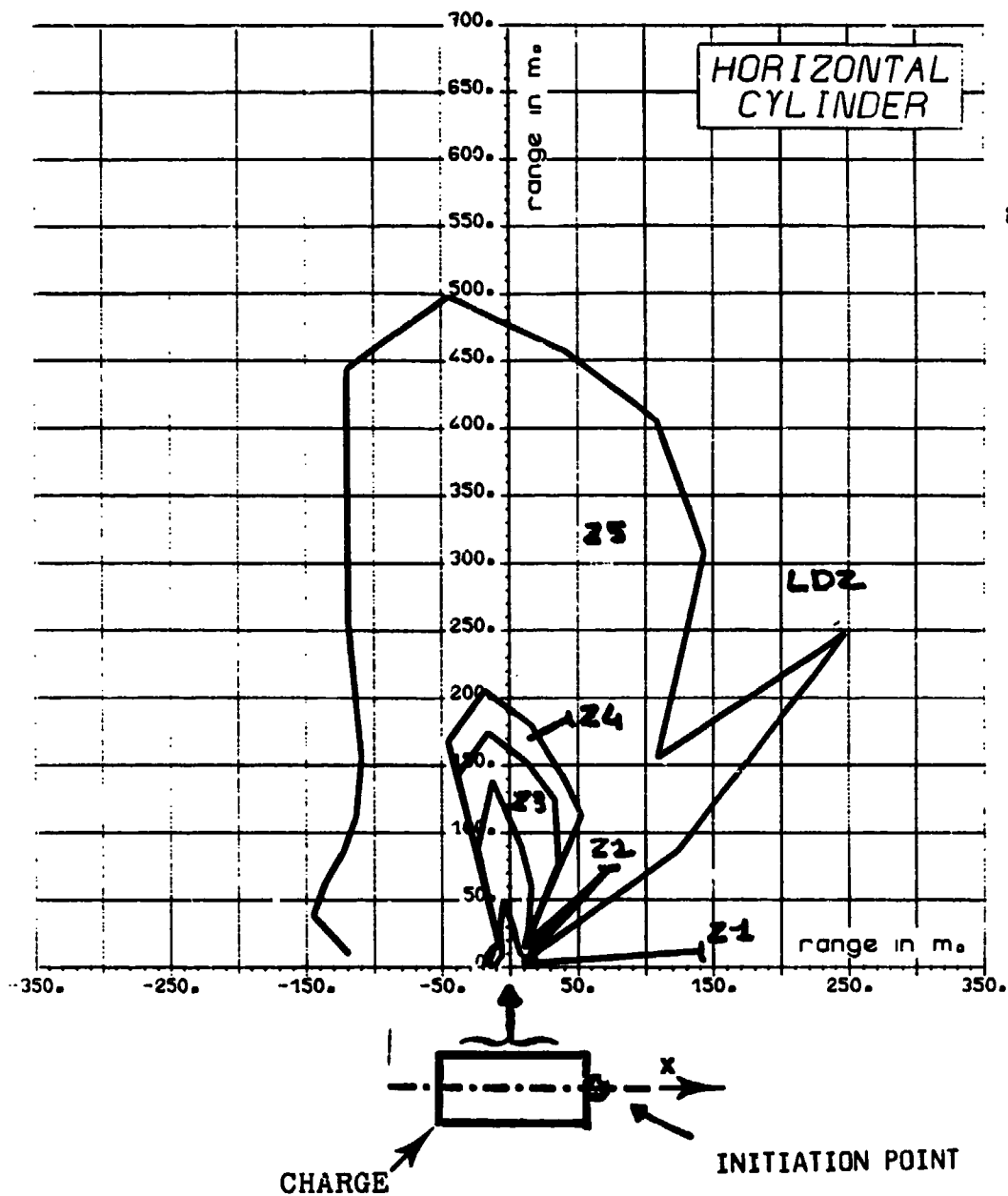


FIGURE 6
LIMITS OF THE HAZARDOUS AREAS

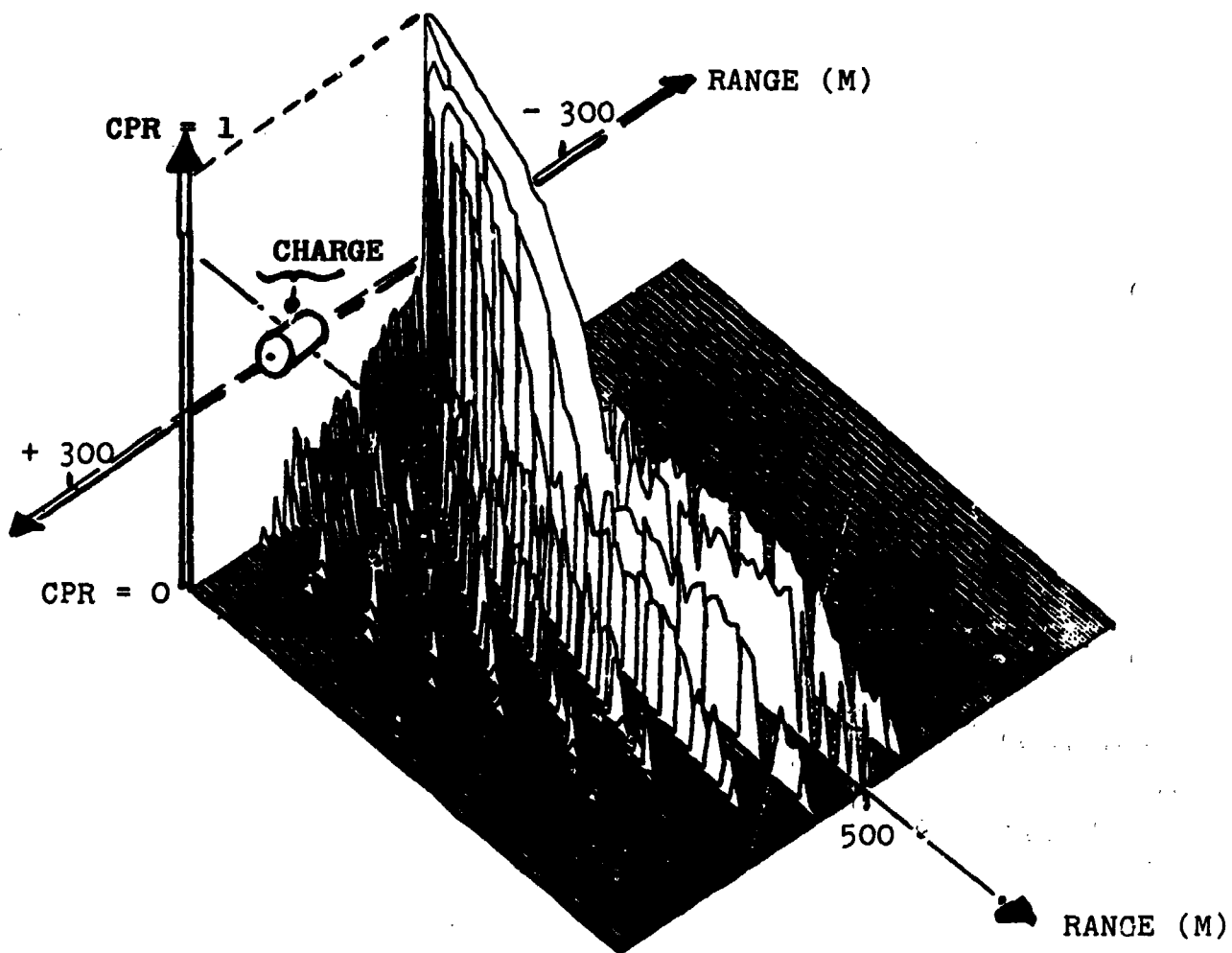


FIGURE 7
CONDITIONAL PROBABILITY OF REACHING VERSUS RANGE
FOR EACH ANGULAR SECTOR OF 10°

7 - CONCLUSIONS

SNPE has now the means of studying the projection hazards. The computer code, Densecla, is one of our tool for such a study. But we still have to develop some particular topics like lethality of projections and particularly lethality of penetrating missiles which is, for the moment, only evaluated in function of its kinetic energy.

1908

VELOCITY MEASUREMENTS OF ACCEPTOR WALL FRAGMENTS FROM
THE MASS DETONATION OF A NEIGHBORING ABOVEGROUND
BARRICADED MUNITION STORAGE MAGAZINE MODEL

G. Bulmash
C. N. Kingery
G. A. Coulter

Ballistic Research Laboratory
Aberdeen Proving Ground, MD 21005-5066

AD-P005 379

$2W$ to the $1/3$ Power Abstract

This report presents the results of a study designed to determine if fragments from the most severely loaded wall of an aboveground brick munition storage magazine would cause a mass detonation of the munitions within the magazine. Unreinforced, scored concrete of similar density was substituted for brick in the wall of the acceptor. The blast loading is the result of a mass explosion in a neighboring magazine which is located at a separation distance of $K_2 (2W)^{1/3}$; the magazines are separated by earth barricades. Responding and non-responding $1/23.5$ scaled models were designed for the tests. Velocity measurements were obtained by using voltage interrupt wire screens. It was determined that the maximum fragment velocity, 10.8 m/s, is too low to initiate a sympathetic detonation.

I. INTRODUCTION

This study was sponsored and funded by the Department of Defense Explosive Safety Board (DDESB). In Machrihanish, Scotland munitions are stored in aboveground brick magazines that are surrounded on three sides by earth barricades and located at a separation distance of $K_2 (2W^{1/3})$. The U.S. Navy stores weapons in this facility. It is the purpose of this report to determine if a mass explosion in one magazine, the donor, would result in a sympathetic mass explosion in the nearest neighbor magazine, the acceptor. The direct cause of a mass explosion in the acceptor would be high velocity fragments from the acceptor wall.

In the test procedure section of this report will discuss the scaling and simplifying assumptions used to go from the full scale Machrihanish site to a feasible test layout. This section will also cover the design and construction of the concrete donor magazine, the concrete acceptor wall, and the steel nonresponding models. Static and dynamic tests to establish the strength of the concrete acceptor wall will be discussed as well as dynamic shock tube tests on the acceptor wall that approximate the blast loading expected in the field tests. The instrumentation used to measure blast pressures and wall fragment velocities will be described, and the test layout and firing program will be presented.

The results section will first present the field blast data, and show it is reasonable and consistent. Data establishing the concrete acceptor wall strength will be presented. Preliminary velocity data from the shock tube velocity tests will be discussed. Fragment velocity data from the field tests will be reduced and analyzed. It will be shown that the fragment velocities measured in this study are less than those calculated when the same blast loads are applied to unbounded fragments. This is the upper limit on the velocity. Comparisons with other model studies concerning fragment or debris velocities will be presented.

Finally, the report will conclude that the maximum velocity obtained, 10.8 m/s, is too low to initiate a sympathetic detonation. A busy reader who has faith and is interested in results may proceed to Section III D, "Field Tests Fragment Velocities," where the essence of this report is presented.

II. TEST PROCEDURE

A. Scaling and Simplifications

The Machrihanish magazines of interest are brick and concrete structures 9.67 x 7.82 x 3.65 meters. The walls are composed of a double layer of brick with an air cavity between the layers; the floor and ceiling are made of concrete. These magazines contain a mixed explosive load, typically mines, torpedoes, and destructors (Reference 1).

The authorized mass of high explosives that may be contained in the Machrihanish magazines that are being studied is 13,000 kg (Reference 1). Kingery made the conservative assumption that 13,000 kg of mixed explosives could be modeled with an equivalent amount of Pentolite (Reference 2). The 13,000 kg full scale charge weight was scaled to a one kg bare, hemispherical Pentolite charge for this experiment. Applying cube root scaling, a one kg test charge results in a 1/23.5 scale model; the donor, acceptors, and barricades are 1/23.5 scale.

The Machrihanish magazines are simple structures designed to protect munitions from the weather and allow for quick access. However, attempting to model the strength of even these basic structures on a 1/23.5 scale was impractical. The best approach was to scale the mass by constructing the responding models of similar materials*.

B. Models

Three scale models were designed for this program: a responding concrete donor structure, a nonresponding acceptor model instrumented with piezoelectric transducers, and a nonresponding steel acceptor with one responding concrete wall.

1. Concrete Donor Model. The concrete donor model, which is used to simulate a mass explosion in a full scale magazine, is composed of five separate concrete slabs and a cardboard door. The cardboard door simulates the relatively unsubstantial door in the real magazine, a door designed to readily fail and focus the blast forward away from neighboring magazines. Refer to Figure 1, a photograph showing the floor, walls, and roof; the door is not present. Also evident on Figure 1 is a small hole for emplacing the detonator and a groove for the detonator wire. The one kg bare Pentolite charge is centered on this hole. These slabs were poured in small wooden forms, and copper wire was placed in the soft concrete in a criss-cross pattern. The rebar was used to prevent the slabs from breaking while being handled. The slabs were made from "Sakrete Sand Mix;" gravel could not be incorporated in the mixture because the stones have a larger diameter than the slab thickness. The roof has the minimum thickness of 0.64 cm, and the floor has the maximum thickness of 1.27 cm. To create a complete donor structure, the slabs and door were placed together. The parts stood on their own; no binding material was used to hold this model together.

In creating this donor magazine model no attempt was made to explicitly match the strength of the full scale magazine. Sand based concrete mix was used because it has a density approximately equal to that of the brick and concrete in the original structure. In this manner, the dimensions and mass were both scaled by 1/23.5. The density of the brick walls in the Machrihanish magazines is $1,910 \text{ kg/m}^3$, and the density of the concrete roof is $2,224 \text{ kg/m}^3$ (Ref. 1). A sample of the concrete models had a density of $1,959 \pm 206 \text{ kg/m}^3$.

* W. E. Baker, Wilfred Baker Engineering, San Antonio, TX, August 1984, private communication).

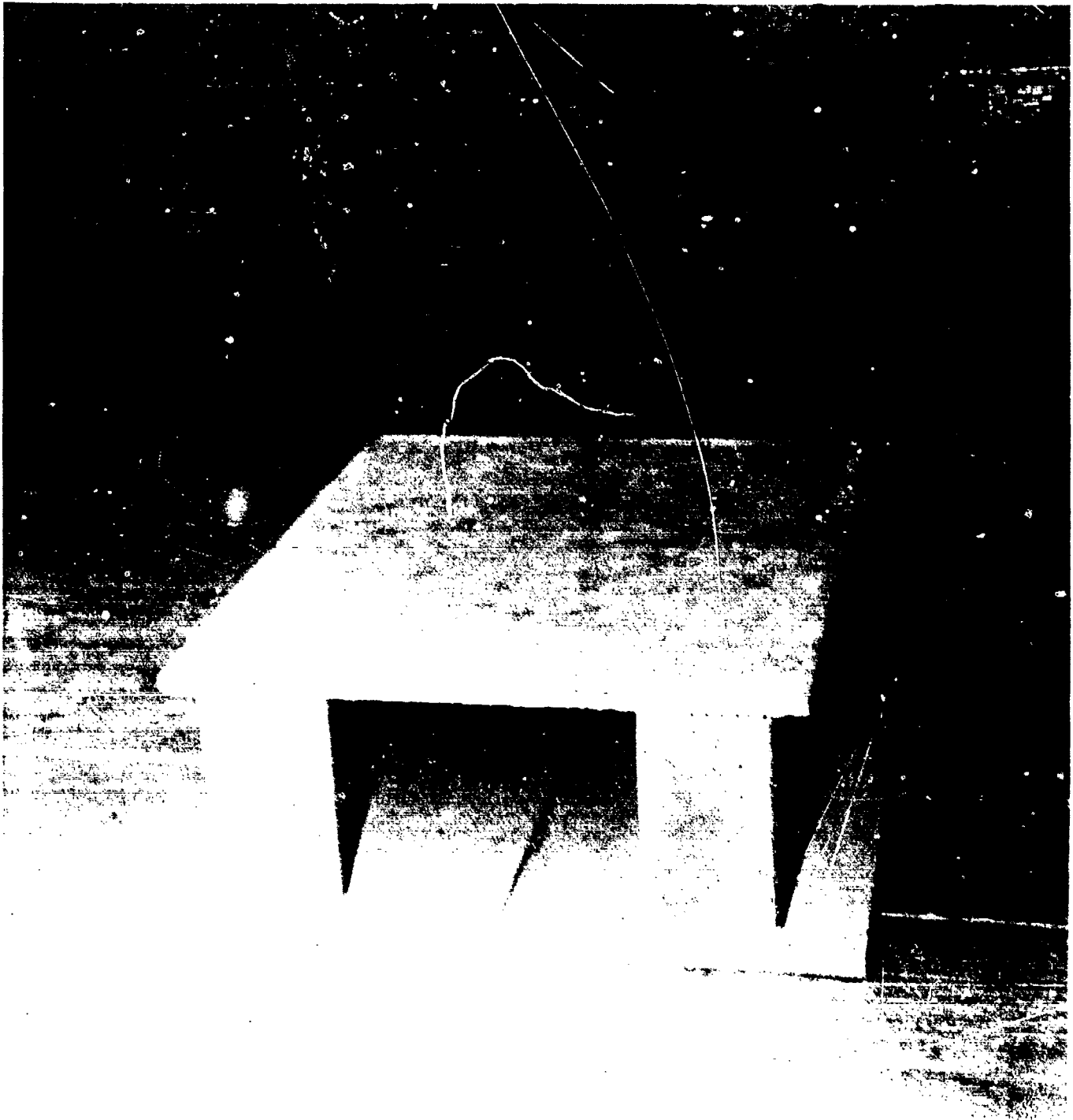


Figure 1. Photograph of Concrete Donor Model

2. Steel Nonresponding Acceptor Model. The purpose of this model is to document the blast loading experienced by the responding concrete wall that will be discussed in Section 3. Dimensions of the steel acceptor model are 30.5 x 33.3 x 41.1 cm (see Figure 2). The model was constructed from 2.54 cm thick steel plate. All surfaces are welded together except for the front wall which was bolted to the model to facilitate emplacing gages, wires, and connectors. For stability the acceptor extends 15 cm below ground level. Therefore, the exposed dimensions are 15.5 x 33.3 x 41.1 cm. There are 5 transducer positions on the model: four on the near sidewall, which experiences the most severe blast loading, and one on the roof. In Figure 2, the five gage positions are labelled 2 through 6.

3. Nonresponding Steel Acceptor Model with One Responding Concrete Wall. The heart of this experiment is the measurement of velocities of fragments from the responding acceptor wall. The concrete acceptor wall is supported by a nonresponding steel acceptor similar to the model described in Section 2. Refer to Figures 3 and 4, a sketch and photograph of this model. This acceptor is also constructed from 2.54 cm steel. In this case, all surfaces are welded together, except for the roof which is bolted to allow for emplacing velocity measurement screens and their supporting structure.

The concrete wall is placed against this steel acceptor as indicated on Figures 3 & 4. It is rigidly supported by the steel side walls of the acceptor and for most shots is attached to the floor and overlapping roof with caulking material. The concrete wall was constructed from the same sand mix used to create the donor structure discussed in Section 1. Reinforcing wire was not used in this 0.9 x 12.7 x 40.6 cm wall. A PCB gage (PCB Electronics Inc. piezoelectric pressure transducer) was placed adjacent to the wall. This is gage position 1; its location is indicated on Figure 4.

Optionally, with the concrete wall removed, 2.54 cm and 1.27 cm diameter concrete plugs 0.9 cm thick could be tested by placing them in a nonresponding steel plate containing two mounting holes. This plate bolts to the side of the steel acceptor as indicated on Figure 5. In this arrangement it was possible to obtain velocity measurements without using blast energy to break up the the responding target. A PCB gage was placed in the center of the plate. This is gage position 1 as indicated on Figure 5.

Although modeling the strength of the full scale wall explicitly was not feasible, it was imperative that the model wall not be too strong. A wall that was excessively strong would consume too much of the blast energy in breaking up, and the consequent fragment velocities would be unrealistically low. For this program it was determined that the wall should fail at approximately 34.5 kPa (5 psi). Two unreinforced brick houses were subjected to nuclear blasts at the Nevada Test Site in 1955 (Reference 3). The building placed at the 11.7 kPa level was structurally intact after the test whereas the one at the 34.5 kPa level was destroyed with most of the debris remaining nearby.

Another important consideration in designing this wall was the break

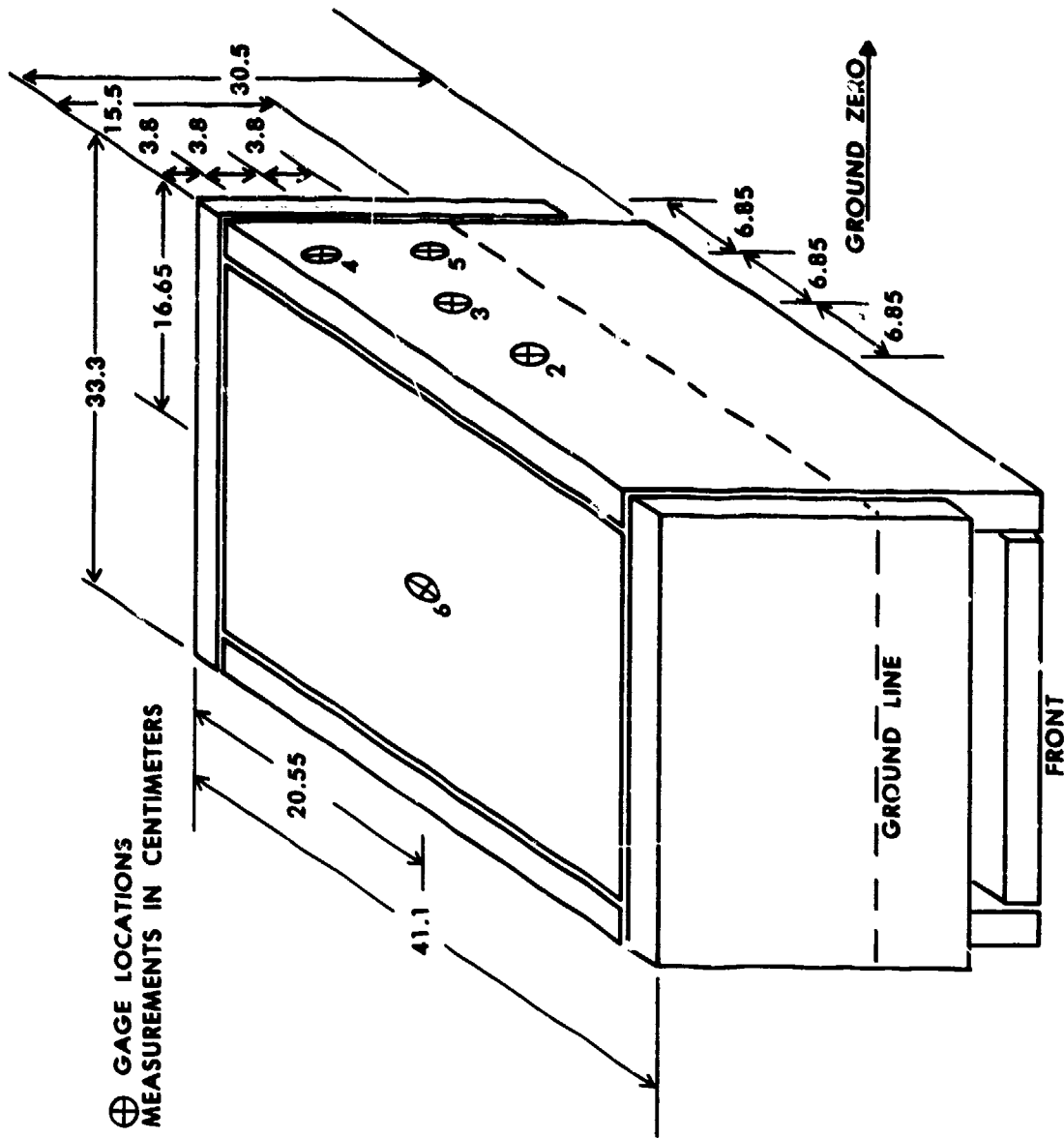


Figure 2. Nonresponding Acceptor Model

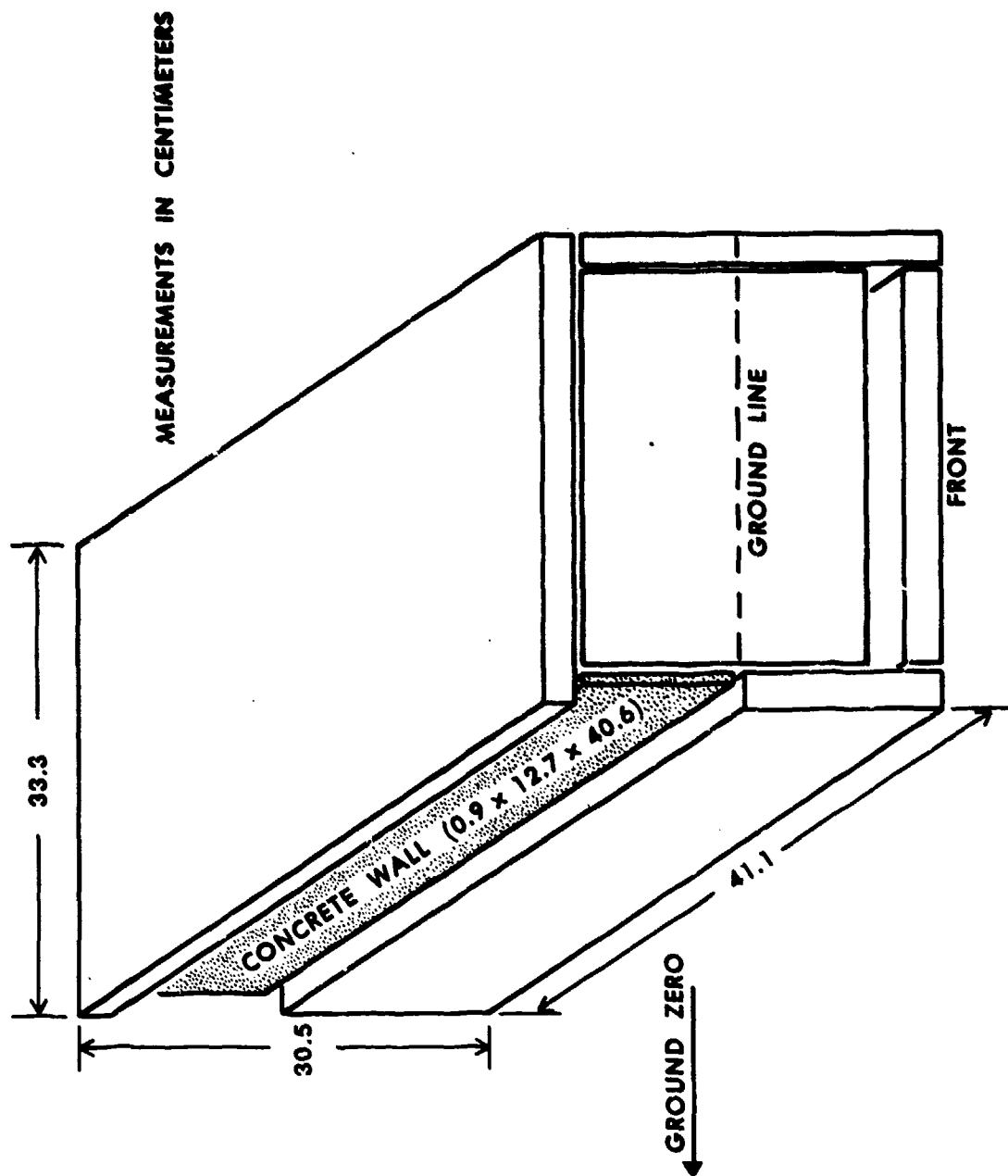


Figure 3. Sketch of the Acceptor Model with One Responding Concrete Wall



Figure 4. Photograph of the Acceptor Model with One Responding Concrete Wall

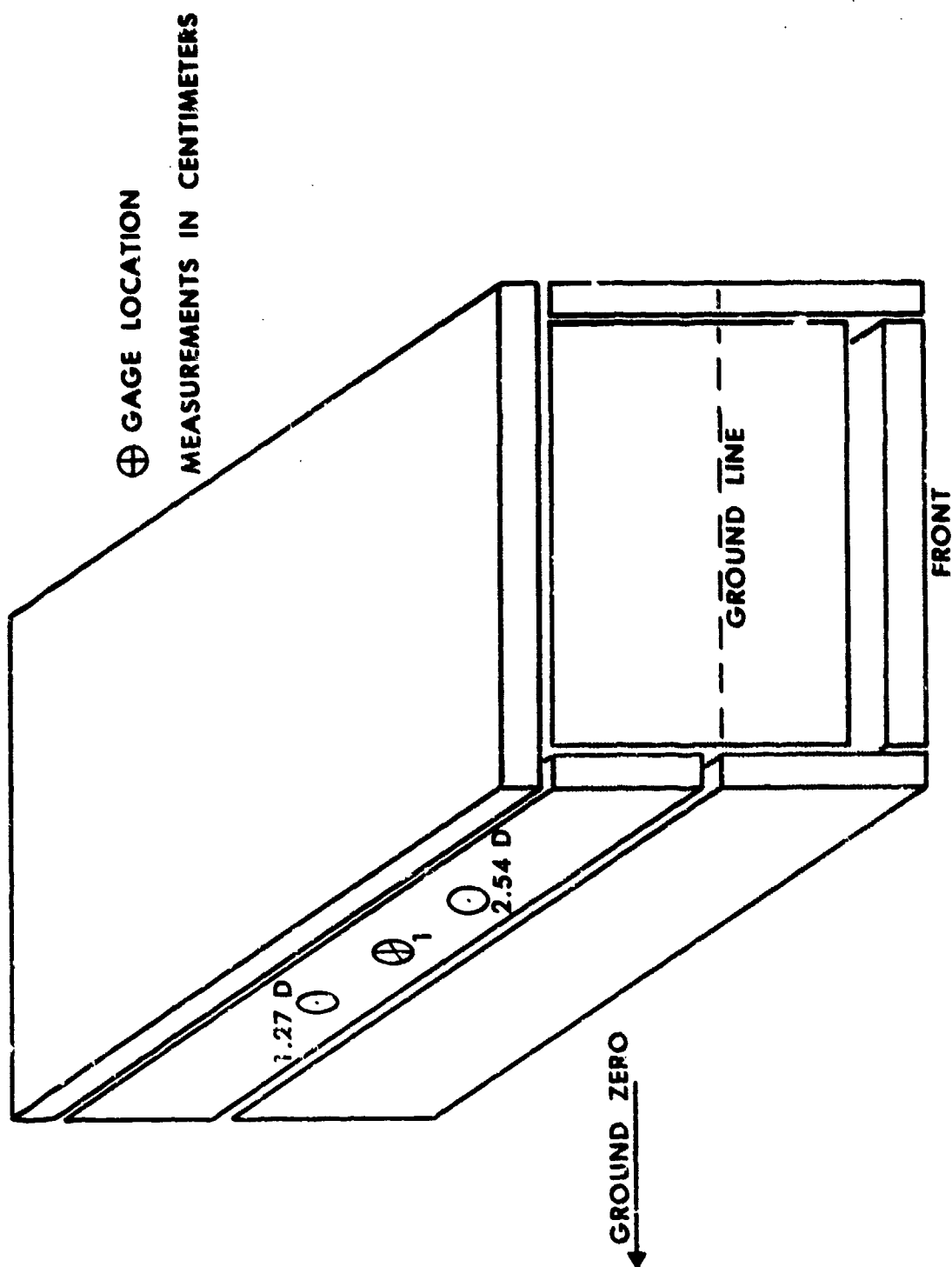


Figure 5. Acceptor Model with a nonresponding Steel Plate Containing Holes for Two Concrete Plugs

up pattern. The wall was scored to break up into regular 2.54 x 2.54 cm squares; the break up pattern was finalized after the strength tests discussed in Section 4. This size corresponds to full scale fragments that are 0.60 meters square, 0.21 meters thick and weigh 147.3 \pm 15.5 kg. Preliminary shock tube velocity tests on concrete acceptor walls showed that an unscored wall broke up into fragments having irregular size and shape. These tests are discussed in Section C.

4. Tests to Determine the Strength of the Concrete Acceptor Wall.
These tests were an essential part of the wall design.

a. Quasi-static Tests. An Instron model TTM hydraulic loading machine was used to apply a quasi-static, uniformly distributed load to a number of the concrete acceptor walls. A Starrett displacement gage was attached to the underside of the wall to simultaneously measure displacement as a function of loading. Figure 6 shows the quasi-static test arrangement. For these tests the wall was simply supported by a wood frame that overlapped the concrete by 1.27 cm on all four sides.

b. Dynamic Tests. The BRL 10.2 x 38.1 cm compressed air shock tube (Reference 4) was used to apply a dynamic load to a number of the concrete walls. Figure 7 is an illustration of this test setup. A wall was situated between two sections of the shock tube and held in place hydraulically. In this arrangement the wall was clamped and the shock tube overlapped the concrete by 1.27 cm on all four sides. These dynamic tests were performed with three different shock tube compression chamber lengths: 147.3 cm, 45.7 cm, and 8.3 cm. The length of the compression chamber or driver determined the shock wave positive phase duration and affected the impulse. By varying the driver length and compression chamber pressure, the wave shape was manipulated in an attempt to simulate a free field blast wave which characteristically exhibits exponential decay and, for a one kg charge, short duration (0.7 msec in the field tests). Each wall was tested at very low overpressure and examined for failure. The pressure was increased incrementally and the wall reexamined after every test until the wall failed. The walls were mounted normal to the shock flow and exposed to full reflected pressure.

Pressure-time records were obtained by placing one or two PCB Electronics Inc. model 113A piezoelectric transducers in the shock tube. One of these gages, which was used on every shot, was mounted against the shock tube wall 58.4 cm upstream from the test location to record the side-on pressure. The other gage was used to determine the full reflected pressure load that the concrete wall would experience. It was mounted in the center of the steel plate described in Section B 3. This steel plate was placed at the test location instead of the concrete wall. A series of shots was fired to determine the reflected pressure at the test location. Then the plate was removed and replaced with the concrete wall. When tests were performed on the concrete wall, only the upstream side-on gage was present. In this way it was possible to correlate the side-on pressures obtained when the plate and wall were tested with the reflected pressure on the plate. Thus, the reflected pressure on the wall was determined. The pressure-time records were stored in a Tektronix 5223 digitizing oscilloscope and transferred to a Tektronix 4051 microcomputer for analysis.

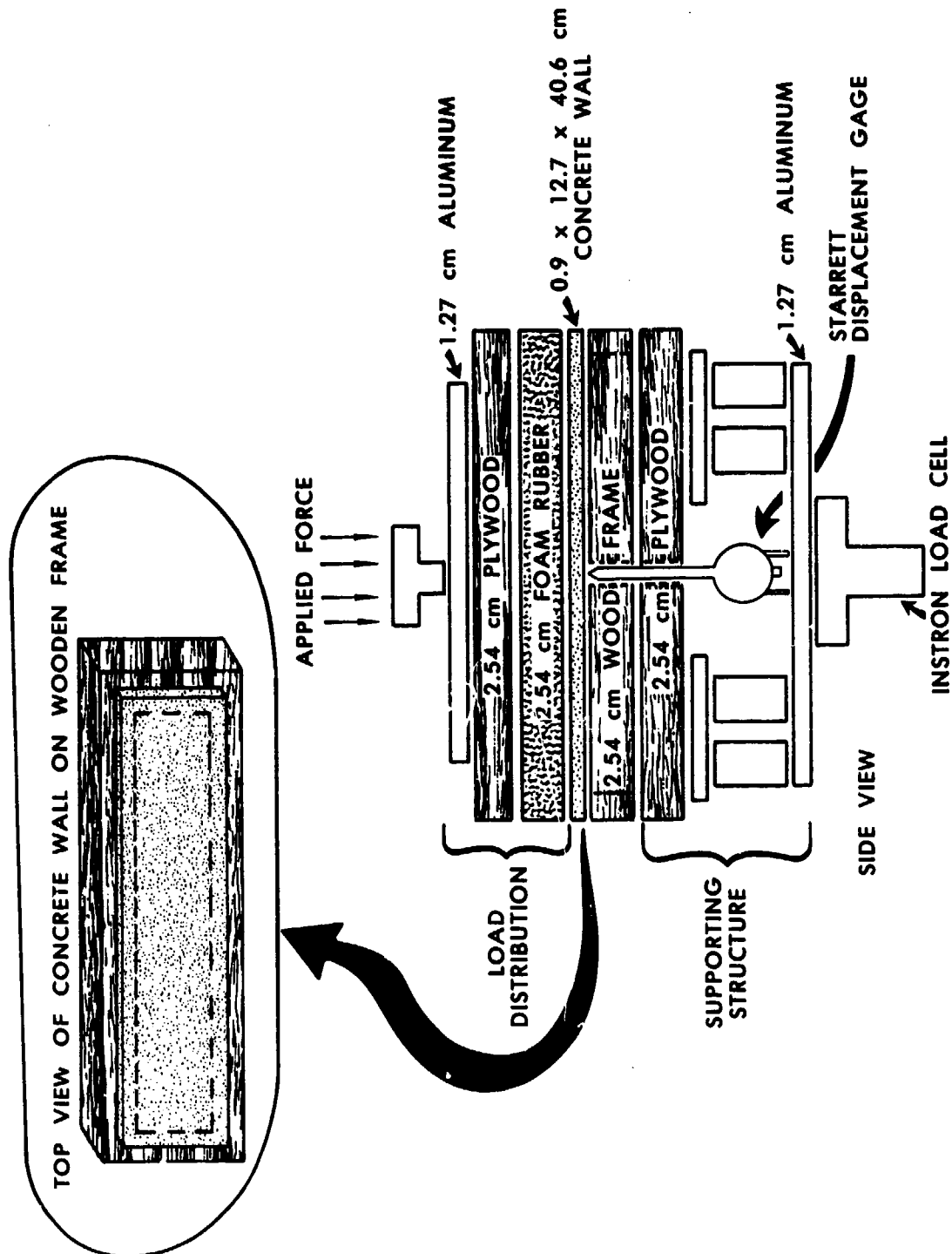
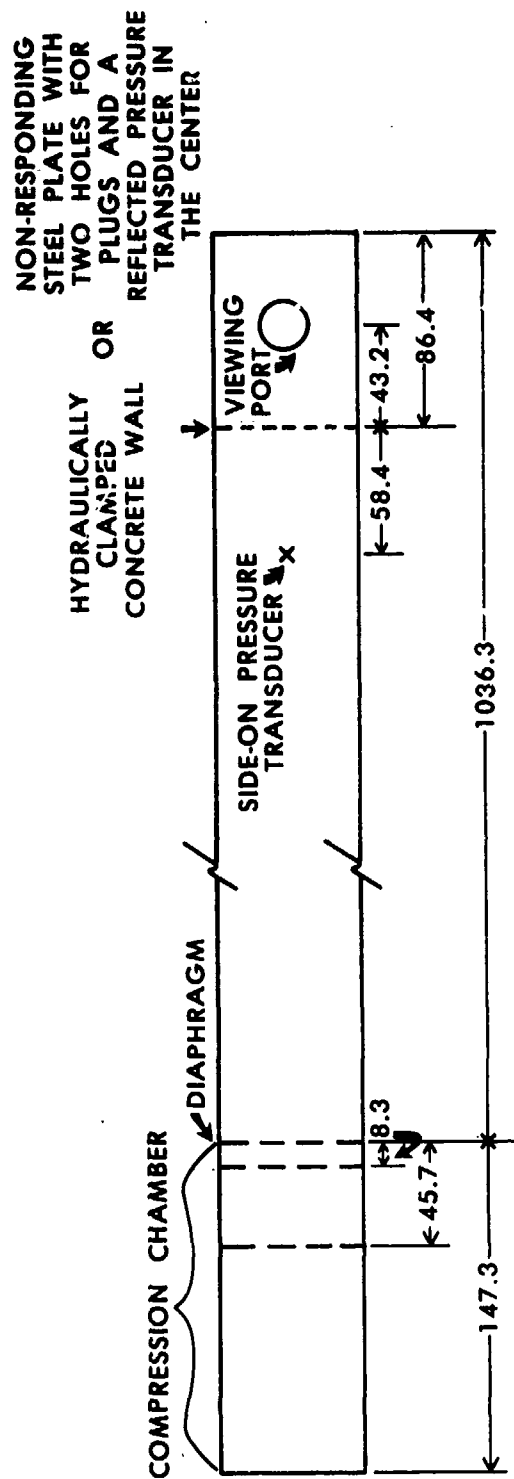


Figure 6. Quasi-static Loading Arrangement Used to Establish Concrete Acceptor Wall Strength



MEASUREMENTS IN CENTIMETERS

Figure 7. BRL 10.2 x 38.1 cm Compressed Air Shock Tube Setup for a Concrete Wall Test

C. Shock Tube Velocity Tests

Shock tube tests were performed to develop an approximation of the fragment velocities expected in the field tests. Employing the same arrangement discussed in Section 4 b above, a number of concrete walls were tested dynamically in the 10.2 x 38.1 cm shock tube at overpressures that caused them to fail and send fragments downstream with measurable velocities. These tests were performed using an 8.3 cm driver. Velocity measurements were obtained at a glass port located 43.2 cm downstream from the concrete wall test site. A 16 mm high speed camera, operating at 1000 frames per second, photographed the fragments as they passed the port. Additionally, a 2.54 cm diameter concrete plug 0.9 cm thick was tested in the shock tube by placing it in a nonresponding steel plate containing a small mounting hole. This is the same plate that attaches to the steel nonresponding model discussed in Section B 3 (refer to Figure 5). The concrete plug was placed in the mounting hole but was not secured. Thus, no blast energy was required to free the plug, and the measured velocity is an upper limit achievable in this test arrangement.

D. Field Tests

The field tests were performed during March 1985 at the Ballistic Research Laboratory outdoor Range 8 located on Spesutie Island, Aberdeen Proving Ground. Previous work, sponsored by the DDESB and performed by the BRL, concerned with the Machrihanish storage facility is reported in references 2 and 5.

1. Test Instrumentation. The pressure recording and velocity measurement instrumentation are described in this section.

a. Pressure Recording Instrumentation. The instrumentation for this test series consisted of pressure transducers, a magnetic tape recorder, and a data reduction system. A block diagram is shown on Figure 8. PCB Electronics Inc. model 113A piezoelectric pressure transducers, having quartz sensing elements and built-in source followers, were used to obtain pressure-time records of the blast event. The Honeywell tape recorder consists of three basic units: a power supply and voltage calibrator, amplifiers, and an FM recorder having a 80 kHz response time. A Honeywell Visicorder oscillograph with 5 kHz response was used for preliminary analysis of the pressure records. Data was processed through an analog to digital converter and transferred to a Textronix 4052 microcomputer that was used to create working plots. Finally, the data was transferred to linked CDC Cyber 750 and 7600 mainframe computers for further analysis.

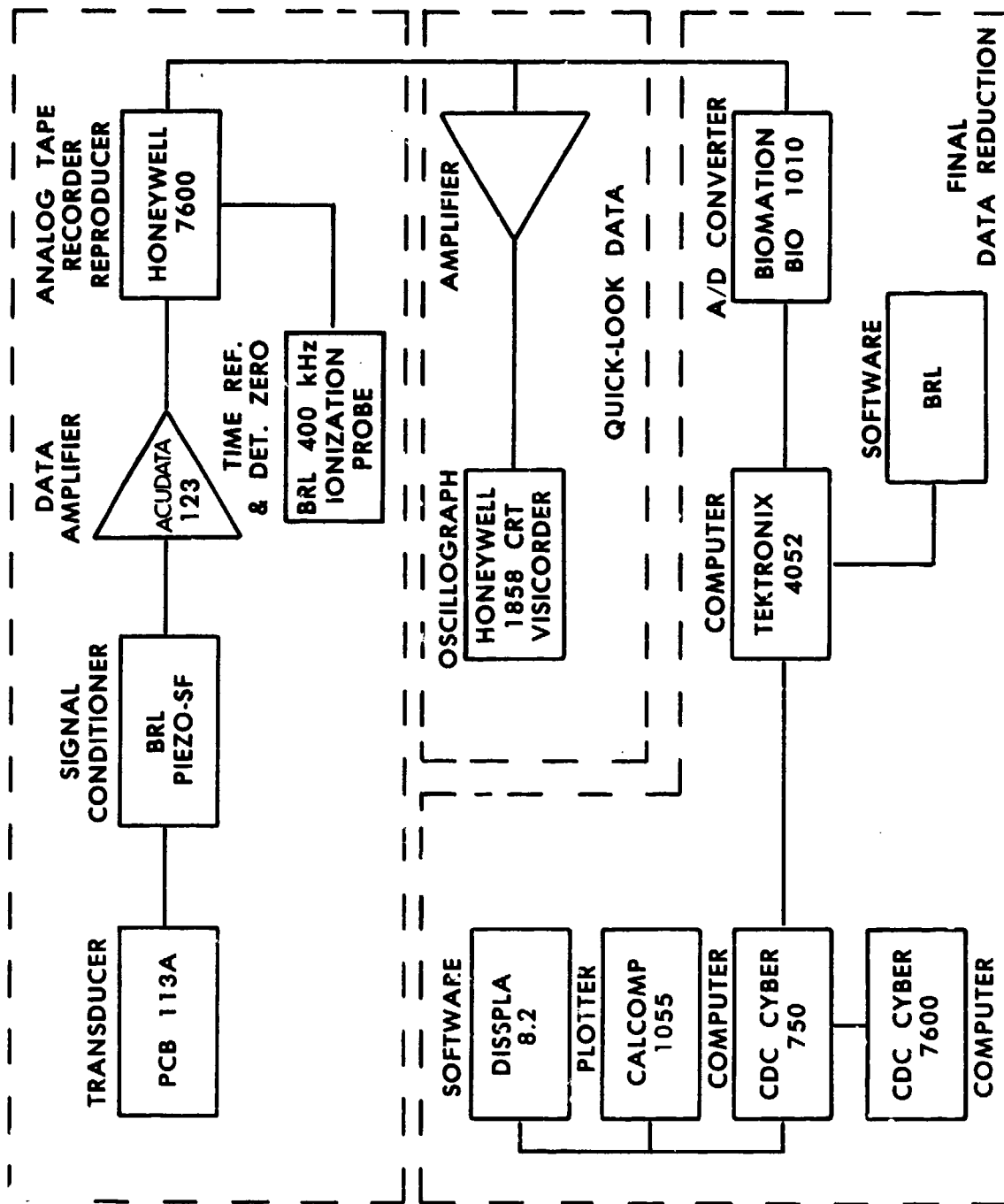


Figure 8. Data Acquisition/Reduction System

b. Velocity Measurement Instrumentation. Velocity measurements were obtained by using a variation of the voltage interrupt or "break screen" method. A break screen is a piece of thin paper coated with an electrically conducting chemical to create a circuit. When a fragment strikes the paper, it interrupts the circuit and a time measurement may be recorded on a digital counter. By placing two break screens within the nonresponding acceptor, one behind the other, concrete wall fragment velocities may be calculated from the start and stop times recorded on a counter and the known distance between the break screens, in theory. However, in early field tests, extraordinarily high velocities were obtained using this method. These velocities, in the range 200-341 m/s, were attributed to the ground shock. The blast event propagates a shock, through the solids on the test site, to the break screens which interrupts the circuits. Realistic fragment velocity measurements were obtained by replacing the paper break screens with single strand wire. Figure 9 displays the velocity measurement setup within the steel acceptor model. Even the thinnest wire offered mechanical resistance to the advancing fragments; this slowed the fragments down. Therefore, a method was required to start the counters without reducing the velocities. A PCB gage, placed adjacent to the concrete wall, was used as the start signal. Notice that there is a second set of looped wire circuits in the background. Velocities recorded here were lower than on the first set of circuits, because breaking the wires impeded the fragments. Measurements from the background circuits were not used.

Figure 10 is a block diagram of the velocity measurement system. The PCB gage is the start source for the Racal-Dana counter, and the wire circuit stops the counter when the wire is cut by a fragment.

2. Test Layout. A diagram and photograph of the test layout are presented on Figures 11 and 12. The entire test site, that is, the barricades, donor and acceptors, is 1/23.5 scale. The barricades are composed of compacted soil, and the test pad is coarse sand. The steel acceptors, which remained in place for all nine shots, were stabilized in several ways. The lower 15.2 cm of the walls were buried in the sand. Four steel straps were placed across and around the floor of each acceptor, and the straps were secured with 61.0 cm spikes driven into the test pad.

The test pad configuration is symmetric about an axis going through the free field gage (Station 7 on Figure 11) and the center line of the donor. Because of this symmetry, the blast loading on both steel acceptors should be the same; four gages on the near wall of the nonresponding acceptor should measure the blast loading experienced by the concrete wall on the other acceptor.

3. Firing Program. Nine test shots were fired during the period 11 March - 27 March 1985 at Range 8 on Spesutie Island. For a concise summary of the firing program, refer to Table 1. On Shots 1 and 2 the concrete plugs were tested. On Shots 3 - 8 the concrete walls were tested. On Shot 9 the plugs were again tested, this time with the barricades removed.

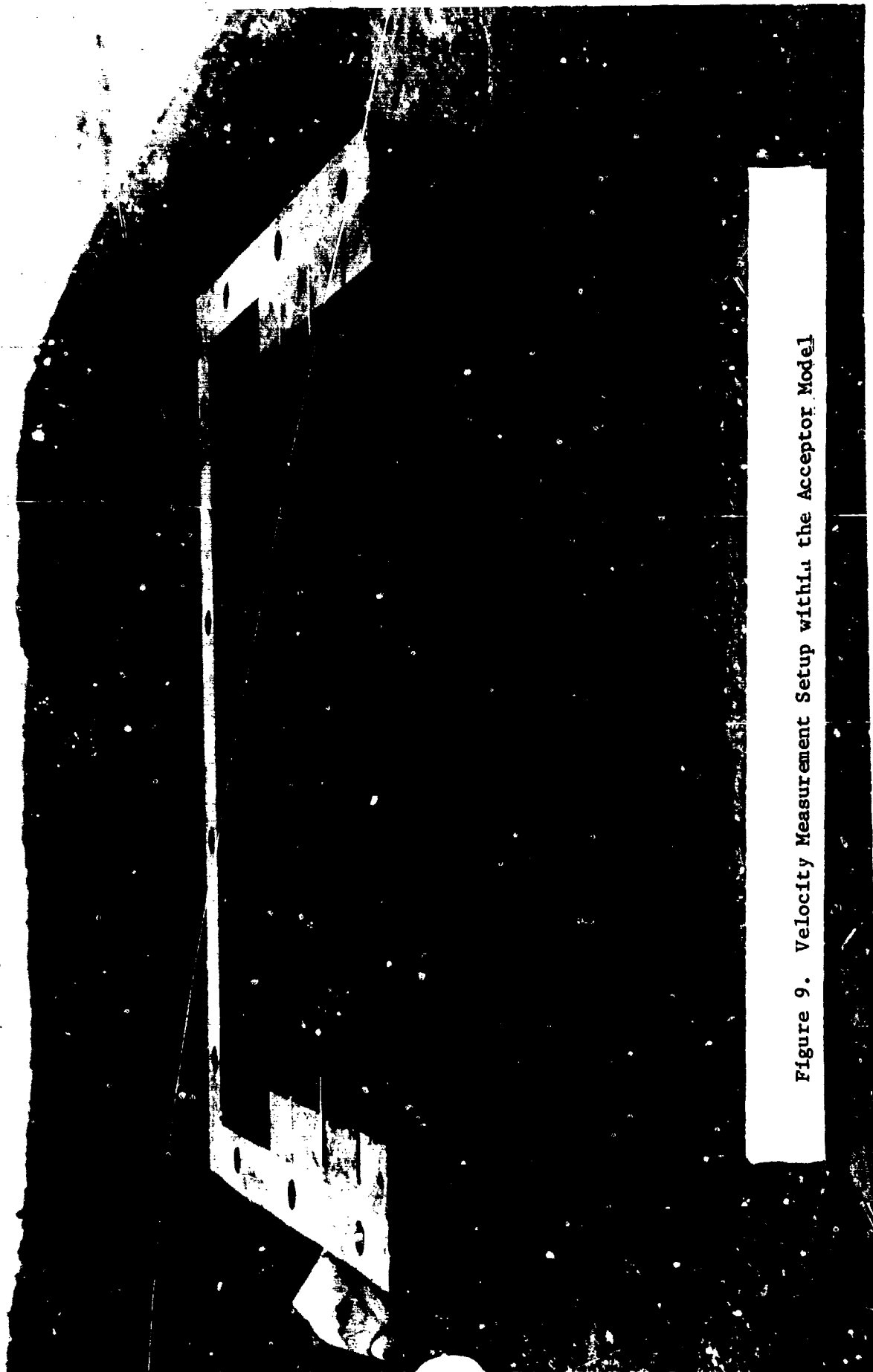


Figure 9. Velocity Measurement Setup within the Acceptor Model

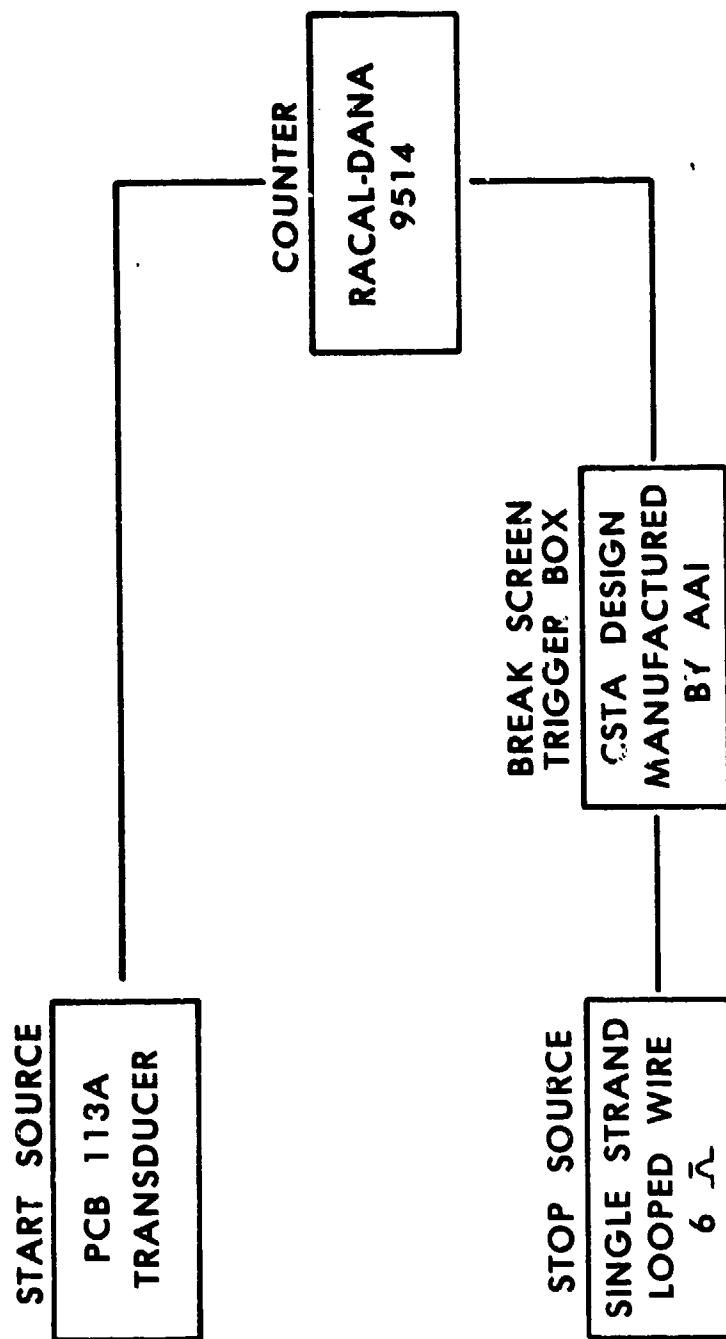


Figure 10. Block Diagram of the Velocity Measurement System

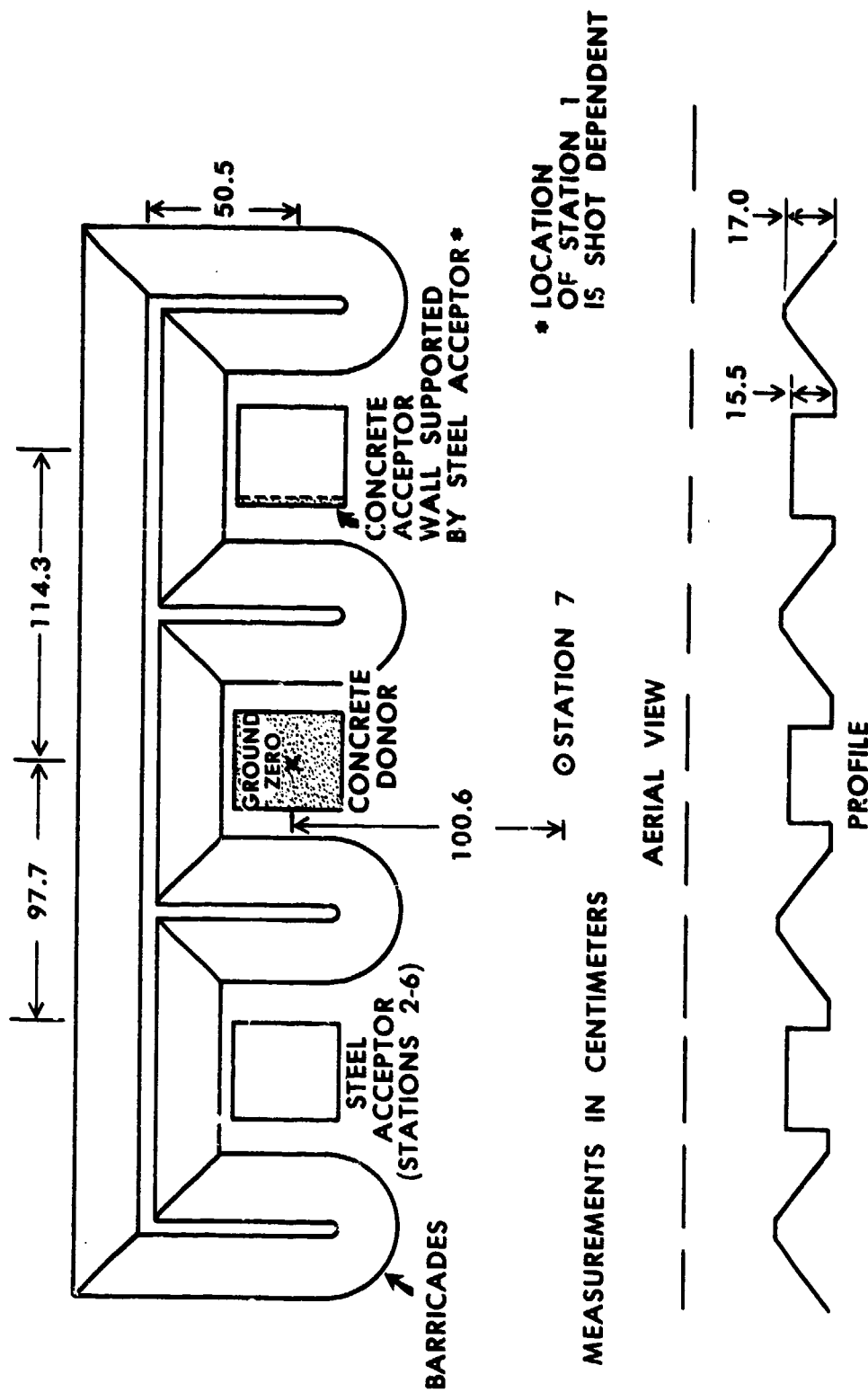
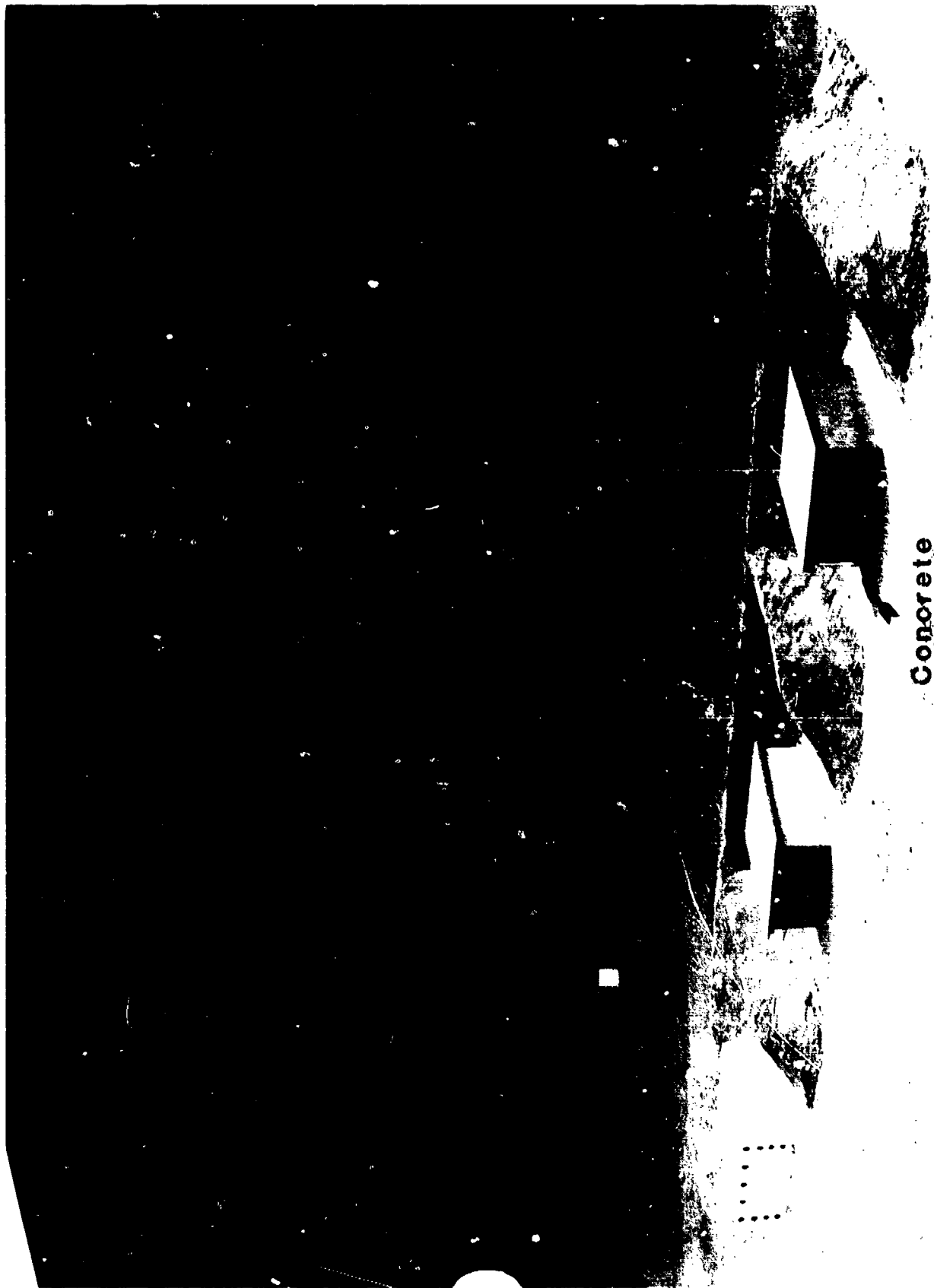


Figure 11. Diagram of the Test Layout



**Concrete
Acceptor Wall**

Figure 12. Photograph of the Test Site

TABLE 1. FIRING PROGRAM

Shot#	Concrete Target	Velocity Instrumentation	Barricades
1	Plugs	Paper Screens	Yes
2	Plugs	Paper Screens	Yes
3	Wall	Wire	Yes
4	Wall	Wire	Yes
5	Wall	Wire	Yes
6	Wall	Wire	Yes
7	Wall	Wire	Yes
8	Wall	Wire	Yes
9	Plugs	Wire	No

III. RESULTS

A. Field Test Blast Data

The acceptor sidewall nearest to the blast experiences the most severe load (Ref. 2). An interpretation of the blast loading on the near sidewall and roof of the acceptor is presented on Figure 13. The shock front strikes the near sidewall at a 33.9 degree angle whereas it strikes the roof at an angle of 56.1 degrees causing the roof to experience a lower loading. Because of the higher loading, the near sidewall is the focus of this study.

The pressure-time (P-T) records for all seven stations from Shot 2 are displayed in Figure 14. Station 1 is located in the center of the nonresponding plate (see Figure 5); this corresponds to the center of the concrete wall. Likewise, Station 2 (see Figure 2) is located at the center of the near wall on the nonresponding steel acceptor. Because of the test site symmetry, Stations 1 & 2 should undergo the same loading. Fragments from the center of the concrete wall have the highest velocities; Station 1 & 2 are of primary interest. Station 3-5 are also located on the nonresponding acceptor's near wall as indicated on Figures 2. Station 6, on the roof is subjected to a much lower load. Station 7 is located 100.6 cm in front of ground zero. The gage at Station 7, mounted flush

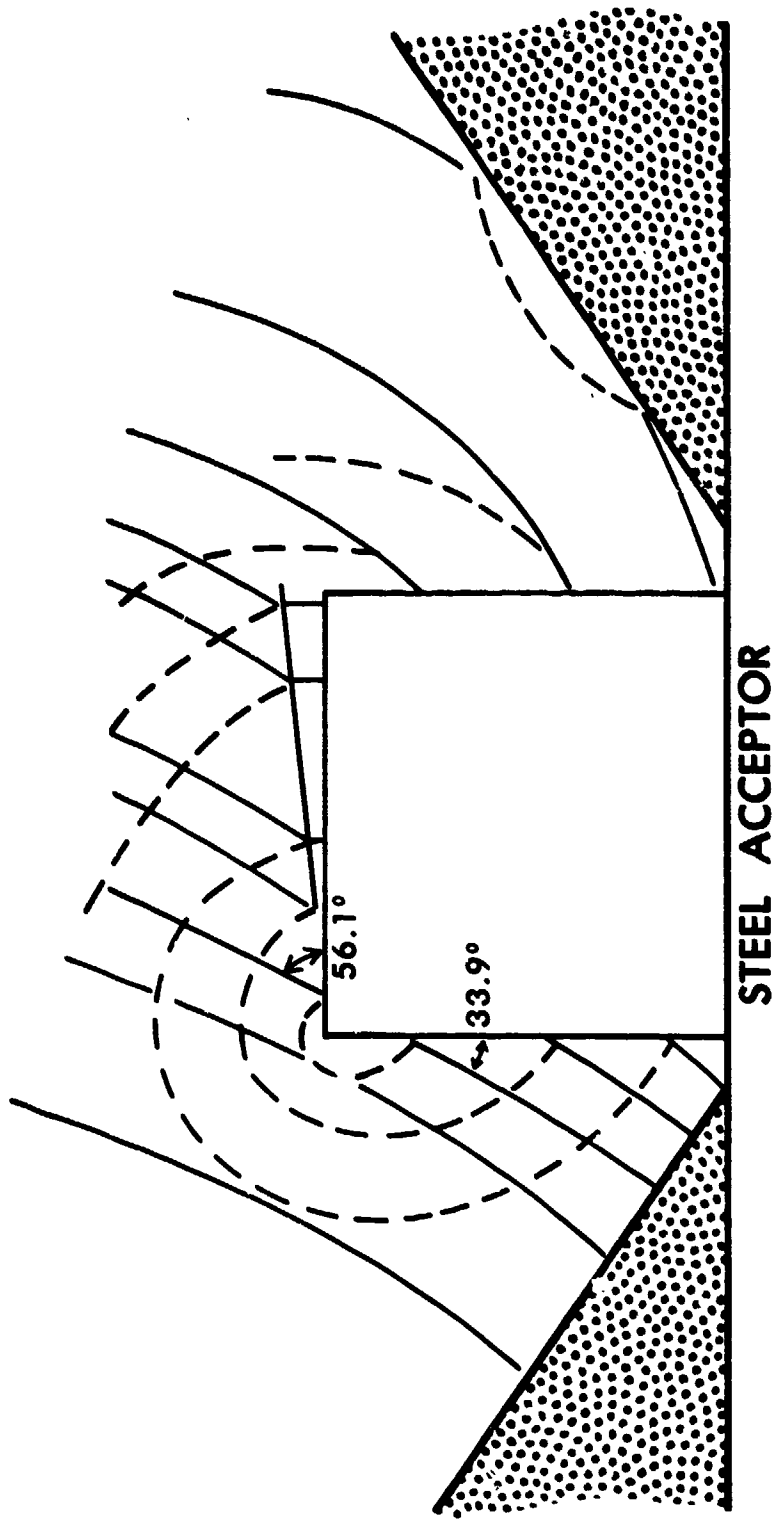


Figure 13. Shock Loading on Acceptor Models

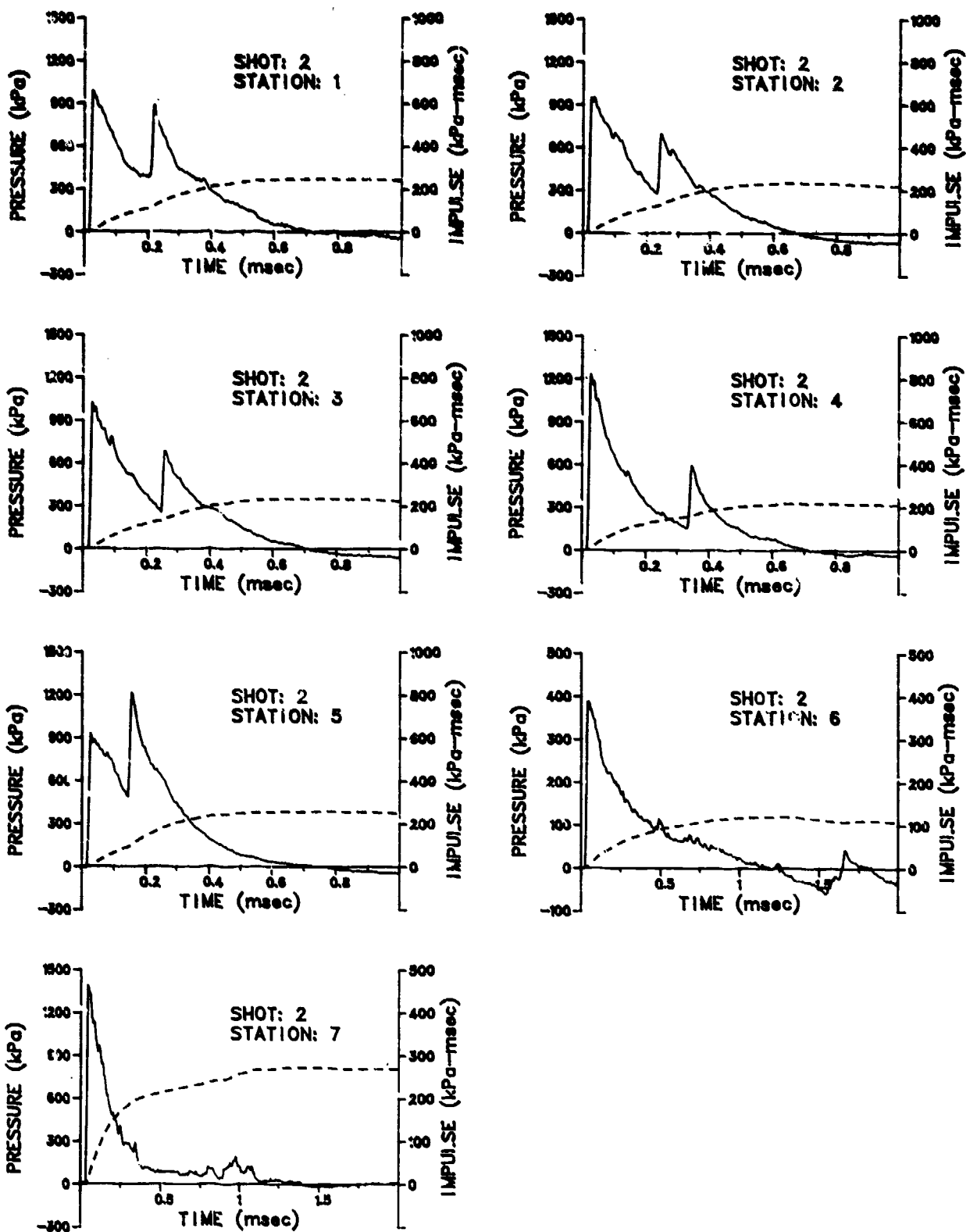


Figure 14. Pressure-time Histories for Shot 2

with the ground, is subjected to side-on pressure and monitors the blast wave propagating in front of the donor. Because the donor door was designed to fail, the blast was focused forward resulting in a peak pressure recorded at Station 7 that is close to side-on pressure for an unconfined 1 kg blast.

Stations 1 & 2 on Figure 14 both show an initial peak pressure of over 900 kPa followed by a lesser peak at 0.2 msec. The secondary peak is caused by a reflection of the shock wave from the ground. Stations 3-5 display similar twin peaks; in each case the relative magnitudes of the two peaks is determined by the distances from the wave sources. The blast wave strikes the upper edge of the wall first and decays as it travels downward to the ground line where it is reflected and travels upward, again decaying as a function of distance. For example, Station 4, located in the upper corner of the acceptor shows an initial peak of 1227 kPa and a 591 kPa secondary peak whereas Station 5, located in the lower corner much closer to the ground, shows a 927 kPa initial peak and a 1214 kPa secondary peak. Clearly, the peak pressure exhibited at Station 6, 388 kPa, is much lower. Station 7, the free field gage position, shows an initial pressure of 1388 kPa which is close to free field side-on pressure for an unconfined Pentolite charge, 1540 kPa (Reference 6).

The impulse for each gage position is also indicated on Figure 14. The impulse is a direct indication of the applied force and is used to calculate the maximum velocity for a freely translating wall which is the upper limit of obtainable velocities. As stated above, Stations 1 and 2 are of primary interest because the greatest fragment velocities should be obtained from the center of the wall. The peak impulses for Stations 1 to 5 are very close: 246.3, 233.7, 234.1, 217.9, and 256.3 kPa-msec. The average value is 237.7 kPa-msec. Peak impulse is defined as the impulse at the end of the blast wave positive phase duration.

For Shots 1-8 the donor structure, charge, and test pad were not varied; the blast loading should be the same for each shot. Therefore, the P-T records from Shot 2 are representative of all eight shots, and records for Shots 1 and 3-8 are presented in the Appendix.

Identical shots were also fired and are reported in References 2 and 5. The pertinent P-T records from those tests show that the blast data are self-consistent.

Peak pressure, impulse, shock arrival time, and positive phase duration for Shots 1-8 are listed in Table 2 for the primary stations of interest, Stations 1 & 2.

TABLE 2. AIRBLAST PARAMETERS FOR SHOTS 1-8

Shot#	Station#	Peak Pressure kPa (1st/2nd)	Impulse* kPa-msec	Arrival Time msec	Duration msec
1	1	1039.2 / 1034.2	276.7	0.9025	0.7050
1	2	800.6 / 621.2	212.4	0.8075	0.7050
2	1	983.9 / 889.3	246.3	0.8900	0.7025
2	2	949.7 / 693.6	233.7	0.8125	0.6725
3	1	884.3 / 873.1	231.0	0.8450	0.6650
4	2	**1091.7 / 850.6	263.1	-	0.6850
5	2	978.9 / 614.2	211.8	-	0.6725
6	2	1062.2 / 806.3	245.8	0.8250	0.6425
7	2	1009.9 / 819.1	258.6	0.8225	0.6800
8	2	***1002.7 / 862.9	257.7	0.8075	0.6825

* Impulse to end of positive phase

** Not considering the spike on Figure A-3

*** Not considering the spike on Figure A-7

The test pad layout was altered for Shot 9 by removing the barricades. Without the barricades to impede the shock wave, dynamic flow, and particle fragments, the blast loading on the near wall of the acceptors should be higher. Also, in this test arrangement, the shock wave strikes the near wall face-on which results in full reflected pressure. The P-T records for Shot 9 are displayed on Figure 15. These records may be compared with Shot 2 (Figure 14) which is an identical test except for the barricades. Comparison of Shots 2 & 9 shows the effects that the barricades have on attenuating the blast loading. Between Reference 2 and the current project, several configurations that are variations of the Machrihanish site have been tested; airblast parameters from these different configurations are presented in Table 3 to show the effects of the barricades and donor structure on confining the blast. Comparison is made at Station 3, a gage location used in each project. Station 4 was used for Shot 9, because it was difficult to measure blast pressure under such severe conditions. The record at Station 4 appears more realistic than that at Station 3. Table 3 lists blast environments from the least to the most severe. Evidently, loose sand barricades attenuate the blast more than hardpacked soil barricades. When the donor structure is removed, the blast pressure increases dramatically, but the impulse is not significantly increased. However, when the barricades are removed, both the pressure and impulse are markedly increased. The enhanced impulse is caused by particles striking the gage.

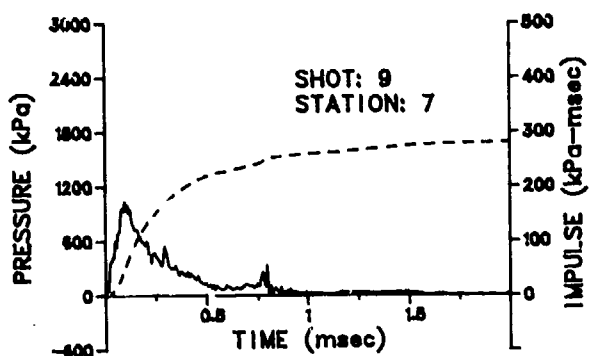
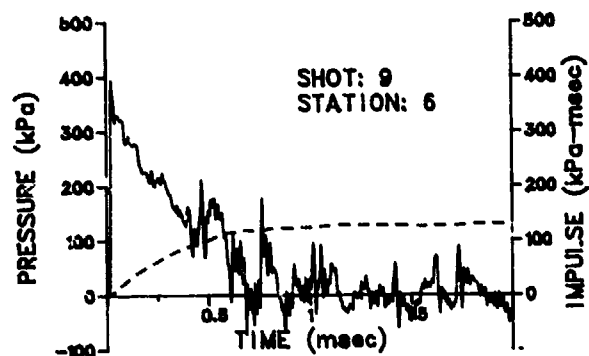
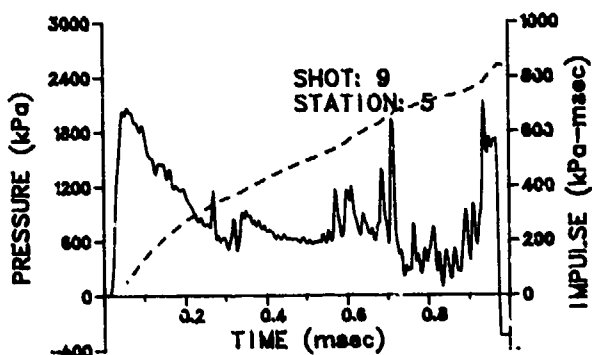
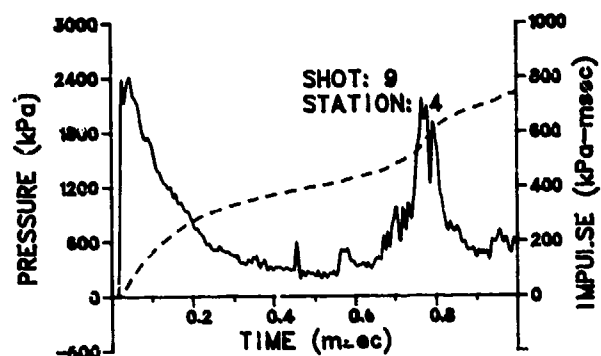
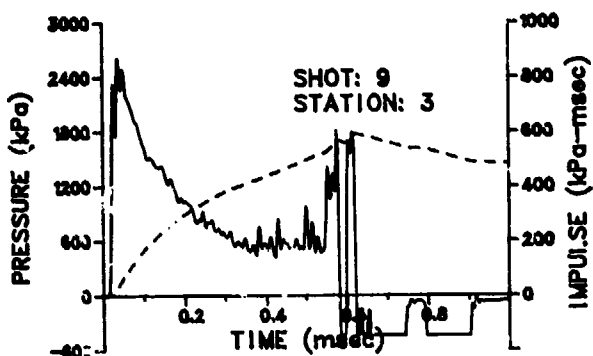
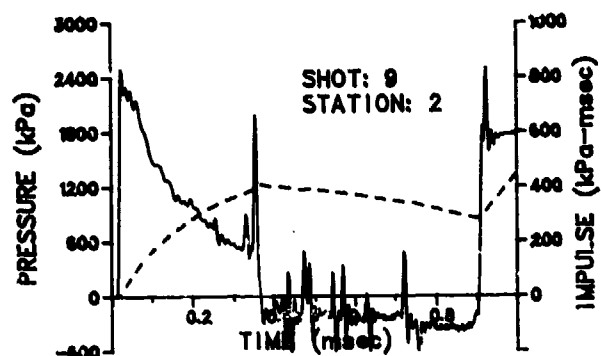
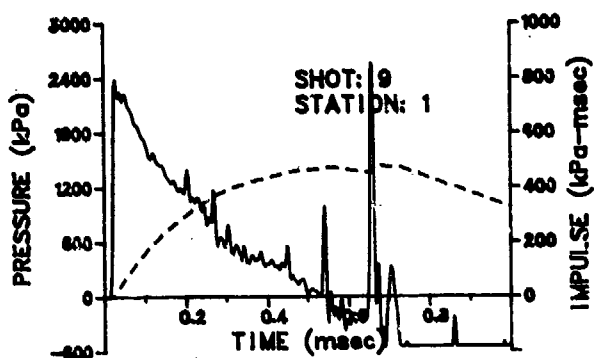


Figure 15. Pressure-time Histories for Shot 9

TABLE 3. EFFECTS OF BARRICADES AND DONOR STRUCTURE ON BLAST LOADING

Source	Station	Donor	Barricade	Pressure kPa	Impulse kPa-msec	Arrival Time msec	Duration msec
Ref. 2 Shot 3	3	Yes	Sand	821	195.0	0.8500	0.70
Shot 6	3	Yes	Soil	1079	245.8	0.8475	0.70
Ref. 2 Shot 4	3	Yes	Soil	1093	239	0.8900	0.71
Ref. 2 Shot 5	3	Floor Only	Soil	2015	240	0.5120	0.58
Shot 9	4	Yes	No	2387	746	1.025	1.1

B. Strength of the Concrete Acceptor Wall

A description of these tests may be found in Section II B 4.

1. Quasi-static Tests. Ten concrete walls of several preliminary designs were tested quasi-statically to obtain an initial approximation for a workable final design. The results of the tests are listed in Table 4. For a sample of eight walls having a mean mass of 0.90 kg, the distributed load required to crack the panels in tension was 34.4 kPa and the displacement to failure was 0.49 mm. As a matter of general interest, the displacement as a function of applied force for the unscored 0.92 kg wall is shown in Figure 16. The walls with the finest scoring pattern, 2.12 x 2.54 cm, failed at lower than the mean pressure, but for the most part, walls with the other scoring patterns did not crack more readily than unscored walls. The scores, when present, were shallow, having a nominal depth of 0.32 mm. The quasi-static tests showed that every concrete wall failed near enough to 34.5 kPa to be acceptable. Quasi-static tests on 1/40 scale brick walls composed of cement-lime mortar and red granite chips are reported in Reference 7 where wall failure occurred at 34.5 \pm 20.7 kPa.

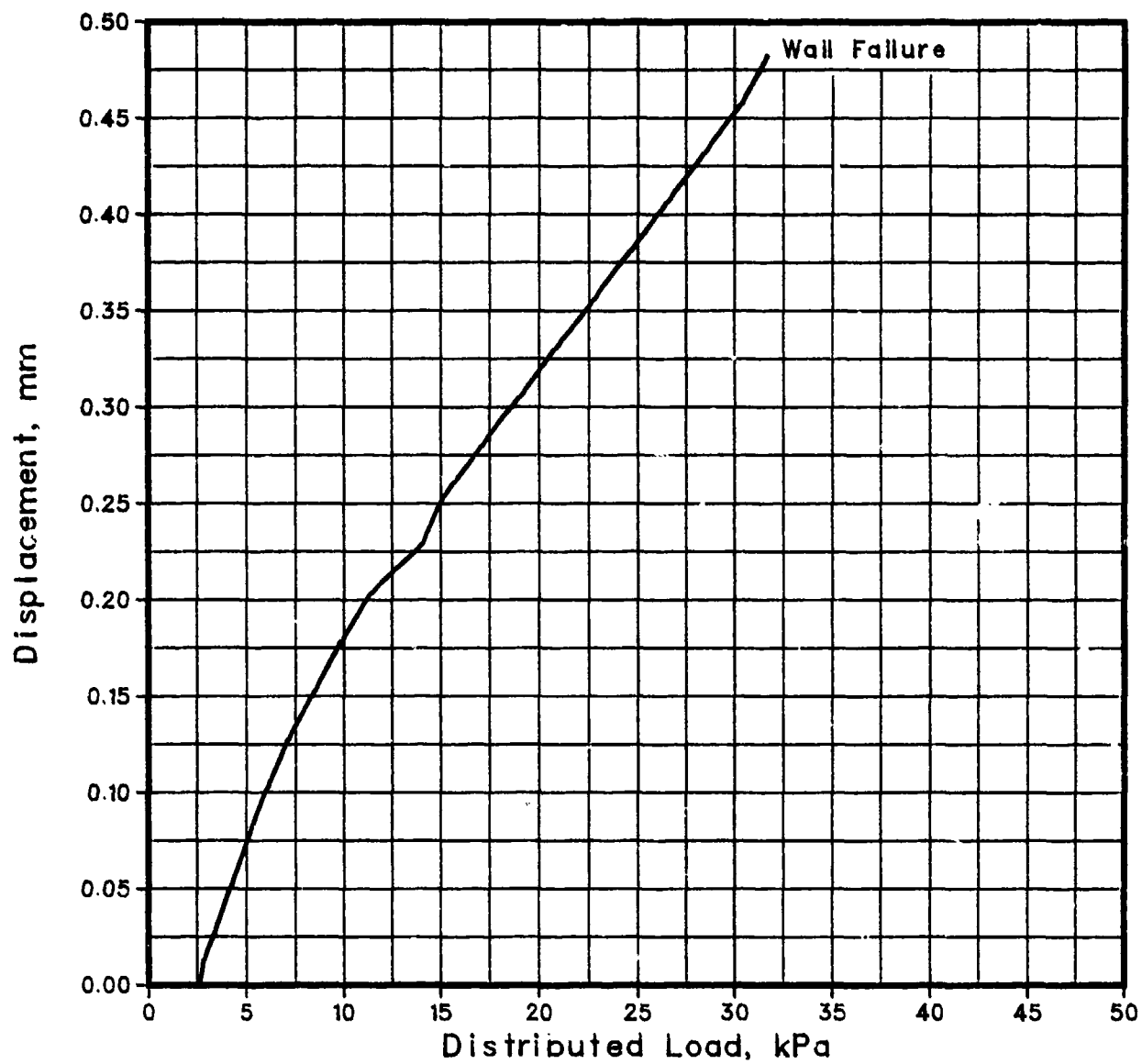


Figure 16. Displacement as a Function of Applied Force for an Unscoored Wall

TABLE 4. CONCRETE WALL QUASI-STATIC STRENGTH TESTS

Mass (kg)	Distributed Load (kPa)	Displacement (mm)	Scoring Pattern (cm)	Curing Period (days)
0.92	31.8	0.48	None	19
0.86	36.4	0.43	None	36
0.86	40.5	0.43	4.66x5.08	29
0.91	33.0	0.58	4.66x5.08	25
0.92	32.6	0.51	4.66x5.08	26
0.90	47.8	0.56	4.66x2.54	19
0.90	28.4	0.46	2.12x2.54	22
0.90	25.0	0.46	2.12x2.54	22

Scoring the walls influenced the breakup pattern. An unscored panel exhibited predictable cracks (see Figure 17) for a wall under tension because of bending moment. A scored wall tended to crack along the scores (see Figure 18).

As a result of these static tests, a 2.54 x 2.54 cm scoring pattern was determined to be suitable for the field tests.

2. Dynamic Tests. Ten concrete walls were tested for strength in tension using the BRL 10.2 x 38.1 cm shock tube. The results are indicated in Table 5. All of the walls tested dynamically have a 2.54 x 2.54 cm scoring pattern except for one unscored wall. The walls were scored in one of two ways. In method I, the walls were scored immediately after being poured resulting in shallow, irregular scores, nominally 0.32 cm. In method II, the walls were allowed to set up for several hours and then scored. This resulted in deeper, regular scores, nominally 0.445 cm. Three driver lengths were used for these tests. The driver length determined the impulse and positive phase duration of the shock wave. The walls were exposed to full reflected pressure; the column labelled "Failure Range" in Table 5 indicates that a wall did not fail at the lower reflected pressure, but did fail at the higher value.

With the long driver installed, five walls tested failed at less than 22.8 kPa. With the medium length driver, two walls tested failed at less than 15.9 kPa. When the driver was shortened to 8.3 cm, 2 of 3 walls tested failed at higher pressure, between 21.4 and 31.7 kPa. The failed slabs showed both cracks caused by failure under tension and cracks caused by shear failure along the supporting edges. The dynamic tests showed that walls with a 2.54 x 2.54 cm scoring pattern would be workable for the field tests. Both the regularly and irregularly scored walls failed close enough to 34.5 kPa to be acceptable.

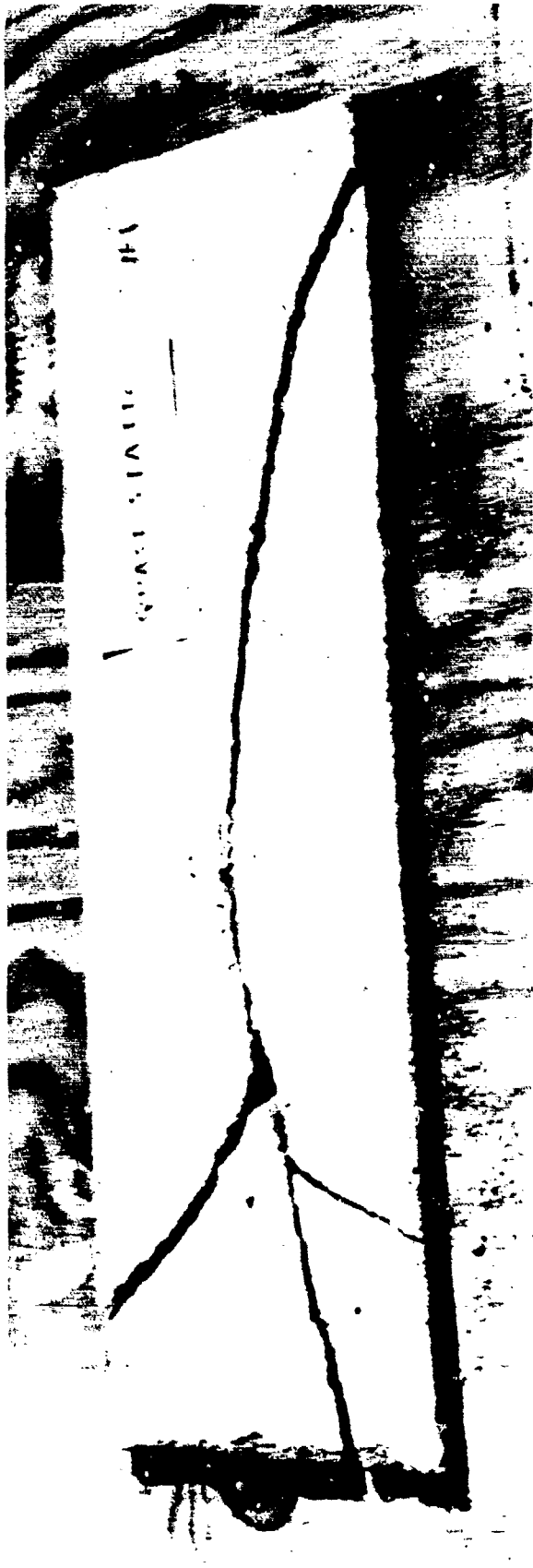


Figure 17. Breakup Pattern of a Quasi-statically Tested Unscored Concrete Wall

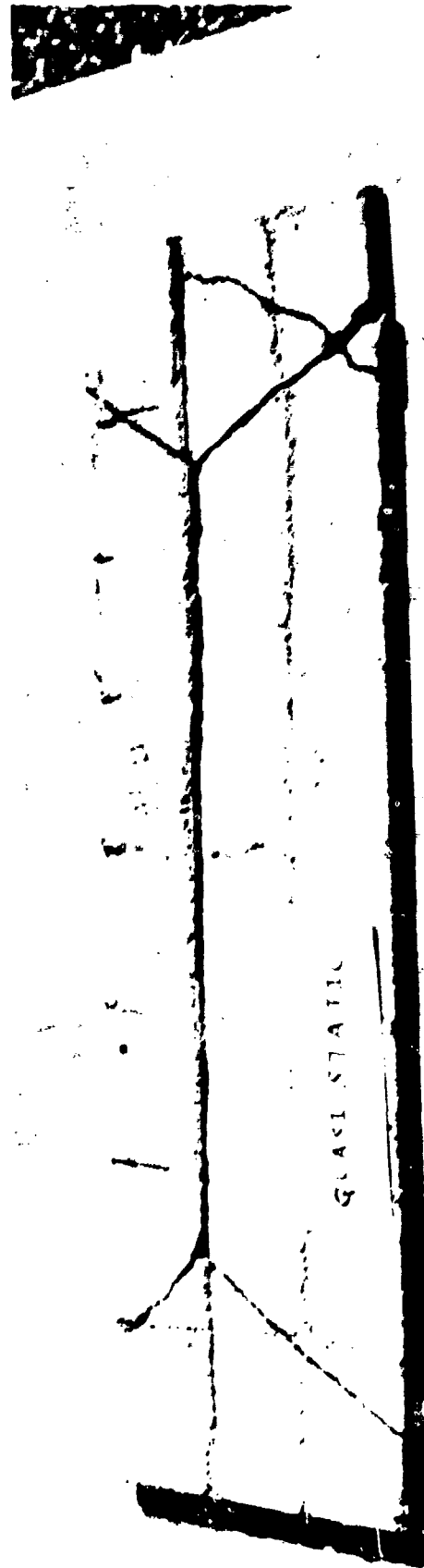


Figure 18. Breakup Pattern of a Quasi-statically Tested Scored Concrete Wall

TABLE 5. CONCRETE WALL DYNAMIC STRENGTH TESTS

Mass (kg)	Failure Range (kPa)	Driver Length (cm)	Load Duration (msec)	Scoring Pattern*	Curing Period (days)
0.96	<22.8	147.3	10	I	25
0.86	17.2-20.7	147.3	10	I	26
0.73	<13.8	147.3	10	I	19
0.77	<16.5	147.3	10	II	23
0.93	15.2-17.2	147.3	10	I	19
0.94	13.8-15.2	45.7	7	I	13
0.91	13.8-15.9	45.7	7	II	23
0.97	21.4-31.7	8.3	3.5	None	20
0.80	15.2-21.4	8.3	3.5	I	23
0.91	21.4-31.7	8.3	3.5	II	30

* I - shallow, irregular scores, nominally 0.32 cm

II - regular scores, nominally 0.445 cm

Apparently, the concrete wall is sensitive to the load duration. It is possible to calculate the fundamental frequency of vibration for the concrete wall if several assumptions are fulfilled (Reference 8). The wall is assumed to be elastic, homogeneous, isotropic, of uniform thickness, and the deflections are small in comparison with the wall thickness.

Let h = wall thickness

Γ = flexural rigidity of wall

E = modulus of elasticity in tension = 3,000,000 LB/sq in (Reference 9)

ν = Poisson's ratio = 0.13

d = weight per unit volume of material in the wall

g = gravitational acceleration

b = wall length

c = wall width

f = fundamental frequency of vibration

Then,

$$D = \frac{E h^3}{12 (1 - \nu^2)} \quad (1)$$

and

$$f = \frac{\pi}{2} \left(\frac{1}{b^2} + \frac{1}{c^2} \right) \sqrt{\frac{gD}{hd}} \quad (2)$$

From Equation 2, it was determined that the fundamental frequency equals 213.2 cycles per second, and the period of vibration is 4.7 msec. The data in Table 5 shows that for the load durations of 10 or 7 msec, the walls failed at lower pressures than for the load duration of 3.5 msec. The period of vibration, 4.7 msec, falls between 3.5 and 7 msec. Evidently, the data in Table 5 indicates that when the duration of the applied load exceeds the period of vibration of the wall, failure occurs at lower pressure than when the period exceeds the load duration. Perhaps under field test conditions, where the load is applied for only 0.7 msec, the wall may require overpressures higher than 34.5 kPa for failure.

C. Shock Tube Fragment Velocity Measurements

A description of these tests was given in Section II C. The BRL 10.2 x 38.1 cm shock tube was used to simulate the blast loading expected in the field tests. Results from Reference 2 were used to predict the blast loading for the field tests reported in this study. Specifically, air blast parameters from Shot 4, Station 3, of Reference 2, which are listed in Table 3 of this report, were used. That record shows 1093 kPa peak pressure, 239 kPa-msec impulse, and 0.71 msec duration. In these shock tube tests it was not possible to reproduce such a high pressure, short duration pulse. The best approach was to match the impulse by creating a 80.0 kPa peak pressure wave of 7.4 msec duration. This resulted in an impulse of 224.5 kPa-msec which is close to the field case. Two walls and two 2.54 cm concrete plugs were tested in this arrangement. The results are listed in Table 6. Since no energy was needed to free the plugs, their velocities are higher than wall fragment velocities. The velocities are very low, the highest value being 11.4 m/s. The vertical velocity as a result of gravity is about 1 m/s; this is not indicated on Table 6.

TABLE 6. SHOCK TUBE FRAGMENT VELOCITY MEASUREMENTS

Target*	Mass (kg)	HORIZONTAL Velocity (m/s)	CURING Period (days)
I	0.88	7.0	17
II	0.90	5.0	39
Plug	0.00595	10.0	39
Plug	0.00595	11.4	39

* I - wall having shallow, irregular scores
 II - wall having regular scores

D. Field Tests Fragment Velocities

1. Data Analysis. The velocity data for nine field shots are presented in Table 7. Velocity measurements were recorded for fragment movement from the back of the near sidewall to a position 9.6 cm from the near sidewall (4.5 cm from the centerline of the model). Several independent circuits were set up to record independent velocity measurements. The measurements obtained from the independent circuits were consistent. When more than one valid measurement was obtained, the value listed in Table 7 is the highest value. The raw velocity data is actually a little lower than the true velocity because it takes the load duration, 0.7 msec, for the fragments to accelerate to maximum speed. During the loading time, the wall has moved 6.3 mm on average based on the equations of motion discussed below. Also, the value recorded by the counters is the horizontal velocity; including gravitational acceleration and any vertical component of the applied load increases the velocity slightly.

The last column of Table 7, labelled "Classical Limit", indicates the maximum velocity a target could reach as a result of an applied load. This value was calculated by using the pressure-time records as input to a computer program that calculated the force applied to the target as a function of time. The assumptions made are that the target translates freely, that is, no blast energy is used to break it up, and the entire blast wave applies a force to the target, that is, the load is applied before the target breaks up. These basic equations of motion are included for completeness.

Let M = target mass

a = instantaneous target acceleration

$F(t)$ = applied force on target as a function of time

$p(t)$ = blast pressure on target as a function of time

A = target cross-sectional area

dt = pressure record time increment (digitizing time step)

dv = instantaneous target velocity

Then,

$$F(t) = A p(t) \quad (3)$$

$$a = \frac{F(t)}{M} = \frac{dv}{dt} \quad (4)$$

$$v = \int a \, dt \quad (5)$$

and the final velocity may be computed by numerically integrating the velocities from shock arrival until the end of the positive phase. The upper limit velocity as a function of time for the concrete wall used on Shot 6 is displayed graphically on Figure 19.

TABLE 7. FIELD TEST VELOCITY DATA

Shot#	Target	Mass (kg)	Scoring Pattern*	Measured Velocity (m/s)	Classical Limit (m/s)
1	Plug	0.0065	-	-	21.6
2	Plug	0.00635	-	6.3	19.7
3	Wall	0.81	II	10.8	14.6
4	Wall	0.95	II	8.5	14.3
5	Wall	0.98	II	6.6	11.2
6	Wall	0.82	I	10.8	15.5
7	Wall	0.94	I	8.0	14.2
8	Wall	0.96	None	4.7	13.9
9	Plug	0.0028	-	35.8	21.4
	Plug	0.00635	-	124.6	37.2

* I - wall having shallow, irregular scores

II - wall having regular scores

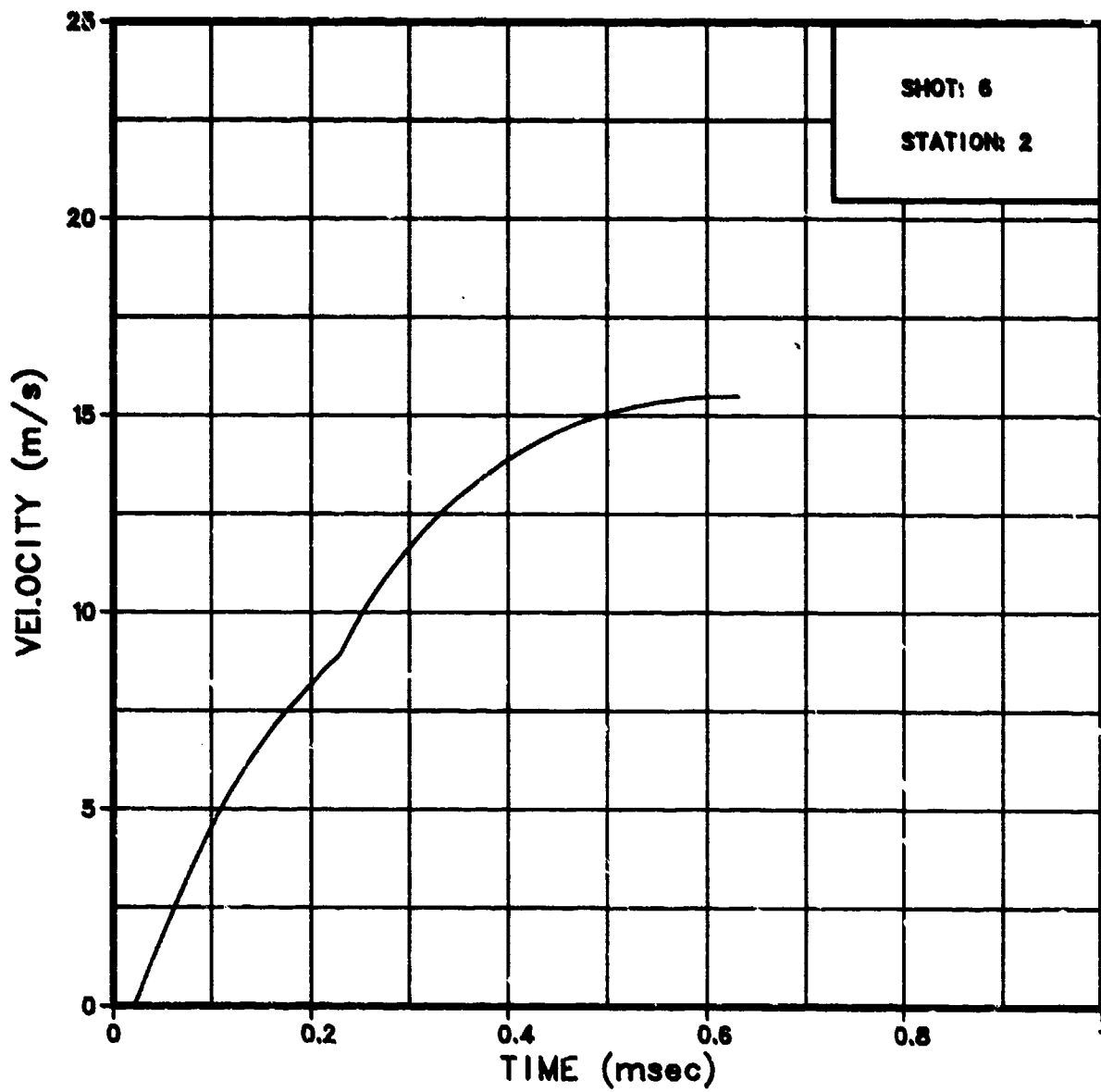


Figure 19. Velocity vs. Time for a Freely Translating 0.82 kg Concrete Wall Using Shot 6, Station 2 as the Applied Load

For the six shots where walls were tested, the measured velocities ranged from 4.7 m/s minimum for an unscored wall to 10.8 m/s maximum for the scored walls. Using Equation 5, the calculated upper limit velocities for walls were in the range 11.2-15.5 m/s. These calculations were based on Station 2, at the center of the nonresponding sidewall, for each shot where a wall was tested. There are several reasons why the measured velocities are lower than the limiting velocities. As previously indicated the true velocity is slightly greater than the measured velocity, because the fragments are accelerating for approximately 0.7 msec while the load is being applied. Furthermore some blast energy is required to breakup the wall; this energy will not accelerate the wall. Also, not all of the blast energy that reaches the fragment will go into fragment motion. Some portion of the blast wave will be diffracted around the fragments.

On Shot 1 valid measurements were not recorded. On Shot 2, a velocity of 6.3 m/s for a 6.35 gram plug was measured. This value is lower than the wall velocities, because the shock wave strikes the plug at a 33.9 degree angle and pushes the plug against its support instead of driving the plug straight through the hole. The upper limit velocity for the plug, 19.7 m/s, is higher than that for walls, because this plug is thinner than the wall and requires less applied force to propel it.

On Shot 9 the barricades were removed. The measured velocities of 35.8 and 124.6 m/s are not considered reliable. These could be measurements of the plugs or blast debris. Likewise, the upper limit velocities for Shot 9 are based on erratic pressure-time histories.

2. Comparisons. In Reference 1, Ward and Porzel used air blast parameters to analytically derive the blast load impinging on the center of the near sidewall of a Machrihanish magazine. The method used to derive the loading profile is discussed in the triservice manual, "Structures to Resist the Effects of Accidental Explosions" (Reference 10). There are several different magazine designs at Machrihanish; the magazine modeled in Reference 1 is 7.62 x 6.10 x 3.05 meters which is smaller than the magazine discussed in this report. Using the equations of motion, the idealized blast load was applied to a unit area fragment of the near sidewall. It was determined that the maximum velocity of a near sidewall fragment would be 58 m/s. These computations do not consider any blast shielding effects produced by the barricades.

Velocity measurements of fragments from 1/8 and 1/40 scale brick walls subjected to a blast wave are reported by Raynham (Ref. 7). The models were exposed to a 100 ton TNT blast; they were placed at the 66.2 kPa and 89.6 kPa side-on pressure level. The 1/8 scale walls were composed of 2.7 x 1.27 x 0.9 cm model bricks joined with a cement-lime mortar. The 1/40 scale walls were an amalgam of cement-lime mortar and red granite chips that simulated standard bricks on the 1/40 scale. Raynham concludes that for the 1/8 scale walls the mean velocity of the large fragments at the 89.6 kPa level is 16.2 m/s and at the 66.2 kPa level is 11.5 m/s. Similarly, for the 1/40 scale walls the mean velocity of the large fragments at the 89.6 kPa level is 19.4 m/s and at the 66.2 kPa level is 14.3 m/s.

IV. CONCLUSIONS

The fragment velocities measured in this 1/23.5 scale model experiment indicates that the mass detonation of one magazine would not cause a sympathetic detonation in the nearest neighbor magazine. The velocities measured were in the range of 4.7 - 10.8 m/s. Reference 1 has a discussion of the velocities required for munition detonation. Virtually all explosives of interest are safe from exposure to massive debris at 60 m/s.

ACKNOWLEDGEMENTS

The authors wish to thank all the players involved in this project. John Sullivan assisted in planning and implementing the quasi-static tests. Dominick DiBerardo performed the quasi-static tests, improvising all the way. Kenneth Holbrook, the charge handler and field technician, kept the field tests running smoothly. Bud Dunbar did his usual excellent job as recording engineer. Alan Trowbridge, of Dynamic Sciences, Inc., showed considerable skill in obtaining valid velocity measurements by modifying the break screen setup to accommodate blast effects. The assistance of Dynamic Sciences, Inc. was provided by the Velocity Measurements Branch of the Combat Systems Test Activity.

REFERENCES

1. F. B. Porzel, J. M. Ward, "Explosive Safety Analysee of the Machrihanish Magazine," NSWC TR 79-359, December 1979.
2. C. N. Kingery, G. Bulmash, P. Muller, "Blast Loading on Above Ground Barricaded Munition Storage Magazines," BRL TR 2557, May 1984 (AD A141677).
3. "The Effects of Nuclear Weapons," Department of the Army Pamphlet No. 50-3, March 1977.
4. G. A. Coulter, B. P. Bertrand, "BRL Shock Tube Facility for the Simulation of Air Blast Effects," BRL MR 1685, August 1965, (AD 475669).
5. G. A. Coulter, C. N. Kingery, P. Muller, "Blast Loading on Above Ground Barricaded Munition Storage Magazines-II," BRL TR-2694.
6. Private Communication.
7. C. J. Raynham, "Model Studies of the Movement of Debris from Brick Panels which Fail under the Action of a Blast Wave," United Kingdom Atomic Energy Authority, AWRE Report E 7/63, March 1963.
8. L. S. Marks, Mechanical Engineers' Handbook, seventh edition, McGraw-Hill, 1967.
9. R. J. Roark, Formulas for Stress and Strain, second edition, McGraw-Hill, 1943.
10. Departments of the Army, Navy, and Air Force, "Structures to Resist the Effects of Accidental Explosions," TM 5-1300, NAVFAC P-397, AFM 88-22, June 1969.

APPENDIX

PRESSURE-TIME RECORDS FOR SHOTS 1 AND 3 TO 8

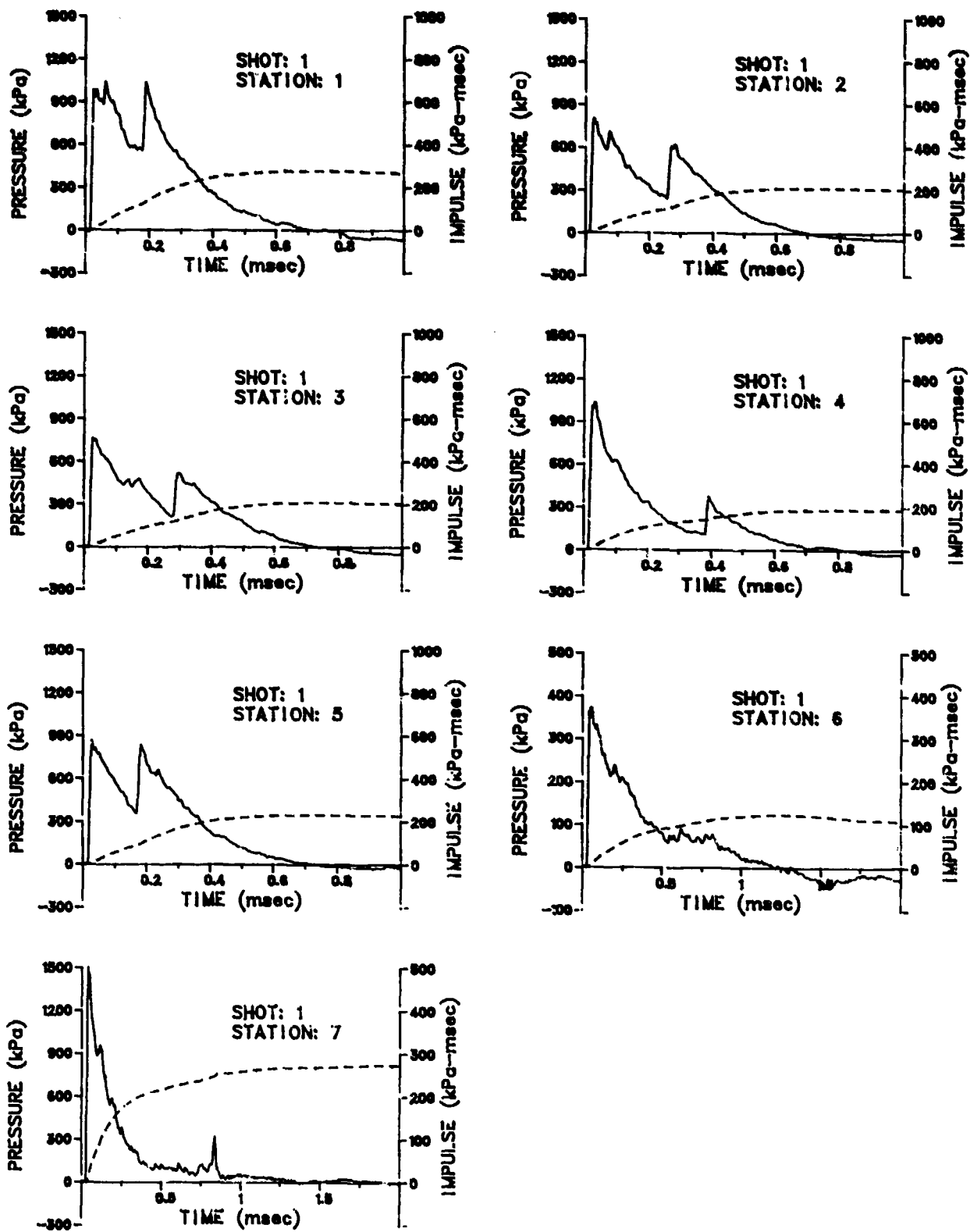


Figure A-1. Pressure-time Histories for Shot 1

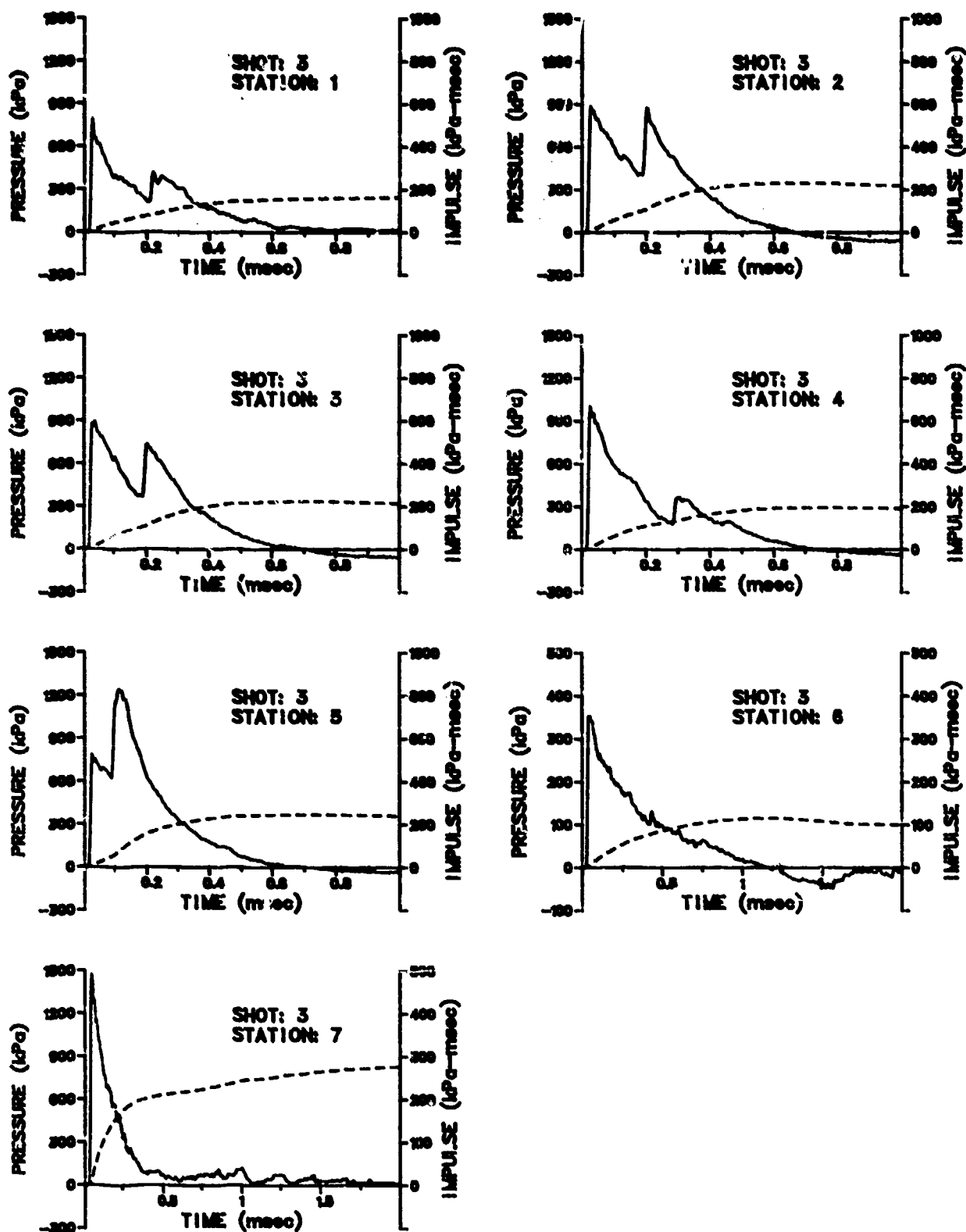


Figure A-2. Pressure-time Histories for Shot 3

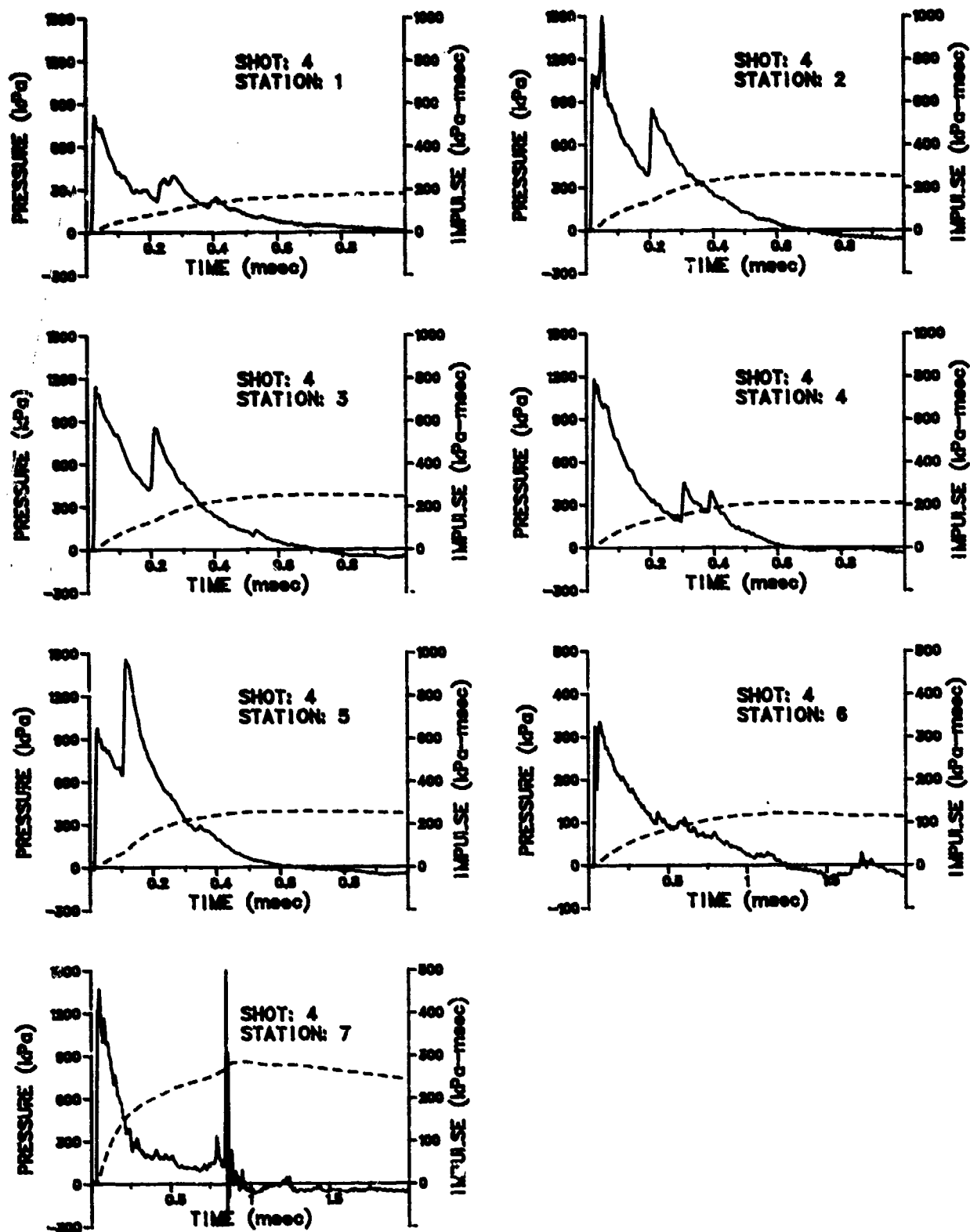


Figure A-3. Pressure-time Histories for Shot 4

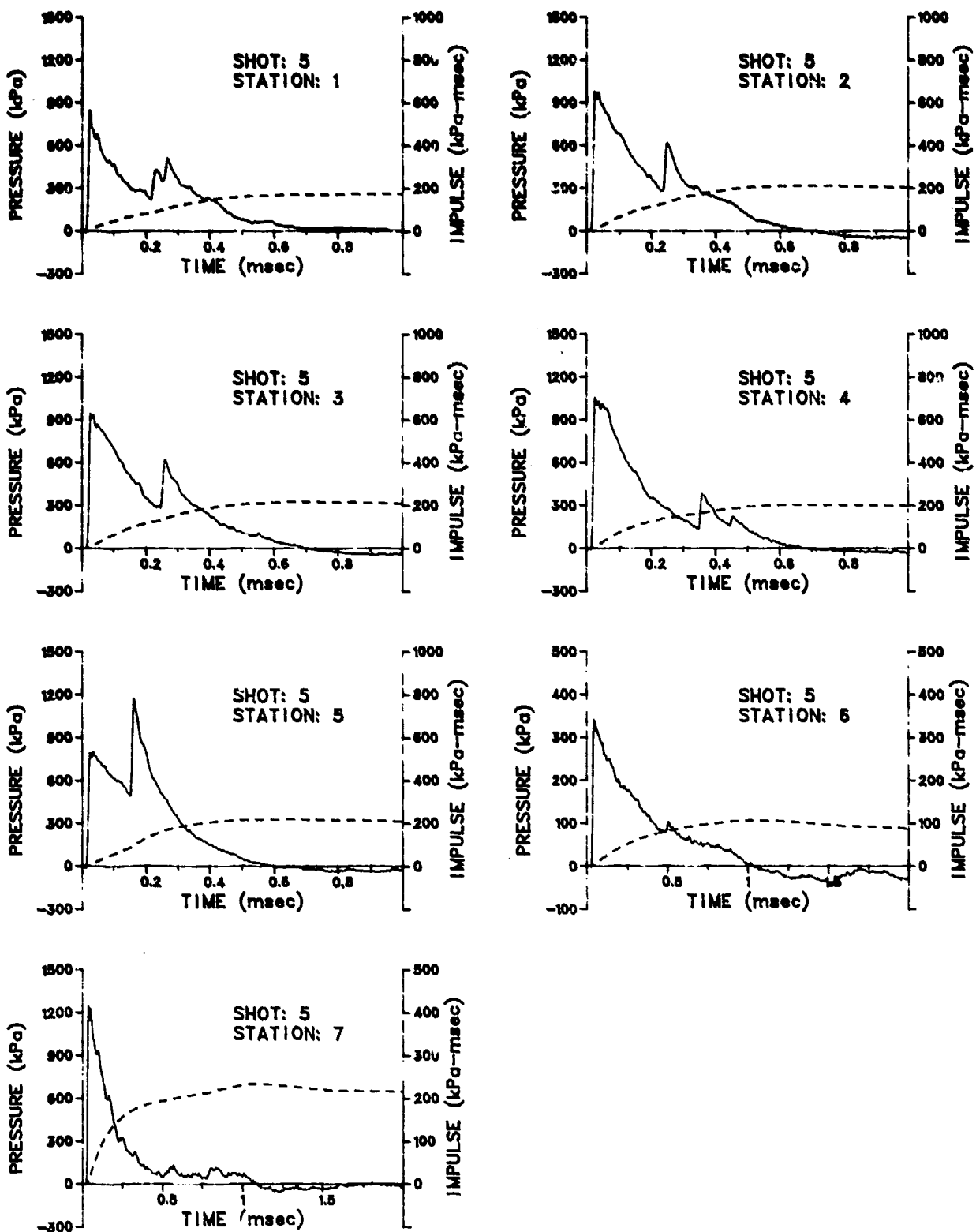


Figure A-4. Pressure-time Histories for Shot 5

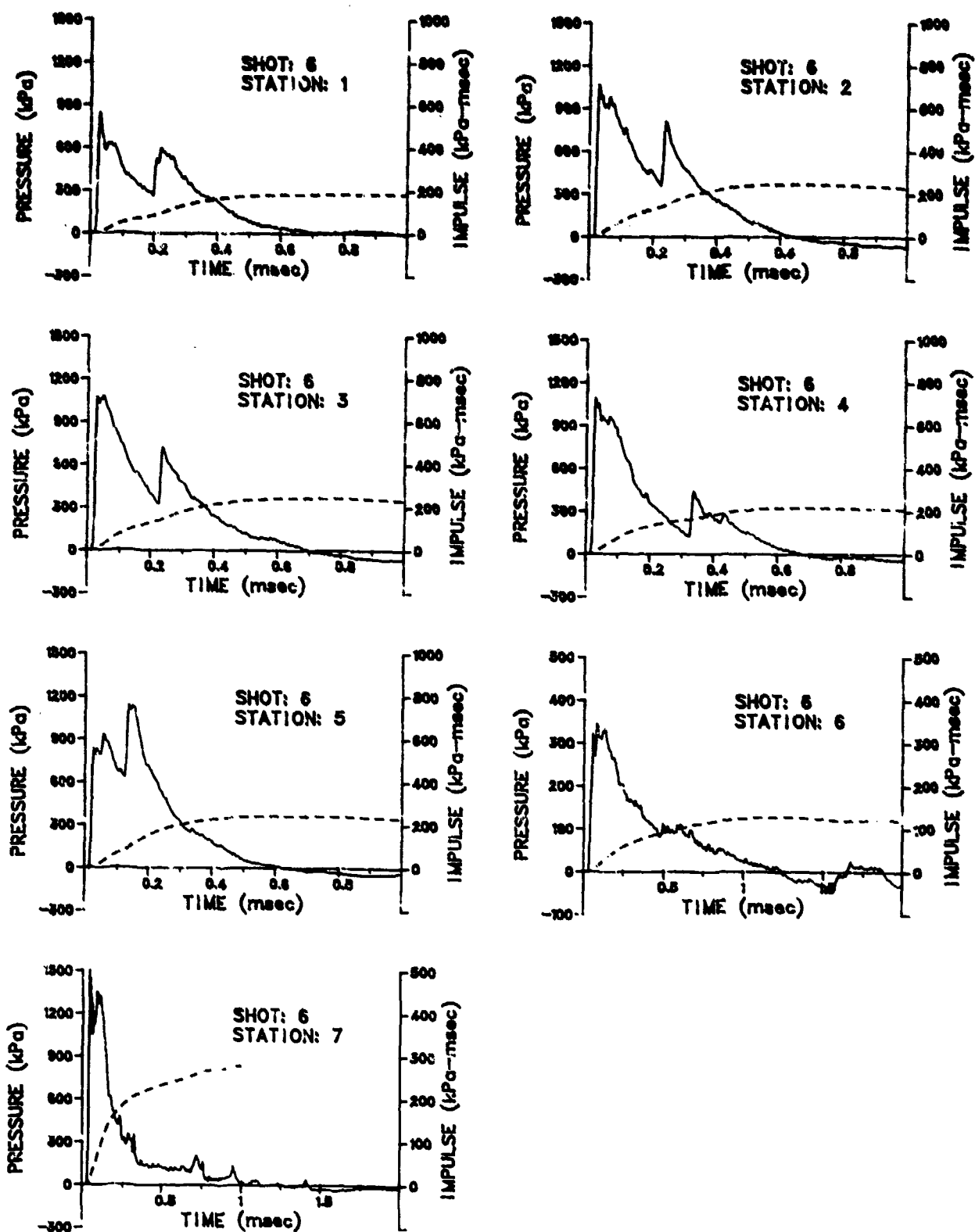


Figure A-5. Pressure-time Histories for Shot 6

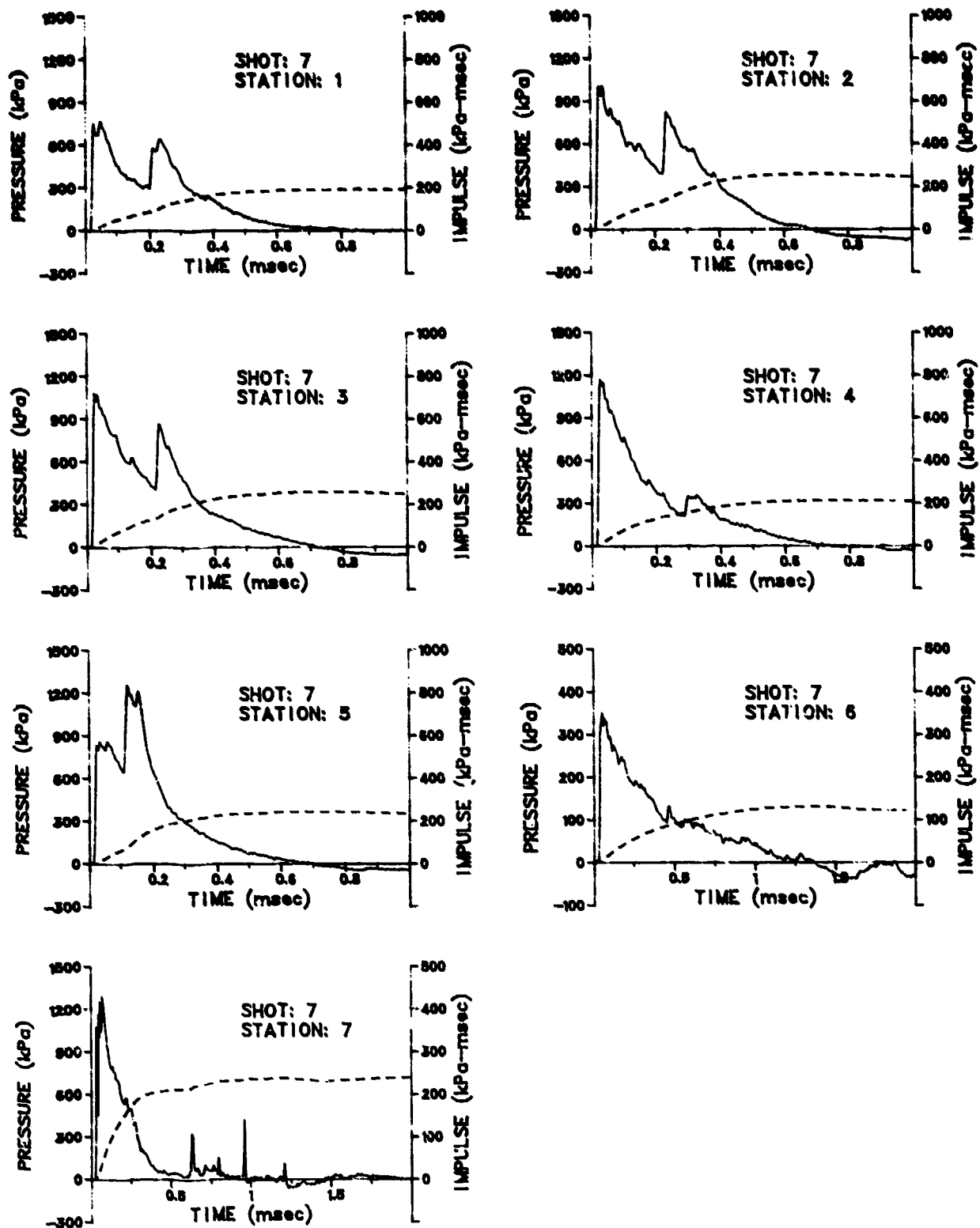


Figure A-6. Pressure-time Histories for Shot 7

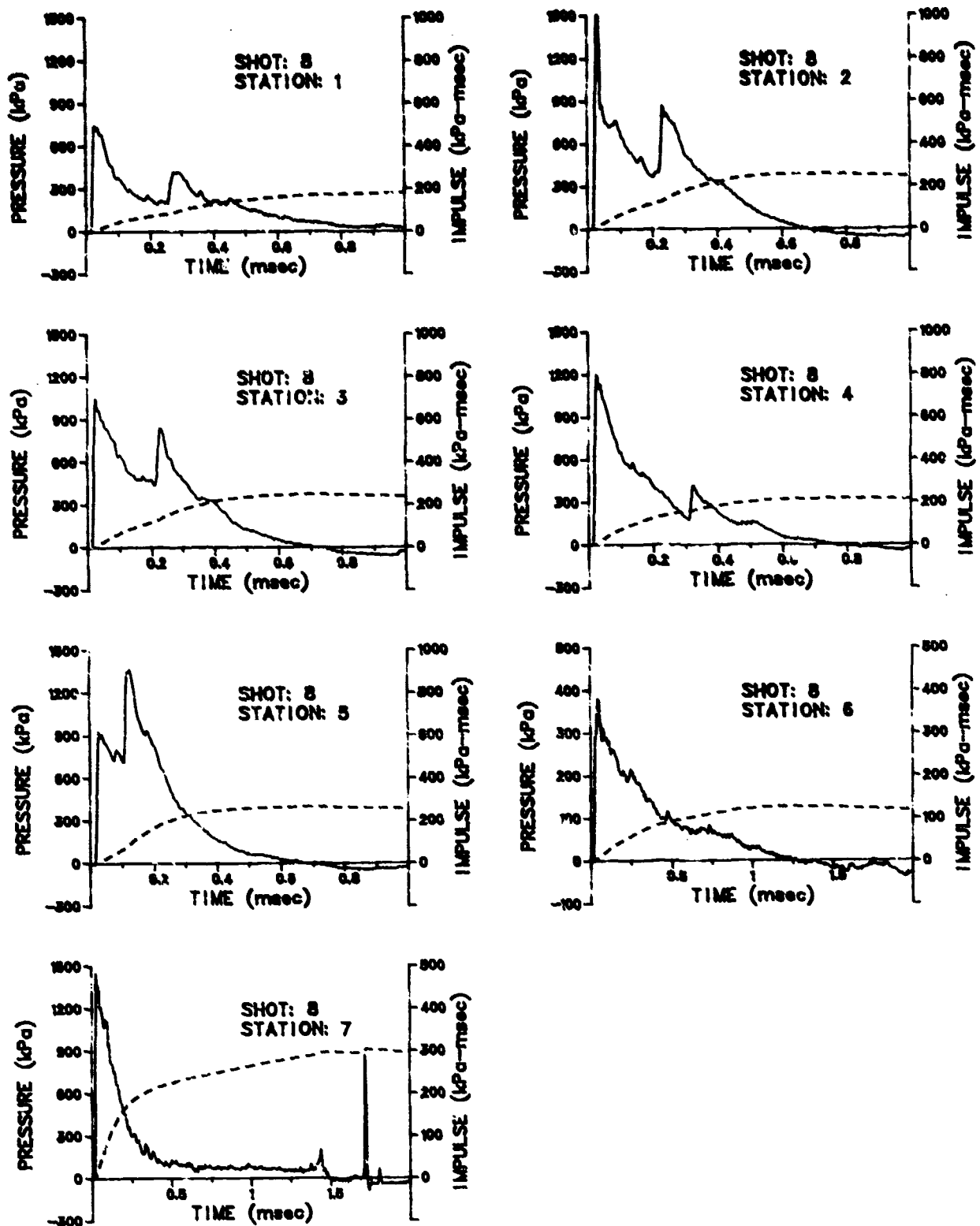


Figure A-7. Pressure-time Histories for Shot 8

1954

LA-UR

Los Alamos National Laboratory is operated by the University of California for the United States Department of Energy under contract W-7408-ENG-36.

AD-P005 380

TITLE: PREDICTIVE MODELS FOR THERMAL HAZARDS

AUTHOR(S): J. L. Janney and R. N. Rogers

SUBMITTED TO: 22nd Explosives Safety Seminar,
August 26-28, 1986
Anaheim Marriott Hotel
Anaheim, CA

By acceptance of this article, the publisher recognizes that the U.S. Government retains a nonexclusive, royalty-free license to publish or reproduce the published form or this contribution, or to allow others to do so, for U.S. Government purposes.

The Los Alamos National Laboratory requests that the publisher identify this article as work performed under the auspices of the U.S. Department of Energy.

Los Alamos Los Alamos National Laboratory
Los Alamos, New Mexico 87545

PREDICTIVE MODELS FOR THERMAL HAZARDS

J. L. Janney and R. N. Rogers

Los Alamos National Laboratory
Los Alamos, NM 87545

Many self-heating accidents with energetic materials have occurred when operations that have been done safely on a small scale are attempted on a larger scale. They have also occurred when a material is heated for a longer time or to a higher temperature than is normal for its processing or storage, such as might be caused by equipment malfunction or power failure.

To prevent self-heating accidents, we must be able to predict the critical temperature for the size and shape of the material we are interested in. The critical temperature ($T_{Sub C}$) is defined as the lowest constant surface temperature at which a material of a given size and shape will self-heat to catastrophic destruction. This can be burning, explosion, or detonation, and because it is related to heat flow, it is dependent on the geometry of the system. As size increases, the critical temperature decreases, as shown in Figure 1. The shape also affects the $T_{Sub C}$, so that a sphere will have a higher $T_{Sub C}$ than any other shape with the same radius or half thickness, as shown in Figure 2 for PBX 9501, plastic-bonded explosive.

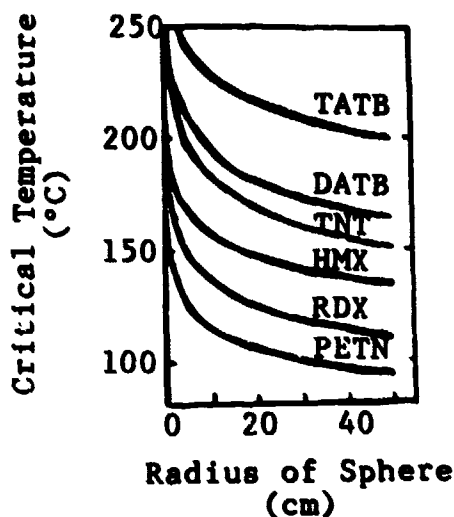


Figure 1. Effect of size on critical temperature.

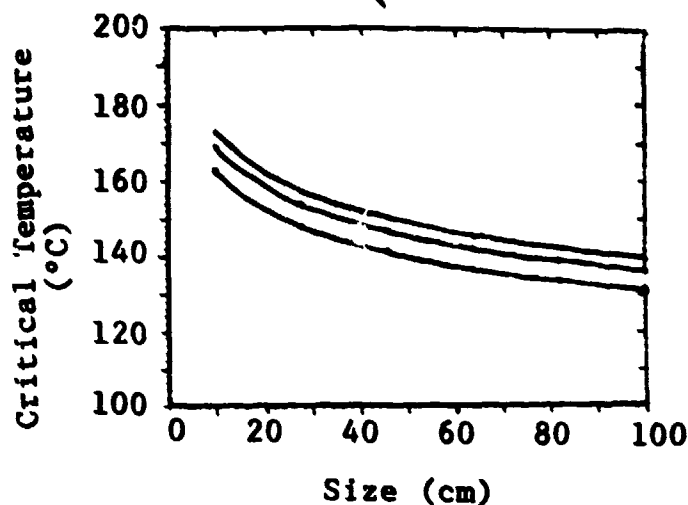


Figure 2. Effect of shape on critical temperature. Shapes shown are sphere (top), cylinder (middle), and slab (bottom).

The critical temperature can be calculated by the Frank-Kamenetskii¹ reactive-heat-flow equation for solid-state, unstirred systems,

$$\frac{E}{T_c} = R \ln \left[\frac{a^2}{6\lambda} \cdot \frac{\rho Q Z E}{T_c^2 R} \right]$$

or the Semenov² equation for liquid, stirred systems,

$$\frac{E}{T_c} = R \ln \left[\frac{V}{Sb} \cdot \frac{\rho Q Z E}{T_c^2 R} \right]$$

- where T_c = critical temperature, Kelvin
 E = Arrhenius activation energy, cal/mole
 Z = pre-exponential (frequency factor), s^{-1}
 R = gas constant, 1.9872 cal/K mole
 a = radius of sphere or cylinder, or half-thickness of slab, cm
 ρ = density, g/cm^3
 Q = heat of reaction, cal/g
 δ = shape factor; 3.32 for sphere, 2.72 for 1-d cyl., 0.88 for an infinite slab
 λ = thermal conductivity, $cal/^{\circ}C \cdot s \cdot cm^2$
 V = volume, cm^3
 S = surface area, cm^2
 b = heat flow coefficient of vessel, $cal/^{\circ}C \cdot s \cdot cm^2$

In order to calculate the critical temperature, we need to know the kinetics of the decomposition. We use a differential scanning calorimeter (DSC) to measure the rate of heat evolution, from several samples at dif-

ferent isothermal temperatures. This rate of heat production is proportional to the absolute rate of the total chemical reactions at any given instant, as follows:

$$\frac{dq}{dt} = Q \frac{d\alpha}{dt} = kQf(\alpha) ,$$

where Q = heat of reaction

α = fraction decomposed at any time

k = chemical rate constant

$f(\alpha)$ = the applicable rate law.

The DSC rate curve will give us the rate of heat production as a function of time. If we calculate the area under the curve with Simpson's rule we can find the fraction decomposed at any given time, α , by dividing the partial area to that time, a , by the total area, A , as shown in Figure 3. We can then calculate $d\alpha/dt$.

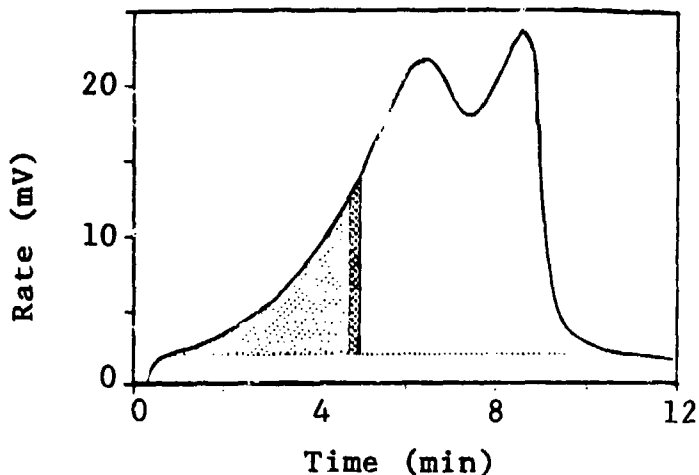


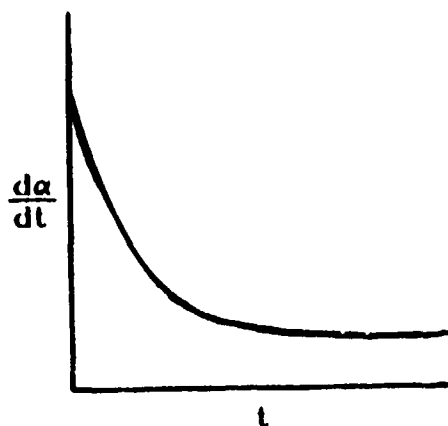
Figure 3. Rate curve.

[] Partial area, a

[] Change in area, $\frac{\Delta a}{\Delta t} ; \lim_{t \rightarrow 0} = \frac{da}{dt}$

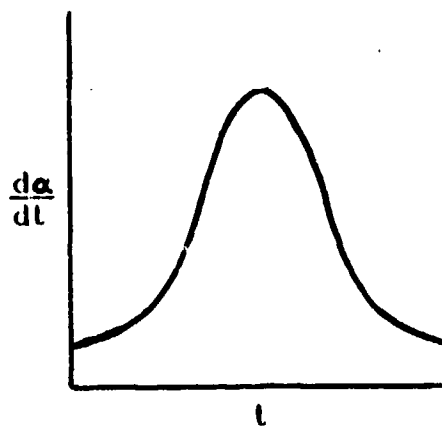
Total area under curve, A , is calculated using an extrapolated final baseline.

To find the rate constant, we must use a rate law that will linearize the data for the part of the reaction that represents catastrophic self-heating. Most computer software programs use a normal rate law for the decomposition. A first-order rate law assumes maximum rate at the beginning, as shown in Figure 4. Most explosives, however, are complex, and decompose more nearly according to an autocatalytic-type rate law as shown in Figure 5, where the heat evolution builds up to a peak after intermediate products have been formed.



$$\frac{d\alpha}{dt} = k(1 - \alpha)$$

Figure 4. Idealized first-order rate curve.



$$\frac{d\alpha}{dt} = k\alpha(1 - \alpha)$$

Figure 5. Idealized autocatalytic-type rate curve.

The total heat evolution may be expressed by the equation

$$\frac{d\alpha}{dt} = k_1 + k_2(1-\alpha)^n + k_3\alpha^p(1-\alpha)^q,$$

where each term may represent several simultaneous or sequential reactions. For thermal hazards predictive models, we use the global heat, since it is the rate of the total heat evolution that will determine whether the decomposition will be catastrophic.

The rate curve for triamino trinitrobenzene (TATB) is shown in Figure 6. If we use its data to calculate the values necessary for an autocatalytic rate law plot, we get the curve shown in Figure 7.

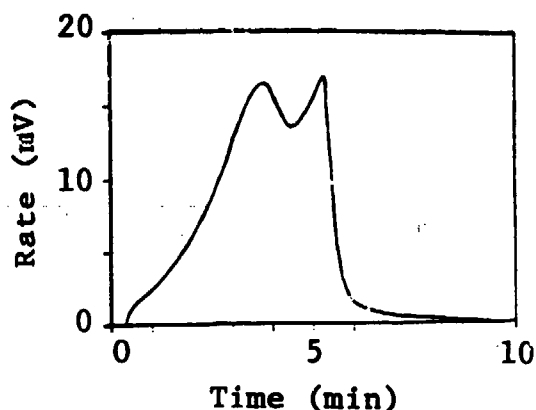


Figure 6. Isothermal DSC rate curve for TATB at 630 K.

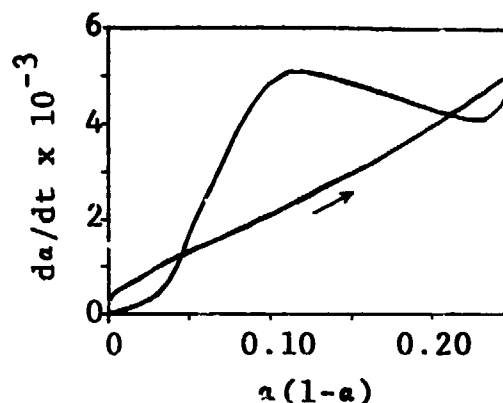


Figure 7. Autocatalytic-type rate law curve for TATB. The curve folds back on itself at $a(1-a) = 0.25$.

The slope of the linear portion is the rate constant, k , for that temperature.

To be valid for our calculations, the rate constants found from runs at different isothermal temperatures must also be from data linearized by the same rate law and for the same per cent decomposition. Otherwise we will not be comparing rate constants for the same decomposition mechanism, and an Arrhenius plot will not be valid.

Occasionally, rate constants for energetic materials can be calculated from normal rate laws. We then find the linear section from a plot such as that shown in Figure 8. The slope of the linearized segment will be the order, and $\ln k$ for that order can be found by extrapolating to 0. Figure 9 shows an order plot for Composition B, a mixture of 59.5/39.5/1 RDX*/TNT/wax. Again, the order at different isothermal temperatures must be the same, or

*Cyclotrimethylene trinitramine

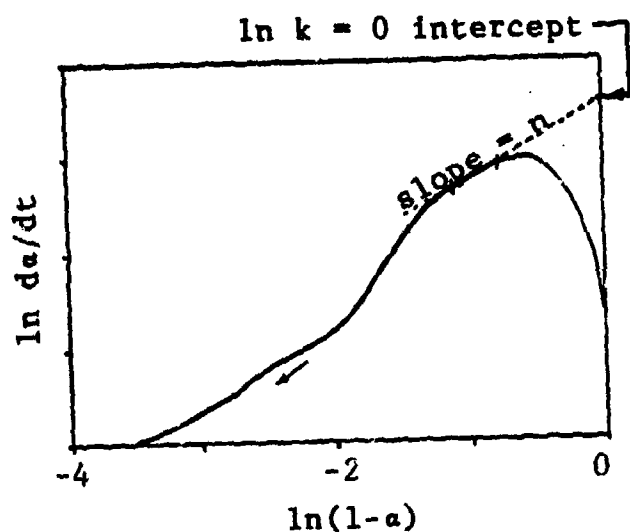


Figure 8. Order plot. Positive slopes represent data from the decay portion of the rate curve.

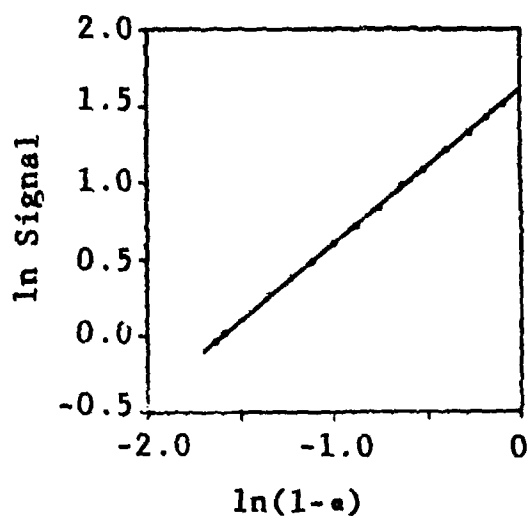


Figure 9. Order plot for Comp B at 500 K. The experimental order is 1.0.

nearly so, for the Arrhenius plot of the rate constants to be valid. When the orders at different temperatures are different, either the mechanisms have changed, or different parallel reactions have become predominant at the new temperatures.

A function might be found that would linearize the data throughout the decomposition, but for energetic materials with different decomposition mechanisms, such a function would have little chemical validity.

After we know the rate constants from the different isothermal runs, as calculated from any rate law that has chemical meaning, an Arrhenius plot can be made, as shown in Figure 10 for Comp B. The activation energy and pre-exponential are determined from the slope, which is equal to $-E/R$.

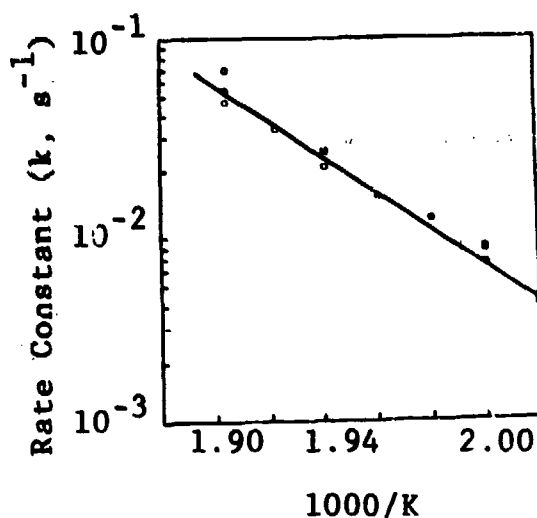


Figure 10. Arrhenius plot for Comp B, obtained from first-order data.

As may be expected, linear segments from different parts of the rate curves may give different rate constants, thus different sets of values for E and Z . Only one set will accurately predict the critical temperature for all sizes and shapes, so we must verify that the values we have chosen are the ones that represent the mechanisms that control self-heating.

The thermal properties of an explosive may differ greatly from batch to batch. The overall rate of the chemical reactions that occur during the induction time is determined by the number and energy of high-free-energy zones present. These may be caused by such things as crystalline imperfections and impurities. Figure 11 shows the differences in the rate curves of several kinds of cyclotetramethylene tetranitramine (HMX).

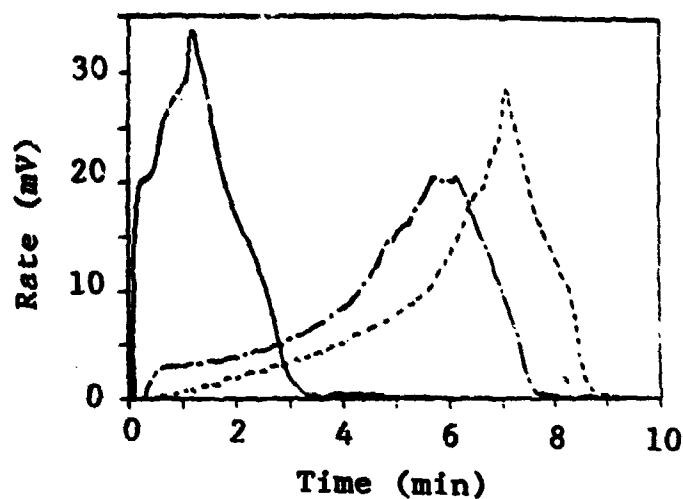


Figure 11. Isothermal rate curve data for three samples of production-grade HMX. Samples approximately 1 mg, run at 545 K.

We use a separate, small-scale laboratory test* to verify our results. A small sample, usually about 40 mg, is sealed into an empty blasting cap, and its thickness is measured. This sample is lowered into a molten metal bath at a constant, known temperature, and the time to explosion is measured. This test is repeated at different temperatures until we have found the temperature below which no explosions will occur.

*The test is a modification of the one described by Henkin and McGill³.

We can calculate the critical temperature for this size and shape with our DSC values for E and Z in the Frank-Kamenetskii equation. If the calculated T_c equals the experimental T_c , we feel we can make predictions for other sizes and shapes with some confidence, and this becomes our predictive model. If the predicted and experimental temperatures do not agree, however, we may not have calculated our kinetics values properly, or there may be errors in the other variables. A discrepancy may also indicate a significant pressure effect. The DSC tests are done at atmospheric pressure under a nitrogen purge gas, and the time-to-explosion test, while not able to withstand high pressures, confines the gases up to several atmospheres.

When the predictive model needs further verification, or when there is no predictive model and information is needed about whether a material will self heat catastrophically at a given temperature, a large-scale test can be done. We use a pair of 1-liter heating mantles around liter flasks of castable explosives, or a pair of machined hemispheres of explosives if they will not melt at the test temperature. Thermocouples are placed at several positions in each mantle, and the temperature controllers are adjusted so that the hottest spot in each mantle controls its temperature. Thermocouples may be placed in the center of the sample if it is desired, and recorders can be attached to the thermocouples to chart the temperature excursion as the sample heats. The explosive assembly is placed in a 6-ft steel-walled containment vessel, and brought to a predetermined isothermal temperature as quickly as possible. It is then left until the sample self heats, which may be as long as several weeks if the experimental temperature is very near the critical temperature.

The small-scale time-to-explosion test is also good for ranking explosives in order of thermal stability. The compatibility of materials in formulations can also be easily checked, as illustrated by the HMX-Pb mixtures in Figure 12.

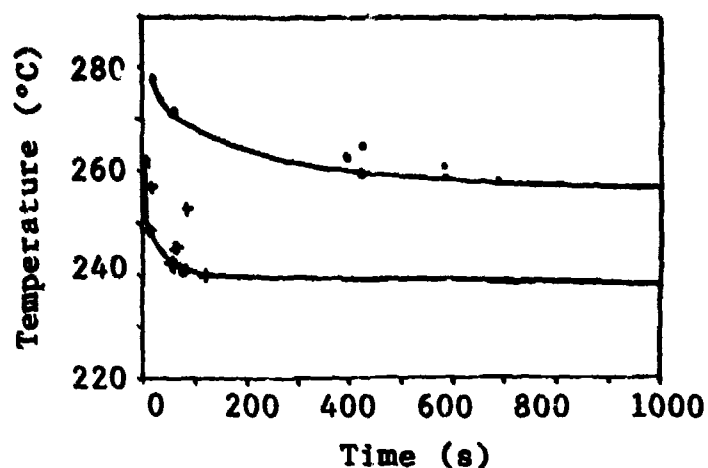


Figure 12. Critical temperature data for HMX (top) and HMX/Pb 50/50 vol% (bottom).

This test can also be used as a quality control test. Times to explosion may be affected by crystalline defects in the material, or particle sizes, even when the critical temperature may not vary significantly. Impurities and additives such as are found in fertilizer-grade ammonium nitrate can cause a difference of about 100° in the critical temperature at these small sizes, as well as a shorter time to explosion at the same temperature. Such decreases might cause an unacceptable decrease in the safety margin for processes conducted near the critical temperature.

REFERENCES

1. D. A. Frank-Kamenetskii, *Diffusion and Heat Transfer in Chemical Kinetics*, Plenum Press, New York, NY, 1969.
2. N. N. Semenov, *Chemical Kinetics and Chain Reactions*, Oxford University Press, London, 1935.
3. H. Henkin and R. McGill, *Ind. Eng. Chem.*, 44 (1952) 1391.

1966

AD-P005 381

MULLER MIXER FIRE
"LESSONS LEARNED"

BY

B. V. DIERCKS
J. E. HAWLEY
M. L. NARON

MORTON THIOKOL INC.
Longhorn Division
Marshall, Texas 75670



1967

↙
The purpose of this paper is to share some of the actions taken by Morton Thiokol, Inc. to enhance safety in pyrotechnic muller mixing operations at Longhorn Army Ammunition Plant. These initiatives resulted from the investigation of a muller mixer fire which occurred on October 30, 1985. It is the safety management philosophy of Morton Thiokol Ordnance Operations that all explosive accidents and significant near miss incidents be thoroughly investigated, by the Engineering and Safety Committee, utilizing a safety systems approach. This committee, which is chaired by the Director of Engineering, B. V. Diercks at the Longhorn Division, was charged with identifying the causative deficiencies and ancillary procedural, equipment design and human engineering changes required to enhance the overall system. To assist Mr. Diercks in this investigation, the following personnel were key contributors in the safety initiatives developed from the analysis of this incident:

J. E. Hawley
T. R. McClellan
M. L. Naron
F. J. Russell
W. M. Teague

Safety & Security Manager
Chief Safety Engineer
Technical Specialist
Mechanical Engineer
Safety Engineer

CONFIDENTIAL 29, 1985

On October 30, 1985 at approximately 0830 hours a flash fire occurred in Bay D of Building B-11 while mixing M22 flash composition. This was a remote video camera monitored operation. The fire initiated in a size 05 dual wheel National Engineering stainless steel Special Simpson Porto Muller equipped with two-200 pound muller wheels plus an inside and outside plow. Both plows were fitted with nylon wipers positioned in direct contact with the bowl surface.

Longhorn AAP has used this blade to bowl contact mulling procedure since the mid-60's. The mixer wheels/plows revolve at approximately 18 RPM and are driven by an 1800 RPM 3 H.P. motor through a double belt sheave and gear box. The bowl diameter is approximately 39 inches and 12 inches deep with the mulling wheels/plows geared to move in a counterclockwise rotation. All bays are equipped with closed circuit TV monitors, Backarack explosive vapor alarms, Detronics UV rapid acting deluge and fusible link wet pipe fire protection systems with electrically interlocked emergency exit doors, fire door and vapor alarms to remote controls. Also provided is 100 percent make up air with temperature and humidity control, vapor/dust removal systems connected to an external wet type Rotoclone dust collector that is electrically interlocked to the control panel. Walls between bays and control room are substantial dividing walls of 12 inch thick reinforced concrete with three feet of sand fill between bay and control station walls. (Figure 1 illustrates B11 configuration)

At the time of the incident, Bays A and B were inactive while Bay C was in same mix cycle as Bay D. The pyrotechnic being manufactured was a M22 flash composition mix which is composed of Magnesium (93.75 lbs.), Teflon (12.5 lbs.), and Viton Binder (18.76 lbs.) dissolved in Methyl Ethyl Ketone (44 lbs.). This was the first mix of the day with bowls in both Bays C and D being charged with only the Magnesium and the dissolved Binder. No Teflon had been added. The remote mix operation had run approximately 7 of the 10 minutes when the flash fire occurred. The fire caused superficial damage to Bay D and equipment with most of the production material either being consumed or tossed out of the bowl by deluge system. No personnel injuries were incurred. The fire ball did not propagate to Bay C due to the rapid acting deluge system but was

forced into the back corridor and out the emergency exit nearest Bay D. The fire ball also vented over the top edge of the sliding corridor fire door igniting contaminated surface along the fire door track and ceiling. In interviewing the operator who was supposed to have been watching the TV monitors, there was no indication of a problem before she heard a boom and looked up and to see Bay D engulfed in flames on the TV monitor. (Figure 2 shows damage in Bay D)

continued
In conducting this investigation a local and worldwide canvassing of industry incidents failed to identify a similar accident that occurred in the production cycle experienced. Not having a comparative data base to draw on, a complete equipment and supporting systems tear down and analysis was conducted. This evaluation included component design, production material quality control and sensitivity testing, electro-mechanical interfaces, manufacturing processes and procedural adequacy. Without belaboring all the causative possibilities considered the following four were considered the most probable in order of priority:

- ✓ Friction due to Mechanically Damaged Lip Seal in Muller Wheel,
- ✓ Friction Between Material Contamination in Bearings,
- ✓ Friction Between Plow Blades and Bowl, and
- ✓ Exothermic Moisture Reaction.

The above scenarios were selected as most probable since a man/machine interface was not evident at the time of the incident coupled with mechanical damage, contamination and fire being identified inside a muller wheel. This was also supported by no unusual observations noted prior to the incident or during post production material screening, chemical analysis, and sensitivity testing. Electro Static Discharge (ESD) was not indicated as all electrical continuity systems checked. The investigation of this incident centered primarily on friction/spark ignition, e.g., ignition temperature of MEK is 960°F with a flash point of 70°F while M22 composition is 752°F. The frictional heat levels indicated were considered achievable in the scenarios hypothesized.

The most probable cause was identified during detailed disassembly of the muller wheels which found a damaged Garlock Klosure Lip Seal. Under microscopic examination it was apparent that the metal spring fingers in the lip seal had made metal to metal contact with the axle plus there was indication of fire in the area. Small amounts of explosive contamination were also found past the lip seals in bearings of both the muller wheel and center support post. To correct this deficiency the muller wheel assembly (Figures 3 and 4) has been redesigned with a redundant Ethylene Propylene "O" ring seal plus potting the void in lip seal with solvent resistant Epon 828 and Versamid 125 filler. The lip seal filler prevents explosive product entrapment and build up at the edge of the lip seal, protects finger springs, and aids in cleaning of center support post lip seal. The effectiveness of this lip seal configuration was tested in inert and live prove out mixes which established a twenty (20) shift replacement schedule of all lip seals and bearings. This preventive maintenance baseline may be extended as future experience warrants. Eight months of continuous operations has seen no migration of product past lip seals. (See Figure 5)

The third alternative focused on friction between pyrotechnic composition entrapped in the rough bowl surface and rubbed by direct contact wipers and plow blades causing hot spots. As indicated at the beginning of this paper, the

Longhorn Division has used nylon wiper/plow blades in "Zero" clearance with bowl surfaces for over ten (10) years without incident. The rough condition of bowl surface was due to years of continuous multi-product use without an adequate program to periodically reface bowl and wheel surfaces. The result was a badly worn bowl and muller wheel surface. In addition, it was also discovered that the Total Indicated Runout (TIR) of the bowl was excessive and that the bowl flexed when torque was applied from drive belts. To correct these deficiencies the bowl and wheels were refaced to remove all scratches, scores and gouges, the high points of the mixer wall and bottom were identified and marked on the bowl plus a drive belt tension stabilizer support was added to drive shaft. The muller wheels were also slightly crowned to push possible foreign material out from under wheel. The nylon blades were replaced with ultra high molecular weight conductive polyethylene blades which are installed with a minimum .030 clearance. This blade to bowl clearance is verified daily by production foreman. The last two initiatives were felt necessary to increase our safety margin by eliminating the possibility of static charge generation buildup on nylon blades. The .030 standoff also reduces the potential for blade/bowl friction points. In addition, a nylon bolt was added between rocker arm and crosshead to prevent metal to metal contact and pinching of material. (See Figure 6)

The last scenario involves the possible introduction of moisture with magnesium causing an exothermic chemical reaction with the release of hydrogen. Due to the rain the night before and morning of the incident, the introduction of moisture was a consideration but could not be substantiated. Post testing of magnesium, MEK and binder lots found no moisture specification discrepancies. Operators interviewed had not noticed any water dripping or condensate forming on the Rotoclone duct. Taking an ultra conservative safety approach, action was taken to preclude this possibility happening by requiring all magnesium, teflon and MEK binder solutions to be preconditioned prior to use at 60°F for sixteen hours (16 hours). Daily moisture samples of MEK are taken plus the Rotoclone duct system has been modified with an internal condensate flange trap with take off piping. Temperature and Relative Humidity Recorders have also been installed in all weigh up and muller mixing operations to accurately document the temperature/humidity conditions at the time of weigh up, mixing and mulling.

In addition to the direct causative refinements discussed, the detailed analysis of operating, maintenance, documentation procedures and equipment design surfaced a number of ancillary initiatives which have enhanced the safety of our muller mixing operations. The following is a summary of those observations with improvements made.

- Crew Leader failed to observe ignition point on TV monitor. Video and audio VCRs have been installed in all remote muller mixing and granulating operations.
- High pressure water used to clean bowls dispersed atomized composition particles which became airborne or floated in run off water becoming attached to walls, ceilings, underside of bowl, drive system compartment and dump door trunnion housing. High pressure water cleaning is no longer used, periodic washing of bay and corridor walls and ceiling is required, drive system compartment has been encapsulized with clear lexan cover to eliminate

motor compartment contamination plus the capability to observe motor and drive belt operations. The dump door has also been modified with "O" ring seal and a product containment chute.

- Millwrights were manually lifting and positioning 200 pound muller wheels in bowls. A large number of dents were caused by dropping or positioning wheels in bowls. A portable lifting device and bracket have been installed on the mixer drive compartment to assist when performing special and preventative maintenance operations.
- During the initial mixing cycle of inert and live testing, pockets of unacceptably high explosive vapor levels were not detected by the Backrack Vapor Alarm mounted just outside bowl lip. To correct this deficiency, the air exhaust system was rebalanced plus an air purge capability installed. In addition, the wiper blade was redesigned to improve mixing flow and homogeneity characteristics which minimizes explosive vapor entrapment. The vapor alarm system was set to activate at 20% of the Lower Explosive Limit (LEL). Also all dual wheel mullers were modified with reverse (clockwise) rotation capability.

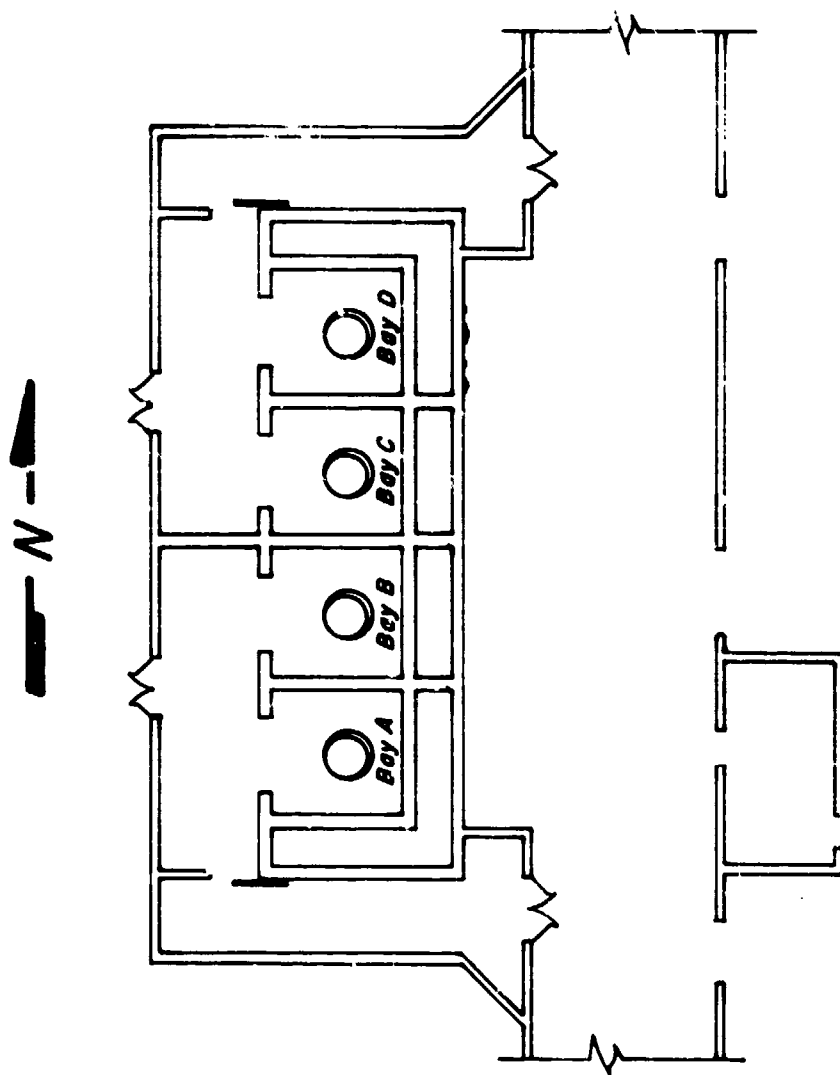
The improvements resulting from our Lessons Learned are being institutionalized at Longhorn AAP. All dual wheel muller mixers have been modified and we are now addressing a detailed design review of single wheel mullers. The procurement specifications for upgrade replacement of mullers have incorporated these refinements plus providing for a side opening dump door to aid in cleaning and maintenance, and thicker bowl construction to minimize flex and hold TIR.

It is the desire of Morton Thiokol that the Lessons Learned presented be of value and where applicable incorporated into the readers safety program. An explosives incident jeopardizes the safety and health of our most important resource - our employees - and tarnishes the credibility of our industry. We must continually strive for safety excellence. At Longhorn AAP our goal is "Zero Accidents" and is reflected in our Safety Creed:

- Pyrotechnics are Unforgiving
- Man can be Unthinking
- Complacency is the Road to Failure

While the tenants of that creed are absolutes the last is the most germane to the case study. The human fallacy of complacency coupled with the mystique of pyrotechnics and the philosophy of "Don't Fix It If It Is Not Broke" was the road to this system failure. Hopefully the Lessons Learned and the initiatives taken will assist our industry in being proactive rather than reactive in the future.

Figure 1



BUILDING B-11

Figure 2

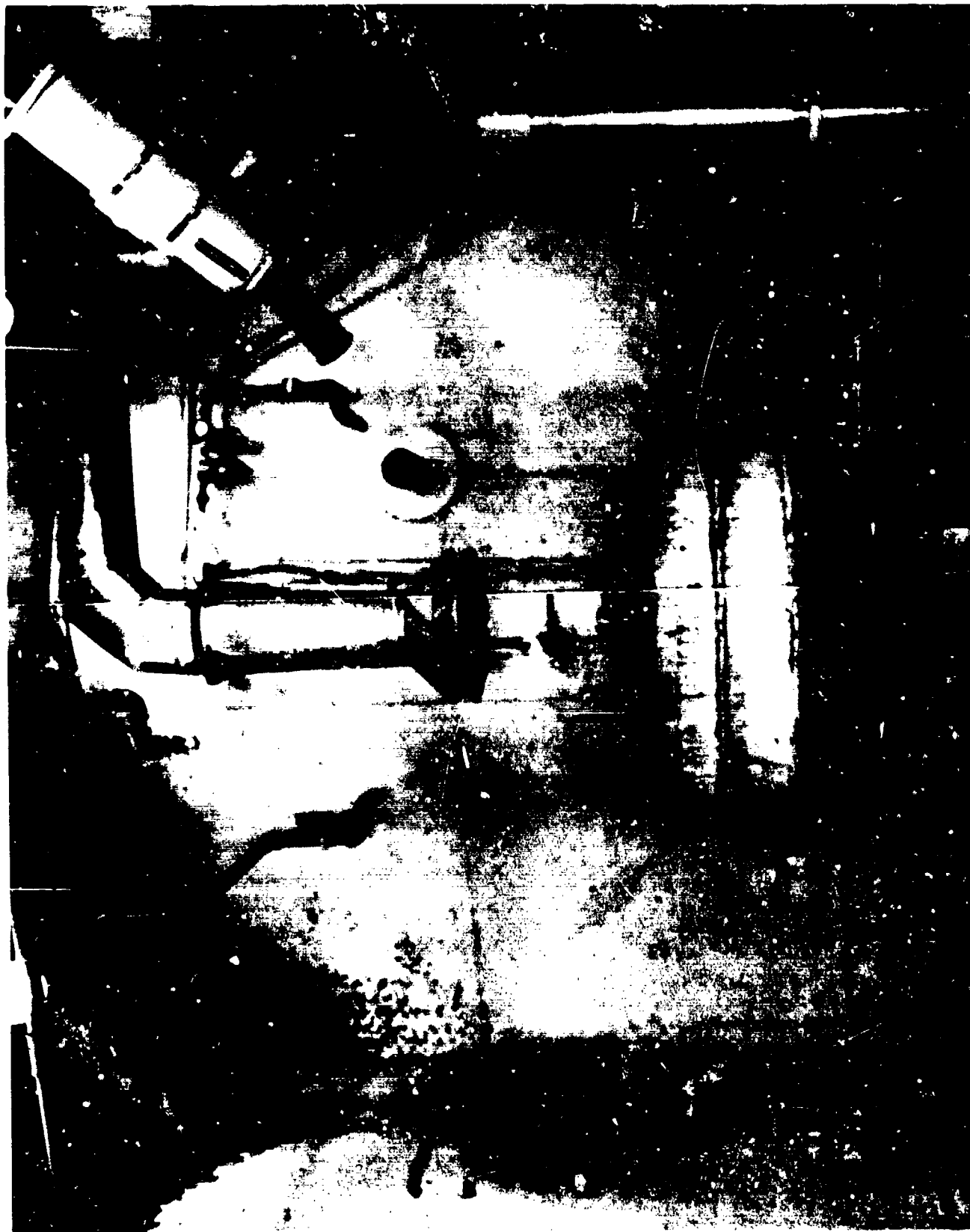


Figure 3

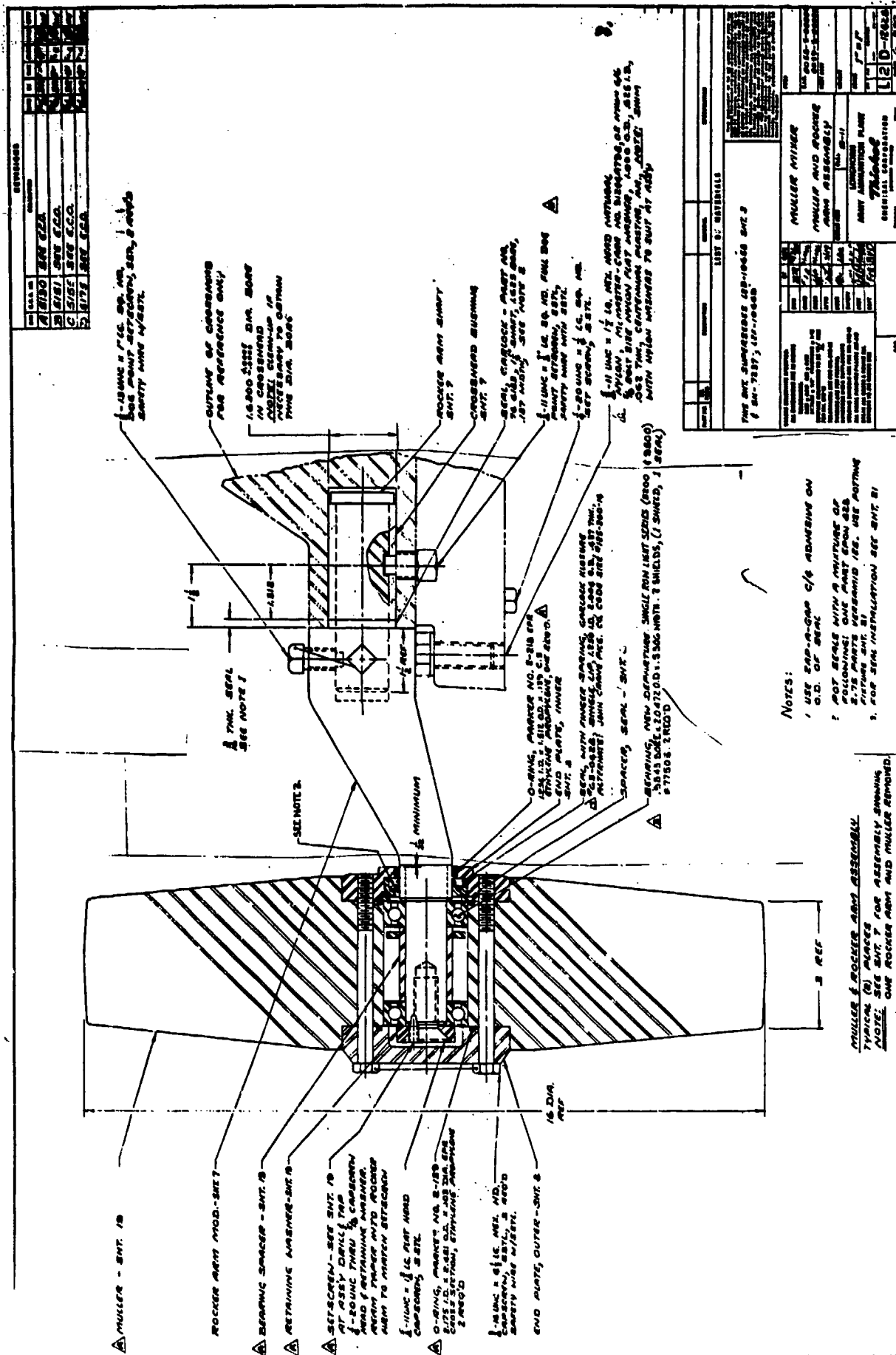


Figure 4

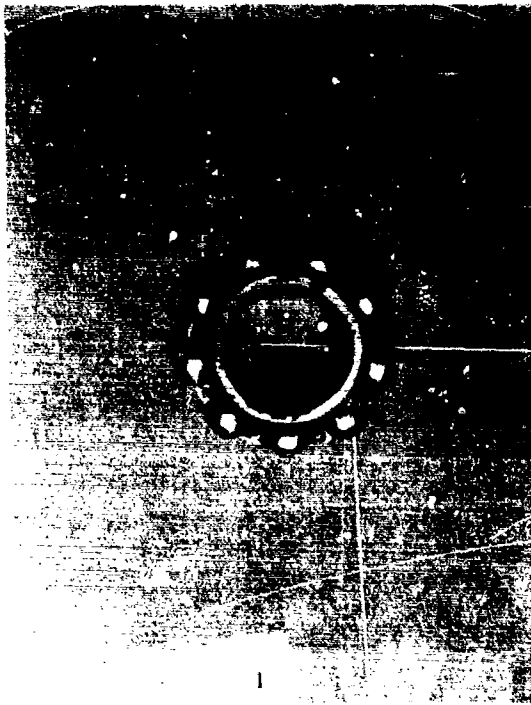


Figure 5

GARLOCK KLOUSURE LIP SEAL

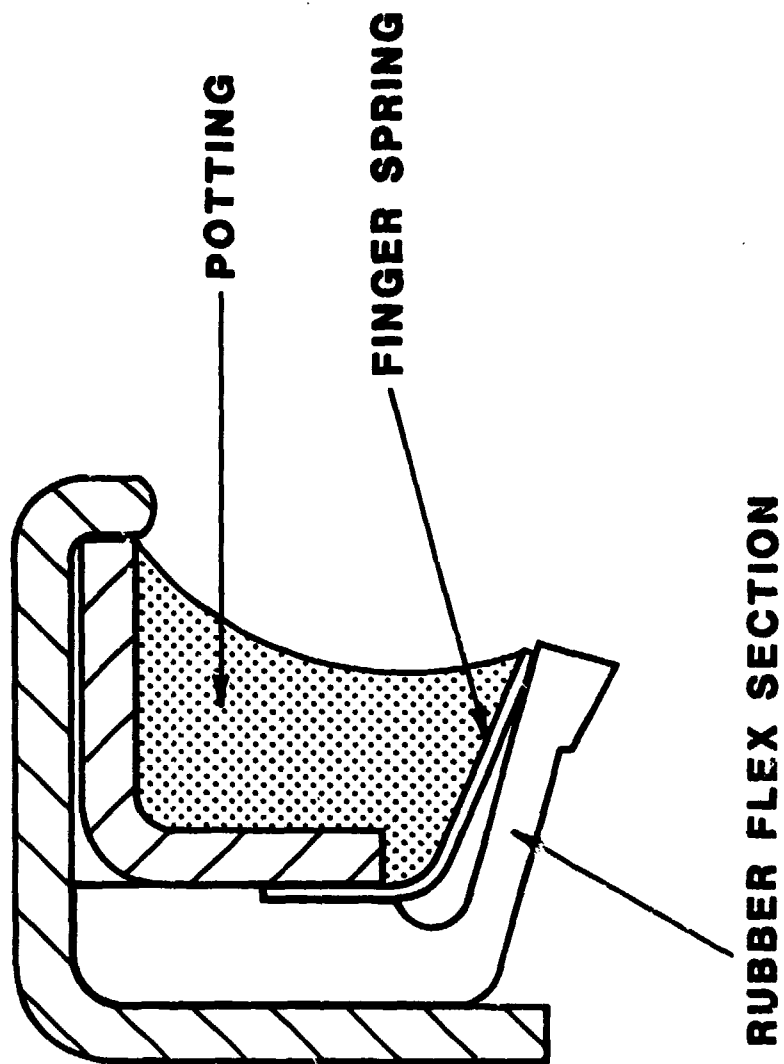
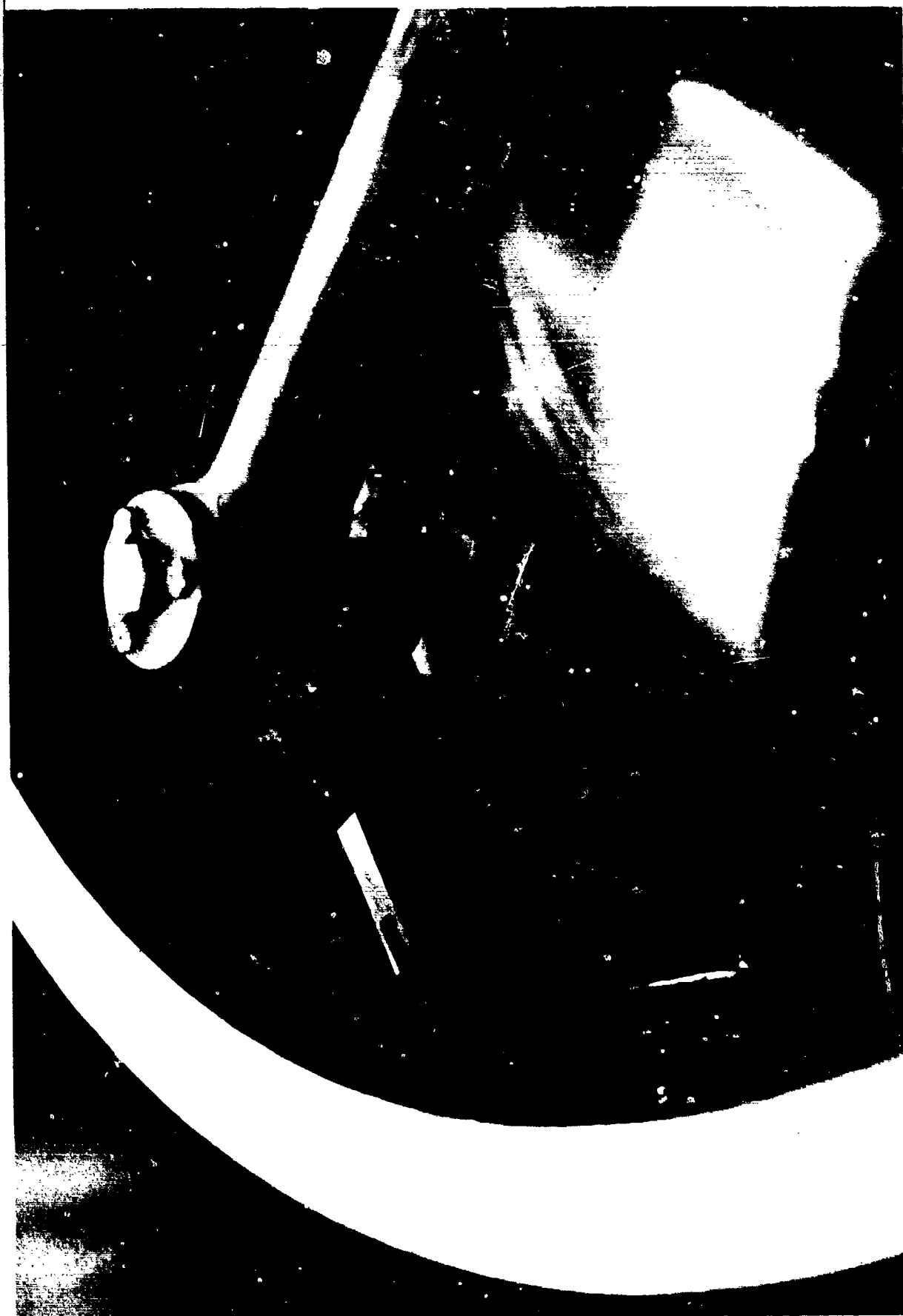


Figure 6



1978

AD-P005 382

FLASH BURN HAZARD CRITERIA
RE-EVALUATION
FOR PROPELLANT FIRES

By
R.B. Crockart
Defence; Research Centre
Salisbury, Australia

1979

INTRODUCTION

1. When thermal radiation effects present the most significant hazard from an explosive material, and any other effects such as blast and fragmentation are of little or no consequence, explosives with these properties are classified as Hazard Division 1.3. This hazard division includes many of the propellants, some of which can burn with great violence and intense heat, emitting considerable radiant energy capable of causing injury and death at significant distances and others which burn for a long time with small flame areas, possibly emitting, sporadic thermal plumes with hazardous effects limited to the immediate environment.
2. Under the NATO system for determining the Quantity distance (Q-D) requirements for HD 1.3, a single relationship, $D = 6.3 Q^{1/3}$ m, with a prescribed minimum distance for quantities over 50 kg of 60 m, is used for the protection at the Inhabited Building Distance (IBD).
3. After a review of the historical basis for the present quantity distance relationship used for HD 1.3, this paper will discuss recent studies in the combustion characteristics of propellants to evaluate any significant factors influencing radiant energy release in storage or processing. Recent studies on the effects of exposure of people and facilities to short duration flashes of radiant heat energy will be reviewed to assess their applicability to the Q-D relationships for HD 1.3. Finally the preliminary tests made to develop a different set of Q-D relationships for HD 1.3 explosives will be presented for consideration.

THE DEVELOPMENT OF THE HD 1.3 Q-D RELATIONSHIPS

4. A careful review of the causes of death and injury in 81 accidents in the explosives and propellant industries over the 1959-1968 period, reported in Reference A, showed that primary blast (over-pressure) damage did not cause a single death but that projected fragments and the effects of exposure to the searing radiant heat accounted for 77 of the 78 fatalities covered by the review. The great majority of these accidents involved a fire which eventually lead to a mass detonation.
5. Although there have been studies undertaken over recent years to understand the hazard mechanism and devise more effective protection for blast and projected fragment injury, the subject of protection from radiant heat has not been well studied.
6. The present Q-D relationship for protection at the IBD was derived by Jarrett and others over 1948-56, Reference B. The radiant heat from burning WM.017 propellant, known as "horse hair" cordite, was measured radiometrically and integrated over the short burn time, 4-6 seconds, to obtain the total flux density, measured in calories per square centimetre, at various distances from the burn sites which

varied in size up to 20,000 kg. The threshold condition for moderate first degree burns to occur on human skin as a result of exposure to radiant heat from the fireball of nuclear explosion had been established at 3 cal/cm². Using this threshold condition, Jarrett developed a relationship between the mass of explosives and the distance at which the flux density from the burning explosives was attenuated to this tolerable level. This Q-D relationship is currently used for all HD 1.3 explosives.

7. During the tests to be discussed in the last section of this paper, digitised thermal representations of the fireball growth were recorded. A qualitative examination of the 50 kg burns of three other propellants were compared with a similar quantity of "horse hair" cordite. Significant differences in both the burn time and the plume sizes are shown. These differences are significant because they cause changes in the intensity of radiation (irradiance) at an exposed site. Three effects of changing irradiance levels require consideration. Firstly there will be propellants which when ignited burn quietly for long periods and there will be a distance from such a fire where an irradiance above 1.4 kilowatts per square metre (kw/m²) will cause pain and, after a period, permanent injury. Secondly there will be locations from burning propellants up to 3 to 4 times above the threshold level which will allow (site) personnel enough time to take cover before permanent injury is caused. Lastly there will be propellants producing large fireballs where both irradiance and burn time measurements will be needed to determine the risk.

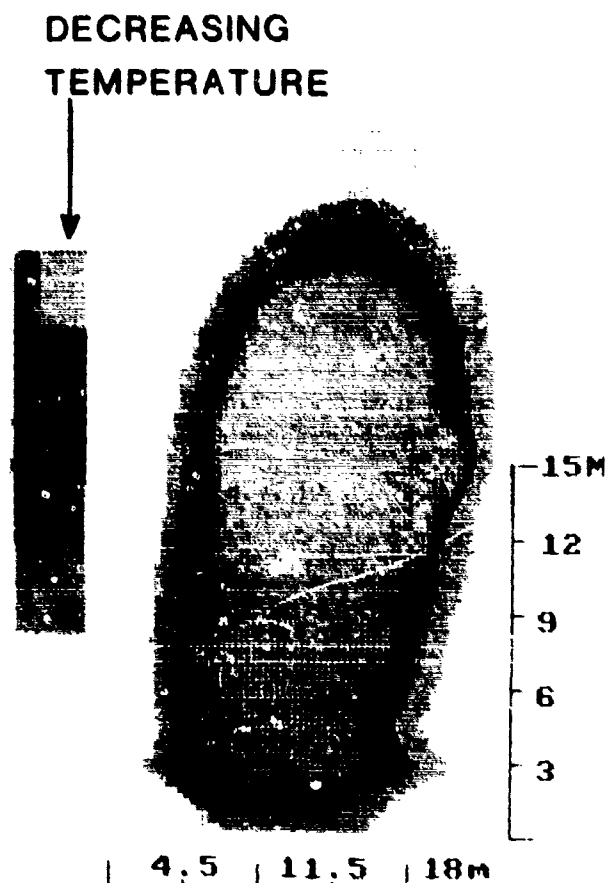
8. The thermal characteristics of a nuclear explosion, being derived from a 10⁷ degrees Kelvin (K) fireball will consist of thermal radiation with shorter wavelengths than the fireballs from propellants burning around 2500 K or from a detonating HD 1.1 explosive around 5000 K. The distribution of energy at a given temperature (2500-5000 K) is in accordance with the well known Planck's Distribution Law, if it can be assumed that the radiation is "black body". The use of thermal injury data from nuclear explosions might not be warranted if similar information was available from sources more closely approximating the temperature of burning propellants. The effect of shorter wavelengths is not known but transmissivity effects through scattering and absorption will be different. BLEVE's or Boiling Liquid Expanding Vapour Explosions is the term given to the fireball incidents associated with either liquid or vapour releases from pressurised storage vessels after rupture. As the temperature of such fireballs is close to 2000 K injury records are considered to be appropriate to the study of propellant fire hazards. From more than 50 BLEVE's, reviewed in Reference 1, including the well known accident at the Spanish Campsite in 1978 when a tanker truck ruptured releasing 23 tonnes of propylene. That part of the hazard analysis of BLEVE incidents where the thermal impact from injury has been developed will be considered in proposing Q-D's for HD 1.3 material.

COMBUSTION CHARACTERISTICS OF PROPELLANTS

9. Numerous studies of the combustion mechanism of rocket and gun propellants has been made. In these studies a different combustion mechanism is known to apply to propellants where the oxidiser and fuel are chemically combined such as the double base propellants compared with propellants where the oxidiser and fuel are simply physically mixed, such as the cast composites. Those chemically combined are known homogeneous propellants and those as mixtures as heterogeneous.

10. Both combustion mechanisms are similar in that the heat being fed back from the flame zone causes the pyrolysis at the surface and the gaseous material so formed undergoes the exothermic reaction which causes the whole process to be self sustaining while there is propellant exposed to the feed back heat.

11. The first diagram is a digitised thermal image of a double base propellant about 2 seconds after ignition with the unburnt propellant relatively cold below the thermal plume.



12. A temperature differential may be seen between the various flame zones and the surface of the propellant. The higher temperature recorded at the higher levels of the thermal plume may be due to additional heat derived from a combination of atmospheric oxygen to complete the oxidation of the essentially fuel rich mixture from the lower level anaerobic burning of the double base propellant material. The plume formed during the burning of a propellant under atmospheric conditions is considered as similar in the overall effect to that formed in a BLEVE. The essential difference is considered to be that combustion in the BLEVE takes place at the fuel air interface while that of the propellant is derived from the contained oxidant in the emitted gas. The essential similarity for the purposes of hazard evaluation, between the BLEVE and a propellant fire is that the hazard in both is created by a radiant volume of gas approximating to a sphere.

13. A digital image of the thermal plumes from composite propellants have not been examined when ignited under atmospheric conditions. Other propellant types possibly requiring analysis for a determination of hazard rating, are the composite modified cast double base propellants (CMBD's). CMBD's are double base propellants which include extra oxidisers to compensate for the fuel rich condition. When AP is added to increase the oxidiser level, the combustion flame characteristics tend towards that described for heterogeneous propellants while if RDX or other active oxidiser is used the double base characteristics are retained and the flame and hence plume temperature is higher. If these derived propellants retain their HD 1.3 rating under the standard classification testing, there appears to be a need for specific radiant heat measurements to evaluate the Q-D requirements in storage.

14. From the foregoing it is concluded that the hazardous effects of an inadvertent initiation of a quantity of HD 1.3 material will not only depend on the total weight of material involved but on the rate at which gaseous material is evolved from the surface and the temperature distribution in the resulting plume. The rate at which propellant is evolved will depend on the exposed surface area to the feed back heat and hence on the physical dimensions of the material. The effects of any obscuration such as packaging or surface inhibition as well as the established burning law applicable to the material will also be important considerations. The temperature distribution of the resulting plume from an inadvertent ignition will depend not only on the exothermic properties of the material but physical factors such as wind and the manner in which it was ignited.

15. The above consideration leads to the conclusion that the hazard rating applicable to HD 1.3 materials needs to be assessed in conditions representative of their storage or processing situations. Tests of this nature are performed during qualification tests in accordance with the UN standards and it will be proposed that appropriate hazard ratings may be undertaken as part of these tests. However, before considering testing, the threshold conditions applicable to thermal impact will be considered.

Thermal Impact

16. The Jarrett studies only considered flux density measured in calories/cm², recent considerations on the effects of thermal radiation on humans considered both the intensity of radiation, usually measured in kilowatts per square metre (kw/m²) and where appropriate, flux density measurements in Joules per square metre (J/m²).

17. The threshold intensity condition is of significance when considering the effects of relatively permanently burning flares. This condition is almost universally accepted as 1.4 kw/m². The basis of this irradiance figure is that pain will be felt when a layer 0.1 mm below the skin surface exceeds 44.8°C. Skin irradiation below the 1.4 kw/m² threshold will not result in pain because an increase in the peripheral blood flow prevents the localised temperature from reaching this condition.

18. The American Petroleum Institute Code (API) (Reference E) provides the details of the time required for humans to register pain at levels above the threshold. At 4.7 kw/m^2 it takes 16 seconds and this is the level recommended in the API code as being tolerable for operators (site personnel) wearing normal clothes and where shelter exists.

19. An Australian risk assessment, Reference F, in considering the radiation risk to residential areas from Petroleum Industrial installation assessed the 4.7 kw/m^2 level a tolerable risk providing the likelihood of such an occurrence did not exceed 50×10^{-6} in any one year. These likelihood levels are in general in keeping with the tolerable risk levels assessed in the NATO Q-D relationships.

20. At levels near the pain threshold, the probability of people exposed being able to take cover before blistering of the skin occurs is considered to be reasonably high (0.9). Where levels reach 20 kw/m^2 , the non-blistering exposure time must be below 5 seconds. This corresponds to a total flux measurement of 2.4 cal/cm^2 and hence the value is in general keeping with the assumptions used by Jarrett in derivation of the conditions considered applicable to "horse hair" cordite burns. The advantage of these recent interpretations is that they provide a sliding scale for the calculation of the tolerable levels for varying burn times, providing a measurement of the intensity and duration has been made.

21. Reference G is a UK study into thermal radiation from fireballs where the blistering threshold is linked in terms of irradiance q , in kw/m^2 and time ' t ' in seconds -

$$q \text{ (threshold)} = 50 * (t)^{-.71}$$

For the 4-5 second burn times recorded by Jarrett in his study, this formula₂ above indicates that the threshold irradiance should be 15.9 kw/m^2 or a total flux density of 2 cal/cm^2 .

22. The conditions relating irradiance and time to determine a threshold condition for tolerable flash burns were developed by various authorities in considering the safety requirements in the petroleum industry, particularly for BLEVE type accidents. There is a general agreement on the threshold conditions as they are based on actual injury studies.

23. The safety distances which have resulted from a study of BLEVE's vary widely in the different authorities. The main reason for the differences is the assumptions made about the time and actual size of the exploding vapour plume, which in most cases is considered to assume a constant diameter of plume and time of burn based on the mass of exploding material. For the study of fireballs from propellants both time and the cross sectional area of the radiating plume may be measured, as will be outlined in the next section.

Preliminary Results of the Burn Trials

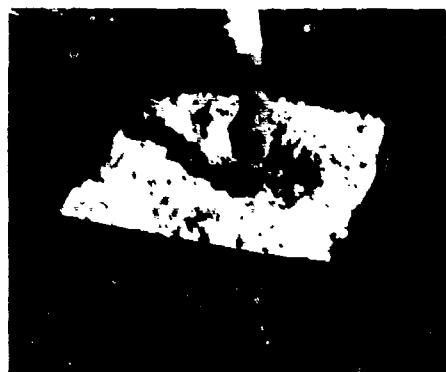
24. The preliminary trials involving propellant in 50 kg lots were made to measure the radiant flux and burn times of three separate propellants in four combinations. The following photographs detail these preliminary burn lots.



Trial 1 and 2 were 50 kg of WM.017 'horse hair' cordite. Trial 1 used 10 kg of NH.025 as an intermediary (not shown).



Trial 3 was 50 kg of NH.025.



Trial 4 was 50 kg of NC-NG Paste (25% water wet) using 10 kg of NH.025 as an intermediary.

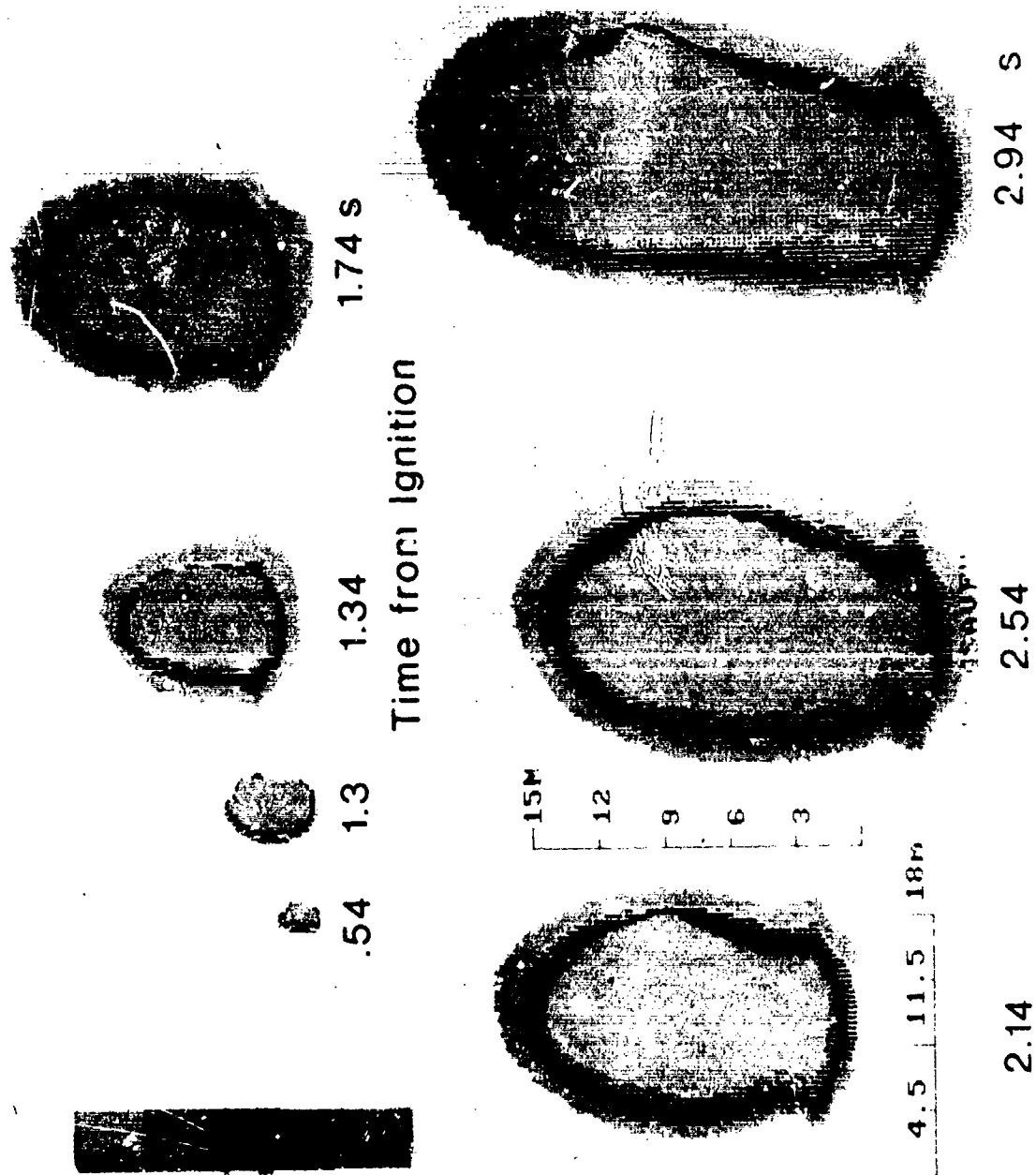
25. The instrumentation used in the preliminary trials included an AGA 782 Thermovision SWB Thermal Imaging Radiometer, a Molelectron Model PR200 broad band radiometer and a cine-camera set to 500 frames per second. The following photographs show the instrumentation layout at the block house and a snap shot taken during the first burn.



26. The specifications of the scanning radiometer, which is considered the essential instrument to take the appropriate measurements, including the lenses used and that of the Radiometer are enclosed as an Annex. The analogue video record of the thermal video image were recorded at 25 fields per second.

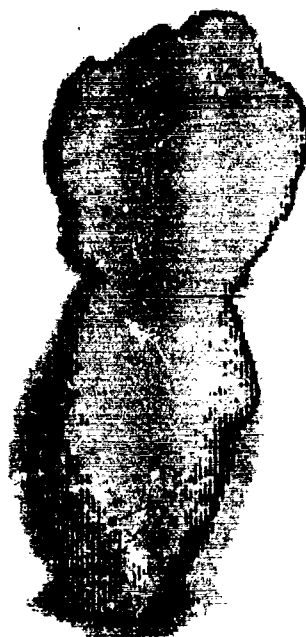
27. The analogue video was converted into a standard TV format, via a scan converter which reduced the resolution to 10 levels, thermal image. Individual frames at selected times during the burn were digitised and the output placed on a floppy disc suitable for processing with an IBM Personal Computer (PC). Software written for the PC selected a grey scale value which segregated the digitised data from the burn into the first six of the 10 levels theoretically available. The digitised pictures were produced on the PC and placed in a chronological sequence. A colour printer was used to provide a hard copy of the results from which the following reproductions have been made.

50kg BURN TRIAL WM PROPELLANT +10kg NH.025

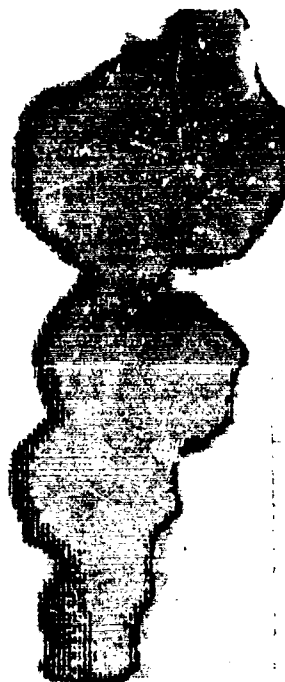




3.34



3.74



4.14 s

Time from Ignition



4.54 s

4.5 11.5 18m

15M

12

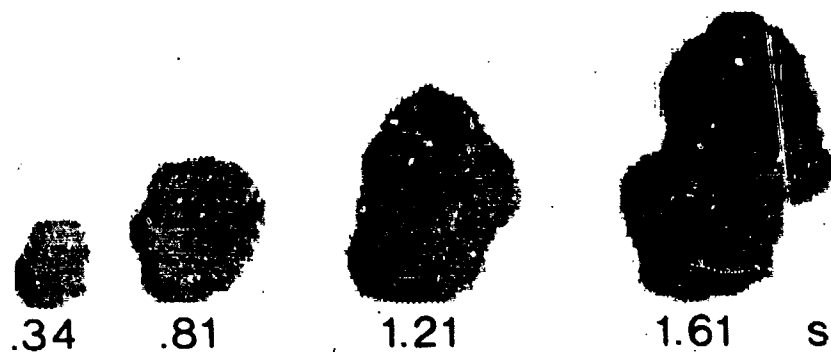
9

6

3

50kg BURN TRIAL WM
PROPELLANT + 10kg NH.025

50kg BURN OF .017 WM PROPELLANT



Time from Ignition



2.01



2.41 s



2.81



3.21



3.61 s



15M

12

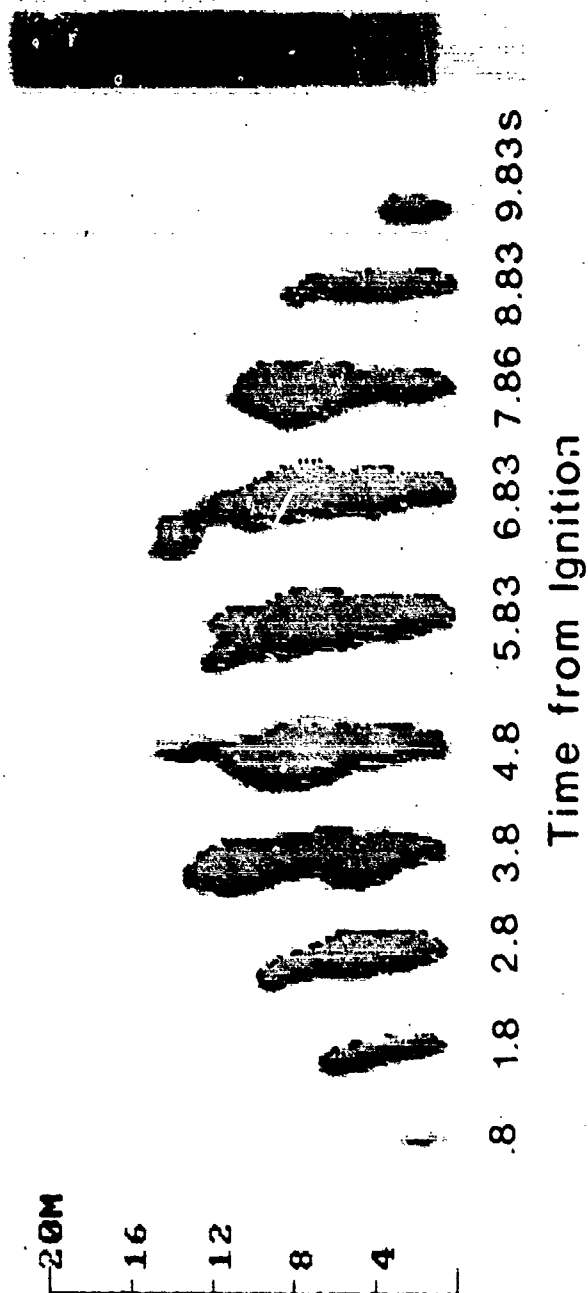
9

6

3

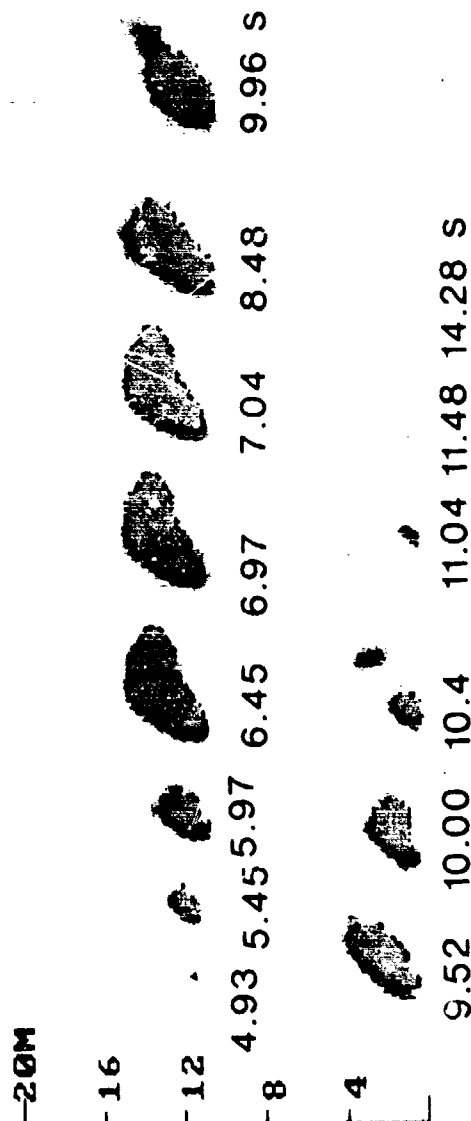
4.5 11.5 18m

50kg BURN OF NH .025 (MONO-PROPELLANT)



6 18 24m

50kg PASTE +10kg NH .025 AS INTERMEDIARY



Time from Ignition

6 18 24m

28. As the trial results being recorded here are still being processed, qualitative interpretations only are being made on the differences clearly seen in the radiant surface presented to an exposed site after an ignition of HD 1.3 material. As the original Q-D relationships in use were determined from the "horse hair" cordite there is considered a demonstrable need to re-appraise of Q-D's to cover the range of HD 1.3 material in terms of irradiance and exposure time. However, completion of the temperature calibration of the radiometric scanner and application of the Stefan Boltzmann equation, to be described in the next paragraphs, will allow irradiance time histories of propellant burns to be made and compared with the irradiance time thresholds established for the tolerable threshold conditions applicable to BLEVE's.

29. The irradiance at distance from a thermal source at temperature T_s in degrees Kelvin in an ambient environment of T_a will be derived from the Stefan Boltzmann relationship using the following formula:

$$q = A t V s (T_s^4 - T_a^4)$$

where q = Target irradiance in kw/m^2

A = Exposed Target Area in m^2

t = Transmissivity

s = Stefan Boltzmann constant $5.67 \times 10^{-11} \text{ kw}(\text{m}^2\text{K}^4)$

T_s, T_a = Surface and Ambient Temperatures

All the factors on the right hand side of this formula will be known after calibration of the scanner. The total irradiance time history will be the sum of the irradiances of each picture element or pixel. The pixel area has been determined from the geometrical optics and verified by burning flares with an IR output on a calibrated frame at the burn location. The placing of a black body source at a fixed temperature to provide a temperature scale at the time of the preliminary burns could not be related to any of the available grey scales. This problem is being reviewed and the possible solution lies in precalibration of the proposed lens-filter combination under laboratory conditions.

30. 'V' in the equation is the view factor and accounts for that fraction of the radiant energy leaving one surface and striking another. As well as incorporating the attenuation at the distance squared it includes the effective diameter of the source (assumed a spherical fireball of diameter D) and any possible angle "O" which a target might make with the axis of the fireball. 'V' is given by a relationship developed in Reference G:

$V = D^2 \cos \theta / 4r^2$ - where 'r' is the distance from plume centre to the target. Under the conditions of the test, $\cos \theta$ will tend to 1 and hence the variables in this factor will be known for calculation of QD's.

31. Various expressions are available for the calculation of the transmissivity factor "t". Transmissivity or attenuation of the radiant flux through passage through the atmosphere is caused by absorption by water vapour and other gases, principally carbon dioxide and scattering (related to visibility). The relationship considered most appropriate for the calculation of transmissivity under the test conditions has been obtained from Reference I, it is :

$$t = 202 * (P_W * \text{Distance})^{-0.09}$$

Where P_W is the partial pressure of water vapour.

32. The number of transformations from scanner imagery to the final digitising is introducing noise into the lower grey-scale levels with the current methods of analysis. The possibility of direct digitising of the scanner output is being considered but if this is not achieved the effect will be minimal, because of the 4th power effect of temperature on the calculation of irradiance.

33. The anticipated outcome of the trials will be a number of hazard divisions within the HD 1.3 classification, possibly four to match the general trend foreseen in the preliminary trials.

34. As proposed, at least two large scale burns up to 2000 kg will be used to assess any scaling effect on the results obtained from sample (50 kg) burns. When this hazard evaluation technique is tested and proved in the current trials, the foreseen application will be during propellant qualification testing, as undertaken by propellant manufacturing facilities such as at Mulwala Explosives Factory NSW.

35. Propellant qualification testing to UN Standards is undertaken under realistic conditions of confinement and external fire. The radiant plumes which result from these tests, validating the HD 1.3 classification, are also clearly capable of analysis by the described digitised thermal imagery technique. A video record of the tests described in this paper are concluded by views of such propellant qualification testing at Mulwala which have been chosen to show the thermal plumes.

Conclusion

36. When thermal radiation effects constitute the greatest single hazard in the storage or processing of an explosive material, there is a considered need to create sub-divisions of hazard levels with the HD 1.3 category.

37. The present Q-D relationships tend to place too stringent storage and processing conditions on some materials which burn for long periods with small flame zones, under ambient conditions. On the other hand, there are propellants and propellant combinations which seem to exceed the radiant intensity and/or flame duration criteria consistent with the present Q-D relationships for HD 1.3 material.

38. An evaluation procedure involving digitising thermal imagery during qualification testing is under assessment to evaluate this proposition and devise a graduated set of Q-D tables within HD 1.3.

39. When the full range of propellants have been tested using the technique being proposed here and the analysis of the hazards they present in storage completed, the details will be submitted to DDESB for consideration and possible adoption.

References

- A. Explosion Hazards and Evaluation, Baker, Cox and others;
Elsevier Publishing Co. USA 1983 Chapter 7.
- B. Jarrett (1966) Prevention of and Protection Against Accidental
Explosion of Munitions, Fuels and other Hazardous Mixtures.
1966 Conference Annals of the New York Academy of Sciences Vol 152
Published by the Academy.
- C. Kubota N. A Survey of Rocket Propellants and their Combustion
Characteristics - Progress in Astronautics and Aeronautics
Volume 90, 1983.
- D. Lengelle, Bizot, Duterque and Trubert : "Steady-State Burning of
Homogeneous Propellants" Progress in Astronautics and Aeronautics
Volume 90, 1983.
- E. American Petroleum Institute Guide (1967)
Guide for pressure relief and depressurising systems, API RP 521 USA.
- F. Haddad (1985) A risk assessment study for the Botany/Roadwick
Industrial Complex, NSW Dept of Planning and Environment.
- G. Lihou D.A. and Maund J.K. (1982) Thermal Radiation Hazard from
fireballs. Symposium on the assessment of major hazards.
I. Chem E. Symp. No. 71
- H. Pitblado (1986) Consequence Models for BLEVE Incidents
- Interim Paper - Dept of Chem. Engineering Warren Centre
Sydney University Australia.
- I. TNO (1979) Yellow Book, Methods for the calculation of the
physical effects of the escape of dangerous material 2 Vols
Dutch Directorate of Labour.

Instrument Specifications :

Scanning Radiometer

Type : AGA 782 Thermovision SWB

IR Detector: Indium Antimonide cooled by liquid nitrogen

Spectral Response: 3-5 Micron

Field frequency: 25 Hz

Lines per frame: 280, interlaced 4:1

Resolving Power: 100 elements/line

Lens: $20^{\circ} \times 20^{\circ}$ fitted to cover spatial extent of
propellant plume at 100 & 125 m.

Monitor used with Scanner:

Type: Thermovision Type 780

Thermal Image Size: 50 x 50 mm

Thermal Range: 9 calibrated ranges.

Broad Band Radiometer

Type: Molelectron Model PR200

Spectral Range : 0.2 to 40 micron \pm 5%
(windowless)

Surface Uniformity: \pm 5%

Field of View: 0.1 Sr

System Response time
at 2, 20 & 200 mW Fast response: 1 sec

AD-P005 383

**SYSTEM SAFETY CONSIDERATIONS FOR THE
DESIGN OF A CHEMICAL SURETY MATERIEL
LABORATORY**

PREPARED BY: GEORGE E. COLLINS, JR.

**CHEMICAL RESEARCH DEVELOPMENT AND ENGINEERING CENTER
SAFETY OFFICE
ABERDEEN PROVING GROUND, MD. 21010-5423**

PREFACE

This document was prepared to show, through example, how established system safety concepts can be applied to the design of a chemical surety materiel (CSM) laboratory. The end result of this effort was the development of safety considerations for incorporation into the design of a CSM laboratory.

REFERENCES

1. Draft Technical Manual, TM XX-XX, Undated, Facility System Safety Program.
2. CSL SOP 70-18, 10 Nov 82, Exhaust Ventilating Systems.
3. DOD 6055.9 - STD, July 1984, Ammunition and Explosives Safety Standards.
4. DARCOMR 335-102, 6 May 1982, Safety Regulations For Chemical Agents GB and VX.
5. CSL SOP 385-1, 2 June 1982, Chemical and Occupational Safety and Health Program.

1.0. INTRODUCTION: The application of system safety concepts to the facility acquisition process has recently gained acceptance throughout the Department of Defense and most recently within the the Department of Army with the conception of SAFEARMY 1990. The Army's goal is to: "fully integrate the total system safety, human factors, and health hazard assessments into continuous comprehensive evaluation of selected systems and facilities." The Chemical Research Development and Engineering Center (CRDEC) has mandated appropriate levels of system safety throughout the lifecycle of facility development for many reasons. These include:

- * Optimum safety and health is required to prevent personnel injury to these agents. Facility System Safety (FSS) is one avenue used to achieve optimum safety and health in our operations.

- * FSS is a proven method to reduce deficiencies during facility acquisition.

- * FSS is a proactive approach which will reduce inconsistencies found in our facilities thereby reducing outside scrutiny.

This article demonstrates one specific effort in Facility System Safety (FSS) currently underway at CRDEC. The intended purpose of this article is to demonstrate, through specific examples, how FSS can be applied to the design/construction/operation of a chemical surety materiel laboratory. The laboratory under study is a 32 million dollar Military Construction, Army (MCA) project designed to replace aging facilities which are currently utilized to perform daily CSM operations. This article will demonstrate the methods used in identifying, analyzing and ultimately eliminating or reducing the effect of a hazard on the facility, equipment and personnel.

2.0. FACILITY SYSTEM SAFETY OVERVIEW: The process of applying system safety to facility acquisition can be divided into the following tasks:

- a. Categorization
- b. Preliminary Hazard List
- c. Preliminary Hazard Analysis
- d. Design Considerations

The remainder of this article will involve a description of each of these tasks followed by an example of how the task was applied to the design of this CSM laboratory. Descriptions of tasks a-c were taken from reference 1.

3.0. CATEGORIZATION: The first step in this process is to clearly define the risk associated with the operation of this laboratory. This step includes a brief description of the operation followed by a risk assessment and a recommendation on the level of system safety required.

3.1. LABORATORY DESCRIPTION: The laboratory under consideration will conduct diversified chemical surety materiel laboratory operations. These materials are anticholinergic agents and are extremely lethal in small concentrations.

The recommended permissible airborne exposure concentration for these agents are in the area of 0.0001 mg/m³ (2 x 10⁻⁵ ppm). Two personnel are required, as a minimum, to perform this operation.

3.2. ASSESSMENT: The most significant hazard present in this laboratory operation is the release of vapor CSM from engineering controls and into the workplace. This mandates further efforts in system safety in the form of a Preliminary Hazard List (PHL) and a Preliminary Hazard Analysis (PHA). The user must in this instance take an active role in the design review process.

4.0. PRELIMINARY HAZARD LIST: Once the risk categorization is completed, the next step is to develop a PHL.

4.1. PURPOSE: The PHL is a user generated listing of hazards which must be controlled. The user must at this stage assign a risk assessment code to each hazard and establish any further requirements for analyses. As a minimum the user should use the following sources of information for PHL development:

- a. Material Safety Data Sheets
- b. Feasibility Studies
- c. Project Development Brochures
- d. Standing Operating Procedures
- e. Operator Interviews

4.2. PRELIMINARY HAZARD LIST DESCRIPTION: The incorporation of this information into a PHL entry is shown as Figure 2. This entry describes; the nature of the hazardous event (column 1), why or how the hazard may result in a mishap (column 2), the effects on operating personnel, equipment, and the facility (column 3), the risk assessment code assigned to the uncontrolled hazard (column 4) and any comments the originator may have (column 5).

5.0. PRELIMINARY HAZARD ANALYSIS: The next step in the process is the development of a PHA. This analysis is the core of the FSS program and as such is vital in eliminating or reducing the inherent hazards associated with this laboratory operation.

5.1. PURPOSE: The PHA is used to further analyze the data identified in the PHL. This enhances the hazard control database and provides specific recommended corrective action for the resolution of hazardous conditions. A combination of the informational sources used in the PHL development and any additional design information should be used in PHA development.

5.2. PRELIMINARY HAZARD ANALYSIS DESCRIPTION: The incorporation of this information into a PHA entry is shown as Figure 3. This entry describes; the proposed actions needed to eliminate or control the hazard (column 6), the risk assessment code assigned after controls (column 7), and the identification of applicable codes and standards (column 8).

5.3. HAZARD TRACKING LOG: In addition to the above analysis, a hazard tracking log should be maintained. This log is to ensure all open loops are

closed and ensures the appropriate level of management is identified as being involved in the acceptance of risk. This log should be initiated during the design phase and maintained throughout the construction portion. A simulated entry is shown in Fig. 4. This entry describes; the specific action taken to eliminate, control or accept the hazard (column 9), the reference of the blueprint/drawing numbers or other documents that address the action taken (column 10), name of individual closing out the action on design (column 11), and the name of the individual closing out the action during construction (column 12). The information contained in this log does not reflect an actual log entry but is shown for information purposes only.

6.0. LABORATORY DESIGN CONSIDERATIONS: As a result of this effort, detailed safety design considerations can be developed to preclude the release of lethal concentrations of vapor CSM into the workplace. This will minimize the potential for death or serious injury to our research scientists. A summary of these requirements is shown in Appendix A.

7.0. CONCLUSIONS: The effort put forth in FSS for this laboratory has many benefits. Most noteworthy are:

- a. Safest possible laboratory
- b. More mission responsive facility
- c. Less expensive facility

This article is a step in the direction we must all head towards and that is total system safety for facilities to reduce inherent hazards associated with their operation.

Risk Assessment. An expression of possible loss, described in terms of hazard severity and mishap probability. Subdefinitions follow:

A. Hazard. Any existing or potential condition that can result in a mishap.

B. Mishap. An unplanned event or series of events that result in death, injury, occupational illness, or damage to or loss of equipment or property (i.e., an accident).

C. Hazard severity. An assessment of the worst potential consequence, defined by degree of injury, occupational illness, or property damage which could occur. Hazard severity categories will be assigned by Roman numeral according to the following criteria:

(1) Category I - Catastrophic: May cause death or loss of a facility.

(2) Category II - Critical: May cause severe injury, severe occupational illness, or major property damage.

(3) Category III - Marginal: May cause minor injury, minor occupational illness, or minor property damage.

(4) Category IV - Negligible: Probably would not affect personnel safety or health, but is nevertheless in violation of specific standards.

D. Mishap Probability. The probability that a hazard will result in a mishap, based on an assessment of such factors as location, exposure in terms of cycles or hours of operation, and affected population. Mishap probability will be assigned an arabic letter according to the following criteria:

(1) Subcategory A - Likely to occur immediately.

(2) Subcategory B - Probably will occur in time.

(3) Subcategory C - May occur in time.

(4) Subcategory D - Unlikely to occur

E. Risk Assessment Code. An expression of risk which combines the elements of hazard severity and mishap probability (e.g., IA, IIIB, etc.). The following table gives the rank order risk assessment codes.

		Mishap Probability			
		A	B	C	D
Hazard Severity	I	1	1	2	3
	II	1	2	3	4
	III	2	3	4	5
	IV	3	4	5	5

F. Imminent Danger. A hazardous situation for which risk assessment code of category IA, IIA, or IB has been assigned.

Figure 1. RISK ASSESSMENT

COLUMN 1	COLUMN 2	COLUMN 3	COLUMN 4	COLUMN 5
HAZARDOUS EVENTS	CAUSAL FACTORS	EFFECTS	RISK ASS. CODE	COMMENTS
Release of vapor CSM from lab hood and into workplace or atmosphere	1. Power failure	1. Loss or lab hood capture. Release of CSM into workplace. Personnel injury or death. System/ facility damage minimal.	I A 1	None
	2. Mech. exhaust fan failure	2. Same as #1 above	I B 1	None
	3. Poor lab hood capture (Design)	3. Turbulence may result in small release of CSM into workplace. Personnel injury or death could result. System/facility damage minimal.	I B 1	None
	4. Operator error	4. Judgement errors could result in an inadvertent release of CSM into the workplace. Personnel injury or death could result. System/facility damage minimal.	I B 1	None
	5. Filters do not remove CSM from exhaust	5. Personnel injury to people surrounding the facility. System/facility damage minimal. Adverse publicity.	II C 3	Scenario less likely and severe due to dilution factor.
	6. Exhaust ductwork not properly sealed	6. Small concentrations CSM in the workplace possible in the event the exhaust system were to go positive. Personnel injury or death possible. System/facility damage minimal.	I C 2	Scenario less likely due to additional requirement for system to go positive.

FIGURE 2 - PRELIMINARY HAZARD LIST

COLUMN 5	COLUMN 6	COLUMN 7
RECOMMENDED ACTIONS	CONTROLLED RISK ASS. CODE	STANDARDS
CAUSAL FACTOR #1: ----- a.) Emergency generator system shall be installed to automatically initiate in the event of a power failure, system phasing shall be accomplished in a manner which will not permit the occurrence of a hazardous condition. b.) Laboratory hoods must be equipped with a mechanism to warn operators of emergency power status and hood function. c.) Standing Operating Procedures should contain provisions for the curtailment of operations, immediate masking and evacuation from areas that experience power failures.	IV D 5	DOD 6055.9-STD DARCOMR 385-102 CSL SOP 385-1
CAUSAL FACTOR #2: ----- a.) Two alternatives are available to prevent a hazardous condition from occurring in the event of a mechanical failure. These include: (1) Redundant exhaust fan units, (2) Procedural controls which require curtailment of operations, donning of protective masks and immediate evacuation during ventilation loss. b.) Laboratory hoods shall be equipped with a means to warn operators of improper ventilation system functioning	IV D 5	DOD 6055.9-STD DARCOMR 385-102 CSL SOP 385-1 LOCAL SOPs
CAUSAL FACTOR #3: ----- a.) Laboratory hoods must be located away from: -Main traffic aisles and doorways -Adjacent walls and operable windows -Cross drafts exceeding 30 lfpm -Heating Units -Exits. b.) Laboratory hoods must perform as follows: -Average inward face velocity of 100 lfpm +/- 10% with the velocity at any point not deviating from the average face velocity by more than 20%	IV D 5	DARCOMR 385-102 AEHA Technical Guide #30 CSL SOP 385-1

FIGURE 3. PRELIMINARY HAZARD ANALYSIS

COLUMN 5	COLUMN 6	COLUMN 7
RECOMMENDED ACTIONS	CONTROLLED RISK ASS. CODE	STANDARDS
CAUSAL FACTOR #3 (Continued):		
c.) Operators must be trained in proper operation within a laboratory hood.		
CAUSAL FACTOR #4:	IV D 5	CSL SOP 385-1
a.) Operating personnel must be properly trained.		
b.) Operating personnel must wear appropriate protective clothing.		
c.) Operating personnel must work under a properly approved SOP.		
CAUSAL FACTOR #5:	IV D 5	CSL SOP 70-18 CSL SOP 385-1
a.) Exhaust filtration system shall meet CSL SOP 70-18.		
CAUSAL FACTOR #6:	IV D 5	DOD 6055.9-STD CSL SOP 385-1
a.) Ductwork shall be sealed to preclude leakage.		
b.) All joints shall be seamless welded.		
c.) Ductwork shall be capable of withstanding 16 inches water column vacuum and 25 inches water column positive pressure.		

FIGURE 3 - PRELIMINARY HAZARD ANALYSIS
(Continued)

COLUMN 8	COLUMN 9	COLUMN 10	COLUMN 11
ACTION TAKEN	TRANSFER	DESIGN CERTIFICATION	CONSTRUCTION CERTIFICATION
CAUSAL FACTOR #1:			
a.) Emergency generator installed and properly phased	Drawing #:099 Specification Section # 09991	Mr. Smith	Mr. Jones
b.) Laboratory hoods equipped with warning devices to notify operator of power loss	Drawing #:061 Specification Section # 08001	Mr. Smith	Mr. Jones
c.) Installation notified of finding	Disposition Form sent 6 Jan 86 to safety office	-----	-----
CAUSAL FACTOR #2:			
a.) Installation safety office determines need to go with procedural controls. SOPs will be developed accordingly.	Disposition Form 10 Jan 86	-----	-----
b.) Laboratories equipped with warning devices to notify operators of ventilation system failure	Drawing #:061 Specification Section # 08001	Mr. Smith	Mr. Jones
CAUSAL FACTOR #3			
a.) Lab hoods meet the following: Away from: -Main traffic aisles -Doorways and Windows -Adjacent walls -Cross drafts > 30 fpm -Heating units -Exits	Drawing #:045	Mr. Smith	Mr. Jones

FIGURE 4. HAZARD TRACKING LOG

COLUMN 8	COLUMN 9	COLUMN 10	COLUMN 11
ACTION TAKEN	TRANSFER	DESIGN CERTIFICATION	CONSTRUCTION CERTIFICATION
CAUSAL FACTOR #3 (Continued)			
b.) Lab hoods perform as follows: -Average face velocity 100 lfpm +/- 10%. No single reading deviating from average by 20% -Smoke testing did not result in a release of visible smoke	Drawing #:046 Specification Section # 07010	Mr. Smith	Mr. Jones
c.) Installation notified of requirement for proper training of operators	Disposition form dated 25 Mar 86	-----	-----
Causal Factor #4			
Installation responsibility	Installation notified 25 Mar 86	-----	-----
Causal Factor #5			
Exhaust system complies with CSL SOP 70-18	Specification Section # 01001	Mr. Smith	Mr. Jones
Causal Factor #6			
Ductwork properly sealed and tested	Specification Section # 02000	Mr. Smith	Mr. Jones
	Disposition form dated 25 Mar 86	-----	-----

FIGURE 4. HAZARD TRACKING LOG
(CONTINUED)

APPENDIX A

Laboratory Design Considerations For Protection Against Vapor CSM Exposure

A. Electrical Design Considerations (Causal Factor #1):

1. Emergency generator systems will be installed to service the following:

- Exhaust ventilation fans
- Make-up air handling units
- Critical operating equipment
- Emergency lighting
- All emergency alarm systems

2. Diesel-powered generators will be used. The emergency generator will be sized to handle 100% of the connected emergency load.

3. Start-up of the exhaust ventilation system and critical equipment must be sequenced to prevent a hazardous condition. In addition, the starting of the supply air handling unit and the exhaust fan services each room shall initiate simultaneously to avoid placing the room under positive pressure. Automatic transfer switching will be used.

B. Warning Systems (Causal Factor #1&2):

1. Facility will be equipped with a master control panel and alarms which permits functional verification of the exhaust blowers, filters, make-up air supply systems, fire control systems and waste treatment processes.

2. Laboratory hoods will be equipped with audible and visual alarms which will be designed to initiate when the average inward face velocity falls below 90 linear feet per minute.

3. Visible alarms must be located so they can be readily seen by personnel while working at the exhaust hood.

A - 1

4. A test switch must be installed on all alarms which will permit the operator to verify that the light has not burned out and the sound alarm will function. This test must be performed while ventilation system is in full operation.

C. Laboratory Hood Location (Causal Factor #3):

1. Laboratory hoods must be located away from:

- Heavy traffic aisles
- Doorways
- Adjacent walls
- Crossdrafts that exceed 30 lfpm
- Heating units
- Exits

2. Sidewall registers and conventional ceiling diffusers shall not be used for laboratory air supply.

3. Perforated ceiling panels shall be used so that distribution of supply air is three feet minimum from the front face of the hood. The exit velocity from these panels shall not exceed 30 lfpm.

D. Laboratory Hood Performance (Causal Factor #3):

1. Laboratory hoods shall have an average inward face velocity of 100 lfpm +/- 10% with the velocity at any point not deviating from the average face velocity by more than 20%.

2. Leakage testing must be done with 30 second or one minute smoke candles placed approximately 20 centimeters inside the hood. Any visible escape of smoke should be considered indicative of unacceptable performance.

3. Laboratory hoods shall be designed as deep and low in height as practical. Rough wall surfaces and recesses in walls and work surfaces are unacceptable.

4. The location of sash tracks and the number of baffles and slots provided are integral to the proper containment of materials.

5. Laboratory hoods will be equipped with a 20 centimeter line taken from the face of the hood. No CSM contaminated equipment should be placed in front of this line during operations.

E. Exhaust Ventilation/Filtration System (Causal Factor #5):

1. All laboratory exhaust air shall be exhausted through a filtration system which complies with CSL SOP 70-18. These systems have been proven to be effective in removing CSN vapor from an exiting airstream.

2. Ventilation exhaust shall not be recirculated.

3. Instrumentation shall be required to monitor and control the airflow through the filter system. Instrumentation shall provide a means to monitor overall pressure drop as well as the pressure drop between each filter element.

4. The filter system shall include a series redundant-parallel Chemical Biological Radiological (CBR) filter assembly with a capability of placing a detector between the adsorber banks to warn of "breakthrough". The system shall provide accessibility to filters for repairs, maintenance and leak testing.

5. The filter system shall be as follows:

Hood-- Prefilter-- HEPA-- Adsorber-- Adsorber-- HEPA-- Exhaust

6. Exhaust stacks shall be designed and constructed to ensure good dispersion of exhaust air to the atmosphere thereby preventing recirculation.

F. Exhaust Ductwork (Causal Factor #6):

1. All ductwork shall be round, and welded with flange connections.

2. All ductwork shall be capable of withstanding 16 inches water column vacuum and 25 inches water column positive pressure.

3. Ductwork shall be designed to facilitate dismantling and to minimize the release of contamination to adjacent areas with bagging or other approved means.

2012

AD-P005 384

SAFETY CONSIDERATIONS FOR THE OPERATION OF A THERMAL DESTRUCTOR
UNIT FOR CHEMICAL SURETY MATERIEL 3"X" ITEMS

GREGORY W. ST. PIERRE: SAFETY ENGINEER, CHEMICAL RESEARCH,
ENGINEERING AND DEVELOPMENT CENTER,
ABERDEEN PROVING GROUND

1.0. INTRODUCTION.

This paper outlines the major safety considerations for the operation of a thermal destructor unit utilized to incinerate 3"x" items previously contaminated by Chemical Surety Materiel (CSM). The portions of the operation of the thermal destructor unit which will be evaluated from a safety standpoint in this paper are the receipt/storage of 3"x" material, the loading of the firepan, the actual operation of the unit, and the disposition of the 5"x" waste and ash. This paper will also outline the engineering controls utilized to ensure that the thermal destructor unit is operating in compliance with all environmental requirements.

2.0. STORAGE/RECEIPT OF 3"x" WASTE.

This section of the paper assesses the packaging, labeling, and transportation of laboratory waste or contaminated material by the using directorate. Wastes generated by the directorates are handled according to their size, form of contamination and the materials physical state. One form of waste generated is used filters, the exposed ends of these filters are sealed with plastic which is secured in place with plywood. Other forms of contaminated bulk material and laboratory waste are decontaminated with the appropriate type and amount of decontamination solution. Generated waste is either placed into small sealed metal storage containers (liquid and small solid waste) and then placed into larger metal containers. Bulk solid waste is double wrapped/bagged with plastic. Items will then be labeled/stenciled with the building number from which it came, organization, name of the person making the shipment, telephone number, and type of contamination. The using directorate will make arrangements with the installation's environmental group to have the necessary waste monitored by analytical methods for determination of 3"x" status. The waste is redecontaminated and remonitored, only if detectable levels are above the 3"x" limits. After items are certified clean and stenciled with the appropriate decontamination marking (xxx), the using directorate will then fill out the appropriate turn-in forms. These turn-in forms contain information on the type of contamination, the type of decontamination solution used, the material contaminated, liquid content within the container, pallet number, and the clearance number (monitoring results). Currently, 3"x" waste is being transported by either the using directorate or Technical Escort Unit (TEU) in government owned vehicles to one of the three existing storage areas.

2.1. WASTE STORAGE.

The 3"x" waste is segregated into three categories, solid waste, liquid waste, and filters. Each type of waste is stored in a separate facility/area.

a. A large gravel pad is used for the storage of solid waste which is contained in metal drums or is double wrapped in plastic and palletized.

b. The liquid waste storage facility is a building constructed of masonry walls and cement floors. Liquid waste is contained in metal drums,

palletized, and placed in the center of a temporary dike constructed of sandbags which are covered by plastic sheeting.

c. Filters are stored in a large warehouse building constructed of masonry walls and cement floors. The particulate filters are stored at the eastern end of the building and the charcoal absorbers are being stored at the western end of the building. All filters are monitored to the 3"x" level, double wrapped in plastic, and palletized. Filters which have not been bubbled by the installation's environmental group and can not be bubbled until the outside temperature warms, are stored at the Chemical Agent Storage Yard (CASY).

d. When the 3"x" waste arrives at one of the three storage areas, personnel from the thermal destructor unit facility will receive the material and sign the transport form for verification of receipt. After receiving the 3"x" waste, the containers will be stenciled with the date of receipt. The containers/items of 3"x" waste are then stored at the site until it is time for the waste to be incinerated.

3.0. LOADING OF THE FIREPAN.

The 3"x" waste being stored at one of the storage sites, when scheduled for incineration, is loaded onto a truck with the use of a forklift, by the operators of the thermal destructor unit. The 3"x" waste is off-loaded onto temporary storage pads outside of the thermal destructor unit facility to await incineration. One pallet of 3"x" waste is lifted, with the use of a forklift, and placed into the firepan. Once the 3"x" waste is placed into the firepan, the pallet is opened (removal of the straps/plastic) and each item is identified by material makeup (i.e. metal, slate, glass, etc.), then weighed. The charging of the firepan is dependent on the combustibility of the material being placed into the incinerator. The combustibility of the material being placed into the firepan for incineration determines the amount of waste incinerated at one time. Personnel at the facility use a chart from the thermal destructor unit operating manual supplied by the contractor, describing the amounts of specific types of combustible materials which may be burned in the incinerator safely. Currently, the personnel at the facility place one or more bulk items into the firepan and cover the larger pieces with smaller material. The drums containing solid waste are lined with plastic bags and the total contents of the drums are removed in the plastic bags and placed into the firepan. When smaller sealed metal cans are placed into the firepan, the lids are removed from the cans or a hole is punched into the can prior to being placed into the firepan. The personnel at the thermal unit wear coveralls, gloves (leather or cloth), and safety shoes when handling the contents in the drums. Wearing of respiratory protection is a option for the operators. A working record log book is kept describing the type of material being incinerated, the weights of the items, and the makeup of each item. The information that is recorded is transcribed into the master record log book kept in the office on site. After loading of the firepan is complete, the firepan is placed into the firecar with the use of an overhead crane. The firecar is then rolled under the primary combustion chamber and sealed to

await incineration. Personnel while conducting the above operations will be wearing coveralls, safety shoes, and leather gloves due to the handling of rough objects. The handling of 3"x" waste is covered under an Internal Operating Procedure (IOP).

4.0. OPERATION OF THE INCINERATOR.

This portion of the paper evaluates the operation of the incinerator. The operation of the incinerator is covered by an IOP. Each individual at the thermal destructor unit facility has read and understands the IOP. Once the firecar is sealed to the primary combustion chamber, a series of start up procedures are initiated prior to the actual incineration of the 3"x" waste (these procedures are outlined in detail in the IOP). In accordance with (IAW) DARCOMR 385-102, Safety Regulations for Chemical Agents GB and VX, 6 May 1982, 3"x" waste when heated to 1000 degrees F for 15 minutes is considered sufficient to achieve a 5"x" condition. The incinerator operates at temperatures and times in excess of the prescribed limits by Army Materiel Command (AMC). There are two combustion chambers within the incinerator, the primary and secondary combustion chambers. The secondary combustion chamber is heated to 1600 degrees F prior to the heating of the primary chamber. The primary burners cannot be lighted until the secondary combustion chamber reaches a temperature of 1600 degrees F (an interlock mechanism). The temperature in the primary combustion chamber is brought up to 1200 degrees F for approximately 90 minutes. Throughout the 90 minute burn time the vapors from the primary combustion chamber are subjected to 1600 degrees F for a 2 second retention time in the secondary combustion chamber. When the burn has been completed, the combustion chambers are allowed to gradually cool down by slowly reducing the intensity of the burners. The current procedure is to shut down the scrubber system when the internal temperature of the combustion chambers reaches 500 degrees F and the force draft fan is left on to pull in cool air. The firecar is allowed to cool to a minimum of 200 degrees F and is then uncoupled from the combustion chamber. The uncoupled firecar is rolled into the loading/unloading control room, to be cleaned out.

5.0. CLEANING OF THE FIREPAN.

The firepan containing the 5"x" material is removed from the firecar weighed, and set on the floor of the facility. Personnel wear coveralls, gloves, safety shoes, and a NIOSH approved respirator when unloading material out of the firepan. One type of material (i.e. scrap metal or slate) at a time is removed from the firepan and placed on a pallet. When the pallet is full, the firepan is reweighed to determine the weight of the scrap metal or slate that has been removed from the firepan, and this weight is recorded. This process continues for each pallet of material removed, until all of the bulk material is removed from the firepan. After the bulk items are removed from the firepan, several ash samples are collected from different portions of the firepan for a composite sample of the burn. The ash samples collected are labeled with the burn number, date of the burn, and the facility where the samples were collected. Samples are held on site until there are approximately 20 samples, which are then sent to a contractor for analysis.

The remaining ash and debris in the firepan is shoveled into a metal drum. The shoveling of the ash generates a dusty condition in the work area. After the firepan is cleaned of ash and debris, the surrounding work area is swept clean and the collected material is placed into the ash drum. The pallets of scrap metal and slate are stenciled and then removed to their respective pads at the thermal destructor unit complex to await pickup for the disposal by the appropriate agencies. The drums of ash are sealed and stored outside of the facility to await transport to its respective storage area. The cleanup operation is then completed and the firepan is ready to be charged for the next burn.

6.0. DISPOSITION OF 5"X" WASTE AND ASH.

The pallets of scrap metal, slate, and drums of ash are transported to separate locations for disposal or storage. Scrap metal is stored on a pad in the thermal destructor unit complex. When a sufficient load of scrap metal is collected (dependent on amount per burn), the scrap metal is transported to the Aberdeen Proving Ground Installation Support Activity (APGISA) scrap metal yard. The scrap slate is stored on a pad in the thermal destructor unit complex. When a sufficient load of scrap slate is collected (dependent on amount per burn), the scrap slate is transported and buried in the APGISA landfill. The drums of ash are stored outside of the thermal destructor unit complex and then after two or three burns, the drums are transported to their respective storage facilities by government personnel. The drums of ash are stored in one end of the building and are separated into three categories. The first category contains the drums for which the samples are being analyzed for hazardous waste and the contents of the drums remain unknown. The second category contains the drums which have been determined by analytical methods to contain no hazardous waste and are transported to a landfill for disposal (color-coded green for "go"). The third category contains the drums which have been determined by analytical methods to contain hazardous waste and are transported to APGISA Environmental Management Office (EMO) for proper storage and subsequent disposal.

7.0. STORAGE OF LIQUID WASTE.

Metal drums containing liquid waste are currently being stored in the eastern end of the storage facility. The drums are stored on top of pallets which are placed on a bare concrete floor. The drums are stacked two high and will not be stacked higher due to height restraints of the facility. For the present, a temporary dike surrounding the drums has been constructed of bags of sand stacked two high and covered with a plastic sheeting. The temporary dike will be used until a permanent dike can be constructed. The existing concrete floor is free of major cracks or gaps. The permanent dike will be constructed in the eastern end of the building, the dike and floor will be coated with an epoxy-type paint which is resistant to strong acid, bases, and flammables. The dimensions of the dike will be 40' (length) x 30" (width) x 6" (minimum height). The floor within the diked area will be sloped to a recessed sump pit which will be equipped with a sump pump. An adequate lighting system will also be installed to aid personnel during the visual

inspections of the drums for leaks. An overhead crane, which is capable of lifting a thousand pounds, has been requested to aid in the movement of liquid constructed which will elevate the liquid waste drums 18" off the floor. The liquid waste drums are inspected on a weekly basis by government personnel. The following are the requirements set for the use and management of containers within a storage area:

a. All containers holding hazardous waste are in good condition and the contents of these containers will be transferred to a new container or an overpack container, if the original container begins to leak.

b. Ensure that the container or liner is made of a material which is compatible with the hazardous waste.

c. Containers holding hazardous waste shall always remain closed when in storage. The containers will not be opened, handled or stored in such a manner which could lead to its rupture.

d. All storage areas shall be inspected on a weekly basis for leaks and deterioration of the containers.

7.1. CONTAINMENT STORAGE.

The containment storage areas shall be designed in the following manner:

a. Base free of cracks or gaps.

b. Base sufficiently impervious to contain leaks and spills.

c. Base designed to provide efficient drainage, so liquid doesn't stand on the base for longer than one hour.

d. All containers be elevated off of the base to prevent contact from leaking liquid.

e. The diked area has sufficient capacity to contain 10% of the volume of the containers, or the contents of the largest container, whichever is larger.

8.0. MAINTAINING OF RECORDS.

Personnel at the thermal destructor unit maintain several sets of records ranging from the receipt of 3 "x" waste to the disposition of 5 "x" conditional material.

8.1 RECORDS FOR RECEIPT.

A copy of all Materiel Courier Receipt forms and Request For Issue or Turn-In forms are kept at the facility, with the receipt of the forms and other

pertinent information being recorded in a log book. These two forms list the type of contamination, decontamination solution used, user's name, organization, date received, pallet number assigned, certified 3 "x", and the clearance number for the bubble analysis results.

8.2. DETAILED CHEMICAL AND PHYSICAL ANALYSIS OF WASTE/ASH.

A written waste analysis plan shall be developed which describes the procedures which will be followed to collect and analyze samples. The following information is required:

- a. The parameters for which each hazardous waste will be analyzed, the rationale for the selection of these parameters, and how the analysis for these parameters will provide sufficient information on waste's properties.
- b. The test methods which will be used to test for these parameters.
- c. The sampling method which will be used to obtain a representative sample of the waste to be analyzed.
- d. The frequency with which the initial analysis of the waste will be reviewed or repeated to ensure that the analysis is accurate and up-to-date.

8.2.1. Monitoring reports will be maintained at the facility containing the following information:

- a. The dates, exact places, and times of sampling or measurements.
- b. Name of the individual who performed the sampling.
- c. The dates that the analyses were performed.
- d. The name of the individual who performed the analyses.
- e. The analytical techniques or methods used.
- f. The results of the analysis.

Specific waste analysis required to determine the following:

- a. The heating value of the waste.
- b. The halogen and sulfur content in the waste.
- c. The concentrations in the waste of lead and mercury, unless there is documented data to show that the element is not present.

8.2.2. Monitoring reports are being maintained at the facility, but the information is maintained in several different records and not in an

individual record. The monitoring information currently being collected is as follows:

- a. The dates, exact places, and times of sampling.
- b. The dates that the analysis were performed.
- c. The name of the contracting firm who is performing the analyses.
- d. The analytical techniques or methods used.
- e. The results of the analysis.

9.0. CONTINGENCY PLAN AND EMERGENCY PROCEDURES.

A contingency plan will be maintained at the facility and submitted to the proper emergency response teams. This plan will incorporate the following:

- a. A spill prevention, control, and countermeasures (SPCC) plan.
- b. Hazardous waste management provisions.
- c. Description of arrangements with local authorities/emergency response teams.
- d. List of the names, addresses, and phone numbers of all persons qualified to act as an emergency coordinator.
- e. List of all the Emergency Equipment and Alarms (communication devices).
- f. Evacuation plan (routes and alternate routes).
- g. Name of qualified individual to be an Emergency Coordinator on site at all times.

9.1. EMERGENCY PLAN.

In case of an emergency situation the Emergency Coordinator will initiate the Emergency Plan in the following sequence:

- a. Activate internal facility alarms.
- b. Contact appropriate agencies.
- c. Assess damage.
- d. Determine if evacuation is necessary.

9.1.1. File report on emergency situation containing the following information:

- a. Name and address of the facility.
- b. Name and telephone number of the individual who reported the emergency situation.
- c. Time and type of emergency situation.
- d. Name and quantity of materials involved.
- e. Extent of injuries (if any).
- f. Possible hazards to human health and environment.
- g. Plans for monitoring for leaks during the emergency situation.
- h. Cleanup procedures of the facility and equipment.
- i. Notification procedures.
- j. Personnel will have immediate access to an internal alarm or an emergency communications device.
- k. There shall be adequate aisle space to allow for the unobstructed movement of personnel, fire protection equipment, spill control equipment, and decontamination equipment within the facility in case of an emergency situation.

9.1.2. The following emergency equipment is required at the facility:

- a. An internal communication/alarm system for emergency instructions to facility personnel.
- b. A telephone/two-way radio for emergency use.
- c. Portable fire equipment, fire control equipment, spill control equipment, and decontamination equipment.
- d. Adequate water volume and pressure for the fire suppression systems.

10.0. MONITORING AND INSPECTING EQUIPMENT.

A written schedule for the inspection of all monitoring equipment, safety and emergency equipment, security devices, operating and structural equipment which are important to preventing, detecting, or responding to environmental

or human health hazards. As a minimum, the following requirements are to be met for the written schedule:

- a. The written schedule will be kept on site.
- b. Will identify the types of problems being looked for during the inspection.
- c. The frequency of inspections.
- d. The following items will be recorded and kept for a minimum of 3 years from the date of inspection:
 - Date and time of inspection.
 - Name of inspector.
 - Observations made during the inspection.
 - Date and nature of any repairs or other remedial actions.

10.1. CALIBRATION RECORDS.

Records will be maintained on all calibration and maintenance records, and all original strip chart recordings for continuous monitoring instrumentation for 3 years.

10.1.1. Before hazardous waste is added, the incinerator will be brought to a steady state condition of operation to include:

- a. Temperatures.
- b. Air flow.

10.1.2. While incinerating hazardous waste the following monitoring and inspecting will be conducted:

- a. Monitor combustion and emission control instruments at least every 15 minutes. (i.e., waste feed, fuel feed auxiliary, airflow, incinerator temperature, scrubber flow, scrubber pH, and relevant level controls).
- b. Observe stack plume visually at least hourly.
- c. The complete incinerator and associated equipment shall be inspected daily for leaks, spills, fugitive emissions, and all emergency shutdown controls/system alarms.

11.0. RECORD ON ALL WASTE INCINERATED.

An operating record will be maintained at the facility until closure and this record will contain, as a minimum, the following:

- a. Description and quantity of each hazardous waste received.
 - type of item being burned (i.e., hoods, filters, etc.).
 - make-up of item being burned (i.e., metal, slate, etc.).
 - weight of the item being burned.
- b. Methods and dates of treatment, storage or disposal.
- c. Location of each hazardous waste within the facility and quantity for each location.
- d. Results of analyses.
- e. Summary reports on all emergency situations.
- f. Results of inspections (kept for 3 years).
- g. Records for spent or discarded laboratory solvents/chemicals exposed to surety agents and then treated by decontamination solutions. The following information will be recorded:
 - The identity of the solvent or chemical.
 - The identity of the surety agent involved.
 - The treatment chemical solution used for decontamination purposes.
 - Date the item was incinerated.
 - The hazardous waste code (if any).
 - The amount of material incinerated.
- h. Records for spent treatment solutions from the treatment of items exposed to surety agents. The following information will be recorded:
 - The identity of the surety agent involved.
 - The name or description of the spent treatment solution.
 - Date the spent treatment solution was incinerated.
 - The amount of spent treatment solution incinerated.

11.1. RECORDS MAINTAINED DURING THE BURN.

One detailed record is maintained during the operation of the incinerator which contains the following information:

- a. The burn number.
- b. The date of the burn.
- c. The pH of the scrubber during the burn.
- d. The 3 "x" individual item weights prior to the burn.
- e. The pallet number.
- f. The type of items placed into the firepan (i.e., hoods, filters, etc.).
- g. Total weight of the items being burned.
- h. Total weight of the items after the burn.
- i. Total weight lost after the burn.
- j. Temperature maintained in the secondary combustion chamber at hourly intervals.
- k. Temperatures in the primary and secondary combustion chambers during the detoxification stage of incineration. The temperatures are recorded at half-hour intervals.
- l. Temperatures in the primary and secondary combustion chambers after the detoxification stage of incineration. The temperatures are recorded at hourly intervals.
- m. Final temperature reading from the two combustion chambers the following morning.
- n. Pertinent remarks dealing with the operation of the incinerator.
- o. A pre-operational checklist for the burn is filled out, signed by the operator, and attached to the log.
- p. A chart reading of the temperatures maintained of the primary and secondary combustion chambers during the burn is signed by the operator and attached to the log.

11.2. RECORDS MAINTAINED AFTER THE BURN.

Several sets of records are maintained after the burning of 3 "x" waste. They are:

11.2.1. One record is maintained on the items removed from the firepan. The following information is contained in this record:

- a. The weight of the burned item.
- b. The identification of the burned item (when possible).
- c. Total weight loss recorded after the burn.
- d. A master log book is maintained in the office at the thermal destructor unit containing total weights, total weights losses, and burn numbers.

11.2.2. Records are kept on 5 "x" conditional scrap metal and slate. The following information is recorded:

- a. The burn number.
- b. The drum/pallet number.
- c. The weight of the 5 "x" items. (the drums/pallets of scrap metal/slate are then stored at the complex pending disposition).

11.2.3. Records are maintained of the Rendered Safe Statement forms which are used for the turn-in of scrap metal being transported to the APGISA scrap yard. The Rendered Safe Statement form contains information pertaining to the burn number, pallet number, weight of the scrap metal, and certification that the scrap metal is 5 "x".

11.2.4. A final set of records are maintained for accountability purposes of 5"x" items. These records contain:

- a. The total weight of the 3 "x" waste being burned.
- b. The total weight of the ash filled drums and the analysis results.
- c. The total weight of slate sent to the APGISA land fill.
- d. The total weight of scrap metal sent to the APGISA scrap metal yard.

12.0. ANNUAL REPORT.

An annual report shall be prepared and submitted to the Secretary of the Maryland Office of Health and Hygiene by 1 March of each year. This report

shall include the following:

- a. Activities at the facility during the previous calendar year.
- b. The EPA identification number, name, and address of the facility.
- c. A description and the quantity of each hazardous waste received during the year.
- d. The method of treatment, storage or disposal for each hazardous waste.
- e. The certification signed by an authorized representative .

13.0. TRAINING FOR PERSONNEL.

Personnel shall successfully complete a program of classroom training or on-the-job training that teaches the operators to perform their duties in a way which ensures the facilities compliance with state requirements. The program shall provide the following:

- a. Hazardous waste management procedures (including contingency plan implementation).
- b. Familiarize personnel with:
 - Emergency procedures.
 - Emergency equipment.
 - Emergency systems.

13.1. DOCUMENTING TRAINING.

Records documenting training received by operating personnel will be retained at the facility and contain the following:

- a. The job title for each position.
- b. The name of each employee filling each position.
- c. A written description for each position.
 - Prerequisite skill.
 - Education or other qualifications.
 - Duties assigned.
- d. A written description of the type and amount of both introductory and continuing training to be given to each person.

- a. Records will be kept until closure of facility.

13.2. ADDITIONAL TRAINING REQUIREMENTS.

The following installational requirements are in addition to the Federal and State requirements.

- a. All thermal destructor unit IOP's will be reviewed with the operational staff when an individual is initially assigned to facility. This form of training will be recorded on the signature sheet of the IOP and the individual's training document.

- b. Emergency procedures will be included as part of the initial and annual training program.

- c. Operational parameters described in the IOP will be included as part of the initial and annual training program.

- d. New personnel will, as a minimum, be trained on the thermal destructor unit equipment for a minimum period of six months and 20 incinerator runs. The competency of the operator will be evaluated after the six months by the first line supervisor who determines whether to extend the training period, reassign or certify the employee. The employee training record will be documented at this time describing operational competency. Noncertified employees will not be allowed to operate switches, valves, etc., without the presence of a certified operator.

14.0. SAFETY CONSIDERATIONS.

Upon the completion of the safety evaluation for the thermal destructor unit the following changes were implemented:

- a. The use of TEU for the transportation of 3"x" waste has been terminated, except for in busy periods. The majority of the 3"x" waste is being picked-up and transported to the respective waste storage facilities/areas by operating personnel at the thermal destructor unit. The personnel from the thermal destructor unit facility are more familiar with the type of waste to be picked up, proper packaging of waste, and what waste is unacceptable for disposal at the thermal unit. Having personnel from the thermal destructor unit transport the 3"x" waste will be a time saver and will relieve TEU of this operation.

- b. Due to the potential build up of pressure within the metal containers of waste, which are being incinerated, the thermal unit personnel have been punching holes into the metal containers prior to the items being placed into the firepan. Non-metal containers are now being utilized for the storage 3"x" waste instead of the metal containers. Such containers would not allow the internal pressures to build up to hazardous levels, but these would have to be

stored in an enclosed area where the drums would not be exposed to the elements. An enclosed area has been constructed right outside of the thermal unit complex for the storage of the non-metal containers of 3"x" waste.

c. As mentioned previously in this paper the removal of ash from the firepan generates a dusty condition at the worksite. To alleviate this situation the operating personnel wet down the ash prior to shovelling the ash into the drums. Other methods being looked into to alleviate this problem are engineering controls, different handling procedures, and possibly developing a mechanical method for emptying the firepan.

d. Additional temperature probes have been added to the primary combustion chamber to ensure that a uniform temperature is being maintained during the burn.

15.0. SUMMARY.

Incineration has been developing as a primary means of disposing of various type of waste materials. To ensure the safe operation of the thermal destructor unit several safeguards were incorporated into the design of the incinerator and a detailed Internal Operating Procedure (IOP) has been developed for operations at the facility. Some of the safeguards incorporated into the design of the incinerator are redundant electronic system within the control panel for the incinerator, redundant pumps for essential portions of the incinerator, pollution control systems, and minor safety features. Possible emissions of hazardous byproducts which could be generated during the incineration of waste within the primary combustion chamber are captured by one of three pollution control devices. The three pollution control devices are in series of one another and are specifically developed to control waste byproducts generated during the incineration of 3"x" waste. The most important safeguard for any operation are the development of detailed operating procedures which describe each portion of the operation and the proper procedures to be followed in the event of an emergency. With the above safeguards being followed and implemented the potential for a hazardous situation to occur is greatly reduced and will enhance the safety for operating personnel.

AIRBLAST MEASUREMENTS AND EQUIVALENCY
FOR SPHERICAL CHARGES AT SMALL SCALED DISTANCES

by

Edward D. Esparza
Southwest Research Institute
San Antonio, Texas

22nd Department of Defense Explosives Safety Seminar
26-28 August 1986

ABSTRACT

AD-P005 385

An experimental investigation was conducted to obtain direct measurements of side-on overpressures from spherical charges of six different high explosives at small scaled distances ranging from 0.74 to 3.5 ft/lb ^{to the 1/3 power} $^{1/3}$. The pressure-time recordings of the incident airblast waves were processed to obtain peak side-on overpressures, shock wave arrival times, side-on impulses, and positive durations. Comparisons of the test data were made with standard blast curves for these four parameters. The side-on overpressure and arrival time data from the TNT tests are in excellent agreement with the standard curves. The impulse and duration data show that at scaled distances less than 3 ft/lb $^{1/3}$, the standard curves are not as well defined as those for pressure and arrival time. TNT equivalencies for each of the six explosives were determined using the standard pressure and impulse curves, as well as the actual TNT test data obtained. These results indicate that the pressure based TNT equivalency at small scaled distances for some of the explosives tested can be significantly different than that based on the heat of detonation.

INTRODUCTION

Background

Characterization of blast waves from high explosive detonations in free air by experimental methods has a long history dating back to World War II, as reported by Kennedy [1]. Stoner and Bleakney [2] in 1948 reported results of free-air experiments conducted with small TNT and Pentolite charges of various shapes. After World War II, a large number of investigators made free-field blast measurements in the United States. Goodman [3] compiled free-field blast measurements from bare, spherical Pentolite charges made by several investigators at the U.S. Army Ballistic Research Laboratories from 1945 to 1960. During this same time period, data were also generated by investigators at the U.S. Naval Ordnance Laboratory. Baker [4] provides an excellent historical summary and presents much of the data from these investigations.

Measurements of blast parameters from other than free air, high explosive detonations have been made by many investigators, also dating back to World War II. For example, measurements of blast wave properties from ground bursts of large hemispherical TNT charges were compiled and analyzed by Kingery [5]. Air blast data from height-of-burst experiments have been measured by several investigators such as Reisler, et al. [6,7]. Measurements of normally reflected waves have been made by Jack [8], Dewey, et al. [9], Wenzel and Esparza [10], and others. Measurements of blast parameters from charges of various geometries, from sequential detonations, from simultaneous detonations, and at real and simulated altitude conditions have also been made by many investigators [10-17]. Good descriptions of the characteristics of air blast waves in general are provided by Baker [4], Swisdak [18], and Glasstone and Dolan [19].

Because air blast data have been obtained by a large number of investigators for different explosives, one can obtain different predictions for blast parameters depending on the source. In attempts to eliminate some of these variations, "standard" blast parameter graphs and tables have evolved over time. Examples of blast curves are presented in References 4, 5, and 18-21. Probably the most widely used set of standard curves is found in the tri-service manual, "Structures to Resist the Effects of Accidental Explosions" [22]. In this manual, curves for free-air detonations and surface

detonations are presented for various blast parameters. These curves are based partly on experiments, and partly on analyses and computer code computations. At distances very close to the charge, direct measurements of many of the blast parameters are either nonexistent or very few. Consequently, these curves are not well defined at distances close to an explosive charge.

The standard curves are usually for spherical TNT explosions. For other high explosives, the concept of TNT equivalency is then often used to predict the blast parameters. TNT equivalency is defined as the ratio of the charge weight of TNT to the weight of the test explosive that will yield the same amplitude of a blast parameter at the same radial distance from each charge. All high explosives generate blast waves which are quite similar in character. However, their equivalence to TNT may vary with distance from the charge, and with the particular blast parameter chosen for comparison. Thus, a single equivalent weight ratio may not be appropriate, particularly at close distances to the charge where experimental verification may not exist. Furthermore, equivalence based on one blast parameter may be significantly different for another, even though the same high explosive is being tested.

Objectives

To obtain direct measurements of blast overpressures at small scaled distances from spherical charges of TNT and five other high explosives, Southwest Research Institute (SwRI) funded a project [23] to conduct a series of free-air experiments using explosive charges that were surplus to some earlier SwRI projects. These precision charges ranged in weight from about 0.5 to 1.3 lb and were cast or pressed from Composition B, PBX-9404, Pentolite, TNT, PBX-9501, and PBX-9502. The data from these spherical charges were to be used to characterize the blast waves generated by the six high explosives at small scaled distances. In addition, the TNT data were to be compared to standard curves, and the data from the other five explosives were to be used to analyze the concept of TNT equivalency at small distances from the charges. This paper presents a brief description of the limited number of experiments conducted and the results obtained. Additional details of the tests, and graphs and tabulations of all the experimental data are provided in Reference 23.

Blast Scaling

Scaling of blast wave properties is a common practice used to generalize blast data from high explosives. Scaling or model laws are used to predict the properties of blast waves from large-scale explosions based on tests at a much smaller scale. The most common scaling law is the one formulated independently by Hopkinson [24] and Cranz [25]. This law states that self-similar blast waves are produced at the same scaled distance when two explosives of similar geometry and of the same explosive material, but of different size, are detonated in the same atmosphere. The Hopkinson-Cranz or cube-root scaling law has become so universally used that high explosive blast data are almost always presented in terms of the scaled parameters generated by this law. A more complete discussion of this law is given by Baker [4]. Another widely used scaling law formulated by Sachs [26] allows prediction of the effects of detonations at different ambient conditions. For the experiments reported here, the ambient conditions were not sufficiently different from standard sea level conditions to warrant the use of Sachs' law. Therefore, all data are presented using Hopkinson-Cranz scaled parameters.

DESCRIPTION OF EXPERIMENTS

The experiments were conducted at the SwRI explosives range using the apparatus depicted in Figure 1. Two pipe stands supported wedge-shaped transducer holders, one reconditioned from earlier work [27] and a similar new one. A cross-member was used to suspend the explosive spheres. The transducer wedges were positioned about 5 ft above the concrete pad surface to preclude any surface reflections from interfering with the initial blast wave. In all tests, the wedge-tipped transducer holders were positioned 180° apart on either side of the high explosive spheres. They were 32 in. long, 6 in. wide, and 2 in. thick, were fabricated from 2024-T4 aluminum rectangular stock, and fitted with hardened 4130 steel tips at the wedge-shaped end. Each transducer holder had provisions for mounting six pressure transducers, all in line with the center line of the flat top surface.

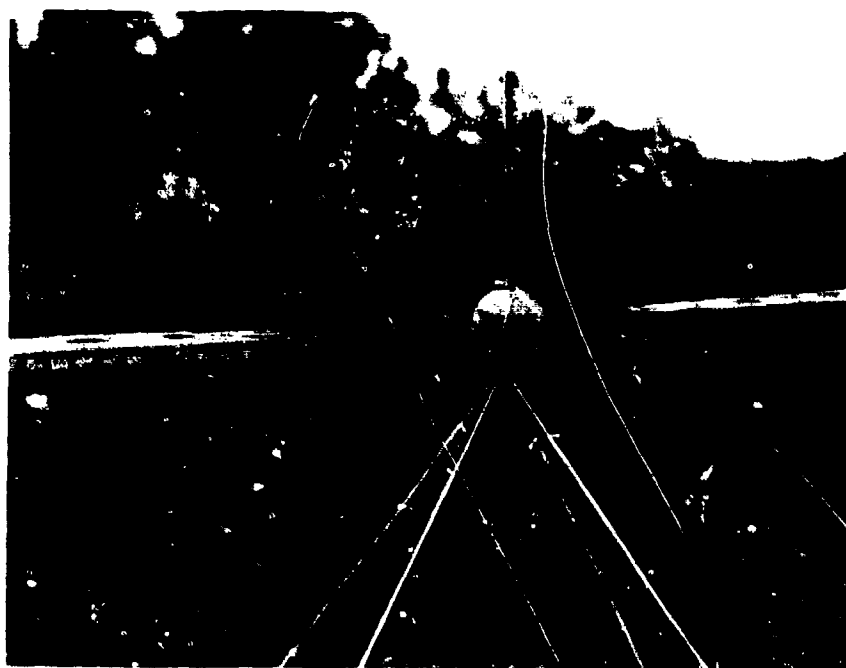
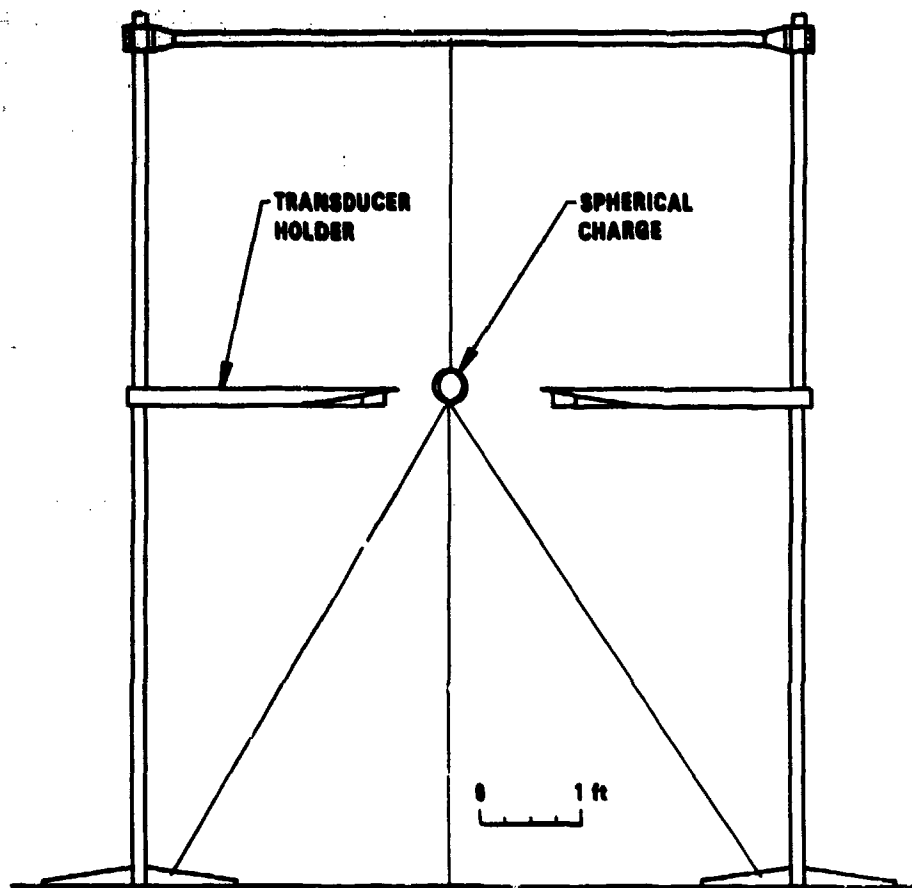


Figure 1. Test Apparatus For Close-in Measurements

The pressure transducers used to measure the blast overpressures are manufactured by PCB Piezotronics. Three different models of the series 102A transducers were used. All models have the same physical configuration differing primarily in their full scale range, sensitivity, and discharge time constant. Each PCB transducer utilizes a piezoelectric, pressure sensing element made of quartz which is coupled with a miniature source follower within the body of the transducer. Power and signal amplification were provided with PCB Model 494A06 six channel units. The blast pressure-time histories were recorded on magnetic tape using a Honeywell Model 101, Wideband II, FM tape recorder at a bandwidth of 0-500 kHz (+1, - 3dB).

The data were processed in sets of four data channels using a Biomation Model 105 transient recorder for digitizing at effective sampling rates of 0.6 to 3.2 million samples per second depending on the measurement location. The digital data were transferred from the transient recorder memory via a CAMAC data buss to a hard disk and a flexible diskette of a DEC 11/23 computer located at the range facility. Final data processing and plotting were then accomplished from the diskette with a DEC 11/70 computer. Figure 2 shows a block diagram of the pressure data record/reduction system. The high-frequency response of this system was 200 kHz.

In addition to the pressure measurements, pin gages of the piezoelectric and ionization types were used to obtain additional time-of-arrival data. Both types used are made by Dynasen, Inc. They were epoxied into copper tube mounts which were held in place by special adapters and pipe stands. The pin gages using the stands were positioned horizontally looking at the center of the sphere and at 90° from the pressure transducer holders. When installed on a test, pin gage tips were located 2 in. and 4 in. from the charge surface. In some cases a third pin was used with the tip on the surface of the charge. This pin was suspended almost vertically along the string holding the charge in place.

EXPERIMENTAL RESULTS AND DISCUSSION

Test data were obtained from 18 experiments using six different types of high explosives as indicated in Table 1. For some of the explosives, more than one explosive weight was available for testing. The pressure-time

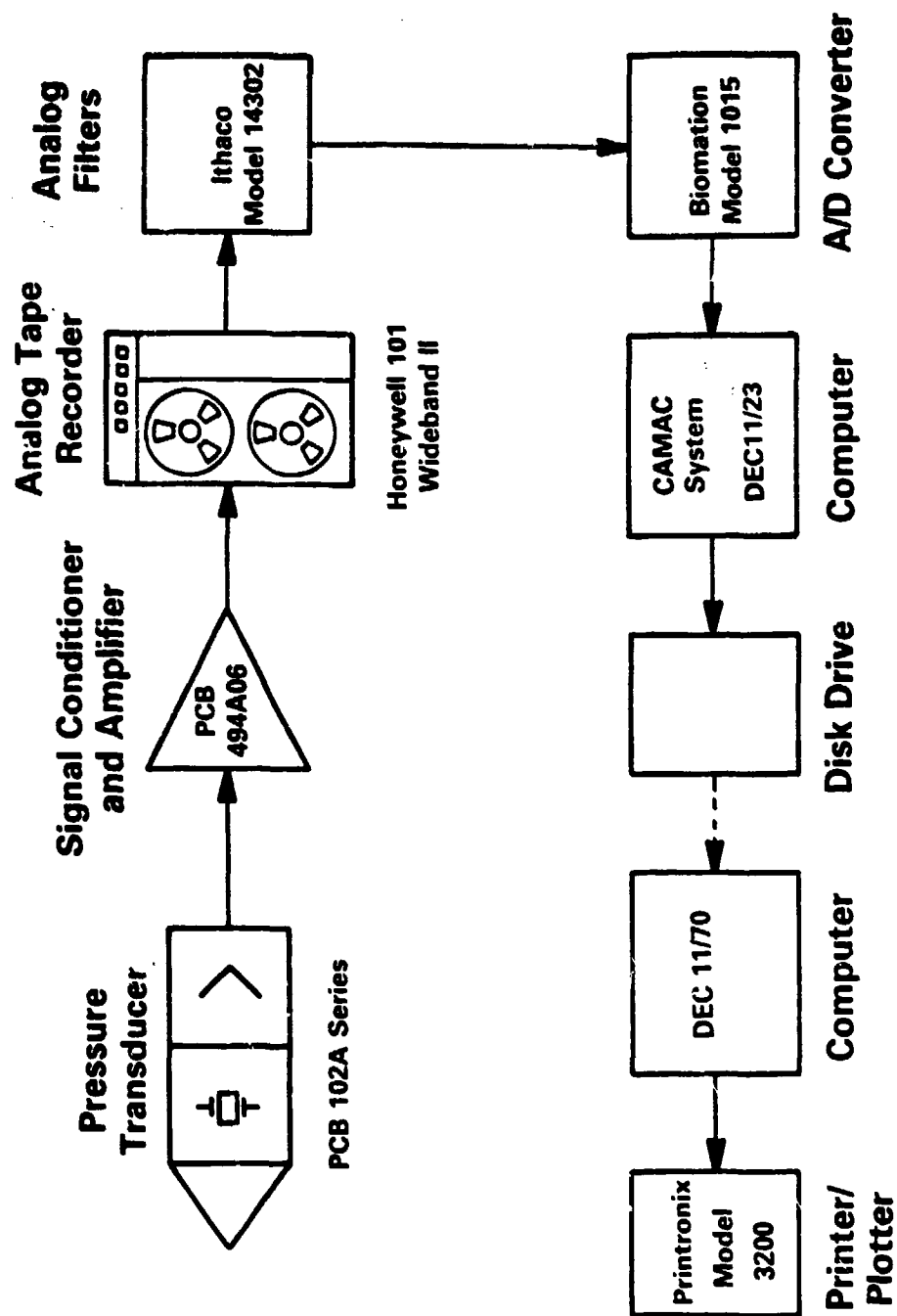


Figure 2. Data Recording and Processing System

recordings made on each test were processed to obtain peak side-on (incident) overpressures, shock wave arrival times, side-on impulses, and positive durations of the incident pressure pulse. Additional arrival time data were obtained with the position pins. The pressure data were obtained at scaled distances ranging from 0.74 to 3.5 ft/lb^{1/3}. In most tests, 12 pressure measurements were made. Arrival time data were obtained at scaled distances as close as the surface of the explosive sphere on some tests.

More than 200 pressure measurements were made in this research program. The shock wave in air from any high explosive is formed when the detonation wave propagating in the explosive reaches the surface. For a spherical charge initiated at the center, the initial shock wave in air will also be spherical, and, consequently, symmetrical about any plane bisecting the charge. High explosives generate blast waves which are quite similar in character. However, the properties of the waves may differ for different explosives, particularly at close proximity. The wave formed in air adjacent to an explosion has properties much influenced by the nature of the explosive source. Once the wave propagates in air independently of its source, it is affected primarily by the properties of air. As the blast wave passes through the air, rapid variations of blast wave properties (such as pressure) occur. The properties which are usually defined and measured are those of the undisturbed or side-on wave as it propagates through the air. Examples of side-on overpressures recorded on this project are shown in Figures 3-6.

Table 1. Summary of Experiments

<u>Explosive Type</u>	<u>Nominal Charge Weight (lb)</u>	<u>No. of Experiments</u>
Composition B	1.074	2
Composition B	0.494	1
PBX-9404	0.495	4
PBX-9404	1.002	3
Pentolite	1.309	3
TNT	1.285	2
PBX-9501	0.805	2
PBX-9502	1.301	1

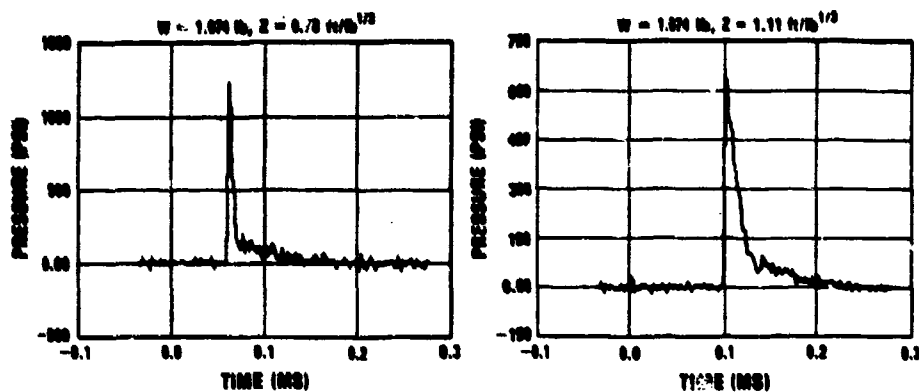


Figure 3. Blast Pressure Data From a Composition B Test

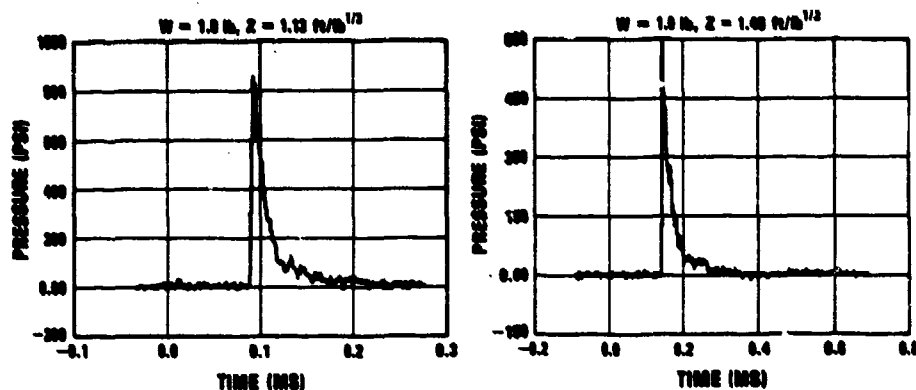


Figure 4. Blast Pressure Data From a PBX-9404 Test

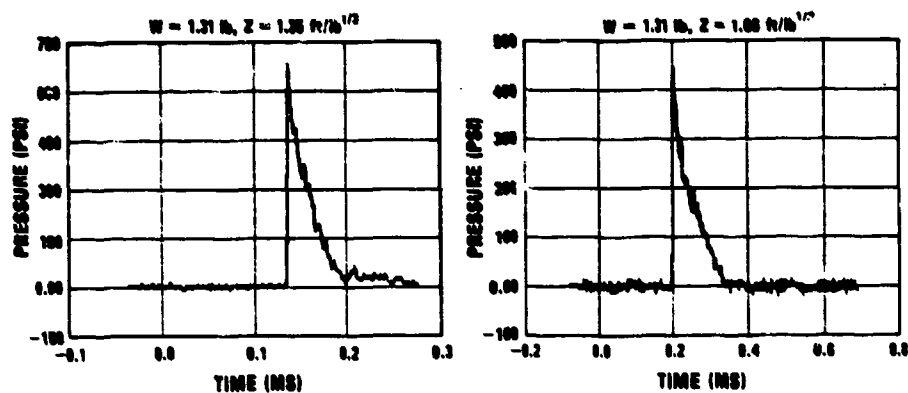


Figure 5. Blast Pressure Data From a Pentolite Test

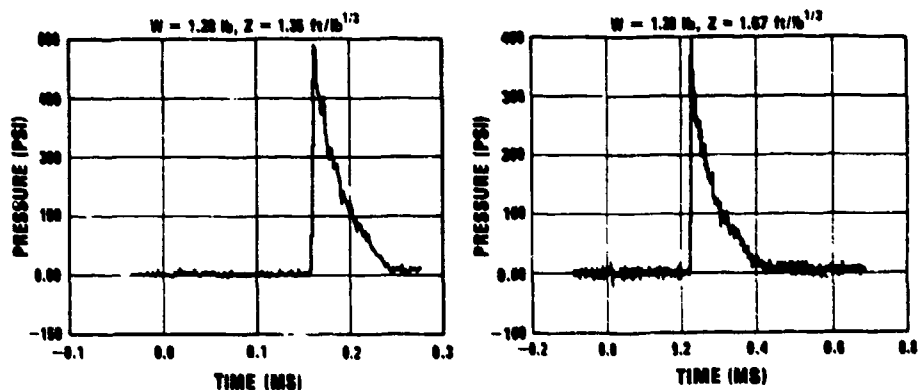


Figure 6. Blast Pressure Data From TNT Tests

Figure 3 presents pressure-time histories recorded at scaled distances (Z) of 0.78 and 1.11 ft/lb^{1/3} on a test using a sphere of Composition B with a mass (M) of 1.074 lb. In Figure 4, two measurements from a PBX-9404 test are presented. The first of these two pressure measurements was taken at a scaled distance of 1.13, about the same as for the second trace in Figure 3. These two traces exemplify the similarity in the character of the data obtained at the same scaled distance from two different explosives. However, the magnitudes of the pressures measured are different. Figure 5 includes a sequence of two measurements made on a Pentolite test at scaled distances Z of 1.35 and 1.66. As was the case with the previous two figures, these two traces depict the gradual decay in the peak pressure with increasing distance, as well as the gradual increase in arrival and duration times. Figure 6 shows two data traces from TNT tests at scaled distances of 1.36 and 1.67, similar to those for the Pentolite data of Figure 5. These last two figures again show the similarity in the character of the incident overpressures from two different high explosives at similar scaled distances and the differences in amplitude.

The pressure measurements made on this program covered a range in scaled distances from 0.74 to 3.5 ft/lb^{1/3}. The examples of data presented concentrated on the closer scaled distances. However, examination of the data plots showed consistency at all scaled distances within each test and within tests using the same type of high explosive, even for those cases in which more than one charge size was available for testing. The observed rise times for the closer-in pressure measurements were approximately 3 microseconds. This value is consistent with the measurement system upper frequency response specification. At the larger scaled distances, the rise times observed were about 7 microseconds, which agree with the time required for the blast wave to travel across the pressure transducer diaphragm.

TNT Data Comparisons

Peak incident or side-on overpressure (P_s) was the primary blast parameter measured on this project. The peak overpressure at the shock front of an air blast wave can be measured directly with pressure transducers or it can be inferred from the velocity of the shock front. All measurements reported here were made directly with pressure transducers located at small scaled distances from the spherical high explosive charges. The arrival time (t_a) of a free-air blast wave is defined here as the time interval between the

initiation of the detonator and the arrival of the blast wave at a measurement location. This interval of time includes the time for the detonation wave to travel through the charge. Measurement of arrival times can be accomplished by several techniques. It can be done using high speed cinematography, blast switches of various types, or pressure transducers. Arrival time is usually the most accurately measured blast parameter. In this program, most measurements were obtained from the pressure transducer records. Some additional data at closer scaled distances were obtained with pin gages. The specific side-on impulse (i_s) is the positive area under the pressure-time history. The side-on impulse is a function of the peak overpressure, the duration of the positive phase, and the rate of decay of the pressure behind the shock front. Of the four blast parameters measured on this project, the positive duration (t_d) is the most subjective measurement. Individual interpretations of the same data will vary and inherently will produce a larger scatter than on the other three blast parameters.

Pressure-time records were obtained from two TNT experiments with spheres weighing 1.285 lb. The four parameters measured on these tests are plotted in Figures 7-10 and are compared to TNT standard curves [28] which will be included in the revised edition of the tri-service manual, Reference 22. The peak overpressures measured are plotted in Figure 7. The new test data [23] are plotted as vertical bars indicating the range measured. These data were measured at scaled distances ranging from 0.75 to 2.59 ft/lb^{1/3}. The new TNT pressure data are self-consistent and the comparison with the reference curve and most of the data base used to develop this curve indicates good agreement. This confirms the validity of the data from the TNT experiments as well as the data from the tests using the other five high explosives since the same measurement system and test procedures were used. Also, it increases the confidence of the results presented later on TNT-equivalency based on peak incident pressures.

It is interesting to note that the TNT reference curve for pressure from Reference 28 is a polynomial curve fit to pressure values found primarily in References 3, 5-7, 18, and 29. The compiled data from Goodman [3] are for Pentolite spheres. These data were converted in Reference 28 to TNT equivalents for use in the TNT curve fit. The TNT equivalency used is not given. For scaled distances less than 1.5 ft/lb^{1/3}, all the peak pressures presented

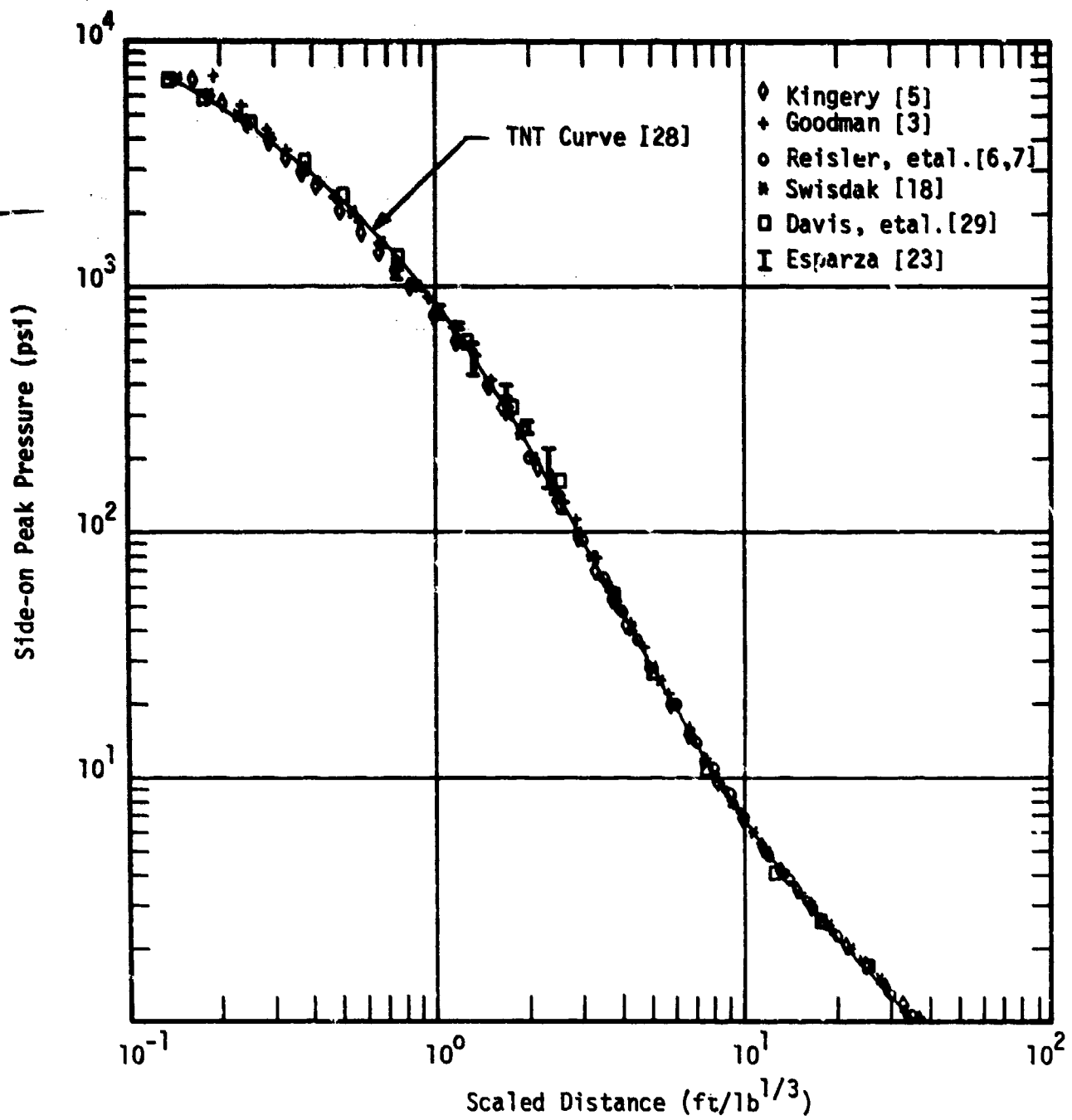


Figure 7. Comparison of TNT Pressure Data With TNT Curve

by Goodman [3] were obtained by Sultanoff and McVey [30] from optical measurements of shock front velocities. The data reported by Kingery [5] are from TNT surface bursts and are converted in Reference 28 to free air equivalent data using a reflection factor of 1.8. The pressure measurements from Reisler, et al. [6,7], were from TNT tests, but are all for scaled distances greater than $2.0 \text{ ft/lb}^{1/3}$. Swisdak [18] states that, at scaled distances less than $1.0 \text{ ft/lb}^{1/3}$, all overpressures given in that reference were obtained by hydrodynamic computer code calculations. Reference 29 presents TNT data tables and curves which were taken from Dobbs, et al. [31], and are identical to those in Reference 22, the tri-service manual. None of these last three references [22, 29 and 31] indicates which portions of the curves are derived from actual measurements. Thus, the lack of actual TNT incident pressure measurements at small scaled distances indicates that even the revised TNT standard curve from Reference 28 is not well defined experimentally close to the charge, and that the new pressure measurements presented in this paper are an important contribution to the experimental data base.

In Figure 8, the scaled time-of-arrival data for the TNT experiments are plotted as vertical bars showing the range of measurements at each scaled distance. As expected, the scatter of the data is less than for the corresponding incident pressure data, and the scatter increases the closer the measurements were made to the charge center. The TNT test data show excellent agreement with the TNT curve from Reference 28. The arrival time of the shock wave at a distance from an explosion depends on the velocity of the wave. The Rankine-Hugoniot equations relate the velocity of a shock front and the peak pressure of the shocked gas. Thus, it is possible to compute the velocity of the shock front from known values of peak incident overpressure and in turn compute arrival times from the derived shock velocities. This is the approach taken in Reference 28 to develop the scaled arrival time curve so that it was consistent with calculated shock velocities and the side-on pressure curve shown in Figure 7. Thus, the new measured arrival times are also consistent with the side-on pressure measurements.

The incident impulse data from the TNT tests [23] are presented in Figure 9. Over the range of scaled distance shown, the measured scaled impulses define a curve which indicates an explosive less energetic than TNT. This result is unlike the peak pressure and arrival time data which agreed with the

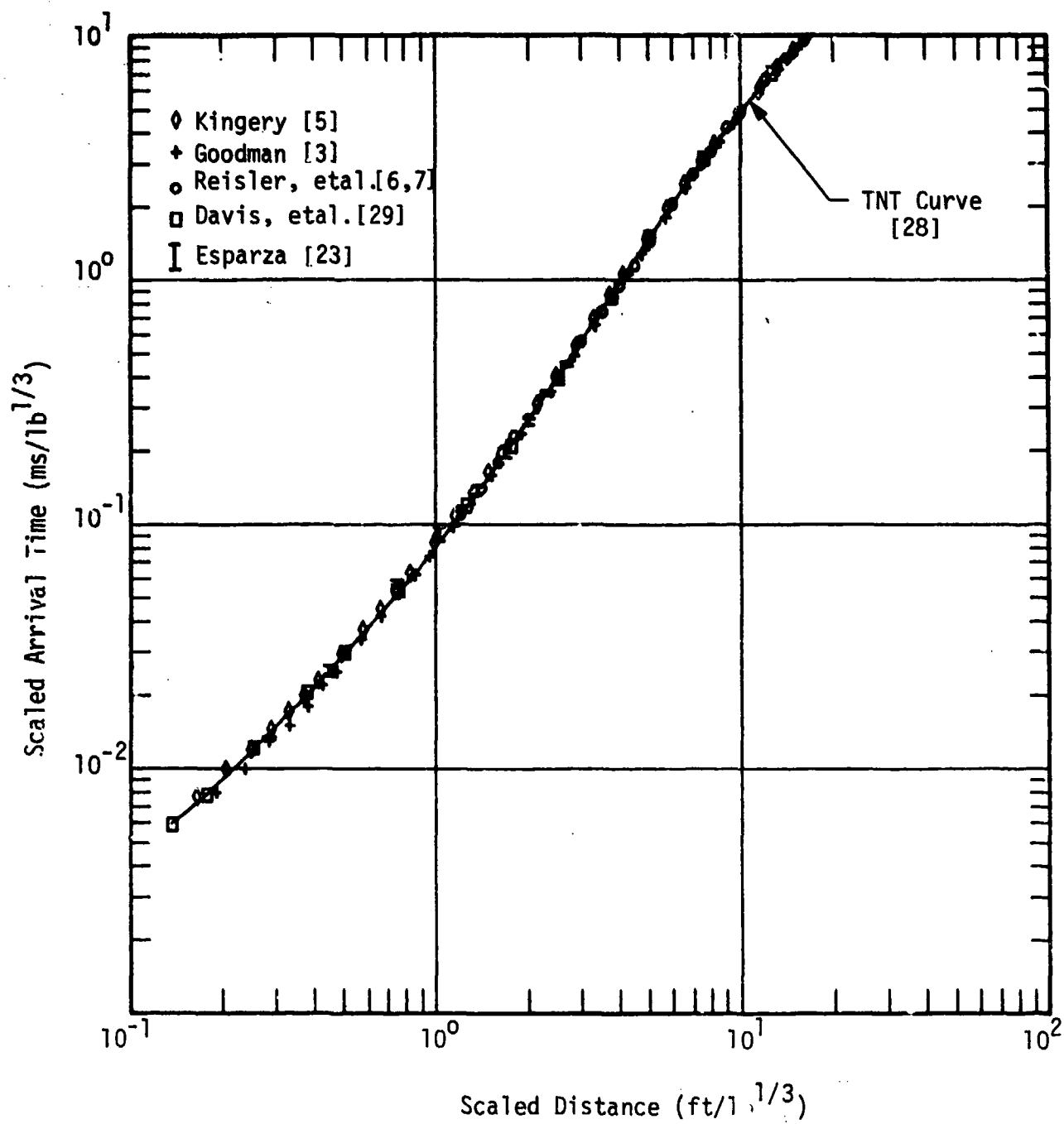


Figure 8. Comparison of TNT Arrival Time Data With TNT Curve

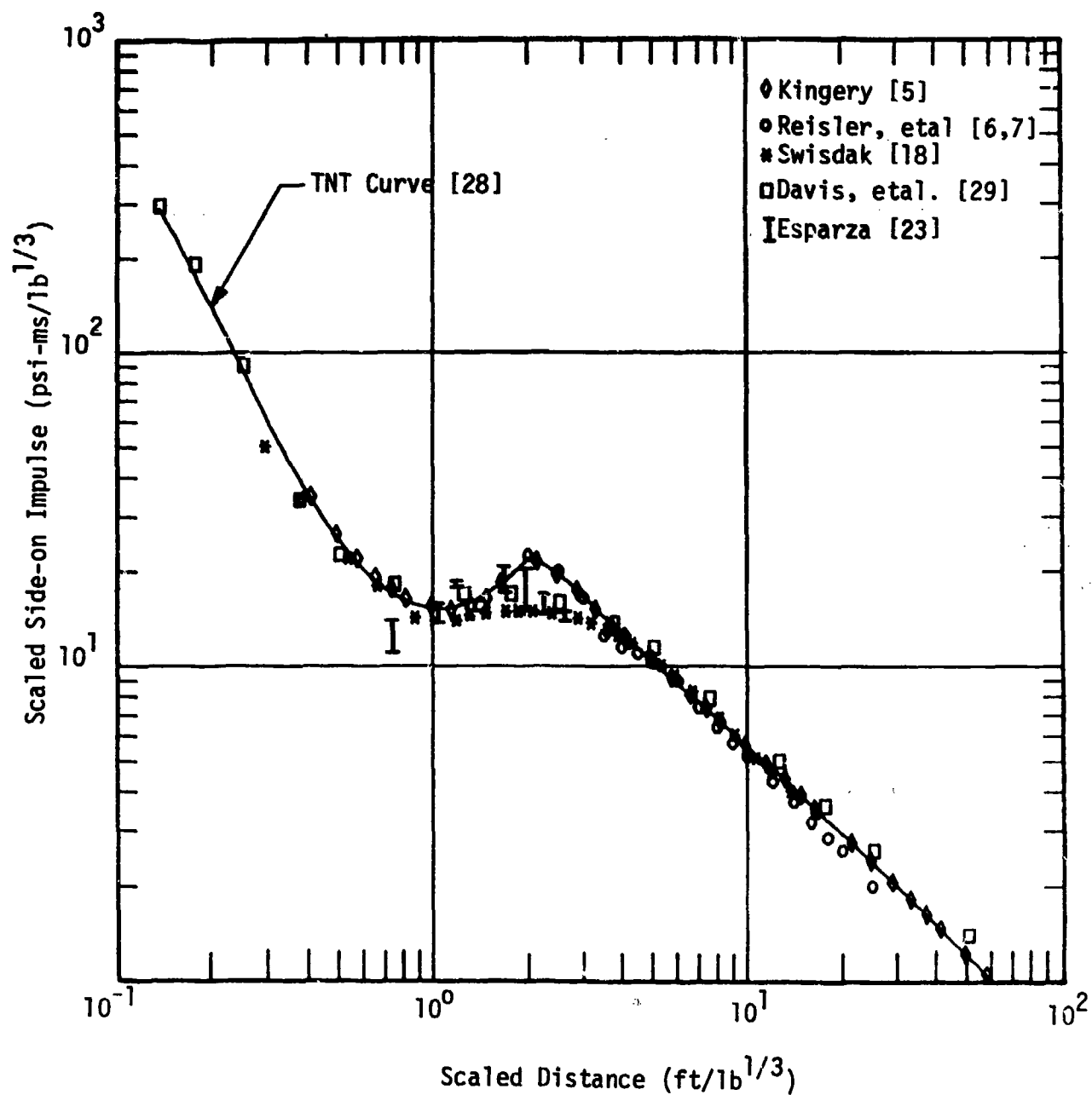


Figure 9. Comparison of TNT Impulse Data With TNT Curve

respective reference curve. However, the range of scaled distances at which the new impulse data [23] were obtained is the same at which major differences are indicated in the data from the referenced literature presented in Figure 9 used to define the TNT curve from Reference 28. In fact, more weight appears to have been given to data converted to free air equivalents from surface and height-of-burst explosions in defining the side-on impulse TNT curve [28], than actual free air data like those measured on this project. Furthermore, the new TNT test data were measured over a scaled distance range of 0.75 to 2.59 ft/lb^{1/3} which includes that portion of the curve with changes in slope, making it the most difficult portion of the curve to define with experiments or curve fits.

Figure 10 is a plot of the new TNT duration data [23] compared to the TNT reference curve and data from other references included in Reference 28. This comparison shows consistently shorter scaled durations for the new test data than the reference curve at respective scaled distances. Over the range of scaled distances at which measurements were made, the scaled times from the reference curve are almost a factor of two longer than the new measured values. The curve fit for the reference TNT curve was based only on data from hemispherical TNT surface bursts assuming a 1.8 reflection factor to convert them to free-air equivalents [28]. However, the other free air, TNT data shown in Figure 10 from References 18 and 29 show the same type of differences between the curve and the new data. The TNT reference curve appears to be more of an upper bound on the scale duration data at scaled distances less than 3 ft/lb^{1/3}.

Data From Other Explosives

Measurements of P_s , t_d , i_s , and t_d for the five other explosives listed on Table 1 were also made. For some of them, two charge weights were available for testing; for some, there was only one charge size. As shown in Figures 3-6, the pressure-time records at comparable scaled distances are quite similar in character, but the various parameters may differ quantitatively. For example, the measured data obtained from the three Composition B experiments are presented in Figure 11. Two tests used 1.07-lb spheres and one test used a 0.494-lb sphere. In Figure 11a, the peak pressure data obtained over a scaled distance range of 0.78 to 3.1 ft/lb^{1/3} are self-consistent and in general were of higher amplitude than the comparable TNT

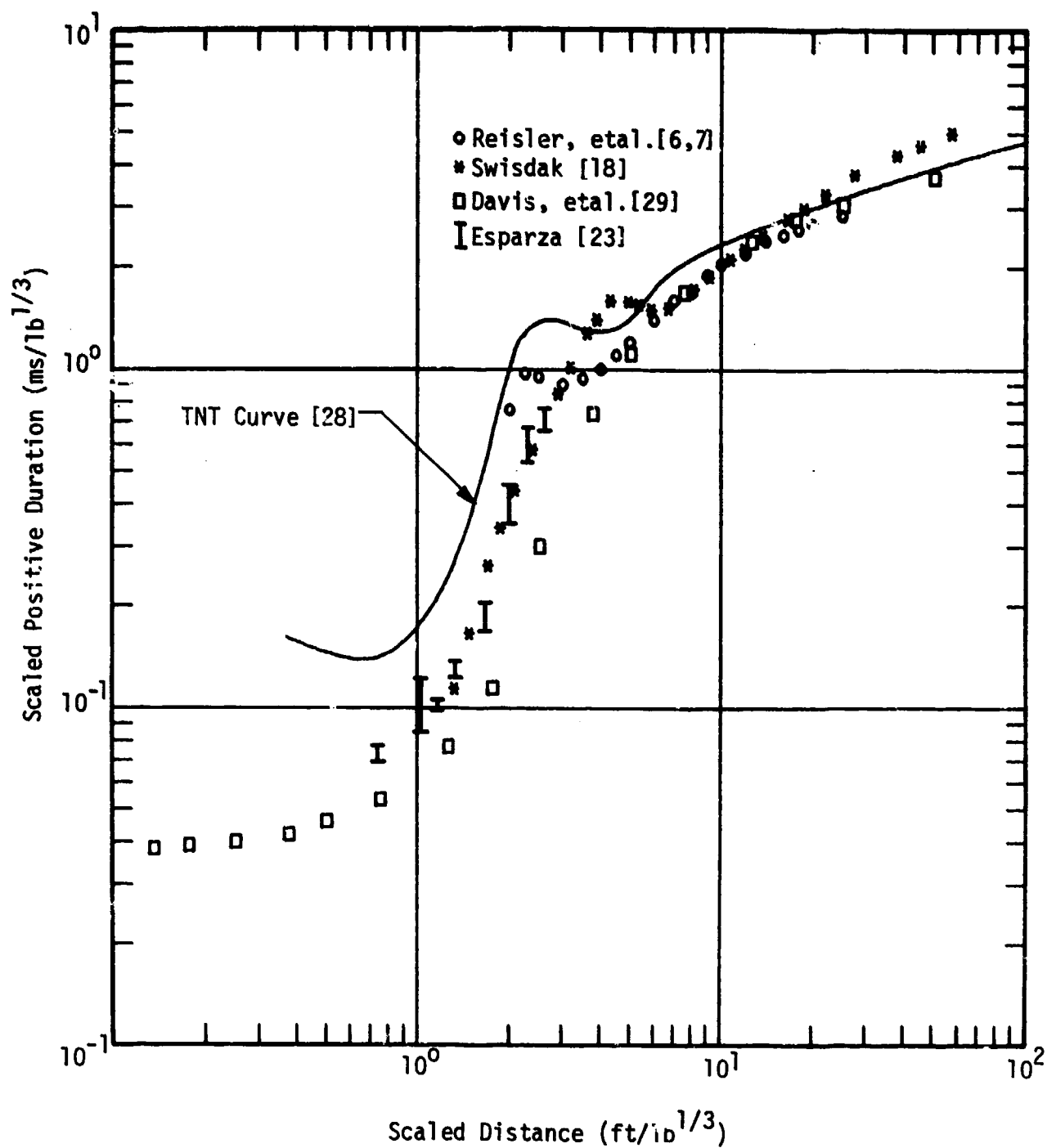


Figure 10. Comparison of TNT Positive Duration Data With TNT Curve

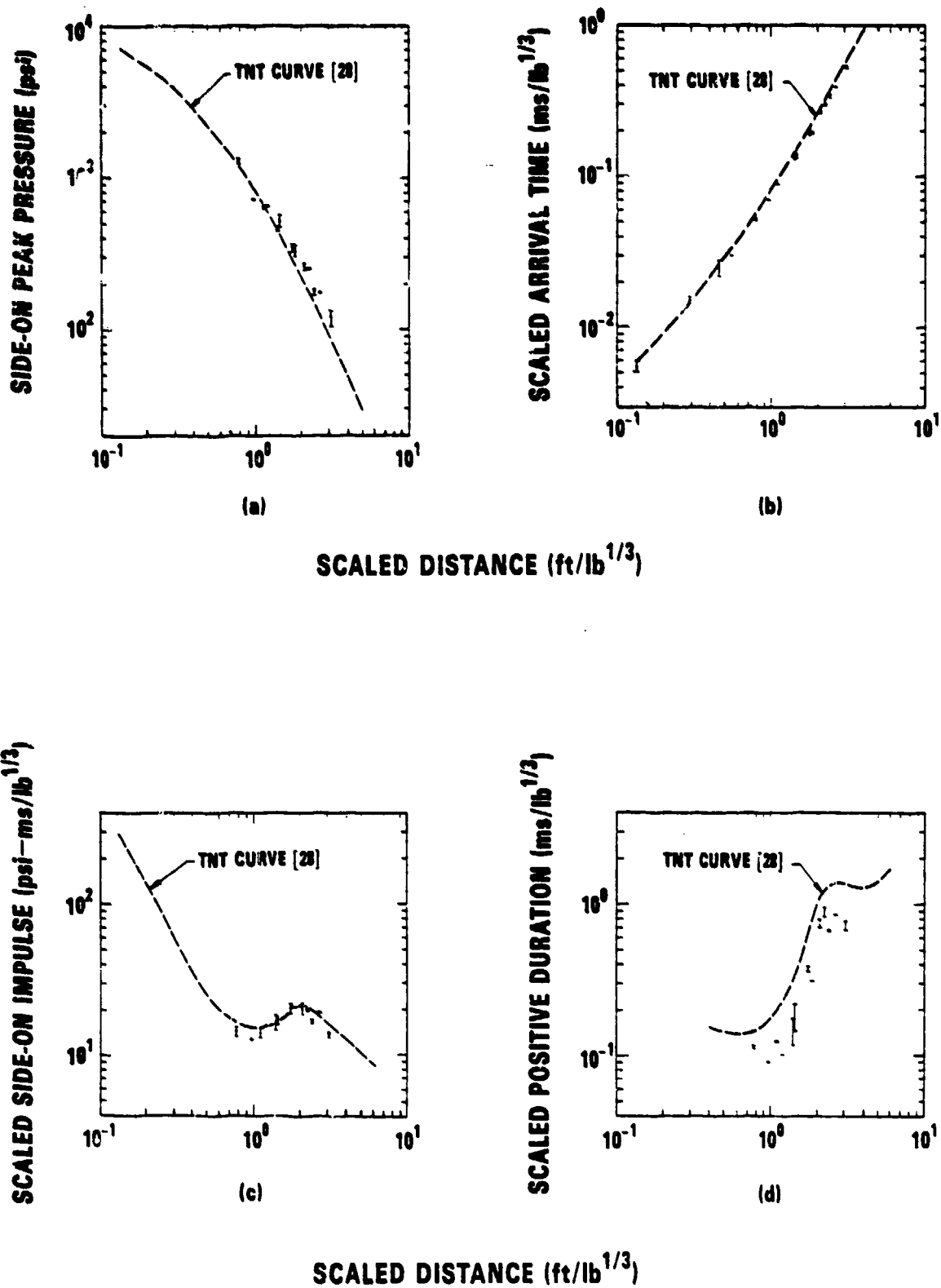


Figure 11. Blast Data from Composition B Experiments

values denoted by the dashed curve taken from Reference 28. This indicates that based on peak pressure measurements, Composition B is more energetic than TNT. Additional discussions on TNT equivalency are presented later in the paper. The Composition B arrival time data are graphed in Figure 11b. Most of the arrival times measured for this explosive are slightly shorter than those indicated by the TNT reference curve [28]. In Figure 11c, the impulse data from the Composition B tests are presented. Generally, the data are of somewhat lower amplitude than indicated by the TNT reference curve [28]. Note that, on a plot of scaled impulse versus scaled distance, an explosive less energetic than TNT, with a constant equivalency, would yield a parallel curve shifted left and down at 45° from the TNT curve. Figure 11d presents the scaled durations from the Composition B tests. It is obvious from this figure that the scatter in the duration data is greater than for other three blast parameters as was the case with the TNT data presented previously.

In Reference 23, similar data comparisons with the TNT reference curves from Reference 28 are also made for the other four high explosives tested. In this paper those results will be summarized. The peak overpressures generated by PBX-9404, Pentolite, and PBX-9501 were of higher amplitude than those indicated for the TNT reference curve. Only the pressures from PBX-9502 were of lower amplitude than the TNT values. The arrival time measurements for these four explosives exhibited less scatter than the pressure data, but were consistent with them. Thus, of the six high explosives tested only the scaled arrival times from the PBX-9502 tests were slower than the TNT values. This result is consistent with that obtained from the overpressure data.

The impulse data from the PBX-9404 tests were generally of higher amplitude than those from the TNT reference curve, while those for the Pentolite tests were generally of lower amplitude. The impulse data from the PBX-9501 tests were in some cases slightly lower and in other cases higher than the TNT reference curve. Finally, the impulse data from the one PBX-9502 test were generally of lower amplitude than analogous TNT curve values. Thus, of the six high explosives tested, only two generated impulse data that were consistently of the same or higher amplitude than the reference TNT curve [28] at scaled distances ranging from 0.74 to 3.5 lb/ft^{1/3}.

As already shown for the TNT and Composition B tests, the positive duration data from the other four explosives tested had greater scatter than any of the other three blast parameters measured. In addition, the scaled durations were in every case significantly shorter than those from the TNT reference curve [28].

Pressure TNT Equivalency

It is common practice to express the blast effects from various explosive sources in terms of the amount of TNT that will produce a blast wave having the same property as the one being characterized. Side-on pressure is the most common parameter used to determine TNT equivalency for high explosives. TNT equivalency based on incident pressure is defined as the ratio of the charge weights (TNT weight/explosive weight) that will give the same peak pressure at the same radial distance from each charge.

The concept of TNT equivalency offers the advantage of providing in one number an identification of a given blast wave in terms of a standard explosive whose blast effects have been extensively documented. The disadvantages are in many instances minor, but must be considered whenever TNT equivalency is applied, particularly at small scaled distances. In the first place, most explosives have not been tested sufficiently or at all at small scaled distances to determine a good equivalency factor based on pressure or other blast parameters. Second, the equivalency factor may vary with scaled distance or may differ whether based on pressure or another parameter. Finally, for high explosives with no comparative data available, TNT equivalency is often approximated by the ratio of the two heats of detonation. This ratio may be adequate at some scaled distances and invalid at others.

Computations of TNT equivalent factors were made for the six explosives tested in this project using the incident pressure data obtained on the 18 experiments. For each explosive, plots of pressure versus scaled distances were made and an approximate fit was made through the average of the pressures measured at each scaled distance. TNT equivalency ratios were computed by determining the scaled distances corresponding to pressures of 100, 320, and 1,000 psig. For TNT, these three incident pressures corresponded to scaled distances of 2.89, 1.69, and $0.9 \text{ ft/lb}^{1/3}$ as obtained from the reference TNT curve [28]. The pressure equivalency E_p for an explosive is then

$$E_p = \frac{W_{TNT}}{W} = \left(\frac{Z}{Z_{TNT}} \right)^3 \quad P_s = \text{constant} \quad (1)$$

where:

- E_p = TNT equivalency of an explosive based on side-on overpressure
- P_s = peak side-on overpressure
- R = distance from the center of the charge
- W = explosive mass
- W_{TNT} = TNT mass
- Z = scaled distance = $R/W^{1/3}$
- Z_{TNT} = scaled distance = $R/W_{TNT}^{1/3}$

The average equivalency for each explosive was obtained by calculating E_p at each of the three pressures and then averaging the three values. The equivalency ratio for each explosive varied slightly over the pressure range of 100 to 1000 psig and the average value and corresponding standard deviation are tabulated in Table 2.

The values listed in Table 2 are based on a limited number of experiments. However, the peak pressures measured were self-consistent for each explosive and the range of the data at each measurement location was for the most part within $\pm 10\%$ of the average. In addition, the TNT experiments generated peak pressures which agreed very closely with values from the TNT

Table 2. Average Pressure TNT Equivalency

<u>Explosive Type</u>	<u>Pressure TNT Equivalency *</u>	<u>Standard Deviation</u>
Composition B	1.2	11%
PBX-9404	1.7	18%
Pentolite	1.5	5%
TNT	1.0	7%
PBX-9501	1.6	5%
PBX-9502	0.9	2%

*For incident pressure range of 100-1000 psig

curve from Reference 28. This reference curve is the result of a polynomial curve fit to large amounts of data from tests and some from computer calculations compiled from 10 different references.

Comparisons of the TNT equivalency ratios based on the pressure data obtained on this project and those based on heats of detonations and other references are presented in Table 3. It is interesting that for some explosives the equivalency ratio based on the pressure data at small scaled distances agrees quite well with that based on the heats of detonation. For other explosives significant differences are apparent. Also, the ratios from Reference 18 are based on a much lower pressure range except for Pentolite whose equivalency ratio agrees well with the new value. The pressure range for the ratios from Reference 22 is given as being applicable from 2 to 50 psi. Note that, since TNT equivalency is the ratio of the weights of TNT to that of a test explosive, the effect on the scaled distance is the cube root of the ratio. In other words, for a particular explosive that is supposed to be 50% more energetic than TNT (TNT equivalency of 1.5) the effect on the scaled distance ($R/W^{1/3}$) becomes only 14.5%. The expected average peak pressure for this more energetic explosive would be about 28% higher than for a comparable weight of TNT at a scaled distance of 1.0 ft/lb^{1/3}. At other small

Table 3. Comparisons of TNT Equivalency Ratios

Explosive Type	Pressure TNT Equivalency	Based on Calculated Heat of Detonation*	From Ref. 18	From Ref. 22
Composition B	1.2 (100-1000 psi)	1.09	1.11 (5-50 psi)	1.10 (2-50 psi)
PBX-9404	1.7 (100-1000 psi)	1.11	1.13 (5-30 psi)	---
Pentolite	1.5 (100-1000 psi)	1.09	1.40 (5-600 psi)	1.17 (2-50 psi)
TNT	1.0 (100-1000 psi)	1.00	1.00 (Standard)	1.00 (2-50 psi)
PBX-9501	1.6 (100-1000 psi)	1.13	---	---
PBX-9502	0.9 (100-1000 psi)	0.82	---	---

* From References 21, 32, and 33

scaled distances the effect on the average peak pressure would be different, but generally the effect is less on the pressure than on explosive weight.

Conversely, note that in determining TNT equivalency ratios a small variation in determining the scaled distances for a particular average peak pressure is amplified because the ratio of scaled distances is cubed as indicated in Equation 1. Thus, it would be difficult to compute a TNT equivalency ratio at a given scaled distance more accurate than about $\pm 10\%$. To obtain an accuracy of $\pm 10\%$ requires that the scaled distance for a particular average peak pressure generated by an explosive be determined more accurately than $\pm 3\%$.

Impulse TNT Equivalency

The second parameter that is sometimes used to compute TNT equivalency is the side-on impulse. Computations were made of TNT equivalent ratios based on the impulse data obtained for the six explosives tested at small scaled distances. A similar procedure was used as for the pressure data. The impulse equivalency E_i for an explosive is simply

$$E_i = \frac{W_{TNT}}{W} = \left(\frac{Z}{Z_{TNT}} \right)^3 i_s = \text{constant} \quad (2)$$

where:

- E_i = TNT equivalency of an explosive based on side-on impulse
- i_s = side-on impulse

However, on a plot of scaled impulse ($i_s/W^{1/3}$) versus scaled distance ($R/W^{1/3}$), constant values for i_s are found at lines oriented 45° to the scaled axes. Thus, the graphical or computational procedure is somewhat more involved than for pressure. Since the test data were measured at small scaled distances over which the TNT reference curve has two different inflection points, computations were made at scaled distances of 0.9 and 2.9 ft/lb^{1/3} and averaged to obtain equivalency ratios based on impulse. The results are presented in Table 4.

Table 4. Average Impulse TNT Equivalency Base on Impulse

<u>Explosive Type</u>	<u>Impulse TNT Equivalency Using TNT Ref. Curve [28]</u>	<u>Impulse TNT Equivalency Normalized to TNT Data</u>
Composition B	0.8 (11%)	1.3
PBX-9404	1.2 (47%)	2.0
Pentolite	0.6 (8%)	1.0
TNT	0.6 (14%)	1.0
PBX-9501	1.0 (6%)	1.7
PBX-9502	0.7 (6%)	1.1

Unlike the excellent agreement between the pressure data from the TNT tests and the TNT reference curve, the TNT impulse data indicated an equivalency significantly less than unity when compared to the TNT impulse curve from Reference 28. This difference is probably due to "the very few and sometimes suspect quality" [28] of the measured incident impulses at scaled distances less than $1 \text{ ft/lb}^{1/3}$, and the wide scatter of the data used to generate the reference curve between a scaled distance of 1 and $3 \text{ ft/lb}^{1/3}$ [28], the range over which most of the measurements reported here were made. In fact, as shown in Figure 9 the reference curve appears to be an upper bound of the scaled impulse over this range of scaled distances. It is not surprising, then, that the test data from the present TNT tests yielded an equivalency ratio less than 1 when compared to the curve from Reference 28. Consequently, the TNT equivalency ratios obtained using the reference curve and the data from the six high explosive tests were normalized to the values of the new TNT data. These results are also tabulated in Table 4 and show a more realistic relationship among the impulse equivalencies, as well as a reasonable comparison with the corresponding pressure equivalences presented in Table 2. However, as has been shown by others [18,29], the ratios for pressure and impulse are not necessarily the same.

SUMMARY

An experimental program was conducted to obtain direct measurement of side-on overpressure at small scaled distances from spherical charges of six different high explosives. The pressure-time recordings made on the 18

experiments were processed to obtain peak overpressures, shock wave arrival times, side-on impulses, and positive durations of the incident or side-on pressure pulse. In addition to comparisons of the data with TNT reference curves for these four parameters, TNT equivalency for each explosive was obtained based on the measurements of side-on peak overpressures and impulses. More than 200 pressure measurements were made on tests with six different high explosives: TNT, Composition B, PBX-9404, Pentolite, PBX-9501, and PBX-9502. The number of tests conducted was limited by the number of spherical charges left over from previous projects.

The observations and conclusions based on the peak overpressure data were:

- o data were self-consistent for each explosive
- o in most cases variations from the average pressure at each scaled distance were less than $\pm 10\%$
- o compared to a TNT reference curve [28], the TNT data showed excellent agreement
- o only PBX-9502 was less energetic than TNT based on the overpressure data.

From the arrival times measured the following can be stated about these data:

- o arrival time data exhibited less scatter than the pressure data
- o TNT test data agreed quite closely with a TNT reference curve [28]
- o comparisons for all six explosives with a TNT reference curve [28] showed consistency with similar comparisons based on pressure.

Comparisons of the impulse data to the TNT reference curve [28] showed that

- o in general, the test data were of lower amplitude for four of the explosives, and of the same or higher amplitude for the other two explosives
- o by using the TNT test data as the basis for comparison, more realistic impulse-based equivalencies were obtained.

Comparisons were also made for the positive duration data from each explosive and the reference TNT curve [28]. This showed that:

- o the scaled durations measured for all six explosives were shorter than those indicated by the reference TNT curve

- o over the range of scaled distances used to make the measurements, the reference curve appears to be more of an upper bound for the new data as it is for the data from other sources [28].

Even though only a limited number of spherical charges were available, the experimental data obtained on this project [23] for the six different high explosives are an important addition to the very limited air burst data (and are in some cases the only known data) available from direct pressure measurements for characterizing their blast parameters at small scaled distances. The side-on pressure and arrival time data from the TNT tests are in excellent agreement with the revised curves in Reference 28. Similar data for the other five explosives show differences that indicate TNT equivalency for some of them can be significantly different than that based on their heat of detonation. The impulse and duration data showed that at scaled distances less than $3 \text{ ft/lb}^{1/3}$, the revised standard TNT curves [28] are definitely not as well defined as those for pressure and arrival time. More experimental air burst data are needed from TNT tests, as well as from other commonly used high explosives to better define TNT equivalency at small scaled distances based on impulse.

Additional experiments similar to those described in this report are recommended to measure pressure-time histories at small scaled distances from spherical charges. These additional data would better characterize the blast waves near different high explosives and increase the confidence of the new data presented. The experimental techniques used on this project to make the pressure measurements are suitable to obtain data at scaled distances as small as $0.75 \text{ ft/lb}^{1/3}$. However, even closer direct measurements of pressure may be possible using small, scaled hemispherical charges detonated on a replaceable hardened steel surface with side-on transducers mounted flush with the steel surface.

ACKNOWLEDGEMENTS

This paper is based on a research project funded by Southwest Research Institute (SWRI) through its Advisory Committee for Research. Special thanks are extended to Dr. W. E. Baker for his invaluable advice and technical consultation in the proposing and performance of the project this paper is

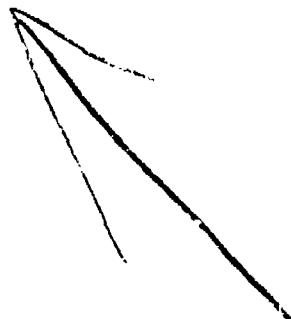
based on. The author appreciates the important contributions made by the SwRI project team to the successful conduct of that project and the resources provided by SwRI for the preparation of this paper.

REFERENCES

1. Kennedy, W. D., "Explosions and Explosives in Air," in *Effects of Impact and Explosion*, M. T. White (ed.), Summary Technical Report of Div. 2, NDRC, Vol. I, Washington, DC, AD 221 586, 1946.
2. Stoner, R. A., and Bleakney, W., "The Attenuation of Spherical Shock Waves in Air," *Journal of Applied Physics*, Vol. 19, No. 7, 1948.
3. Goodman, H. J., "Compiled Free Air Blast Data on Bare Spherical Pentolite," BRL Report 1092, Aberdeen Proving Ground, MD, February 1960.
4. Baker, W. E., *Explosions in Air*, University of Texas Press, Austin, Texas, 1973.
5. Kingery, C. N., "Air Blast Parameters versus Distance for Hemispherical TNT Surface Bursts," BRL Report No. 1344, Aberdeen Proving Ground, MD, September 1966.
6. Reisler, R., Pellet, B., and Kennedy, L., "Air Blast Data from Height-of-Burst Studies in Canada, Vol. I: HOB 5.4 to 71.9 Feet," BRL Report No. 1950, Aberdeen Proving Ground, MD, December 1976.
7. Reisler, R., Pettit, B., and Kennedy, L., "Air Blast Data from Height-of-Burst Studies in Canada, Vol. II: HOB 45.4 to 144.5 Feet," BRL Report No. 1990, Aberdeen Proving Ground, MD, May 1977.
8. Jack, W. H., Jr., "Measurements of Normally Reflected Shock Waves from Explosive Charges," BRL Memorandum Report No. 1499, Aberdeen Proving Ground, MD., AD 422886, July 1963.
9. Dewey, J. M., Johnson, O. T., and Patterson, J. D., II, "Mechanical Impulse Measurements Close to Explosive Charges," BRL Report No. 1182, Aberdeen Proving Ground, MD, November 1962.
10. Wenzel, A. B., and Esparza, E. D., "Measurements of Pressures and Impulses at Close Distances from Explosive Charges Buried and in Air," Final Report on Contract No. DAAK 02-71-C-0393 with U. S. Army MERDC, Ft. Belvoir, VA, August 1972.
11. Wisotski, J. and Snyder, W. H., "Characteristics of Blast Waves Obtained from Cylindrical High Explosives Sources," DRI No. 2286, Denver, CO, 1965.
12. Reisler, R. E., Giglio-tos, L., and Teel, G. D., "Air Blast Parameters from Pentolite Cylinders Detonated on the Ground," BRL Memorandum Report No. 2471, Aberdeen Proving Ground, MD, 1975.
13. Kulesz, J. J., Esparza, E. D., and Wenzel, A. B., "Blast Measurements at Close Standoff Distances for Various Explosive Geometries," *Minutes of the 18th Explosives Safety Seminar*, Vol. I, San Antonio, TX, Department of Defense Explosives Safety Board, September 1978.

14. Guerke, G. and Scheklinski-Glueck, G., "Blast Parameters from Cylindrical Charges Detonated on the Surface of the Ground," **Minutes of the 20th Explosives Safety Seminar**, Vol. 1, Norfolk, VA, 1982; and **Proceedings I, Eighth International Symposium on Military Applications of Blast Simulation**, Spiez, Switzerland, 1983.
15. Zaker, T. A., "Blast Pressures from Sequential Explosions," IIT Research Institute, Chicago, Illinois, Phase Report II, Project J6166, March 25, 1969.
16. Hokanson, J. C., Esparza, E. D., Wenzel, A. B., and Price, P. D., "Measurements of Blast Parameters on a Barricade Due to Simultaneous Detonations of Multiple Charges," Contractor Report ARLCD-CR-78032, U. S. Army Armament Research and Development Command, Dover, NJ, 1978.
17. Jack, W. H., and Armendt, B. F. Jr., "Measurements of Normally Reflected Shock Parameters under Simulated High Altitude Conditions," BRL Report No. 1280, Aberdeen Proving Ground, MD, AD 469014, April 1965.
18. Swisdak, M. M., Jr., "Explosion Effects and Properties: Part I--Explosion Effects in Air," NSWC/WOL/TR 75-116, Naval Surface Weapons Center, White Oak, Silver Spring, MD, October 1975.
19. Glasstone, Samuel and Dolan, Philip J., "The Effects of Nuclear Weapons," United States Department of Defense and U. S. Department of Energy, 1977.
20. "Suppressive Shields Structural Design and Analysis Handbook," U. S. Army Corps of Engineers, Huntsville Division, HNDEM-1110-1-2, November 1977.
21. **A Manual for Prediction of Blast and Fragment Loadings on Structures**, U. S. Department of Energy, DOE/TIC-11268, 1980.
22. **Structures to Resist the Effects of Accidental Explosions**, Department of the Army Technical Manual TM-5-1300, Department of the Navy Publication NAVFAC P-397, Department of the Air Force Manual AFM 88-22, Department of the Army, the Navy, and the Air Force, June 1969.
23. Esparza, E. D., "Side-on Blast Measurements and Equivalency at Small Scaled Distances for Spherical Charges," Final Report 06-9386, Southwest Research Institute, San Antonio, Texas, May 1985.
24. Hopkinson, B., **British Ordnance Board Minutes** 13565, 1915.
25. Cranz, C., **Lehrbuch der Ballistic**, Springer-Verlag, Berlin, 1926.
26. Sachs, R. G., "The Dependence of Blast on Ambient Pressure and Temperature," BRL Report 466, Aberdeen Proving Ground, MD, 1944.
27. Esparza, E. D., and Baker, W. E., "Measurements of Blast Waves from Bursting Pressurized Frangible Spheres," NASA CR-2843, Washington, DC, May 1977.
28. Kingery, C. N., and Bulmash, G., "Airblast Parameters from TNT Spherical Air Burst and Hemispherical Surface Burst," Ballistic Research Laboratory Technical Report ARBRL-TR-02555, Aberdeen Proving Ground, MD, April 1984.
29. Davis, V. W., Goodale, T., Kaplan, K., Kriebel, A. R., Mason, H. B., Melichar, J. F., Morris, P. J., and Zaccor, J. N., "Nuclear Weapons Blast Phenomena, Volume IV--Simulation of Nuclear Airblast Phenomena with High Explosives (U)," DASA Report 1200-IV, Washington, DC, July 1973 (SECRET-FRD).

30. Sultanoff, M. and McVey, G., "Shock-Pressure at and Close to the Surface of Spherical Pentolite Charges Inferred from Optical Measurements," BRL Report No. 917, Aberdeen Proving Ground, MD, August 1954.
31. Dobbs, N., Cohen, E., and Weissman, W., "Blast Pressures and Impulse Loads for Use in the Design and Analysis of Explosive Storage and Manufacturing Facilities," *Annals of the New York Academy of Sciences*, Vol. 152, Art 1, October 1968.
32. Hokanson, J. C., Esparza, E. D., Baker, W. E., Sandoval, N. R., and Anderson, C. E., "Determination of Blast Loads in the DWF," Volume 1, Phase II, SwRI-6578, San Antonio, TX, July 1982.
33. Dobratz, B. M. and Crawford, P. C., "Properties of Chemical Explosives and Explosive Simulants," LLNL Explosives Handbook, Lawrence Livermore National Laboratory, January 1985.



Safety Analysis for Vented Dust Explosions

by James J. Kulesz and Wilfred E. Baker

Abstract

Below some critical particle size, magnesium powder is pyrophoric in air. Techniques for producing fine magnesium powder therefore require use of an inert atmosphere in an enclosed system. For added safety, these systems are set up in strong, vented explosion test bays, and all operations are conducted remotely from control consoles located outside the test bays. This paper describes methods for determining the pressure loads on and structural response of two vented explosion test bays subjected to hypothetical explosions involving fine magnesium powder. The analyses predicted catastrophic failure of the bays in their original configuration. By increasing the vent area in the original structures, however, the bays could survive the predicted worst case explosions. Thus, minor modifications in the existing structures ensured safe operation without a decrease in production quantities.

Acknowledgements

The authors wish to express our gratitude to Mr. Jim Herrington and Tracor, MBA for supporting the analyses described in this paper.

I. Introduction

Tracor MBA is developing new techniques for producing fine magnesium powder. Because magnesium powder below some critical particle size is pyrophoric in air, these techniques require that the fine powder be produced in an inert atmosphere. This is done in the systems under development by totally enclosing the process in stainless steel vessels and piping, and by inerting with argon.

Although a number of safety devices are built into these developmental systems, the systems are also set up in strong, vented explosion test bays, and all operations are conducted remotely from control consoles located outside the test bays. The test bays are modified from old Navy ordnance facilities. Although the safety precautions taken in these operations make the chance for a worst case magnesium powder explosion in a test bay quite small, there is undoubtedly still some small probability of occurrence of such an accident. The authors performed a safety analysis which considered such explosions in each of two test bays, with the explosion

source assumed to be a cloud of magnesium powder rapidly released from the test vessel into the test bay. The amount of powder assumed per bay is the maximum which could be in the vessel in that bay (100 lb. in Bay 1 and 20 lb. in Bay 2), and ignition is assumed to be certain, because of the pyrophoric nature of the fine magnesium powder.

A. Test Bay Number 1

The larger test bay has internal dimensions of 32'8" x 25' x 16', and has two large vent openings, entirely uncovered, with dimensions of 9'6" x 8' and 7'6" x 7'. There is also a 5' x 5' hole cut in the ceiling for a spiral stairway access to equipment installed on the roof. There is a single, steel plate entrance door in the rear wall of the bay. This door covers a 3' x 7' opening, overlapping it by 1.5"-2" on both vertical edges and the top. The door is not supported at the bottom.

The bay structure is reinforced concrete. The front and rear walls are 12 inches thick and have reinforcing consisting of #4 rebars, 12 inches on centers, both ways, both sides. The rebar grids are displaced on opposite sides of the wall such that the center of the outermost rebars are nominally 1.5" from the wall face. Both end walls are double-wall, sand-filled structures. Each wall in the double wall has a section identical to the above, but these are formed with vertical end and central webs to make a vertical caisson with total thickness of 40 inches. The 16 inch cavity in the caisson is filled with sand.

The roof of the bay varies somewhat in thickness, being thickest along a transverse centerline and tapering uniformly to an edge which overhangs the fore and aft walls by several feet. The average thickness is about 8 inches and reinforcing consists of #3 rebars, 12 inches on centers, both ways, both sides. The rebar grids are displaced on opposite sides of the roof such that the center of the outermost rebars are nominally 1.0 inch from the wall face.

To analyze wall response, one must know (or assume) strengths for the rebar steel and for the concrete. The structure is of World War II vintage, and we therefore assume that the rebar was Grade 40, the most common grade then in use. This steel has a static yield strength (f_y) of 40,000 psi. At the time the structure was made, the concrete compressive strength was probably about 4000 psi. But, undamaged concrete continuously increases in strength with age. So, we estimated that the strength of the concrete (f'_c) was 6000 psi.

B. Test Bay Number 2

The smaller test bay has internal dimensions of 16' x 25' x 16', and has a single uncovered vent opening, 7'6" x 7'. After some planned modifications, a door would be installed which opened to the control room. We assumed a door opening of 3' x 7', and a door made of 0.5 inch thick, A36 steel plate which overlapped the door opening and opened inward.

This bay is adjacent to the large test bay, and shares one of the double, sand-filled barrier walls. The opposite cross wall is of identical construction. The cross sections of front and rear walls are identical to those for the first bay and the roof construction is also identical. Steel and concrete strengths are therefore assumed to be the same as for Test Bay Number 1.

II. Pressure Loading

To our knowledge, there is no documented case in the literature, either experimental or theoretical, which supports the possibility of a detonation involving magnesium powder and air. Instead, tests have shown (reference 1) that magnesium powder and air can produce a violent dust explosion reaction. From tests performed in a one cubic meter vessel, the results given in Table 1 (reference 1) were obtained. According to Palmer (reference 2), for particles sized below about 50 μ m, the explosion strength still increases as particle size decreases, but at a much slower rate. The rate of pressure rise is dependent on the room size and obeys Bartknecht's scaling law (reference 3):

$$\left(\frac{dP}{dt}\right)_{\max} V^{1/3} = k_{st} \quad (1)$$

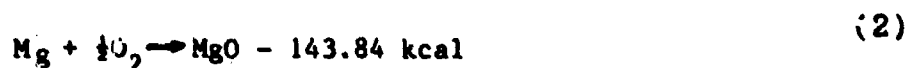
where dP/dt is the maximum rate of pressure rise
 V is room volume
 k_{st} is a constant dependent upon the dust.

From equation (1) and the test data in Table 1, the value for the constant k_{st} is 24,167 psi-ft/sec. Also, the minimum explosible concentration in English units is 1.873×10^{-3} lb/ft³. The data presented above was acquired from tests in closed vessels. However, the two bays being examined in this analysis are both vented. For reasonably well vented structures, the maximum pressures are lower and the maximum pressure rise rate may or may not have been reached before the pressure decreases. Even if the bays were closed, the maximum pressure would not be attained since the mixtures in either bay are below stoichiometric.

Table 1. Cubic Meter Explosion Chamber Test Results for Magnesium Powder (reference 1).

Mean Particle Size - 28 μ m
 Minimum Explosive Concentration - 30 g/m³
 Maximum Explosion Pressure - 17.5 bar (254 psi)
 Maximum Rate of Pressure Rise - 508 bar/s (7366 psi/sec)

When magnesium reacts with oxygen in the air, the following exothermic reaction occurs:



(Note: The reaction can proceed to MgO_2 with a heat of formation of 148.9 kcal.)

Heat produced during the reaction will raise the temperature of MgO , which is a powder, and the surrounding air. Since we do not know how to partition the energy between the powder and the gas during the time of the reaction, we can be conservative by assuming all of the energy is absorbed by the surrounding air and raises its temperature according to

$$\Delta T = \frac{Q}{m_{(\text{O}_2)} c_{v(\text{O}_2)} + m_{(\text{N}_2)} c_{v(\text{N}_2)}} \quad (3)$$

where Q is energy in calories
 $m_{(\text{O}_2)}$ and $m_{(\text{N}_2)}$ are mass of oxygen and nitrogen in grams, respectively
 $c_{v(\text{O}_2)}$ and $c_{v(\text{N}_2)}$ are heat capacity at constant volume for oxygen and nitrogen in cal/g °C, respectively

One can then use the ideal gas law to calculate peak absolute pressure in a closed chamber from:

$$P = \frac{\mu RT}{V} \quad (4)$$

where P is absolute pressure
 μ is number of moles of gas
 R is ideal gas constant
 V is room volume

(Note: P_{max} is lesser of $(P-p_0)$ or 254 psi where p_0 is 1 atm.)

Sapko et al. (reference 4) gives the relationship between burning velocity and pressure rise for gas explosions in a closed vessel as

$$\Delta P = p_o E^2 (E-1) \gamma_u \left(\frac{S_u t}{a} \right)^3 \leq P_m \quad (5)$$

where ΔP is pressure rise
 p_o is initial pressure (1 atm)
 γ_u is ratio of specific heats for unburned gas (1.4)
 S_u is burning velocity
 t is time
 a is vessel radius (for a spherical vessel)
 E is expansion ratio
 P_m is maximum gage pressure in a closed vessel

Since equation 5 was developed for a spherical vessel, we used an equivalent radius a described by

$$a = \left(\frac{3V}{4\pi} \right)^{1/3} \quad (6)$$

where a is radius of equivalent sphere
 V is room volume

The expansion ratio E is given by

$$E = \frac{\rho_u}{\rho_b} = \frac{M_u T_b P_u}{M_b T_u P_b} \quad (7)$$

where ρ is density
 M is molecular weight
 T is temperature
 P is pressure
 $"b"$ denotes burned gas
 $"u"$ denoted unburned gas

For our case, P_u equals P_b since there are no shock waves anticipated. Differentiating equation 5 with respect to time, assuming a constant burning rate, one has

$$\frac{dp}{dt} = 3 p_o E^2 (E-1) \gamma_u \frac{S_u^3}{a^3} t^2 \quad (8)$$

Simultaneously solving equations 5 and 8, one has

$$t = \frac{3P}{(dp/dt)} \quad (9)$$

Substituting P and $(dp/dt)_{\max}$ in equation 3, one can determine the time t_m to peak pressure in a closed chamber:

$$t_m = \frac{3P}{(dp/dt)_{\max}} \quad (10)$$

Rearranging equation 5 and substituting P_{\max} and t_m for P and t , one has

$$S_o = \left[\frac{P_{\max}^3}{P_o E^2 (E-1) \gamma_u t_m^3} \right]^{1/3} \quad (11)$$

where P_{\max} is lesser of $(P-p_o)$ from eq. 4 or 254 psi

Since the rooms at the Tracor facility are vented, the peak pressure P_{\max} will not be reached due to substantial gas venting. From Bradley and Mitcheson (references 5 and 6), the scaled vent area \bar{A} is defined as

$$\bar{A} = \frac{c_d A_v}{A_s} \quad (12)$$

where c_d is discharge coefficient (0.6)
 A_v is vent cross section area
 A_s is total area

The scaled burning velocity \bar{S}_o is defined as

$$\bar{S}_o = \frac{S_o}{a_{uo}} \left(\frac{\rho_{uo}}{\rho_{bo}} - 1 \right) \quad (13)$$

where S is burning velocity
 a is acoustic velocity
 ρ is density
 $"c"$ denotes initial conditions
 $"u"$ and $"b"$ denote unburned and burned, respectively

Note that (p_{uo}/p_{bo}) is the expansion coefficient E given in equation 7. From Bradley and Mitcheson, one then has

$$\Delta P_m = \frac{(0.7)}{(\bar{A}/\bar{S}_o)^2} \text{ for } \Delta P_m < 1 \text{ atm} \quad (14)$$

$$\Delta P_m = 0.64 - 4.6 \log_{10} (\bar{A}/\bar{S}_o) \text{ for } \Delta P_m > 1 \text{ atm} \quad (15)$$

Thus far we have described the increasing phase of the pressure-time curve where ΔP_m is the maximum gage pressure and the time history to the peak pressure is given in equation 5.

For the decreasing phase of the pressure-time curve, we use the method described by Anderson, Baker et al. (reference 7) to determine the time t_{max} to return to atmospheric pressure given by

$$t_{max} = \frac{V}{a_o A_v} (0.4284) \left[\frac{P_{Qs} + P_o}{P_o} \right]^{0.3638} \quad (16)$$

where V is volume
 a_o is acoustic velocity
 P_{Qs} is peak quasistatic pressure
 (same as P_m above)
 P_o is atmospheric pressure

The pressure-time history from peak pressure to atmospheric pressure P_o was calculated from

$$p(t) = (P_{Qs} + P_o) e^{-ct} \quad (17)$$

where

$$c = \frac{1}{t_{max}} \ln \left(\frac{P_{Qs} + P_o}{P_o} \right) \quad (18)$$

and t is in seconds and $p(t)$ is in psig

Thus, the pressure-time history for the loading is completely described.

A summary of the approximate method we used to determine the pressure loading over time for rapid burning of magnesium powder in a vented chamber is as follows:

1. Calculate the room volume and vent area.
2. Calculate $(JP/dt)_{max}$ from equation 1.
3. Calculate the moles of fuel and air, balance the reaction equation, and calculate energy Q from the reaction using equation 2.
4. Calculate temperature rise using equation 3.
Convert temperature rise to absolute temperature.
5. Calculate absolute pressure using equation 4.
6. Calculate gage pressure and compare to see if below maximum explosion pressure P_m (254 psi). Choose the lower pressure for P_{max} .
7. Calculate t_m from equation 10. This is the time to

- peak pressure in a closed vessel for optimum conditions and dust concentration.
8. Calculate adjusted burning velocity S_u using equation 11.
 9. Calculate scaled vent area \bar{A} using equation 12.
 10. Calculate scaled burning velocity S_0 using equations 13 and 7.
 11. Calculate peak pressure ΔP_m in vented chamber using equations 14 or 15.
 12. Calculate pressure versus time during increasing phase of pressure-time curve using equation 5
 13. Calculate the completion time t_{max} for pressure venting using equation 16.
 14. Calculate pressure decay constant c from equation 18.
 15. Calculate pressure versus time for decreasing phase using equation 17.
 16. Plot results from steps 12 and 15. Simplify load by drawing straight-line segments. Translate time axis if needed so that $t=0$ when $P=0$. Make a table to record time, pressure, and pressure times loading area. Values from this table are used to describe loads on members of structure during structural analysis.

III. Structural Response

The dynamic analysis methods we used are described in references 8-10. In these methods, the real structural elements are first converted to equivalent single-degree-of-freedom (sdof) dynamic systems, and then their elastic-plastic responses computed for applied transient forces. The methodology is well described in Chapters 1 and 5 of reference 8, and in Chapter 5 of reference 10. To aid in the computations, we ran a computer program written in BASICA for the IBM PC computer. The program gives numerical solutions for the sdof, elastic-plastic structural elements, and both prints out and graphs the displacement-time histories of the responses.

To use Biggs' sdof response calculation methods, we make a number of preliminary calculations to convert properties for the real elements to the equivalent, elastic-plastic sdof analog. First, we use dynamic strength properties for the concrete and steel, rather than static properties. From tables in reference 9, we see that

$$\text{Concrete: } f'_{dc} = 1.25 f'_c = 1.25 \times 6000 = 7500\text{psi} \quad (19a)$$

$$\text{Steel: } f_{dy} = 1.1 \times 40,000 = 44,000\text{psi} \quad (19b)$$

The elastic modulus for concrete is calculated from

$$E_c = 33w^{1.5} \sqrt{f'_c} \quad (20)$$

where w is specific weight in lb/ft^3
(reference 8)

If we assume that $w = 160 \text{ lb/ft}^3$, then

$$E_c = 33 \times 160^{1.5} \times \sqrt{6000} = 5.17 \times 10^6 \text{ psi} \quad (21)$$

Percent reinforcing is calculated from (references 8 and 9)

$$p = A_s / bd \quad (22)$$

where A_s is the cross-section area of reinforcing steel on one side, b is the rebar spacing, and d is the distance from the center of a rebar nearest the surface to the farthest wall surface. For reinforced concrete, plastic moment of a section b inches wide is given by (references 8 and 9):

$$M_p = pf_{dy} bd^2 (1 - 0.59 pf_{dy} / f'_{dc}) \quad (23)$$

Moment of inertia per unit width for reinforced concrete is given by (wall short dimension)

$$I_a = \frac{d^3}{2} (5.5 p + 0.083) \quad (24)$$

Biggs (reference 8) gives tables of conversion factors which allow calculation of various quantities needed to convert these section properties to equivalent sdof properties. We assume fully-clamped boundary conditions for the rear wall and the roof, and simply-supported on the long edges for the steel door.

For the steel door, plastic section modulus is

$$Z = bh^2/4 \quad (25)$$

and moment of inertia is

$$I = bh^3/12 \quad (26)$$

Modulus of elasticity is

$$E_s = 30 \times 10^6 \text{ psi} \quad (27)$$

From Table 5.5 in reference 8, we establish conversion factors for the wall and roof panels as two-way slabs, clamped on all four edges.

IV. Results

The results of the pressure loading calculations for Bays 1 and 2 are shown in Figures 1 and 2, respectively. The dashed lines in the figures show the approximation used for the structural analyses.

The dynamic response calculations show that, in all instances, the natural vibration periods of the structural elements considered in both Bays 1 and 2 are much shorter than total vented dust explosion times. Responses are therefore primarily determined by maximum vented gas pressure amplitudes (not durations), by loaded areas of elements, and by inherent strengths of elements.

The maximum response amplitudes for the transformed sdof representations of bay walls, roofs and doors are given in Table 2. Our calculations predict that, in both Bays 1 and 2, the front walls, rear walls and roof all fail catastrophically. Only the steel doors and the interbay wall withstand the explosion pressures.

The only reasonable way to alleviate this potential problem was to drastically increase the vent areas in the bay rear walls. We therefore calculated a series of new pressure-time curves for both bays, assuming enlarged vent areas, up to a maximum of removal of the entire rear wall. The load-time pairs and structural details were then input into our structural response computer program and the responses of the structural elements were calculated. Enough different vent areas were chosen to allow graphical interpolation of vent area required to achieve a specified structural response level. The results, plotted in Figure 3, show that vent areas considerably less than the full rear wall area will assure structural survival. The roof response controls, because it is weaker than the walls. Reading values from Figure 3, we can establish vent areas for each bay to just have the roof survive ($\mu = 15$), and to have it remain elastic, for each bay. Table 3 shows these values.

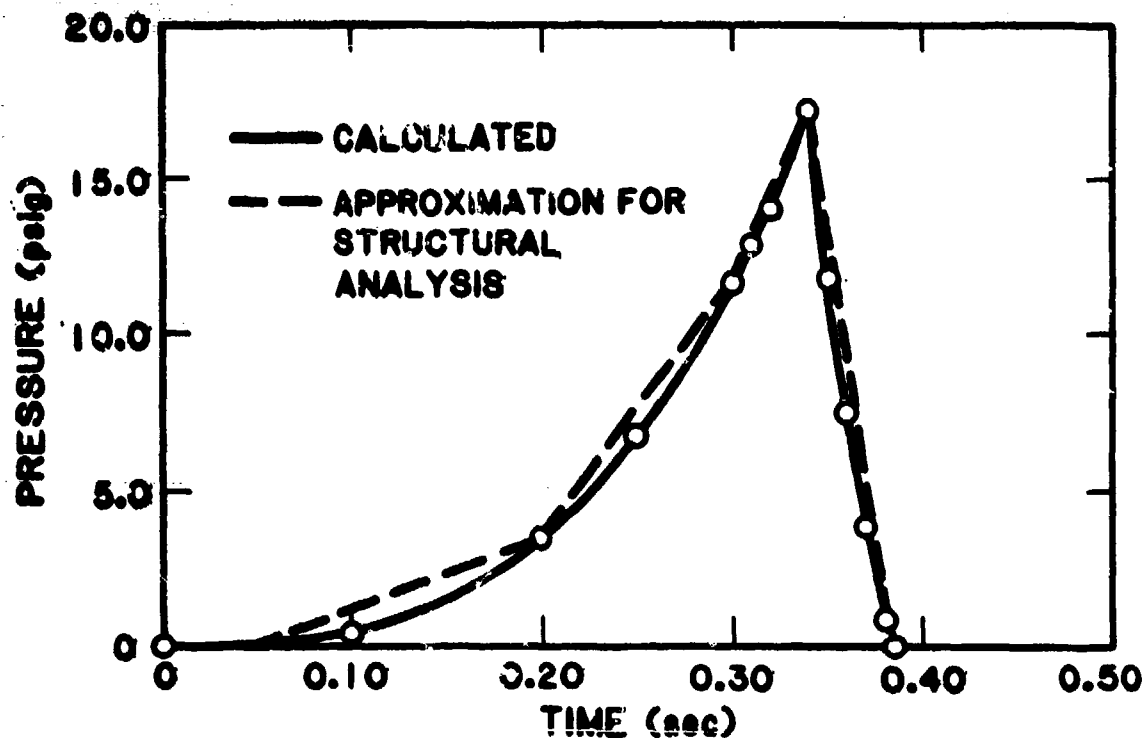


Figure 1. Pressure Loading in Bay 1 (100 lb. Mg.)

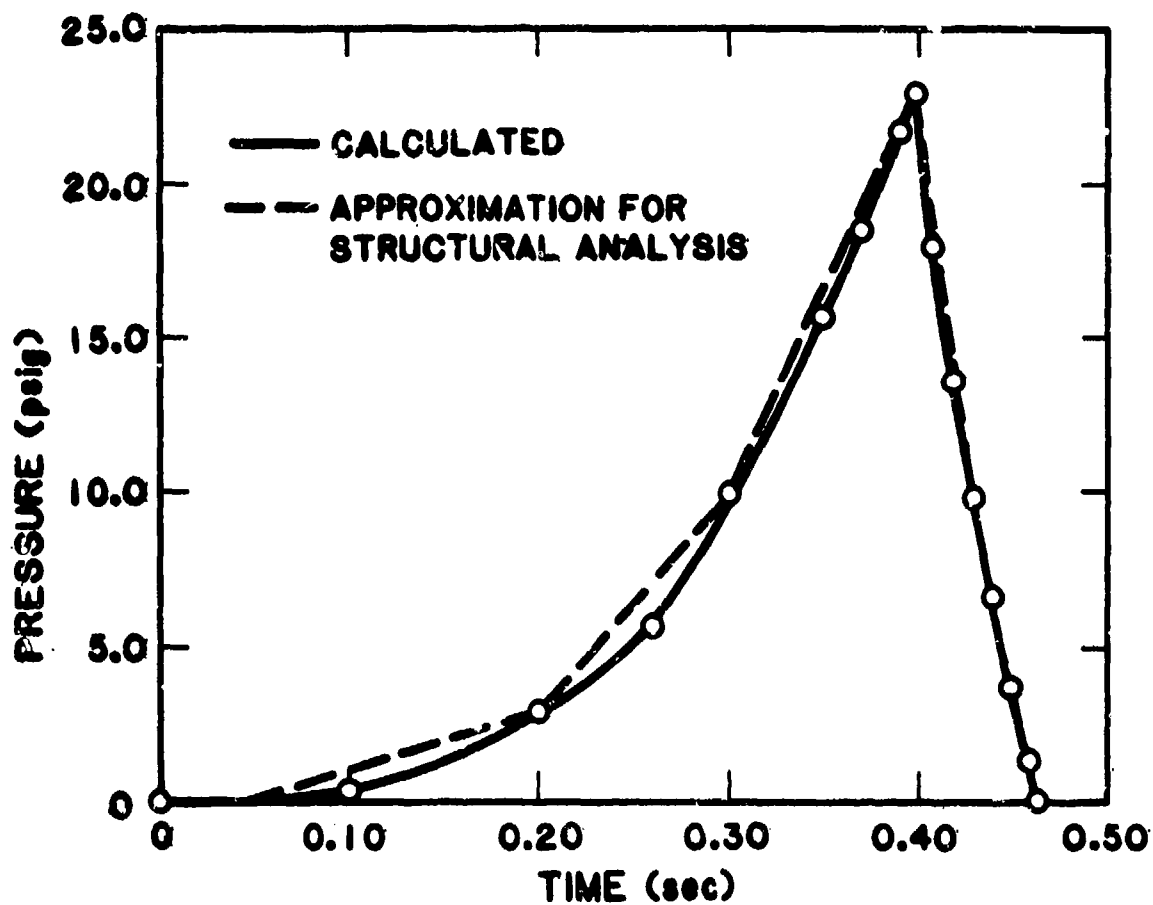


Figure 2. Pressure Loading in Bay 2 (20 lb. Mg.)

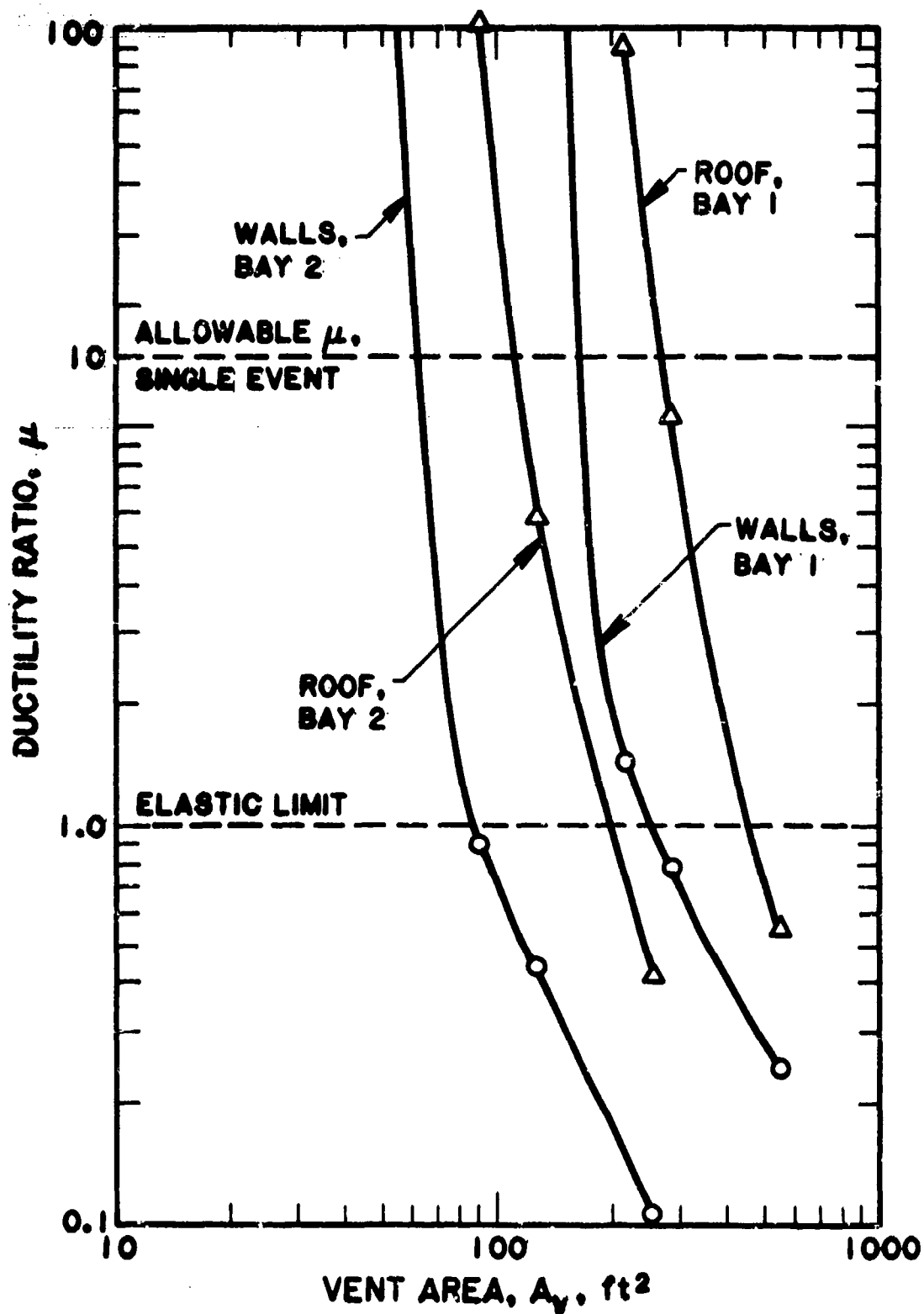


Figure 3.
Maximum Ductility Ratios for Walls and Roofs vs. Vent Areas.

Table 2. Maximum Responses of Structural Elements

Element	y_m (in.)	y_{el} (in.)	μ^*
Bay 1			
Outside Wall	45.5	0.306	149
Roof	364	0.361	1010
Door	1.19	42.8	$\ll 1$
Interbay Wall	0.0199	0.0777	0.256
Bay 2			
Outside Wall	67.5	0.193	350
Roof	1110	0.361	3070
Door	1.618	42.8	$\ll 1$
Interbay Wall	0.0272	0.0777	0.350

* $\mu \leq 15$ is acceptable.

Table 3. Vent Areas to Limit Roof Response.

Bay Number	A_v for $\mu = 15$ (sq ft)	A_v for $\mu = 1$ (sq ft)
1	270	460
2	110	200

V. Summary

In this paper, we described a procedure for estimating pressure versus time in a vented chamber containing rapidly burning magnesium powder. We also briefly described the method used for predicting structural response. The analyses predicted catastrophic failure of the original design if the postulated accident should occur. The vent area was subsequently increased in the analysis until the existing structure could safely tolerate the pressure loads.

VI. References

1. P. Field, Handbook of Powder Technology, Volume 4, Dust Explosions, Elsevier Scientific Publishing Company, Amsterdam, 1982.
2. K.N. Palmer, Dust Explosions and Fires, Chapman and Hall, Ltd., London, England, 1973.
3. W. Bartknecht, Explosionen, Ablauf und Schutzmassnahmen, Springer-Verlag, Berlin, 1978.
4. M.J. Sapko, A.L. Furno, and J.M. Kuchta, "Flame and Pressure Development of Large-Scale CH₄-Air-N₂ Explosions," U.S. Bureau of Mines, Report of Investigations 8176, 1976.
5. Derek Bradley and Alan Mitcheson, "The Venting of Gaseous Explosions in Spherical Vessels. I - Theory," Combustion and Flame 32, 221-236 (1978).
6. Derek Bradley and Alan Mitcheson, "The Venting of Gaseous Explosions in Spherical Vessels. II - Theory and Experiment," Combustion and Flame 32, 237-255 (1978).
7. Charles E. Anderson, Jr., W.E. Baker, Donna K. Wauters and Bruce L. Morris, "Quasi-static Pressure, Duration, and Impulse for Explosions (e.g. HE) in Structures," International Journal of Mechanical Science, Vol. 25, No. 6, 455-464, 1983.
8. J.M. Biggs, Introduction to Structural Dynamics, McGraw-Hill Book Co., New York, 1964.
9. "Suppressive Shields. Structural Design and Analysis Handbook," HNDEM-1110-1-2, U.S. Army Corps of Engineers, Huntsville Division, 18 November 1977.
10. W.E. Baker, P.A. Cox, P.S. Westine, J.J. Kulesz and R.A. Strehlow, Explosion Hazards and Evaluation, Elsevier Scientific Publishing Company, Amsterdam, 1983.

TNT EQUIVALENCE OF TWO PLASTIC-BONDED
EXPLOSIVES FOR INTERNAL BLAST AND GAS PRESSURES

Wilfred E. Baker
Wilfred Baker Engineering
Donna W. O'Kelley
Southwest Research Institute

ABSTRACT

Past internal blast testing within an eight-scale loads model of a multi-bay containment structure has provided a data base for both reflected internal blast loads and long-term gas phase pressures within a strong containment structure. These data are analyzed to determine TNT equivalence for internal blast loading, and separate values for TNT equivalence for gas phase pressures, for two plastic-bonded explosives, PBX-9404 and PBX-9502. Different values are obtained for the two phases of the internal blast loading, and both differ from values which would be estimated on the basis of heats of explosion relative to TNT.

1. INTRODUCTION

It is common practice in estimating hazards or blast loads from detonating high explosives to express the masses or energies of the explosives as equivalent masses or energies of TNT. One reason for this conversion is that many of the "standard" curves or equations for air blast wave properties for high explosives (Refs. 1-3) are based on data fits to tests with TNT. Another reason is that some methods for predicting transient loads on blast-resistant structures are applicable only for blast loading from TNT explosive (Ref. 3).

The two most prevalent methods for estimating TNT equivalence are comparisons based on free-field blast testing, and comparisons based on relative heats of explosion.

Generally, the comparisons based on free-field blast measurements show somewhat different equivalence values for peak overpressure as opposed to specific impulse (Ref. 4), and/or variation of equivalence with scaled distance (Ref. 5). One of the latest set of comparisons of this nature appears in Ref. 6.

The use of relative heats of explosion has the virtue of ease of measurement (via bomb calorimetry), and simplicity. A single conversion number results, rather than one which differs for different blast parameters or varies with distance.

In internal blast loading of structures from high explosive detonations, the loading on various interior surfaces consists of an initial reflected

shock wave, followed by several later waves arriving after reflection from other surfaces, superimposed on a much longer duration gas pressure which has a relatively slow rise time. Fig. 1. shows a record of this loading in a model containment structure with no venting. Usually, the shock loading and gas pressure phases are considered separately in estimating their properties (see Ref. 7), and then recombined in some simplified form to estimate combined internal blast loading for structural response calculations (again, see Ref. 7).

One phase of an extensive internal blast test program conducted by SwRI for Pantex Plant was directed toward establishing internal explosion TNT equivalence values for several explosives. All tests were run in an eighth-scale loads model of the Damaged Weapons Facility, which was repeatedly subjected to a number of internal detonations with no damage to the model. Ref. 8 contains a description of the tests in this phase, as well as tables of all reduced data from the many transducers flush-mounted in the model. Figs. 2 and 3 are sections through the model, showing some of the transducer locations.

In tests within this unvented model, the internal configuration was varied in two ways. The equipment and personnel locks were left open for some tests, or closed for some tests by bolted and sealed covers shown in Fig. 3. For this phase, we also installed a cover inside the entrance to the high bay for some tests. By varying the type of explosive, charge weight and effective internal volume, we could obtain extensive internal blast and gas pressure data over a range of "loading densities" W/V. A series of TNT charges of a single weight were detonated for comparison.

This paper presents TNT equivalents for the plastic-bonded explosives PBX-9404 and PBX-9502 for internal explosions, based on the test data from Ref. 8.

II. DESCRIPTION OF TESTS

A total of 37 tests were conducted during the Phase II series. All explosive charges were detonated within the high bay section of the model, and all but a few were in the same location (location A in Ref. 8). Most of the charges were bare explosive spheres, centrally initiated.

Three 1.280 lb TNT spheres were detonated to give base data for comparing internal blast loads from other explosives. The most extensive data obtained for other explosives were for PBX-9404 and PBX-9502 plastic-bonded explosives. Charge shapes for these explosives were also spherical, and weights ranged from 0.495lb to 0.993lb for PBX-9404, and 0.639lb to 1.285lb for PBX-9502. Table 1 gives the composition by weight of these two explosive mixtures. For complete test details, see Ref. 8.

The primary test data were the pressure-time traces recorded at various locations on the interior surfaces of the model. Data were reduced to separate shock loads (initial and later reflected) from quasi-static or gas pressure loads. Following sections cover methods for estimating TNT

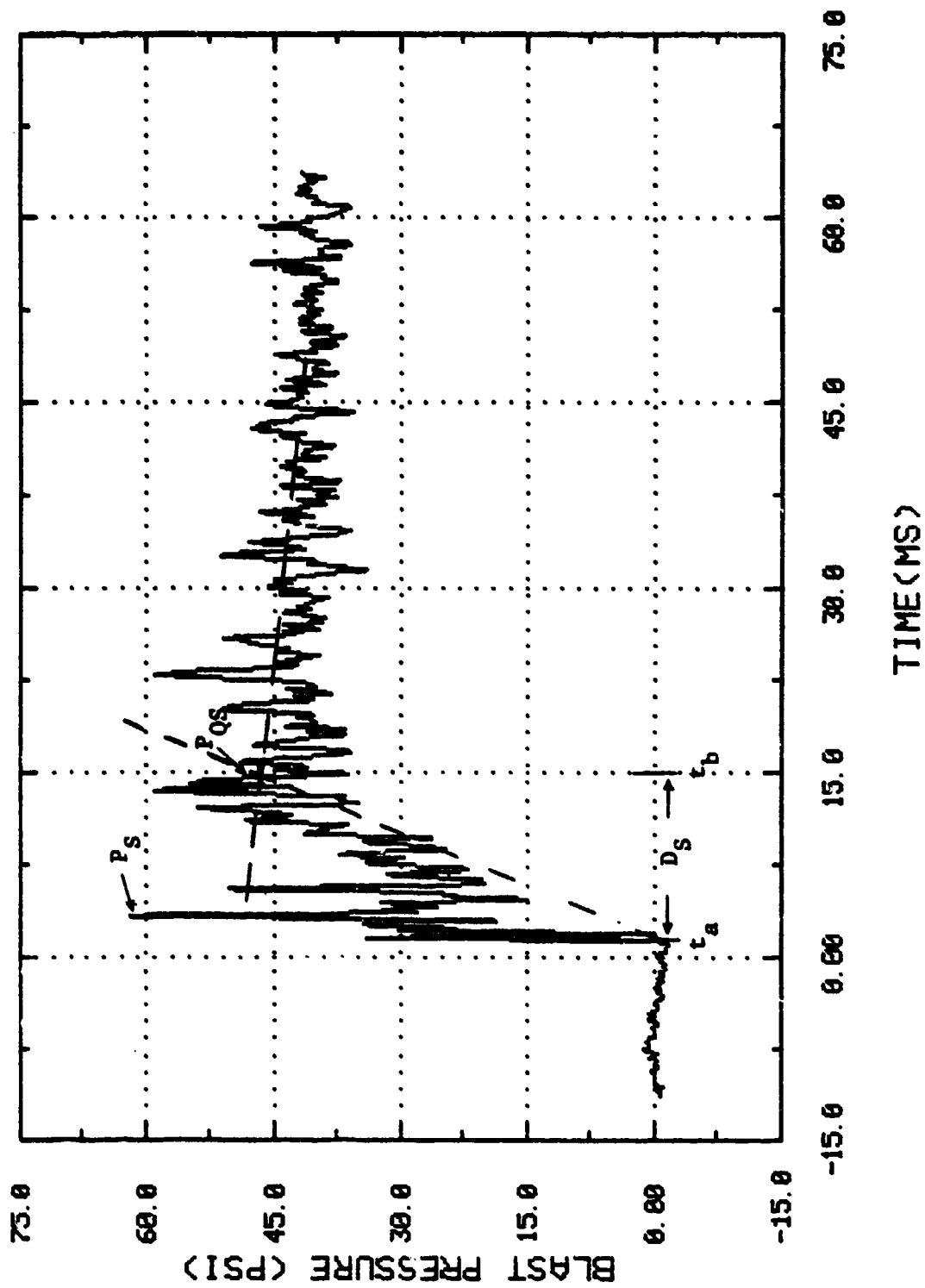


Figure 1

Typical Internal Blast and Gas Pressure Trace
for a Blast Containment Structure

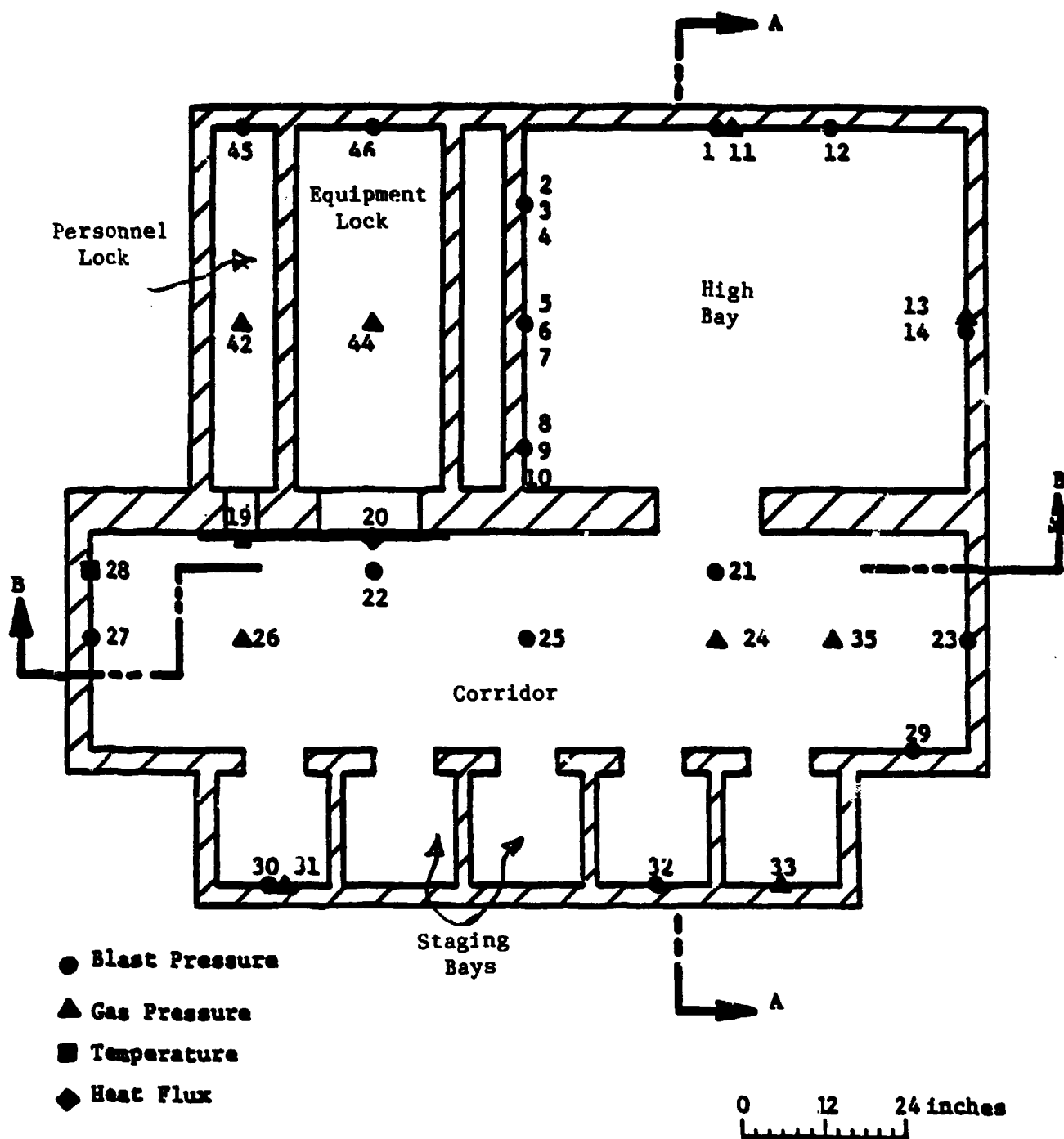
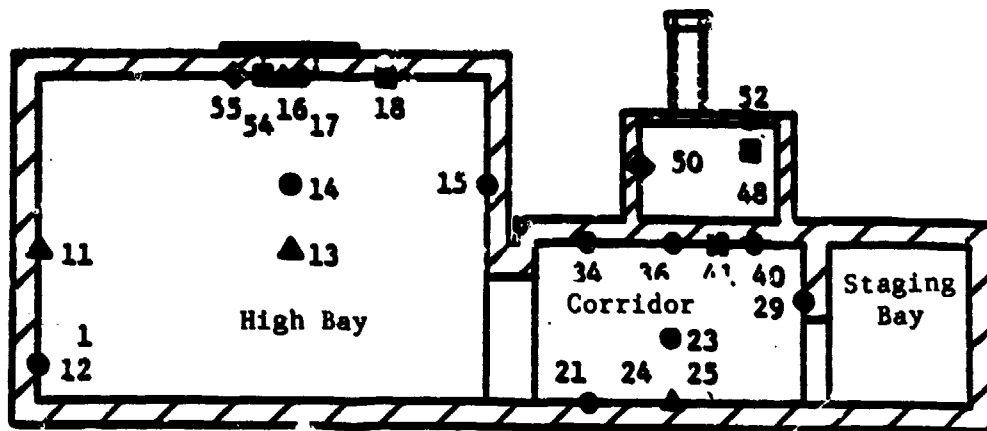
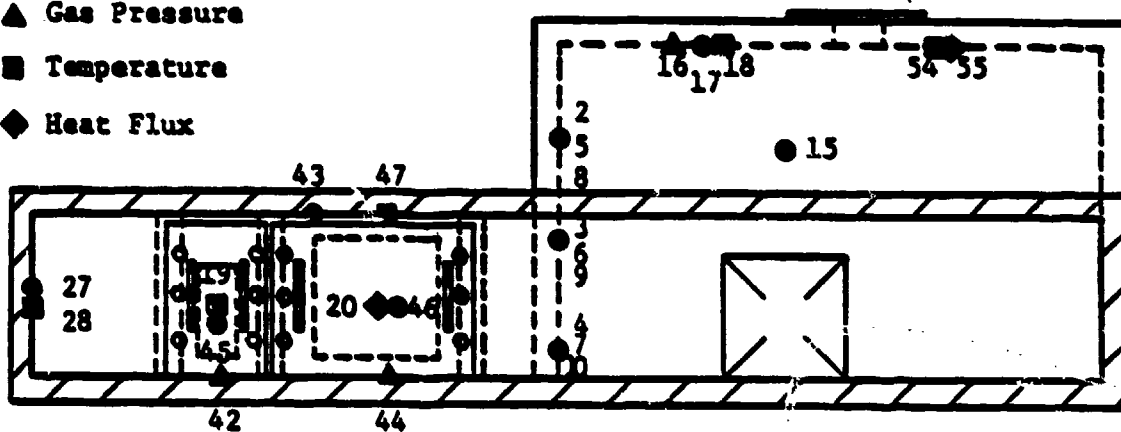


Figure 2
Horizontal Section through DWF Model



SECTION A-A

- Blast Pressure
- ▲ Gas Pressure
- Temperature
- ◆ Heat Flux



SECTION B-B

0 12 24 inches

Figure 3

Vertical Sections through DWF Model

equivalence from the pressure records, for the two phases of internal blast loading.

TABLE 1

Composition of Two Plastic-Bonded Explosives

<u>Explosive</u>	<u>Composition</u>	<u>% by Weight</u>
PBX-9404	HMX	94
	NC (12.0% N)	3
	CEF*	3
PBX-9502	TATB	95
	Kel-F 800**	5

* CEF is Tris-~~2~~-chloroethyl-phosphate

** Kel-F 800 is Chlorotrifluoroethylene/vinylidene fluoride copolymer, 3:1.

III. TNT EQUIVALENCE FOR INTERNAL BLAST LOADING

A. Method of Analysis

The method of analysis is based on direct, gage-by-gage comparisons of reduced internal blast data. We restrict the comparisons to those tests with the same charge locations and the same model configuration (open interior doors). In this manner, we eliminate all variations in data except charge weight and type.

There were fourteen blast gage locations in the high bay used during these tests, three TNT tests of the same weight, nine PBX-9404 tests divided among four charge weights, and eight PBX-9502 tests divided among four charge weights. These data are given in Tables 5-9 and 12-15 in Ref. 8, but are too voluminous to repeat here.

The procedure for estimating TNT equivalence for blast from these data is as follows:

- 1) For each gage location, make a least-squares fit to a linear relation between peak overpressure values and charge weight of PBX-9404 or PBX-9502.
- 2) Determine a value for PBX charge weight from the fit which gives the same overpressure as the average of the three TNT tests for the same gage location.
- 3) Divide PBX charge weight by weight of TNT charge, i.e., 1.280 lb. This value is one number for TNT equivalence, based on peak overpressure.

- 4) Repeat steps 1) through 3) for each gage location.
- 5) Average TNT equivalents to get overall TNT equivalence based on overpressures. Calculate a standard deviation, as well as the average.
- 6) Repeat steps 1) through 5) for impulse data, and obtain TNT equivalence based on impulse.

B. Results

Table 2 gives the results of this procedure, for PBX-9404 explosive, by gage location and means and standard deviations. Blanks in the table indicate no reasonable intercept of our straight-line data fit. Table 3 gives results for PBX-9502 explosive. For these data, we were always able to get intercepts for the data fit.

Table 2. Internal Blast TNT Equivalents
for PBX-9404 Explosive

<u>Gage Loc.</u>	<u>Overpressure TNT Equivalent</u>	<u>Impulse TNT Equivalent</u>
1	0.898	0.757
2	0.620	0.527
3	1.095	0.836
4	0.915	0.877
5	0.811	0.773
6	0.920	0.680
7	0.755	0.846
8	0.579	--
9	0.827	0.987
10	0.759	0.803
12	0.687	0.577
14	0.488	0.573
15	0.738	--
17	1.073	0.838
Average	0.798	0.756
Std. Dev.	± 0.175	± 0.140

**TABLE 3. Internal Blast TNT Equivalence
for PBX-9502 Explosive**

<u>Gage Loc.</u>	<u>Overpressure TNT Equivalent</u>	<u>Impulse TNT Equivalent</u>
1	1.33	0.968
2	1.196	0.869
3	1.347	1.038
4	1.196	1.034
5	0.844	1.062
6	1.786	1.057
7	1.215	1.157
8	0.928	0.848
9	0.932	1.10
10	1.152	1.165
12	1.568	0.972
14	0.717	0.756
15	1.056	1.403
17	1.1996	0.957
Average	1.176	1.028
Std. Dev.	± 0.283	0.159

IV. TNT EQUIVALENCE FOR INTERNAL GAS PRESSURES.

A. Method of Analysis

The method of analysis for TNT equivalence for peak internal gas pressure P_{Qs} is much simpler than analysis for TNT equivalence for internal blast loading, because peak gas pressures were found to be independent of gage location for any model configuration. So, it was possible to average all of these values for all gas gages for a given test, and compare to averages for the TNT series as well as past data for TNT. This was done and reported in Ref. 8.

The method is best described by referring to Fig. 4, which shows peak quasi-static pressures from these tests plotted as a function of the "loading density", W/V . Also plotted is a portion of the curve for TNT, fitted to earlier TNT data (see Ref. 7). Then, each data point was adjusted to lie on the curve by choosing the value of W/V which corresponded to the measured pressure. TNT equivalence for that point was then taken as the ratio of equivalent W/V to actual W/V . For a given explosive, the equivalence values were then averaged, and a standard deviation was calculated.

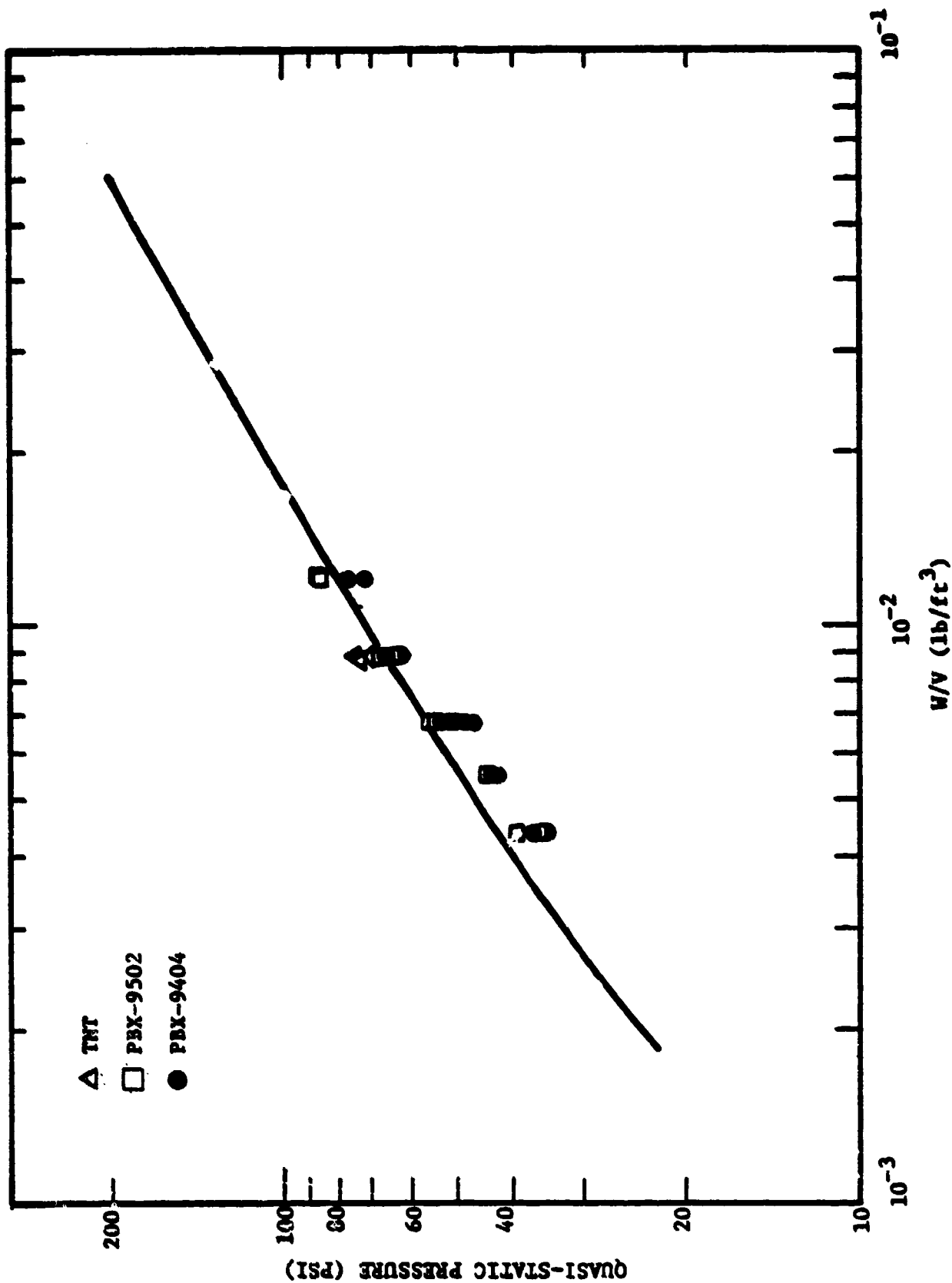


Figure 4
Summary of Quasi-Static Pressure Data

B. Results

Table 4 gives the results of estimating TNT equivalence for quasi-static pressure for PBX-9404 and PBX-9502 explosives. Note that both show values less than one, when compared to the "standard" P_{Qs} curve in Ref. 7. Also note that the average quasi-static pressure for the three TNT charges fired in this program was somewhat greater than the standard curve value. We retained the conversions to the standard curve for the other explosives, however, because it is in fairly wide use.

V. DISCUSSION

We can summarize the TNT equivalencies estimated in this paper, and those predicted relative to TNT, and have done this in Table 5. The numbers in parenthesis under equivalence based on quasi-static pressure are normalized to the measured values for TNT during these tests, rather than to a "standard" curve based on previous tests. We suspect that the earlier values are lower than the current ones because all earlier tests were conducted in vented structures, while these test were conducted in a pressure-tight, nonvented structure. The values for P_{Qs} in our test were easily read from the records because they did not decay, while values from vented tests were always estimates requiring extrapolation of the early parts of the gas pressure records.

Table 5. Comparison of TNT Equivalences
on Various Bases

<u>Explosive</u>	<u>Bases</u>	<u>TNT Equivalence</u>
PBX-9404	Internal blast overpressure	0.798
	Internal blast impulse	0.756
	Quasi-static pressure	0.813 (0.680)
	Relative heats of explosion**	1.11
	Relative heats of combustion*	0.630
PBX-9502	Internal blast overpressure	1.176
	Internal blast impulse	1.028
	Quasi-static pressure	0.920 (0.770)
	Relative heats of explosion**	0.815
	Relative heats of combustion*	0.746

* Measured in Ref. 7

** Based on calculated values.

Review of Table 5 indicates the following:

- o Values for TNT equivalence for internal blast based on overpressures and impulses are close enough for a given explosive to average these values and use a single conversion number.

Table 4. TNT Equivalence of Two Plastic-Bonded Explosives for Quasi-Static Pressure

TEST NOS.	EXPLOSIVE	F_{OS} (PSI)	(W/V) (LB/FT ³) EQUIVALENT	(W/V) (LB/FT ³) ACTUAL	TNT EQUIV., ϵ_g
42,43	PBX-9404	75.7	1.05×10^{-2}	1.23×10^{-2}	0.854
18,19	PBX-9404	62.3	7.60×10^{-3}	8.86×10^{-3}	0.857
27,28,29	PBX-9404	51.5	5.6×10^{-3}	6.82×10^{-3}	0.821
13,24,25	PBX-9404	49.5	5.4×10^{-3}	6.82×10^{-3}	0.792
14	PBX-9404	48.6	5.2×10^{-3}	6.80×10^{-3}	0.765
20,21	PBX-9404	43.1	4.4×10^{-3}	5.54×10^{-3}	0.815
22,23	PBX-9404	36.1	3.5×10^{-3}	4.43×10^{-3}	0.790
					0.813 ± 0.034
15,16,17	TNT	75.3	1.05×10^{-2}	8.79×10^{-3}	1.195
40,41	PBX-9502	87.6	1.35×10^{-2}	1.22×10^{-2}	1.107
32,33	PBX-9502	65.2	7.8×10^{-3}	8.85×10^{-3}	0.881
38,39	PBX-9502	54.3	6.4×10^{-3}	6.80×10^{-3}	0.941
34,35	PBX-9502	44.2	4.6×10^{-3}	5.56×10^{-3}	0.827
36,37	PBX-9502	37.8	3.7×10^{-3}	4.39×10^{-3}	0.843
					0.920 ± 0.113

- o The TNT equivalence values for internal blast do not correlate with either relative heats of explosion, or relative heats of combustion, for either PBX-9404 or PBX-9502 explosives.
- o TNT equivalence for quasi-static pressure correlate reasonably well, when based on these test results rather than compared to standard curves, to relative heats of combustion for both test explosives compared to TNT.

These comparisons point out again that the concept of TNT equivalence is inexact, and that simple conversions based on relative heats of explosion (as in Ref. 7) can lead to either overprediction or underprediction of blast loads. Similarly, TNT equivalencies for quasi-static pressure differ from equivalencies for internal blast loads. But, for the specific range of loading densities employed for these tests, a simple conversion based on relative heats of combustion is reasonably accurate.

VI. REFERENCES

1. W. E. Baker, Explosion in Air, Univ. of Texas Press, Austin, TX, 1973. (Second printing, Wilfred Baker Engineering, San Antonio, TX, 1983)
2. C. N. Kingery & G. Bulmash, "Airblast Parameters from TNT Spherical Air Burst and Hemispherical Surface Burst", Technical Report ARBRL-TR-02555, Ballistic Research Laboratory, Aberdeen Prov. Gr., MD, April 1984.
3. "Structures to Resist the Effects of Accidental Explosions", Dept. of the Army Technical Manual TM5-1300, Department of the Navy Publication NAVFAC P-397, Department of the Air Force Manual AFM 88-22, June 1969.
4. W. D. Kennedy, "Explosions and Explosives in Air", Chapt. 2, Vol. 1, Effects of Impact and Explosions, Summary Tech. Rep. of Div. 2, NDRC, Wash., D.C., 1946.
5. M. M. Swisdak, Jr., "Explosion Effects and Properties: Part I - Explosion Effects in Air", NSWC/WOL/TR 75-116, Naval Surface Weapons Center, White Oak, MD, Oct. 1975.
6. E. D. Esparza, "Side-On Blast Measurements and Equivalency at Small Scaled Distances for Spherical Charges", Final Report, SwRI Project No. 06-9386, Southwest Res. Inst., San Antonio, TX, May 1985.
7. W. E. Baker, P. S. Westine, J. J. Kulesz, J. S. Wilbeck and P. A. Cox, "A Manual for the Prediction of Blast and Fragment Loading on Structures", DOE/TIC-11268, U. S. Dept. of Energy, Amarillo, TX, Nov. 1980.
8. J. C. Hokanson, E. D. Esparza, W. E. Baker, N. R. Sandoval, and C. E. Anderson, "Determination of Blast Loads in the Damaged Weapons Facility. Vol. 1, Final Report for Phase II", SwRI for MHSM, Pantex Plant, Amarillo, TX, July 1982.

AD-P005 388

HAZARD ANALYSIS OF EXPLOSIVES BY ACCELERATING RATE CALORIMETRY

Jack L. Johnston and Maria P. Flores

Naval Weapons Station, Yorktown, Virginia

ABSTRACT

This work aims at one important aspect of hazard analysis: compatibility testing of explosives with other materials. We discuss preliminary testing of the Accelerating Rate Calorimeter (ARC) for use in determining compatibility of a widely used military plastic bonded explosive (PBX), PBXN-106, with a material of known incompatibility. A series of tests was done to determine: that the ARC can maintain a typical polyurethane/RDX based PBX in an adiabatic environment; precision of repeat runs; effect of sample size; effect of testing the PBX in contact with an alkaline material. Relative precision for onset of exotherm for six runs was $\pm 1.24\%$. Over the mass range tested, 100-400mg, effect of sample size was small (6% change in exotherm onset). Testing the PBX in contact with an alkaline substrate significantly reduced the onset of temperature of exotherm onset.

Safe, but energetic PBXs can become unstable when in contact with a seemingly inert material. This is important over the short term during processing, but sensitive incompatibility detection methods are needed in light of the fact that weapons systems are often expected to store safely for 20-30 years in a variety of climates. It is well known that heat accelerates deteriorative chemical reactions, some of which may already be the result of unfavorable combinations of materials. New PBXs contain many new components for which we have no long term storage data. Our work parallels efforts in the chemical industry to use adiabatic calorimetry to study thermal runaway reactions and to develop criteria for predicting instability. One primary screening method, vacuum thermal compatibility (VTC), uses gassing as a measure of reactivity caused by incompatibility, although some reactions do not produce gas. Differential scanning calorimetry (DSC) is another technique in which lowering of exotherm onset temperature and activation energy or changes in endotherm/exotherm curves suggest incompatibility. Using the ARC, we can expect greater sensitivity of several orders of magnitude and detection of exotherms at lower levels. We anticipate some materials will fit a window of incompatibility detectable on the ARC but not on VTC. As we compare data for materials routinely placed in contact with explosives, our ability to assess incompatibilities of materials on the basis of empirical results may lead to structural and compositional criteria for predicting hazards.

INTRODUCTION

The stability of high explosives is affected not only by the intrinsic stability of the energetic chemicals in use but by the materials in contact with the explosive. Table (1) gives some basic definitions that will be used throughout this paper. Rogers [1] defines thermally incompatible materials as those which, when combined with an explosive, lower the thermal stability of that explosive. A major responsibility of this organization is the development and documentation of safe loading procedures for in service Naval weapons and explosive loading of weapons and shapes for development work. We often select materials of construction, select coatings and liners, sealants, gaskets, and design loading fixtures that will touch the explosive. These materials can affect the stability of the explosives over the short mixing cycles often at elevated temperatures, during loading and special test programs and over the long term - maybe twenty to thirty years or more. Some underwater mines are over forty years old. Elevated storage temperatures, notorious for accelerating deteriorative chemical reactions, may reach over 130 degrees F. inside a weapon in the sun. As a guideline, a chemical reaction doubles in rate for each ten deg. C. rise in temperature. Reference (2) describes an amine-cured epoxy system in use with propellants for twenty years which showed signs of incompatibility depending on which test was used. Thus, we seek new, more sensitive ways to predict incompatibility of materials with explosives. The Accelerating Rate Calorimeter (ARC) is a relatively new instrument developed about 1980 and used in the chemical process industry to predict runaway chemical reactions, basically, reactions generating heat faster than either reaction vessel or storage container can draw it away. References [3], [4] and [5] describe some uses of the ARC in the chemical industry. References [6] and [7] describe recent applications in the explosives industry. Because of parallels between the need to accurately predict runaway chemical reactions in the chemical industry and to detect unsafe material combinations in weapons, particularly over the long term, we performed preliminary testing of a typical PBX to evaluate the ARC. The aim is to eventually detect latent incompatible combinations of materials and explosives, none of which by themselves are especially unstable. Since reactions of explosives are complex and don't follow consistent rate laws, we evaluated data for empirical indicators of incompatibility, not for kinetics or reaction mechanisms.

WHY EVALUATE PBXs?

PBXs are mixtures of explosives, plasticizers, energetic plasticizers, stabilizers, polymeric binders and sometimes metals. Initially PBXs satisfied requirements to load weapons of various shapes and resisted aerodynamic heating. Then, they satisfied insensitive munitions objectives. The number of formulations is

rising, and because these explosives are so new and complex, we know little about long term storage stability in contact with various materials. In the current set of experiments, PBXN-106 was chosen since it is in several weapons and it is one of the best characterized.

WHY EVALUATE THE ARC?

References [3], [4] and [8] show that the ARC typically detects onset of an exothermic reaction (used as a measure of incompatibility) at lower temperatures than the differential scanning calorimeter (DSC) and may be a more sensitive predictor of incompatibility. Figure (1) shows this graphically in a plot of log heat rate versus $1/T$. The ARC determines self heating usually 50-100 deg. C. lower than the DSC. The ARC automatically records a number of parameters including pressure as a reaction proceeds. The closed, adiabatic system approximates the internal environment of a weapon which is undergoing self heating, keeps

gasses which may catalyze the reaction in contact with the reactants and permits easy collection of gasses and solid reactants. Thus, the ARC may provide more information than other methods. Sample size is larger than that of DSC techniques giving a more representative sample. Finally the metal bomb and outer vessel are ideally suited to contain heat tests on explosives. The instrument is described in more detail below.

COMPARISON OF THE ARC TO OTHER METHODS OF DETERMINING INCOMPATIBILITY

Table (2) lists many of the stability methods now in use. These are compatibility methods if materials are put in contact with the explosives. The two most commonly used methods are the vacuum stability or vacuum thermal compatibility (VTC) test and differential scanning calorimetry (DSC). In the VTC method the sample is heated to about 100 deg. C. for 48 hours under a vacuum in a glass manometer system. The volume of evolved gas is used as a compatibility criterion after correction to standard conditions. NATO Standard Agreement 4147 and OD 44811, among others, describe variations of this test. Figure (2) shows typical apparatus. The test is inexpensive, a number of them can be run simultaneously and it is fairly reliable. However, some reactions do not produce gas, volatiles may interfere with results, toxic mercury is used in the manometer and the glass does not contain the occasional violent overgassing. Figure (3) shows the lump form of the samples with probably little actual contact area, but this problem exists with many methods. The DSC technique uses a reference and a sample, heats the two and monitors the heat needed to maintain constant temperature between the two. Figure (4) shows sample size comparison among several methods. note that the DSC sample size is very small, possibly leading to inhomogeneous samples. Unless a pressure DSC is used, reaction gasses escape. Also, increases in pressure cannot be monitored.

WHAT IS THE ARC?

References [9] and [10] Describe the ARC and its theory in detail. Columbia Scientific Industries of Austin, TX, makes the commercial instrument used in these experiments. Briefly, the ARC is an adiabatic calorimeter which heats the sample in the pattern shown in Figure (1). The sample, typically 0.1-0.5 grams, is sealed in the 0.032 inch walled Hastelloy bomb shown in Figure (5). Figures (6) and (7) show the entire assembly of bomb to instrument which is programmable for parameters such as an isothermal cycle, heating rate changes or start/stop temperatures. The ARC heats the sample in increments looking at preset intervals for onset of exotherm. When a self sustaining reaction starts generating heat at over 0.02 deg. C. per minute, the ARC adds heat to the calorimeter to match the calorimeter temperature to the bomb temperature, thus the true adiabatic nature of the test. Several parameters are monitored including heat rate, pressure increase and time to explosion. The instrument has a correction factor for the thermal mass of the bomb. Evolved gas can be routed to other instruments and the sample residue collected from the bomb and analyzed. A sample run generally takes an hour to prepare and overnight to run so the ARC is best used after a prescreening of samples. Sample bombs are expensive, about \$75 each and cannot be cleaned and reused, but they are strong and inert. Development of an inert but less costly bomb is feasible.

Experimental

Three experiments were performed using a PBXN-106 cured production lot B/P 966 dated Mar 1986:

1. Determine repeatability of runs on constant mass of a PBX. Note if the ARC can follow the exotherm generated by the explosive. Results are summarized in Table (3). TA and TB indicate start and finish of the exotherm.
 2. Change the sample mass and thus the thermal inertia of the sample bomb and note the effects. Results are summarized in Table (3).
 3. Combine the PBXN-106 with solid sodium hydroxide dispersed on reagent grade aluminum oxide (alumina) and note effects. Compare to VTC and DEC data. Table (4) compares ARC and DSC data. Figure (8) shows effect of sodium hydroxide on DSC results. Table (5) compares ARC and VTC data. The sodium hydroxide was used as a material of known incompatibility with nitro groups. The aluminum oxide was an inert diluent.
- The sodium hydroxide/aluminum oxide mixtures were prepared by coating the alumina powder with known masses of sodium hydroxide dispersed in water. Dried samples were used in the experiment. The PBX was mashed between fingers only to avoid affecting RDX size. Mixtures prepared were 0, 1, 5, 10, 25 and 50 percent sodium

hydroxide on alumina. A melting point capillary and stainless steel push rod were used to fill the bombs to the desired weights. Figure (9) shows the filling setup. Sample masses for experiments 1 and 2 were as shown. Explosive mass for experiment 3 was 0.2 grams. Total mass of alumina and sodium hydroxide was 0.2 grams to keep a constant thermal mass of 0.4 grams in the bombs.

Bombs were 0.032 inch wall Hastelloy C with 1/16 inch neck. Thermocouple was held in place at bottom by a manufacturer supplied clip. The original spring was removed.

Instrument settings were:

Start Temp 100, End Temp 350, Slope Sens, Heat Step 2.00, Data Step 0.50, Wait Time 10.00, burst Diff 100.

The DSC was a Perkin Elmer DSC 4. Sample mass was about 3mg; heating rate was 10 deg. cent per min.

Vacuum thermal compatibilities were run for 48 hours at 100 deg. C. Sample size was 0.2gram of each component.

DISCUSSION

1. Overall aim in comparing various ARC parameters is to evaluate data not dependent on kinetics, and not affected by auto catalysis or changes in reaction order. Heat rate curves (not shown) suggest auto catalysis. Data show that the exotherm onset and exotherm maximum are stable indicators of neat PBXN-106 self heating. The pressure variations indicate that the system had periodic leaks. As delivered, the ARC has no self-check for the pressure transducer plumbing.

2. Effect of sample mass over the range tested of 0.1 to 0.43 grams showed a variation onset of 6.4 percent. The PBXN-106 had a range of 0.2 to 0.3 grams which shows little variation. The main criteria for sample mass were to limit pressures to the 2500 PSI max for the transducer, to enable the calorimeter to follow the exotherm and to avoid disastrous explosions. Some explosives will not generate heat faster than the instrument can track. An inert filler may dampen the exotherm rate by acting as a heat absorber.

3. The comparison between ARC and DSC data shows that the ARC sees the onset of exotherm for neat PBXN-106 55 degrees before the DSC detects it. This difference holds for each concentration of alkaline sodium hydroxide. The DSC 'sees' the 0.5 percent sodium hydroxide shown by an exotherm drop of 2.06 degrees. However, the exotherm onset temperatures reverse with the next increase in concentration by 1.79 degrees. Vacuum thermal compatibility also detects the 0.5 percent sodium hydroxide by gassing more than the arbitrary 2.0 g per cubic centimeter cutoff. At higher concentrations, the reactions were so severe we stopped the tests after about 10-20 minutes. Other materials must be tested to show that the ARC can detect incompatibilities undetected by DSC or VTC.

CONCLUSIONS

1. Based on the preliminary study of PBXN-106 the ARC can supplement other methods in compatibility testing.

2. The ARC can follow the self heating of at least one PBX, and because of formulation similarities, will work on others. Pure explosives such as RDX have not been evaluated.

3. The ARC proved to be more sensitive than the DSC in detecting exotherm onset, but more experiments are necessary to find if there is a window of incompatibility detectable by the ARC but not by DSC or VTC.

PLANNED WORK

1. Evaluate more systems of known incompatibility. Demonstrate that improved sensitivity is significant.

2. Correlate ARC data to VTC data.

3. Improve ARC sample bomb system and pressure system.

4. Incorporate modern microcomputer hardware and software to process data.

5. Develop hazard index.

REFERENCES

1. Rogers, R., I&EC Product R&D, 3, 109 (1962).

2. Caldwell, D., R. Rogers, et al., "Use of Gasometric Time to Explosion and Isothermal Differential Scanning Calorimetry to Assess Compatibility of Double Base Propellants and Epoxy Resin Systems," American Defense Preparedness Association Joint Symposium on Compatibility and Processing of Plastics/Materials, (31Oct-2Nov 1983).

3. Fenlon, W., Plant Operations Progress, 4, 197-202 (1984).

4. Coates, C., Chemistry and Industry, 212-216 (Mar 1984).

5. Duch, M. et al., Plant Operations Progress, 1, 19-26 (1982).

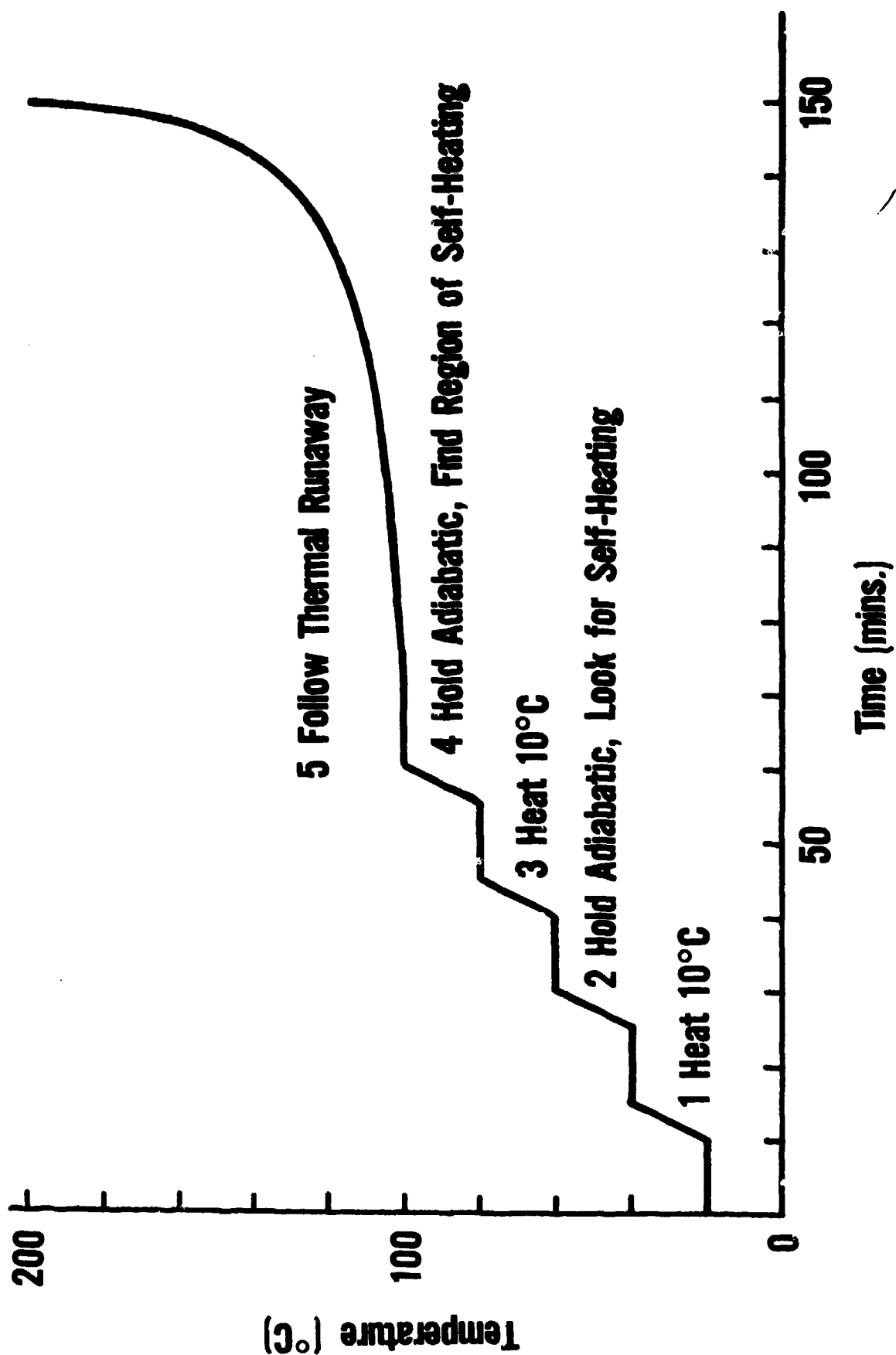
6. Lee, P., et al., "Evaluation of Thermal Runaway of High Explosives Using Accelerating Rate Calorimetry," 41st Calorimetry Conference, Somerset, NJ (17-22 Aug, 1986).

7. Harris, B. Propellants, Explosives, Pyrotechnics, 19, 7-11, (1984).

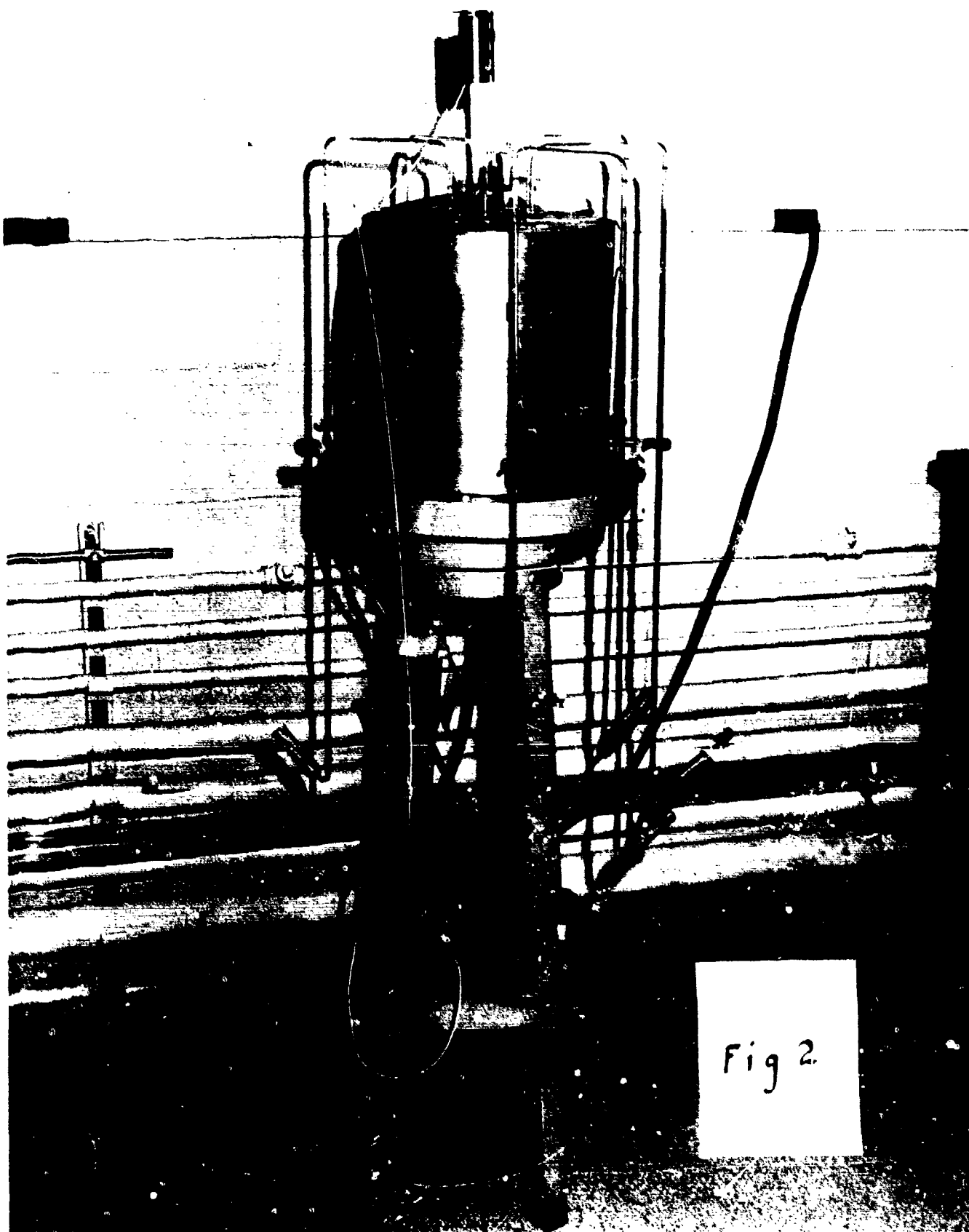
8. Columbia Scientific Industry Technical Information Bulletin No. 3.

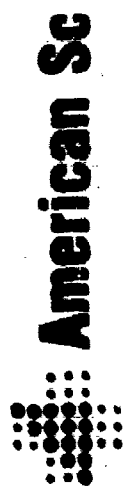
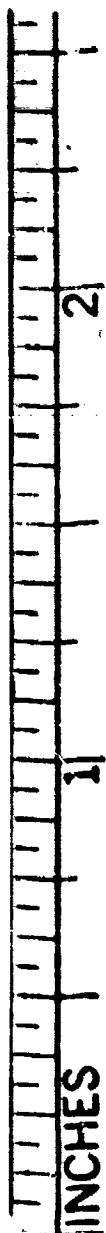
9. Townsend, D. and J. Tou, Thermochemica Acta, 37, 1-30 (1980).

10. Smith, D., et al., American Laboratory, 1-9, (Jun 1980).



Typical ARC Experiment





American Sc

A Single Source For A

Cat. M1075



Fig 3

Relative Size Of Sample Holders And Samples

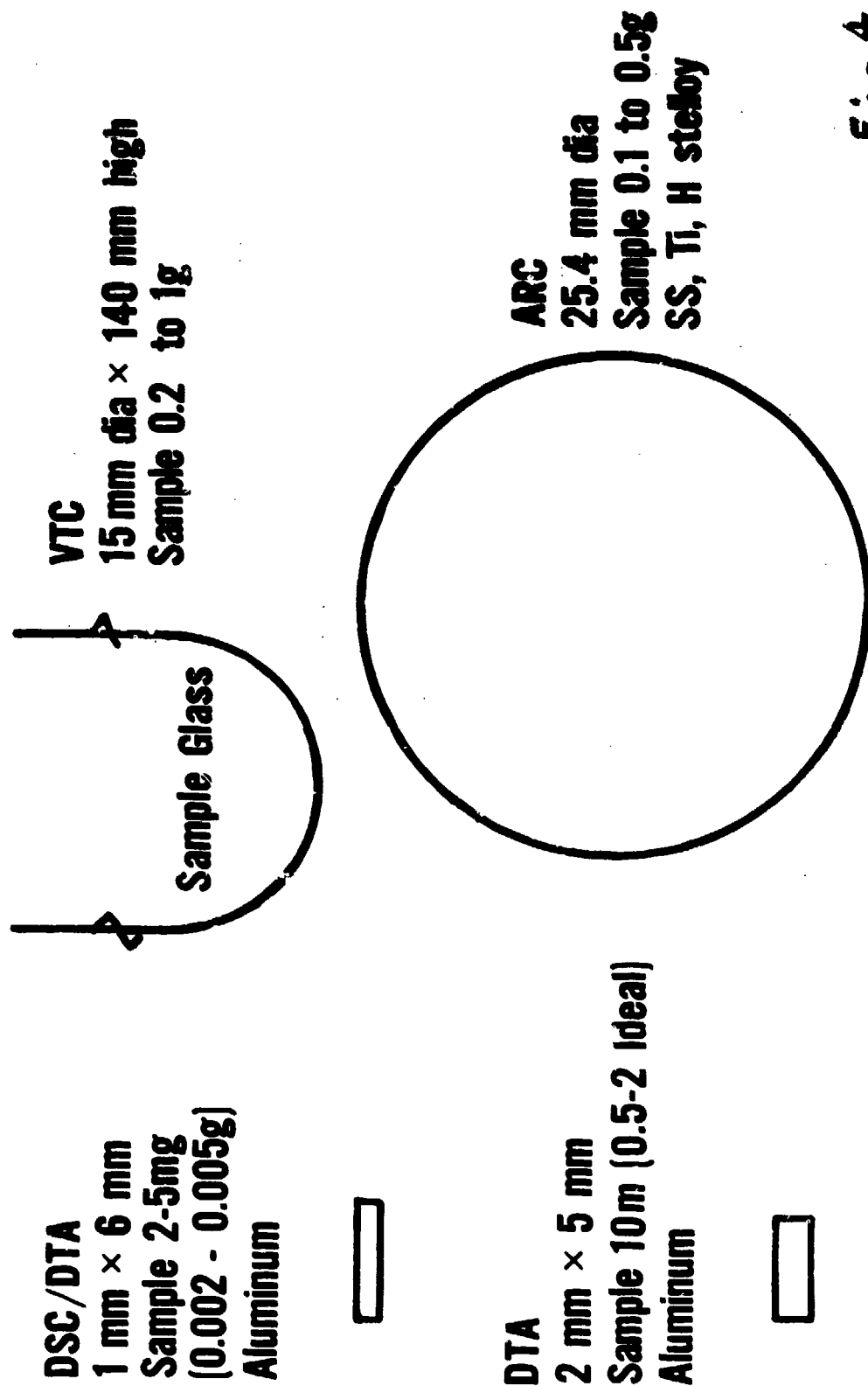


Fig 4

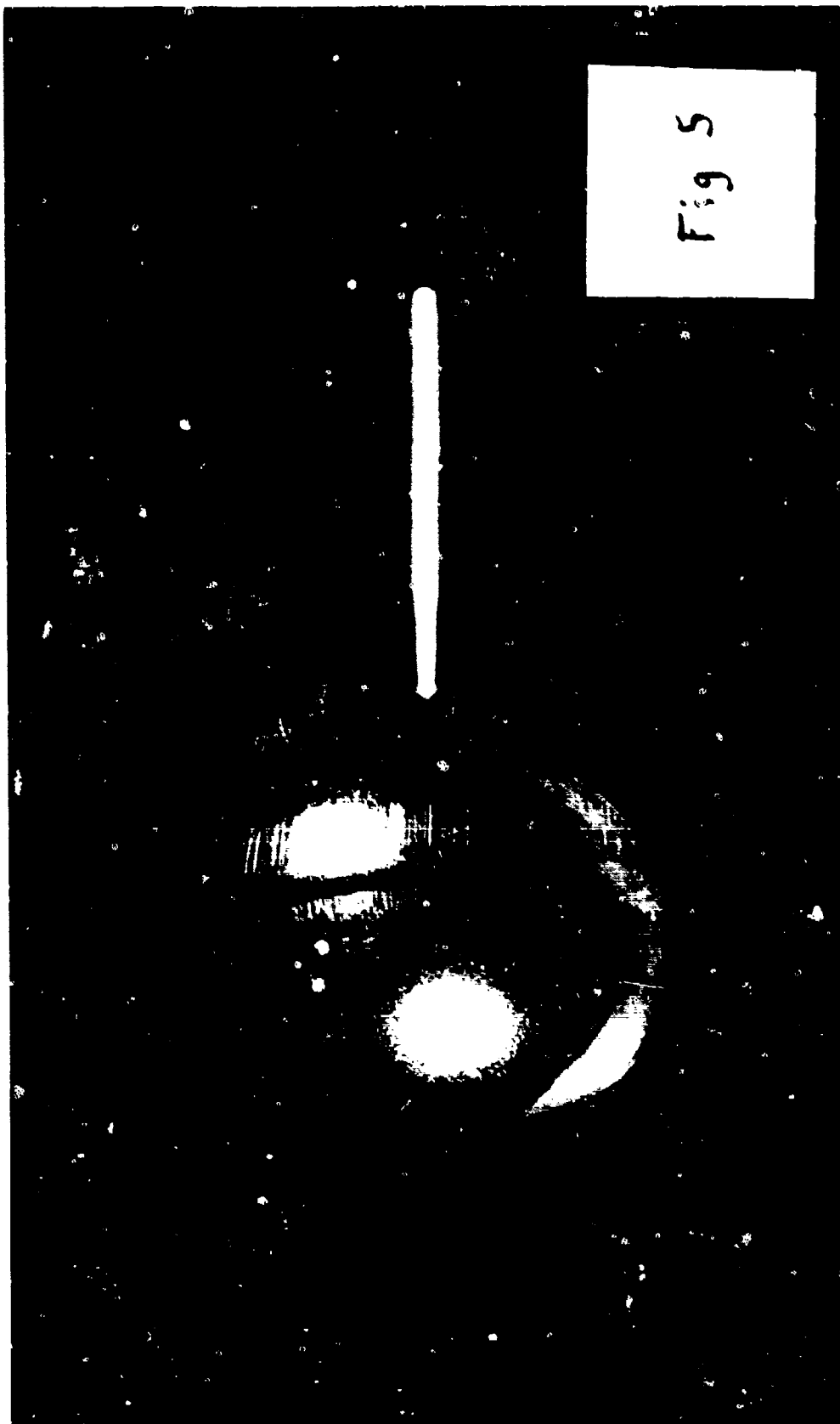
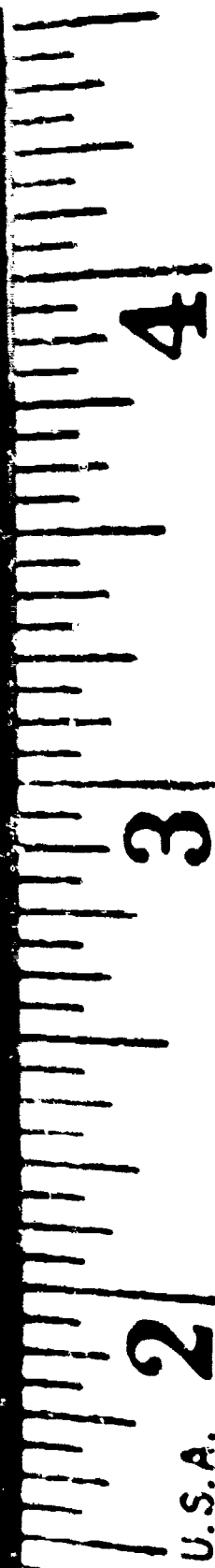
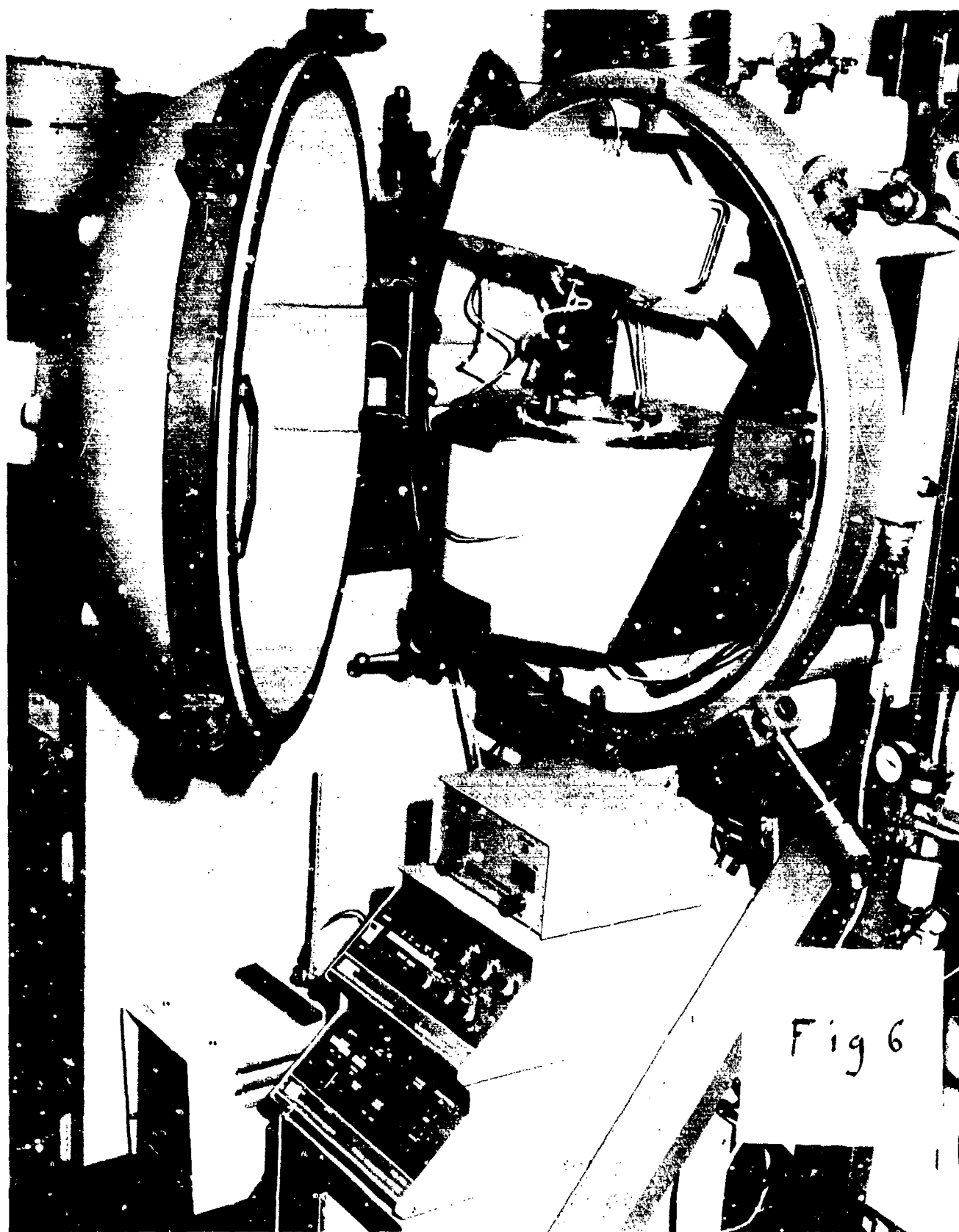


Fig 5





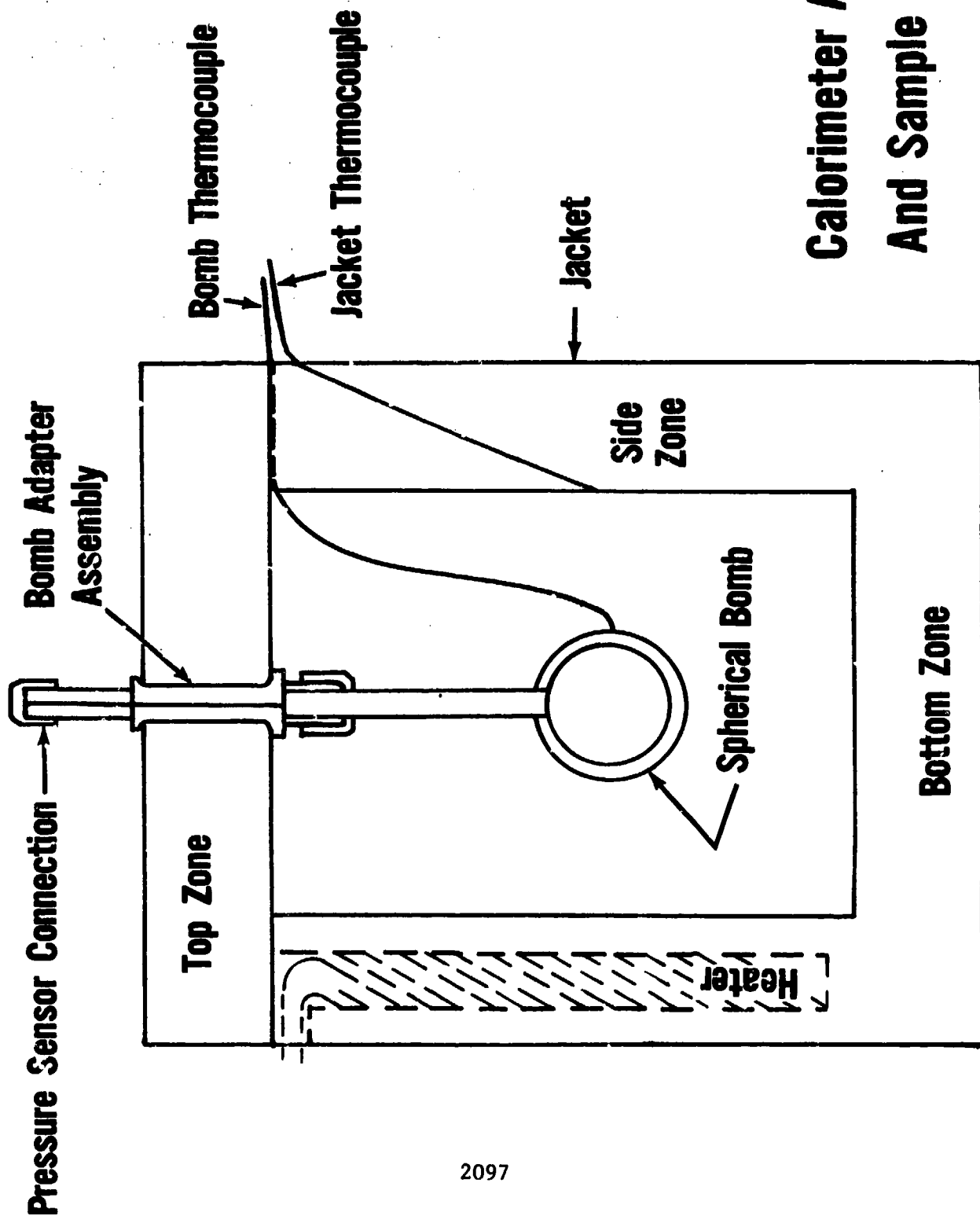


Fig 7

Calorimeter Assembly And Sample System

Fig 8



DSC SCANS PBXN 106 WITH $\text{Al}_2\text{O}_3/\text{NaOH}$

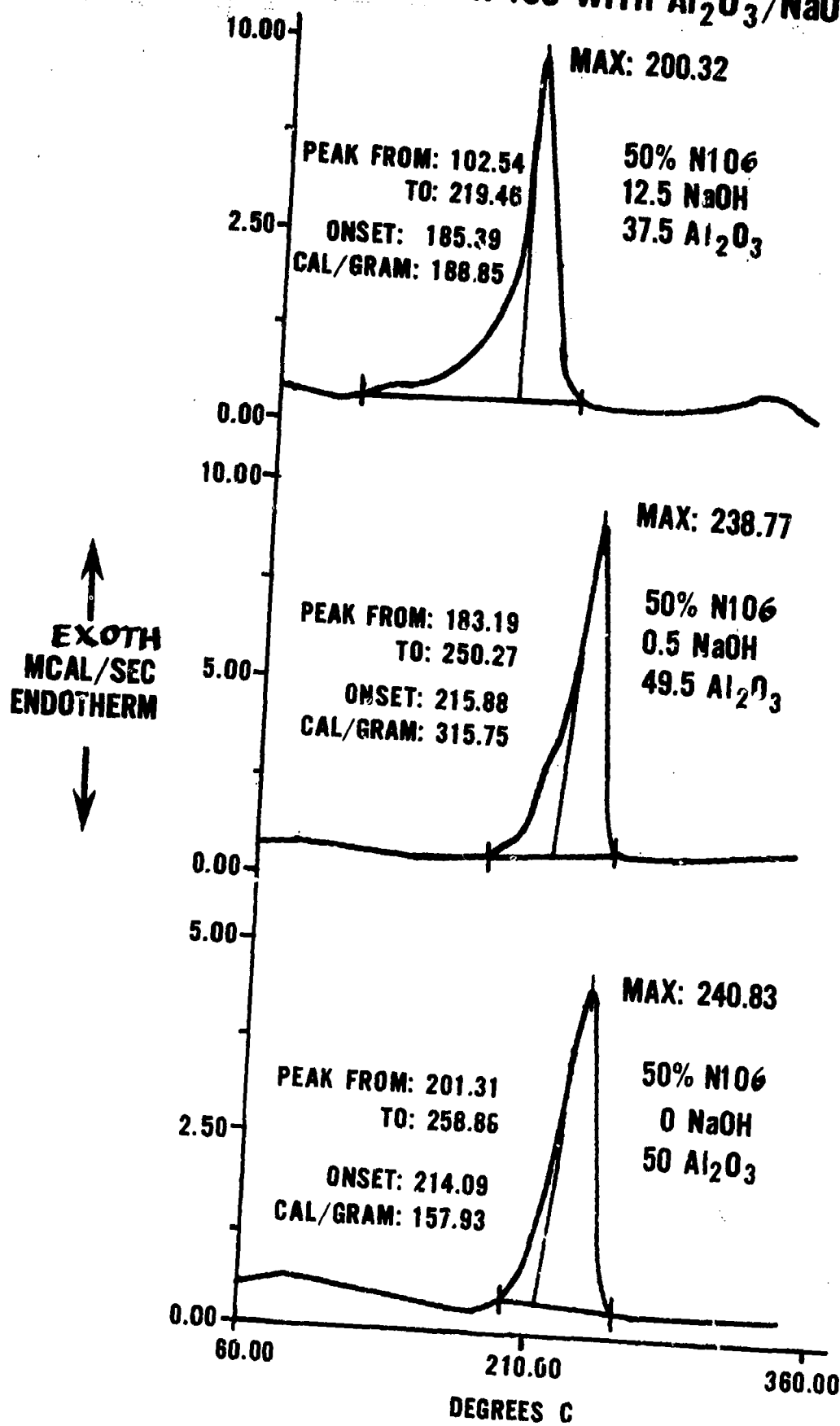


Fig 9

SCAN RATE 10°C/MIN.

● BASIC DEFINITIONS

● **EXPLOSIVE** - Substance capable, by chemical reaction, of producing gas at such a temperature, pressure and rate as to be capable of causing damage to the sur roundings.

● **HIGH EXPLOSIVES** - Substances which, in their application as primary, booster or main charges are required to detonate. Examples, RDX, HMX and TNT

● **PBX** - Plastic Bonded Explosive

Table 1

BASIC DEFINITIONS cont'd

● **PBXN 106**

Nitramine High Explosive - RDX Or Hexogen Or Cyclonite

Energetic Plasticizer Mixture - Bis(2.2 Dinitropropyl)

Acetal/Formal

Crosslinked Polyurethane Binder

Stabilizer

Catalyst

● **RDX**

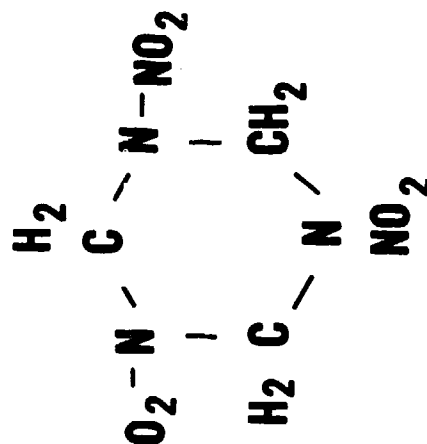


Table 1

COMPATIBILITY METHODS NOW IN USE

- DSC
- DTA
- VACUUM STABILITY
- TALIANI
- TGA
- ASTM E 698-79 ARRHENIUS KINETIC CONSTANTS
- HENKIN TIME TO EXPLOSION TEST
- ASTM E 476-73 THERMAL INSTAB. OF CONFINED
CONDENSED PHASE SYSTEMS
- ARC

Table 2

ARC-PBXN 106

REPRODUCIBILITY AND EFFECT OF SAMPLE MASS

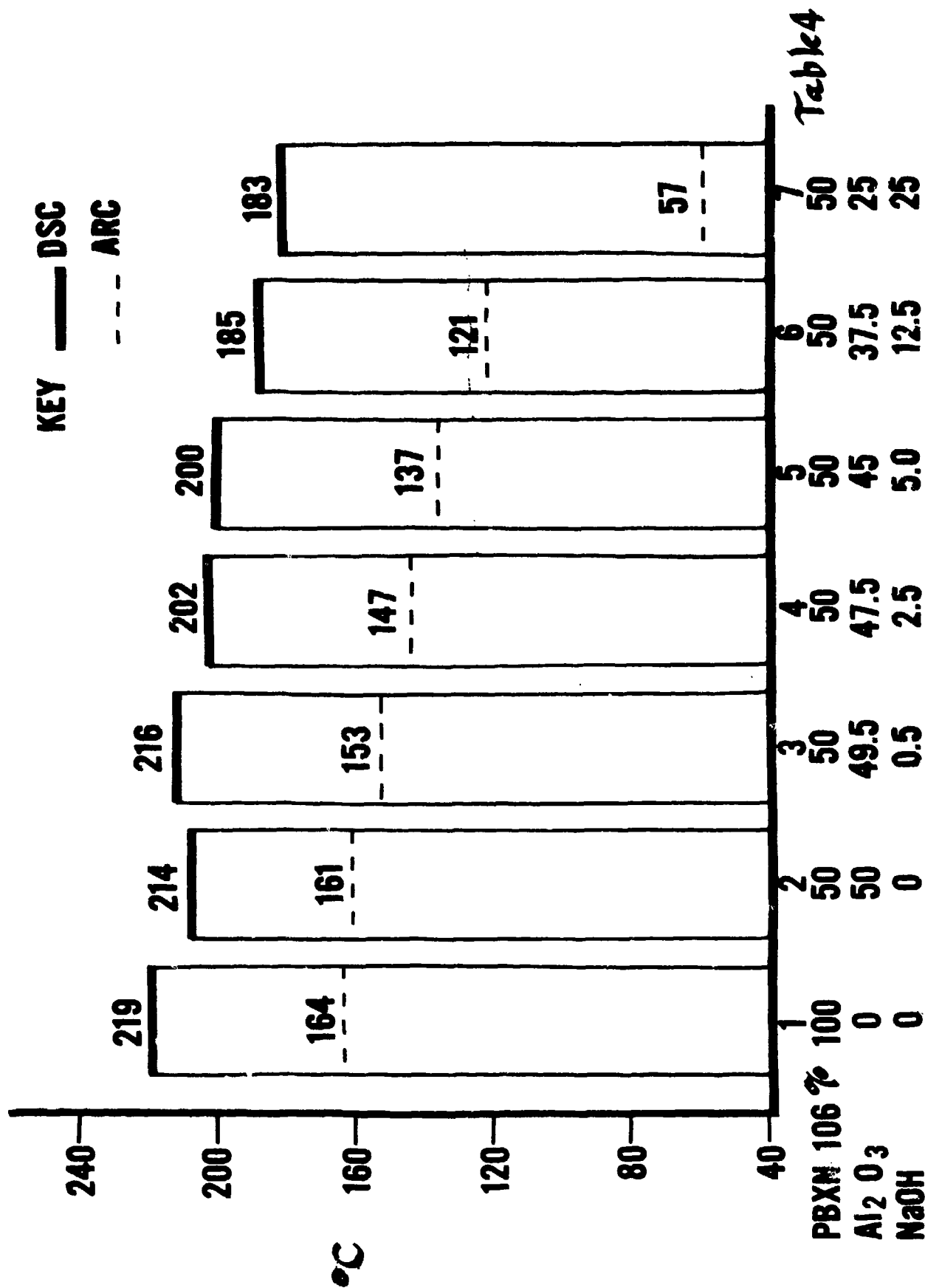
●REPRODUCIBILITY

SAMPLE MASS GRAMS	PRESSURE PSI	EXOTHERM ONSET, °C TA	EXOTHERM MAX, °C	TA-TB
0.2002	511	165.9	223.1	63.3
0.2000	513	161.2	226.7	67.9
0.1998	350	163.1	223.1	64.1
0.1998	503	163.9	225.6	66.2
0.2003	476	167.0	227.7	60.2
0.1998	525	162.2	230.3	66.9
MEAN 0.2000	475	163.9	226.1	64.7
PREC ±0.11%	±16.3%	±1.13%	±1.24%	±4.29%

●EFFECT OF SAMPLE MASS

0.1001	148.2	167.1	208.6	41.5
0.2000	513	161.2	226.7	67.9
0.3155	684	161.0	240.9	79.5
0.3945	1089	158.7	239.2	99.9
0.4207	1362.1	157.2	206.9	49.6
0.4309	1171.4	156.7	245.9	109.0
		△ 6.2%	Table 3	

EXOTHERM ONSET PBXN 106/NaOH ARC VS DSC



ARC-VTC DATA FOR PBXN 106/NaOH

	PERCENT	EXOTHERM ONSET °C	EXOTHERM MAX °C	TIME TO MAX TEMP	VAC COMP CC/G
PBXN 106	100	163.90	226.09	967.24	0.2
PBXN 106	50				TEST
NaOH	0	160.94	207.14	1293.15	ABORTED
Al ₂ O ₃	50				
	50	152.98	171.07	1337.69	3.4
	0.5				
	49.5				
	50	147.19	169.78	1199.56	TEST
	2.5				ABORTED
	47.5				
	50	137.18	142.78	1226.87	TEST
	5.0				ABORTED
	45				
	50	121.12	133.63	1075.99	GASSED
	12.5				THROUGH
	37.5				
	50	57.01	66.07	158.94	GASSED
	25				THROUGH
	25				

Table 5


Paper Distributed at the:

Twenty-Second DoD Explosives Safety Seminar
Anaheim, California

AD-P005 389

DETERMINATION OF METAL SPARKING CHARACTERISTICS
AND THE EFFECTS ON EXPLOSIVE DUST CLOUDS

by
C. James Dahn
&
Bernadette N. Peyes


Safety Consulting Engineers, Inc.
Rosemont, Illinois 60018

ABSTRACT

Of major concern in industry are hazards posed by metal-to-metal sparking in environments where potentially explosive dusts are present. The probability of ignition of a dust cloud by metal sparking is dependent on many factors including the type of metal, the contact speed of the metal surfaces, the contact time of the metal surfaces, the pressure on the contact surface and the type and concentration of the dust cloud present.

Metal sparking tests were performed as part of a hazard analysis program. Safety Consulting Engineers, Inc. conducted for ICI Americas, Inc.

The purpose of the test was to determine the sparking characteristics of a series of metals and the effects of the sparks produced on several types of dust clouds.



INTRODUCTION

Explosibility tests have been performed in the past to determine the relative destructive output of various types of dusts. Test chambers were used to simulate dust explosion. Figure 1 is a sketch of Bureau of Mines 20-liter chamber equipped with a sample dust dispersion mechanism. The 20-liter chamber was modified to contain the mechanical sparking system. Figure 2 is a sketch of the modified Bureau of Mines 20-liter chamber.

The spherical shape of the 20-liter chamber helps provide a uniform dust suspension. A 7.62 cm (3-inch) diameter by 0.635 cm (1/4-inch) thick 304L stainless steel contact wheel mounted on a shaft, which protrudes through the side wall of the chamber, is driven by an electric motor located outside the chamber. A 0.635 cm (1/4-inch) diameter by 5.08 cm (2-inch) long rod is held by a lever bar against the circumference of the metal wheel. A dead weight of 1362 grams (3 pounds) is located at the outside portion of the lever bar. A viewing window and mirror allowed remote observation of the tester.

PROCEDURE

Each rod material/dust combination test was performed as follows. The preweighed dust sample was first placed in the bottom of the chamber. The rod material was raised using a pulley mechanism before the test chamber was closed. The electric motor was turned on to start the contact wheel. Pressurized air from the test chamber nozzle dispersed the sample dusts uniformly while the rod material was dropped to make contact with the rotating wheel. Ignition of the dust cloud was then observed through the view mirror. The setup is illustrated in Figure 3.

TEST RESULTS

The first series of tests consisted of testing six metal rods to determine the minimum contact wheel speed which would produce sparking for each rod. The following metal rods were tested: 1018 Mild Steel, 316 Stainless Steel, 304 Stainless Steel, 304L Stainless Steel, 3003-H14 Aluminum and 6061-T6 Aluminum. By determining the minimum wheel rotation speed that produced sparking for each one of the metal rods tested, the types of metals more likely to produce sparking were identified. Table 1 contains results of these tests and shows that 304 Stainless Steel rod produced sparking at the lowest wheel speed. Neither aluminum rods produced no sparking at the maximum wheel speed available.

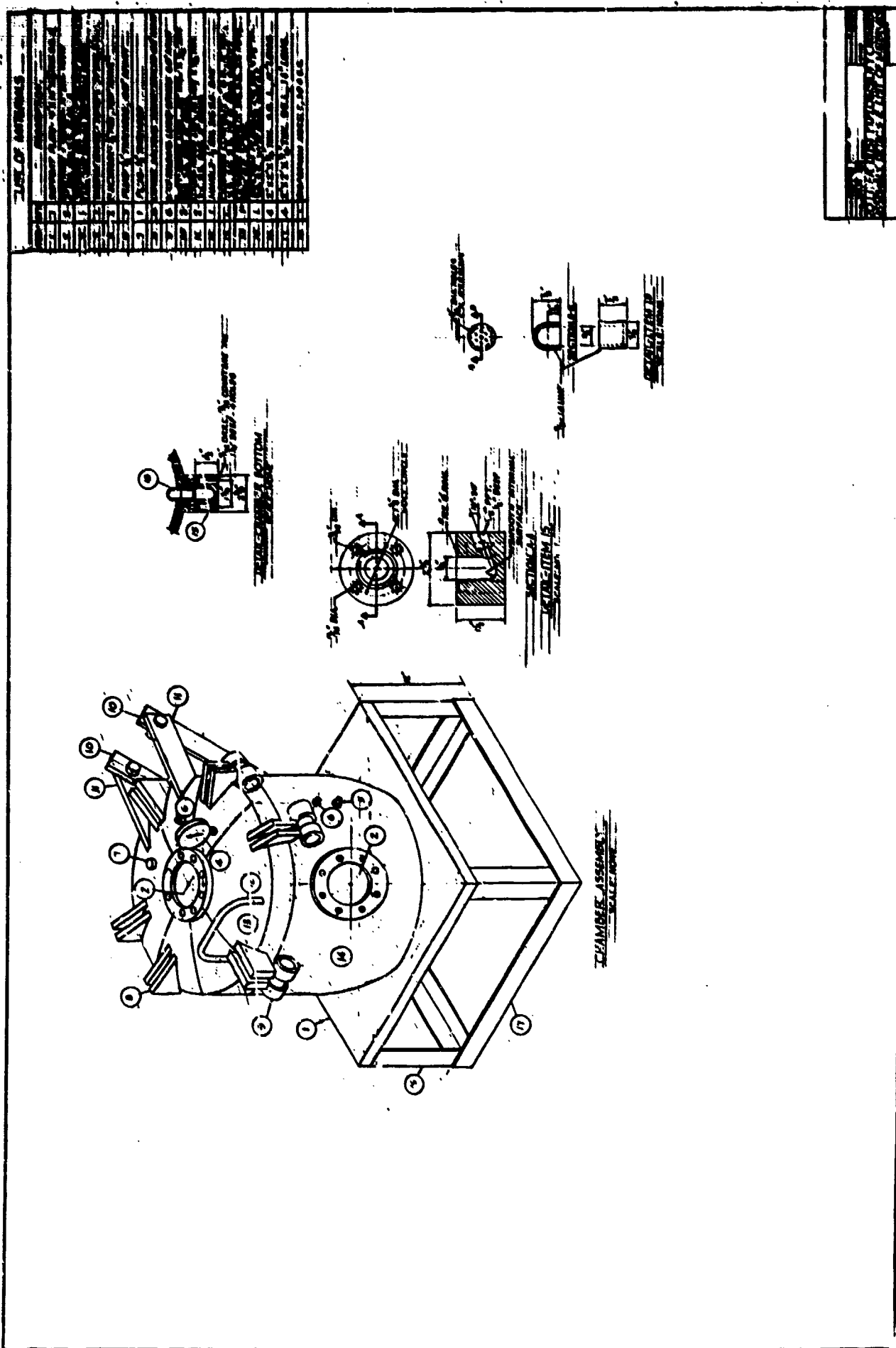


Figure 1. U. S. Bureau of Mines 20-liter chamber.

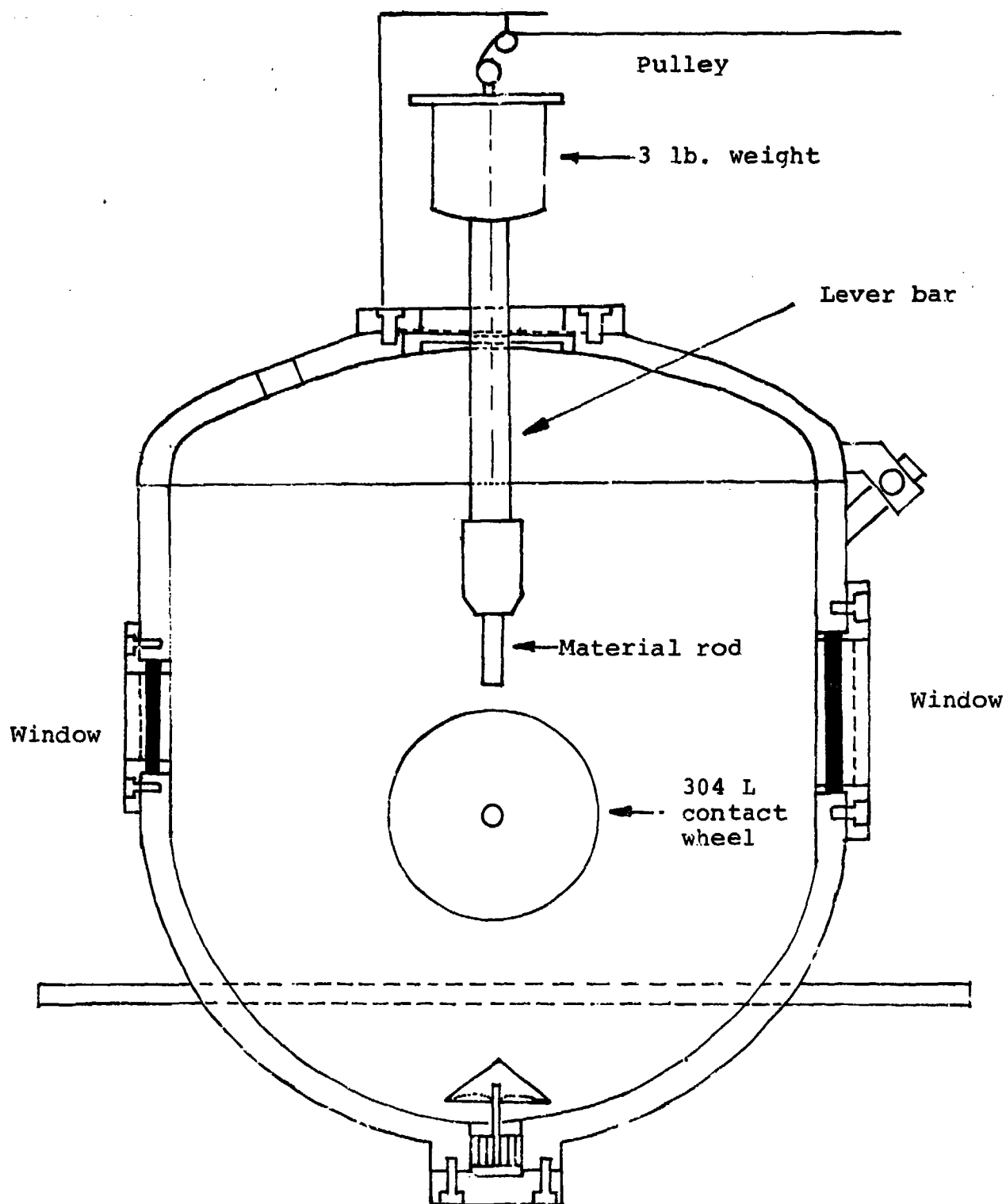


Figure 2. Modified Bureau of Mines 20-liter chamber.

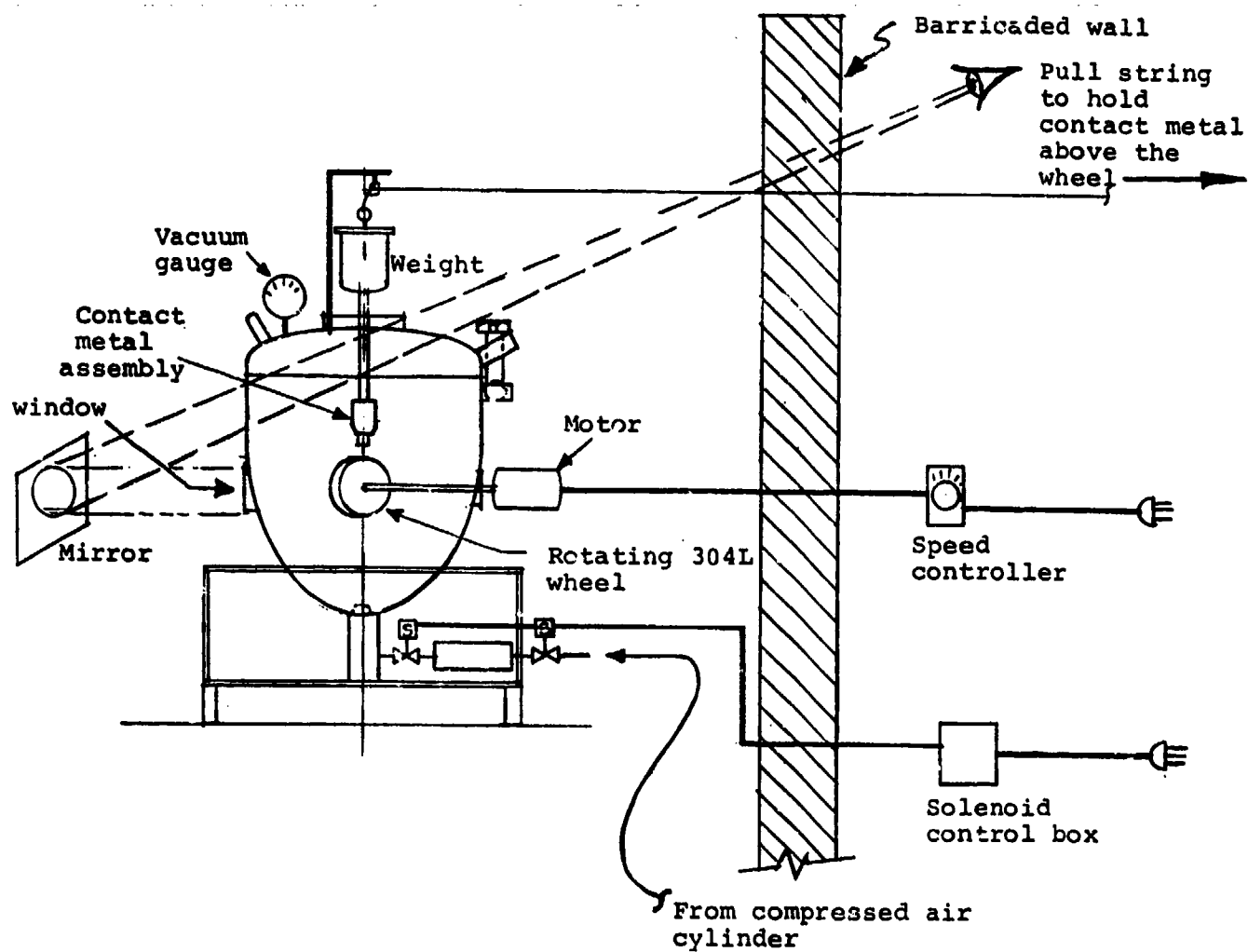


Figure 3. Metal sparking test setup.

After the minimum sparking speeds were found, five different propellant dusts, M6, M30Al, M31Al, CBI, Black Powder, one carbonaceous dusts, Pittsburgh coal dust and one commercial product, cornstarch, were tested to determine the minimum sparking speed for each rod type that would ignite each sample dust. The sample materials tested were ground and sieved through mesh screen (-200 and -100). Table 2 lists the minimum sparking speed for each rod tested that would ignite each sample dust. Results of testing indicated that 1018 Mild Steel was the material aluminum rods failed to produce sparking at low speeds, these materials did not ignite the sample dusts.

The third test series was conducted at a peripheral wheel speed of 14.0 meter/sec (≈ 45.8 ft/sec) for all rod material-sample dust combinations. This test series allowed a ranking of the sample dusts based on ignition sensitivity. The most sensitive dust was M6 propellant with sensitivity decreasing respectively for CBI, cornstarch, M30Al, M31Al, Black Powder and Pittsburgh coal dust. The test rod materials, in order from the most likely to least likely to produce ignition were 1018 Mild Steel, 304L Stainless Steel, 304 Stainless Steel, 316 Stainless Steel, 3003-H-14 Aluminum and 6061-T6 Aluminum. Table 3 illustrates the decreasing ignition sensitivity for the dust samples tested with rods in the order of least likely to produce ignition.

The fourth series of tests consisted of testing all rod material sample dust combinations that produced ignition in the third series of tests, at a peripheral wheel speed of 14.0 meter/sec. The contact time of the rod material and wheel was limited to 0.5 sec. Again this test series allowed a ranking of the sample dusts based on ignition sensitivity during a relatively short exposure to sparking. Table 4 shows that all sample dusts tested ignited when 1018 Mild Steel was used. Cornstarch, CBI, M6 and Black Powder also ignited when tested with 316 Stainless Steel rod.

CONCLUSIONS

Metal sparking tests, on various metals in several dust cloud environments, showed a distinction between metals that are relatively safer to handle in an explosive dust cloud atmosphere and those that may be unsafe.

Metals found to present a lower sparking hazard include both 3003-H14 and 6061-T6 Aluminum.

Metals tested that are not well suited to an explosive dust cloud atmosphere include 1018 Mild Steel, 304L Stainless Steel, 304 Stainless Steel and 316 Stainless Steel because of their greater tendency to produce sparking.

The potential for explosive dust initiation appears to be greater when contact speed with metals exceeds 9.2 meter/sec (30.1 ft/sec) for 1018 Mild Steel, 8.4 meter/sec (27.5 ft/sec) for 304L Stainless Steel, 7.2 meters/sec (23.6 ft/sec) for 304 Stainless Steel, 7.2 meters/sec (23.6 ft/sec) for 304 Stainless Steel, 8.4 meter/sec (27.5 ft/sec) for 316 Stainless Steel.

At longer metal contact times (with speed greater than the minimum contact speed which would produce sparking for each metal), a greater potential hazard of ignition may also be possible.

TABLE 1
MINIMUM CONTACT WHEEL SPEED
WHICH WOULD PRODUCE SPARKING FOR EACH ROD

Contact Force: 13.3 N (3 lbf)

MATERIAL ROD	MINIMUM CONTACT WHEEL SPEED		
	(m/s)	(rpm)	(ft/s)
.018 Mild Steel	9.2	2300	30.1
304L Stainless Steel	8.4	2100	27.5
304 Stainless Steel	7.2	1800	23.6
316 Stainless Steel	8.4	2100	27.5
6003-H14 Aluminum	No visible spark at maximum speed of		
	19.9	5000	65.4
6061-T6 Aluminum	No visible spark at maximum speed of		
	19.9	5000	65.4

**MINIMUM SPARKING SPEED FOR EACH MATERIAL ROD
THAT WOULD IGNITE THE SAMPLE DUST**

SAMPLE DUST TEST	DUST PARTICLE SIZE (µm)	DUST CONC. (g/liter)	POD MATERIAL				MINIMUM SPEED TO CAUSE IGNITION
			1018 MILD STEEL	304L STAINLESS STEEL	304 STAINLESS STEEL	316 STAINLESS STEEL	
M6	75	0.0029	12.4 (40.6)	14.0 (45.8)	14.0 (45.8)	13.5 (44.5)	-
M30A1	75	0.0029	11.2 (36.6)	13.2 (43.2)	13.2 (43.2)	13.5 (44.5)	-
M31A1	150	0.0059	10.4 (34.0)	14.0 (45.8)	14.0 (45.8)	14.0 (45.8)	-
CBI	150	0.0059	8.8 (28.8)	14.0 (45.8)	14.0 (45.8)	14.0 (45.8)	-
Black Powder	75	0.0029	11.6 (37.9)	13.2 (43.2)	>19.9 (>65.4)	14.0 (45.8)	-
Pittsburgh coal dust	75	0.0029	10.0 (32.7)	>19.9 (>65.4)	>19.9 (>65.4)	>19.9 (>65.4)	-
Cornstarch	75	0.0029	8.0 (26.2)	14.0 (45.8)	14.0 (45.8)	14.0 (45.8)	-

-- showed no ignition up to a maximum speed of 19.9 m/s (65.4 ft/s)

TABLE 3

METAL SPARKING TEST RESULTS AT METAL
WHEEL SPEED OF 14.0 m/s (45.8 ft/s)

SAMPLE DUST TESTED	DUST PARTICLE SIZE (μ m)	DUST PARTICLE SIZE (in)	SAMPLE DUST CONC. (g/liter)	ROD MATERIAL (Number of ignitions in 20 runs)					
				1018 MILD STEEL	304L STAINLESS STEEL	304 STAINLESS STEEL	316 STAINLESS STEEL	3003-H14 ALUMINUM	6061-T6 ALUMINUM
M6	75	0.0029	0.25	20	19	18	18	-	-
CBI	150	0.0059	0.41	19	17	18	18	-	-
Cornstarch	75	0.0029	0.35	20	9	7	16	-	-
M30A1	75	0.0029	0.41	19	18	15	15	-	-
M31A1	150	0.0059	0.32	14	13	11	9	-	-
Black powder	75	0.0029	0.25	17	8	6	8	-	-
Pittsburgh coal dust	75	0.0029	0.35	5	-	-	-	-	-

- showed no ignition

TABLE 4

METAL SPARKING TEST RESULTS AT METAL WHEEL SPEED
OF 14.0 m/s (45.8 ft/s) WITH ROD MATERIAL CONTACT
TIME OF 0.5 SEC.

SAMPLE DUST TESTED	DUST PARTICLE SIZE (μ m)	DUST PARTICLE SIZE (in.)	SAMPLE DUST CONC. (g/liter)	ROD MATERIAL (Number of ignitions in 20 runs)					
				1018 MILD STEEL	316 STAINLESS STEEL	304 STAINLESS STEEL	304L STAINLESS STEEL	3003-H14 ALUMINUM	6061-T6 ALUMINUM
Cornstarch	75	0.0029	0.35	15	10	3	-	-	-
M6	75	0.0029	0.25	12	2	-	-	-	-
CBI	150	0.0059	0.41	10	5	-	-	-	-
Black Powder	75	0.0029	0.25	10	2	-	-	-	-
M31A1	150	0.0059	0.32	9	-	-	-	-	-
M30A1	75	0.0029	0.41	8	-	-	-	-	-
Pittsburgh coal dust	75	0.0029	0.35	-	-	-	-	-	-

- showed no ignition

Paper Distributed at the:

Twenty-Second DoD Explosives Safety Seminar
Anaheim, California

AD-P005 390

WC-814 PROPELLANT BURNING IN A
SCAMP-TYPE HOPPER

by

C. James Dahn
Safety Consulting Engineers, Inc.
Rosemont, Illinois

August 28, 1986

ABSTRACT

Before a SCAMP-Type hopper could be used to load a 5.56-mm blank round with propellant WC-814, it was necessary to determine the maximum quantity of the propellant that could be used in the hopper without yielding a burning-to-explosion transition. A hopper was tested in a remote area with 60, 110, 160, and 210 lb of propellant; five tests were conducted at each weight level. None of the tests resulted in an explosion or detonation after the propellant was ignited. In all of the tests the propellant did burn, causing damage to the vent pipe and sometimes the hopper.

INTRODUCTION

The 5.56 mm Blank M200 round had been loaded with HPC-13 propellant using conventional plate loading equipment. An available SCAMP Load and Assemble Submodule located at LCAAP was converted to load the 5.56 mm Blank round. Due to the 1.1 DoD hazard classification for the HPC-13 propellant, it cannot be used in SCAMP-Type equipment. Use of an alternate propellant, WC-814, with a 1.3 hazard classification would permit use of the SCAMP-Type equipment and yield a higher production rate at a reduced unit cost.

The testing conducted for this project was to determine the maximum quantity of the WC-814 propellant that can be used in a SCAMP-Type hopper without yielding a burning-to-explosion transition. Testing was initiated with 60 lb of propellant and increased by 50-lb increments to a maximum of 210 lb.

The pressure rise time and total pressure were measured for each test. Also recorded was the surface temperature of the hopper. Photographic coverage for each test consisted of film coverage at 64 fps and 1000 pps and 35-mm color still shots.

The propellant weight and height in the hopper were recorded for each test. Five tests were run using 60 lb of the propellant. The propellant weight was then increased to 110 lb, then 160 lb, and then 210 lb for five runs each.

TEST EQUIPMENT AND SETUP

SCAMP-Hopper

The hopper used in the testing was constructed per AMCCOM Drawing No. 12624485, "SCAMP-Hopper". Details for the hopper legs and discharge opening (Detail A) were added to the drawing by Safety Consulting Engineers, Inc. See Figure 1.

The hopper was constructed of 14 gauge carbon steel. The aluminum vent pipes were constructed of 1100 aluminum sheets with crimped seams. The vent pipe and feed pipe tubing were replaced after each test run.

The hopper was placed in the center of a remote test area. Four guy wires attached to the hopper legs anchored the hopper down. See Figure 2.

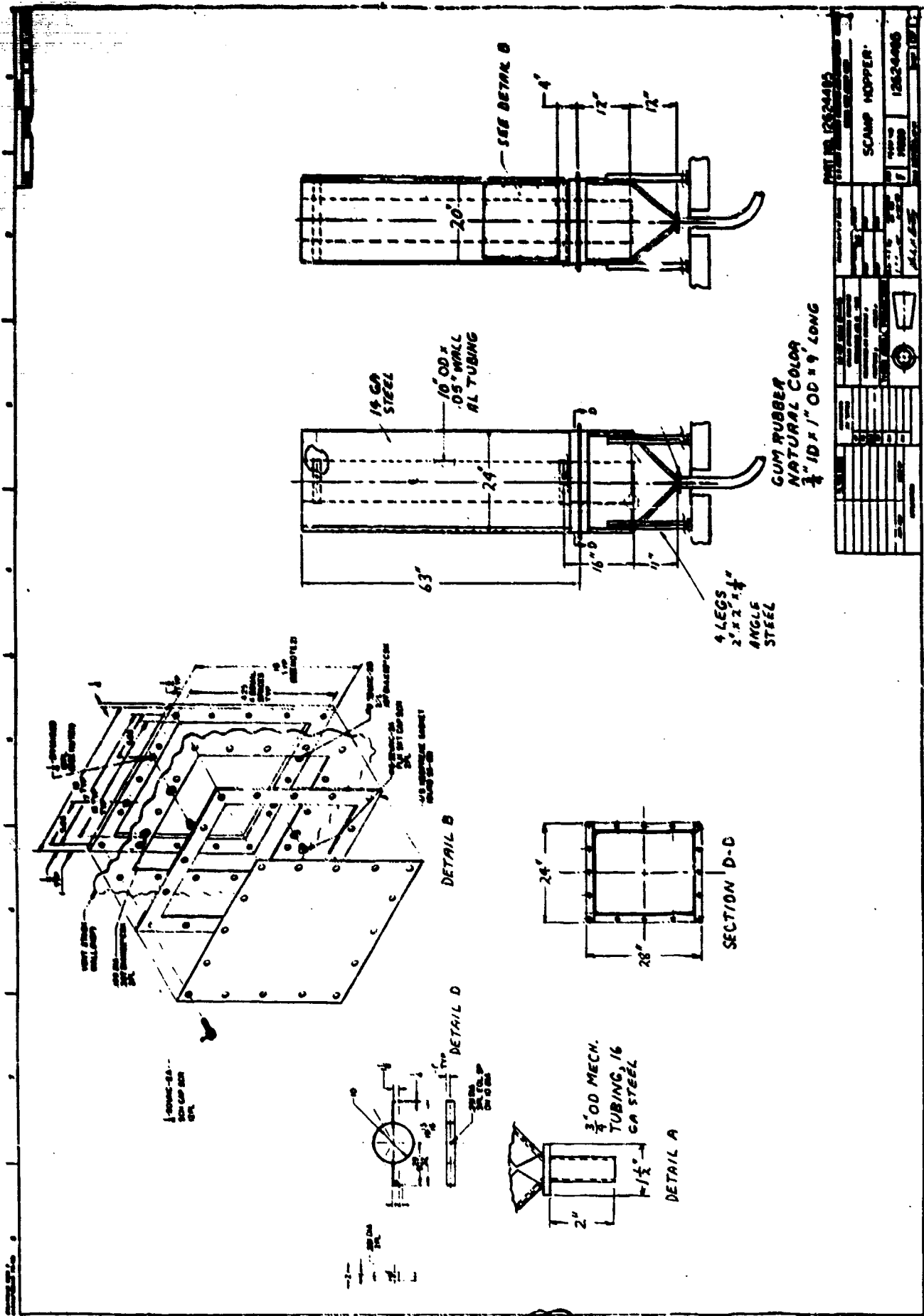


Figure 1. Drawing for SCAMP-hopper construction.

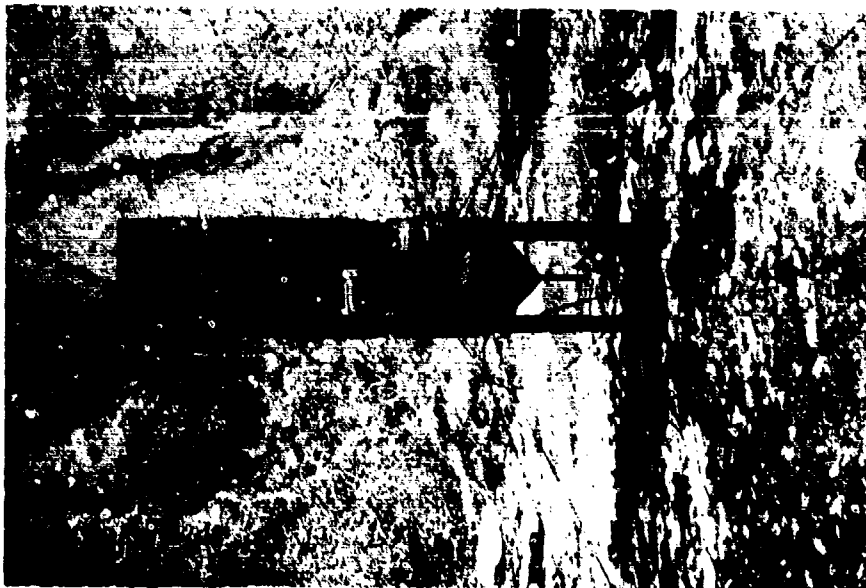


Figure 2. Test setup.

Instrumentation

The pressure rise rate and peak pressure were measured using two Celesco LD-25 pressure transducers. The transducers were placed outside of the hopper 7.5 feet and 15 feet from the point of ignition. See Figure 3. Each transducer was connected to an amplifier, and a monitor/calibration chassis. See Figure 4. The transducer signal was then recorded on magnetic tape and recorded on a light beam recorder. As an alternate, the pressure signal could be monitored via an oscilloscope. The blast pressure measuring system was calibrated using three different weights of pentolite (1, 2, and 5 lb).

The temperature of the hopper wall was measured using three thermocouples. The thermocouples were attached to the outside wall at distances of one foot, two feet and three feet above the point of ignition. See Figure 3. The thermocouples were attached to a datalogger which recorded the temperatures.

Film coverage of the tests was provided at both 64 fps and 1000 pps. A Bolex camera, set up approximately 200 feet from the hopper, was used to film each test at 64 fps. See Figure 5. Coverage at 1000 pps was accomplished using a Hycam high-speed camera placed approximately 300 feet from the hopper and 90 degrees from the Bolex camera. Closed circuit TV was used to monitor the hopper and test area during each test.

Equipment Setup

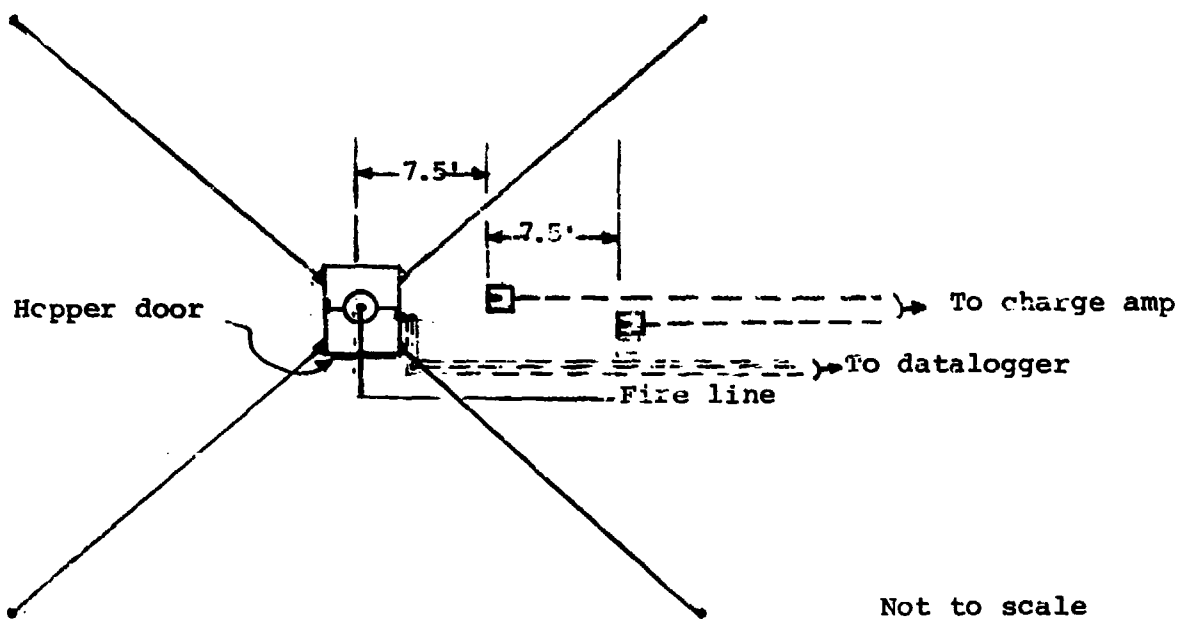
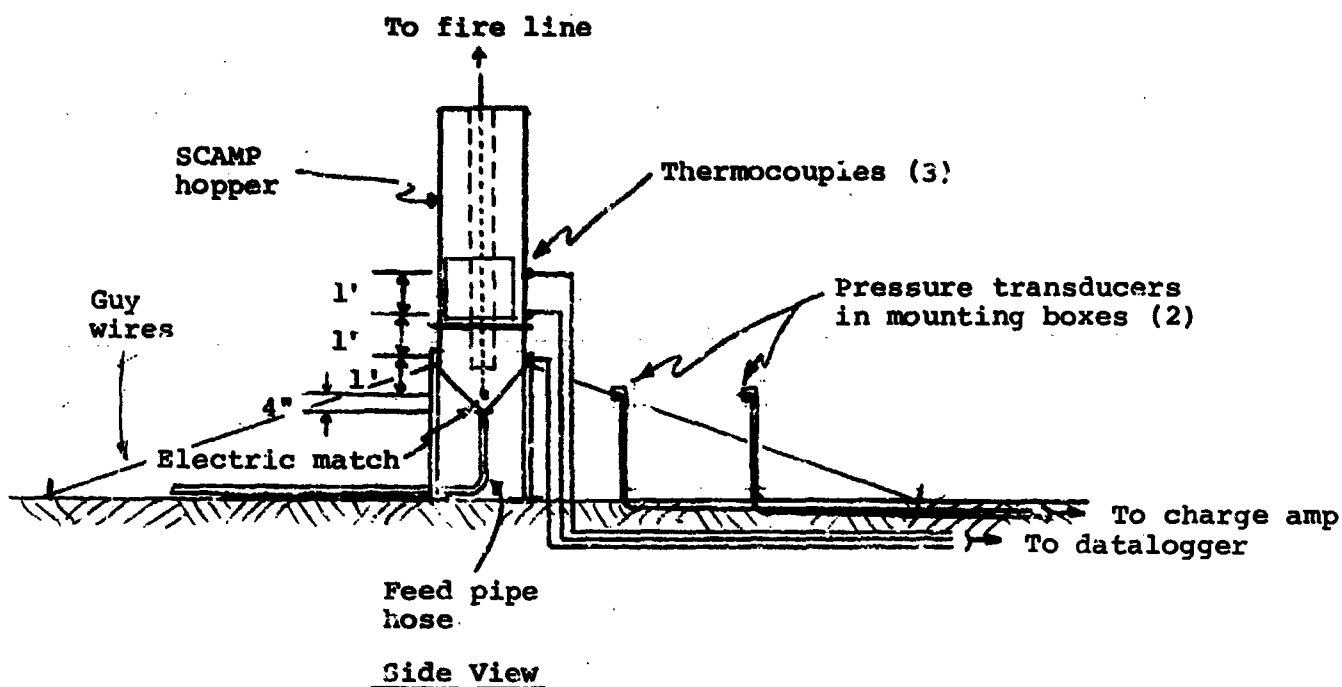
The hopper, pressure transducer, thermocouples, and cameras were set up as shown in Figures 3 and 5. Operations were controlled and monitored from two remote buildings.

The ignition source was an M100 electric match. A 12V DC battery connected through the high-speed camera was used to fire the electric match. One operator controlled the cameras and fire line. A second operator monitored the test via CCTV and controlled the temperature and pressure recording instrumentation. Radios provided communication between the two operators.

TEST PROCEDURE

Prior to each test, the equipment and instrumentation were set up as described previously and checked. The fire line was left shorted and disconnected from the 12V DC battery. The cameras were loaded with film and focused.

Once the equipment, instrumentation, and cameras were set up, the test area was cleared of all personnel but one operator. The operator weighed out the amount of propellant to be tested. Out of this weighed amount, propellant was taken and poured into



Not to scale

Figure 3. SCAMP hopper test setup.

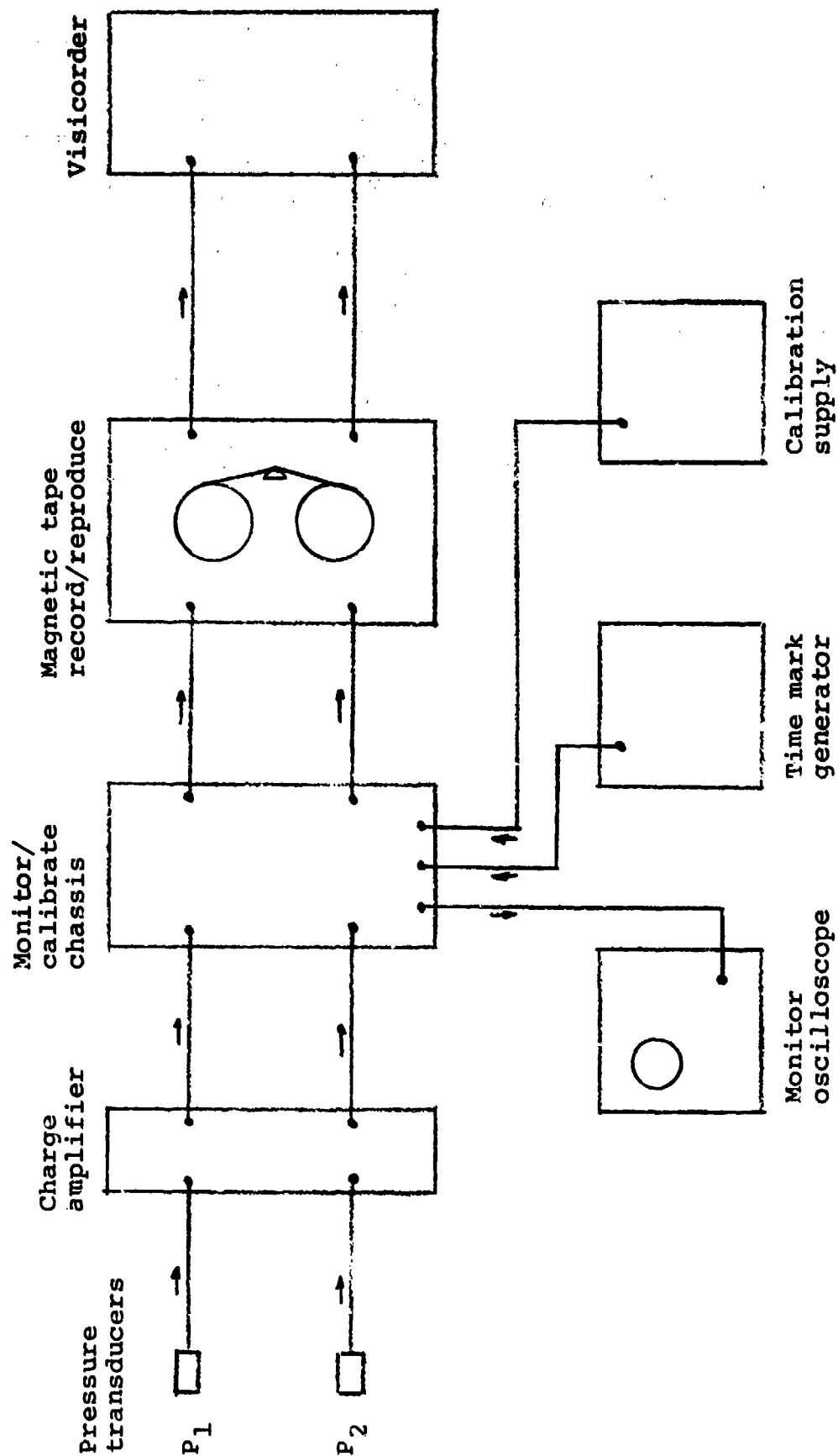


Figure 4. Block diagram of pressure instrumentation setup.

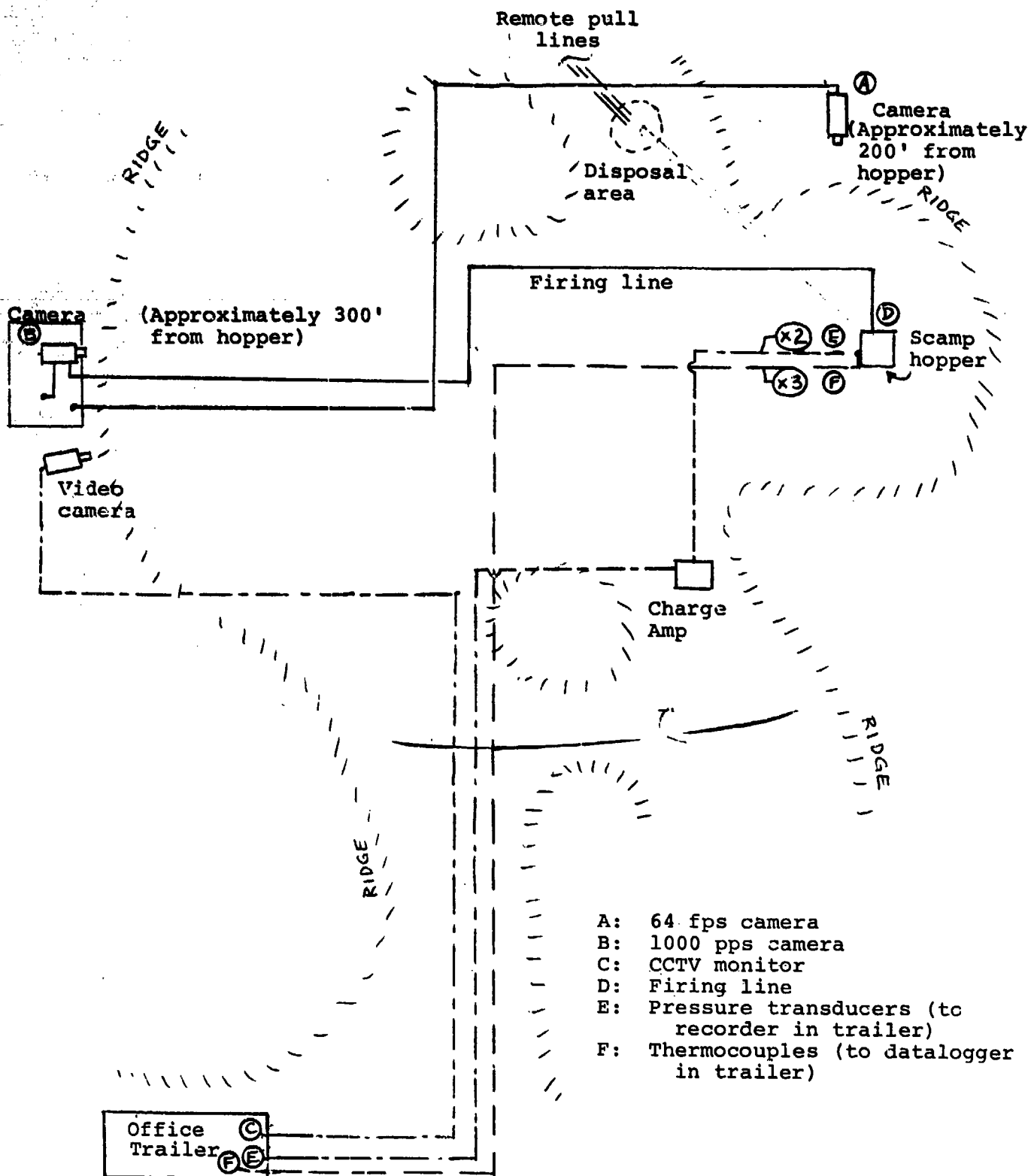


Figure 5. Equipment setup.

the nine foot long rubber feed hose which had been sealed with duct tape at one end. The filled feed pipe was then attached to the hopper discharge.

A small guide tube was positioned down the center of the hopper for use in placement of the electric match. The remainder of the weighed propellant was then poured into the hopper, around the vent pipe. After being leveled, the height of the propellant in the hopper (outside the vent pipe) was measured.

Next, a shorted electric match was lowered into the hopper down the guide tube. This placed the electric match four inches above the bottom discharge opening of the hopper. The guide tube was then carefully removed, allowing the propellant to flow in around the electric match. The electric match leads were connected to the firing line (which was disconnected from the 12V DC battery and shorted).

Once the test area was cleared of all personnel, a warning siren was sounded. The recording instruments were started and the firing line was connected to the battery. The firing signal was controlled through the high-speed camera. (This allowed the film to reach the desired speed before the electric match was fired). After a countdown, the high-speed camera was started and the electric match fired. The reaction was monitored on the CCTV screen. Once the reaction was complete, the cameras and recording instruments were shut off.

After waiting a period of time to ensure the test area was safe to enter, the hopper was examined for evidence of damage. Color still shots were taken of the hopper and vent pipe. Damaged vent pipes and feed pipes were removed after each test and replaced with new ones.

TEST RESULTS

None of the tests resulted in an explosion or detonation. In all of the tests, the propellant did burn, causing damage to the vent pipe and sometimes the hopper.

A summary of the test results is shown in Table 1. In the majority of cases, the entire amount of propellant burned, causing the vent pipe to collapse and the feed pipe to partially burn. In a few cases (Runs 2, 10, 14 and 16) the vent pipe was thrown out of the hopper from the force of the burning. In two of the tests (Run 10 with 110 lb, and Run 14 with 160 lb) the vent pipe was also fragmented.

TABLE 1
SCAMP HOPPER TEST RESULTS

RUN NO.	PROPELLANT WEIGHT (lb)	PROPELLANT HEIGHT (in)	BURNING OR DETONATION	OBSERVATIONS
1	60.0	12.0	Burn	Vent, feed pipes damaged.
2	60.0	13.0	Burn	Vent pipe thrown from hopper, feed pipe burned.
3	60.0	13.0	Burn	Vent, feed pipes damaged.
4	60.0	13.0	Burn	Same
5	60.0	12.5	Burn	Same
6	110.0	17.0	Burn	Vent pipe damaged, torn out of top bracket.
7	110.0	17.0	Burn	Propellant in feed pipe did not burn.
8	110.0	17.0	Burn	Vent, feed pipes damaged.
9	110.0	17.0	Burn	Same
10	110.0	17.0	Burn	Vent pipe fragmented into 8 pieces thrown 10 to 100 feet from hopper. Hopper deformed.
11	160.0	20.5	Burn	Vent, feed pipes damaged.
12	160.0	20.5	Burn	Same
13	160.0	20.5	Burn	Same
14	160.0	20.5	Burn	Vent pipe fragmented and thrown 20-30 feet from hopper. Top bracket thrown 30 feet from hopper.

TABLE 1 (Continued)

SCAMP HOPPER TEST RESULTS

RUN NO.	PROPELLANT WEIGHT (lb)	PROPELLANT HEIGHT (in)	BURNING OR DETONATION	OBSERVATIONS
15	160.0	20.5	Burn	Vent, feed pipes damaged.
16	210.0	25.0	Burn	Vent pipe thrown 20 feet from hopper, feed pipe burned.
17	210.0	25.0	Burn	Vent, feed pipes damaged.
18	210.0	25.0	Burn	Same
19	210.0	25.0	Burn	Same
20	210.0	25.0	Burn	Same

By the end of the fifth run (the 60-lb tests completed), some slight deformation of the hopper was noticed. The deformation was in the form of warpage to the upper portion of the hopper walls. The intense burning of Run 10 (110 lb) resulted in more extensive deformation of the hopper. The damage was confined to the upper portion of the hopper, which was deformed one to two inches on the two wider sides of the hopper. The top bracket, which holds the vent pipe in place, was pulled from the hopper walls. The vent pipe was also fragmented and thrown from the hopper during Run 14 (160 lb). In this test, the top bracket was torn completely from the hopper walls and was thrown about 30 feet.

The maximum hopper wall temperatures, and the times it took to reach those temperatures, are shown in Table 2. Since no detonation occurred, the pressures measured by the transducers remained at ambient. The pressure traces showed no increases during any of the tests.

TABLE 2
MAXIMUM HOPPER WALL TEMPERATURES

RUN NO.	AVERAGE WALL TEMP. START (°F)	BOTTOM (1 ft)		MIDDLE (2 ft)		TOP (3ft)	
		TEMP (°F)	TIME (sec)	TEMP (°F)	TIME (sec)	TEMP (°F)	TIME (sec)
1	23	147	59	153	38	150	56
2	26	141	48	132	76	167	42
3	ND	ND	-	ND	-	ND	-
4	15	121	73	127	73	131	73
5	46	113	77	134	77	137	77
6	65	126	76	135	68	167	71
7	28	85	67	103	51	118	51
8	19	95	78	ND	-	ND	-
9	82	152	80	151	80	173	80
10	83	132	78	142	72	160	69
11	32	235	150	179	74	170	21
12	58	133	58	117	58	153	42
13	30	101	52	86	52	129	52
14	8	75	55	68	55	107	55
15	60	114	62	110	56	131	62
16	15	95	69	117	59	145	65
17	58	117	107	133	47	130	47
18	18	173	88	161	39	191	77
19	68	160	118	120	35	176	115
20	58	126	105	124	33	124	54

ND: No data.

AN AUTOMATED EXPLOSIVE REMOVAL SYSTEM USING CAVITATING WATER JETS

Andrew F. Conn

Division Head, Jet Technology Systems Division
Tracor Hydronautics, Inc.
7210 Pindell School Road
Laurel, Maryland 20707
USA

AD-P005 391

ABSTRACT

A remotely-controlled automated system has been built for safely and rapidly removing explosives from 105 and 155 mm warheads. This system was acquired by the Israel Military Industries to clear a stockpile of obsolete munitions, and allow reclamation of the shells and HE constituents. Using the CAVIJET® cavitating water jet method, the HE is fully washed out from the warhead, and then the effluent water is filtered and reused. After one operator loads a warhead into the washout machine and leaves the area, all subsequent functions are monitored and controlled from a remote location. The 16 lb load of HE in a 155 mm warhead can be removed in well under two minutes with this new system. With adaptations this type of equipment can be used for the demilitarization of any warhead size, bombs, and solid-propellant rocket motors.

1. INTRODUCTION

1.1 Background

The demilitarization equipment described in this paper was specifically designed and built for use by the Israel Military Industries (IMI) in their munitions factory at Ramat Hasharon, Israel. Although this particular equipment is being used to remove explosives from 105 and 155 mm warheads, it is emphasized that this CAVIJET® washout system can be used for cleaning out virtually any type of cylindrical munition, from small shells to bombs, and for removing solid-propellants from missile or rocket motors.

The design and safety validations for this system were developed under several R&D projects (see Refs. 1-8) with the U.S. Army and Navy. These studies (see summaries in Appendix A) proved that CAVIJET® cavitating water jet nozzles could safely, rapidly, and efficiently remove explosive and propellant materials from munitions.

1.2 The CAVIJET® Cavitating Water Jet Technology

The staff at Tracor Hydronautics has developed and patented a number of methods for enhancing the erosive action of a water jet, by stimulating the creation of cavitation in or around the jet. This technology has proven capable of maximizing the cleaning or cutting

performance for a given input of hydraulic power, and such nozzle systems have significantly outperformed comparable conventional water jet systems for a wide range of commercial and military applications.

The CAVIJET cavitating fluid jet method (see Fig. 1) is one of the very few successful attempts to harness, for useful purposes, the destructive power of cavitation, which for decades has plagued the designers of hydrodynamic equipment. The basic concept simply consists of nozzle designs which induce the rapid growth of vapor-filled cavities within a relatively low velocity liquid jet. By proper adjustment of the distance between the nozzle and the surface being worked on, these cavities are induced after their growth to violently collapse on or near that surface in the high-pressure stagnation region where the jet impacts the solid material. Because the collapse energy of the cavitation field is concentrated over many very small areas at collapse, extremely high, very localized stresses are produced. This local pressure amplification provides the cavitating fluid jet with a great advantage over a steady noncavitating jet operating at the same pump pressure and flow rates.

During the past few years, an entirely new generation of cavitating jet nozzles has been developed, motivated initially by our ongoing effort to find improved nozzle designs for augmenting the action of deep-hole drill bits. These "self-resonating" cavitating nozzles, known as STRATOJETs (see Fig. 1b), have proven to be substantially more erosive than what we are now calling the "conventional" CAVIJET nozzles for situations which involve submerged cleaning or cutting, as in this demilitarization application. Here advantage is taken of the natural tendency of the shear layer of a jet to structure. By hydroacoustical resonance, large vortical motions concentrated in "organized structures" at the periphery of the jet are induced. This has the advantage of generating a very early cavitation inception (e.g., at 2.5 times lower jet velocities for the same submergence conditions) and therefore a higher degree of erosion for the same cavitation conditions.

2. DESCRIPTION OF SYSTEM

2.1 General Description

Schematic drawings of the CAVIJET demilitarization system are shown in Figs. 2 and 3. Some of the principal system units are shown in Figs. 4 to 10. Note that only the components which come in direct contact with HE are located in the Process Room. The control and power units are placed at any convenient remote location outside the room which contains the munitions. Once the warhead or motor is placed within the Washout Unit, an operator runs the system and monitors the cleanout action from the Control Console, which can be at any desired distance or position for safety. If desired, a robot can be used to place palletized warheads into the Washout Unit. This allows for a faster operation, with an operator only required to enter the Process Room after cleanout of a complete pallet instead of after each shell is cleaned.

The effluent (water, with particles of explosive or propellant) flows out of the Washout Unit, and the HE particles are then separated and filtered out of the water in a series of steps. The water is then recirculated back to the high pressure water pump and reused. This water reuse process therefore greatly minimizes the treatment costs associated with preparing "once-through" water for disposal in a municipal sewer system.

2.2 Safety Features

The CAVIJET demilitarization system has been designed to inherently minimize the chances of either overstressing or heating the explosive materials. In addition, the system is operated by remote control, and contains a number of interlocks which will automatically shutdown the system if operator errors or component failures should occur.

To maximize safety, this CAVIJET washout system:

- Operates at up to one-half the pressure required by conventional water jet methods.
- Utilizes jet velocities well below the levels capable of detonating explosive materials.
- Provides man-in-the-loop observation and sequence-decision-making to allow shut-down, if needed, well in advance of potential problems (caused, for instance, by failures in water or air supplies).
- Is a fully integrated facility, with built-in safety interlocks to provide automatic high-pressure water diversion in case of system or operator errors.
- Has only stainless steel, brass, or plastic materials in contact with water containing explosive particles; is fully grounded; and uses plastic or other nonsparking materials such as nylatron overlays at any machine locations where impact-sparking might occur.
- Maintains a "fully flooded" mode within the shell, motor, or bomb being cleaned, thus providing a safer, more efficient, foam-free explosive-removal process.
- Uses only hydraulic and pneumatic actuators to control and move components in Process Room.
- Has sensors and transducers of the intrinsically safe design.

3. SYSTEM COMPONENTS

3.1 CAVIJET Washout Unit

This unit is shown in the drawing in Figure 4 and the photograph in Figure 5. The principal parts of this unit are: the CAVIJET cutting head; the lance and its drive and control components; the shell rotation subsystem; and the effluent control and removal components.

3.1.1 CAVIJET cutting head - this head contains three self-resonating cavitating jet nozzles. The positioning and orientation of these three nozzles was established after a development effort (Ref. 6), which led to the present design. Two nozzles face forward, to cut away

successive segments of explosive. The third nozzle is aimed backward, to clean off any remaining residues on the shell wall, and to cut up any chunks that are too large to escape from the shell. The jet thrusts are balanced, so that no net lateral loading is felt by the lance.

3.1.2 Lance components - the high pressure water is fed to the cutting head via the lance, a segment of stainless steel, smooth-walled, one-inch diameter high pressure pipe (Item 3, Fig. 4). The lance is caused to translate by two hydraulic cylinders (Item 6, Fig. 4). The stroke length for these cylinders is controlled by a pair of sealed, Reed-type switches, which are magnetically coupled to a steel piece at the tip of one hydraulic cylinder. The positions of these stroke-limiting switches are preset for each size of munition to be cleaned. The stroke of the cutting head is automatically reversed at a position which is typically an inch or more from the shell base. At the end of the withdrawal stroke, the system automatically stops the lance, and diverts the water flow away from the washout unit. Further discussion of the operating sequence is in Sec. 4.

3.1.3 Shell rotation - a hydraulic motor rotates the shell. The base of the shell is clamped by a soft-plastic insert in the shell base holder (Item 8, Fig. 4). The entire shell rotation subassembly is mounted on a sliding table (Item 15) which is moved by a hydraulic cylinder (Item 13). To clamp the shell in place, preparatory to rotation, the operator activates the hydraulic control valve (Item 12), which slides the shell-base holder over the shell-base.

3.1.4 Effluent control and removal - all effluent (water and explosive particles) are kept fully contained during and after the washout cycle. This is accomplished by a molded soft-plastic shell-nose holder (Item 9) which seals around the shell nose. The effluent escapes around the lance and out of the shell during the washout cycle, thence through the hollow shell-spindle bearing block (Item 10), and into a large tee which connects to the effluent-removal hose (Item 11). The effluent flows through this hose to the Settling Tank (see Fig. 3).

3.2 Control Console

Once the shell (or motor) has been placed into the washout unit, and secured into the ready-for-rotation position, all further operations are performed via the remote control console (Figs. 7, 8). This console has the controls for turning on the system, starting and stopping the rotation of the shell and the feed of the lance, and an emergency interrupt which will stop all functions and divert the water flow away from the washout unit. Readouts on the control panel include: pump pressure, differential pressure across the final filter unit (Sec. 3.4.5), and status indications for water flow, operating pressure, and lance retraction.

In case of loss of water pressure during the cleaning cycle, the system will automatically stop the forward feeding of the lance and shut down all controlled functions. This safety feature assures that the cleaning head cannot be driven into contact with the explosive if no erosive jetting is occurring.

3.3 Hydraulic Power Unit

This unit provides the hydraulic oil flow to the cylinders and motor discussed in Sec. 3.1. Included is an electric motor, hydraulic pump, oil sump, flow and pressure control valves, and automatically-actuated solenoid valves which sequence the feed and retraction of the lance. Timers which control the automatic purge valves for the centrifugal separators (Sec. 3.4.3) are also housed here.

3.4 Effluent Treatment Units

A multistep approach is used to separate the particles of explosive (or propellant) from the process water, so that this water can be recirculated back to the high pressure water pump. Refer to the schematic in Fig. 3 for the positioning of the several effluent treatment units.

3.4.1 Transfer pumps - air-powered, diaphragm type pumps are used to transfer the explosive-laden water through each part of the system.

3.4.2 Settling tank - the effluent enters this tank directly from the washout unit. Baffles and a mesh basket are used to trap the larger particles and many of the finer particles.

3.4.3 Centrifugal separators - a two-stage, passive separator unit (Fig. 9) is used to remove particles larger than 325 mesh (44 microns). The sludge which builds up in the collection chambers of this unit are periodically purged by air-actuated valves. These valves are programmable to open at desired intervals, for any required purging duration.

3.4.4 Water reservoir - this tank is used to store the system water, and to allow settling of fine particles. Some radiative cooling is also achieved at this reservoir. Makeup water, as required, is added to the system here.

3.4.5 Final filter unit - this cartridge type filter (Fig. 10) removes all particles larger than 5 microns, thus rendering the water suitable for reuse in the system. A differential pressure transducer across this unit provides a readout on the control console. Thus, the operator is advised when it is time to replace the cartridge filter elements.

3.4.6 Water chiller (optional) - under certain conditions it may be necessary to include a chiller in the system to remove the heat imparted to the water by the 150 hp high pressure pump.

3.5 High Pressure Pump Unit

The pump which supplies high pressure water to the CAVIJET cutting head may be driven by either an electric motor (as shown in Fig. 6) or a diesel engine. Typical pump specifications are 5,000 psi at 38 gpm flow rate, which requires a 150 hp (112 kW) prime mover. Features of this unit include an automatic pressure relief valve to prevent inadvertent overpressurization in the system; automatic shutdown in the case of loss

of feedwater, to prevent pump damage due to cavitation; and a remotely actuated diverter valve which controls water flow either to the washout unit, or (in the normally-open-mode) to a low-pressure dump line.

4. OPERATIONAL STEPS

The following steps briefly outline the operation and safety-interlocks of the system:

4.1 Shell Placement and Securing

One operator places the shell (or motor) into the washout unit, and clamps it into position. (NOTE: shells and bombs are rotated in this system. However, missile and rocket motors are clamped in a fixed position. In this case, the CAVIJET cutting head is rotated.) The operator then leaves the Process Room.

4.2 Initiation of Operations

After TV verification that the shell is in position and the process room is cleared of personnel, the control room operator then pushes the "ROTATION" start button which causes the projectile to begin to spin. the "LANCE FEED" start button is then pushed, causing the lance to begin to translate forward towards the shell. If there is a problem at any point in the operation, a red "EMERGENCY STOP" button can be pushed to stop all controlled functions.

4.3 Automatic Sequencing

The lance will feed into the shell until it first activates the high pressure water diverter valve and the "WATER" light comes on. This valve is automatically activated by a Reed-type switch of the same type as used to control the stroke-length for the lance. When the required pressure is achieved in the system, the "RATED PRESSURE" light will go on. Thereafter, should this pressure drop, e.g., due to loss of feed water to the pump, then an automatic shutdown of all functions will occur.

When the lance reaches the preset position of full forward travel into the shell, it automatically reverses, and retracts until reaching the full retraction position. The "LANCE RETRACTED" light then comes on to signal the operator that the cleanout is completed. Note, the water is automatically diverted away from the unit near the end of the lance retract sequence; the same switch accomplishes both the water on and off functions.

4.4 Completion of Cycle

The control room operator then pushes the "ROTATION AND FEED STOP" button to stop the shell rotation. At this time, the operator can enter the process room, unclamp the cleaned shell and replace it with the next shell to be cleaned.

5. CONCLUDING REMARKS

A safe and efficient system is now available to replace the slow and costly steam-out or melt-out methods for removing high explosives from shells and bombs. This CAVIJET demilitarization system can also be used to remove solid propellant materials from missile or rocket motors. Studies have demonstrated the inherent safety of this cavitating water jet system, which operates at one-half the pressures required by conventional water jet equipment. Using remote controls, and built-in safety interlocks, the CAVIJET method can, for instance, remove the 16 pound load of HE in a 155 mm warhead in well under two minutes.

6. ACKNOWLEDGMENTS

The following Tracor Hydronautics staff members participated in the design, fabrication, assembly, or documentation of the equipment described in this paper: George Arrington, Paul Bolander, John Bosque, Dale Dahlheimer, Roger Dorsey, Gary Frederick, Michael Gracey, Kae Guy, Herbert Hickey, Blair Holtschneider, Cal Lockner, George Matusky, Gary Poquette, Donna Vanek, and Ronald Watson. The author expresses deep appreciation to each of his coworkers -- needless to say, it couldn't have been done without you.

7. REFERENCES

1. Conn, A. F. and Rudy, S. L., "Development of a CAVIJET™ System for Removing Missile Propellants," Hyronautics Incorporated Technical Report 7446-1, February 1975.
2. Conn, A. F., Wechsler, L., and Rudy, S. L., "Field Trials of a CAVIJET™ System for Removing Missile Propellants," Hydronautics, Incorporated Technical report 7446-2, March 1976.
3. Conn, A. F. and Rudy, S. L., "Using Cavitating Water Jets for Demilitarization," Proceedings of the Symposium on Demilitarization of Conventional Explosives, ADPA, April 1976.
4. Conn, A. F. and Rudy, S. L., "Using Cavitating Water Jets for Demilitarization," Proceedings of the Seventeenth Explosives Safety Seminar, Denver, September 1976.
5. Conn, A. F. and Krajkowski, E. A., "Explosive Removal with CAVIJET™ Cavitating Water Jets," Proceedings of the Eighteenth Explosives Safety Seminar, San Antonio, September 1978.
6. Conn, A. F., Krajkowski, E. A., and Shapira, N. I., "Using the CAVIJET® Process to Remove Explosives from Army Munitions," Proceedings Second Demilitarization and Disposal Technology Conference, ADPA, pp. 38-40, April 1979.

7. Conn, A. F., Liu, H. L., Frederick, G. S., and Rudy, S. L., "Removal of Explosives from Projectiles Using CAVIJET® Cavitating Fluid Jets," Hydronautics, Incorporated Technical Report 7723-1, August 1979. (Also ARRADCOM Contractor Report ARLCD-CR-79015, with E. A. Krajkowski).
8. Lindenmuth, W. T., Conn, A. F., and Aymar, R. H., "Demonstration of Explosive Removal from Projectiles Using CAVIJET® Cavitating Fluid Jets," Hydronautics, Incorporated Technical Report 7984-1, January 1981.

APPENDIX A

DEVELOPMENT OF THE CAVIJET DEMILITARIZATION SYSTEMS

During a series of studies conducted for the U.S. Army and Navy, it was demonstrated that cavitating water jets could safely and rapidly remove materials (explosives and propellants) from warheads and munitions. In each case lower pressures and/or energy-consumptions, relative to conventional water jet methods, were required. Some highlights of these projects are given in the following sections.

A.1 Explosive Removal

The effort involved in this project for the U.S. Army (see Refs. 7 and 8) required a series of laboratory trials which served to define optimum system and operating parameters, followed by retrofitting the cavitating jet technology into an existing water jet demilitarization facility at the Iowa Army Ammunition Plant.

During the first phase of this study, an extensive series of safety tests were conducted in order to establish the suitability of using the CAVIJET cavitating jet technology. Over 200 safety tests were run on samples of TNT and Composition B, as well as on Composition B-filled 105 mm shells. Pressures up to 68.9 MPa (10,000 psi) were used in these tests -- representing an over-pressure level more than double the 33.1 MPa (4,800 psi) required to remove these explosives from ammunition. No reaction of any kind occurred, and analyses of the results by the U.S. Army resulted in the acceptance of the CAVIJET method for U.S. Government demilitarization applications (Ref. 7).

The primary objective of this project for the U.S. Army R&D Command was to reduce the amount of energy required to remove TNT and Composition B explosives from warheads such as the 105 and 155 mm types. As may be seen from Table A-1, introduction of CAVIJET cavitating jet nozzles into the existing facility reduced the energy per warhead by 20.5 percent. We also satisfied several secondary objectives: (a) reducing the time required per warhead (a 31.9 percent improvement), and (b) reducing the operating pressure (a 52 percent reduction). The reduction in operating pressure, coupled with the energy and time savings, combined to reduce substantially the cost per warhead for this demilitarization operation.

A fourth objective, which was achieved by our redesign of the facility, was to eliminate the foam which had been created during ammunition washout by the Army's existing high-pressure water jet method. The creation of copious quantities of foam by their facility had caused the Army to virtually abandon its use because of the hazardous handling required. We designed a water-filled shell-handling and washout method which, combined with the substantial reduction in jet velocity afforded by the CAVIJET method, served to virtually eliminate the air-water-explosive particle amalgam which had shut down the Army's washout facility.

Table A-1
Comparison of Explosive Removal with
Conventional and Cavitating Jets

Parameter	Existing Water-Jet System	Modified System with CAVIJET Nozzles
Energy required to remove 16 pounds of Composition B from 155 mm warhead	3.36 kW-hr	2.67 kW-hr
Time required	2.10 minutes	1.43 minutes
Operating pressure	10,000 psi (68.9 MPa)	4,800 psi (33.1 MPa)

Operating a water-jet system at a reduced pressure serves to decrease maintenance costs by extending the life of pump seals and packings, nozzles, and virtually any component in the high-pressure circuit. Lower pressure operation is also intrinsically safer in situations involving human error and/or component failure. In virtually every application we have investigated, it was possible with CAVIJET nozzles -- operating at reduced pressure relative to conventional nozzles -- to produce comparable or improved rates of cleaning or cutting. Conversely, operating the CAVIJET system at an equivalent pressure allowed for increased rates of production. The optimum choice of system parameters requires examination of all tradeoffs within the system's economic model.

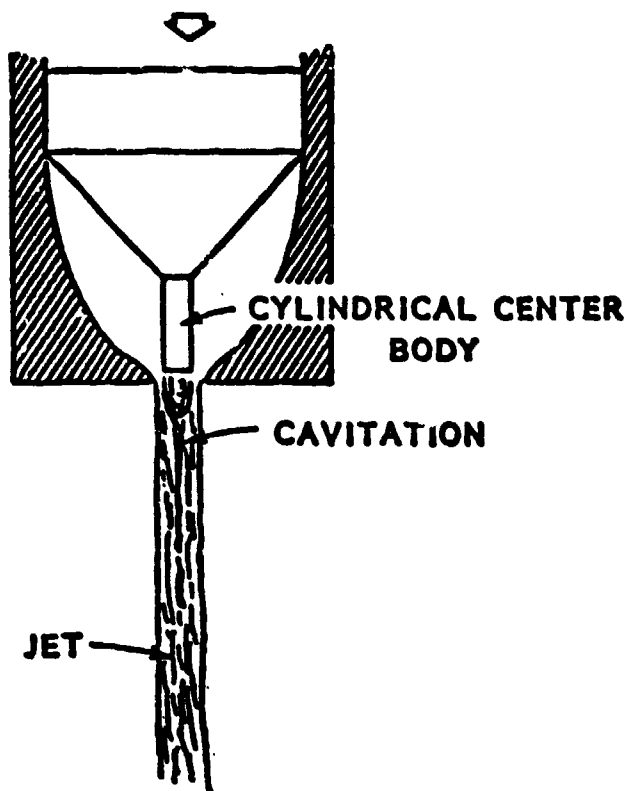
A.2 Solid Propellant Removal

This project which we conducted for the U.S. Navy required -- as with the U.S. Army project described in the previous subsection -- a development of optimum operating parameters followed by design of a retrofit of our CAVIJET technology into an existing water-jet propellant removal facility. This existing facility had been plagued by a number of problems, each related to system pressure: namely, rapid wear of nozzles and frequent shut-downs for replacement of pump seals and packings. As summarized in Table A-2, the introduction of a CAVIJET cleaning tool greatly improved the system performance.

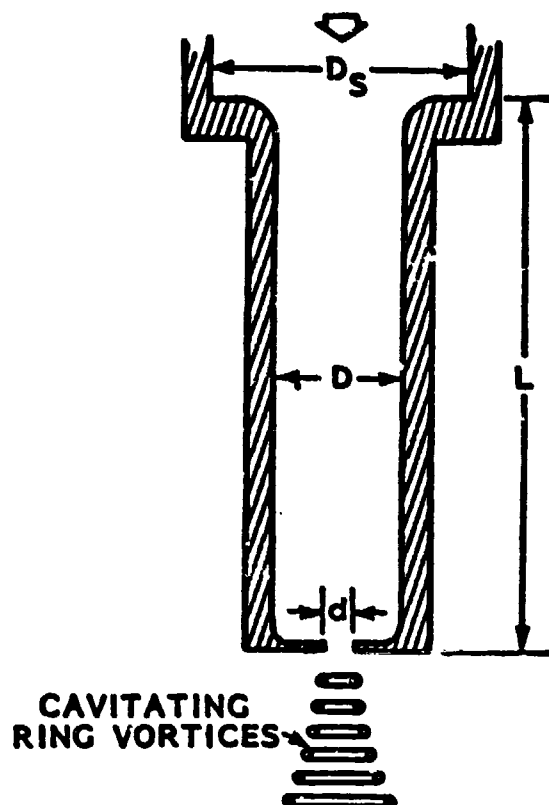
Table A-2
Comparison of Cleaning TARTAR Missile Motor
Casings with Conventional and Cavitating Jets

Parameter	Existing Water-Jet System	Modified System with CAVIJET Nozzles
Energy required to clean motor	351 kW-hr	117 kW-hr
Time required	3.0 hours	1.92 hours
Operating pressure	5,000 psi (34.5 MPa)	2,600 psi (17.9 MPa)

The CAVIJET technology was able to reduce the total energy required to clean a TARTAR missile motor to one-third of that needed with conventional, noncavitating jets. The cavitating action allowed this motor to be cleaned at almost half the pump pressure and in over one-third less time. Furthermore, the larger orifice diameters of the CAVIJET nozzles served to minimize the probability of nozzle-clogging, which had frequently occurred with the previous, smaller-nozzle system, causing blowouts of seals and pump packings due to excess pressure pulsations.

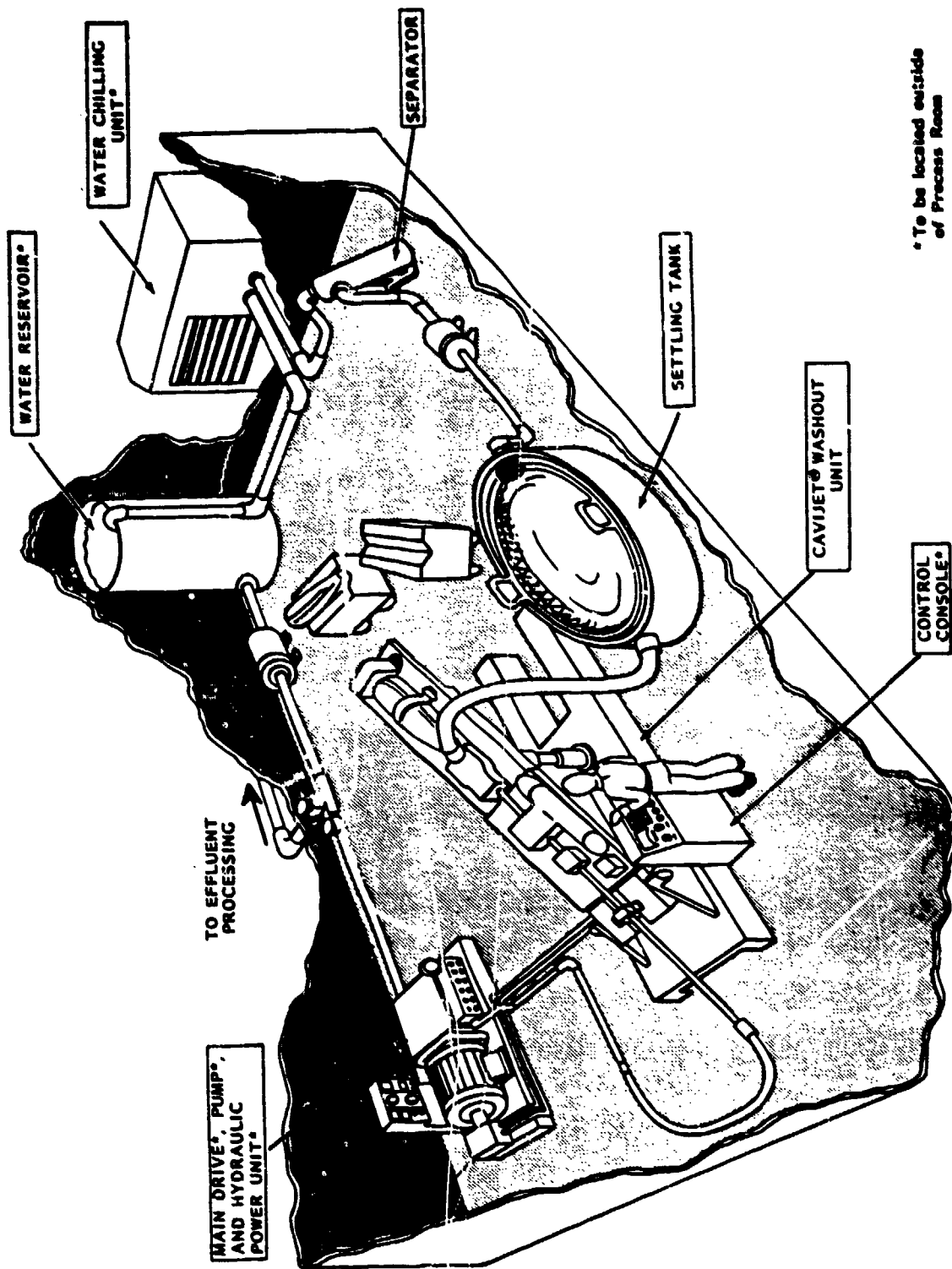


- a. **CENTERBODY CAVIJET®**; This nozzle system induces cavitation by flow separation.



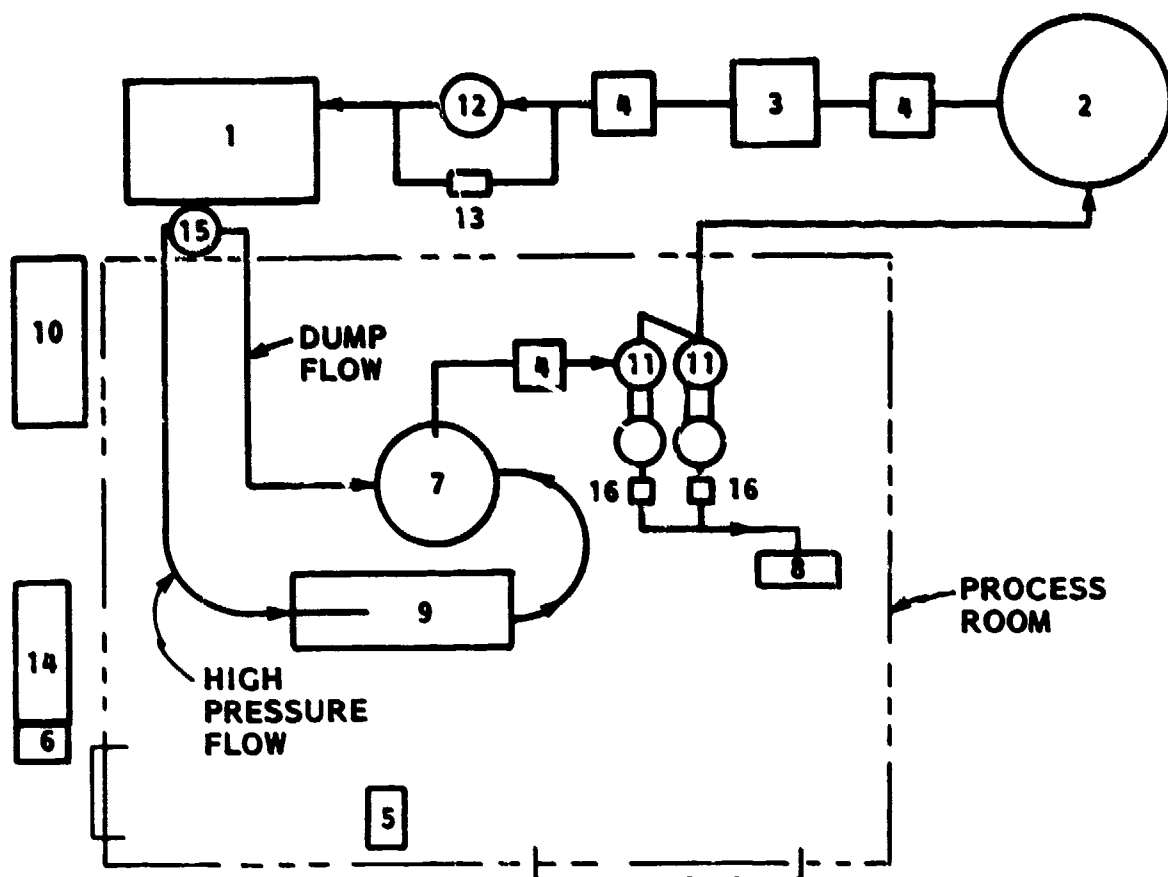
- b. **ORGAN-PIPE STRATOCJET**; This nozzle creates a series of structured vortices by internal, resonant self-modulation of the jet pressure.

FIGURE 1 - EXAMPLES OF CAVITATING JET NOZZLE CONFIGURATIONS



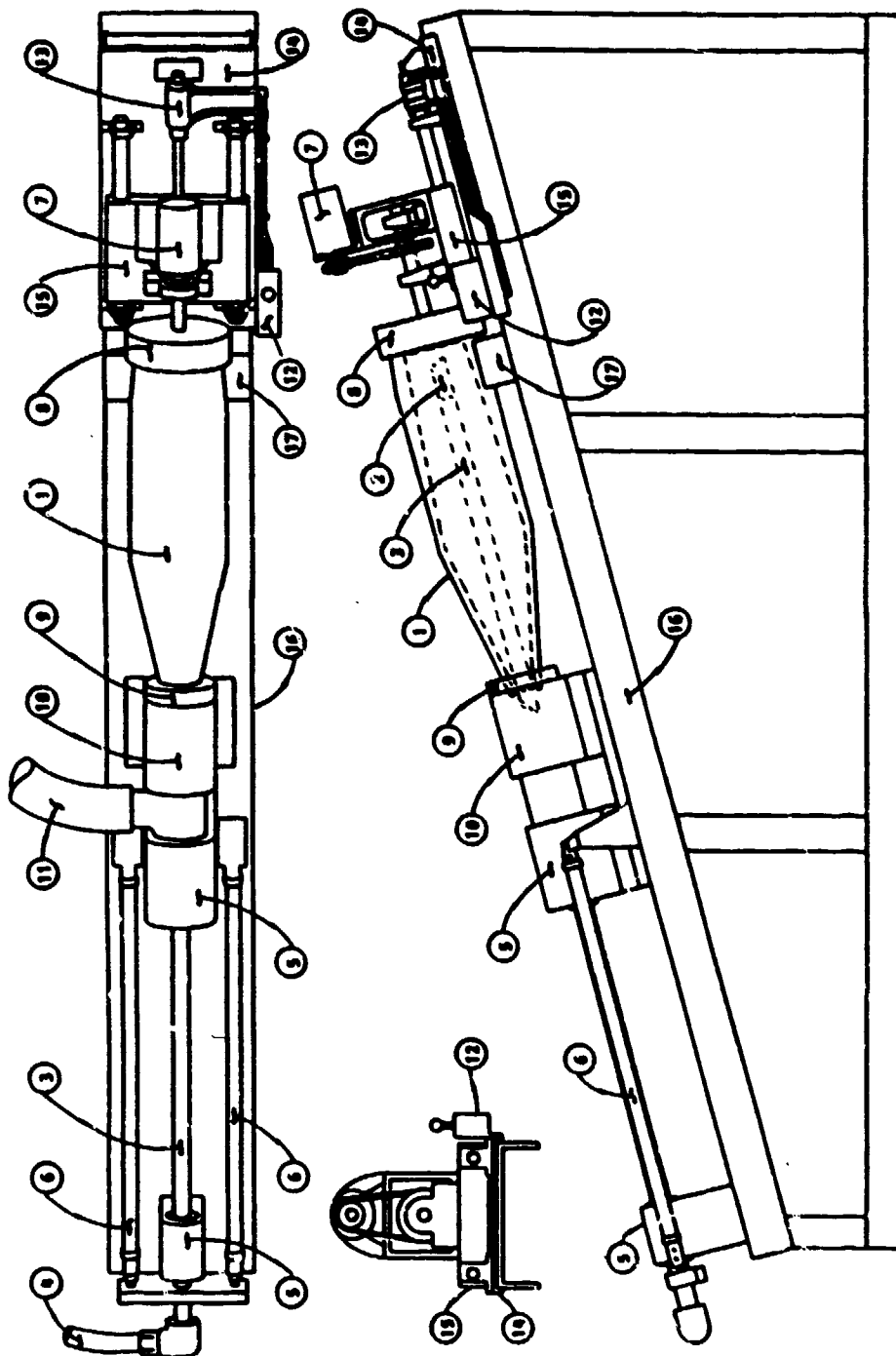
*To be located outside of Process Room

FIGURE 2 - CONCEPT DRAWING OF CAVIJET® DEMILITARIZATION FACILITY



1. HIGH PRESSURE WATER PUMP UNIT
2. WATER RESERVOIR
3. WATER CHILLER
4. AUXILIARY PUMPS (3)
5. T.V. CAMERA
6. T.V. MONITOR
7. SETTLING TANK WITH BASKET
8. SLUDGE CONTAINER
9. CAVIJET WASHOUT UNIT
10. HYDRAULIC POWER UNIT
11. CENTRIFUGAL SEPARATORS
12. FINAL FILTRATION
13. FILTER PRESSURE TRANSDUCER
14. CONTROL CONSOLE
15. DIVERTER VALVE
16. AUTOMATIC PURGING VALVES

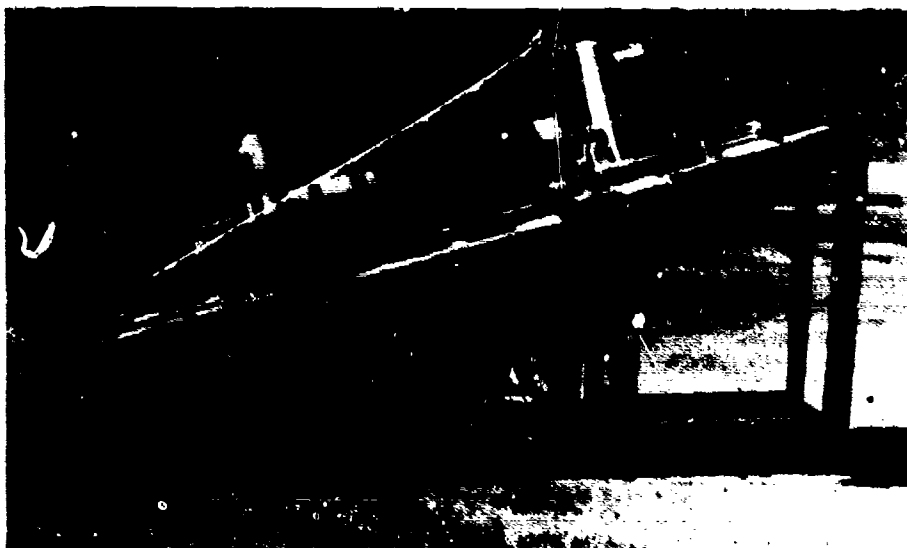
**FIGURE 3 - SCHEMATIC OF SYSTEM COMPONENTS IN CAVIJET®
DEMILITARIZATION FACILITY**



COMPONENTS LIST:

1. Shell to be cleaned
2. CAVIJET cutting head
3. Lance
4. High pressure water supply hose
5. Lance bearing blocks
6. Lance-feed hydraulic cylinders
7. Shell-rotating hydraulic motor
8. Shell-base holder
9. Shell-base holder (replaceable for each shell type)
10. Shell-rotating hydraulic motor
11. Shell-rotating hydraulic motor (replaceable for each shell type)
12. Bearing block for shell-rotating hydraulic motor
13. Effluent-removal hose
14. Control-valve for shell-clamping cylinder
15. Shell-clamping hydraulic cylinder
16. Movable table (manually set for each shell type)
17. Sliding table, for shell clamping
18. Main-bed plate
19. Guide (replaceable for each shell type)

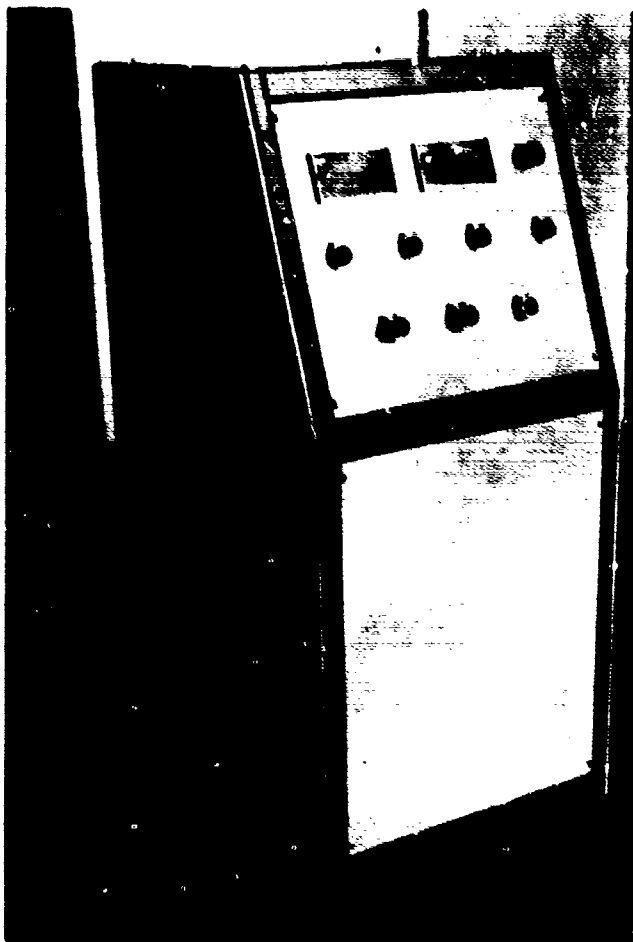
**FIGURE 4 - CAVIJET® EXPLOSIVE WASHOUT UNIT -
LAYOUT AND LIST OF COMPONENTS**



**FIGURE 3 - CAVIJET • WASHOUT UNIT - with 155mm
warhead in position for washout**



**FIGURE 6 - HIGH PRESSURE WATER PUMP UNIT - shown
is the 150 hp electric motor driven design,
skid-mounted, with motor controller, feed-water
tank and diverter-valve assembly**



**FIGURE 7 - CONTROL CONSOLE -
for remote control and
monitoring of system
functions**

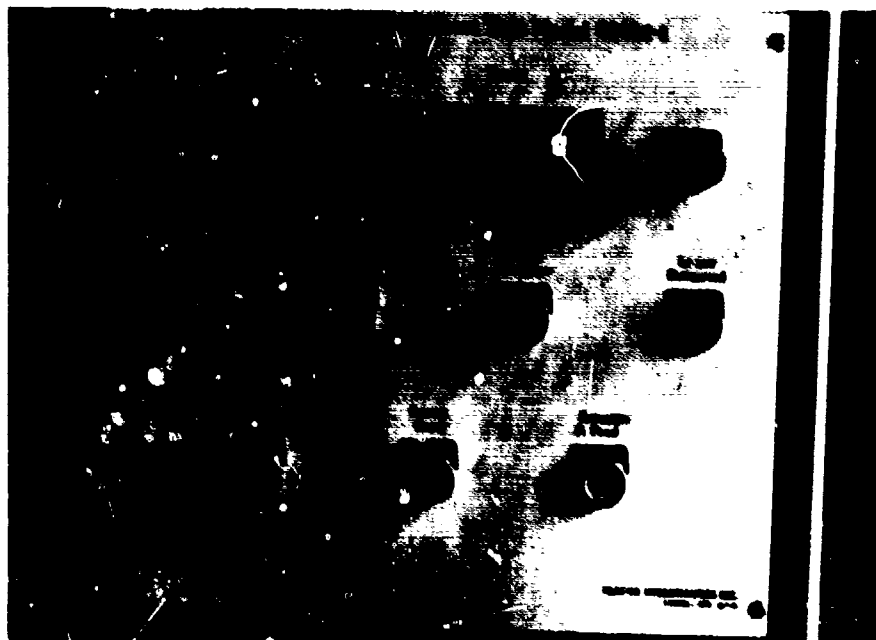
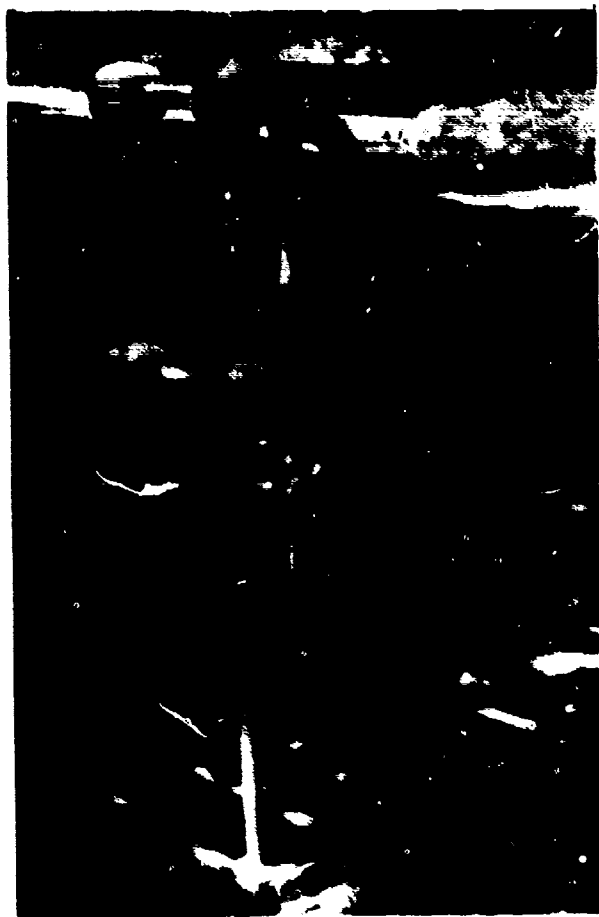
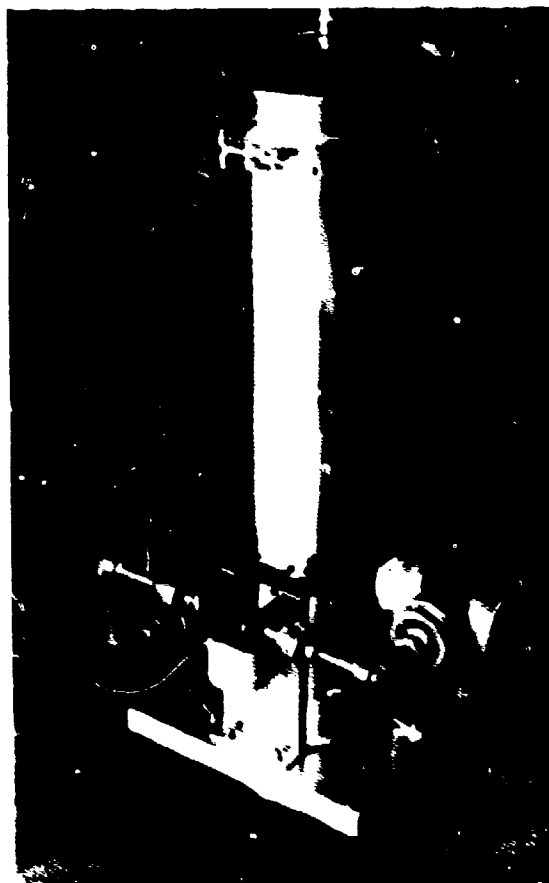


FIGURE 8 - CONTROL PANEL
2148



**FIGURE 9 - CONTRIFUGAL SEPARATOR -
with automatic, timed purge
valves**



**FIGURE 10 - FINAL FILTER - cartridge
elements for 5 micron
particles; with differential
pressure transducer (read-
out is on Control Console)**

AD-P005 392

IDENTIFICATION AND CHARACTERIZATION OF EMISSIONS AND
AND RESIDUES FROM OPEN BURNING AND DETONATION OF MUNITIONS

by

MARK M. ZAUGG
DIRECTOR FOR AMMUNITION EQUIPMENT
TOOELE ARMY DEPOT
TOOELE, UT 84074-5004

ABSTRACT

This paper presents background and information about the ongoing study to sample air emissions and soil residues from open burning and open detonation operations. Test methods are presented along with summary of the project status.

INTRODUCTION

Passage and implementation of the Environmental Protection Act (EPA), Clean Air Act (CAA) and Resource Conservation and Recovery Act (RCRA) have brought increasing pressure by state and federal environmental protection agencies on open burning and open detonation (OBOD) operations at Department of Defense installations. In the mid 1970's, the Army initiated plans to construct several incinerators to minimize the need for OBOD operations, as part of the Army Pollution Abatement Program. Since 1980, five Explosive Waste Incinerators (EWI), and eight Contaminated Waste Processors (CWP) have been installed at various Army installations. However, operational experience has proven that disposal of munitions using incinerators, including the existing deactivation furnaces, is more costly than using OBOD operations.

In view of the increased competition for funds with demilitarization generally having lowest priority for funding, the most economical method of demil consistent with environmental policy, must be available to destroy the growing stocks of munitions awaiting disposal. However, actual data to prove/disprove that OBOD is/is not a polluting method of disposal was limited. For this reason, four projects have been conducted, starting as early as 1980, to evaluate the environmental impact of OBOD operation. They include two studies by the U.S. Army Environmental Hygiene Agency of soil residues and analyses of ground water at OBOD sites, a study of parameters affecting migrations of residues by U.S. Army Toxic and Hazardous Materials Agency, and a study of emissions from OBOD operations.

DISCUSSION

The latter project, the Identification and Characterization of Emission and Residues from Open Burning and Detonation of Munitions was begun in November 1983 by the Ammunition Equipment Directorate (AED) at Tooele Army Depot (TEAD), Utah, under funding and guidance from U.S. Army Armament, Munitions and Chemical Command (AMCCOM). Purposes of the study are to obtain actual OBOD emissions data for use in:

1. Supporting development of standards and regulations that DOD will propose to state and federal EPAs for adoption, to permit and control OBOD sites.
2. Supporting the preparation of OBOD permits.
3. Negotiating with state EPAs for obtaining/renewing OBOD permits for DOD installations.

Published theoretical calculations of OBOD products, and results from small scale tests conducted by Battelle Columbus Laboratories inside of a detonation chamber in 1980-1982 were used as a starting point for the project. The tests planned for in the study have been conducted at Dugway Proving Ground (DPG), Utah, with the support of DPG personnel, under the project management and direction of the U.S. Army Armament, Munitions and Chemical Command (AMCCOM), technical direction of the U.S. Army Environmental Hygiene Agency (USAEHA), with consultation of the Environmental Protection Agency at Research Triangle Park for quality and audit assistance.

The Navy is providing assistance in computer model development to predict emissions from OBOD operations.

TEST SUMMARY

Thirty-two tests have been conducted during the period of 19 November 1985 to 13 August 1986. In general, tests where ammunition and explosives were detonated involve five different size detonations, 100 lbs., 500 lbs., 1,000 lbs., 2,000 lbs., and 5,000 lbs. Propellant burns, in general, involve burns of 5,000 and 10,000 lbs. quantities. A summary of the tests and test items is shown in Table 1. It should be noted that some of the earlier test items were repeated to gain confidence in and better validate the data by having repetitions for comparison. In all cases, weight of explosive includes weight of explosive in the munitions or bulk being tested, plus weight of booster and initiator explosive.

A UH-1H helicopter provided by the U.S. Army Aviation Development and Test Activity, Ft. Rucker, Alabama, has been equipped with air sampling and monitoring equipment for collecting data from the plumes produced from the above tests.

Air samples are drawn into a sampling manifold through a 20 ft. long probe which extends forward of the helicopter. The instruments and equipment collecting data are of two types, real time/direct reading instruments, and air sample collecting equipment. Data output from direct reading instruments is recorded as millivolt readings onto an on-board computer which records the millivolt output of each instrument every 0.5 seconds. The time of helicopter entry and exit from the plume is also recorded on the computer. A list of information recorded real time by the computer is shown on Table 2.

In addition to information from direct reading instruments, air samples are collected with an evacuated cylinder, a Volatile Organic Sampling Train or VOST and a bulk particulate filter. These samples have been sent to three separate laboratories for analysis. The evacuated cylinder that has been used for all but last test is a 2.8 l stainless steel canister. Attempts are being made to collect a larger bulk air sample of approximately 100 l to increase lower detection levels in the plume. The VOST consists

Table 1
SUMMARY OF PHASE I TESTS

<u>Date</u>	<u>Item</u>	<u>Tests Quantities in lbs.</u>
19 Nov 1985	Bulk TNT	100, 500, 1000, 2000, 5000
11 Dec 1985	Bulk TNT	100, 500, 1000, 2000, 5000
12 Dec 1985	Bulk Explosive D	100, 500, 1000, 2000, 5000
22 Jan 1986	Bulk Explosive D	100, 500, 1000, 2000, 5000
22 Jan 1986	3.5" Rockets (Comp B)	100, 500, 1000 *1
5 Mar 1986	Bulk Comp B	100, 500, 1000, 2000, 5000
16 Apr 1986	MK 54-1 Depth Bombs (HBX)	250, 495, 990, 1985, 4950 *3
16 Apr 1986	M82 500 lb Bombs (tritonol)	100, 500, 1000, 2000, 5000 *3
12 May 1986	MK 4-0 Depth Charge (HBX)	95, 500, 1000, 2025, 5010 *3
12 May 1986	Hand Grenades (TNT)	100, 500, 1000, 2000, 5000
14 May 1986	MK 4-0 Depth Charge (TNT)	100, 500, 1000, 2000, 5000 *3
14 May 1986	50mm M71 Projectiles (TNT)	100, 500, 1000, 2000, 5000
14 May 1986	M26E1 Propellant	5440, 10560
16 May 1986	MK 16-6 Torpedo Warhead (HBX)	643, 643, 1286, 1929, 5144 *3
16 May 1986	Propellant SPDF	5333, 10667
21 May 1986	Propellant SPCF	5000, 10000 *4
21 May 1986	Military Dynamite	100, 500, 1000, 2000, 5000
22 May 1986	Navy Manufacturing Waste	2677, 5329
29 May 1986	Bulk Explosive D	100 *2
4 Jun 1986	Bulk Explosive D	100, 500, 1000, 2000, 5000
4 Jun 1986	Bulk TNT	100, 500, 1000, 2000, 5000
5 Jun 1986	Propellant SPD	5333, 10666
5 Jun 1986	3.5" Rockets (Comp B)	100, 500, 1000, 2000, 5000
5 Jun 1986	175mm Projectiles (TNT)	92, 488, 1005, 2010, 5025
5 Jun 1986	Bulk Comp B	100, 500, 1000, 2000, 5000
10 Jun 1986	M30 Propellant	4915, 9830
10 Jun 1986	MK 82 500 lb Bombs (H6)	100, 500, 1000, 2000, 5000 *3
17 Jun 1986	MK 81 250 lb Bombs (H6)	192, 576, 960, 1920, 4992 *3
17 Jun 1986	M10 Propellant	5333, 10666 *4
17 Jun 1986	5"/38 Projectiles (Expl D)	100, 500, 1000, 2000, 5000
1 Jul 1986	Bulk Explosive D	100, 500, 1000, 2000, 5000
1 Jul 1986	5"/38 Projectiles (A3)	100, 500, 1000, 2000, 5000
13 Aug 1986	90mm M71 Projectiles (TNT)	100, 500, 1000, 2000, 5000 *5

Table 1 (cont'd)
SUMMARY OF PHASE I TESTS

- *1 Fragments from the 1000 lb. test ignited the 2000 lb. stack of rockets. Test was aborted due to subsequent helicopter mechanical problems.
- *2 Test aborted due to helicopter mechanical problems.
- *3 Quantities vary from the 100, 500, 1000, 2000, 5000 lb. quantities due to the fixed explosive of the item. Quantities of each item were used such that overall explosive weight would be as close to the 100, 500, etc., quantities as practicable.
- *4 Heat generated from initial burn resulted in ignition of second propellant train resulting in a single burn of the total quantity.
- *5. Munitions were buried under 12 feet of earth cover, except for 2000 lbs detonation, which was buried under 4 feet of earth cover.

Table 2

INFORMATION OBTAINED FROM REAL TIME/DIRECT READING INSTRUMENTS

Altitude (feet above ground level)
Sulfur Dioxide concentration (ppm)
Chlorine concentration (ppm)
Hydrogen chloride concentration (ppm)
Hydrogen cyanide concentration (ppm)
Nitric oxide concentration (ppm)
Nitrogen dioxide concentration (ppm)
Hydrogen sulfide concentration (ppm)
Carbon monoxide concentration (ppm)
Ozone concentration (ppm)
Hydrogen concentration (ppm)
Oxygen concentration (%)
Ammonia concentration (ppm)
Carbon dioxide concentration (ppm)
Temperature (°C)
Sampling Manifold Pressure (inches water)
Air speed of helicopter (knots)
Manifold velocity (ft/sec)
Relative humidity (%)
Time in the plume of each pass (sec)
Cumulative particle count in the following ranges:
 0.3- 0.5 microns
 0.5- 0.7 microns
 0.7- 1.0 microns
 1.0- 5.0 microns
 5.0- 10.0 microns
 >10.0 microns *

* Particles greater than 20.0 microns are removed with a Stokes Separator to avoid plugging of the sensor.

of two cartridges in series, one packed with conditioned XAD-2 resin and the other with XAD-2 resin and activated charcoal separated by a glass wool filter. Purpose for these sample methods is to detect organic species that may result from incomplete destruction of explosives or products of formation during the OBOD reaction.

In addition fallout trays are placed as close to the 5,000 lb. detonation as possible without them being overturned by the explosion. Throw out from the detonation and soil fallout after the detonation is collected in these trays. The soil fallout samples from the nine trays on each 5,000 lb. test are composited and homogenized into one sample which is sent for analysis. All of the above samples are analyzed for the presence of any of the items listed in Table 3, which includes RCRA listed hazardous materials.

Video records of each test are made such that the volume of the plume could be estimated for each pass of the helicopter. By combining the cloud volume with the measured concentration of each emission product, an estimate of the total quantity of the product emitted to the atmosphere is obtained. The accuracy of the estimate is limited to the accuracy of the cloud volume measurements and instrument detection capabilities of the emission product concentrations. This information will also aid in the prediction of down wind concentrations of each emission product measured.

Reduction of Data from Real-Time Direct Reading Instruments

Instruments selected for the study had to be portable and light weight due to the limited load carrying capacity of the helicopter. This limited the selection of instruments. The short sampling time available for each helicopter pass through the plumes created an additional major challenge in the determination of product concentrations. The majority of the instruments do not reach full steady state response for 25-30 seconds or longer (This is a problem not only of the instruments selected but of most other instruments that could have been used except for space and weight restrictions). Without a specific and unique calibration method, the instrument readings at shorter sampling times do not give accurate values of

Table 3

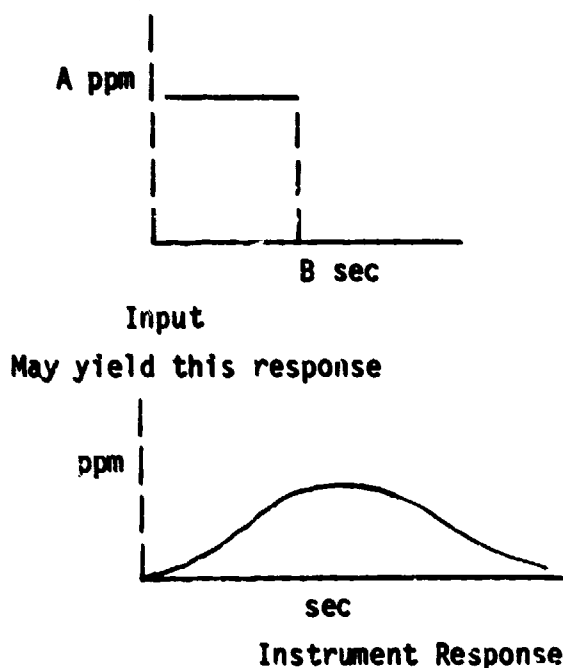
SPECIES TO BE ANALYZED IN FALLOUT PARTICULATES, VOST,
BULK FILTER PARTICULATES, AND SOIL SAMPLES

Acetophenone	Picric Acid
Ammonium Picrate	Polycyclic Aromatic Hydrocarbon
Aniline	RDX
Benzene	Tetryl
Dibutyl Phthalate	Toluene
Mono- and dinitrobenzenes	1,3,5-Trinitrobenzene
Mono- and dinitrophenols	2,4,6-Trinitrotoluene
Mono- and dinitrotoluenes	Arsenic and Compounds
Diphenylamine	Barium and Compounds
HMX	Cadmium and Compounds
Nitrocellulose	Chromium and Compounds
Nitroglycerins	Lead and Compounds
Nitroguanidine	Mercury and Compounds
PETN	Silver and Compounds
Phenol	Selenium and Compounds
Phthalic Anhydride	Carbon
Phthalic Acid	

the concentrations entering the instruments. To resolve this problem, AED personnel developed a five point calibration method which generates calibrated instrument response curves for sample times of 5, 10, 15, 20 and 30 seconds, with input gas concentrations of 0, 10, 20, 30 and 40% or 0, 20, 40, 60, and 80% of the full scale of the instrument.

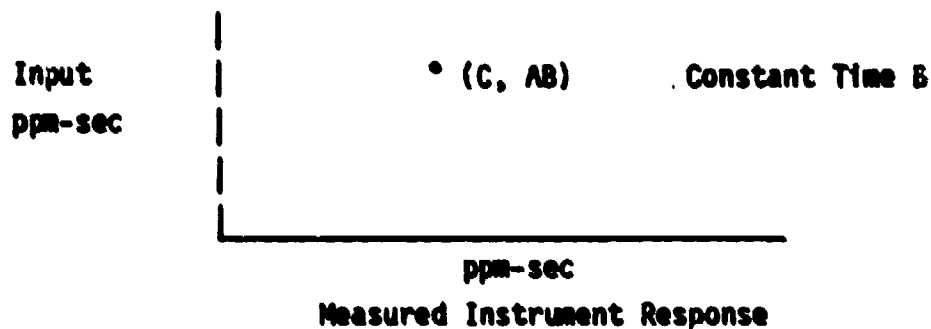
The resulting information recorded by the computer is a concentration curve rising from the background concentration to some point, then falling back to the background concentration with time. By integrating the area under the curve, a value of recorded concentration (in parts per million (ppm)) x time (seconds) is obtained. Plotting each measured concentration x time point versus the input concentration x time pulse that the calibrated input gas is fed to the instrument, a calibrated instrument response curve is generated. During plume sampling, the recorded concentration x time value can be compared to the calibration curve which corresponds to the length of time in the plume and the actual concentration determined.

For example, an input of A ppm for B seconds

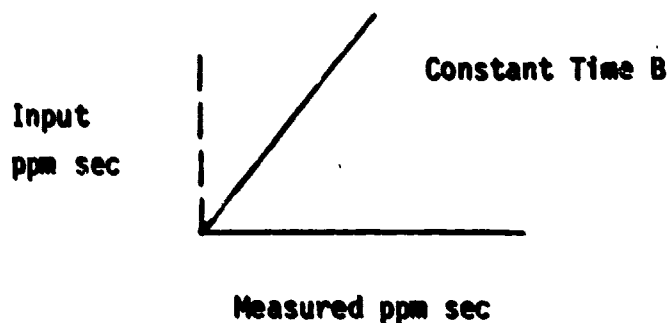


Integrating the area under the curve yields an input of $A \times B$ ppm-sec and an instrument response of some corresponding value C ppm-sec.

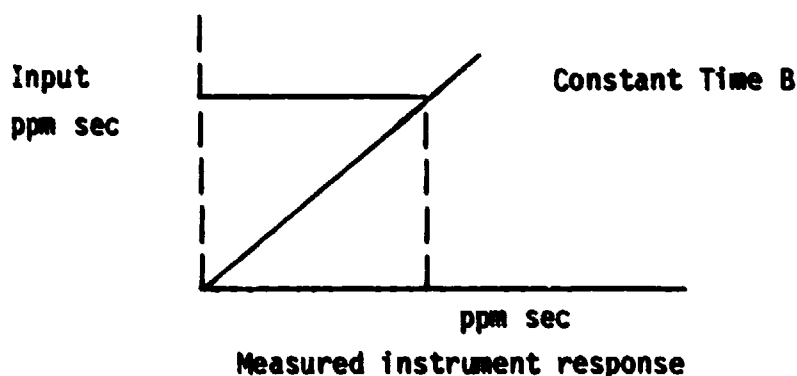
Plotting these values on an XY graph yields one point (C, AB) as follows:



Inputting a number of different concentrations over the same time B, yields a calibration curve for the time pulse B as follows:



For a sample time of B seconds in a plume, the measured instrument response can be found on the calibration graph and the input ppm sec determined from the curve as follows:



Dividing the input ppm-sec by the time B yields the true concentration in ppm that is in the plume for any particular helicopter pass. It should be noted that this would be an average concentration for that pass.

A computer program developed by AED personnel and programmed by a software consultant, takes the raw data from the instruments in millivolts, converts the millivolt readings to appropriate engineering units, i.e., ppm, temperature, ft/min, etc., integrates the areas under the concentration curves for the instruments measuring concentration, to yield the measured instrument response in ppm-seconds. The program then compares this value to the most recent calibration curve equations before and after the test, and the actual concentration in the plume for each pass is determined as explained above. The program has greatly reduced the time required to process the thousands of data points generated for each test and simplifies a very complex data reduction process.

PLUME VOLUME DETERMINATION

In order to determine the total quantity of a particular combustion/detonation product emitted from OBOD operations, it is necessary to compute the volume of the plume at a point in time when the concentration of that product is measured. Multiplying the concentration by the plume volume results in the total quantity of the product emitted.

Initial tests used two video cameras at fixed locations to record the detonations/burns and track the plume progression.

As efforts to calculate the plume volume progressed, it was determined that additional information was necessary to more accurately determine the volume. Two additional video cameras, four Auto-max film cameras and two thermal imaging cameras were added for all tests in June 1986 to obtain better plume data and permit more accurate plume tracking. Plume volumes are currently being calculated using the measured wind speed and direction to track the location of plume and hence determine the distance from the camera location to the plume. The irregularities in the plume shape and lack of good definition of plume boundaries, especially against backgrounds of other clouds, make the plume volumes difficult to measure accurately. Determination of plume shapes and sizes is subjective and will vary with the operator making measurements. Some variation will occur even when the same operator repeats the measurements as a quality control check. More refined, and hopefully more accurate, plume volume calculation methods and programs are being jointly developed by AED and DPG.

CONCLUSIONS

The data reduction, validation, and analysis have not progressed to the point of making exact statements about test results. However, the concentrations of emission products from OBOD of the munitions tested measured at approximately two minutes after detonation when the helicopter can safely enter the plume, appear to be well below levels generally considered as safe in places such as the occupational environment.

This information coupled with the results from the other three OBOD related studies indicate that OBOD of munition produces negligible impact on the environment while providing for safety and efficiency of operations.

TOMAHAWK (BGM-109 B/C-2) SYMPATHETIC DETONATION TESTING
AND HAZARD ARC DETERMINATION

By

Michael M. Swisdak, Jr.
Naval Surface Weapons Center
White Oak, Silver Spring, Maryland 20903-5000

ABSTRACT

The Naval Surface Weapons Center (NSWC) has previously conducted studies to determine the Explosive Safety Quantity Distance (ESQD) arcs associated with the handling of one BGM-109 TOMAHAWK missile. It has also examined the safety/vulnerability of the TOMAHAWK in Armored Box Launchers. The current study addressed the sympathetic detonation characteristics of pairs of TOMAHAWK missiles for several shipping/handling scenarios. The specific objective was the determination of the Maximum Credible Event (MCE) for TOMAHAWK cruise missiles in shipping/handling configurations. Pre-test predictions will be presented and discussed. Four tests were conducted. The results of these tests will be presented and compared with the pre-test predictions. Based on the results of these tests, a hazard arc is determined for handling up to four missiles simultaneously.

INTRODUCTION

The Naval Surface Weapons Center (NSWC) has previously conducted studies to determine the Explosive Safety Quantity Distance (ESQD) arcs associated with the handling of one BGM-109 encapsulated TOMAHAWK missile in its shipping container (on a truck).¹ This study (tests and analyses) indicated that a conservative estimate of an acceptable hazard arc was 500 feet. This is the currently accepted value, reported in Table 5-3 of Navy publication OP-5, Ammunition and Explosives Ashore.²

Subsequent to the adoption of this 500-foot value for one missile, the Joint Cruise Missile Project Office (JCMPO) raised the question and asked the NSWC to determine what an acceptable arc would be when handling up to four missiles. NSWC responded that the Maximum Credible Event (MCE) could be limited to one warhead detonation, provided the TOMAHAWKS were maintained in a side-by-side nose-to-tail configuration. The JCMPO then requested NSWC to consider non nose-to-tail situations. Based on this request, NSWC was tasked to determine (by testing with associated analyses) the sympathetic detonability for several "worst-case" handling scenarios. The specific objective for the NSWC effort was to determine the MCE for two submarine-launched BGM-109 TOMAHAWK cruise missiles with the WDU-25/B (formerly MK40 MOD 0 BULLPUP) warhead in shipping/handling configurations. Based on the results for two missiles, the four missile case could be calculated by analogy/extrapolation. With the MCE defined, a four missile hazard arc could then be determined.

ITEM DESCRIPTION

Missile. The item under test was the submarine-launched version of the BGM-109 B/C-2 TOMAHAWK cruise missile with the WDU-25/B warhead (formerly the MK 40 MOD 0 BULLPUP warhead). Figure 1a is a schematic of the all-up round, and Figure 1b is a sketch of the warhead. Previous analyses¹ had shown that only the warhead would be involved in the MCE determination. The solid propellant booster and the jet fuel did not contribute to the reactions. Therefore, for the purpose of these tests, only that part of the missile located in the vicinity of the warhead needed to be considered. Since complete TOMAHAWKS were not available for testing, the airframe and launch capsule had to be simulated. A previous NSWC study developed a detailed simulant for a TOMAHAWK missile. These simulant techniques were used on this study. Figure 2 is a sketch of the airframe simulant. On the real missile, the ring stiffeners are on the inside of the airframe. For the purpose of these tests, and as a cost savings, they were placed on the outside of the airframe. Thus, the forebody section simulant consisted of a BULLPUP warhead, surrounded by an externally stiffened aluminum cylinder of the proper thickness simulating the airframe. Figure 3 is a photograph of the airframe simulant being placed on the warheads.

Launch Capsule. Figure 4 is a sketch of the TOMAHAWK capsule. It was simulated for these tests with a steel cylinder having an 11/64" wall thickness.

Shipping Container. The shipping container used for this missile is the CNU-308 Shipping Container. Figure 5 is a simplified sketch of the container. As can be seen in this figure, the shipping container is not symmetrical. There are two steel rails, running along the sides of the container--these are not present in the top or the bottom. There is also a fiberglass support cradle below the launch capsule; this is not present on the sides or the top.

The fiberglass in the walls of the container was simulated with plexiglass of approximately the same density. Figure 6 is a photograph of one of the completed assemblies. The shipping container simulation in Figure 6 represents horizontal stacks (steel rail included).

SCENARIOS CONSIDERED

A previous study³ established that in nose-to-tail arrangements, the TOMAHAWK missiles would not sympathetically detonate. This can be seen in Figure 7 for two shipping containers/missiles. In a side-by-side nose-to-tail configuration, the donor warhead does not line up with anything detonable. Therefore, only nose-to-nose configurations were considered. Further guidance from the JCMPO limited the study to submarine-launched configurations (i.e., those containing a launch capsule). As was just illustrated, the shipping container is not symmetrical; i.e., it is not the same side-to-side and top-to-bottom. Assuming a nose-to-tail arrangement is not maintained, several configurations are possible:

- (a) Shipping containers stacked horizontally (side-by-side).
- (b) Shipping containers stacked vertically (one on top of another).

(c) Shipping container placed next to a launch capsule.

(d) Launch capsule placed on top of a shipping container.

Evaluation of these four arrangements leads to seven possible configurations which should be considered. These are detailed in Table 1.

TABLE 1 HANDLING CONFIGURATIONS CONSIDERED

<u>Number</u>	<u>Configuration</u>
1	SC* to SC (Side-by-Side)
2	SC to SC (Side-by-Side: Offset)
3	SC to SC (Vertical Stack - Top Initiation)
4	SC to SC (Vertical Stack - Bottom Initiation)
5	LC** to SC (Side-by-Side)
6	LC to SC (Side-by-Side: Offset)
7	LC to SC (Vertical Stack)

*SC is a CNU-308 shipping container.

**LC is the submarine launch capsule.

Configuration 1 represents two side-by-side shipping containers. Configuration 2 offsets one of the containers with respect to the other. This has the effect of misaligning the steel side rails and could affect the fragmentation characteristics. Configurations 3 and 4 represent vertical stacks of shipping containers (the difference being the point of initiation (upper or lower round)). In one instance, the fiberglass support is between the donor warhead and acceptor rounds. Configuration 5 is similar to Configuration 1, except that one missile is removed from its shipping container and the launch capsule is exposed. Configurations 6 and 7 are similarly analogous to Configurations 2 and 3 with one missile outside of its shipping container. Each of these configurations is shown schematically in Figure 8.

PREDICTIONS

Sympathetic Detonation. Each of the configurations listed in Table 1 were analyzed for sympathetic detonation using techniques developed as part of the Naval Explosives Safety Improvement Program (NESIP).^{4,5} The results are presented in Table 2.

The fragment induced pressures were calculated using a fragment velocity of over 7000 ft/s. This is the maximum fragment velocity in the primary beam spray as determined by arena test data. The fragment size was based on NESIP determinations that the average fragment has a thickness of 1/2 the case thickness for naturally-fragmenting munitions.

Based on these predictions and discussions with the JCMPD, Configurations 1, 3, 4, and 6 were selected for testing. It was felt that the predicted detonation cases did not require testing. Configuration 2 was not considered as much of a "worst case" as was Configuration 1.

Airblast. Airblast pressure-distance curves were predicted for both one and two warhead detonations. The predictions were made using the computer program UTE,⁵ with the following assumptions:

Explosive Weight:	470 pound TNT Equivalent
Case Weight:	560 pounds
Reflection Factor:	2.0 (surface burst)

The results of these calculations are presented in Figure 9.

TEST DESCRIPTION

Of the seven configurations presented in Tables 1 and 2, four were selected and tested. Each test consisted of one donor and one acceptor. Airframes, launch capsules, and shipping containers were simulated as needed for each test. The donor was detonated and the consequences of the detonation were determined. Airblast was measured at six positions along two radial lines on each test. High speed photography, with frame rates up to 44,000 pps, monitored each event. In addition the action of the acceptor on a steel witness plate was also observed.

MCE DETERMINATION RESULTS

Sympathetic detonation occurred for three of the four configurations tested. Configuration 1 did not sympathetically detonate; Configurations 3, 4 and 6 did. These findings were supported by three independent observations--witness plates, high speed photography, and airblast.

Configurations 3, 4, and 6. All three of these configurations behaved in a similar manner. Figure 10 is a post-detonation photograph of one of the witness plates (the three plates were indistinguishable).

The high speed cameras did not operate during the test of Configuration 3. On Configurations 4 and 6, the overhead cameras showed that the fireball from the donor reached the acceptor about 380 microseconds after first light. By 475 microseconds, the acceptor is engulfed in the fireball. At 500 microseconds, the acceptor begins to detonate. These detonation times are consistent with those reported by Ward⁶ for MK82 bombs, when the increased spacing present on these tests is taken into account.

The airblast measured on these three configurations was identical. The pressure data are also plotted in Figure 11 and compared with the pre-test prediction for a two warhead detonation.

Configuration 1. This configuration did not sympathetically detonate. The acceptor case was broken apart and pieces thrown about 900 feet. Three pieces representing almost the entire case were recovered. Figure 12 is a photograph of the largest case piece located.

The overhead photography showed the acceptor being engulfed by the fireball with no reaction.

The airblast also indicated only a single warhead detonation. The pressure-distance data are presented in Figure 13 and compared with the pre-test single bomb detonation.

MCE Summary. Three of the four selected scenarios which were predicted either to be marginal or to sympathetically detonate, did indeed detonate. The only configuration which did not detonate was the one containing steel channels along each side of the shipping container. Even though these channels were not entirely in the main beam spray, they effectively acted as shields or diverters for the acceptor warhead.

Based on the above described tests and analyses, the following are the MCEs for the various scenarios:

- (a) For all nose-to-tail configurations, the MCE is one warhead.
- (b) For nose-to-nose configurations with the shipping containers stacked side-by-side, the MCE is one warhead.
- (c) For nose-to-nose configurations with the shipping containers stacked vertically, the MCE is the number of warheads in the stack.
- (d) For nose-to-nose configurations with one missile removed from its shipping container, the MCE is the number of warheads in the stack for both horizontal and vertical stacks.

Thus, in order to maintain the MCE at one warhead, several options could be considered:

- (a) Insure by handling procedures/regulations that the missiles (either in or out of their shipping containers) are always maintained in a nose-to-tail configurations.
- (b) Modify the shipping container so that nose-to-nose vertical stacks are not possible. In addition, by rules/handling procedures insure that missiles outside their shipping containers are maintained in a nose-to-tail attitude with respect to other shipping containers.
- (c) By means of rules/handling procedures insure that nose-to-nose vertical stacks are never used, and that missiles outside their shipping containers are maintained in a nose-to-tail attitude with respect to their shipping containers.

Using a combination of options (a) and (c) the JCMPO felt that it could maintain the MCE at one warhead, even while handling four missiles. The question then to be determined was what the hazard arc should be for this operation.

FOUR-MISSILE ESQD ARC

A "worst-case" four-missile scenario was developed jointly with the JCMP0 and then examined.

Two TOMAHAWK missiles, in their launch capsules and shipping containers are loaded side-by-side in a nose-to-tail configuration on the bed of a truck. The truck is then driven onto the pier. As this is occurring, two additional TOMAHAWK missiles in their launch capsules are being removed from a nearby submarine and placed nose-to-tail in specially positioned chocks on the pier. When this operation is complete, the truck arrives--giving a total of four TOMAHAWK missiles on the pier simultaneously (there are two on the truck and two on the pier). All four are maintained in a nose-to-tail configuration. One of the missiles on the truck detonates. What is the associated Maximum Credible Event (MCE) and the explosive hazard quantity-distance (ESQD) arc?

As has been previously demonstrated, the MCE for a horizontal row of TOMAHAWK missiles maintained in a nose-to-tail configuration is one (1) warhead, regardless of the number of missiles. With this MCE, what are the potential debris sources? Obviously, the pieces of the donor missile/capsule/shipping container, as well as the truck on which it is sitting. The adjacent acceptor missile, even though it does not detonate, is close enough to the donor explosion to be a major source of debris. The two additional missiles sitting on the pier are spaced sufficiently far away from the detonation to not become major sources of debris. Certainly they will be thrown about. However, they will not fragment into large numbers of pieces and the pieces that are formed will not be thrown significant distances.

The ESQD arc for one missile in a launch capsule in a shipping container was determined experimentally by Ward several years ago. A re-examination of his results indicated that his scenario (one missile/launch capsule/shipping container on a truck) had an expected hazard range of 384 feet, with a value of 454 feet at the 95% Confidence Level. This was the basis for the 500-foot arc for the handling of one missile.

As part of Ward's original study, he analyzed in detail the debris which was recovered. This included cataloging each piece of debris as to source (warhead, capsule, airframe, shipping container, truck, etc.), material (steel or aluminum), final location, and whether or not each piece was hazardous.

A conservative approach to our scenario is the following: Use Ward's data for a one missile detonation on a truck, but double the fragment contribution from the airframe, launch capsule, and shipping container. When this is done, a new hazard range-distance relationship is obtained--one that has an expected value of 420 feet with a 95% Confidence Level value of 617 feet.

ESQD ARC DISCUSSION

The value of 617 feet obtained in this manner is very conservative. It assumes that the acceptor missile/shipping container will be broken up and thrown, just as if it had detonated. Obviously, this is not the case. The pieces of the acceptor missile would be larger and heavier, there would be

fewer of them, and they would not go as far. During the sympathetic detonation testing described above, a piece of the non-detonating acceptor warhead was thrown almost 900 feet. It should be pointed out that this was the only piece recovered, and represented only one hazardous fragment. Also in this test, the configuration was not nose-to-tail, but nose-to-nose.

For the four TOMAHAWK missiles on a pier with a truck scenario, the hazard arc should be taken as 600 feet. This is a rounding off of the 617 feet determined above. It must be remembered that this is a conservative estimate.

The use of a 600-foot ESQD arc when handling four TOMAHAWKS was recently proposed to the DDESB with the above test data and analyses as part of the back-up data package. It has been accepted by them and is currently being implemented.

REFERENCES

1. Ward, J. M., "Simulated TOMAHAWK Missile Handling Arc Test Results," Minutes of the Eighteenth Explosives Safety Seminar, Volume II, San Antonio, TX, 12-14 Sep 1978.
2. Ammunition and Explosives Ashore: Safety Regulations for Handling, Storing, Production, Renovation, and Shipping, NAVSEA OP-5, Volume 1, Fourth Revision, Change 12, 15 Oct 1984.
3. Swisdak, M., "ESQD Arcs for TOMAHAWK, HARPOON, ASROC, and PENGUIN," Formal presentation to the DDEGB, 13 Apr 1983.
4. Porzel, F. B., "Technology Base of the Navy Explosives Safety Improvement Program," Minutes of the Nineteenth Explosives Safety Seminar, Los Angeles, CA, Sep 1980.
5. Porzel, F. B., "Introduction to a Unified Theory of Explosions," NOLTR 72-209, 14 Sep 1972.
6. Ward, J. M., "Blast/Fragment Hazards Associated with the Accidental Explosion of a MK82 Bomb Pallet," Minutes of the Nineteenth Explosives Safety Seminar, Los Angeles, CA, Sep 1980.

TABLE 2 SYMPATHETIC DETONATION PREDICTIONS

CONFIGURATION	SEPARATION* DISTANCE (ft)	OVERPRESSURE IN ACCEPTOR			SYMPATHETIC DETONATION PREDICTION***
		DETONATION** THRESHOLD (Kbars)	SHOCK INDUCED (Kbars)	FRAGMENT INDUCED (kbars)	
1 ¹	1.4	25	17.2	21.3	Marginal
2 ¹	1.5	25	14.8	21.3	Marginal
3	1.9	25	9.6	20.6	Marginal
4	1.9	25	9.6	20.6	Marginal
5 ¹	0.9	25	40.5	22.7	Yes
6 ¹	2.1	25	7.4	22.7	Yes
7	1.1	25	28.0	22.7	Yes

¹The presence of the side rails are not considered in this calculation, as they are not totally in the main fragment pattern.

*Measured from charge surface to charge surface.

**NOL Large Scale Gap Test (LSGT) data are used to establish the threshold for detonation. This is the 50% LSGT pressure of H-6.

***Sympathetic detonation is predicted when either the shock or fragment induced pressure is 0.85 * LSGT pressure.

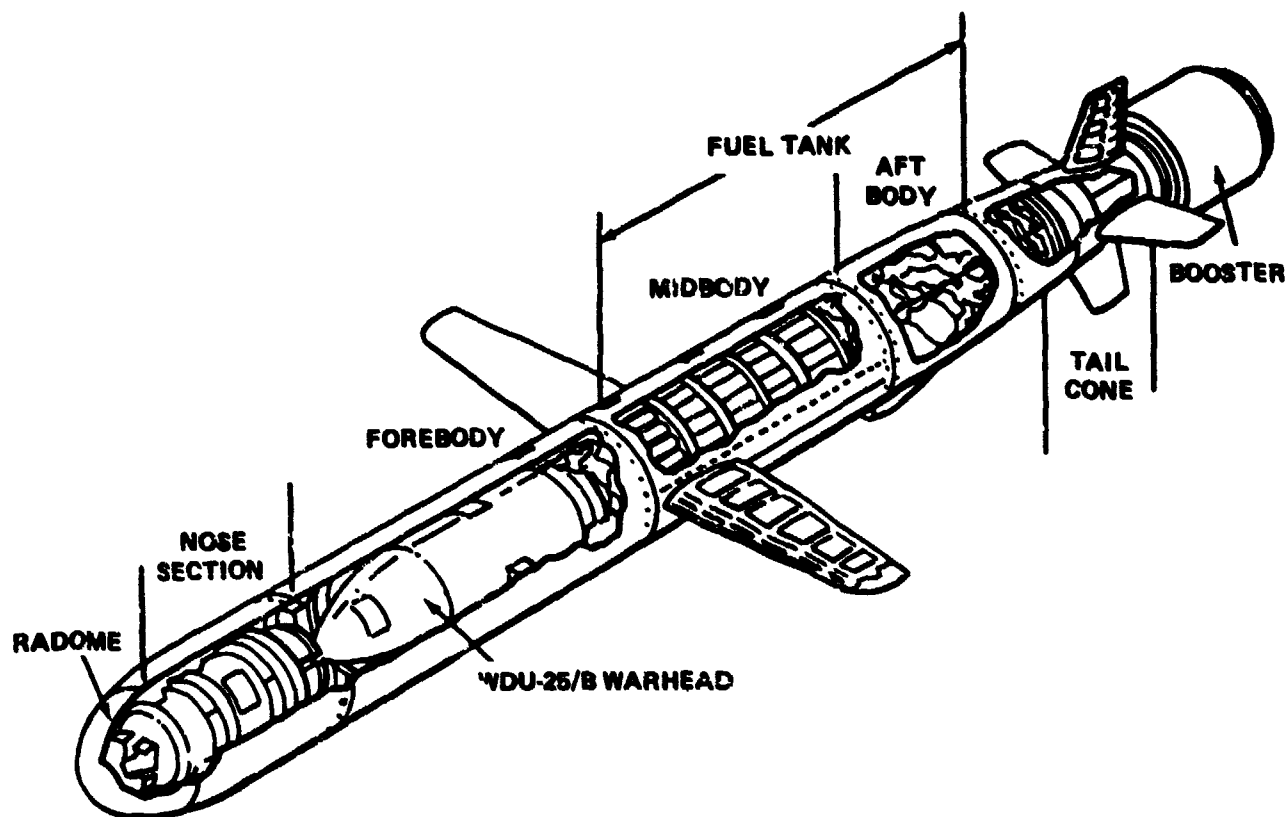


FIGURE 1A. TOMAHAWK ALL-UP ROUND

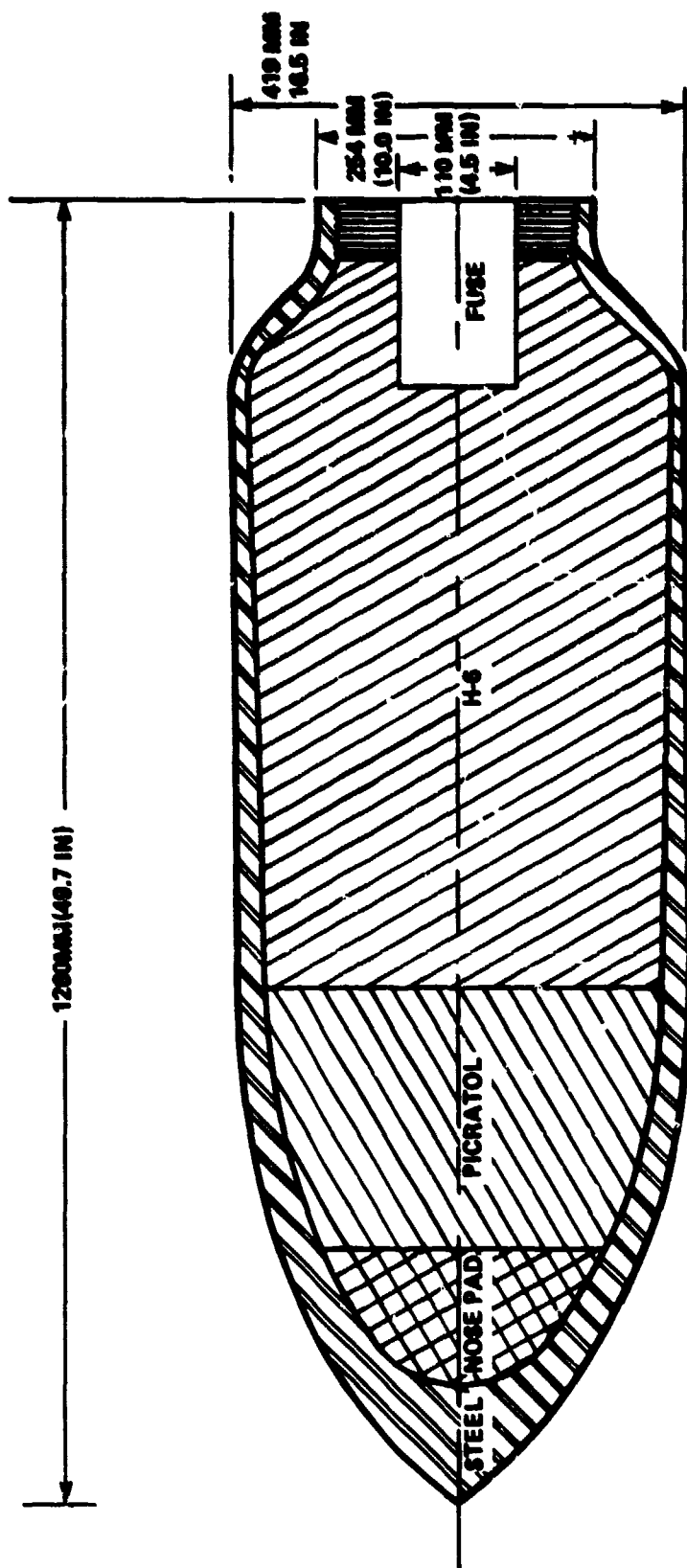


FIGURE 1b. WDU-25/B WARHEAD ASSEMBLY

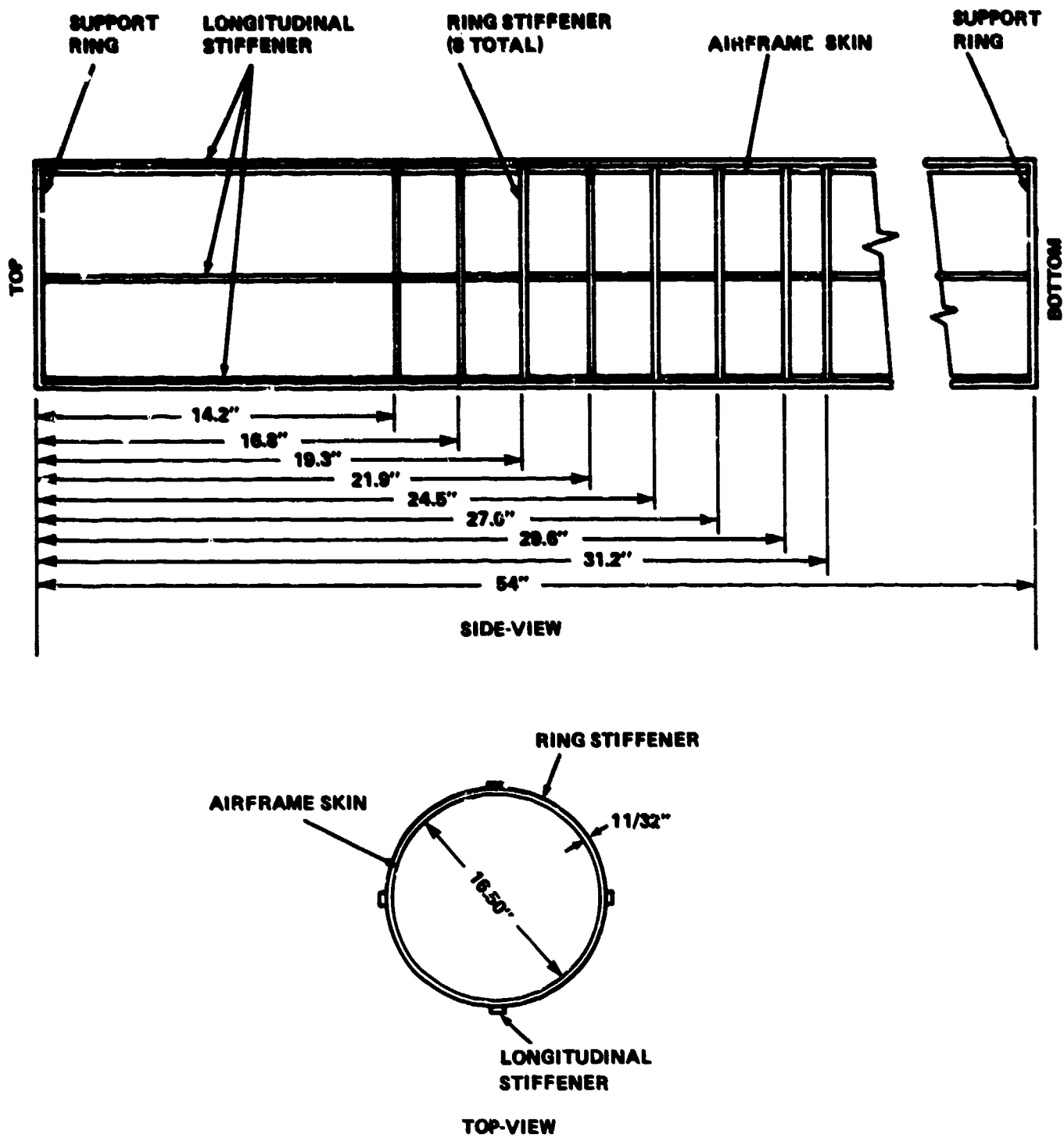


FIGURE 2. AIRFRAME SIMULANT



FIGURE 3. AIRFRAME SIMULANT INSTALLATION

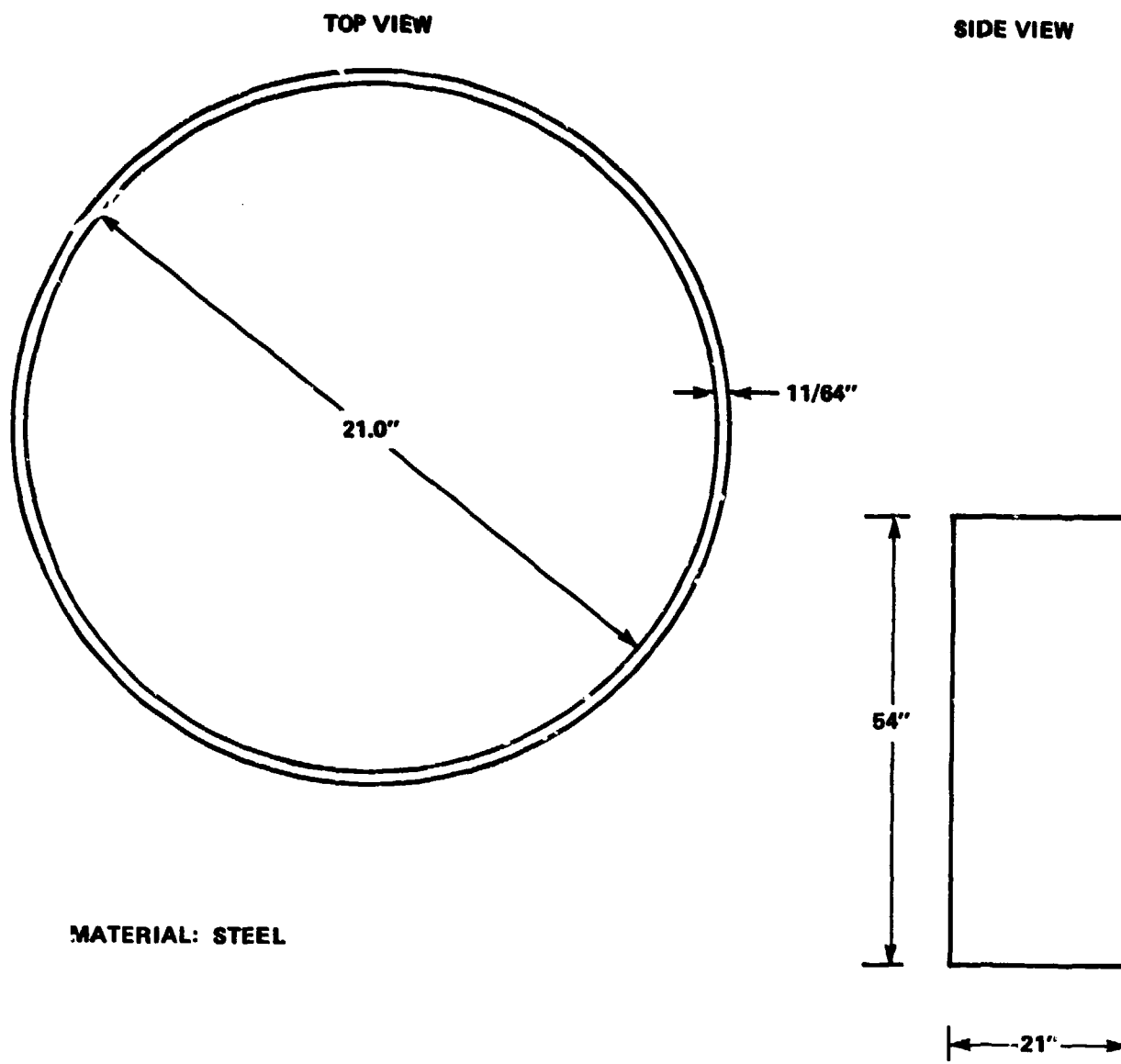


FIGURE 4. LAUNCH CAPSULE SIMULANT

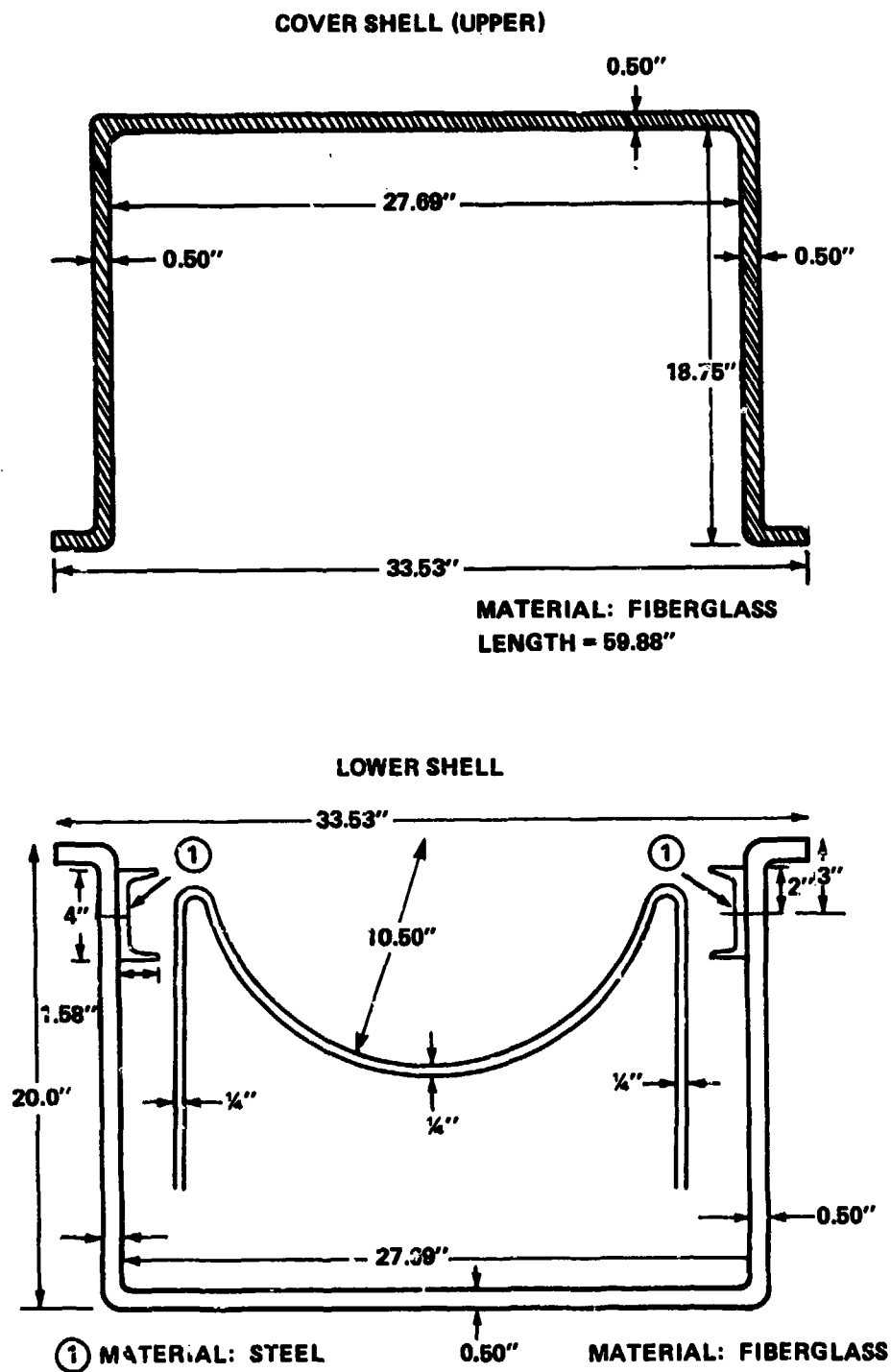


FIGURE 5. SIMPLIFIED CROSS SECTION OF CNU 308 SHIPPING CONTAINER

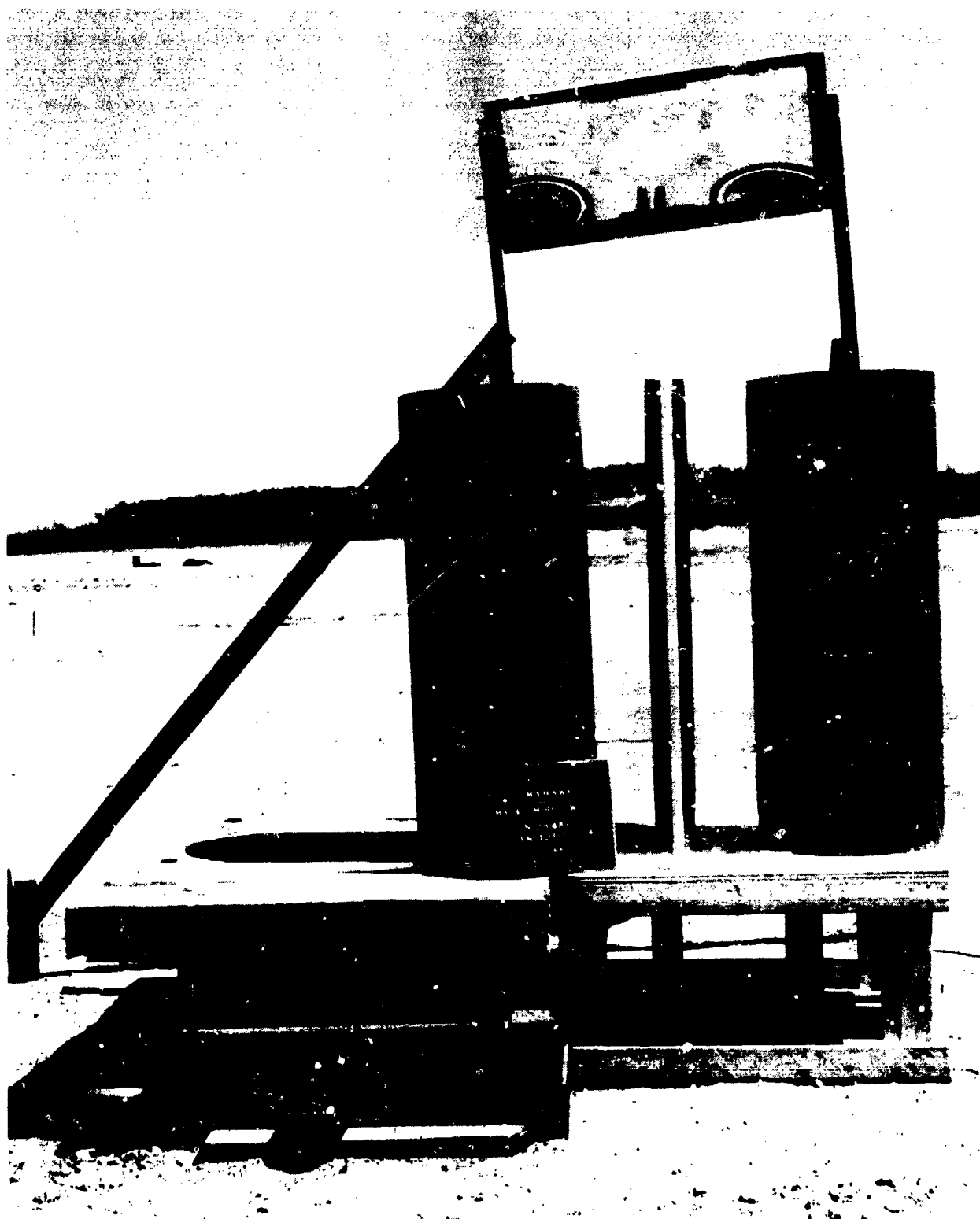


FIGURE 6. HORIZONTAL STACK SIMULATION

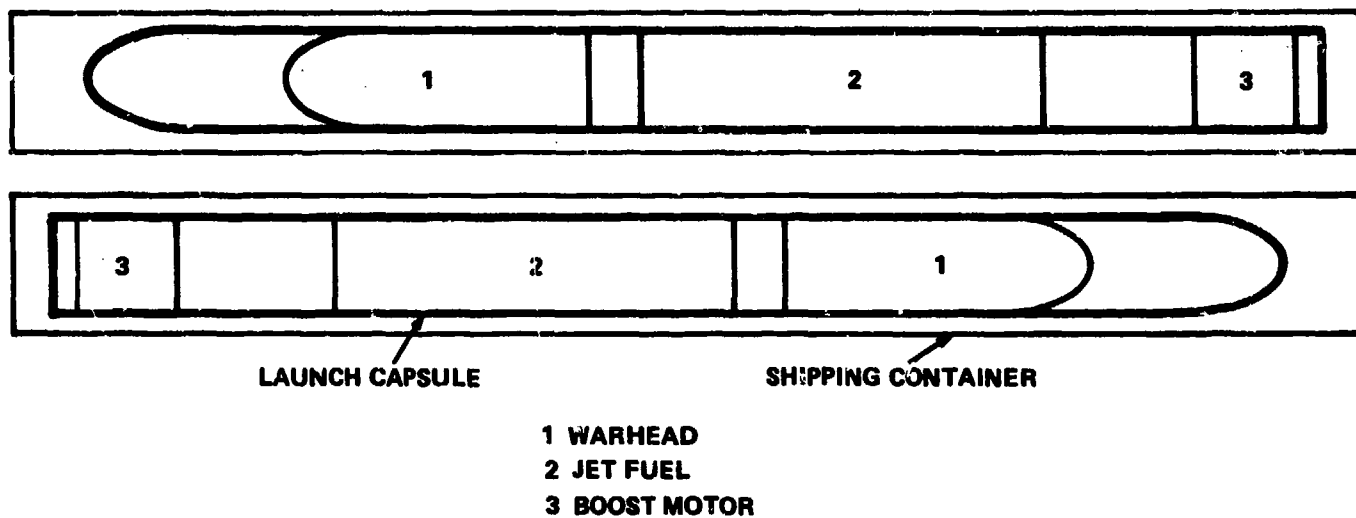
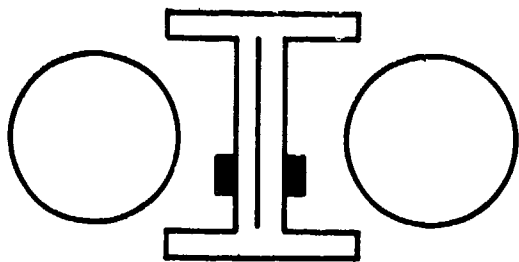
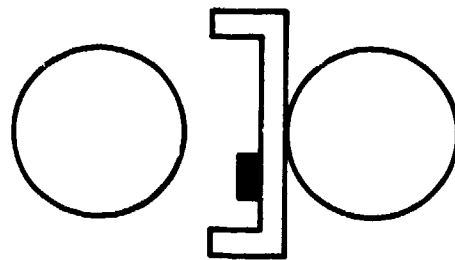


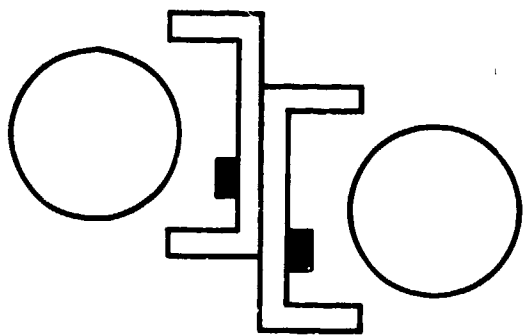
FIGURE 7. NOSE-TO-TAIL TOMAHAWK ALIGNMENT



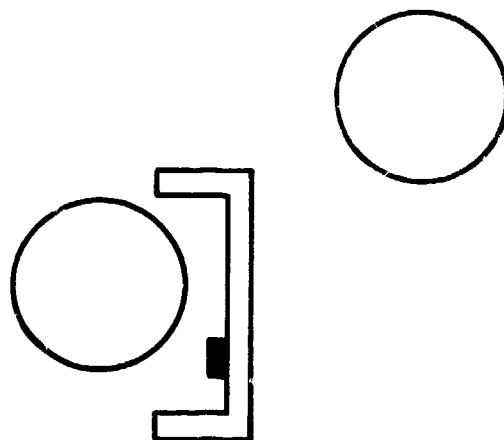
CONFIGURATION 1



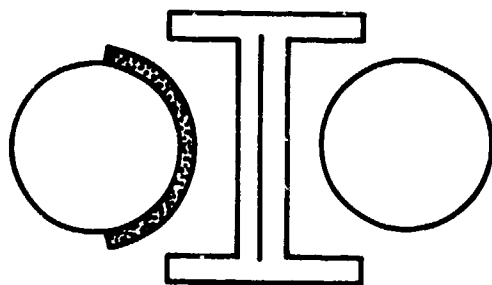
CONFIGURATION 5



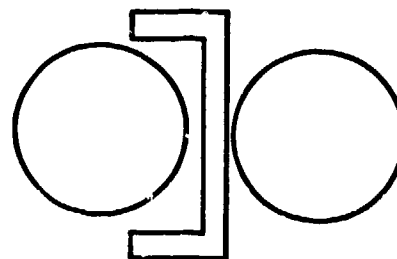
CONFIGURATION 2



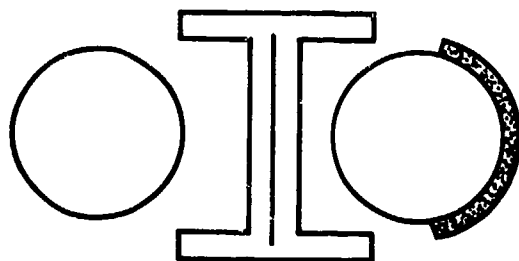
CONFIGURATION 6



CONFIGURATION 3



CONFIGURATION 7



CONFIGURATION 4

**NOTE: ALL OF THESE ARE TOP VIEWS WITH
THE WARHEAD STANDING ON END.**

FIGURE 8. POSSIBLE CONFIGURATIONS

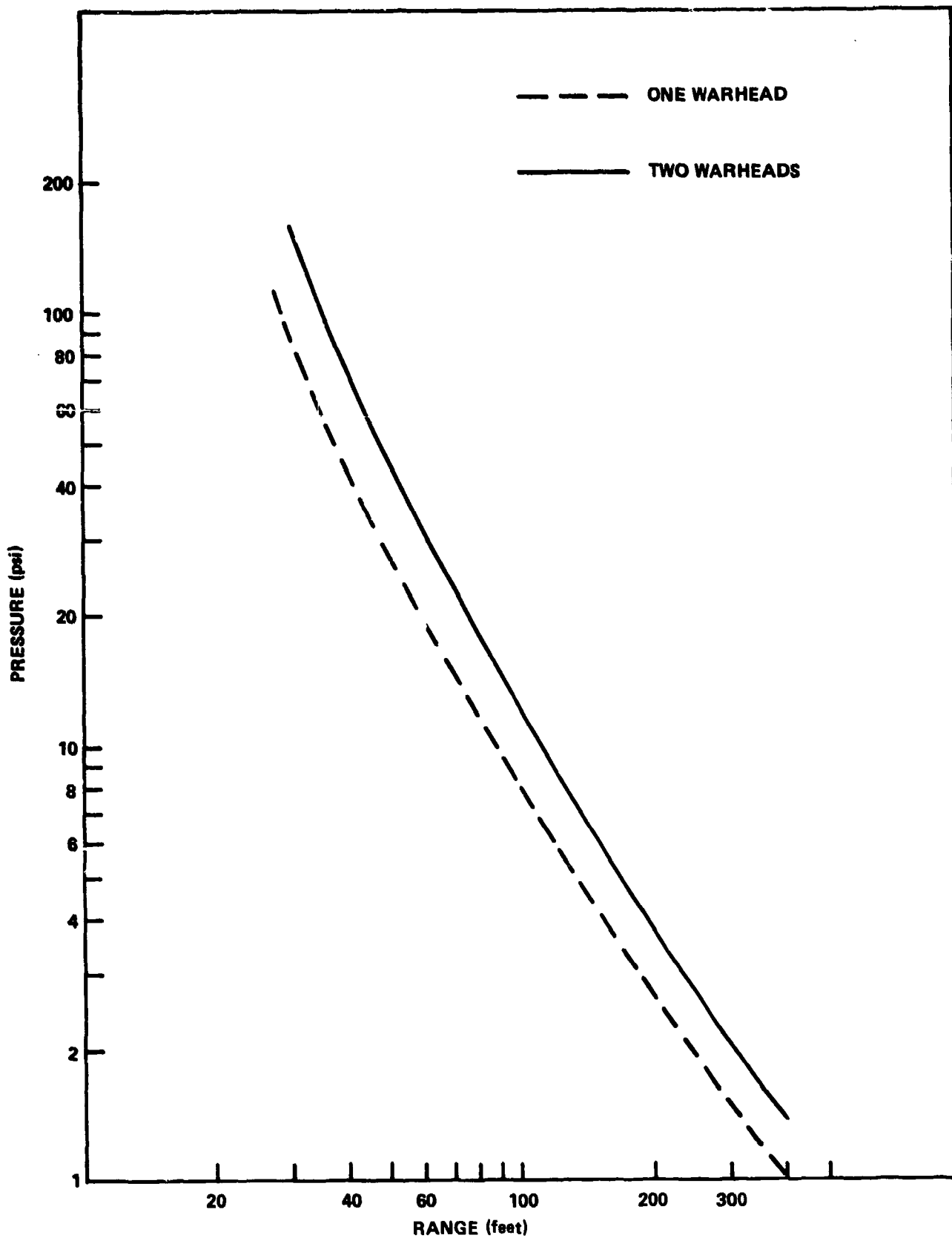


FIGURE 9. PRETEST PREDICTIONS



FIGURE 10. WITNESS PLATE POST-TEST

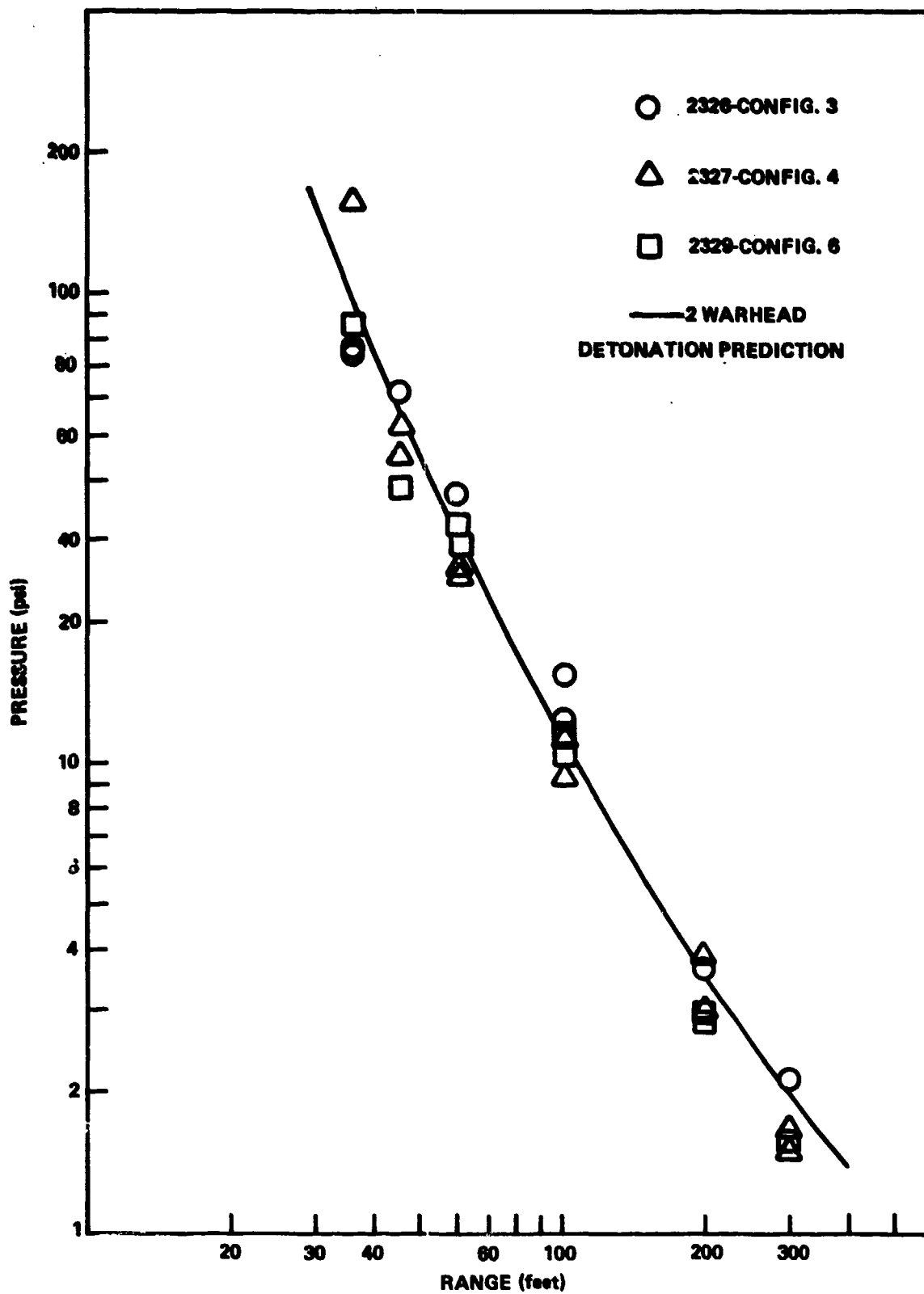


FIGURE 11. CONFIGURATIONS 3, 4, AND 6, PRESSURE-DISTANCE DATA



FIGURE 12. CONFIGURATION 1, ACCEPTOR CASE PIECE

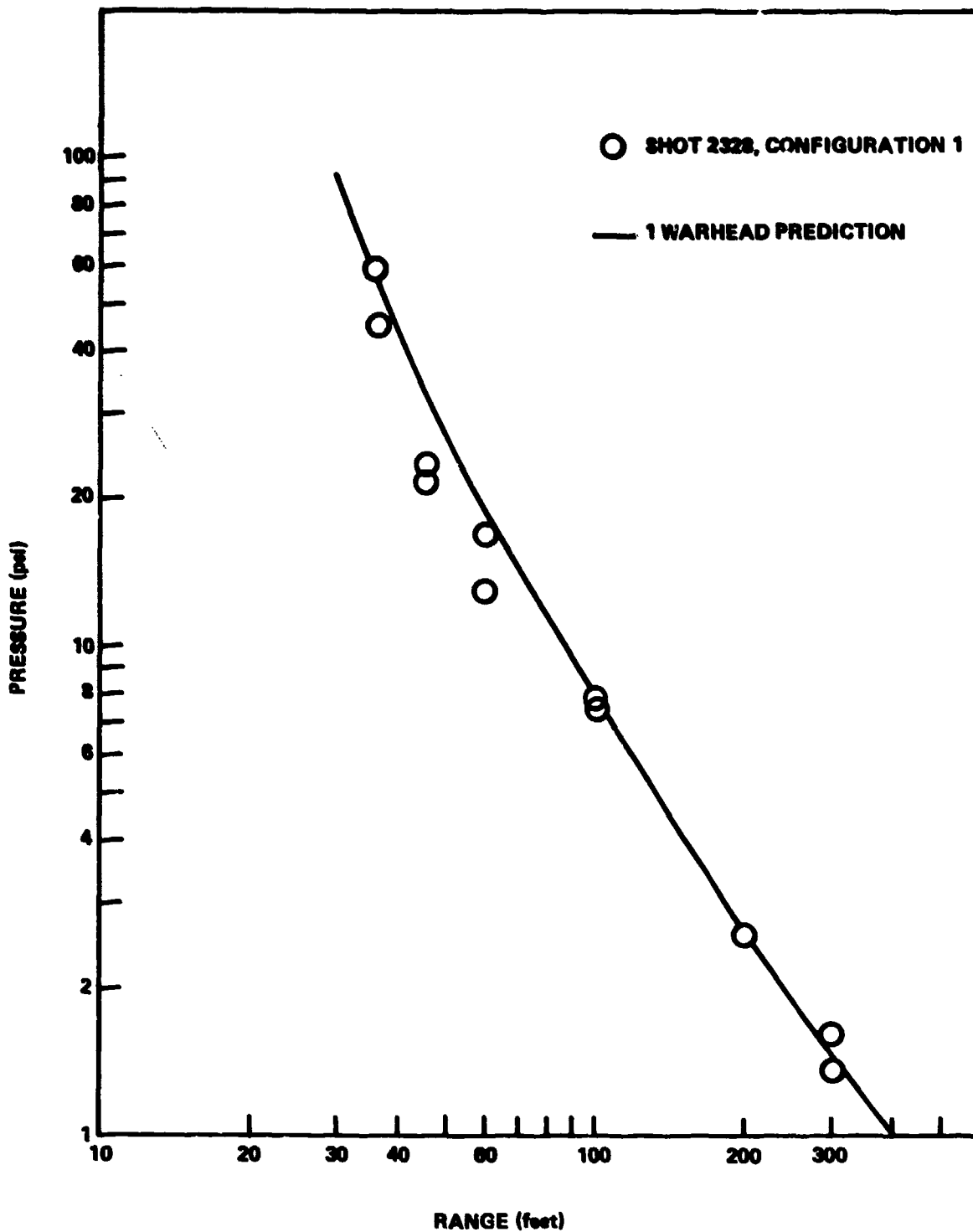


FIGURE 13. CONFIGURATION 1, PRESSURE-DISTANCE CURVE

CHAIRMAN'S CLOSING REMARKS

We have fulfilled the purpose of this seminar and more. The seminar has provided a forum or an opportunity to actively exchange information (state-of-the-art) information among 830 of ourselves and over 90 representatives from twenty friendly nations throughout the world. In addition, we have ample proof that the senior leadership in DoD and the Services recognize and support our continuing efforts in explosive safety. We have taken the opportunity provided to talk to people we might have not otherwise have had the chance to talk to and we have renewed old acquaintances and met new friends. In short, we have tied our profession close together. For these reasons and none other, the seminar has been successful. In that regard, please let us know how we can make it better next time. Use your critique sheets to voice your concerns. You don't need to take much time to tell us about the registration problems. We know how to correct that and we thank you for your patience in working with us during that trying time. Next time, we will handcarry our pre-registration envelopes and not rely on the Postal Service.

C. Several Thanks are due:

1. Marriott staff and management.
2. Members of the Secretariat and Mr. Ray Sawyer.
3. The General Officers who volunteered or were pushed into

service to provide us their guidance and support.

4. The moderators for their advance preparation and assistance in controlling the special session.

5. The authors of the papers that were presented. Their efforts have paid off because most of them are now recognized as the vanguard in advancing explosive safety standards in our ever increasing complex environment.

6. And last, but far from least, all of us who faithfully attended the seminar sessions, debated the papers, discussed mutual problems and who, in the future, will carry the word back to the explosives community.

D. In closing, I hope you all had as much fun as I did and that you gained as much as I did from the proceedings. Wouldn't mind doing this more often. Have a safe trip home, God Speed and we hope to see you all on the East Coast in August of 1988.

Thank you.

ATTENDANCE LIST
22d DoD Explosives Safety Seminar

ABRISZ, Gary W.	US Army Safety Center, Fort Rucker, AL 36362
ABROL, Satish C.	HQ USAF/LEEE, Bolling AFB, Wash., DC
ADAMS, Ardine	Travis AFB, CA 94535
ADAMS, AVILLE E	AFLC, Wright-Patterson AFB, OH 45433
ADAMS, Richard T.	Naval Fac Engr Command, Alex., VA 22332
ADAMS, Robert L.	Boeing Military Airplane Co., Wichita, KS 67277
AIKEN, Charles C.	NAVSEA Safety School, Bloomington, IN 47401
ALLES, John W.B., Cdr	Royal Netherlands Navy, Netherlands
AMEND, Mark A.	AF Armament Laboratory, Eglin AFB, FL 32542
AMIALE, Rene Vital, ING GEN	Inspec de L'Armement Pour Les Explos, France
AMIRAM, Eitan	Ministry of Def, Israel Military Industries, NY, NY
ANDERSON, Donald R., LTC, USA	HQ, DNA, Wash., DC 20305
ANDERSON, Ray W.	Agbabian Associates, El Segundo, CA 90245
ANDREWS, Jack E.	Explosive Technology, Inc., Fairfield, CA 94533
ANDREWS, Sidney B.	Naval Surface Wpn Ctr, Dahlgren, VA 22448
ANSPACH, Earl E.	Sverdrup Tech., Inc., Arnold AFB, TN 37389
ANTHONY, Phillip D.	Center for Explo Tech Research, Socorro, NM 87801
ARMSTRONG, Lawrence H.	Ministry of Defence(Navy), Bath, England
ASH, Richard W.	USAMC Field Safety Activity, Charlestown, IN 47111
ATHEY, Crystal J.	Aberdeen Proving Ground, MD 21010-5401
ATHOW, Lewis F., CDR	Chief of Naval Operations, Washington, DC 20350
ATTEBERRY, Jeff D.	Naval Station San Diego, CA 92136
AUYER, Joseph L.	Wyle Laboratories, Huntsville, AL 35807
BACK, Robert J.	Aerojet Ordnance Co., Chino, CA 90740
BAGGEN, Albert J., Jr.	Quantic, San Carlos, CA 94070
BAHL, David K.	DCASMA, Van Nuys, CA 91408-2713
BAIRD, Richard L.	Western Space & Msl Ctr, Vandenberg, CA 93437
BAKER, Charles	Lawrence Livermore Nat'l Lab, Livermore, CA 94550
BAKER, Wilfred E.	Wilfred Baker Engineering, San Antonio, TX 78209
BALLOU, Richard D.	DLA, DCASR, O'Hare IAP, Chicago, IL 60666-0475
BARCLAY, Don E.	Lone Star Army Ammo Plant, Texarkana, TX 75505
BARKER, Donna C.	DDESB Secretariat, Alex., VA 22331
BARNES, Robert T.	Lexington-Blue Grass Army Depot, Lexington, KY 40511
BARNETTE, Jerry	Naval Surface Weapons Center, Dahlgren, VA 22448
BARRIOS, Daniel R.	Tracor M.B.A., San Ramon, CA 94583
BAXTER, Leland K.	Hercules, Inc., Magna, UT 84044
BECHTOLD, Kirk P.	Delco Systems Operations, Goleta, CA 93117
BECKER, Brian A.	Bulova Systems & Instr Corp., Valley Stream, NY 11582
BECKFR, Randall L.	LA Police Department, BS, LA, CA 90012
BEDFORD, John D.	NASA/Marshall Space Flight Ctr, AL 35812
BENDER, Urs F., MG	DCSO Logistics, Swiss DOD, Berne, Switzerland
BENNETT, George T.	1776 ABW, Andrews AFB, DC 20331
BEREZA, Steven	Rockwell Int'l - Rocketdyne Div, Canoga Park, CA 91303
BERK, Joseph H.	Aerojet Ordnance Co., Downey, CA 90241

BEROGGI, Giambiera	Ernst Basler & Partners, Zurich, Switzerland
BERRY, Sharon L.	Naval Weapons Center, China Lake, CA 93555
BESSON, Jacques C.	Del Generale Pour L'Armement, France
BETTS, Curt P.	USA COE, Omaha District, Omaha, NE 68102
BEYER, Marv E.	Naval Civil Engr Lab, Port Hueneme, CA 93043
BIGELOW, Donald, SSgt	1 SOW/Safety (Exp), Hurlburt Field, FL 32544
BIGGER, Julian R.	U.S. Dept of Energy, Albuquerque, NM 878115
BLOOM, Thomas J.	Quantic Ind., Inc., San Carlos, CA 94070
BLOUNT, Wilson E.	AF Inspection & Safety Center, Norton AFB, CA 92409
BOBASH, B.	Ministry of Def, Israel Military Industries, NY 10022
BOBCZYNSKI, Sigmund A.	Naval Ocean Systems Center, San Diego, CA 92152
BODINE, Paul L., COL	Eighth AF Safety, Barksdale AFB, LA 71110
BODINE, W.M.	Ford Aerospace & Comm Corp., Newport Beach, CA 92658
BOGARD, Robert L., Jr., LTC	AMC Siret Field Ctr, Dover, NJ 07801-5299
BOIMEL, A.	Ministry of Def, Israel Military Industries, NY, NY
BOISSEAU, Francois-Xavier	SNPE, France
BOLTON, Robert M., MAJ	322 ALD 1SE, Ramstein AB, GE
BONITATI, John	Army Materials Tech Lab, Watertown, MA 02172
BOOM, Jan	Ministry of Defence & Materiel, Royal Netherlands Army
BORG, George, Dr.	Embassy of Australia, Wash., DC 20036
BOSSARD, R.K.	Eldorado Engr., Inc., West Valley, UT 84119
BOSTON, David	GOEX, Inc.
BOTT, Ronald J.	G.A. Technologies, Inc. 92138
BOTTJER, Gary M.	US Army Safety Center, Fort Rucker, AL 36330
BOWEN, Elmon R.	60 Military Airlift Wing, Travis AFB, CA 94535
BOWEN, Guv P., BG	USAMC, Dep Exec Dir for Conventional Ammo, Alex., VA
BOWERS, Robert F., COL	DDESB Secretariat, Alex., VA 22111
BOWLES, Patricia M.	Southwest Research Institute, San Antonio, TX 78284
BOZDECK, Larry	MP Assoc., Oakland, CA 94610
BRACE, Gerald G.W.	Chief, Inspector of Naval Ordnance, Bath, England
BREAZEL, Vern	Omark Industries, Lewiston, ID 83501
BREEDEN, Gary T., SMS	AF Inspection & Safety Center, Norton AFB, CA 92409
BRINKMAN, Earl J.	Olin Corporation, East Alton, IL 62024
BROCK, Brian	General Dynamics, Pomona, CA 91769
BROOKS, Alfred	Fed Railroad Admin. DOT, Wash., DC 20590
BROSNIHAM, TIM	Naval Air Test Center, Patuxent River, MD 20670
BROWER, Jerome S.	Broco, Inc., 2824 N. Locust Ave., Rialto, CA 92376
BROWN, Warren R.	Olin Corporation, Badger AA Plant, Baraboo, WI 53959
BUCHHOLTZ, Walter C.	AF Eng & Svcs Ctr, Tyndall AFB, FL 32403
BUTWILOWITZ, Ernst	NL/MOD/DQM/M11 Cmte on Dangerous Goods, The Hague
BUFORD, Alfred J.	United Technologies, San Jose, CA 95150
BULMASH, Gerald	US Army Ballistic Research Lab, APG, MD 21005
BURRELL, Sam	AF Rocket Propulsion Lab, Edwards AFB, CA 93523
BUTCHER, Dennis H., 1LT	419TFW, Hill AFB, UT 84056
BUTCHER, Michael A.	Naval Weapons Station, Concord, CA 94520
BYRD, John L.	Dir, USA Defense Ammo Ctr & School, Savanna, IL 61074
BYUN, Choong Koo, COL	DCSLOG, Ammo Div, HQ, Republic of Korea, Seoul, Korea
CADJUS, Robert N.	Baggett Transp. Co., Irvine, CA 92720
CALTAGIKONE, Joseph P.	USA Arma Research Dev & Engr Ctr, Picatinny AR, NJ

CAMPBELL, Clarence J.
 CANNON, Paul C.
 CANTRELL, Frederick, LtCol
 CARDIN, Jacques C., CAPT
 CAREW, Donald L.
 CARTER, James M., CAPT
 CATES, Charles A.
 CAUDLE, David A.
 CAUNDAY, Mariano
 CAUTHEN, Charles B.
 CESSARIO, Thomas R.
 CHANG, James D.C.
 CHANPONG, Udorn
 CHEW, Don A.
 CHIZALLET, Maurice
 CHRETIEN, Francis
 CHRISTENSEN, Roger D., 2LT
 CHURCHILL, Frank H.
 CHURILO, Charles J.
 CLARY, Val
 CLEVELAND, Leroy
 CLINTON, Stephen P.
 COAD, Roger D.
 COLLINS, David L.
 COLLINS, George E., Jr.
 COLLINS, Jon D.
 COLLINS, William B.
 COMBS, Harold K.
 CONLEY, John H.
 CONN, Andrew F.
 COOK, Johnnie L.
 COOPER, Clarence J., MSgt
 COOPER, Robert R., CAPT
 COOVER, Don W.
 COPELAND, Jackson M.
 CORLEY, John D., 2LT, USAF
 COULTER, George
 COURSON, Leonard A., CAPT
 COURTRIGHT, W. Clarence
 COX, James C.
 COX, Phineas A.
 CRAIG, Bobby G.
 CRATEN, Joseph D.
 CROCHET, Herman J.
 CROCKETT, Kim
 CROTTY, Kenneth
 CRUZ, Ignacio
 CUMMINGS, Bruce E.
 CUTHBERT, Leon G.
 CYR, Lynda C., CAPT, USAF

AMC Field Safety Activity, Charlestown, IN 47111
 Olin Corp-Ordnance Products, Marion, IL 62959
 Royal Military College of Science, UK
 Ministere de la Defense, Paris, France
 HQ, First AF/SE, Langley AFB, VA 23665
 5th Bombardment Wing (SAC), Minot AFB, ND 58705
 US Army Safety Center, Fort Rucker, AL 36362
 US Naval Weapons Center, China Lake, CA 93555
 SRI International, Menlo Park, CA 94025
 CAL/OSHA Consultation, San Bernardino, CA 92401
 Morton Thiokol, Inc., Elkton Div, Elkton, MD 21921
 DCSNGR, HQ WESTCOM, Fort Shafter, HI 96858-5100
 Bernard Johnson Inc., Houston, TX 77040
 USAMC Field Safety Activity, Charlestown, IN 47111
 MATRA, Velizy, France
 AEROSPATIALE, Les Hureaux Cedex France
 2701 Exp Ord Disp Squad, Hill AFB, UT 84056
 Ogden Air Logistics Center, Hill AFB, UT 84056
 AFSC Armament Division, Eglin AFB, FL 32542
 Space Div, Worldwide Postal Ctr, LA, CA 90009-2960
 Day & Zimmermann, Inc., Kansas AAP, Parsons, KS 67357
 HSMM, Roanoke, VA 24034
 Los Alamos Nat Lab, Los Alamos, NM 87545
 New Mexico Tech-Tera Group, Socorro, NM 87801
 Chemical Research Dev Engr Ctr, APG, MD 21010
 ACTA Inc., Torrance, CA 90505
 Armament Division, Eglin AFB, FL 32542
 Lexington-Blue Grass AD, Lexington, KY 40511
 USA Combat Systems Test Act, APG, MD 21005
 Tracor Hydronautics, Inc., Laurel, MD 20707
 Red River Army Depot, Texarkana, TX 75507
 AEDC/SE, Arnold Engr Dev Ctr, Tullahoma, TN 37389
 AF Weapons Laboratory, Kirtland AFB, NM 87118
 Kresky Signs, Inc., Petaluma, CA 94953
 Naval Air Test Center, Patuxent River, MD 20670
 Air Force Armament Lab, Eglin AFB, FL 32542
 Ballistic Research Lab, APG, MD 21005
 Field Cmd, Def Nuclear Agency, Kirtland AFB, NM 87115
 Los Alamos Nat Lab, Los Alamos, NM 87545
 USA Combat & Sys Test Act, APG, MD 21005
 Southwest Research Institute, San Antonio, TX 78284
 CETR, New Mexico Tech, Socorro, NM 87801
 USATHAMA, Aberdeen Proving Ground, MD 21010
 Mason Chamberlain Inc., Picayune, MS 39466
 Naval Air Test Center, Patuxent River, MD 20670
 US Army Tech Escort Unit, APG, MD 21010
 DDESB Secretariat, Alex., VA 22331-0600
 SRS Technologies, Vandenberg AFB, CA 93437
 Aerojet Ordnance Co., Downey, CA 90241
 Eighth AF Safety, Barksdale AFB, LA 71110

DADD, Alan C., Cdr
 DAHN, Carl J.
 DAUGHERTY, Edward A.
 DAVIDSON, Robert
 DAVIS, Dickey P., CAPT, USN
 DAVIS, Jo O.
 DAVIS, L.K.
 DAY, Douglas
 DAY, J. Donald
 DAY, Robert D.
 DAYWALT, Raymond A.
 DEAN, Herman A.
 DEDMAN, Oneal
 DEMARCO, Richard J.
 DEMPSEY, Robert D.
 DENISON, Thomas S.
 DENNY, Richard
 DESHPANDE, Pralhad M.
 DICKENSON, H.
 DILTS, Chuck
 DINSMORE, Frederick E., CAPT
 DITTMAN, Harry A.
 DIXON, Ward R.
 DODGEN, James E.
 DONALDSON, Lyle
 DONLEY, William J.
 DORN, Dennis
 DOTTS, James E.
 DOTY, Delbert
 DOUGHERTY, Charles M., MAJ
 DOUMA, Larry A.
 DOUMA, Patricia
 DOUTHAT, C. David
 DOVE, Richard C.
 DOWDY, Ross W.
 DRAKE, James T.
 DRESSLER, Enge D.
 DROUX, M. Rolland
 DRUM, William S.
 DRURY, A. Chuck
 DUNSETH, Clifford A.
 DUPUIS, Gary J.
 DeSANDO, Richard J.
 EASTWOOD, Terry W.
 ECKELBARGER, Donald E., MG
 EDDINGTON, Russel
 EDDY, John R.
 EDWARDS, Charles L.
 EISAMAN, Jack V.
 ELI, Mark W.

NAB Coronado, CA 92155
 Safety Consulting Engineers, Inc., Rosemont, IL 60018
 Applied Ordnance Tech, Inc., Arlington, VA 22202
 Naval Air Test Center, Patuxent River, MD 20670
 DDESB, Alexandria, VA 22331-0600
 Sandia National Lab, Albuquerque, NM 87185
 USAE Waterways Experiment Sta, Vicksburg, MS 39180
 Radford AAP, Radford, VA 24141
 EDM Corporation, Vicksburg, MS 39180
 AFPRO/DET16, Anaheim, CA 92803
 Naval Weapons Supt Ctr, Crane, IN 47522
 HQ, ATC/IGFG, Randolph AFB, TX
 Pine Bluff Arsenal, Pine Bluff, AR 71602
 Naval Weapons Center, China Lake, CA 93555
 USAEDH, Huntsville, AL 35807
 Honeywell Inc., Defense Systems Div, Hopkins, MN 55343
 Army Materials Tech Lab, Watertown, MA 02172
 Ex-Indian Ordnance Factories Services, India
 Hayes, Seay, Mattern, & Mattern, Roanoke, VA 24034
 McDonnell Douglas Astro Co., Titusville, FL
 96 BMW/Weapons Safety Ofc, Dyess AFB, TX 79607
 DLA/DCASR Cleveland, OH 44199
 Lawrence Livermore Nat'l Lab, Livermore, CA 94550
 Dodgen Engineers, Colorado Springs, CO 80934
 HQs 22AF/SEV, Travis AFB, CA 94535
 NAS, Patuxent River, MD 20670
 The Nathan Hale Group, Fairfax, VA 22030
 Sandia Nat'l Lab, Albuquerque, NM 87185
 Quantic Industries, Inc., Salinas, CA 93902
 Munitions Mgmt Div, Hill AFB, UT 84056
 Honeywell Inc., Minneapolis, MN 55112
 Honeywell Inc., Minneapolis, MN 55112
 USAEDH, Huntsville, AL 35807
 USAE-WES, Vicksburg, MS 39180
 Agbabian Associates, Hawthorne, CA 90250
 DDESB, Alexandria, VA 22331-0600
 Nav Exp Ord Disp Tech Ctr, Indian Head, MD 20640
 Com a l'Energie, Ctr d'Etudes de Vaujours, France
 Maryland Assemblers, Inc., Perry, FL 32347
 Federal Cartridge Co., Anoka, MN 55303
 HQ, 60th Ord Group, APO, NY 09052
 62 MAW, McChord AFB, WA 98438
 Monsanto Res. Corp., Miamisburg, OH 45342
 Lockheed Msl & Space Co., Inc., Sunnyvale, CA 94088
 Director of Human Resources Dev, Wash, DC 20310
 NASA, Edwards, CA 93523
 Defense Nuclear Agency, Alex., VA 22310
 Field Cmd, DNA, Kirtland AFB, NM 87115
 Boeing Aerospace Corp., Seattle, WA 98124
 Lawrence Livermore Laboratory, Livermore, CA 94550

ELLENBERG, John R.
 ELLIS, B.J., Wing Cmdr
 ELMORE, Richard E.
 ENDICOTT, David W.
 EPPERT, Frank P.
 ESPARZA, Edward D.
 EVANS, A. Donald
 EVANS, Michael D.
 EYTAN, Reuben
 FABER, Jan J., MAJ, RNLA
 FADORSEN, Gary
 FAHY, Robert J.
 FANNIN, Gerald F.
 FARLEY, Francis P.
 FATZ, Raymond J.
 FAUX, Neal D.
 FAWKES, Gordon A.
 FELLER, Shaul, Dr.
 FERRARO, Carlo
 FERRITTO, John M.
 FICK, Rudi E., CAPT. GAF
 FIERZ, Gerard, Dr.
 FINLEY, Dennis K.
 FISHER, Penelope
 FITZGERALD, Patrick
 FLEMING, Herman T.
 FLORY, Robert A.
 FLOYD, James Q.
 FLOYD, Thomas G.
 FOULK, David W.
 FRANCIS, Chretien
 FRAZIER, Wayne R.
 FREEMAN, Anthony
 FREEMAN, Raymond W.
 FRENCH, Stephen H., COL, USA
 FREY, Leo J.
 FRITTS, Arthur B.
 FROM, F.
 GAENZLE, Ronald W.
 GALLAGHER, Richard N.
 GARCIA, Carlos E.
 GARCIA, Esteban A.
 GARCIA, John R.
 GARDNER, Charles C.
 GARLAND, Thomas L.
 GARVIN, Joe

Martin Marietta Missile Ord Dept., Orlando, FL 32855
 Royal Australian AF, Wash., DC 20036
 Naval Surface Weapons Center, Dahlgren, VA 22448
 Live Process Development, Brigham City, UT 84302
 Booker Associates, Inc., St. Louis, MO 63101
 Southwest Research Institute, San Antonio, CA 78284
 Holston Defense Corporation, Kingsport, TN 37660
 Calspan Corporation, Arnold AFS, TN 37389
 Evtan Building Design Ltd, Tel Aviv, Israel
 MOD NL, The Netherlands
 Automatic Sprinkler Corp., Cleveland, OH 44147
 HQs, AMC, Alex., VA 22333
 317 TAW, Pope AFB, NC
 DCASR, Boston, Boston, MA 02210
 HQDA Safety Office, Washington, DC 20310
 Weapons Safety Ofc. Hill AFB, Utah 84056
 Naval Weapons Center, China Lake, CA 93555
 Israel Armament Dev Auth., Haifa, Israel 31021
 Chief of Naval Operations, Washington, DC 20350
 Pacific Airfield Tech Co., Ventura, CA 93003
 FMOD GE Armed Forces Staff, Bonn, Germany
 Dr. Ing. MARIO BIAZZI S.A., Vevey, Switzerland
 MIMC, Southport, NC 28461
 Berrite Div of Whittaker, Sausalito, CA 91350
 DOS, SA6, Washington, DC 20502
 General Dynamics, San Diego, CA 92138
 Tech Reps Inc., Springfield, VA 22152
 USAF, Robins AFB, Warner Robins, GA 31098
 US Air Force (HERD), FL 32542
 USA Central Ammo Mgmt, Ft. Shafter, HI 96858
 AEROSPATIALE, Les Mureaux, France
 NASA Hqs. Safety Div. Wash., DC 20546
 Micronics International, Inc., Brea, CA 92621
 USAMC, Alexandria, VA 22333-0001
 USA Ctrl Ammo Mgmt Ofc(PAC), Ft Shafter, HI 96858
 USA ARDFC, Dover, NJ 07801
 21AF (MAC), McGuire AFB, NJ 08641
 Ministry of Def, Israel Military Industries, NY, NY
 Ammo Br. Fort Bliss, TX 79916
 AF Rep, Morton Thiokol, Brigham City, UT 84302
 US Dept. of Energy, Albuquerque, NM 87115
 HO USAFE, APO New York, NY 09012
 Sandia National Lab, Albuquerque, NM 87185
 Radford Army Ammo Plant, Radford, VA 24141
 NASA, Kennedy Space Center, FL 32899
 LTV Aerospace & Defence Co., Prairie, TX 75051

GEMAR, Charles
 GENEST, Ronald G.
 GIBB, Roderick
 GIBSON, Richard W.
 GOLDIE, Roger H.
 GOLDSTEIN, Selma
 GOLIGER, Jean G.
 GORDON, Rex
 GUTHERBERG, Martin J.
 GRACE, Paul J.
 GRANT, Horace
 GRAY, John J.
 GREAR, Jay W.
 GREEN, Greg
 GREENBERG, Paul J., BG
 GREENFIELD, Gary
 GREENMAN, Robert B.
 GREENWADE, Edward R.
 GROSSMAN, Boas
 GROVES, John E. Jr.
 GRYTING, Harold J., Dr.
 GUARIENTI, Richard P.
 GUNTER, Wayne D.
 GURKE, Gerhard H.
 GUTHRIE, Mitchell A.
 GJY, Roy E.
 HAINES, Robert O.
 HALE Nathan C.
 HALL, Eugene
 HALL, Paul H.
 HALSEY, Carl C.
 HALSTEAD, Bruce B., COL, USA
 HALTON, Phillip T.
 HAMILTON, Delbert T.
 HAMMER, William R.
 HANNAH, Maurice M.
 HANNUM, John A.E.
 HANSEN, Kevin E.
 HARGIS, Harold L.
 HARRIS, Alma T.
 HARRIS, Nolan W., CAPT
 HARROD, Charles E.
 HARRUFF, Gaylord L., MSgt
 HART, James H.
 HART, Steven M.
 HARTLEY, Frank R.
 HARTMAN, Edward A., SMSgt
 HARTON, Erskine E., Jr.
 HARVEY, Raymond A.
 HASSLER, John W.

Technical Ord., Inc., St. Bonifacious, MN 55375
 McDonnell Douglas Helicopters, Mesa, AZ 85205
 1 STRAD, Vandenberg AFB, CA 93437
 Lockheed Msl & Space Co., Inc., Sunnyvale, CA 94088
 Los Alamos Nat'l Lab, Los Alamos, NM 87545
 Los Alamos National Lab, Los Alamos, NM 87545
 SNPE, France
 San Jose, CA 95125
 Ford Aerospace & Com Corp., Newport Beach, CA 92658
 Aerojet Strategic Prop Co, Sacramento, CA 95813
 Baggett Transp. Co., Birmingham, AL 35233
 Universal Prop Co., Phoenix, AZ 85029
 Sandia Nat'l Lab, Albuquerque, NM 87185
 Martin Marietta, Denver, CO 80102
 Dep OG for Procurement & Readiness, AMCCOM, Rock Is., IL
 SRI International, Menlo Park, CA 94025
 Naval Surface Wpns Ctr, Dahlgren, VA 22448
 Pan Am World Svcs, Patrick AFB, FL 32925
 Ministry of Def, Israel Military Industries, NY, NY
 BEI Defense Sys Co., Inc., Camden, AR 71701
 Southwest Research Institute, San Antonio, TX 78684
 Lawrence Livermore Nat'l Lab, Livermore, CA 94550
 NASA GSFC/Wallops Is., VA 23337
 Ernst-Mach-Institut, FRG
 Naval Surface Wpns Ctr, Dahlgren, VA 22448
 VP Special Devices Inc., Newhall, CA 91321
 Iowa Army Ammunition Plant, Middletown, IA 52638
 The Nathan Hale Group, Fairfax, VA 22030
 Nav Plant Rep, McDonnell Douglas Corp., St. Louis, MO
 Polaris Missile Fac Atlantic, Charleston, SC 29408
 Naval Weapons Center, China Lake, CA 93555
 DDESB, Alexandria, VA 22331-0600
 Day & Zimmermann Inc., Lone Star AAP, Texarkana, TX
 HQs, Military Airlift Command, Scott AFB, IL 62225
 HQ, Air Force Systems Command, Andrews AFB, MD 20334
 63d Mil Airlift Wing, Norton AFB, CA 92409
 JHU-APL/Chem Prop Info Agency, Laurel, MD 20707
 IRECO Inc., West Jordan, UT 84084
 SRS-Technologies, Vandenberg AFB, CA 93437
 Rocky Mountain Arsenal, Commerce City, CO 80022
 HQ, PACAF Hickam AFB, HI 96818
 Atlantic Research Corp., Gainesville, VA 22065
 Air Force Flight Test Ctr, Edwards AFB, CA 93523
 Teledyne McCormick Selph, Hollister, CA 95023
 USASC Progs Div, Fort Rucker, AL 36362
 Royal Military College of Science, UK
 HQ, Tac Air Cmd, SEW, Langley AFB, VA 23665-5001
 Falls Church, VA 22046
 Martin Marietta Denver Aerospace, Denver, CO 80201
 Halex, Inc., Hollister, CA 95023

HATHAWAY, James W.
 HAWES, James M.
 HAWLEY, James E.
 HEDGES, Michael D.
 HEFELFINGER, Richard
 HEIL, John B.
 HEILMANN, Volker O., Lt Col
 HELLE, Charles J.
 HENDERSON, Jimi
 HENDERSON, Johnathan
 HENDERSON, Lester D.
 HENDERSON, William R.
 HENRY, Robert E.
 HERCHBERGER, Chester K.
 HERRON, Roger A.
 HERVEY, A.E., COL
 HESTER, Phil B.
 HICKMAN, John C.
 HIGGS, Maynard W.
 HILBERT, Gary L.
 HILL, Daniel B.
 HILLMAN, Robert S.
 HILLS, Dan J.
 HJORTH, Iwan
 HOFFMAN, Norman
 HOLBROOK, Douglas L.
 HOLDEN, Clifford A.
 HOLDERNESS, Gene R.
 HOLMES, Fred L.
 HOLT, James D.
 HORNIG, Howard C., Dr.
 HOSTLER, Gerald L.
 HOUSTEAU, Larry
 HOWELL, Edward D.
 HUDSON, Fred M.
 HUDSON, Melvin C.
 HUDSON, Thomas W., CMSgt
 HUGHES, J. Garth, Brig.
 HUNT, Monica E.
 HUNT, Raymond G.
 HUTCHINGS, William D.
 INBAR, A.
 ISBELL, Daniel R.
 JABLOVSKIS, B.Z.
 JACKSON, Wilber
 JACOBS, Edward M., Lt Col
 JANG, Joseph F.
 JANNEY, Joan L.
 JEFFERSON, Joseph E., COL
 JENKINS, James P.

USA Arma Research Dev & Engr Ctr, Yuma PG, AZ 85365
 Mason Chamberlain Inc., NSTL Base, MS 39529
 Morton Thiokol, Inc./Longhorn Div, Marshall, TX 75670
 DOE/PSA, Surrey, England
 McDonnell Douglas Astronautics, Titusville, FL 32780
 Motorola Inc., Gov'n't Elec Group, Scottsdale, AZ 85252
 Fed Armed Forces, Ofc for Studies & Exercises, GE
 CIA Brasileira de Cartuchos, San Paulo, SP., Brazil
 NAVPRO, Sunnyvale, CA 94088
 Saferry Svc Organ, Ministry of Defence, Kent, UK
 NWS, Seal Beach, CA 90740
 Naval Surface Weapons Center, Dahlgren, VA 22448
 Lawrence Livermore Nat'l Lab, Livermore, CA 94550
 DCASR-LA, El Segundo, CA 90245
 USA Ballistic Research Lab, APG, MD 21005
 US Army Safety Center, Fort Rucker, AL
 Jet Research Center, Inc., Arlington, TX 76004
 NASA/Computer Science Corp., Wallops Is., VA 23337
 Holston Army Ammo Plant, Kingsport, TN 37660
 Martin Marietta Corp., Vandenberg AFB, CA 93437
 Ammunition Equip. Dir., Tooele Army Depot, UT 84074
 Martin Marietta Denver Aerospace, Denver, CO 80201
 Plans & Oper Div, Fort Ord, CA 93941
 Forsvarets Eksplosivstofkommission, Hvidovre, Denmark
 Technical Ord. Inc., St. Bonifacius, MN 55375
 CSTA, FSSD, TSD, Ammo Proc Br, APG, MD 21005
 Aberdeen Proving Ground, CSTA, MD 21005-5059
 Hi-Shear Technology, Torrance, CA 90505
 Martin Marietta Aerospace, Vandenberg AFB, CA 93437
 Day & Zimmerman, Hawthorne A&P, Hawthorne, NV 89615
 Lawrence Livermore Lab, Livermore, CA 94550
 HQ, 56th Field Artillery Cmd, APO, NY 09281
 Wyle Laboratories, Noro, CA 91760
 DDESB Secretariat
 Atlantic Research Corp., Gainesville, VA 22065
 Safety Dept., Naval Ord Station Indian Head, MD 20640
 HQ, SAC, Offutt AFB, NE 68113
 President, Australian Ord Council, Canberra, AS
 Naval Air Test Center, Patuxent River, MD 20670
 Hercules Inc., Allegany Ballistics Lab, Rocket Ctr, WVA
 USAF, Robins AFB, GA 31098
 Ministry of Def, Israel Military Industries, NY, NY
 White Sands Missile Range, New Mexico 88002
 Naval Surface Wpns Ctr, Dahlgren, VA 22448
 MATCU, Travis AFB, CA 94535
 AF Inspection & Safety Center, Norton AFB, CA 92409
 Quant'c Industries, Inc., San Carlos, CA 94070
 Los Alamos Nat'l Lab, Los Alamos, NM 87545
 DDESB Secretariat, Alex., VA 22331
 Martin Marietta Aero Corp., Vandenberg AFB, CA 93437

JENKS, Albert J.
 JENSSEN, Arnfinn
 JENUS, Joseph
 JERNIGAN, Alfred E.
 JISA, James P.
 JOEH-PENG, Ng
 JOHNSON, Billy F., CAPT
 JOHNSON, Jeffrey L.
 JOHNSON, Robert
 JOHNSON, Theodore A.
 JOHNSTON, David A.
 JOHNSTON, Jack L.
 JOINER, Charles W.
 JONES, Donovan J.
 JONES, Forest M.
 JONES, Jerry W.
 JONES, Kenneth P.
 JONES, William L.
 JOSEPHSON, Larry H.
 JOYNER, Taylor B.
 JUSTICE, Fred C.
 KAMENIK, Peter H.
 KARTACHAK, Thomas S.
 KATICH, Michael S.
 KATSABANIS, P.
 KATSANIS, David J.
 KAUFMAN, Susan J., CAPT, USAF
 KAYS, Janice D.
 KEENAN, William A.
 KELLER, Bill H.
 KELLEY, Philip G.
 KELLY, Francis J.
 KELLY, William M.
 KENNEDY, James C., Jr.
 KENNEDY, Lynn W.
 KERNS, Avery J.
 KETCHEN, Donald W.
 KIDD, Harold L.
 KIESSLING, Michael S.
 KIGER, Sam A., Dr.
 KINDTLER, Gert W., MAJ
 KING, Chi Y.
 KING, David P., LTC, USAF
 KING, Francis
 KINGERY, Charles
 KITA, Terry J.
 KLAPMEIER, Kenneth M.
 KLASSEN, Bret T., CAPT, USAF
 KLOMPENHONNER, Greg D.
 KNAUR, J.

Hercules Aerospace Ord Div, Desota, KS 66018
 Norwegian Defence Constr Svc, Oslo, Norway
 AF Systems Command, Armament Div, Eglin AFB, FL 32542
 Yuma Proving Ground, Yuma, AZ 85365
 McDonnell Douglas Helicopter Co., Mesa, AZ 85205
 Def Materials Organ, Min of Def, Paya Lebar Airport
 US Army Chemical Activity WESTCOM, APO SF, CA 96305
 NSWSS, Port Hueneme, CA 93043
 Micronics International, Inc., Brea, CA 92621
 Log Dir, Sup & Svcs, Ammo Storage Br, APG, MD 21005
 NWS, Yorktown, VA 23691
 Naval Weapons Station, Yorktown, VA 23691
 Martin Marietta Missile Ord Dept, Orlando, FL 32855
 Talley Defense Systems, Inc., Mesa, AZ 85201
 Aerojet General, Sacramento, CA 95853
 Baker perkins Inc., Saginaw, MI 48601
 Munitions Support Br., Dugway, Utah 84022
 Watervliet Arsenal, Watervliet, NY 12019
 Naval Weapons Center, China Lake, CA 93555
 Ctr for Explosives Tech Research, Socorro, NM 87801
 Baker Perkins Inc., Saginaw, MI 48601
 US Army TECOM, Aberdeen Proving Ground, MD 21005
 USA Toxic & Haz Materials Agency, APG, MD 21010
 Stresan Lab, Inc., Spooner, WI 54801
 Mining Resource Engineering Limited, Ontario, Canada
 T&E International, Inc., Bel Air, MD 21014
 Air Staff-Safety & Nuclear Surety, Wash, DC 20330
 Martin Marietta Aerospace, Denver, CO 80201
 Naval Civil Engr Lab, Port Hueneme, CA 93043
 Nav Ord Test Unit, Cape Canaveral, FL 32920
 Mason & Hanger, Amarillo, TX 79177
 Army Materials Tech Lab, Watertown, MA 02172
 Marguardt Company, Van Nuys, CA 91409
 Battelle, Columbus, OH 43201
 S-Cubed-Div of Maxwell Labs, Albuquerque, NM 87198
 Dr. Ing. MARIO BIAZZI S.A., Vevey, Switzerland
 GA Technologies, Inc., San Diego, CA 92138
 Martin Marietta Aerospace, Cocoa Beach, FL 32931
 Bowmar Aerospace, Fort Wayne, IN
 USAE Waterways Experiment Station, Vicksburg, MS
 Forsvarets Eksplosivstofkommission, Hvidovre, Denmark
 Lawrence Livermore Laboratory, Livermore, CA 94550
 6595 ATG, Edwards AFB, CA 93523
 Boeing Aerospace Operations, Dahlgren, VA 22448
 Ballistic Research Lab, APG, MD 21005
 Federal-Hoff, Inc., Anoka, MN 55303
 Detector Electronics Corp., Mpls., MN 55438
 AF Systems Cmd, Eglin AFB, FL 32542
 Naval Surface Weapons Center, Silver Spring, MD 20903
 Cdr, USA Missile Command, Redstone Arsenal, AL 35898

KNIEPP, Norbert R.
 KNOWLTON, Robert E.
 KNUTSON, Roger L.
 KNUTSSON, L. R.
 KOHLBECK, Donald F.
 KOHRN, Marvin
 KOK-WAH, Tan, MAJ
 KOMOS, John N.
 KONCERNSERVICE, Nobel
 KOONTZ, Robert A.
 KOPLOY, Maria
 KOSGOVER, David C.
 KRACH, Fred G.
 KRENCIK, Dick
 KREPS, Raymond E.
 KRIETZ, Terry E.
 KRONICK, Richard A.
 KRUG, Gary R.
 KRUMM, Alan G.
 KRUPA, Mike
 KRUPKO, Edmund J.
 KWAK, Solim S.W.
 KYLEN, Deverle
 LAATSCH, Edward M.
 LAIDLAW, B.G.
 LAIN, David
 LAKE, Rickey B., TSgt
 LALONDE, Richard J.
 LAMB, Alfred L.
 LAMB, Layfield L.
 LAMPE, Lewis B.
 LANHAM, Katherine P.
 LARSEN, Wallace P.
 LAURITZEN, Erik
 LECHKO, Michael
 LEDDEN, William J.
 LEE, Chang H.
 LEE, Gary E.
 LEE, Greg
 LEE, Kim Chye, CPT
 LFE, Robert A.
 LEGALUPPI, Marco
 LENNERTZ, Gudio
 LEVEY, David V.
 LIGHTHISER, T.P.
 LIND, Larry L.
 LIPP, Curtis
 LITTLEFIELD, Dorothy R.
 LITWAK, Gerald M.
 LLOYD, James D.

USA AVISCOM, St. Louis, MO 63120
 Chemetics International Co., Vancouver, Canada
 Honeywell, Hopkins, MN 55343
 AB Bofors, BOFORS, Sweden
 Camarillo, CA 83010
 SM-ALC/SEFW, McClellan AFB, CA 95652-5990
 Ministry of Defence, Republic of Singapore
 Olin-Winchester Corp., Lake City AAP, Indep, MO 64050
 Nat'l Swedish Inspektorate of Explo & Flam, Sweden
 Naval Weapons Ctr, China Lake, CA 93555
 GA Technologies, Inc., San Diego, CA 92138
 Ammann & Whitney, New York, NY 10014
 Monsanto Research Corp., Miamisburg, Ohio 45342
 Aerojet Ordnance Co., Chino, CA 91709
 Eastern Space & Missile Ctr, Patrick AFB, FL 32925
 HQ, USA Depot Systems Command, Chambersburg, PA 17201
 Lockheed Missile & Space Co., Charleston, SC 29411
 Federal Cartridge Co., Anoka, MN 55303
 Naval Ocean Systems Ctr, San Diego, CA 92152
 3009 Roxboro Road, Euless, TX 76039
 Morton Thiokol, Inc./Huntsville Div, Huntsville, AL
 AED-TEAD, Tooele Army Depot, Tooele, UT 84074
 MAQX, Hill AFB, UT 84056
 The Nathan Hale Group, Fairfax, VA 22030
 Defense Research Estab., Ralston, Alberta, Canada
 Micronics International, Inc., Brea, CA 92621
 Explosives Safety Div, Wright-Patterson AFB, OH 45433
 Rockwell International, Anaheim, CA 92803
 Dugway Proving Ground, Dugway, UT 84022
 Naval Weapons Station Charleston, SC 29408
 Exec Dir for Conventional Ammo, AMC, Alex., VA 22333
 Naval Exp Ord Disp Tech Ctr, Indian Head, MD 20640
 Morton Thiokol, Inc., Brigham City, UT 84302
 OILOCONSULT, Danish Ministry of Defense, Denmark
 Automatic Sprinkler, Cleveland, OH 44147
 Naval Weapons Center, China Lake, CA 93555
 Ford Aerospace & Com Corp., Newport Beach, CA 92658
 GA Technologies, Inc., San Diego, CA 92138
 HQ, PACAF/DEEV, ARAEC, Dover, NJ 07801-5001
 Ministry of Defence, Republic of Singapore
 Morton Thiokol, Inc., Louisiana AAP, Shreveport, LA
 Whitney, Bailey, Cox & Magnani, Timonium, MD 21093
 Federal Republic of Germany, ARAEC, Dover, NJ 07801
 JOEX, Inc., Cleburne, TX 76031
 USA Ammo Ctr & School, Savanna, IL 61074
 Western Div, Nav Fac Engr Cmd, San Bruno, CA 94066
 Aerojet General, Sacramento, CA 95853
 Aerojet Ordnance Co., Tustin, CA 92680
 HQs, SAC, Offutt AFB, NE 68113
 USAMC Field Safety Activity, Charlestown, IN 47111

LOFTON, Layne B.
 LONG, Everett A., Jr.
 LONG, William R.
 LONGO, Vito
 LOPEZ, Manuel
 LORENZ, Richard A.
 LOUSHINE, Tom M.
 LOVE, Jim M.
 LOWE, William F.
 LOYD, Robert A.
 LUCAS, Deborah B.
 LIND, Bob
 LYNAM, Robert D.
 LYNN, Jeffrey L.
 LAHOUD, Paul M.
 MAINES, Gary L.
 MANEY, Joe L.
 MANNSCHRECK, W.
 MANSELL, Charles
 MANVELL, Robert
 MARDON, Pierre, MG
 MASON, Kevin M.
 MATHIEU, Raymond A.
 MAIZEY, Peter
 MCCALLA, Alan
 MCCLESKEY, Frank
 MCCOMAS, James H.
 MCCORKLE, Clyde L.
 MCCOWN, Leland A.
 McDONALD, Jack L.
 McDOUGAL, Charles B.
 MCGILL, R.J.
 MCGRAW, Richard P.
 MCKEEM, William R.
 MCKENZIE, Allen K.
 MCKIEL, Kenneth R.
 McLAIN, J.P.
 McMILLAN, Erik
 McQUEEN, Jerry E.
 MELVIN, Felix N.
 MERZ, Hans A.
 MEYER, Gerald
 MEYER, Wallace M., Lt Col
 MEYERS, Gerald
 MICHAUD, Christian
 MIHALYI, Harry
 MIKULA, James J.
 MILES, Donald P.
 MILES, Kurt W., CAPT
 MILLER, Craig A.

Longhorn AAP, Marshall, TX 75671
 US Naval Weapons Center, China Lake, CA 93555
 Naval Wpns Ctr, China Lake, CA 93555
 SPF Incorporated Safety Svcs, Leesburg Pike, VA 22041
 US AMCCOM, Chem Research Dev & Engr Ctr, APG, MD 21010
 Boeing Mil Airplane Co., Wichita, KS 67277
 Sunflower AAP, DeSota, KS
 Aerojet Strategic Prop Co, Sacramento, CA 95813
 AF Armament Lab, Eglin AFB, FL 32542
 USA Armament, Munitions & Chem Cmd, Rock Is., IL 61299
 Naval Air Test Center, Patuxent River, MD 20670
 Motorola Inc., Govn't Elec Group, Scottsdale, AZ 85252
 314th Tac Airlift Wing, Little Rock AFB, AR 72099
 USANICOM Safety Office, Redstone Arsenal, AL 35898
 US Army Engr Div, Huntsville, AL 35807
 Broco, Inc., 2824 N. Locust Ave., Rialto, CA 92376
 Det 1 AFISC/SNI, Kirtland AFB, NM 87117
 Cdr, Naval Safety Ctr, Norfolk, VA 23511
 NTC Safety, AFZJ-PAS, Fort Irwin, CA 92310-500
 Martin-Marietta Aerospace Co., Vandenberg AFB, CA 93437
 Min Def, Inspec de L'Armement Poudres et Explos, France
 Hq, Laboratory Command, Adelphi, MD 20783
 General Electric Co., Burlington, VT 05401
 GA Technologies, Inc., San Diego, CA 92138
 Hardley Industries, Godfrey, IL
 Naval Surface Wpns Ctr, Dahlgren, VA 22448
 Winchester, Olin Corp, Lake City AP, Independence, MO
 HQ, US Army Materiel Command, Alex., VA 22333
 USA Chemical Act, WESTCOM, APCA-SA, APO SF 96305
 San Antonio, TX 78298
 Lexington-Blue Grass AD, Lexington, KY 40511
 Aerojet General Corp., Sacramento, CA 95853
 Ensign Bickford Co., Simsbury, CT 06070
 Naval Weapons Supt Ctr, Crane, IN 47522
 Morton Thiokol, Inc., Ogden, UT 84405
 PMIC, Pt. Mugu, CA 93041-5000
 New Mexico Inst. of Mining & Tech, Socorro, NM 87801
 USAF Tac Fighter Wpns Ctr, Nellis AFB, NV 89191
 Motorola Inc., Govn't Elec Group, Scottsdale, AZ 85252
 Hawthorne Army Ammo Plant, Hawthorne, Nevada 89415
 Ernst Basler & Partners, Zurich, Switzerland
 Naval Civil Engr Lab, Port Hueneme, CA 93043
 AF Inspec & Safety Ctr, Norton AFB, CA 92409
 Naval Civil Engr Lab, Port Hueneme, CA 93043
 Center D Etude de Vaujours a la Mission, France
 DCASR Dallas, Dallas, TX 75250
 US Army Armament RD&E Center, Dover, NJ 07801
 Ministry of Defence (Navy), Bath, UK
 Dugway Proving Ground, Dugway, UT 84022
 Kresky Signs, Inc., Petaluma, CA 94953

MILLER, Henry R.	Uniroyal Chemical Co., Inc., Joliet AAP, IL 60434
MILLER, Jerry R.	Tooele Army Depot, Tooele, UT 84074
MILLER, John R.	PPG Ind., Inc., Huntsville, AL 35801
MILLER, Paul L.	Honeywell, MN 55343
MILLER, Robert A. TSgt	343 TFW, Eielson AFB, Alaska 99702
MILLS, Clifton E.	USAF, Robins AFB, GA 31098
MIX, Claire L.	Northrop Corp./Vantura Div, Newbury Park, CA 91320
MOHANTY, B.	C-I-L Inc., Exp Rech Lab, McMasterville, Quebec, Canada
MONCOS, Michael I.	Pacific Missile Test Ctr, Point Mugu, CA 93042
MOORE, C. J.	AF Military Training Ctr, SEV, Lackland AFB, TX 78236
MOORE, Kenneth J.	Rockwell Intr Satellite Sys Div, Kennedy Space Ctr, FL
MOORE, Thomas M.	HQ USCENAF, Shaw AFB, S.C. 29152-5002
MOORE, Verence D.	NSWC/WD, Silver Spring, MD 20903
MORAN, Edward P.	DDSB Secretariat, Alex., VA 22331
MOREAU, Bernard	Societe Nat Des Poudres et Explosifs, Paris, France
MORGAN, Charles E.	NUWES, Keyport, WA 98345
MORGAN, Larry	USAMC Field Safety Activity, Charlestown, IN 47111
MORI, George L.	Honeywell-USD, Hopkins, MN 55343
MORIN, Gerald E.	Rockwell International, Anaheim, CA 92803
MORRISON, William C., COL	AF Inspection & Safety Center, Norton AFB, CA 92409
MORSE, Carl E., LTC, USA	Hq, Defense Nuclear Agency, Alex., VA 22310
MORTENSEN, Dell L.	Day & Zimmermann Corp., Hawthorne Army Ammo Plant, NV
MOSELEY, Kenneth E.	USA Strategic Def Cmd, APO San Francisco, CA 96555
MOSLEY, Kenneth E.	Ford Aerospace & Communications Corp, Newport Beach, CA
MOSS, Laudy	Aerojet Strategic Prop Co., Sacramento, CA 95813
MOSSA, Martin	USA Combat Sys Test Act, APG, MD 21005
MUELLER, Billy D., TSgt	443 MAW/SEF, Altus AFB, OK 73523
MUELLER, Heinz	Tudor Engineering Company, San Francisco, CA 94105
MUTLU, Matti E.	Finish Defence Forces Research Ctr, Finland
MULKEY, Robert J.	Mason & Hanger, Amarillo, TX 79177
MULLIN, Jonathan B., Lt Col	Western Space & Msl Test Ctr, Vandenberg AFB, CA 93437
MUNOZ, George R.	Hollister, CA 95024
MURPHY, Francis X.	Dir for Quality Assurance, Seneca AD, Romulus, NY 14541
MURRAY, Robert K.	Ford Aerospace & Communications Corp, Newport Beach, CA
MURTHA, Robert N.	Naval Civil Engr Lab., Port Hueneme, CA 93043
MUSACCHIO, John M.	Paul C. Rizzo Assoc., Inc., Pittsburgh, PA 15235
NAPADENSKY, Hyla	IIT Research Institute, Chicago, IL 60616
NASH, John T.	HQ, Dept. of Army, Washington, DC 20310
NASH, Phil	Southwest Research Institute, San Antonio, TX 78284
NAVARRO, Ernesto A.	Honeywell, Hopkins, MN 55343
NEADES, David N.	USA Ballistic Research Lab, APG, MD 21005-5006
NEFF, Ronald A.	Kansas Army Ammo Plant, Parsons, Kansas 67357
NELSON, Gerald A.	Naval Ocean Systems Center, San Diego, CA 92152
NELSON, Olen	Star Glove & Safety Products Corp., LA, CA 90021
NETT, Dal M.	USA Combat Sys Test Act, APG, MD 21005
NEW, Willie	US Army Technical Escort Unit, APG, MD 21010
NEYRINCK, Ronny G., CAPT	Belgian Army, Leuven, Belgium
NICKERSON, Howard D.	Naval Fac Engr Command, Alex., VA 22332
NIERGARTH, Charles C.	Aerojet Ordnance Co., Chino, CA 90740
NILSSON, Erik O.	Nat Swedish Inspectorate of Explo & Flam, Solna, SW

NOLTE, Gerry C.
 NORBERG, Donald W.
 NUDD, Edward J.
 O'BRIAN, Richard B.
 OLSON, David W.
 OLSON, Eric T.
 OLSON, R. G.
 OPEL, Mervin C.
 OPFERMANN, Albert B.
 OPSCHOOR, Gerard
 ORR, Madeleine
 OVERBAY, Larry W.
 OWEN, Michael C., Brig.
 OXLEY, Jimmie C.
 PAIGE, John A.
 PAKULAK, Jack M.
 PAKULAK, Mary S.
 PALLITTO, Joseph, MSgt, USAF
 PAPP, A.G.
 PARIS, William F., COL
 PARK, Cindy
 PARKES, David A.
 PARRISH, Alan
 PARRISH, Charles A.
 PARRISH, David D.
 PARSONS, Gary W.
 PATRICK, Gwyn C.
 PATTESON, Macon
 PAYNE, David G.
 PEARSON, Stanley L.
 PELEG, A.
 PENROD, Steven K.
 PEREIRA, William C., CPT
 PERRY, John G.
 PERRY, Robert B.
 PETENS
 PETERS, Charles R.
 PETERSEN, Carl G.
 PETTY, Paul
 PHILO, William H.
 PIPER, Charles J.
 PLATE, Stanley
 POHL, A. David
 POJMANN, David M., COL
 POPE, Alvin L.
 POPE, Barbara S.
 PORTNOY, Seymour
 PRENDERGAST, James D., Dr.
 PRESTON, H. Joe
 PRICE, Donna

Ctrl Ammo Mgmt Ofc(PAC), Ft. Shafter, HI
 Stearns Catalytic Corp., Denver, CO 80210
 Science Applications International Corp., Las Vegas, NV
 Aerojet General Corporation, La Jolla, CA 92037
 Kresky Signs, Inc., Petaluma, CA 94953
 AMC Field Safety Activity, Charlestown, IN 47111
 Lockheed Missile & Space Co., Sunnyvale, CA 94086
 ICI Americas Inc., Charlestown, IN 47111
 E.I. DuPont Co., Wilmington, DE 19803
 Prins Maurits Lab TNO, Netherlands
 FMC Corporation, San Jose, CA 95108
 Combat Sys Test Activity, APG, MD 21005
 Dir of Land Svcs Ammo, Vauxhall Barracks, Oxon, England
 Ctr for Explosives Tech Research, Socorro, NM 87801
 Space Ordnance Systems, Canyon Country, CA 91351
 Naval Weapons Center, China Lake, CA 93555
 Naval Weapons Center, China Lake, CA 93555
 HQ USCINCPAC, Camp h.M. Smith, HI 96861
 Mason & Hanger-Silasmason Co., Inc., Amarillo, TX
 HQDA, DALO-SMA, Washington, DC 20310
 Lake City AA, SMCCLC-SF, Independence, MO 64050-0330
 Black & Veatch, Kansas City, MO 64114
 Hercules Inc., P.O. Box, Radford, VA 24141
 Hercules Inc., Radford, VA 24141
 Lockheed, Sunnyvale, CA 94086
 Whittaker Corp., Bermite Div, Saugus, CA 91355
 USATECOM, Aberdeen Proving Ground, MD 21005
 Command Support Division, Dahlgren, VA 22448
 USA Depot Act Umatilla, Hermiston, OR 97838
 Space Ordnance Systems, Canyon Country, CA 91351
 Ministry of Def, Israel Military Industries, NY 10022
 Umatilla Army Depot, Hermiston, OR 97838
 Republic of Singapore AF, Paya Lebar Airport
 USAMC, Alexandria, VA 22333
 DDESB, Alexandria, VA 22331-0600
 Cdr, ARDEC, Dover, NJ 07801-5001
 USA Armament Research, Dev, & Engr Ctr, Dover, NJ
 OILOCONSULT, Danish Ministry of Defense, Denmark
 General Dynamics, Pomona, CA 91769
 DOS SA6, Washington, DC 20520
 Quantic, San Carlos, CA 94070
 Tri-State Motor Transit Company, Alex., VA 22311
 TRW, Redondo Beach, CA 90278
 HQ, AMCCOM, Rock Island, IL 61299
 Mason & Hanger Engr Inc., Lexington, KY 40505
 DASD (Family Support, Ed, & Safety), Washington, DC
 Armament, Research, Dev & Engr Ctr, Dover, NJ 07801
 USA-CERL-EM, PO Box 4005, Champaign, IL 61820-1305
 Strategic Weapons Fac Pacific, Bremerton, WA 98315
 NSWC/WD, Silver Spring, MD 20903-5000

PRICE, Paul D.
 PROCTOR, James F.
 PROHASKA, Frank B.
 PROPER, Kenneth W.
 PROUDMAN, W.
 PULS, Kenneth C.
 PURVIS, James E.
 QUINN, Keith M.
 RAGAN, Elmer W.
 RAMBAUT, Michel Louis
 RANEY, Gary
 RASH, Ray C.
 RAU, Stephen J.
 RAZ, Ray
 REED, Jack
 REES, Norman J.M.
 REEVES, Harry J.
 REEVES, Peter, Commodore, UK
 REGOPOULOS, Ken J.
 REINHARD, E. Daniel
 RENFRO, William
 REYES, Bernadette N.
 REYNAUD, Raymond J.
 REZETKA, Wilbert L.
 RHEA, Richard L.
 RICHARDSON, David E.
 RICHER, Kevin R., SSgt
 RICHMOND, Donald R.
 RIEDER, William E.
 RIFE, Richard
 RIGGS, John I.
 RILEY, William E.
 RISBECK, Tom R.
 ROBERTS, Charles E.
 ROBERTS, Robin
 ROBERTSON, Tom R.
 ROBINSON, E.A., Dr.
 ROBINSON, Eddie G.
 ROBINSON, Ralph D.
 ROEDSON, William J.
 ROESLER, Helmut
 ROOT, George L.
 ROSBERG, Al
 ROSEN, Robert S., CAPT, USN
 ROSENTHAL, William D.
 ROVELL, Charles A.
 ROY, Edward M.
 RUCKER, Klaus G.
 RUSSAKOV, Loren
 RUTISHAUSER, Paul W.
 DDES Secretariat, Alex., VA 22331
 Naval Surface Weapons Ctr, Silver Spring, MD 20901
 Naval Sea Supt Ctr, Pacific, San Diego, CA 92138
 USA Def Ammo Center & School, Savanna, IL 61074
 Maryland Assemblers, Inc., Perry, FL 32347
 Ensign Bickford Co., Simsbury, CT 06070
 Western Space & Msl Test Ctr, Vandenberg AFB, CA 93437
 Arnold Eng. Dev. Center, Arnold AFS, TN 37389
 2750 ABW Safety, Wright-Patterson AFB, OH 45322
 Commissariat a L'Energie Atomique, Paris, France
 Aerojet Ordnance Corp., Downey, CA 90241
 Cdr Off, Naval Weapons Supt Ctr, Crane, IN 47522
 Monsanto Research Corp., Miamisburg, Ohio 45342
 HQs, AFRES/SEW, Robins AFB, GA
 Sandia Nat'l Laboratory, Albuquerque, NM 87185
 MOD, UK, Kent, Great Britain
 Ballistic Research Lab., USABRL, APG, MD 21005
 Ministry of Defence, Ordnance Board, London, UK
 The Marguard Co., Van Nuys, CA 91409
 Ofc Asst Sec Navy (S&L), Wash., DC 20360
 Micronics International, Inc., Brea, CA 92621
 Safety Consulting Engineers, Inc., Rosemont, IL 60018
 NASA - Johnson Space Center, Las Cruces, NM 88001
 Pacific Missile Test Ctr, Point Mugu, CA 93042
 Olin Corporation, St. Marks, FL 32355
 Hercules Incorporated, Bacchus Works, Magna, UT 84044
 2701 Exp Ord Disp Squad, Hill AFB, UT 84056
 Los Alamos Nat'l Lab, Los Alamos, NM 87545
 HQ AF Logistics Cmd, Wright-Patterson AFB, OH 45433
 AMKPM-CD, APG, MD
 Aerojet Strategic Prop Co, Sacramento, CA 95813
 Western Space & Missile Ctr, Vandenberg AFB, CA 93437
 Chamberlain Manufacturing Corp., Waterloo, IA 50704
 DCASMA Twin Cities, St. Paul, MN 55116
 Aerojet Ordnance Co., Chino, CA 91709
 Explosives Branch, Ottawa, Canada
 British Defense Staff, British Embassy, Wash., DC 20008
 Pine Bluff Arsenal DA, AR 71602
 Field Cmd, Def Nuclear Agency, Kirtland AFB, NM 87115
 United Technologies, San Jose, CA 95150
 Stearns Catalytic Corp., Philadelphia, PA 19102
 Jet Propulsion Lab, Edwards Fac, Edwards, CA 93523
 Nobel Koncernservice AB, Sweden
 Naval Magazine Lualualei, HI 96792
 Whittaker Corp., Bermite Div, Saugus, CA 91355
 LTV Aerospace & Def Co., Dallas, TX 75265
 Ctr for Explosive Tech Research, Socorro, NM 87801
 E.I. DUPONT de NEMOURS, Pompton Lakes, NJ 07442
 Micronics, Brea, CA 92621
 Ammo Surveillance Div, Tooele AD, Tooele, UT 84074

RUTLEDGE, Peter J.
 SACK, James L.
 SALLY, John
 SAMUELSON, Alan F.
 SAND, Larry D.
 SAUERBAUM, Richard J.
 SAUNDERS, Duane E.
 SAWYER, Ray B.
 SAYLORS, James A.
 SCHAEFER, Dennis H., MAJ
 SCHAEFER, Siegfried F.
 SCHILLING, Robert W.
 SCHULZE, William F.
 SCHUM, Robert R.
 SCOTT, Dick
 SCOTT, Ralph A.
 SEAL, Warren G., LCDR
 SEYMOUR, Richard B.
 SHANNAN, Joe E.
 SHEARIN, Walter F.
 SHIMIZU, Haruaki
 SHIPMAN, D. R.
 SHOPHER, Kenneth R.
 SHRIVER, Jerry R.
 SHROYER, William
 SHULTS, Richard H.
 SHURTLEFF, E.M.
 SILER, A. Ken
 SIMON, Brian P.
 SIMON, Elvis D.
 SIMPSON, Douglas K.
 SINAI, J.
 SINGH, Ashok K.
 SKIDMORE, Frank M., CAPT, USMC
 SLOAN, Robert E.
 SMALLWOOD, Robert J., Dr.
 SMITH, Alan J.
 SMITH, C. Richard
 SMITH, Dale W.
 SMITH, Douglas D.
 SMITH, Gary H.
 SMITH, Lawrence E.
 SMITH, Obie A., Jr.
 SMITH, Paul D.
 SMITH, Richard E.
 SMITH, Robert L.
 SMITH, Roger W., LCdr
 SMITH, Ronald A.
 SMITH, Samuel I.
 SMITH, Terence E.

OASD (FM&P), Washington, DC 20301-4000
 USA COE, Omaha District, Omaha, NE 68108
 Comarco Inc., Ridgecrest, CA 93555
 Defense Contrac Admin., Santa Ana, CA 92712
 Omaha Dist Corps of Engrs, Omaha, NE 68101-1294
 438 MAW, McGuire AFB, NJ 08641
 Magnavox, Fort Wayne, IN 46808
 DDESB Secretariat, Alex., VA 22331
 Bernard Johnson Inc., Houston, TX 77056
 Canadian Forces, Ontario, Canada K1C2K9
 German Armament Administration, Meppen, West Germany
 Federal Ministry of Defence, Bonn, Germany
 Monsanto Research Corp., Miamiburg, Ohio 45342
 DCASMA Twin Cities, St. Paul, MN 55116
 Garrett Fluid Systems Co., Tempe, AZ 85282
 DDESB Secretariat, Alex., VA 22331
 COMNAIRPAC, San Diego, CA 92135
 Martin Marietta Denver Aerospace, Denver, CO 80201
 Mason & Hanger-Silas Mason Co., Inc, Iowa AAP, IA 52638
 Crane Army Ammo Activity, Crane, IN 47522
 Nippon Oil & Fats Co., New York, NY 10166
 TRW, San Clemente, CA 92672
 AF Inspection & Safety Center, Norton AFB, CA 92409
 Det 35 AFPRO/SE, Aerojet-Gen Corp., Sacramento, CA
 Aerojet Ordnance Co., Chino, CA 91709
 Atlantic Research Corp., Gainesville, VA 22065
 Ford Aerospace & Comm Corp., Newport Beach, CA 92658
 Defense Logistics Agency, Marietta, GA 30062
 Naval Weapons Station, Concord, CA 94520
 Martin Marietta Corp., Denver, CO 80201
 Olin Corporation, Cheshire CT 06410
 Ministry of Def, Israel Military Industries, NY, NY
 CRS Sirmine, Greenville, SC 29606
 Marine Corps Air Station, Yuma, AZ 85369
 Naval Ammo Prod. Engr Ctr, Crane, IN 47522
 UK Health & Safety Exec, Bootle, England
 UK Min of Def, UK Rep McDonnell Douglas, St. Louis, MO
 General Dynamics/Pomona Div, Pomona, CA 91769
 Ford Aerospace & Communications Corp, Newport Beach, CA
 Broco, Inc., 2824 N. Locust Ave., Rialto, CA 92376
 Spescom International Inc., Irvine, CA 92718
 USA Armament Mun & Chem Cmd, Rock Is., IL 61299
 Anniston Army Depot, AL 36201
 Los Alamos Nat'l Lab, Los Alamos, NM 87545
 Sandia Nat'l Lab, Albuquerque, NM 87185
 Hercules Aero Co, Sunflower AAP, DeSota, KS 66018
 DNA, Kirtland AFB, Albuquerque, NM 87112
 NUWES Indian Island Det, Hadlock, Washington 98339
 Honeywell LAP Facility, Joliet, IL 60434
 Rockwell International, Anaheim, CA 92803

SMITH, Walter C.
 SPELL, Daniel
 SPENCE, Wesley F.
 SPERLING, Michael
 ST. PIERRE, Gregory N.
 STANCKIEWITZ, Charles
 STANFORD, Angela
 STATON, James W.
 STEINBAKKEN, S.
 STEINER, Wendell E.
 STEPHENS, David J.
 STERANKA, Patricia J.
 STEVENSON, Randy N.
 STEWART, Bob W.
 STILES, Wayne, LT
 STOREY, Ray E.
 STRATMAN, George E.
 STRONG, David R.
 STUDDERT, William T.
 STUMPH, Charles
 SUEKER, Wayne R.
 SUGARMAN, Samuel H.
 SUTHERLAND, Michael J.
 SUVER, Elizabeth M.
 SVEC, Sue A.
 SVENSSON, Sven-Erik, Col Lt
 SWAFFORD, Chester
 SWISDAK, Michael M., Jr.
 TAN, Richard, LTC
 TANCRETO, James E.
 TANIGAWA, Clifford N.
 TARAS, Darwin N.
 TAYLOR, Truman
 TAYLOR, William J.
 TERRY, Kenneth L.
 THILL, Frank L.
 THOMAS, Garland L., Dr.
 THOMPSON, Kenneth A.
 THURMAN, James T.
 THYSSEN, Michael W., 1LT
 TOENJES, Kurt A., CAPT, GAF
 TOLLEY, Gilbert O.
 TOZER, Noel H.
 TRAUGH, William H.
 TRICK, John J.
 TROCINO, Joseph L.
 TSUCHIYA, James H.
 TUCKER, Del
 TUCKER, Steve
 TUOKKO, Seppo S.

Micronics International, Inc., Brea, CA 92621
 USA White Sands Missile Range, NM 88072
 E.I. du Pont de Nemours & Co., Wilmington, DE 19398
 Aerojet Ordnance Co., Downey, CA 90240
 Chem R&D & Engr Ctr, APG, MD 21010-5423
 USAMC Field Safety Activity, Charlestown, IN 47111
 DDESB Secretariat, Alex., VA 22331
 6515 MMS/MAW, Edwards AFB, CA 93523
 Haerens Forsyningskommando, Norway
 Pacific Msl Test Ctr, Pt. Mugu, CA 93042-5000
 UK Ministry of Defence, Portland Dorset, UK
 USA Depot Activity, Pueblo, Pueblo, CO 81001
 Martin Marietta Missile Ord Dept, Orlando, FL 32355
 Loral Electro-Optical Systems, Pasadena, CA 91109
 HQ, AAC/ICFW, Elmendorf AFB, Alaska 99506-7000
 Weapons Safety Office, Hill AFB, UT 84056
 Hill AFB Weapons Safety Ofc, Hill AFB, Utah 84056
 Rockwell Int'l-Rocketdyne Div, Canoga Park, CA 91303
 AMC Surety Field Ctr, Dover, NJ 07801-5299
 Orange Co. Sherriff Dept., Orange, CA 92667
 Honeywell, Inc., Joliet, IL 60434
 Bulova Systems & Instruments Corp., Valley Stream, NY
 1005A Crimson Tree Way, Edgewood, MD 21040
 Air National Guard, Andrews AFB, MD 20331
 Anniston Army Depot, AL 36201
 Forsvarets Materielverk, Karlstad
 DCASMA, Santa Ana, CA
 Nav Surface Weapons Ctr, Silver Springs, MD 20903
 Ministry of Defence, Republic of Singapore
 Navy Civil Engr Lab, Port Hueneme, CA 93043
 The Marquardt Co., Van Nuys, CA 91409
 HQ, US Army Materiel Command, Alex., VA 22333
 US Army Safety Center, Fort Rucker, AL 36362
 Ballistic Research Lab., APG, MD 21014
 Hq, US Army Japan, APO SF 96343-0054
 NAS North Island, CA 92135
 SF-ENG, Kennedy Space Center, FL 32899
 USA Msl & Space Ctr & Sch, Redstone AR, AL 35897
 Explo Unit, FBI Lab., Washington, DC 20535
 AR Weapons Laboratory, Kirtland AFB, NM 87118
 FMOD GE Armed Forces Staff, Bonn, Germany
 HQ US Army Europe, APO NY 09403
 Dept. of Defence(Australia), St. Marys, Australia 2760
 Morton Thokol, Brigham City, UT 84302
 Naval Ordnance Station, Indian Head, MD 20640
 15233 Van Turen Blvd., Sherman, CA 91403
 Hercules Inc., McGregor, TX 76557
 HQ, Depot Sys Command, Chambersburg, PA 17201
 Sandia Nat'l Lab., Livermore, CA 94550
 Ministry of Defence, Helsinki, Finland

TUTTLE, Peter G.
 UNGER, Ronald J.
 VAGNONE, Eugene H.
 VAN DOLAH, Robert W.
 VAN EVERDINK, Leo
 VAN SLYKE, Milton R.
 VANEK, Chester F.
 VARNER, Kenneth W.
 VAUSHER, A.L.
 VENKATECH, Mandyam C.
 VERNON, Gregory A.
 VETTER, Eric S.
 VETTER, Leo M.
 VICKERS, Marvin E.
 VINCOLI, Jeff
 VIOLA, Ed
 VOGT, Michael G.
 VRETLAD, Bengt E., Dr.
 WAGER, Phillip C.
 WALKER, Raymond F., Dr.
 WALTER, James R.
 WALTERS, James O.
 WANGLER, R.B.
 WARD, Jerry M.
 WARNER, Al
 WATANABE, Wallace A.
 WATSON, Jerry L.
 WATSON, Richard W.
 WATTS, Howard D.
 WAY, Norman L.
 WEARE, Christopher
 WEAVER, Frances L.
 WEBB, Samuel D.
 WEBSTER, Larry D.
 WEIGEL, Ulrich
 WERNSMAN, Robert L., CAPT
 WEST, Buddy
 WHEELER, Ronald H.
 WHITFIELD, Lorenzo
 WHITNEY, Christine
 WHITNEY, Mark G.
 WILCOX, Gary L.
 WILLIAMS, Andre R.
 WILLIAMS, Doyle G.
 WILLIAMS, Vernon, SGT
 WILLIOTT, E.G., MG
 WILSON, Donald E.
 WILSON, John P.
 WILSON, Robert L.
 WING, Walter G.

DCAR Boston, Boston, MA 02210
 Sverdrup Technology, Inc., Arnold AFS, TN 37389
 Northrop Corporation, Anaheim, CA 92801
 Consultant, Pittsburgh, PA 15241
 MIMC, The Netherlands
 NAVSEA, Washington, DC 20362
 Lockheed Missile & Space Co., Sunnyvale, CA 94086
 Surv Div, Camp Stanley Storage Act, San Antonio, TX
 McDonnell Douglas Corp., Huntington Beach, CA 92647
 GA Technologies, Inc., San Diego, CA 92138
 Naval Weapons Center, China Lake, CA
 Rockwell International, Downey, CA 90241
 375th Aeromedical Airlift Wing, Scott AFB, IL 62225
 Naval Sea Supt Ctr, Pacific, San Diego, CA 92110
 McDonnell Douglas Astro Co., Titusville, FL 32780
 VP Kinross Mfg Corp., Kincheloe, MI 49788
 US Army Corps of Engineers, Washington, DC 20314
 FORTF-RSFA, Eskilstuna, Sweden
 Naval Civil Engr Laboratory, Port Hueneme, CA 93043
 Walker Associates, Morris Plains, NJ 07950
 Naval Weapons Sta, Seal Beach, CA 90740
 US Army Nuclear & Chem Agent, Springfield, VA 22150
 Southwest Research Institute, San Antonio, TX 78284
 DDESB, Alexandria, VA 22331-0600
 United Technologies, San Jose, CA 95150
 US Army Corps of Engineers, Huntsville, AL 35807
 BRL-TBL-EEB, Aberdeen Proving Ground, MD 21005
 U.S. Bureau of Mines, DOI, Pittsburgh, PA 15236
 Naval Surface Weapons Ctr, Silver Spring, MD 20903
 Monsanto Research Corp., Miamisburg, Ohio 45342
 Orange Co. Sherriff Dept., Orange, CA 92667
 Ballistic Research Lab, APG, MD 21005
 Lockheed Missile & Space Co., St. Marys, GA 31558
 Naval Sea Systems Cmd, Washington, DC 20362
 UNB Frau Theresia, Koisdorfer Str. 80, 5485 Sinzig
 Chief of Naval Operatins, Washington, DC 20350
 AD/SES, Eglin AFB, FL 32542
 Schneider Services International, Arnold AFS, TN 37389
 436 MAW, Dover AFB, Dover, DE 19902
 US DOT, Washington, DC 20590
 Southwest Research Institute, San Antonio, TX 78284
 Chamberlain Manufacturing Corp., Waterloo, IA 50704
 34th Ord Det(EOD), Sierra AD, Herlong, CA 96113
 LA Army Ammo Plant, Shreveport, LA 71130
 USA White Sands Missile Range, NM 88002
 President, UK Ordnance Board, England
 Public Works Dept., Nav Ord Sta, Indian Head, MD 20640
 USAF, McClellan AFB, AL 95652
 Propellux Corporation, Edwardsville, IL 62025
 Bowmar Aerospace, Fort Wayne, IN

WINKLER, Melvin E.
 WOFFORD, Robert K.
 WOLFE, Larry K.
 WOODSUM, Mark E., 1LT, USA
 WORSHAM, W.K.
 WRIGHT, Howard G.
 WRIGHT, Terry P.
 WU, D. L.
 WUENNENBERG, Thomas C.
 YAMAMOTO, Hitomi G.
 YATES, Mitchell D.
 YEE, Kan
 YEN, Chong Lian
 YIP, Harry H.
 YONG-KWANG, Sim
 YOUNG, John H., LCDR, USN
 YUTMEYER, William P.
 ZAKER, Bernadette
 ZAKRZEWSKI, Peter H.
 ZAUGG, Mark M.
 ZHAO, Zhuang-Hua
 ZIENTEK, Ronald J.
 ZIMMERMAN, John R., Dr.

Navy Plant Br Rep Ofc, Hercules Inc, Magna, UT 84044
 Dir for Quality Assurance, Sierra AD, CA 96113
 HQs, Military Airlift Command, Scott AFB, IL 62225
 70th Ord Disp Det, San Diego, CA 92106
 Martin Marietta Aerospace, Orlando, FL 32855
 Chemetics International Co., B.C., Canada
 NSWSES, Code 4R40, Port Hueneme, CA 93043
 Bechtel National, Inc., San Francisco, CA 94119
 Booker Associates, Inc., St. Louis, MO 63101
 Reynolds industries Sys Incorp., San Ramon, CA 94550
 AFPRO/DET-36, LAAFS, CA 90009
 Naval Underwater Systems Ctr, Newport, RI 02840
 Republic of Singapore AF, Paya Lebar Airport
 G.A. Technologies, San Diego, CA 92138
 Ministry of Defence, Republic of Singapore
 COMEABASEDASWWINGSLANT, Jacksonville, FL 32212
 US Army Materiel Command, Charlestown, IN 47111
 DDESB Secretariat (Invitational)
 Defense Logistics Agency, St. Louis, MO 63101
 Ammo Equip. Dir., Tooele Army Depot, UT 84074
 Xian Modern Chemistry Institute, Xian, China
 USA White Sands Msl Range, NM 88002
 USA Armament Resch & Dev Ctr, Pic Ar, Dover, NJ 07801